Jörg Klekamp
Madjid Samii

Surgery of Spinal Tumors

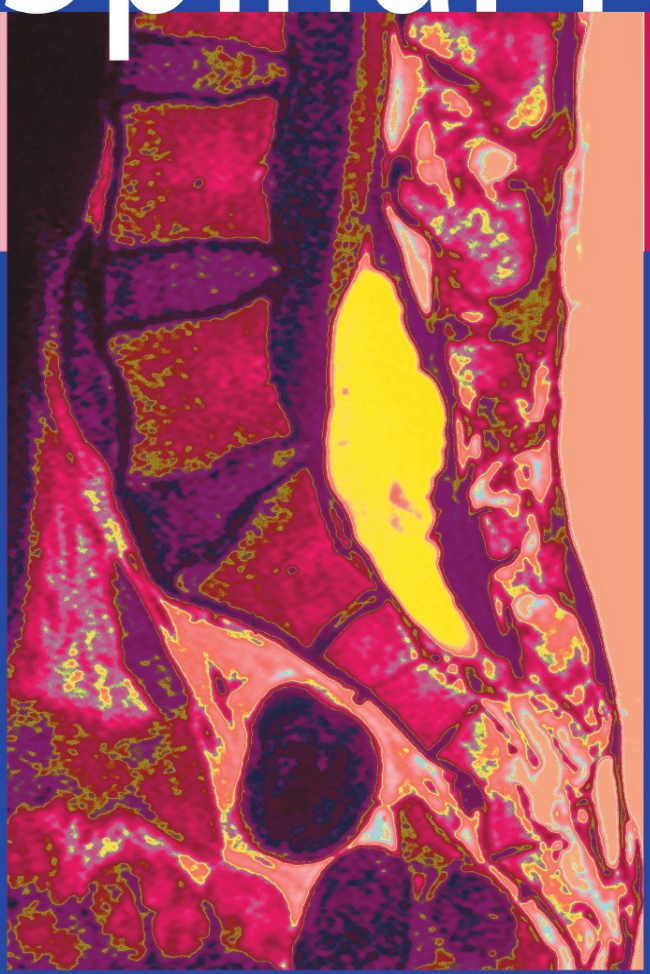

Springer

Jörg Klekamp, Madjid Samii

Surgery of Spinal Tumors

Jörg Klekamp, Madjid Samii

Surgery of Spinal Tumors

With 1879 Figures and 105 Tables

Springer

Jörg Klekamp, MD
Christliches Krankenhaus Quackenbrück
Chirurgisches Zentrum
Fachbereich Neurochirurgie
Danziger Straße 2
49610 Quackenbrück
Germany

Madjid Samii, MD
International Neuroscience Institute (INI)
Rudolf-Pichlmayr-Straße 4
30625 Hannover
Germany

ISBN 978-3-540-44714-6 Springer Berlin Heidelberg New York

Library of Congress Control Number: 2006940545

Springer is a part of Springer Science+Business Media
springer.com

Editor: Gabriele Schröder, Heidelberg, Germany
Desk Editor: Stephanie Benko, Heidelberg, Germany
Production: LE-TEX Jelonek, Schmidt & Vöckler GbR, Leipzig, Germany
Cover design: Frido Steinen-Broo, EStudio, Calamar, Spain
Reproduction and typesetting: am-productions GmbH, Wiesloch, Germany

Printed on acid-free paper 24/3100/YL 5 4 3 2 1 0

Dedications

For my wonderful wife Ulrike and our son Lukas, whose continuing love and understanding provided so much support for me throughout this project.

Jörg Klekamp

To my beloved family.

Madjid Samii

This book is dedicated to all patients suffering from spinal tumors. Their courage and enthusiasm to withstand progressive immobility or even life-threatening situations has been a tremendous inspiration for us.

Jörg Klekamp
Madjid Samii

Foreword

The request from Professor Jörg Klekamp for me to write the foreword for this monograph was an appealing challenge. Prior to the era of microneurosurgery, I was firmly involved in the surgery of spinal lesions, and achieved surgical removal of spinal arteriovenous malformations (AVMs) on 12 patients in the years between 1960 and 1965. Microneurosurgical techniques were introduced in Zurich in 1962, and since then I have applied these techniques to the exploration of the various spinal lesions: 182 herniated discs, 78 spinal cord AVMs, and 263 spinal tumors (46 epidural, 94 extramedullary, and 123 intramedullary tumors). These have been published in a preliminary paper only, for I was unable to accomplish completion of the planned Volume V in my Microneurosurgery series within an adequate time frame. I therefore admire the achievement of Klekamp and Samii, who present to us a most comprehensive work.

This monograph is outstanding in many aspects, providing an overview of the clinical experiences gained in a single neurological institution over a period of 25 years between 1978 and 2003, consisting of 1081 spinal tumors treated in 868 patients, with 973 operations (intramedullary tumors in 198 patients, extramedullary tumors in 446 patients, and epidural tumors in 329 patients). The entire cohort of patients was explored surgically by applying microsurgical techniques. The history of spinal surgery, spinal anatomy, neuroradiology, clinical neurophysiology, surgical approaches, and surgical techniques in the treatment of intramedullary, extramedullary, and epidural tumors in cervical, thoracic, and lumbosacral areas, postoperative results and outcome, complications, morbidity, recurrences, survival, and adjuvant therapies are all meticulously analyzed and thoroughly documented in numerous informative statistical tables and in educative pictures. In addition, multivariate analyses were performed to determine the factors predicting surgical results or outcome. For each factor, a β-value is given, which indicates its predictive power compared to others.

Three distinct time periods can be traced throughout the approximately 120-year history of spinal surgery.

1. The Previsualization Period (1880–1920). A precise neurologic examination of the patient revealed a reliable topographic diagnosis of a spinal lesion. Extramedullary tumors were successfully removed by Macewen (1183, 1884), Horsley (1887), Thornburn (1888), Abbe (1889), Chipault (1894), and Starr (1895). The surgery of intramedullary tumors, however, was pioneered by von Eiselberg (1907), Fedor Krause (1908), Braun (1910), Röpke (1911), and Charles Elsberg (1914). Cushing had explored an intramedullary tumor in 1905, but did not remove it.

Klekamp and Samii emphasize the impact of the paper by Horsley, as he passionately recommended surgery on patients with spinal tumors, because the alternative, "conservative treatment" was associated with a very high mortality rate. The worldwide highly respected pioneer of spinal tumor surgery was Charles Elsberg. In 1925 and 1941, Elsberg published his series of cases (168 with extramedullary tumors, 73 with epidural tumors, and 19 with intramedullary tumors), wherein he recorded remarkably reduced mortality rates.

2. The Myelography Period (1921–1975). The introduction of myelography (1921) by Sicard and Forestier was a welcome and reliable diagnostic advance, for it displayed the precise localization of the lesions. The publication of Guidetti and Fortuna (1967) reflects the positive impact of myelography technology on spinal surgery. They collected in the literature published prior to 1965, 473 operated cases of intramedullary tumors: 119 ependymomas, 125 astrocytomas, 11 oligodendrogliomas, 59 glioblastomas, 113 lipomas, 29 hemangioblastomas, and 17 melanomas. In addition to the effectiveness of myelography for topographic diagnosis, another innovation became essential for the successful treatment of spinal tumors, namely the introduction of the first generation of bipolar coagulation tools by James Greenwood. In 1941, 1942, 1952, and 1953 Dr. Greenwood successfully operated on four patients with spinal cord lesions, none of whom suffered either pre- or postoperative neurological deficits. Previous to Dr. Greenwood's success, there had been a great reluctance to attempt surgery on an intramedullary tumor, especially on a patient having no, or only discrete neurological deficits.
3. The introduction of selective spinal angiography by M. Djindjian (1970), and noninvasive neurovisualization technology (computed tomography in 1970 and magnetic resonance imaging in 1985). These innovations signified very relevant breakthroughs in achieving precise topographic and differential diagnoses of spinal lesions, as well as delineating their vascularization pattern. This knowledge is of great benefit when evaluating the location of the lesion, and when devising a plan for surgical exploration.

Many developments and innovations followed that represented enhancing factors for the continually evolving microsurgical techniques; for example, the introduction of the operating microscope, the development of greatly improved bipolar coagulation technology by L. Malis, with specifically modeled bipolar coagulation forceps and bipolar coagulation balls, cavitron ultrasound surgical aspirator suction technology, and intraoperative monitoring. In addition, intense laboratory training, the experiences of the surgeon, and a certain talent are components that contribute to expertise, and these elements are substantiated by Klekamp and Samii.

Analysis of the operative results of the authors, as well as evaluation of the experiences of other authors in this field, strongly indicate the great importance of operating on patients with spinal lesions in an early phase, when they present with no or minor neurologic deficits. The more severe the preoperative neurologic condition of the patient, the less the injured cord will recover. Further advances in neurovisualization technology with diffusion and perfusion modalities promise to differentiate accurately the neuroplastic lesion from demyelinating, degenerative, vascular, or infection diseases.

The generally observed postoperative course is characterized by transient worsening of neurologic symptoms for a few days or even months before functional recovery occurs. There are reasonable hopes that the research activities of molecular biologists will offer effective treatment for faster recovery of the operated spinal cord patient.

This monumental work of Klekamp and Samii represents an impressive document recounting their neurosurgical endeavors in the last quarter of the 20th century. The meticulous statistical analyses will be of great value as a reliable source of reference. This unique monograph will undoubtedly be of great interest to neurosurgeons, neurologists, neuroradiologists, neuromolecular biologists, neurophysiotherapists, and occupational therapists alike.

Little Rock, July 2006 M.G. Yaşargil

Preface

Spinal tumors are rare and potentially devastating lesions that threaten the patient's mobility or even life. Despite their rarity, every neurosurgeon in clinical practice has to deal with them regularly. With modern imaging, microsurgical techniques, and improved understanding of spinal biomechanics and modern instrumentation systems, the fate of complete paraplegia can be avoided if therapy is instituted in time. Whereas intramedullary and extramedullary tumors are the domain of the neurosurgeon, extradural tumors are treated by neurosurgeons and orthopedic surgeons alike.

The aim of this book is to give an overview about the clinical experience gained in a single neurosurgical institution over a period of 25 years. This series consists of 1081 spinal tumors treated in 868 patients who underwent 973 operations between 1978 and 2003 (Table 1). Thus, this entire series consists of patients undergoing surgery with microsurgical techniques. The great majority of them were diagnosed using modern imaging techniques such as computerized tomography and magnetic resonance imaging. We do not claim to cover every aspect or every pathology of spinal tumors, but rather concentrate on what we have seen, found, learned, and achieved during this time. The results presented here represent this entire period. The treatment recommendations and descriptions of surgical techniques are based on these experiences and our ongoing analyses, and reflect our current state of the art. We hope that this book will aid neurosurgeons and spine surgeons in counseling and treating patients with spinal tumors.

Table 1. Data of 1081 spinal tumors treated in 868 patients with 973 operations between 1978 and 2003

Type of tumor	Number of patients	Number of tumors	Number of operations	No surgery
Intramedullary	182	199	198	9
Extramedullary	406	553	446	20
– Intradural	349	466	385	18
– Intra-extradural	57	87	61	2
Epidural	280	329	329	4
Total	868	1081	973	33

Each chapter of this book has been written in such a way that it can be read as a separate section. First, we would like to outline how patients were evaluated and what statistical methods were employed.

Patients were examined on outpatient visits and during their hospital stay before and after surgery. Each pre- and postoperative neurological symptom was documented and analyzed individually according to a scoring system

(Table 2) [3]. In addition, their overall clinical condition was evaluated according to the Karnofsky score [2]. These parameters were used to describe the preoperative condition and the short-term clinical course after surgery. To describe the preoperative course, we asked for the first clinical symptom the patient had noticed and which symptom was the major complaint at the time of surgery (i.e., the main symptom).

Table 2. Neurological scoring system

Score	Sensory disturbance, pain, dysesthesias	Motor weakness	Gait ataxia	Sphincter function
5	No symptom	Full power	Normal	Normal
4	Present, not significant	Movement against resistance	Unsteady, no aid	Slight disturbance, no catheter
3	Significant, function not restricted	Movement against gravity	Mobile with aid	Residual, no catheter
2	Some restriction of function	Movement without gravity	Few steps with aid	Rarely incontinent
1	Severe restriction of function	Contraction without movement	Standing with aid	Often catheter
0	Incapacitated function	Plegia	Plegia	Permanent catheter

Success of treatment for spinal tumors can be analyzed in several ways. Could the tumor be completely removed? Did the patient improve clinically? Did the patient deteriorate clinically during follow-up? Did the tumor recur? How long did the patient survive? For each section of the book we used the same data acquisition and statistical methods.

Long-term results were analyzed by calculating recurrence rates according to survival statistics [1], because this method allows us to account for varying follow-up times and gives a much more realistic picture regarding long-term postoperative results. Two types of recurrences were distinguished: (1) whenever a patient developed progressive neurological symptoms after surgery, this was defined as a clinical recurrence; (2) whenever a tumor recurred or a tumor remnant progressed on neuroradiological imaging, this was called a tumor recurrence.

To determine the factors predicting surgical results or outcome, multivariate analyses were performed. For each factor, a β-value is given, which indicates its predictive power compared to others.

Most, but not all of the case illustrations show pathologies treated within the study period between 1978 and 2003. The intraoperative photographs, in particular, are intended to demonstrate our current way of treatment rather than to present examples of how we used to operate on them.

The overwhelming majority of operations were performed with the patient in the prone position. As far as intraoperative photos are concerned, all are oriented according to the surgeon's view. If the semisitting position was used, this is mentioned in the figure legend

Gore-Tex® is a registered trademark of W. L. Gore & Associates, 555 Papermill Road, Newark, DE 19711, USA. TachoSil® is a registered trademark of Nycomed, PO Box 88, Langebjerg 1, DK-4000 Roskilde, Denmark.

Jörg Klekamp and Madjid Samii

References

1. Kaplan EL, Meier P (1958) Nonparametric estimation from incomplete observations. J Am Stat Assoc 53:457–481
2. Karnofsky DA, Burchenal JH (1949) The clinical evaluation of chemotherapeutic agents in cancer. In: MacLeod CM (ed) Evaluation of Chemotherapeutic Agents. Columbia University Press, New York, pp. 191–205
3. Klekamp J, Samii M (1993) Introduction of a score system for the clinical evaluation of patients with spinal processes. Acta Neurochir (Wien) 123:221–223

Acknowledgments

We would like to thank all of our colleagues listed below, who were trained by the senior author and have contributed to the surgical treatment of the patients of this series: S. Al Zaher, L.M. Auer, H. Baumann, M. Bellinzona, M. Berger, H.W. Bothe, D.K. Böker, G. Carvalho, G. Chhadeh, R. Eghbal, M. El Azm, T. Günther, B. Hermans, K.D. Lerch, T. Lutz, C. Matthies, F. Meyer, S. Mirzai, J.R. Moringlane, G. Mtafu, M. Nakamura, G. Penkert, A. Piepgras, W. Prösamer, R. Ramina, S. Rosahl, R. Schönmayr, A. Sepehrnia, M. Tatagiba, S. Thomas, K. Turel, H.G. Töppich, P. Van Ouwerkerk, P. Vorkapic, H. Voss, D. Völkening, K. Von Wild, and P.M. Zink.

We express our thanks to Prof. Dr. J. Freyschmidt, Klinikum Bremen Mitte, who provided figures of some of the spinal bone tumors, and to Dr. F. Meyer Evangelisches Krankenhaus Oldenburg, for his help with photographic documentation of spine tumors and proof reading. Steffi Dieke and Stefan Gallwitz helped with the photographic documentation.

Contents

5 Epidural Tumors

History 1

Contents

Today, surgery of spinal tumors is a very gratifying part of neurosurgery. With modern imaging techniques the diagnosis has become quite simple. Tumors can now be detected early, and with modern microsurgical techniques the neurological function of the spinal cord can almost always be preserved and often even improved. This is the result of a long period of development that started way before Victor Horsley's first operation of a spinal meningioma in 1887.

1.1 Surgical Approaches

Claudius Galen, born in the year 129 in Pergamon in Turkey, was probably the first anatomist to note the segmental representation of the spinal cord. He performed experiments and dissections on dogs to better understand the human anatomy and the consequences of spinal cord injuries. This was 1800 years before Darwin's evolution theory. Examining victims of gladiator fights, he observed specific neurological deficits according to the level of the spinal cord and was able to specify the spinal level of injury according to his clinical examination [10].

First attempts on spinal surgery were undertaken by the French army surgeon Ambroise Paré as early as 1549 for patients with spinal dislocations. He diagnosed the level of injury by palpation and crepitation, excised bony splinters compressing the cord, and applied traction for spinal dislocations with the aid of a wooden frame [35]. However, throughout the middle ages and well into the 19th century, spinal surgery was met with great scepticism. Most physicians considered injuries and tumors of the spine and spinal canal as untreatable. For instance, Nicolaus Petreus Tulpius described a patient with spina bifida aperta in 1641, who presented with a cystic mass attached to the underlying spinal cord by a small pedicle. The pedicle was ligated, the cystic mass became necrotic, and the patient died [18]. At that time, spina bifida was thought to be related to osteomyelitis of the spine. Associated cysts were considered to be connected to the urinary bladder [18]. The first attempt to close a spina bifida with a musculoskeletal flap can be attributed to Bayer in 1892 [18].

Systematic spinal surgery started in the 19th century with attempts at spinal cord decompression by performing laminectomies. The first description dates back to 1814 and was performed on a 26-year-old patient with a thoracic injury and complete paraplegia after falling from the roof of a house. The surgeon was unable to reduce the associated dislocation, and the patient demonstrated no recovery of function and died soon thereafter [24]. Obviously, this experience did not help to make spinal surgery more acceptable in the neurological community. The major problems at the time were inadequate anesthesia and pain control, leading to intraoperative shock and infections.

The first patient to survive a laminectomy was operated in 1828. This patient had fallen from a horse and suffered a complete paralysis of both legs. Some improvement of his sensory function was observed postoperatively [48]. Until 1840, just 12 spinal surgery patients were described in the literature. This number rose to 29 by 1867 [36]. A first systematic description of the surgical technique for laminectomy was given by Chipault in 1894 [5]. Further modifications and technical improvements were reported subsequently. To limit blood loss, Krause introduced what he called a laminotome. This was a kind of a strong biting forceps, which worked its way through bone by cutting and compressing the lamina [30]. By 1894, Menard

described the technique of costotransversectomy for treatment of Pott's disease [37]. The first description of a hemilaminectomy was provided by Bonomo in 1902 [4]. Several surgeons preferred to operate on patients in the right lateral position so that the part of the spine that was targeted could be elevated with cushions. In that way, cardiac function was considered to be more easily managed [29, 43].

Surgical approaches to the spine from the anterior direction were developed considerably later. Early attempts by Albee [2] and Hibbs [25] were associated with considerable mortality rates. They were performed for patients with Pott's disease, and the lack of antimicrobial drugs meant that postoperative infections were the major problem. Ito et al. [28] developed the extraperitoneal approach to the lumbar spine in 1934. A series of transthoracic decompressions with somewhat acceptable morbidity and mortality figures was finally published by Hodgson and Stock in 1956 [26] at a time with better anesthesia, diagnostic techniques, and operating skills, and when antibiotics were being developed in increasing numbers.

1.2 Tumor Removal

So, with the technique of laminectomy, the standard approach to spinal lesions was available in the second half of the 19th century. The first spinal tumor operation is widely attributed to Victor Horsley, who described the removal of a spinal meningioma, performed on June 9th in 1887 [20]. However, Lecat operated on a spinal tumor as early as 1753 [32]. Macewen reported on two patients in whom he had removed fibrous neoplasms of the dura in 1883 and 1884, respectively [33, 34]. As he was not a neurosurgeon, however, not much credit was given to these successful operations. Furthermore, the two patients were victims of Pott's disease with spinal deformities, suggesting that granulation tissue rather than true neoplasms were probably removed [44]. Horsley himself listed in his paper 58 patients with spinal tumors from the literature, of which 2 had been operated on previous to his own operation. Horsley's operation did not go smoothly. He opened the spine of this 42-year-old man at the wrong level at first and only after one of his assistants, Charles Ballance, who had studied the anatomy of the spinal cord and its roots carefully, had pointed out that due to the descending course of spinal nerve roots the lesion may be located higher than the clinical evaluation would predict, did Horsley extend the exposure cranially finding the meningioma at last. Postoperatively, the patient made a very gratifying recovery with preservation of his neurological functions. However, he suffered from a cerebrospinal fluid fistula for 6 weeks before it subsided spontaneously. Fortunately, no infection had developed. The patient was able to work 16 h a day 1 year after the operation, and finally died 20 ears later from causes unrelated to his spinal meningioma [42].

Horsley's paper had a tremendous impact on the medical community. He passionately recommended operating on patients with spinal tumors, as the alternative – conservative treatment – was associated with a very high mortality: 74% of patients with unoperated extradural tumors and 83% of patients with unoperated intradural tumors died due to respiratory failure, pneumonia, urinary septicemia, or decubitus ulcera, to mention the commonest causes of death. Horsley was convinced that surgery could prevent grave complications and death for a significant number of patients even given the prevailing enormous diagnostic and technical restraints. His paper was so stimulating that Starr could report on 19 spinal tumor operations as early as 1895, adding three cases of his own [49]. Eleven of these, however, died from postoperative complications. With increasing experience, however, mortality figures could be reduced. Even attempts on intraoperative functional studies were undertaken at that time and probably started with Abbe, who performed motor root stimulations during operations [1].

Whereas the first removals of extradural tumors can be attributed to Thorburn in 1888 [52] and Abbe in 1889 [1], surgery on intramedullary tumors started in the early 20th century. Cushing had exposed an intramedullary tumor by a myelotomy, but thought the lesion to be inoperable. Despite that, the patient recovered well from his procedure [8]. The first intramedullary tumor removal was successfully undertaken in 1907 by Freiherr von Eiselsberg in Vienna, with recovery of function after transient aggravation of his preoperative deficits [13].

The first series of spinal tumors was presented by Fedor Krause in 1908 [29]. He reported on 25 operated patients. Eight died from postoperative complications. In his former publication 2 years earlier, 6 of his first 11 patients had died [40]. In other words, he was able to improve operative mortality from 55% to 14% within a very short time. Listed among his spinal tumors were two enchondromas. These have to be considered the first operations on spinal disc prolapses, which he mistook for neoplasms [30]. Harvey Cushing concentrated on cranial surgery, but he did perform a considerable number of operations on spinal

tumors as well. Between 1912 and 1932, he treated 60 cases of spinal tumors: 23 meningiomas, 4 neurofibromas, 8 sarcomas, 3 ependymomas, and 4 astrocytomas to mention the intradural tumors [6].

The pioneer of spinal tumor surgery, however, is Charles A. Elsberg. His first major publication on his clinical work with intramedullary and extramedullary tumors was published in 1925; this book remains a landmark publication [15]. His results on 54 extramedullary, 13 intramedullary, and 14 epidural tumors compare favorably even with the first series published in the microsurgical era. He described the concept of a two-stage operation for the removal of intramedullary tumors, which he had discovered by accident. In a patient with the assumed diagnosis of an extramedullary tumor, he had injured the pia mater upon opening the dura. Unexpectedly, he observed that the intramedullary tumor extruded out of the cord almost by itself. The cord was reexposed in a second operation, performed after the patient had recovered from the first. At that time, the tumor had exposed itself almost completely out of the cord, so that he was able to resect it completely with a good functional result [17, 14]. However, this technique was used only a few times. In the second edition of his book in 1941, he summarized his work and presented his experience on the basis of 168 extramedullary, 73 epidural, and 19 intramedullary tumors. He had achieved complete resections for 150 extramedullary, 63 epidural, and 7 intramedullary tumors. His mortality rates were 5%, 7%, and 16% for extramedullary, epidural, and intramedullary tumors, respectively [16].

1.3 Diagnostic Imaging

The first endeavors on spinal cord surgery were performed without any imaging of the lesions. Radiological signs of a spinal tumor, such as a widening of the spinal canal or erosion of bony elements, were rarely encountered [7, 30, 39, 40, 45]. Neurologists determined the spinal level of the suspected tumor clinically and the surgeon had to do the operation to confirm the diagnosis and to remove the tumor. The major differential diagnostic sign was an increased intensity of neurological deficits without an ascending spinal level [50]. Only if the preoperative assumptions and clinical evaluations were correct could the patient expect to profit from surgery. In von Eiselsberg and Ranzi's series of 17 patients operated for suspected tumors, 5 patients underwent surgery without a tumor being discovered [13]. This illustrates the enormous diagnostic difficulties faced during that time. The commonest misdiagnosis was a circumscribed area of arachnoiditis [30].

Therefore, further imaging techniques were needed desperately. Dandy introduced air myelography in 1919. He injected air into the lumbar area and measured the time until the air could be detected intracranially [9]. Obviously, this was a very unprecise way of diagnosing a spinal tumor. The major neuroradiological breakthrough was the discovery of myelography with contrast material injected into the subarachnoid space by Sicard and Forestier [47]. It was a discovery by accident. Originally, the contrast material was aimed for the epidural space because they considered an intrathecal injection to be harmful. However, the intradural injection did not cause any apparent problems in this patient and a diagnostic method was born that gained immediate acceptance worldwide. A few years later, Peiper described the technique of myelography systematically and provided criteria for the differential diagnosis of myelographic findings [41].

1.4 Spinal Reconstruction and Fusion

With the introduction of approaches to the spine and increasing surgical attempts to treat spinal tumors as well as spinal trauma and degenerative disorders, little concern existed for spinal stability among neurosurgeons – not to mention for the side effects of surgery on spinal stability. First attempts to reconstruct the vertebral column were met with great scepticism by many respected neurosurgeons because reconstruction and stabilization meant longer surgery, a risk of insufficient vascularization of the reinserted laminae, and a higher risk of infection at a time without sufficient anesthetic techniques and antibiotics [29, 30, 40, 50].

As early as 1889, Dawbarn performed an H-type opening with lateral transection over the transverse processes and a horizontal transection connecting the two. In this way he could reflect two flaps of soft tissue together with bony elements cranially and caudally [11]. Urban and Bickham used U-shaped incisions for the same purpose [3, 53]. Röpke described a similar technique to thin out the lamina with a chisel, transecting it in the midline and then retracting both lamina halves together with attached soft tissues laterally [43]. With closure of the soft tissues, these authors approximated the lamina sufficiently to allow fusion.

Spinal stabilization was first developed to treat patients with Pott's disease. Hadra used wiring of the

spinous processes to prevent kyphotic deformities [21]. In 1910, Lange suggested steel bars for fusion of a spondylitic spine [31]. Albee, Hibbs, and Ito used bone grafts to achieve bony fusion [2, 25, 28]. However, it was not until the advent of better anesthetic techniques and antibiotic treatment, as well as a better understanding of spinal biomechanics, that stabilization techniques for the spine finally became practical. A major step was the pioneering work of Sir Frank Holdsworth, who classified spinal fractures according to the mechanism into pure flexion, flexion-rotation, extension, and compression fractures. He also introduced a two-column model of spinal stability [27]. This work provided an important background for the development of the first successful spinal instrumentation system for posterior spinal fusion by Paul Harrington in the 1960s [22, 23]. The first ventral instrumentation system was introduced soon thereafter by Dwyer et al. in 1969 [12].

1.5 Modern Advances

With good anesthetic techniques, antibiotic treatment, and reasonable diagnostic imaging established, the next major advance was the introduction of the operative microscope in the 1960s. Before the introduction of microsurgery, surgeons were most of all concerned for the patients' survival after spinal cord surgery. With the advent of the operative microscope, it became possible to preserve the patients' neurological function with increasing frequency. In 1975, Yasargil and De Preux published the first paper on a series of microsurgically removed intramedullary angioblastomas with excellent clinical outcomes [54]. This paper was followed by a congress report on 37 intramedullary tumors undergoing microsurgical removal. Of these, 24 had been resected completely (11 of 12 angioblastomas, 8 of 11 ependymomas, and 1 of 4 astrocytomas), of which 13 demonstrated postoperative improvement, while 6 remained unchanged and just 5 were neurologically worse. Apart from the operative microscope, he emphasized the bipolar coagulation technique as the second major technical advance for treatment of these patients, the correlation between preoperative neurological status and postoperative functional results, and recommended surgical removal before serious neurological deficits were present. Each step for microsurgical resection as outlined in this paper describes the state-of-the-art technique up to today [55]. In a later publication he advised against laminectomies to remove intra- or extramedullary tumors to avoid problems of postoperative spinal instability. He had used osteoplastic laminotomies – cutting laminae with an oscillating saw, removal in one bloc and reinsertion with sutures – since 1973 for extensive tumors and advocated partial hemilaminectomies for smaller tumors – a technique he developed in 1980 [56]. Apart from concerns regarding spinal stability after resection of intradural tumors, he also applied a telescoping screw for reconstruction of the T11 and T12 vertebrae after resection of a giant-cell tumor, which can be considered the prototype for the expandable cages employed today [46].

A large number of publications have since dealt with intramedullary tumors. By comparison, little has been published on extramedullary tumors. The largest series on extramedullary tumors with a detailed analysis of the literature was published by Nittner in 1976. He analyzed 4885 patients [38].

With the introduction of magnetic resonance imaging in the 1980s, the diagnosis of spinal tumors has finally become much easier and more reliable. Patients can now be discovered before severe neurological deficits are present. This enables surgeons even to improve neurological symptoms in patients with intramedullary tumors. A recent monograph on a large series of intramedullary tumors presenting the current therapeutic standard was published by Fischer and Brotchi in 1996 [19].

Whereas intradural spinal tumors are the domain of neurosurgeons, different concepts were followed for the management of epidural tumors by neurosurgeons and orthopedic surgeons. Initially, neurosurgeons focused solely on neurological function and performed surgery with the intention of decompressing the spinal cord and nerve roots. They had little concern for spinal stability. For instance, the potentially devastating long-term effects of laminectomies were overlooked by most neurosurgeons for decades. On the other hand, orthopedic surgeons tended to concentrate only on the biomechanical problems associated with tumors. Achievement of stability was the foremost goal.

Today, surgical approaches that respect the integrity of the intervertebral joints and spinal stability are available for any part of the spine. If the tumor has caused spinal instability or tumor removal has to compromise stability, a variety of fusion techniques are available for each segment of the vertebral column from any angle. In this respect, patients and neurosurgeons have profited a great deal from the work of orthopedic and trauma surgeons [51]. In fact, there still is a large field for interdisciplinary research and clinical work to improve even further the management of patients with spinal tumors.

References

1. Abbe R (1889) Spinal surgery – a report of eight cases. Med Rec 38:85–92
2. Albee FH (1911) Transplantation of a portion of the tibia into the spine for Pott's disease: a preliminary report. JAMA 57:885–886
3. Bickham WS (1905) Technique of exposure of the spinal cord and canal: osteoplastic resection and laminectomy. Ann Surg 41:372–398
4. Bonomo L (1902) Laminectomia laterale: nuovo metodo di apertura des canale rachidiano. Gior Med Regio-Esercito 50:1132–1157
5. Chipault A (1894) Études de Chirurgie Médullaire. Historique, Chirurgie Opératoire, Traitement. F. Alcan, Paris
6. Cohen-Gadol AA, Spencer DD, Krauss WE (2005) The development of techniques for resection of spinal cord tumors by Harvey W. Cushing. J Neurosurg Spine 2:92–97
7. Collins J, Marks HE (1915) The early diagnosis of spinal cord tumors. Am J Med Sci 149:103–112
8. Cushing H (1905) The special field of neurosurgery. Bull Johns Hopkins Hosp 16:77–87
9. Dandy W (1919) Röntgenography of the brain after the injection of air into spinal canal. Ann Surg 70:397–403
10. Daremberg C (1854) Oeuvres Anatomiques, Physiologique et Medicales de Galien. Baliere, Paris
11. Dawbarn RHM (1889) A successful case of spinal resection. NY Med J 49:711–715
12. Dwyer AF, Newton NC, Sherwood AA (1969) An anterior approach to scoliosis. A preliminary report. Clin Orthop 62:192–202
13. Eiselsberg A Freiherr von, Ranzi E (1913) Über die chirurgische Behandlung der Hirn- und Rückenmarkstumoren. Arch Klin Chir 102:309–468
14. Elsberg CA (1912) Surgery of intramedullary affections of the spinal cord: anatomical basis and technique. JAMA 59:1532–1536
15. Elsberg CA (1925) Tumors of the Spinal Cord, and the Symptoms of Irritation and Compression of the Spinal Cord Nerve Roots: Pathology, Symptomatology, Diagnosis and Treatment. PB Hoeber, New York
16. Elsberg CA (1941) Surgical Diseases of the Spinal Cord, Membranes and Nerve roots: Symptoms, Diagnosis, and Treatment. PB Hoeber, New York
17. Elsberg CA, Beer E (1911) The operability of intramedullary tumors of the spinal cord. Am J Med Sci 142:636–647
18. Fisher RG (1951) Surgery of the congenital anomalies. In: A History of Neurological Surgery (Ed.) Walker AE, Williams Wilkins, Baltimore, pp 334–361
19. Fischer G, Brotchi J (1996) Intramedullary spinal cord tumors. Thieme, Stuttgart
20. Gowers WR, Horsley V (1888) A case of tumour of the spinal cord. Removal; recovery. Med Chir Trans 53:377–428
21. Hadra BE (1881) Wiring of the spinous process in injury and Pott's disease. Trans Am Orthop Assoc 4:206
22. Harrington PR (1962) Treatment of scoliosis. J Bone Joint Surg Am 44:591–610
23. Harrington PR (1973) The history and development of Harrington instrumentation. Clin Orthop 93:110–112
24. Hayward G (1815) An account of a case of fracture and dislocation of the spine. N Engl J Med Surg 4:1–3
25. Hibbs RA (1911) An operation for progressive spinal deformities. N Y Med J 93:1013–1016
26. Hodgson AR, Stock FE (1956) Anterior spinal fusion: a preliminary communication on the radical treatment of Pott's disease and Pott's paraplegia. Br J Surg 44:266–275
27. Holdsworth FW, Hardy A (1953) Early treatment of paraplegia from fractures of the thoraco-lumbar spine. J Bone Joint Surg Br 35:540–550
28. Ito H, Tsuchiya J, Asami G (1934) A new radical operation for Pott's disease. J Bone Joint Surg 16:499–515
29. Krause F (1908) Erfahrungen bei 26 operativen Fällen von Rückenmarkstumoren mit Projektionen. Dtsch Z Nervenheilkd 36:106–113
30. Krause F (1911) Die Chirurgie des Rückenmarks. In: Die Chirurgie des Gehirns und Rückenmarks nach eigenen Erfahrungen, II. Urban Schwarzenberg, Berlin, pp 649–820
31. Lange F (1910) Support of the spondylitic spine by means of buried steel bars attached to the vertebra. Am J Orthop Surg 8:344–361
32. Lecat CNL (1765) Traité de l´existence, de la nature et des propriétés du fluide des nerfs et principalement de son action dans le mouvement muculaire. Ouvrage couronné, en 1753, par l'Académie de Berlin; suivi des dissertations sur la sensibilité des méninges, des tendons etc, l`insensibilité du cerveau, la structure des nerfs, l´irritabilité hallerienne, Berlin
33. Macewen W (1884) Trephining of the spine for paraplegia. Glasgow Med J 22:55–58
34. Macewen W (1885) Two cases in which excision of the laminae of portions of the spinal vertebrae had been performed in order to relieve pressure on the spinal cord causing paraplegia. Glasgow Med J 25:210–212
35. Markham JW (1951) Surgery of the spinal cord and vertebral column. In: Walker AE (Ed) A History of Neurological Surgery. Williams Wilkins, Baltimore, pp 364–392
36. Markham JW (1952) The history of laminectomy prior to 1866. Bull Hist Med 26:375–384
37. Ménard V (1894) Causes de la paraplégie dans le mal de Pott. Son traitement chirurgical par l'ouverture direct du foyer tuberculeux des vertébres. Rev Orthop 5:47–64
38. Nittner K (1976) Spinal meningiomas, neurinomas and neurofibromas. In: Vinken PJ, Bruyn GW (eds) Handbook of Clinical Neurology, Volume 20. Tumours of the Spinal Cord. Part II. North Holland, Amsterdam, pp 177–322
39. Nonne M (1913) Weitere Erfahrungen zum Kapitel der Diagnose von komprimierenden Rückenmarkstumoren. Dtsch Z Nervenheilkd 47: 436–503
40. Oppenheim H, Krause F (1906) Über die operative Behandlung der Hirn- und Rückenmarkstumoren. Verh Ges Dtscher Natur Ärzte 2:194–202
41. Peiper H (1926) Die Myelographie im Dienste der Diagnostik von Erkrankungen des Rückenmarkes. Ergeb Med Strahlenforsch 2:107–195
42. Rogers L (1935) The surgery of spinal tumours. Lancet 1:187–191

43. Röpke W (1911) Über die operative Entfernung intramedullärer Rückenmarkstumoren, zugleich ein Beitrag zur Kenntnis über die Beschaffenheit des Lumbalpunctats bei Rückenmarkstumoren. Arch Klin Chir 96:963–980
44. Scarff JE (1955) Fifty years of neurosurgery, 1905–1955. Int Abstr Surg 101:417–513
45. Schlesinger H (1898) Beiträge zur Klinik der Rückenmarks- und Wirbeltumoren. Gustav Fischer, Jena
46. Senning A, Weber G, Yasargil MG (1962) Zur operativen Behandlung von Tumoren der Wirbelsäule. Swiss Med J 92:1574–1576
47. Sicard J, Forestier J (1921) Méthode radiographique d'exploration de la cavité épidurale par le lipiodol. Rev Neurol (Paris) 36:1264–1266
48. Smith AG (1829) An account of a case in which portions of three dorsal vertebrae were removed for the relief of paralysis from fracture, with partial success. North Am Med Surg J 8:94–97
49. Starr MA (1895) A contribution to the subject of tumors of the spinal cord, with remarks upon their diagnosis and their surgical treatment, with a report of six cases, in three of which the tumor was removed. Med News N Y 66:222–224
50. Stursberg H (1908) Die operative Behandlung der den Rückenmark und die Cauda equina komprimierenden Neubildungen. Zentralbl Grenzgeb Med Chir 11:91–110
51. Sundaresan N, Schmidek HH, Schiller AL, Rosenthal DI (1990) Tumors of the Spine. Diagnosis and Clinical Management. W.B. Saunders, Philadelphia
52. Thorburn W (1889) A Contribution to the Surgery of the Spinal Cord. Charles Griffin, London
53. Urban B (1892) Über operative Eingriffe bei Compression des Rückenmarks durch Verschiebung der Wirbelkörper. Verh Dtsch Ges Chir 21:211–219
54. Yasargil MG, De Preux J (1975) Experiences microchirurgicales dans 12 cas d'hemangioblastomes intramedullaires. Neurochirurgie 21:425–434
55. Yasargil MG, Pernecky A (1976) Operative Behandlung der intramedullären spinalen Tumoren. In: Schiefer W, Wieck HH (eds) Spinale raumfordernde Prozesse – Diagnostische und therapeutische Fortschritte in Praxis und Klinik. Perimed, Erlangen, pp 299–312
56. Yasargil MG, Tranmer BI, Adamson TE, Roth P (1991) Unilateral partial hemi-laminectomy for the removal of extra- and intramedullary tumours and AVMs. Adv Tech Stand Neurosurg 18:113–132

Anatomy

2

Contents

This chapter provides some anatomical information to help the reader to understand the pathophysiology of tumors of the spine and spinal cord as well as to guide surgeons to particular configurations and important aspects for planning and performing surgery in the safest and least traumatic manner.

2.1 Cervical Spine

The cervical spine consists of two "special" vertebrae – the atlas and axis – connecting the spine with the cranium in a complex set of joints and ligaments, and five "ordinary" vertebrae in a slightly lordotic curve (Figs. 2.1–2.3). In young adults, the average length of the cervical spine measures 12.5 cm from the lower border of C7 to the tip of the dens axis. In retroflexion, the average length is 11.5 cm, compared to 12.69 cm in anteflexion [9, 10]. This needs to be considered for correct intraoperative localization of intradural tumors; radiological examinations are performed in a different neck position than the operative one!

The atlas is formed like a ring with small lateral masses, which articulate with the occipital condyles of the cranium above and the lateral masses of the axis underneath. A fifth joint provides the rotation of the head and is formed between the atlas and the dens axis (i.e., the odontoid process). The axis articulates with the lateral masses of C1 above and supports the dens axis in the midline (Figs. 2.2 and 2.3). The remaining vertebral bodies are rectangular in shape, with a slight depression of the superior surface, giving rise to bony edges on either side (i.e., the uncinate processes). Thus, the intervertebral discs rest on a cup-like surface of the lower vertebra, whereas the lower surface of a cervical vertebra (i.e., the upper surface of the intervertebral space) is flat (Fig. 2.2).

The posterior elements of the second to seventh vertebra form the neural arches consisting of pedicles, the lamina, and spinous processes. The short pedicles connect the vertebral body with the facet joints, which are formed by articular processes above and below. These processes are named according to their orientation: the articular of the inferior vertebra projecting upward is called the superior articular process, and vice versa for articular process from the superior vertebra facing downward (Fig. 2.1). In axial sections through the facet joints, the posterior facet belongs to the superior neural arch representing the inferior articular process and vice versa for the anterior facet (Fig. 2.3). A neuroforamen is formed by pedicles above and below the vertebral body and uncinate process medially, the transverse process laterally, and the articular processes posteriorly. The cervical foraminae are oriented about 30° anterolaterally. The neural arches project posteriorly to meet at the base of the spinous process. On cross section, they are ovoid in shape, with a flattened anterior surface. The spinous processes point downward in the midline (Fig. 2.1). There is no spinous process at C1, but there are particularly large processes at C2 and C7. The average anterior–posterior diameter of the bony spinal canal measures 18–20 mm at C1 and C2, and 15–17 mm between C3 and C7. The thecal sac measures 10–14 mm throughout the cervical spine, and the spinal cord 6–9 mm. In other words, the spinal cord normally occupies about 40–50% of the spinal canal.

As far as ligamentous structures are concerned, the atlantoaxial ligaments, anterior and posterior longitudinal ligaments, the yellow ligament, the interspinous ligament, and the supraspinous ligament should

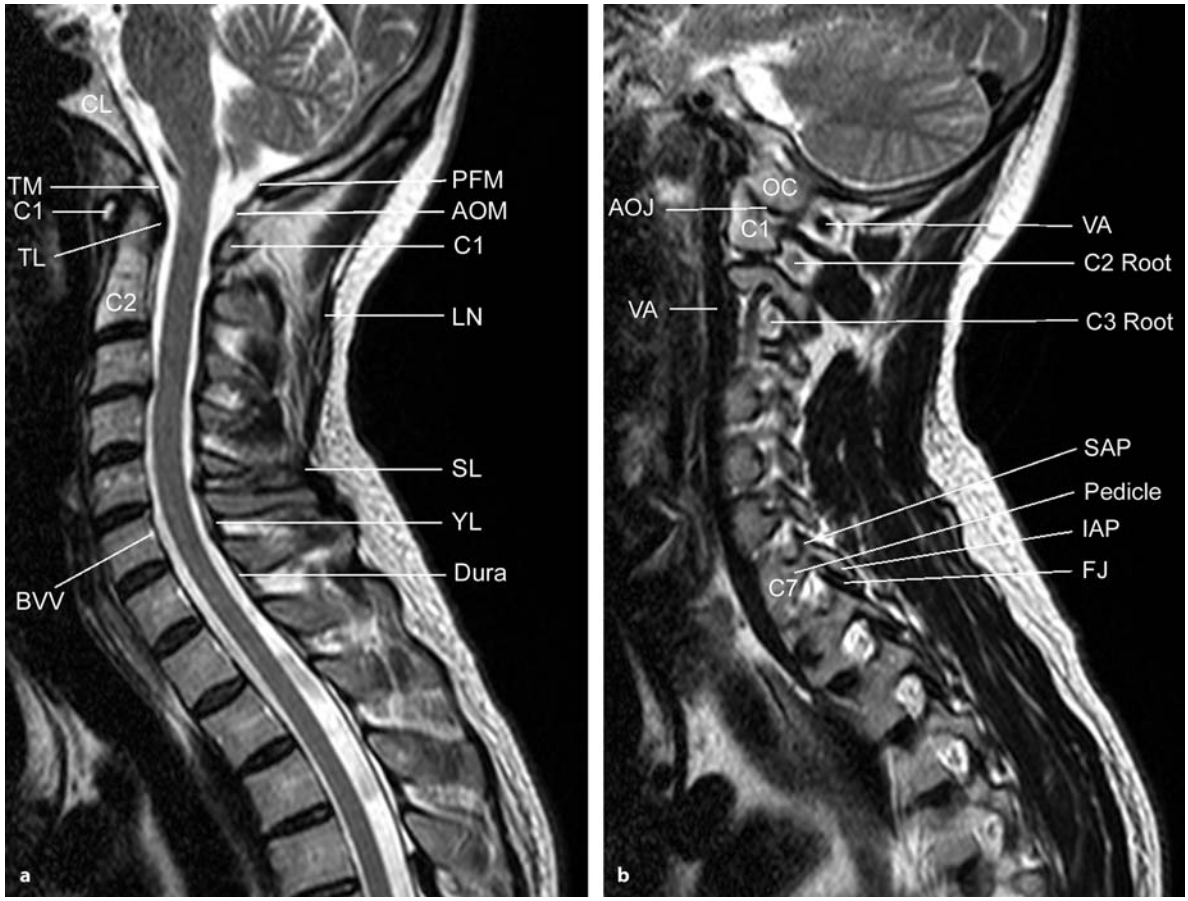

Fig. 2.1. a Sagittal T2-weighted magnetic resonance imaging (MRI) scan of the cervical spine in the midline: *CL* Clivus, *PFM* posterior rim of the foramen magnum, *TM* tectorial membrane, *AOM* atlantooccipital membrane, *TL* transverse ligament, *LN* ligamentum nuchae, *SL* supraspinous ligament, *YL* yellow ligament, *BVV* basivertebral vein. **b** Sagittal paramedian T2-weighted MRI scan of the cervical spine. *OC* Occipital condyle, *AOJ* atlantooccipital joint, *VA* vertebral artery, *SAP* superior articular process, *IAP* inferior articular process, *FJ* facet joint

be mentioned. The medial atlantoaxial joint is stabilized by a complex set of ligaments. The most important of these is the cruciform ligament, which lies immediately behind the dens in the coronal plane (Fig. 2.3). The vertical and horizontal arms of this ligament explain its name. The horizontal arms form the so-called transverse ligament between the lateral masses of C1 and the posterior surface of the dens to hold it firmly against the anterior arch of C1 (Fig. 2.1). The vertical arms run between the anterior rim of the foramen magnum and the body of C2. The dens is linked to the skull base by the apical ligament extending from its tip to the anterior foramen magnum and the alar ligaments laterally toward the occipital condyles. The vertebral bodies are connected by anterior and posterior longitudinal ligaments from C1 right down to the sacrum along their anterior and posterior surfaces, respectively. The anterior longitudinal ligament ends in the anterior atlantooccipital membrane at the level of the foramen magnum. The posterior longitudinal ligament is connected with the posterior foramen magnum via the tectorial membrane (Fig. 2.1). The posterior vertebral elements are stabilized by yellow, interspinous, and supraspinous ligaments. The yellow ligament links the vertebral laminae and, thus, forms the posterior border of the spinal canal in the interlaminar space and is connected to the posterior atlantooccipital membrane cranially. The interspinous ligament serves as an important posterior anchor and runs between spinous processes, whereas the supraspinous ligament extends between the tips of the spinous processes (Fig. 2.1).

The vascular anatomy consists of the vertebral arteries and a venous plexus. This plexus runs along the posterior surface of the vertebral bodies mainly in the midline, where it elevates the posterior longitudinal

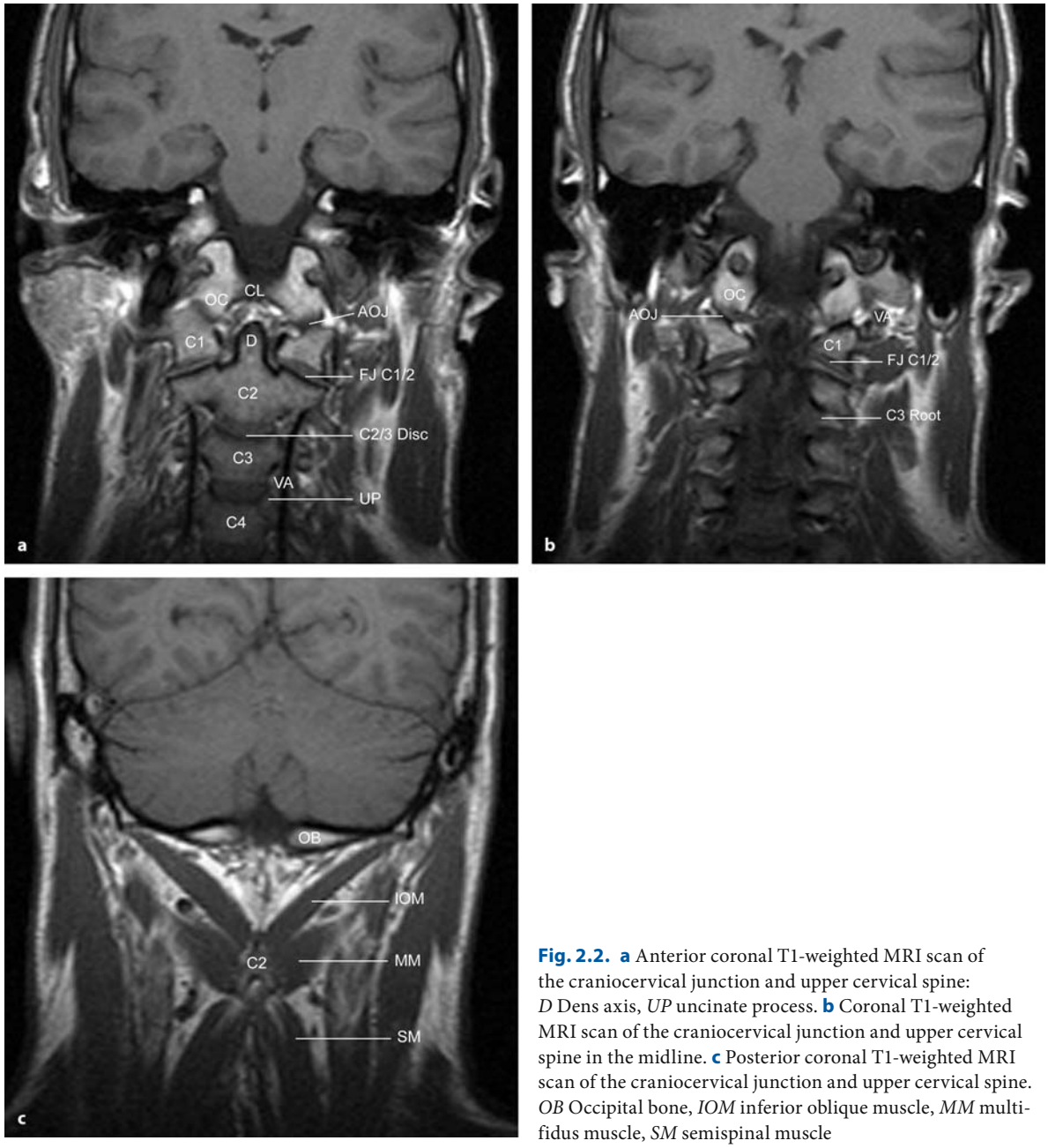

Fig. 2.2. **a** Anterior coronal T1-weighted MRI scan of the craniocervical junction and upper cervical spine: *D* Dens axis, *UP* uncinate process. **b** Coronal T1-weighted MRI scan of the craniocervical junction and upper cervical spine in the midline. **c** Posterior coronal T1-weighted MRI scan of the craniocervical junction and upper cervical spine. *OB* Occipital bone, *IOM* inferior oblique muscle, *MM* multifidus muscle, *SM* semispinal muscle

ligament. The vertebral arteries arise from the subclavian arteries in 90% of patients. In rare instances, the left vertebral artery may arise from the aortic arch. Other unusual origins such as the inferior thyroid and the common carotid artery have been described. The arteries travel anterolaterally of the neuroforaminae between C6 and C1 through foraminae in the transverse processes. However, the vertebral artery may enter the spine at other levels such as C3, C4, C5, and C7 [10]. In about 89% of cases the artery arises in a straight line through these transverse foraminae. However, medial loops at C4, C5, and C6 may occur in rare cases [10]. Above C2, the artery turns posteriorly and superiorly, traverses the transverse foramen of C1 and continues medially along the superior margin of the atlas in a sulcus to form a loop toward the dura of the foramen magnum. In some cases, a foramen is formed in this area (i.e., the arcuate foramen). The vertebral artery is surrounded by a venous plexus, which is particularly prominent between C2 and its intracranial section (Figs. 2.1–2.3).

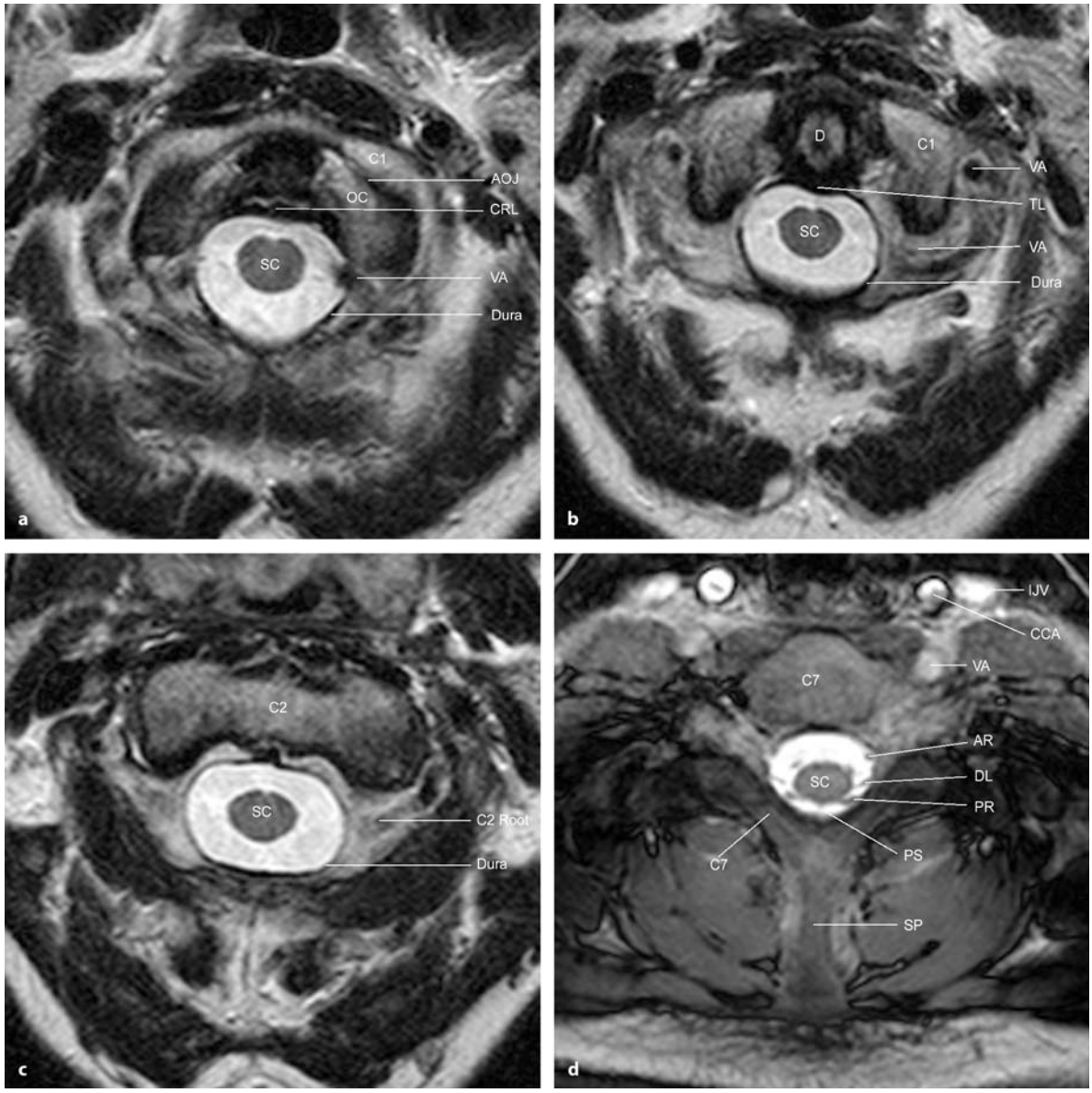

Fig. 2.3. **a** Axial T2-weighted MRI scan at C1. *CRL* Cruciate ligament, *SC* spinal cord. **b** Axial T2-weighted MRI scan at C1/2. **c** Axial T2-weighted MRI scan at C2. **d** Axial T2-weighted MRI scan at C7. *IJV* Internal jugular vein, *CCA* common carotid artery, *AR* anterior root, *DL* dentate ligament, *PR* posterior root, *PS* posterior septum, *SP* spinous process

2.2 Thoracic Spine

The 12 thoracic vertebral bodies are rectangularly shaped with flat superior and inferior surfaces. The neural foraminae exit almost laterally. From top to bottom, the height of the bodies gradually increases. The intervertebral discs appear flatter than their cervical and lumbar counterparts. The pedicles of the thoracic vertebrae extend from the superior half of the vertebral body. The neuroforaminae are directed laterally. The laminae form an almost circular spinal canal of constant width throughout the thoracic spine. As this part of the spine forms a slight kyphosis, the thecal sac and spinal cord seem slightly displaced anteriorly in the upper thoracic canal (Figs. 2.4 and 2.5). The major difference in the bony anatomy of the thoracic spine is the articulation with the ribs. The heads of ribs 2–10 articulate with their posterior surfaces to the posterolateral aspects of vertebral bodies. Half of the joint surface is on the superior and half on the inferior body. Ribs 1, 11, and 12 articulate only

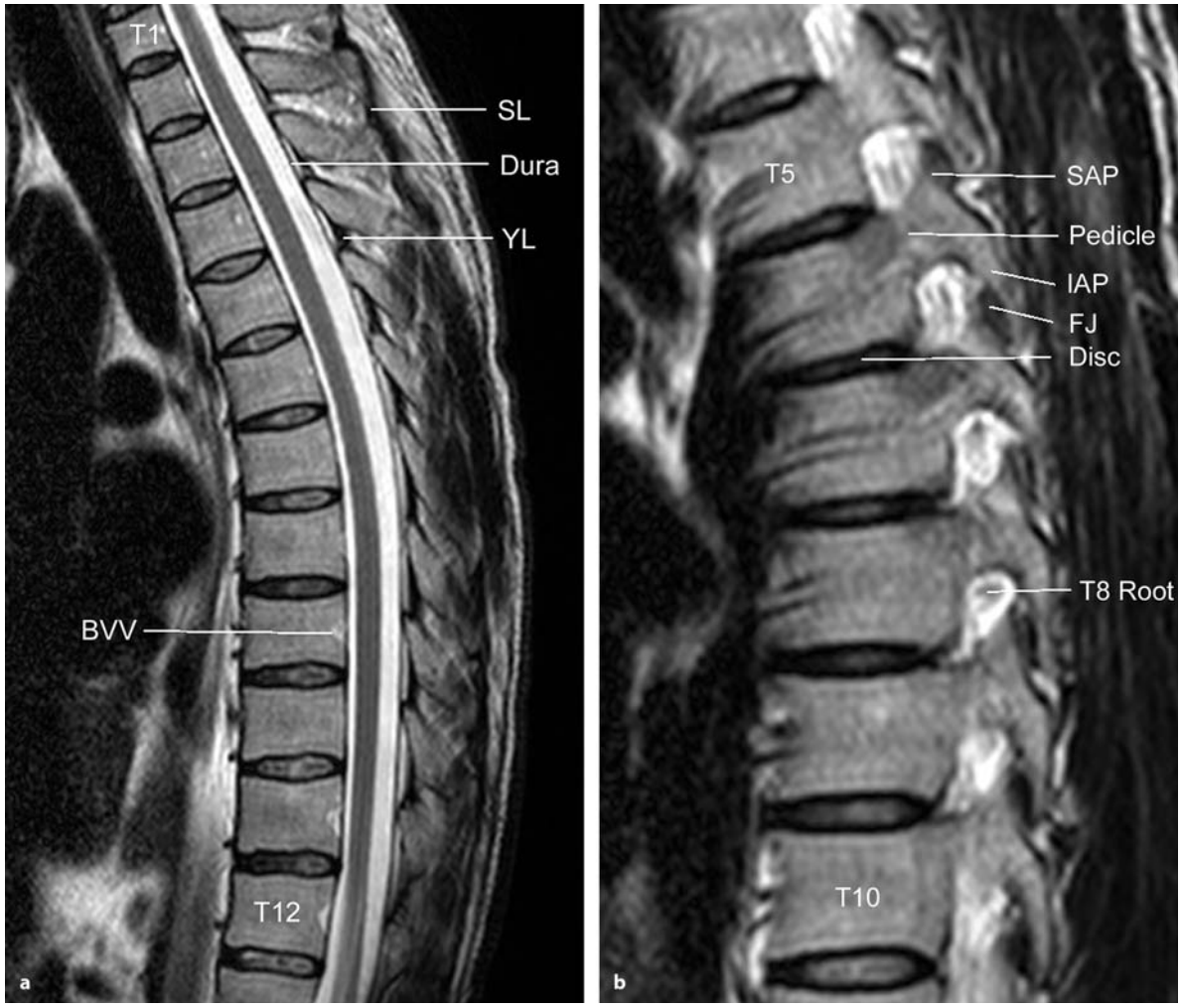

Fig. 2.4. **a** Sagittal T2-weighted MRI scan of the thoracic spine in the midline. **b** Paramedian sagittal T2-weighted MRI scan of the thoracic spine

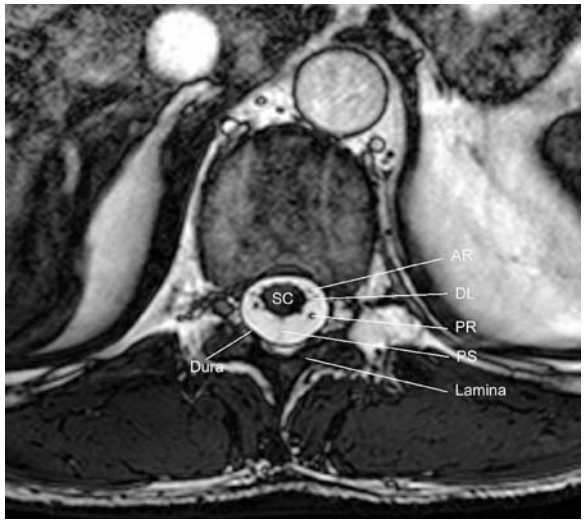

Fig. 2.5. Axial T2-weighted MRI scan of the midthoracic spine

with the upper part of the corresponding vertebral body. Furthermore, the tubercles of ribs 1–10 articulate on their posterior surfaces with the transverse processes of the same-numbered vertebral body.

As far as the vascular anatomy is concerned, the external venous plexus around the vertebral bodies is of particular importance in the thoracic and lumbar spine. Changes in intrathoracic and intra-abdominal pressure are transferred to the epidural internal venous plexus through anastomoses and affect the cerebrospinal fluid (CSF) pressure in the thoracic and lumbar spine. Furthermore, interconnections exist between the external venous plexus and the azygos venous system. This connection provides a parallel drainage system that bypasses the superior and inferior vena cava.

Fig. 2.6. **a** Sagittal T2-weighted MRI scan of the lumbar spine in the midline. *CE* Cauda equina. **b** Paramedian sagittal T2-weighted MRI scan of the lumbar spine. *EV* Epidural vein, *PI* pars interarticularis

2.3 Lumbar Spine and Sacrum

Similarly to the thoracic vertebrae, the five lumbar vertebral bodies are rectangular in shape, with flat superior and inferior surfaces. The pedicles project posterolaterally. The neural foraminae exit almost laterally. The posterior border of each foramen is formed by the articular processes. These processes are comparably long and form the facet joints, which are oriented in the coronal plane. The lumbar laminae form an oval spinal canal in the upper lumbar spine. In the lower part, the shape becomes more triangular, with bony recesses anterolaterally; these are formed by indentations of the superior articular processes of the facet joints (Figs. 2.6 and 2.7). The sacrum is composed of four or five fused vertebrae that form a triangle. It articulates laterally with the iliac bones (Fig. 2.8).

Fig. 2.7. **a** Axial T2-weighted MRI scan of the lumbar spine at Th12/L1. **b** Axial T2-weighted MRI scan of the lumbar spine at L3. **c** Axial T2-weighted MRI scan of the lumbar spine at L3/4. **d** Axial T2-weighted MRI scan of the lumbar spine at the pedicle level of L5. *AVP* Anterior epidural venous plexus. **e** Axial T2-weighted MRI scan of the lumbar spine at foraminal level of L5. **f** Axial T2-weighted MRI scan of the lumbar spine at L5/S1

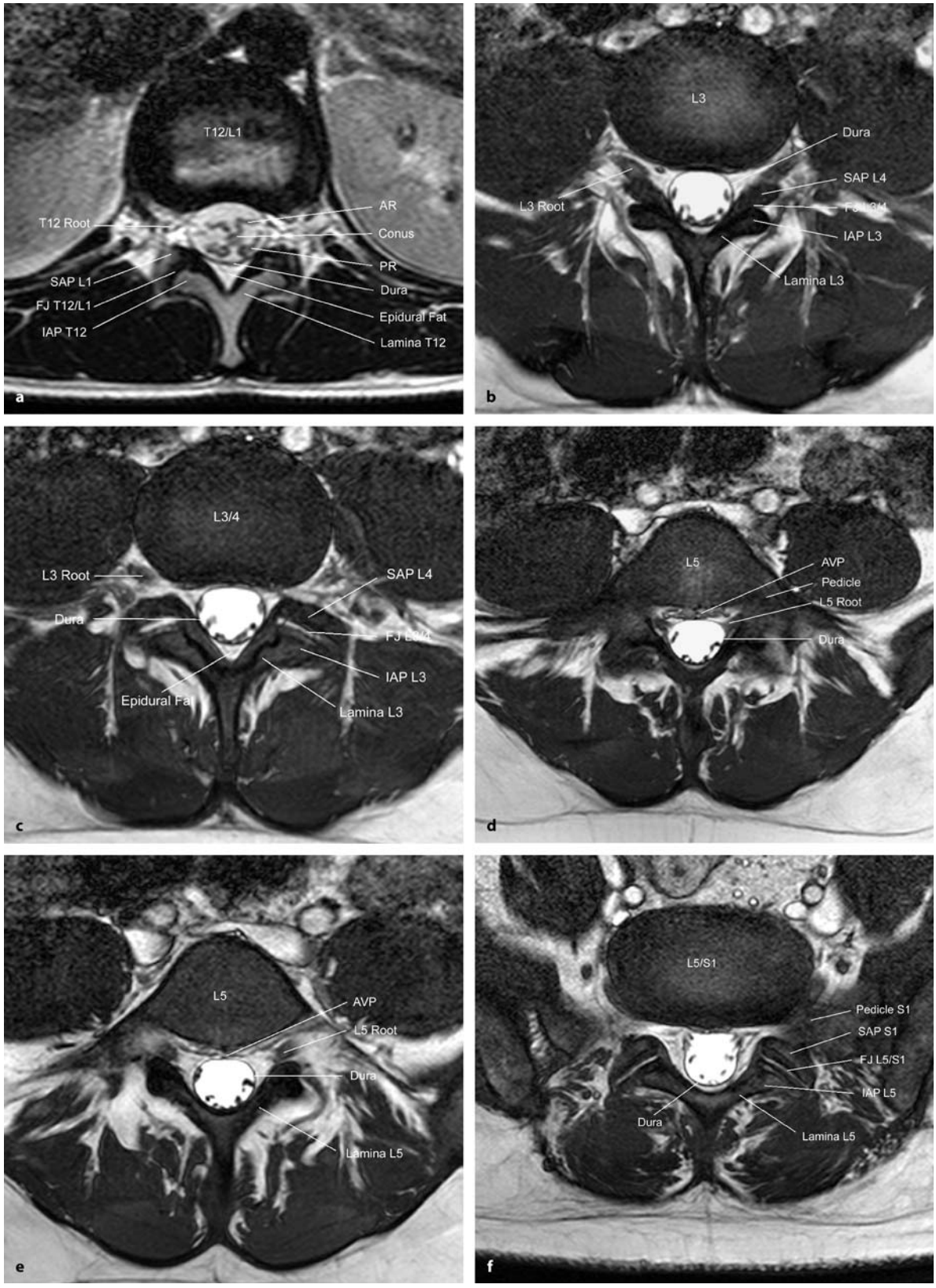
T12/L1
T12 Root
AR
Conus
PR
SAP L1
Dura
FJ T12/L1
Epidural Fat
IAP T12
Lamina T12
a
L3
Dura
SAP L4
L3 Root
FJ L3/4
IAP L3
Lamina L3
b
L3/4
L3 Root
SAP L4
Dura
FJ L3/4
IAP L3
Epidural Fat
Lamina L3
c
L5
AVP
Pedicle
L5 Root
Dura
d
L5
AVP
L5 Root
Dura
Lamina L5
e
L5/S1
Pedicle S1
SAP S1
FJ L5/S1
IAP L5
Dura
Lamina L5
f

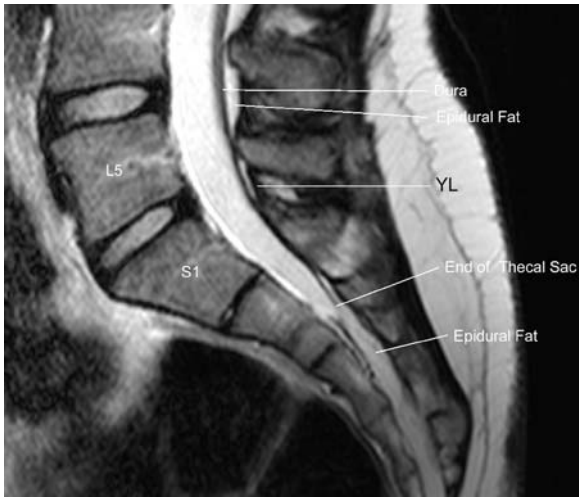

Fig. 2.8. Sagittal T2-weighted MRI scan of the sacrum

Lumbar nerve root sleeves lie anterolateral to the thecal sac at the level of the pedicle, and continue into the upper half of the neuroforamen. The epidural fat of the spinal canal contains a venous plexus and connective tissue. This plexus communicates with the external venous plexus surrounding vertebral body and posterior elements. Individual veins may accompany the nerve root on its way through the neuroforamen, and are positioned in the lower part of the foramen (Fig. 2.7). The thecal sac extends approximately to S2 (Fig. 2.8).

2.4 Spinal Biomechanics

The line of the center of gravity of the erect human body lies anterior to the vertebral column. As a consequence, axial loads to the body in the upright position result in a combination of spinal axial compression and bending movements. A simple biomechanical concept of the spine is as two columns, an anterior column and a posterior column [6].

The anterior column provides the weight-bearing part of the spine. About 80% of the axial load is absorbed by this column, whereas the remaining 20% is spread to posterior elements as a shearing force. Vertebral bodies and intervertebral discs are constructed to withstand these weight-bearing forces, whereas the annulus fibrosus of the disc absorbs torque and shear movements. Thus, the anterior column acts like a distraction device.

The posterior column, on the other hand, consists of laminae and facet joints, which work as a chain of articulators. The remaining 20% of the axial load is absorbed mainly by the facet joints. This articulation chain is controlled by ligaments and muscles, which compress the posterior elements like a tension band. In other words, the posterior column serves as a compression device.

The posterior compressing forces of the muscles provide a balance between the anterior column and posterior articulation chain. Movements are possible due to deformations of the intervertebral discs and the facet joints. Ligaments limit the amount of motion possible within each segment. The stability of the spine requires intact anterior and posterior elements. Neoplasms of the spine, which destroy parts of the anterior and/or posterior column structures, will tend to cause kyphotic deformities, because the weight-bearing capability of the anterior and/or the compressive action of the posterior column is compromised. For restoration of stability, anterior reconstructions require distraction, whereas posterior devices have to apply compression. In each individual case, anterior and posterior elements have to be analyzed carefully to select the appropriate reconstruction: anterior, posterior, or a combined approach [4].

2.5 Spinal Meninges

The dura mater is about 0.8 mm thick and consists of collagen and elastic fibers. At the foramen magnum, the dura mater of the head and the external periost merge into the spinal dura mater. Here, the dura mater consists of three layers: (1) the innermost layer of the spinal dura is in continuity with the inner dural layer of the skull, (2) the middle spinal layer continues to form the external dural layer of the skull, and (3) the outer layer transgresses into the periost of the skull (Fig. 2.1) [10]. A complex set of fiber bundles inside the dura allows head movements without displacing the dural sac out of the midline of the spinal canal.

The arachnoid membrane is the outer wall of the CSF space. It is watertight, loosely attached to the dura [13], and ensheathes the spinal nerves toward the root sleeves, where it fuses with the dura. In the subarachnoid space, numerous strands run between the arachnoid membrane and cord surface, mainly in the posterior, and to a lesser degree in the anterior subarachnoid space. These septations have been described to be derived from an intermediate, fenestrated leptomeningeal layer, which is attached to the inner surface of the arachnoid membrane and surrounds nerve roots and blood vessels on the cord surface as a fenestrated layer (Fig. 2.9) [13]. Posteriorly, a septum

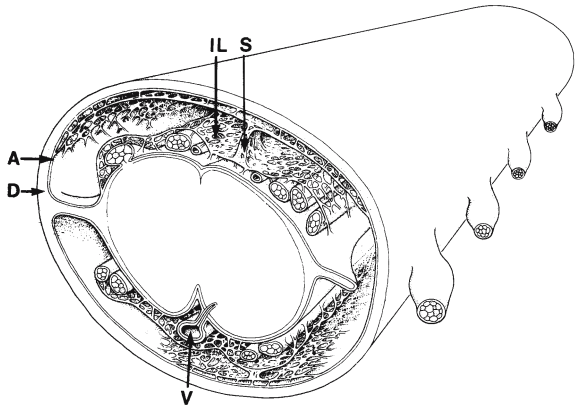

Fig. 2.9. This diagram of the human spinal cord and its meninges shows the arachnoid membrane (*A*) close to the dura mater (*D*). An intermediate leptomeningeal layer (*IL*), which lies between arachnoid membrane and pia mater, is fenestrated and attached to the inner aspect of the arachnoid membrane. It is reflected to form the posterior septum (*S*) and is spread over the cord surface including blood vessels (*V*) and nerve roots with fine trabeculae. Reprinted with permission from Nicholas and Weller (1988) [13]

runs in longitudinal direction between the pia mater and the arachnoid membrane. It separates the posterior subarachnoid space into a left and right half (Figs. 2.3, 2.5, and 2.9) [8]. Toward the cervical area, it becomes more and more fenestrated and tapers off toward the cisterna magna. Similar fenestrations are evident toward the conus medullaris. The insertion of the septum at the spinal cord surface follows the course of the midline dorsal vein. In other words, pulling the arachnoid membrane may apply tension to the midline septum, and hence to this attached vein! Further septations have been described more laterally along the posterior roots from the dorsal root entry zone toward the arachnoid membrane, into the root sleeve, mainly in the lower cervical and thoracic spine. The anterior subarachnoid space does not demonstrate any such septations. Thus, anterior roots do not display such enveloping arachnoid membranes. The posterior septations may ease the dissection of large extramedullary tumors off the spinal cord, as they may provide a nice dissection plane [12].

The denticulate ligament is a transverse plate of fibers originating from the pia mater and running to the inner surface of the dura, usually inserting about 1.5–2 mm dorsal to the dural nerve root sleeve. It courses alongside the spinal cord on either side between the anterior and posterior roots (Figs. 2.3 and 2.5) [10].

The pia mater ensheathes the spinal cord. It contains fiber bundles, forming a complex support system for the spinal cord together with its extensions – the denticulate ligaments – and the dura mater. It holds the spinal cord in the center of the dural sac and protects it from undue extension as a result of spine movements [10]. The pia mater is not permeable to water and provides a barrier between the subarachnoid space and perivascular spaces of the cord [13].

Several observations, however, suggest that the extracellular space of the spinal cord and subarachnoid space should be considered as two compartments of the same fluid space that require free communication between each other. According to Rennels et al. [15], CSF enters the extracellular space of the central nervous system along the perivascular spaces of arteries, whereas extracellular fluid leaves it along the perivascular spaces of veins toward the subarachnoid space. This exchange depends on normal arterial and venous blood flow and can be abolished by interfering with the arterial blood supply. Studies with contrast medium injected into the subarachnoid space support this concept [3, 7, 11]. The required communication between the subarachnoid space and the perivascular spaces was demonstrated along posterior root entry zones, where Cloyd and Low [1] demonstrated the existence of fenestrations in the pia mater.

2.6 Spinal Cord and Nerve Roots

The spinal cord is about 45.9 cm long in males and 41.5 cm in females [10]. In the cervical and lumbar regions, the spinal cord is enlarged in its transverse diameter. The cervical enlargement between C4 and C7 is most pronounced at C5/6 (Fig. 2.1). According to magnetic resonance imaging measurements, the cervical cord varies in length corresponding to neck movements between 12.69 cm in anteflexion and 11.5 cm in retroflexion [9]. The lumbar enlargement is located approximately at the level of Th12, depending on the conus position (Fig. 2.6). The conus medullaris ends normally at about L1 and is surrounded by the nerve roots of the cauda equina. Caudally to the conus, the filum terminale is located in the center of the dural sac (Fig. 2.6).

The spinal cord contains white matter, which consists of axons, myelin-forming oligodendroglial cells, and fibrous astrocytes, and gray matter, which consists of neuronal cells, dendrites, neuroglial processes, oligodendroglia, and astrocytes. White matter is less vascularized than gray matter. The axons are organized in tracts with major motor or sensory functions. Most of these tracts are myelinated and either interconnect different spinal levels with each other or

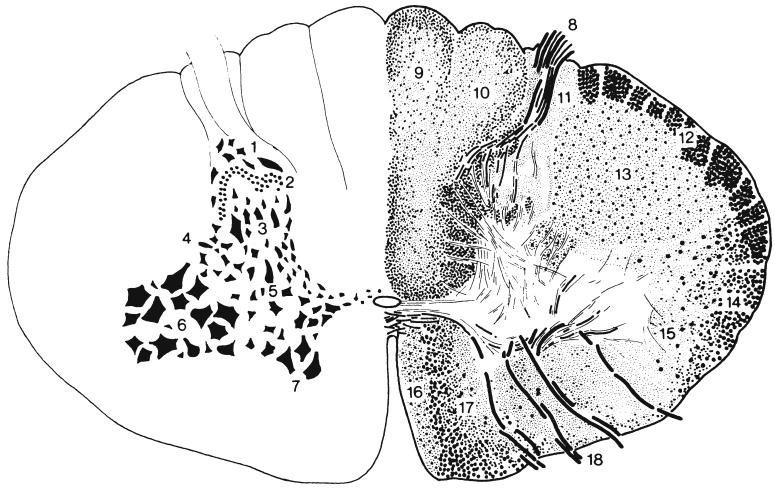

Fig. 2.10. Horizontal section through the fifth to sixth cervical segment of the spinal cord: *1* marginal cells, *2* substantia gelatinosa, *3* nucleus proprius, *4* reticular process, *5* substantia intermedia, *6* lateral motoneurons, *7* medial motoneurons, *8* posterior root, *9* fasciculus gracilis, *10* fasciculus cuneatus, *11* fasciculus dorsolateralis, *12* posterior spinocerebellar tract, *13* lateral pyramidal tract, *14* anterior spinocerebellar tract, *15* fasciculus anterolateralis, *16* anterior pyramidal tract, *17* fasciculus longitudinalis medialis, *18* anterior root. Reprinted with permission from Nieuwenhuys et al. (1978) [14]

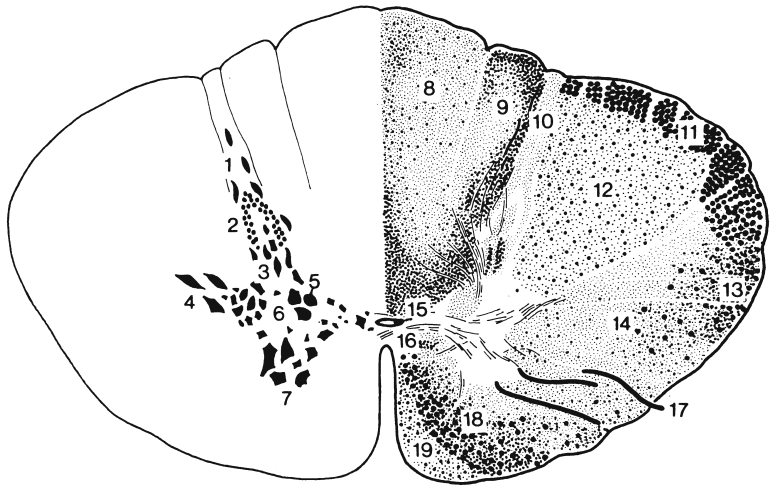

Fig. 2.11. Horizontal section through the fifth thoracic segment of the spinal cord: *1* marginal cells, *2* substantia gelatinosa, *3* nucleus proprius, *4* nucleus intermediolateralis, *5* nucleus thoracicus, *6* substantia intermedia, *7* motoneurons, *8* fasciculus gracilis, *9* fasciculus cuneatus, *10* fasciculus dorsolateralis, *11* posterior spinocerebellar tract, *12* lateral pyramidal tract, *13* anterior spinocerebellar tract, *14* fasciculus anterolateralis, *15* central canal, *16* commissura alba, *17* anterior root, *18* fasciculus longitudinalis medialis, *19* anterior pyramidal tract. Reprinted with permission from Nieuwenhuys et al. (1978) [14]

Fig. 2.12. Horizontal section through the fifth lumbar segment of the spinal cord: *1* marginal cells, *2* substantia gelatinosa, *3* nucleus proprius, *4* processus reticularis, *5* substantia intermedia, *6* nucleus cornu commissuralis, *7* motoneurons, *8* funiculus posterior, *9* posterior root, *10* fasciculus dorsolateralis, *11* funiculus posterolateralis, *12* funiculus anterolateralis, *13* funiculus anterior, *14* anterior root. Reprinted with permission from Nieuwenhuys et al. (1978) [14]

contain long descending or ascending fibers. The posterior midline tracts (i.e., the lateral fasciculus cuneatus and medial fasciculus gracilis) carry sensory information from the upper and lower part of the body, respectively, to the brain. Fibers enter these columns from posterior nerve roots. Thus, axons from lower segments of the body gradually become placed more medially the higher the spinal level. Between these two fascicles, a small intermediate sulcus may be detectable on the posterior surface. The lateral segments of white matter contain the spinocerebellar, lateral spinothalamic, and lateral corticospinal tracts. The anterior spinothalamic and anterior corticospinal tracts are found anteriorly (Figs. 2.10–2.12).

The gray matter of the spinal cord forms an H-shaped structure in the axial plane and varies in size according to the spinal level. It is greatest in the cervical and lumbar cord and considerably smaller in the thoracic cord due to the larger numbers of neurons required for motor function of upper and lower extremities, respectively. In the center of the cord and white matter lies the central canal, which is lined by ependymal cells. This canal is surrounded by fiber tracts of the anterior and posterior commissures. The gray matter is organized in the posterior and anterior horn on either side. The posterior horn contains sensory neurons organized in layers. In the cervical region, the posterior horn also contains the spinal nucleus of the trigeminal nerve. Thus, upper cervical pathologies may cause sensory dysfunctions in the face. The ventral horns, on the other side, contain motoneurons and interneurons. Of particular importance is the nucleus of the phrenic nerve, which is located between C3 and C6. Operations at these levels may cause phrenic dysfunctions and, thus, respiratory functions should be monitored carefully after operations at this level (Figs. 2.10–2.12).

Blood is supplied through the radicular arteries, which branch off the vertebral, aortic intercostal, and lumbar arteries and run along the anterior surface of the roots. They form the anterior and the paired posterior spinal arteries. In the cervical area, the anterior spinal artery is derived from paired branches of the distal vertebral arteries. The rest of the vascular supply to anterior and posterior spinal arteries is extremely variable. In most cases, there are two or three radicular branches to the cervical cord. Between one and six anterior radicular arteries connect to the anterior spinal artery in the cervical region, while none to eight posterior radicular arteries may supply the paired posterior spinal arteries [16]. In other words, sacrificing a radicular artery in the cervical region may be considered safe for most patients, but it may cause serious deficits in a patient with a low number of radicular arteries in the cervical area. A watershed region between the upper and lower spinal cord supplies is at about Th4. A regular lower major artery (i.e., the arteria radicularis magna or artery of Adamkiewicz) enters from the left side in 75% of patients, mostly (85% of cases) between Th9 and L2 and less often (in 15% of cases) between Th5 and Th8, to supply the anterior spinal artery [2]. Further radicular arteries supplying the anterior spinal artery may be encountered more often on the left side [5]. The anterior spinal artery courses along the anterior median sulcus. Anastomoses to the posterior spinal arteries exist, which are located on the dorsolateral surface of the cord. Branches of the anterior spinal artery penetrate the cord to supply the anterior white matter, ventral horns of the gray matter, base of the posterior horns, and the lateral columns. Distances between these central spinal arteries are larger in the thoracic cord compared to the conus area, where they are shortest, and the cervical cord. Arteries within the spinal cord are considered as end-arteries, as no anastomoses are detectable. Branches of the posterior spinal arteries supply the remaining posterior parts of the cord [16].

Veins run in a longitudinal direction on the cord surface and continue along the nerve roots toward the epidural venous plexus. About one-third to one-half of all roots carry radicular veins [16].

As far as vegetative functions of spinal nerves are concerned, sympathicoafferent and sympathicoefferent fibers can be distinguished. Neurons of the intermediolateral and intermediomedial nuclei of the thoracic and upper lumbar cord send out efferent fibers, which terminate either in the ganglia of the sympathetic trunk on the same level, in adjacent ganglia, or further cranially in cervical ganglia [10].

Little is known about sympathicoafferent fibers, which mediate vasoconstriction upon a cold stimulus to the skin. Even after complete transection of the cord, a cold stimulus to a lower extremity can still trigger vasoconstriction in the upper extremity via the sympathetic trunk. As far as efferent, vasoconstrictor fibers are concerned, those for the neck and head exit through the roots of C8–Th3, those for the upper extremities at Th3–Th6, and those for the lower extremities at Th4–L3. Vasodilator control is exerted through purely spinal reflex mechanisms and cannot be mediated across a level of cord transection. Its spinal representation is thought to correspond to the sensory distribution [10].

Sweat secretion is controlled by thermoregulatory centers of the brainstem, and efferent fibers leave the

anterior horns corresponding to the vasoconstrictor fibers of the sympathetic system [10].

Sensory fibers enter the spinal cord through posterior roots in the paramedian dorsal root entry zone, while motor fibers leave the cord via anterior roots at the corresponding ventral surface of the cord. Among posterior roots, anastomoses exist within the spinal subarachnoid space between neighboring segments in up to 61% of cases (dependent on the spinal level) [10]. Such anastomoses are much rarer among anterior root fibers and were identified only in up to 21% [10].

Posterior and anterior roots traverse the subarachnoid space in a lateral, caudal direction and in most cases penetrate the dura in separate pouches. The arachnoid fuses with the anterior and posterior roots several millimeters central to the spinal ganglion and merges with the dura of the root pockets [10]. The dorsal root ganglia lie posteriorly in the neural foramen just medial to the junction between the dorsal and anterior roots. Connective tissue, fat, and vascular structures surround the spinal nerve in its foramen. From a surgical standpoint, the venous plexus is the most important of these structures.

References

1. Cloyd MW, Low FN (1974) Scanning electron microscopy of the subarachnoid space in the dog. I. Spinal cord levels. J Comp Neurol 153:325–368
2. Djindjian R (1984) Vascular malformations. In: Shapiro R (ed) Myelography, 4th edn. Year Book Medical Publishers, Chicago, pp 318–344
3. Dubois PJ, Drayer BP, Sage M, Osborne D, Heinz ER (1981) Intramedullary penetrance of metrizamide in the dog spinal cord. AJNR 2:313–317
4. Harms J, Tabasso G (1999) Instrumented Spinal Surgery. Principles and Technique. Thieme, Stuttgart
5. Hassler O (1966) Blood supply to human spinal cord. A microangiographic study. Arch Neurol 15:302–307
6. Holdsworth FW, Hardy A (1953) Early treatment of paraplegia from fractures of the thoraco-lumbar spine. J Bone Joint Surg Br 35:540–550
7. Ikata T, Masaki K, Kashiwaguchi S (1988) Clinical and experimental studies on permeability of tracers in normal spinal cord and syringomyelia. Spine 13:737–741
8. Key EAH, Retzius MG (1875) Studien der Anatomie des Nervensystems und des Bindegewebes. Samson Wallin, Stockholm
9. Koschorek F, Jensen HP, Terwey B (1987) The dynamic evaluation of the cervical spinal canal and spinal cord by magnetic resonance imaging during movement. In: Voth D, Glees P (eds) Diseases of the Craniocervical Junction. De Gruyter, Berlin, pp 99–103
10. Lang J (1993) Clinical Anatomy of the Cervical Spine. Thieme, Stuttgart
11. Li KC, Chui MC (1987) Conventional and CT metrizamide myelography in Arnold-Chiari I malformation and syringomyelia. AJNR 8:11–17
12. Nauta HJW, Dolan ED, Yasargil MG (1983) Microsurgical anatomy of spinal subarachnoid space. Surg Neurol 19:431–437
13. Nicholas DS, Weller RO (1988) The fine anatomy of the human spinal meninges. A light and scanning electron microscopy study. J Neurosurg 69:276–282
14. Nieuwenhuys R, Voogd J, Van Huizen C (1978) The Human Central Nervous System. A Synopsis and Atlas. Springer, Heidelberg
15. Rennels ML, Gregory TF, Blaumanis OR, Fujimoto K, Grady PA (1985) Evidence for a "paravascular" fluid circulation in the mammalian central nervous system, provided by the rapid distribution of tracer protein throughout the brain from the subarachnoid space. Brain Res 326:47–63
16. Turnbull IM, Brieg A, Hassler O (1966) Blood supply of cervical spinal cord in man. A microangiographic cadaver study. J Neurosurg 24:951–965

Intramedullary Tumors 3

Contents

Intramedullary tumors account for 16% of the spinal tumors in our series [43]. Among all central nervous system tumors, figures for intramedullary tumors range between 2 and 4% in the literature [57, 204, 215, 314, 318, 344]. In other words, intramedullary tumors are rare. A minority of these tumors is associated with genetic diseases such as von-Hippel-Lindau disease (VHL), causing hemangioblastomas and neurofibromatosis type 2 (NF-2) associated with ependymomas or astrocytomas. Intramedullary tumors are observed in 19% of patients with NF-2 and 20% of those with VHL [251]. In neurofibromatosis type 1 (NF-1), intramedullary tumors are rare. So far, only astrocytomas have been encountered in NF-1 [348].

With the introduction of magnetic resonance imaging (MRI), an increasing number of patients with intramedullary tumors are now diagnosed at an early stage of the disease. This imaging modality has certainly benefited patients enormously [356]. However, some problems in differential diagnosis between intramedullary tumors and demyelinating or inflammatory diseases of the spinal cord still exist. Associated cysts (i.e., syringomyelia) may be present with a small underlying tumor that can be easily overlooked. So quite clearly, MRI has made the diagnosis of intramedullary tumors easier but not foolproof.

In this chapter we will describe the clinical symptoms of intramedullary tumors and their neuroradiological features, provide a description of surgical techniques, and finally give a detailed analysis of postoperative results and outcomes on the basis of 182 patients treated in the past 25 years. These patients underwent 198 operations for treatment of 199 tumors (Table 3.1). Fourteen patients underwent multiple operations.

Table 3.1. Intramedullary tumors of 182 patients treated in the past 25 years

Type of tumor	Adults	Children	Total
Ependymoma	76	3	79
Astrocytoma	40	25	65
Angioblastoma	20	1	21
Hamartoma	10	–	10
Glioependymal cyst	7	–	7
Cavernoma	6	–	6
Metastasis	4	–	4
Melanocytoma	4	–	4
Ganglioglioma	1	1	2
Schwannoma	1	–	1
Total	**169**	**30**	**199**

3.1 History and Diagnosis

In our series, about one-third of patients experienced some form of pain as their first symptom. The remainder complained about sensory deficits, paresthesias, motor weakness, or gait problems as their first manifestation in about equal proportions. With malignant tumors, almost all patient complained about pain, gait ataxia, or motor weakness right form the start (Table 3.2). In general, the case history averaged about 33±44 months, with considerable variability, ranging between 1 week and 28 years. Benign tumors had a significantly longer history compared to malignant tumors (36±46 months and 7±13 months, respectively; $p<0.0001$).

Approximately 36% of tumors were located in the cervical cord, 50% in the thoracic cord, and the remaining 14% in the conus area [98]. According to our experience, the advent of MRI has not led to a faster diagnoses in general (30±32 months before and 33±41 months after the introduction of MRI). After all, intramedullary tumors are so rare that they are quite often not included in the differential diagnosis when the first symptoms have appeared. However, patients are in better neurological condition at the time of surgery now compared to the pre-MRI era [356]. In our series, the average preoperative Karnofsky score has improved from 55±20 to 70±17 ($p=0.0001$) since the introduction of MRI. Patients who for years are thought to have multiple sclerosis while neurological symptoms continue to progress due to an overlooked intramedullary tumor, should be a phenomenon of the past.

The average age at presentation was 38±17 years. The typical clinical history was characterized by a gradual and slow progression without intermittent remission of symptoms. This is a very important point for the differential diagnosis to inflammatory or demyelinating syndromes. The latter almost always develop significant deficits quickly, within days or weeks, and then fluctuate and display some variability in terms of intensity and/or localization of symptoms with time. Sudden clinical progressions occur in intramedullary tumors only in exceptional cases. We have encountered them in association with either tumor hemorrhages [4, 163, 242, 301, 324] or highly malignant tumors [130].

On admission, the clinical situation had progressed to affect motor functions to some degree for at least 80% of patients. Motor weakness or a gait problem was considered their major concern for 22% and 38% of patients, respectively. Even though pain was still present in 52% of patients, just 19% wanted surgery predominantly for pain relief. Sensory deficits were found in 87% of cases and dysesthesias in 56% (Table 3.3). The preoperative Karnofsky score averaged about 67±18. In the literature, most studies describe a progressive course of neurological deterioration prior to surgery. However, unusual presentations due to affections of the autonomic nervous system are also reported. Fricke and Romine [102] described a patient with a thoracic ependymoma presenting with ortho-

First symptom	Benign tumors	Malignant tumors	Adults	Children	Total
Pain	34%	43%	38%	21%	35%
Gait ataxia	18%	33%	17%	24%	19%
Motor weakness	16%	19%	14%	42%	17%
Sensory deficits	14%	–	15%	–	13%
Dysesthesias	15%	5%	15%	4%	14%
Sphincter Problems	3%	–	2%	4%	2%
Scoliosis	1%	–	–	4%	1%

Table 3.2. Initial symptoms of intramedullary tumors

Table 3.3. Symptoms at presentation for intramedullary tumors

Symptom	Benign tumors	Malignant tumors	Adults	Children	Total
Pain	52%	53%	53%	42%	52%
Gait ataxia	78%	95%	78%	96%	80%
Motor weakness	76%	89%	77%	85%	78%
Sensory deficits	86%	95%	89%	69%	87%
Dysesthesias	58%	42%	63%	23%	56%
Sphincter problems	35%	47%	35%	39%	36%

Fig. 3.1. a, b T1-weighted, contrast-enhanced sagittal and axial magnetic resonance imaging (MRI) images of an intramedullary World Health Organization (WHO) grade I astrocytoma at Th2–Th6 in a 10-year-old girl. The tumor enhances brightly with contrast, and is associated with a considerable syrinx above and below the solid tumor, which affects predominantly the left side, compressing the remaining cord to the right (*arrowhead* in **b**)

static hypotension and diarrhea. Both resolved after tumor removal.

Comparing adults and children, astrocytomas were the predominating tumor in children (83%), with all other pathologies almost exclusively occurring in adults (Table 3.1). Looking at clinical presentations for children with intramedullary tumors, we noticed a higher proportion of motor weakness or gait problems as the first (66% compared to 31%; Table 3.2; chi square test: $p<0.0001$) and the major complaint on admission compared to adults (86% compared to 56%; chi square test: $p=0.0023$) [54, 68, 131, 152, 215, 325]. Correspondingly, at presentation, sensory affections, pain or dysesthesias were encountered less often in children (Table 3.3).

In small children, the symptoms and signs of an intramedullary tumor may not be easy to detect. Unusual presentations such as abdominal pain [75], painless muscle atrophies without sensory disturbances [88], or torticollis [31, 54, 131] may be observed.

Of children with intramedullary tumors, 4% became symptomatic with a progressive scoliosis [152]. DeSousa et al. [68] observed abnormal spine radiographs in 58% of children with intramedullary tumors (e.g., scoliosis, kyphotic angulations). The distinguishing feature pointing toward a spinal tumor is the association of scoliosis with pain [46] or other neurological symptoms.

3.2 Neuroradiology

Without any doubt, MRI has revolutionized our preoperative possibilities to establish the diagnosis, determine the exact extent of the tumor (Figs. 3.1 and 3.2), and visualize associated cysts (Figs. 3.1 and 3.2) [37, 282, 357]. Nobody will operate on an intramedullary tumor anymore without an adequate preoperative MRI scan. Except for patients unable to undergo an MRI, computed tomography (CT) with contrast or myelography is no longer required [161, 165, 247].

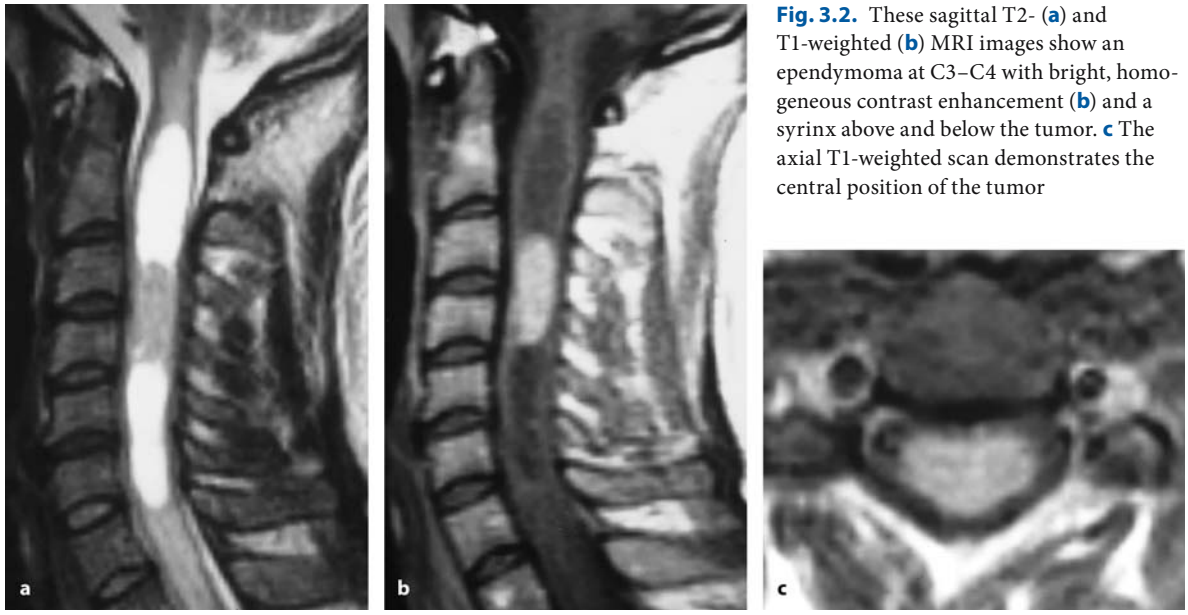

Fig. 3.2. These sagittal T2- (**a**) and T1-weighted (**b**) MRI images show an ependymoma at C3–C4 with bright, homogeneous contrast enhancement (**b**) and a syrinx above and below the tumor. **c** The axial T1-weighted scan demonstrates the central position of the tumor

With modern imaging and microsurgical techniques, percutaneous needle aspirations and biopsy procedures are rendered obsolete [269]. Positron emission tomography may be capable to distinguish between an active tumor and scar tissue or gliosis, but is mainly of scientific interest in intramedullary tumors [295].

Standard X-rays, however, should still be performed to visualize the bony anatomy of the spine, evaluate the stability in the affected segment, and to facilitate the intraoperative identification of the correct spinal level. In rare instances, slow-growing tumors may erode vertebral pedicles (Fig. 3.3), widen the spinal canal (Fig. 3.4), or even cause vertebral and spinal deformities (Fig. 3.4) [322]. The latter may be observed especially in children. Quite often, the preoperative radiological study already demonstrates significant biomechanical problems in younger patients [68, 162, 199, 300].

If a recurrent tumor has to be operated, functional X-rays may be helpful to rule out instability provoked by the previous operation. Furthermore, a CT scan with bone window may be extremely helpful for exposure of the dura, as it demonstrates bony landmarks for the dissection of epidural scar tissue.

As for the MRI diagnosis of intramedullary tumors, the preoperative examination has to provide the following information:

1. Imaging has to demonstrate the precise spinal level of the tumor, its upper and lower limits in T1- and T2-weighted images. This has to be done in such a way that the surgeon can determine this level by intraoperative roentgenography; the cervical or lumbar spine has to be shown in upper and lower thoracic tumors, respectively, as well [322].
2. An examination with gadolinium is mandatory. Contrast enhancement is an indicator concerning the vascularity of the tumor and the homogenous or inhomogenous uptake of contrast may aid in the differential diagnosis between tumors such as ependymomas or angioblastomas and an astrocytoma, for instance. Inhomogenous uptake of contrast may also be a feature of anaplastic or malignant tumors.
3. Axial scans have to show the demarcation toward the normal cord tissue and the orientation of the tumor inside the cord: midline versus eccentric, posterior, or anterior position. Furthermore, exophytic parts of the tumor can be demonstrated on axial scans.

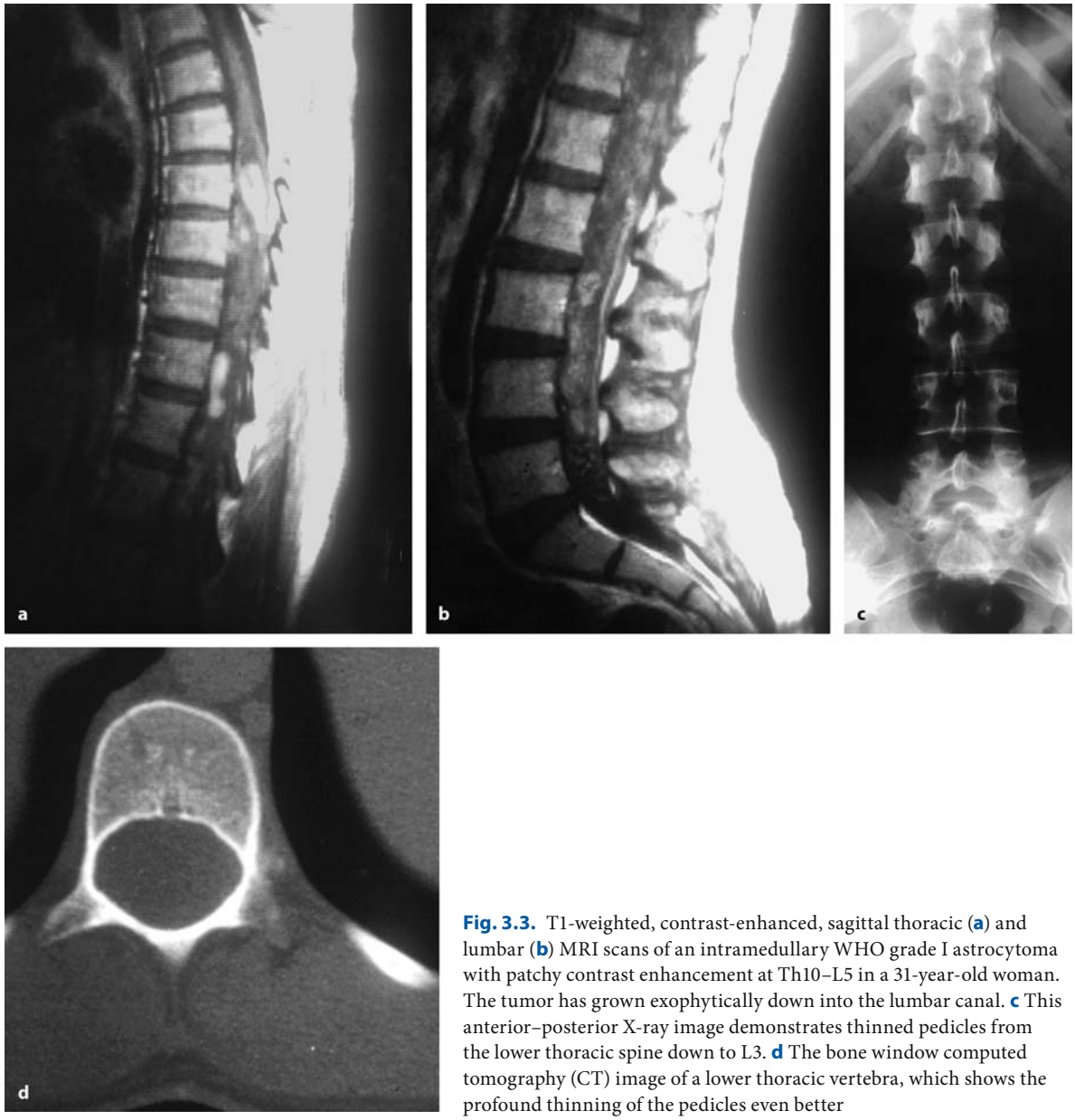

Fig. 3.3. T1-weighted, contrast-enhanced, sagittal thoracic (**a**) and lumbar (**b**) MRI scans of an intramedullary WHO grade I astrocytoma with patchy contrast enhancement at Th10–L5 in a 31-year-old woman. The tumor has grown exophytically down into the lumbar canal. **c** This anterior–posterior X-ray image demonstrates thinned pedicles from the lower thoracic spine down to L3. **d** The bone window computed tomography (CT) image of a lower thoracic vertebra, which shows the profound thinning of the pedicles even better

4. A significant number of intramedullary tumors is associated with a syrinx [15, 56, 57, 111, 265, 267]. The MRI has to distinguish between a solid tumor and an associated cyst.
5. In patients with suspected or known systemic diseases such as NF-2 or VHL, the entire neuraxis has to be examined [76, 189, 214, 254, 284].

However, as informative as an MRI scan is, it does not provide an answer to the question almost every patient will ask when confronted with the diagnosis: is the tumor resectable? Although there are signs that may suggest that the tumor is well demarcated and removable, such as a bright homogenous enhancement with gadolinium or a clear-cut demarcation on T2-weighted images, we were unable to define radiological criteria to predict respectability or histology accurately (Fig. 3.5) [196].

In general, ependymomas are centrally located, sharply defined intramedullary lesions that are isointense on T1- and T2-weighted images and will take up contrast homogenously in most instances (Fig. 3.2) [86, 93, 173, 224, 322, 323]. Miyazawa et al. [224] analyzed the contrast-enhancing patterns of ependymo-

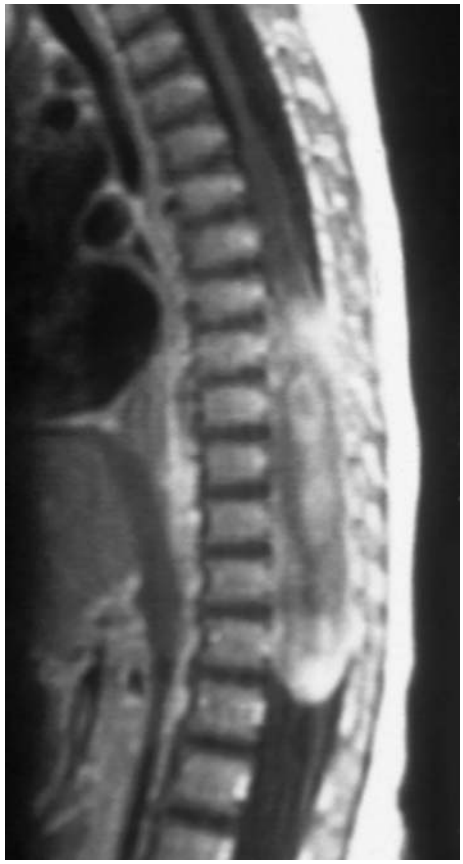

Fig. 3.4. T1-weighted, contrast-enhanced sagittal MRI scan of a huge WHO grade II–III astrocytoma at Th6–L1 in a 4-month-old boy. The tumor appears partly cystic and has widened the spinal canal. The lower thoracic spine is straightened and a slight kyphosis is apparent at Th12/L1

Fig. 3.5. The resectability of an intramedullary tumor cannot be predicted by MRI. These contrast-enhanced, sagittal, T1- (**a**) and T2-weighted (**b**) MRI images demonstrate a WHO grade I astrocytoma at C6–C7 in a 33-year-old woman. The tumor takes up little contrast and there appears to be no clear demarcation toward the spinal cord at either the lower or upper pole on either image. Yet, the tumor could be completely resected. **c**, **d** Contrast-enhanced, sagittal T1- (**c**) and T2-weighted (**d**) MRI images showing an astrocytoma at C3–C6 in a 17-year-old girl. The tumor takes up some contrast and appears particularly well demarcated in **d**. The tumor turned out to be infiltrative and could be only partly resected. The histology disclosed a WHO grade III anaplastic astrocytoma

mas further and found 4 different types in 28 tumors: homogeneous (Fig. 3.2), heterogeneous (Fig. 3.6), heterogeneous with cyst wall enhancement (Fig. 3.7), and enhancing nodule with a cyst wall (Fig. 3.8). In T2-weighted images, dark caps of hemosiderin may be observed at the upper and lower tumor poles (Fig. 3.6) [93, 196, 239, 322]. However, this feature is not pathognomonic for ependymomas, as it was also observed with malignant astrocytomas [156]. The association with intramedullary cysts is common [323] and was observed in 60.5% of our patients (Figs. 3.2, 3.6, and 3.7). Ependymomas with exophytic components are reported, but are extremely rare [122].

Angioblastomas are brightly enhancing lesions in T1-weighted images and are commonly associated with an intramedullary cyst – 88% in our series (Fig. 3.9) [52, 78, 125, 134, 145, 173, 334]. Sometimes tiny tumors may give rise to enormous cysts (Fig. 3.10). Therefore, every intramedullary cyst must be examined without and with contrast on MRI [86]. Although cardiac gated cine MRI studies are considered by some authors to distinguish between tumor associated cysts, which do not display flow phenomena, and syringomyelia, which do present flow signals inside syrinx cavities, this imaging modality is not reliable for this purpose in our experience. Tumor-associated cysts may also show signs of flow (Fig. 3.10). Angioblastomas may be associated with a significant amount of peritumoral edema. They are often vascularized by radicular arteries and, therefore, tend to be located in the subpial area toward the dorsal root entry zone (Fig. 3.10) [134]. However, anteriorly located angioblastomas fed by anterior arteries do occur (Fig. 3.9) [134, 148]. The intramedullary location is the most common among angioblastomas, but extramedullary and epidural angioblastomas may also be observed [78, 134, 322], especially in patients with VHL. Intramedullary angioblastomas may be entirely surrounded by spinal cord tissue or may protrude into the subarachnoid space like an exophytic tumor [58, 134, 145]. Veins on the spinal cord surface may be so enlarged that they can be detected by myelography or MRI as meningeal varicosis [29, 322, 341]. With the modern technique of magnetic resonance angiography, feeding and draining vessels can be demonstrated [210]. If an angioblastoma is suspected, the entire neuraxis should be examined, as multiple tumors associated with VHL are not so rare (Fig. 3.11) [29, 78, 134]. Even leptomeningeal spreading of angioblastomas has been described [11].

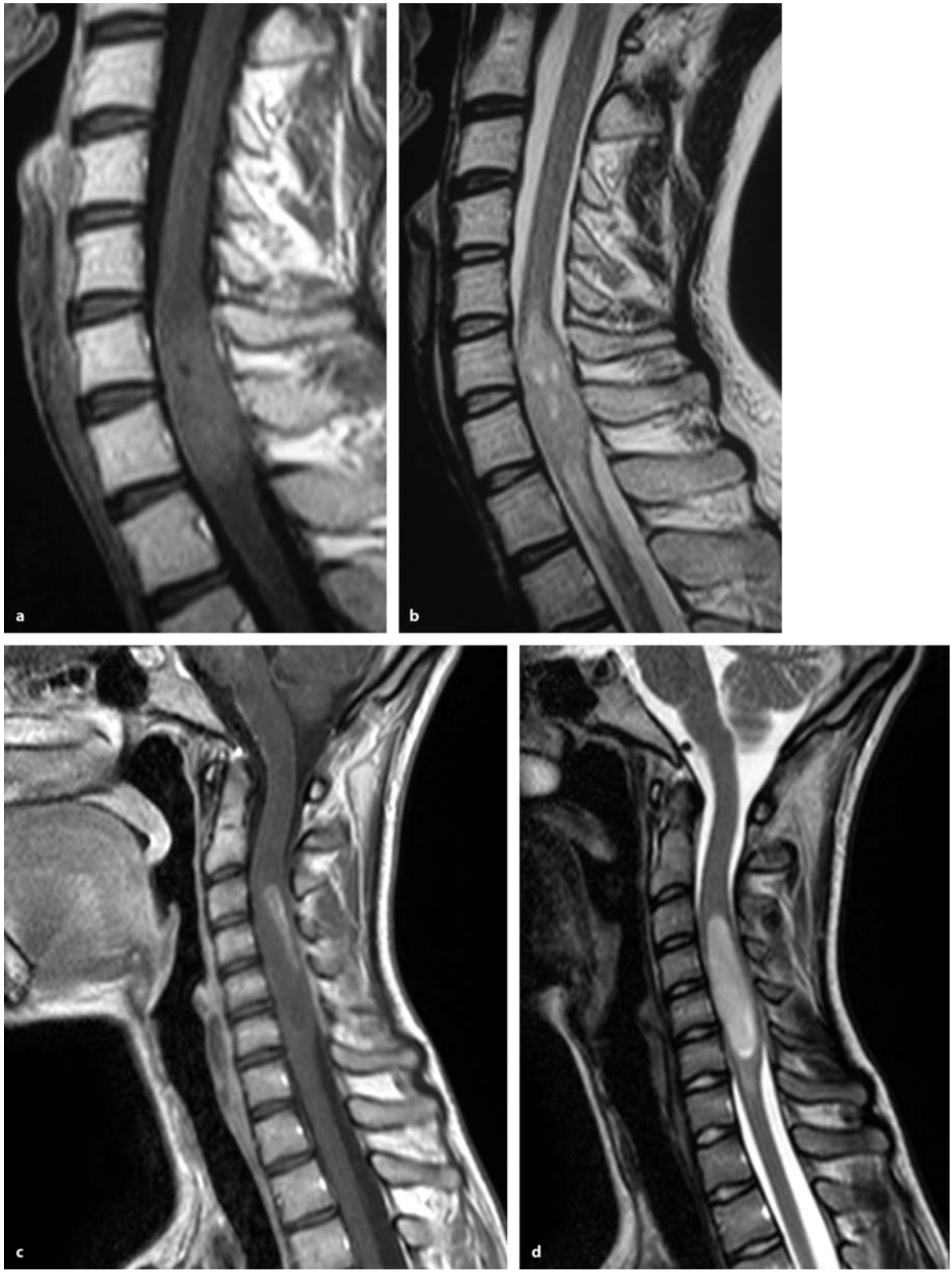

Fig. 3.5.

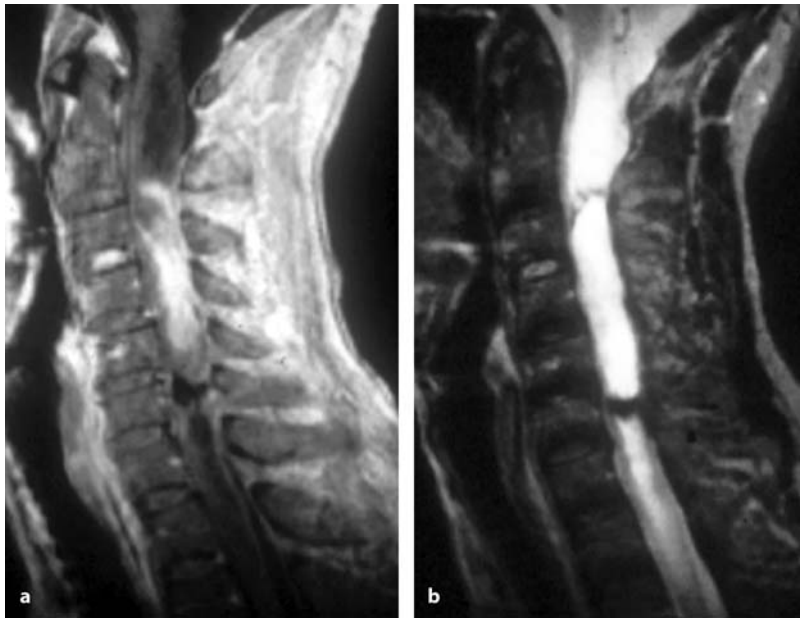

Fig. 3.6. **a** T1-weighted sagittal MRI after contrast application, of an ependymoma at C3–C6 with inhomogenous contrast enhancement. **b** This T2-weighted scan shows hemosiderin caps at either tumor pole related to tumor hemorrhages. Once again, syrinx cavities accompany this tumor

Fig. 3.7. This sagittal, contrast-enhanced, T1-weighted MRI scan shows an ependymoma at C3–C7 with heterogenous contrast enhancement as well as enhancement of the cyst wall, which is part of the tumor. A syrinx extends from C2 cranially into the lower brainstem

Fig. 3.8. T1-weighted, contrast-enhanced MRI of a patient with neurofibromatosis type 2 (NF-2) and an ependymoma at C1/2. The contrast-enhancing, solid tumor is part of a cyst wall. The remainder of the cyst wall does not take up gadolinium and is not part of the tumor. The other contrast-enhancing lesions most likely represent schwannomas

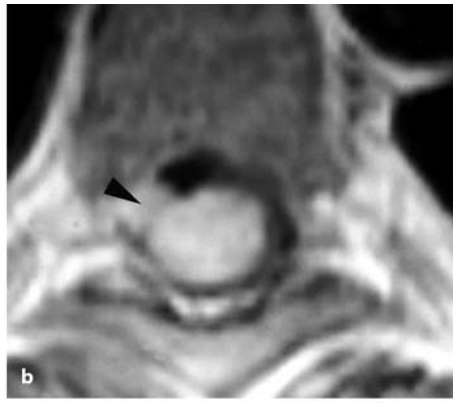

Fig. 3.9. T1-weighted, contrast-enhanced sagittal (**a**) and axial (**b**) MRI scans of a sizable intramedullary angioblastoma at Th6–Th7 in a 47-year-old woman. The tumor is accompanied by large syrinx cavities above and below. There appears to be an exophytic component anteriorly on the right side, corresponding to the major arterial supply of this lesion (*arrowheads*)

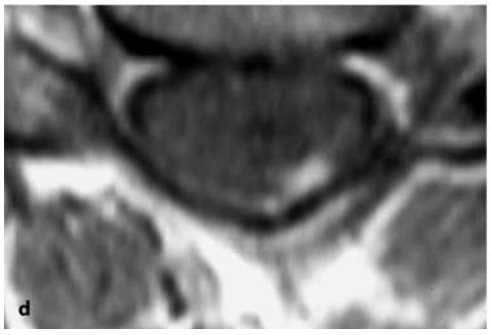

Fig. 3.10. This series of MRI scans is an example of a small angioblastoma associated with a large syrinx in a 45-year-old woman. **a** This T2-weighted image displays a syrinx without any apparent tumor. **b** In the T1-weighted image (without contrast), a solid tumor at C5/6 could be suspected. **c, d** Only the sagittal and axial, contrast-enhanced T1-weighted images disclose the pathology correctly: a small angioblastoma in the left dorsal root entry zone at C4/5. (*Continuation see next page*)

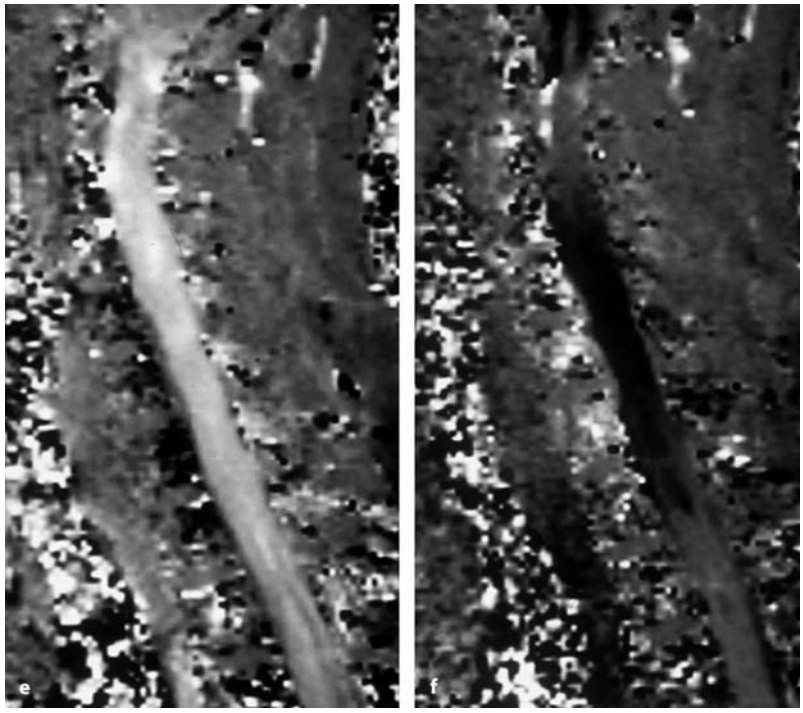

Fig. 3.10. (*Continued*) **e, f** These cardiac gated cine MRIs demonstrate flow signals in the associated syrinx in cerebrospinal fluid (CSF)-systole and diastole (i.e., flow inside a syrinx does not prove the absence of an intramedullary tumor)

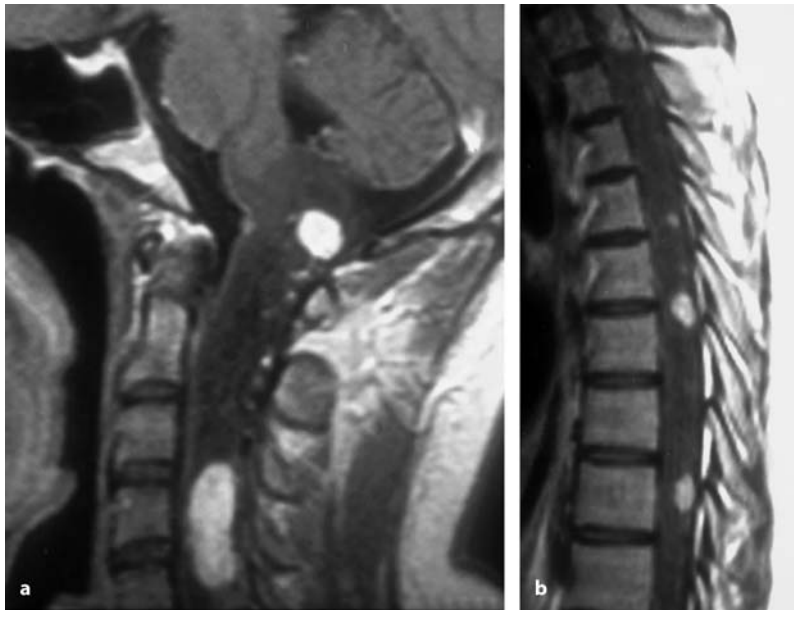

Fig. 3.11. Craniocervical (**a**) and thoracic (**b**) T1-weighted, contrast-enhanced MRI scans in a 34-year-old patient with von Hippel-Lindau disease (VHL), displaying multiple intramedullary angioblastomas at C1, C2–C4, Th1, Th4, Th5/6, and Th8

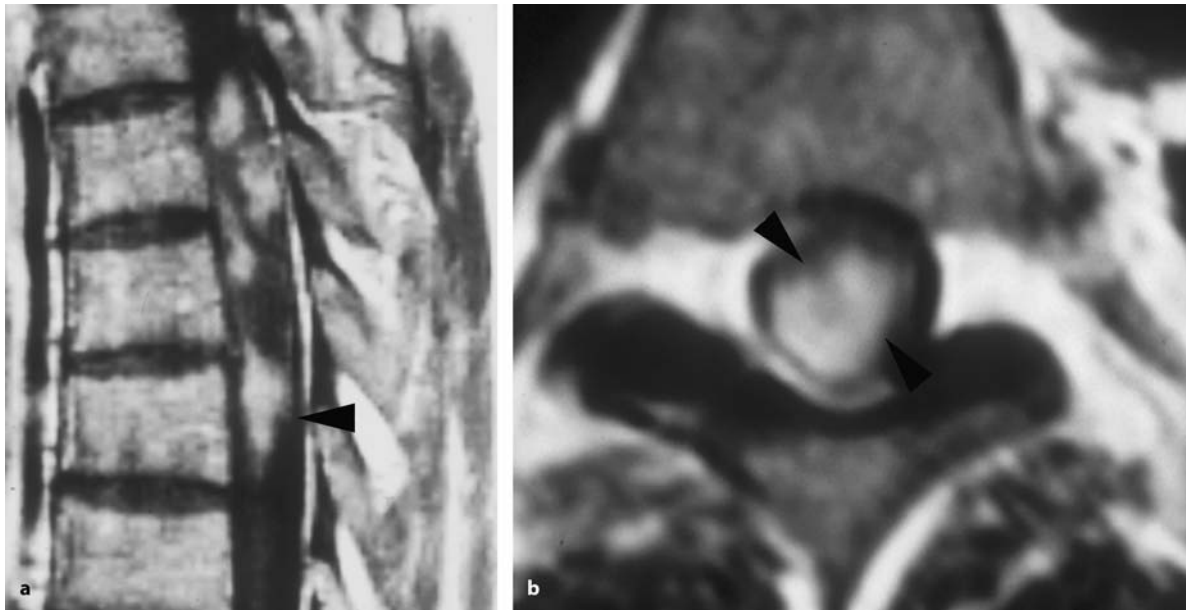

Fig. 3.12. Contrast-enhanced, sagittal (**a**) and axial (**b**) T1-weighted MRI scans of a WHO grade III astrocytoma at Th5–Th7 in a 49-year-old patient. The tumor shows patchy contrast enhancement and protrudes out of the cord posteriorly on the right side (*arrowheads*)

Fig. 3.13. Sagittal, contrast-enhanced T1-weighted MRI images of a large intramedullary WHO grade I astrocytoma in a 9-year-old boy extending from the midthoracic cord (**a**) into the posterior fossa (**b**)

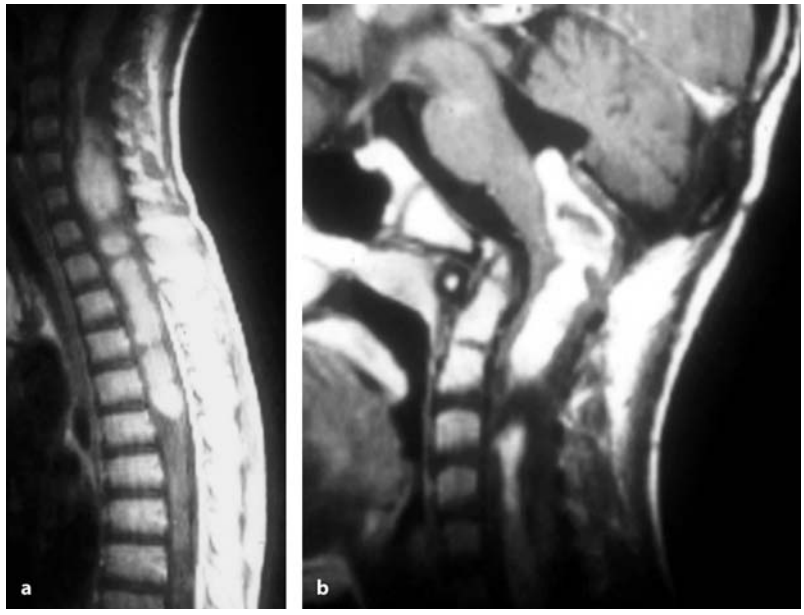

Astrocytomas often take up contrast inhomogeneously in T1-weighted images (Figs. 3.1, and 3.3–3.5). Cysts accompany these tumors less often – 42.5% in our series [156]. On axial scans, astrocytomas are often eccentric (Fig. 3.1) and may transgress the pia mater to grow exophytically (Fig. 3.12) [86, 130, 142, 173, 322]. Exophytic growth has been reported to be more common in the conus region [142]. Rare extensions from the cervical cord into the cranial cavity have also been described (Fig. 3.13) [136]. Astrocytomas may torquate the spinal cord and infiltrate spinal nerve roots (Fig. 3.12). Some astrocytomas do not take up gadolinium at all (Fig. 3.14); in that instance, the differential diagnosis to inflammatory reactions in

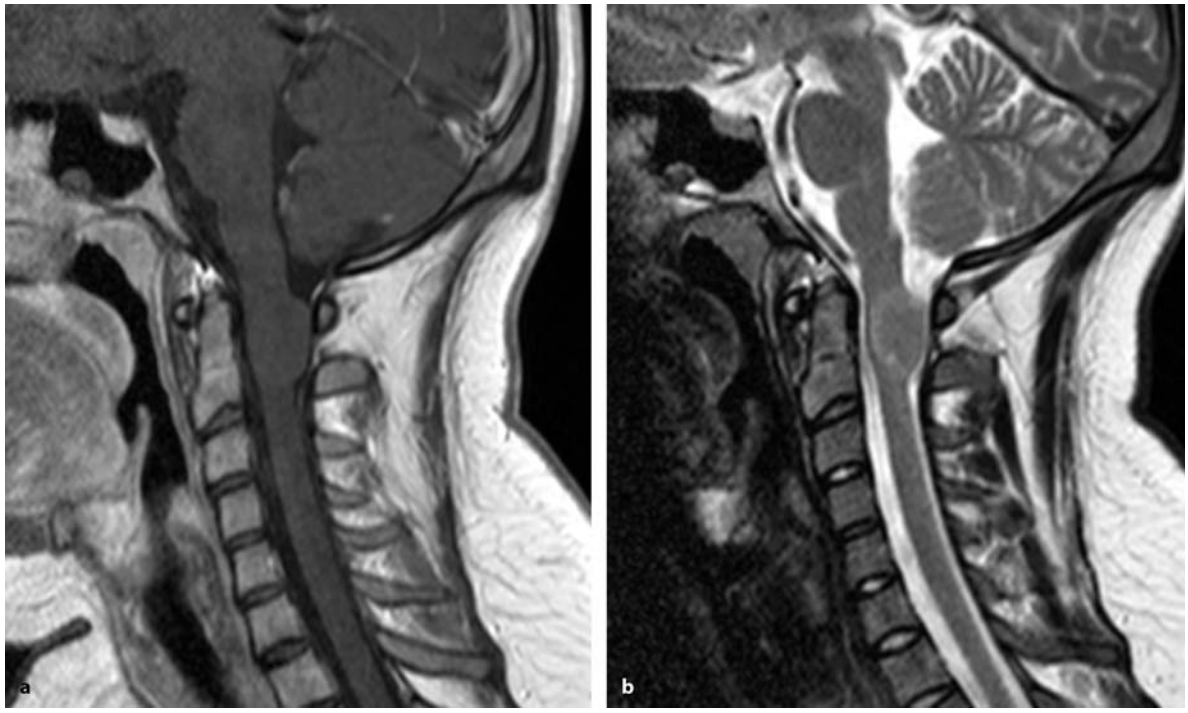

Fig. 3.14. Sagittal, contrast-enhanced T1-weighted MRI image (**a**) and T2-weighted image (**b**) of a WHO grade I intramedullary astrocytoma at C1–C2 in a 21-year-old patient. The tumor does not take up contrast at all and is isodense to the spinal cord on the T1-weighted image. Only the T2-weighted image demonstrates a demarcation toward the cord with a slightly hyperdense rim

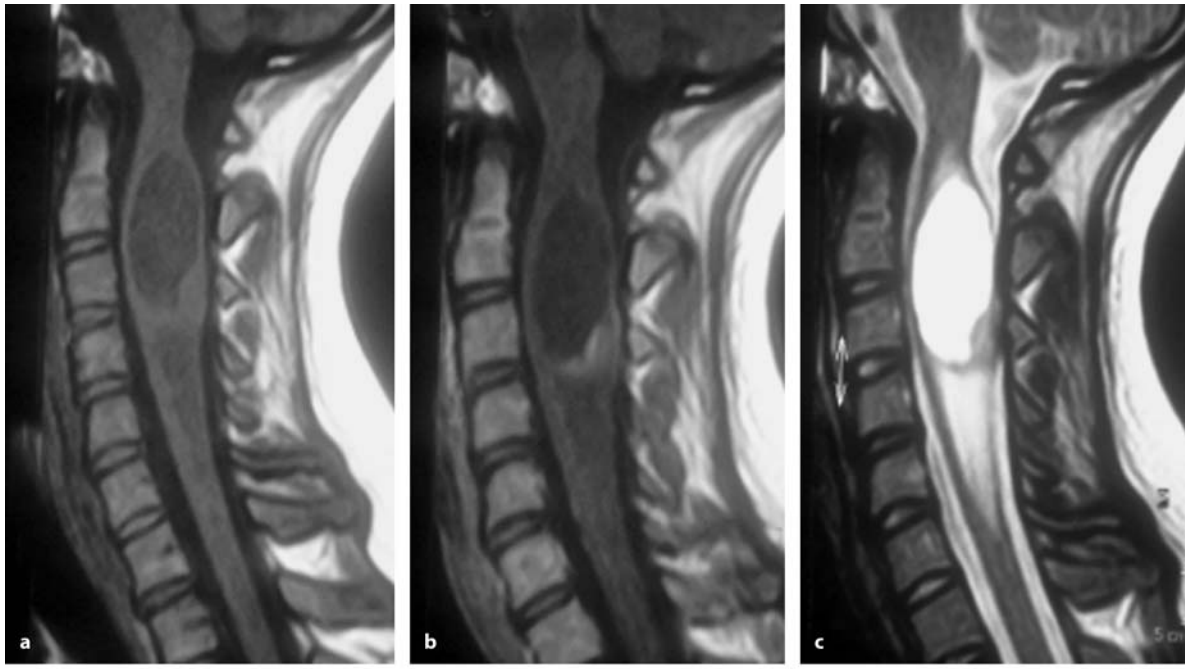

Fig. 3.15. Sagittal T1-weighted MRI without (**a**) and with contrast enhancement (**b**), of a cystic WHO grade I astrocytoma at C2–C4 in a 22-year-old woman. Just the solid part at C3/4 takes up contrast. **c** The T2-weighted scan shows the demarcation of the cystic tumor toward the edematous spinal cord. (*Continuation see next page*)

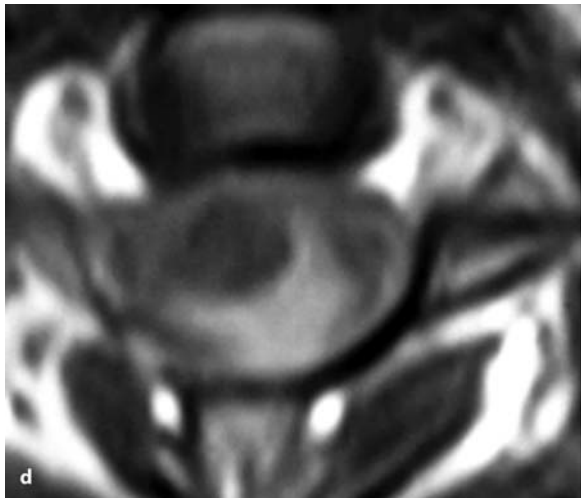

Fig. 3.15. (*Continued*) **d** This contrast-enhanced axial T1-weighted scan shows the solid, enhancing part of this cystic tumor

the spinal cord may be extremely difficult. Likewise, the distinction between cystic astrocytomas and a syrinx may be almost impossible, if the cyst wall appears like gliotic tissue rather than a contrast-enhancing tumor (Fig. 3.15) [86, 140]. In intratumoral cysts, the protein content tends to be higher compared to a syrinx cavity or the subarachnoid space. However, this is not always the case (Fig. 3.15). To determine the exact extension of an astrocytoma, T2-weighted images may be extremely helpful as they tend to show a better demarcation toward normal cord tissue than do T1-weighted images (Figs. 3.14 and 3.15).

Mixed signal intensities on T1-weighted images and high signal intensity on T2-weighted images but a clear-cut limitation of the tumor is displayed by intramedullary gangliogliomas (Fig. 3.16). Patchy enhancement with contrast is common [173]. Again, the T2-weighted image may be the most helpful to determine the extent of the tumor.

Cavernous hemangiomas are extremely rare and can be distinguished from other pathologies by their characteristic patchy contrast uptake in T1-weighted images and signs of hemosiderin in the surrounding cord tissue in T2-weighted scans (Fig. 3.17) [35].

Glioependymal cysts are mostly, but not exclusively observed in the conus area (Figs. 3.18 and 3.19). The lining does not enhance with contrast and the fluid inside the cyst gives a signal identical to cerebrospinal fluid (CSF). The cysts may be quite sizeable and do not contain septations (Fig. 3.19) [213]. The differential diagnosis to syringomyelia may pose some problems. Apart from septations, which are a common feature of syrinx cavities (Fig. 3.20) but are absent in glioependymal cysts, flow void signals on T2-weighted images and flow signals in cardiac gated cine MRI scans may help to distinguish a syrinx (Fig. 3.20) from an ependymal cyst (Fig. 3.21). However, this imaging modality is not absolutely reliable. Flow signals may be absent in syrinx cavities. Finally, the asymmetric shape of a syrinx on sagittal images (Fig. 3.22) compared to the symmetric appearance of ependymal cysts (Fig. 3.19) may be helpful for differential diagnosis.

Within the group of intramedullary hamartomas, dermoid cysts and lipomas should to be mentioned. These lesions are often, but not always, accompanied by manifestations of spinal dysraphism. In patients with dermoid cysts, an associated dermal sinus is not uncommon [14, 108, 181, 310]. Likewise, a diastematomyelia [108, 306], a tethered cord [108, 257], incomplete vertebral arches [260], or an additional lipoma [257] may be encountered. The cyst wall may enhance with contrast. The cyst contents vary in signal intensity as they may contain almost any type of tissue or substance. Most of them have been found in the conus medullaris (Fig. 3.23) [3, 9, 20, 49, 260]. However, dermoid cysts have also been described at other spinal levels [64], such as the thoracic [30] or cervical medulla [10, 65].

Intramedullary lipomas are quite rare if we restrict this category to lipomas with a sizable intramedullary portion (Fig. 3.24). Almost all intramedullary lipomas that we have encountered displayed an exophytic extension into the subarachnoid space. Whenever the extramedullary part was considered larger than the intramedullary part, we put that lipoma into the extramedullary category. Cooper and Epstein [57] described 29 spinal lipomas, of which just 2 were located inside the spinal cord. The radiological features are quite clear on MRI, with the characteristic high signal intensity on T1-weighted images [27]. With fat-suppression techniques, an MRI examination nowadays provides an accurate preoperative diagnosis [255]. As already mentioned for dermoid cysts, intramedullary lipomas may be associated with other features of spinal dysraphism [101]. However, this is less often observed compared to extramedullary lipomas, which demonstrate signs of spina bifida occulta in the majority of patients. Any spinal level may be involved [188]. In children, intramedullary lipomas of remarkable extension have been described reaching from the cervical spine into the posterior fossa [40, 63, 174, 227, 232, 236, 342] or throughout the entire spinal cord [274].

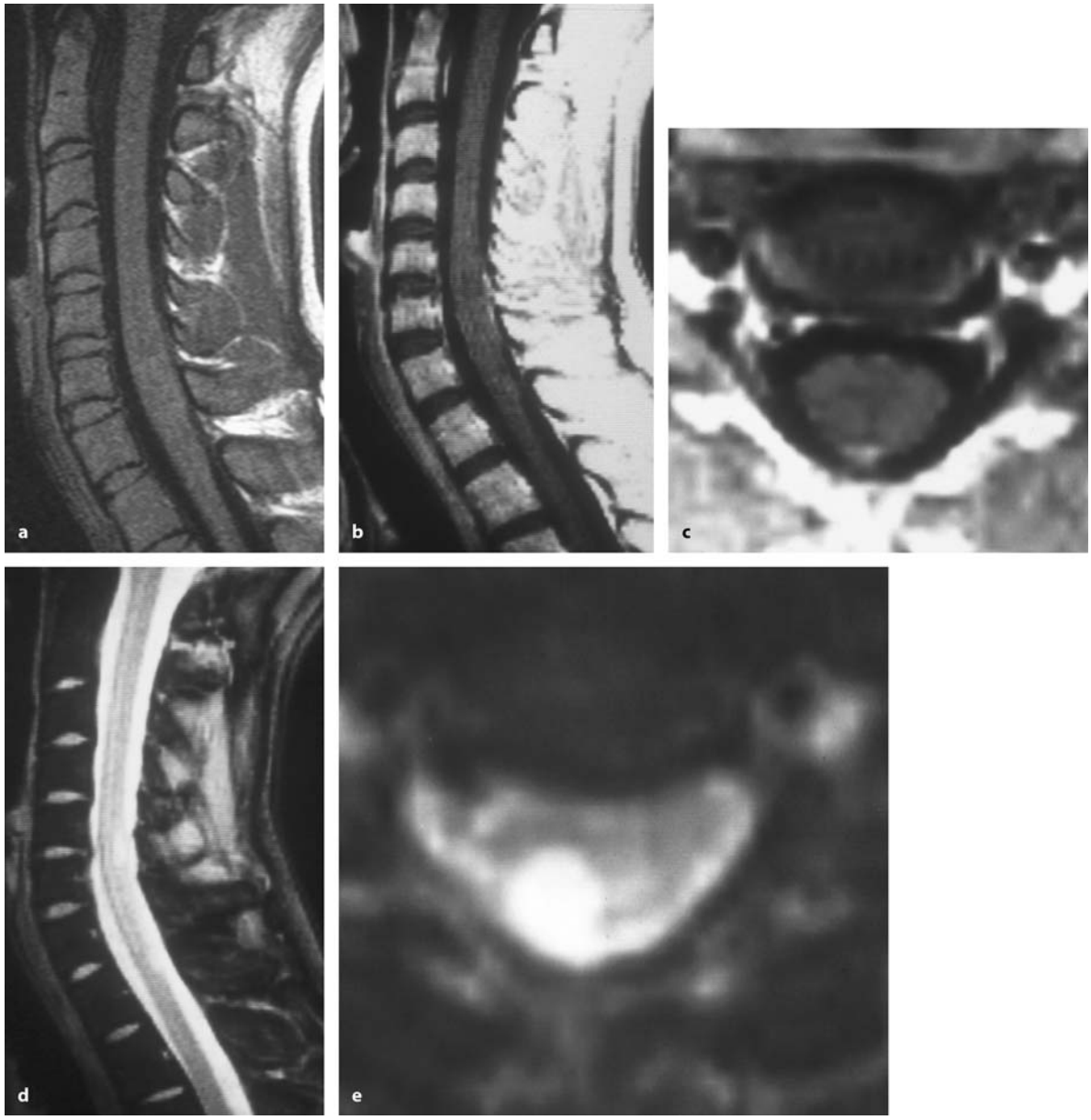

Fig. 3.16. T1-weighted sagittal MRI scans without (**a**) and with contrast enhancement (**b**), of a ganglioglioma at C5/6 in a 27-year-old woman. The tumor appears isodense and without contrast enhancement. There is, however, some enhancement on the posterior cord surface related to dilated veins, which can be better appreciated on the axial image (**c**). The T2-weighted sagittal (**d**) and axial (**e**) MRI scans disclose the tumor as a hyperdense lesion in the posterior part of the cord on the right side at C5/6

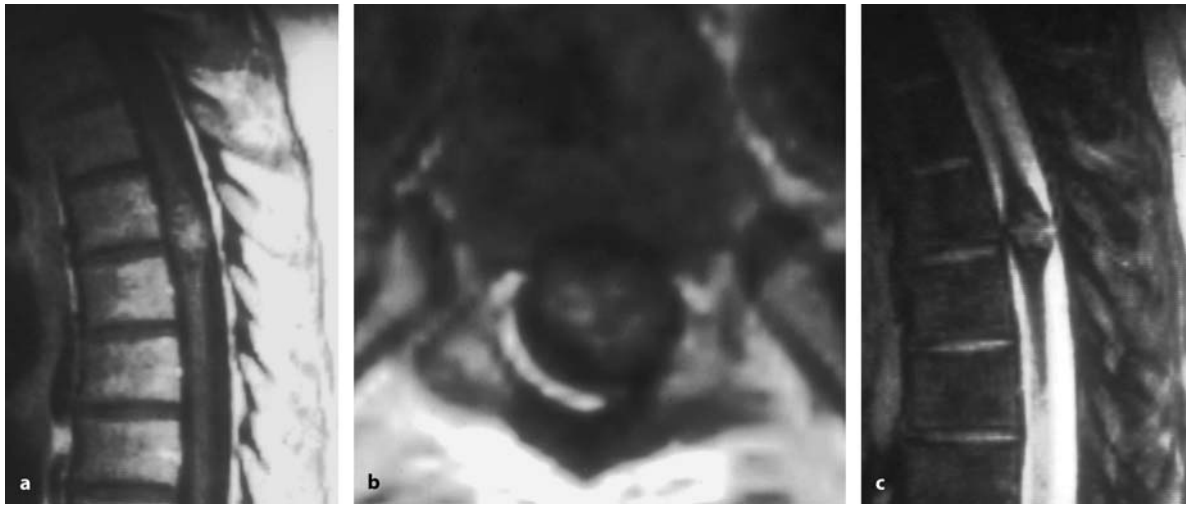

Fig. 3.17. T1-weighted, contrast-enhanced, sagittal (**a**) and axial (**b**) MRI scans of a cavernoma at Th4 in a 57-year-old patient. The patchy contrast enhancement and irregular shape of the tumor as well as the black hemosiderin remnants on T2 (**c**) are typical for this tumor

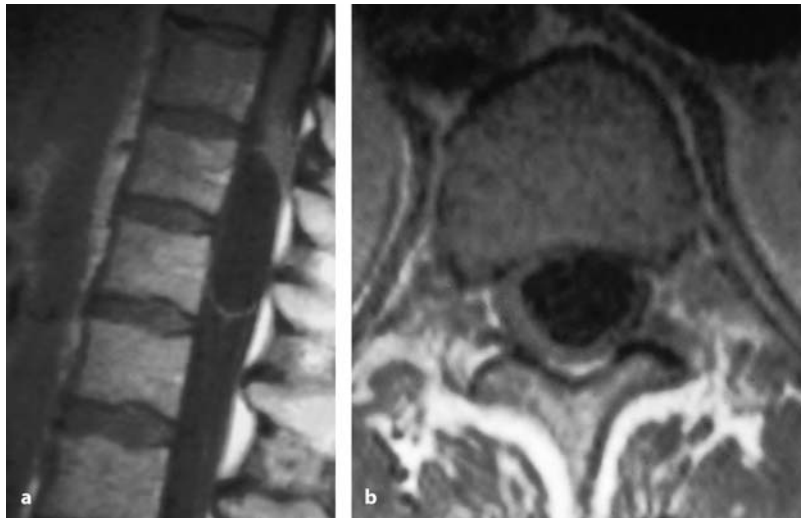

Fig. 3.18. T1-weighted sagittal (**a**) and axial (**b**) MRI scans of an ependymal cyst of the conus in a 45-year-old woman. The cyst is located anteriorly on the left side. Please note the considerable space-occupying effect of this cyst

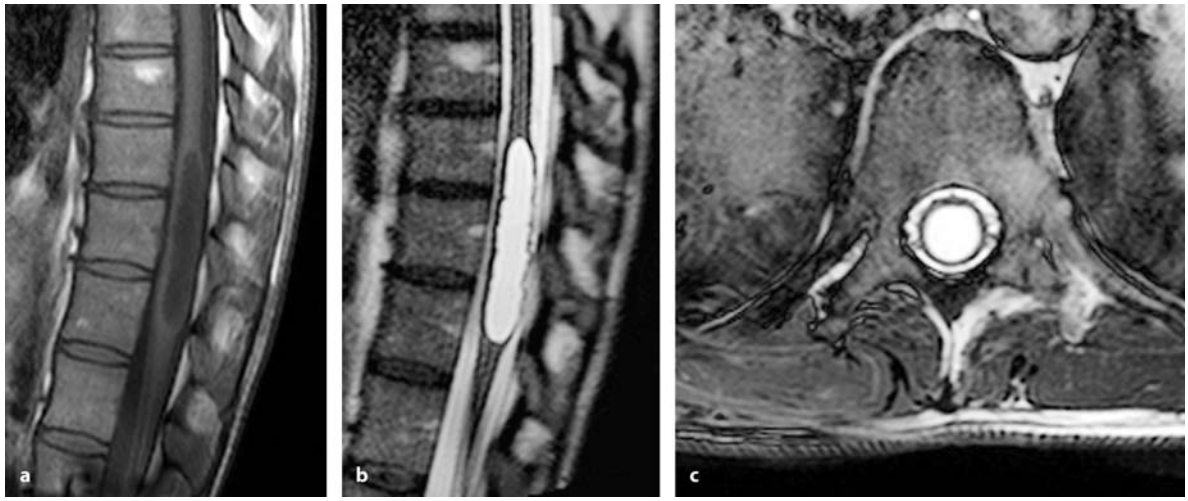

Fig. 3.19. T1- (**a**) and T2-weighted (**b**) MRI scans of an ependymal cyst at Th10–Th12 in a 42-year-old woman with an 18-month history of pain in her right leg. The cyst is in a central position, as apparent on the axial T2-weighted image (**c**). The cyst causes marked expansion of the cord and appears like a regular, symmetric cyst with sharp demarcation toward the spinal cord. There are no septations inside the cyst

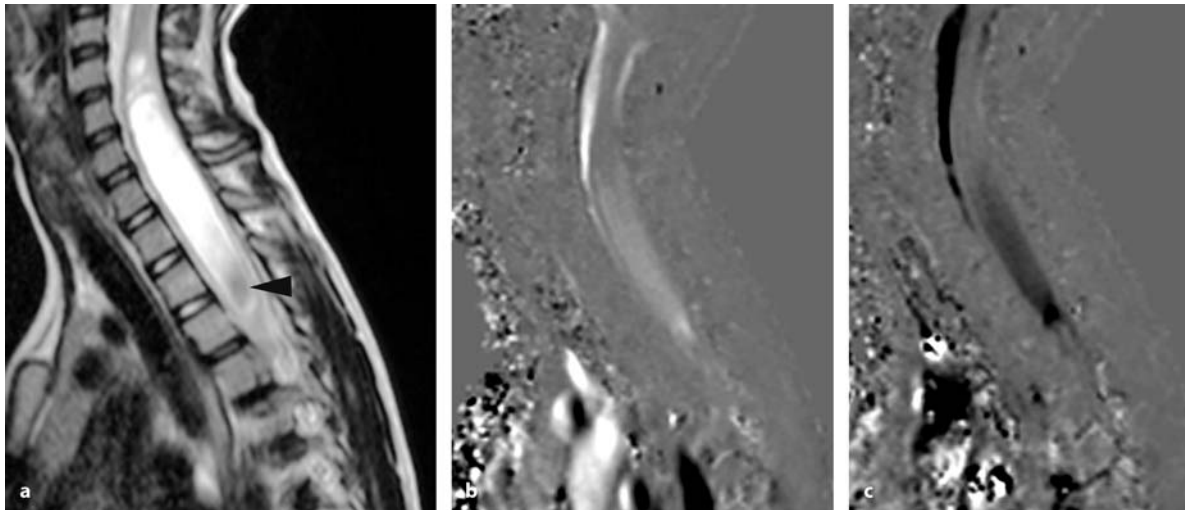

Fig. 3.20. (**a**) T2-weighted sagittal MRI scan of a cervicothoracic syrinx with flow void signals inside the cyst (*arrowhead*). The cardiac gated cine MRI scans demonstrate flow signals within the syrinx in systole (**b**) and diastole (**c**)

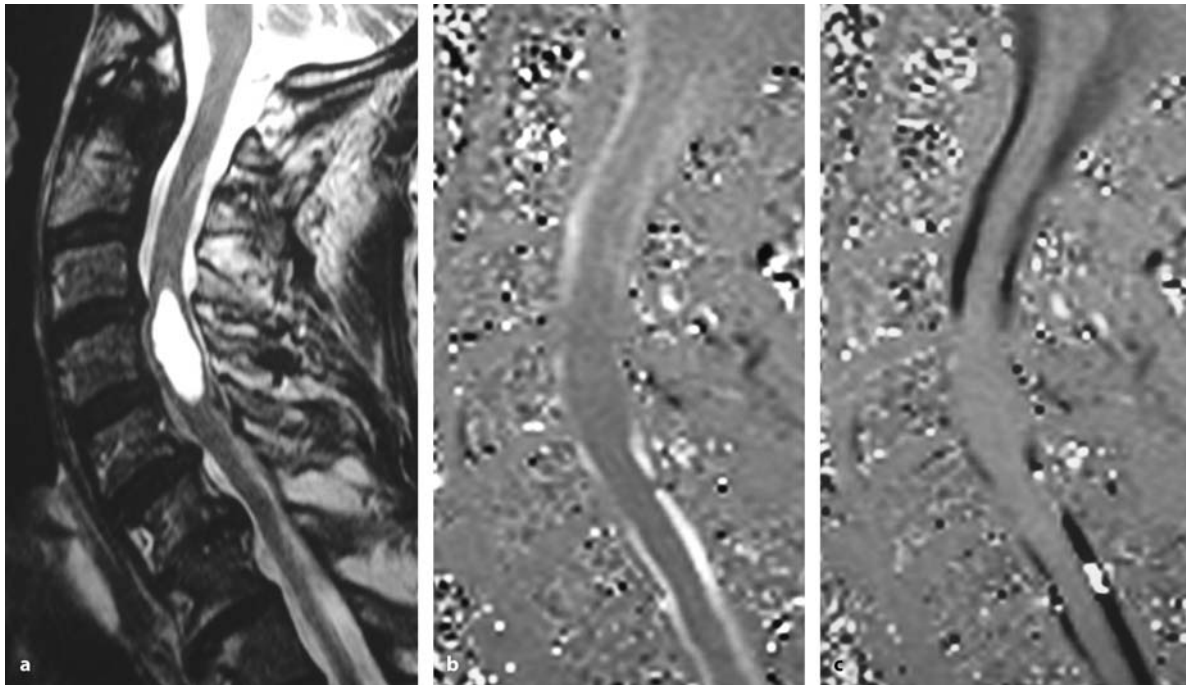

Fig. 3.21 (**a**) T2-weighted sagittal MRI scan of an ependymal cyst at C4–C5 in a 62-year-old woman. The cardiac gated cine MRI scans display no flow signals within the cyst in systole (**b**) or diastole (**c**)

Fig. 3.22. This T2-weighted sagittal MRI scan shows a syrinx at C4–Th3 caused by an arachnopathy at Th3. The syrinx expands in an upward direction away from the area of CSF flow obstruction. This causes an asymmetric shape of the syrinx: its diameter is largest close to the arachnopathy at Th3 (*arrowhead*) and gradually tapers off toward C4

Fig. 3.23. T1-weighted sagittal MRI scan (without contrast) of a predominantly intramedullary dermoid cyst at L1–L2 in a 42-year-old woman. The hyperdense signal of the cyst wall and part of the cyst contents represent fatty components

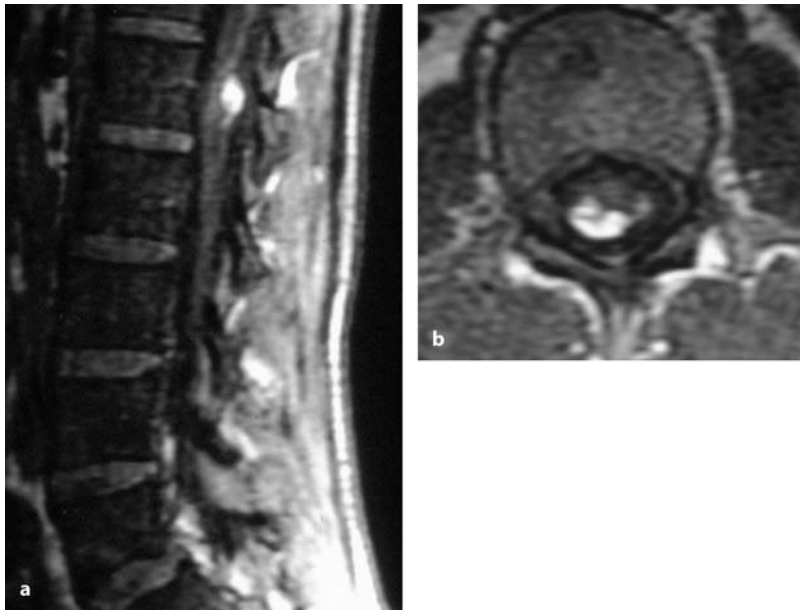

Fig. 3.24. Sagittal (**a**) and axial (**b**) T1-weighted images (without contrast) of an intramedullary lipoma at L1 in a 32-year-old patient with an additional tethered cord related to a low conus position. The typical hyperdense signal of the lesion is apparent

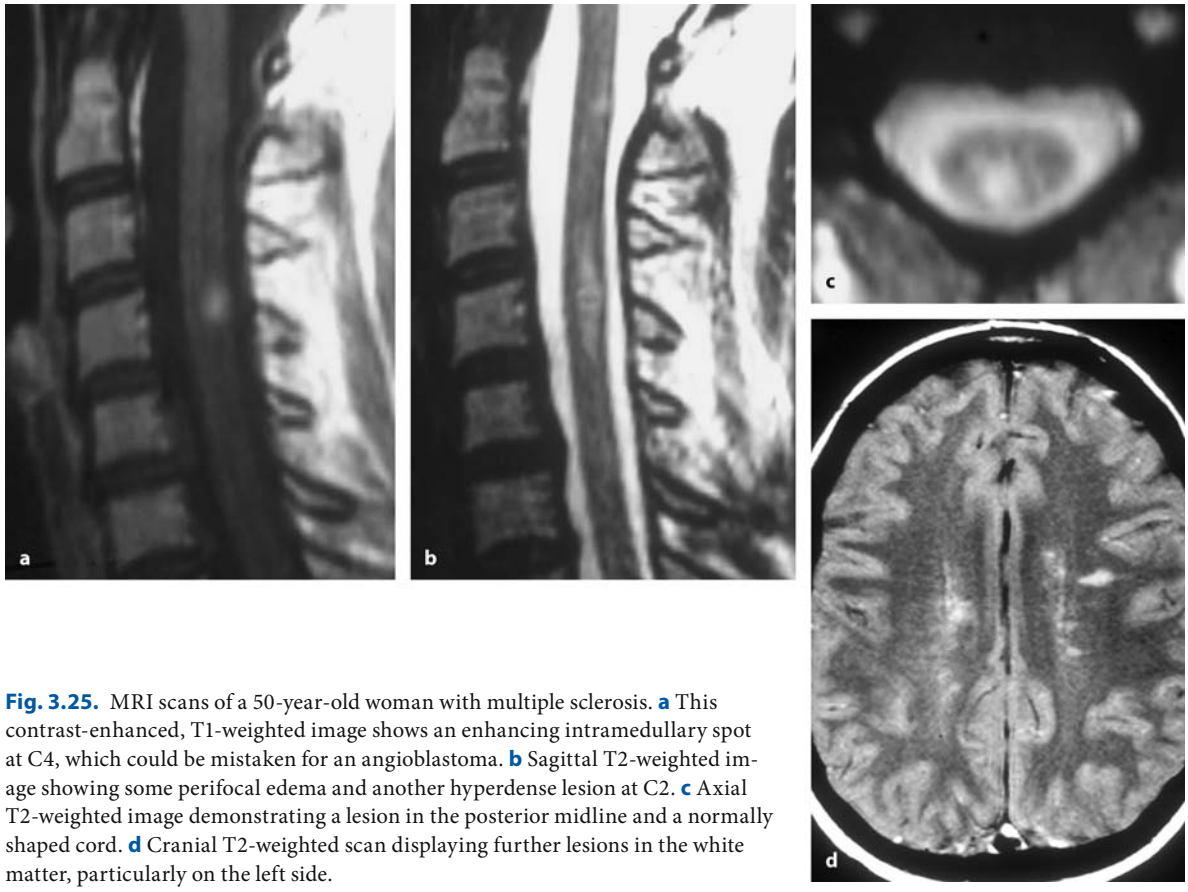

Fig. 3.25. MRI scans of a 50-year-old woman with multiple sclerosis. **a** This contrast-enhanced, T1-weighted image shows an enhancing intramedullary spot at C4, which could be mistaken for an angioblastoma. **b** Sagittal T2-weighted image showing some perifocal edema and another hyperdense lesion at C2. **c** Axial T2-weighted image demonstrating a lesion in the posterior midline and a normally shaped cord. **d** Cranial T2-weighted scan displaying further lesions in the white matter, particularly on the left side.

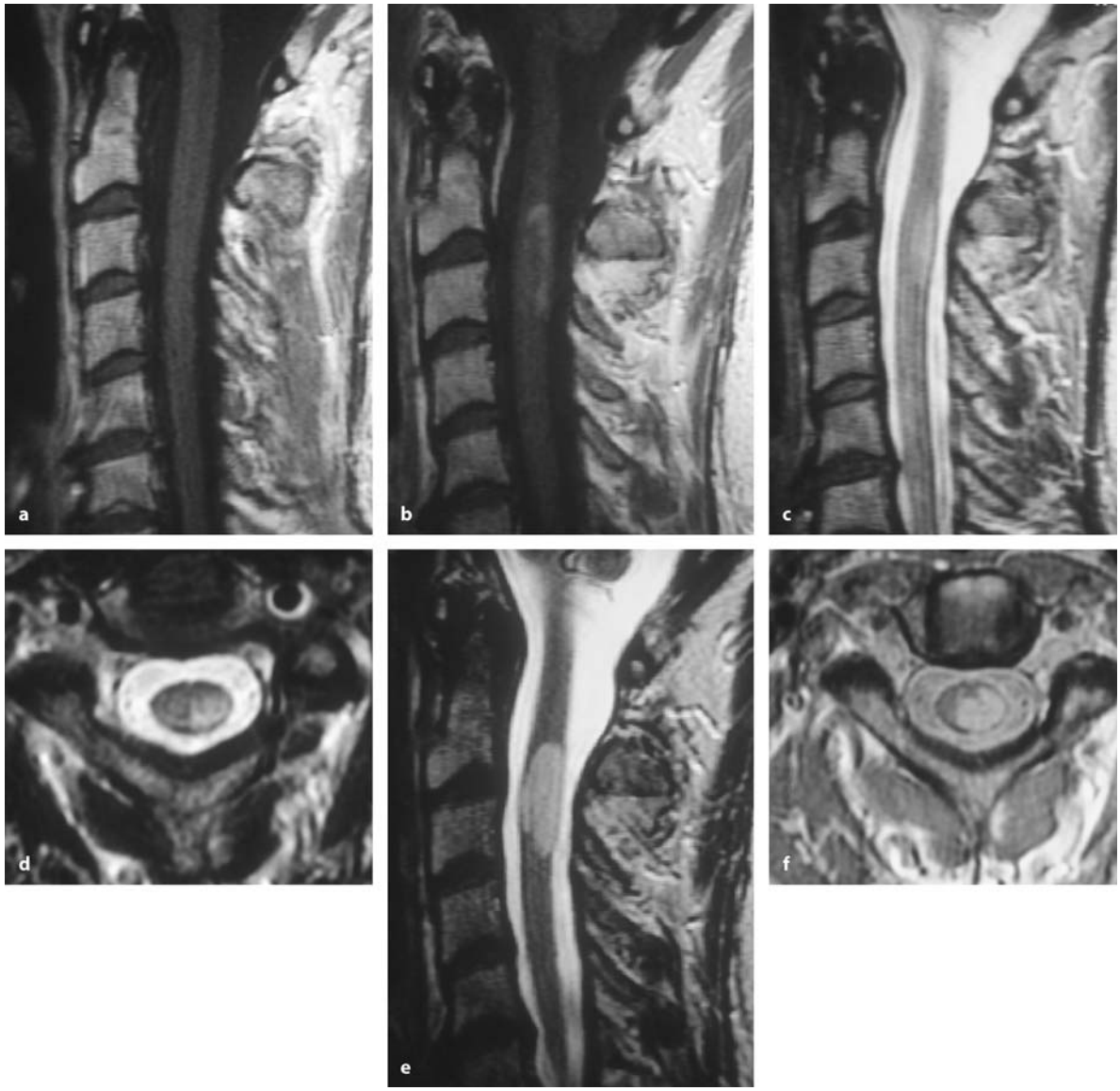

Fig. 3.26. Signal characteristics of inflammatory lesions may change with time. These T1-weighted sagittal MRI scans without (**a**) and with contrast (**b**), show an inflammatory lesion at C2–C3. The lesion does not cause a space-occupying effect. Without contrast, the cord looks absolutely normal. After contrast application, there is some enhancement surrounding the lesion. The sagittal (**c**) and axial (**d**) T2-weighted images present an ill-defined, hyperdense lesion in the left side of the cord. On follow up after 12 weeks, the lesion appears larger and better demarcated on the sagittal (**e**) and axial (**f**) T2-weighted image, but there is still no space-occupying effect

The differential diagnosis to inflammatory and demyelinating diseases may be difficult, especially with lesions that take up no or little contrast. If an intramedullary lesion is suspected to be a tumor, the following questions should be asked:

1. Is the lesion space occupying?
2. Does the lesion display different signal characteristics with time?
3. Does the pathology affect different parts of the spinal cord with time?

As a general rule, inflammatory and demyelinating lesions almost never displace cord tissue at all, or to an extent that would explain the clinical symptoms (Figs. 3.25–3.29) [173, 190]. Multiple spinal cord lesions may be detected in demyelinating (Fig. 3.25) and

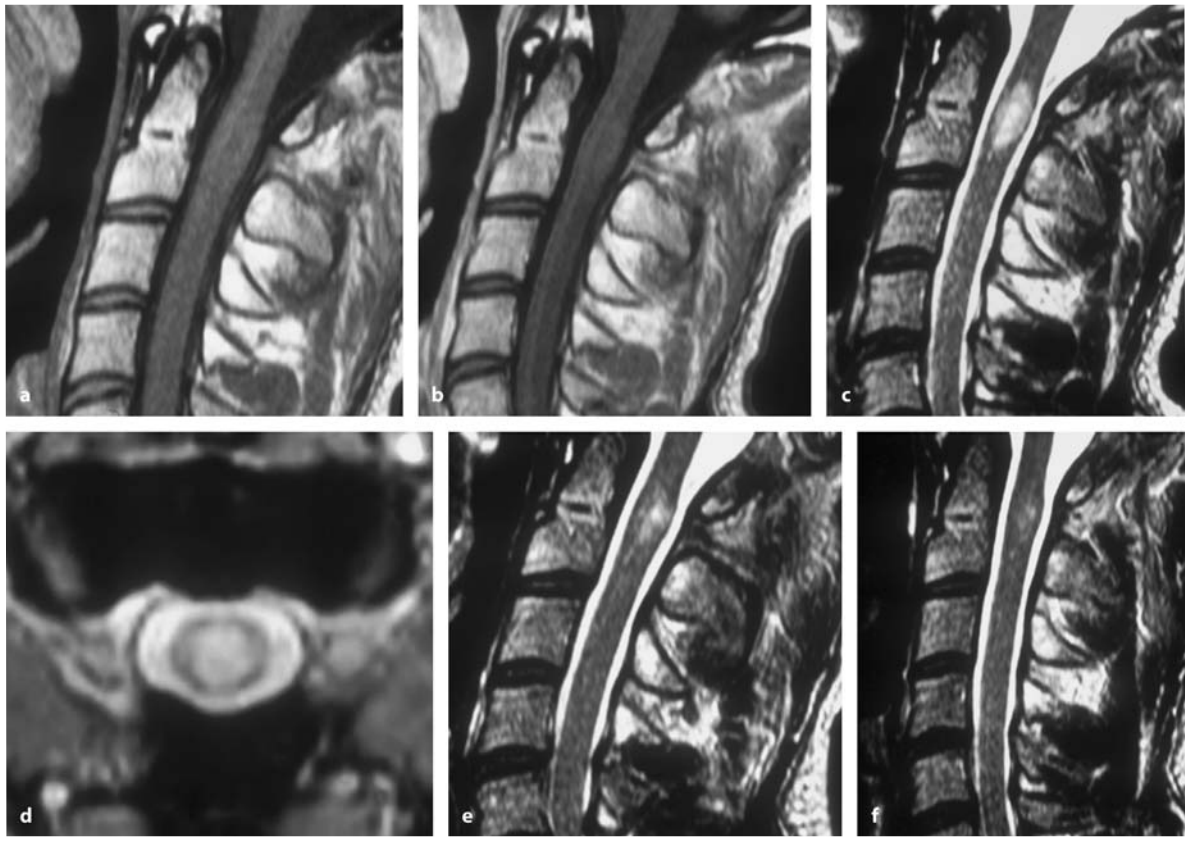

Fig. 3.27. T1-weighted sagittal MRI scans without (**a**) and with contrast (**b**), of a 35-year-old patient with an inflammatory lesion at C2 and fluctuating paresthesias in his arms and legs. There is no contrast enhancement at all on T1, but a discrete enlargement of the cord is seen at this level. The sagittal (**c**) and axial (**d**) T2-weighted images demonstrate an ill-defined, hyperdense, and centrally located lesion. On follow up after 6 months (**e**) and 1 year (**f**), the lesion gradually regressed

inflammatory diseases. If in doubt, the safest way to arrive at the most likely diagnosis is to repeat the MRI after a couple of weeks. Inflammatory and demyelinating reactions vary in intensity with time, leading to different radiological appearances within a few weeks or months (Figs. 3.26 and 3.27). Tumors never change their MRI appearance in such a short time. Contrast enhancement, on the other hand, does not prove that the lesion is a tumor (Figs. 3.25, 3.26, and 3.28) [302, 332]. Furthermore, in most demyelinating diseases such as multiple sclerosis, additional areas of pathology will often be detected in other parts of the central nervous system so that additional MRI scans of the brain can be helpful in such cases (Fig. 3.25) [196]. However, multiple sclerosis can present with an isolated spinal lesion. Another pathology to be considered is subacute necrotizing myelopathy with spinal cord edema and rim-like contrast enhancement (Fig. 3.29). With time, spinal cord atrophy develops [302].

Lee et al. [190] presented a series of nine patients with nonneoplastic histologies who had been operated for suspected intramedullary tumors. Four patients had demyelinating lesions, two had sarcoidosis, two had amyloid angiopathy, and one patient an inflammatory pseudotumor. The only feature common to all of these lesions was a lack of spinal cord expansion.

In some instances after postoperative radiotherapy, it may be very difficult to differentiate postradiation myelopathy from a recurrent tumor on MRI [261, 302, 351]. Again, the presence of a space-occupying lesion and repeated scans may solve the diagnostic dilemma.

With increasing experience, surgeon and neuroradiologist may be expecting a certain pathology and may find their preoperative assumptions to be correct with increasing frequency. However, one should not base operative decisions on MRI morphology. Whether the tumor is resectable or not has to be determined

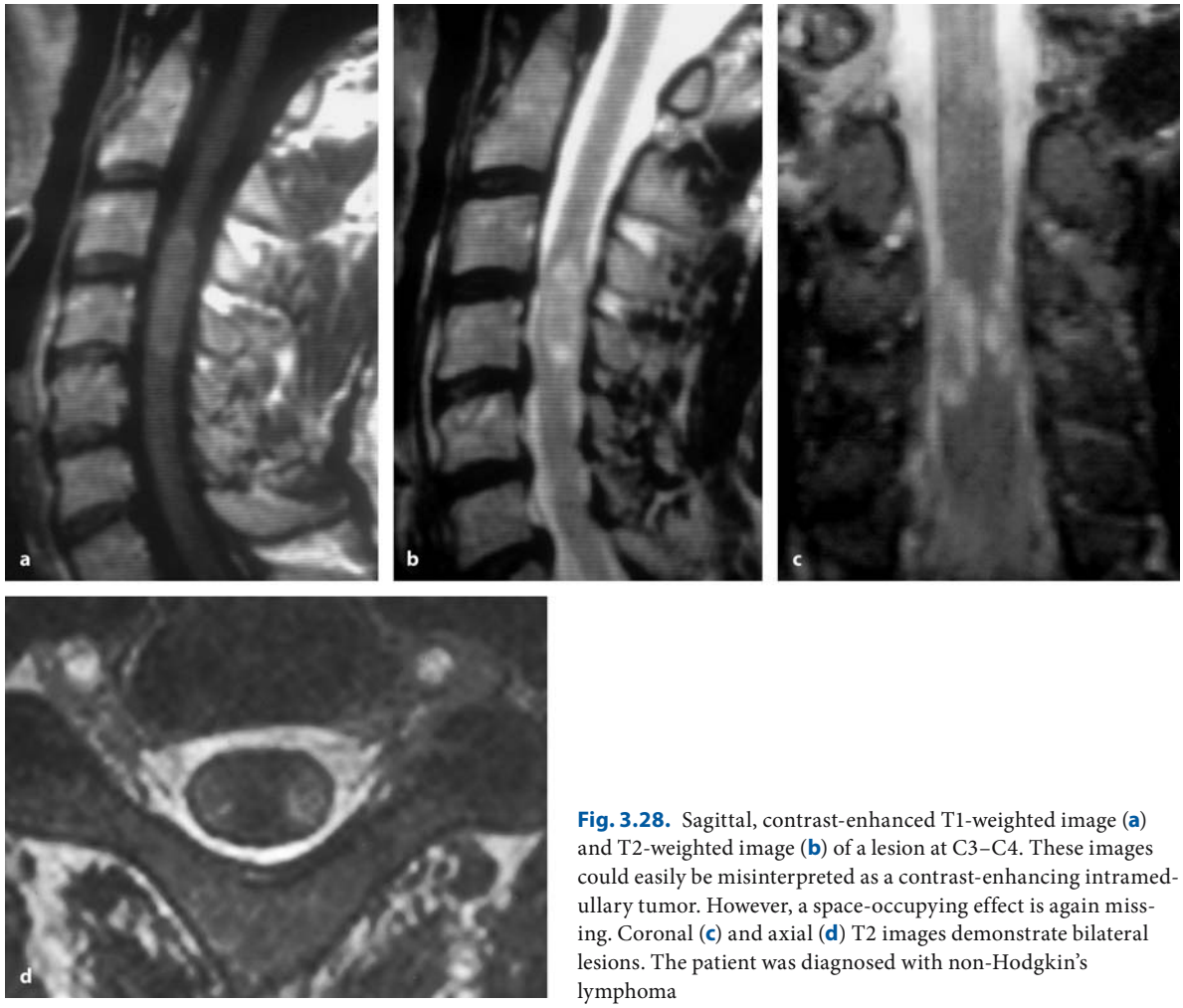

Fig. 3.28. Sagittal, contrast-enhanced T1-weighted image (**a**) and T2-weighted image (**b**) of a lesion at C3–C4. These images could easily be misinterpreted as a contrast-enhancing intramedullary tumor. However, a space-occupying effect is again missing. Coronal (**c**) and axial (**d**) T2 images demonstrate bilateral lesions. The patient was diagnosed with non-Hodgkin's lymphoma

in the operative theater. The surgeon should begin with the intention to remove the tumor completely [57] rather than expecting that not much can be done anyway because the tumor looks like an infiltrating glioma on MRI, for instance. Similarly, radical tumor removal should not be forced without a clear-cut demarcation just because the MRI suggests a clearly demarcated and, thus, resectable tumor.

Finally, one should remember the rare association of hydrocephalus with an intramedullary tumor [266, 268, 278]. If the clinical examination and patient history suggest the possibility of hydrocephalus, a CT or MRI of the head should be performed. In patients with malignant astrocytomas, the presence of hydrocephalus is an ominous sign as it indicates a fast progressing and possibly disseminating tumor disease [278]. We observed hydrocephalus in one patient at the time of recurrent growth of his thoracic anaplastic astrocytoma.

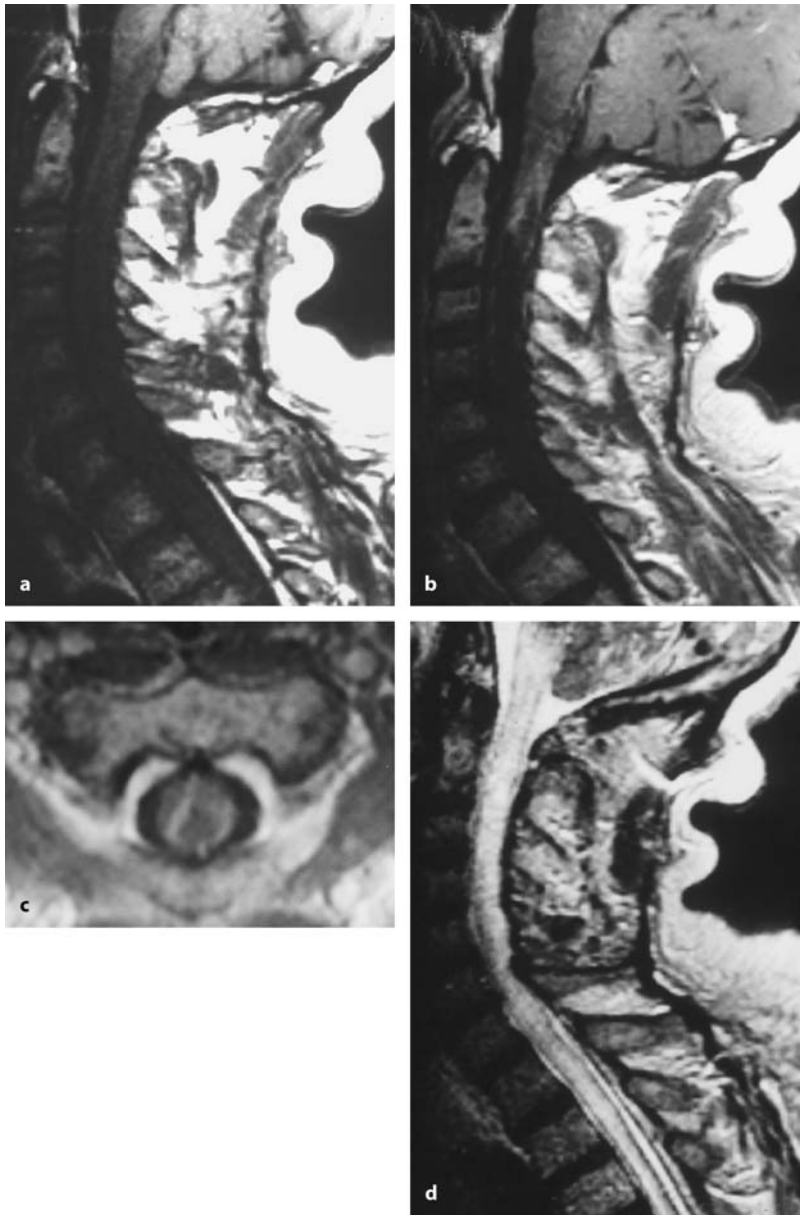

Fig. 3.29. T1-weighted sagittal MRI scans without (**a**) and with contrast (**b**), of a 60-year-old patient with a necrotizing myelopathy (Foix-Alajouanine syndrome) of the upper cervical cord. The lesion is hypodense due to edema formation with perifocal contrast enhancement and centrally located (**c**). **d** The T2-weighted image displays marked edema extending into the thoracic cord

3.3 Surgery

Before describing the surgical techniques and strategies for removal of intramedullary tumors, we would like to comment on the perioperative use of corticosteroids. Several colleagues give high-dose corticosteroids before, during, and 24 h after surgery for an intramedullary tumor [130, 263]. In 1990 the results of the Second National Acute Spinal Cord Injury Study (NASCIS II) were published, which showed that the administration of a high-dose regimen of methylprednisolone could improve neurological recovery in spinal-cord-injured patients [25]. As several experimental studies demonstrated that steroids work even better if they are administered before injury, patients undergoing intramedullary surgery should benefit from such a regimen. However, the NASCIS II and III studies have also been heavily challenged [51]. This leaves a considerable amount of controversy to be resolved. At the moment, no general recommendation can be given until further studies have established a benefit. We have not routinely administered corticosteroids for spinal cord surgery.

3.3.1 Exposure

The exposure of an intramedullary tumor is done exclusively from the posterior position. Except for cervical tumors, we operate with the patient in the prone position. In the prone position, care should be taken to support the abdomen and thorax sufficiently to facilitate central venous flow in order to limit epidural venous bleeding and to prevent pressure-related injuries during a procedure that will often take several hours. For cervical tumors down to a level of about Th1/2 we prefer the semisitting position. Provided an anesthesiological team experienced with this position is at hand, it does offer considerable advantages. In particular, a clean surgical field is easy to maintain at all times by simple irrigation. This minimizes the necessity for additional suction next to or within the spinal cord. During positioning we monitor sensory evoked potentials (SEPs) to avoid undue pressure on the cord during this maneuver. Especially for the cervical area, the spinal canal may be completely filled with cord and tumor, so that additional osteophytic changes in elderly patients or the physiological mobility of the spine in juvenile patients have to be considered.

Once the positioning is completed we determine the correct spinal level under fluoroscopic control. We perform a midline incision down to the fascia. The fascia is incised next to the spinous processes on both sides. Small arterial bleeders are usually found directly on the tips of the spinous processes where the fascia is attached, and can be easily coagulated. Next, we detach the muscles from the spinous processes and vertebral arches with the periosteum. We recommend use of a blunt instrument like a raspatorium to put the muscles fibers under lateral tension. In this way muscular attachments can be identified and transected. Starting at one end of the exposed vertebral arches, we proceed in this manner and put cotton tamponades next to the now-exposed bony elements. In this way, blood loss should be minimal.

Once all vertebral arches are exposed to about the intervertebral joints we check once more the correct spinal level with fluoroscopy. Before starting to remove any bone we establish complete hemostasis. For intramedullary tumors, we perform a small medial laminotomy, which is about 10–15 mm wide. For this purpose we cut the vertebral arches with a small craniotome and remove all laminae including the interspinous and yellow ligaments together in one block (Fig. 3.30). Some authors prefer to use a small diamond drill. To avoid shrinkage of the interspinous ligaments we store laminae and ligaments under tension during the remainder of the procedure and keep them moist with isotonic saline solution (Fig. 3.31). In this fashion, we ensure a good fit of the laminae for reinsertion at the end of the operation.

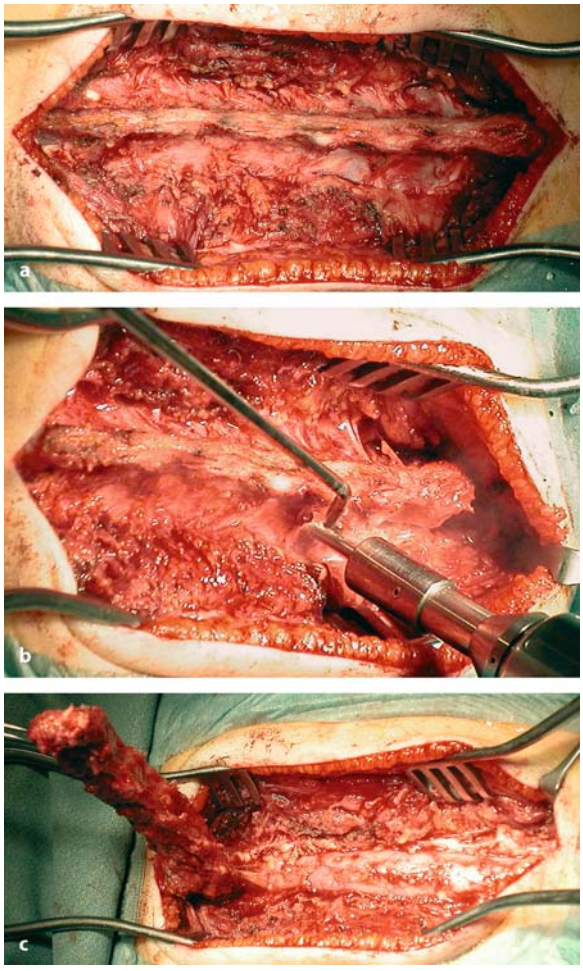

Fig. 3.30. a Intraoperative view on the thoracic spine of a 3-year-old child with an extensive intramedullary tumor. The muscles have been detached laterally from vertebral arches to about the level of intervertebral joints. **b** A small craniotome is used to cut laminae and yellow ligaments together starting at the lowest spinal level of the exposure. To insert the craniotome correctly underneath the ligament, a small interlaminar fenestration should be performed at the entry level. The craniotome is angled laterally and the cutting is performed right along the spinous processes on either side. **c** With transection of the interspinous ligaments, the laminotomy block can be elevated in one piece

Conventional laminectomies should be avoided whenever possible. If a laminectomy is performed, we use a flat-footed Kerrison punch to avoid pressure on the spinal cord. We recommend leaving the yellow ligament intact during bone removal. In this way, injury to the epidural veins can be easily avoided. Once

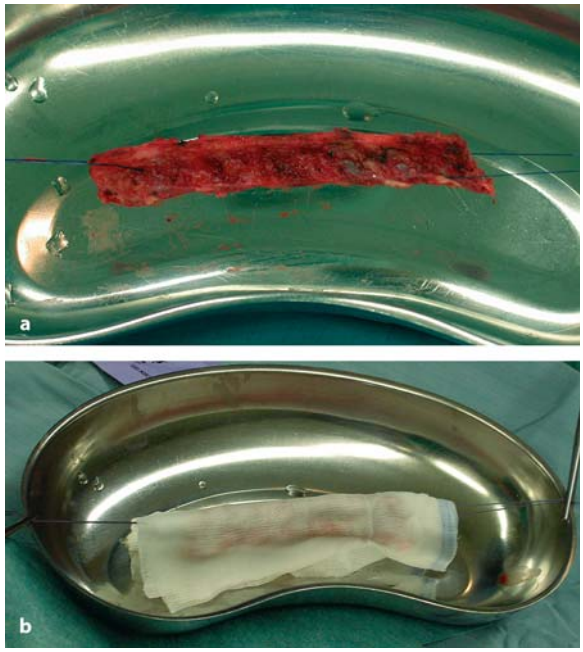

Fig. 3.31. a The laminotomy block is put under tension and is kept moisturized during tumor removal to prevent shrinkage of interlaminar ligaments (**b**). This ensures a good fit at the time of reinsertion

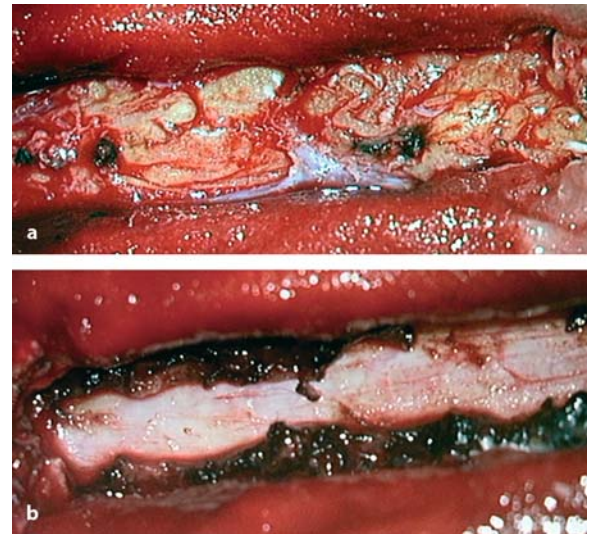

Fig. 3.32. a This close-up view shows the epidural fat containing the epidural venous plexus covering the dura after removal of the laminae. With large tumors, the epidural fat may be completely absent, only to reappear above and below the tumor, indicating the major tumor extension. The cutting of the lamina and the yellow ligament avoids pulling on epidural fat and its veins and, thus, limits blood loss. **b** With coagulation and shrinkage of the epidural fat medially, the dura becomes exposed in the midline. This dura exposure is sufficient for removal of an intramedullary tumor

the vertebral arches are removed, the yellow ligament is resected sharply. Care should be taken not to pull on the epidural fat during this maneuver as profuse bleeding from epidural veins may result, especially in the thoracic spine.

After removal of the yellow ligament or the laminotomy block, the epidural fat may be cut longitudinally in the midline and then mobilized laterally by shrinking it with bipolar coagulation. In this way, blood loss should be minimal during the exposure (Fig. 3.32). Quite often, however, epidural fat and veins are compressed and displaced laterally by the intramedullary tumor and veins will only start bleeding after the tumor is removed.

An alternative technique has been described by Yasargil et al. [350]. They used a modified multilevel hemilaminectomy to approach and remove intramedullary angioblastomas. The advantage of this approach is the preservation of posterior ligaments in the midline and the laminae on the contralateral side. As angioblastomas are generally located in a mediolateral position within the spinal cord, this approach is sufficient for a laterally located tumor. In recent years, selected cases with small lateral located tumors were removed, even via interlaminar fenestrations, to preserve the integrity of the laminae.

From this point on, surgery is performed with the aid of the operative microscope. The dura is opened in the midline. Dural retention sutures are used to keep the dura open and under tension. The arachnoid membrane should be left intact during opening of the dura to avoid injury to the spinal cord and its vessels. A more detailed description on the microsurgical anatomy of the subarachnoid space is given in the sections on anatomy and extramedullary tumors. Once the dura is opened entirely, the arachnoid membrane is opened with microscissors. Arachnoid septations and adhesions should be dissected sharply to avoid tearing of small blood vessels and tension on the spinal cord.

3.3.2 Tumor Removal

Once the arachnoid membrane is opened with microscissors, the cord is inspected for a suitable area for opening. In most instances, the posterior aspect of the cord will not present any signs of the underlying

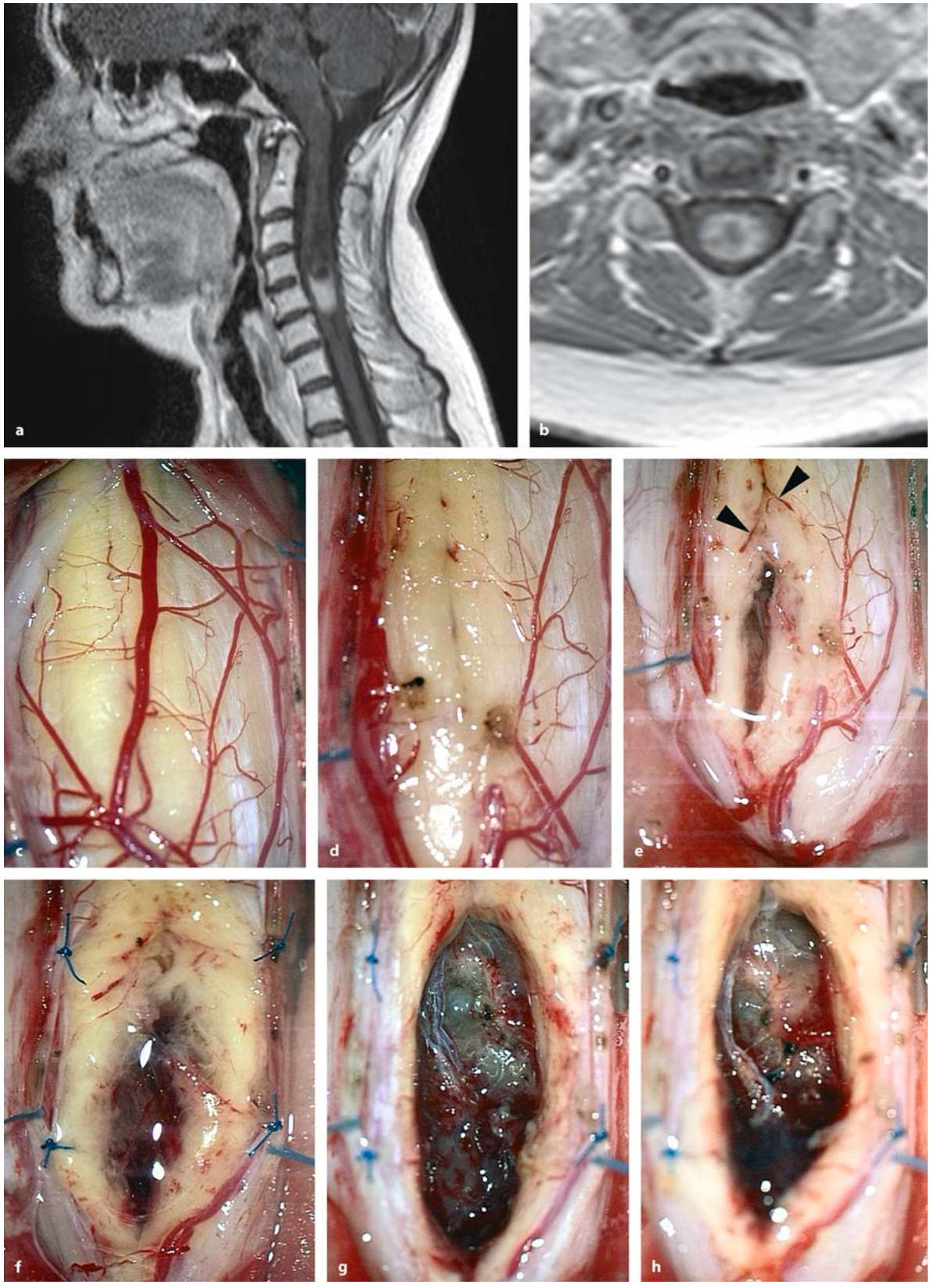

Fig. 3.33. (*Continuation see next page*)

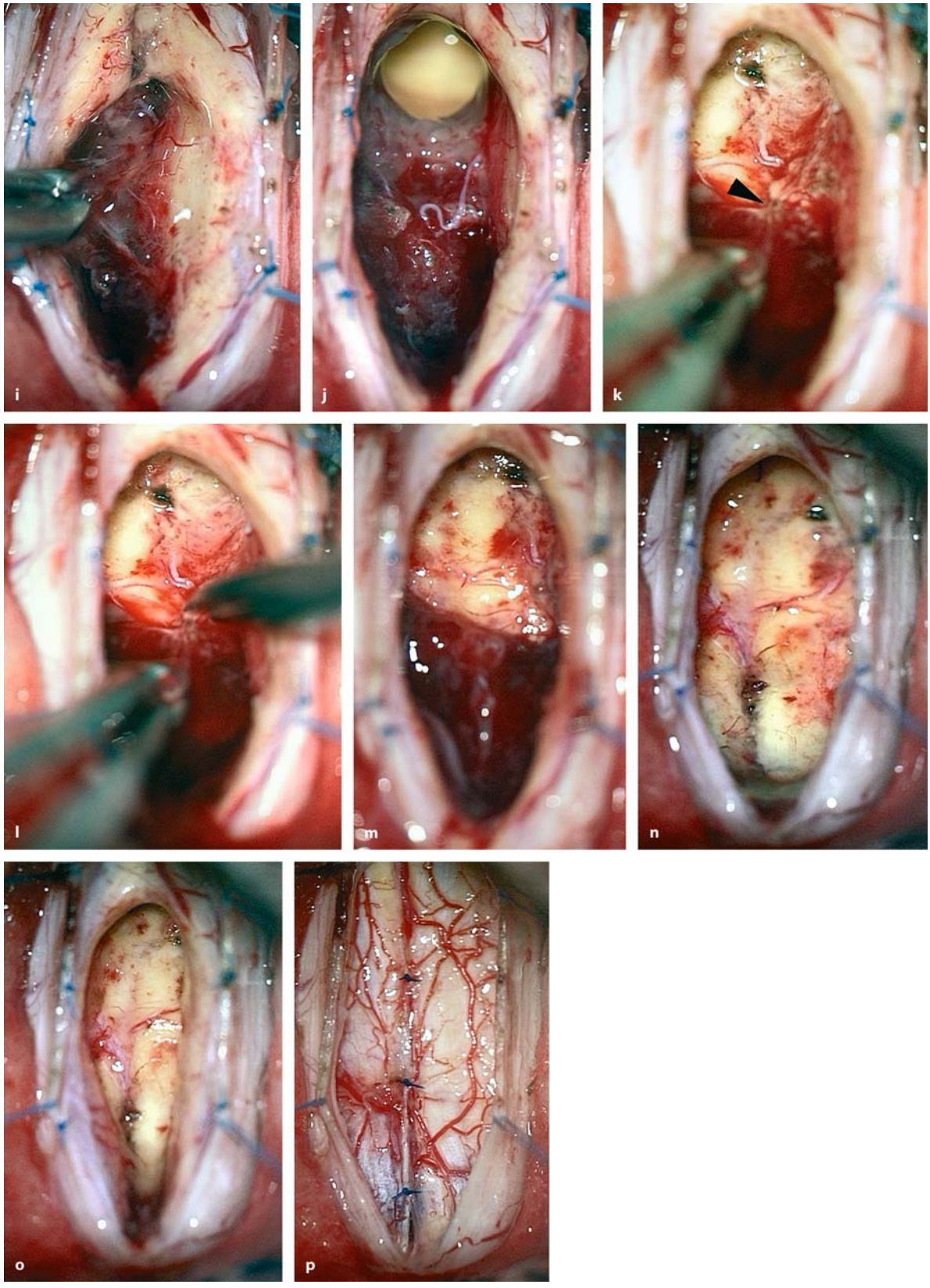

Fig. 3.33. (*Continuation see next page*)

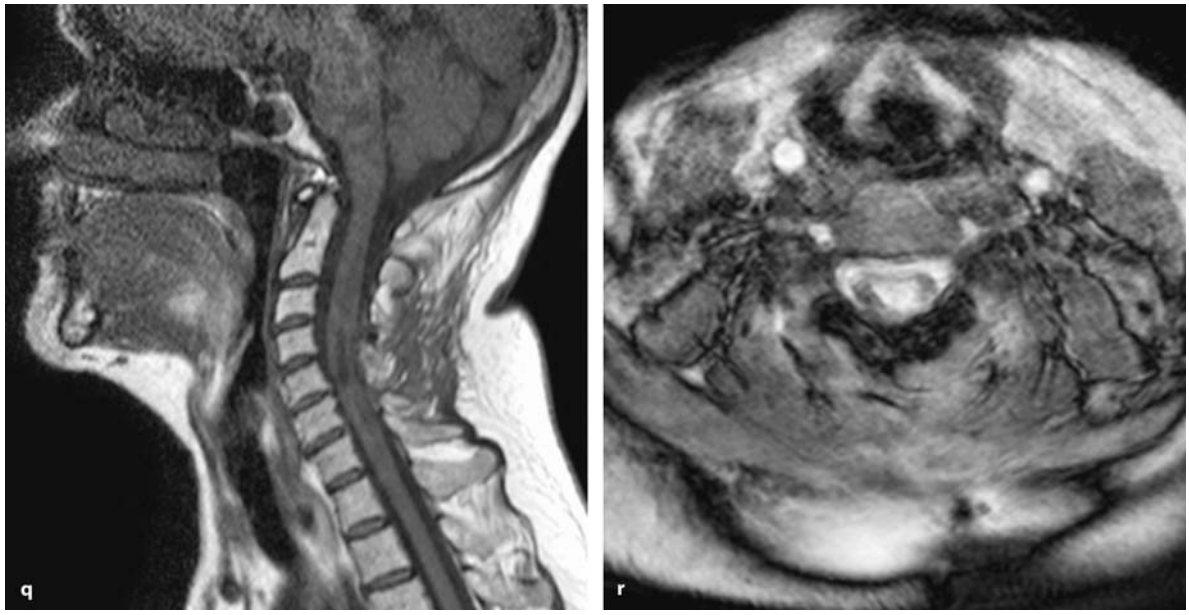

Fig. 3.33. (*Continued*) T1-weighted, contrast-enhanced, sagittal (**a**) and axial (**b**) MRI images of an ependymoma at C5 in a 64-year-old woman with a 2-month history of sensory disturbances in both arms. A small syrinx accompanies the tumor cranially. **c** Appearance of the spinal cord after opening of the dura in the semisitting position. The cord appears swollen but otherwise normal on inspection. Small surface vessels enter the cord in the midline. **d** After cutting the pia mater, the cord is carefully opened in the midline. **e** The posterior surface of the tumor is reached. In the upper half of the picture, the midline vessels converging from both sides toward the median raphé of the spinal cord can be appreciated (*arrowheads*). **f** Pia retention sutures are applied. **g** The entire tumor is exposed. **h** Debulking of the tumor has started with small forceps. **i** Gently pulling on the remainder of the tumor allows to bluntly dissect the surrounding cord along a clearly defined dissection plane. **j** Entering the syrinx, the upper pole of the tumor is reached. Now the tumor can be dissected out of the cord anteriorly. Small feeding vessels in the midline (*arrowhead*) can be identified (**k**), coagulated and cut (**l**). **m** This view shows the appearance after resection of the upper half of the tumor. After complete resection (**n**), the pia sutures are cut (**o**) and the pia is closed with 8-0 sutures (**p**). The postoperative MRI scans in T1 (**q**) and T2 (**r**) reveal a complete resection with collapse of the associated syrinx and the resection cavity. The patient is without any additional neurological deficits in unchanged condition 1 year postoperatively

tumor – unless the neoplasm has reached the pia mater or even grown exophytically. Sometimes superficial discoloration as a result of tumor hemorrhages may indicate the underlying pathology. However, especially in patients with an additional syrinx, the extension of the solid intramedullary tumor cannot be determined by inspection of the cord as the cord will appear swollen over a more extensive area. Therefore, we recommend the use of ultrasonography to check that the exposure is adequate and to determine the exact position of the solid tumor before embarking on the myelotomy [83, 164, 200, 203, 272, 275].

Basically, three options exist. In most instances, the myelotomy is done in the midline (Fig. 3.33). If the tumor is located laterally, the dorsal root entry zone may be used. With angioblastomas, arterialized veins and enlarged feeding arteries often indicate the position of the tumor (Fig. 3.34). With tumors reaching the surface or those with exophytic growth, the spinal cord can be entered in that area (Fig. 3.35). Care should be taken to avoid unnecessary coagulation of the posterior surface vessels, as this may cause significant sensory problems. Monitoring of SEPs is particularly helpful during this part of the operation. Even though only a portion of the sensory fibers can be stimulated and a complete picture of sensory functions cannot be obtained [116], SEP monitoring educates the surgeon to proceed in a manner that will not put undue stress on the spinal cord, and the posterior pathways in particular [135]. In addition, monitoring of motor evoked potentials is recommended and extremely helpful during all steps of tumor removal [151–153, 178, 183, 229].

We recommend that the spinal cord be opened over the entire tumor as the first step of dissection [301, 318]. We use a diamond knife or microscissors to cut the pia mater. The remainder of the cord opening should be performed with blunt instruments. We

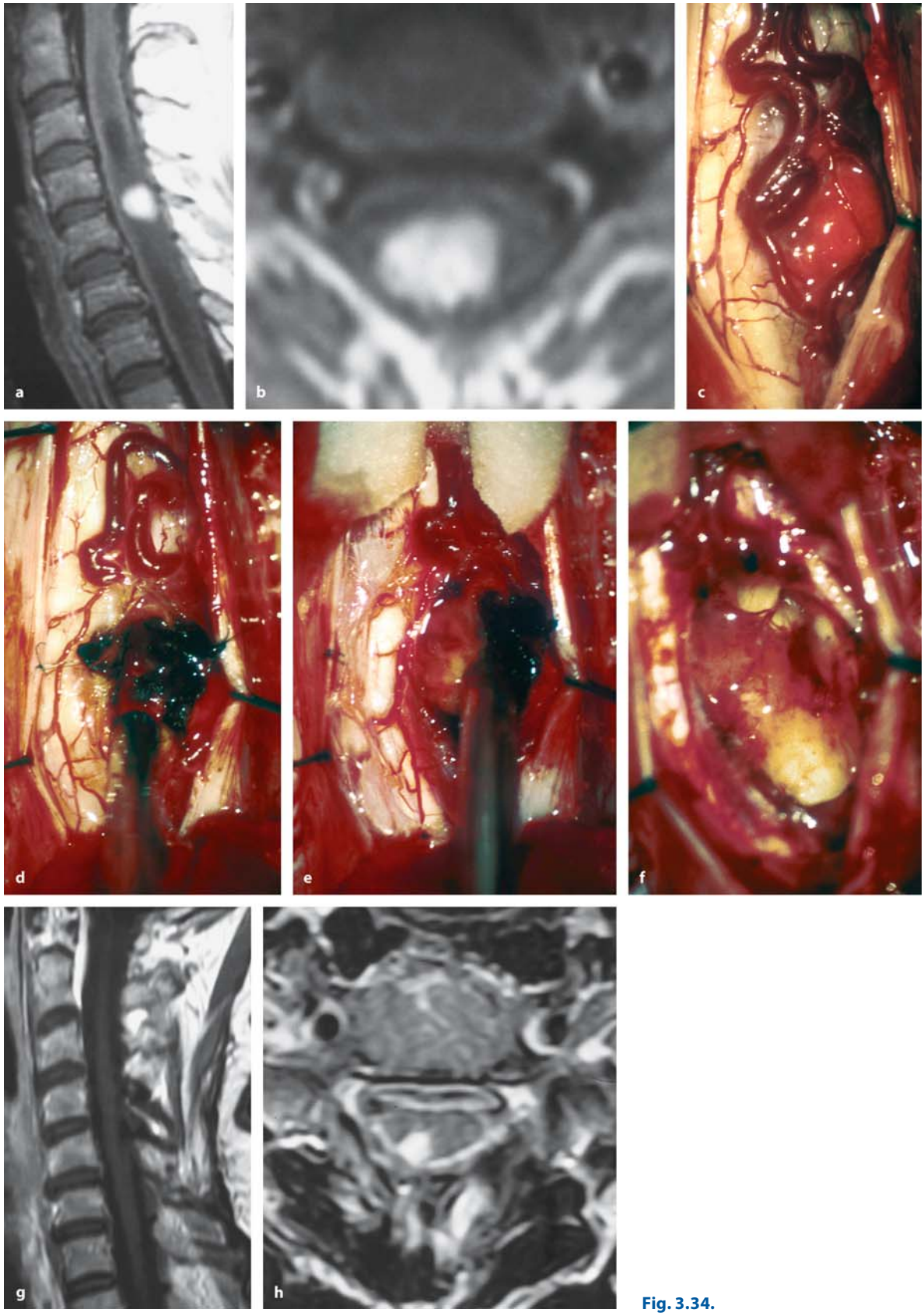

Fig. 3.34.

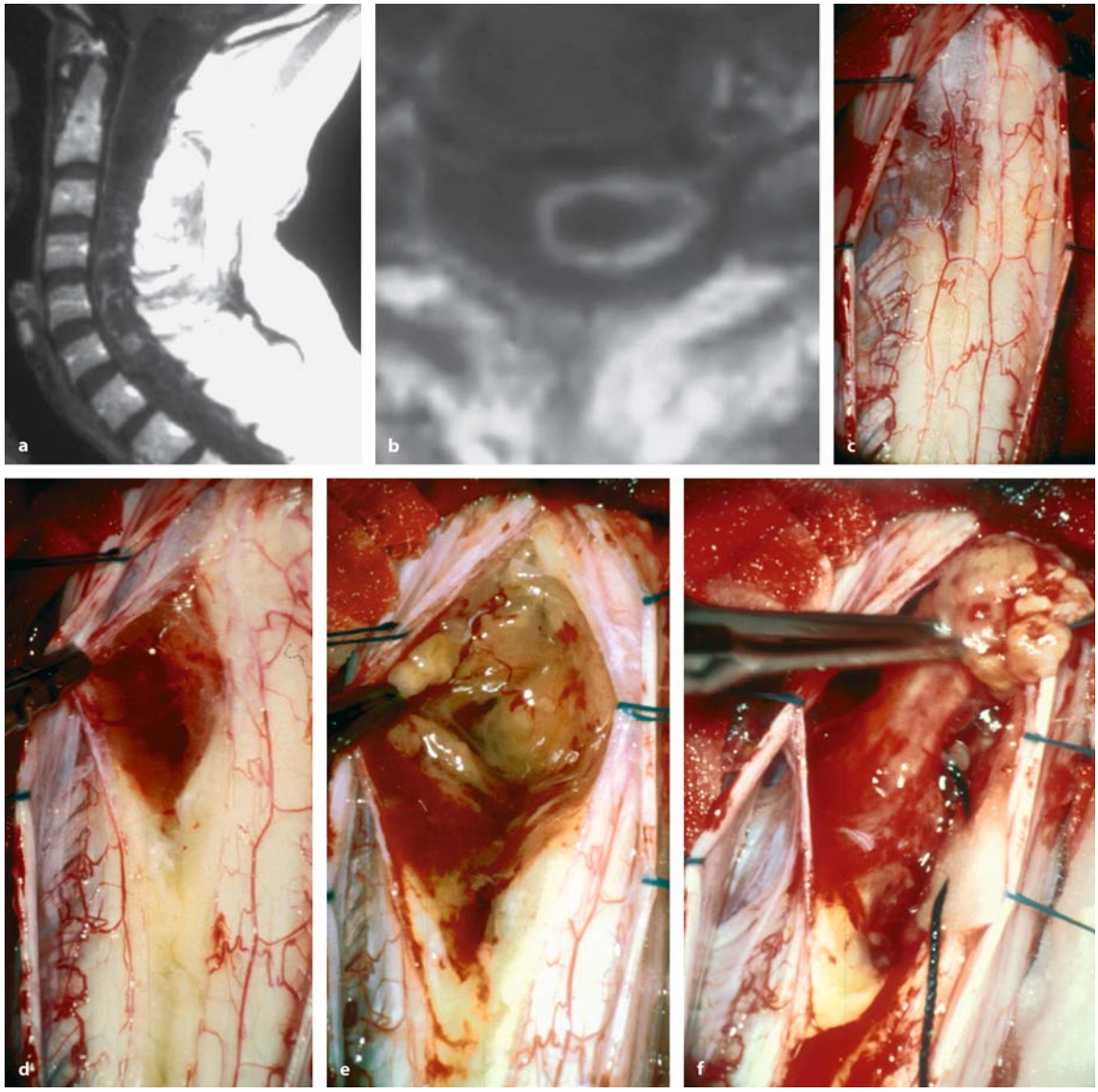

Fig. 3.35. T1-weighted, contrast-enhanced sagittal (**a**) and axial (**b**) MRI images of an intramedullary WHO grade I astrocytoma at C3–C7 in a 37-year-old man with a 9-year history of a progressive tetraparesis. Other institutions advised against surgery, so he had been reluctant to undergo surgery, until he finally presented with a severe tetraparesis and was unable to walk. The tumor appears mostly cystic with a significant syrinx above and below it. **c** The intraoperative view on the spinal cord in the semisitting position indicates, that the tumor has reached the pia mater on the left side and occupies mainly the left side of the cord. **d** The pia mater is opened in the midline and the tumor becomes immediately apparent. **e**, **f** Dissection with tumor forceps allows delivery of the tumor step by step. (*Continuation see next page*)

Fig. 3.34. T1-weighted, contrast-enhanced sagittal (**a**) and axial (**b**) MRI images of an angioblastoma at C5 in a 52-year-old woman with a 4-year history of pain and a slight tetraparesis. There is a marked syrinx above and below the tumor which reaches the posterior cord surface on the right side. **c** The intraoperative view on the spinal cord in the semisitting position shows the characteristic orange color of the tumor surrounded by feeding arteries and dilated veins. **d** With bipolar coagulation of feeding arteries and the tumor surface, slight suction on the tumor allows blunt dissection around the tumor. Further feeding vessels within the cord were not present in this case so that the angioblastoma could be lifted out of the cord in toto (**e**). **f** This photograph demonstrates the view inside the syrinx after removal of the tumor. Five years later, the T1-weighted, contrast-enhanced MRI image (**g**), shows no recurrence. The T2-weighted axial scan (**h**) shows the resection area. Postoperatively, the patient remained in unchanged condition

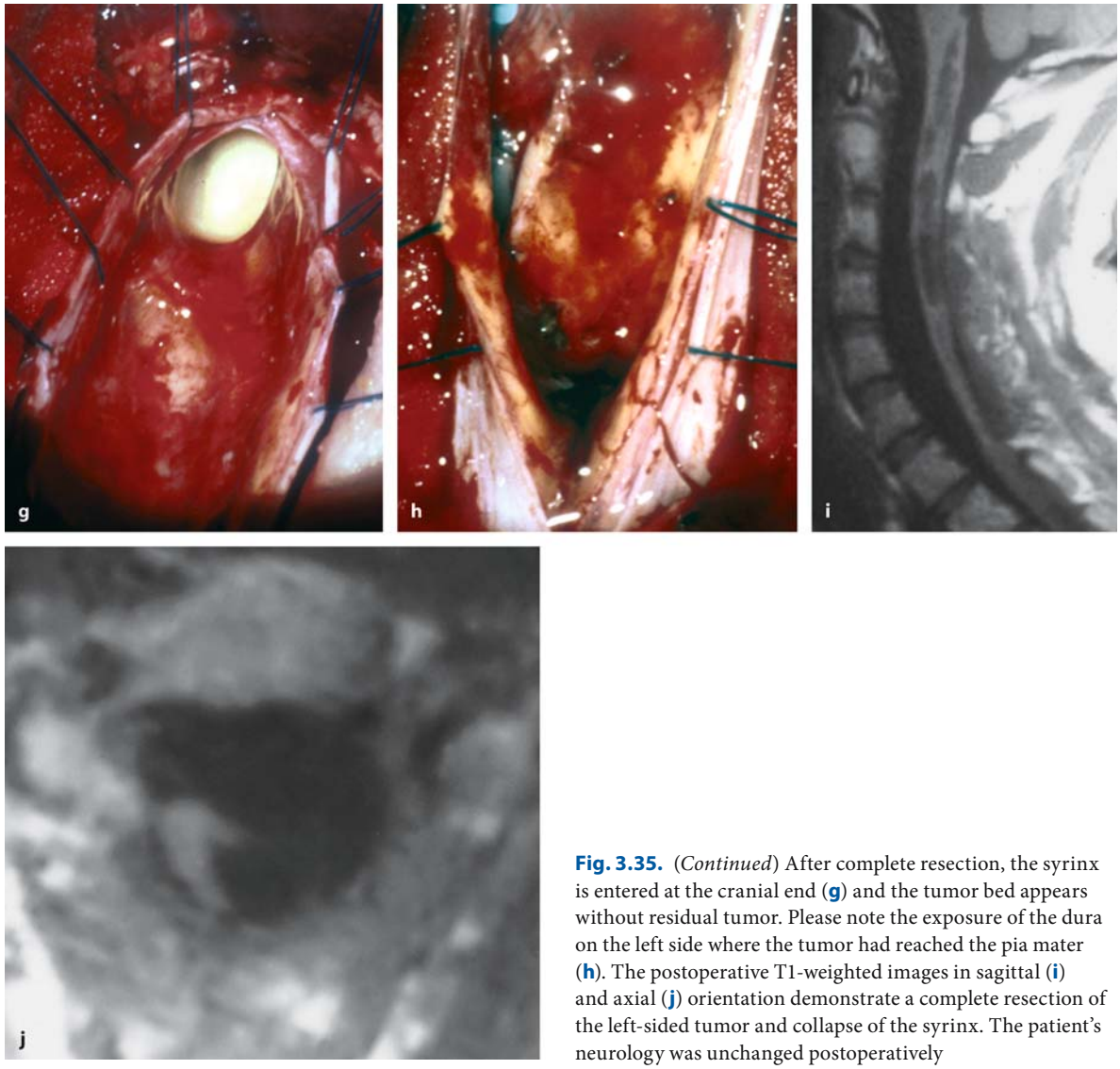

Fig. 3.35. (*Continued*) After complete resection, the syrinx is entered at the cranial end (**g**) and the tumor bed appears without residual tumor. Please note the exposure of the dura on the left side where the tumor had reached the pia mater (**h**). The postoperative T1-weighted images in sagittal (**i**) and axial (**j**) orientation demonstrate a complete resection of the left-sided tumor and collapse of the syrinx. The patient's neurology was unchanged postoperatively

spread the overlying cord fibers apart with two microdissectors to go deeper. In this way, we can minimize the amount of sharp dissection [85]. Therefore, we would rather like to avoid the term "myelotomy" and use "opening of the spinal cord" instead. A good landmark as to the position of the midline is the posterior median septum, a thin fibrous structure that separates the spinal cord in two halves posteriorly. Small vessels on both sides converging to this septum guide the surgeon to the exact midline (Fig. 3.33). However, medial structures may be displaced to either side if the tumor has not grown in the center (Fig. 3.36). Next, we use 6-0 sutures, which we anchor in the pia mater and connect to the dura to keep the cord open (Figs. 3.33, 3.35, and 3.36) [130, 301]. This maneuver minimizes manipulation of the spinal cord during tumor removal, protects the lateral spinal cord surfaces from injury, and may later facilitate the determination of tissue planes considerably once the tumor has been debulked.

The next step of the operation should concentrate on reducing the size of the intramedullary tumor. The only exception to this rule applies to angioblastomas (Fig. 3.34). They have to be resected en bloc to avoid profuse bleeding. For the remaining pathologies, tumor size reduction may be achieved by either coagulation or debulking of the tumor. Any lateral dissection right at the beginning carries the risk of applying a lot of pressure to the surrounding cord. Debulking can be done with tumor forceps, sharp dissection, or ultrasound aspiration (cavitron ultrasonic aspiration, CUSA) depending on the consistency of the tumor

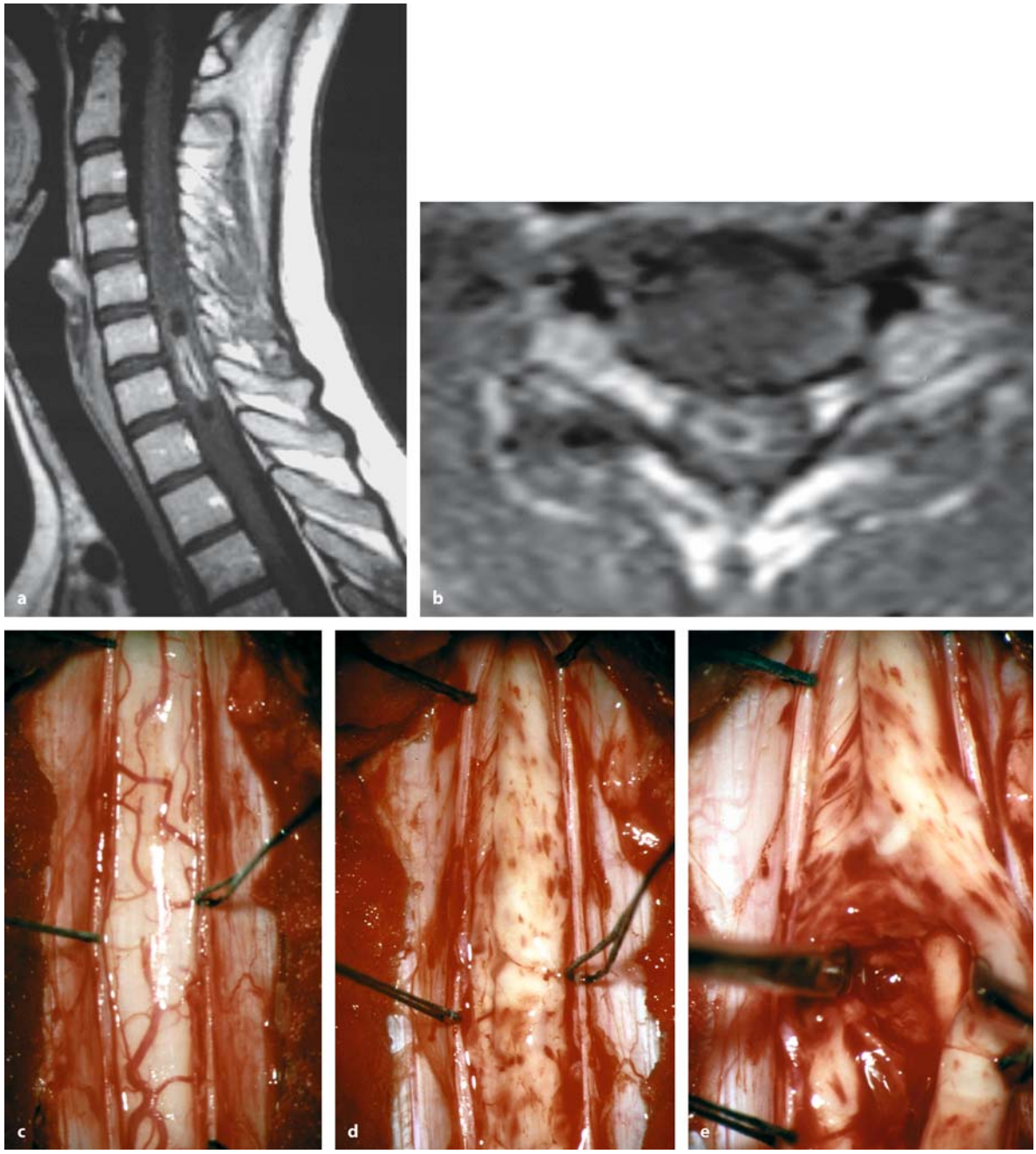

Fig. 3.36. T1-weighted, contrast-enhanced sagittal (**a**) and axial (**b**) MRI images of an intramedullary WHO grade I astrocytoma at C6-C7 in a 23-year-old woman with a 10 year history of right sided arm pain progressing to a slight tetraparesis. There is no significant syrinx associated with the tumor that is located on the right side. **c** The intraoperative view on the spinal cord in the semisitting position displays no visible abnormality. **d** Opening of the cord in the midline displays a normal cord on the left side with small vessels indicating the midline, which is displaced to the left side. The tumor affects exclusively the right side of the cord. **e** With gradual debulking of the tumor from inside, a dissection plane appears on the right side. (*Continuation see next page*)

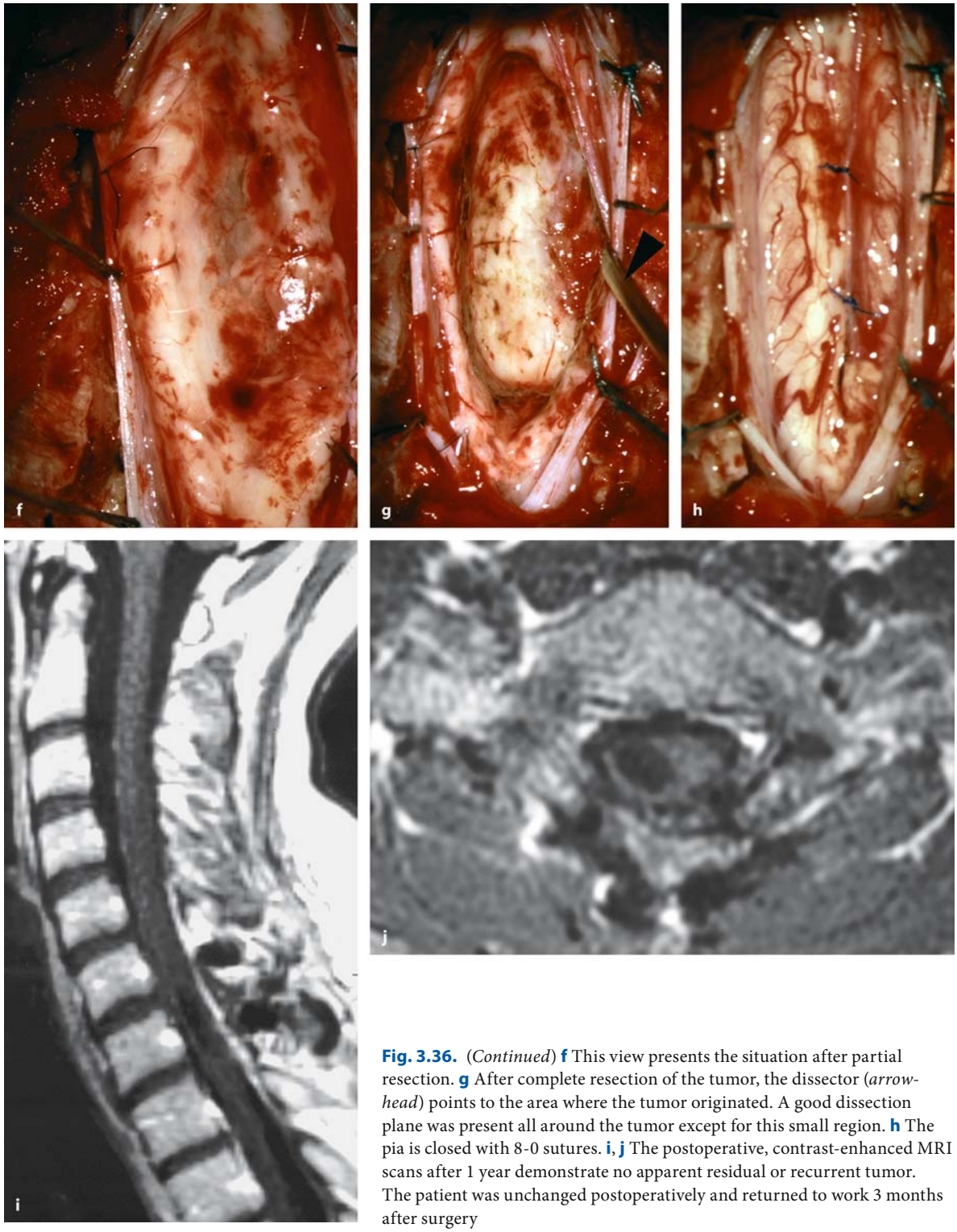

Fig. 3.36. (*Continued*) **f** This view presents the situation after partial resection. **g** After complete resection of the tumor, the dissector (*arrowhead*) points to the area where the tumor originated. A good dissection plane was present all around the tumor except for this small region. **h** The pia is closed with 8-0 sutures. **i, j** The postoperative, contrast-enhanced MRI scans after 1 year demonstrate no apparent residual or recurrent tumor. The patient was unchanged postoperatively and returned to work 3 months after surgery

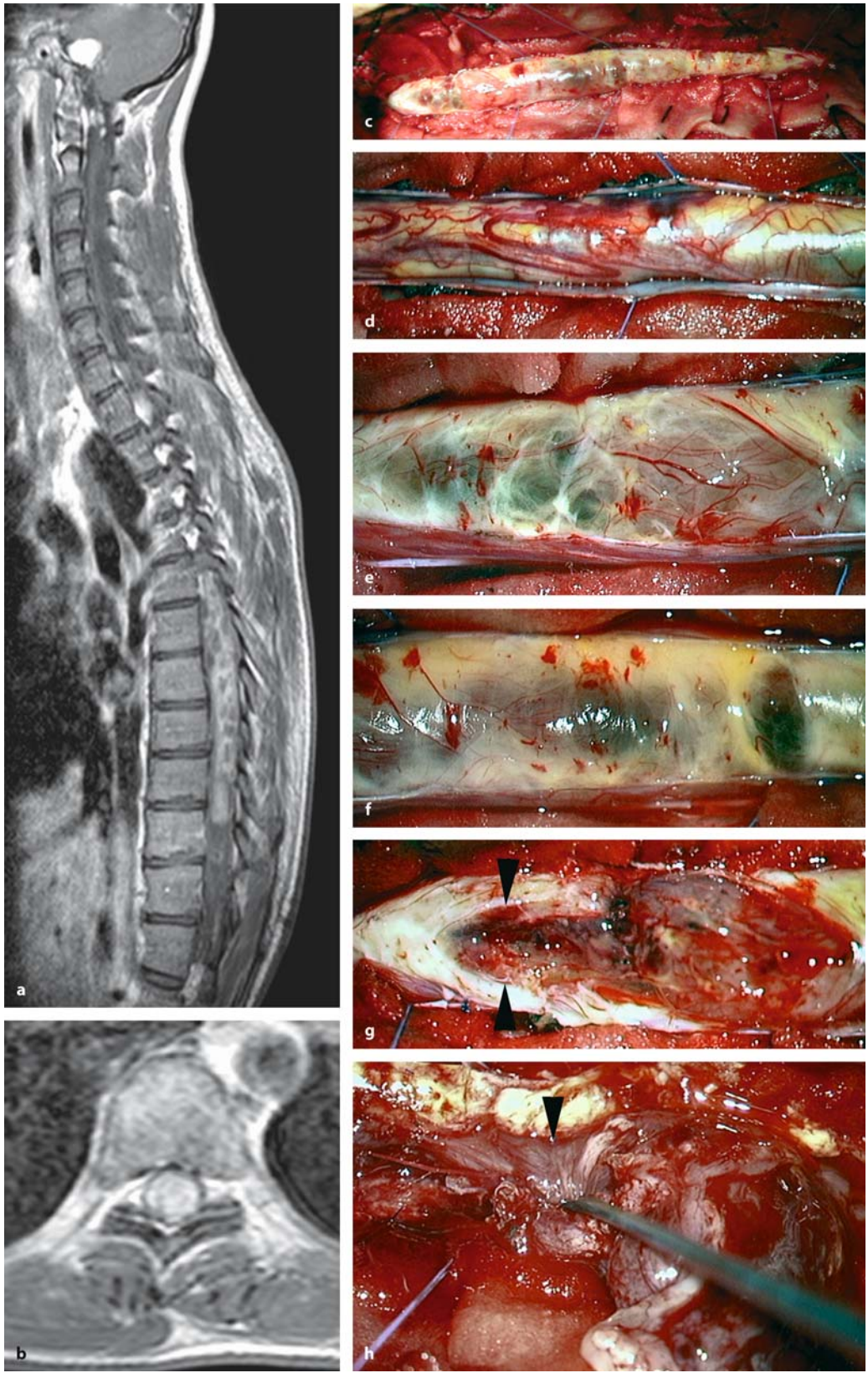

Fig. 3.37. (*Continuation see next page*)

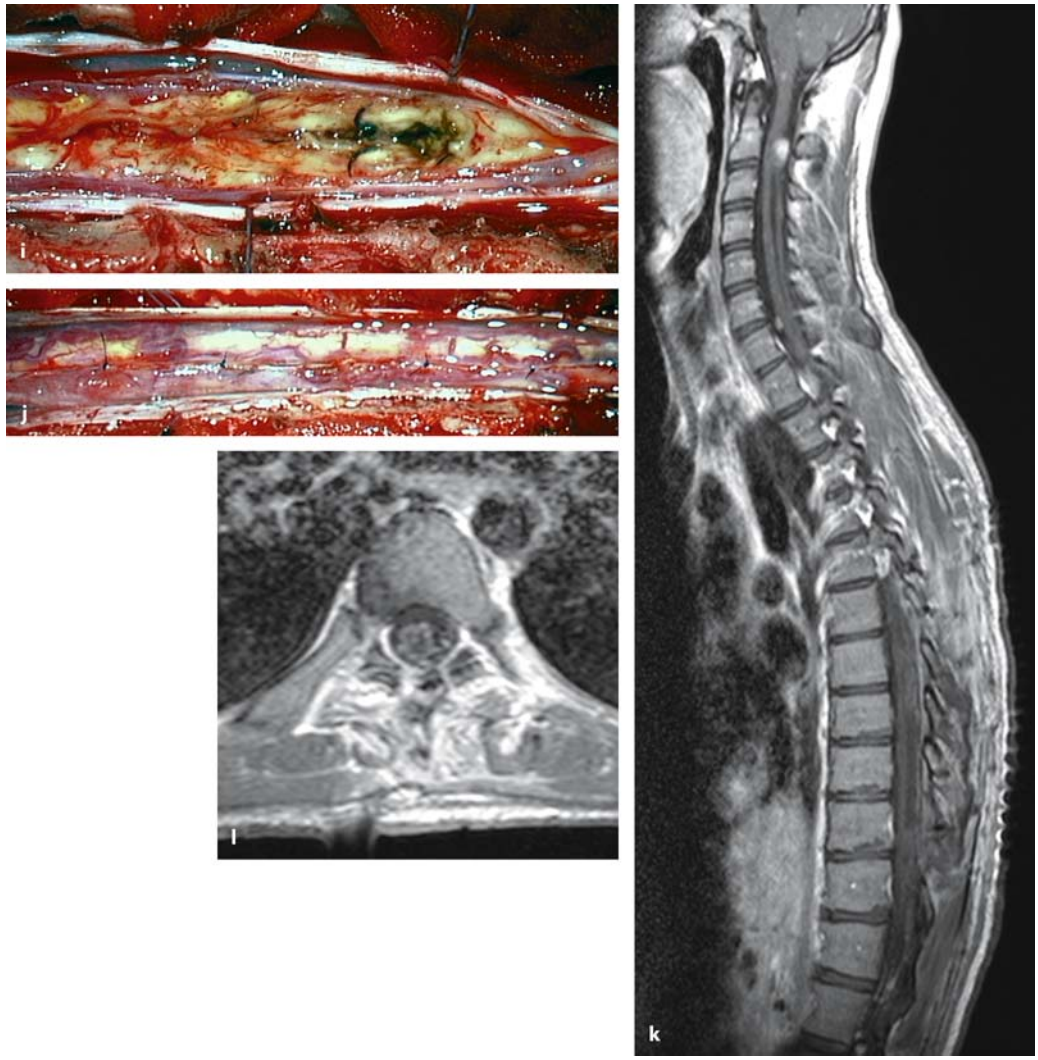

Fig. 3.37. (*Continued*) T1-weighted, contrast-enhanced sagittal (**a**) and axial (**b**) MRI images of an intramedullary ependymoma at Th5–Th10 in a 19-year-old man with NF-2 and a 1-month history of a progressive left-sided paraparesis. The tumor appears partly cystic and is associated with a syrinx above. **c** The intraoperative overview on the spinal cord reveals a grossly abnormal surface with parts of the tumor having reached the pia and discolorations related to small tumor hemorrhages. **d** This view demonstrates a closer view of the cord surface before opening of the arachnoid membrane. **e**, **f** After the arachnoid membrane has been opened, pial vessels can be seen on the cord surface with tumor tissue right underneath. The yellowish hazy-appearing structures are posterior white matter tracts that have been displaced by the tumor. **g** The pia has been opened in the midline. With debulking of the tumor, the lateral dissection plane becomes visible (*arrowheads*; **g**, **h**). After complete removal of the tumor (**i**), the cord is closed with 8-0 pia sutures (**j**). The postoperative sagittal (**k**) and axial (**l**) T1-weighted, contrast-enhanced MRI images demonstrate a complete tumor resection and shrinkage of the syrinx. The patient experienced a significant neurological deterioration after surgery. He regained his preoperative status within 6 months and is free of a recurrence 1 year after surgery

and its vascularity (Figs. 3.33 and 3.35–3.37). Only if sufficient debulking or shrinking of the tumor has been achieved should one try to dissect tumor margins toward the surrounding cord (Figs. 3.33 and 3.35–3.37). With infiltrating tumors, debulking is continued as long as one can safely remain inside the tumor. Once the transition zone toward normal cord tissue is reached, tumor removal is stopped (Fig. 3.36).

Whether a dissection plane between tumor and cord can be determined is of paramount importance for radicality. Several techniques may be used to achieve this goal. In some instances it may be possible to almost wipe the covering layer of spinal cord tissue

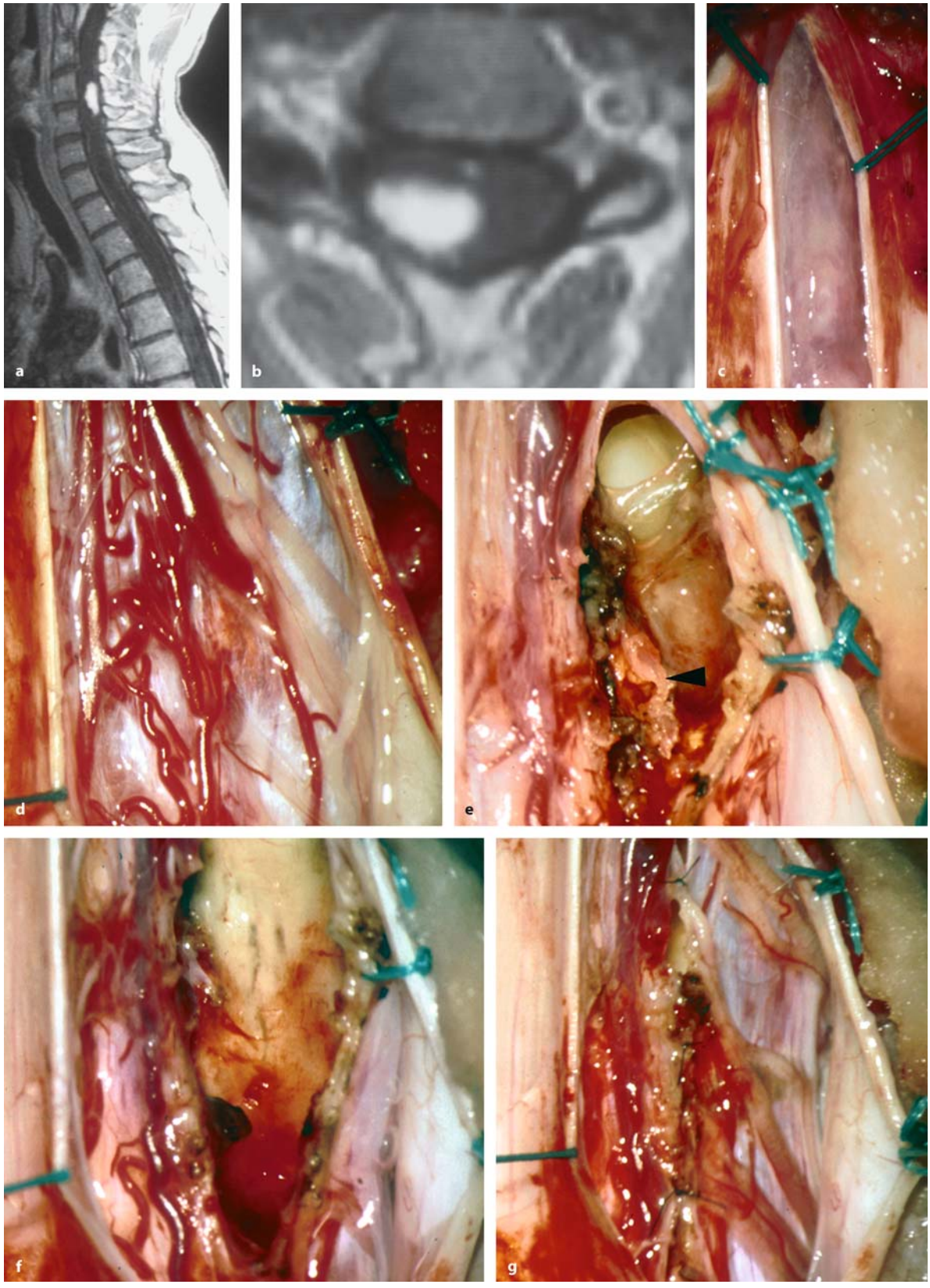

Fig. 3.38. (*Continuation see next page*)

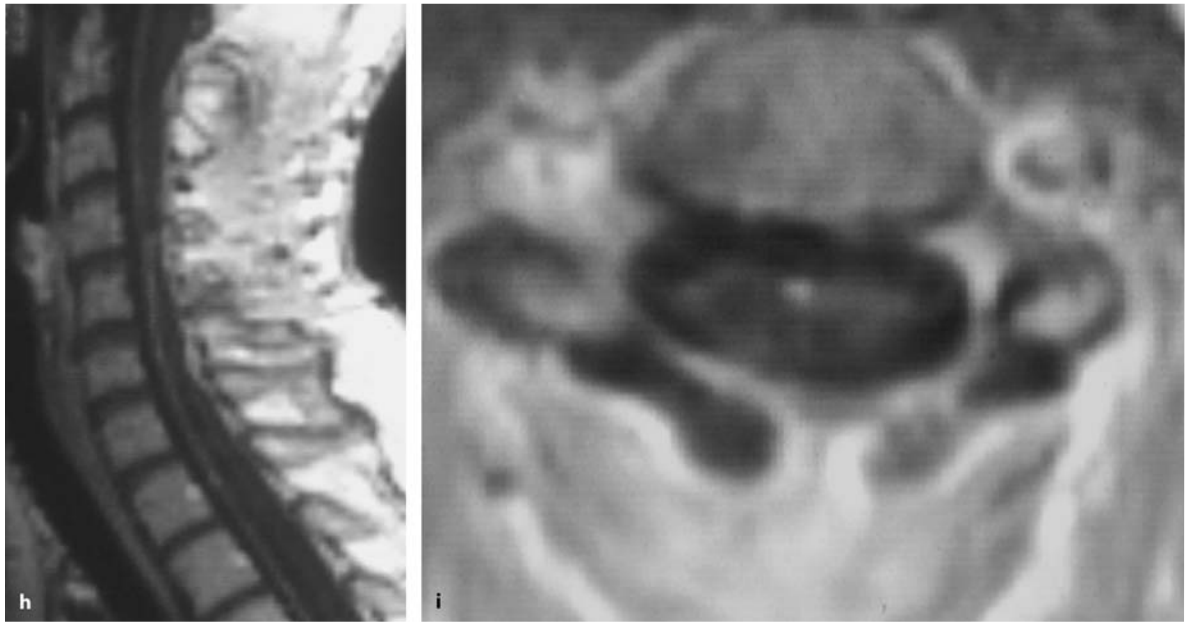

Fig. 3.38. (*Continued*) T1-weighted, contrast-enhanced sagittal (**a**) and axial (**b**) MRI images of an intramedullary angioblastoma at C4–C5 on the right side in a 44-year-old woman with a 10-year history of sensory disturbances in her right arm. She underwent radiotherapy, which did not prevent further deterioration. At the time of surgery, her entire right arm was plegic with gait ataxia becoming apparent. Again, a significant syrinx is visible. **c** This intraoperative view in the semisitting position after dura opening demonstrates arachnoid scarring as a result of the radiotherapy. **d** After opening of the arachnoid, the tumor is just appearing as an orange spot in the dorsal root entry zone on the right side surrounded by tumor-feeding vessels and posterior roots. **e** The tumor appeared somewhat brittle. After shrinking of the tumor with bipolar coagulation, most of it could be removed in one piece. Parts of it, however, remained attached to the surrounding gliotic zone visible on the left (*arrowhead*). The syrinx at the top is entered and serves as a valuable adjunct to determine the correct dissection plane. After complete resection (**f**), the cord is closed with 8-0 pia sutures (**g**). The postoperative sagittal (**h**) and axial (**i**) T1-weighted, contrast-enhanced MRI images, demonstrate a complete tumor resection. The patient's neurological condition was left unchanged

off the tumor capsule with fine forceps and microdissectors (Figs. 3.37). Alternatively, two fine forceps can be used to separate cord and tumor tissue from each other (Figs. 3.33, 3.35). In other instances the spinal cord may be very adherent to the tumor, and even with a clear definition of a dissection plane preparation along this plane may be difficult. In such cases, sharp dissection is required to remove the tumor. With vascular lesions such as angioblastomas and cavernomas, coagulation of the tumor opens the cleavage plane (Fig. 3.34). In patients who have been irradiated, a gliotic plane has been generated by radiotherapy (Fig. 3.38). This may render dissection and identification of a correct cleavage plane very difficult [346, 347].

Of particular help to define a correct dissection plane may be an associated syrinx at the lower and/or the upper pole of the tumor. A syrinx clearly defines the limit of the tumorous process, and may help considerably to determine the margins of the tumor (Figs. 3.33–3.35 and 3.38) [89, 217, 317, 318].

Similarly, a gliotic wall around a former tumor hemorrhage may be helpful for dissection. On the other hand, a fresh intramedullary tumor hemorrhage may make the determination of dissection planes impossible. Therefore, radical tumor removals should not be attempted in the acute phase after an intramedullary hemorrhage unless the dissection plane can be clearly determined. In such instances, surgery should first aim to decompress the cord by opening the pia and removing the clot. If tumor resection is judged too risky in such an operation, a second attempt can be scheduled once the glial tissue around the hemorrhage has formed and the patient has recovered some function (Fig. 3.39).

Once tissue planes are determined, the remainder of the tumor can be removed. Care has to be taken to identify tumor feeding vessels, which have to be

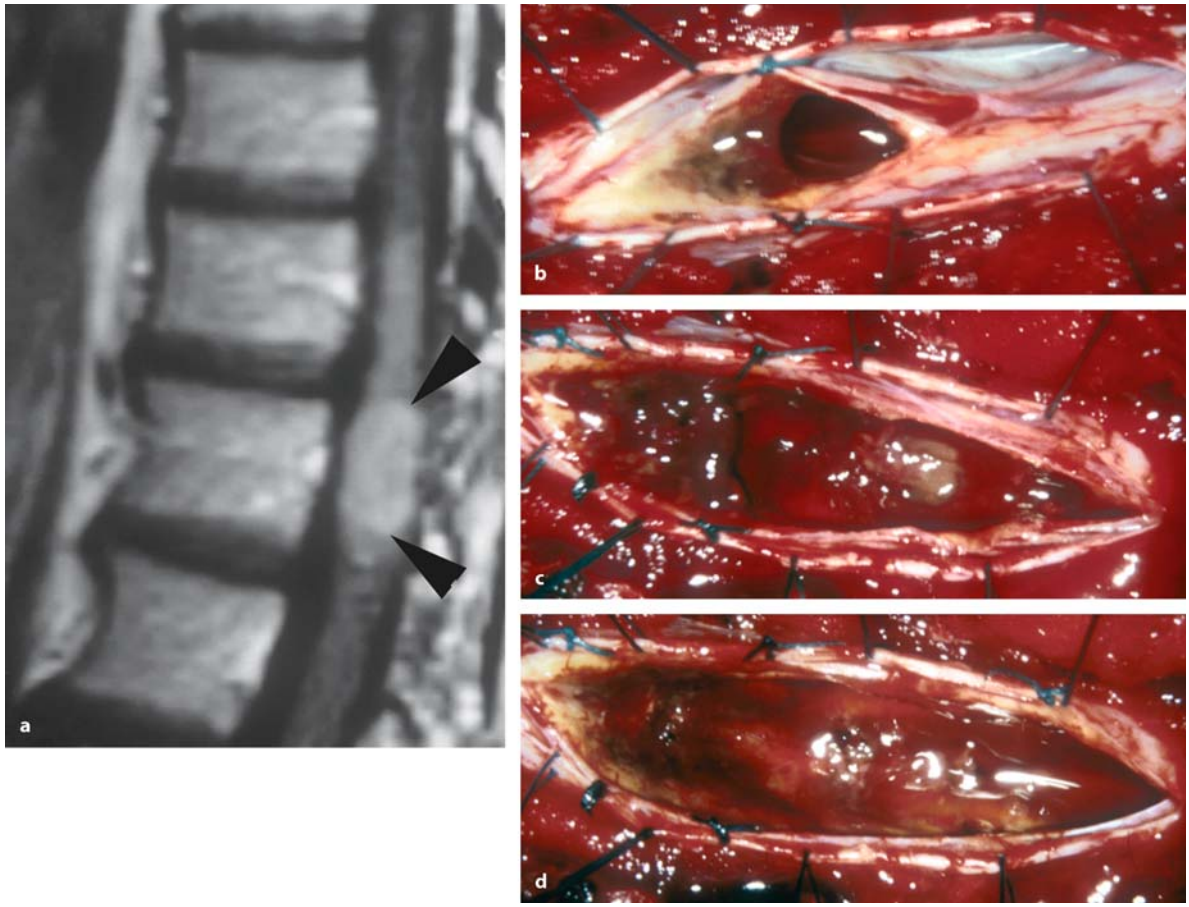

Fig. 3.39. a T1-weighted, contrast-enhanced sagittal MRI scan of an intramedullary ependymoma at Th8–Th9 in a 44-year-old woman with a 5-month history of sensory disturbances in her right leg. A few weeks before surgery she experienced a sudden neurological deterioration with development of a paraparesis. The scan shows the contrast-enhancing tumor (*arrowheads*) and signal changes above and below due to a hemorrhage. **b** The intraoperative view after opening the cord in the midline and applying pia retention sutures displays the hematoma cavity and the tumor. Note the collapsed cord to the right after evacuation of the clot. **c** This view demonstrates the situation after partial removal of hematoma and tumor. The dissection was very difficult in the edematous cord due to ill-defined tumor borders obscured by the hemorrhage. **d** After complete resection, the tumor bed looks fine. Postoperatively, the patient deteriorated significantly with loss of walking abilities and sphincter control and made only a partial recovery. In retrospect, just the hematoma should have been evacuated and the tumor removal postponed until some function had been recovered and the remaining hematoma resorbed

coagulated and cut. Important feeding vessels may derive from the anterior spinal artery, especially in ependymomas (Fig. 3.33). Dissection has to minimize any undue tension on these feeding vessels to avoid any compromise to this important artery. By often changing the area of dissection from left to right and superior to inferior, one can distribute the stress one puts on the cord and its vessels during removal. In this way, a radical resection is generally possible for tumors that do not infiltrate the spinal cord [84, 85].

In most instances, the surgeon will have to operate on the intramedullary tumor without knowing the exact histology – with the exception of vascular tumors such as cavernomas and angioblastomas, which can be easily identified even before surgery in most patients. For the remainder, intraoperative frozen sections should not be relied upon [318]. They can give information as to the benign or malignant nature of the tumor, but due to the small specimen available for analysis, the rate of false diagnoses is higher compared to intracranial tumors, for instance. Therefore, the surgeon has to rely foremost on his own intraoperative judgment. Nevertheless, a few points specific for the most common pathologies are worth mentioning.

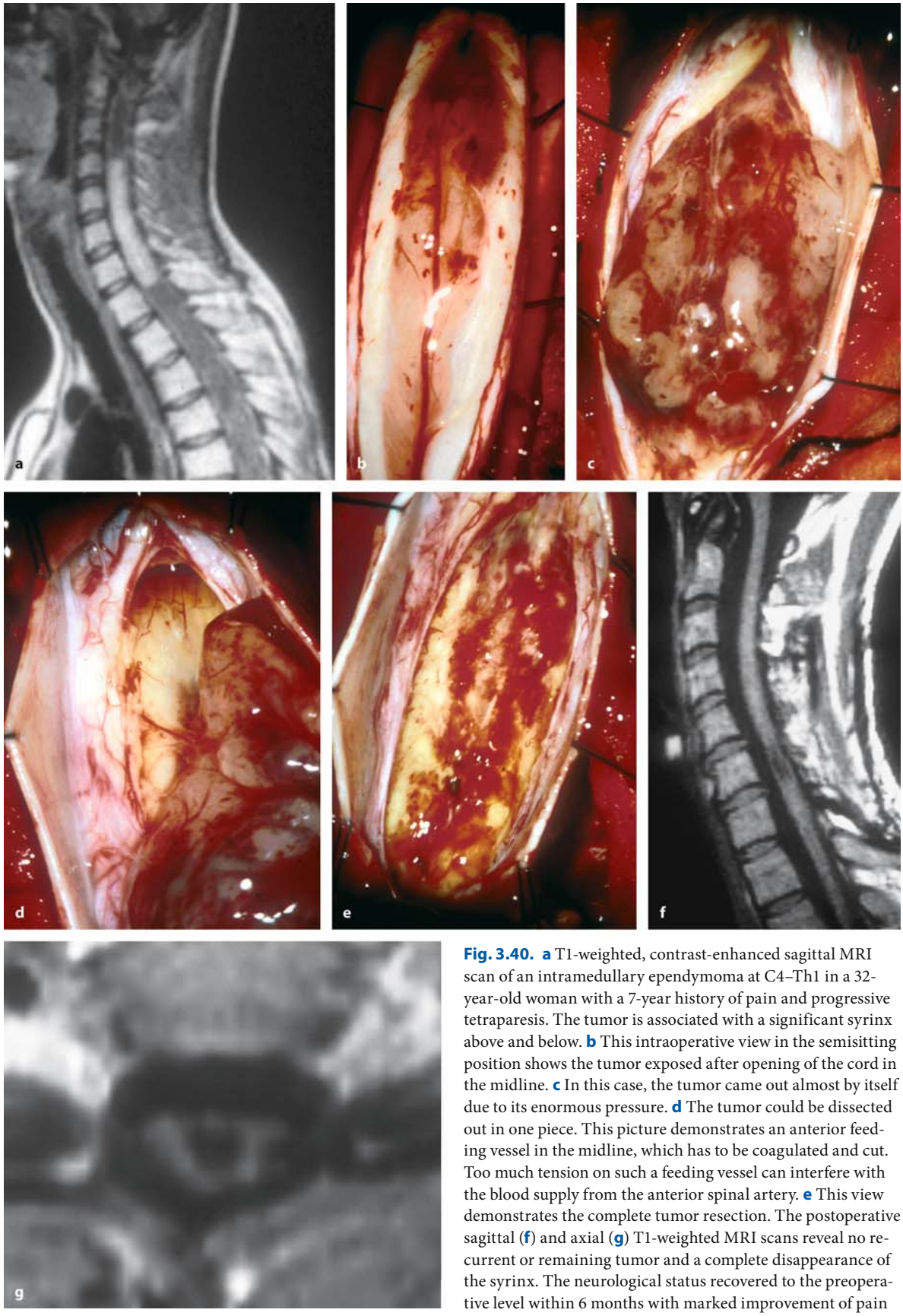

Fig. 3.40. **a** T1-weighted, contrast-enhanced sagittal MRI scan of an intramedullary ependymoma at C4–Th1 in a 32-year-old woman with a 7-year history of pain and progressive tetraparesis. The tumor is associated with a significant syrinx above and below. **b** This intraoperative view in the semisitting position shows the tumor exposed after opening of the cord in the midline. **c** In this case, the tumor came out almost by itself due to its enormous pressure. **d** The tumor could be dissected out in one piece. This picture demonstrates an anterior feeding vessel in the midline, which has to be coagulated and cut. Too much tension on such a feeding vessel can interfere with the blood supply from the anterior spinal artery. **e** This view demonstrates the complete tumor resection. The postoperative sagittal (**f**) and axial (**g**) T1-weighted MRI scans reveal no recurrent or remaining tumor and a complete disappearance of the syrinx. The neurological status recovered to the preoperative level within 6 months with marked improvement of pain

3.3.2.1 Removal of Ependymomas

In general, ependymomas are completely resectable [204, 301]. They displace rather than infiltrate the spinal cord. Some ependymomas may exert such enormous pressure that they almost come out by themselves once the pia has been opened (Fig. 3.40) [217]. In such instances, the pia has to be opened quickly over the entire extension of the tumor and blunt instruments should be used for posterior and lateral dissection of the tumor. With an insufficient pial opening, on the other hand, posterior pathways may be injured by the extruding tumor. With ependymomas associated with a syrinx, the cyst may be lined by a gliotic wall. This gliosis can be left in place and has to be distinguished from tumor tissue. It is sufficient to remove the solid tumor part (Fig. 3.41).

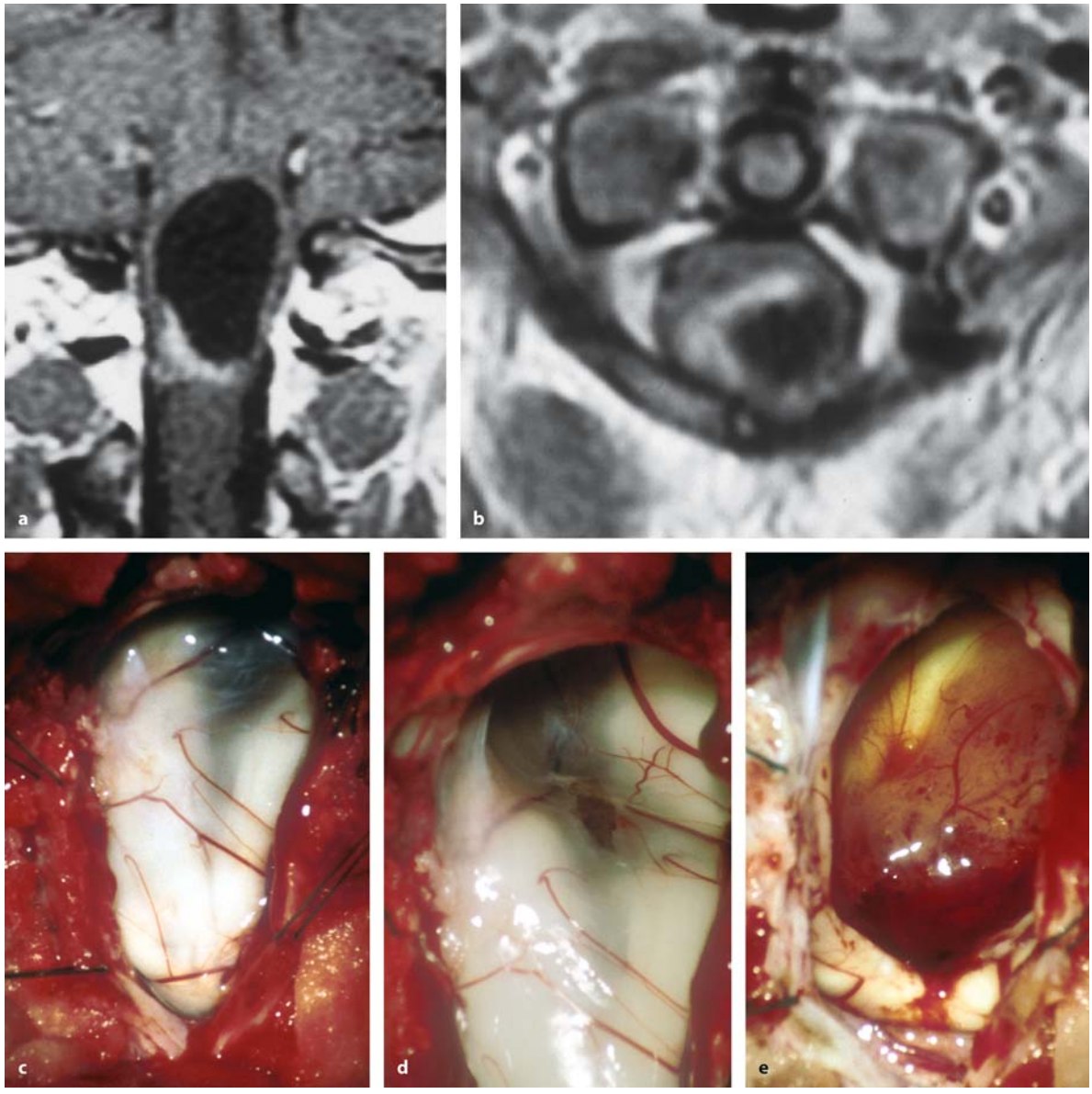

Fig. 3.41. T1-weighted, contrast-enhanced coronal (**a**) and axial (**b**) MRI images of an intramedullary ependymoma at C1–C2 in a 32-year-old woman with NF-2 and a 6-month history of gait and sensory disturbances. The solid tumor demonstrates bright contrast enhancement and is located at the bottom of the associated cyst on the right side. **c** This intraoperative photograph in the semisitting position demonstrates the view on the upper cervical cord after dura and arachnoid membrane opening. The tumor cyst is visible underneath the pia. **d** The pia is incised to evacuate some of the cyst fluid. **e** The solid tumor becomes apparent after opening of the pia and the posterior cyst wall. (*Continuation see next page*)

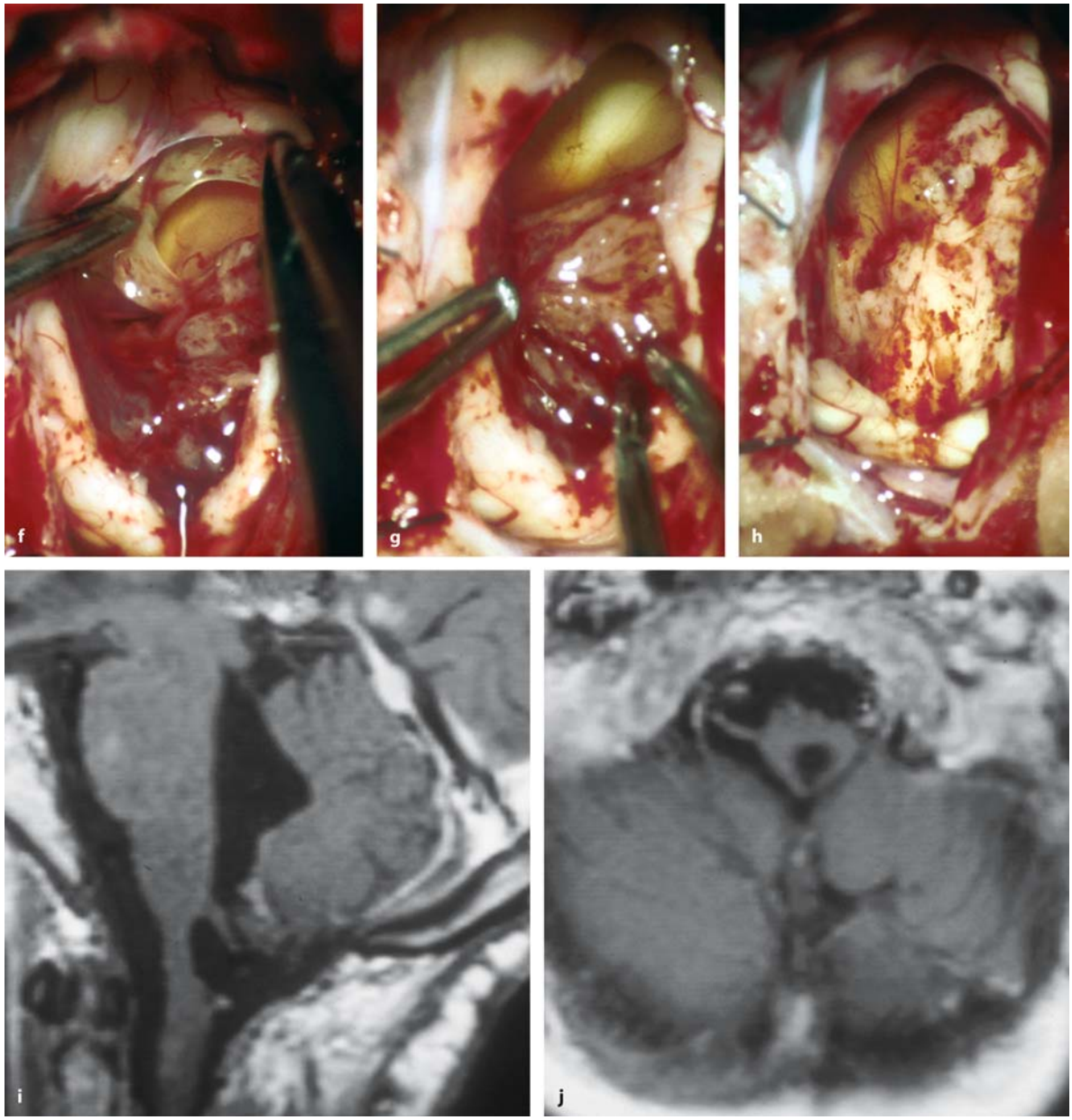

Fig. 3.41. (*Continued*) The tumor can be dissected from the cyst wall with two fine tumor forceps (**f**) and removed almost in one piece (**g**). **h** This view demonstrates the complete tumor resection. The postoperative T1-weighted, contrast-enhanced sagittal (**i**) and axial (**j**) MRI scans show no tumor remnant or recurrence 5 years after operation. The patient's neurological symptoms improved postoperatively

In all cases, tumor feeding vessels have to be identified and cut. Of particular importance are those arising from the anterior spinal artery in the midline. In any case, care should be taken to avoid too much tension on these feeding vessels as this may compromise spinal cord blood supply. Sufficient tumor debulking and coagulation and transection of these feeders are required to prevent such problems (Figs. 3.33, 3.40, and 3.42). Ependymomas may extend toward the pia mater so that the dura may be exposed after a complete resection (Fig. 3.42).

In the absence of associated cysts it may not always be easy to identify the upper and lower margins of an ependymoma [217]. In such instances the tumor may transgress into a fine thin structure towards the central canal. At that stage, this structure should be

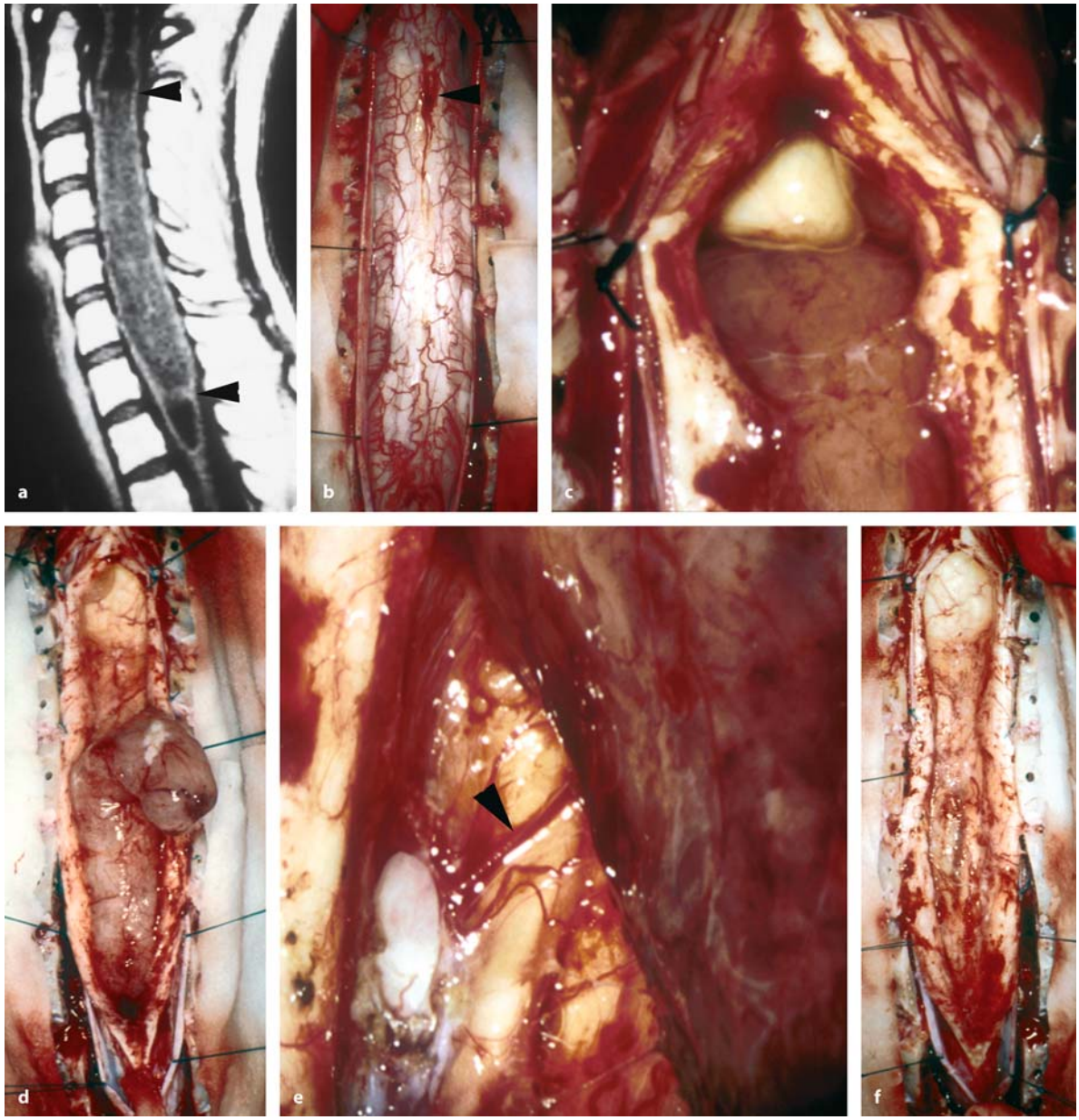

Fig. 3.42. **a** This T1-weighted sagittal MRI scan shows an intramedullary ependymoma at C2–C7 (*arrowheads*) with small syrinx cavities above and below in a 25-year-old woman with a 1-year history of progressive tetraparesis. **b** This view in the semisitting position reveals the grossly swollen spinal cord. Note the injury to the cord surface with dura opening in the upper part of the exposure (*arrowhead*). With opening of the cord in the midline, the pressure of the tumor allowed it to be dissected out in one piece, starting at the upper pole entering the syrinx (**c**) and working carefully downward (**d**). **e** Once again, it has to be emphasized that care must be taken to avoid the small anterior feeding vessels coming from the anterior spinal artery (*arrowhead*). Note that this tumor had penetrated the cord anteriorly close to the anterior spinal artery, exposing the ventral dura on the left side. **f** The final intraoperative view shows a clean resection field. (*Continuation see next page*)

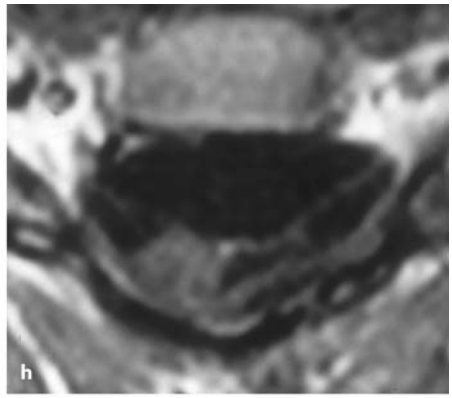

Fig. 3.42. (*Continued*) The postoperative sagittal (**g**) and axial (**h**) T1-weighted, contrast-enhanced MRI scans reveal a complete resection, but also an extensive posterior fixation of the cord to the dura. The excellent postoperative neurological outcome lasted for 1 year. Since then the has patient suffered from a severe dysesthesia syndrome and myelopathy. Within 8 years, no tumor recurrence has developed

transected rather than followed further, which would require additional dissection deep in the center of the cord.

Ependymomas may extend over several spinal levels and reach enormous sizes (Fig. 3.37). This should not deter the surgeon from recommending surgery. Even tumors affecting the entire spinal cord have been removed successfully in single or multiple stages [66]. Likewise, ependymomas extending into the medulla oblongata are amenable to surgery [129].

3.3.2.2 Removal of Astrocytomas

In general, astrocytomas have to be considered as infiltrating tumors. Therefore, the identification of cleavage planes carries considerable risks and may even be outright impossible [130, 204]. However, some astrocytomas do present cleavage planes, allowing a complete resection using similar dissection techniques as described for ependymomas. The strategy of choice is to remove them from inside out [80]. In tumors with ill-defined margins, CUSA is ideal to debulk the mass. Astrocytomas may display varying characteristics during dissection: they may show a nice cleavage plane in some areas, but in other parts infiltrate surrounding tissue diffusely [152]. Tumor feeding vessels may come from all angles and do not originate from the anterior spinal artery as regularly as in ependymomas. Regardless of dissection technique, the danger of creating an artificial cleavage plane that does not exist is real. As long as the tissue appears pathologic – consistency, color, and structure may be used as guidelines – debulking can be continued. In some cases, a clear dissection plane can be followed all around the tumor (Figs. 3.35, 3.43, and 3.44) or in most places (Fig. 3.36). In the remainder, one reaches a kind of transitional zone toward normal tissue at some stage. Without a clear-cut plane of dissection, no further removal should be attempted once the mass of the tumor has been removed (Fig. 3.45) [80, 130, 318].

Astrocytomas may extend over several spinal segments (Fig. 3.45) and may even occupy the entire spinal cord, especially in young children. Such tumors have been removed in two-staged operations [19, 36, 81, 241].

With malignant astrocytomas, a complete resection is impossible, as all of them display an infiltrating growth pattern (Figs. 3.46 and 3.47), which may also involve nerve roots (Fig. 3.46). In patients with a rather short clinical history and an infiltrating tumor, we do use frozen sections to establish the anaplastic or highly malignant nature of such a tumor. In these instances, conservative debulking is performed to remove the mass. But no attempt is undertaken to search for a cleavage plane in order to prevent any postoperative neurological deterioration, as a recurrence is certain irrespective of the amount of resection.

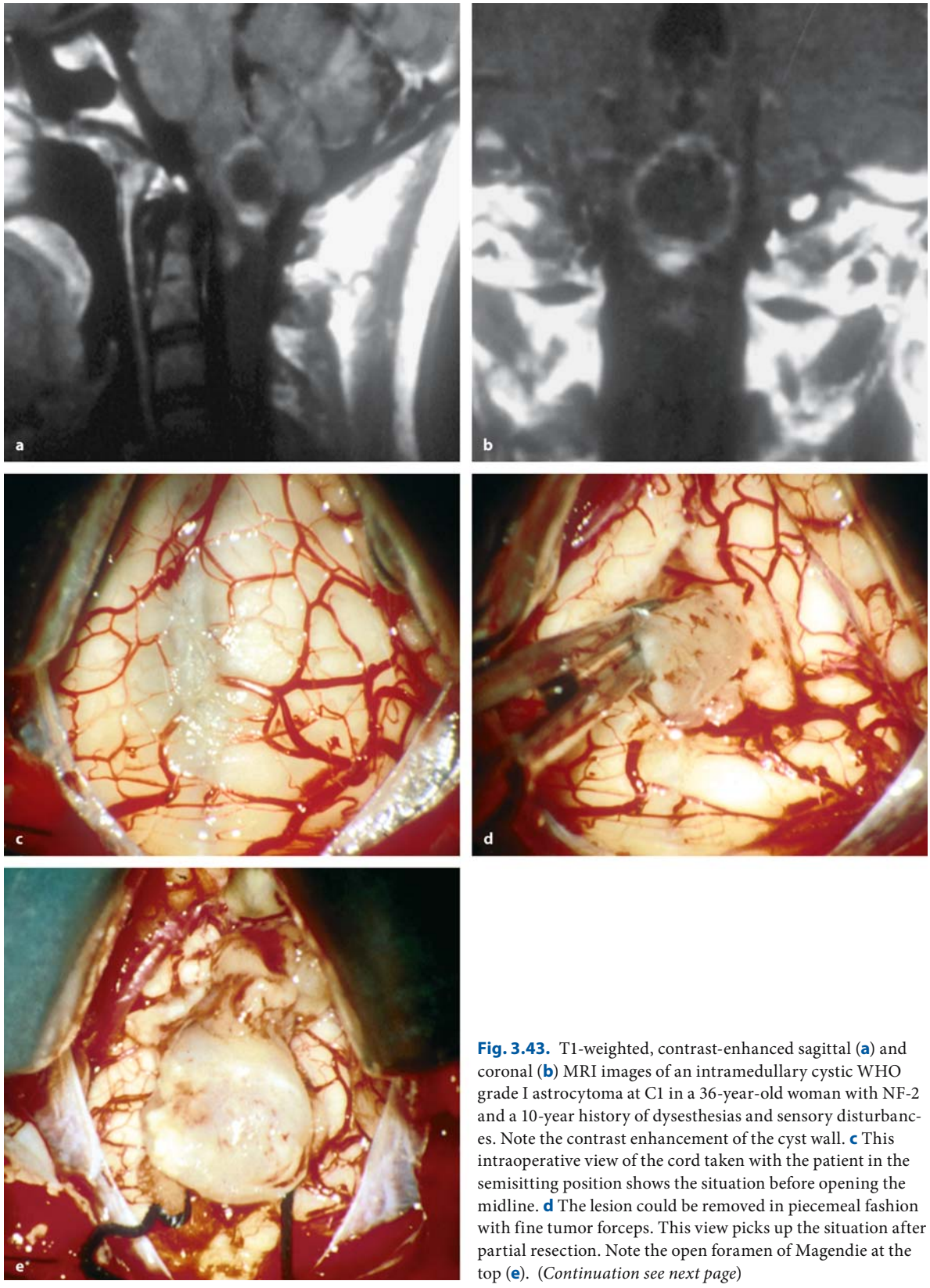

Fig. 3.43. T1-weighted, contrast-enhanced sagittal (**a**) and coronal (**b**) MRI images of an intramedullary cystic WHO grade I astrocytoma at C1 in a 36-year-old woman with NF-2 and a 10-year history of dysesthesias and sensory disturbances. Note the contrast enhancement of the cyst wall. **c** This intraoperative view of the cord taken with the patient in the semisitting position shows the situation before opening the midline. **d** The lesion could be removed in piecemeal fashion with fine tumor forceps. This view picks up the situation after partial resection. Note the open foramen of Magendie at the top (**e**). (*Continuation see next page*)

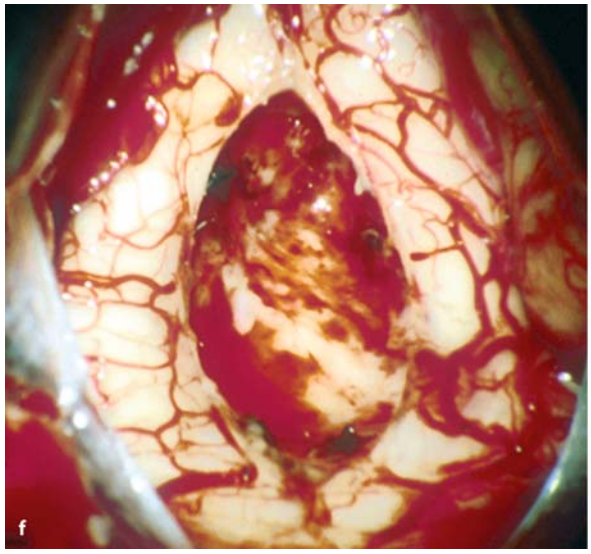

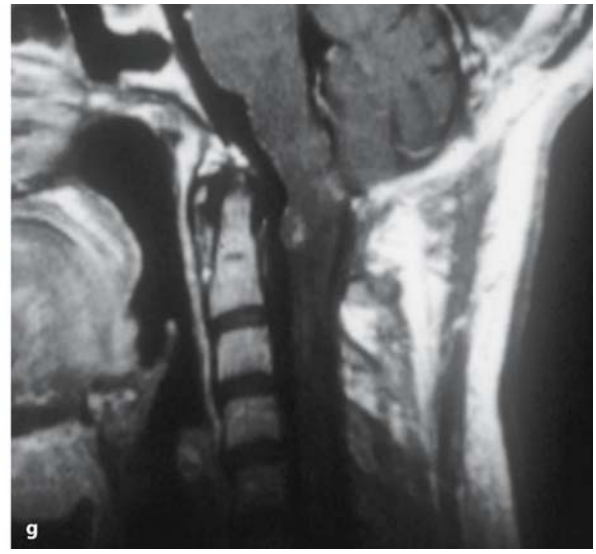

Fig. 3.43. f (*Continued*) The tumor could be resected completely. **g** The postoperative sagittal T1-weighted, contrast-enhanced MRI scan shows no residual tumor. The patient's gait improved postoperatively. No recurrence has been observed within 4 years follow-up

Fig. 3.44. This series of sagittal and axial MRI scans show an intramedullary WHO grade I astrocytoma at C1–C2 in a 21-year-old patient with a 3-month history of sensory disturbances and dysesthesias in his arms. T1-weighted scans without (**a**) and with contrast (**b**), reveal no uptake by the tumor at all. (*Continuation see next page*)

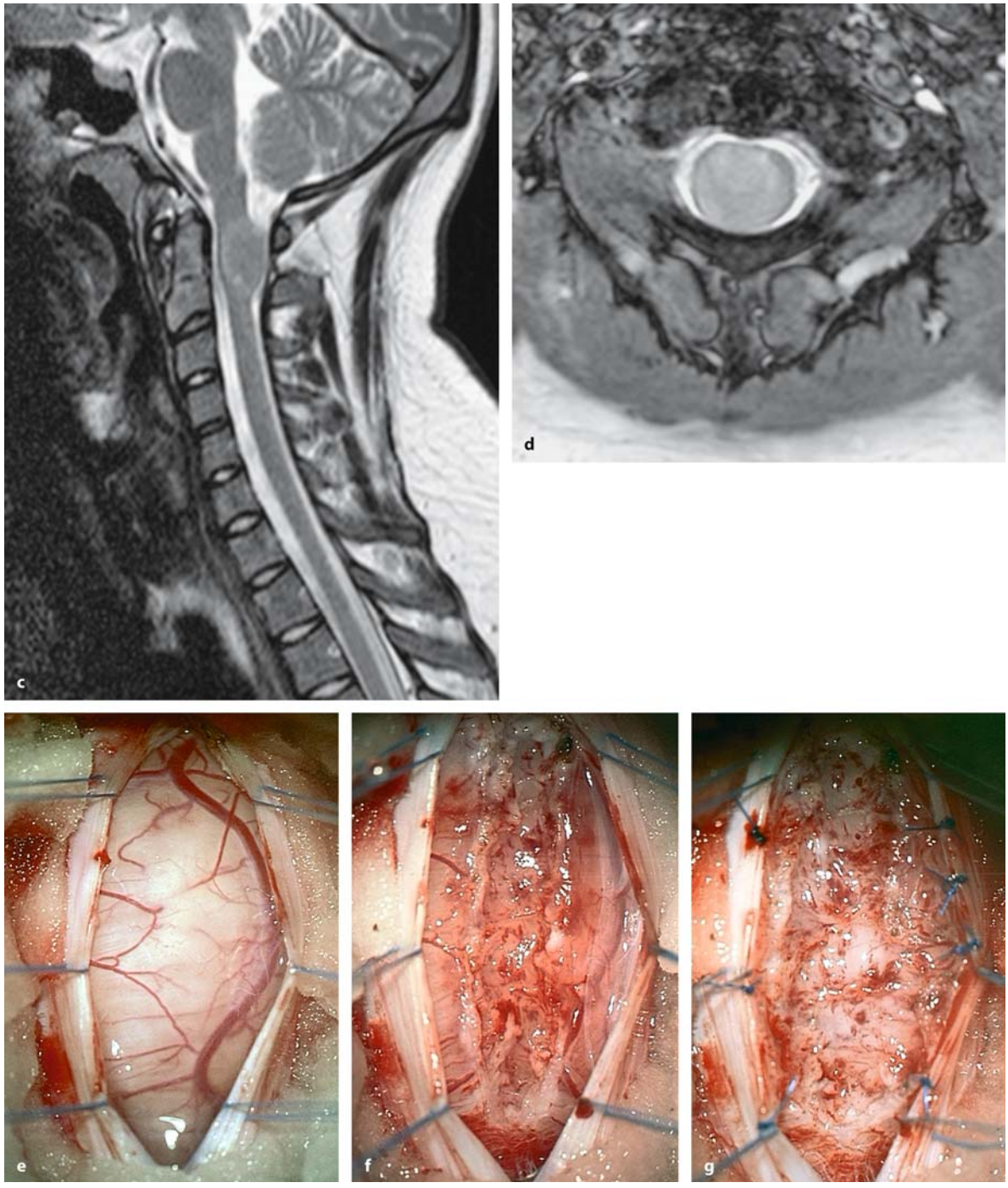

Fig. 3.44. The T2-weighted images in the sagittal (**c**) and axial planes (**d**) give the best radiological demarcation of this large tumor. **e** The intraoperative view after dura opening, taken with the patient in the semisitting position, demonstrates the grossly swollen cord. With opening of the pia in the midline, the tumor is encountered immediately (**f**), and protrudes out slightly due to its pressure after applying pial sutures (**g**). (*Continuation see next page*)

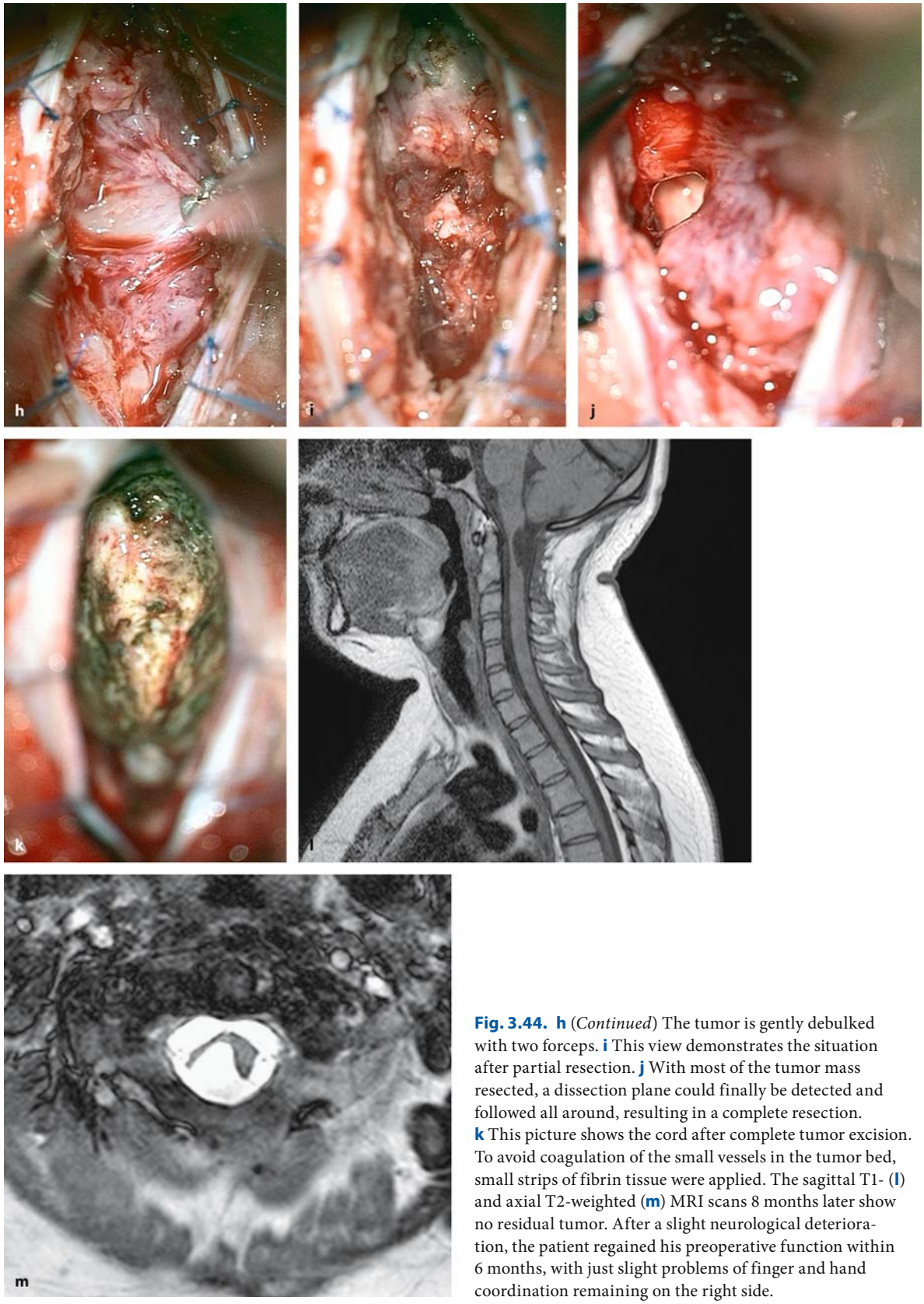

Fig. 3.44. h (*Continued*) The tumor is gently debulked with two forceps. **i** This view demonstrates the situation after partial resection. **j** With most of the tumor mass resected, a dissection plane could finally be detected and followed all around, resulting in a complete resection. **k** This picture shows the cord after complete tumor excision. To avoid coagulation of the small vessels in the tumor bed, small strips of fibrin tissue were applied. The sagittal T1- (**l**) and axial T2-weighted (**m**) MRI scans 8 months later show no residual tumor. After a slight neurological deterioration, the patient regained his preoperative function within 6 months, with just slight problems of finger and hand coordination remaining on the right side.

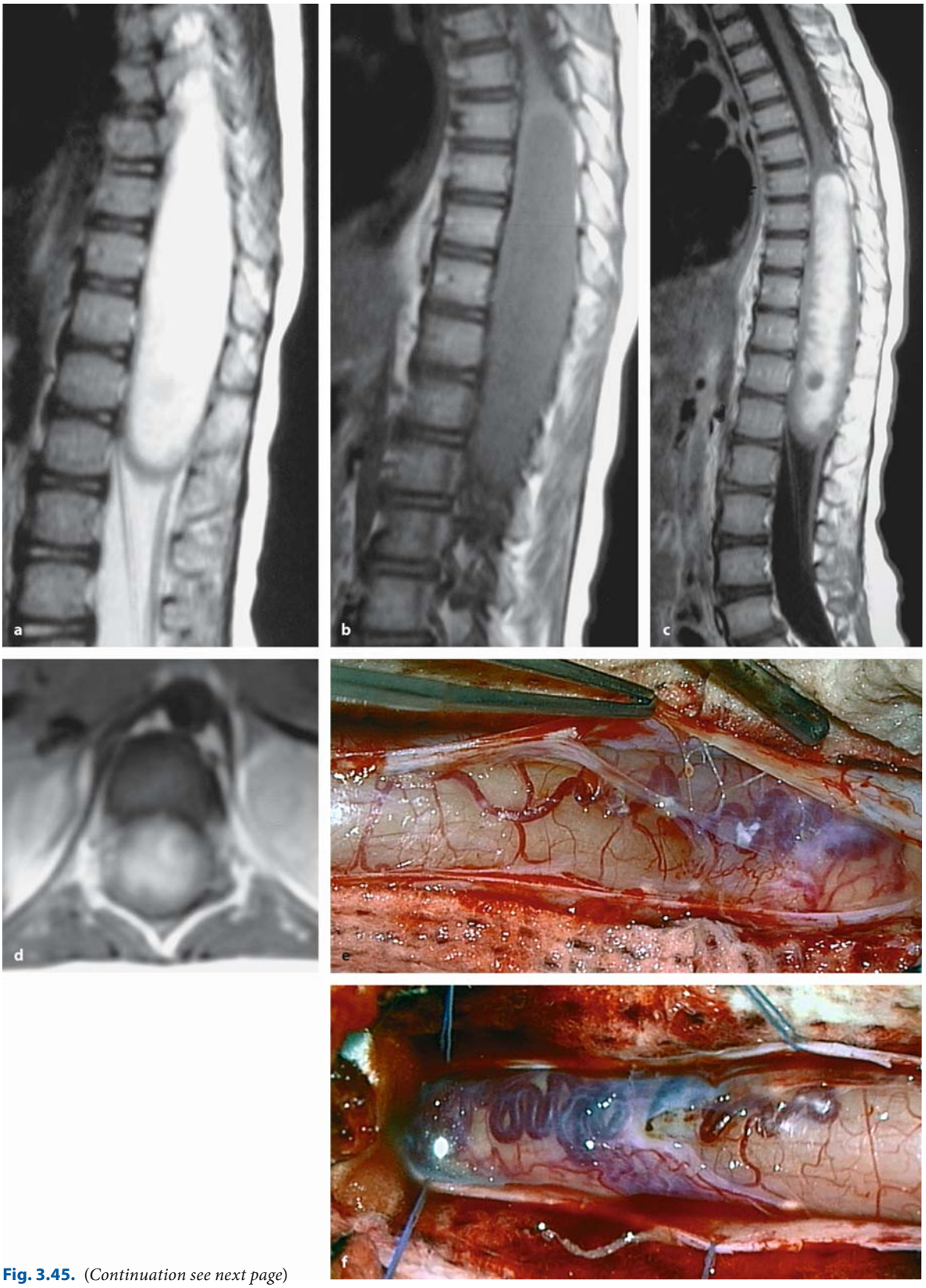

Fig. 3.45. (*Continuation see next page*)

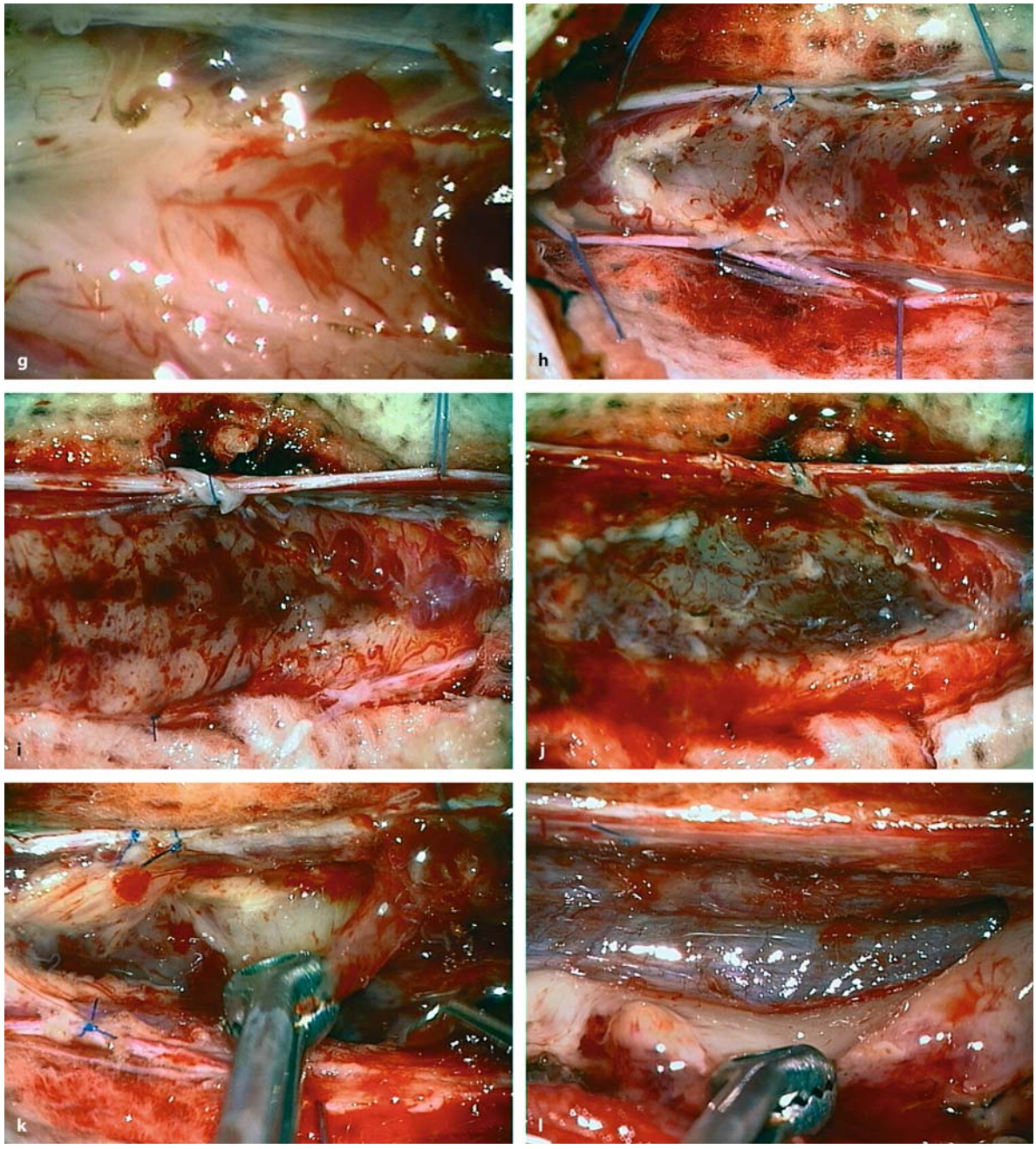

Fig. 3.45. Sagittal T2- (**a**) and T1-weighted MRI images without (**b**) and with contrast (**c**), of an intramedullary astrocytoma WHO grade II–III at Th7–L2 in a 3-year-old girl with a 1-year history of a progressive paraparesis. There is irregular contrast enhancement and a marked enlargement of the cord. The spinal canal is widened. **d** The axial scan demonstrates a tumor with ill-defined margins. After opening of the dura and the arachnoid membrane, a grossly abnormal cord surface appears with arachnoid adhesions at the lower (**e**) and upper (**f**) tumor poles. **g** Opening the cord in the midline at the upper pole discloses the characteristic surface vessels converging in the midline in the left half, and tumor tissue appearing in the right half of the photo. **h**, **i** Applying pia sutures after cord opening, the tumor seems to fill out the entire cord and starts to protrude out in the lower part (**i**). **j** This image shows the situation half way through debulking of the mass. **k** With most of the pressure on the cord relieved by debulking, a plane appears in the upper part of the tumor, which can be followed with blunt dissection in most areas. **l** The anterior pia mater is reached by following the tumor margin. The tumor had split the cord into two halves longitudinally. (*Continuation see next page*)

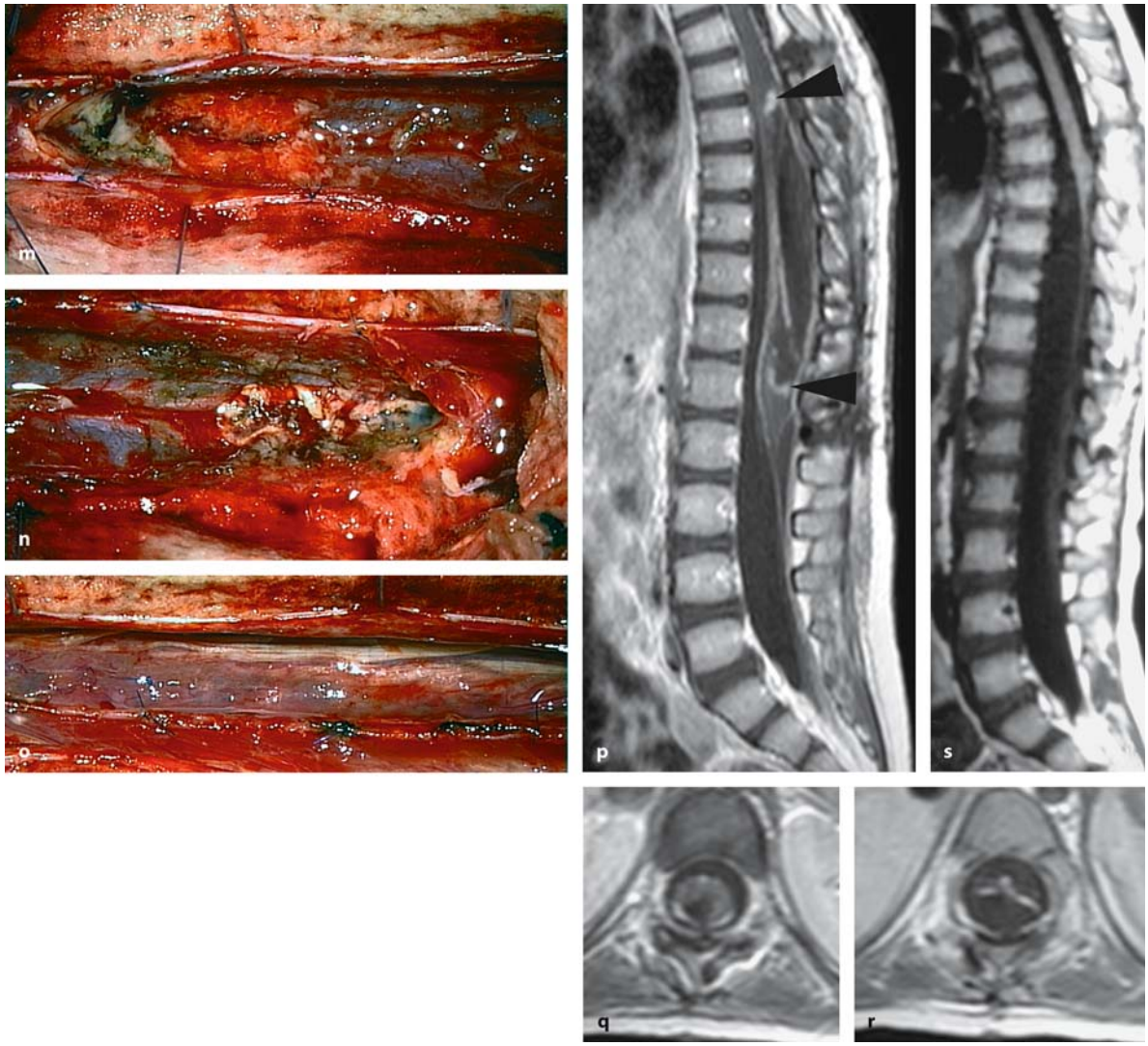

Fig. 3.45. (*Continued*) After resection of the tumor, the upper (**m**) and lower parts (**n**) of the tumor bed are demonstrated. **o** The pia mater is closed with 8-0 sutures. The postoperative T1-weighted, contrast-enhanced MRI scans in the sagittal (**p**) and axial planes (**q**, **r**) show a complete resection of this tumor. At Th7/8 and L1, small areas of contrast enhancement are visible, suggesting small tumor remnants (*arrowheads* in **p**). Postoperatively, the patient experienced an almost complete paralysis of both legs. With intensive rehabilitation, the girl started to walk again after 1 year. Sphincter functions, however, did not recover. Despite tremendous problems with the histopathological grading and recommendations by pediatric oncologists to give chemotherapy to this child, it was decided against any adjuvant therapy. The girl is free of a recurrence for 2 years. The last follow-up scan shows no tumor and a slight kyphosis (**s**)

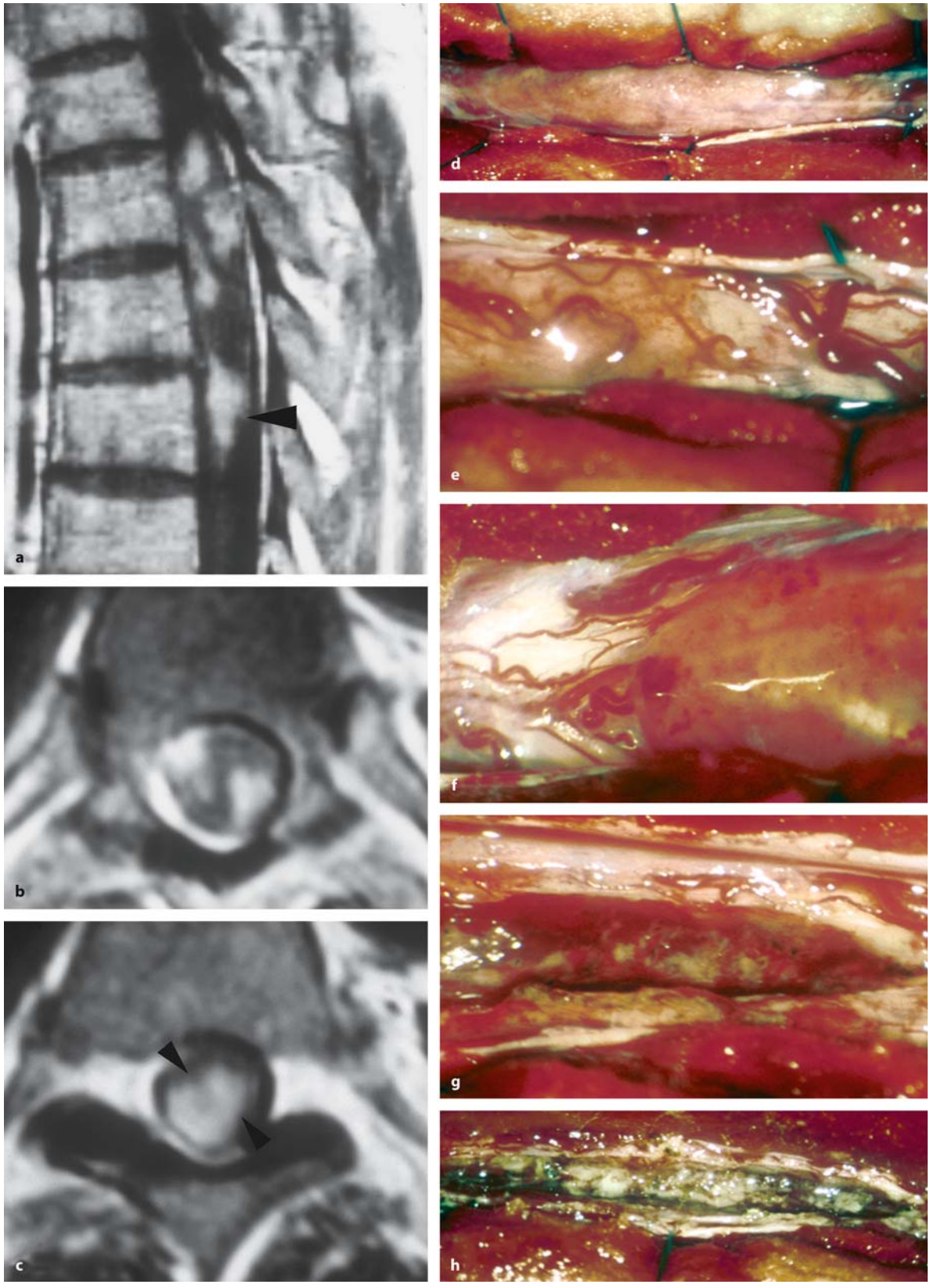

Fig. 3.46. (*Continuation see next page*)

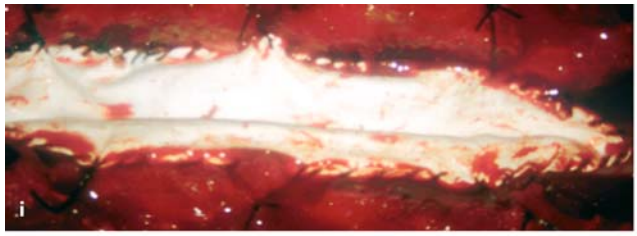

Fig. 3.46. (*Continued*) T1-weighted, contrast-enhanced sagittal (**a**) and axial (**b**, **c**) MRI images of an intramedullary WHO grade III astrocytoma at Th5–Th8 in a 49-year-old man with a 12-month history of a painlessly progressing paraparesis. There is patchy contrast enhancement of the tumor, which displays an exophytic component (*arrowheads* in **a** and **c**). **d** The intraoperative view after dura opening reveals the tremendous pressure of this tumor. The cord surface is obscured by tumor tissue, which has grown through the pia infiltrating posterior nerve roots. Closer views at the lower (**e**) and upper pole (**f**) after arachnoid opening make this obvious. **g** After partial resection, no cleavage plane was present, so that tumor removal was stopped at this stage (**h**). **i** A Gore-Tex® duraplasty was inserted. The postoperative sagittal (**j**) and axial (**k**) contrast-enhanced MRI scans demonstrate the decompression of the cord. The patient maintained his neurological status for 6 months, when a recurrence of tumor growth caused a rapidly developing paraplegia. In the following weeks, dissemination of the tumor led to hydrocephalus, and the patient finally died after 17 months

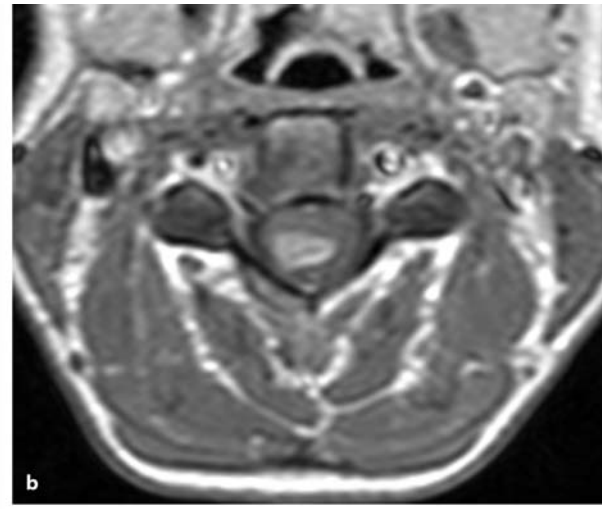

Fig. 3.47. T1-weighted, contrast-enhanced sagittal (**a**) and axial (**b**) MRI images of an intramedullary WHO grade III astrocytoma at C3–C6 in a 16-year-old girl with a 2-month history of a rapidly progressive tetraparesis. There is a patchy uptake of contrast. The tumor appears well demarcated toward the spinal cord and on the right side. (Continuation see next page)

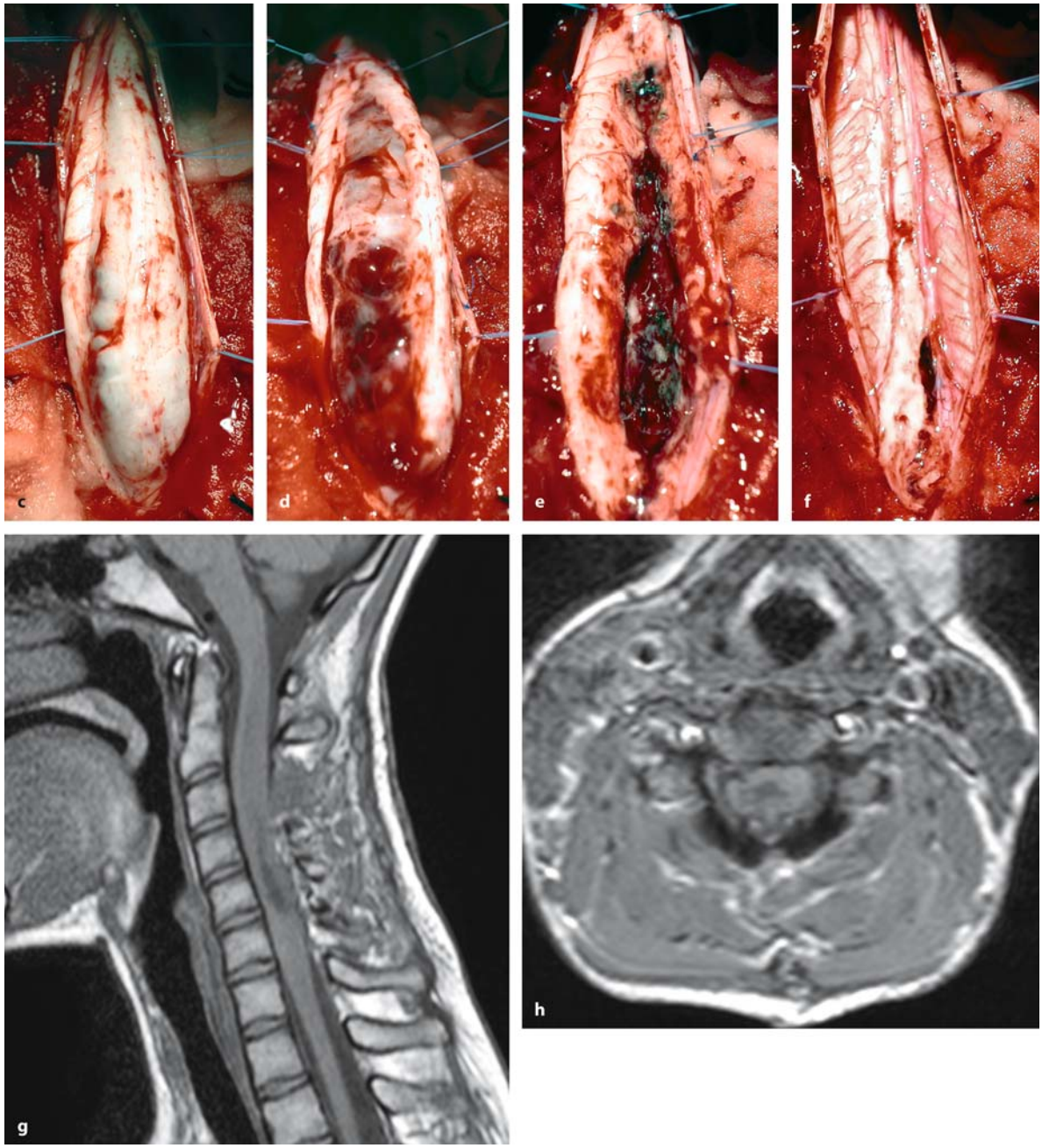

Fig. 3.47. (*Continued*) **c** This intraoperative view, taken with the patient in the semisitting position and after opening the pia in the midline, demonstrates the normal appearing cord on the left side with small midline vessels and the grossly abnormal tissue in the right half (see Fig. 3.36 for comparison). Note the displacement of the midline toward the left side. **d** Some of the posterior cord substance could be dissected and gently spread laterally revealing additional intratumoral hemorrhages. **e** After resection of the major tumor mass, no dissection plane could be determined, so tumor removal was stopped at this point. **f** Closing the cord with pia sutures confirms a significant decompression. The postoperative sagittal (**g**) and axial (**h**) T1-weighted, contrast-enhanced images show a good reduction of the tumor mass. The patient underwent chemotherapy and radiotherapy and recovered well with no significant neurological deficits for 11 months. A local recurrence and subarachnoid spreading of the tumor subsequently resulted in a rapidly developing tetraplegia and death 12 months after surgery

3.3.2.3 Removal of Angioblastomas

As a considerable number of intramedullary angioblastomas are associated with a syrinx, the precise localization of the solid tumor part is of particular importance. In most instances, arterialized and dilated veins cover the posterior surface of the cord at and next to the angioblastoma. In some instances, the characteristic orange color of the lesion is apparent right underneath the pia mater (Figs. 3.34, 3.38, and 3.48). In all other cases, ultrasound is a valuable tool to determine the limits of the tumor [83, 144, 164, 200, 203, 272, 275, 290].

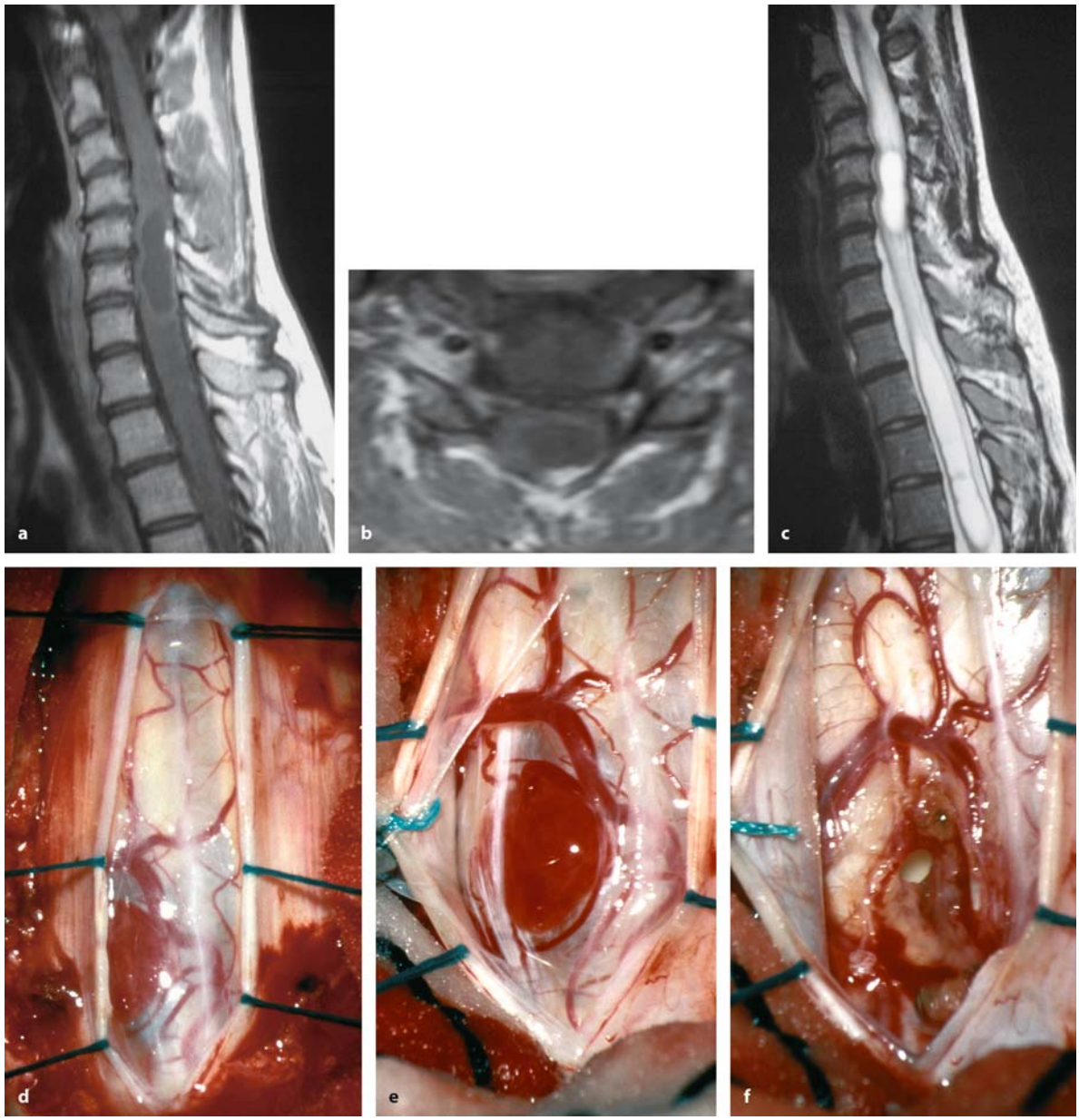

Fig. 3.48. T1-weighted, contrast-enhanced sagittal (**a**) and axial (**b**) MRI images of an intramedullary angioblastoma at C5 in the left dorsal root entry zone in a 30-year-old woman with VHL and a 10-month history of dysesthesias, sensory dysfunctions, and mild motor weakness in her left arm. She had been operated previously on a thoracic angioblastoma. Next to the residual syrinx from the thoracic tumor, a new one developed between C5 and C6, as can be seen on the sagittal T2 image (**c**). The intraoperative pictures, taken with the patient in the semisitting position before (**d**) and after arachnoid opening (**e**), display the tumor in the left dorsal root entry zone. **f** After resection of the tumor, gliotic tissue appears towards the syrinx. (*Continuation see next page)*

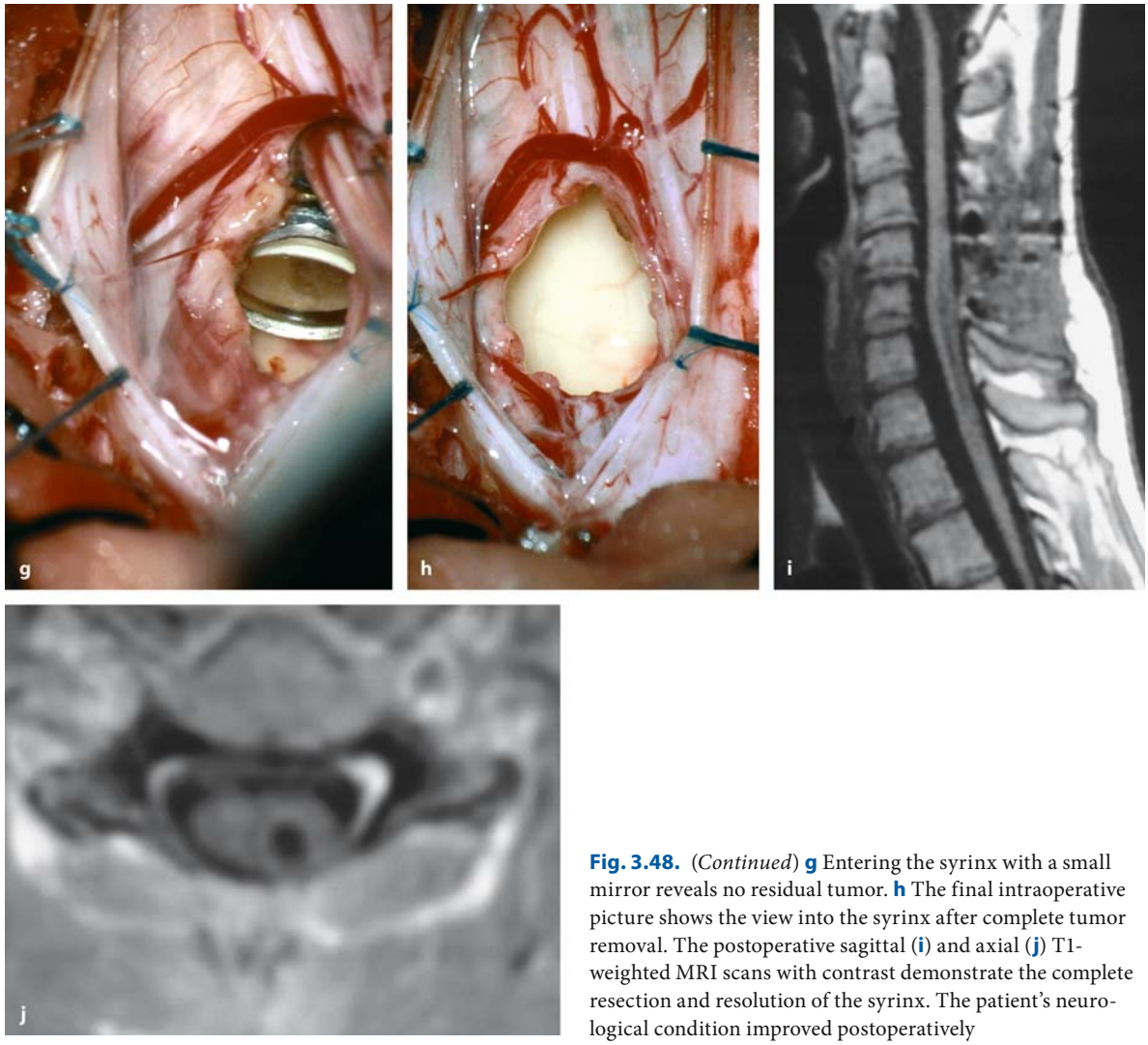

Fig. 3.48. (*Continued*) **g** Entering the syrinx with a small mirror reveals no residual tumor. **h** The final intraoperative picture shows the view into the syrinx after complete tumor removal. The postoperative sagittal (**i**) and axial (**j**) T1-weighted MRI scans with contrast demonstrate the complete resection and resolution of the syrinx. The patient's neurological condition improved postoperatively

With highly vascularized tumors such as angioblastomas, it is advisable to remove the tumor in toto to avoid profuse bleeding with debulking [185, 252], which may pose enormous problems finding the right dissection plane between tumor and spinal cord. With pial incision, the dilated surface vessels next to the tumor have to be dealt with. They cannot be mobilized and tend to bleed as soon as they are touched. The bipolar system should be set low so that they shrink gradually rather than rupture. The subpial localization of most angioblastomas then allows coagulation of the tumor surface as soon as the pia has been transected (Figs. 3.34, 3.38, and 3.48). With coagulation, the tumor can be shrunk slightly so that dissection around the lesion becomes possible. Quite often, they are associated with either an intramedullary cyst or considerable edema. We place small cuttonoids around the tumor and apply a little bit of suction on these cuttonoids to facilitate further dissection. Going around the tumor, feeding arteries are dissected, coagulated, and transected. Having completed dissection around the tumor, the angioblastoma can be delivered in toto [198, 233, 252, 318, 350]. To check for remnants of the tumor in cases with an additional syrinx, a small mirror can be used (Fig. 3.48).

With anteriorly located tumors fed from branches of the anterior spinal artery, one can also approach the tumor from posterior, especially in cases with a large syrinx (Fig. 3.49). Alternatively, an anterior approach with corpectomy has been described [148, 264].

In large tumors, however, debulking may be necessary. In such instances, preoperative embolization should be considered – provided an experienced interventional radiologist is available [125, 134, 185, 245, 327].

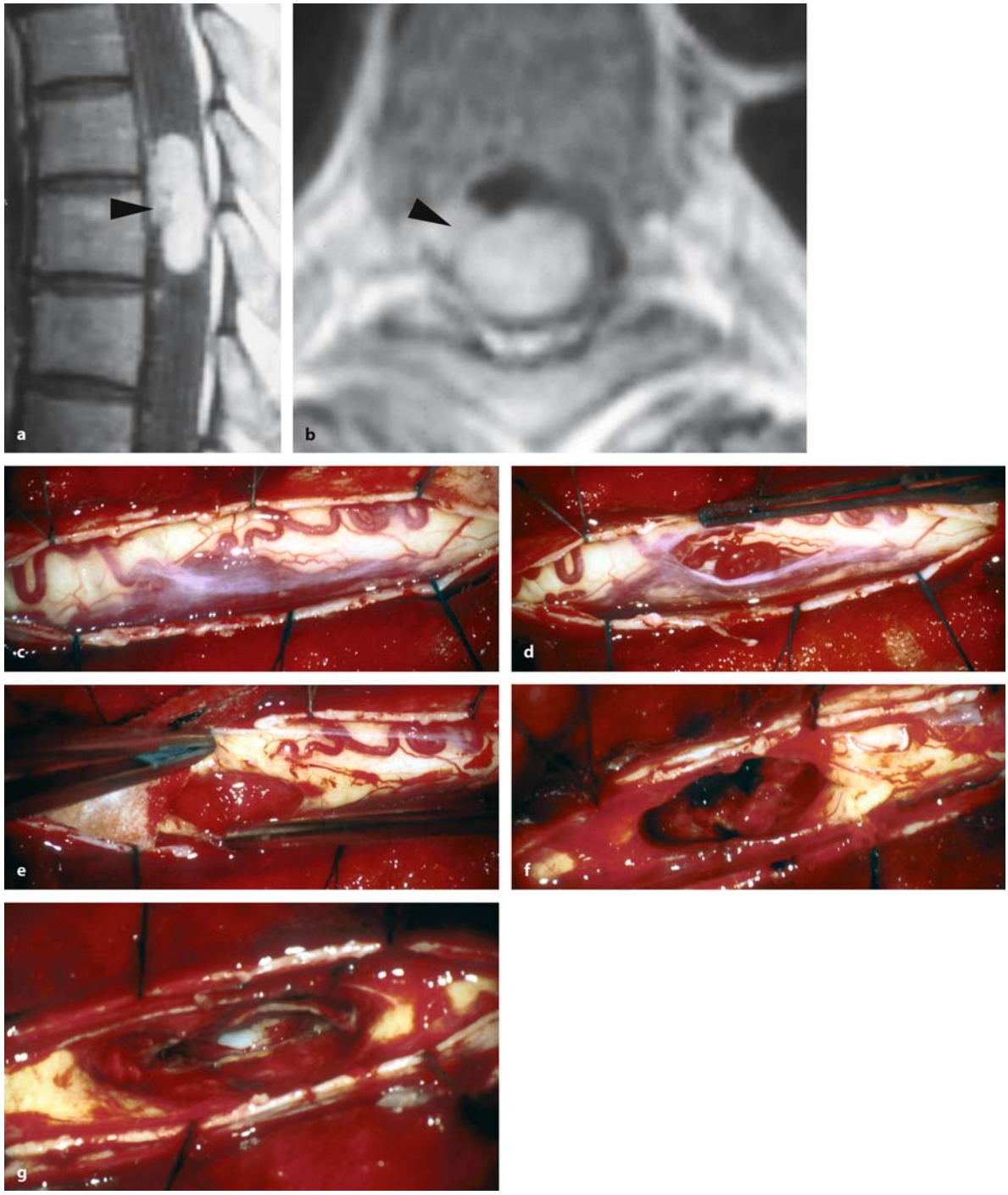

Fig. 3.49. T1-weighted, contrast-enhanced sagittal (**a**) and axial (**b**) MRI images of an intramedullary angioblastoma at Th6–Th7 in a 47-year-old woman with a 4-month history of pain and progressive paraparesis. Both scans reveal that the main feeders of this tumor come from the right anterior side (*arrowheads*). The intraoperative views before (**c**) and after arachnoid opening (**d**) show engorged vessels on the cord surface. **e** After opening of the cord in the midline, the tumor could be dissected from the spinal cord. While lifting out the tumor (**f**), the anterior feeders could be coagulated and transected, revealing the penetration of the tumor anteriorly on the right side, and exposing the ventral dura (**g**). (*Continuation see next page)*

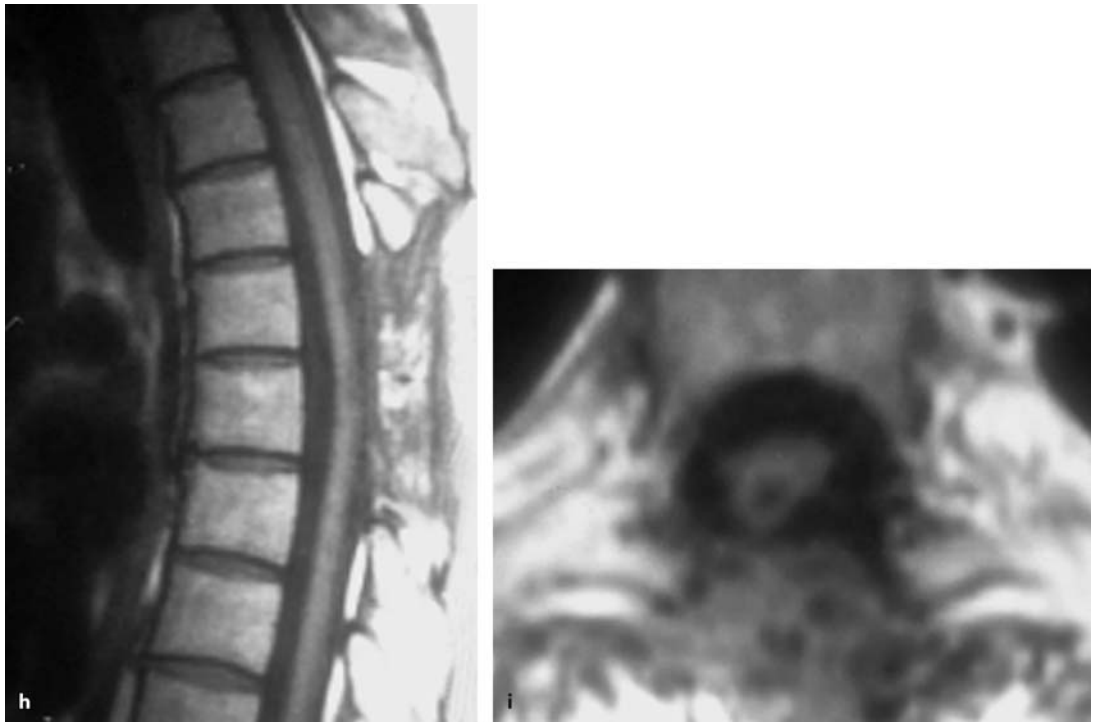

Fig. 3.49. (*Continued*) The postoperative sagittal (**h**) and axial (**i**) T1-weighted images confirm a complete resection and a posterior fixation of the cord to the dura. Except for some sensory deficits, the patient retained her neurological status. At this spinal level she developed an extramedullary recurrence posteriorly 6 years later, which could be resected completely

In patients with VHL disease, the symptomatic tumor is removed (Fig. 3.48), while other tumors, if present, are controlled with MRI on a yearly basis [62].

3.3.2.4 Removal of Hamartomas

Intramedullary dermoid cysts are growing lesions due to the metabolic activity of the cells in the cyst wall. These do not proliferate, but continue to produce substances that fill the cyst causing its expansion. Thus, radical excision of the entire cyst and its wall is the goal of surgery. Otherwise, a recurrence is almost certain. Unfortunately, this may be extremely difficult to achieve. The cyst wall may be extremely adherent to the spinal cord tissue requiring sharp dissection to deliver the cyst wall. If the cyst contents spill into the subarachnoid space during surgery, aseptic meningitis may result. If the cyst had ruptured prior to surgery, severe arachnoid adhesions may have formed (Fig. 3.50) [65] or the cyst contents may gradually spread inside the expanded central canal in a cranial direction [170]. Even abscess formations have been described [49]. Complete removal of a dermoid cyst may be impossible without damaging the cord in such instances. Partial resections or cyst evacuations are sometimes all that can be done (Fig. 3.50).

The intramedullary part of a spinal lipoma does not display a cleavage plane toward the spinal cord tissue. Therefore, attempts of radical resection are not recommended. As the lipoma does not display proliferative potential, decompression is all that is required. This may involve a partial resection of the extramedullary component in some cases. Usually, we just perform a laminotomy with a duraplasty (Fig. 3.51). As lipomas may be associated with arachnoid scarring [73, 171, 281] we prefer to leave the arachnoid membrane intact if no debulking is required.

Surgery for an intramedullary hamartoma may have to involve more than removal or decompression. Additional tethering mechanisms such as a diastematomyelia or a thick filum terminale may also have to be addressed. These techniques are described in the section on extramedullary tumors.

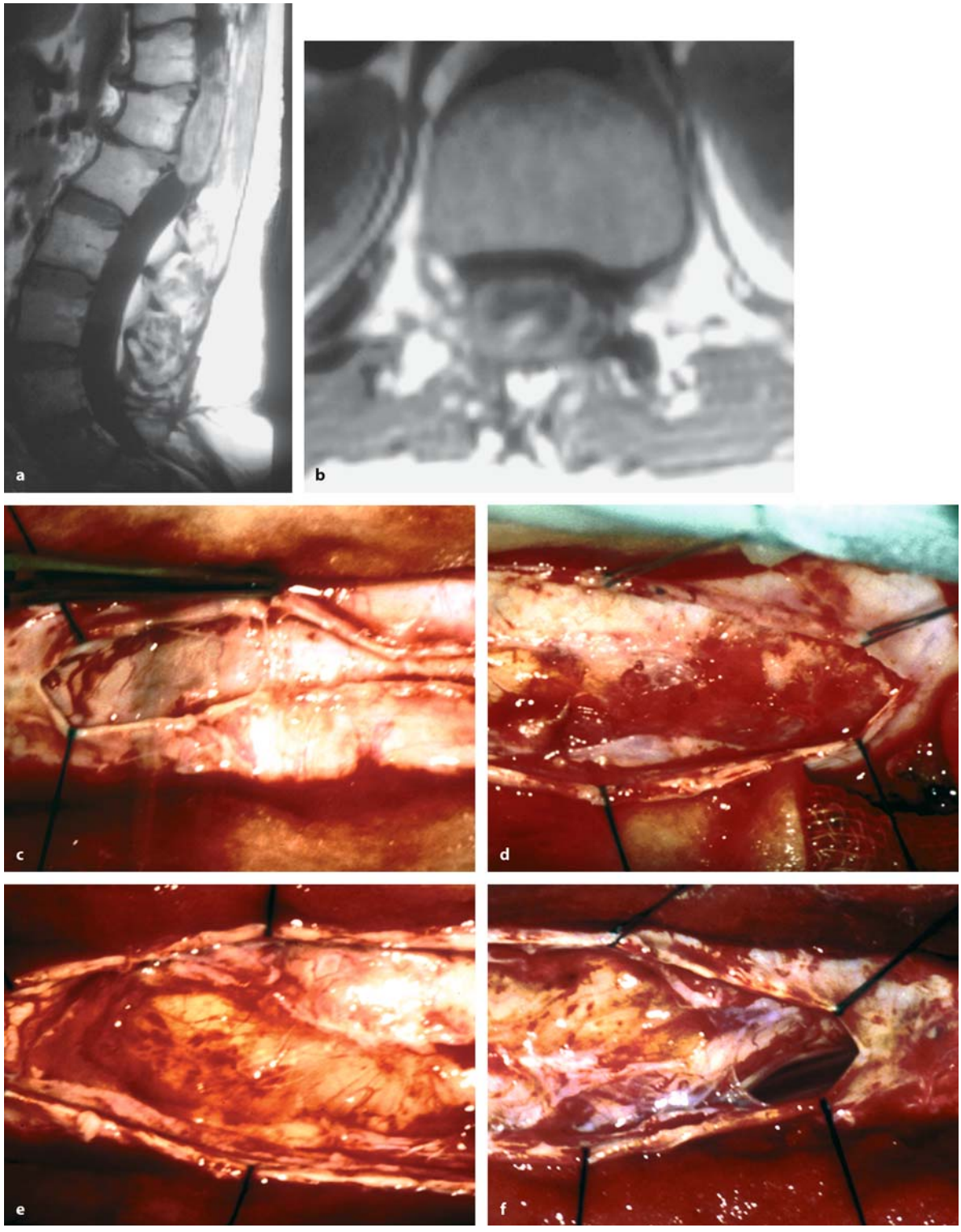

Fig. 3.50. T1-weighted, contrast-enhanced sagittal (**a**) and axial (**b**) MRI images of a recurrent intramedullary dermoid cyst at Th11–L1 in a 31-year-old woman with a 9-month history of pain and a slight paraparesis with intact sphincter functions. **c** This intraoperative view at dura opening shows the underlying adhesions between the dura, arachnoid membrane, and cord. The dermoid cyst is completely intramedullary at this level. **d** At the lower pole, arachnoid adhesions with the capsule of the exophytic dermoid cyst are visible. After partial resection, the upper (**e**) and lower (**f**) sections of the tumor bed reveal the amount of decompression. It was judged too hazardous to dissect the densely adherent capsule out of the cord. (*Continuation see next page*)

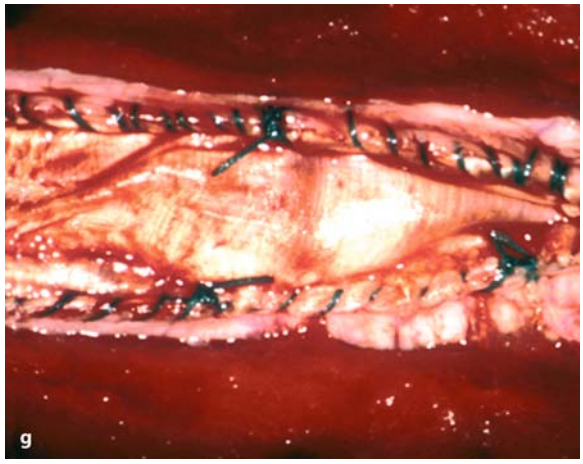

Fig. 3.50. (*Continued*) **g** The dura was closed with a fascia lata duraplasty. Postoperatively, the patient has been free of a recurrence for 4 years with an unchanged neurological status, improved pain, but distressing dysesthesias

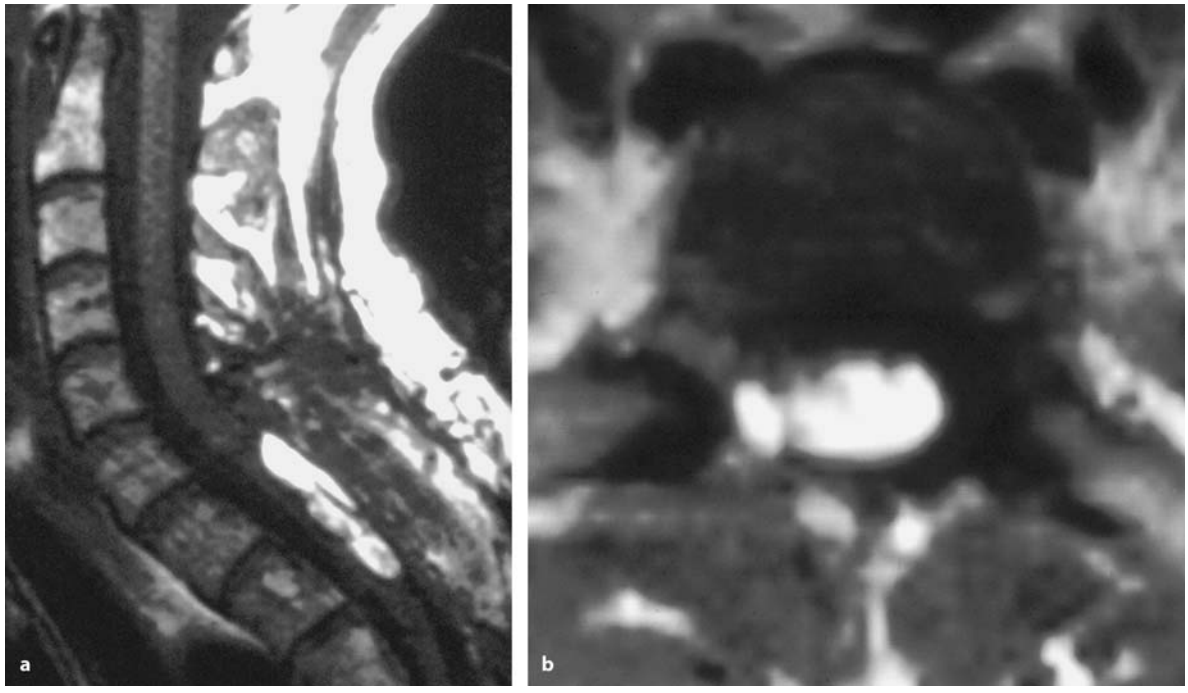

Fig. 3.51. T1-weighted sagittal (**a**) and axial (**b**) MRI images of an intramedullary lipoma at C7–Th1 in a 42-year-old woman with a 4-year history of severe pain and a moderate paraparesis. She had undergone a previous operation elsewhere without beneficial effect. (*Continuation see next page*)

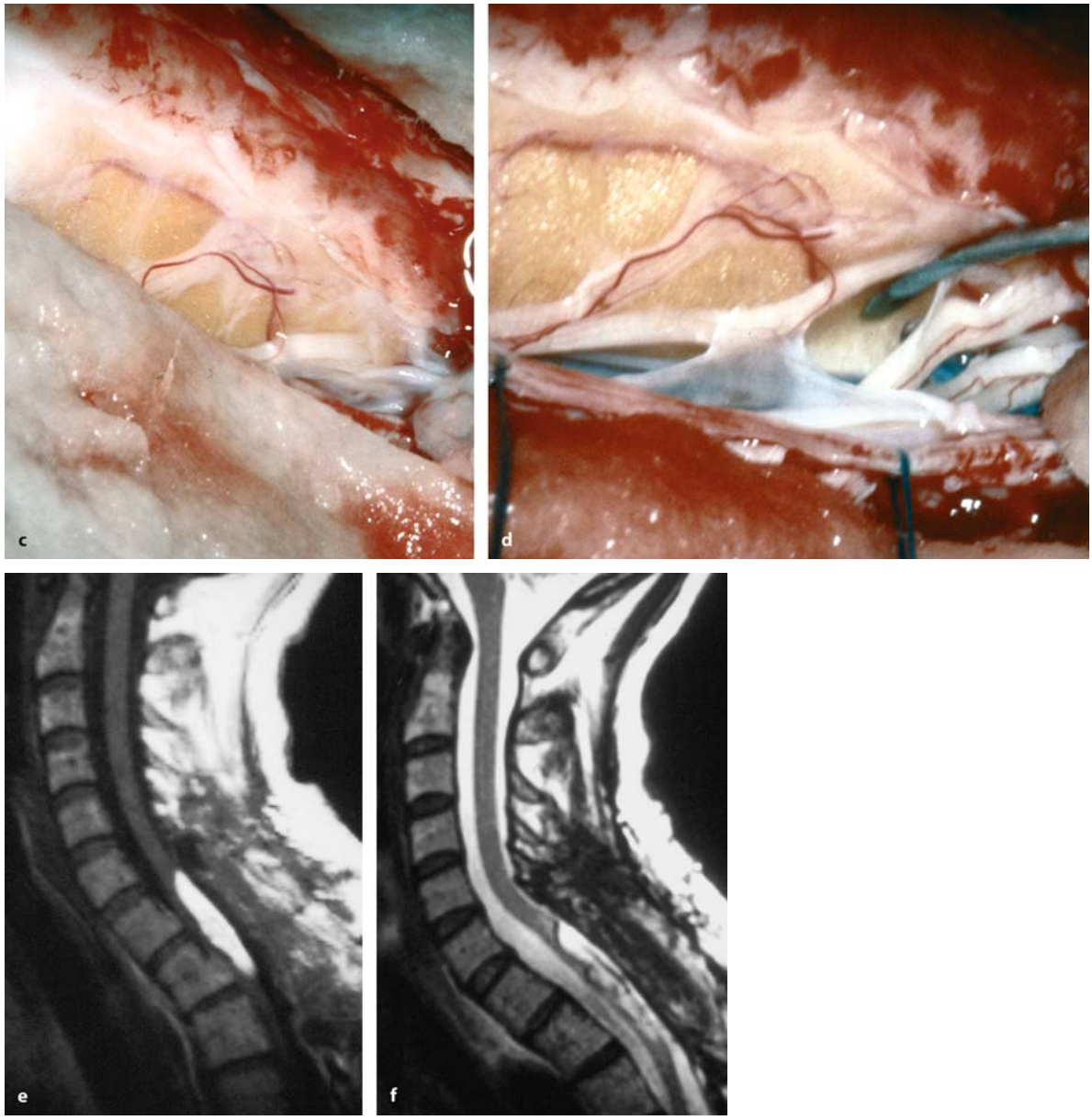

Fig. 3.51. (*Continued*) There is no major space-occupying effect detectable from this lipoma. **c**, **d** Intraoperative views after dura opening displayed a partly exophytic lipoma covered by posterior roots. After arachnoid dissection to untether the cord, no further attempts to remove the lipoma were undertaken. The dura was closed with a fascia lata duraplasty to avoid retethering. The post-operative sagittal T1- (**e**) and T2-weighted (**f**) images reveal no major cord tethering 3 months after surgery. Neurological symptoms gradually improved with a marked relief of pain

3.3.2.5 Removal of Cavernomas

With cavernomas, coagulation of the lesion will shrink it to such a degree that feeding vessels become identifiable, which then can be closed and transected. The hemosiderin-stained glial tissue around a cavernoma should not be removed. It is the result of repeated minor hemorrhages, does not belong to the pathology, and helps to preserve the surrounding cord tissue as a good protective layer (Fig. 3.52) [34, 216, 246]. Furthermore, some cavernomas are accompanied by large veins, so called developmental venous anomalies (DVAs). These veins have to be preserved as they drain normal tissue and do not represent tumor vessels [293]. However, it appears that DVAs are not a common feature of spinal cavernomas compared to other central nervous system locations.

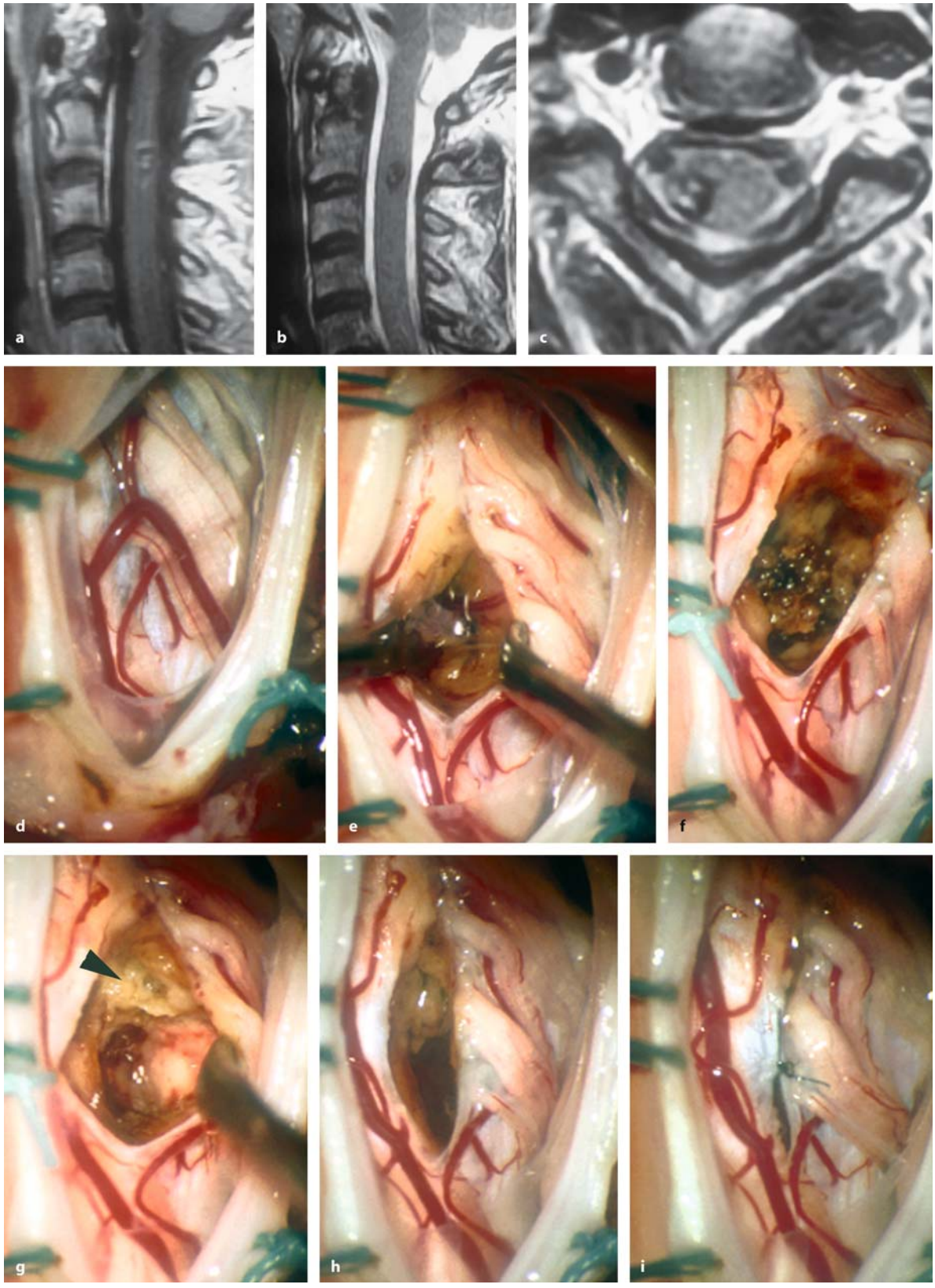

Fig. 3.52. (*Continuation see next page*)

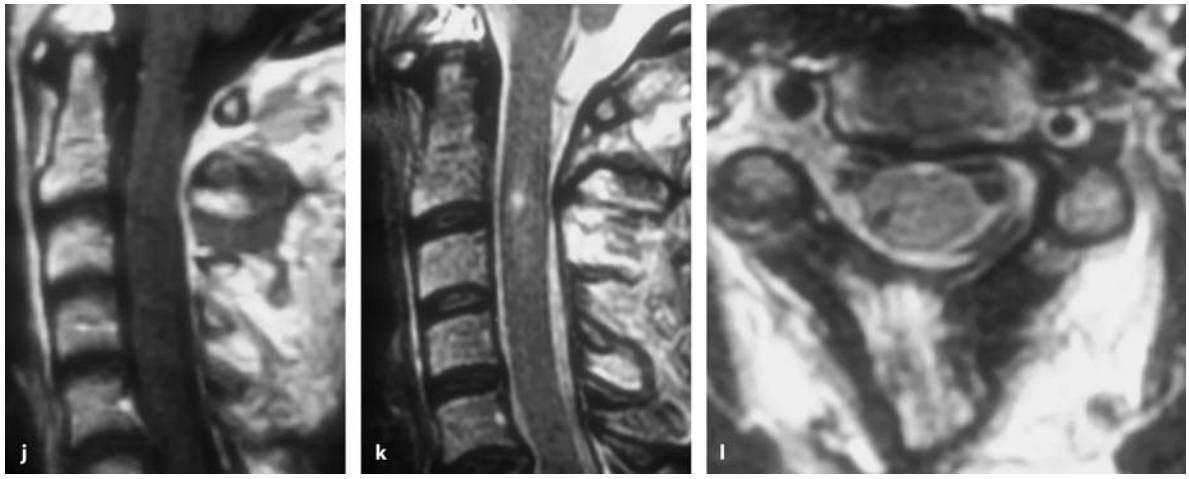

Fig. 3.52. (*Continued*) T1-weighted, contrast-enhanced sagittal MRI images (**a**), and sagittal (**b**) and axial (**c**) T2-weighted MRI images of an intramedullary cavernoma at C2/3 on the right side in a 51-year-old woman with occipital pain on the right side. **d** This intraoperative picture after dura and arachnoid opening, taken with the patient in the semisitting position, shows a completely normal cord surface. **e** With opening of the pia at the dorsal root entry zone with two microdissectors, the gliotic tissue and remnants of small hemorrhages are visible. **f** With bipolar coagulation and application of suction on a very low setting, the cavernoma became visible, shrank, and disclosed the dissection plane. **g** After removal of the cavernoma, some of the surrounding gliosis is visible in the upper half (*arrowhead*). After releasing the pia retention sutures (**h**) the cord was closed with a 8-0 pia sutures (**i**). The postoperative, contrast-enhanced T1-weighted image (**j**) and the T2-weighted sagittal (**k**) and axial (**l**) scans after 1 year reveal a complete resection. The patient had no postoperative neurological deficits and reported a marked relief of pain

With anteriorly located cavernomas, several surgical options can be used. With sutures applied to dentate ligaments, the spinal cord may be rotated so that the anterolateral section of the cord becomes accessible even from a posterior approach. With resection of facet joints and pedicles, an even better access is achieved with this technique [208]. Another alternative is a ventral approach with partial or complete corpectomy and stabilization [97, 292].

3.3.2.6 Removal of Recurrent Tumors

For reoperation of an intramedullary tumor, the removal of the epidural scar may cause some problems. As a general principle, the dissection of the dura should start in an area not involved with the previous operation, preferably at the upper and lower margins of the first operation. With a small part of the neighboring lamina removed, the dura is identified and further dissection can be done much easier. If the first laminectomy has been extended further laterally than required, we just expose the dura in the midline leaving scar tissue on the dura laterally.

If the previous operation involved a laminotomy, exposure of the dura is much easier. The muscles can be detached from the laminae as usual. The miniplates or sutures are removed and the laminotomy block can be taken out or – if a bony fusion has occurred – is prepared with a small craniotome as described earlier. As the muscular layer is not attached to the dura in scar tissue, no further dissection is required once the laminae are taken out.

Before opening the dura, ultrasound may be useful to determine areas of intradural scarring that may attach the cord to the dura posteriorly. The strongest adhesions should always be expected right underneath the dura suture line. Therefore, the dura should not be opened through the old suture line, but lateral or medial to it (Fig. 3.53). In recurrent tumors, dura retention sutures should only be set under tension very carefully as the cord may be attached to the dura and, thus, any tension on the dura may affect the cord and its vascular supply. The arachnoid membrane should be left intact during opening of the dura to avoid injury to the spinal cord and its vessels. Once the dura is opened entirely, the arachnoid is opened with microscissors. If arachnoid adhesions exist, they should be dissected with sharp instruments to avoid tearing of small blood vessels and tension on the spinal cord (Figs. 3.50 and 3.53). If arachnoid scarring is severe, a complete arachnoid dissection should not be

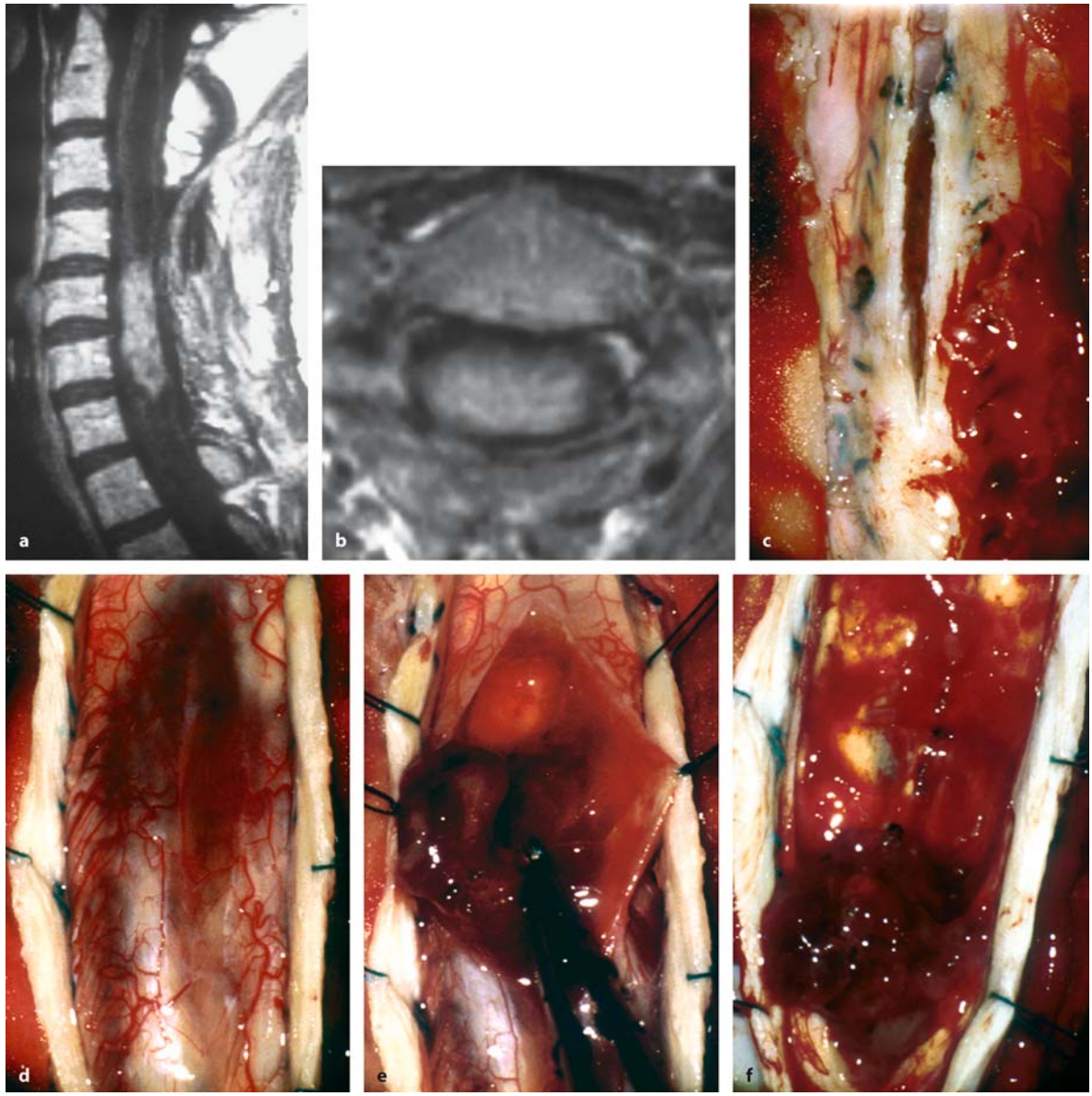

Fig. 3.53. T1-weighted, contrast-enhanced sagittal (**a**) and axial (**b**) MRI images of a recurrent intramedullary ependymoma at C5–C7 in a 42-year-old man with a 4-month history of a progressive tetraparesis. The tumor is accompanied by a large syrinx. **c** This intraoperative view, taken with the patient in the semisitting position, demonstrates the strategy of dura opening in such cases. The previous suture line was avoided and the duraplasty incised in the midline instead. **d** With opening of the arachnoid membrane, the tumor was apparent, protruding out of the previous area of the myelotomy. Starting at the top in the area of the syrinx (**e**) the tumor could be removed gradually, completely, and in one piece (**f**). (*Continuation see next page*)

performed. The chances are that these adhesions will reform postoperatively anyway and injury to the spinal cord during arachnoid dissection may be considerable. In some instances of recurrent tumors it was even difficult to differentiate between the arachnoid membrane and the spinal cord surface. In these instances, arachnoid preparation should be kept to a minimum and the surgeon should concentrate on exposure of the posterior midline aspect of the cord using the nerve roots on either side as guidelines.

Depending on the previous operation, the intramedullary tumor may already protrude out of the previous myelotomy (Fig. 3.53), thus guiding the surgeon to the target. Depending on the ultrasound im-

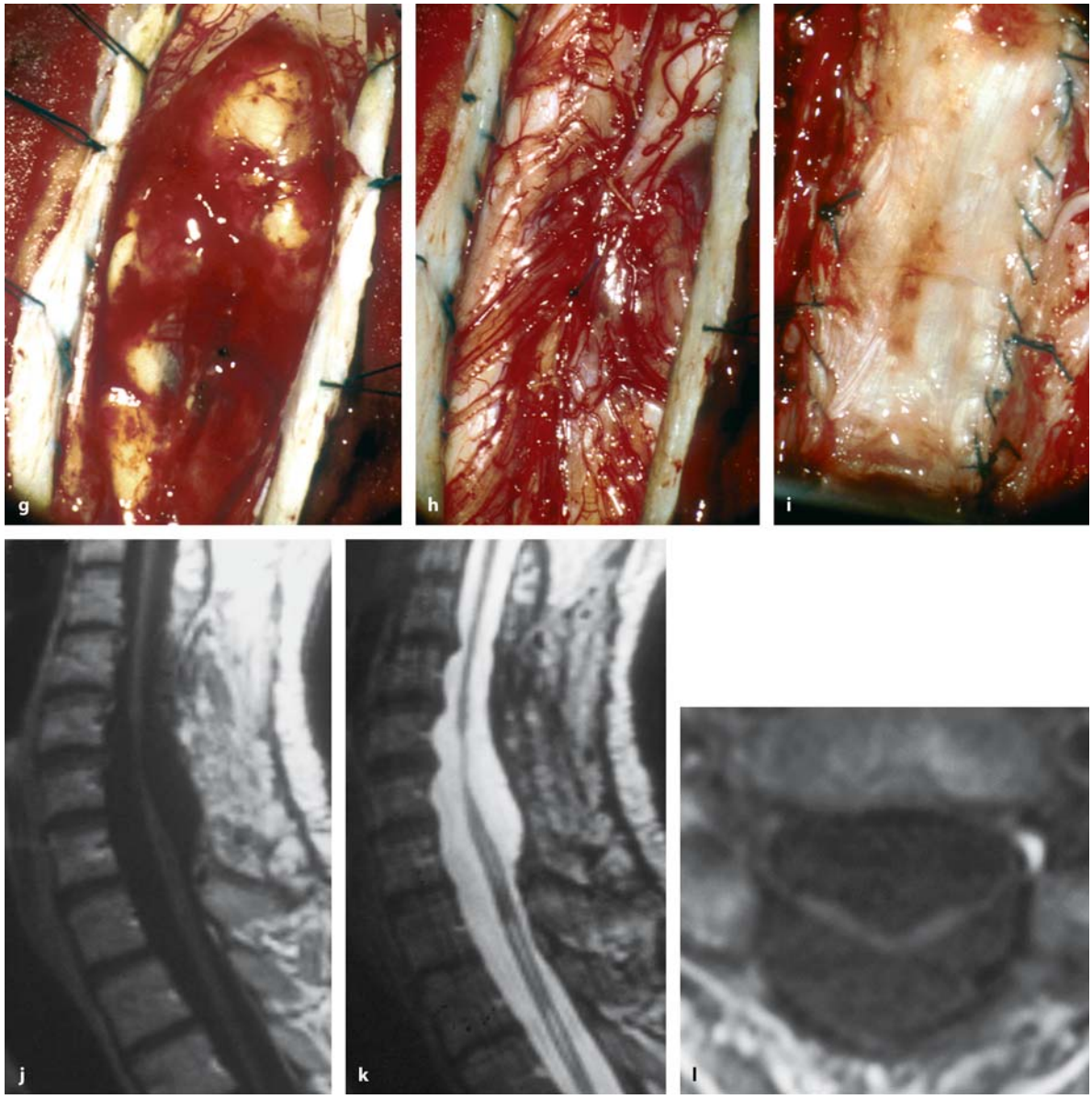

Fig. 3.53. (*Continued*) After complete resection (**g**) the cord was closed with 8-0 pia sutures (**h**) and a fascia lata duraplasty was inserted (**i**) to avoid cord tethering. The postoperative sagittal, contrast-enhanced T1-weighted image with contrast (**j**), the sagittal T2-image (**k**) and the axial T1-scan (**l**) display a complete resection with no postoperative cord tethering. The postoperative neurological status was unchanged except for aggravated sensory deficits. The patient has been free of a recurrence for 6 years. However, despite this perfect postoperative result, the patient developed a dysesthesia syndrome within 6 months of the operation

age, it may be necessary to extend the cord opening. Once this is achieved, further resection is undertaken as described earlier (Fig. 3.53). On the other hand, if only a biopsy procedure had been done, one can proceed just as in a primary operation.

As arachnoid scarring is the rule rather than the exception in these cases, dura closure is achieved with a duraplasty to prevent formation of further arachnoid adhesions after removal of the recurrent tumors (Figs. 3.50 and 3.53).

3.3.3 Closure

Once the tumor is removed we check that hemostasis is adequate. Inside the tumor bed we use as little coagulation as possible and recommend small cotton paddies, irrigation, and simply taking some time. To avoid adhesions between the tumor bed and the dura, we use a few 8-0 sutures to close the pia of the cord provided the tumor mass could be removed (Figs. 3.33, 3.36–3.38, 3.47, 3.52, and 3.53) [204]. Although recommended by some authors to prevent arachnoid scarring, we do not close the arachnoid membrane. Finally, the dura is closed watertight. In cases with severe arachnoid adhesions or after incomplete tumor removals we insert a dural graft to enlarge the subarachnoid space [301]. For this purpose we recommend Gore-Tex®, which offers good protection against intradural and epidural scarring [252]. Autologeous grafts revascularize and tend to form severe adhesions to the spinal cord. We elevate the duraplasty with a few retention sutures to lift the suture line off the cord surface. We then reinsert the laminae with titanium miniplates (Fig. 3.54) [263]. We do not use sutures for this purpose as they do not hold the lamina in a firm position. We had to revise two patients for lamina dislocations after suturing and have not seen this complication since we changed to miniplates. If required, the laminae can be supported or substituted with hydroxyapatite, as ingrowth of bone has been demonstrated for this material (Fig. 3.55) [175]. Steel miniplates should be avoided as they interfere with MRI.

The muscle layer should be closed with single sutures. This layer of closure is extremely important to prevent CSF fistulas [130, 355]. Fascia, subcutaneous tissue, and skin are closed in the conventional manner.

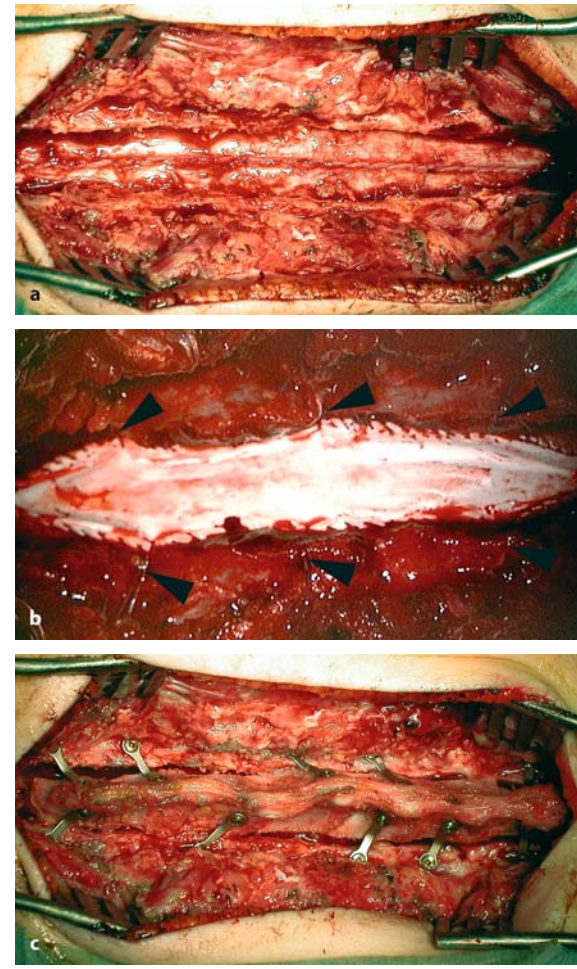

Fig. 3.54. Closure of the dura is either done with a primary running suture (**a**) or in patients with incomplete resections, a Gore-Tex® duraplasty (**b**) is inserted. Note the tenting sutures lifting the suture line. **c** The laminotomy bloc is inserted with small titanium plates and self-cutting screws. With long exposures, as depicted here, alternating plate fixations are sufficient.

3.3.4 Adjuvant Therapy

The treatment of choice in patients with an intramedullary tumor is surgery aiming at complete removal of the tumor. To perform a biopsy procedure with subsequent radiotherapy is no longer acceptable. If complete resection cannot be achieved, radiotherapy has been recommended for ependymomas [43, 283, 305, 338] and for astrocytomas [157, 176]. On the other hand, Chigasaki and Pennybacker [43], Epstein et al. [84], and Roux et al. [283] denied a beneficial effect for astrocytomas, and Mork and Loken [228] and McCormick et al. [217] for ependymomas. It appears, that radiation doses above 40 Gy have to be applied to achieve a response [104]. The possible role of stereotactic radiosurgery for the treatment of benign intramedullary tumors is not yet established. Ryu et al. [285] presented a series of seven patients with ten tumors; two patients improved, four remained stable, and one patient died within a maximum follow up of 2 years.

Currently, we recommend radiotherapy only for World Health Organization (WHO) grade III and IV tumors [137, 301, 312, 356]. In our series, 13 (7%) were classified as grade III and 7 (4%) as grade IV tumors. In other words, almost 90% of intramedullary tumors were benign, requiring surgery only. The role of chemotherapy for high-grade intramedullary tumors still needs to be determined [234].

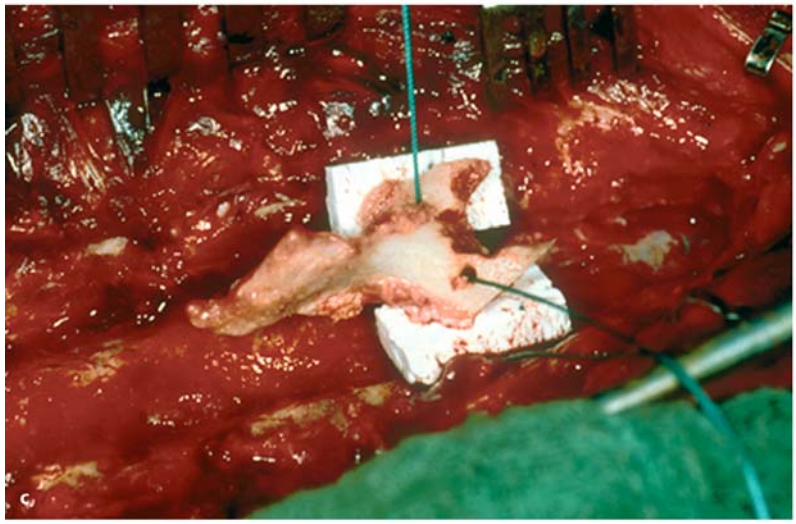

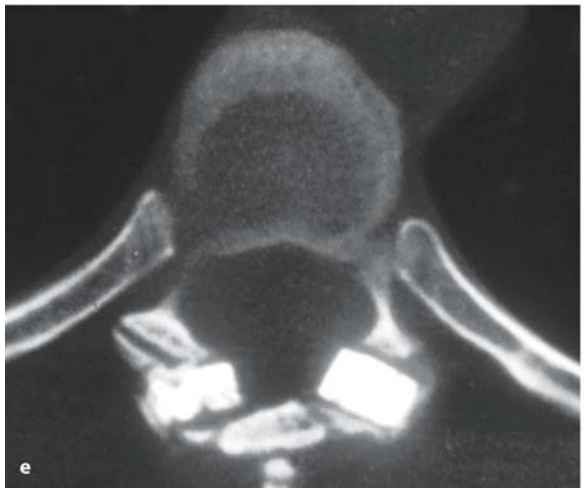

Fig. 3.55. This set of figures demonstrates an alternative method for decompression of the spinal canal. **a**, **b** T1-weighted, contrast-enhanced sagittal MRI scans of an intramedullary WHO grade I astrocytoma at Th10–L5 in a 31-year-old woman with an incomplete paraparesis and preserved sphincter control. The tumor has grown exophytically down the lumbar canal. A radical resection was judged too hazardous. We had particular concerns regarding the infiltrated caudal nerve roots (see also Fig. 3.3). **c** This view after dura closure shows the technique: the lamina is sutured to the pedicle with a small block of hydroxyapatite set in between. The postoperative X-ray (**d**) and CT image (**e**) demonstrate the amount of spinal canal enlargement and bony fusion in the depicted thoracic level. The neurological status could be preserved for 3 years. With 10 years of follow up, this patient has retained significant motor function in her legs and has control of sphincter functions

3.4 Postoperative Results and Outcome

The histological types of the operated intramedullary tumors are given in Table 3.1. The predominance of ependymomas and astrocytomas among intramedullary tumors in adults is well documented [222, 271, 312]. In children, low-grade astrocytomas are the most common type [222, 319].

3.4.1 Tumor Resection

Of 199 intramedullary tumors, 53% were removed completely, 32% were resected subtotally, and the remaining 15% were decompressed and underwent either a biopsy procedure or cystostomies with and without additional drains (Table 3.4). There were significant differences related to tumor histology, spinal level, and experience of the surgeon. With ependymomas (82%), cavernomas (83%), and with angioblastomas (90%) the great majority were resected completely. Astrocytomas, however, were classified as complete removals in only 18% of cases. Among cervical tumors, 70% were resected completely compared to 51% for thoracic and 18% for conus tumors (chi square test: p=0.0004). Comparing children and adults, the rate of total removal was considerably lower in children due to the higher proportion of astrocytomas (18% vs 58% for children and adults, respectively; p=0.0002).

In the literature, rates of complete resections vary greatly [98, 115, 120, 204, 271, 289, 312]. The series of Guidetti et al. [115] was collected in the premicrosurgical era. They achieved complete removals of ependymomas in 56% and in 6% for other intramedullary tumors. With the introduction of the operative microscope, rates of complete resections have increased significantly with consistently higher complete resection rates reported for ependymomas and angioblastomas compared to astrocytomas. Malis [204] removed 95% of ependymomas completely and achieved complete resections of astrocytomas in 19% of cases. Fornari et al. [98] gave figures for complete removals of 81% for ependymomas and of 50% for astrocytomas. These series represent the state of the art before the introduction of MRI. With the advent of MRI, rates of complete resection have increased for astrocytomas in particular. On the other hand, without modern imaging and microsurgical equipment, a recent paper from Africa recommended revival of the technique of Elsberg, with a two-stage operation within 2–3 weeks [158].

But what is a complete resection of an infiltrative tumor? We have classified tumor removal as complete if there was no detectable tumor tissue at the end of surgery and postoperative MRI scans demonstrated no visible tumor remnants. With terms like radical subtotal removal and 99% removal, for example, in the literature, one wonders about the criteria some investigators might have used for their analyses. Hejazi and Hassler [120] claimed complete resections for 85% of their intramedullary tumors. Fischer and Brotchi [95] reported complete resections of ependymomas in 94% and for astrocytomas in 37%. Raco et al. [271] reported on 202 intramedullary tumors and obtained complete resections for 81% of their ependymomas and grade I astrocytomas, with 12% complete resections for grade II astrocytomas and no complete removals for high-grade tumors. Shrivastava et al. [312] reported on 30 patients older than 50 years and obtained complete resections in 65%. They found no differences in resection rates according to the spinal level. Sandalcioglu et al. [289] reported a series of 78 intramedullary tumors with an average follow up of 34.4 months. Their series comprised 32 ependymomas, 15 astrocytomas, 10 metastases, 9 cavernomas, and 8 angioblastomas to mention the commonest entities. The low percentage of astrocytomas and the relatively high numbers of metastases and cavernomas is quite unusual. With this in mind, the rates of 83.3% for complete resections, 11.5% for subtotal resections, and 5% for biopsies become explainable. On the other hand, focusing on conus tumors, Mathew and Todd [211] achieved a complete resection in 2 out of 22 patients. This underlines the specific problems encountered with tumors in that region.

Although complete tumor removal should always be attempted [57], we emphasize that radicality should

Surgery	Benign tumors	Malignant tumors	Total
Complete	104 (58%)	2 (10%)	106 (53%)
Subtotal	46 (26%)	17 (81%)	63 (32%)
Decompression/ Biopsy/Cystostomy	28 (16%)	2 (10%)	30 (15%)

Table 3.4. Surgical results for intramedullary tumors

not be forced, especially when a clear-cut cleavage plane cannot be identified – as in patients with astrocytomas – or the experience of the surgeon is limited. If we analyze the resection rates of ependymomas, angioblastomas, and cavernomas related to surgical experience in our series, we observed a high rate of complete resection (>80%) for experienced surgeons and a lower rate of less than 70% with less experienced surgeons. Throughout the years, a learning curve could be observed. Rates for complete resections of these tumor entities rose in our series from 50% before 1985, to 72% between 1986 and 1990, to 81% between 1991 and 1995, and finally to 97% for the last period between 1996 and 2003.

The neuroradiological evaluation of the amount of resection is often complicated by postoperative intramedullary signal changes that take up gadolinium and are difficult to differentiate from tumor remnants [312]. One distinguishing feature between intramedullary scar tissue and tumor is the presence of cord enlargement associated with tumor remnants [23, 26]. Quite often, however, only repeated MRI scans can provide the decisive information. In patients who have undergone radiotherapy, the distinction between tumor recurrence and radiation-induced signal changes may be even more difficult [262].

3.4.2 Clinical Results

The immediate postoperative result is related to the preoperative status, the spinal level of the tumor, and the experience of the surgeon regardless of tumor histology [6, 38, 54, 60, 80, 82, 84, 85, 94, 95, 115, 118, 124, 204, 252, 271, 301, 317, 335, 346, 347]. The extent of tumor removal has only a minor influence on the short-term postoperative outcome [6, 56, 118, 215].

Table 3.5. Clinical course for patients with benign and malignant intramedullary tumors

Symptom	Preoperative status	Postoperative status	3 Months postop.	6 Months postop.	1 Year postop.
Pain					
Benign	4.1±1.0	3.9 ±0.9	4.3±0.9	4.3±0.9	4.3±0.9**
Malignant	4.1±1.2	4.2±0.9	4.5±0.7	4.5±0.7	
Hypesthesia					
Benign	3.3±1.0	2.4±1.2	2.6±1.2	2.7±1.2	2.7±1.2**
Malignant	3.0±0.7	2.1±1.3	2.3±1.3	2.3±1.3	
Dysesthesias					
Benign	4.1±0.9	4.1±0.9	4.0±0.9	4.0±1.0	3.9±1.0
Malignant	4.2±0.9	4.5±0.5	4.4±0.7	4.4±0.7	
Gait					
Benign	3.5±1.3	2.9±1.4	3.2±1.4	3.5±1.5	3.5±1.4
Malignant	2.5±1.4	2.0±1.6	2.3±1.8	2.2±1.7	
Motor power					
Benign	3.6±1.3	3.2±1.4	3.5±1.3	3.6±1.3	3.7±1.3
Malignant	2.9±1.5	2.4±1.7	2.6±1.8	2.6±1.8	
Sphincter function					
Benign	4.2±1.3	3.7±1.8	4.0±1.5	4.1±1.4	4.1±1.4
Malignant	4.1±1.5	3.5±2.1	3.5±2.1	3.5±2.1	
Karnofsky score					
Benign	70±16	62±17	67±17	69±17	69±18
Malignant	56±21	53±19	56±21	57±20	

*$p<0.05$, **$p<0.01$; statistically significant difference between preoperative status and 1 year or 6 months postoperatively; abbreviation: postop. = postoperatively

In our series, the postoperative course was characterized by transient worsening of neurological symptoms in 44% of patients for a few days or even months before functional recovery occurred [38, 60, 120, 215, 217]. In 68% of these, the preoperative status was reached again within 3 months, in 98% within 1 year, and for one patient it took 2 years. We attribute this transient deterioration to edema or interference with spinal cord blood flow, especially on the venous side. The transient deterioration affected gait, motor power, and bladder and bowel function. Therefore, the radiological and clinical examination after 3 months can be considered as a landmark evaluation for a patient who underwent surgery for an intramedullary tumor. Once the operative region has healed, the MRI becomes reliable to assess the radicality of removal, and arachnoid scarring leading to tethering of the cord – if it occurs – can be detected. Most patients have recovered from their postoperative deterioration and one can cautiously make a prognosis as to how the clinical course will probably continue.

As a general rule, the patient can nowadays expect to retain the preoperative neurological status with a successful operation in the long term. This empha-

Table 3.6. Clinical course for patients with benign intramedullary tumors related to tumor removal

Symptom	Preoperative status	Postoperative status	3 Months postop.	6 Months postop.	1 Year postop.
Pain					
Complete	4.1±1.0	4.0±0.8	4.2±0.8	4.3±0.9	4.2±0.9
Subtotal	4.1±1.1	3.7±1.1	4.3±1.0	4.5±0.8	4.5±0.8*
Biopsy	4.1±1.0	4.2±0.9	4.5±0.8	4.3±0.8	4.3±0.9
Hypesthesia					
Complete	3.3±0.8	2.3±1.0	2.5±1.0	2.6±1.0	2.6±1.0**
Subtotal	3.1±1.3	2.2±1.4	2.3±1.4	2.5±1.4	2.6±1.4**
Biopsy	3.3±1.3	3.2±1.4	3.3±1.4	3.2±1.7	3.2±1.7
Dysesthesias					
Complete	3.8±0.9	3.9±0.9	3.8±0.9	3.8±0.9	3.8±1.0
Subtotal	4.2±1.0	4.2±1.0	4.0±1.0	3.9±1.1	3.9±1.1
Biopsy	4.3±1.0	4.4±0.9	4.5±0.8	4.6±0.8	4.6±0.7
Gait					
Complete	3.7±1.1	3.0±1.3	3.3±1.3	3.6±1.3	3.6±1.3
Subtotal	3.0±1.6	2.2±1.6	2.8±1.7	2.8±1.7	2.9±1.7
Biopsy	4.0±0.9	3.8±1.1	3.9±1.0	4.1±1.0	4.0±1.1
Motor power					
Complete	3.9±1.1	3.4±1.4	3.7±1.2	3.8±1.2	3.9±1.1
Subtotal	3.1±1.5	2.7±1.4	3.0±1.4	3.1±1.5	3.1±1.6
Biopsy	3.3±1.1	3.2±1.4	3.5±1.5	3.7±1.3	3.9±1.2
Sphincter function					
Complete	4.3±1.2	3.8±1.7	4.1±1.4	4.2±1.3	4.2±1.3
Subtotal	4.1±1.6	3.3±2.1	3.7±1.9	3.7±1.8	3.8±1.8
Biopsy	4.3±1.0	4.4±1.0	4.4±1.0	4.4±1.0	4.4±1.0
Karnofsky score					
Complete	71±15	63±17	68±16	71±17	71±17
Subtotal	66±19	54±17	61±18	63±19	64±19
Biopsy	74±9	71±13	72±15	74±14	73±15

Statistically significant difference between preoperative status and 1 year or 6 months postoperatively: *$p<0.05$, **$p<0.01$

sizes that surgery has to be recommended early. This statement is valid regardless of age or histology. Very good results of surgery can be obtained for small children under the age of 3 years as well as for elderly patients [54, 312]. In the series of Sandalcioglu et al. [289], about two-thirds of the patients were unchanged or improved postoperatively, whereas 34.6% were worse. The preoperative state determined the postoperative result. Thoracic tumors were associated with higher morbidity, according to these authors.

We have analyzed the postoperative clinical course for individual symptoms separately for benign and malignant tumors in detail for the first 12 and

Table 3.7. Multivariate analysis for prediction of a high postoperative Karnofsky score for patients with intramedullary tumors

Factor	β-value
High preoperative Karnofsky score	0.7290
No recurrence	0.3899
Radiotherapy	0.2109
Syrinx	0.1366
Long history	0.1325
Female sex	0.1127
No dysesthesia syndrome	0.0878

Correlation: r=0.8222, p<0.0001

Table 3.8. Clinical course for patients with intramedullary tumors related to the preoperative Karnofsky score

Symptom	Preoperative status	Postoperative status	3 Months postop.	6 Months postop.	1 Year postop.
Pain					
Preop. score					
≥70	4.2±0.9	4.1±0.8	4.3±0.7	4.4±0.7	4.4±0.8*
<70	3.6±1.1	3.6±1.2	4.1±1.0	4.3±1.0	4.4±0.9*
Hypesthesia					
Preop. score					
≥70	3.5±0.8	2.7±0.8	2.8±0.9	2.9±0.9	2.9±0.9**
<70	2.3±1.2	1.3±1.4	1.4±1.5	1.6±1.6	1.6±1.6*
Dysesthesias					
Preop. score					
≥70	4.0±0.9	4.1±0.8	4.0±0.8	4.0±0.9	3.9±0.9
<70	3.6±1.0	3.8±1.1	3.8±1.1	3.9±1.1	4.0±1.1
Gait					
Preop. score					
≥70	4.0±0.7	3.2±1.1	3.7±1.0	3.9±1.0	3.9±1.0
<70	1.6±1.2	1.1±1.2	1.3±1.2	1.4±1.4	1.5±1.5
Motor power					
Preop. score					
≥70	4.1±0.9	3.6±1.2	3.9±1.0	4.0±0.9	4.0±0.9
<70	2.0±1.3	1.6±1.2	1.8±1.3	2.0±1.4	2.1±1.6
Sphincter function					
Preop. score					
≥70	4.7±0.7	4.4±1.3	4.5±1.0	4.6±0.9	4.6±0.9
<70	2.8±1.9	1.7±1.9	2.3±1.7	2.5±1.8	2.6±1.8
Karnofsky score					
Preop. score					
≥70	77±6	67±13	73±12	75±11	75±12
<70	43±12	40±11	42±11	45±14	46±17

Statistically significant difference between preoperative status and 1 year postoperatively: *p<0.05, **p<0.01; abbreviation: preop. socre = preoperative Karnofsky score

6 months after surgery, respectively (Table 3.5). As far as subjective symptoms are concerned, pain may improve postoperatively, whereas dysesthesias are generally left unchanged. Sensory deficits, however, tend to increase almost always as a result of the operative approach, with only slight subsequent recovery. These observations are made for benign and malignant tumors alike. For benign tumors, the remainder of the neurological symptoms after 1 year are on average as preoperatively, whereas with malignant tumors a trend toward deterioration becomes detectable after 6 months.

In Table 3.6 the effect of surgery on postoperative outcome is outlined. Comparing complete and subtotal resections, no differences become apparent considering that the preoperative state was significantly worse for patients undergoing subtotal removal as far as gait ataxia, motor weakness, and the average Karnofsky score are concerned. With biopsy procedures and decompression, postoperative deteriorations can be avoided and satisfactory results for the first postoperative year were observed. However, subsequent tumor growth will lead to worse clinical results later in the course.

To predict a high Karnofsky score after 1 year, we performed a multiple regression analysis. This score can be expected to be high provided the patient has a high Karnofsky score before surgery, does not experience a tumor recurrence, and undergoes radiotherapy (for high-grade tumors). Less important predictors were the presence of a syrinx, a long preoperative history, female sex, and no postoperative dysesthesia syndrome (Table 3.7). The amount of resection was not an independent factor.

Finally, the clinical course was analyzed according to the preoperative Karnofsky score (Table 3.8). For patients with preoperative scores between 70 and 100 and those below 70, identical postoperative courses were observed with stabilization of the preoperative status. In other words, even for patients with more severe preoperative deficits, surgery can still preserve function. However, what has been lost before surgery will not be regained. The final result will always remain worse compared to patients with the same pathology but operated before severe deficits had developed.

3.4.3 Syringomyelia

Of 199 intramedullary tumors, 48% presented with an associated syrinx [15, 265, 267]; 33% were above and 11% below the tumor level, 56% exhibited a syrinx above and below the tumor, and 9% were associated with syringobulbia. A tumor-associated syrinx was found more often in adults than in children (49% and 40%, respectively). Ependymomas (65%) and hemangioblastomas (90%) showed the highest proportion of syrinx formation. Astrocytomas (31%), cavernomas (33%), or hamartomas (20%) were less often accompanied by syringomyelia. The proportion of tumors associated with syringomyelia declined with the spinal level: it was highest for cervical tumors (58%), intermediate for thoracic tumors (48%), and considerably lower for conus tumors (21%).

Whereas syringomyelia is generally related to disturbances of CSF flow, such as in arachnoid scarring [169, 170], this association is not evident in patients with tumor-associated syringomyelia. Arachnoid scars at the tumor level were found in equal proportions for tumors with and without syringomyelia (30% and 32% cases, respectively). Evidence for tumor hemorrhages were present in 26% patients with syringomyelia and 23% without an accompanying syrinx. This indicates that syrinx formation is not related to arachnoid changes, tumor hemorrhages, or hematomyelia in patients with intramedullary tumors.

Most authors consider disruptions of the blood–brain barrier as the most likely mechanism based on analyses of the protein content of the syrinx fluid [194]. This, however, would imply that tumor-associated cysts are observed throughout the spinal canal in equal proportions.

We consider changes of extracellular fluid dynamics due to the space-occupying intramedullary lesion as the major mechanism leading to syrinx formation in association with intramedullary tumors, and interpret a syrinx as a chronic interstitial edema [169]. Different rates of associated cysts in cervical, thoracic, and conus tumors may be explained due to different CSF and extracellular fluid dynamics in these spinal segments.

The presence of a syrinx favored resectability of the tumor [38, 39]. The rate of total tumor removal was higher in patients with accompanying syrinx compared to those without (72% and 35%, respectively; chi square test: $p<0.0001$), mainly due to the higher proportion of ependymomas. Tumor removal alone was sufficient to decrease syrinx size, as confirmed for 92% of patients with adequate pre- and postoperative MRI scans. A syrinx associated with an intra-

medullary tumor does not need any additional surgical maneuvers such as shunts or myelotomies. With removal of the tumor, the syrinx will regress automatically, as demonstrated in several figures above.

3.4.4 Complications

3.4.4.1 Short-Term Complications

Complications were encountered in 15% of patients (Table 3.9). The commonest problem was a postoperative CSF fistula. This complication is avoidable with a meticulous dura suture and tight soft-tissue closure, especially of the muscular layer. In recurrent cases, soft-tissue scarring puts the patient at an increased risk for fistula formation. In such instances we recommend insertion of a lumbar drain at surgery and to keep it for about 1 week as a preventive measure, especially if a Gore-Tex® duraplasty has been inserted. Depending on the intraoperative situation, it may even be advisable in selected cases to insert a layer of fascia lata to reinforce the dura suture.

As already mentioned, we have encountered two lamina dislocations in patients in whom the lamina had been fixed with sutures. We have not seen this complication since we have changed to miniplates for this purpose (Fig. 3.56).

We observed a surgical mortality within the first 30 days of 1.1%. One 70-year-old patient with an intramedullary metastasis died 3 weeks after surgery. Another 33-year-old patient with a recurrent, high cervical ependymoma died due to sudden respiratory failure 3 weeks after an uneventful operation and preserved neurological function. Unfortunately, an autopsy was denied. Brotchi and Fischer [28] observed a surgical mortality rate of 3.2% in a series of 93 ependymomas.

Table 3.9. Complications for patients with intramedullary tumors

Type	Total
Cerebrospinal fluid leak	11
Wound infection	7
Hemorrhage	2
Lamina dislocation	2
Instability	1
Delayed cord edema	1
Urinary tract infection	4
Gastrointestinal infection	1
Acute psychosis	1
Total	**30** **15%**

3.4.4.2 Long-Term Complications

Late complications may be associated with spinal instability or postsurgical myelopathy. To avoid instabilities, intervertebral joints should be left intact during the exposure. It is not necessary to extend the exposure so wide that these joints are compromised. However, postoperative instabilities cannot be prevented by a small laminotomy alone. This complication becomes more common the higher the spinal level and the younger the patient is [131, 234], even though Yeh et al. [352] found a particularly high incidence of postoperative deformities in the thoracolumbar region. Lunardi et al. [199] observed postlaminectomy deformities in 24% and Takahashi et al. [325] in 40% of children operated for intramedullary tumors. Jallo et al. [152] reported postoperative spinal deformities in 66% of children, with 35% requiring stabilization procedures. Within a series predominantly of adult patients we observed no spinal instabilities after removal of an intramedullary tumor that would have required an intervention; however, we have seen kyphotic deformities, especially in children after laminectomies (Fig. 3.57).

Reinsertion of the vertebral lamina is supposed to protect against this late complication. However, such an effect has not been proven in adults and could only be demonstrated for children [234, 316, 352]. Even after reinsertion of the lamina, one important posterior anchor remains unrestored – the interspinous ligament. Furthermore, atrophy and abnormal innervation of neck and back muscles may cause muscular imbalances, which alone may be sufficient to induce spinal instability despite reinserted laminae. Furthermore, spinal deformities may above be present before surgery, as demonstrated earlier. Nevertheless, we recommend reinsertion of the laminae in all patients with miniplates after removal of the tumor, to restore the anatomy as far as possible. Avoiding fixation of the neck and back muscles to an epidural scar, one may consider a favorable effect to avoid neck and back pain related to muscular tension on the dura. Reinserted laminae also make a reoperation easier in the case of a tumor recurrence. We believe that these are reasons enough, even if a postoperative deformity cannot be prevented in all cases and monitoring by

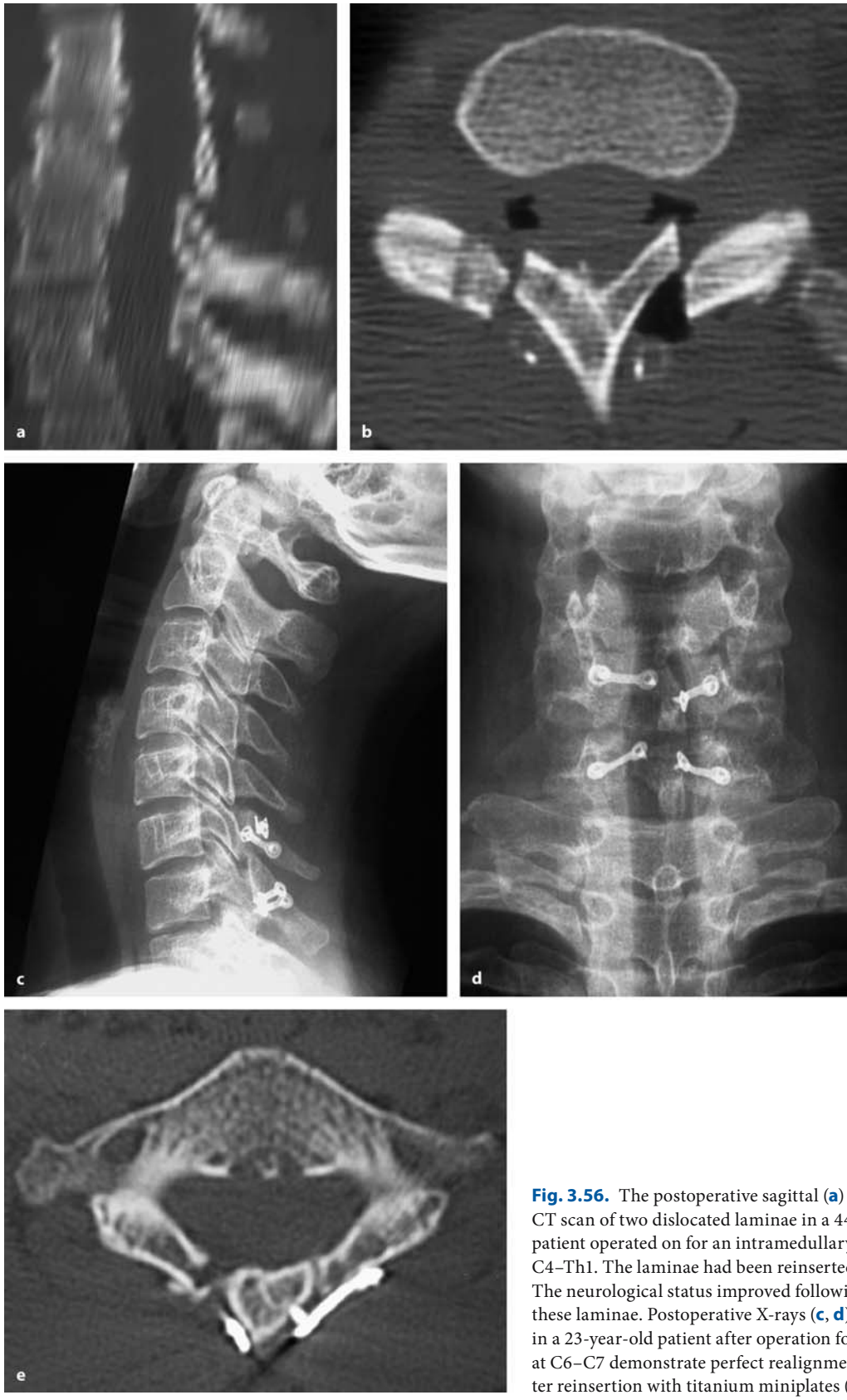

Fig. 3.56. The postoperative sagittal (**a**) and axial (**b**) CT scan of two dislocated laminae in a 44-year-old patient operated on for an intramedullary astrocytoma at C4–Th1. The laminae had been reinserted with sutures. The neurological status improved following removal of these laminae. Postoperative X-rays (**c**, **d**) and CT scan (**e**) in a 23-year-old patient after operation for an astrocytoma at C6–C7 demonstrate perfect realignment and fusion after reinsertion with titanium miniplates (see also Fig. 3.36)

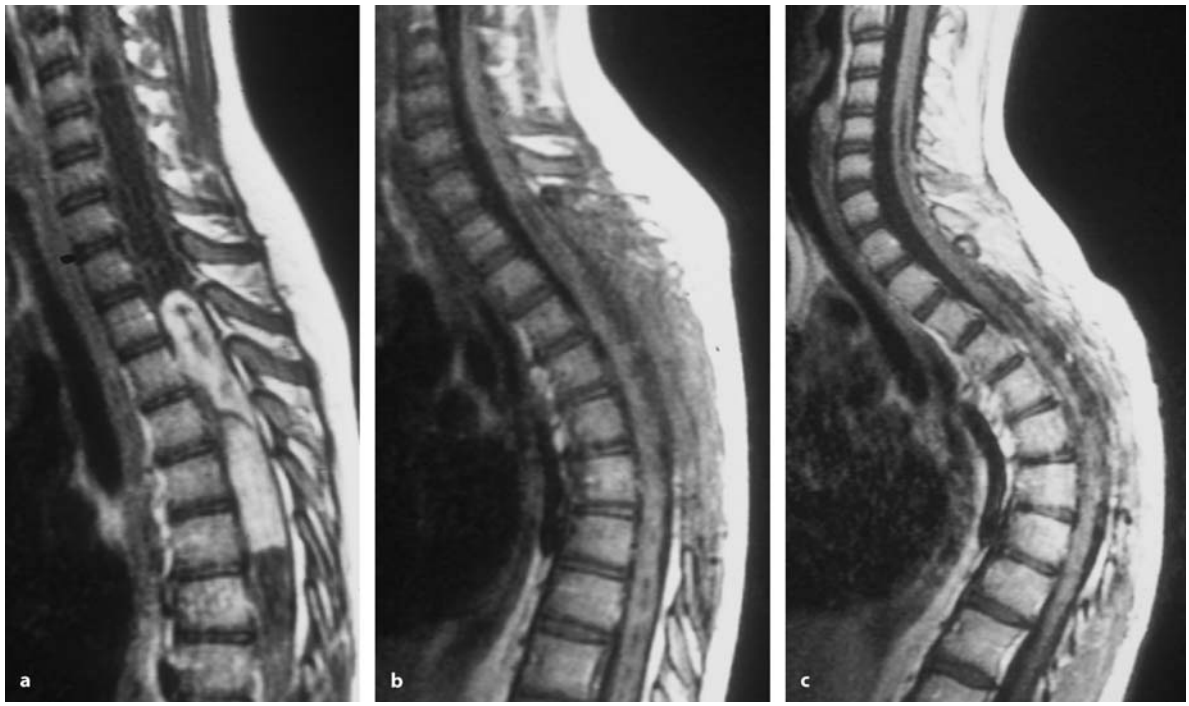

Fig. 3.57. This series of sagittal MRI scans of a WHO grade I astrocytoma at Th2–Th6 in a 10-year-old girl demonstrate the stability problems associated with these tumors, which may be aggravated by laminectomies. Compared to the preoperative scan (**a**), a kyphotic deformity started to develop as soon as 3 months after subtotal resection (**b**), and progressed further within 1 year (**c**)

experienced orthopedists is still recommended, and mandatory – especially in children [231].

A significant proportion of patients develop a postoperative dysesthesia syndrome, which is characterized by unpleasant dysesthesias – sometimes described as burning type – and pain. In a small number of these patients, even a progressive deterioration of neurological functions in the form of a progressive myelopathy in the absence of a tumor recurrence can be observed [113, 128, 215, 256, 271, 317, 318]. The etiology of this myelopathy is not entirely clear and is probably related to several factors. Greenwood [113] attributed these to worsening gliosis. Peker et al. [256] found a correlation with the number of affected spinal segments in ependymomas and attributed this syndrome to injury of the dorsal columns. Hoshimaru et al. [128] suggested that arachnoid scarring and cord atrophy predispose a patient to postsurgical myelopathy. Raco et al. [271] also suggested that postoperative cord tethering was responsible. Tethering was observed in 17% of their patients and was thought to be responsible for pain and dysesthesias in 8% of their patients. They recommended gabapentin and buprenorphine for treatment of this syndrome, while nine patients were reoperated for cord tethering, four patients experiencing considerable improvement and two patients some improvement.

We have observed this syndrome after 44 operations for intramedullary tumors, (22%). So far, we have not reoperated any patient for this problem. The symptoms usually began after about 2–3 months postsurgery and then either remained stable or progressed to neurological deterioration in six patients. Evaluation of the rates after complete resections (26%), subtotal removals (20%) and biopsy procedures (18%) revealed a correlation of this problem with the amount of resection. A similar correlation was found with the spinal level. While 23% were affected after removal of a cervical tumors, these figures dropped to 20% and 14% for thoracic and conus tumors, respectively. Furthermore, this problem is more common in adults than in children (23% and 15%, respectively). Its likelihood also varies with the tumor histology: we observed it in 56% of patients after surgery of a hamartoma, in 33% of cavernomas, and in 30% of ependymomas, but to a lesser degree for astrocytomas (14%) and angioblastomas (19%).

We have tried to establish a relationship between this syndrome and postoperative tethering of the cord to the overlying dura. Tethering was observed in 46%

Table 3.10. Multivariate analysis for prediction of a postoperative dysesthesia syndrome for patients with intramedullary tumors

Factor	β-value
Syringomyelia	0.2118
High preoperative Karnofsky score	0.2046
Adult age	0.1545
Female sex	0.1133

Correlation: r=0.3383, p=0.0113

of patients. Dysesthesia syndromes were more common in patients with postoperative cord tethering (35%) compared to those without (25%). However, this difference was not statistically significant. Such adhesions between dura and cord on MRI could be observed in 58% of patients after removal of intramedullary tumors early in our series. This figure was reduced to 26% by applying pial sutures to close the cord after tumor removal (Fisher test: p=0.0069). However, comparing the rate of patients developing a dysesthesia syndrome in those with and without cord suturing revealed no advantage for those with cord suturing. In summary, no relationship with postoperative cord tethering could be clearly established among our patients.

A multivariate analysis showed that the presence of a syrinx, a high preoperative Karnofsky score, adult age, and female sex were independent factors predisposing to this syndrome (Table 3.10, r=0.3383, p=0.0113). Comparison of tumors with and without syringomyelia showed a significantly higher proportion of dysesthesia syndromes for patients with a syrinx (27% and 14%, respectively; Fisher test: p=0.0244). In analogy to our experience with syringomyelia related to arachnoid scarring [170], one may decompress the area of surgery by a dural graft to maintain the patency of the subarachnoid space. This maneuver reduced significantly the rate of dysesthesia syndromes from 27% to 13% (Fisher test: p=0.0283).

3.4.5 Morbidity, Recurrences, and Survival

3.4.5.1 Morbidity

We observed permanent surgical morbidity (i.e., postoperative neurological worsening within 30 days of surgery without subsequent recovery) in 13% of cases. Combined with the aforementioned rate for transient postoperative neurological deterioration in 44% of patients, these figures combine to 57% of patients who experience an immediate postoperative worsening of neurological functions. Of these, about three-quarters will regain their preoperative status. This is essential information for every patient scheduled for such an operation.

Looking at possible factors influencing surgical morbidity, we observed a similar learning curve in terms of postoperative morbidity, as already mentioned for resection rates. Before 1985, permanent surgical morbidity was observed for 34% of patients. Between 1986 and 1995, this figure dropped to 12%. Since 1996, this rate declined further to 8%. The advent of MRI, however, seems to have had the most profound impact. Before 1988, the diagnosis of an intramedullary tumor relied on myelography, postmyelographic CT, or CT with intravenous contrast. During that period, surgical morbidity was 33%, dropping to 8% thereafter.

The major factor determining permanent morbidity, however, is the preoperative status of the patient. Numerous studies emphasized that the major factor determining long-term outcome is the preoperative neurological status [55, 57, 82, 98, 115, 124, 137, 215, 271, 317]. This can be attributed to marked differences in surgical morbidity in relation to the preoperative status. For patients with a preoperative Karnofsky score above 70 (i.e., patients able to live independently without assistance), permanent morbidity was 9%. For patients with scores between 40 and 70 the figure rose to 18%, and for patients with scores below 40, surgical morbidity was 30%. Moreover, a new postoperative deficit had considerably more serious functional consequences for those patients who were already significantly disabled preoperatively.

Cervical and thoracic tumors were associated with considerably less morbidity compared to tumors in the conus area (5.6%, 14.3%, and 26.5%, respectively; log-rank test: p=0.039) [38, 60, 211, 289, 318, 347]. The more precarious vascular supply in the thoracic cord, the smaller size of the cord in the lower spinal segments, and the dense concentration of important neurological functions in the small confined structure of the conus may explain this observation.

Arachnoid scarring was observed in 30% of operations for intramedullary tumors [43] and especially common in recurrent tumors (63% compared to 23% without a previous operation; Fisher test: p<0.0001). However, dissection of preexisting arachnoid scars did not increase surgical morbidity, as others have observed [96, 128].

3.4.5.2 Tumor Recurrences and Clinical Recurrences

Apart from a tumor recurrence, other mechanisms can lead to clinical deterioration of a patient after surgery for an intramedullary tumor. Therefore, it appears appropriate to distinguish between a tumor recurrence – as observed on postoperative imaging – and a clinical recurrence – as becomes apparent clinically.

Overall, tumor recurrence rates of 24% and 26% were observed after 5 and 10 years, respectively (Fig. 3.58) [107]. A multivariate analysis revealed that a complete resection (Fig. 3.59), a benign tumor grade (Fig. 3.60), and a high spinal level (Fig. 3.61) predicted a low tumor recurrence rate (Tables 3.11 and 3.12).

After complete resections, local recurrence rates of 3%, 8%, and 13% were observed after 1, 5, and 10 years, respectively (Table 3.12, Fig. 3.59; log-rank test: $p<0.0001$). Such a correlation between the amount of resected tumor and probability of a local recurrence has not been reported as so clear-cut in most studies [6, 43, 56, 107, 130, 137, 215, 318].

The significant difference in local recurrences between benign and malignant tumors, on the other hand, is self-explanatory (Fig. 3.60) [107]. With benign grades, recurrence rates of 9% and 18% were observed after 1 and 5 years, respectively, whereas malignant tumors recurred at rates of 44% and 68%, respectively (log-rank test: $p<0.0001$). The third independent factor was the spinal level, with particularly

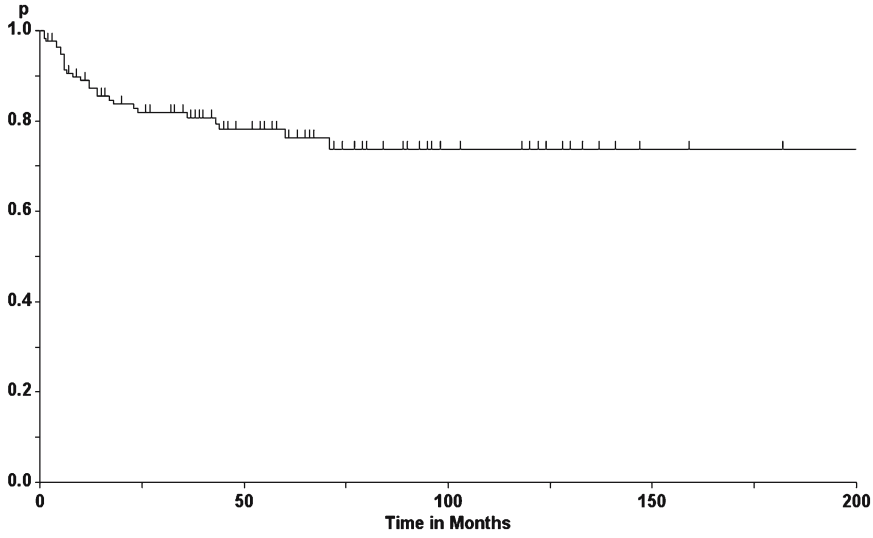

Fig. 3.58. Overall tumor recurrence rates for patients with intramedullary tumors

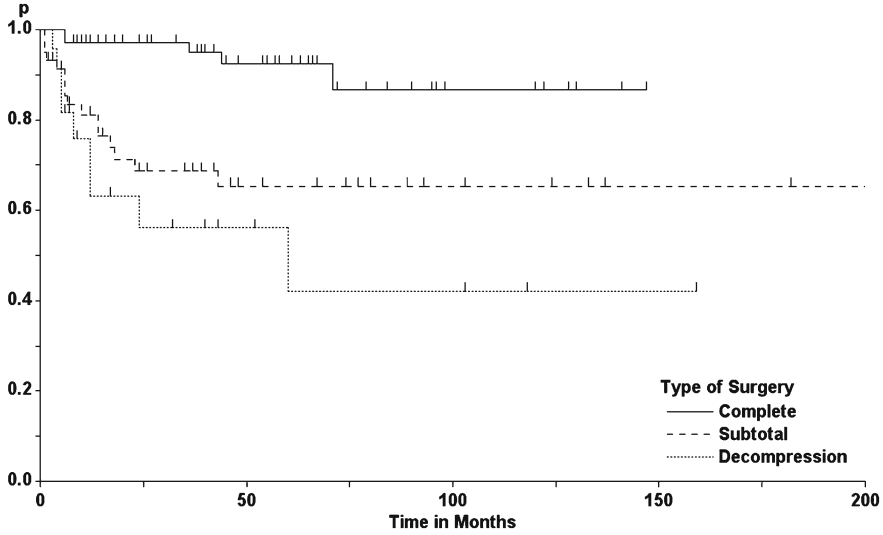

Fig. 3.59. Tumor recurrence rates for patients with intramedullary tumors as a function of the extent of tumor resection (log-rank test: $p<0.0001$)

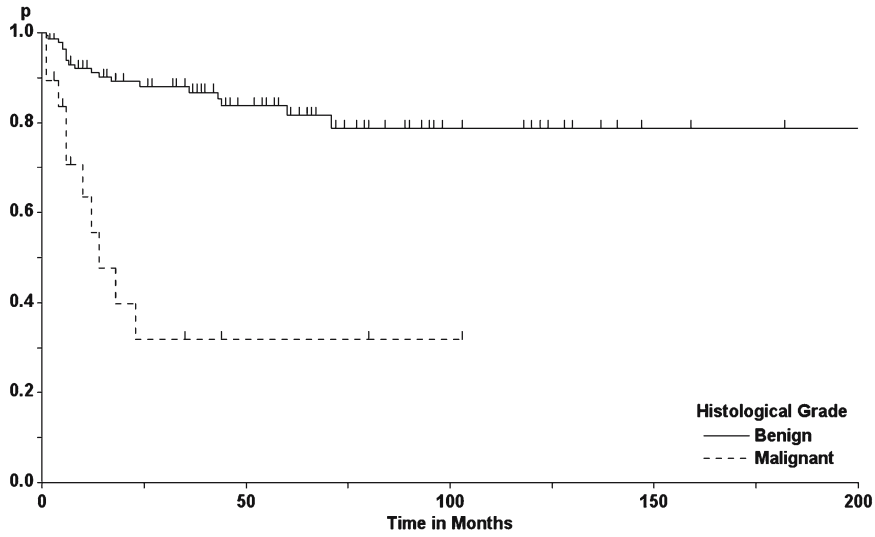

Fig. 3.60. Tumor recurrence rates for patients with intramedullary tumors as a function of histological grade (log-rank test: $p<0.0001$)

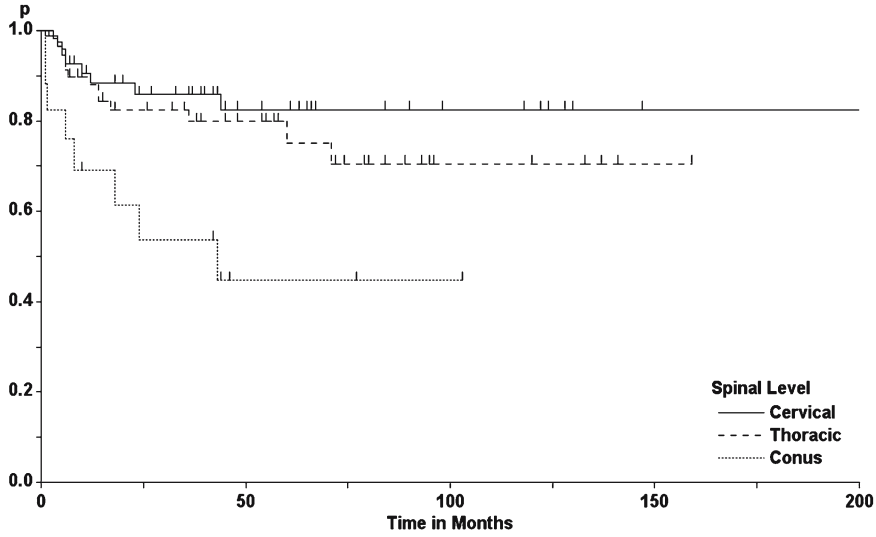

Fig. 3.61. Tumor recurrence rates for patients with intramedullary tumors as a function of spinal level (log-rank test: $p=0.0056$)

high recurrence rates for conus tumors (Fig. 3.61; log-rank test: $p=0.0056$).

If we then analyze which factors predispose to long-term stabilization of the patient's clinical condition (i.e., a low clinical recurrence rate), additional factors come into play apart from local tumor control. A multiple regression analysis was performed to predict a low clinical recurrence rate for patients with intramedullary tumors (Table 3.13). As for tumor recurrences, again a complete resection and a high spinal level were determined as independent factors. In addition, absence of arachnoid scarring, dissection of arachnoid scars, and no preoperative radiotherapy predicted a low rate of clinical deteriorations. This finding supports the concept that avoidance of cord tethering benefits patients in the long term.

Table 3.11. Multivariate analysis for prediction of a low tumor recurrence rate for patients with intramedullary tumors

Factor	β-value
Complete resection	0.2446
Benign grade	0.1660
High spinal level	0.1654

Correlation: $r=0.3422$, $p=0.0001$

Table 3.12. Tumor recurrence rates for patients with intramedullary tumors

Group	1 Year	5 Years	10 Years
Benign grade	9%	18%	21%
Malignant grade	44%	68%	68%
Complete resection	3%	8%	13%
Partial resection	19%	35%	35%
Biopsy/decompression	37%	58%	58%
Cervical	12%	18%	18%
Thoracic	12%	25%	30%
Conus	31%	55%	55%
Total	**13%**	**24%**	**26%**

Table 3.13. Multivariate analysis for prediction of a low clinical recurrence rate for patients with intramedullary tumors

Factor	β-value
Complete resection	0.3218
High spinal level	0.2101
No preop. arachnoid scar	0.1693
Arachnoid scar dissected	0.1114
No preop. radiotherapy	0.0995

Correlation: r=0.4536, p=0.0002

3.4.5.3 Survival

Finally, we analyzed postoperative survival rates: 87% of patients survived for 1 year, 76% for 5 years, and 73% for 10 years (Fig. 3.62). Multiple regression analysis determined that a benign histological grade (Fig. 3.63), no tumor recurrence, no arachnoid scarring, a high preoperative Karnofsky score (Fig. 3.64), and a long preoperative history predicted long survival (Table 3.14). For grade I tumors, survival rates of 84% after 5 and 10 years, respectively, were observed. With grade II tumors, even 92% survived for 5 and 10 years, respectively. The results for malignant intramedullary tumors were nothing but frustrating for patients with grade IV tumors and somewhat variable for patients with grade III tumors (Table 3.15) [107, 318]. For grade IV tumors, 80% died within 12 months of surgery, with all patients dead within 2 years regardless of the amount of resection or the type of adjuvant therapy. With grade III tumors, we observed higher survival rates, with three patients surviving more than 5 years. We also observed subarachnoid dissemination in many patients with malignant intramedullary tumors. Once this occurred, patients died within a few weeks or months at the latest.

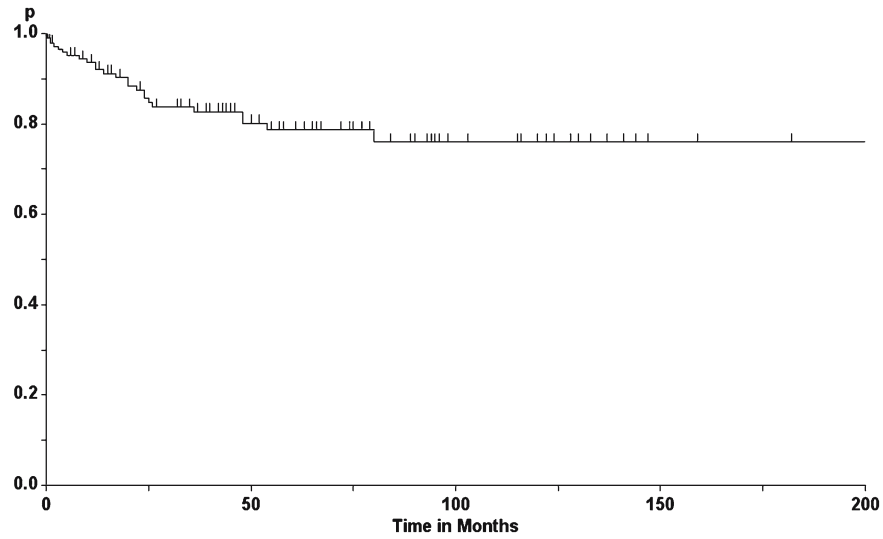

Fig. 3.62. Overall survival rate of patients with intramedullary tumors

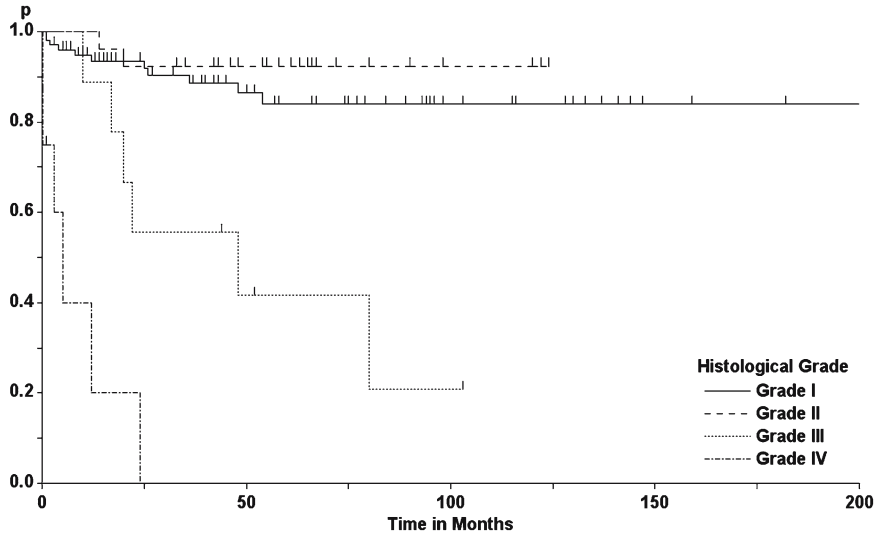

Fig. 3.63. Survival rates for patients with intramedullary tumors as a function of histological grade (log-rank test: $p<0.0001$)

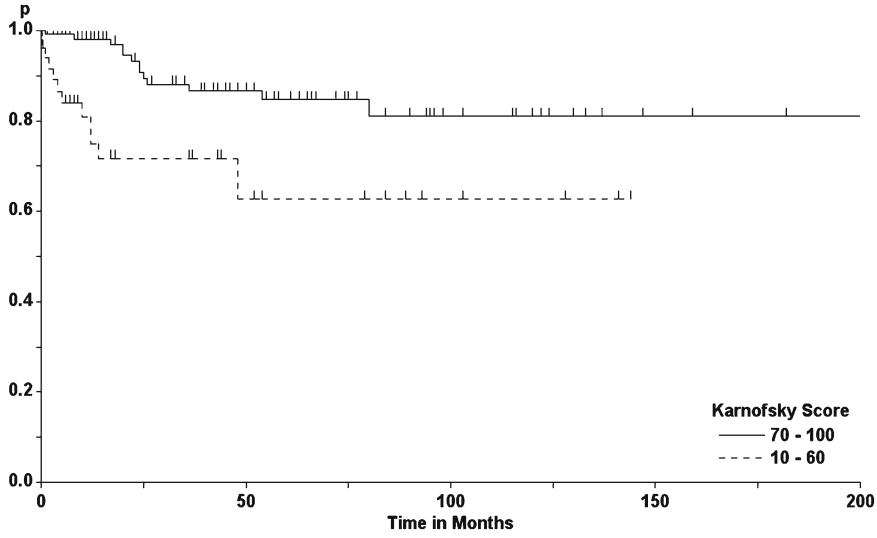

Fig. 3.64. Survival rates for patients with intramedullary tumors as a function of the preoperative Karnofsky score (log-rank test: $p=0.0012$)

Table 3.14. Multivariate analysis for prediction of a low mortality rate for patients with intramedullary tumors

Factor	β-value
Benign grade	0.1788
No local recurrence	0.1775
No preop. arachnoid scar	0.1270
High preop. Karnofsky score	0.1211
Long history	0.0795

Correlation: $r=0.3680$, $p=0.0002$

Table 3.15. Survival rates for patients with intramedullary tumors

Group	1 Year	5 Years	10 Years
Grade I	93%	84%	84%
Grade II	100%	92%	92%
Grade III	89%	42%	21%
Grade IV	20%	0%	–
Karnofsky score ≥70	98%	85%	81%
Karnofsky score <70	75%	63%	63%
Total	**87%**	**76%**	**74%**

3.5 Specific Entities

3.5.1 Ependymomas

Ependymomas and astrocytomas are the most frequent intramedullary tumors. Ependymomas of the spinal canal may be located intramedullarly, attached to the filum terminale, or even extradurally originating from heterotopic ependyma cells [226, 230]. Unlike some authors, we have eliminated ependymomas of the filum terminale from the analysis of intramedullary ependymomas. They are discussed in the section on extramedullary tumors.

Intramedullary ependymomas are solitary tumors that are located centrally in the spinal cord in the overwhelming majority of patients (Figs. 3.33, 3.40, 3.42, and 3.53). However, patients with intramedullary ependymomas and disseminated disease [195, 207] and with exophytic components [122] have been described. A significant proportion of NF-2 patients also harbor intramedullary ependymomas (Figs. 3.37 and 3.41) [189, 214, 254, 284, 301]. Analyses of the genetic features of ependymomas even disclosed links to the NF-2 gene [21, 74].

We have observed 84 intramedullary ependymomas in this series; 5 patients refused surgery, so that 79 ependymomas were included in our analysis of surgical results. They presented at an average age of 43±15 years (range 8–74 years) after a quite variable history ranging from 1 month to 12 years (mean 30±30 months). We observed an equal sex distribution in this subgroup and followed these patients for 37±38 months (maximum 12 years).

At the beginning of the history, signs are often quite unspecific, with some additional sensory impairment in about 70% of patients according to Schwartz and McCormick [301] or pain [195]. In our series, pain and gait ataxia were the commonest initial symptoms (Table 3.16). By the time of surgery, gait ataxia was the major concern for 43% of patients. The overall clinical picture before surgery is presented in Table 3.17. Compared to the second major group of intramedullary tumors (i.e., astrocytomas), there were no significant differences detectable.

Quite often, small tumor hemorrhages can be observed on MRI, particularly at the tumor poles [28, 217, 239], leading to the somewhat characteristic capping sign on the T2-weighted images mentioned above. Usually, such hemorrhages remain clinically insignificant as long as they are minor or the blood can accumulate in a preexisting cyst (Fig. 3.65). But we have also seen one patient with a sudden hemorrhage leading to a permanent paraparesis before surgery could be undertaken (Fig. 3.39) [301]. In terms of the spinal distribution of these tumors, 36 were encountered in the cervical cord, 38 in the thoracic cord, and 5 in the conus area; 65% of ependymomas showed an associated syrinx.

Table 3.16. Initial symptoms of intramedullary ependymomas and astrocytomas

First symptom	Ependymoma	Astrocytoma
Pain	39%	28%
Gait ataxia	21%	23%
Motor weakness	8%	27%
Sensory deficits	16%	8%
Dysesthesias	14%	11%
Sphincter problems	1%	–
Scoliosis	–	2%

Table 3.17. Symptoms for intramedullary ependymomas and astrocytomas at presentation

Symptom	Ependymomas	Astrocytomas
Pain	51%	44%
Gait ataxia	75%	88%
Motor weakness	73%	88%
Sensory deficits	90%	85%
Dysesthesias	58%	51%
Sphincter problems	29%	36%

The majority of ependymomas can be removed completely. In the literature, rates for complete resections vary between 69% [89], 70% [195], 74% [149], 81% [271], 90% [28], 95% [204], and 97% [39]. We have removed 82% of ependymomas completely, while a subtotal removal was achieved in 15% and a biopsy procedure and decompression was performed in 3%. Incomplete resections were associated with significantly higher, permanent surgical morbidity (42% compared to 11% after complete resections, respectively; log-rank test: p=0.0124), indicating lack of surgical experience as a major contributor to this difference. Complications occurred in 17%, with CSF leaks and wound infections as the commonest problems.

Postoperatively, the majority of patients demonstrated an unchanged clinical picture so that early surgery is recommended (Table 3.18) [28, 39, 195, 256,

Fig. 3.65. Sagittal T1- (**a**) and T2-weighted (**b**) MRI scans of an ependymoma at Th2–Th3 with an intramedullary hemorrhage into an associated cyst in a 53-year-old man with a 6-month history of dysesthesias. There was no clinical sign of a sudden deterioration suggesting this hemorrhage. T1- (**c**) and T2-weighted (**d**) axial scans demonstrate the changes in the intramedullary signal due to hemosiderin in the solid tumor part and the sedimentation of blood in the associated cyst, respectively. (*Continuation see next page*)

271]. In a series by Chang et al. [39], 64% of patients were unchanged postoperatively, 26% improved, and 10% worsened. In a study on 93 ependymomas, the condition of 9 patients had improved 1 year postoperatively, 14 were worse, and the remainder unchanged [28]. In a study on 20 children with intramedullary ependymomas, Lonjon et al. [195] reported postoperative improvements for 40%, unchanged neurology for 50%, and deteriorations for 10%. Raco et al. [271] determined improvements for 25%, while 66% remained unchanged. In our series, 29% experienced a transient deterioration of neurological function after surgery. Once recovery had occurred, 15% reported postoperative improvement and 48% stabilization of their neurological function after complete tumor resection, whereas 37% demonstrated a worse clinical condition. After subtotal resection, no patient reported a postoperative improvement. Two-thirds were left unchanged, whereas one-third were worse. Table 3.18 gives an overview of the postoperative course for individual symptoms within the first postoperative year after complete and subtotal resections. A significant improvement was only seen for the postoperative course of pain, whereas scores for sensory function, gait ataxia, and the Karnofsky score were significantly reduced after 1 year compared to preoperatively.

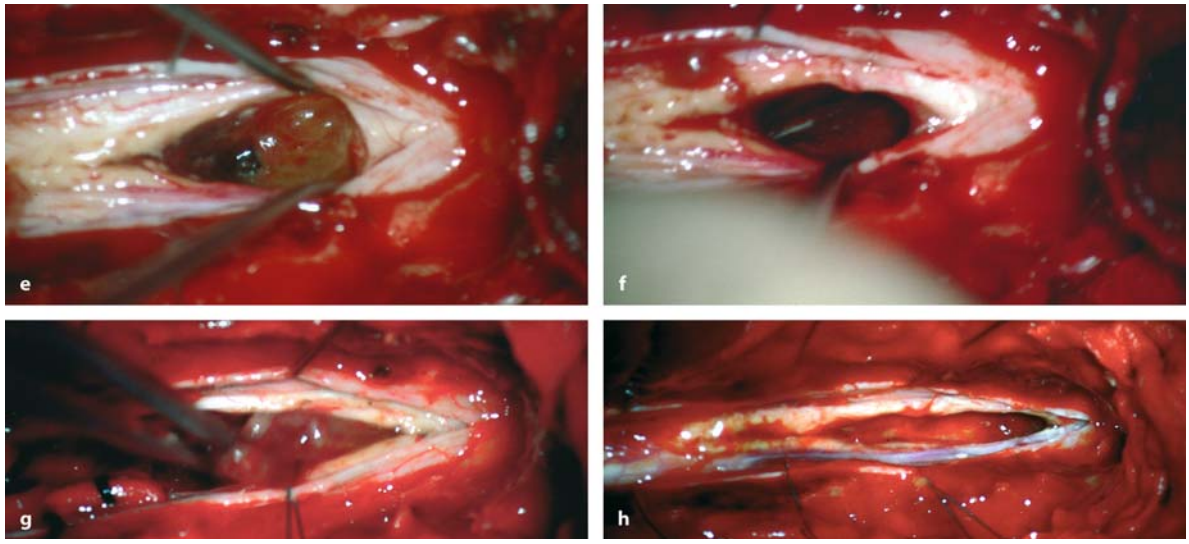

Fig. 3.65. (*Continued*) **e** Intraoperative view after opening the cord in the midline, showing part of the tumor and a hematoma. With removal of the blood (**f**), the tumor could finally be dissected in conventional manner (**g**). **h** The final view shows the situation after complete resection of the tumor and evacuation of the hemorrhage. After a short period of neurological deterioration, the patient recovered his preoperative functions

Table 3.18. Clinical course for patients with intramedullary ependymomas related to tumor removal

Symptom	Preoperative status	Postoperative status	3 Months postop.	6 Months postop.	1 Year postop.
Pain					
Complete	4.1±0.9	4.0±0.8	4.3±0.8	4.4±0.9	4.3±0.9*
Subtotal	4.2±1.0	3.9±1.1	4.6±0.7	4.8±0.4	4.8±0.4
Hypesthesia					
Complete	3.3±0.8	2.2±1.0	2.3±1.0	2.4±1.0	2.4±1.0**
Subtotal	3.1±0.9	2.4±1.3	2.4±1.3	2.6±1.3	2.6±1.3
Dysesthesias					
Complete	4.0±0.9	4.0±0.9	3.8±0.9	3.8±1.0	3.7±1.0
Subtotal	4.2±1.0	4.2±1.0	4.0±0.9	4.0±1.0	3.9±0.9
Gait					
Complete	3.8±1.1	2.8±1.4	3.2±1.4	3.4±1.5	3.4±1.5*
Subtotal	3.2±0.7	2.3±1.1	2.8±1.5	3.0±1.4	3.0±1.4
Motor power					
Complete	4.0±1.1	3.1±1.3	3.4±1.2	3.5±1.3	3.6±1.2
Subtotal	3.8±1.0	3.1±1.6	3.3±1.6	3.4±1.5	3.4±1.5
Sphincter function					
Complete	4.5±1.0	3.7±1.8	4.1±1.4	4.2±1.3	4.2±1.3
Subtotal	4.7±0.7	3.9±1.7	4.1±1.7	4.1±1.7	4.1±1.7
Karnofsky score					
Complete	73±13	61±17	66±17	68±18	69±18*
Subtotal	71±14	61±18	63±18	67±18	68±18

Statistically significant difference between preoperative status and 1 year postoperatively: *$p<0.05$, **$p<0.01$

Table 3.19. Multivariate analysis for prediction of a high postoperative Karnofsky score after 1 year for intramedullary ependymomas

Factor	β-value
Preop. Karnofsky score	0.6798
No dysesthesia syndrome	0.3986
No recurrence	0.2697
High spinal level	0.2464
No preop. arachnoid scar	0.1943
No postop. tethering	0.1728
Young age	0.1176

Correlation: r=0.9063, p<0.0001

A multiple regression analysis to predict a high postoperative Karnofsky score after 1 year disclosed a high preoperative Karnofsky score and no dysesthesia syndrome as the most significant factors. Other less important influences were no recurrence, young age, high spinal level, and neither preoperative nor postoperative arachnoid scarring (Table 3.19). The amount of tumor resection and the histological grade had no influence on the postoperative Karnofsky score according to this analysis.

The histological classification of low-grade ependymomas does not appear to be of prognostic significance in intramedullary ependymomas [228]. Among our patients, just one 14-year-old girl was diagnosed with a grade III tumor and underwent postoperative radiotherapy after complete resection of her tumor (Fig. 3.66); 44 months later there was no evidence of recurrent tumor. However, with anaplastic ependymomas, the overall prognosis is generally poor in terms of local control and survival [228].

Intramedullary ependymomas provide a much better prognosis than their intracranial counterparts [149, 228, 273]. This is due to the fact that the spinal cord contains this tumor, the cord substance is displaced rather than infiltrated and, thus, the tumor is usually completely resectable with minimal risk of subarachnoid seeding, which is often observed with extramedullary ependymomas or ependymomas of the fourth ventricle [273].

With complete removal of an intramedullary ependymoma, tumor recurrences are rare and the patient can expect a good prognosis [56, 195, 217, 252, 256, 271, 273, 305]. Tumor removal should be recommended as soon as the diagnosis is made, regardless of extension (Fig. 3.67). According to multiple regression analysis, incomplete resection was the most important factor predicting a recurrence [273, 338]. Other less important factors were postoperative radiotherapy, a high spinal level, and female sex (Table 3.20). We observed no local recurrences after complete resections at all, with a maximum follow up of 12 years. After subtotal resections, two recurrences within 14 months were observed, providing a recurrence rate of 21% (Fig. 3.68). Likewise, Schick et al. [297] determined a recurrence rate of 20% after subtotal resections within a period of 29–118 months without using Kaplan-Meier statistics. Chang et al. [39] reported a 5-year rate without recurrence of 70% and determined in a multivariate analysis that the extent of resection was the decisive factor. Lonjon et al. [195] gave no postoperative radiotherapy and obtained recurrence rates of 7% after 5 years and 30% after 10 years.

Examination of postoperative survival statistics disclosed a 1-year survival rate of 95% and rates of 91% after 5 and 10 years, respectively (Fig. 3.69). Shirato et al. [311] reported a 5-year survival rate of 96%. Lonjon et al. [195] observed a survival rate of 90% after 5 and 10 years. Ferrante et al. [89] reported a 10-year survival rate of 80%. Raco et al. [271] and Sgouros et al. [305] determined postoperative survival rates of 83% and 85.5%, respectively, for 5 years after complete removal, and observed a strong relationship between survival rates and amount of resection. This relationship was not evident in our series as both groups demonstrated virtually identical survival rates of 91% and 89% after 5 years for complete and subtotal removal, respectively.

In terms of adjuvant radiotherapy, low doses of below 40 Gy are certainly not effective [89]. With higher doses, some studies report a benefit. However, most of them mix intramedullary and extramedullary ependymomas together [47, 207, 259, 305, 309, 338] or do not compare groups with and without postoperative radiotherapy [47, 176, 207, 259, 283, 309]. Nevertheless, these studies recommend applying radiotherapy to all patients operated for spinal ependymomas, even claiming that the amount of tumor resected is irrelevant for the patient's outcome [309]. Shaw et al. [309] gave a disease-free rate of 81% for 5 years and 71% for 10 years; 95% of their patients survived 5 or 10 years. Marks and Adler [207] reported a 5-year survival rate of 57% for intramedullary ependymomas after radiotherapy. Compared to surgical series, however, these numbers certainly do not support a major role for radiotherapy in the treatment of intramedullary ependymomas.

From our review of the literature, there is no conclusive evidence that radiotherapy has a beneficial effect for patients with incompletely resected intramedullary ependymomas [133]. For extramedullary

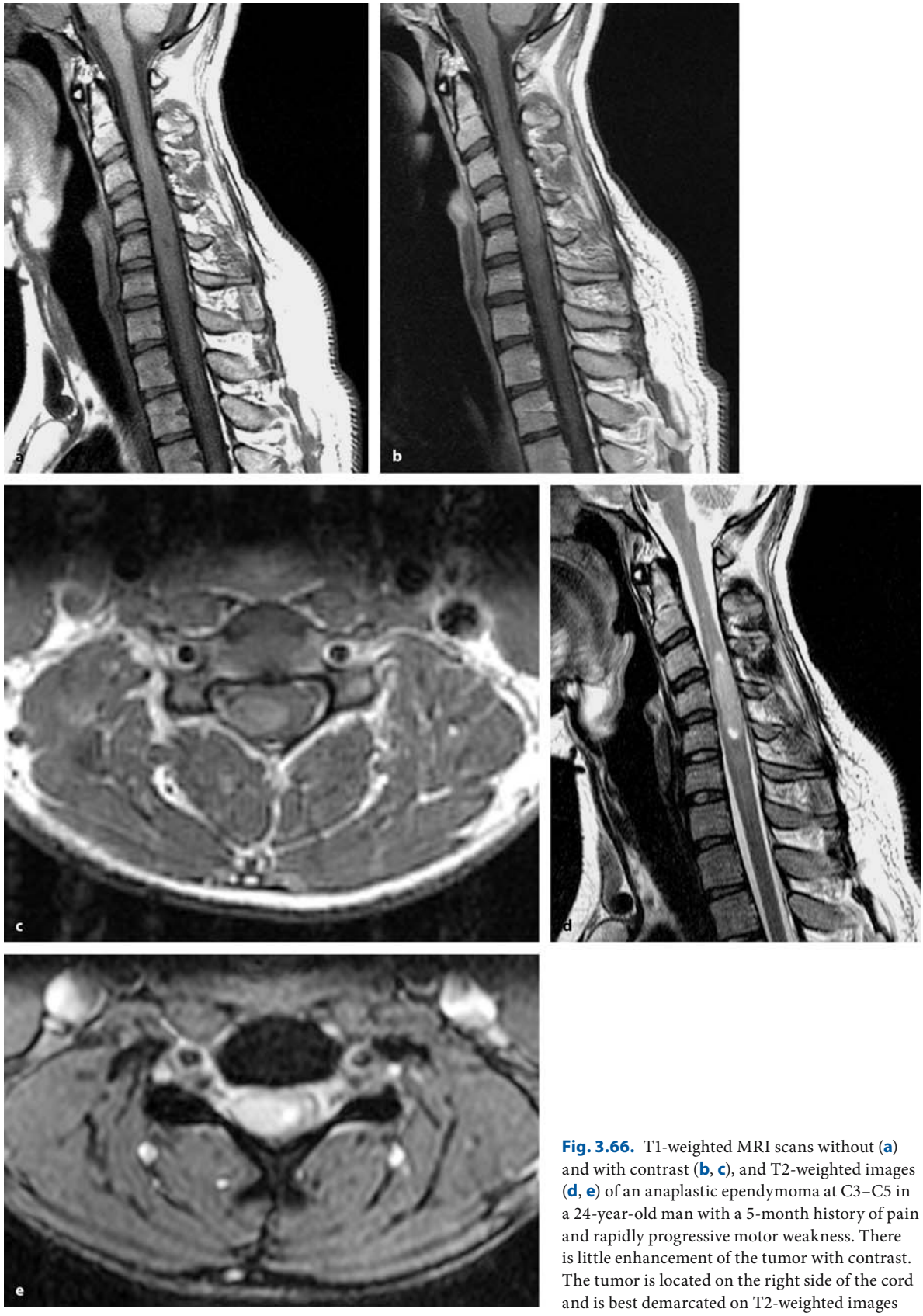

Fig. 3.66. T1-weighted MRI scans without (**a**) and with contrast (**b**, **c**), and T2-weighted images (**d**, **e**) of an anaplastic ependymoma at C3–C5 in a 24-year-old man with a 5-month history of pain and rapidly progressive motor weakness. There is little enhancement of the tumor with contrast. The tumor is located on the right side of the cord and is best demarcated on T2-weighted images

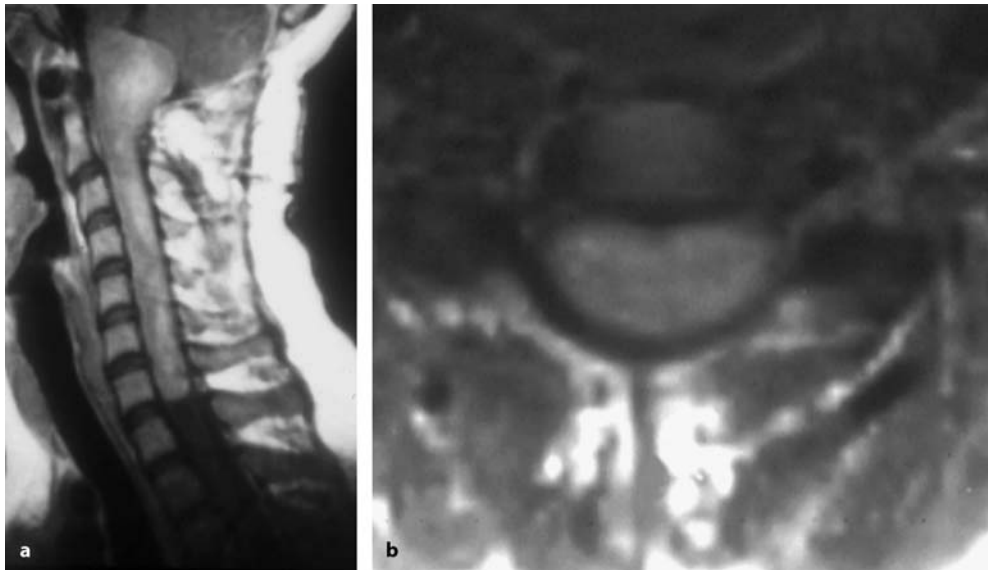

Fig. 3.67. These, contrast-enhanced sagittal (**a**) and axial (**b**) MRI scans show an intramedullary ependymoma extending from the posterior fossa to Th2 in a 25-year-old woman presenting with a 5-year history of slight gait ataxia and tetraparesis. Surgery was recommended as the only chance for preserving neurological functions in the long term. The patient repeatedly refused surgery and died 2 years later from respiratory failure

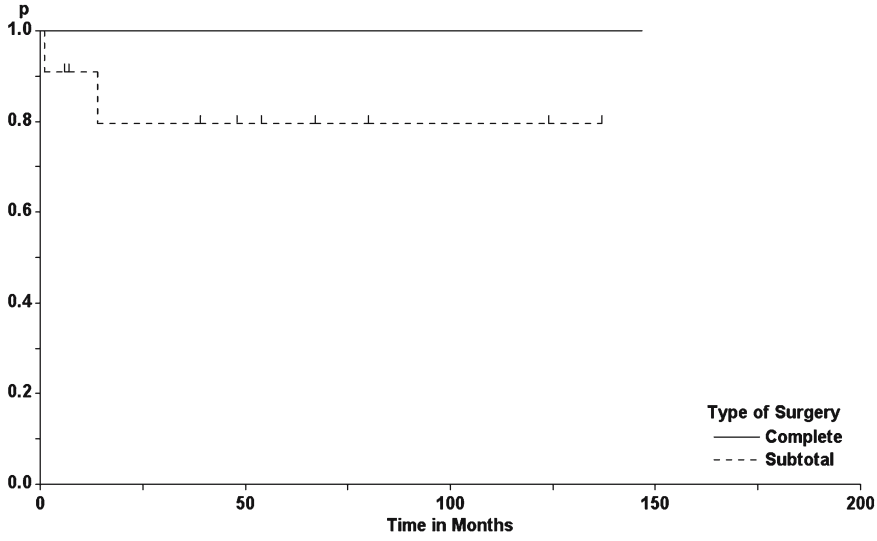

Fig. 3.68. Tumor recurrence rates for patients with intramedullary ependymomas as a function of the amount of tumor resected (log-rank test: p=0.0026)

Table 3.20. Multivariate analysis for prediction of a low clinical recurrence rate for patients with intramedullary tumors

Factor	β-value
Complete resection	0.5338
Radiotherapy	0.3967
High spinal level	0.2028
Female sex	0.1062

Correlation: r=0.6818, p<0.0001

ependymomas of the filum terminale, radiotherapy seems to be more efficient [207]. If surgery has to be performed after radiotherapy, cleavage planes may be much more difficult to define due to the gliosis, which may have formed in the radiation field [89].

Given the excellent long-term results in terms of local recurrences and survival rates after surgery alone, there is a general agreement among neurosurgeons not to recommend postoperative radiotherapy for intramedullary ependymomas [217, 234, 273]. Even after incomplete resections, we rather

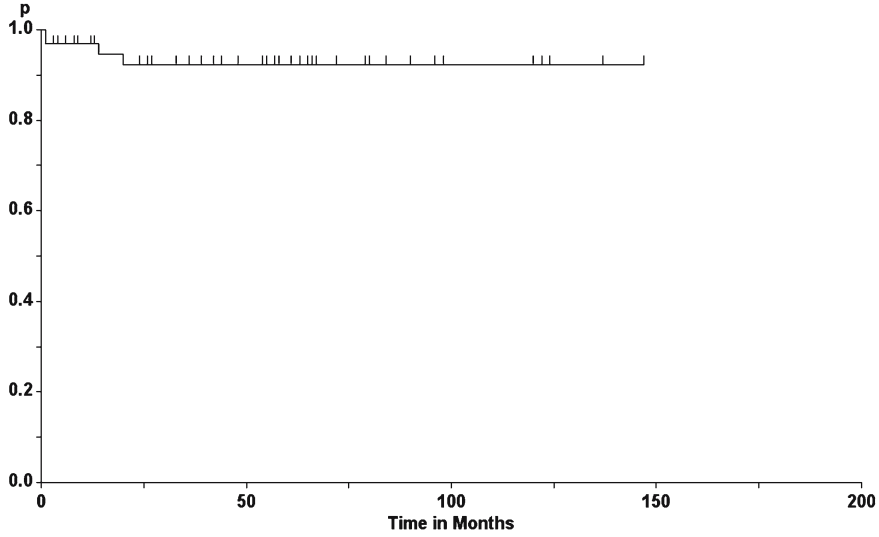

Fig. 3.69. Survival rate of patients with intramedullary ependymomas

perform a second operation than advise radiotherapy [195]. Currently, we recommend radiotherapy only for patients with WHO grade III tumors. This recommendation is given basically for lack of alternatives.

3.5.2 Astrocytomas

Astrocytomas are the commonest intramedullary tumors in children and occur secondary to ependymomas in adults [130]. The great majority of patients with intramedullary astrocytomas have solitary tumors (Figs. 3.35, 3.36, and 3.44–3.47). However, in patients with NF-1 or NF-2, intramedullary astrocytomas may be encountered together with other spinal tumors (Fig. 3.43) [189, 214, 254, 284, 348].

According to the literature, the average patient history can be expected to last 13 months, with a considerably shorter history for malignant as compared to benign astrocytomas [45, 168, 291]. The patient history was longer in our series and lasted 29±41 months. One patient gave a history of dysesthesias for more than 10 years before the diagnosis was made. There was a marked difference between benign and malignant astrocytomas. In the former, the average history was significantly longer compared to malignant tumors (38±46 months and 7±14 months, respectively; $p<0.0001$). Patients presented at an average age of 29±18 years with an equal age distribution spanning from 1 week to 69 years. Twenty-two children (<18 years) underwent 23 operations, while 38 adults were operated for 42 tumors. Two additional patients had refused surgery.

Pain is the commonest initial symptom [24, 130, 151]; however, gait ataxia and motor weakness were mentioned almost as often as the initial complaint (Table 3.16). At presentation, gait ataxia and motor weakness predominated the clinical picture in 75% of patients (Table 3.17). A comparison of benign and malignant tumors revealed no significant differences in the clinical picture apart from the considerably shorter history for malignant tumors, as already mentioned. Eighteen tumors were located in the cervical cord, 32 in the thoracic, and 15 in the conus area; 31% had an associated syrinx.

Astrocytomas are infiltrating tumors, so radical resection is not possible in most instances. The goal of treatment is to reduce the tumor size as much as possible (Figs. 3.45–3.47). We were able to achieve complete resections in 18% of our patients (i.e., no visible tumor left intraoperatively and on postoperative MRI; Figs. 3.35, 3.36, 3.43, and 3.44); 62% were removed subtotally and the remaining patients underwent a biopsy procedure and decompression (11%), or cystostomy for cystic tumors (9%).

Table 3.21. Histological grades for intramedullary astrocytomas

Grade	Adults	Children	Total
I	27 (64%)	14 (61%)	41 (63%)
II	3 (7%)	5 (22%)	8 (12%)
III	9 (21%)	3 (13%)	12 (18%)
IV	3 (7%)	1 (4%)	4 (6%)

Table 3.22. Clinical course for patients with intramedullary astrocytomas related to tumor resection and histological grade

Symptom	Preoperative status	Postoperative status	3 Months postop.	6 Months postop.	1 Year postop.
Pain					
Complete	4.3±0.9	4.3±0.5	4.4±0.5	4.3±0.7	4.1±1.0
Subtotal	4.9±0.4	4.4±0.8	4.6±0.5	4.9±0.4	5.0
Benign	4.1±1.1	3.9±0.9	4.4±0.7	4.4±0.7	4.5±0.8
Malignant	4.2±1.2	4.3±0.9	4.6±0.7	4.4±0.7	
Hypesthesia					
Complete	3.5±1.1	2.4±0.7	2.9±0.6	2.9±0.6	2.8±0.9
Subtotal	3.9±0.7	2.6±1.0	2.6±1.0	2.6±1.0	2.7±1.0*
Benign	3.0±1.4	2.0±1.1	2.2±1.2	2.1±1.3	2.2±1.3**
Malignant	3.0±0.7	2.3±1.1	2.6±1.1	2.6±1.1	
Dysesthesias					
Complete	3.9±0.8	4.0±0.8	4.1±0.6	4.1±0.6	4.3±0.5
Subtotal	4.7±0.5	4.6±0.5	4.3±0.8	4.3±0.8	4.3±0.8
Benign	4.1±0.9	4.1±1.0	4.2±0.9	4.1±1.0	4.2±0.9
Malignant	4.1±0.9	4.4±0.5	4.3±0.7	4.3±0.7	
Gait					
Complete	3.1±1.6	3.0±0.9	3.1±1.1	3.5±0.9	3.5±0.9
Subtotal	3.9±0.4	2.3±1.3	3.1±1.2	3.3±1.6	3.6±1.3
Benign	3.0±1.7	2.5±1.3	2.8±1.5	3.0±1.6	3.1±1.6
Malignant	2.6±1.5	2.2±1.5	2.6±1.7	2.4±1.6	
Motor power					
Complete	3.6±1.4	3.3±1.5	3.5±1.2	3.8±0.9	3.8±0.9
Subtotal	3.6±1.3	3.0±1.3	3.1±1.2	3.6±1.4	3.6±1.4
Benign	3.0±1.6	2.6±1.5	2.8±1.5	3.1±1.5	3.1±1.6
Malignant	3.0±1.6	2.7±1.6	2.9±1.6	2.9±1.6	
Sphincter function					
Complete	4.3±1.2	3.5±1.9	3.9±1.3	4.0±1.3	3.9±1.6
Subtotal	4.9±0.4	3.7±2.2	4.1±1.9	4.1±1.9	4.1±1.9
Benign	4.2±1.6	3.6±2.0	4.0±1.6	4.0±1.6	4.0±1.6
Malignant	4.0±1.6	3.9±1.8	3.9±1.8	3.9±1.8	
Karnofsky score					
Complete	68±19	66±15	70±12	74±11	72±15
Subtotal	75±8	56±15	66±14	73±10	73±10
Benign	66±19	58±17	63±17	67±18	66±19
Malignant	55±21	54±18	57±19	58±19	

Statistically significant difference between preoperative status and 1 year postoperatively: *$p<0.05$, **$p<0.01$

Similar figures were reported by Kim et al. [168]. They obtained 3 total removals among 28 patients, while subtotal resections were performed in 6 and partial resections in 14 patients. Five patients underwent a biopsy procedure and decompression. In a French multicenter study on pediatric intramedullary astrocytomas, total or subtotal removal was achieved in 43% of 73 patients [24].

Raco et al. [271] were able to resect 31% of intramedullary astrocytomas completely. While none of the high-grade tumors were completely removed, a complete resection was achieved mainly for pilocytic

astrocytomas (81%) and, to a much lower degree, for grade II tumors (12%).

The rate of complete resection has increased over the years in our hands, while the percentage of patients undergoing biopsy procedures and decompression has dropped. Before 1985, 8% were completely resected and 77% subtotally or partially. Between 1986 and 1995, 14% were removed completely and 69% subtotally, with still 17% undergoing a biopsy procedure and decompression. In the last period since 1996, 29% were removed completely, 67% subtotally, and 4% biopsied. MRI and growing experience can be held responsible for this development.

Looking at histological grades, differences between adults and children appeared with a higher proportion of malignant tumors in adults (17% and 28%, respectively; Table 3.21) [152, 168]. However, this did not reach statistical significance.

Postoperatively, 30% experienced a transient aggravation of neurological deficits that recovered within 1 year. Permanent surgical morbidity was seen after 14% of operations. An analysis of morbidity figures over the years once again demonstrated a significant improvement from 39% before 1985 to 7% after 1986, and 8% since 1996. The precise preoperative localization of the tumor on MRI seems the most plausible explanation. Complications were observed in 17%, with CSF leaks and wound infections predominating.

Postoperative improvement was observed in 25%, and a stable and unchanged postoperative neurological status was seen in 58%, while 17% were worse compared to preoperatively. Similar outcomes were observed by Raco et al. [271], with functional improvements restricted mainly to pilocytic astrocytomas. On average, sensory function significantly decreases, with the remainder of the neurology being left unchanged during the first postoperative year for completely and subtotally removed tumors alike. Similar clinical trends are observed irrespective of histological grades (Table 3.22).

To predict a high Karnofsky score after 1 year a multiple regression analysis determined the preoperative Karnofsky score [168], no tumor recurrence, postoperative radiotherapy (for high-grade tumors), and a long history as the most powerful predictors (Table 3.23).

Evaluation of tumor recurrence rates for astrocytomas revealed low spinal level (Fig. 3.70), malignant grade (Fig. 3.71), and adult age (Fig. 3.72) as important independent predictors (Table 3.24). The amount of resection did not influence recurrence rates as an independent factor, even though a trend for higher recurrence rates for incompletely resected tumors could be observed (Fig. 3.73).

Table 3.23. Multivariate analysis for prediction of a high Karnofsky score after 1 year for intramedullary astrocytomas

Factor	β-value
High preop. Karnofsky score	0.5600
No recurrence	0.4429
Postop. radiotherapy	0.3837
Long history	0.3336
Female sex	0.1747

Correlation: $r=0.9285$, $p<0.0001$

Overall, 87% survived for 1 year and 63% and 57% survived for 5 and 10 years, respectively (Fig. 3.74). Shirato et al. [311] observed a considerably worse survival rate of 50% after 5 years, and Huddart et al. [132] found a 5-year survival rate of 59%. Both of these studies incorporated a significant number of patients with postoperative radiotherapy. Survival rates were influenced by local recurrences, histological grade (Fig. 3.75), and patient age (Fig. 3.76, Table 3.25) [132]. For benign tumors, 92% survived 1 year and 77% for 5 and 10 years. Malignant tumors reduced these numbers to 74% after 1 year, 27% after 5 years, and 14% after 10 years. Children had a better survival prognosis than adults, with 87% surviving for 5 years compared to 52% for adults [132, 291]. Similar results were documented in a series of 65 intramedullary astrocytomas, with the length of history, the preoperative Karnofsky score, and the histological grade influencing survival [139].

Numerous studies have documented that neither progression-free intervals nor survival are influenced significantly by the amount of resection, provided a reduction of tumor volume to decompress the spinal cord was achieved [6, 43, 56, 107, 130, 139, 151, 152, 215, 318]. On the other hand, Constantini et al. [55] did observe a correlation between the amount of resection and progression-free survival in low-grade astrocytomas.

Kim et al. [168] calculated the median survival as 184 and 8 months for low and high grade tumors, respectively, with a benefit of radiated compared to nonradiated patients. In a French multicenter study on pediatric intramedullary astrocytomas, 36 patients underwent postoperative radiotherapy and 9 chemotherapy. Good outcome was related to young age, history longer than 2 months, preoperative spinal deformity, and low histological grade [24]. Radiotherapy

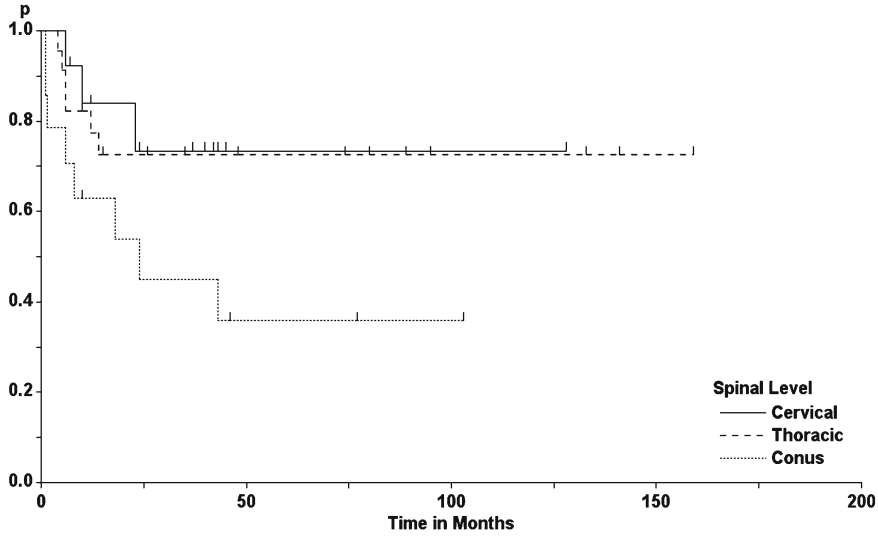

Fig. 3.70. Tumor recurrence rates for patients with intramedullary astrocytomas as a function of spinal level (log-rank test: p=0.07)

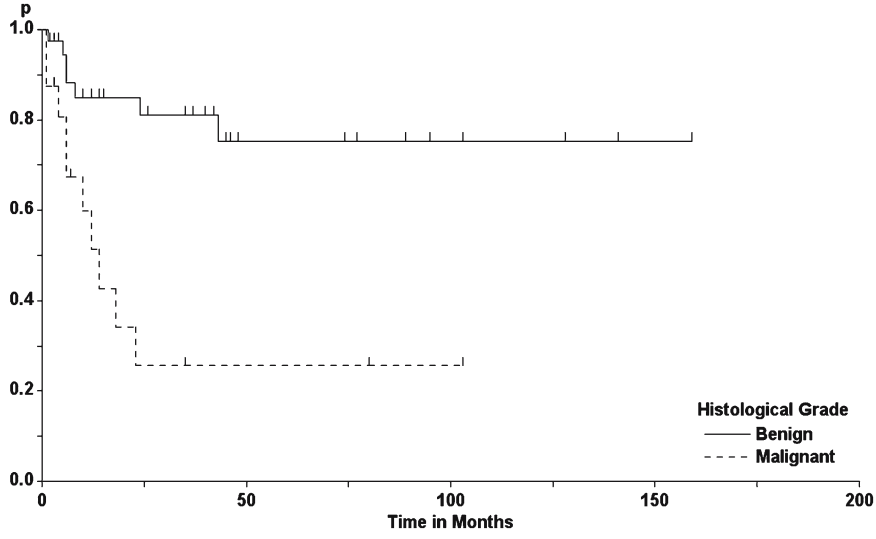

Fig. 3.71. Tumor recurrence rates for patients with intramedullary astrocytomas as a function of histological grade (log-rank test: p=0.0007)

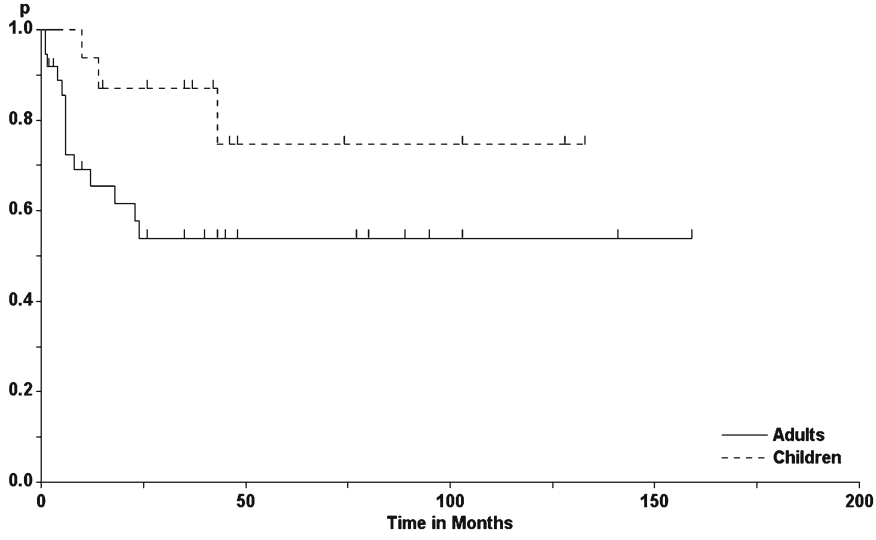

Fig. 3.72. Tumor recurrence rates for patients with intramedullary astrocytomas as a function of patient age (log-rank test: p=0.06)

Table 3.24. Multivariate analysis for prediction of a low recurrence rate for intramedullary astrocytomas

Factor	β-value
High spinal level	0.3380
Benign grade	0.2973
Young age	0.2137
High preop. Karnofsky score	0.1563

Correlation: r=0.5607, p=0.0014

had no influence on survival, while extent of surgery was marginally not significant (p=0.08).

Jallo et al. [151] reported a series of 17 low-grade astrocytomas in adult patients. They had presented after an average history of 20 months (range: 1–48 months). Four patients with subtotal removals underwent postoperative radiotherapy. Three patients died due to tumor progression 24–36 months after surgery. Fourteen patients are alive with stable disease and a median follow up of 7.4 years. In nine of these patients, MRI demonstrated no evidence of tumor. The 5- and 10-year survival rates were 82%. Twelve patients (86%) had improved or kept their preoperative status postoperatively.

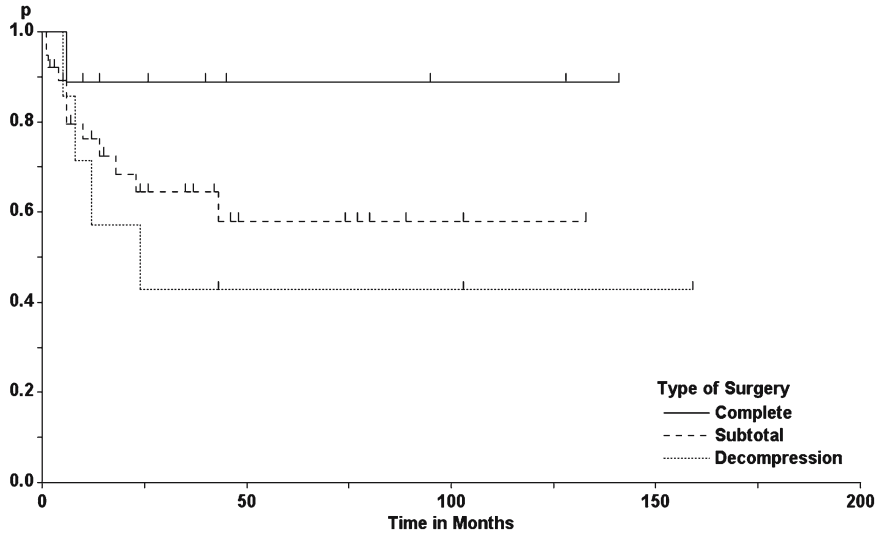

Fig. 3.73. Tumor recurrence rates for patients with intramedullary astrocytomas as a function of the amount of tumor resected (log-rank test: not significant)

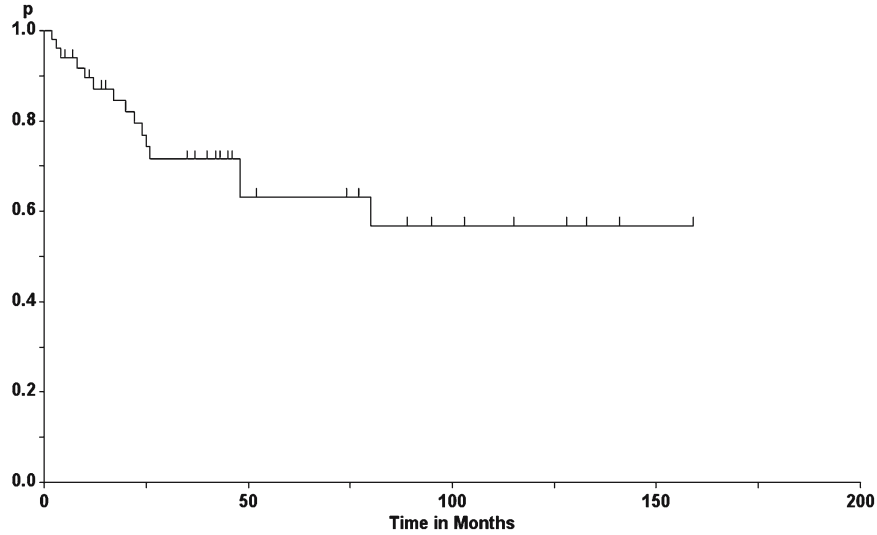

Fig. 3.74. Survival rate for patients with intramedullary astrocytomas

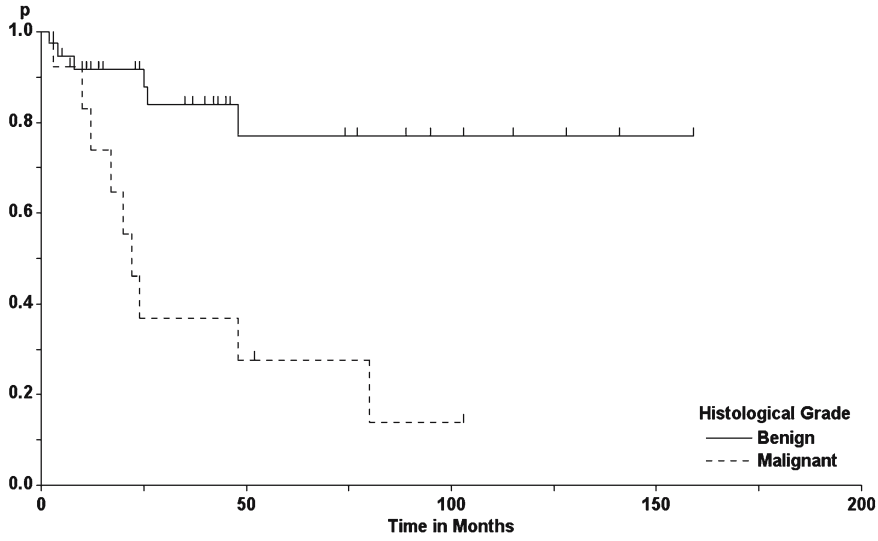

Fig. 3.75. Survival rates for patients with intramedullary astrocytomas as a function of histological grade (log-rank test: p=0.0004)

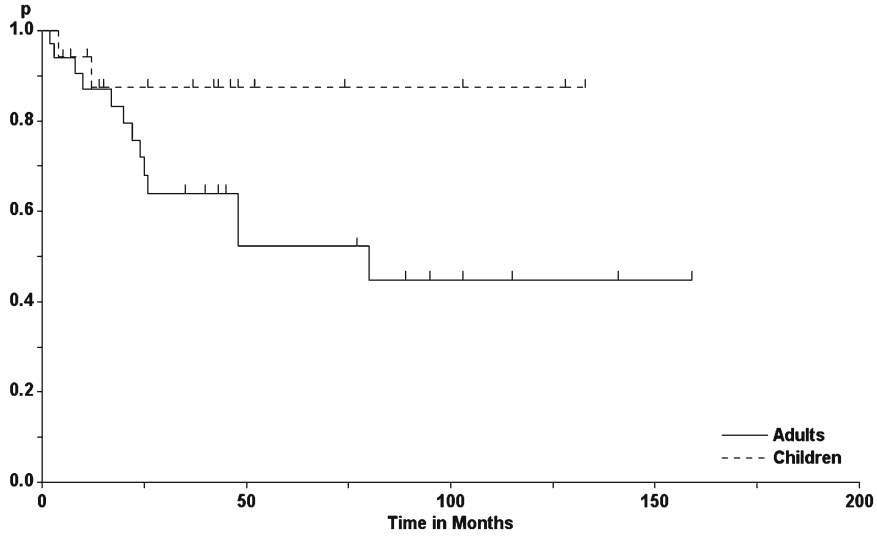

Fig. 3.76. Survival rates for patients with intramedullary astrocytomas as a function of age (log-rank test: p=0.074)

Table 3.25. Multivariate analysis for prediction of high survival rate for intramedullary astrocytomas

Factor	β-value
No recurrence	0.3045
Benign grade	0.2875
Young age	0.2110

Correlation: r=0.5745, p=0.0001

Overall, this analysis shows that pediatric and adult patients demonstrate different biological behaviors of these tumors. In children, the postoperative course is more often benign after complete or subtotal resection compared to adults [54, 68, 130, 131, 152, 252], even though Hardison et al. [118] made the opposite observation with 39% and 14% of children with low-grade astrocytomas dead and without clinical progression within 5 years, respectively.

A point of continuing controversy is the value of postoperative radiotherapy. Epstein et al. [84] reported long progression-free intervals after resection of low-grade astrocytomas without radiotherapy in adults. Houten and Weiner [131] reported a 5-year survival rate of 57% in children with low-grade astrocytomas, while Bouffet et al. [24] gave a figure of 76% and Jallo et al. [152] of 88% for this group and time. The postoperative course of incompletely removed low-grade astrocytomas is considered by most neuro-

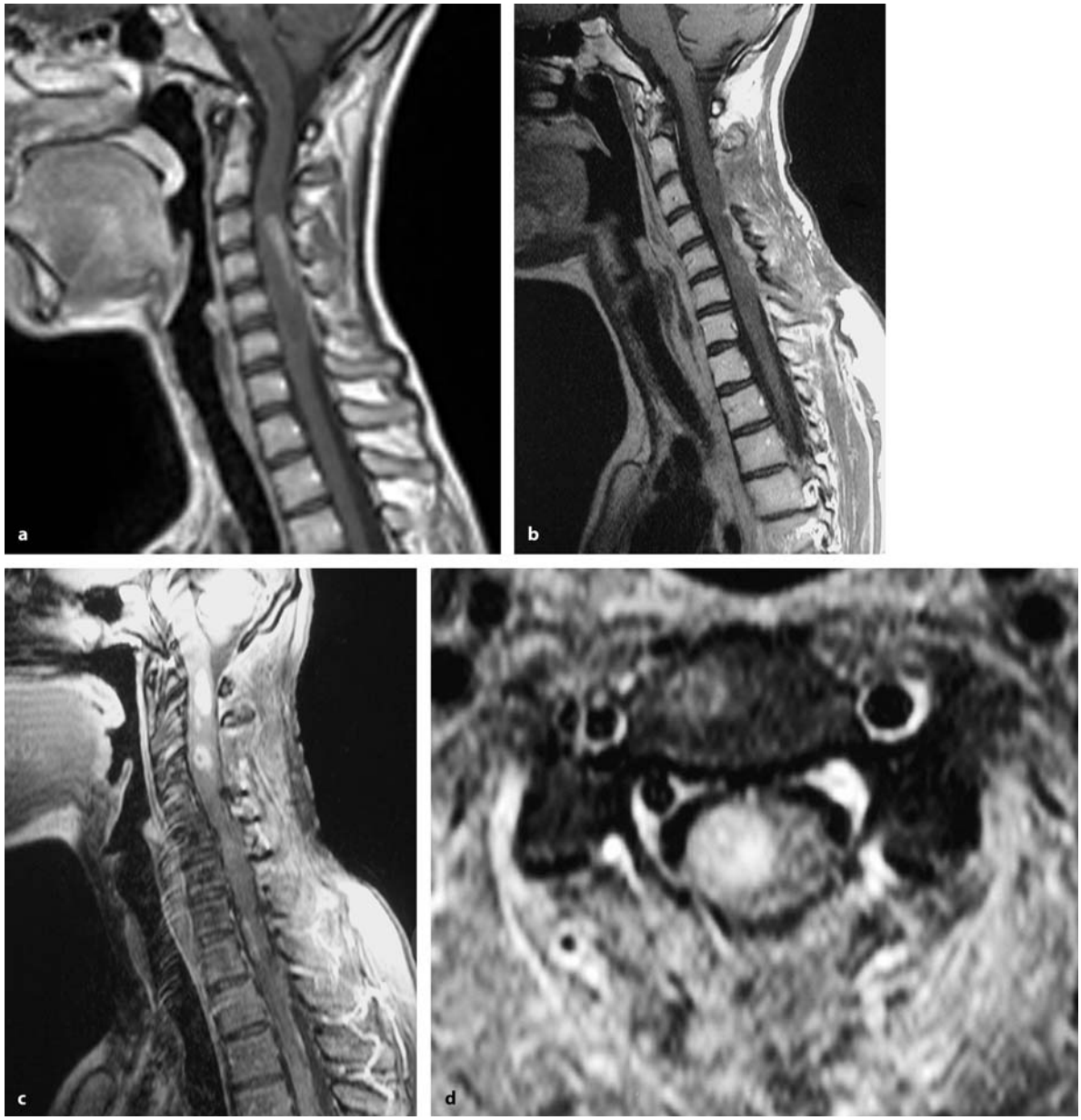

Fig. 3.77. Sagittal T1- weighted MRI scans of an WHO grade III astrocytoma at C3–C6 in a 16-year-old girl before (**a**) and after partial resection (**b**; see also Fig. 3.47). Despite chemo- and radiotherapy, the patient demonstrated a local recurrence and subarachnoid spreading (**c**, **d**), and died 12 months after surgery

surgeons as being so benign that radiotherapy should be withheld and rather, repeated surgeries undertaken [54, 151]. The major factor influencing the long-term clinical course and survival is the histological grade and not the mode of treatment [55, 107, 130, 132, 137, 157].

Nevertheless, several authors recommend postoperative radiotherapy for intramedullary astrocytomas [45, 132, 133, 141, 157, 311]. High radiation doses may provide survival times of 4 years in some cases for malignant astrocytomas [141]. However, a clinical randomized study is still not available. Other studies denied such an effect for high-grade tumors and pointed toward the risk of radiation-induced myelopathy if sufficient doses are applied [333]. Even radiation-induced gliomas have been reported [17, 112].

In a study on 36 spinal cord astrocytomas – 21 glioblastomas (grade IV), 13 anaplastic astrocytomas

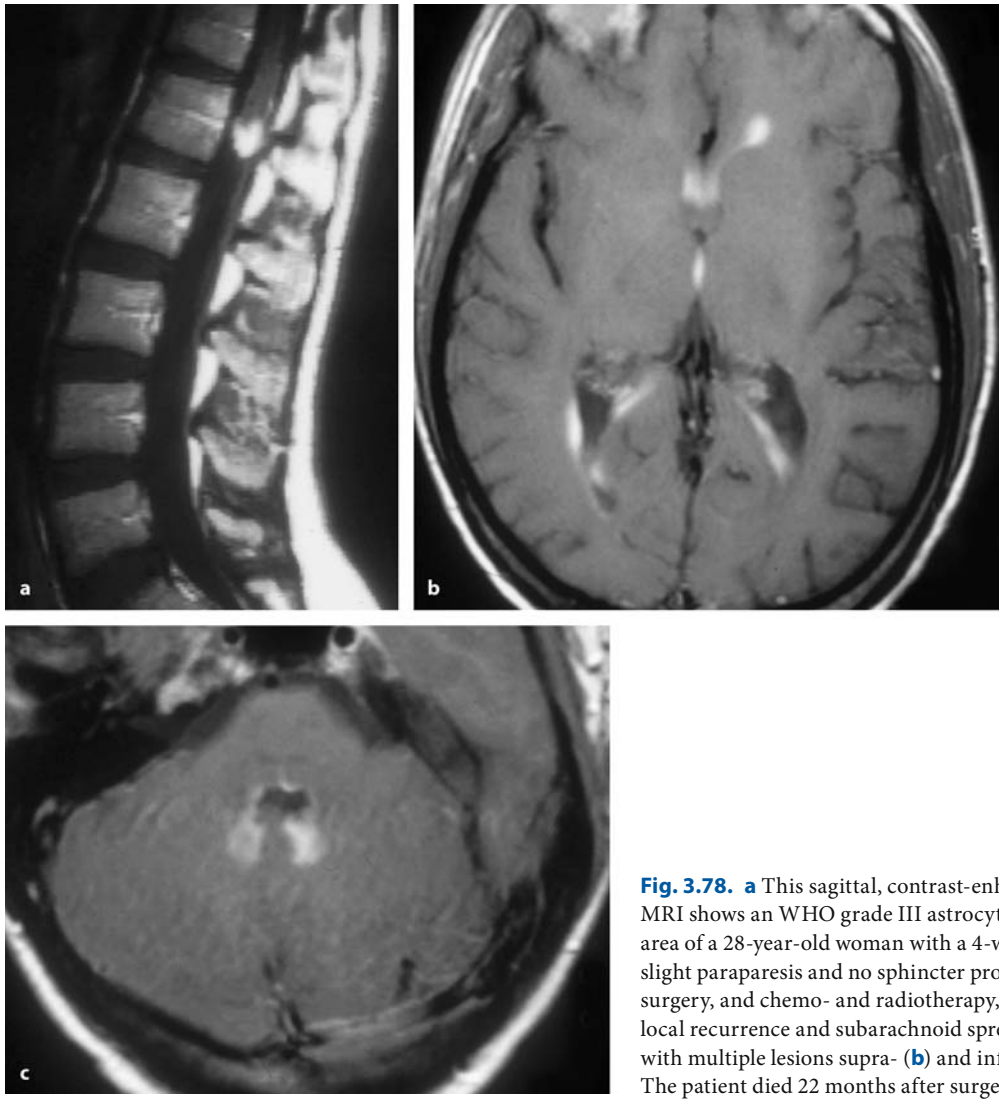

Fig. 3.78. a This sagittal, contrast-enhanced T1-weighted MRI shows an WHO grade III astrocytoma in the conus area of a 28-year-old woman with a 4-week history of a slight paraparesis and no sphincter problems. Despite surgery, and chemo- and radiotherapy, she developed a local recurrence and subarachnoid spreading of the tumor with multiple lesions supra- (**b**) and infratentorially (**c**). The patient died 22 months after surgery

(grade III), 2 grade II astrocytomas – by Santi et al. [291], 29% received postoperative radiotherapy and 19% a combination of radiotherapy and chemotherapy. The two grade II tumors and six anaplastic tumors progressed to glioblastomas. The authors observed 15 central nervous system metastases in this group plus 2 extraneural metastases. The overall median survival time was 10 months for both grade III (range 1–84 months) and grade IV (range 1–43 months) tumors. Patients older than 40 years had a shorter survival (in the range of a few months) compared to younger patients, who survived for 1 year on average. The authors concluded that there is no prognostic difference between grade III and IV tumors or survival advantage for patients who had undergone aggressive surgery, radiotherapy, or chemotherapy. Shirato et al. [311] recommended high doses of radiation – so called radiocordectomy – for high-grade astrocytomas, claiming two long-term survivors (i.e., longer than 4 years) among six high-grade tumors.

Cohen et al. [48] reported 19 malignant astrocytomas with an average history of 7 weeks. All but one patient received postoperative radiotherapy and 53% received additional chemotherapy. All but one patient died after a mean survival of 6 months; 58% had evidence of dissemination. The authors recommended postoperative adjuvant radiotherapy for the entire neuraxis.

We advise radiotherapy for patients with WHO grade III and IV tumors only. A high-grade astrocytoma of the spinal cord is an eventually fatal disease. From our experience, the length of survival is quite

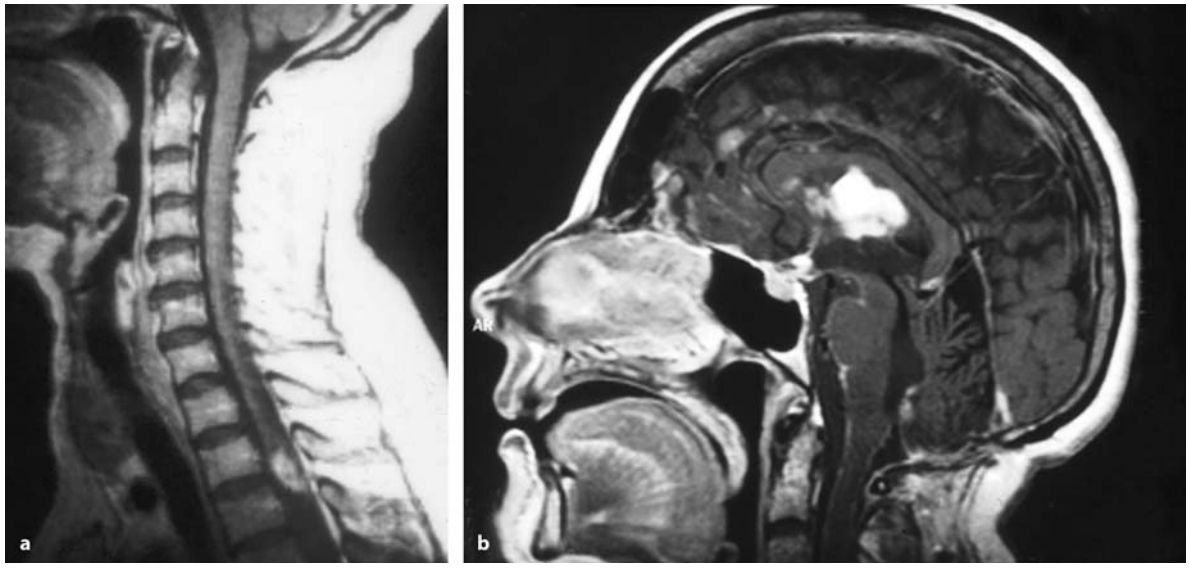

Fig. 3.79. Sagittal T1-weighted MRI scan (**a**) of a WHO grade III astrocytoma at Th2/3 in a 47-year-old woman with a 5-month history of a progressive paraparesis. The patient underwent radiotherapy subsequent to surgery. No local recurrence developed, but she presented 3 years later with a WHO grade III cerebellar astrocytoma. This was also removed and treated with adjuvant radiotherapy, but the patient returned with subarachnoid seeding (**b**) and hydrocephalus, and finally died almost 7 years after the initial operation

variable for grade III patients (Figs. 3.45–3.47) but limited to months for grade IV patients [24, 45, 84, 130, 157]. Subarachnoid dissemination is very common in high-grade astrocytomas of the spinal cord and should be suspected in patients who deteriorate after therapy for these tumors (Figs. 3.77–3.79) [18, 45, 48, 121, 141, 258, 294]. Intramedullary glioblastomas have also been described after removal of intracranial high-grade astrocytomas [117], as was the case in one of our patients who developed a thoracic intramedullary glioblastoma after partial resection of an anaplastic thalamic astrocytoma.

Among our series of 16 high-grade astrocytomas, 9 underwent postoperative radiotherapy, 1 patient received chemotherapy, and 1 patient a combination of both. All four grade-IV patients were dead within 2 years. Of nine patients with grade III tumors, five patients survived longer than 2 years, with three patients still alive at 7, 52, and 103 months after surgery and six patients dead 10, 17, 20, 22, 48, and 80 months postoperatively. One explanation for the great variability in outcome of patients with grade III tumors may be related to difficulties with a correct histological classification. Even though reference centers were consulted in all cases, we have observed quite diverse opinions, especially with grading of astrocytomas in young children. Among such children with grade III tumors, two patients have not undergone any adjuvant therapy at all, with no evidence of tumor recurrence or progression on follow up.

First reports on chemotherapy of intramedullary gliomas in children are promising [333], even for high-grade tumors [13]. But these reports are still based on very low patient numbers. As malignant tumors in this localization are very rare, hardly any single institution acquires enough patients to perform an appropriate prospective study [13]. Given the fact that intramedullary astrocytomas behave differently compared to their intracranial counterparts, different clinical courses are apparent for children and adults, and the problems of a correct classification of spinal astrocytomas, it seems problematic to simply transfer experiences with chemotherapy of intracranial gliomas to intramedullary cases.

Allen et al. [5] described the results of a pilot study for 13 of 18 children with anaplastic astrocytomas and glioblastomas. The 5-year rate for recurrence-free survival was 46% and the overall 5-year survival rate was 54% for these 13 children. No survivors were encountered among glioblastomas; all except two surviving patients have evidence of disease. Doireau et al. [72] treated eight children with unresectable or recurrent tumors with a regimen of carboplatin, procarbazine, vincristine, cyclophosphamide, etoposide, and cisplatin over 16 months. Three patients had evidence of subarachnoid dissemination. The authors claimed

a complete remission in four children, with all but one child alive and clinically stable after 59, 55, 40, 35, and 16 months. However, among this small series of eight patients was one patient with an unclassified astrocytoma and two patients with pilocytic astrocytomas, while the remainder were anaplastic. Townsend et al. [333] observed a beneficial effect with chemotherapy for low-grade astrocytomas in children. This conclusion was based on four children. Quite clearly, an appropriate prospective study on a larger scale is needed to prove a beneficial effect for chemotherapy of spinal cord astrocytomas [13].

3.5.3 Angioblastomas

Angioblastomas represent about 2.1% [145, 247] to 5% [276] of spinal tumors according to the literature, and about 1.9% of all spinal and 11.8% of intramedullary tumors in our series. They tend to occupy the posterior, paramedian aspect of the spinal cord (Figs. 3.34 and 3.48) [185, 198, 223, 336]. However, centrally or anteriorly located angioblastomas do occur (Fig. 3.49) [134, 264].

We have operated on 21 intramedullary angioblastomas affecting nine female and eight male patients (Table 3.26). Ten tumors (48%) were associated with VHL. Among VHL patients, between 13% [202] and 38% [105] harbor spinal angioblastomas. In unselected series, about 22–25% of patients with an angioblastoma will turn out to have VHL [105, 263]. With identification of the VHL tumor suppression gene, molecular genetic screening has become available and should be offered to patients with angioblastomas [336]. VHL patients require yearly MRI scans of the brain and spinal canal. Radiological examinations of these patients should not only concentrate on measuring individual tumor sizes, but also monitor the associated cysts. We consider an increase of an intramedullary cyst associated with an unchanged angioblastoma as an indication for surgery as much as evidence of tumor growth. In one study, surgery was recommended even for asymptomatic patients with increasing cysts [336].

In our series, 12 tumors were situated in the cervical area and the remaining 9 in the thoracic cord; all but 2 demonstrated an associated syrinx. Patients presented at an average age of 39±14 years (range 13–65 years) after a history of 39±41 months, ranging between 2 months and 13 years. A comparison of patients with and without VHL revealed that patients with VHL were slightly younger (34±13 years and 42±14 years, with vs. without VHL, respectively; not significant) and presented a shorter history (19±23 and 51±48 months, respectively; p=0.03) than those without. Patients were followed for 53±59 months. One-third of patients each reported pain or sensory deficits as the initial symptoms, with motor weakness (14%), dysesthesias (14%), and sphincter disturbances (5%) being less common initially. At presentation, pain (29%), and sensory (24%) and motor deficits (24%) were mentioned as the major concerns by most patients [62, 185]. Dysesthesias (14%) and gait ataxia (10%) were reported as the main symptoms less often. This is in contrast to most other intramedullary pathologies where gait ataxia and motor weakness predominate the clinical picture on admission. Acute presentations due to an intramedullary hemorrhage have been reported, but are very rare [243, 280, 353].

Surgical resection is the treatment of choice. Radiation treatment has been performed in the past (Fig. 3.38) [277], but is no longer acceptable. In our series, there was no permanent surgical morbidity. All but two angioblastomas were removed completely. In these two cases, postoperative MRI demonstrated small tumor remnants.

In terms of local control of the angioblastoma and neurological outcome, we did not observe a difference between patients with and without VHL. Two-thirds of patients experienced some postoperative improvement and 29% an unchanged postoperative status [233, 345, 350], while one patient described a postoperative worsening. Pain in particular responds favorably to complete excision [62, 78, 304]. Yasargil et al. [350] achieved 11 complete resections among a series of 12 patients with intramedullary angioblastomas. Ten of these demonstrated postoperative clinical improvement.

The postoperative clinical result is determined by the preoperative status [62, 198, 263, 336] and the presence of VHL [78, 193]. Van Velthoven et al. [336] reported 28 patients with intramedullary angioblastomas; 18 (64%) were associated with VHL. All tumors were completely removed, with postoperative improvement in 28.6% and stabilization in 71.4% of patients.

Pluta et al. [264] compared their results for eight patients with anteriorly located angioblastomas according to the approach that was used. They encountered significant morbidity associated with posterior approaches in such tumors and obtained better results with anterior approaches using a corpectomy with subsequent fusion. We have not seen significant clinical worsening for any of our patients using the conventional posterior pathway.

Table 3.26. Overview of patients with intramedullary angioblastomas

Sex	Age (years)	Level	History (months)	VHL	Symptoms	Surgery	Outcome
F	13	Th9–12	60	No	Hypesth., Gait, Dysesth., Pain, Motor, Sphincter	Subtotal	Improved Rec. 17 months
M	46	C3–5	36	No	Hypesth., Dysesth., Pain, Motor	Subtotal	Improved No Rec. 211 months
F	47	C4–5	60	No	Hypesth., Gait, Motor	Complete	Improved No Rec. 11 months
F	65	C2	36	No	Hypesth., Gait, Dysesth., Pain, Motor	Complete	Improved No Rec. 130 months
F	47	Th6–7	4	No	Hypesth., Gait, Dysesth., Pain, Motor, Sphincter	Complete	Improved Rec. 36 months
M	23	C1	16	No	Hypesth., Gait, Dysesth.	Complete	Improved No Rec. 84 months
F	52	C5	48	No	Hypesth., Gait, Dysesth., Pain	Complete	Improved No Rec. 66 months
F	45	C6–7	156	No	Hypesth., Gait, Dysesth.	Complete	Worse No Rec. 9 months
F	44	C4–5	120	No	Hypesth., Gait, Dysesth., Motor	Complete	Unchanged Lost to follow up
M	42	C1	3	No	Hypesth., Gait, Dysesth.	Complete	Improved No Rec. 18 months
M	36	Th11	24	No	Dysesth., Pain	Complete	Unchanged Lost to follow up
M	24	C1–2	48	Yes	Hypesth., Gait, Dysesth., Pain, Motor	Complete	Improved Rec. 44 months
	24	Th10–11	2		Hypesth., Gait, Dysesth., Pain	Complete	Improved Rec. 6 months
	25	Th10	3		Hypesth., Gait, Dysesth., Pain, Motor, Sphincter	Complete	Improved No Rec. 38 months
	28	C1–3	6		Hypesth., Gait, Dysesth., Pain, Motor, Sphincter	Complete	Unchanged Lost to follow up
M	62	C4–6	12	Yes	Hypesth., Gait, Pain, Motor, Sphincter	Complete	Improved Died 12 months
M	38	C3	18	Yes	Hypesth., Gait, Pain, Motor, Sphincter	Complete	Unchanged Died 36 months

Abbreviations: F = female, M = male, VHL = von Hippel-Lindau disease, Hypesth. = hypesthesia, Dysesth. = dysesthesia, Gait = gait ataxia, Motor = motor weakness, Sphincter = sphincter disturbances, Rec. = recurrence

Table 3.26. (*Continued*)

Sex	Age (years)	Level	History (months)	VHL	Symptoms	Surgery	Outcome
F	23	Th5–6	14	Yes	Hypesth., Gait, Dysesth., Pain	Complete	Improved Rec. 71 months
	30	C5	10		Hypesth., Gait, Dysesth., Pain, Motor, Sphincter	Complete	Improved No Rec. 4 months
M	37	Th3–4	6	Yes	Hypesth., Dysesth.	Complete	Unchanged Lost to follow up
F	47	Th1	72	Yes	Hypesth., Gait, Motor, Sphincter	Complete	Unchanged Lost to follow up

Recurrences were observed among three out of six patients with VHL and for one patient each after a complete and an incomplete resection without VHL. In VHL, clinically relevant angioblastomas on different spinal levels were observed after varying intervals of a few months to 6 years.

De la Monte and Horowitz [67] observed a recurrence rate of 27% among 26 patients harboring lesions in the cerebellum (24 patients), spinal cord (1 patient), or cervicomedullary junction (1 patient). Recurrences were associated with young age (<30 years), VHL, and the presence of multiple tumors. Recurrent angioblastomas were less often accompanied by a syrinx.

Lee et al. [185] presented a series of 14 patients with angioblastomas with a male predominance of 11:3 and a median follow up of 47 months; 6 patients were affected by VHL and 13 had intramedullary tumors. They concluded that patients undergoing a complete resection had a better postoperative neurological state compared to incompletely removed tumors and emphasized the benefit of preoperative embolization to achieve complete resections.

In conclusion, intramedullary angioblastomas are not only completely resectable, but are also associated with the lowest surgical morbidity and the best neurological outcome among all intramedullary tumors. Therefore, the radiological diagnosis of an angioblastoma should lead to surgery as soon as symptoms have developed or repeated MRI scans have demonstrated tumor growth or progression of an associated syrinx [336].

In patients with VHL, the extraspinal affections of this syndrome ultimately determine the patient's fate [202], apart from multiple tumors requiring a series of operations over time. Such manifestations caused death in two of our VHL patients. As renal cell carcinomas and other neoplasms may occur in these patients, regular check-ups with ultrasound examinations of the abdomen are mandatory [78, 221, 237]. The median expected survival for VHL patients has been calculated at 49 years, with renal cell carcinomas as the commonest cause of death [202].

3.5.4 Hamartomas

We have observed four dermoid cysts, four lipomas, and one patient with a combination of both in this category of intramedullary tumors. Whereas hamartomas are not tumors in a strict sense – they do not contain proliferating cells – they are space occupying and displace spinal cord tissue. Quite regularly, they are not completely surrounded by cord substance and protrude out of the cord. The overwhelming majority of spinal hamartomas are located extramedullarly. We have only classified them as intramedullary if the major component of the lesion was embedded inside the spinal cord. Therefore, a more detailed discussion is provided in the section on extramedullary tumors. Among intramedullary hamartomas, one dermoid cyst and four lipomas were associated with a tethered-cord syndrome.

3.5.4.1 Lipomas

Lipomas may display an increasing size with time due to hypertrophy of the lipomatous tissue whenever there are changes of body fat in general. In other words, it may be possible to reduce the size of a lipoma by instigating a low-fat diet and weight reduction [79]. They have also been shown to increase during steroid therapy [2].

Table 3.27. Overview of patients with intramedullary hamartomas

Sex	Age (years)	Level	Type	History (months)	Symptoms	Surgery	Outcome
M	32	L1 TCS	L	36	Hypesth., Sphincter	Dec. Duraplasty	Unchanged No Rec. 9 months
F	42	C7–Th1	L	48	Hypesth., Gait, Dysesth., Pain, Motor, Sphincter	Dec. Duraplasty	Improved No Rec. 7 months
F	29	S1–S4 TCS	L	72	Hypesth., Gait, Pain, Motor, Sphincter	Dec. Duraplasty	Unchanged No Rec. 52 months
F	31	S1–S4 TCS	L	9	Hypesth., Gait, Motor, Sphincter	Dec. Duraplasty	Unchanged No Rec. 6 months
F	42	L1–2 TCS	L+D	120	Hypesth., Gait, Dysesth., Pain, Motor, Sphincter	D Compl. L Partial Duraplasty	Improved No Rec. 16 months
F	25	L5–S1 TCS	D	1	Hypesth., Gait, Dysesth., Pain, Motor, Sphincter	Subtotal	Worse No Rec. 182 months
M	29	Th11–L1	D	6	Gait, Motor	Subtotal	Improved No Rec. 3 months
F	32	Th3–5	D	10	Hypesth., Gait, Motor	Dec. Duraplasty	Improved No Rec. 40 months
F	31	Th11–L1	D	9	Hypesth., Gait, Pain, Motor	Subtotal	Improved No Rec. 48 months

Abbreviations: L = lipoma, D = dermoid cyst, TCS = tethered cord syndrome, Dec. = decompression, Compl. = complete resection

The preoperative history tends to be longer compared to other intramedullary entities [101, 188]. The five patients in this series presented after a history of 57±42 months (range 9 months to 10 years) at a mean age of 35±6 years (range 29–42 years) and were followed for 21±21 months (maximum 52 months). Symptoms were dominated either by pain (three patients) or sphincter disturbances (two patients). One lipoma was encountered in the cervicothoracic junction and the other four in the conus area (Table 3.27).

Lipomas do not demonstrate a good dissection plane toward the spinal cord, similarly to an infiltrating neoplasm. Therefore, a complete resection of an intramedullary lipoma is not recommended [73, 167]. Decompression of the affected spinal segments is the procedure of choice (Figs. 3.51 and 3.80) [77, 174]. If at all, partial resection of the extramedullary portion of the lipoma is all that should be attempted (Fig. 3.80) [63, 167].

Several authors recommend the use of carbon dioxide lasers for removal of lipomas. This technique is reported to reduce blood loss during removal and to shorten the operation considerably [218, 347]. We have no experience with this technique.

We have removed one lipoma partially (Fig. 3.80) and decompressed the other four with a generous dura graft (Fig. 3.51). No postoperative neurological improvements should be expected for intramedullary lipomas [167]. Pain may be reduced, but otherwise no clinical change is the common outcome [188]. Among this series, two patients improved and three were left unchanged, with no subsequent recurrences (Table 3.27). However, due to dysesthesia syndromes, three patients deteriorated, with two demonstrating a progressive myelopathy related to retethering.

Fig. 3.80. Sagittal (**a**) and axial (**b**) T1-weighted MRI scans of an intramedullary lipoma at L1 associated with a tethered cord syndrome in a 32-year-old man with a 3-year history of sphincter problems. The postoperative T1- (**c**) and T2-weighted (**d**) MRI scans show the desired result with a good decompression of the conus, release of the tethered cord, and no postoperative scar formation leading to retethering. However, the patient developed a disturbing dysesthesia syndrome 4 months later

3.5.4.2 Dermoid Cysts

With dermoid cysts the situation is different; they contain cells that produce some kind of gradually accumulating product. This will increase the size of the cyst with the potential of progressive pressure on the spinal cord. The history is considerably shorter compared to lipomas – 29±51 months in this series, ranging from 1 month to 10 years. Even acute presentations related to aseptic meningitis [65, 296] or abscess formation [49] have been described. The average age was 32±6 years (range 25–42 years), with pain in three patients and motor weakness in two patients as the major clinical problems (Table 3.27) [197].

The goal of treatment should be a radical excision. Unfortunately, the cyst wall may be extremely adherent to the cord substance, making it almost impossible to achieve a complete resection without damaging the cord. Sharp dissection is often required (Figs. 3.50 and 3.81). Furthermore, the cyst material may be very irritating for the arachnoid membrane, with a significant risk of aseptic meningitis, if the subarachnoid space becomes contaminated [197]. Therefore, we consider dermoid cysts to be one of the most difficult surgical challenges among intradural spinal pathologies. If a complete resection can be performed, the outcome will be favorable [30, 179]. On the other hand, it may be wiser to leave part of the cyst wall in

Fig. 3.81. a Sagittal T1-weighted MRI scan of an intramedullary dermoid cyst at L1–L2 and a tethered cord in a 42-year-old woman with a 10-year history of pain and progressive paraparesis. The postoperative T1-weighted image (**b**) demonstrates the result after partial resection of the cyst and release of the tethering. No duraplasty was inserted, but despite postoperative fixation of the conus to the dura, no progressive myelopathy developed

place rather than to force the issue of radical excision (Figs. 3.50 and 3.81). After incomplete resections, recurrence rates appear to be low [197]. We have resected one dermoid cyst completely, performed subtotal resections in the other three instances, and a decompression in one patient. No recurrences were observed for these patients (Table 3.27). Again, two patients were affected by a dysesthesia syndrome, of which one progressed to a myelopathy associated with cord retethering.

3.5.5 Glioependymal Cysts

Intramedullary glioependymal cysts are observed predominantly in the area of the conus medullaris (Figs. 3.82 and 3.83), but may occur anywhere in the spinal canal (Fig. 3.84) [279]. The cyst contains fluid that is similar to CSF [279]. Some authors have called these cysts terminal ventricles or considered them to be an isolated eccentric syrinx of the conus medullaris. The majority of them are observed in adults, with most pediatric cases being asymptomatic [50].

The differential diagnosis to cystic tumors can be made after gadolinium application. The wall of an ependymal cyst will not take up contrast [279, 313]. The distinction form syringomyelia, however, may pose some problems (Figs. 3.19–3.22). With cysts in the conus area that protrude out of the cord, the diagnosis of an ependymal cyst is quite easy (Fig. 3.18). However, at other spinal levels it may be not so obvious. The best guideline is the caliber and shape of the ependymal cyst. They cause significant and symmetric cord expansion at both ends whereas a syrinx tends to taper off gradually at either the caudal or cranial pole. Furthermore, septations are not a feature of ependymal cysts [313].

As far as the pathophysiology of these cysts is concerned, no widely accepted theory exists. One case report dealt with an ependymal cyst and an associated tethered cord – as in one of our patients (Fig. 3.82) – raising the question of a dysraphic background [12, 50]. Coleman et al. [50] examined 418 spinal MRI scans in children and young adults between 5 days and 20 years of age and found 11 (2.6%) children under 5 years of age with ovoid dilatations of the central canal in the conus medullaris; 53% of studied patients were older than 5 years and did not show such dilatations. They concluded that dilatations of the conus are a developmental phenomenon representing a normal variant in young children. This theory, however, does not explain why some patients retain these dilatations and become symptomatic. The theory favored by most authors explains these cyst as a result of proliferating ectopic ependymal cells [99].

The often eccentric position of symptomatic cysts in the conus area, the high pressure inside these cysts, and the lack of craniocaudal expansion with time suggest that ependymal cysts never had, or no longer have, a communication with the central canal, and that they do not communicate with the extracellular space of the spinal cord (Fig. 3.83). Unlike syringomy-

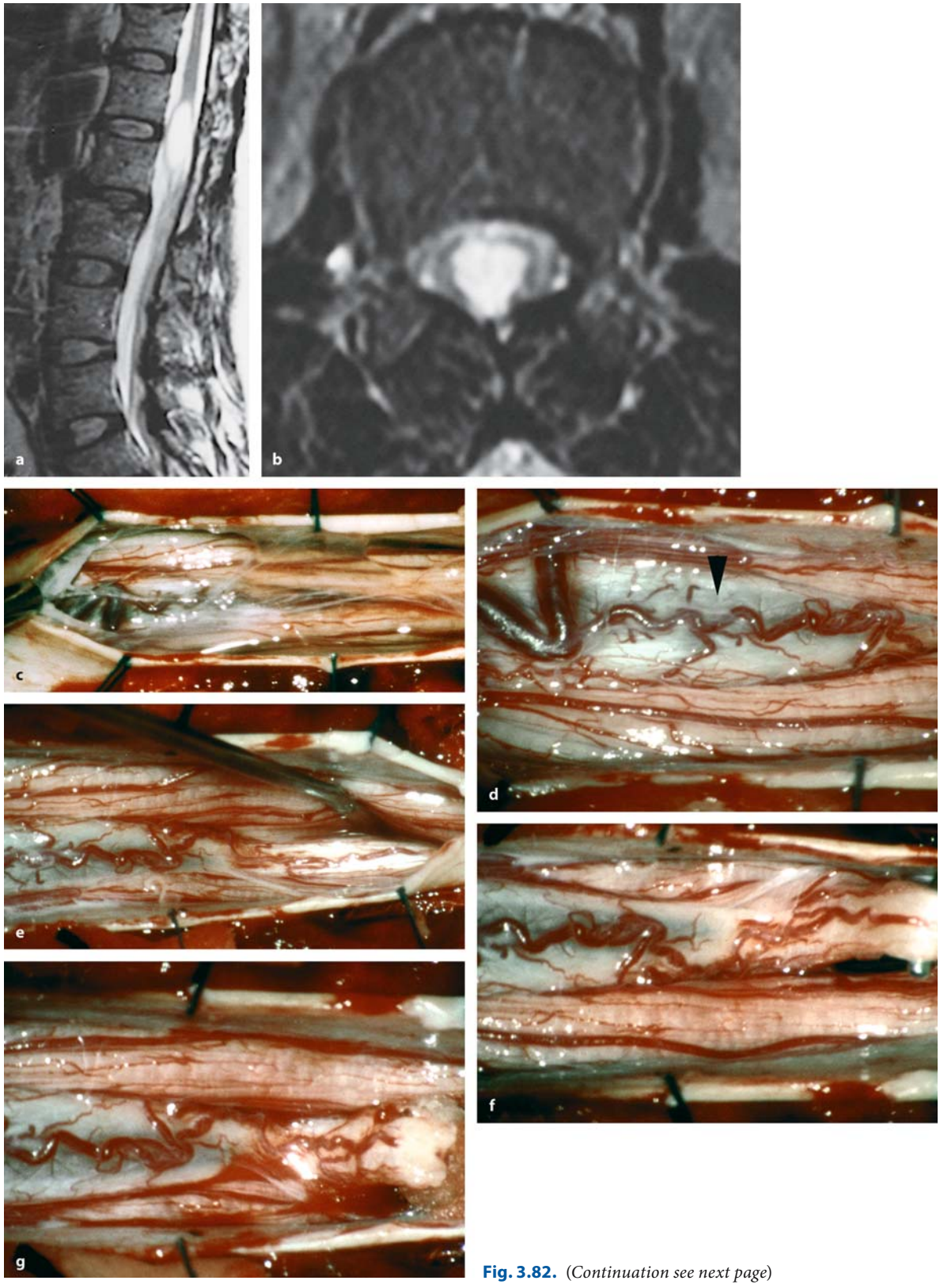

Fig. 3.82. (*Continuation see next page*)

Fig. 3.82. (*Continued*) Sagittal (**a**) and axial (**b**) T2-weighted MRI scans of an ependymal cyst at L1–L2 and an associated tethered cord in a 58-year-old woman with an 18-month history of progressive paraparesis and pain, but preserved sphincter functions. **c** This intraoperative view was taken after dura opening and demonstrates slight arachnoid adhesions and thickening. **d** After arachnoid opening, the cyst was almost visible through the pia mater and thinned out posterior tracts in the midline (*arrowhead*). **e** The thickened filum terminale is displayed and clearly distinguishable by its brighter color compared to neighboring nerve roots. The filum was then isolated (**f**), coagulated, and cut (**g**) to untether the cord. **h** Finally, the ependymal cyst was opened in the midline. A wide fenestration was not performed to avoid damage to white matter tracts. Postoperatively, the patient showed improvement of walking, sensory disturbances, and pain

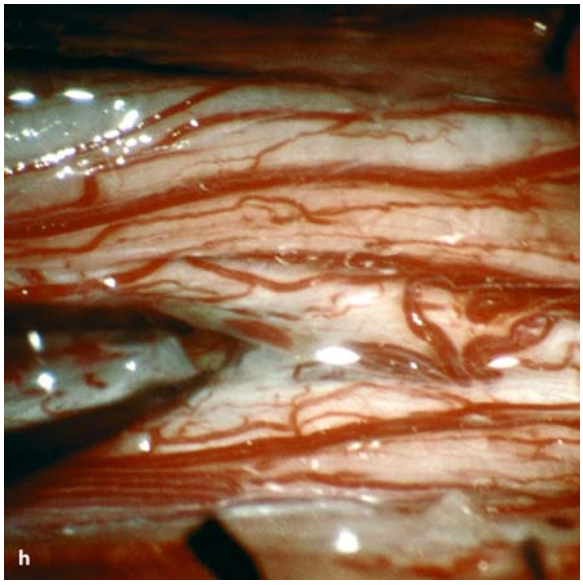

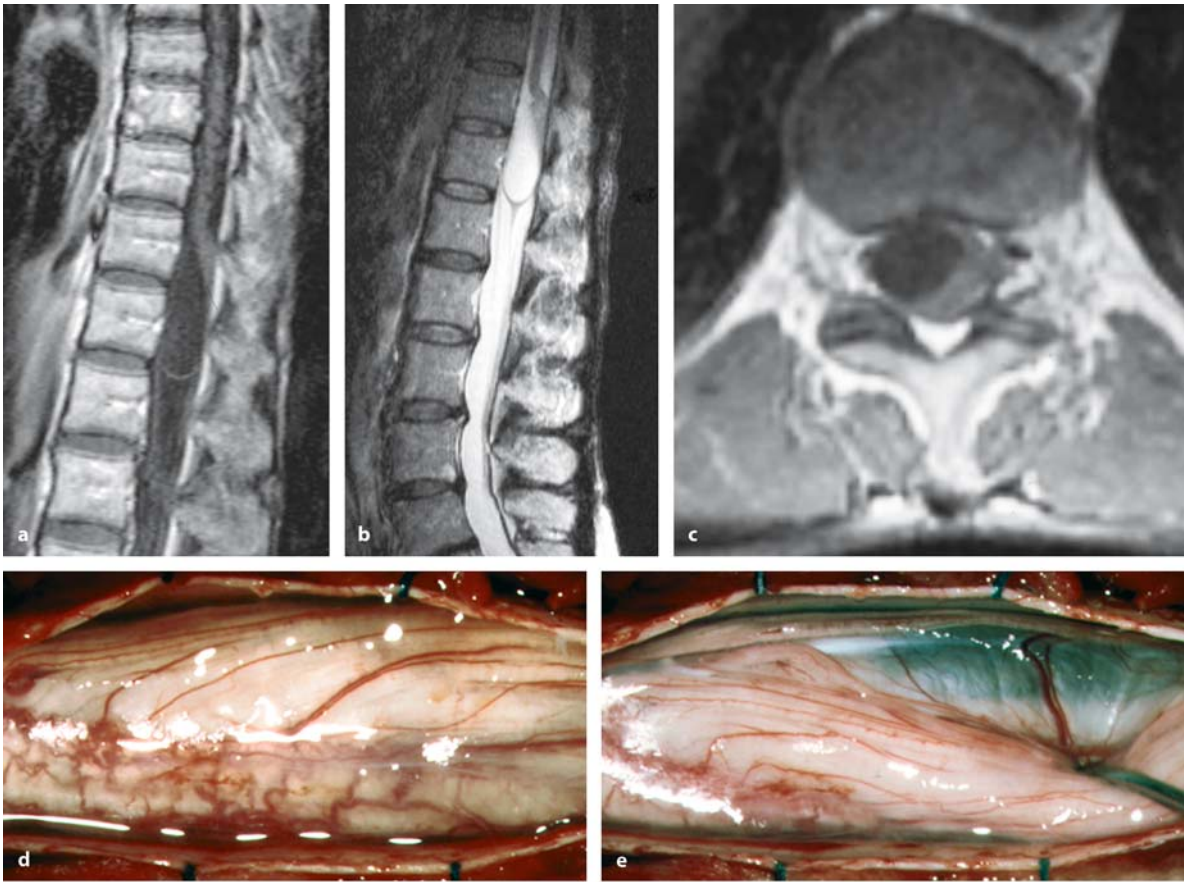

Fig. 3.83. Sagittal T1- (**a**) and T2-weighted (**b**), and axial T1-weighted (c) MRI scans of an ependymal cyst of the conus at Th11–Th12 in a 66-year-old woman with a 7-year history of a progressive quadriceps paresis on the right side. Note the eccentric position of the cyst in the sagittal and axial plane and the significant space-occupying effect. **d** This intraoperative view, taken after dura opening, demonstrates a completely normal, translucent arachnoid membrane, and an anticlockwise rotation of the conus due to the cyst. **e** Mobilizing the right-sided roots with a dissector exposed the cyst wall. (*Continuation see next page*)

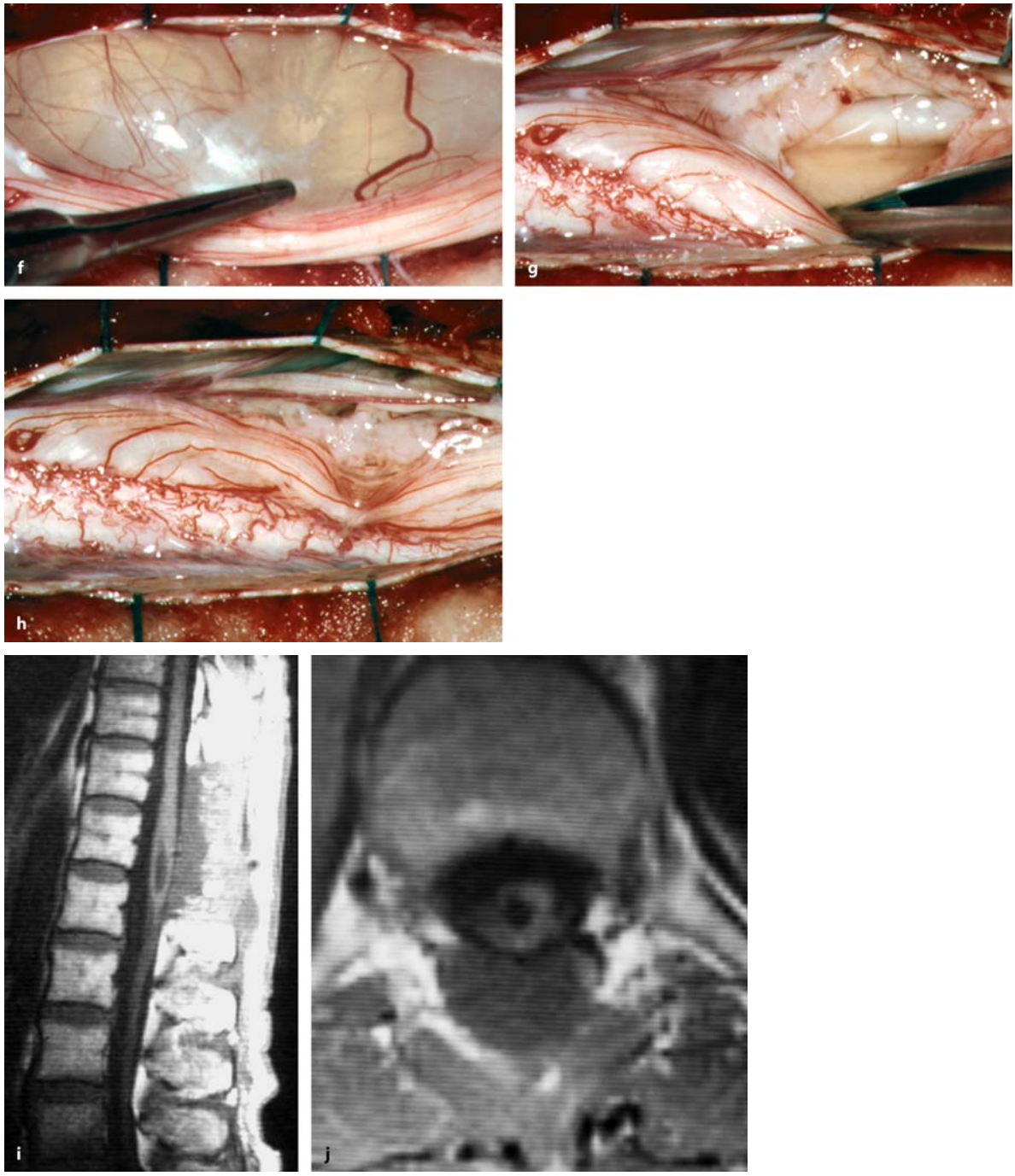

Fig. 3.83. (*Continued*) **f** Slight further rotation of the conus provided access to the anterior cyst wall, which was translucent and covered by the pia mater. There were no nervous structures in this part of the cyst wall. With wide fenestration of the cyst wall (**g**), the cyst collapsed (**h**). The postoperative sagittal (**i**) and axial (**j**) T1-weighted scans demonstrate a good decompression of the conus. The paresis improved postoperatively. No recurrence has occurred within 3 years

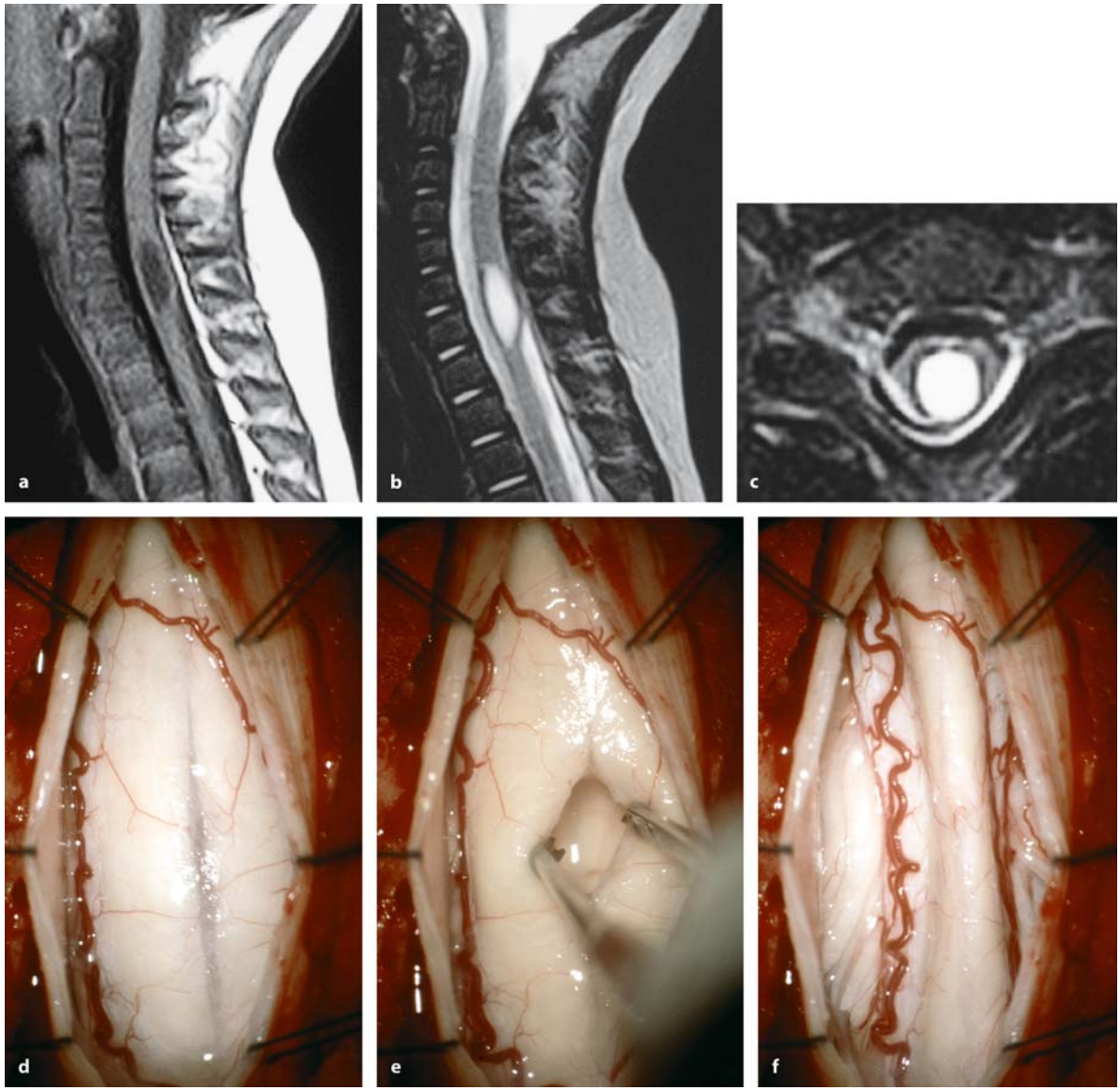

Fig. 3.84. Sagittal T1- (**a**) and T2-weighted (**b**), and axial T2-weighted (**c**) MRI scans of an ependymal cyst at C6–C7 in a 51-year-old woman with a 4-month history of pain and dysesthesias in her left arm. **d** This intraoperative view, taken with the patient in the semisitting position after dura and arachnoid membrane opening, displays a swollen cord with diminished vascularization of the posterior cord surface. The pia appears translucent in the midline. The cyst was opened in the midline (**e**), after which it collapsed (**f**). (*Continuation see next page*)

elia, ependymal cysts are not related to disturbances of CSF flow, so a different mechanism must be operating, which still needs to be elucidated.

The cysts are lined with collagenous tissue and cuboidal cells with no separate basement membrane [12, 92, 99, 147, 180, 279, 307]. The literature provides case reports or small series of patients. The recommended treatment is either drainage [279, 286, 320] or partial resection of the cyst wall [12, 92, 147, 180, 238, 279] with good results for both techniques. Sharma et al. [307] excised the cyst wall completely at Th4/5 in a 7-year-old child with progressive paraparesis and observed a good postoperative recovery.

We have encountered seven patients with ependymal cysts. All but two were located in the conus, with one patient demonstrating an additional tethered cord. Patients presented at an average age of 51±9 years after a history of 31±30 months (range 2 weeks to 7 years). They were followed for 43±57 months (maximum 10 years; Table 3.28). Pain was the most promi-

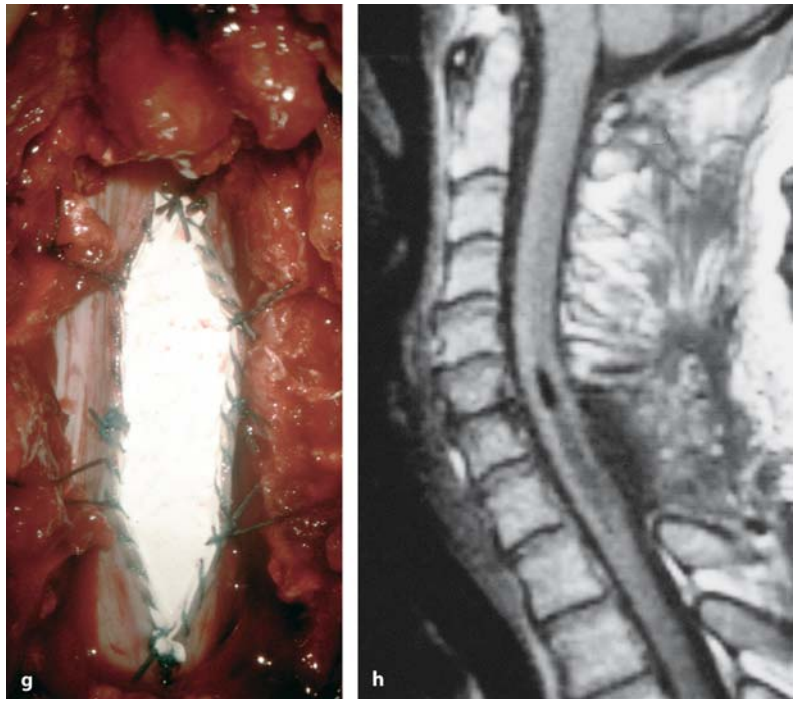

Fig. 3.84. (*Continued*) **g** A Gore-Tex® duraplasty was inserted. **h** The postoperative T1-weighted MRI demonstrates a good decompression of the cervical cord and a free CSF passage in the operated area. Preoperative symptoms improved

Table 3.28. Overview of patients with intramedullary ependymal cysts

Sex	Age (years)	Level	History (months)	Symptoms	Surgery	Outcome
M	44	C2–C6	48	Hypesth., Dysesth., Pain, Motor, Sphincter	Drainage	Improved No Rec. 118 months
F	52	Th11–12	12	Pain	Cystostomy Duraplasty	Unchanged No Rec. 17 months
F	45	Th11–12	48	Hypesth., Gait, Dysesth., Pain, Motor, Sphincter	Cystostomy Duraplasty	Unchanged Rec. 60 months
F	66	Th11–12	84	Gait, Motor	Fenestr.	Improved No Rec. 32 months
F	58	Th11–L1 TCS	18	Hypesth., Gait, Dysesth., Pain, Motor	Cystostomy Duraplasty	Improved Lost to follow up
F	51	C5–Th1	4	Hypesth., Pain	Cystostomy Duraplasty	Improved No Rec. 4 months
F	41	Th12–L1	0.5	Gait, Pain	Fenestr.	Unchanged Lost to follow up

Abbreviation: Fenestr. = fenestration

nent clinical problem [99], with four patients developing motor deficits.

According to our experience with syringomyelia, we have been reluctant to place shunts in these cysts. Only one patient underwent cyst shunting to the subarachnoid space with a good clinical and radiological result. Whenever the cyst wall had displaced the cord to a degree that only the pia mater covered the cyst lining, wide fenestrations were performed (Fig. 3.83) [99]. In all other instances, we have opened the cyst in the midline and then decompressed the subarachnoid space with a generous dura graft (Figs. 3.82 and 3.84). One recurrence was observed among this latter group with postoperative improvements reported by four patients and unchanged situations by three patients.

3.5.6 Cavernomas

Intramedullary cavernomas are rare pathologies and represented 3% of our intramedullary pathologies [69]. On even rarer occasions they may be associated with familial multiple cavernomas of the central nervous system (Fig. 3.85) [69, 187]. Despite being so rare, this entity has attracted a considerable number of publications [1, 32, 34, 61, 69, 70, 109, 216, 219, 244, 246, 293, 308, 315, 337, 354]. The majority of patients are women [32, 61, 244].

The preoperative clinical course tends to be characterized by a stepwise neurological progression due to repeated hemorrhages [34, 61, 69, 109, 219, 244, 288, 354]. Years may go by between such phases of deterioration [246]. Other patients present a slowly deteriorating course due to smaller hemorrhages and increasing gliosis [34, 61, 69, 244, 246] or an acute onset of symptoms associated with major bleedings [32, 69, 70, 244, 246]. Pediatric patients tend to present acutely more often than adult patients [70]. Pain and sensory problems usually predominate the clinical picture [32, 109], but acute paraplegias due to massive hemorrhages are described [123]. Patients have also been described with subarachnoid hemorrhages [205] and large intramedullary bleedings causing hematomyelia [235].

A controversial discussion centers around the question of what to recommend for incidentally discovered intramedullary cavernomas. Cantore et al. [34] and Cristante and Hermann [61] recommend observation of such patients. Ojemann et al. [246] suggest removal of incidentally found intramedullary cavernomas if they are located posteriorly (i.e., in a favorable position for resection). The risk of hemorrhage is thought to be about 1.6% per year [32]. Sandalcioglu et al. [288] calculated a higher bleeding rate of 4.5% per patient year and a rebleeding rate of 66% per patient year in those with a previous hemorrhage,

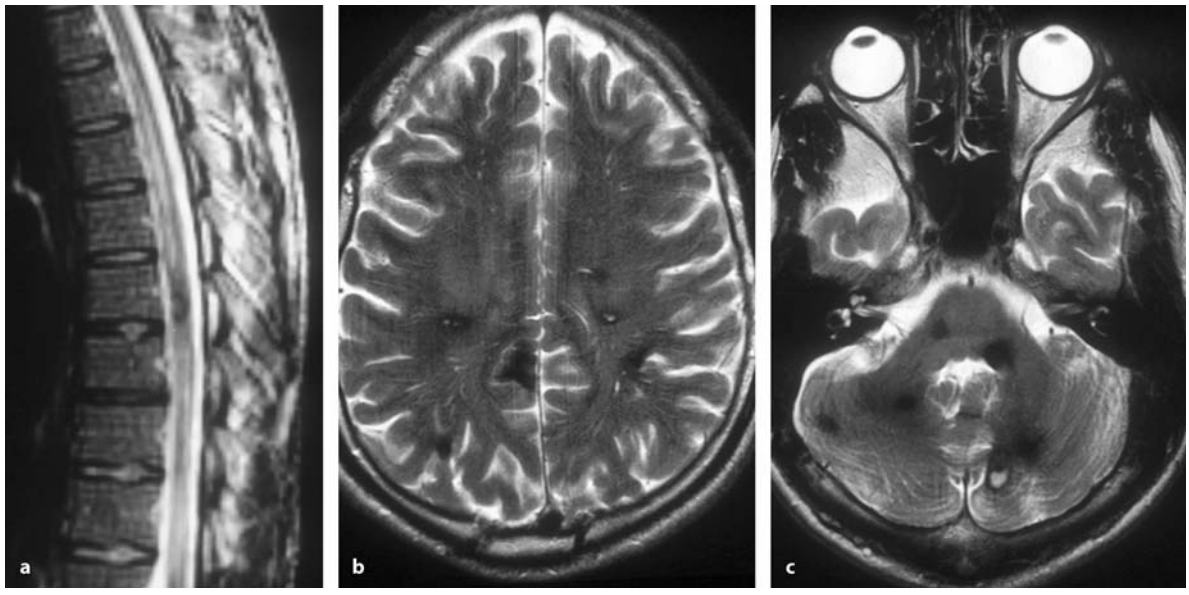

Fig. 3.85. These T2-weighted MRI scans of the thoracic cord (**a**), cerebrum (**b**), and cerebellum (**c**) demonstrate multiple cavernomas in a father of a boy with a cavernoma of the third ventricle. The father complained of minor headaches but no neurological symptoms. Given the pathology of his son, he had asked for this MRI scan. No recommendation for surgery has been given so far because of the small sizes of the lesions

Table 3.29. Overview of patients with intramedullary cavernomas

Sex	Age (years)	Level	History (months)	Symptoms	Surgery	Outcome
F	43	Th7–9	4	Hypesth., Gait, Dysesth., Pain, Motor, Sphincter	Complete	Unchanged No Rec. 54 months
M	57	Th3	16	Hypesth., Gait, Dysesth., Pain, Motor, Sphincter	Complete	Improved No Rec. 18 months
M	22	Th7–8	0.1	Hypesth., Gait, Dysesth., Pain, Motor, Sphincter	Subtotal	Improved Lost to follow up
F	59	Th3	12	Hypesth., Gait, Dysesth., Pain, Motor, Sphincter	Complete	Improved No Rec. 58 months
F	38	Th6	120	Hypesth., Gait, Dysesth., Pain, Motor	Complete	Improved No Rec. 4 months
F	51	C2	1	Dysesth., Pain	Complete	Improved No Rec. 3 months

according to their experience with ten patients. Cervical cavernomas are considered especially prone to clinical deterioration [32, 69]. Given the enormous consequences of a significant intramedullary hemorrhage and the low surgical morbidity, we would agree with Ojemann's view and recommend resection of all symptomatic intramedullary cavernomas and those asymptomatic ones that are located posteriorly [246].

Postoperative results for cavernomas are gratifying. Almost all can be resected completely, and a considerable proportion of patients can be expected to improve clinically (Fig. 3.52) [1, 34, 61, 109, 288, 293, 315].

We observed four female and two male patients. All but one cervical cavernoma were located in the thoracic cord. Except for the cervical cavernoma, these patients were admitted with significant neurological deficits: four patients had significant motor deficits, of which two were unable to walk, and four patients had significant sphincter problems. All but one cavernoma could be removed completely. Five patients in our series improved postoperatively, while the other remained stable. There was no recurrence or morbidity of late onset among this group of patients (Table 3.29). These numbers certainly support our view to operate these lesions before severe deficits have developed.

3.5.7 Metastases

Intramedullary metastases are rare complications of cancerous diseases. In the literature, case reports predominate for this topic. In a recent review, Kalayci et al. [159] evaluated 284 patients reported in the English literature. Of these, just 32 had been treated surgically. Prior to MRI, such lesions were usually diagnosed at autopsy [53, 110]. Miller and McCutcheon [223] gave a figure of 24% for cerebral metastases among autopsied cancer patients, compared to 0.014% with intramedullary metastases. In a survey of 627 patients with cancerous disease by Costigan and Winkelman [59], 153 patients showed metastases to the central nervous system. Among these, 13 patients harbored an intramedullary metastasis (i.e., 2.1% of all cancer patients and 8.5% of those with central nervous system involvement). Just 4 of these 13 patients showed clinical evidence of a myelopathy [59]. Intramedullary metastases indicate an end stage of the disease [114, 177]. In their literature review, Kalayci et al. [159] found other metastases in 55% of these patients, with 41% also demonstrating brain metastases. Therefore, surgery should not be generally recommended, even though longer survival has been claimed for patients undergoing surgery [159].

Intramedullary metastases are the result of hematogenous spread [59, 119, 155, 328]. On rare occasions, multiple intramedullary metastases have been reported (Fig. 3.86) [159]. Leptomeningeal dissemination is

exceptional [59, 154, 262, 328]. Lung (Fig. 3.87) [8, 42, 59, 71, 87, 90, 103, 146, 159, 166] and breast carcinomas [22, 41, 155, 177, 182, 184, 321] are the commonest primary tumors [114, 225], but others have also been reported [7, 114, 126, 127, 143, 154, 201, 212, 287, 299, 329, 330, 349].

Fig. 3.86. Sagittal, contrast-enhanced T1-weighted image of multiple thoracic intramedullary metastases of a bronchial carcinoma in a 54-year-old patient. Due to the small size of the tumor and the terminal stage of his disease, no surgery was recommended.

Most patients are in a much reduced general health status with a history of rapid neurological deterioration [114, 143, 177, 298, 303, 331, 339]. However, as intramedullary metastases are very rare, the diagnosis is often only made at surgery [186, 270].

We observed four intramedullary metastases originating from a bronchial carcinoma in two patients (Figs. 3.86 and 3.87) and from hypernephroma and urothel carcinoma in the other two patients. The patients' ages varied between 60 and 71 years. There were one cervical, one cervicothoracic, and two thoracic metastases. The history was short, and varied between 1 week and 5 months. All presented with a severe paraparesis unable to walk. The patient with kidney metastasis underwent a complete resection of the intramedullary metastasis, improved neurologically, and died 5 months after surgery. Two metastases were resected partially and one only decompressed. None of these three benefitted from surgery and died within 1 month. Similar results are reported in the literature in terms of survival, with the majority of patients dying within 6 months after operation [43, 53, 114, 177, 298, 328]. In their literature survey analyzing 44 sufficiently documented cases, Kalayci et al. [159] calculated that conservative treatment led to improvement in 50% of cases, while 28% were unchanged and 22% deteriorated further. After surgery,

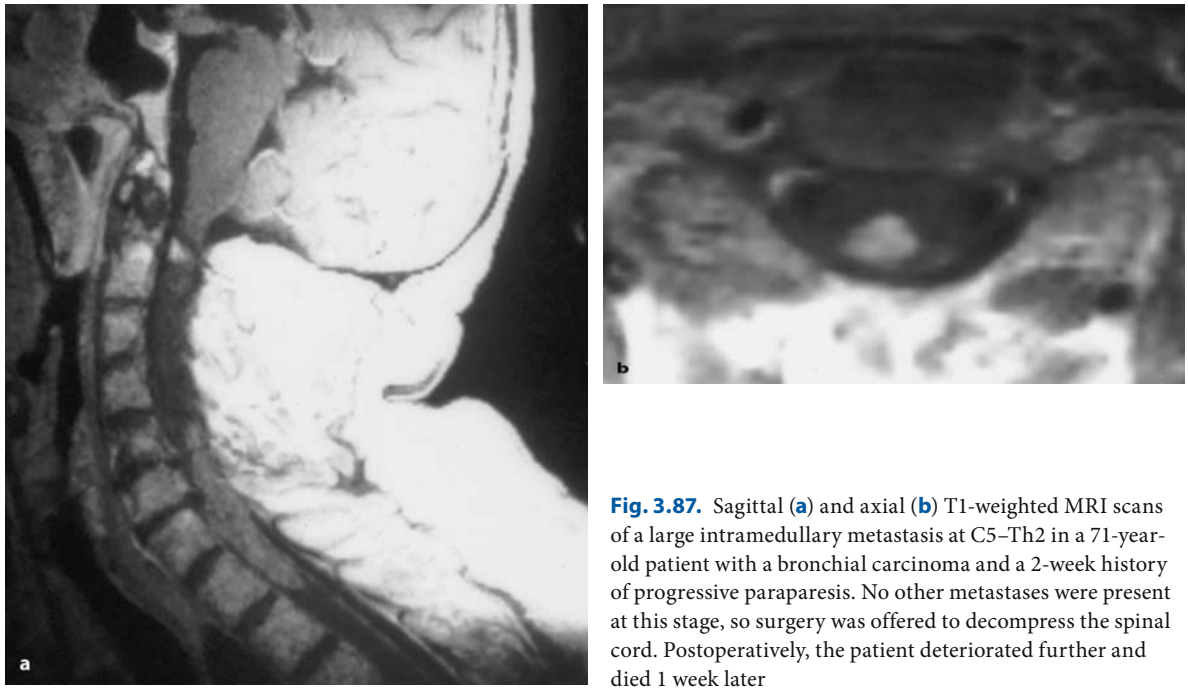

Fig. 3.87. Sagittal (**a**) and axial (**b**) T1-weighted MRI scans of a large intramedullary metastasis at C5–Th2 in a 71-year-old patient with a bronchial carcinoma and a 2-week history of progressive paraparesis. No other metastases were present at this stage, so surgery was offered to decompress the spinal cord. Postoperatively, the patient deteriorated further and died 1 week later

77% improved and 23% were left unchanged. Considering, that surgery was probably offered for patients who were in a better condition, it is our opinion that these numbers do not substantiate their conclusion that surgery should be more widely recommended for these patients.

In cancer patients, the differential diagnosis includes paraneoplastic myelopathies, radiation myelopathy, and chemotherapy-induced myelopathy [44, 172, 206, 343]. The distinguishing feature may be the rapidly deteriorating symptoms accompanied by pain [343]. Intramedullary metastases may even be accompanied by a syrinx [100, 166, 262] or intramedullary hemorrhages [192].

Given the limited life expectancy of these patients, surgery should be undertaken only in selected patients who are in comparably good clinical condition, without disseminated disease, and with progressive neurological deficits [87, 91, 126, 143, 186]. Attempts at radical resection are not warranted. We rather rec-

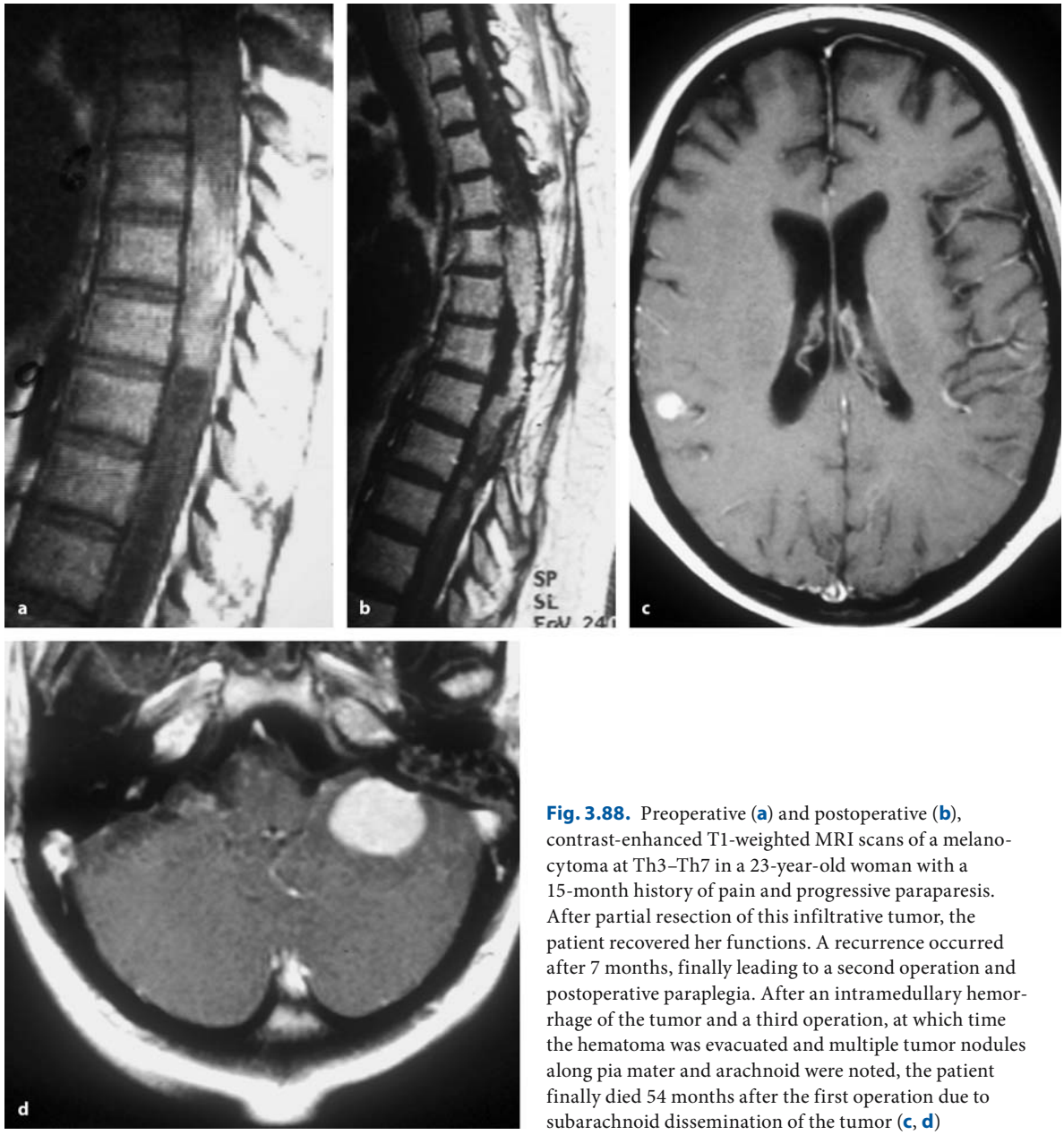

Fig. 3.88. Preoperative (**a**) and postoperative (**b**), contrast-enhanced T1-weighted MRI scans of a melanocytoma at Th3–Th7 in a 23-year-old woman with a 15-month history of pain and progressive paraparesis. After partial resection of this infiltrative tumor, the patient recovered her functions. A recurrence occurred after 7 months, finally leading to a second operation and postoperative paraplegia. After an intramedullary hemorrhage of the tumor and a third operation, at which time the hematoma was evacuated and multiple tumor nodules along pia mater and arachnoid were noted, the patient finally died 54 months after the first operation due to subarachnoid dissemination of the tumor (**c**, **d**)

ommend concentrating on decompressing the spinal cord with moderate debulking of the tumor and insertion of a duraplasty, followed by postoperative irradiation or chemotherapy if applicable [120]. Alternatively, radiotherapy and corticosteroid medication [41, 103, 114, 166, 298, 330, 339, 343], or chemotherapy [90, 349] have been reported to benefit patients with intramedullary metastases.

3.5.8 Melanocytomas

Intramedullary melanocytomas are extremely rare. They have to be differentiated from melanomas and melanoma metastases. Glick et al. [106] published a series of seven patients. They performed detailed pathological examinations and concluded that melanocytomas lack anaplastic features but demonstrate local aggressive behavior.

On the other hand, two case reports of patients with melanocytomas have been published with rather rapid neurological progression and death. Barth et al. [16] reported on a primary intramedullary melanocytoma of the thoracic cord in a 49-year-old woman. The tumor was resected twice and disseminated to the sacral as well as intracranial subarachnoid space. The patient died 4 years after the diagnosis had been established. Takenaka et al. [326] reported on a melanocytoma of the medulla oblongata. The patient died 7 months after surgery.

We have seen two female patients with thoracic melanocytomas with completely different outcomes. One 23-year-old female patient presented with a 15-month history of a moderate paraparesis. She underwent two incomplete tumor resections in 2 years with complete paraplegia and postoperative radiotherapy after the second operation. She progressed further and presented 3 years after the initial diagnosis with a massive intramedullary hemorrhage and increasing tetraparesis requiring a third operation with evacuation of the hematoma. After that operation, her upper extremity function improved again but she developed subarachnoid dissemination with intracranial seeding and died 54 months after the first operation (Fig. 3.88).

The other 62-year-old female patient demonstrated a 3-month history of increasing paraparesis due to a tumor at Th10–T12. She underwent a subtotal resection and recovered significantly after this operation. Despite incomplete resection, she received no adjuvant postoperative therapy but is free of tumor regrowth for 93 months.

3.5.9 Gangliogliomas

Gangliogliomas are rare intramedullary tumors. We have encountered two such patients: one 4-year-old boy showed a tumor at Th2–T5 that was resected subtotally, while the cervical tumor at C5/6 in a 27-year-old woman could be removed completely (Fig. 3.89) with excellent outcomes in both patients.

Gangliogliomas have been reported in pediatric series of intramedullary tumors, while adult patients are usually affected at a comparably young age [131, 153, 250, 253, 340]. Constantini et al. [54] found them in 8 out of 23 children under the age of 3 years. Of these, two patients demonstrated a recurrence after surgery. Epstein et al. [84] found them in 3 out of 25 adult patients with intramedullary tumors. In later publications, this group described the radiological features in 27 patients [253] and treatment results for 56 patients [153]. These tumors may extend over several spinal segments, contain cysts, and display mixed signal intensities on T1-weighted MRI scans [153, 223]. They show a patchy enhancement with gadolinium and enhancement of the spinal cord surface [173, 253].

The great majority can be resected completely as demonstrated by Jallo et al. [153] with 46 completely and 12 subtotally removed tumors. Patients had presented at an average age of 6 years (range: 7 months to 25 years). The commonest presenting symptoms were paraparesis and pain. There were 8 tumors of the cervicomedullary junction, 7 cervical, 21 cervicothoracic, 16 thoracic, and 4 conus tumors in this series. The long-term outlook after complete resections is excellent, with 72% of patients reporting improved or unchanged neurological function and a 5-year progression-free survival of 67%. The 5- and 10-year survival rates were 88% and 77%, respectively. Radiotherapy appeared to be unnecessary [153, 223].

Good results with complete surgical removal have also been claimed by Park et al. [250], whereas incomplete resections were followed by a high recurrence rate. Even leptomeningeal dissemination has been reported with gangliogliomas [18]. Apart from these series, case reports on gangliogliomas have been published [160, 340].

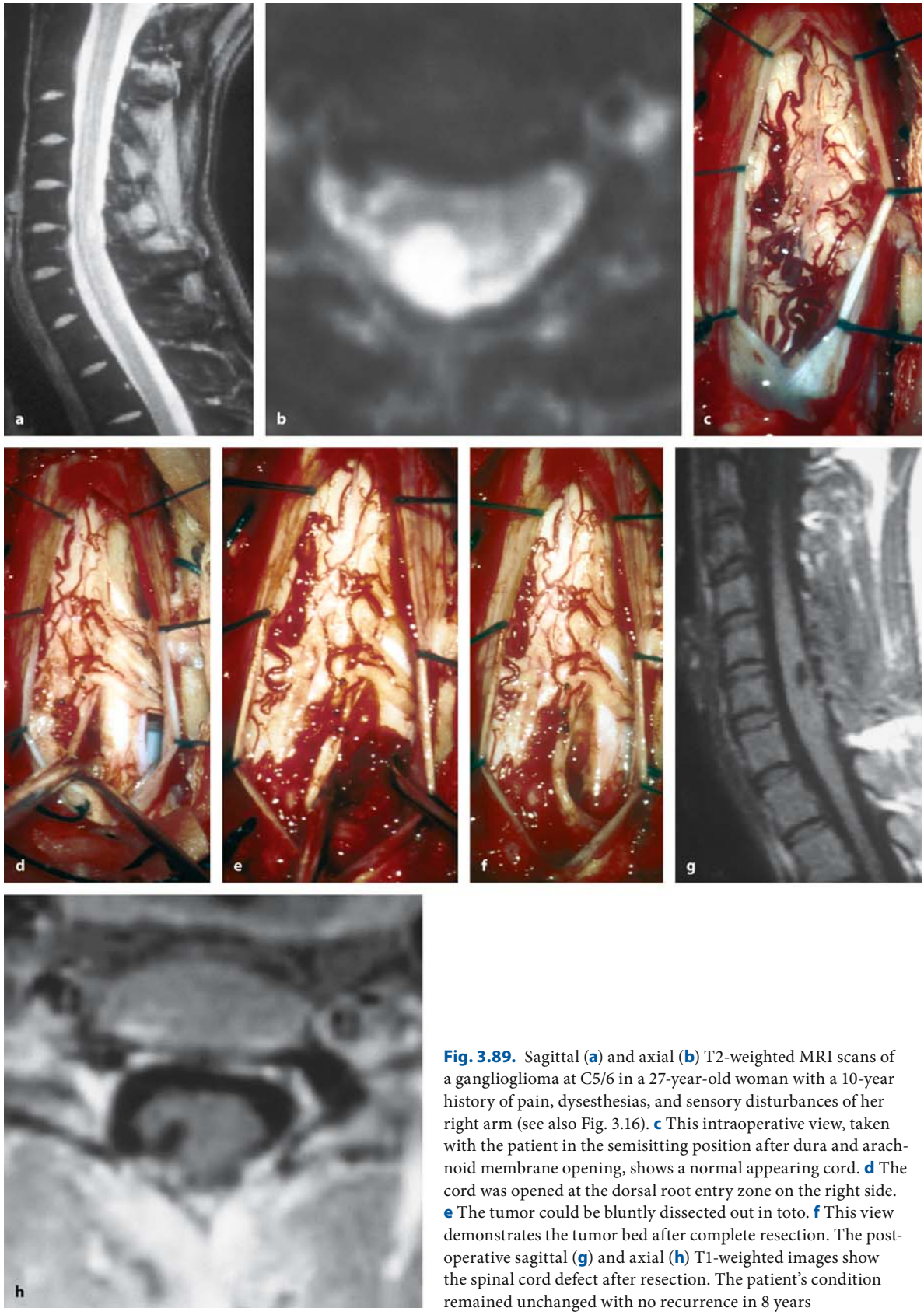

Fig. 3.89. Sagittal (**a**) and axial (**b**) T2-weighted MRI scans of a ganglioglioma at C5/6 in a 27-year-old woman with a 10-year history of pain, dysesthesias, and sensory disturbances of her right arm (see also Fig. 3.16). **c** This intraoperative view, taken with the patient in the semisitting position after dura and arachnoid membrane opening, shows a normal appearing cord. **d** The cord was opened at the dorsal root entry zone on the right side. **e** The tumor could be bluntly dissected out in toto. **f** This view demonstrates the tumor bed after complete resection. The postoperative sagittal (**g**) and axial (**h**) T1-weighted images show the spinal cord defect after resection. The patient's condition remained unchanged with no recurrence in 8 years

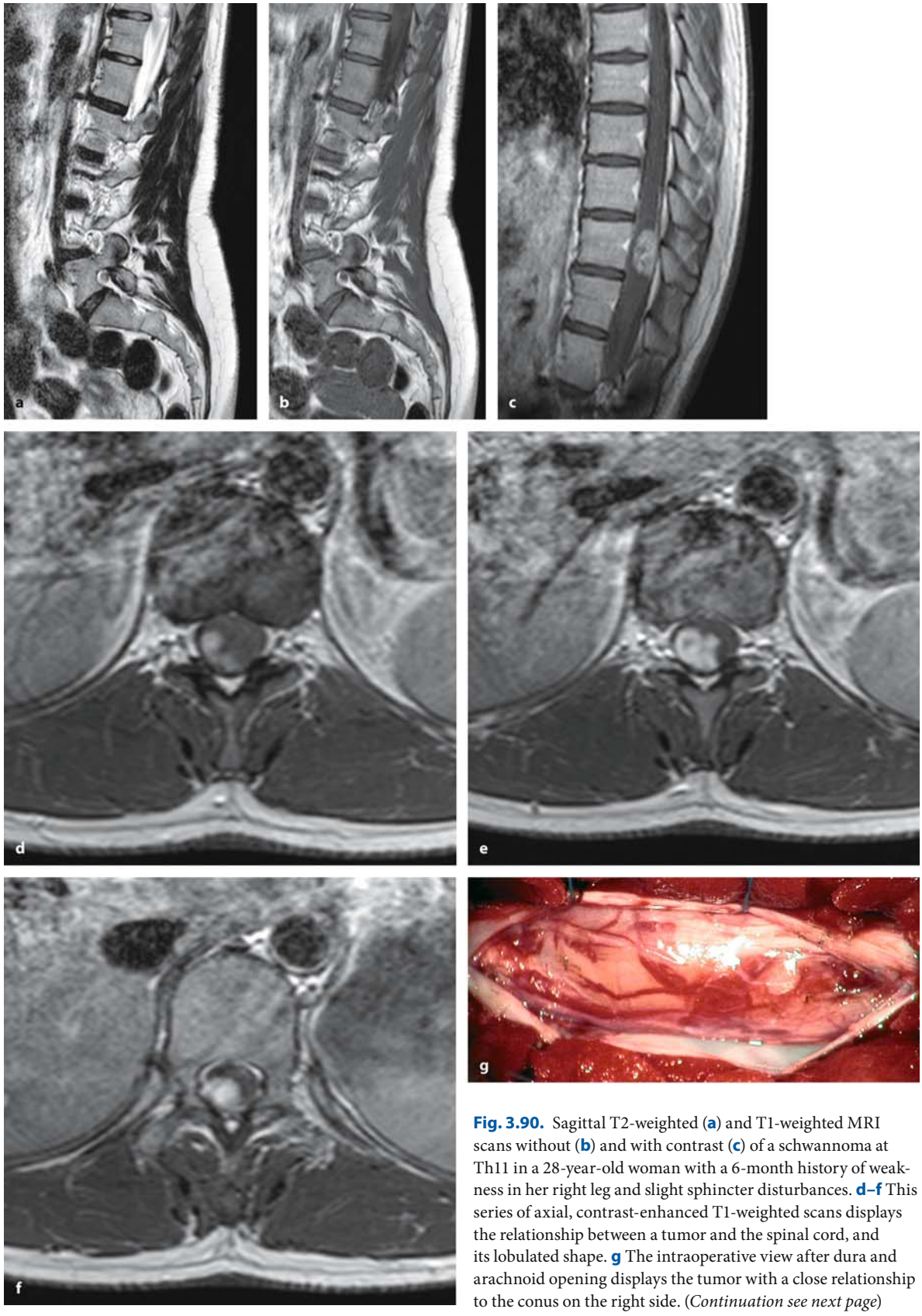

Fig. 3.90. Sagittal T2-weighted (**a**) and T1-weighted MRI scans without (**b**) and with contrast (**c**) of a schwannoma at Th11 in a 28-year-old woman with a 6-month history of weakness in her right leg and slight sphincter disturbances. **d–f** This series of axial, contrast-enhanced T1-weighted scans displays the relationship between a tumor and the spinal cord, and its lobulated shape. **g** The intraoperative view after dura and arachnoid opening displays the tumor with a close relationship to the conus on the right side. (*Continuation see next page*)

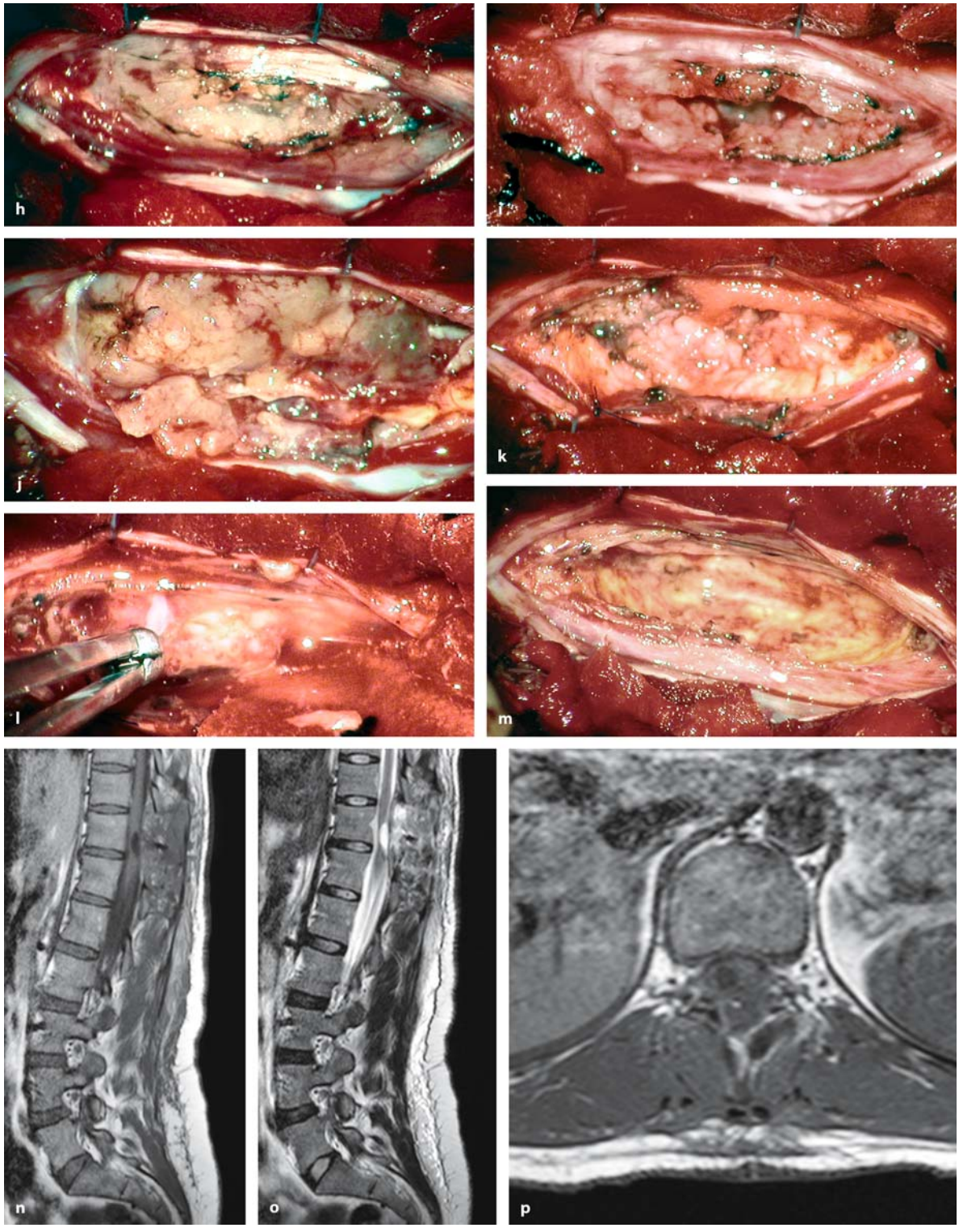

Fig. 3.90. (*Continued*) **h** After incision of the tumor capsule, tumor removal could be started. **i–k** With stepwise debulking of the tumor, decompression was achieved and the capsule could finally be grasped with forceps and dissected (**l**). **m** With complete resection of the capsule, the considerable intramedullary extension of this tumor became apparent. The postoperative T1- (**n, p**) and T2-weighted (**o**) MRI scans demonstrate a complete resection and a defect in the spinal cord representing the former tumor bed. The patient recovered her neurological function within 3 months and has been free of a recurrence for 1 year

3.5.10 Schwannomas

Intramedullary schwannomas resemble an even rarer entity. In the literature, a number of case reports have been published [33, 95, 138, 150, 191, 209, 220, 240, 248, 249]. These tumors have grown into the spinal cord originating from a nerve root right at the entry zone. We have seen one such tumor in a 28-year-old woman with a 6-year history of slightly progressive gait ataxia. She demonstrated a contrast-enhancing tumor above the conus at Th11. At surgery, more than half of this tumor was deeply embedded inside the thoracic cord and had to be dissected out of a slightly gliotic tumor bed to achieve a complete resection. Postoperatively, the patient recovered after a short period of deterioration and finally improved her condition compared to the preoperative status (Fig. 3.90).

3.6 Conclusions

We conclude that intramedullary tumors should be operated on as soon as neurological symptoms have appeared. Waiting for further neurological progression raises the risk of surgery dramatically.

If a syrinx accompanies the tumor, this should be interpreted as a favorable prognostic sign as it indicates a displacing rather than infiltrating tumor, and thus suggests its resectability. It is sufficient to operate on the solid tumor part. The accompanying syrinx will decrease automatically if the tumor has been removed.

Complete tumor removal should be attempted irrespective of the tumor appearance on preoperative MRI. Tumors well defined on MRI may show no reliable dissection planes intraoperatively and vice versa. On the other hand, complete resections should not be attempted at any cost. The long-term result does not always depend on the amount of resection.

To minimize the risk of postoperative tethering, which may cause considerable morbidity, we suggest closing the pia with sutures after complete tumor resections and to decompress the subarachnoid space with a Gore-Tex® dural graft.

Finally, and most importantly, no group of tumors described in this book requires as much experience to achieve the modern standard of therapy (i.e., complete or subtotal resection with preservation of preoperative function). Therefore, we urge that these patients be transferred to neurosurgeons experienced with their treatment. In return, these colleagues have an obligation to train surgeons who wish to operate on these challenging tumors.

References

1. Acciarri N, Padovani R, Giulioni M, Gaist G (1993) Surgical treatment of spinal cavernous angiomas. J Neurosurg Sci 37:209–215
2. Agraharkar A, McGillicuddy G, Ahuja T, Agraharkar M (2000) Growth of intramedullary lipoma in a renal transplant recipient. Transplantation 69:1509–1511
3. Akhaddar A, el Hassani MY, Ghadouane M, Hommadi A, Chakir N, Jiddane M, Boukhrissi N (1999) [Dermoid cyst of the conus medullaris revealed by chronic urinary retention. Contribution of imaging]. J Neuroradiol 26:132–136
4. Alberdi J, Eiras J, Gomez J, Carcavilla L, Cantero J, Gimenez J (1987) [Sudden tetraplegia caused by hemorrhage in a central-medullary astrocytoma]. Neurochirurgie 33:62–65
5. Allen JC, Aviner S, Yates AJ, Boyett JM, Cherlow JM, Turski PA, Epstein F, Finlay JL, Children's Cancer Group (1998) Treatment of high-grade spinal cord astrocytoma of childhood with "8-in-1" chemotherapy and radiotherapy: a pilot study of CCG-945. J Neurosurg 88:215–220
6. Alvisi C, Cerisoli M, Giulioni M (1984) Intramedullary spinal gliomas: long-term results of surgical treatment. Acta Neurochir (Wien) 70:169–179
7. Amin R (1999) Intramedullary spinal metastasis from carcinoma of the cervix. Br J Radiol 72:89–91
8. Aoki H, Fujimoto H, Harada K, Tomonari A, Nakamura Y, Kanazawa K, Masuda K, Shinomiya S, Kawai H (1992) Intramedullary spinal cord metastasis from lung cancer presenting with paraparesis: an autopsied case. Tokushima J Exp Med 39:89–93
9. Arseni C, Danaila L, Constantinescu A, Carp N (1977) Spinal dermoid tumours. Neurochirurgia (Stuttg) 20:108–116
10. Awwad EE, Backer R, Archer CR (1987) The imaging of an intraspinal cervical dermoid tumor by MR, CT, and sonography. Comput Radiol 11:169–173
11. Bakshi R, Mechtler LL, Patel MJ, Lindsay BD, Messinger S, Gibbons KJ (1997) Spinal leptomeningeal hemangioblastomatosis in von Hippel-Lindau disease: magnetic resonance and pathological findings. J Neuroimaging 7:242–244
12. Balasubramaniam C, Balasubramaniam V, Santosh V (2004) Intramedullary glioependymal cyst and tethered cord in an infant. Childs Nerv Syst 20:496–498
13. Balmaceda C (2000) Chemotherapy for intramedullary spinal cord tumors. J Neurooncol 47:293–307
14. Barkovich AJ, Edwards M, Cogen PH (1991) MR evaluation of spinal dermal sinus tracts in children. AJNR Am J Neuroradiol 12:123–129
15. Barnett HJM, Rewcastle NB (1973) Syringomyelia and tumors of the nervous system. In: Barnett HJM, Foster JB, Hudgson P (eds) Syringomyelia. Major Problems in Neurology. Volume 1. WB Saunders, London, pp 261–301
16. Barth A, Pizzolato GP, Berney J (1993) [Intramedullary meningeal melanocytoma]. Neurochirurgie 19:188–194
17. Bazan Cd, New PZ, Kagan-Hallet KS (1990) MRI of radiation induced spinal cord glioma. Neuroradiology 32:331–333

18. Bell WO, Packer RJ, Seidel KR, Rorke LB, Sutton LN, Bruce DA, Schut L (1988) Leptomeningeal spread of intramedullary spinal cord tumors. Report of three cases. J Neurosurg 69:295–300
19. Benzel EC, Mirfarkhraee M, Hadden T, Fowler M (1987) Holocord astrocytoma: a two-staged operative approach. Spine 12:746–749
20. Biliciler B, Vatansever M, Fuat Erten S, Sarac K, Colak A (1996) A huge intramedullary epidermoid cyst: mimicking cauda equina ependymoma. Diagnostic failure of myelography and myelo-CT. J Neurosurg Sci 40:149–152
21. Birch BD, Johnson JP, Parsa A, Desai RD, Yoon JT, Lycette CA, Li YM, Bruce JN (1996) Frequent type 2 neurofibromatosis gene transcript mutations in sporadic intramedullary spinal cord ependymomas. Neurosurgery 39:135–140
22. Bizzozero L, Ferrara M, Villa F, Fontana R, Brusamolino R, Collice M (1994) Intramedullary spinal cord metastasis. Case report. J Neurosurg Sci 38:193–195
23. Borocco A, Idir A, Joubert E, Lacroix C, Hurth M, Doyon D (1995) [Intramedullary glioma. Postoperative MRI aspects]. J Neuroradiol 22:123–130
24. Bouffet E, Pierre-Kahn A, Marchal J C, Jouvet A, Kalifa C, Choux M, Dhellemmes P, Guerin J, Tremoulet M, Mottolese C (1998) Prognostic factors in pediatric spinal cord astrocytoma. Cancer 83:2391–2399
25. Bracken MB, Shepard MJ, Collins WF, Holford TR, Young W, Baskin DS, Eisenberg HM, Flamm E, Leo-Summers L, Maroon J, et al (1990) A randomized, controlled trial of methylprednisolone or naloxone in the treatment of acute spinal-cord injury. Results of the Second National Acute Spinal Cord Injury Study. N Engl J Med 322:1405–1411
26. Breger RK, Williams AL, Daniels DL, Czervionke LF, Mark LP, Haughton VM, Papke RA, Coffer M (1989) Contrast enhancement in spinal MR imaging. AJR Am J Roentgenol 153:387–391
27. Brophy JD, Sutton LN, Zimmerman RA, Bury E, Schut L (1989) Magnetic resonance imaging of lipomyelomeningocele and tethered cord. Neurosurgery 25:336–340
28. Brotchi J, Fischer G (1998) Spinal cord ependymomas. Neurosurg Focus 4:Article 2
29. Browne TR, Adams RD, Roberson GH (1976) Hemangioblastoma of the spinal cord. Review and report of five cases. Arch Neurol 33:435–441
30. Buge A, Chamouard JM, Schadeck B, Sichez JP, Fabiani JM (1985) [Spinal cord congenital epidermoid cyst (a dorsal case)]. Rev Neurol (Paris) 141:810–813
31. Bussieres A, Cassidy JD, Dzus A (1994) Spinal cord astrocytoma presenting as torticollis and scoliosis. J Manipulative Physiol Ther 17:113–118
32. Canavero S, Pagni CA, Duca S, Bradac GB (1994) Spinal intramedullary cavernous angiomas: a literature meta-analysis. Surg Neurol 41:381–388
33. Cantore G, Ciappetta P, Delfini R, Vagnozzi R, Nolletti A (1982) Intramedullary spinal neurinomas. Report of two cases. J Neurosurg 57:143–147
34. Cantore G, Delfini R, Cervoni L, Innocenzi G, Orlando ER (1995) Intramedullary cavernous angiomas of the spinal cord: report of six cases. Surg Neurol 43:448–451
35. Chabert E, Morandi X, Carney MP, Riffaud L, Louail C, Carsin-Nicol B (1999) Intramedullary cavernous malformations. J Neuroradiol 26:262–268
36. Chacko AG, Chandy MJ (2001) Favorable outcome after radical excision of a 'holocord' astrocytoma. Clin Neurol Neurosurg 102:240–242
37. Chamberlain MC, Sandy AD, Press GA (1991) Spinal cord tumors: gadolinium-DTPA-enhanced MR imaging. Neuroradiology 33:469–474
38. Chandy MJ, Babu S (1999) Management of intramedullary spinal cord tumours: review of 68 patients. Neurol India 47:224–228
39. Chang UK, Choe WJ, Chung SK, Chung CK, Kim HJ (2002) Surgical outcome and prognostic factors of spinal intramedullary ependymomas in adults. J Neurooncol 57:133–139
40. Chaskis C, Michotte A, Geffray F, Vangeneugden J, Desprechins B, D'Haens J (1997) Cervical intramedullary lipoma with intracranial extension in an infant. Case illustration. J Neurosurg 87:472
41. Chen YJ, Fan FS, Chen PM (1995) Intramedullary spinal cord metastasis: a case report. Chung Hua I Hsueh Tsa Chih (Taipei) 56:58–61
42. Chermann JF, Miaux Y, Migaud I, Gerber F, Hirsch A (1992) [Value of magnetic resonance imaging in the detection of intramedullary metastases of bronchial epidermoid carcinoma]. Rev Mal Respir 9:636–637
43. Chigasaki H, Pennybacker JB (1968) A long follow-up study of 128 cases of intramedullary spinal cord tumours. Neurol Med Chir (Tokyo) 10:25–66
44. Choucair AK (1991) Myelopathies in the cancer patient: incidence, presentation, diagnosis and management. Oncology (Williston Park) 5:25–31; discussion 35–37
45. Ciapetta P, Salvati M, Capoccia G, Artico M, Raco A, Fortuna A (1991) Spinal glioblastomas: report of seven cases and review of the literature. Neurosurgery 28:302–306
46. Citron N, Edgar MA, Sheehy J, Thomas DG (1984) Intramedullary spinal cord tumours presenting as scoliosis. J Bone Joint Surg Br 66:513–517
47. Clover LL, Hazuka MB, Kinzie JJ (1993) Spinal cord ependymomas treated with surgery and radiation therapy. A review of 11 cases. Am J Clin Oncol 16:350–353
48. Cohen AR, Wisoff JH, Allen JC, Epstein F (1989) Malignant astrocytomas of the spinal cord. J Neurosurg 70:50–54
49. Cokca F, Meco O, Arasil E, Unlu A (1994) An intramedullary dermoid cyst abscess due to Brucella abortus biotype 3 at T11–L2 spinal levels. Infection 22:359–360
50. Coleman LT, Zimmerman RA, Rorke LB (1995) Ventriculus terminalis of the conus medullaris: MR findings in children. AJNR Am J Neuroradiol 16:1421–1426
51. Coleman WP, Benzel D, Cahill DW, Ducker T, Geisler F, Green B, Gropper MR, Goffin J, Madsen PW III, Maiman DJ, Ondra SL, Rosner M, Sasso RC, Trost GR, Zeidman S (2000) A critical appraisal of the reporting of the National Acute Spinal Cord Injury Studies (II and III) of methylprednisolone in acute spinal cord injury. J Spinal Disord 13:185–199

52. Colombo N, Kucharczyk W, Brant-Zawadzki M, Norman D, Scotti G, Newton TH (1986) Magnetic resonance imaging of spinal cord hemangioblastoma. Acta Radiol Suppl 369:734–737
53. Connolly ES Jr, Winfree CJ, McCormick PC, Cruz M, Stein BM (1996) Intramedullary spinal cord metastasis: report of three cases and review of the literature. Surg Neurol 46:329–337; discussion 337–338
54. Constantini S, Houten J, Miller DC, Freed D, Ozek MM, Rorke LB, Allen JC, Epstein FJ (1996) Intramedullary spinal cord tumors in children under the age of 3 years. J Neurosurg 85:1036–1043
55. Constantini S, Miller DC, Allen JC, Rorke LB, Freed D, Epstein FJ (2000) Radical excision of intramedullary spinal cord tumors: surgical morbidity and long-term follow-up evaluation in 164 children and young adults. J Neurosurg 93:183–193
56. Cooper PR (1989) Outcome after operative treatment of intramedullary spinal cord tumors in adults: intermediate and long-term results in 51 patients. Neurosurgery 25:855–859
57. Cooper PR, Epstein F (1985) Radical resection of intramedullary spinal cord tumors in adults. J Neurosurg 63:492–499
58. Corr P, Dicker T, Wright M (1995) Exophytic intramedullary hemangioblastoma presenting as an extramedullary mass on myelography. AJNR Am J Neuroradiol 16:883–884
59. Costigan DA, Winkelman MD (1985) Intramedullary spinal cord metastasis. A clinicopathological study of 13 cases. J Neurosurg 62:227–233
60. Cristante L, Herrmann HD (1994) Surgical management of intramedullary spinal cord tumors: functional outcome and sources of morbidity. Neurosurgery 35:69–74, discussion 74–76
61. Cristante L, Hermann HD (1998) Radical excision of intramedullary cavernous angiomas. Neurosurgery 43:424–430; discussion 430–431
62. Cristante L, Herrmann HD (1999) Surgical management of intramedullary hemangioblastoma of the spinal cord. Acta Neurochir (Wien) 141:333–339; discussion 339–340
63. Crols R, Appel B, Klaes R (1993) Extensive cervical intradural and intramedullary lipoma and spina bifida occulta of C1: a case report. Clin Neurol Neurosurg 95:39–43
64. Cybulski GR, Von Roenn KA, Bailey OT (1984) Intramedullary cystic teratoid tumor of the cervical spinal cord in association with a teratoma of the ovary. Surg Neurol 22:267–272
65. de Baecque C, Snyder DH, Suzuki K (1977) Congenital intramedullary spinal dermoid cyst associated with an Arnold-Chiari malformation. Acta Neuropathol (Berl) 38:239–242
66. de Divitiis E, Spaziante R, Stella L (1978) Giant intramedullary ependymoma. A case report. Neurochirurgia (Stuttg) 21:69–72
67. de la Monte SM, Horowitz SA (1989) Hemangioblastomas: clinical and histopathological factors correlated with recurrence. Neurosurgery 25:695–698
68. DeSousa AL, Kalsbeck JE, Mealey J, Jr, Campbell RL, Hockey A (1979) Intraspinal tumors in children. A review of 81 cases. J Neurosurg 51:437–445
69. Deutsch H, Jallo GI, Faktorovich A, Epstein F (2000) Spinal intramedullary cavernoma: clinical presentation and surgical outcome. J Neurosurg 93:65–70
70. Deutsch H, Shrivistava R, Epstein F, Jallo GI (2001) Pediatric intramedullary spinal cavernous malformations. Spine 26:E427–E431
71. Dietl RH, Winkler R, Lumenta CB (1996) [Intramedullary spinal metastasis of bronchial carcinoma coincident with intramedullary spinal angioma]. Zentralbl Neurochir 57:25–29
72. Doireau V, Grill J, Zerah M, Lellouch-Tubiana A, Couanet D, Chastagner P, Marchal JC, Grignon Y, Chouffai Z, Kalifa C (1999) Chemotherapy for unresectable and recurrent intramedullary glial tumours in children. Brain Tumours Subcommittee of the French Society of Paediatric Oncology (SFOP) Br J Cancer 81:835–840
73. Dyck P (1992) Intramedullary lipoma. Diagnosis and treatment. Spine 17:979–981
74. Ebert C, von Haken M, Meyer-Puttlitz B, Wiestler OD, Reifenberger G, Pietsch T, von Deimling A (1999) Molecular genetic analysis of ependymal tumors. NF2 mutations and chromosome 22q loss occur preferentially in intramedullary spinal ependymomas. Am J Pathol 155:627–632
75. Eeg-Olofsson O, Carlsson E, Jeppsson S (1981) Recurrent abdominal pains as the first symptom of a spinal cord tumor. Acta Paediatr Scand 70:595–597
76. Egelhoff JC, Bates DJ, Ross JS, Rothner AD, Cohen BH (1992) Spinal MR findings in neurofibromatosis types 1 and 2 [see comments]. AJNR Am J Neuroradiol 13:1071–1077
77. el Khamlichi A, el Ouahabi A, Amrani F, Agdach R, Bellakhdar F (1989) [Spinal cord lipoma. Apropos of 3 cases]. Neurochirurgie 35:366–370
78. Emery E, Hurth M, Lacroix-Jousselin C, David P, Richard S (1994) [Intraspinal hemangioblastoma. Apropos of a recent series of 20 cases]. Neurochirurgie 40:165–173
79. Endoh M, Iwasaki Y, Koyanagi I, Hida K, Abe H (1998) Spontaneous shrinkage of lumbosacral lipoma in conjunction with a general decrease in body fat: case report. Neurosurgery 43:150–151; discussion 151–152
80. Epstein F (1986) Spinal cord astrocytomas of childhood. Adv Tech Stand Neurosurg 13:135–169
81. Epstein F, Epstein N (1981) Surgical management of holocord intramedullary spinal cord astrocytomas in children. J Neurosurg 54:829–832
82. Epstein F, Epstein N (1982) Surgical treatment of spinal cord astrocytomas of childhood: a series of 19 patients. J Neurosurg 57:685–689
83. Epstein FJ, Farmer JP, Schneider SJ (1991) Intraoperative ultrasonography: an important surgical adjunct for intramedullary tumors. J Neurosurg 74:729–733
84. Epstein FJ, Farmer JP, Freed D (1992) Adult intramedullary astrocytomas of the spinal cord. J Neurosurg 77: 355–359
85. Epstein FJ, Farmer JP, Freed D (1993) Adult intramedullary spinal cord ependymomas: the results of surgery in 38 patients. J Neurosurg 79:204–209

86. Evans A, Stoodley N, Halpin S (2002) Magnetic resonance imaging of intraspinal cystic lesions: a pictorial review. Curr Probl Diagn Radiol 31:79–94
87. Faillot T, Roujeau T, Dulou R, Blanc JL, Chedru F (2002) [Intramedullary spinal cord metastasis: is there a place for surgery? Case report and review of literature]. Neurochirurgie 48:533–536
88. Felice KJ, DiMario FJ (1999) Cervicomedullary astrocytoma simulating a neuromuscular disorder. Pediatr Neurol 20:78–80
89. Ferrante L, Mastronardi L, Celli P, Lunardi P, Acqui M, Fortuna A (1992) Intramedullary spinal cord ependymomas – a study of 45 cases with long-term follow-up. Acta Neurochir (Wien) 119:74–79
90. Ferroir JP, Cadranel J, Khalil A, Lebreton C, Contant S, Milleron B (1998) [Intramedullary metastases of bronchogenic carcinoma. Two cases]. Rev Neurol (Paris) 154:166–169
91. Findlay JM, Bernstein M, Vanderlinden RG, Resch L (1987) Microsurgical resection of solitary intramedullary spinal cord metastases. Neurosurgery 21:911–915
92. Findler G, Hadani M, Tadmor R, Bubis JJ, Shaked I, Sahar A (1985) Spinal intradural ependymal cyst: a case report and review of the literature. Neurosurgery 17:484–486
93. Fine MJ, Kricheff, II, Freed D, Epstein FJ (1995) Spinal cord ependymomas: MR imaging features. Radiology 197:655–658
94. Fischer G, Brotchi J (1994) [Intramedullary spinal cord tumors. Report. French Society of Neurosurgery. 45th annual congress. Angers, June 12–15 1994]. Neurochirurgie 40 Suppl 1:1–108
95. Fischer G, Brotchi J (1996) Intramedullary Spinal Cord Tumors. Thieme, Stuttgart
96. Fischer G, Mansuy L (1980) Total removal of intramedullary ependymomas: follow-up study of 16 cases. Surg Neurol 14:243–249
97. Fontaine D, Lot G, George B (1999) Intramedullary cavernous angioma. Resection by oblique corpectomy. Surg Neurol 51:435–441; discussion 441–442
98. Fornari M, Pluchino F, Solero CL, Giombini S, Luccarelli G, Oliveri G, Lasio G (1988) Microsurgical treatment of intramedullary spinal cord tumours. Acta Neurochir Suppl (Wien) 43:3–8
99. Fortuna A, Mercuri S (1983) Intradural spinal cysts. Acta Neurochir (Wien) 68:289–314
100. Foster O, Crockard HA, Powell MP (1987) Syrinx associated with intramedullary metastasis. J Neurol Neurosurg Psychiatry 50:1067–1070
101. Freund M, Thale A, Hutzelmann A (1998) Radiologic and histopathologic findings in a rare case of complex occult spinal dysraphism with association of a lumbar fibrolipoma, neurenteric cyst and tethered cord syndrome. Eur Radiol 8:624–627
102. Fricke RD, Romine JS (1977) Thoracic spinal cord tumor presenting with dysautonomic diarrhea. Gastroenterology 73:1152–1156
103. Fujimoto N, Hiraki A, Ueoka H, Kiura K, Bessho A, Takata I, Hiramatsu Y, Ikeda K, Harada M (2000) Intramedullary spinal cord recurrence after high-dose chemotherapy and autologous peripheral blood progenitor cell transplantation for limited-disease small cell lung cancer. Lung Cancer 30:145–148
104. Garcia DM (1985) Primary spinal cord tumors treated with surgery and postoperative irradiation. Int J Radiat Oncol Biol Phys 11:1933–1939
105. Gläsker S, Berlis A, Pagenstecher A, Vougioukas VI, Van Velthoven V (2005) Characterization of hemangioblastomas of spinal nerves. Neurosurgery 56:503–509
106. Glick R, Baker C, Husain S, Hays A, Hibshoosh H (1997) Primary melanocytomas of the spinal cord: a report of seven cases. Clin Neuropathol 16:127–132
107. Goh KY, Velasquez L, Epstein FJ (1997) Pediatric intramedullary spinal cord tumors: is surgery alone enough? Pediatr Neurosurg 27:34–39
108. Gok A, Bayram M, Coskun Y, Ozsarac C (1995) Unusual malformations in occult spinal dysraphism. Turk J Pediatr 37:391–397
109. Gordon CR, Crockard HA, Symon L (1995) Surgical management of spinal cord cavernoma. Br J Neurosurg 9:459–464
110. Gose K, Imajo Y, Takimoto S, Ichiyanagi A, Oshitani T, Kimura S, Hiratsuka J, Ueda N, Yamaguchi T (1984) [Two autopsy cases of intramedullary spinal cord metastasis]. Gan No Rinsho 30:319–323
111. Goy AM, Pinto RS, Raghavendra BN, Epstein FJ, Kricheff II (1986) Intramedullary spinal cord tumors: MR imaging with emphasis on associated cysts. Radiology 161:381–386
112. Grabb PA, Kelly DR, Fulmer BB, Palmer C (1996) Radiation-induced glioma of the spinal cord. Pediatr Neurosurg 25:214–219
113. Greenwood J Jr (1963) Intramedullary tumors of spinal cord: a follow-up study after total surgical removal. J Neurosurg 20:665–668
114. Grem JL, Burgess J, Trump DL (1985) Clinical features and natural history of intramedullary spinal cord metastasis. Cancer 56:2305–2314
115. Guidetti B, Mercuri B, Vagnozzi R (1981) Long-term results of the surgical treatment of 129 intramedullary spinal gliomas. J Neurosurg 54:323–330
116. Haghighi SS, York DH, Ebeling J, Gumerlock MK, Oro JJ, Gaines RW (1992) Dissociation of somatosensory and motor evoked potentials in a patient with an intramedullary spinal tumor. Mo Med 89:790–794
117. Hamilton MG, Tranmer BI, Hagen NA (1993) Supratentorial glioblastoma with spinal cord intramedullary metastasis. Can J Neurol Sci 20:65–68
118. Hardison HH, Packer RJ, Rorke LB, Schut L, Sutton LN, Bruce DA (1987) Outcome of children with primary intramedullary spinal cord tumors. Childs Nerv Syst 3:89–92
119. Hashizume Y, Hirano A (1983) Intramedullary spinal cord metastasis. Pathologic findings in five autopsy cases. Acta Neuropathol (Berl) 61:214–218

120. Hejazi N, Hassler W (1998) Microsurgical treatment of intramedullary spinal cord tumors. Neurol Med Chir (Tokyo) 38:266–271; discussion 271–273
121. Hely M, Fryer J, Selby G (1985) Intramedullary spinal cord glioma with intracranial seeding. J Neurol Neurosurg Psychiatry 48:302–309
122. Hentschel SJ, McCutcheon IE, Ginsberg L, Weinberg JS (2004) Exophytic ependymomas of the spinal cord. Acta Neurochirurgica (Wien) 146:1047–1050
123. Hernandez D, Moraleda S, Royo A, Martinez M, Garcia J, Vazquez MJ (1999) Cavernous angioma of the conus medullaris as a cause of paraplegia. Spinal Cord 37:65–67
124. Herrmann HD, Neuss M, Winkler D (1988) Intramedullary spinal cord tumors resected with CO_2 Laser microsurgical technique: recent experience in fifteen patients. Neurosurgery 22:518–522
125. Hoff DJ, Tampieri D, Just N (1993) Imaging of spinal cord hemangioblastomas. Can Assoc Radiol J 44:377–383
126. Honma Y, Kawakita K, Nagao S (1996) Intramedullary spinal cord and brain metastases from thyroid carcinoma detected 11 years after initial diagnosis – case report. Neurol Med Chir (Tokyo) 36:593–597
127. Hori A, Hirose G, Kataoka S, Matsuno H, Negami T (1990) [Intramedullary spinal cord metastasis documented by MR imaging]. Rinsho Shinkeigaku 30:796–798
128. Hoshimaru M, Koyama T, Hashimoto N, Kikuchi H (1999) Results of microsurgical treatment for intramedullary spinal cord ependymomas: analysis of 36 cases. Neurosurgery 44:264–269
129. Hoshimaru M, Koyama T, Hashimoto N (2000) [Microsurgery of cervical intramedullary ependymomas extending into the medulla oblongata]. No Shinkei Geka 28:517–522
130. Houten JK, Cooper PR (2000) Spinal cord astrocytomas: presentation, management and outcome. J Neurooncol 47:219–224
131. Houten JK, Weiner HL (2000) Pediatric intramedullary spinal cord tumors: special considerations. J Neurooncol 47:225–230
132. Huddart R, Traish D, Ashley S, Moore A, Brada M (1993) Management of spinal astrocytoma with conservative surgery and radiotherapy. Br J Neurosurg 7:473–481
133. Hulshof MC, Menten J, Dito JJ, Dreissen JJR, van den Bergh R, Gonzalez Gonzalez D (1993) Treatment results in primary intraspinal gliomas. Radiother Oncol 29:294–300
134. Hurth M (1975) [Intraspinal hemangioblastomas]. Neurochirurgie 21:1–136
135. Ibanez V, Fischer G, Mauguiere F (1992) Dorsal horn and dorsal column dysfunction in intramedullary cervical cord tumours. A somatosensory evoked potential study. Brain 115:1209–1234
136. Inagawa T, Kamiya K, Nagasako R (1995) A case of spinal low-grade astrocytoma with exophytic and intracranial extension. Surg Neurol 43:261–264
137. Innocenzi G, Raco A, Cantore G, Raimondi AJ (1996) Intramedullary astrocytomas and ependymomas in the pediatric age group: a retrospective study. Childs Nerv Syst 12:776–780
138. Innocenzi G, Cervoni L, Caruso R (1997) [Intramedullary cervical neurinoma. A case report and review of the literature] Minerva Chir 52:697–682
139. Innocenzi G, Salvati M, Cervoni L, Delfini R, Cantore G (1997) Prognostic factors in intramedullary astrocytomas. Clin Neurol Neurosurg 99:1–5
140. Irikura T, Johki T, Tanaka H, Nakajima M, Yasue M, Sakai H, Nakamura N (1990) Holocord astrocytoma – case report. Neurol Med Chir (Tokyo) 30:966–971
141. Isaacson SR (2000) Radiation therapy and the management of intramedullary spinal cord tumors. J Neurooncol 47:231–238
142. Ishikawa T, Iwasaki Y, Isu T, Akino M, Koyanagi I, Hida K, Abe H, Miyasaka K, Abe S (1988) [Spinal intramedullary tumor with exophytic growth]. No Shinkei Geka 16:1339–1345
143. Isla A, Paz JM, Sansivirini F, Zamora P, Garcia Grande A, Fernandez A (2000) Intramedullary spinal cord metastasis. A case report. J Neurosurg Sci 44:99–101
144. Isu T, Iwasaki Y, Imamura H, Akino M, Abe H (1987) [Intra-operative spinal sonography in spinal intramedullary tumor]. No Shinkei Geka 15:947–954
145. Isu T, Abe H, Iwasaki Y, Akino M, Koyanagi I, Hida K, Miyasaka K, Saito H (1991) [Diagnosis and surgical treatment of spinal hemangioblastoma]. No Shinkei Geka 19:149–155
146. Ito K, Sudo A, Imai Y, Yoshizawa H, Suzuki E, Arakawa M (1999) [Intramedullary metastasis of small cell lung cancer]. Nihon Kokyuki Gakkai Zasshi 37:485–488
147. Iwahashi H, Kawai S, Watabe Y, Chitoku S, Akita N, Fuji T, Oda T (1999) Spinal intramedullary ependymal cyst: a case report. Surg Neurol 52:357–361
148. Iwasaki Y, Koyanagi I, Hida K, Abe H (1999) Anterior approach to intramedullary hemangioblastoma: case report. Neurosurgery 44:655–657
149. Iwasaki Y, Hida K, Sawamura Y, Abe H (2000) Spinal intramedullary ependymomas: surgical results and immunohistochemical analysis of tumour proliferation activity. Br J Neurosurg 14:331–336
150. Jacquet G, Czorny A, Godard J, Steimle R, Wendling D (1992) [Intramedullary neurinoma. Apropos of a case. Review of the literature] Neurochirurgie 38:315–321
151. Jallo GI, Danish S, Velasquez L, Epstein F (2001) Intramedullary low-grade astrocytomas: long-term outcome following radical surgery. J Neurooncol 53:61–66
152. Jallo GI, Freed D, Epstein F (2003) Intramedullary spinal cord tumors in children. Childs Nerv Syst 19:641–649
153. Jallo GI, Freed D, Epstein FJ (2004) Spinal cord gangliogliomas: a review of 56 patients. J Neurooncol 68:71–77
154. Jardin F, Stamatoullas A, Fruchart C, D'Anjou J, Clement JF, Tilly H (1999) [Intramedullary spinal cord metastasis and leptomeningeal involvement in Hodgkin's disease. Case report and review of the literature]. Rev Med Interne 20:267–271

155. Jellinger K, Kothbauer P, Sunder-Plassmann E, Weiss R (1979) Intramedullary spinal cord metastases. J Neurol 220:31–41
156. Joubert E, Idir AB, Carlier R, Belal N, Hurth M, Lacroix-Ciaudo C, Ducot B, Doyon D (1995) [MRI symptomatology of primary intraspinal cord gliomas]. J Neuroradiol 22:28–42
157. Jyothirmayi R, Madhavan J, Nair MK, Rajan B (1997) Conservative surgery and radiotherapy in the treatment of spinal cord astrocytoma. J Neurooncol 33:205–211
158. Kalangu KKN, Couto MT (1996) Radical resection of intramedullary spinal cord tumors without cavitron ultrasonic aspirator or CO_2 laser: a "two stage" technique. Surg Neurol 46:310–316
159. Kalayci M, Cagavi F, Gül S, Yenidünya S, Acikgöz B (2004) Intramedullary spinal cord metastases – an illustrated review. Acta Neurochir (Wien) 146:1347–1354
160. Kamikaseda K, Takaki T, Hikita T (1989) Intramedullary ganglioglioma of spinal cord – case report. Neurol Med Chir (Tokyo) 29:838–841
161. Kan S, Fox AJ, Vinuela F, Barnett HJ, Peerless SJ (1983) Delayed CT metrizamide enhancement of syringomyelia secondary to tumor. AJNR Am J Neuroradiol 4:73–78
162. Kaufman BA, Park TS (1992) Congenital spinal cord astrocytomas. Childs Nerv Syst 8:389–393
163. Kawakami K, Kasai H, Yamada A, Numa Y, Sakai N, Kawamoto K (1995) [A case of spinal astrocytoma presenting spinal transverse sign due to hematomyelia]. No Shinkei Geka 23:327–331
164. Kawakami N, Mimatsu K, Kato F (1992) Intraoperative sonography of intramedullary spinal cord tumours. Neuroradiology 34:436–439
165. Kendall B, Symon L (1977) The radiological investigation of intramedullary spinal tumours. Zentralbl Neurochir 38:19–28
166. Keung YK, Cobos E, Whitehead RP, Roberson GH (1997) Secondary syringomyelia due to intramedullary spinal cord metastasis. Case report and review of literature. Am J Clin Oncol 20:577–579
167. Kim CH, Wang KC, Kim SK, Chung YN, Choi YL, Chi JG, Cho BK (2003) Spinal intramedullary lipoma: report of three cases. Spinal Cord 41:310–315
168. Kim MS, Chung CK, Choe C, Kim IH, Kim HJ (2001) Intramedullary spinal cord astrocytoma in adults: postoperative outcome. J Neurooncol 52:85–94
169. Klekamp J (2002) The pathophysiology of syringomyelia – historical overview and current concept. Acta Neurochir (Wien) 144:649–664
170. Klekamp J, Samii M (2002) Syringomyelia. Diagnosis and Treatment. Springer, Heidelberg
171. Klekamp J, Raimondi AJ, Samii M (1994) Occult dysraphism in adulthood. Clinical course and management. Childs Nerv Syst 10:312–320
172. Koehler PJ, Verbiest H, Jager J, Vecht CJ (1996) Delayed radiation myelopathy: serial MR-imaging and pathology. Clin Neurol Neurosurg 98:197–201
173. Koeller KK, Rosenblum RS, Morrison AL (2000) Neoplasms of the spinal cord and filum terminale: radiologic-pathologic correlation. Radiographics 20:1721–1749
174. Kogler A, Orsolic K, Kogler V (1998) Intramedullary lipoma of dorsocervicothoracic spinal cord with intracranial extension and hydrocephalus. Pediatr Neurosurg 28:257–260
175. Kokubun S, Kashimoto O, Tanaka Y (1994) Histological verification of bone bonding and ingrowth into porous hydroxyapatite spinous process spacer for cervical laminoplasty. Tohoku J Exp Med 173:337–344
176. Kopelson G, Linggood RM, Kleinman GM, Doncette J, Wang CC (1980) Management of intramedullary spinal cord tumors. Radiology 135:473–479
177. Kosmas C, Koumpou M, Nikolaou M, Katselis J, Soukouli G, Markoutsaki N, Kostopoulou V, Gaglia A, Mylonakis N, Karabelis A, Pectasides D (2005) Intramedullary spinal cord metastases in breast cancer: report of four cases and review of the literature. J Neurooncol 71:67–72
178. Kothbauer KF, Deletis V, Epstein FJ (1998) Motor-evoked potential monitoring for intramedullary spinal cord tumor surgery: correlation of clinical and neurophysiological data in a series of 100 consecutive procedures. Neurosurg Focus 4:Article 1
179. Krishna KK, Agarwal PA, Agarwal SI, Jain MM (2004) Dermoid of the conus medullaris. J Clin Neurosci 11:796–797
180. Kumar R, Nayak SR, Krishnani N, Chhabra DK (2001) Spinal intramedullary ependymal cyst. Report of two cases and review of the literature. Pediatr Neurosurg 35:29–34
181. Kumar S, Gulati DR, Mann KS (1977) Intraspinal dermoids. Neurochirurgia (Stuttg) 20:105–108
182. Kurtz JE, Andres E, de la Palavesa MM, Deplanque G, Limacher JM, Duclos B, Bergerat JP (1994) [Value of MRI in the detection of spinal cord metastases. Apropos of a case]. Bull Cancer 81:808–810
183. Lang EW, Chesnut RM, Beutler AS, Kennelly NA, Renaudin JW (1996) The utility of motor-evoked potential monitoring during intramedullary surgery. Anesth Analg 83:1337–1341
184. Lauvin R, Cornu P, Philippon J, Gautier JC, Jacquillat C, Khayat D, Doyon D (1988) [Isolated cervical intramedullary metastasis from breast cancer. Value of magnetic resonance imaging]. Rev Neurol (Paris) 144:40–42
185. Lee DK, Choe WJ, Chung CK, Kim HJ (2003) Spinal cord hemangioblastoma: surgical strategy and outcome. J Neurooncol 61:27–34
186. Lee JP, Wang AD, Chang CN (1991) Intramedullary spinal cord metastasis: report of a case and review of the literature. J Formos Med Assoc 90:415–418
187. Lee KS, Spetzler RF (1990) Spinal cord cavernous malformation in a patient with familial intracranial cavernous malformations. Neurosurgery 26:877–880
188. Lee M, Rezai AR, Abbott R, Coelho DH, Epstein FJ (1995) Intramedullary spinal cord lipomas. J Neurosurg 82:394–400
189. Lee M, Rezai AR, Freed D, Epstein FJ (1996) Intramedullary spinal cord tumors in neurofibromatosis. Neurosurgery 38:32–37

190. Lee M, Epstein FJ, Rezai AR, Zagzag D (1998) Nonneoplastic intramedullary spinal cord lesions mimicking tumors. Neurosurgery 43:788–795
191. Lesoin F, Rousseaux M, Pruvo JP, Villette L, Jomin M (1986) [Solitary intraspinal dorsal neurinoma. A case report] Rev Med Interne 7:387–390
192. Li Y, Takayasu M, Takagi T, Yoshimoto M, Mitsui Y, Yoshida J (2000) [Intramedullary spinal cord metastasis associated with hemorrhage: a case report]. No Shinkei Geka 28:453–457
193. Lodrini S, Lasio G, Cimino C, Pluchino F (1991) Hemangioblastomas: clinical characteristics, surgical results and immunohistochemical studies. J Neurosurg Sci 35:179–185
194. Lohle PN, Wurzer HA, Hoogland PH, Seelen PJ, Go KG (1994) The pathogenesis of syringomyelia in spinal cord ependymoma. Clin Neurol Neurosurg 96:323–326
195. Lonjon M, Goh KY, Epstein FJ (1998) Intramedullary spinal cord ependymomas in children: treatment, results and follow-up. Pediatr Neurosurg 29:178–183
196. Lowe GM (2000) Magnetic resonance imaging of intramedullary spinal cord tumors. J Neurooncol 47:195–210
197. Lunardi P, Missori P, Gagliardi FM, Fortuna A (1989) Long-term results of the surgical treatment of spinal dermoid and epidermoid tumors. Neurosurgery 25:860–864
198. Lunardi P, Cervoni L, Maleci A, Fortuna A (1993) Isolated hemangioblastoma of spinal cord: report of 18 cases and a review of the literature. Acta Neurochir (Wien) 122:236–239
199. Lunardi P, Licastro G, Missori P, Ferrante L, Fortuna A (1993) Management of intramedullary tumours in children. Acta Neurochir (Wien) 120:59–65
200. Lunardi P, Acqui M, Ferrante L, Fortuna A (1994) The role of intraoperative ultrasound imaging in the surgical removal of intramedullary cavernous angiomas. Neurosurgery 34:520–523
201. Lyding JM, Tseng A, Newman A, Collins S, Shea W (1987) Intramedullary spinal cord metastasis in Hodgkin's disease. Rapid diagnosis and treatment resulting in neurologic recovery. Cancer 60:1741–1744
202. Maher ER, Yates JRW, Harries R, Benjamin C, Harris R, Moore AT, Ferguson-Smith MA (1990) Clinical features and natural history of von Hippel-Lindau disease. Q J Med 77:1151–1163
203. Maiuri F, Iaconetta G, Gallicchio B, Stella L (2000) Intraoperative sonography for spinal tumors. J Neurosurg Sci 44:115–122
204. Malis LI (1978) Intramedullary spinal cord tumors. Clin Neurosurg 25:512–539.
205. Marconi F, Parenti G, Giorgetti V, Puglioli M (1995) Spinal cavernous angioma producing subarachnoid hemorrhage. Case report. J Neurosurg Sci 39:75–80
206. Margolis L, Smith ME, Fortuin FD, Chin FK, Liebel SA, Hill DR (1981) Intramedullary tumor metastasis simulating radiation myelitis: report of a case. Cancer 48:1680–1683
207. Marks JE, Adler SJ (1982) A comparative study of ependymomas by site of origin. Int J Radiat Oncol Biol Phys 8:37–43
208. Martin NA, Khanna RK, Batzdorf U (1995) Posterolateral cervical or thoracic approach with spinal cord rotation for vascular malformations or tumors of the ventrolateral spinal cord. J Neurosurg 83:254–261
209. Maruki C, Ito M, Sumie H, Sato K, Ishii S (1986) [Intramedullary schwannoma with extradural extension: case report] No Shinkei Geka 14:579–584
210. Mascalchi M, Quilici N, Ferrito G, Mangiafico S, Scazzeri F, Torselli P, Petruzzi P, Casottini M, Tessa C, Bartolozzi C (1997) Identification of the feeding arteries of spinal vascular lesions via phase-contrast MR angiography with three-dimensional acquisition and phase display. AJNR Am J Neuroradiol 18:351–358
211. Mathew P, Todd NV (1993) Intradural conus and cauda equina tumours: a retrospective review of presentation, diagnosis and early outcome. J Neurol Neurosurg Psychiatry 56:69–74
212. Mathur S, Law AJ, Hung N (2000) Late intramedullary spinal cord metastasis in a patient with lymphoblastic lymphoma: case report. J Clin Neurosci 7:264–268
213. Matsubayashi R, Uchino A, Kato A, Kudo S, Sakai S, Murata S (1998) Cystic dilatation of ventriculus terminalis in adults: MRI. Neuroradiology 40:45–47
214. Mautner VF, Tatagiba M, Lindenau M, Funsterer C, Pulst SM, Baser ME, Kluwe L, Zanella FE (1995) Spinal tumors in patients with neurofibromatosis type 2: MR imaging study of frequency, multiplicity, and variety. AJR Am J Roentgenol 165:951–955
215. McCormick PC, Stein BM (1990) Intramedullary tumors in adults. In: Stein BM, McCormick PC (eds) Neurosurgery Clinics in North America. Volume 1, no. 3. Intradural Spinal Surgery. WB Saunders, Philadelphia, pp 609–630
216. McCormick PC, Michelson WJ, Post KD, Carmel PW, Stein BM (1988) Cavernous malformations of the spinal cord. Neurosurgery 23:459–463
217. McCormick PC, Torres R, Post KD, Stein BM (1990) Intramedullary ependymoma of the spinal cord. J Neurosurg 72:523–532
218. McLone DG, Naidich TP (1986) Laser resection of fifty spinal lipomas. Neurosurgery 18:611–615
219. Mehdorn HM, Stolke D (1991) Cervical intramedullary cavernous angioma with MRI-proven haemorrhages. J Neurol 238:420–426
220. Meisel HJ, Patt S, Brock M (1990) [Intramedullary neurinoma. Case report] Zentralbl Neurochir 51:171–173
221. Michels VV (1988) Investigative studies in von Hippel-Lindau disease. Neurofibromatosis 1:159–163
222. Miller DC (2000) Surgical pathology of intramedullary spinal cord neoplasms. J Neurooncol 47:189–194
223. Miller DJ, McCutcheon IE (2000) Hemangioblastomas and other uncommon intramedullary tumors. J Neurooncol 47:253–270
224. Miyazawa N, Hida K, Iwasaki Y, Koyanagi I, Abe H (2000) MRI at 1.5T of intramedullary ependymoma and classification of pattern of contrast enhancement. Neuroradiology 42:828–832
225. Moffie D, Stefanko SZ (1980) Intramedullary metastasis. Clin Neurol Neurosurg 82:199–202

226. Morantz RA, Kepes JJ, Batnitzky S, Masterson BJ (1979) Extraspinal ependymomas. Report of three cases. J Neurosurg 51:383–391
227. Mori K, Kamimura Y, Uchida Y, Kurisaka M, Eguchi S (1986) Large intramedullary lipoma of the cervical cord and posterior fossa. Case report. J Neurosurg 64:974–976
228. Mork SJ, Loken AC (1977) Ependymoma: a follow-up study of 101 cases. Cancer 40:907–915
229. Morota N, Deletis V, Constantini S, Kofler M, Cohen H, Epstein FJ (1997) The role of motor evoked potentials during surgery for intramedullary spinal cord tumors. Neurosurgery 41:1327–1336
230. Moser FG, Tuvia J, LaSalla P, Llana J (1992) Ependymoma of the spinal nerve root: case report. Neurosurgery 31:962–964
231. Mottl H, Koutecky J (1997) Treatment of spinal cord tumors in children. Med Pediatr Oncol 29:293–295
232. Mrabet A, Zouari R, Mouelhi T, Khouaja F, Ghariani MT, Hila A, Haddad A (1992) [Cervicobulbar intramedullary lipoma. Apropos of a case with review of the literature]. Neurochirurgie 38:309–314
233. Murota T, Symon L (1989) Surgical management of hemangioblastoma of the spinal cord: a report of 18 cases. Neurosurgery 25:699–708
234. Nadkarni TD, Rekate HL (1999) Pediatric intramedullary spinal cord tumors. Critical review of the literature. Childs Nerv Syst 15:17–28
235. Nagashima C, Masuda T, Nagashima R, Enomoto K, Watabe T, Morita H, Takahama M (1996) [Spinal intramedullary cavernous angioma associated with hematomyelia: case report with sequential MRI follow-up and histological verification of hematoidin deposits]. No Shinkei Geka 24:1125–1132
236. Naim Ur R, Salih MA, Jamjoom AH, Jamjoom ZA (1994) Congenital intramedullary lipoma of the dorsocervical spinal cord with intracranial extension: case report. Neurosurgery 34:1081–1083; discussion 1084
237. Nakashima H, Tokunaga K, Tamiya T, Matsumoto K, Ohmoto T, Furuta T (1999) [Analysis of spinal cord hemangioblastoma in von Hippel-Lindau disease]. No Shinkei Geka 27:533–540
238. Nassar SI, Correll JW, Housepian EM (1968) Intramedullary cystic lesions of the conus medullaris. J Neurol Neurosurg Psychiatry 31:106–109
239. Nemoto Y, Inoue Y, Tashiro T, Mochizuki K, Oda J, Kogame S, Katsuyama J, Hakuba A, Onoyama Y (1992) Intramedullary spinal cord tumors: significance of associated hemorrhage at MR imaging. Radiology 182:793–796
240. Nicoletti GF, Passanisi M, Castana L, Albanese V (1994) Intramedullary spinal neurinoma: case report and review of 46 cases. J Neurosurg Sci 38:187–191
241. Nunes ML, Coutinho LM, Janisch C, Ehlers JA (1999) Congenital intramedullary tumor with neonatal manifestations. J Child Neurol 14:467–469
242. Oertel J, Gaab MR, Piek J (2000) Partial recovery of paraplegia due to spontaneous intramedullary ependyma haemorrhage. Acta Neurochir (Wien) 142:219–220
243. Ogasawara KK, Ogasawara EM, Hirata G (1995) Pregnancy complicated by von Hippel-Lindau disease. Obstet Gynecol 85:829–831
244. Ogilvy CS, Louis DN, Ojemann RG (1992) Intramedullary cavernous angiomas of the spinal cord: clinical presentation, pathological features, and surgical management. Neurosurgery 31:219–229; discussion 229–230
245. Ohtakara K, Kuga Y, Murao K, Kojima T, Taki W, Waga S (2000) Preoperative embolization of upper cervical cord hemangioblastoma concomitant with venous congestion – case report. Neurol Med Chir (Tokyo) 40:589–593
246. Ojemann RG, Crowell RM, Ogilvy CS (1993) Management of cranial and spinal cavernous angiomas (honored guest lecture). Clin Neurosurg 40:98–123
247. O'Keefe T, Ramirez H, Jr, Huggins MJ, Bennett WF, Blumenkopf B (1985) Computed tomography detection of cervical spinal cord hemangioblastoma: a case report. J Comput Tomogr 9:249–252
248. Okuda Y, Tamaki N, Nameta A, Izawa I, Tomita Y, Kokunai T, Ehara K, Matsumoto S (1988) [Intramedullary invasion by a cervical cystic neurinoma––a case report] No Shinkei Geka 16:173–178
249. Pardatscher K, Iraci G, Cappellotto P, Rigobello L, Pellone M, Fiore D (1979) Multiple intramedullary neurinomas of the spinal cord. Case report. J Neurosurg 50:817–822
250. Park CK, Chung CK, Choe GY, Wang KC, Cho BK, Kim HJ (2000) Intramedullary spinal cord ganglioglioma: a report of five cases. Acta Neurochir (Wien) 142:547–552
251. Parsa AT, Fiore AJ, McCormick PC, Bruce JC (2000) Genetic basis of intramedullary spinal cord tumors and therapeutic implications. J Neurooncol 47:239–251
252. Parsa AT, Lee, J, Parney IF, Weinstein P, McCormick PC, Ames C (2004) Spinal cord and intradural-extraparenchymal spinal tumors: current best care practices and strategies. J Neurooncol 69:291–318
253. Patel U, Pinto RS, Miller DC, Handler MS, Rorke LB, Epstein FJ, Kricheff II (1998) MR of spinal cord ganglioglioma. AJNR Am J Neuroradiol 19:879–887
254. Patronas NJ, Courcoutsakis N, Bromley CM, Katzman GL, MacCollin M, Parry DM (2001) Intramedullary and spinal canal tumors in patients with neurofibromatosis 2: MR imaging findings and correlation with genotype. Radiology 218:434–442
255. Patwardhan V, Patanakar T, Armao D, Mukherji SK (2000) MR imaging findings of intramedullary lipomas. AJR Am J Roentgenol 174:1792–1793
256. Peker S, Ozgen S, Ozek MM, Pamir MN (2004) Surgical treatment of intramedullary spinal cord ependymomas. Can outcome be predicted by tumor parameters? J Spinal Disord Tech 17:51–521
257. Pelissou-Guyotat I, Sindou M, Pialat J, Goutelle A (1988) [Intramedullary mature teratoma associated with an attached cord and an intradural lipoma. Apropos of a surgically treated case. Review of the literature]. Neurochirurgie 34:205–209
258. Peraud A, Herms J, Schlegel J, Müller P, Kretzschmar H, Tonn JC (2004) Recurrent spinal cord astrocytoma with intraventricular seeding. Childs Nerv Syst 20:114–118

259. Peschel RE, Kapp DS, Cardinale F, Mannelidis EE (1983) Ependymomas of the spinal cord. Int J Radiat Oncol Biol Phys 9:1093–1096
260. Peter JC, Sinclair-Smith C, de Villiers JC (1991) Midline dermal sinuses and cysts and their relationship to the central nervous system. Eur J Pediatr Surg 1:73–79
261. Phuphanich S, Jacobs M, Murtagh FR, Gonzalvo A (1996) MRI of spinal cord radiation necrosis simulating recurrent cervical cord astrocytoma and syringomyelia. Surg Neurol 45:362–365
262. Phuphanich S, Zachariah S, Zachariah B, Ku NN, Murtagh FR (1996) Magnetic resonance imaging of syrinx associated with intramedullary metastases and leptomeningeal disease. J Neuroimaging 6:115–117
263. Pietilä TA, Stendel R, Schilling A, Krznaric I, Brock M (2000) Surgical treatment of spinal hemangioblastomas. Acta Neurochir (Wien) 142:879–886
264. Pluta RM, Iuliano B, DeVroom HL, Nguyen T, Oldfield EH (2003) Comparison of anterior and posterior surgical approaches in the treatment of ventral spinal hemangioblastomas in patients with von Hippel-Lindau disease. J Neurosurg 98:117–124
265. Poser CM (1956) The Relationship Between Syringomyelia and Neoplasms. CC Thomas, Springfield
266. Prasad VS, Basha A, Prasad BC, Reddy DR (1994) Intraspinal tumour presenting as hydrocephalus in childhood. Childs Nerv Syst 10:156–157
267. Pullucino P, Kendall BE (1982) Computed tomography of 'cystic' intramedullary lesions. Neuroradiology 23:117–121
268. Purohit AK, Dinakar I, Sundaram C, Ratnakar KS (1990) Anaplastic astrocytoma of the spinal cord presenting with features of raised intracranial pressure. Childs Nerv Syst 6:113–115
269. Quencer RM (1980) Needle aspiration of intramedullary and intradural extramedullary masses of the spinal canal. Radiology 134:115–126
270. Raco A, Delfini R, Salvati M, Innocenzi G, Ciappetta P (1992) Intramedullary metastasis of unknown origin: a case report. Neurosurg Rev 15:135–138
271. Raco A, Esposito V, Lenzi J, Piccirilli M, Delfini R, Cantore G (2005) long-term follow-up of intramedullary spinal cord tumors: a series of 202 cases. Neurosurgery 56:972–981
272. Raghavendra BN, Epstein FJ, McCleary L (1984) Intramedullary spinal cord tumors in children: localization by intraoperative sonography. AJNR Am J Neuroradiol 5:395–397
273. Rawlings CE, Giangaspero F, Burger PC, Bullard DE (1988) Ependymomas: a clinicopathologic study. Surg Neurol 29:271–281
274. Razack N, Jimenez OF, Aldana P, Ragheb J (1998) Intramedullary holocord lipoma in an athlete: case report. Neurosurgery 42:394–396; discussion 396–397
275. Regelsberger J, Langer N, Fritzsche E, Westphal M (2003) [Intraoperative ultrasound of intra- and extramedullary tumours]. Ultraschall Med 24:399–403
276. Resche F, Moisan JP, Mantoura J, de Kersaint-Gilly A, Andre MJ, Perrin-Resche I, Menegalli-Boggelli D, Lajat Y, Richard S (1993) Haemangioblastoma, haemangioblastomatosis, and von Hippel-Lindau disease. Adv Techn Stand Neurosurg 20:197–304
277. Richardson RG, Griffin TW, Parker RG (1980) Intramedullary hemangioblastoma of the spinal cord: definitive management with irradiation. Cancer 45:49–50
278. Rifkinson-Mann S, Wisoff JH, Epstein F (1990) The association of hydrocephalus with intramedullary spinal cord tumors: a series of 25 patients. Neurosurgery 27:749–754
279. Robertson DP, Kirkpatrick JB, Harper RL, Mawad ME (1991) Spinal intramedullary ependymal cyst. Report of three cases. J Neurosurg 75:312–316
280. Rothstein TL (1985) Paraplegia resulting from rupture of previously asymptomatic intramedullary hemangioblastoma during coitus. Ann Neurol 17:519
281. Roth-Vargas AA, Rossitti SL, Balbo RJ, Oliveira MA (1989) So-called tethered cervical spinal cord. Neurochirurgia (Stuttg) 32:69–71
282. Rothwell CI, Jaspan T, Worthington BS, Holland IM (1989) Gadolinium-enhanced magnetic resonance imaging of spinal tumours. Br J Radiol 62:1067–1074
283. Roux FX, Rey A, Lecoz P, George B, Thurel C, Cophignon J, Mikol J (1984) Astrocytomes et ependymomes intramedullaires de l'adulte: La tactique therapeutique influetelle sur les resultats a long terme? Bilan de 23 cas operes et discussion de la litterature. Neurochirurgie 30:99–105
284. Rubinstein LJ (1986) The malformative central nervous system lesions in the central and peripheral forms of neurofibromatosis. A neuropathological study of 22 cases. Ann N Y Acad Sci 486:14–29
285. Ryu SI, Kim DH, Chang SD (2003) Stereotactic radiosurgery for hemangiomas and ependymomas of the spinal cord. Neurosurg Focus 15:Article 10
286. Saito K, Morita A, Shibahara J, Kirino T (2005) Spinal intramedullary ependymal cyst: a case report and review of the literature. Acta Neurochir (Wien) 147:443–446
287. Sakuma S, Iwasaki Y, Isu T, Akino M, Sugimoto S, Takahashi A, Abe H, Inoue K (1990) [A case of intramedullary spinal cord metastasis from adenocarcinoma of corpus uteri]. No Shinkei Geka 18:653–657
288. Sandalcioglu IE, Wiedemayer H, Gasser T, Asgari S, Engelhorn T, Stolke D (2003) Intramedullary spinal cord cavernous malformations: clinical features and risk of hemorrhage. Neurosurg Rev 26:253–256
289. Sandalcioglu IE, Gasser T, Asgari S, Lazorisak A, Engelhorn T, Egelhof T, Stolke D, Wiedemayer H (2005) Functional outcome after surgical treatment of intramedullary spinal cord tumors: experience with 78 patients. Spinal Cord 43:34–41
290. Sanders WP, Ausman JI, Dujovny M, Madrazo BL, Ho KL, Jack CR Jr, Mehta BA (1986) Ultrasonic features of two cases of spinal cord hemangioblastoma. Surg Neurol 26:453–456
291. Santi M, Mena H, Wong K, Koeller K, Olsen C, Rushing EJ (2003) Spinal cord malignant astrocytomas. Clinicopathologic features in 36 cases. Cancer 98:554–561

292. Santoro A, Innocenzi G, Bellotti C, Cancrini A, Delfini R, Cantore GP (1998) Total removal of an intramedullary cavernous angioma by transthoracic approach. Ital J Neurol Sci 19:176–179
293. Santoro A, Piccirilli M, Frati A, Salvati M, Innocenzi G, Ricci G, Cantore G (2004) Intramedullary spinal cord cavernous malformations: report of ten new cases. Neurosurg Rev 27:93–98
294. Sarabia M, Millan JM, Escudero L, Cabello A, Lobato RD (1986) Intracranial seeding from an intramedullary malignant astrocytoma. Surg Neurol 26:573–576
295. Sasajima T, Mineura K, Itoh Y, Kowada M, Hatazawa J, Ogawa T, Uemura K (1996) Spinal cord ependymoma: a positron emission tomographic study with (11C-methyl)-L-methionine. Neuroradiology 38:53–55
296. Sattar MT, Bannister CM, Turnbull IW (1996) Occult spinal dysraphism – the common combination of lesions and the clinical manifestations in 50 patients. Eur J Pediatr Surg 6 Suppl 1:10–14
297. Schick U, Marquardt G, Lorenz R (2001) Recurrence of benign spinal neoplasms. Neurosurg Rev 24:20–25
298. Schiff D, O'Neill BP (1996) Intramedullary spinal cord metastases: clinical features and treatment outcome. Neurology 47:906–912
299. Schijns OE, Kurt E, Wessels P, Luijckx GJ, Beuls EA (2001) Intramedullary spinal cord metastasis as a first manifestation of a renal cell carcinoma: report of a case and review of the literature. Clin Neurol Neurosurg 102:249–254
300. Schoche J, Fried H (1971) [Scoliosis in patients with intramedullary tumors]. Dtsch Gesundheitsw 26:1700–1703
301. Schwartz TH, McCormick PC (2000) Intramedullary ependymomas: clinical presentation, surgical treatment strategies and prognosis. J Neurooncol 47:211–218
302. Schwartz TH, McCormick PC (2000) Non-neoplastic intramedullary pathology. Diagnostic dilemma: to Bx or not to Bx. J Neurooncol 47:283–292
303. Sebastian PR, Fisher M, Smith TW, Davidson RI (1981) Intramedullary spinal cord metastasis. Surg Neurol 16:336–339
304. Seifert V, Trost HA, Stolke D (1990) [Microsurgery of spinal angioblastoma]. Neurochirurgia (Stuttg) 33:100–105
305. Sgouros S, Malluci CL, Jackowski A (1996) Spinal ependymomas – the value of postoperative radiotherapy for residual disease control. Br J Neurosurg 10:559–566
306. Sharma A, Sharma R, Goyal M, Vashisht S, Berry M (1997) Diastematomyelia associated with intramedullary tumour in a hemicord: a report of two cases. Australas Radiol 41:185–187
307. Sharma BS, Banerjee AK, Khosla VK, Kak VK (1987) Congenital intramedullary spinal ependymal cysts. Surg Neurol 27:476–480
308. Sharma R, Rout D, Radhakrishnan VV (1992) Intradural spinal cavernomas. Br J Neurosurg 6:351–356
309. Shaw EG, Evans RG, Scheithauer BW, Ilstrup DM, Earle JD (1986) Radiotherapeutic management of adult intraspinal ependymomas. Int J Radiat Oncol Biol Phys 12:323–327
310. Shen WC, Chiou TL, Lin TY (2000) Dermal sinus with dermoid cyst in the upper cervical spine: case note. Neuroradiology 42:51–53
311. Shirato H, Kamada T, Hida K, Koyanagi I, Iwasaki Y, Miyasaka K, Abe H (1995) The role of radiotherapy in the management of spinal cord glioma. Int J Radiat Oncol Biol Phys 33:323–328
312. Shrivastava RK, Epstein FJ, Perin NI, Post KD, Jallo GI (2005) Intramedullary spinal cord tumors in patients older than 50 years of age: management and outcome analysis. J Neurosurg Spine 2:249–255
313. Sigal R, Denys A, Halimi P, Shapeero L, Doyon D, Boudghéne F (1991) Ventriculus terminalis of the conus medullaris: MR imaging in four patients with congenital dilatation. AJNR Am J Neuroradiol 12:733–737
314. Slooff JL, Kernohan JW, MacCarty CS (1964) Primary Intramedullary Tumors of the Spinal Cord and Filum Terminale. Saunders, Philadelphia
315. Spetzger U, Gilsbach JM, Bertalanffy H (1995) Cavernous angiomas of the spinal cord clinical presentation, surgical strategy, and postoperative results. Acta Neurochir (Wien) 134:200–206
316. Staudte HW, Busch G (1993) [10-year follow-up of C3–C7 cervical laminectomy for intramedullary grade I astrocytoma]. Z Orthop Ihre Grenzgeb 131:225–228
317. Stein BM (1979) Surgery of intramedullary spinal cord tumours. Clin Neurosurg 26:529–542
318. Stein BM, McCormick PC (1992) Intramedullary neoplasms and vascular malformations. Clin Neurosurg 39:361–387
319. Steinbok P, Cochrane DD, Poskitt K (1992) Intramedullary spinal cord tumors in children. Neurosurg Clin N Am 3:931–945
320. Stewart DH Jr, King RB, Lourie H (1970) Surgical drainage of cyst of the conus medullaris. Report of three cases. J Neurosurg 33:106–110
321. Stranjalis G, Torrens MJ (1993) Successful removal of intramedullary spinal cord metastasis: case report. Br J Neurosurg 7:193–195
322. Struffert T, Grunwald I, Roth C, Reith W (2004) Spinal intradurale tumore. Radiologe 44:1211–1228
323. Sun B, Wang C, Wang J, Liu A (2003) MRI features of intramedullary spinal cord ependymomas. J Neuroimaging 13:346–351
324. Sweasey TA, Brunberg JA, McKeever PE, Sandler HM, Chandler WF (1994) Cystic cervical intramedullary ependymoma with previous intracyst hemorrhage. Magnetic resonance imaging at 1.5 T. J Neuroimaging 4:111–113
325. Takahashi I, Iwasaki Y, Hida K, Koyanagi I, Abe H (1996) [Clinical study of intraspinal neoplasms in children]. No Shinkei Geka 24:605–611
326. Takenaka N, Imanishi T, Kondoh A, Ohnumata A, Fukuda J, Yagishita S (1996) [Primary intramedullary melanocytoma of the medulla oblongata: a case report]. No Shinkei Geka 24:247–252
327. Tampieri D, Leblanc R, TerBrugge K (1993) Preoperative embolization of brain and spinal hemangioblastomas. Neurosurgery 33:502–505

328. Tanghetti B, Fumagalli GL, Giunta F, Marini G, Zorzi F (1983) Intramedullary spinal cord metastases. J Neurosurg Sci 27:117–124
329. Taniura S, Tatebayashi K, Watanabe K, Watanabe T (2000) Intramedullary spinal cord metastasis from gastric cancer. Case report. J Neurosurg 93:145–147
330. Thomas AW, Simon SR, Evans C (1992) Intramedullary spinal cord metastases from epithelial ovarian carcinoma. Gynecol Oncol 44:195–197
331. Tognetti F, Lanzino G, Calbucci F (1988) Metastases of the spinal cord from remote neoplasms. Study of five cases. Surg Neurol 30:220–227
332. Tomura N (2000) [Imaging of tumors of the spine and spinal cord]. Nippon Igaku Hoshasen Gakkai Zasshi 60:302–311
333. Townsend N, Handler M, Fleitz J, Foreman N (2004) Intramedullary spinal cord astrocytomas in children. Pediatr Blood Cancer 43:629–632
334. Trost HA, Seifert V, Stolke D (1993) Advances in diagnosis and treatment of spinal hemangioblastomas. Neurosurg Rev 16:205–209
335. Vandertop WP, van Wanroij JL, Rosenberg WW, Tulleken CA (1991) [Surgical resection as treatment of spinal intramedullary tumors]. Ned Tijdschr Geneeskd 135:664–668
336. Van Velthoven V, Reinacher PC, Klisch J, Neumann HPH, Gläsker S (2003) Treatment of intramdedullary hemangioblastomas, with special attention to von Hippel-Lindau disease. Neurosurgery 53:1306–1314
337. Vaquero J, Salazar J, Martinez R, Martinez P, Bravo G (1987) Cavernomas of the central nervous system: clinical syndromes, CT scan diagnosis, and prognosis after surgical treatment in 25 cases. Acta Neurochir (Wien) 85:29–33
338. Vijayakumar S, Estes M, Hardy RW Jr, Rosenbloom SA, Thomas FJ (1988) Ependymoma of the spinal cord and cauda equina: a review. Cleve Clin J Med 55:163–170
339. Vindlacheruvu RR, McEvoy AW, Kitchen ND (1997) Intramedullary thoracic cord metastasis managed effectively without surgery. Clin Oncol (R Coll Radiol) 9:343–345
340. Wald U, Levy PJ, Rappaport ZH, Michowitz SD, Schuger L, Shalit MN (1985) Conus ganglioglioma in a 2½-year-old boy. Case report. J Neurosurg 62:142–144
341. Wilms G, Marchal G, Decrop E, van Fraeyenhoven L, Baert AL, Beuls E, Plets C, van Hauwaert L (1989) Hypertrophic retromedullary venous drainage in spinal cord tumours: MR visualisation. Rofo Fortschr Geb Rontgenstr Neuen Bildgeb Verfahr 151:720–724
342. Wilson JT, Shapiro RH, Wald SL (1996) Multiple intradural spinal lipomata with intracranial extension. Pediatr Neurosurg 24:5–7
343. Winkelman MD, Adelstein DJ, Karlins NL (1987) Intramedullary spinal cord metastasis. Diagnostic and therapeutic considerations. Arch Neurol 44:526–531
344. Woltman HW, Kernohan JW, Adson AW, Craig WM (1951) Intramedullary tumors of spinal cord and gliomas of intradural portion of filum terminale. Fate of patients who have these tumors. Arch Neurol Psychiatr 65:378–393
345. Xu QW, Bao WM, Mao RL, Yang GY (1994) Magnetic resonance imaging and microsurgical treatment of intramedullary hemangioblastoma of the spinal cord. Neurosurgery 35:671–675; discussion 675–676
346. Xu Q, Bao W, Mao R (1996) Microsurgery of intramedullary cervical cord tumor. Chin Med J (Engl) 109:756–761
347. Xu QW, Bao WM, Mao RL, Yang GY (1996) Aggressive surgery for intramedullary tumor of cervical spinal cord. Surg Neurol 46:322–328
348. Yagi T, Ohata K, Haque M, Hakuba A (1997) Intramedullary spinal cord tumour associated with neurofibromatosis type 1. Acta Neurochir (Wien) 139:1055–1060
349. Yamasaki T, Kikuchi H, Yamashita J, Asato R, Fujita M (1989) Primary spinal intramedullary malignant melanoma: case report. Neurosurgery 25:117–121
350. Yasargil MG, Antic J, Laciga R, De Preux J, Fideler RW, Boone SC (1976) The microsurgical removal of intramedullary spinal hemangioblastomas. Report of twelve cases and a review of the literature. Surg Neurol 6:141–148
351. Yasui T, Yagura H, Komiyama M, Fu Y, Nagata Y, Tamura K, Khosla VK, Hakuba A (1992) Significance of gadolinium-enhanced magnetic resonance imaging in differentiating spinal cord radiation myelopathy from tumor. Case report. J Neurosurg 77:628–631
352. Yeh JS, Sgouros S, Walsh AR, Hockley AD (2001) Spinal sagittal malalignment following surgery for primary intramedullary tumours in children. Pediatr Neurosurg 35:318–324
353. Yu JS, Short MP, Schumacher J, Chapman PH, Harsh GR (1994) Intramedullary hemorrhage in spinal cord hemangioblastoma. Report of two cases. J Neurosurg 81:937–940
354. Zentner J, Hassler W, Gawehn J, Schroth G (1989) Intramedullary cavernous angiomas. Surg Neurol 31:64–68
355. Zide BM, Wisoff JH, Epstein FJ (1987) Closure of extensive and complicated laminectomy wounds. Operative technique. J Neurosurg 67:59–64
356. Zileli M, Coskun E, Ozdamar N, Ovul I, Tuncbay E, Oner K, Oktar N (1996) Surgery of intramedullary spinal cord tumors. Eur Spine J 5:243–250
357. Zimmerman RA, Bilaniuk LT (1988) Imaging of tumors of the spinal canal and cord. Radiol Clin N Am 26:965–1007

Extramedullary Tumors 4

Contents

Extramedullary tumors account for 51% of the spinal tumors in our series. The great majority are strictly intradural (84%), while the remainder extend into extradural compartments to varying degrees – some even with considerable extraspinal components. Even though extramedullary tumors are much more common than intramedullary neoplasms, they feature less in publications or scientific meetings. In this chapter we will first describe the clinical symptoms of extramedullary tumors and the typical clinical his-

Table 4.1. Histology of extramedullary intradural tumors

Type of tumor	Number
Meningioma	166
Nerve sheath tumor	158
Arachnoid cyst	35
Hamartoma	29
Ependymoma	26
Neuroblastoma	12
Metastasis	10
Melanocytoma	8
Malignant teratoma	6
Chordoma	5
Angioblastoma	4
Cavernoma	2
Medulloblastoma	2
Germinoma	1
Hemangiopericytoma	1
Exophytic astrocytoma	1
Total	**466**

Table 4.2. Histology of extramedullary intradural tumors with extradural extension

Type of tumor	Number
Nerve Sheath tumor	67
Meningioma	14
Hamartoma	4
Sarcoma	2
Total	**87**

tory on the basis of 553 tumors operated in our clinic. Of these, 466 were intradural, while 87 originated intradurally and demonstrated extradural extension (Tables 4.1 and 4.2). We will then continue with their neuroradiological features, followed by a description of surgical techniques, and finally a detailed analysis of postoperative results and outcomes.

4.1 History and Diagnosis

Most patients follow a rather typical clinical course, with pain of varying character at the beginning, followed by radicular symptoms, and finally a progressive myelopathy. The latter may start just on one side – a Brown-Sequard syndrome – before bilateral signs appear. Usually this course is slowly progressive; however, rapid deteriorations do occur and may be caused by intratumoral hemorrhages or vascular compression of spinal cord vessels. Therefore, the diagnosis of an extramedullary tumor should lead to surgery without much delay. Acute deteriorations may be provoked by lumbar punctures. The sudden pressure decrease associated with loss of cerebrospinal fluid (CSF) is particularly dangerous. Therefore, lumbar punctures or myelograms are contraindicated if an extramedullary tumor is suspected.

Extramedullary tumors were evenly spread along the spinal axis in our series, with 26% in the cervical, 47% in the thoracic, 23% in the lumbar, and the remaining 4% in the sacral spine. There was, however, a significant difference between intradural tumors and those with extradural extension. The latter were more common in the cervical (51% vs. 22%), but less frequently found in the thoracic (34% vs. 48%) and lumbar spine (10% vs. 25%), and in equal proportions in the sacrum (5% vs. 4%) (chi-square test: $p<0.0001$).

Of patients with extramedullary tumors, 51% reported pain as their first symptom. The second commonest symptom was gait ataxia (seen in 18% of our patients). The remaining patients described motor weakness (12%), sensory deficits (8%), dysesthesias (8%), or sphincter problems (2%) as their first manifestation. There were no differences between tumors with and without extradural extension in this respect (Table 4.3). One patient developed hydrocephalus as the first symptom. This is a rare complication of spinal tumors that has stimulated a number of publications trying to explain this phenomenon [217, 280]. The most likely explanation is the blocking of spinal CSF resorption along nerve roots [280].

Table 4.3. Initial symptoms for extramedullary tumors

First symptom	Intra	Intra-Extra	Total
Pain	51%	53%	51%
Gait ataxia	18%	19%	18%
Motor weakness	13%	7%	12%
Sensory deficits	8%	9%	8%
Dysesthesias	8%	11%	8%
Sphincter problems	2%	2%	2%

Abbreviations: Intra = intradural, Intra-Extra = intradural with extradural extension

Table 4.4. Symptoms for extramedullary tumors at presentation

Symptom	Intra	Intra-Extra	Total
Pain	77%	80%	77%
Gait ataxia	71%	66%	70%
Motor weakness	70%	70%	70%
Sensory deficits	76%	82%	77%
Dysesthesias	43%	43%	43%
Sphincter problems	40%	30%	38%

On average, about 26±51 months elapsed between admission to hospital and diagnosis. One patient presented a history of 34 years before being operated at the age of 61 years. The average age was 48±18 years on admission. The most distressing symptoms before surgery were pain (41%) and gait problems (41%), while 12% were most concerned about their motor deficit. Again, there was no difference between tumors with and without extradural extension. Table 4.4 gives an overview of the clinical pictures of patients with extramedullary tumors at presentation. With extradural extensions, radicular rather than medullary symptoms are more common, depending on the size of intra- and extradural components. The average Karnofsky score on admission was 70±15.

4.2 Neuroradiology

In adult patients, intradural tumors are rarely detectable on spinal X-rays. If the tumor has grown very slowly, the spinal canal may be widened and pedicles thinned out (Fig. 4.1). This phenomenon is particularly common in hamartomas (Fig. 4.2). Incomplete laminae (i.e., spina bifida) may be associated with intradural tumors (Figs. 4.2 and 4.3). With hamartomas related to split-cord malformations, dysplasias and

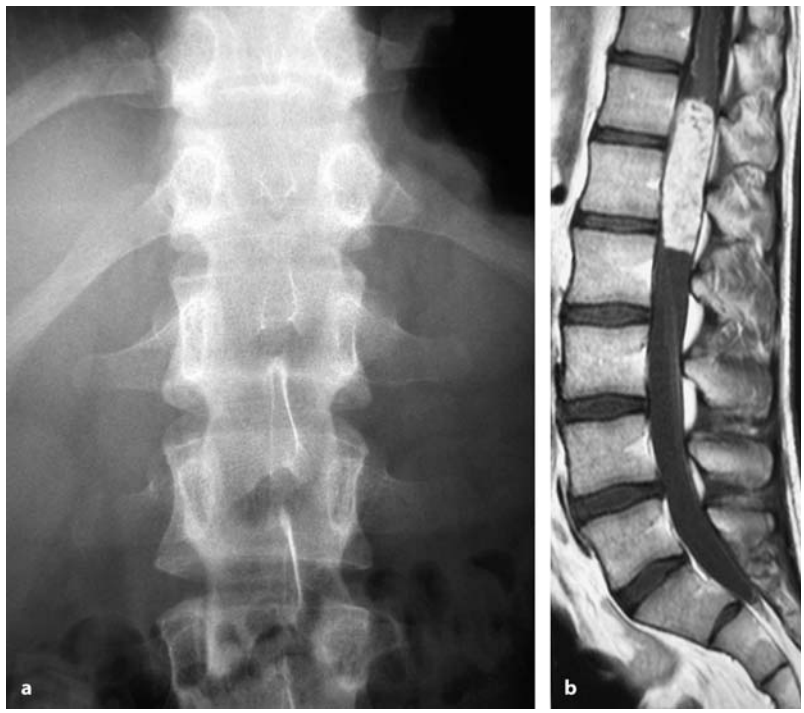

Fig. 4.1. Native anterior-posterior X-ray (**a**) and sagittal T1-weighted magnetic resonance imaging (MRI) scan (**b**) of a 21-year-old man with an extramedullary ependymoma at Th12–L2 and a 10-year history of back pain. The absence of neurological deficits despite this long history and the considerable size of this tumor indicate a very slow growth and explain the thinning of pedicles in the thoracolumbar junction

Fig. 4.2. Native anterior-posterior X-ray (**a**) and sagittal T1-weighted MRI scan (**b**) of a 44-year-old patient with a 9-month history of back pain and a dermoid cyst at L2–L3 with an associated tethered cord. The L2 and L3 pedicles on the right side appear thinned

malformations of the vertebral body may be observed (Fig. 4.4). In the growing spine, deformities may develop whenever a tumor affects the spinal canal. Depending on the age of the child, deformities such as incomplete lamina or dysplastic changes of the vertebral body and instabilities may be observed. Skeletal anomalies are described for phakomatoses associated with spinal tumors, such as neurofibromatosis (NF) [137]. In exceptional cases, calcifications of an extramedullary tumor can be seen on X-ray or computed tomography (CT) scans (Fig. 4.5). With tumors growing along the spinal nerve root, the foramen may be widened (Fig. 4.6) [257].

A bone window CT is quite helpful for a detailed demonstration of the bony anatomy of the affected vertebral bodies, intervertebral joints, pedicles, and laminae. This can be very useful during operations for recurrent tumors, when epidural scar tissue may

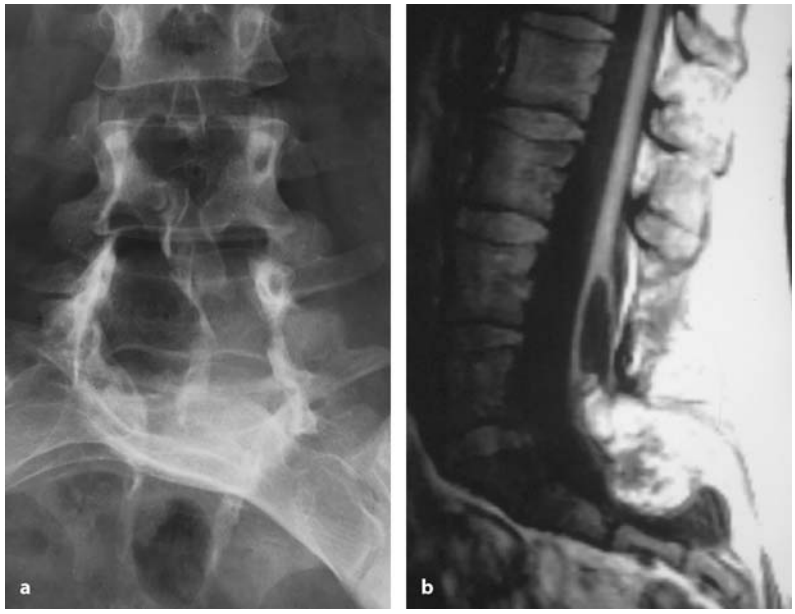

Fig. 4.3. Native anterior-posterior X-ray (**a**) and sagittal T1-weighted MRI scan (**b**) of a 34-year-old woman with a conus lipoma and extradural extension. The lumbar canal is widened with incomplete laminae at L4 and L5 and absent sacral roof

Fig. 4.4. These anterior-posterior (**a**) and lateral (**b**) X-rays demonstrate a complex vertebral anomaly associated with a split-cord malformation and an associated arteriovenous malformationin a 46-year-old woman with an 18-month history of progressive paraparesis and pain. (*Continuation see next page*)

Fig. 4.4. (*Continued*) There is an incomplete segmentation at Th11/Th12 (*arrowheads* in **a** and **b**) with a midline defect in the body of Th11 (**c**) and in-complete laminae at Th11 and Th12 (**d**)

Fig. 4.5. **a** Sagittal T2-weighted MRI of a posterolateral, calcified meningioma at Th10 in a 58-year-old man with an 18-month history of pain and slight gait ataxia. **b** The axial bone window computed tomography (CT) scan demonstrates the calcifications of this tumor

render orientation difficult, tumors with extradural extension (Fig. 4.6), and for tumors associated with spinal dysraphism, such as a split-cord malformation (Fig. 4.4) [198]. In such instances, bony landmarks are the best guides during surgery. In complex dysraphic malformations and tumors with significant extradural extension, a three-dimensional reconstruction of CT images can be helpful (Fig. 4.7). However, such examinations do expose the patient to quite high doses of radiation. Therefore, they should be performed only if required, and be reserved for adult patients.

Fig. 4.6. **a** Oblique X-ray of a 25-year-old patient with a dumbbell schwannoma of the left C7 nerve root expanding the left neuroforamen at C6/7. The sagittal (**b**) and axial (**c**) T1-weighted MRI scans with contrast demonstrate the corresponding tumor. **d** This sagittal T1-weighted scan shows a large schwannoma at C2–C3 in a 68-year-old woman. The coronal scans show the considerable intra- (**e**) and extradural components. **f** The extradural portion grows around the vertebral artery, displacing the external carotid artery on the left side (*arrowhead*). (*Continuation see next page*)

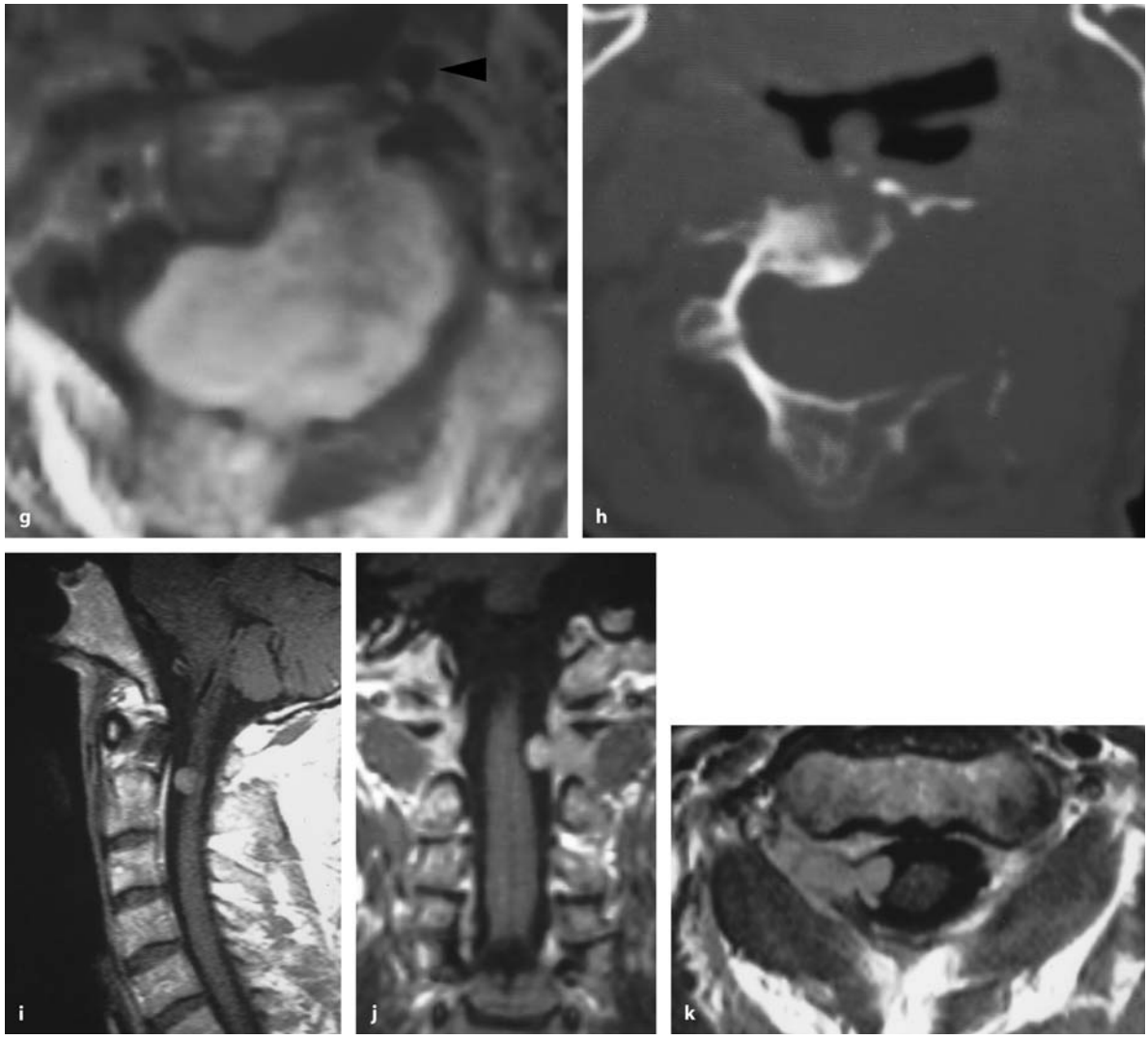

Fig. 4.6. (*Continued*) The axial MRI scan at C2 (**g**) demonstrates the relationship of the schwannoma to the left vertebral artery (*arrow*), whereas the CT scan in bone window technique (**h**) is the ideal modality for visualizing the altered bony anatomy. **i** This sagittal T1-weighted, contrast-enhanced MRI scan shows a schwannoma at C1–C2 in a 64-year-old patient. The coronal (**j**) and axial (**k**) scans give the impression that the small intradural tumor part is an extension of a primarily extradural schwannoma, rather than the other way around

Magnetic resonance imaging (MRI) is the diagnostic procedure of choice for all patients who can undergo this study. The examination has to demonstrate the tumor in at least two planes – sagittal and axial. T1-weighted images without and with gadolinium (contrast) enhancement are essential to demonstrate the exact position of the tumor and its topographical relationship with the spinal cord. Contrast enhancement provides a clue in terms of the vascularity of the process (Figs. 4.1, 4.5, and 4.6). To differentiate between intra- and extradural tumors, sagittal T1- and T2-weighted images are recommended: on T2, the dura is clearly visible as a dark line, and can be easily distinguished from tumors, which are almost always hyperintense in this mode (Fig. 4.8 and 4.9); on T1, the relationship between tumor and epidural fat can disclose the intra- or extradural position of a tumor (Fig. 4.8). Once again, the examination of thoracic tumors has to include a sagittal view of the neighboring spinal segment, so that the exact level of the tumor can be determined by counting from the top or bottom of the spine during surgery [257].

In tumors with extradural extension, the radiological examination has to demonstrate the intra-

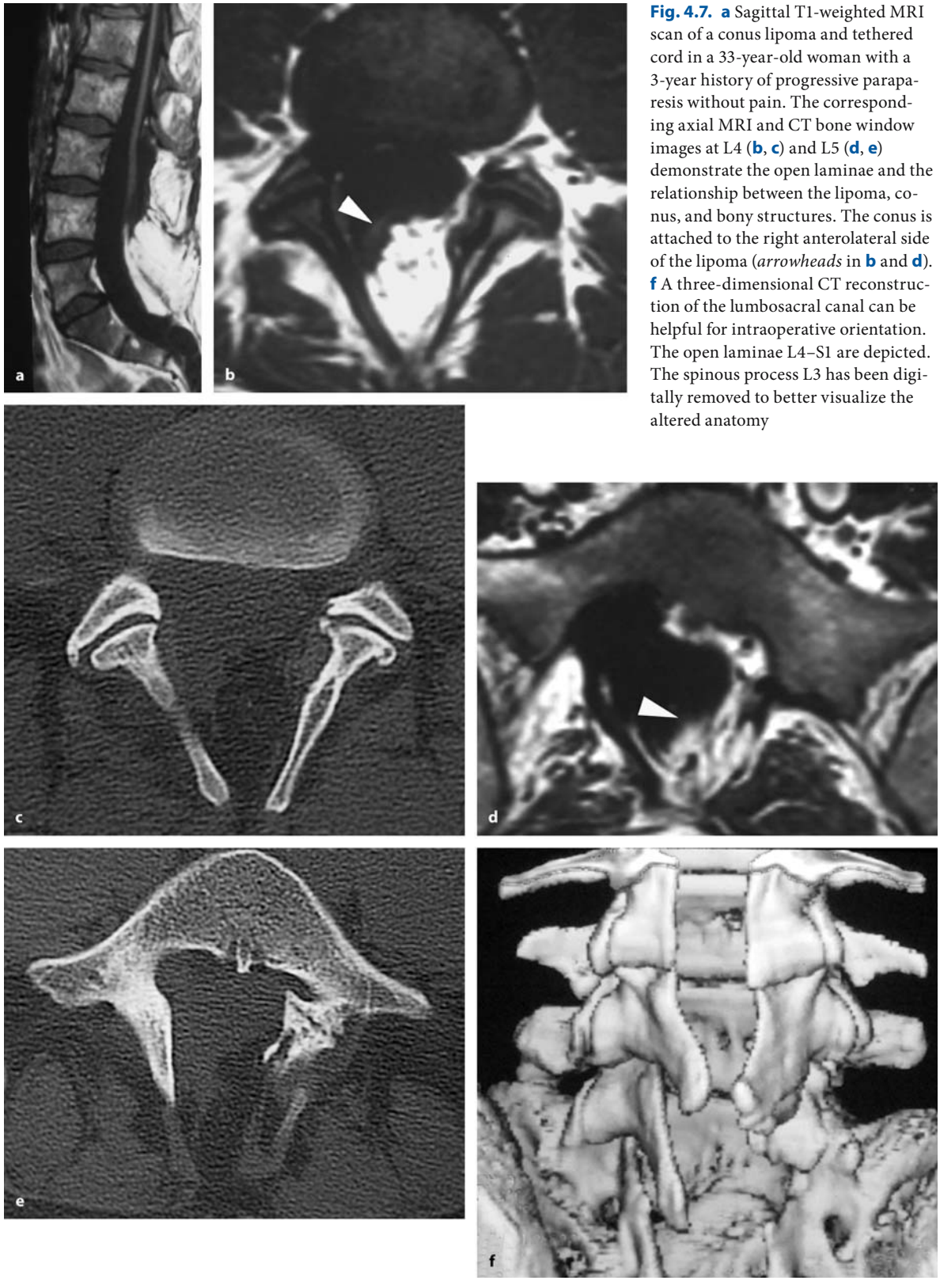

Fig. 4.7. **a** Sagittal T1-weighted MRI scan of a conus lipoma and tethered cord in a 33-year-old woman with a 3-year history of progressive paraparesis without pain. The corresponding axial MRI and CT bone window images at L4 (**b**, **c**) and L5 (**d**, **e**) demonstrate the open laminae and the relationship between the lipoma, conus, and bony structures. The conus is attached to the right anterolateral side of the lipoma (*arrowheads* in **b** and **d**). **f** A three-dimensional CT reconstruction of the lumbosacral canal can be helpful for intraoperative orientation. The open laminae L4–S1 are depicted. The spinous process L3 has been digitally removed to better visualize the altered anatomy

Fig. 4.8. Sagittal T1-weighted MRI scan with contrast of a 25-year-old woman with neurofibromatosis type 2 (NF-2) and multiple spinal tumors. This image depicts an extradural schwannoma at Th5–Th6 and an intradural schwannoma at Th8–Th9. The epidural fat helps to differentiate the relationships between these two tumors and the dura

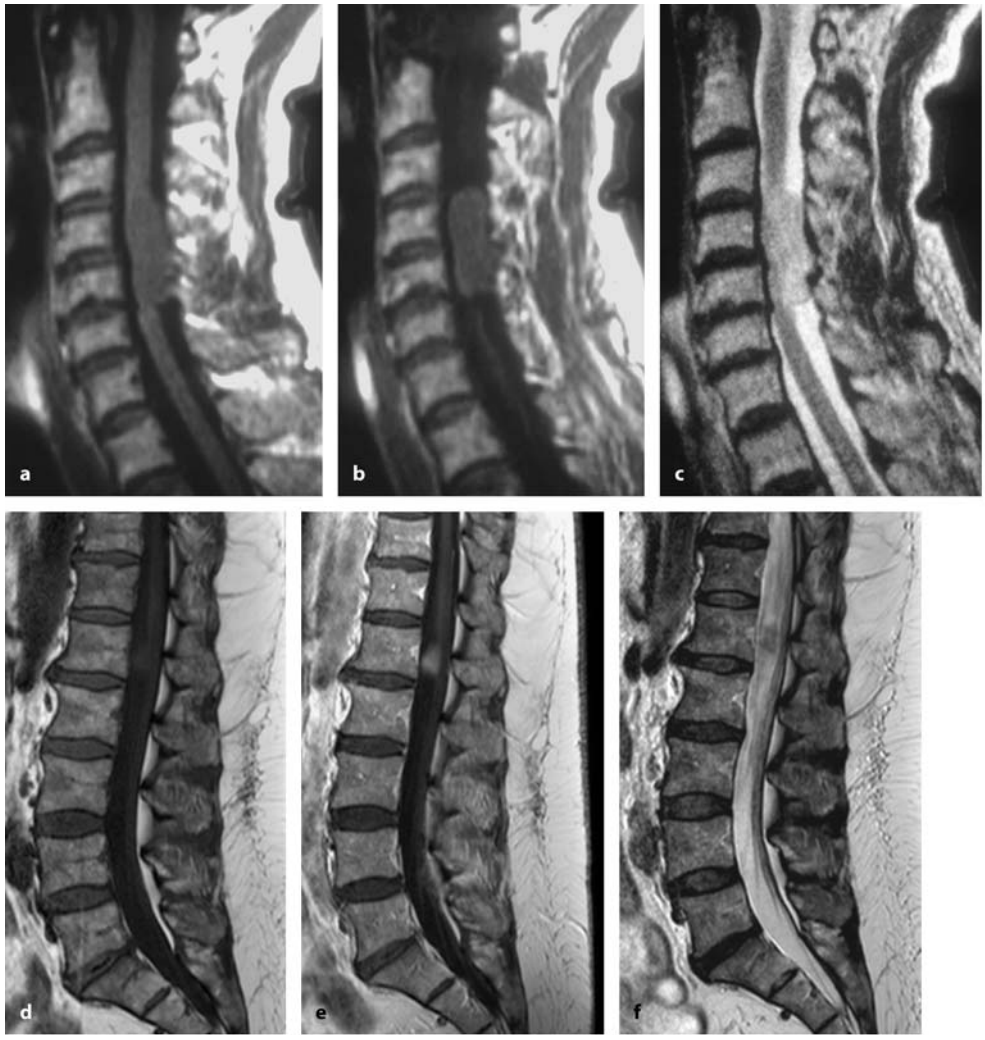

Fig. 4.9. (*Continuation see next page*)

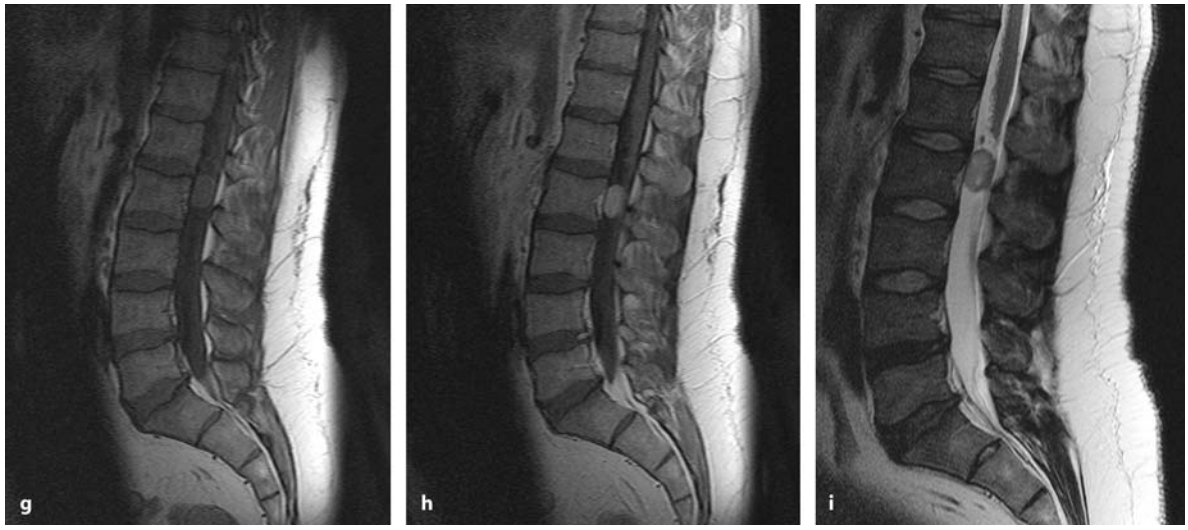

Fig. 4.9. (*Continued*) Sagittal T1-weighted MRI scans without (**a**) and with contrast (**b**), and T2-weighted images (**c**) of a meningioma at C4–C5, a schwannoma of the cauda equina at L1 (**d**, **e**, **f**), and an ependymoma at L2 (**g**, **h**, **i**). All tumors are isodense on T1, hyperdense on T2, and take up contrast

Fig. 4.10. Sagittal T1-weighted MRI scan with contrast of an en plaque growing meningioma at Th2–Th3 with a dura tail sign (*arrowheads*) in the cranial and caudal direction in a 71-year-old man

Fig. 4.11. Sagittal T1-weighted MRI scan of a meningioma at C7–Th1 in a 72-year-old woman. There is a hypodense rim demarcating the tumor from the cord (*arrowhead*). There were no adhesions between tumor and cord surface intraoperatively

and extradural components of the tumor, their relation to neighboring structures such as the vertebral artery, and the altered bony anatomy. The ratio between intra- and extradural tumor extensions can vary markedly. A combination of MRI, CT, and conventional X-ray is recommended for these tumors (Figs. 4.6 and 4.7).

The commonest extramedullary tumors – meningiomas, schwannomas, and ependymomas – display almost identical signal characteristics: isodense on T1-weighted images and hyperdense on T2-weighted images (Fig. 4.9) [257]. They are clearly demarcated toward the spinal cord and subarachnoid space, and

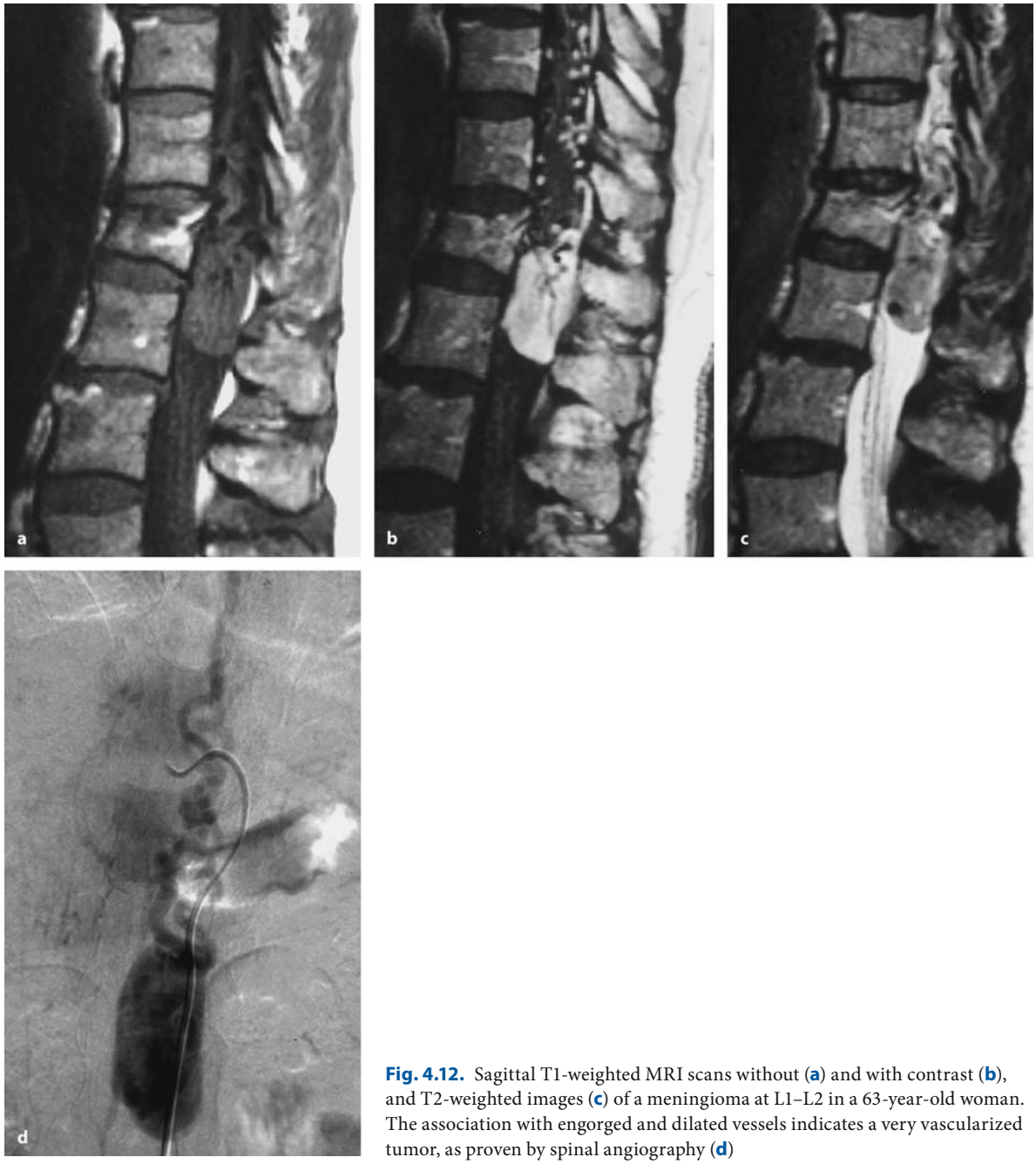

Fig. 4.12. Sagittal T1-weighted MRI scans without (**a**) and with contrast (**b**), and T2-weighted images (**c**) of a meningioma at L1–L2 in a 63-year-old woman. The association with engorged and dilated vessels indicates a very vascularized tumor, as proven by spinal angiography (**d**)

usually take up gadolinium homogeneously. Thus, they may be hard to differentiate on MRI.

However, some distinguishing features may be observed: contrast enhancement of the neighboring dura may indicate a meningioma (Fig. 4.10), but this sign can be missing (Fig. 4.9). Furthermore, demonstration of a hypointense rim around a meningioma on T1-weighted images has been shown to indicate no adhesion of the tumor to the spinal cord surface (Fig. 4.11) [227]. Meningiomas may be highly vascularized (Fig. 4.12), giving the appearance of an angioblastoma (Fig. 4.13). An enlarged neuroforamen may correspond to a nerve sheath tumor that has grown along the nerve root (Fig. 4.6). However, an epidural extension of an extramedullary tumor is not an exclusive feature of schwannomas: 20% of spinal meningiomas in our series, for instance, also demonstrated an extradural component (Fig. 4.14).

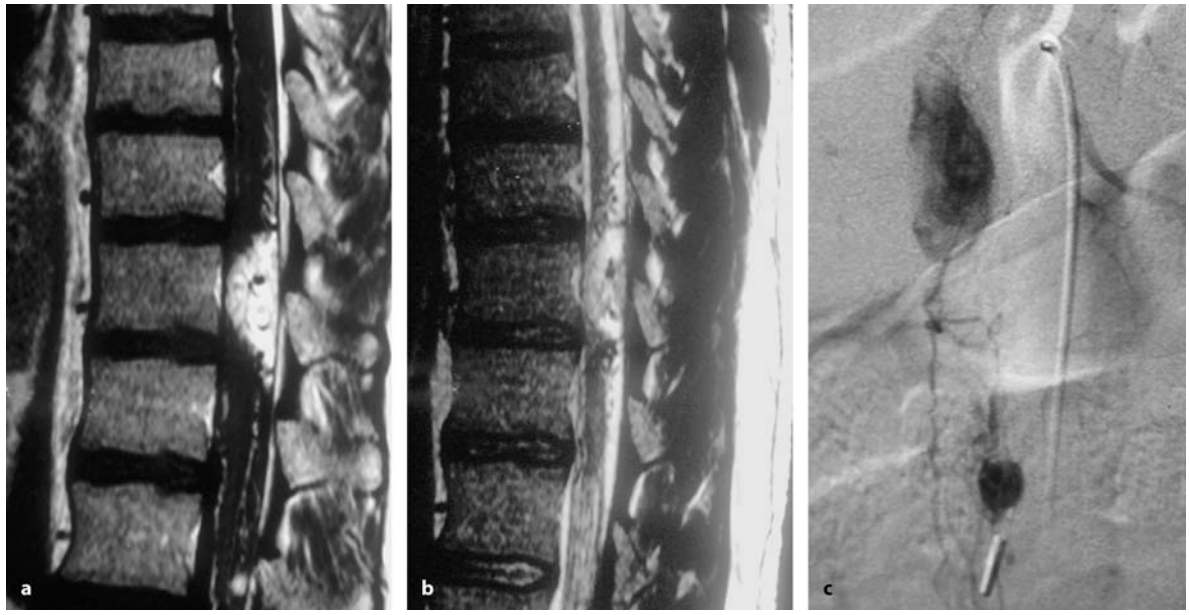

Fig. 4.13. Sagittal T1-weighted MRI scan with contrast (**a**) and T2-weighted image (**b**) of an angioblastoma at Th11 in a 33-year-old man with von-Hippel-Lindau disease (VHL). Again the engorged and dilated vessels next to this tumor indicate a highly vascularized lesion, as demonstrated on spinal angiography (**c**). A second tumor is visible at L1

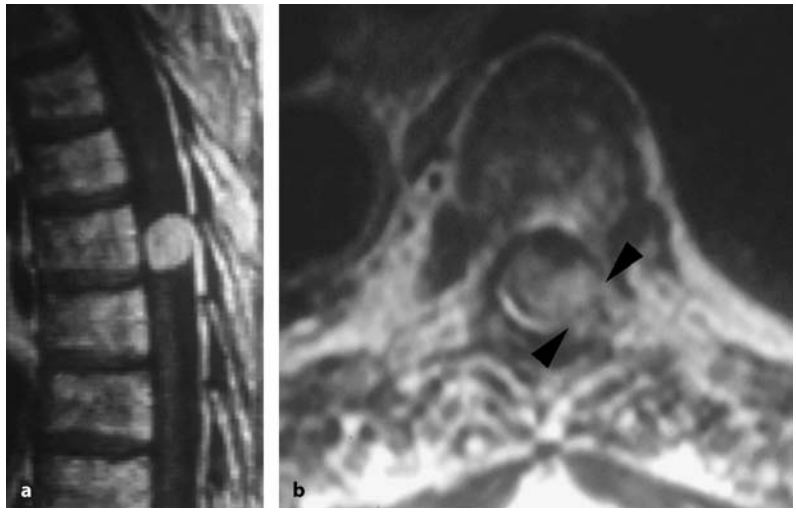

Fig. 4.14. Sagittal (**a**) and axial (**b**) T1-weighted, contrast-enhanced MRI images of a meningioma at Th6 in a 67-year-old man. The axial scan discloses an extradural component on the posterolateral left side (*arrowheads* in **b**)

Schwannomas lack dural signal changes, but may display variable signal intensities if they contain cystic components (Figs. 4.15 and 4.16). Cystic components may also be observed with ependymomas (Fig. 4.17), but are not a feature of meningiomas.

Apart from small ependymomas in the cauda equina region (Fig. 4.9), some may grow to enormous sizes, filling out the entire lumbar and sacral subarachnoid space (Fig. 4.18). They may also be observed elsewhere in the spinal canal due to subarachnoid seeding from a lumbar (Figs. 4.18 and 4.19) or fourth-ventricle tumor.

Spinal intradural lipomas do not usually display diagnostic difficulties due to their hyperintense signal on T1-weighted images, which demonstrate the exact limitations better than conventional T2-weighted images [141]. The major task in preoperative diagnosis is the localization of the conus and filum termi-

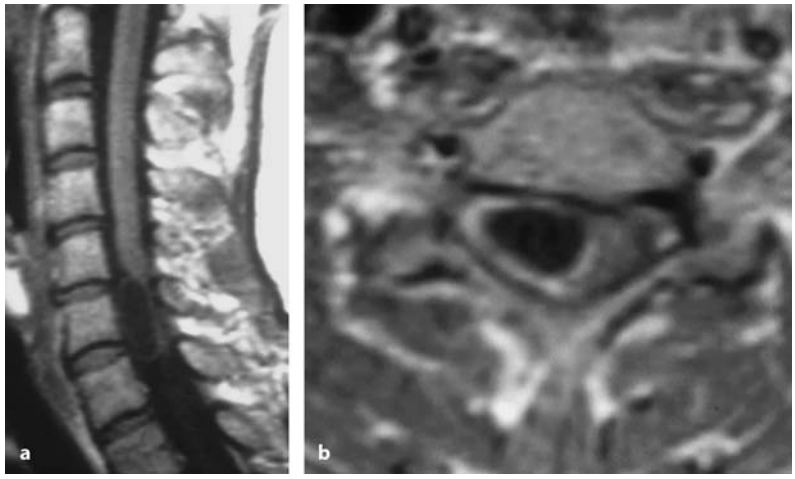

Fig. 4.15. Sagittal T1-weighted MRI scan (**a**) and axial T1-weighted image with contrast (**b**) of a cystic schwannoma at C6–C7 on the right side in a 47-year-old woman. The cyst wall is isodense and enhances contrast. The cyst content appears isodense to cerebrospinal fluid (CSF)

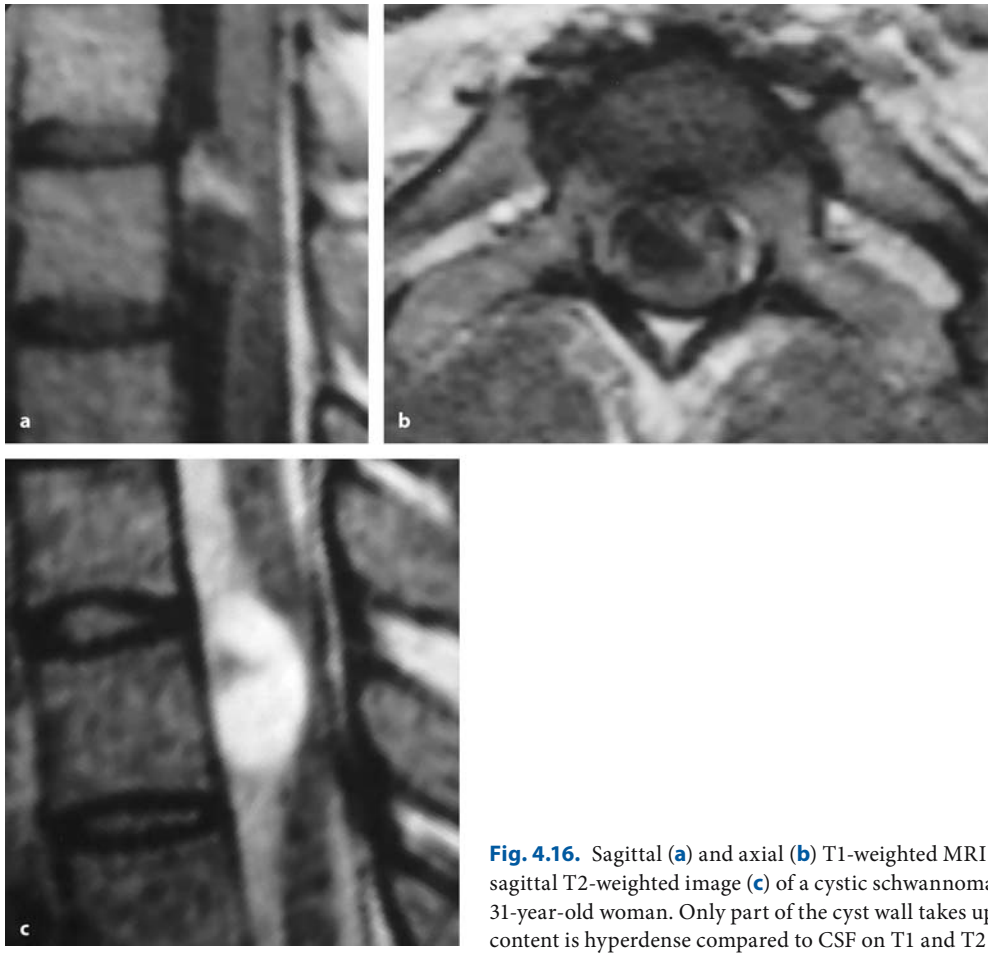

Fig. 4.16. Sagittal (**a**) and axial (**b**) T1-weighted MRI with contrast and sagittal T2-weighted image (**c**) of a cystic schwannoma at Th2–Th3 in a 31-year-old woman. Only part of the cyst wall takes up contrast. The cyst content is hyperdense compared to CSF on T1 and T2

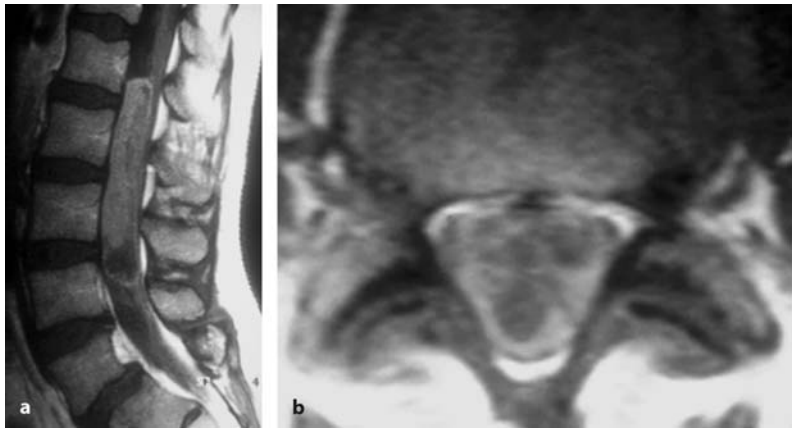

Fig. 4.17. Sagittal (**a**) and axial (**b**) T1-weighted, contrast-enhanced MRI of a large ependymoma at L1–L4 in a 39-year-old woman. Part of the tumor is cystic with inhomogenous contrast uptake due to intratumoral hemorrhages

Fig. 4.18. Sagittal T1-weighted, contrast-enhanced MRI scans of the lumbar (**a**) and thoracic spine (**b**) of a 20-year-old patient with an 8-year history of pain and slight gait ataxia. The entire lumbosacral canal up to Th12 is completely filled by an ependymoma of the filum terminale. The thoracic scan discloses further lesions due to subarachnoid seeding

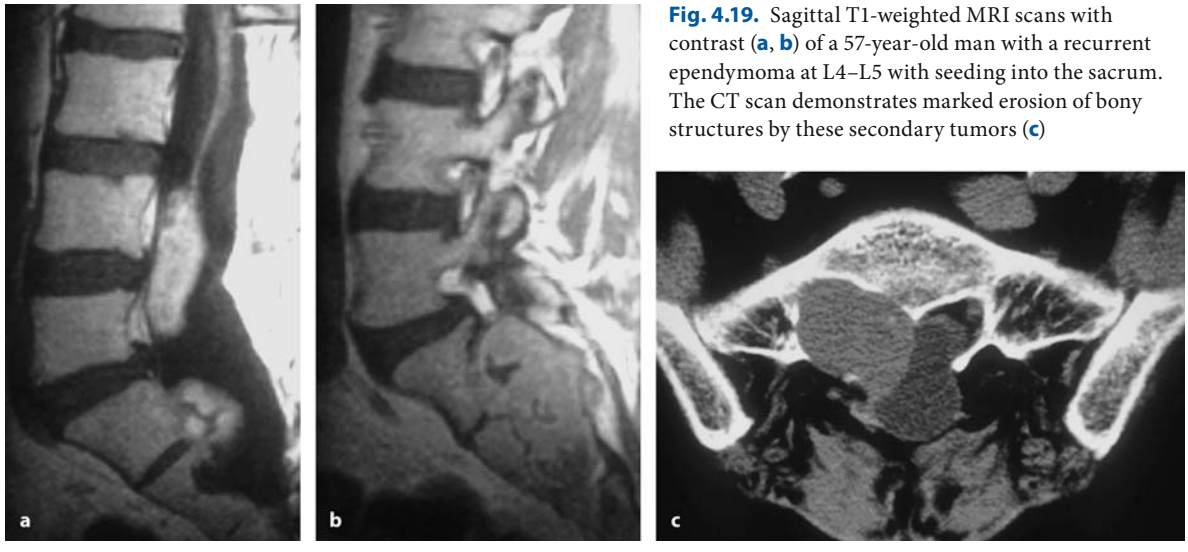

Fig. 4.19. Sagittal T1-weighted MRI scans with contrast (**a**, **b**) of a 57-year-old man with a recurrent ependymoma at L4–L5 with seeding into the sacrum. The CT scan demonstrates marked erosion of bony structures by these secondary tumors (**c**)

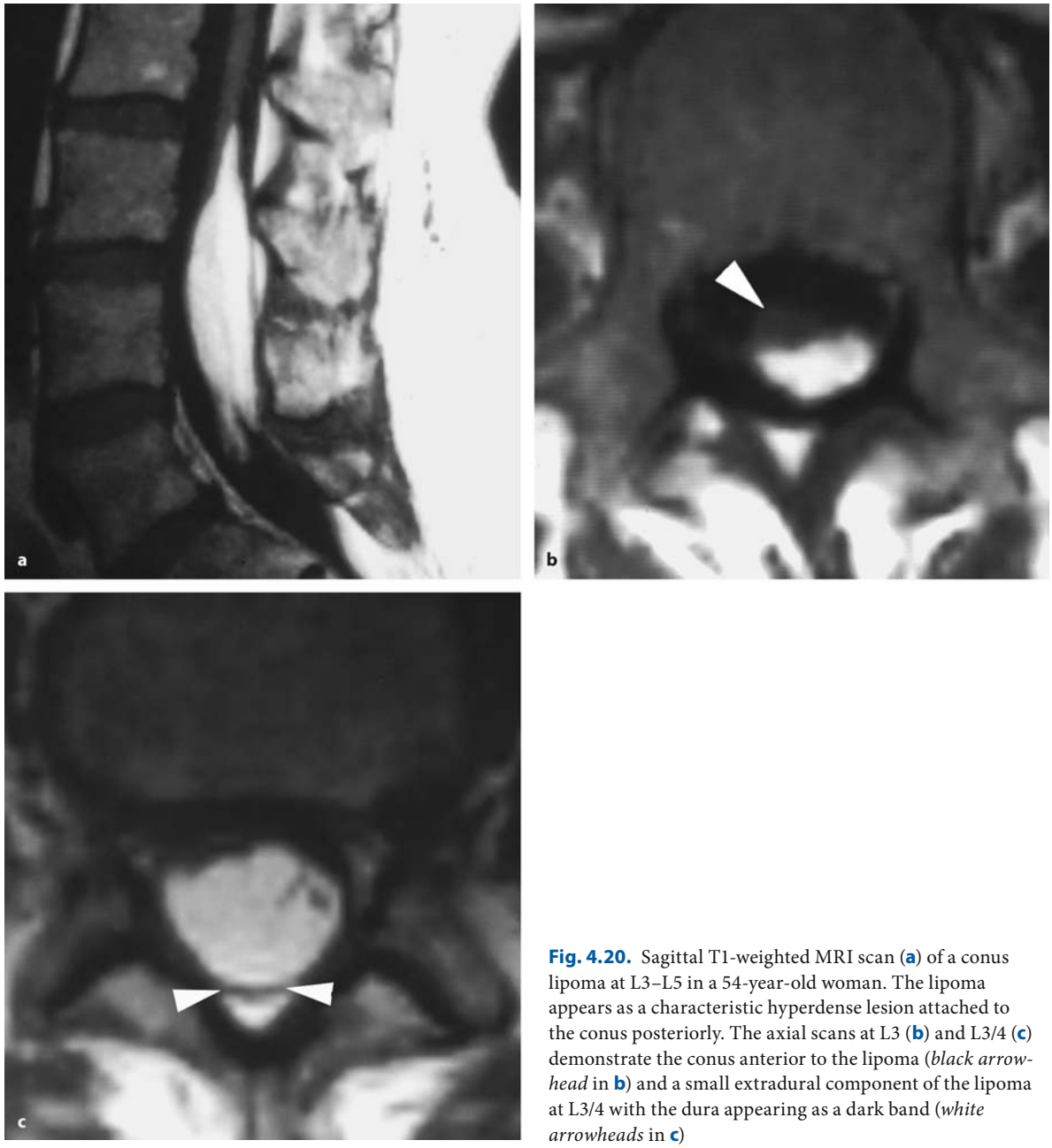

Fig. 4.20. Sagittal T1-weighted MRI scan (**a**) of a conus lipoma at L3–L5 in a 54-year-old woman. The lipoma appears as a characteristic hyperdense lesion attached to the conus posteriorly. The axial scans at L3 (**b**) and L3/4 (**c**) demonstrate the conus anterior to the lipoma (*black arrowhead* in **b**) and a small extradural component of the lipoma at L3/4 with the dura appearing as a dark band (*white arrowheads* in **c**)

nale, the demonstration of extradural extensions of the lipoma, and additional spinal malformations (Figs. 4.20 and 4.21).

Cystic extramedullary tumors may pose diagnostic problems unless the wall is thick and takes up contrast, as in schwannomas (Figs. 4.15 and 4.16), ependymomas (Fig. 4.17), or dermoid cysts (Fig. 4.22) [66]. With dysraphic cysts, the signal intensity of the cyst fluid is almost always different from that of CSF and hyperintense on T2-weighted images in most instances. Dermoid cysts display variable signal characteristics related to the cyst content. As most of them contain some amount of fat or fatty fluid, they usually display a bright signal on T1-weighted images (Fig. 4.22) [66, 176]. The cyst wall may enhance with gadolinium. Most of them are located in the conus region, but other locations along the spinal cord up to the craniocervical junction are possible (Fig. 4.22).

Neurenteric cysts may display a signal intensity identical or hyperintense to that of CSF. The cyst wall

Fig. 4.21. Sagittal (**a**) and axial (**b**) T1-weighted MRI of a conus lipoma at L4–S1 in a 34-year-old man. This lipoma has rotated the conus anticlockwise (*white arrowhead* in **b**) and is extending into the subcutaneous tissue through a sacral dura and fascia defect (*black arrowhead* in **a**). **c** The CT scan also depicts the relationship between lipoma and conus (*white arrowhead*)

Fig. 4.22. This series of images displays the different signal characteristics of dermoid cysts according to their respective contents. Sagittal (**a**) and axial (**b**) T1-weighted MRI scans with contrast of a dermoid cyst at the conus at Th12–L1 in a 19-year-old man, sagittal T1-weighted MRI scans without (**c**) and with contrast (**d**) of a dermoid cyst at Th4–Th5 in a 32-year-old woman, and sagittal (**e**) and axial (**f**) T1-weighted scans without contrast of a dermoid cyst at C1–C2. Hyperintense areas are related to fat components. There were no other associated features of dysraphism such as a tethered cord or spina bifida in either of these patients

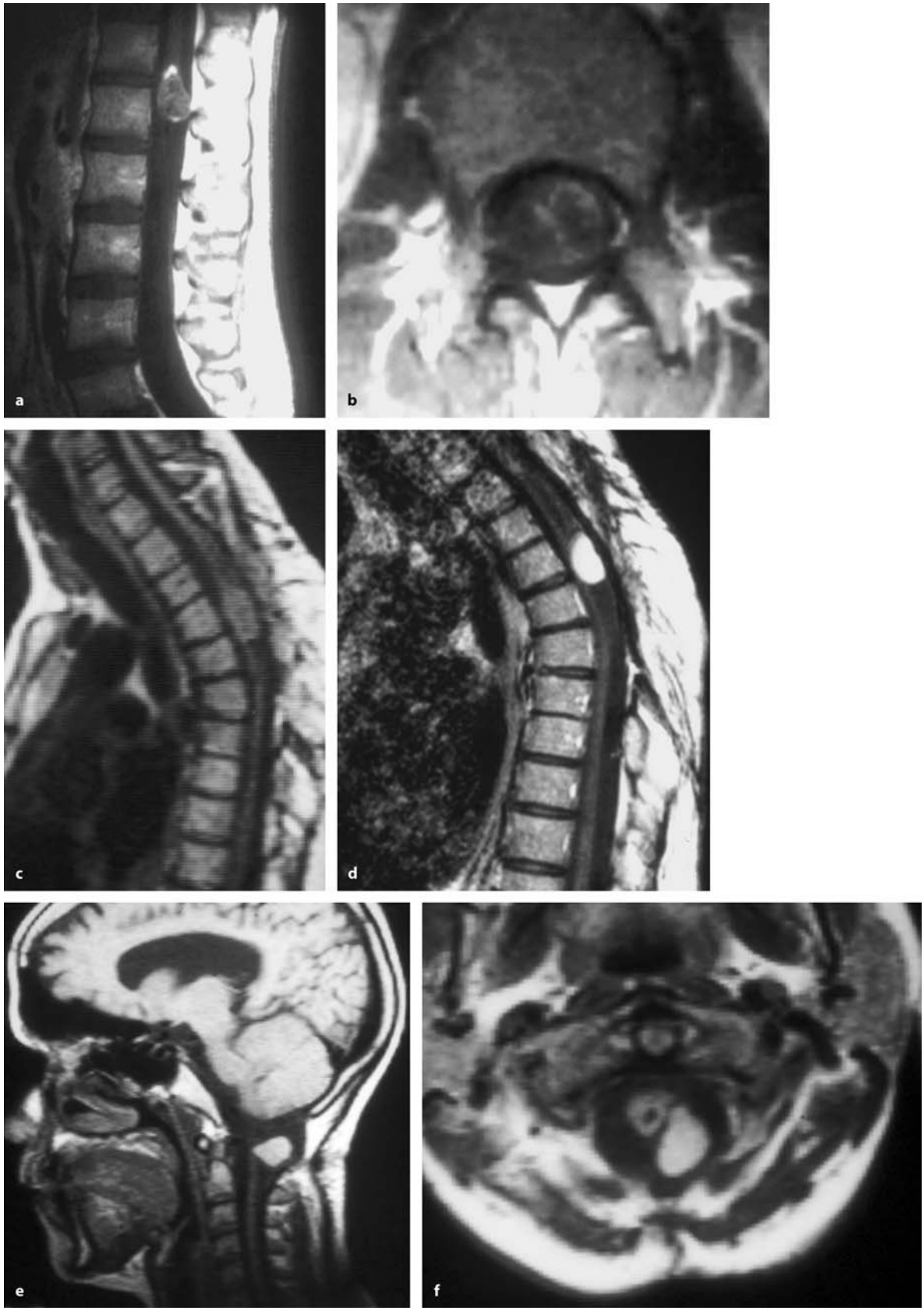

Fig. 4.22.

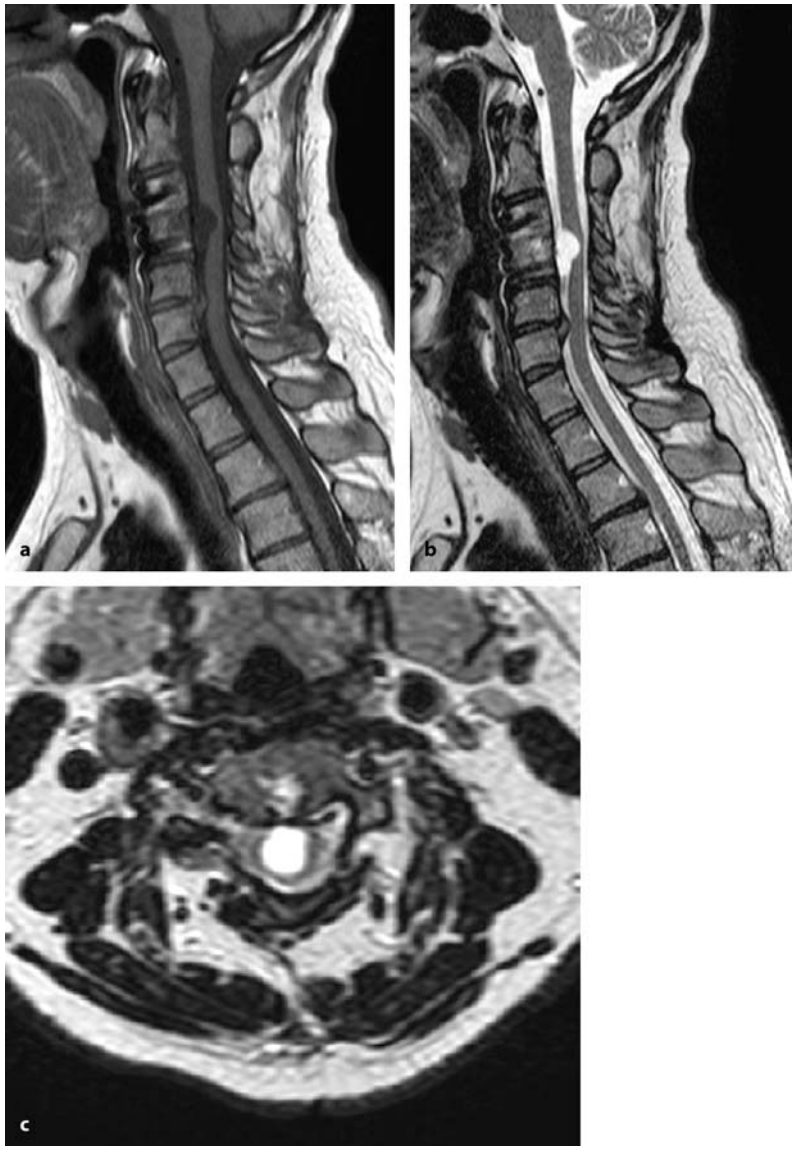

Fig. 4.23. Sagittal T1- (**a**) and T2-weighted (**b**) MRI scans of a neurenteric cyst at C4–C5 in a 44-year-old man. There is no contrast enhancement of the cyst wall. The cyst content appears hyperdense to CSF in both images. **c** This axial image displays a considerable ventral compression of the cord, which appears to be wrapped around this cyst

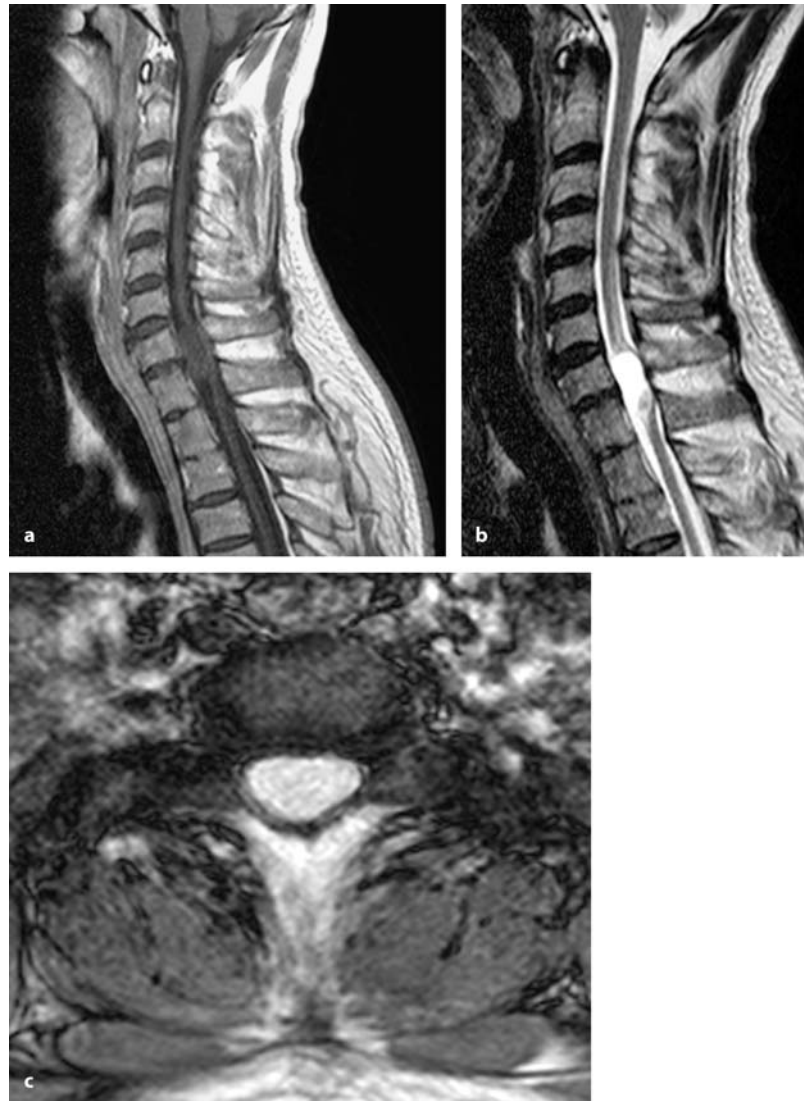

Fig. 4.24. Sagittal T1-weighted MRI scan with contrast (**a**), and sagittal (**b**) and axial (**c**) T2-weighted images of a neuroepithelial cyst at C7–Th1 in a 53-year-old patient. The signal characteristics are indistinguishable from a neurenteric cyst (see Fig. 4.23)

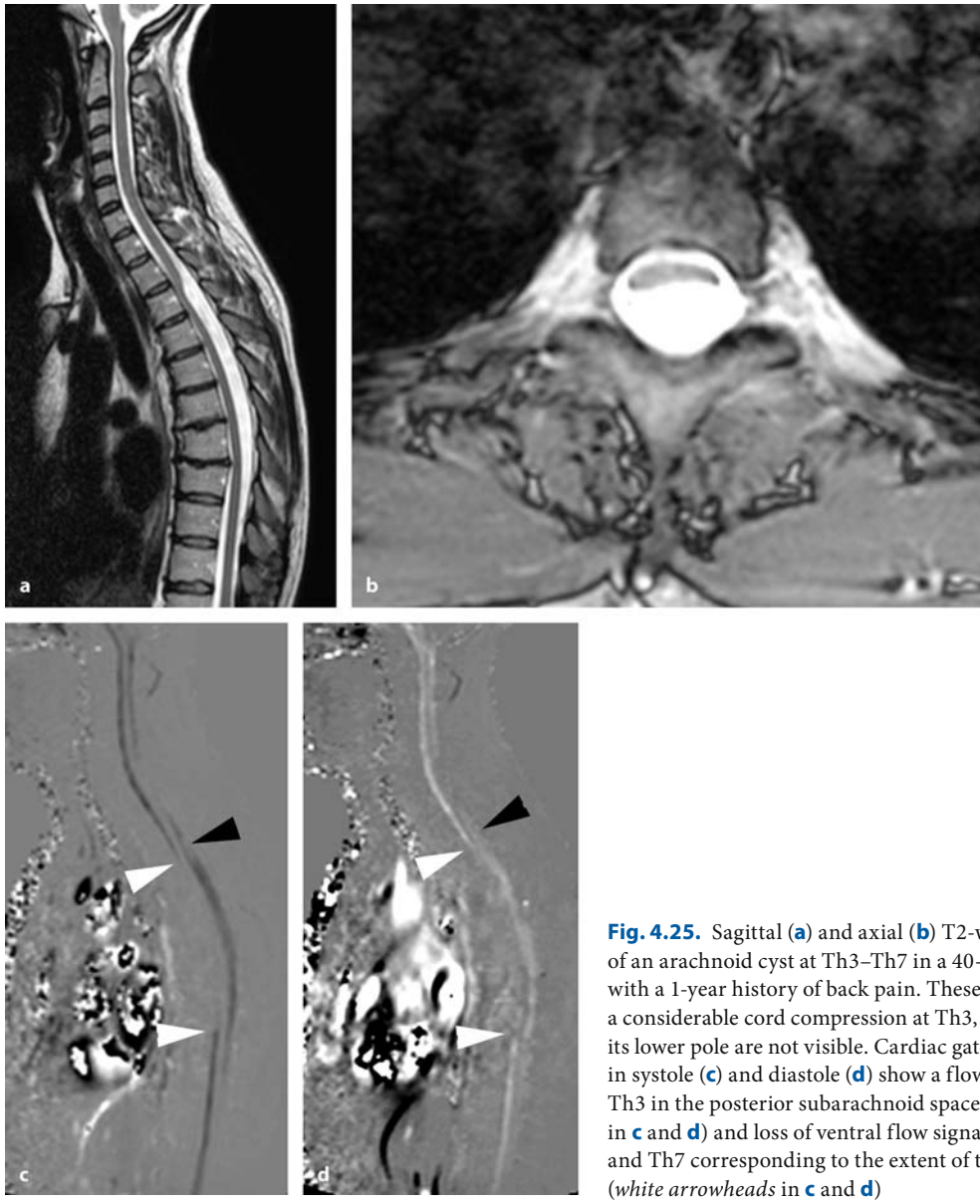

Fig. 4.25. Sagittal (**a**) and axial (**b**) T2-weighted MRI scan of an arachnoid cyst at Th3–Th7 in a 40-year-old woman with a 1-year history of back pain. These images demonstrate a considerable cord compression at Th3, but the cyst wall and its lower pole are not visible. Cardiac gated cine MRI scans in systole (**c**) and diastole (**d**) show a flow disturbance at Th3 in the posterior subarachnoid space (*black arrowhead* in **c** and **d**) and loss of ventral flow signals between Th3 and Th7 corresponding to the extent of the arachnoid cyst (*white arrowheads* in **c** and **d**)

Fig. 4.26. **a** This sagittal T2-weighted MRI scan shows small syrinx cavities above and below an arachnoid cyst at Th4–Th7 in a 32-year-old woman with a 1-year history of pain and slight gait ataxia. The cyst wall is not detectable, nor is there a compressive effect on the cord. **b** The cardiac gated cine MRI image demonstrates the extent of the cyst due to its flow signals, which are different from those in the surrounding subarachnoid space throughout the cardiac cycle (*arrowheads*)

does not enhance with gadolinium [208]. Commonly they appear as lobulated, space-occupying lesions [25]. In most instances, the cyst wall tends to be thicker and is visible on standard MRI scans. Typically, neurenteric cysts lie anterior or anterolateral to the spinal cord (Fig. 4.23) [12, 25, 66], except for cysts at the conus medullaris, which may be located posteriorly [208]. As neurenteric cysts are related to split-cord malformations, corresponding malformations of the vertebral body may be observed. Neuroepithelial cysts show identical signal characteristics to neurenteric cysts (Fig. 4.24).

Arachnoid cysts may extend over several spinal segments. Not all cysts will cause such a significant compression of the cord that they can be easily detected (Fig. 4.25). Cyst walls may be quite thin and move slightly with the pulsatile motion of CSF so that standard MRI images cannot pick them up [66]. The cyst content of arachnoid cysts is indistinguishable from CSF (Figs. 4.25 and 4.26). In such instances, cardiac gated cine MRI is a very sensitive method as the cyst will cause some degree of CSF flow obstruction or turbulence, which may provide indirect evidence of its extension (Figs. 4.25 and 4.26) [275]. If in doubt, myelography and postmyelographic CT are still useful for this pathology, especially using delayed scans for CT (Fig. 4.27) [133]. However, a negative myelogram does not rule out an arachnoid cyst!

Rare extramedullary pathologies such as metastases (Fig. 4.28), melanocytomas (Fig. 4.29), or metastasized chordomas (Fig. 4.30) display similar signal characteristics to more common pathologies such as schwannomas and meningiomas. They all enhance brightly with contrast and show a sharp demarcation toward the spinal cord. Unless a specific clinical history points to a particular pathology, the correct diagnosis is usually not suspected before surgery.

Unlike inflammatory and demyelinating diseases, which can appear on MRI like an intramedullary tumor, there is almost no pathology that could be mistaken for an intradural extramedullary tumor. Only one such case was encountered in our series, with a woman who presented with pain, sensory and motor disturbances, and an extramedullary lesion, who was operated with the preoperative assumption of a tumor but turned out to be a spinal subdural hematoma (Fig. 4.31).

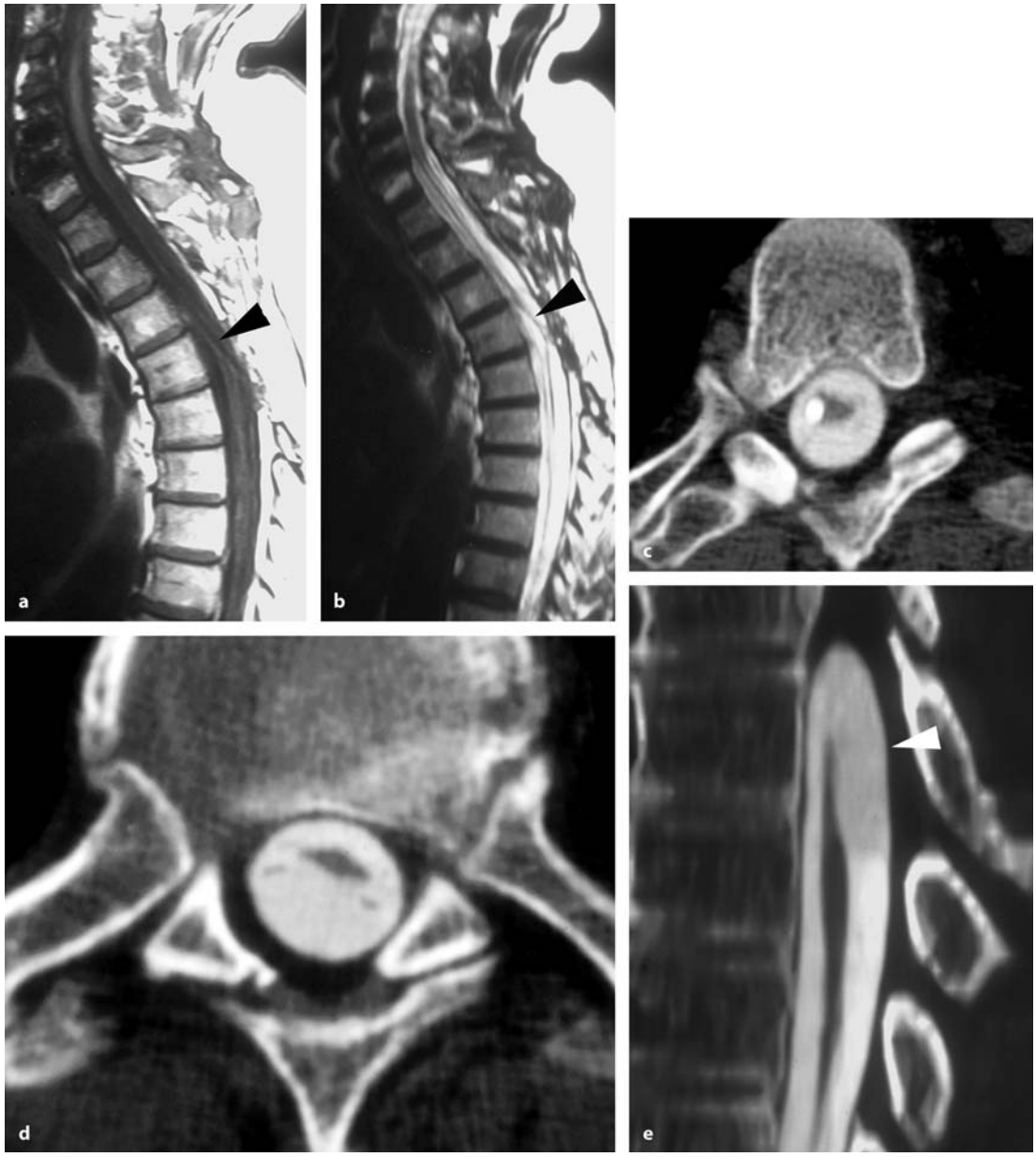

Fig. 4.27. Sagittal T1- (**a**) and T2-weighted (**b**) MRI scans of a 54-year-old man who was treated with a syringosubarachnoid shunt for a cervicothoracic syrinx (*black arrowheads*). The postmyelographic CT scan shows the intramedullary catheter at Th4 (**c**) and an area of posterior cord compression at Th6/7 (**d**). **e** A delayed postmyelographic CT scan with sagittal reconstruction finally demonstrates an arachnoid cyst at Th6–Th7 as the cause for the progressive symptoms and the syrinx (*white arrowhead*)

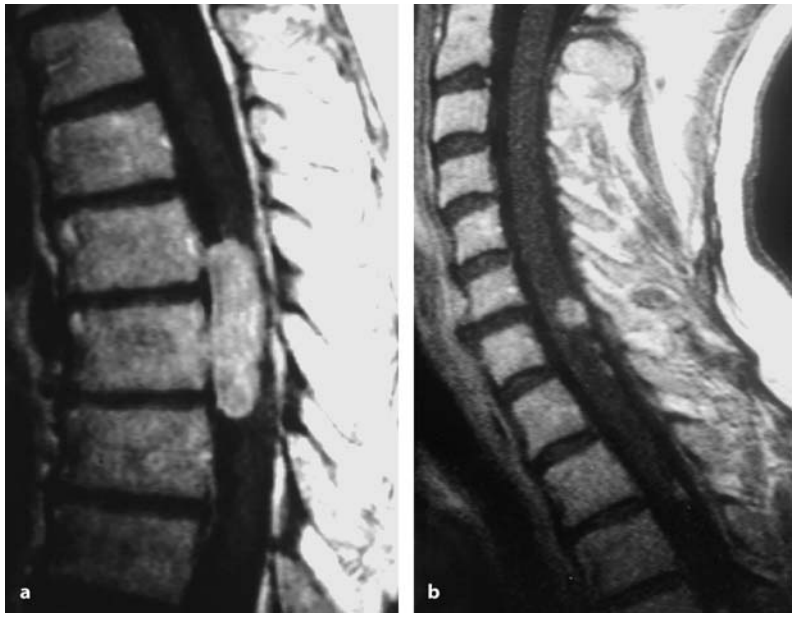

Fig. 4.28. Sagittal T1-weighted, contrast-enhanced MRI images of the thoracic (**a**) and cervical (**b**) spine of melanoma metastases at Th6–Th7 and C7 in a 63-year-old woman with a 3-month history of a slight paraparesis and radicular pain

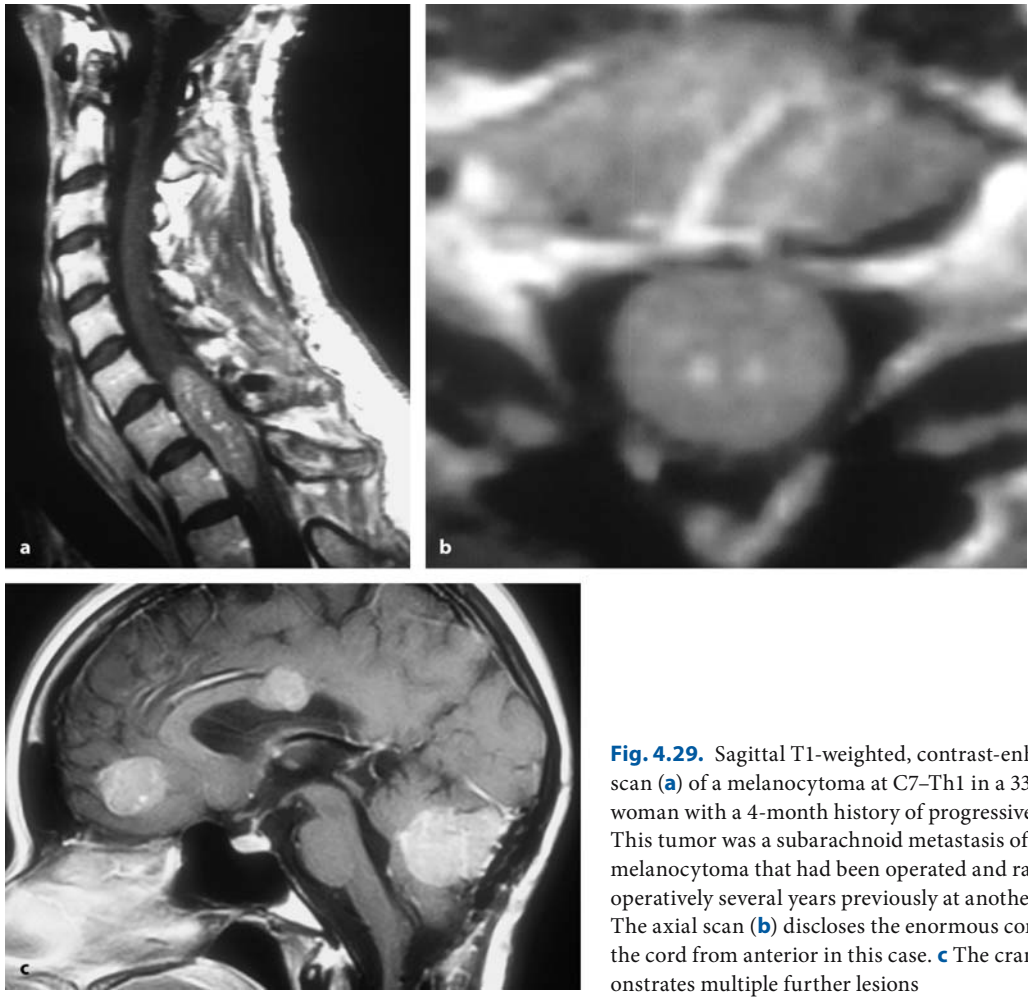

Fig. 4.29. Sagittal T1-weighted, contrast-enhanced MRI scan (**a**) of a melanocytoma at C7–Th1 in a 33-year-old woman with a 4-month history of progressive paraparesis. This tumor was a subarachnoid metastasis of a cerebellar melanocytoma that had been operated and radiated postoperatively several years previously at another institution. The axial scan (**b**) discloses the enormous compression of the cord from anterior in this case. **c** The cranial MRI demonstrates multiple further lesions

Fig. 4.30. Sagittal T1-weighted, contrast-enhanced MRI scans of a 28-year-old man with a short history of a progressive tetraparesis. The extramedullary tumor at C3–C4 turned out to be a chordoma. An extradural chordoma as the primary site could not be demonstrated

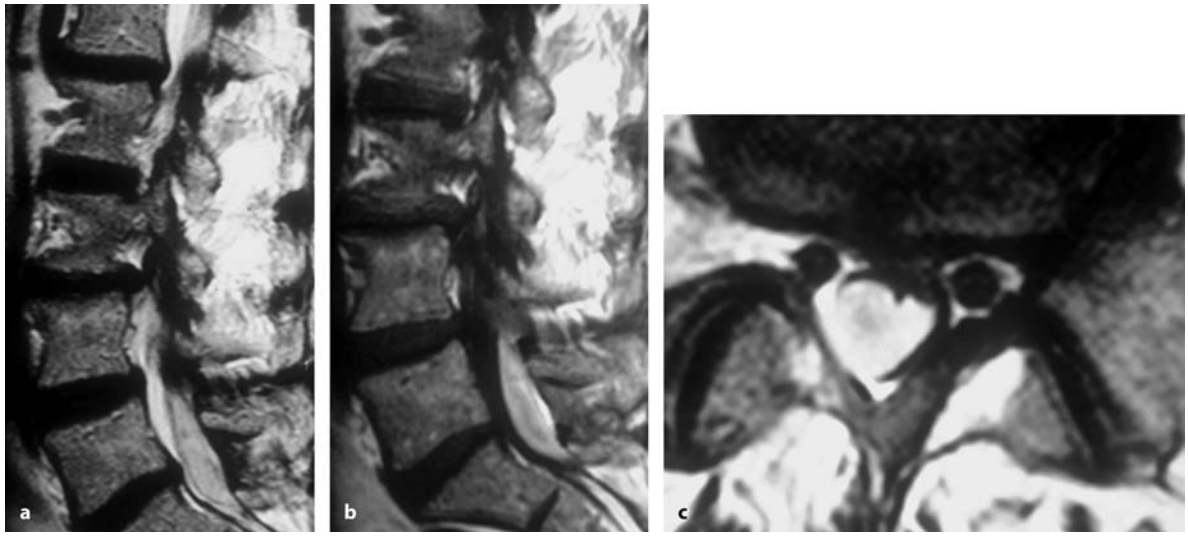

Fig. 4.31. Sagittal T2- (**a**) and T1-weighted (**b**) MRI scans of a subdural hematoma at L5–S1 in a 64-year-old woman with a 2-week history of pain and paraparesis. **c** The axial T1-weighted image shows the considerable diameter of this hematoma. Signal characteristics vary depending on the age of the hematoma. The blood is hypodense on T2 and hyperdense on T1

4.3 Surgery

4.3.1 Exposure

Patients with intradural tumors of the thoracic or lumbar spine are operated in the prone position. We prefer the semisitting position for cervical intradural tumors. We use the same monitoring features as described for intramedullary tumors. For the overwhelming majority of extramedullary tumors, a standard laminotomy and dural exposure for a midline approach as described for intramedullary tumors are sufficient. The required exposure is about 1 cm wide. With small lateral tumors, a hemilaminectomy (Fig. 4.32), or even an interlaminar fenestration, may be adequate.

Alternative anterior approaches have been described for selected cases of anteriorly placed extramedullary tumors. Crockard and Bradford [51] described a patient with transoral removal of an intradural schwannoma. Jenny et al. [125] have employed a transthoracic, transvertebral approach for successful removal of an anteriorly placed, calcified meningioma; Dickman and Apfelbaum [54] employed a similar anterior thoracoscopic approach for removal of a schwannoma, while O'Toole and McCormick [195] reported a complete resection of a ventral schwannoma via an anterior cervical corpectomy with reconstruction, and Arai et al. [12] used a subtotal cervical corpectomy for a neurenteric cyst, which was resected subtotally. In our opinion, extended anterior approaches are not required for the overwhelming majority of solid extramedullary tumors, because the tumor usually provides sufficient space in front of the cord for a safe, piecemeal removal. However, with cystic tumors, calcified or recurrent tumors accompanied by significant arachnoid scarring, the situation may be different. Once the cyst is open and has collapsed, the working space for removal from posterior is gone. With anteriorly placed calcified tumors or recurrent tumors adherent to the arachnoid membrane or pia mater, safe removal requires direct vision of the interface towards the spinal cord. In such cases, it may be too risky to mobilize the cord, so a direct anterior approach may be safer.

With the dura exposed, the operation is continued with the aid of a surgical microscope. To protect the spinal cord against any damage during tumor removal requires most importantly protection of its vessels. In patients with severe preoperative neurological deficits in particular, the spinal cord blood supply may be on the verge of decompensation. The arachnoidal layer can be useful for protecting the spinal cord during surgery, provided the anatomy of the subarachnoid space and the relationship between the tumor and the arachnoid membrane are respected.

The spinal subarachnoid space is divided into five longitudinal compartments. The posterior septum runs in the posterior midline attached to the pia mater of the spinal cord. It separates the posterior subarachnoid space in a left and right compartment and can be followed from the cervical to the lower thoracic region. Other names applied to this structure are septum arachnoidale, septum subarachnoidale, septum intermedium, or septum leptomeningeum dorsale. It has been extensively studied by Key and Retzius [134] (Fig. 4.33). The posterior roots traverse the posterior subarachnoid space from the dural sleeve in the neuroforamen toward the posterolateral sulcus of the spinal cord. Anterior roots run from the anterior spinal cord surface toward the neuroforamen. Between posterior and anterior roots, the dentate ligaments anchor the spinal cord laterally to the dura (Fig. 4.33). Correspondingly, lateral compartments between the anterior and posterior roots and an anterior compartment can be distinguished. Depending on the origin and direction of growth of a particular extramedullary tumor, individual compartments may be expanded or compressed. Arachnoid layers may engulf the entire tumor, providing a safety layer toward the spinal cord surface and its blood vessels. Therefore, the arachnoid can and should be left intact throughout the entire procedure in such instances to avoid injuries to spinal cord vessels and nerve roots and postoperative arachnoid scarring [251].

Before dura opening, we like to locate the exact position of the tumor with ultrasound (Figs. 4.34 and 4.35) [164]. As some of the tumors are mobile to some degree, the position of the tumor in the supine position (i.e., when the MRI scan is done) may differ from the one in the operative room with the patient in the prone position by more than a centimeter! Ultrasound ensures an adequate exposure and provides a clue as to the best position for the dura incision.

We advise leaving the arachnoid membrane intact during dura opening. Important blood vessels reach the spinal cord along anterior and posterior nerve roots. These may be adherent to the arachnoid membrane in any patient with an extramedullary tumor. Therefore, pulling and tearing of the arachnoid membrane should be avoided and sharp dissection used instead to ensure the safety of the cord's blood supply. Once the dura is open and the arachnoid membrane

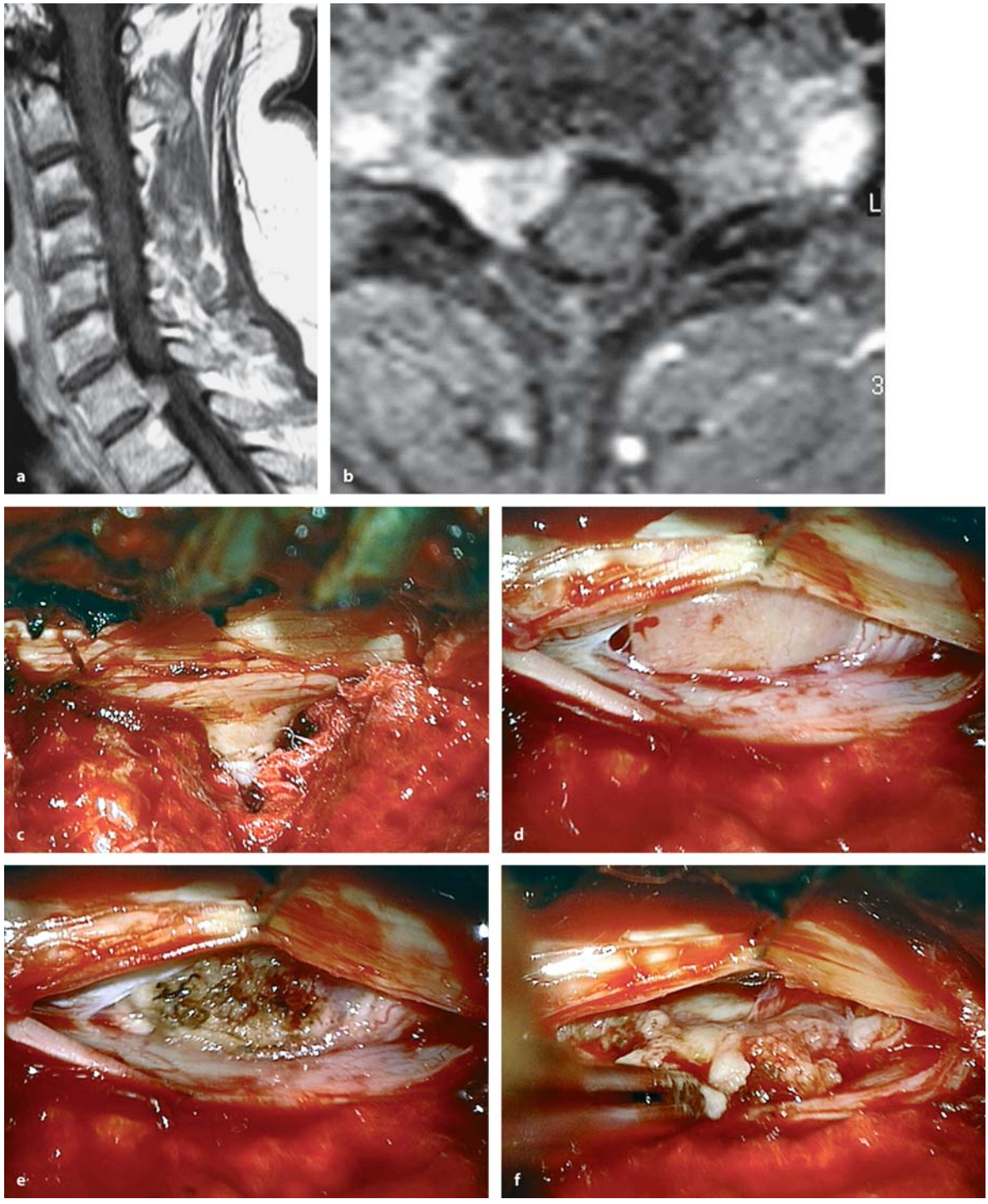

Fig. 4.32. Sagittal (**a**) and axial (**b**) T1-weighted, contrast-enhanced MRI scan of a meningioma at C7/Th1 on the right side in a 66-year-old woman with a 4-month history of pain and sensory disturbances in her right arm. **c** This intraoperative picture demonstrates the exposure of the dura after interlaminar fenestration and partial hemilaminectomies of C7 and Th1 on the right side. As the tumor lies in the dural sleeve of the neuroforamen, the exposure follows the nerve root accordingly. **d** With mediolateral incision of the dura and arachnoid membrane, the tumor becomes visible, pushing the nerve root cranially. With partial resection of the tumor (**e**), the capsule can be mobilized laterally (**f**). (*Continuation see next page*)

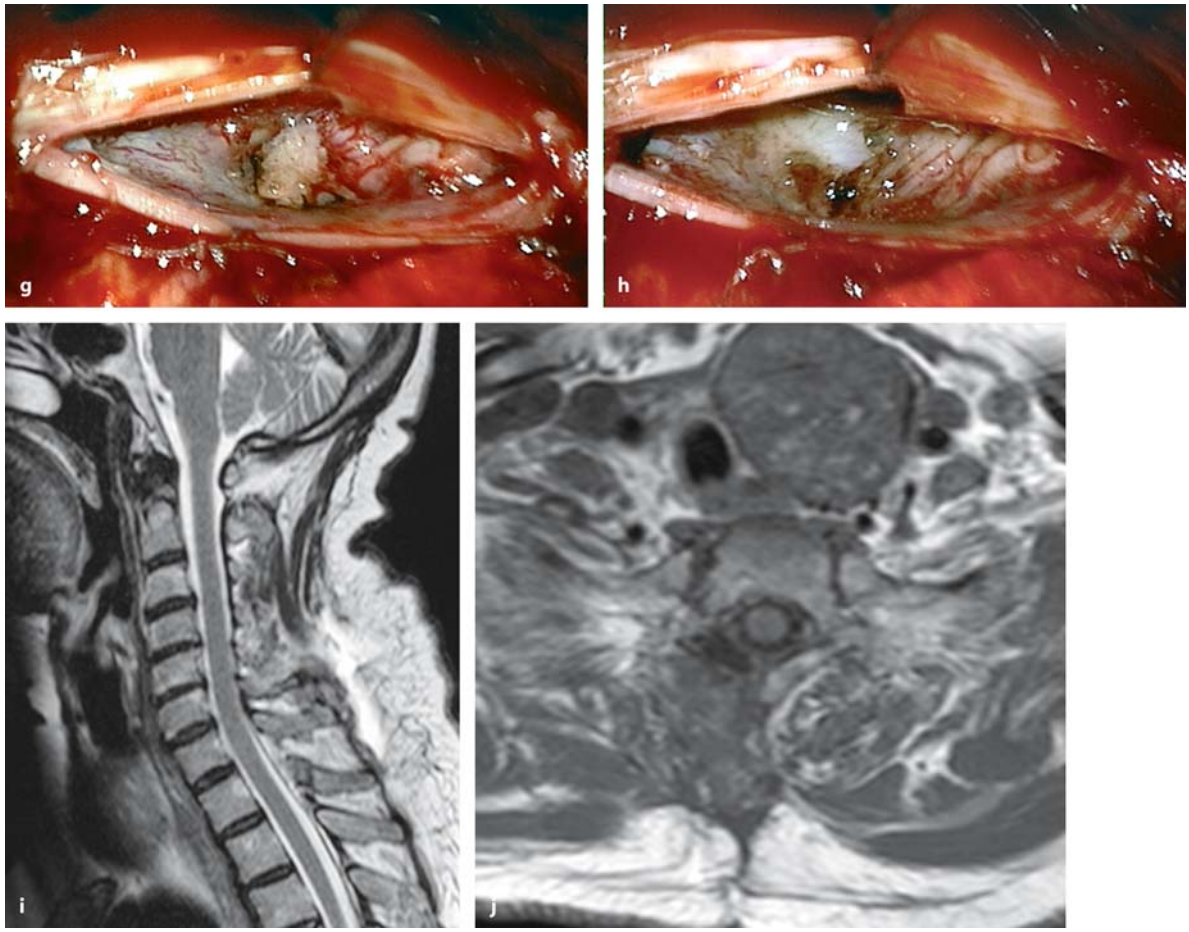

Fig. 4.32. (*Continued*) **g** Finally, the attachment zone in the dura sleeve is exposed. **h** After resection of parts of the inner dural layer, remaining tumor remnants could be removed and the area cauterized, avoiding injury to the nerve root. The postoperative sagittal, contrast-enhanced, T2-weighted (**i**) and axial T1-weighted images (**j**) taken 1 year later show no evidence of a tumor recurrence or arachnoid adhesions. The patient experienced improvement of her pain, but the sensory changes remained unchanged

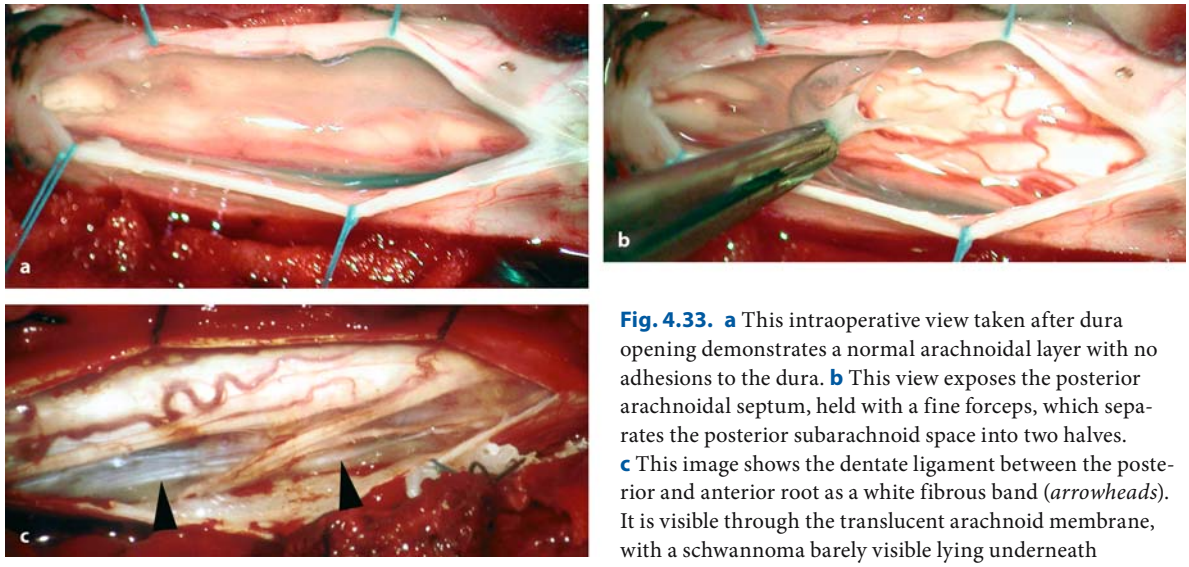

Fig. 4.33. **a** This intraoperative view taken after dura opening demonstrates a normal arachnoidal layer with no adhesions to the dura. **b** This view exposes the posterior arachnoidal septum, held with a fine forceps, which separates the posterior subarachnoid space into two halves. **c** This image shows the dentate ligament between the posterior and anterior root as a white fibrous band (*arrowheads*). It is visible through the translucent arachnoid membrane, with a schwannoma barely visible lying underneath

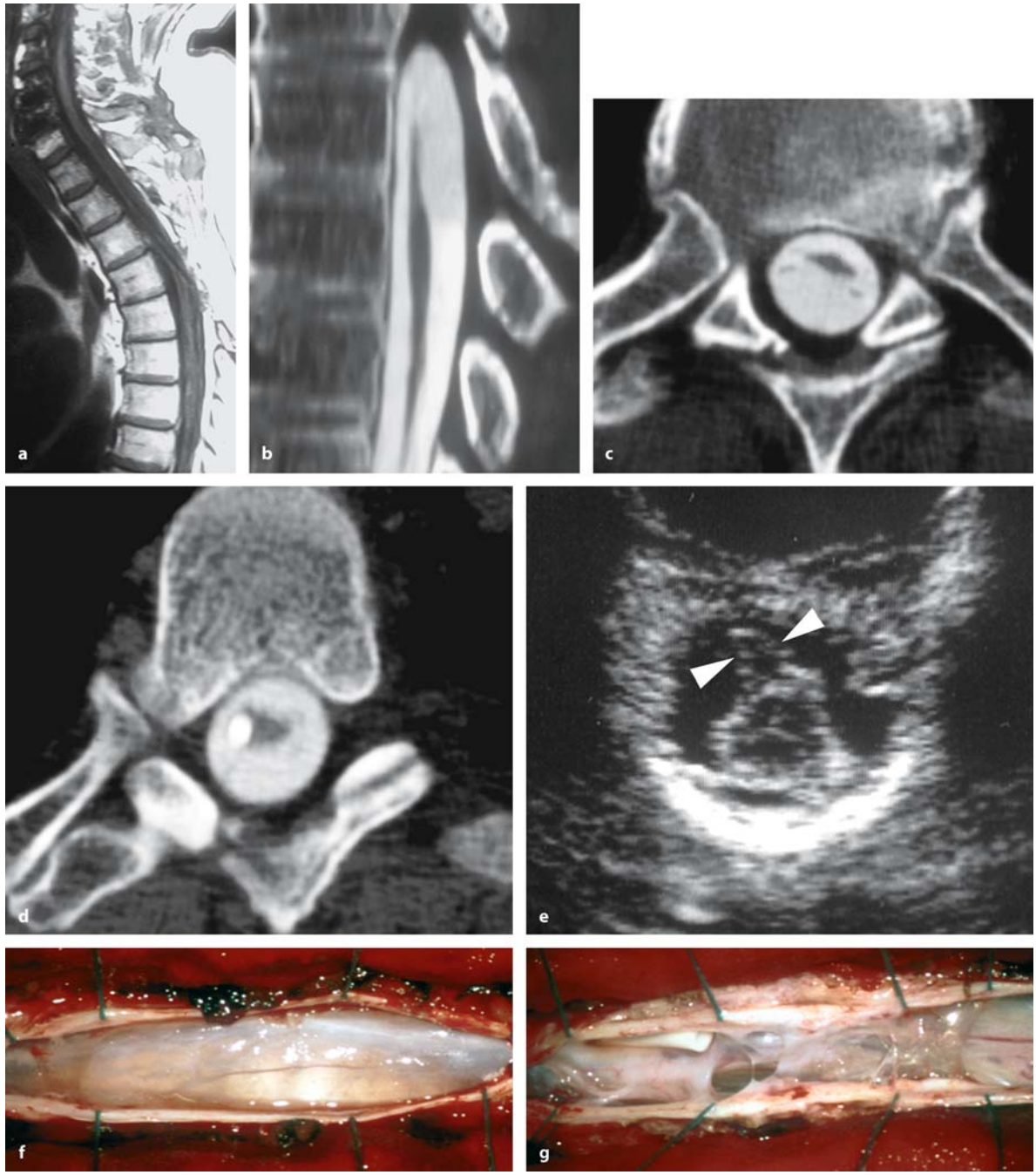

Fig. 4.34. Sagittal T1-weighted MRI scan (**a**) and postmyelographic CT images (**b**, **c**, **d**) of an arachnoid cyst at Th6–Th7 and a cervicothoracic syrinx in a 54-year-old man with a 15-year history of progressive paraparesis predominantly on the right side (see also Fig. 4.27). The paraparesis progressed despite a persistent decrease of syrinx size making him wheelchair dependent. The axial ultrasound image (**e**) demonstrates the spinal cord and thickened arachnoid webs related to the arachnoid cyst (*arrowheads*). **f** This intraoperative view after dura opening demonstrates the clear translucent arachnoid in the area of the cyst at Th6–Th7. **g** By comparison, this image depicts the situation in the area of the previous operation after insertion of a syringosubarachnoid shunt. The arachnoid membrane is thickened in places to a dense fibrous structure adherent to the cord surface. (*Continuation see next page*)

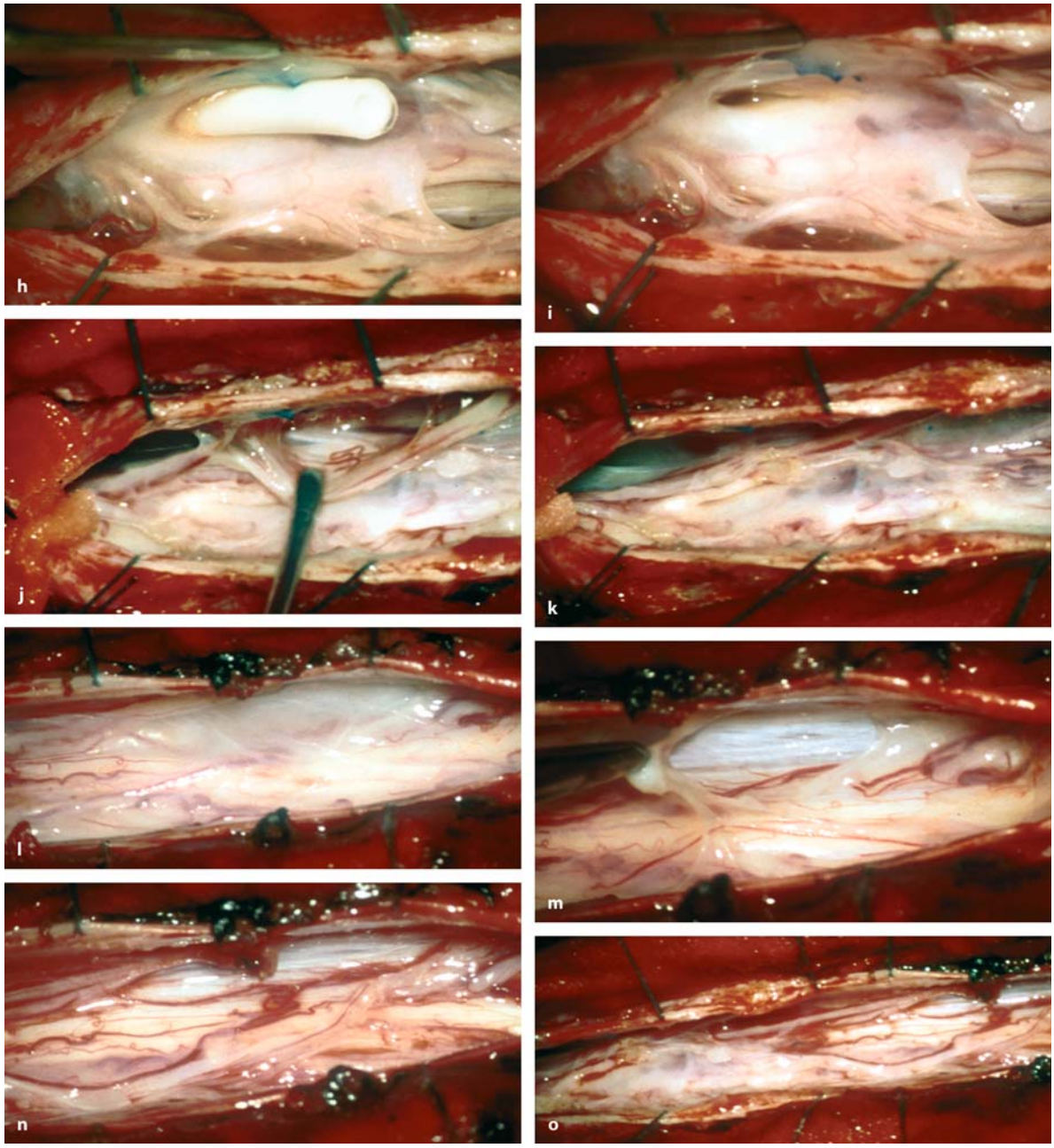

Fig. 4.34. **h** A closer view demonstrates the catheter sutured to the dura. After removal of the catheter, dense arachnoid adhesions next to the former catheter position can be seen posteriorly (**i**) and laterally (**j**). After sharp dissection of these adhesions (**k**), the underlying pathology can be treated: the arachnoid cyst is on the right side of the cord (**l**). **m** This image demonstrates the view into the cyst after opening its posterior wall. After complete resection of the cyst (**n**) the overview image (**o**) once again demonstrates the profound arachnoid changes due to the first operation in the left half of the exposure compared to the 'virgin' area on the right. (*Continuation see next page*)

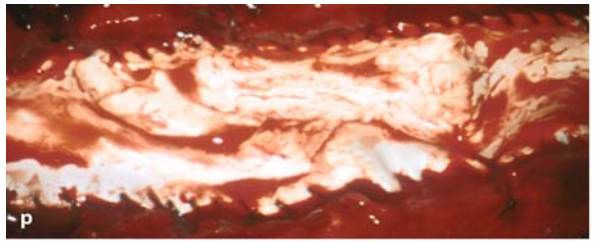

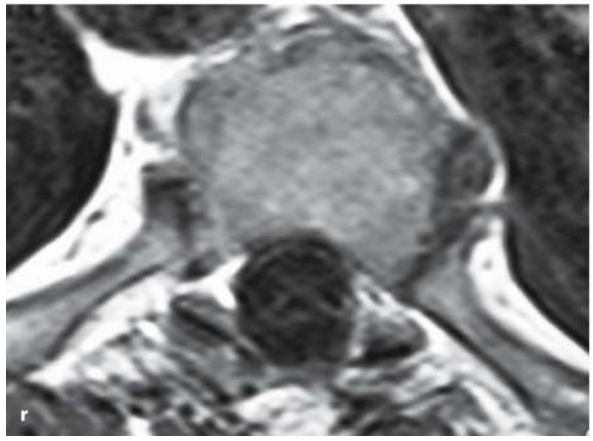

Fig. 4.34. (*Continued*) **p** To avoid postoperative tethering of the spinal cord, the dura is closed with a Gore-Tex® graft. The postoperative sagittal (**q**) and axial (**r**) T1-weighted MRI shows a good decompression of the spinal cord, no syrinx, and a free CSF passage in the area of surgery. There is no evidence of postoperative tethering. The walking ability of this patient improved postoperatively; he now uses his wheelchair only for longer distances. He has been free of a recurrence for 3 years

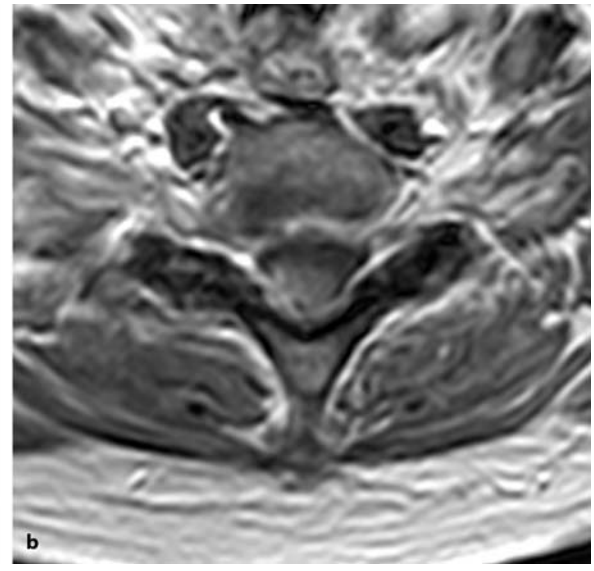

Fig. 4.35. Sagittal (**a**) and axial (**b**) T1-weighted, contrast-enhanced MRI scan of a posterior meningioma at C7–Th1 in a 72-year-old woman with a 2-year history of pain and slight gait ataxia. **c** The intraoperative ultrasound shows the tumor (*white arrowhead*) and the compressed spinal cord (*black arrowheads*). The intraoperative views after dura (**d**) and arachnoid opening (**e**) display the well-encapsulated tumor. After coagulation of the capsule (**f**), the intracapsular tumor removal can be performed (**g**). In this case, the tumor could be peeled out of the capsule with ease. Finally, the dura attachment on the inner dura layer is mobilized (**h**) and resected (**i**). **j** This final view depicts the situation after radical resection of the tumor. The postoperative T1-weighted MRI scans (**k**, **l**) demonstrate no tumor remnant, but also a small hypodense lesion in the cord due to the long-standing compression by the tumor. Pain improved postoperatively with the gait ataxia left unchanged (*Continuation see next page*)

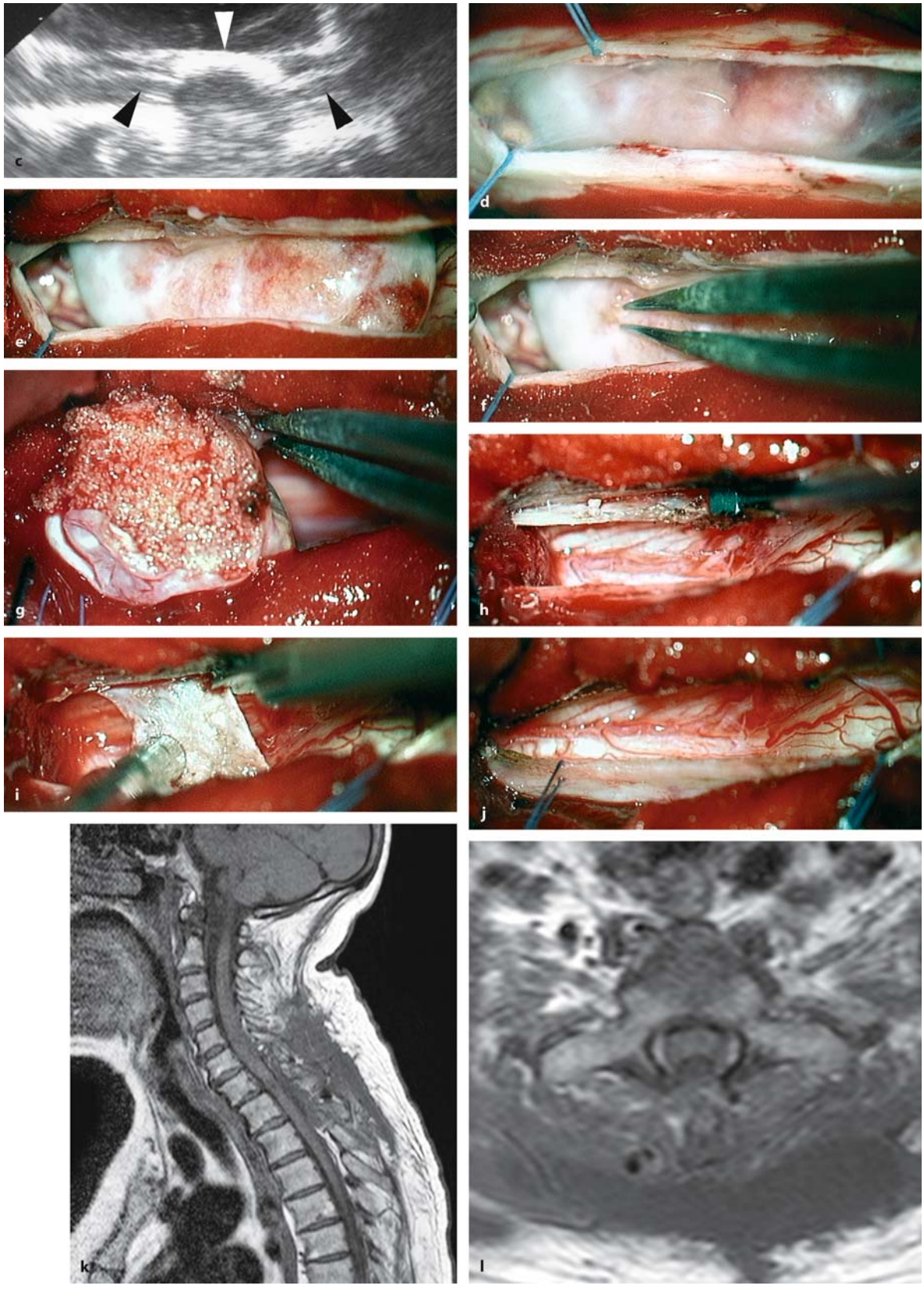

Fig. 4.35. (*Continued*)

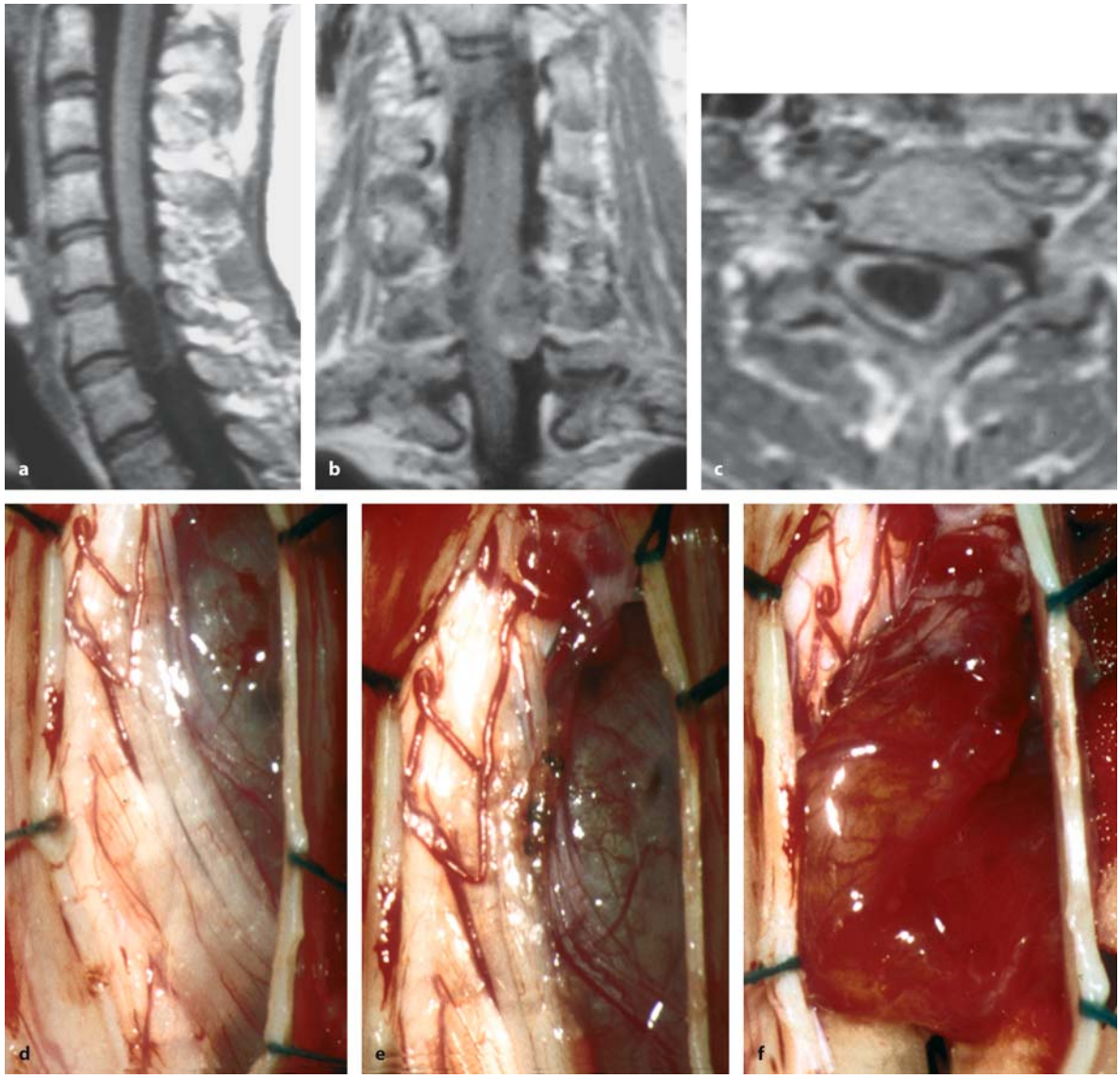

Fig. 4.36. Sagittal T1-weighted MRI scan without (**a**), and coronal (**b**) and axial (**c**) T1-weighted scans with contrast of a cystic schwannoma at C6–C7 on the right side in a 47-year-old woman with a 6-month history of pain in her right arm. **d** This intraoperative view in the semisitting position after dura and arachnoid opening shows the tumor underneath the posterior nerve root. After mobilization of these roots (**e**), the tumor could be incised, decompressed, and mobilized (**f**). (*Continuation see next page*)

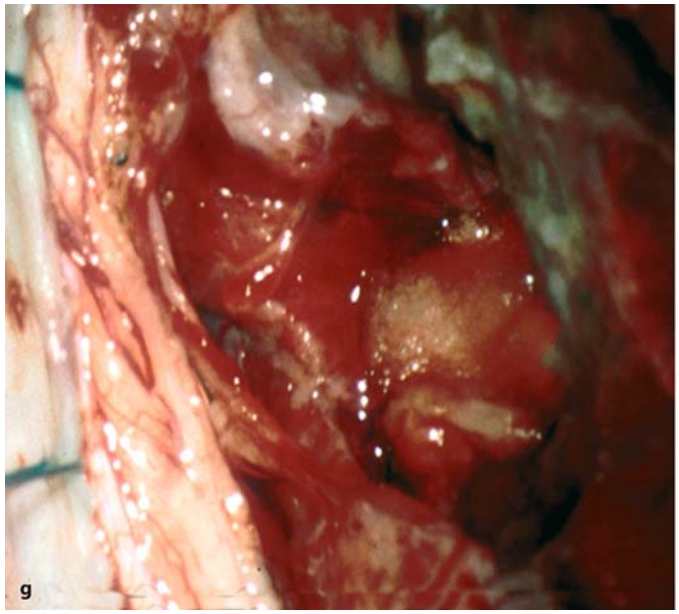

Fig. 4.36. g (*Continued*) The final intraoperative view demonstrates the situation in the dural sleeve toward the neuroforamen after resection of the tumor. The major part of the affected root could be preserved, achieving hemostasis with a small piece of Gelfoam. **h** The postoperative, contrast-enhanced, T1-weighted MRI demonstrates no tumor remnant. The patient's symptoms remained unchanged postoperatively and there has been no recurrence for 4 years

is still intact, the subarachnoid space can be checked for arachnoid changes, and the relationship between the tumor and arachnoid membrane can be evaluated. Normally, the arachnoid membrane is attached loosely to the inner dura layer and can be separated from it bluntly with a microdissector (Figs. 4.34 and 4.35). In cases of trauma, inflammatory processes, long-standing compression, or after previous surgeries, however, the arachnoid membrane may be densely adherent to the inner dura layer, requiring sharp dissection to open the dura without tearing on the arachnoid (Fig. 4.34). Pulling on arachnoid scars should be avoided, as this will also put tension on the spinal cord and its feeding vessels, which may be embedded in them.

With posteriorly placed tumors, a midline incision is chosen (Fig. 4.35). The line of incision should be placed along the medial border of laterally placed tumors. In that way, the medial part of the dura can be left to cover and protect the spinal cord, which is displaced to the contralateral side by the neoplasm (Fig. 4.36). Depending upon the amount of lateral access needed, it may be advisable to suture the dura laterally to facet joints or the periosteum for a better lateral view. With anteriorly placed tumors, the incision is done in the midline. The dura is then retracted laterally with sutures on one side. In most cases anterior tumors can be managed without mobilizing the cord. The space provided by solid tumors is usually sufficient (Fig. 4.37). Alternatively, the spinal cord may be rotated, provided the exposure of the cord extends well above and below the tumor (Fig. 4.38). Sutures can be applied to the dentate ligaments or arachnoid membrane, fixing them toward the dura on the opposite side for this purpose (Fig. 4.38). Furthermore, the exposure can be modified to a posterolateral approach with removal of a pedicle and intervertebral joint [81], or to a lateral approach with removal of the lateral mass [248].

If the tumor extends extradurally along the spinal nerve sheath, the intervertebral foramen is enlarged (Fig. 4.39). In such a case, we follow the spinal dura laterally and remove the remaining bone with small rongeurs or a diamond drill to expose the extradural part of the tumor (Fig. 4.39). In the cervical area, care has to be taken to avoid injury to the vertebral artery. In selected cases, a three-dimensional reconstruction of a CT with contrast enhancement may be useful to demonstrate the tumor, vertebral artery, and bony structures in a single image (Fig. 4.39). If the tumor extends to or even beyond the intervertebral foramen, the dura incision is curved along the nerve root rather than using a T-type incision, which is notoriously difficult to close tightly (Fig. 4.39).

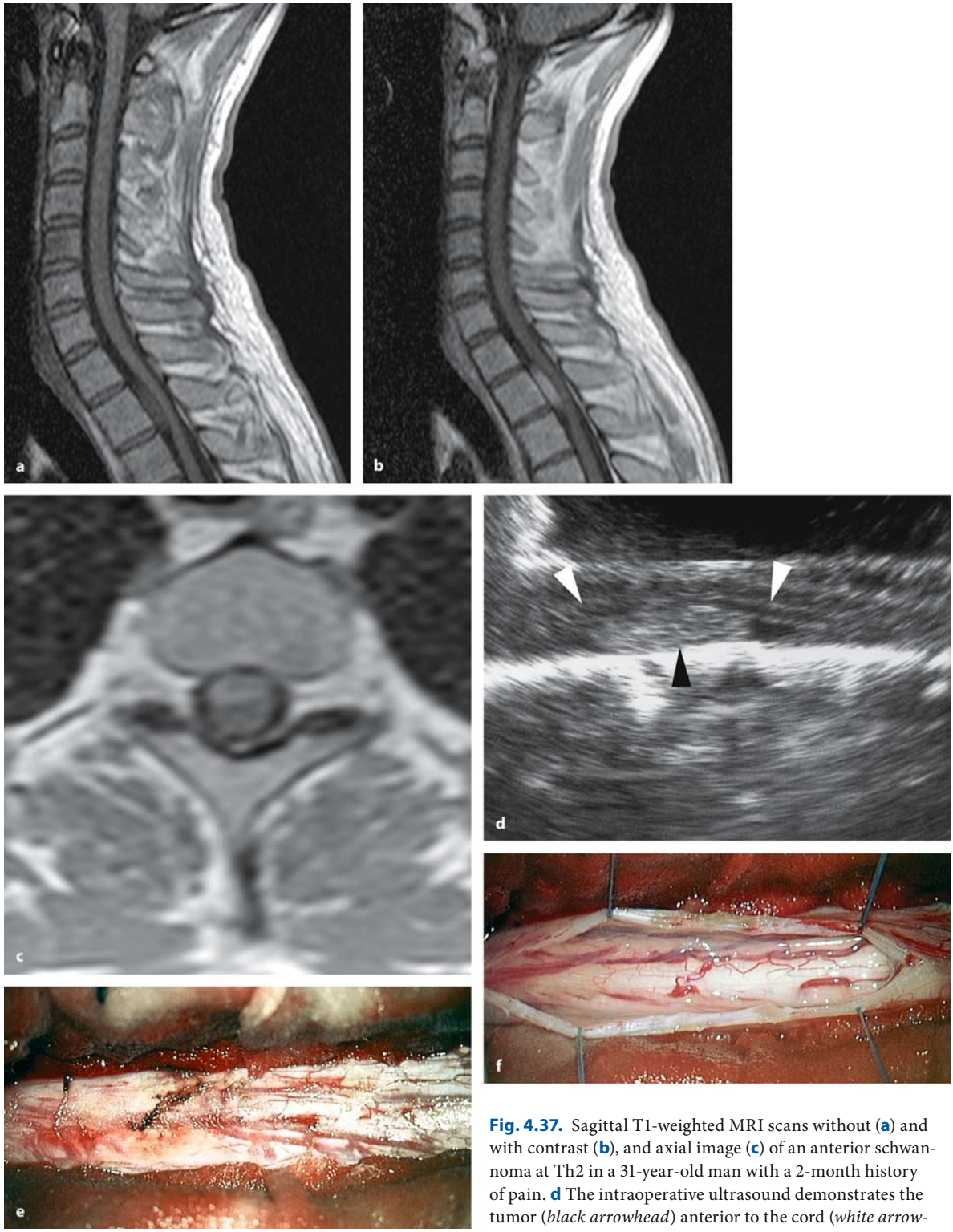

Fig. 4.37. Sagittal T1-weighted MRI scans without (**a**) and with contrast (**b**), and axial image (**c**) of an anterior schwannoma at Th2 in a 31-year-old man with a 2-month history of pain. **d** The intraoperative ultrasound demonstrates the tumor (*black arrowhead*) anterior to the cord (*white arrowheads*). The tumor moved with the pulsatile motion of CSF up and down in relation to the spinal cord (i.e., the tumor was not adherent to the anterior cord surface!). The approach to this tumor involved a standard laminotomy (**e**) and midline dura opening (**f**). (*Continuation see next page*)

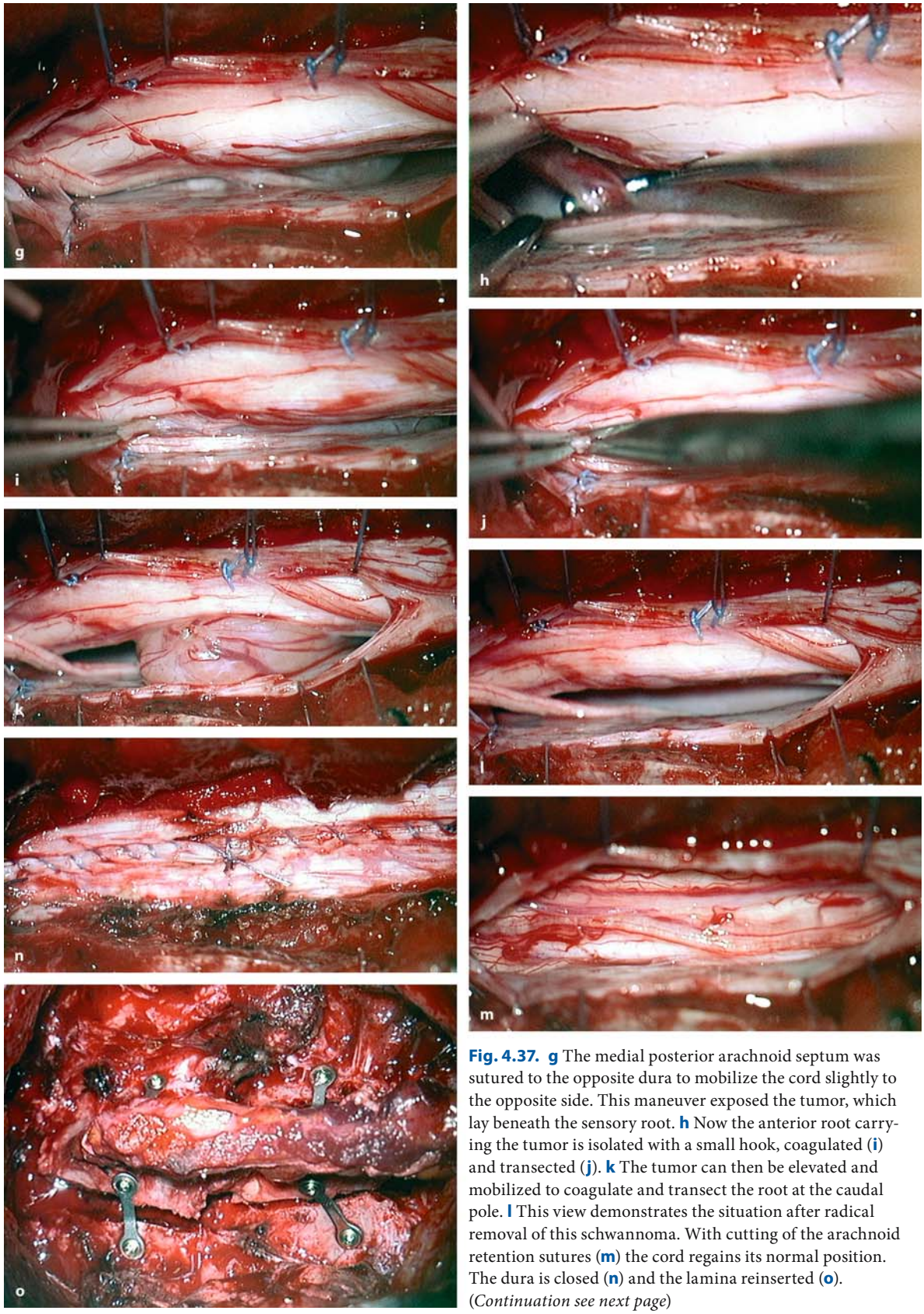

Fig. 4.37. **g** The medial posterior arachnoid septum was sutured to the opposite dura to mobilize the cord slightly to the opposite side. This maneuver exposed the tumor, which lay beneath the sensory root. **h** Now the anterior root carrying the tumor is isolated with a small hook, coagulated (**i**) and transected (**j**). **k** The tumor can then be elevated and mobilized to coagulate and transect the root at the caudal pole. **l** This view demonstrates the situation after radical removal of this schwannoma. With cutting of the arachnoid retention sutures (**m**) the cord regains its normal position. The dura is closed (**n**) and the lamina reinserted (**o**).
(*Continuation see next page*)

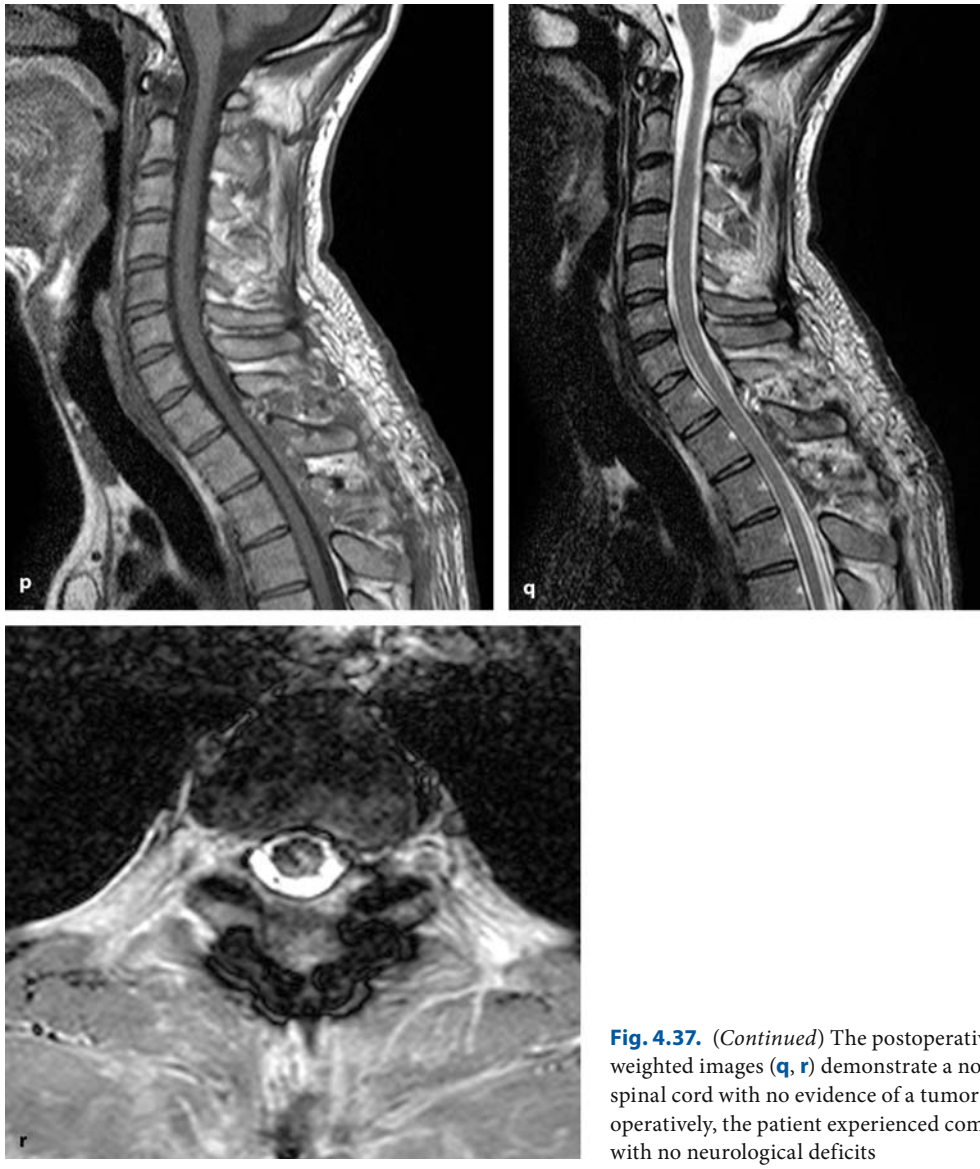

Fig. 4.37. (*Continued*) The postoperative T1- (**p**) and T2-weighted images (**q**, **r**) demonstrate a normal-appearing spinal cord with no evidence of a tumor remnant. Postoperatively, the patient experienced complete pain relief with no neurological deficits

4.3.1.1 Removal of Solid Tumors

Depending on the posterior, lateral, or anterior location of the tumor and its attachment to the dura, nerve roots, blood vessels, or filum terminale, mobilization of extramedullary tumors may apply pressure to the spinal cord and its vessels. As the first surgical step, solid tumors should be debulked (Figs. 4.32, 4.35 and 4.39) or cystic components evacuated (Figs. 4.36 and 4.37). With posterior and lateral tumors, at least part of the tumor is immediately visible after dura opening even without touching any nervous structure (Figs. 4.32, 4.35, 4.36, and 4.39). Once part of the tumor is removed or decompressed, further dissection can be performed to mobilize the remainder of the tumor away from the cord. In this way any pressure on the cord can be avoided.

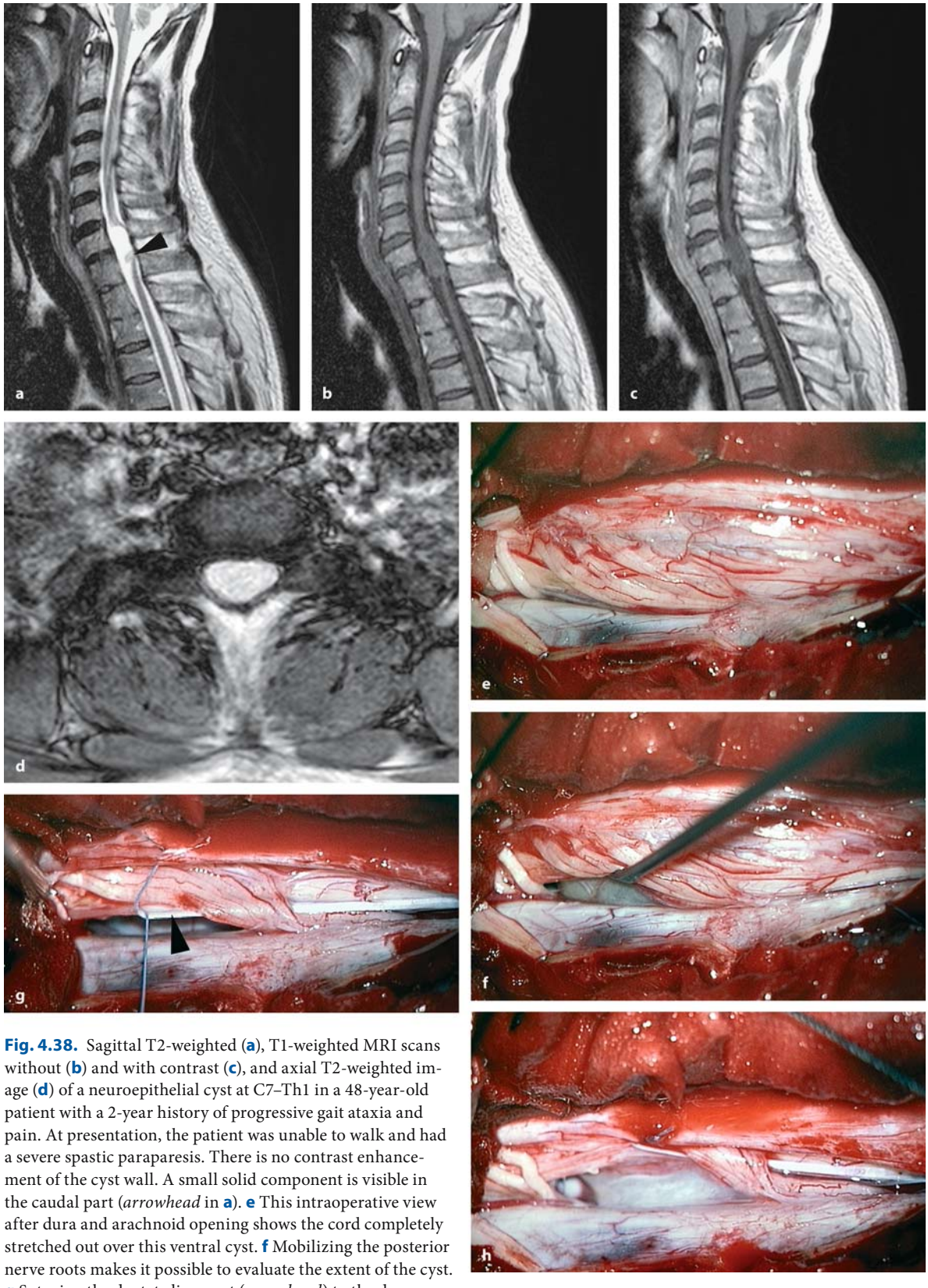

Fig. 4.38. Sagittal T2-weighted (**a**), T1-weighted MRI scans without (**b**) and with contrast (**c**), and axial T2-weighted image (**d**) of a neuroepithelial cyst at C7–Th1 in a 48-year-old patient with a 2-year history of progressive gait ataxia and pain. At presentation, the patient was unable to walk and had a severe spastic paraparesis. There is no contrast enhancement of the cyst wall. A small solid component is visible in the caudal part (*arrowhead* in **a**). **e** This intraoperative view after dura and arachnoid opening shows the cord completely stretched out over this ventral cyst. **f** Mobilizing the posterior nerve roots makes it possible to evaluate the extent of the cyst. **g** Suturing the dentate ligament (*arrowhead*) to the dura on the opposite side provides enough access (**h**). (*Continuation see next page*)

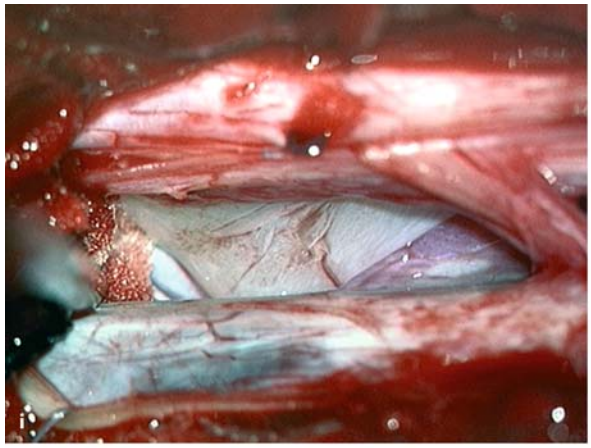

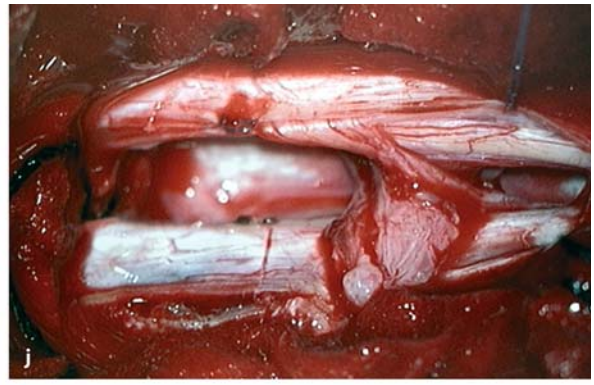

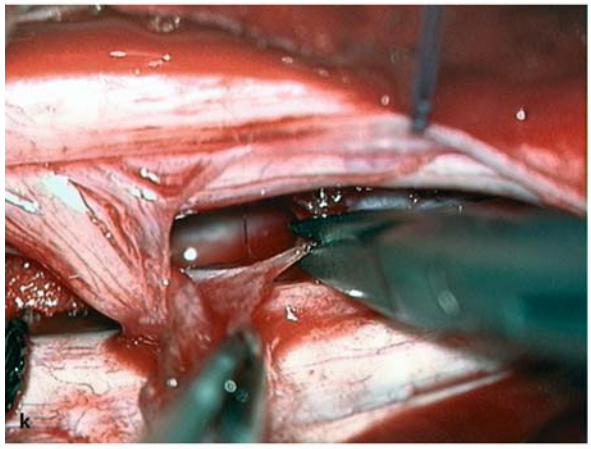

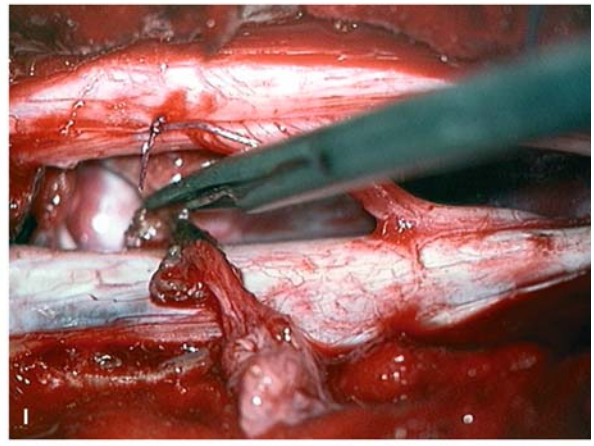

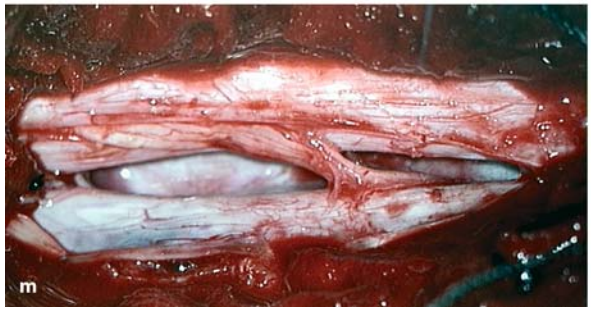

Fig. 4.38. After opening the cyst for decompression (**i**), the cyst wall can be dissected off the spinal cord surface with two fine forceps and mobilized laterally (**j**). The remaining attachments to the arachnoid membrane (**k**) and ventral nerve root (**l**) can be transected. **m** This final view shows the situation after complete resection of the cyst and removal of the dentate sutures. (*Continuation see next page*)

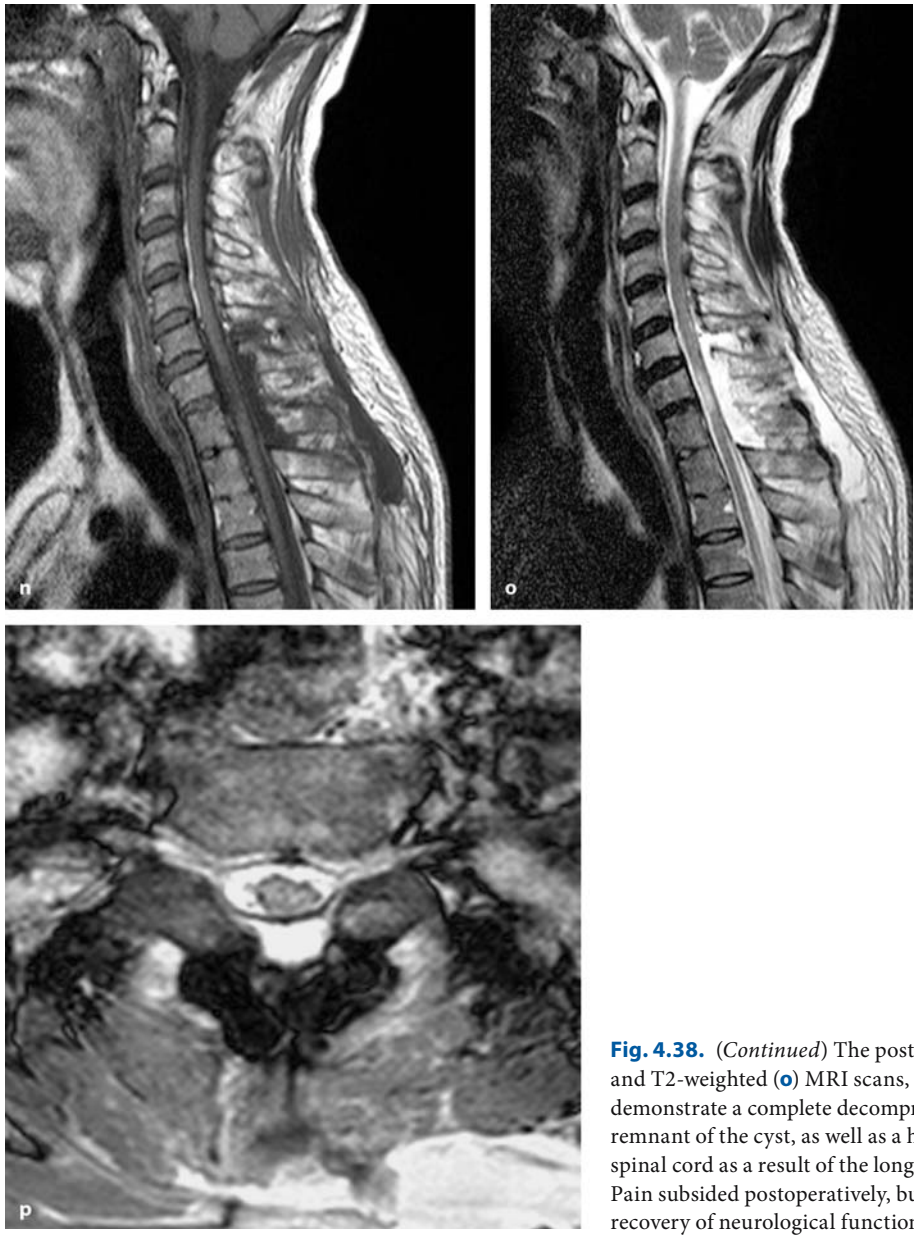

Fig. 4.38. (*Continued*) The postoperative sagittal T1- (**n**) and T2-weighted (**o**) MRI scans, and an axial T2-image (**p**) demonstrate a complete decompression of the cord with no remnant of the cyst, as well as a hypodense lesion in the spinal cord as a result of the long-standing compression. Pain subsided postoperatively, but there was only marginal recovery of neurological function

Fig. 4.39. Sagittal (**a**) and axial (**b**, **c**) T1-weighted, contrast-enhanced MRI scans of a dumbbell schwannoma at C4 in a 22-year-old patient with NF-2. **d** The tumor is growing along the right C4 nerve root out of the enlarged neuroforamen, as documented on this oblique X-ray (*arrowhead*). Above the level of the neuroforamen, the intra- and extradural part are separated by the dura (*arrowhead* in **b**). The posterior (**e**) and anterior (**f**) view of a three-dimensional CT reconstruction with contrast demonstrates the relationship to the vertebral artery, which is displaced medially but not narrowed or engulfed by tumor. (*Continuation see next page*)

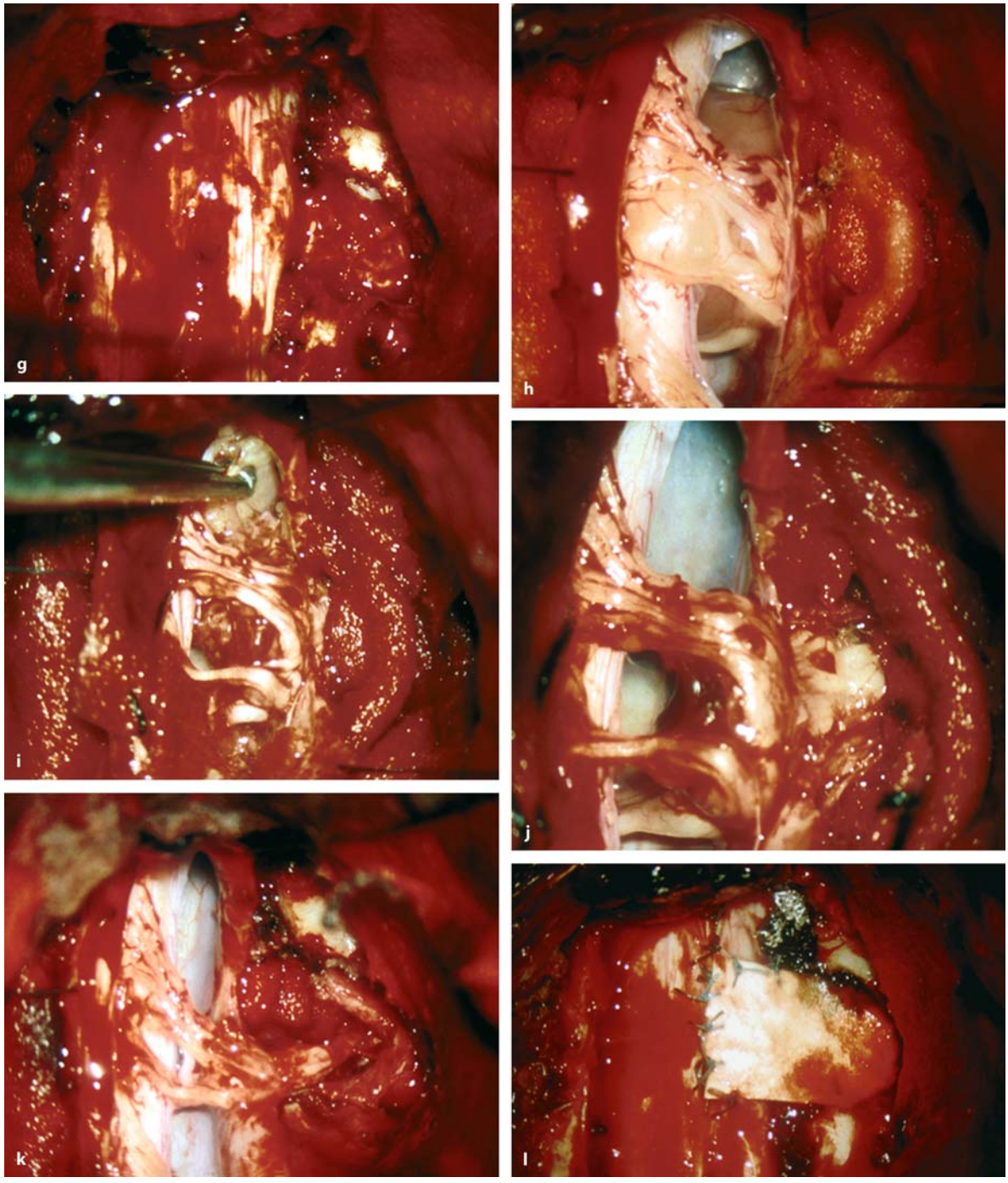

Fig. 4.39. (*Continued*) **g** This intraoperative view shows the dura exposure with the patient in the semisitting position with opening of the neuroforamen on the right side. **h** After dura and arachnoid opening the intradural tumor is visible between posterior and anterior roots. **i** With stepwise removal of the tumor, the intradural mass is resected, preserving both the anterior and posterior root. **j** Now the tumor can be followed and resected along the foramen. **k** After resection of the extradural part, preserving the nerve root, the extradural resection area is filled with Gelfoam. **l** The dura is closed with a small duraplasty. The patient experienced no neurological deficit from this operation and has experienced no recurrence for 5 years

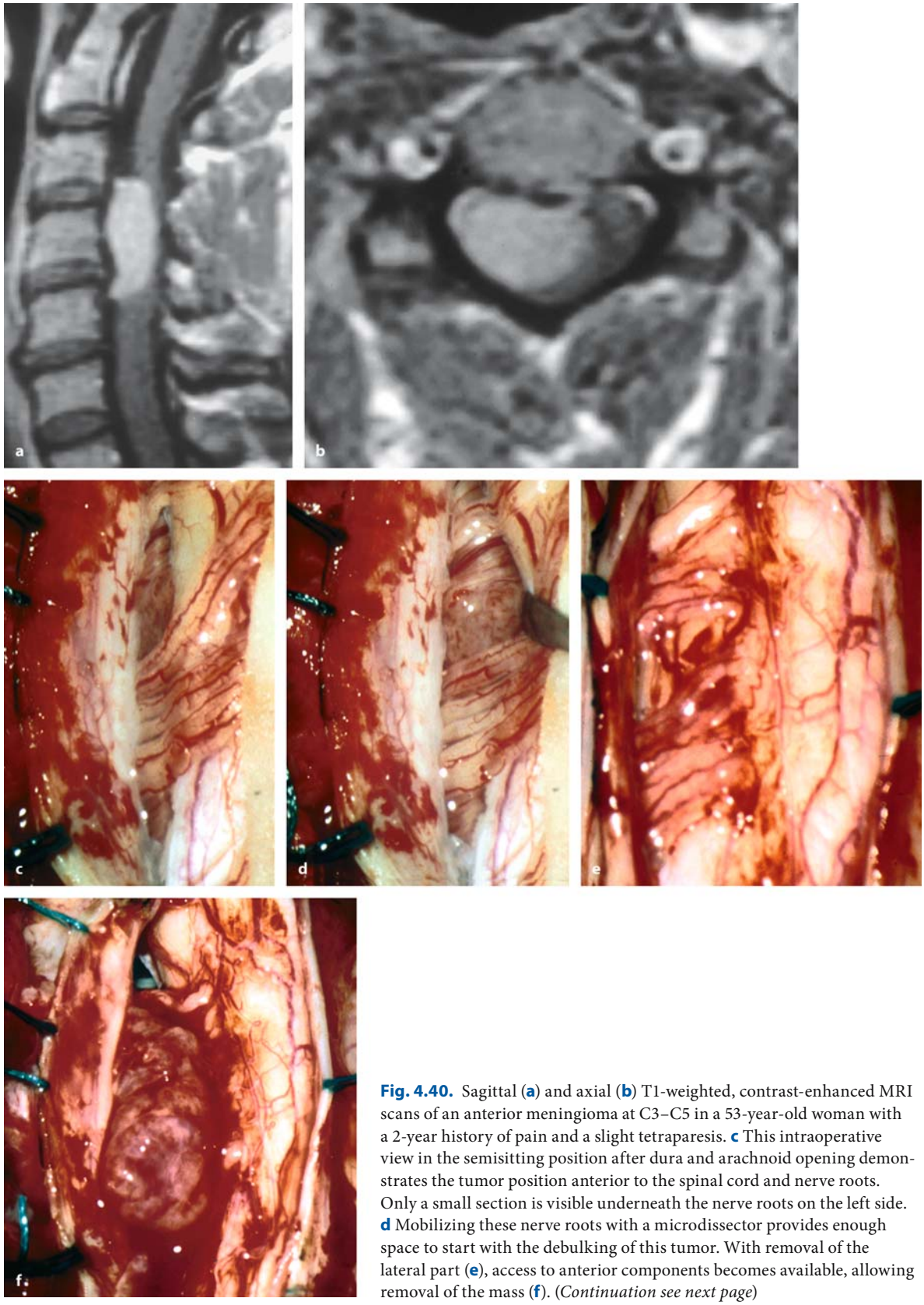

Fig. 4.40. Sagittal (**a**) and axial (**b**) T1-weighted, contrast-enhanced MRI scans of an anterior meningioma at C3–C5 in a 53-year-old woman with a 2-year history of pain and a slight tetraparesis. **c** This intraoperative view in the semisitting position after dura and arachnoid opening demonstrates the tumor position anterior to the spinal cord and nerve roots. Only a small section is visible underneath the nerve roots on the left side. **d** Mobilizing these nerve roots with a microdissector provides enough space to start with the debulking of this tumor. With removal of the lateral part (**e**), access to anterior components becomes available, allowing removal of the mass (**f**). (*Continuation see next page*)

With anterior cottonoids, lateral access as outlined above is the key to a safe removal. Anterior nerve sheath tumors can be mobilized and removed without much difficulty once the tumor is debulked or decompressed and the tumor carrying the nerve root transected (Fig. 4.37). Anterior meningiomas, however, cannot be mobilized until they are disconnected from their dura attachment (Fig. 4.40).

Extramedullary tumors in the cauda equina may also present specific problems. The numerous nerve roots in this area may cover the tumor completely. They may be attached to the tumor surface, may penetrate the tumor mass, or even be infiltrated. In general, it is advisable to dissect nerve roots off the tumor surface first and to push them gently aside with small cottonoids. In this way, slight suction on the cottonoids can remove some of the CSF, so that nerve roots no longer float into the surgical field, as well as blood during tumor removal avoiding direct contact with nerve roots (Fig. 4.41).

After debulking, it will no longer be difficult to remove the remainder of the tumor mass and capsule to decompress the spinal cord. For radicality, it is mandatory to finally deal with the tumor origin. Depending on the histology, extramedullary tumors are attached to the dura mater, nerve roots, filum terminale, or blood vessels.

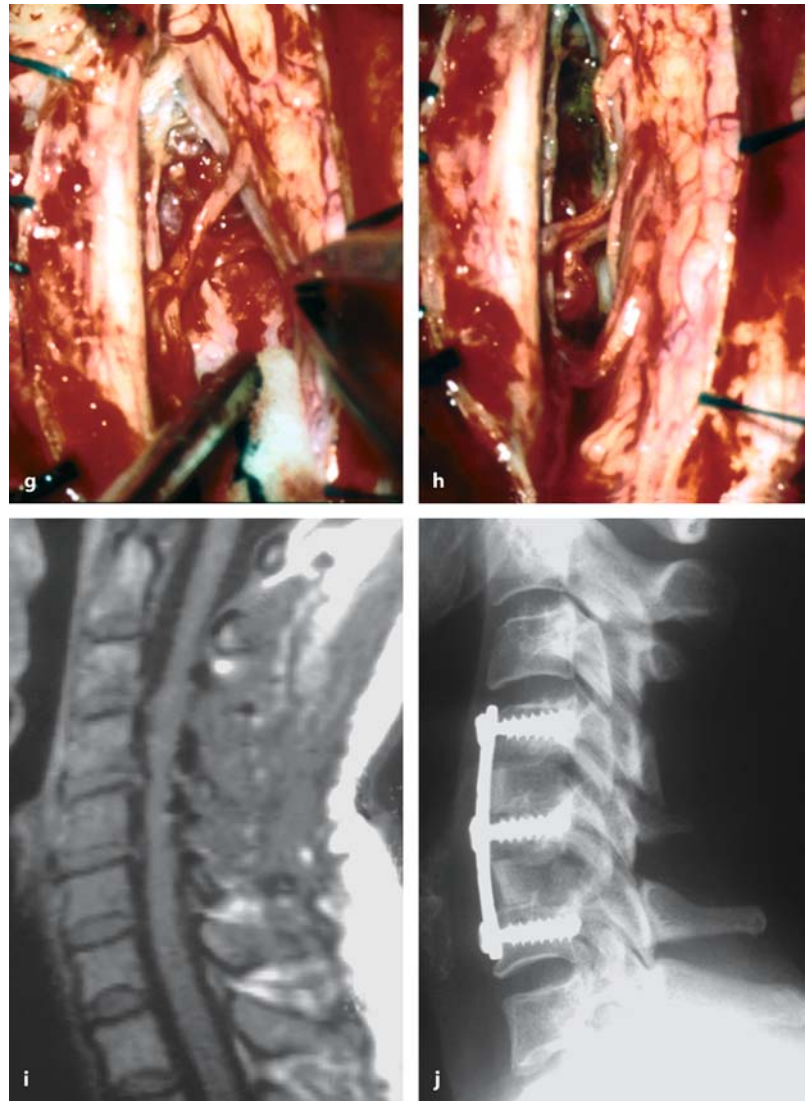

Fig. 4.40. (*Continued*) **g** With the tumor mass removed, the attachment area can be cauterized. **h** This view shows the situation after complete resection of this meningioma. **i** This postoperative T1-weighted MRI scan shows no evidence of a tumor remnant. The patient has been free of a recurrence for 8 years but required a ventral fusion for degenerative disc disease at C4–C6 2 years after this operation (**j**)

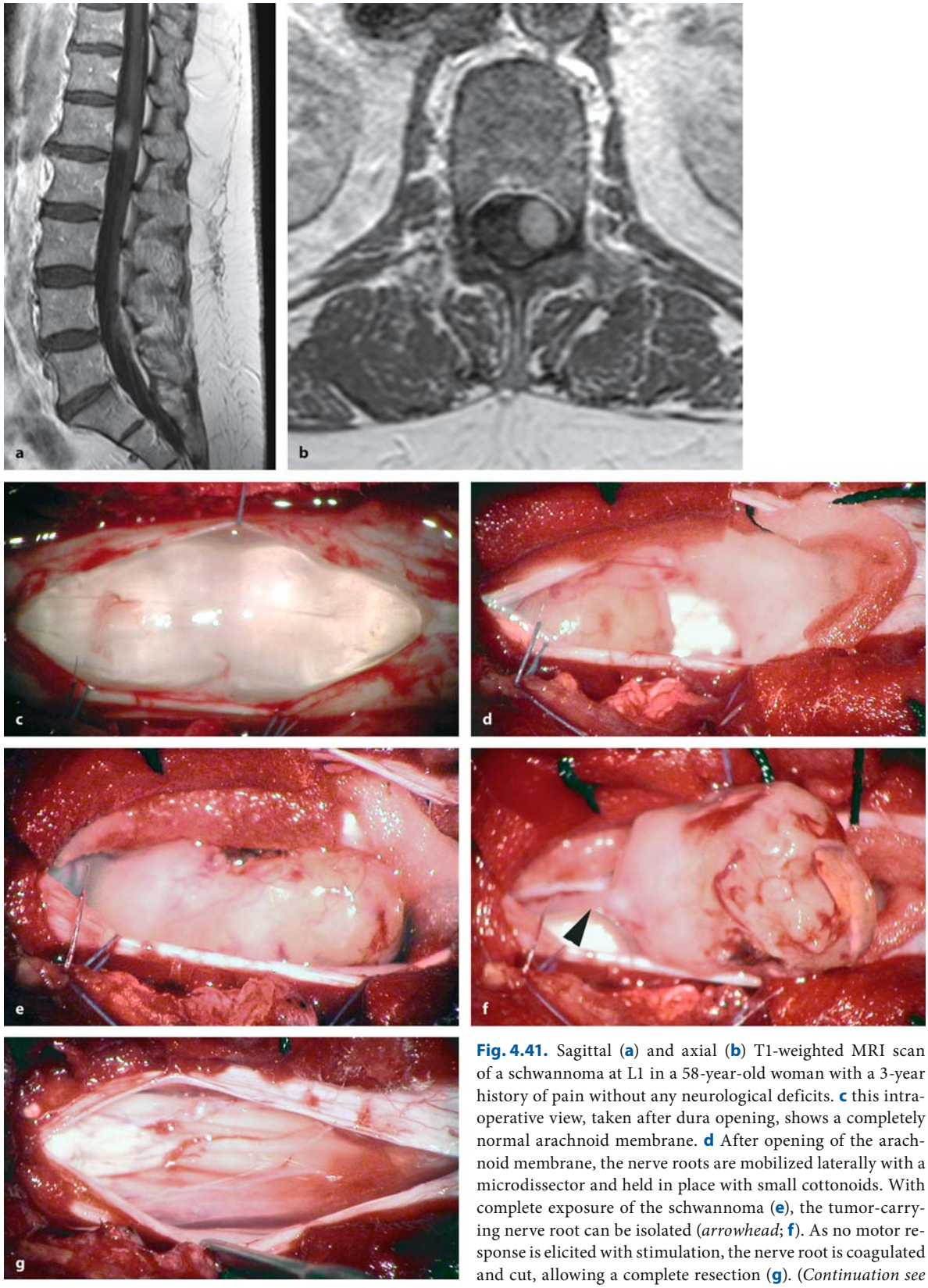

Fig. 4.41. Sagittal (**a**) and axial (**b**) T1-weighted MRI scan of a schwannoma at L1 in a 58-year-old woman with a 3-year history of pain without any neurological deficits. **c** this intraoperative view, taken after dura opening, shows a completely normal arachnoid membrane. **d** After opening of the arachnoid membrane, the nerve roots are mobilized laterally with a microdissector and held in place with small cottonoids. With complete exposure of the schwannoma (**e**), the tumor-carrying nerve root can be isolated (*arrowhead*; **f**). As no motor response is elicited with stimulation, the nerve root is coagulated and cut, allowing a complete resection (**g**). (*Continuation see next page*)

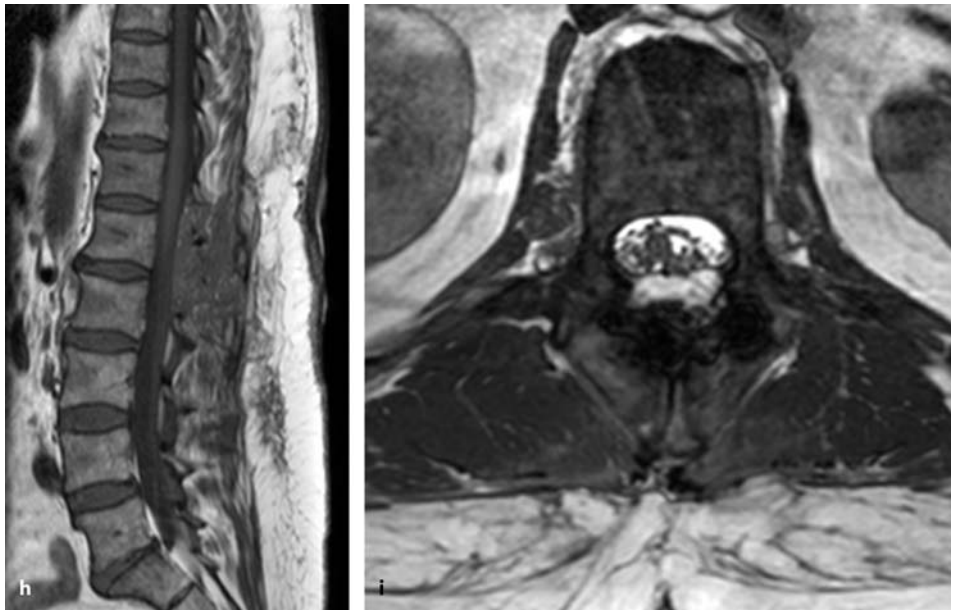

Fig. 4.41. (*Continued*) The postoperative T1-weighted sagittal (**h**) and the T2-weighted axial (**i**) MRI scans demonstrate a complete resection. Postoperatively, no neurological deficits were present and pain improved

4.3.1.1.1 Removal of Meningiomas

The consistency of a spinal meningioma is quite variable. Most of them can be shrunk with bipolar coagulation, debulked, and removed in a piecemeal fashion with tumor forceps. With encapsulated tumors, no pial invasions into the spinal cord are present (Figs. 4.32, 4.35, 4.40, and 4.42) [227]. Even without any adherence to the spinal cord, meningiomas cannot be mobilized until the tumor mass is disconnected from the dura attachment zone. Therefore, the preoperative axial MRI should be studied carefully: the meningioma will compress and displace the spinal cord according to its direction of expansion (i.e., away from the attachment zone). Therefore, the position of the cord will be directly opposite to the attachment zone. The approach and direction of dissection should account for this: the tumor should be dissected away from the cord toward the attachment area (i.e., in the opposite direction of its growth).

However, some tumors such as infiltrating, en plaque growing meningiomas may be densely adherent to the cord, even infiltrate it or recruit some of their blood supply from pial vessels [29]. These tumors have to be dissected sharply off the spinal cord and may not be completely resectable (Fig. 4.43) [29].

Calcified meningiomas pose another problem, as conventional debulking may not be possible [76]. We have used small Kerrison rongeurs or tumor forceps for this purpose (Fig. 4.44). With calcified anterior meningiomas, a direct anterior approach may be required if the tumor cannot be delivered safely from posterior.

Once the tumor mass is resected, radicality demands removal of the dura attachment zone. If the attachment is posterior to the dentate ligament, it can be resected easily and reconstructed with a duraplasty (Fig. 4.44). An alternative strategy leaves the outer dura layer intact and removes just the inner dura layer with the attachment zone, thus avoiding a duraplasty (Figs. 4.32 and 4.35). In particular, for anteriorly placed tumors and attachment zones in the dural sleeve along the nerve root, this area may be coagulated (Figs. 4.40 and 4.42).

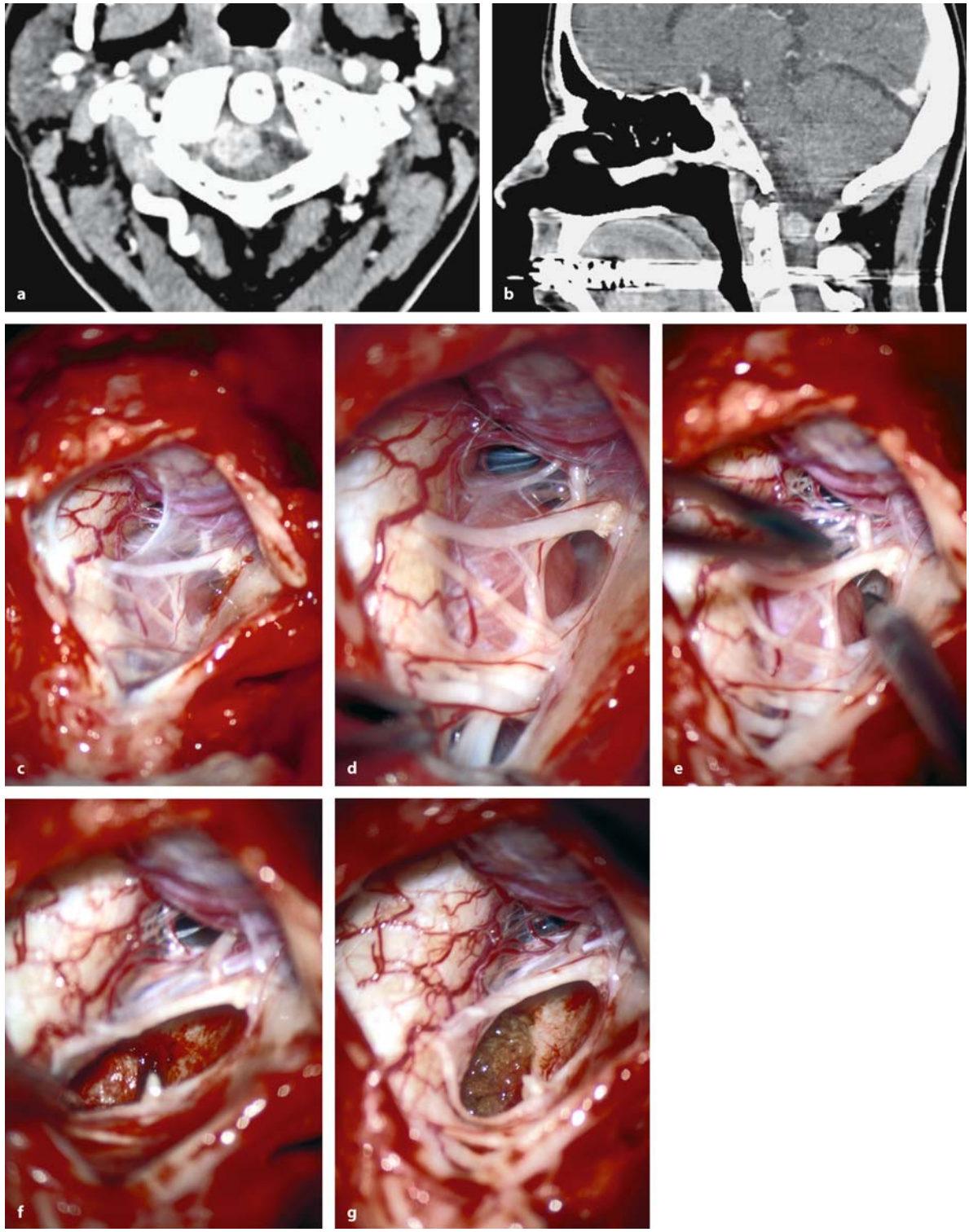

Fig. 4.42. Axial (**a**) and sagittal reconstruction (**b**) of contrast-enhanced CT scans of an anterior meningioma at C1–C2 with displacement of the spinal cord to the left in a 56-year-old woman with a 3-month history of sensory changes in her right arm. **c** This intraoperative view, taken from a posterolateral approach on the right, demonstrates the tumor after mediolateral dura incision. **d** After arachnoid membrane dissection, the tumor appears well encapsulated behind the C2 nerve root. Disconnection of the tumor from the attachment zone (**e**) allowed resection of the tumor mass (**f**). **g** This final view demonstrates a complete resection with coagulation of the attachment area, which is covered with fibrin tissue. (*Continuation see next page*)

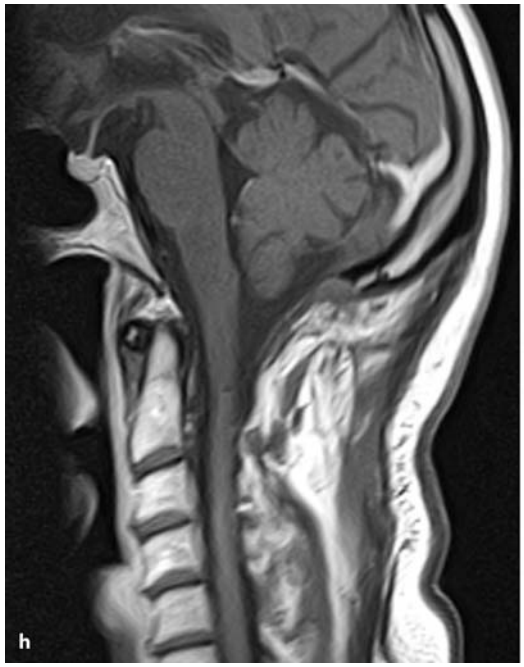

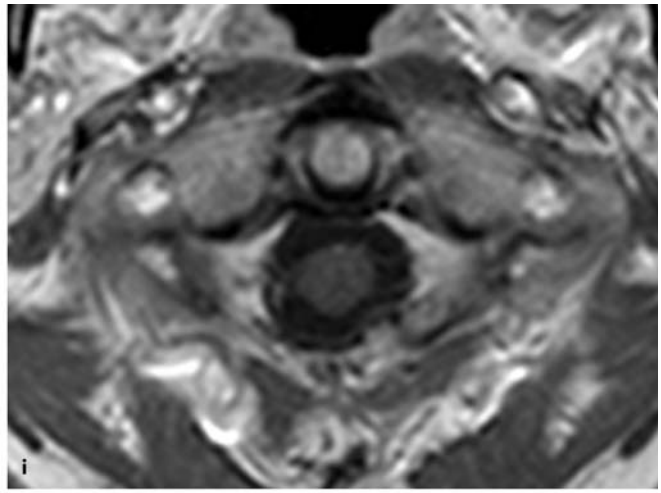

Fig. 4.42. (*Continued*) The patient's sensory changes improved postoperatively, and has been free of a recurrence for 1 year, as demonstrated on these contrast-enhanced sagittal (**h**) and axial (**i**) MRI scans

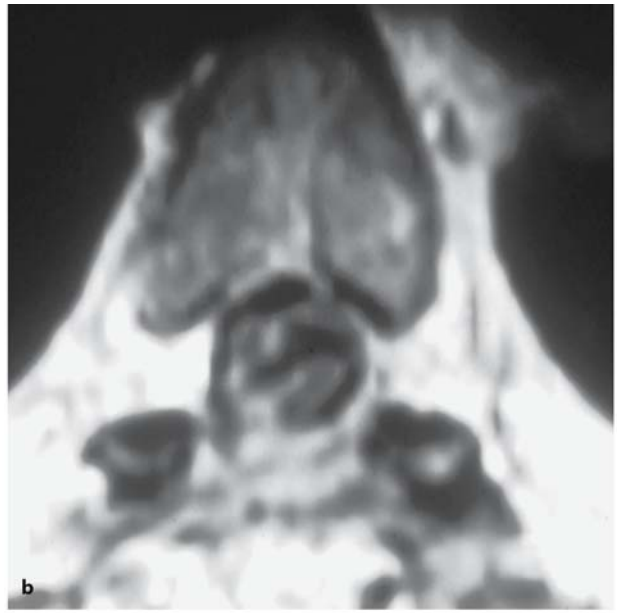

Fig. 4.43. Sagittal (**a**) and axial (**b**) T1-weighted, contrast-enhanced MRI scans of a recurrent, en plaque growing meningioma at Th1–Th3 in a 58-year-old woman with a 1-year history of pain and a moderate paraparesis. The tumor encircles the cord almost completely. (*Continuation see next page*)

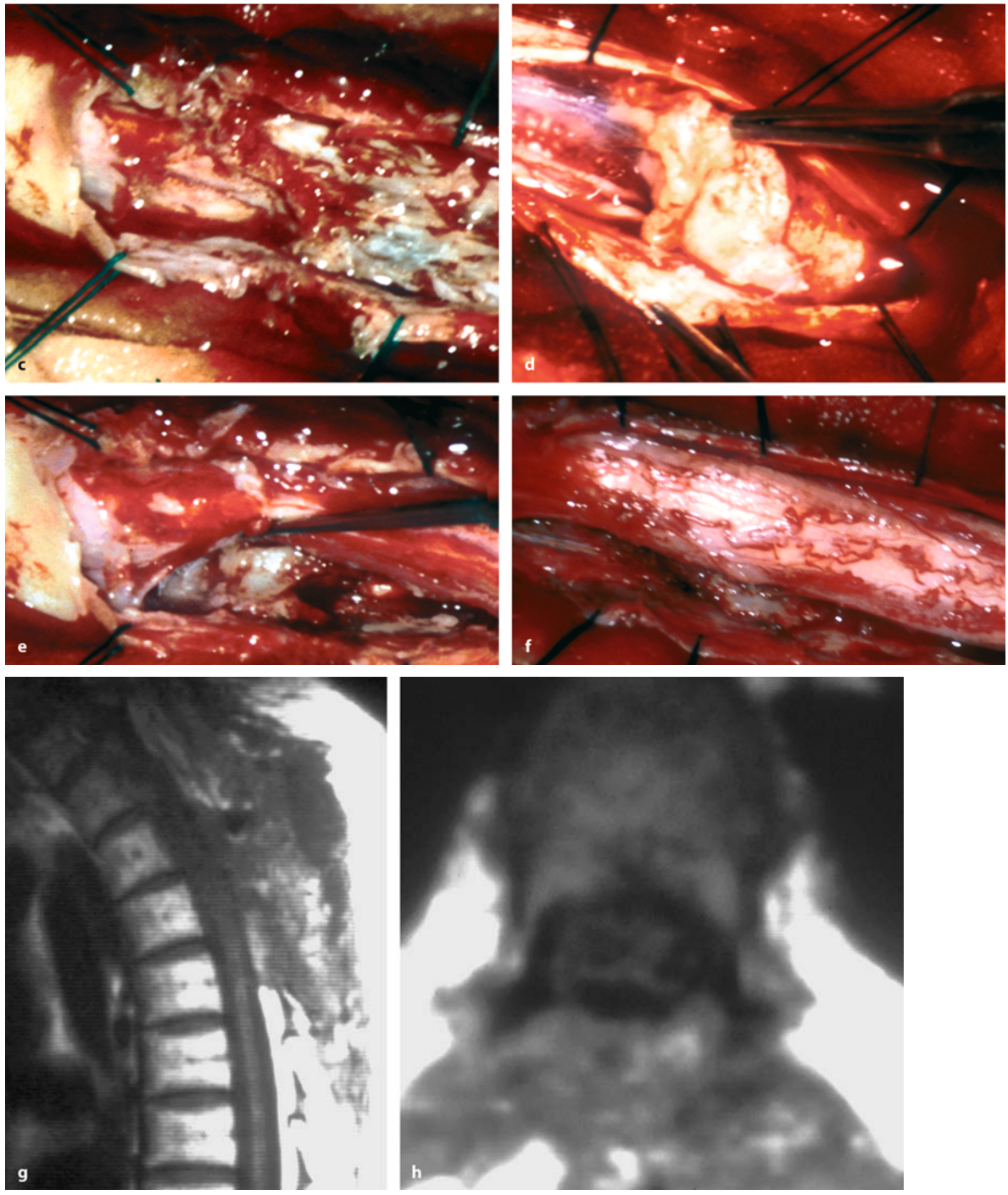

Fig. 4.43. (*Continued*) **c** The intraoperative view after dura opening demonstrates scarring of the arachnoid membrane and the ill-defined limitation of the tumor. **d** Sections of the posterior tumor were calcified and had to be taken out with small rongeurs. **e** Some of the anterior parts were left in place as a removal would have been too risky. **f** This final view shows the decompressed cord with no tumor posteriorly and laterally. The sagittal (**g**) and axial (**h**) T1-weighted MRI scans demonstrate a good decompression of the cord. Pain improved postoperatively; however, the paraparesis remained unaltered. A recurrence occurred 1 year later followed by another operation and a further recurrence after 8 months. At that stage the patient was wheelchair dependent and refused to undergo another operation

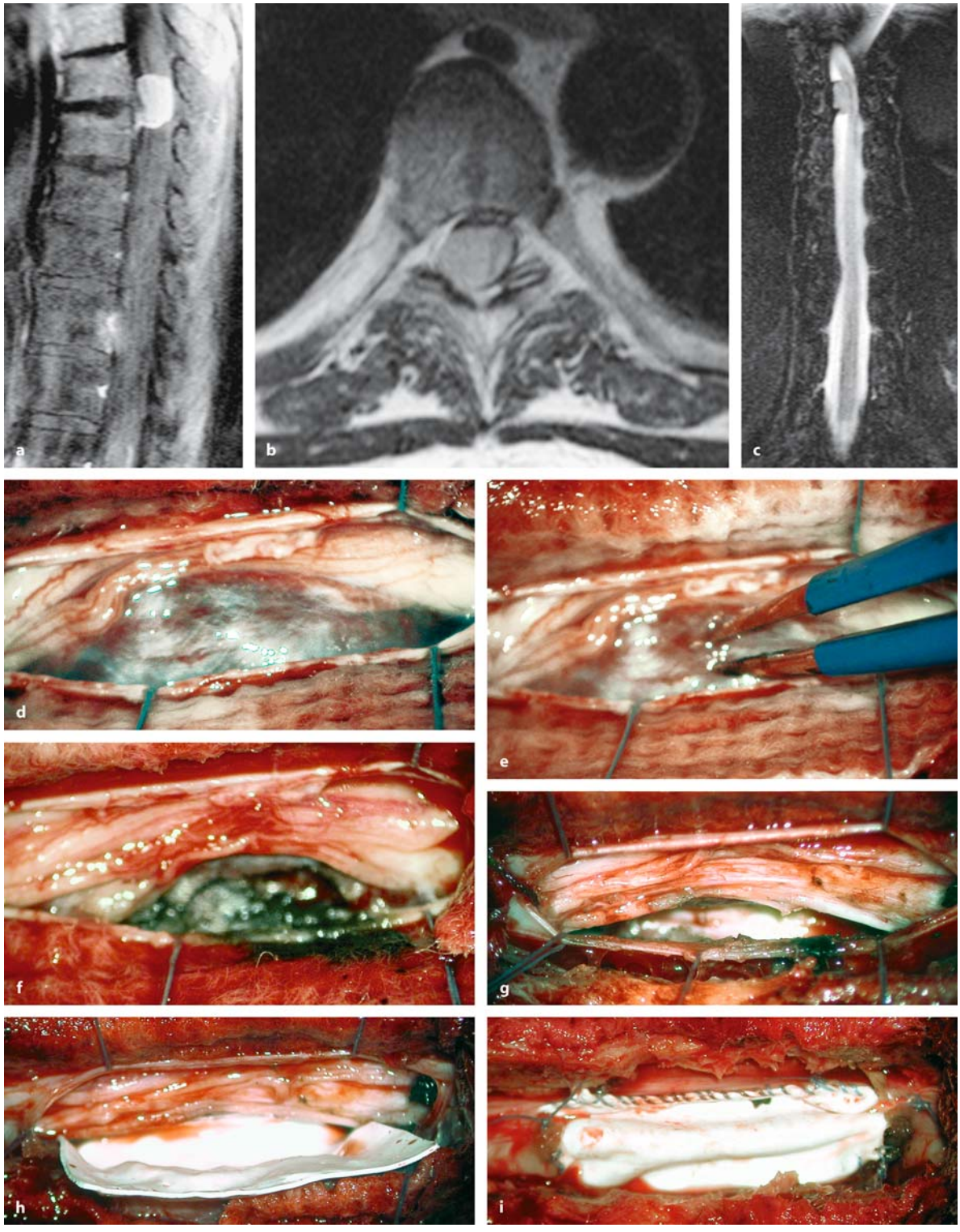

Fig. 4.44. Sagittal (**a**) and axial (**b**) T1-weighted, contrast-enhanced MRI scans of a meningioma at Th6–Th7 in a 65-year-old woman with a 2-year history of pain and progressive paraparesis. **c** This coronal T2-weighted scan indicates the tumor position on the left side of the cord. **d** This intraoperative view, taken after dura opening, shows the tumor compressing the cord to the right. After coagulation of the capsule (**e**), the tumor could be debulked with tumor forceps (**f**). **g** After removal of the tumor mass, the lateral attachment zone remains to be resected. After dura resection on the left, a Gore-Tex® patch is placed anterolaterally (**h**) and sutured to the dura medially with a running suture (**i**). (*Continuation see next page*)

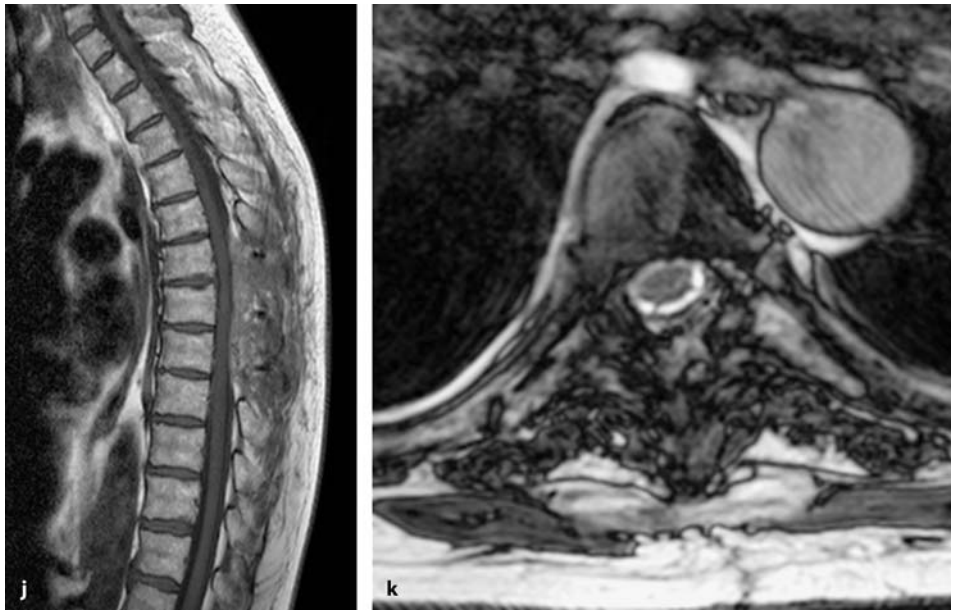

Fig. 4.44. (*Continued*) The postoperative T1-weighted, contrast-enhanced MRI (**j**) and the T2-weighted axial image (**k**) show no tumor recurrence or cord tethering 1 year postoperatively. The patient's symptoms recovered completely except for a slight sensory loss in her left leg

4.3.1.1.2 Removal of Nerve Sheath Tumors

Nerve sheath tumors (i.e. schwannomas and neurofibromas) may be cystic or solid. Neurofibromas contain more fibrous tissue and tend to be tougher. As these tumors originate from nerve roots, they are almost always located lateral of the cord and can be debulked from a standard laminotomy or hemilaminectomy (Fig. 4.36). However, anterior (Fig. 4.37) and extensive schwannomas reaching over several spinal segments (Fig. 4.45) do occur. Radicality requires resection of the affected nerve sheath only. It is not necessary to resect the entire nerve root. Even though most schwannomas originate from sensory nerve roots [33], we recommend preservation of the tumor-carrying nerve root whenever it appears to be normal on inspection and/or a motor response is elicitable on direct stimulation (Fig. 4.36). In other patients it may be possible to preserve most of the rootlets (Fig. 4.46). In patients with no motor response on direct stimulation, the root is usually resected together with the tumor (Figs. 4.37, 4.41, and 4.45). In patients with NF type 2 (NF-2), a more conservative approach is generally taken and the tumor-carrying root is preserved in most instances (Fig. 4.39). On the other hand, one should take care to resect the entire tumor capsule, as neuropathological examinations have shown it to contain tumor tissue [104].

With intradural schwannomas that show extradural extension (i.e. dumbbell-tumors), the intradural part is removed before the extradural part is dissected (Figs. 4.39 and 4.47) [120]. Here, the tumorous nerve sheath is located in close proximity to or in the neuroforamen itself. Motor and sensory fibers are compressed in this very confined space. All fascicles may be jammed together to such a degree that it becomes impossible to single out the tumor-originating nerve sheath (Figs. 4.39 and 4.47). With dumbbell tumors of the thoracic spine, the decision to resect the affected root together with the tumor will have no significant functional consequences [204]. However, in the cervical or lumbar spine, preservation of nerve root function is an essential requirement, especially for patients with NF-2. Another problem that may be encountered with dumbbell tumors of the cervical spine is displacement, encasement, or even occlusion of the vertebral artery (Figs. 4.39 and 4.47).

With intraoperative stimulation, the motor and sensory response can be tested. Only if no response is elicitable should radical excision with removal of the root be performed (Fig. 4.47). Otherwise, the tumor should be debulked and – if in doubt – the risk of leaving small remnants on a functioning nerve root should be taken if further dissection appears too risky, especially in patients with NF-2 (Fig. 4.39).

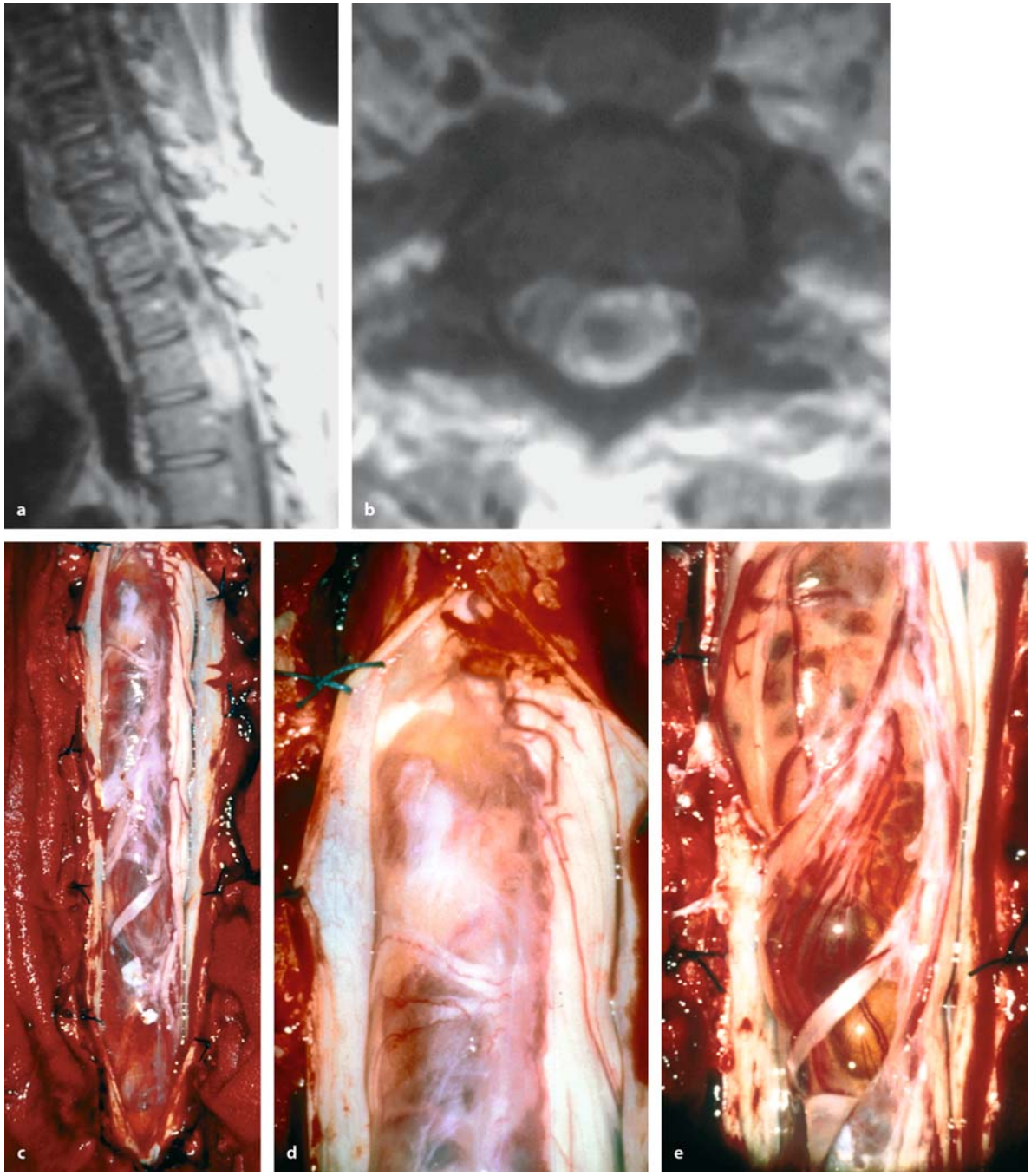

Fig. 4.45. Sagittal (**a**) and axial (**b**) T1-weighted, contrast-enhanced MRI scans of a partly cystic schwannoma at C6–Th4 in a 65-year-old man with a 10-year history of pain in his left arm, shoulder, and upper trunk, and recent development of a moderate tetraparesis. **c** Intraoperative view taken with the patient in the semisitting position after dura and arachnoid opening, displaying this extensive tumor on the left side. Posterior roots can be seen on the surface of this tumor. These detailed views demonstrate the upper (**d**) and lower (**e**) tumor poles. (*Continuation see next page*)

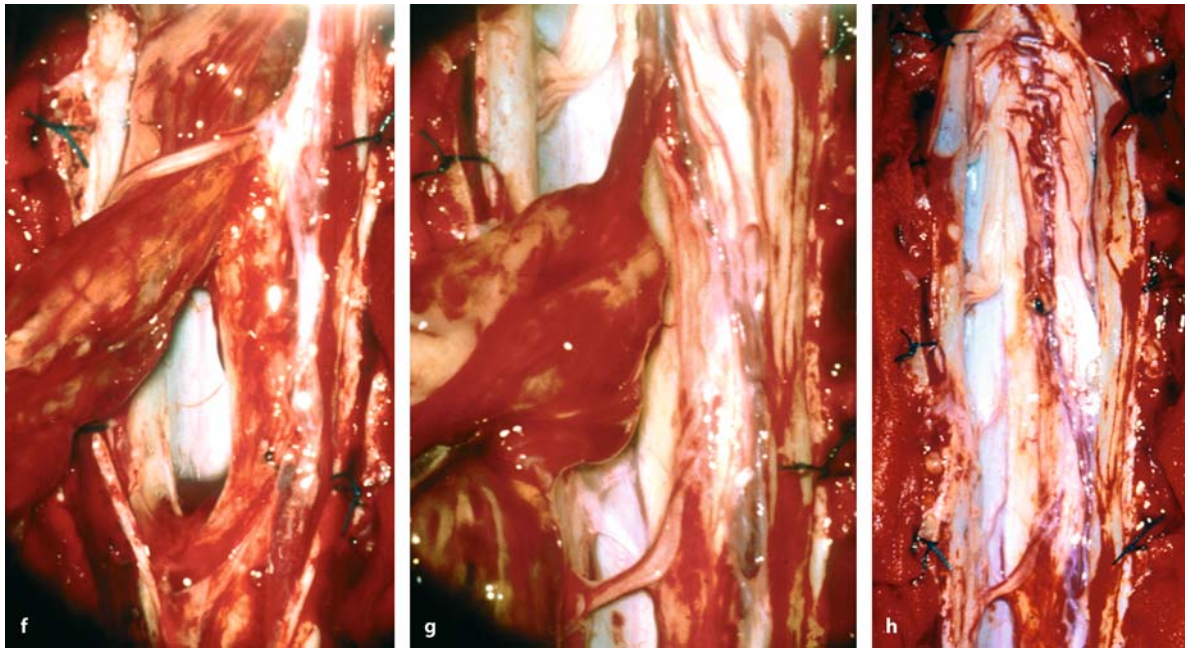

Fig. 4.45. (*Continued*) **f** Starting from the lower pole, the tumor could be easily separated from posterior and anterior nerve roots and spinal cord with microdissectors and small tumor forceps. The tumor had expanded between anterior and posterior roots and could be mobilized in this fashion from one spinal segment to the next. **g** Finally, the tumor carrying nerve root could be isolated and transected. **h** This final picture demonstrates the situation after complete resection of this tumor. The spinal cord has taken its normal position again. Postoperatively, neurological symptoms and pain improved

For radicality, not only the handling of the nerve root in the neuroforamen is critical, but also an adequate exposure of the extradural or even extraspinal extension of the tumor. Sometimes the extraspinal component may reach tremendous proportions, requiring a separate operation from an anterior approach.

4.3.1.1.3 Removal of Ependymomas

Extramedullary ependymomas are almost always found in the lumbar and sacral region. They may grow to enormous sizes, filling out the entire lumbar and sacral subarachnoid space (Fig. 4.18). Due to the significant risk of subarachnoid seeding, extramedullary ependymomas should be resected in toto whenever possible, together with the filum terminale (Fig. 4.48) [204]. If debulking is required, this can be performed safely with well-encapsulated ependymomas, covering the surrounding surgical field with cottonoids and applying suction to avoid contamination of the subarachnoid space with tumor cells (Fig. 4.49). Without a surrounding capsule, ependymomas tend to infiltrate nerve roots, making it much more difficult to achieve a complete resection without damaging important roots (Fig. 4.50). Care has to be taken to avoid injury of the conus. The conus may be displaced and twisted, depending on the growth directions the ependymoma has taken (Fig. 4.49).

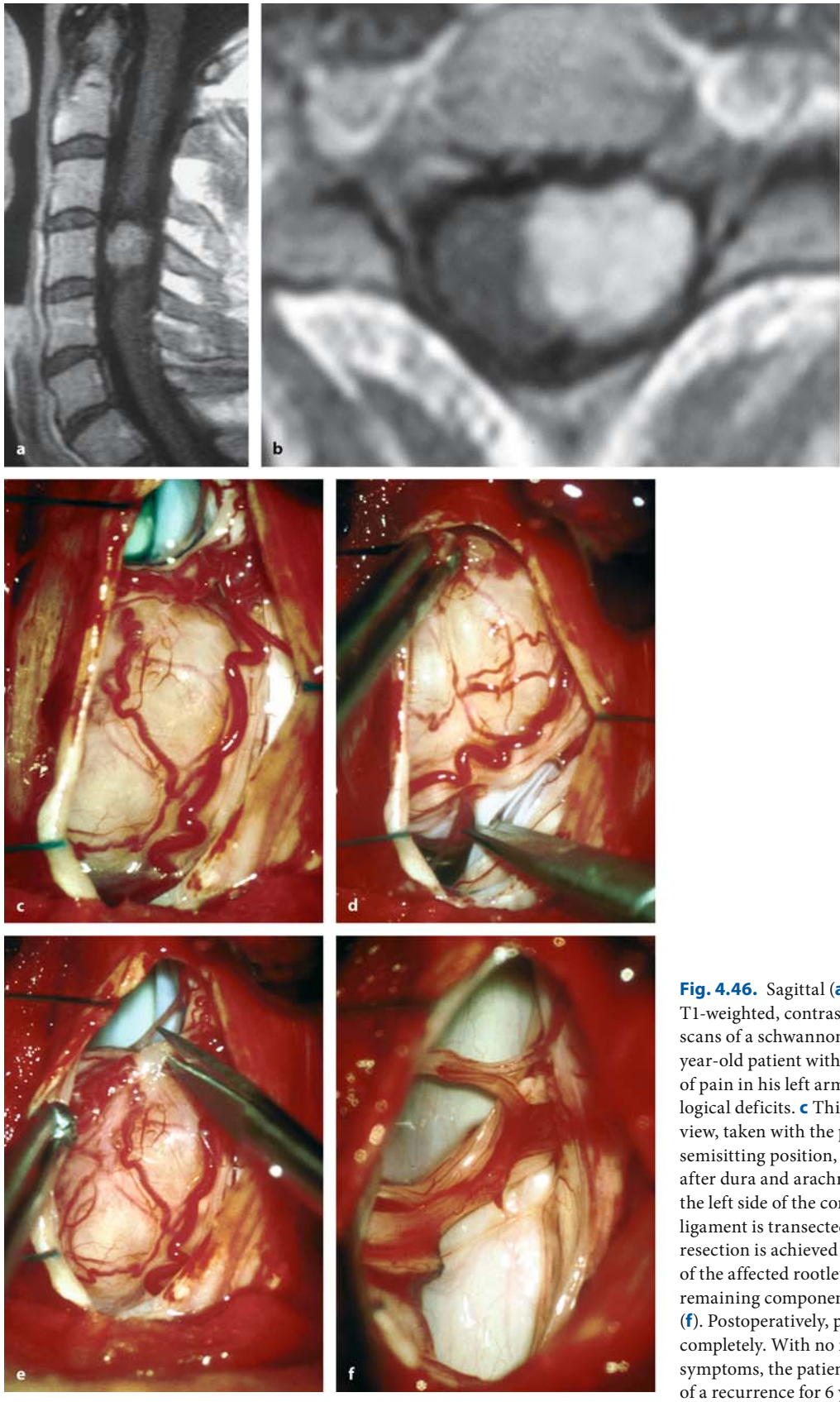

Fig. 4.46. Sagittal (**a**) and axial (**b**) T1-weighted, contrast-enhanced MRI scans of a schwannoma at C4 in a 56-year-old patient with a 10-year history of pain in his left arm without neurological deficits. **c** This intraoperative view, taken with the patient in the semisitting position, shows the tumor after dura and arachnoid opening on the left side of the cord. **d** The dentate ligament is transected. **e** A radical resection is achieved with transection of the affected rootlet, preserving the remaining components of this root (**f**). Postoperatively, pain vanished completely. With no new neurological symptoms, the patient has been free of a recurrence for 6 years

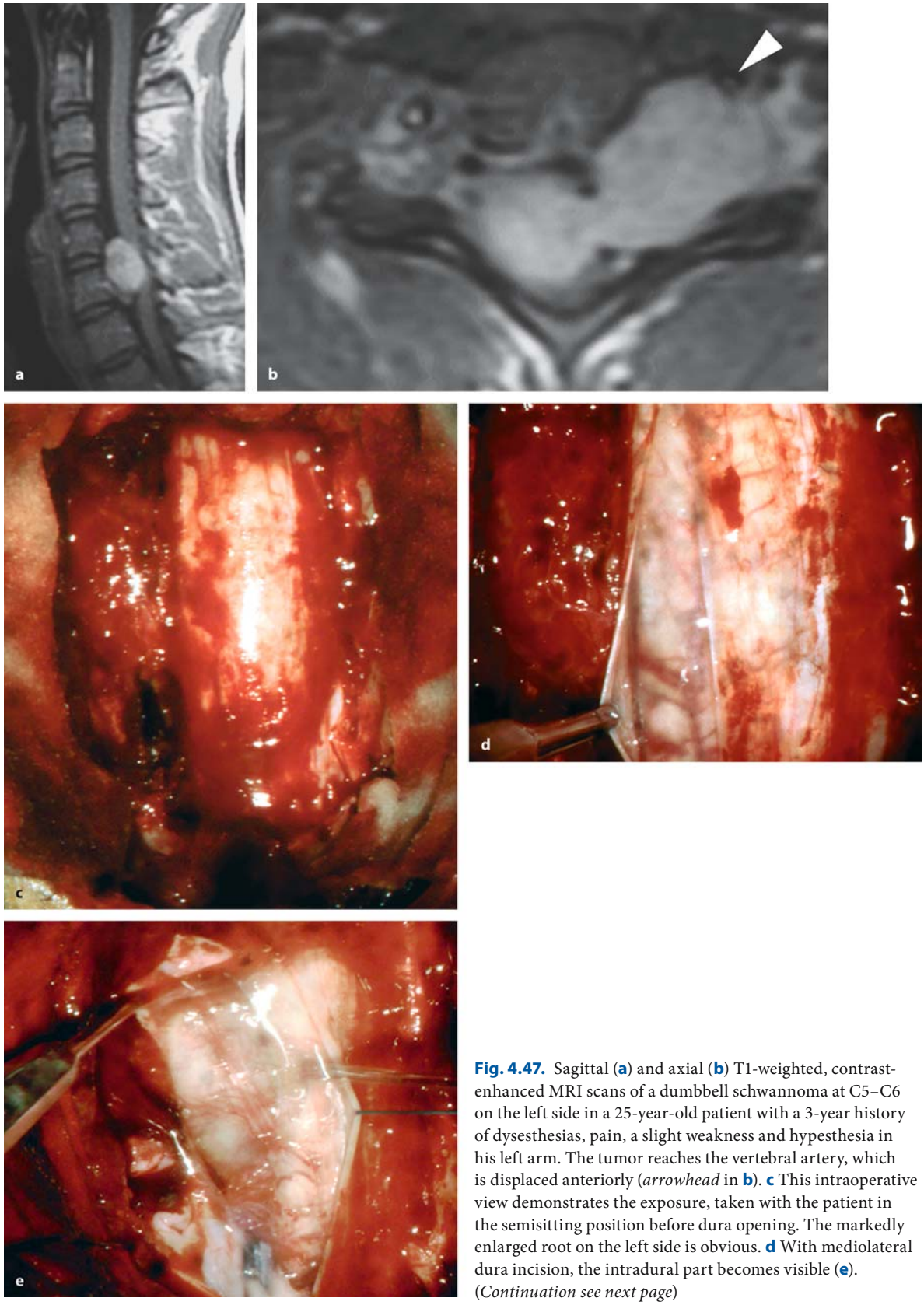

Fig. 4.47. Sagittal (**a**) and axial (**b**) T1-weighted, contrast-enhanced MRI scans of a dumbbell schwannoma at C5–C6 on the left side in a 25-year-old patient with a 3-year history of dysesthesias, pain, a slight weakness and hypesthesia in his left arm. The tumor reaches the vertebral artery, which is displaced anteriorly (*arrowhead* in **b**). **c** This intraoperative view demonstrates the exposure, taken with the patient in the semisitting position before dura opening. The markedly enlarged root on the left side is obvious. **d** With mediolateral dura incision, the intradural part becomes visible (**e**). (*Continuation see next page*)

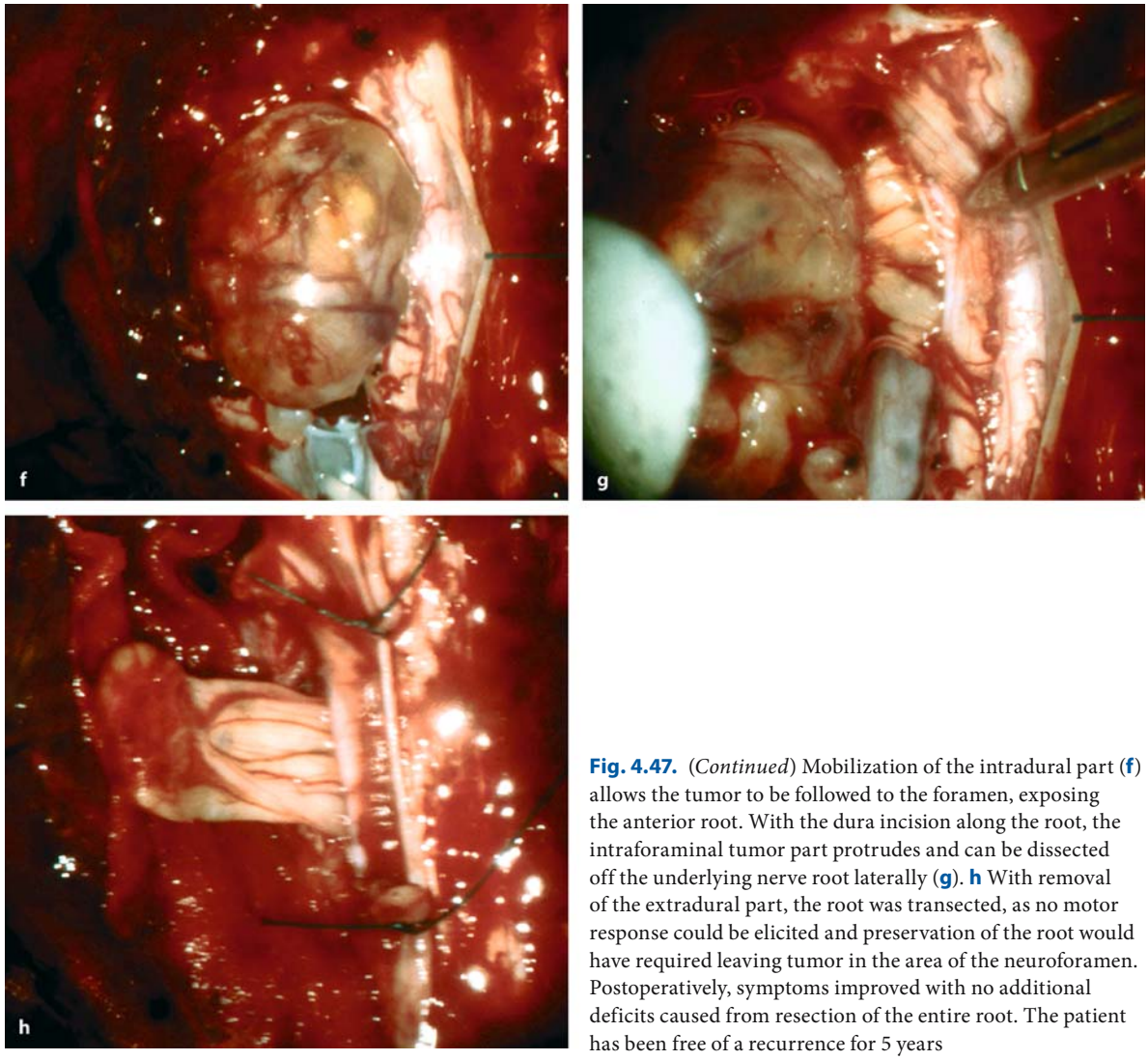

Fig. 4.47. (*Continued*) Mobilization of the intradural part (**f**) allows the tumor to be followed to the foramen, exposing the anterior root. With the dura incision along the root, the intraforaminal tumor part protrudes and can be dissected off the underlying nerve root laterally (**g**). **h** With removal of the extradural part, the root was transected, as no motor response could be elicited and preservation of the root would have required leaving tumor in the area of the neuroforamen. Postoperatively, symptoms improved with no additional deficits caused from resection of the entire root. The patient has been free of a recurrence for 5 years

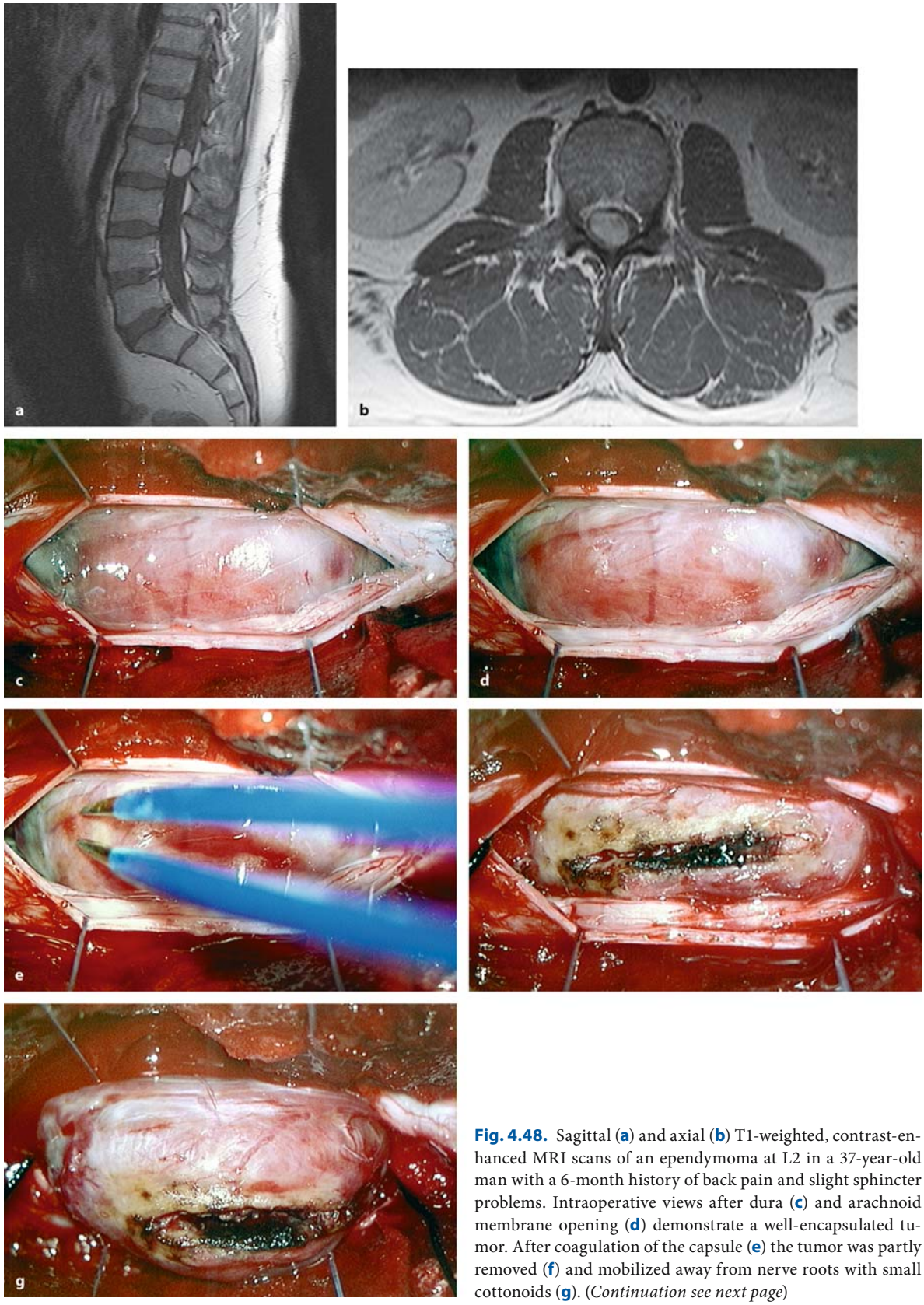

Fig. 4.48. Sagittal (**a**) and axial (**b**) T1-weighted, contrast-enhanced MRI scans of an ependymoma at L2 in a 37-year-old man with a 6-month history of back pain and slight sphincter problems. Intraoperative views after dura (**c**) and arachnoid membrane opening (**d**) demonstrate a well-encapsulated tumor. After coagulation of the capsule (**e**) the tumor was partly removed (**f**) and mobilized away from nerve roots with small cottonoids (**g**). (*Continuation see next page*)

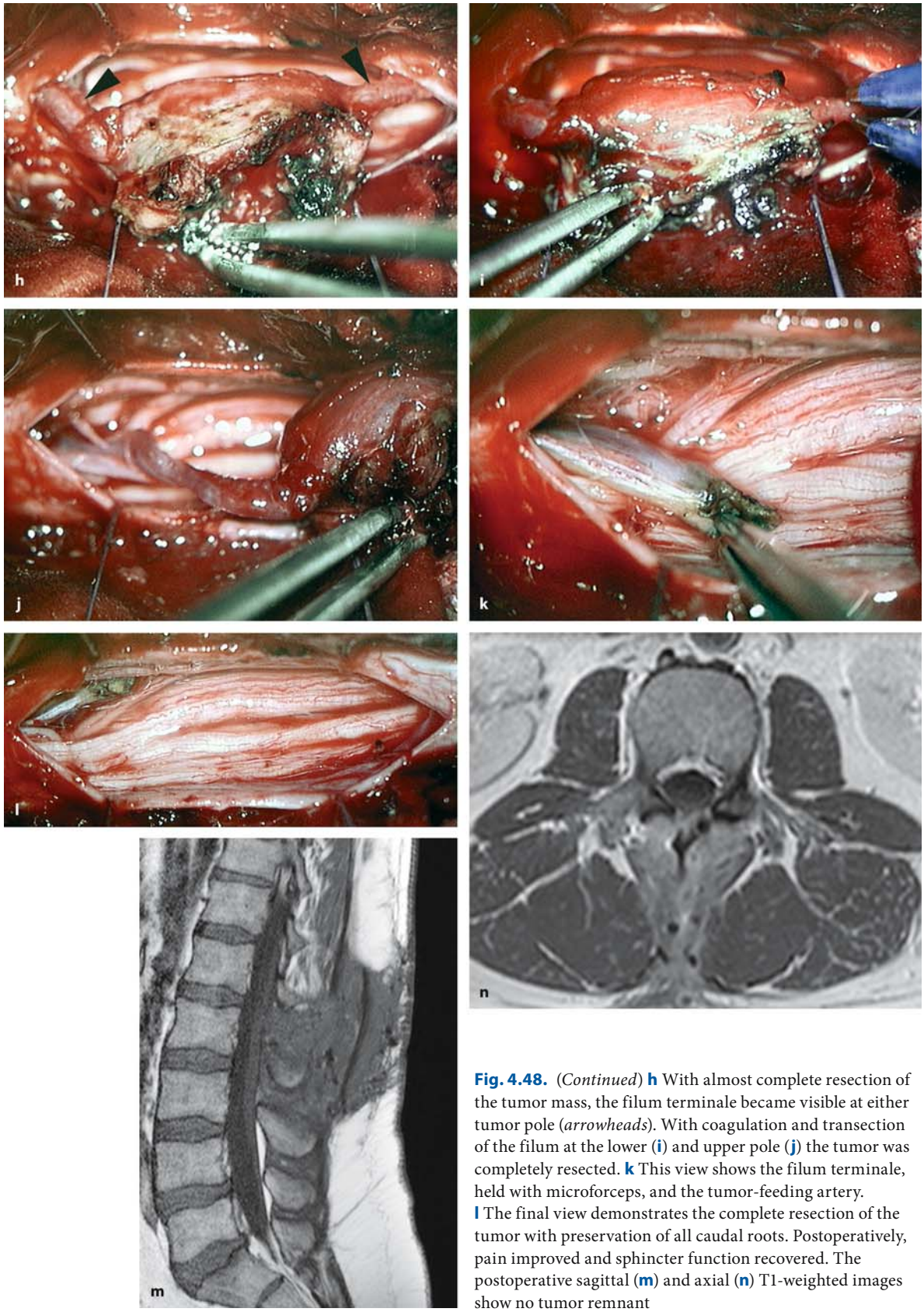

Fig. 4.48. (*Continued*) **h** With almost complete resection of the tumor mass, the filum terminale became visible at either tumor pole (*arrowheads*). With coagulation and transection of the filum at the lower (**i**) and upper pole (**j**) the tumor was completely resected. **k** This view shows the filum terminale, held with microforceps, and the tumor-feeding artery. **l** The final view demonstrates the complete resection of the tumor with preservation of all caudal roots. Postoperatively, pain improved and sphincter function recovered. The postoperative sagittal (**m**) and axial (**n**) T1-weighted images show no tumor remnant

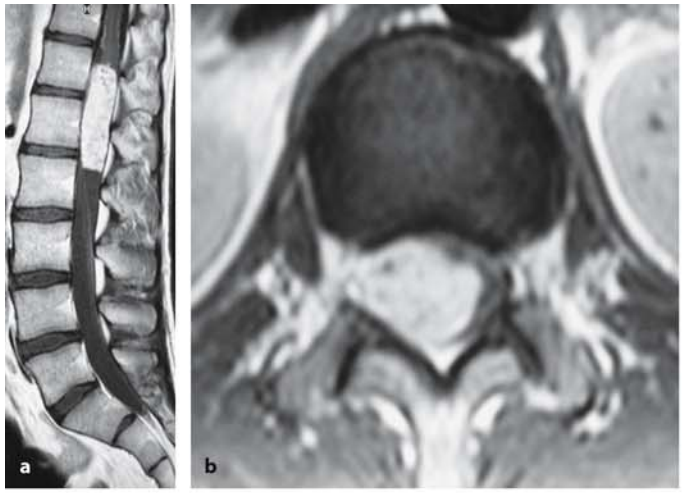

Fig. 4.49. Sagittal (**a**) and axial (**b**) T1-weighted, contrast-enhanced MRI scans of an ependymoma at Th12–L2 in a 21-year-old man with a 10-year history of pain without any neurological deficits. The tumor displaces the conus to the left side. **c** The intraoperative view after dura opening demonstrates this extensive tumor. **d** Xanthochrome CSF is visible below the lower pole. **e** The arachnoid membrane is incised in this area and, after placing cottonoids into the caudal subarachnoid space to avoid any tumor dissemination, the capsule is coagulated (**f**) and debulking is undertaken with suction on a low setting, tumor forceps, and microscissors (**g**). Tumor removal proceeds in this fashion in cranial direction (**h**) until the area of the conus, which is displaced to the left (*arrowhead* in **i**), is reached (**i**). (*Continuation see next page*)

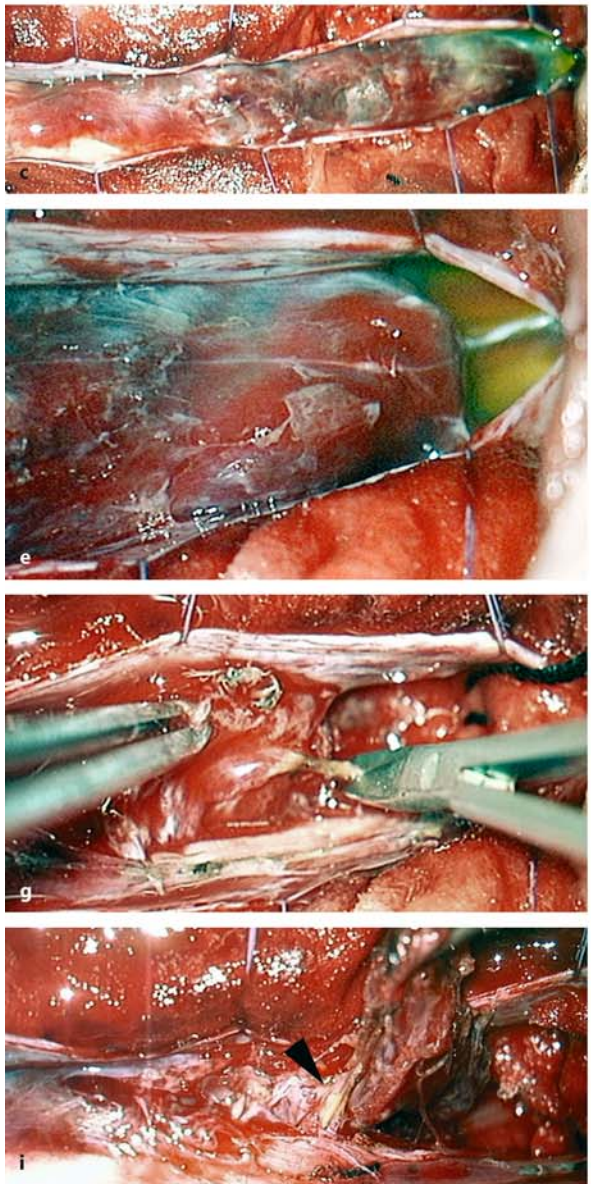

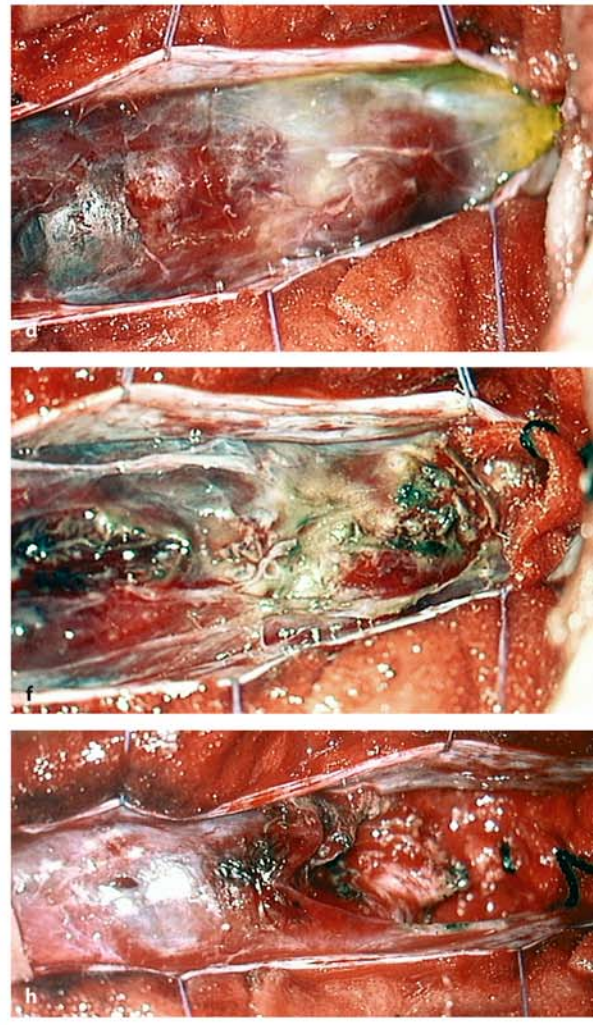

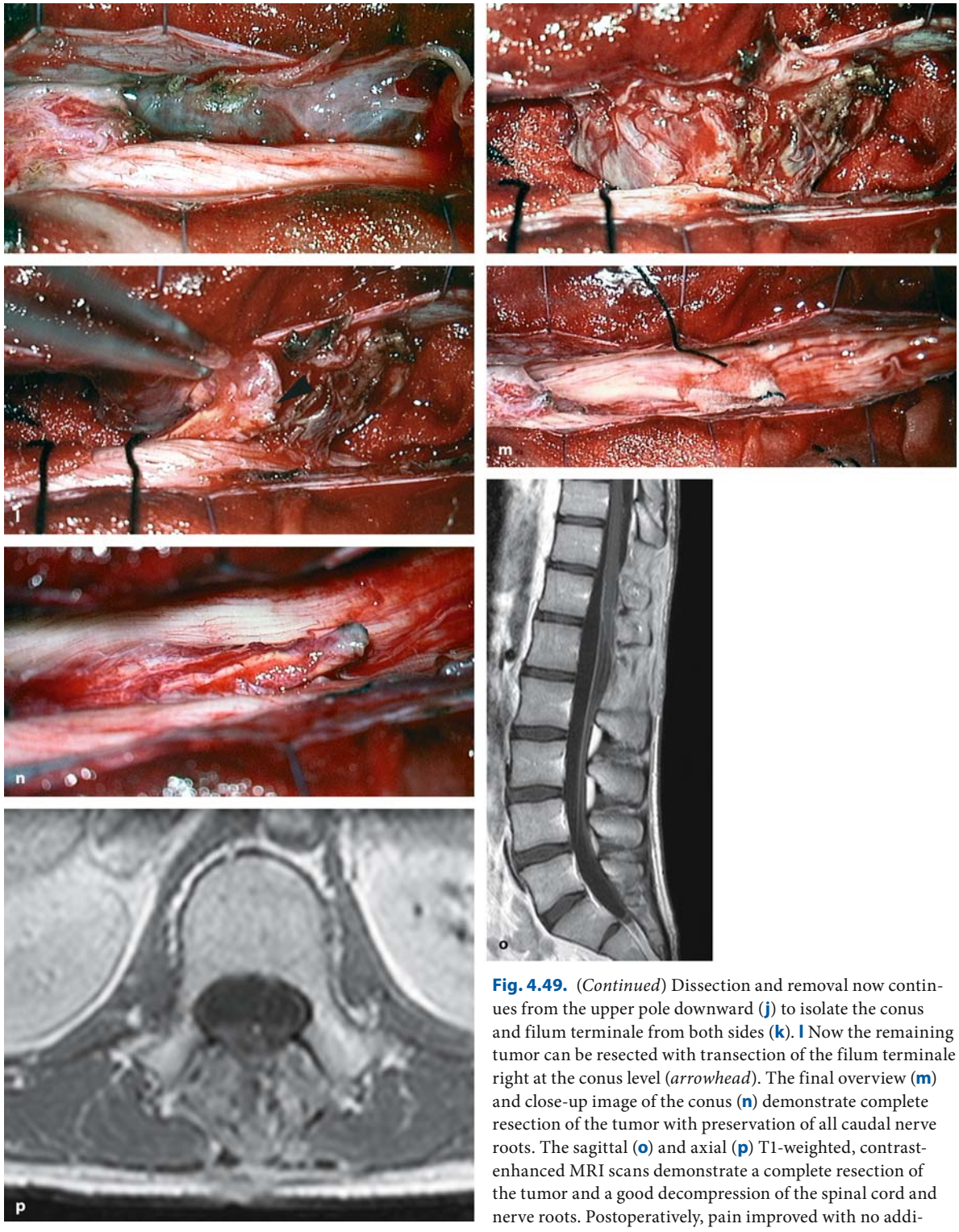

Fig. 4.49. (*Continued*) Dissection and removal now continues from the upper pole downward (**j**) to isolate the conus and filum terminale from both sides (**k**). **l** Now the remaining tumor can be resected with transection of the filum terminale right at the conus level (*arrowhead*). The final overview (**m**) and close-up image of the conus (**n**) demonstrate complete resection of the tumor with preservation of all caudal nerve roots. The sagittal (**o**) and axial (**p**) T1-weighted, contrast-enhanced MRI scans demonstrate a complete resection of the tumor and a good decompression of the spinal cord and nerve roots. Postoperatively, pain improved with no additional neurological deficit except for a slight hypesthesia in the left leg

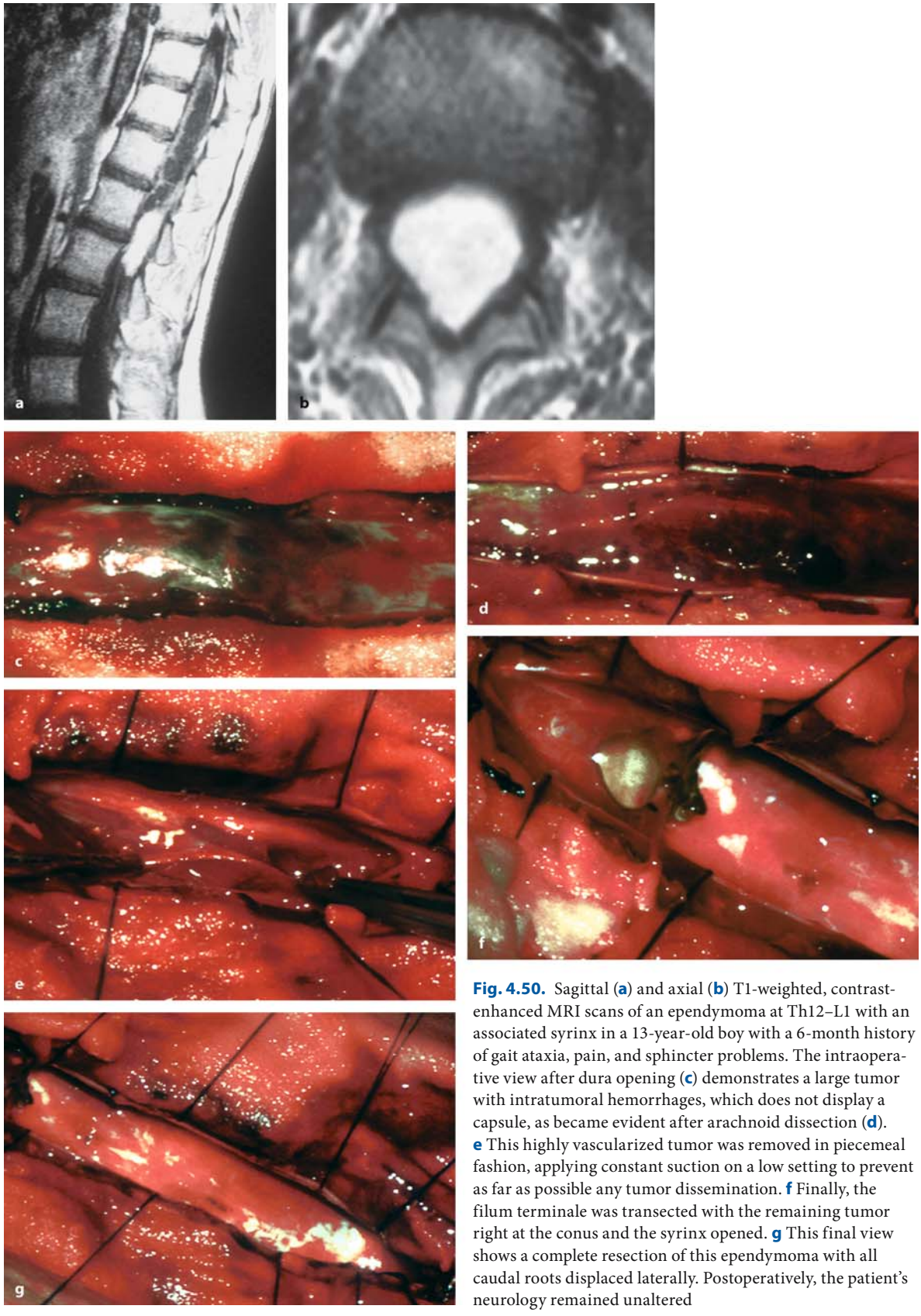

Fig. 4.50. Sagittal (**a**) and axial (**b**) T1-weighted, contrast-enhanced MRI scans of an ependymoma at Th12–L1 with an associated syrinx in a 13-year-old boy with a 6-month history of gait ataxia, pain, and sphincter problems. The intraoperative view after dura opening (**c**) demonstrates a large tumor with intratumoral hemorrhages, which does not display a capsule, as became evident after arachnoid dissection (**d**). **e** This highly vascularized tumor was removed in piecemeal fashion, applying constant suction on a low setting to prevent as far as possible any tumor dissemination. **f** Finally, the filum terminale was transected with the remaining tumor right at the conus and the syrinx opened. **g** This final view shows a complete resection of this ependymoma with all caudal roots displaced laterally. Postoperatively, the patient's neurology remained unaltered

4.3.1.1.4 Removal of Angioblastomas

Highly vascularized tumors such as angioblastomas should be resected in toto to avoid considerable bleeding from the tumor with piecemeal removal. Such tumors can be shrunk with bipolar coagulation on the surface to facilitate resection (Fig. 4.51). Suction and bipolar coagulation should be on a low setting to avoid rupture of the quite vulnerable feeding vessels. If the tumor appears too large for removal in toto, preoperative embolization may be considered (Fig. 4.52). Extramedullary angioblastomas receive their blood supply from the arteries accompanying the spinal nerve roots; such roots have to be preserved. The tumor-feeding vessels have to be identified and transected to ensure radicality (Fig. 4.51).

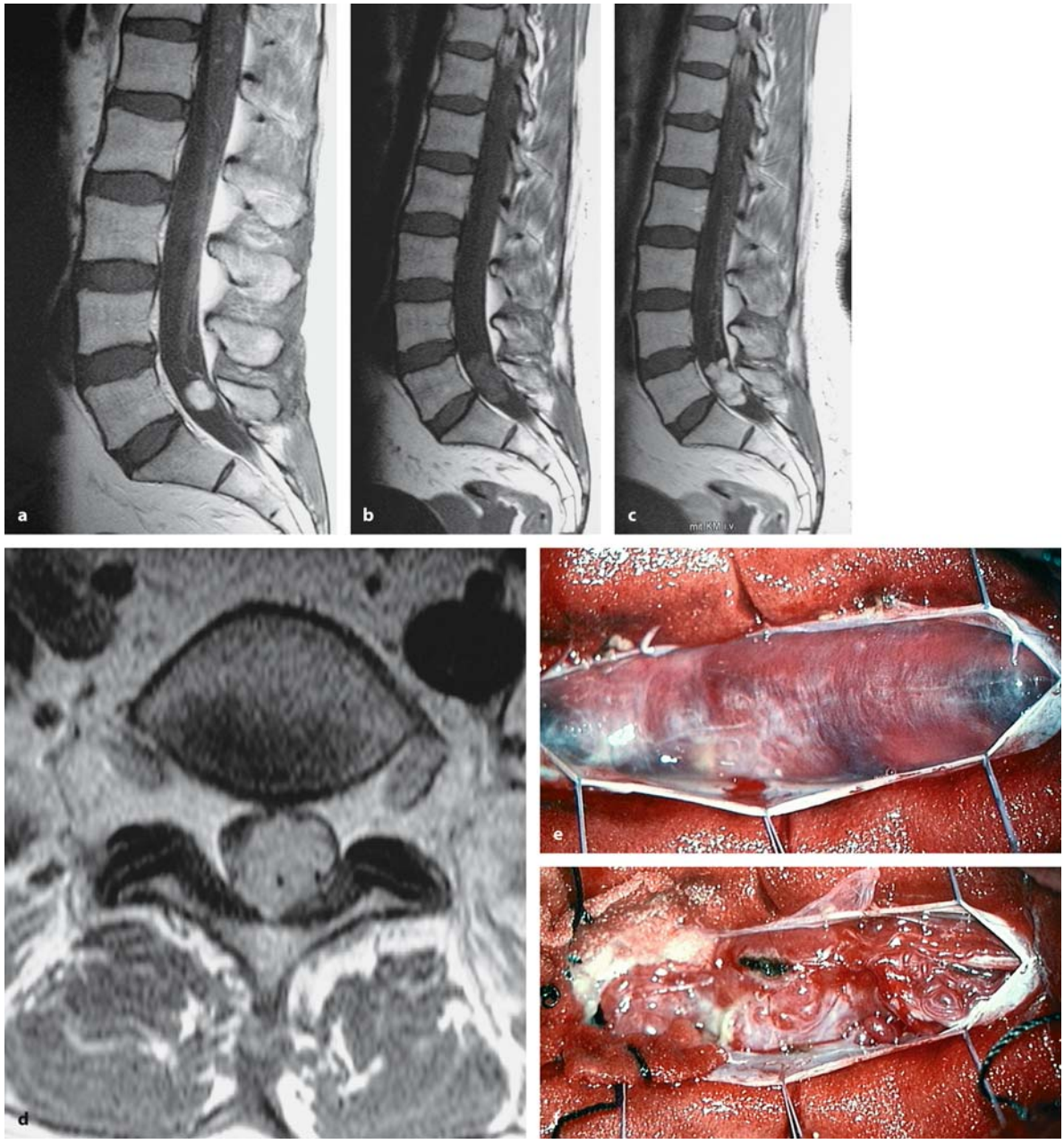

Fig. 4.51. a Within 2 years, this angioblastoma at L5/S1 doubled its size in a 46-year-old woman with VHL and a 1-year history of increasing pain in both legs without additional neurological deficits. The preoperative T1-weighted MRI scans without (**b**) and with contrast (**c**, **d**) demonstrate a large, multilobulated angioblastoma with displacement of caudal nerve roots to the right. **e** The intraoperative view after dura opening displays a tense arachnoid. **f** With opening of the arachnoid, the highly vascularized tumor is visible, surrounded by arterialized veins and feeding arteries. (*Continuation see next page*)

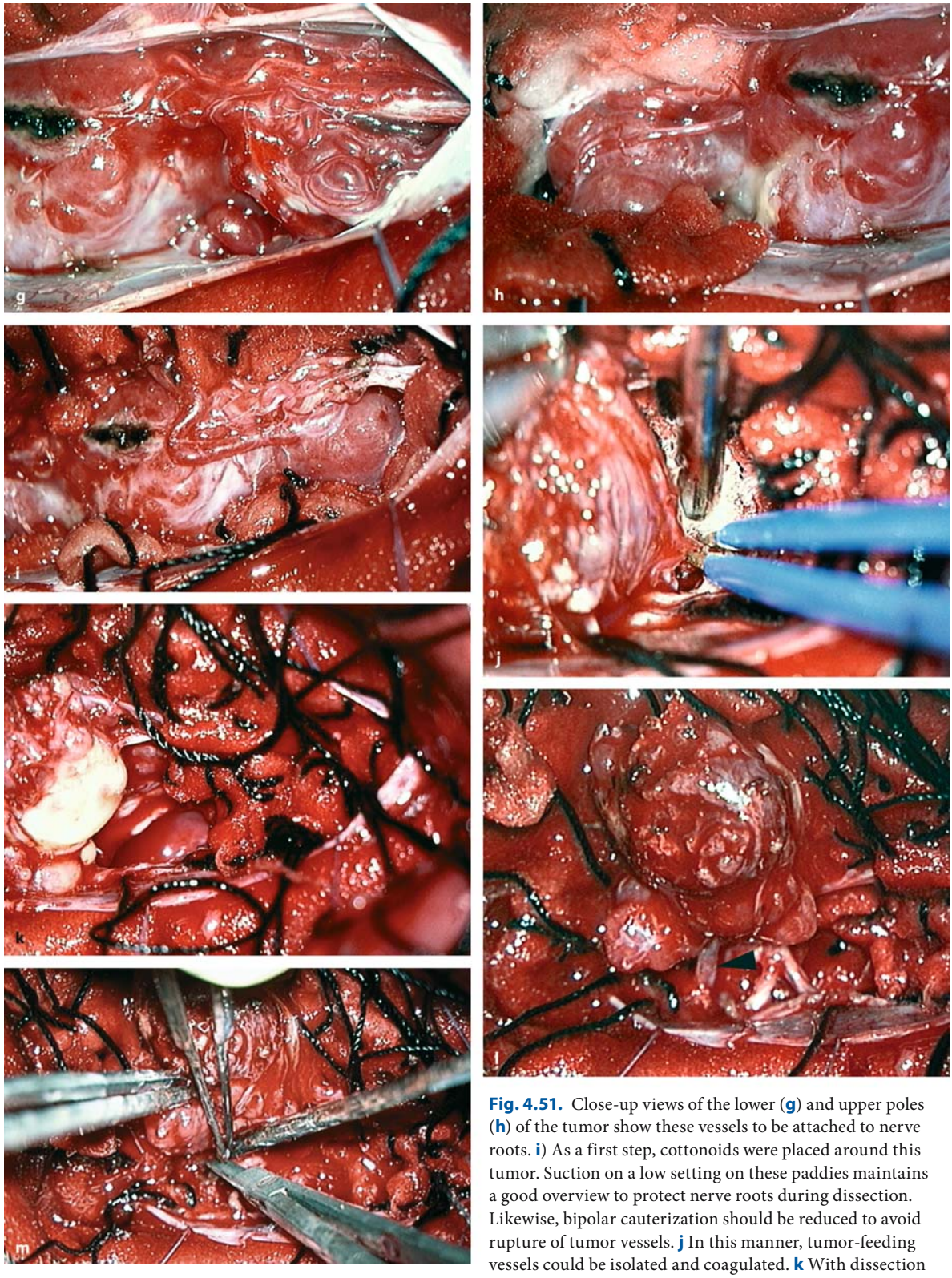

Fig. 4.51. Close-up views of the lower (**g**) and upper poles (**h**) of the tumor show these vessels to be attached to nerve roots. **i**) As a first step, cottonoids were placed around this tumor. Suction on a low setting on these paddies maintains a good overview to protect nerve roots during dissection. Likewise, bipolar cauterization should be reduced to avoid rupture of tumor vessels. **j** In this manner, tumor-feeding vessels could be isolated and coagulated. **k** With dissection of all feeders from below, the tumor could be mobilized and elevated. Finally, the last feeder was isolated on the left side (*arrowhead in* **l**) and transected (**m**). (*Continuation see next page*)

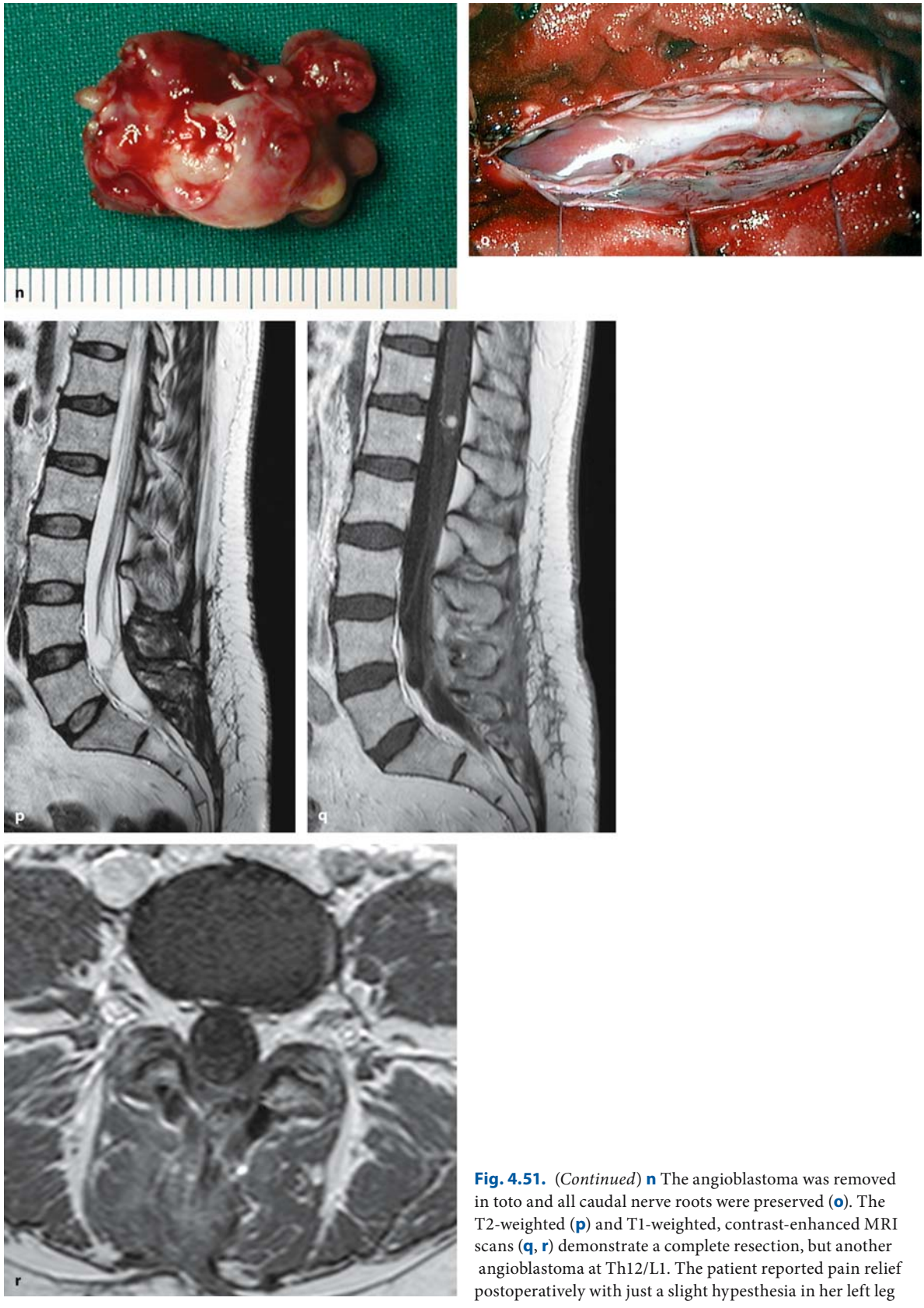

Fig. 4.51. (*Continued*) **n** The angioblastoma was removed in toto and all caudal nerve roots were preserved (**o**). The T2-weighted (**p**) and T1-weighted, contrast-enhanced MRI scans (**q**, **r**) demonstrate a complete resection, but another angioblastoma at Th12/L1. The patient reported pain relief postoperatively with just a slight hypesthesia in her left leg

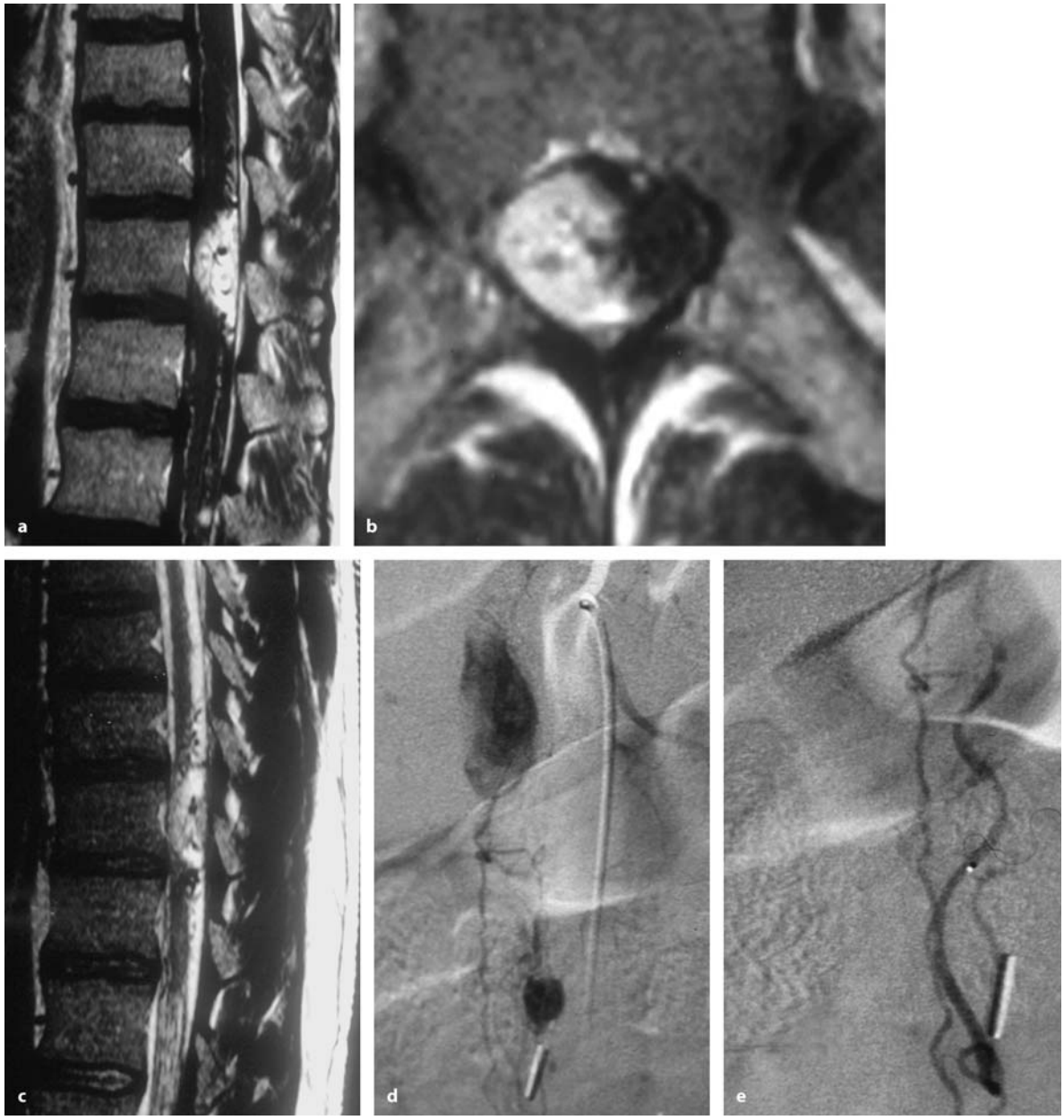

Fig. 4.52. Sagittal (**a**) and axial (**b**) T1-weighted MRI scan with contrast and T2-weighted scan (**c**) of an angioblastoma at Th9 in a 33-year-old patient with VHL and severe back pain but no neurological deficits. This highly vascularized lesion (**d**) was embolized before surgery with a good result (**e**). A further lesion at Th11 was also embolized. (*Continuation see next page*)

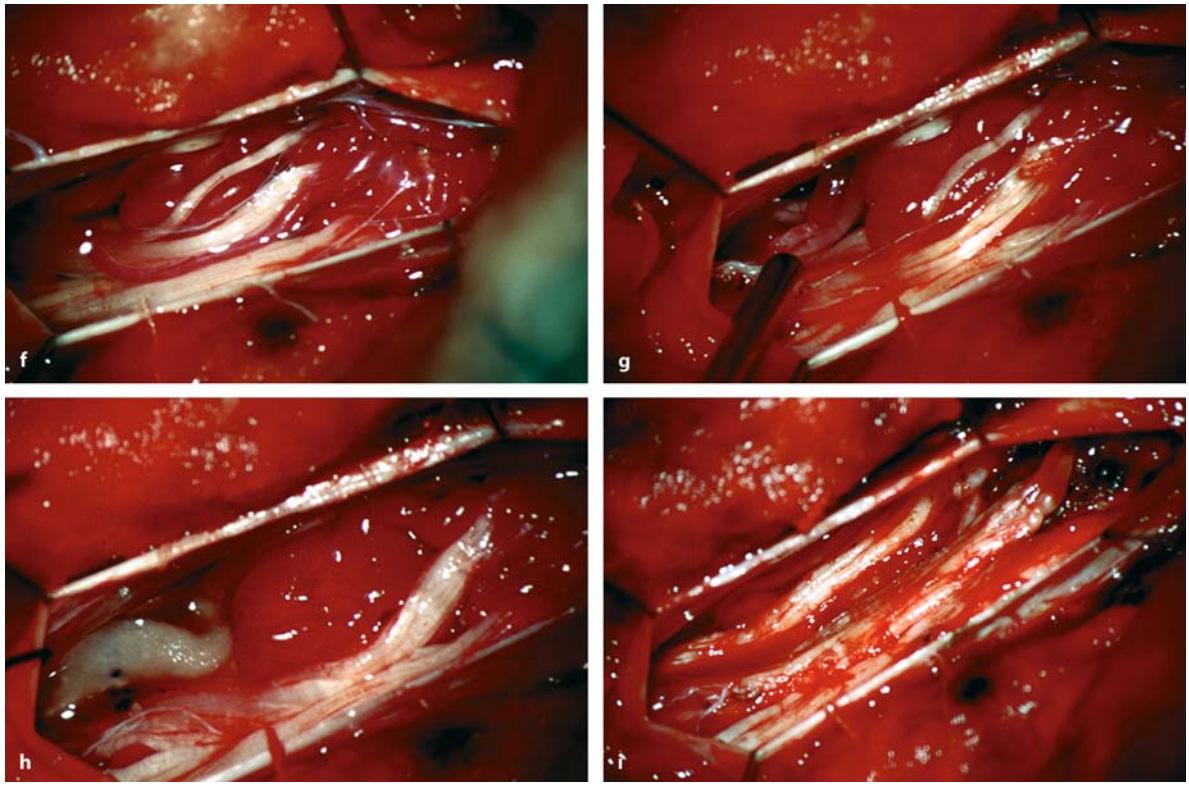

Fig. 4.52. (*Continued*) **f** This intraoperative view after dura and arachnoid opening shows the tumor on the right side covered by nerve roots. Sucking on small cottonoids (**g**) allows isolation of the upper tumor pole (**h**). Mobilizing the nerve roots with a microdissector, the lower tumor pole is also dissected. With coagulation and transection of feeding arteries, a complete resection is finally achieved (**i**). Postoperatively, pain improved without appearance of new deficits. Two years later, another operation was required for the Th11 tumor

4.3.1.1.5 Removal of Hamartomas

Solid hamartomas (i.e., lipomas) may affect the spinal cord or cauda equina in two ways: compression and tethering. Lipomas do not proliferate. The mass of this hamartoma will change according to the entire body fat. If the lipoma is of considerable size, it may compress the spinal cord (Fig. 4.53) or cauda equina (Fig. 4.54). The lipoma is always firmly attached to the cord tissue, with a transition zone that displays no definite cleavage plane. The second mechanism – tethering of the spinal cord – can be caused in several ways: the lipoma may be associated with a low position of the conus with a tight filum terminale (Fig. 4.54), the filum terminale may harbor the lipoma (Fig. 4.55), or the lipoma may have grown into the epidural space transgressing the dura mater (Fig. 4.56) [41]. Furthermore, shortened, but nonetheless functional nerve roots may cause a tethering effect (Figs. 4.57 and 4.58) [38]. Quite often, a lipoma will be associated with other dysraphic defects such as, for example, a dermal sinus (Fig. 4.59), a split-cord malformation, or a dermoid cyst (Fig. 4.54). Finally, lipomas may be associated with significant arachnoid scarring, which may complicate the dissection to a degree that a satisfactory untethering of the conus cannot be achieved without significant risks to inflict neurological deficits [57, 210, 222]. Unfortunately, postoperative arachnoid scarring may be a severe problem in patients with dysraphic hamartomas and lipomas in particular. Therefore, the surgical procedure should focus strictly on what is required, avoiding any unnecessary dissections.

Each of the aforementioned aspects has to be dealt with [41]. If the lipoma is of small size and the spinal cord or cauda appears not to be compressed by it, neurological symptoms will most likely be caused by a tethering mechanism. In such an instance, we do not remove the lipoma, but just untether the cord (Fig. 4.55). This may involve sharp arachnoid dissection, transection of the filum terminale, and/or removal of a bony spur and mesenchymal tissue be-

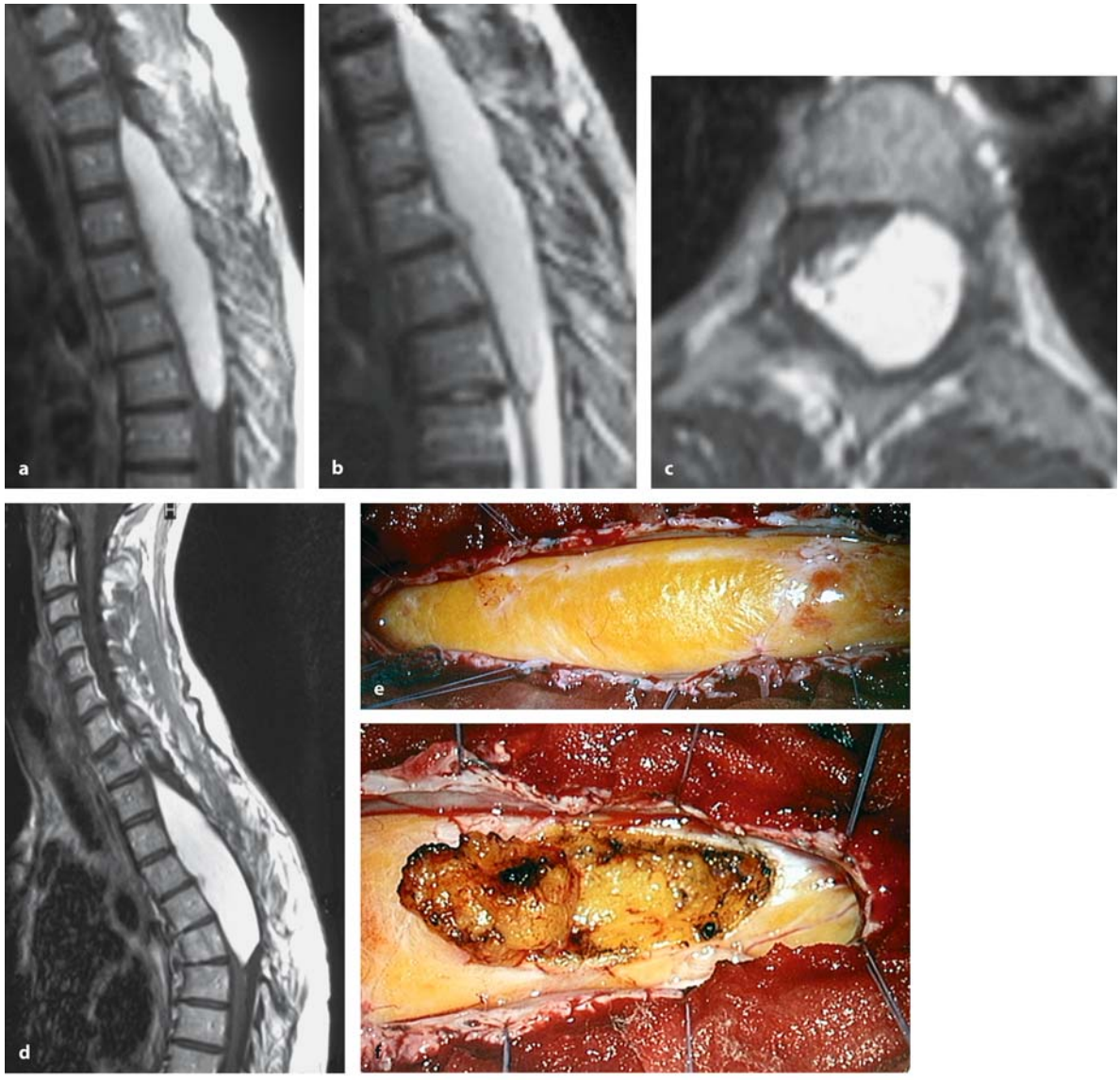

Fig. 4.53. Sagittal T1- (**a**) and T2-weighted (**b**) MRI scans and an axial T1-weighted image (**c**) of an extramedullary lipoma at Th1–Th6 in a 32-year-old woman with a 5-month history of progressive paraparesis. The hamartoma has widened the spinal canal. A kyphosis has formed at Th6/7. In a first operation, a laminectomy and decompression of the cord had been performed. After considerable initial improvement the paraparesis returned after 3 years due to progressive kyphosis at Th6/7 (**d**). Unfortunately, the patient postponed a second operation until she was wheelchair dependent. For this second operation, a reduction of the lipoma mass and a stabilization was planned. **e** The intraoperative view after dura opening shows the enormous size of this lipoma. On opening the capsule, the tumor could be debulked (**f**) leaving the capsule intact, using tumor forceps and sharp dissectors (**g**).
(*Continuation see next page*)

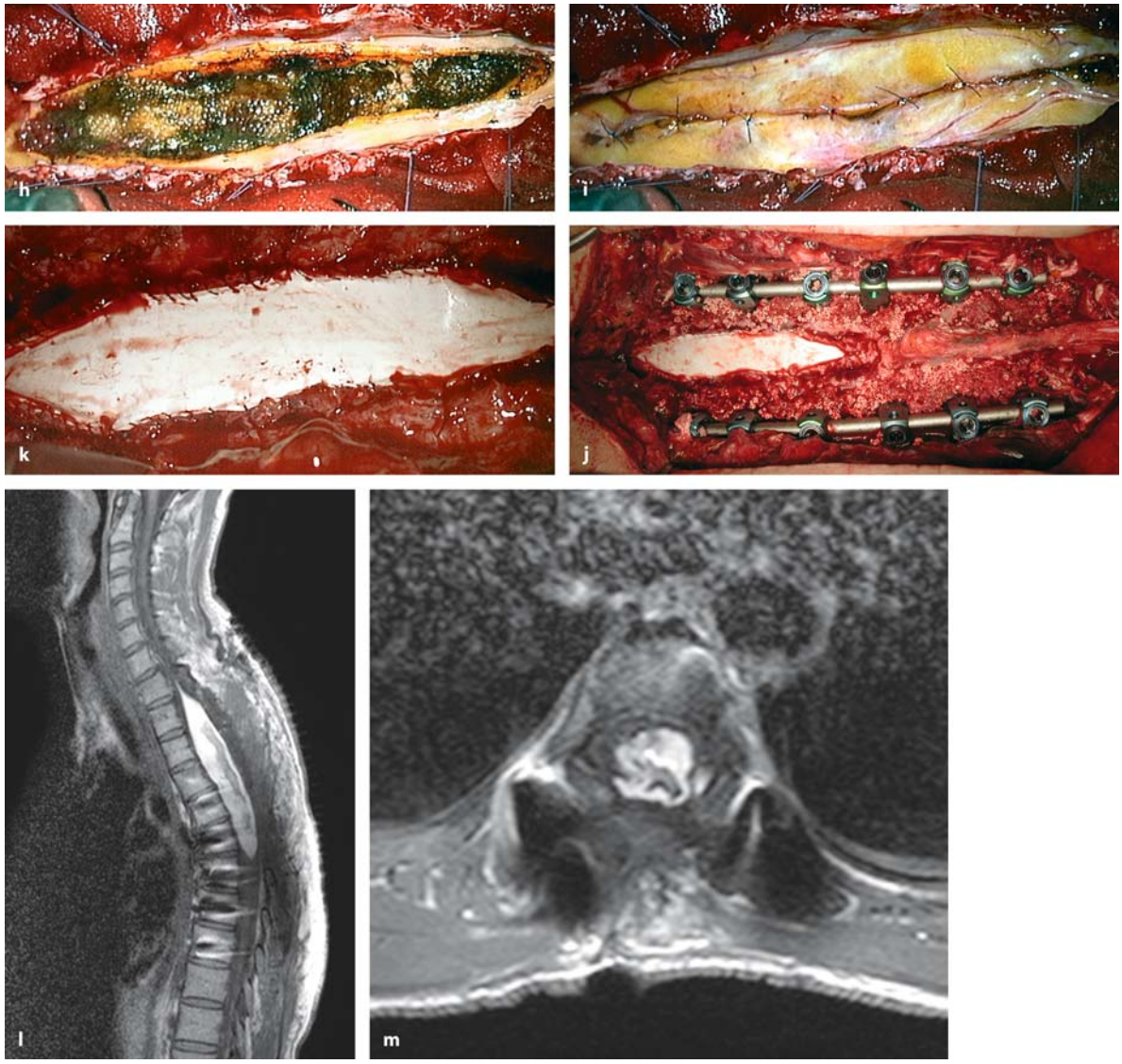

Fig. 4.53. (*Continued*) **h** This image shows the end of the tumor debulking. Intratumoral hemostasis is achieved with fibrin tissue. The closure involves a suture of the lipoma capsule (**i**) and a Gore-Tex® duraplasty (**j**). **k** Finally, a transpedicular stabilization is performed at Th4–Th9. The postoperative T1-weighted sagittal (**l**) and axial (**m**) MRI images show the amount of decompression

tween hemicords, such as aberrant roots and fibrous bands in cases of split-cord malformations [198]. The filum can be identified by its characteristic texture and paler color compared to a nerve root. An artery will always accompany it. Nerve roots may be attached to the filum and have to be dissected off [210]. The filum should be coagulated before it is transected (Figs. 4.54 and 4.55).

If the lipoma appears to be of considerable size and to compress spinal cord or cauda, we reduce its mass (Figs. 4.53, 4.54, 4.58, and 4.59). In such cases we try to leave the outer capsule of the lipoma, so that we can suture it at the end of the debulking. This may limit the risk of postoperative arachnoid scarring, analogous to suturing the pia mater after removal of an intramedullary tumor (Figs. 4.53 and 4.54). Lipomas may be quite vascularized, and several authors recommend the use of lasers for this pathology [172]. If the lipoma transgresses the dura it causes tethering of the spinal cord at the site of dura penetration. Therefore, it is important to detach the epidural and intradural parts from each other at the level of the

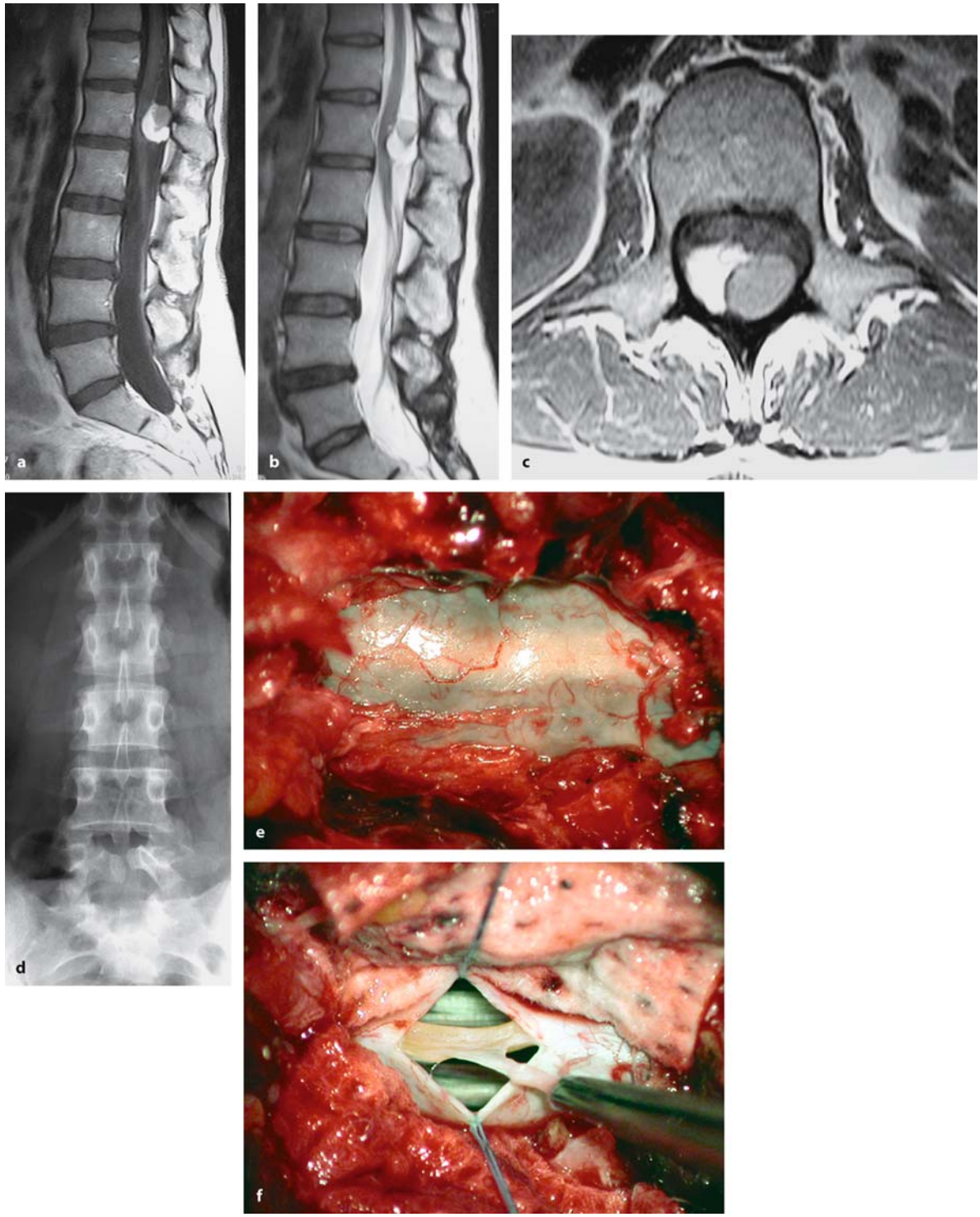

Fig. 4.54. Sagittal T1- (**a**) and T2-weighted (**b**) MRI scans of a mixed hamartoma at L1 combined with a tethered cord in a 51-year-old woman with a 2-month history of back and radicular pain and hypesthesia in her right leg. The upper part of this hamartoma represents a dermoid cyst with a lipoma underneath. The conus ends at L2. **c** The axial image demonstrates the relationship between lipoma on the right, dermoid cyst on the left and spinal cord, which is displaced anteriorly. **d** The conventional X-ray of the lumbar spine shows an incomplete lamina at L5. **e** In a first step the tethered cord is treated exposing the dura at L5. The thickened filum is visible even before dura opening. **f** After dura opening the filum is exposed and found to contain fat; arachnoid adhesions are dissected off to ensure that no caudal roots are attached to the filum. (*Continuation see next page*)

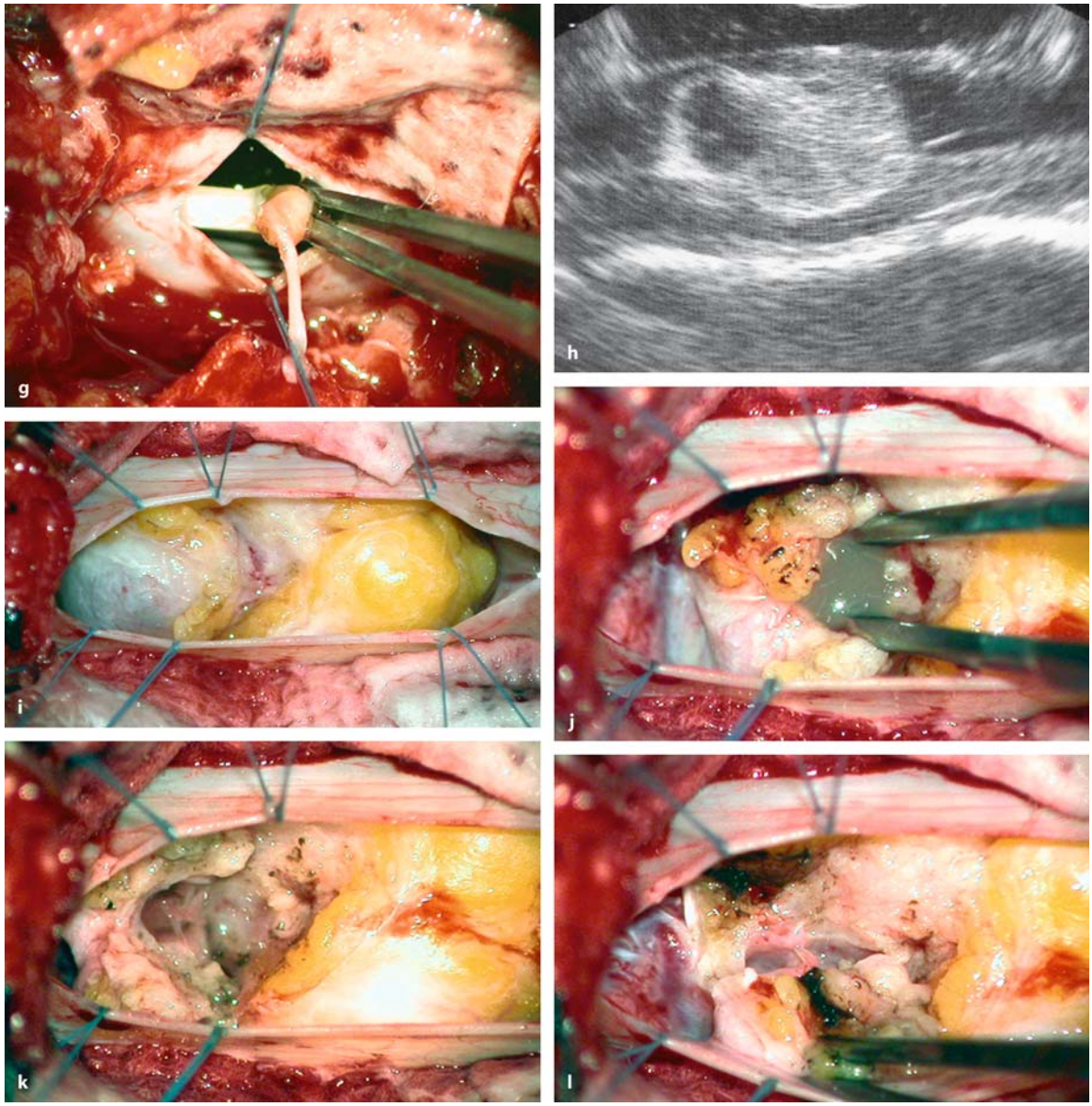

Fig. 4.54. **g** After coagulation and transection of the filum, the dura is closed. **h** After a laminotomy at L1, this ultrasound image depicts the dermoid cyst on the left, the lipoma to the right, and the spinal cord underneath. **i** This intraoperative view after dura and arachnoid opening shows the two components of this hamartoma with the spinal cord hidden underneath. **j** First, the dermoid cyst is incised releasing a mucinous substance that could be sucked away. **k** This view demonstrates the interior of the dermoid cyst. **l** The capsule is now resected stepwise using sharp dissection and leaving a layer of gliosis as a safety barrier for the cord. (*Continuation see next page*)

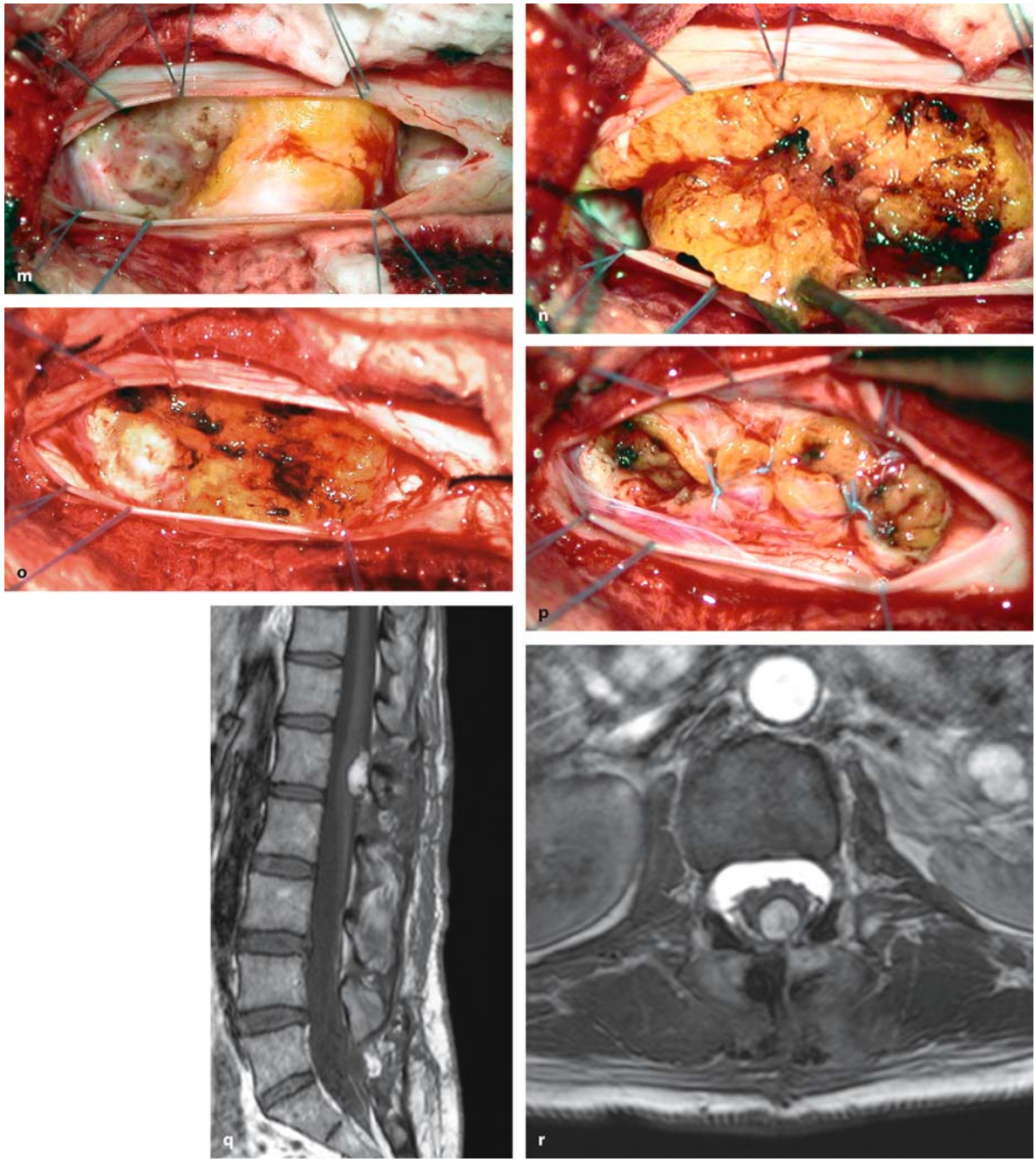

Fig. 4.54. (*Continued*) **m** This photograph demonstrates the situation after complete resection of the dermoid cyst and exposes this gliosis. **n** Debulking of the lipoma is undertaken with tumor forceps and sharp microdissectors. After partial removal of the lipoma (**o**) the capsule is sutured (**p**). The dura was closed with a Gore-Tex® patch and the lamina reinserted with miniplates. The postoperative T1- (**q**) and T2-weighted (**r**) MRI images demonstrate the untethering of the cord, the partial removal of the lipoma, and no remnant of the dermoid cyst. Pain and hypesthesia improved postoperatively. Without any new neurological deficits, the patient is free of a recurrence for 1 year

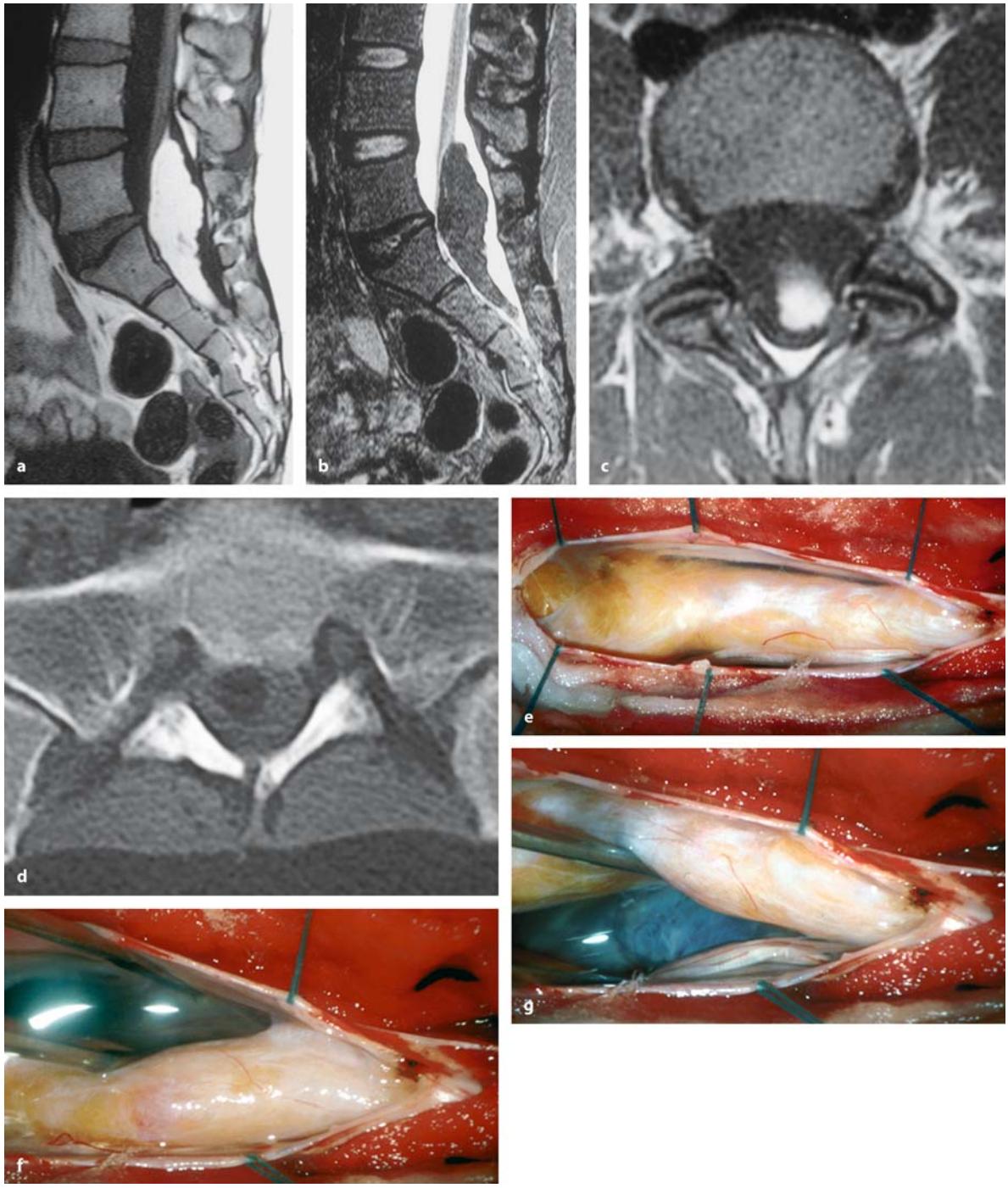

Fig. 4.55. Sagittal T1- (**a**) and T2-weighted (**b**) MRI scans of a lipoma of the filum terminale and conus position at L5 in a 32-year-old woman with a 9-year history of pain, a slight weakness of her left leg, and beginning sphincter disturbances. Axial MRI (**c**) and CT scans (**d**) both demonstrate this pathology and the surrounding bony anatomy. **e** This intraoperative view after dura opening shows the sizeable lipoma with nerve roots attached to its capsule on the left side. After arachnoid opening, the lipomatous filum is checked on either side for adherent nerve roots (**f**, **g**). (*Continuation see next page*)

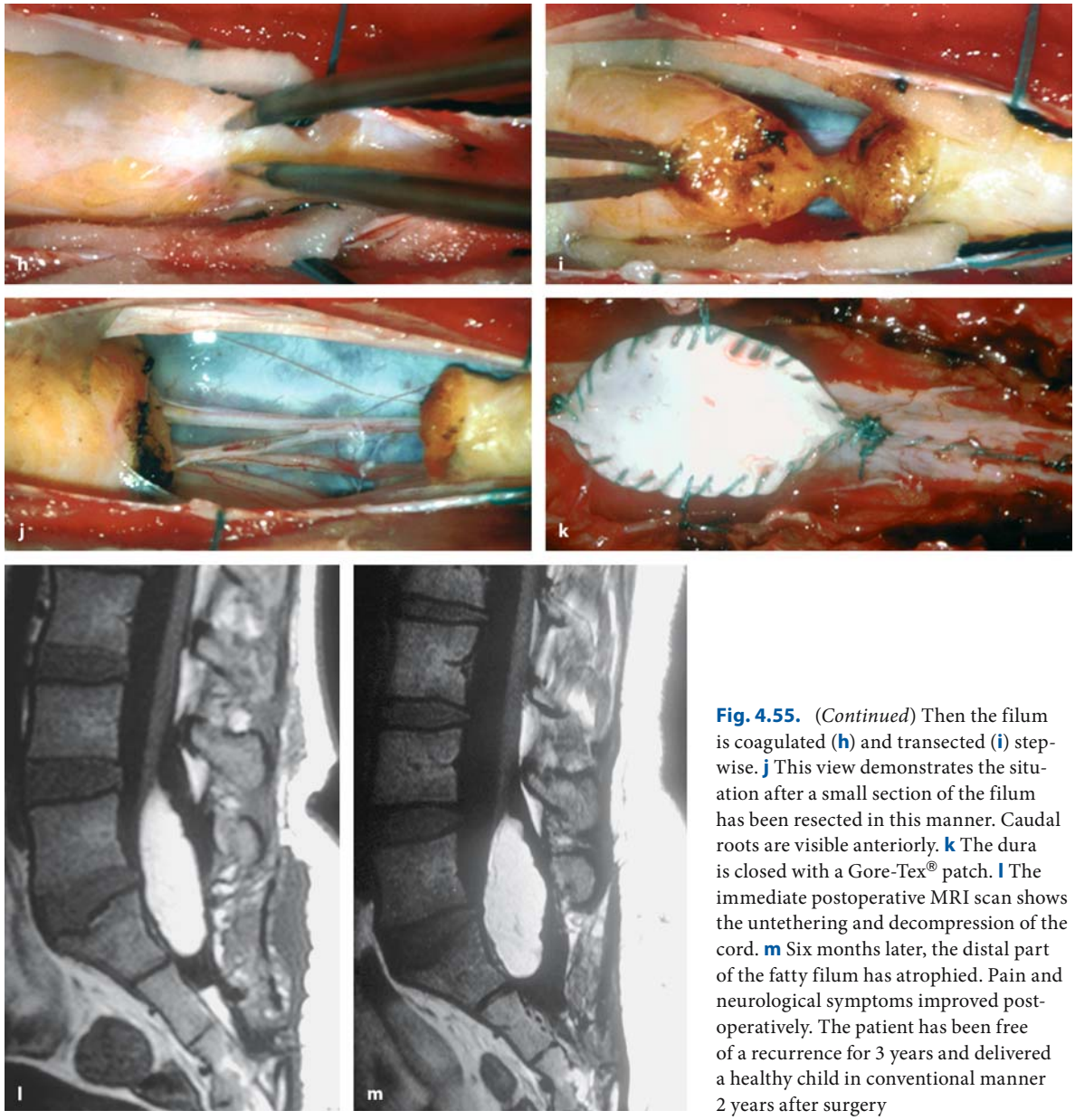

Fig. 4.55. (*Continued*) Then the filum is coagulated (**h**) and transected (**i**) stepwise. **j** This view demonstrates the situation after a small section of the filum has been resected in this manner. Caudal roots are visible anteriorly. **k** The dura is closed with a Gore-Tex® patch. **l** The immediate postoperative MRI scan shows the untethering and decompression of the cord. **m** Six months later, the distal part of the fatty filum has atrophied. Pain and neurological symptoms improved postoperatively. The patient has been free of a recurrence for 3 years and delivered a healthy child in conventional manner 2 years after surgery

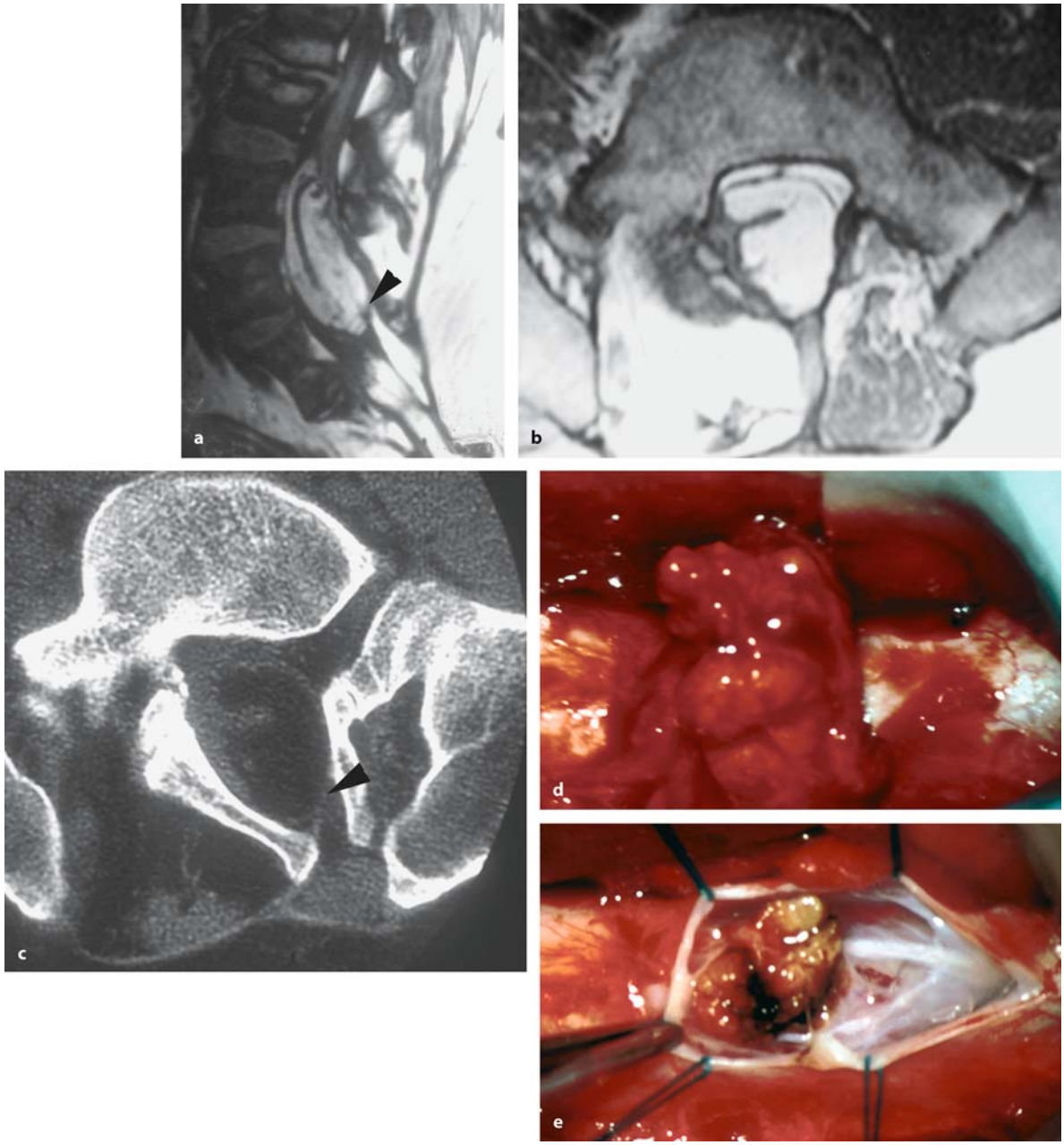

Fig. 4.56. Sagittal (**a**) and axial (**b**) T1-weighted MRI scans of a conus lipoma with extradural extension in a 34-year-old man with a 1-year history of hypesthesia and motor weakness in his right leg accompanied by pain and severe sphincter problems. The sagittal scan shows the extradural extension at L5/S1 (*arrowhead* in **a**) with an intact fascial layer. The axial image demonstrates the conus turned anticlockwise and displaced to the right. **c** The bone window CT scan demonstrates the incomplete lamina of L5 and the connection between intra- and extradural part of the lipoma (*arrowhead*). **d** This intraoperative view shows the extradural part of the lipoma after laminectomy L4 and L5. **e** At this stage, the epidural component of the lipoma has been cut off at the dural entry point and the dura circumcised in this area exposing a thickened arachnoid membrane and the connection of the lipoma to the spinal cord underneath. (*Continuation see next page*)

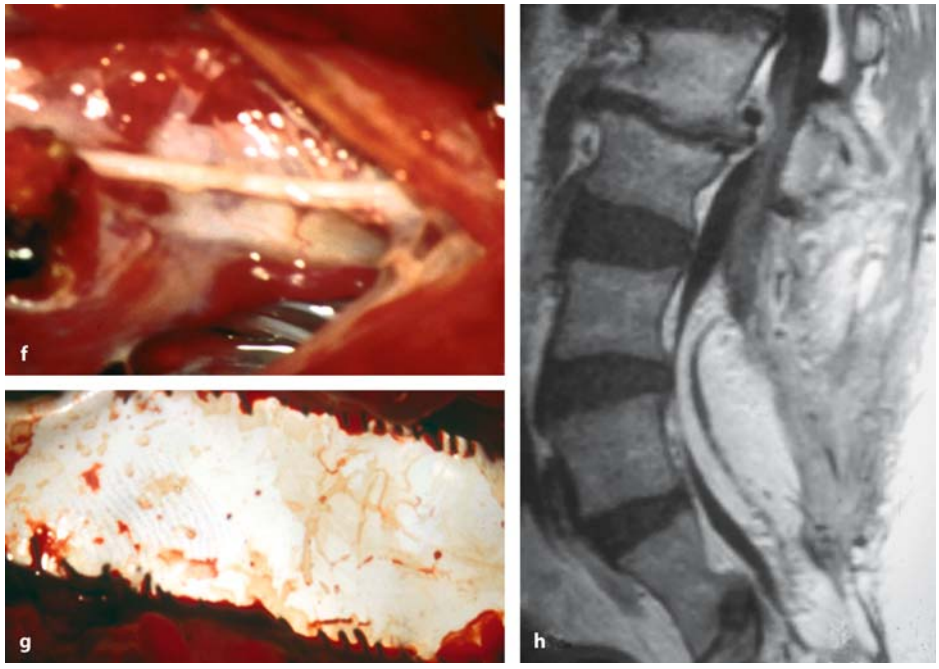

Fig. 4.56. (*Continued*) **f** This close-up view demonstrates the displaced and twisted conus on the right side attached to this lipoma. Further untethering or a reduction of the lipoma mass was judged very hazardous, so that dissection was terminated at this stage. **g** The dura was closed with a Gore-Tex® patch. **h** The postoperative T1-weighted MRI demonstrates the partially untethered spinal cord and the enlarged spinal canal. Postoperatively, the patient experienced considerable pain relief with neurological symptoms unchanged. The patient is free of a recurrence for 2 years

dura in order to untether the cord (Figs. 4.56 and 4.57) [41].

With split-cord malformations (i.e., diastematomyelia), two types can be distinguished: in type 1 the two hemicords are in separate dural tubes, which are separated by a rigid osseocartilagenous septum (Figs. 4.60 and 4.61), whereas in type 2 both hemicords are in one single dura tube but are separated by a nonrigid fibrous septum (Fig. 4.62) [200]. In such cases, the spinal cord is tethered at the site where either intradural mesenchymal (Fig. 4.62) and/or an epidural bony spur (Figs. 4.60 and 4.61) splits the cord into two halves. In either case, aberrant nerve roots on the medial surfaces of both hemicords, hamartomas, and other mesenchymal tissues may connect the hemicords to these separating structures, depending on the type of split-cord malformation, and contribute to the tethering (Figs. 4.60–4.62). In patients with a purely intradural fibrous band splitting the spinal cord, the two hemicords may be so closely attached to each other that on inspection, they may almost appear not to be split at all. In such instances, only the band has to be transected posteriorly and – if present – also anteriorly to relieve the tethered cord. On the other hand, if aberrant mesenchymal tissue is found between both hemicords, all of it needs to be removed [198]. For this purpose, the dural sleeve is circumcised and then removal of the bony spur with its surrounding dural and all aberrant nerve roots or arachnoid scar tissue attached to it can be undertaken (Fig. 4.61). At the end of the dissection, the two hemicords should pulsate freely in the subarachnoid space. The resulting anterior dura defect can be closed with a small Gore-Tex® graft, but this is not mandatory (Fig. 4.61). The posterior defect, however, always requires a dura graft (Figs. 4.61 and 4.62).

Whenever tethering of the spinal cord is part of the pathology, we recommend using a duraplasty to enlarge the subarachnoid space and to limit the risk of retethering [49, 130, 281]. Artificial materials for dura grafting such as Gore-Tex® give much better results in our experience than autologous grafts, as these regularly cause dense adhesions [210].

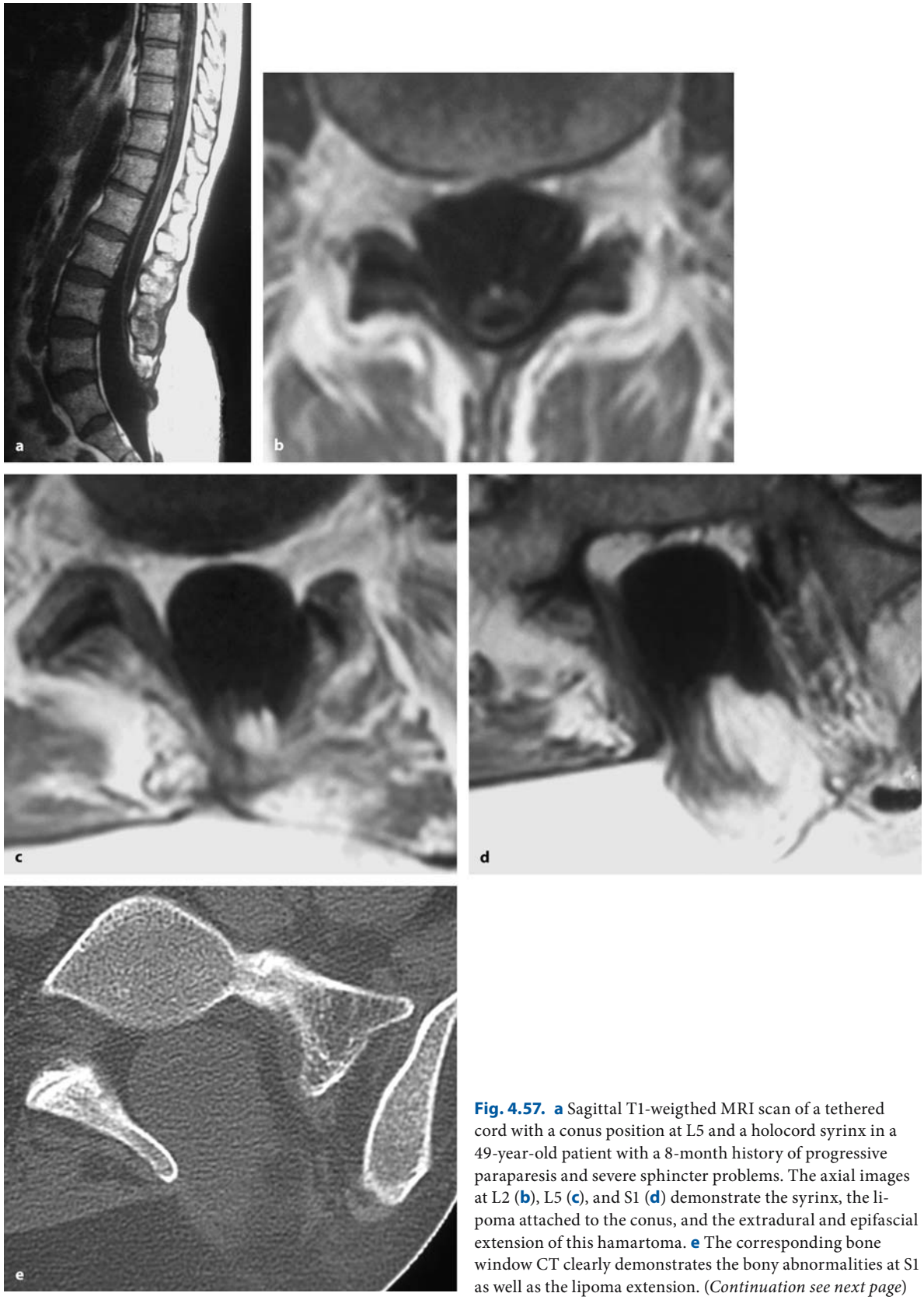

Fig. 4.57. **a** Sagittal T1-weigthed MRI scan of a tethered cord with a conus position at L5 and a holocord syrinx in a 49-year-old patient with a 8-month history of progressive paraparesis and severe sphincter problems. The axial images at L2 (**b**), L5 (**c**), and S1 (**d**) demonstrate the syrinx, the lipoma attached to the conus, and the extradural and epifascial extension of this hamartoma. **e** The corresponding bone window CT clearly demonstrates the bony abnormalities at S1 as well as the lipoma extension. (*Continuation see next page*)

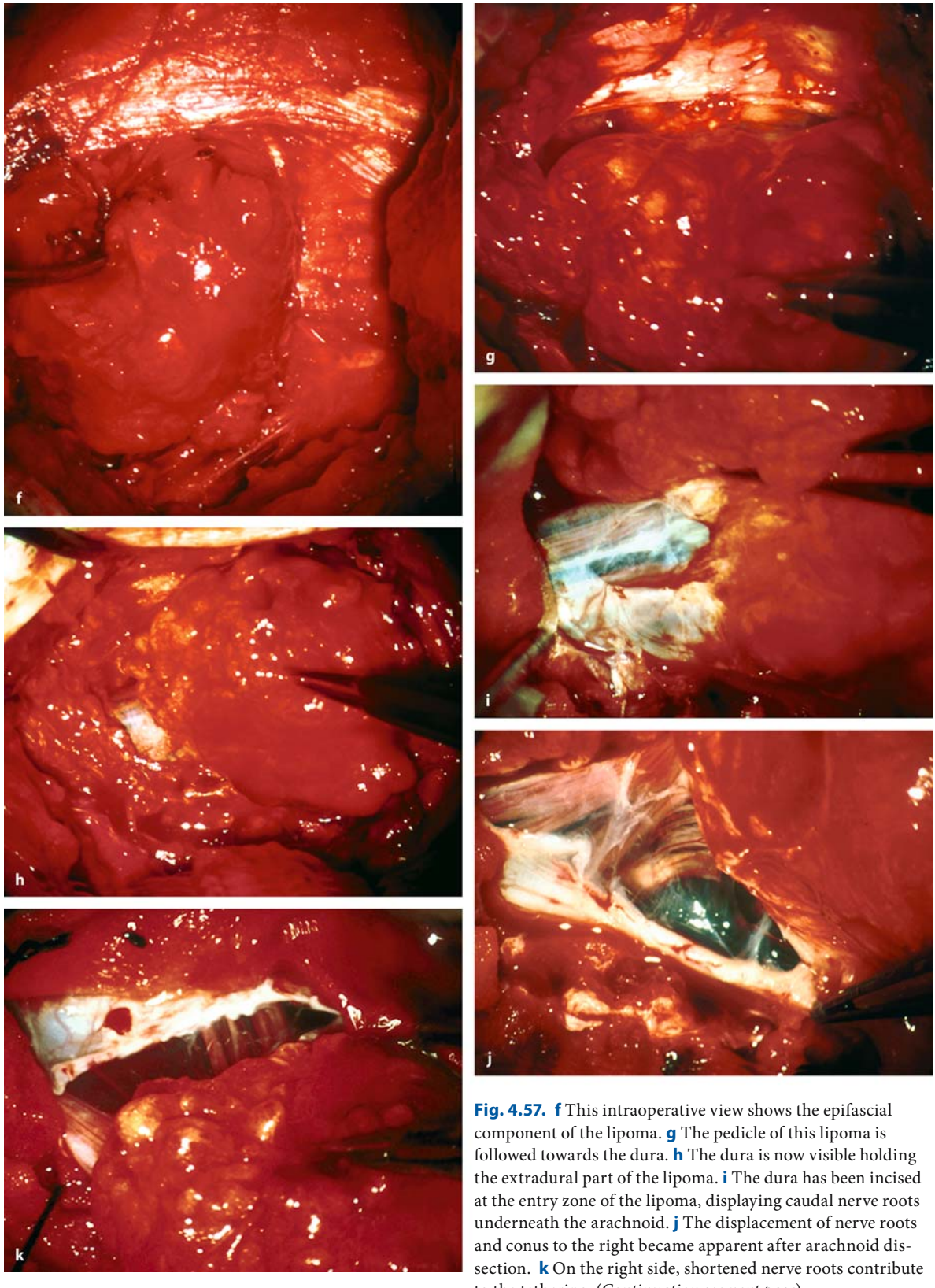

Fig. 4.57. **f** This intraoperative view shows the epifascial component of the lipoma. **g** The pedicle of this lipoma is followed towards the dura. **h** The dura is now visible holding the extradural part of the lipoma. **i** The dura has been incised at the entry zone of the lipoma, displaying caudal nerve roots underneath the arachnoid. **j** The displacement of nerve roots and conus to the right became apparent after arachnoid dissection. **k** On the right side, shortened nerve roots contribute to the tethering. (*Continuation see next page*)

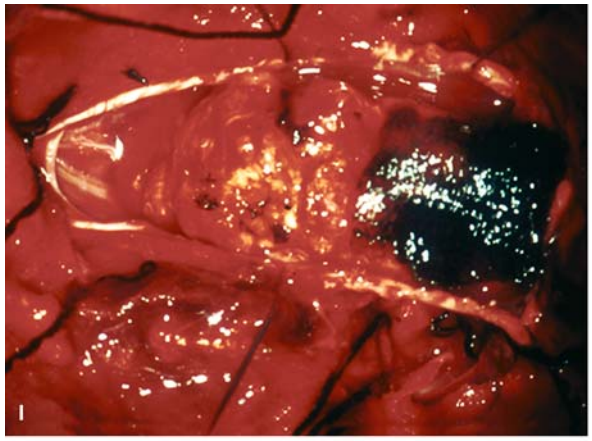

Fig. 4.57. (*Continued*) **l** At this stage, further intradural dissection was terminated. The mass of the well-vascularized lipoma had been reduced and hemostasis achieved with fibrin tissues. The dura was closed with a Gore-Tex® patch. **m** The postoperative T1-weighted MRI scan after 3 months shows a remarkable decrease of syrinx size and the healed area of surgery at L5–S1. Gait and sensory disturbances improved, while sphincter dysfunctions remained unchanged

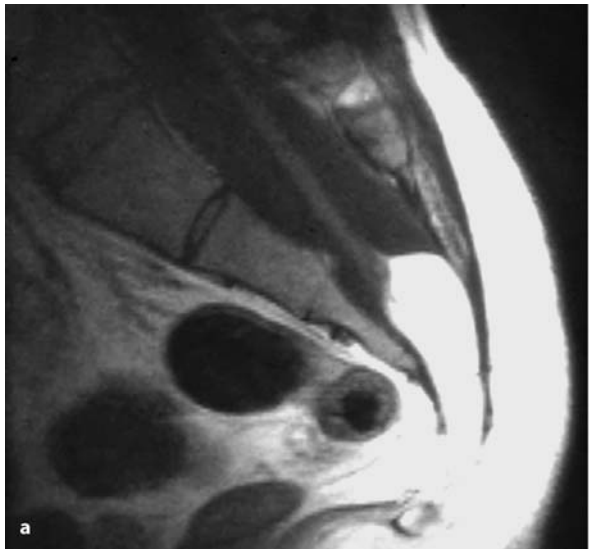

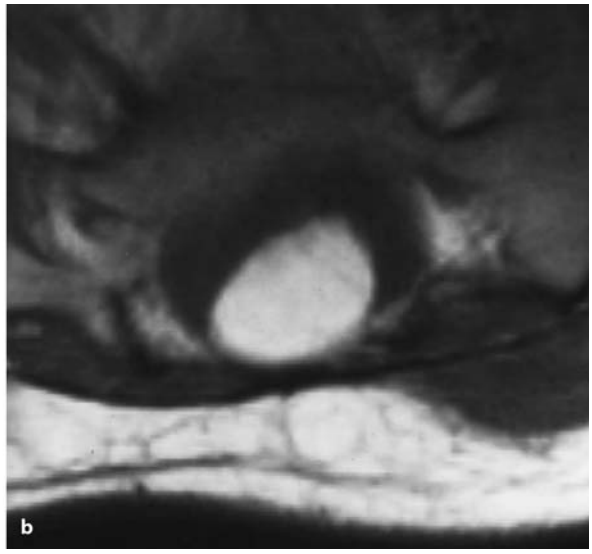

Fig. 4.58. Sagittal (**a**) and axial (**b**) T1-weighted MRI scan of a sacral conus lipoma in a 23-year-old man with a 10-year history of sphincter dysfunction and pain. (*Continuation see next page*)

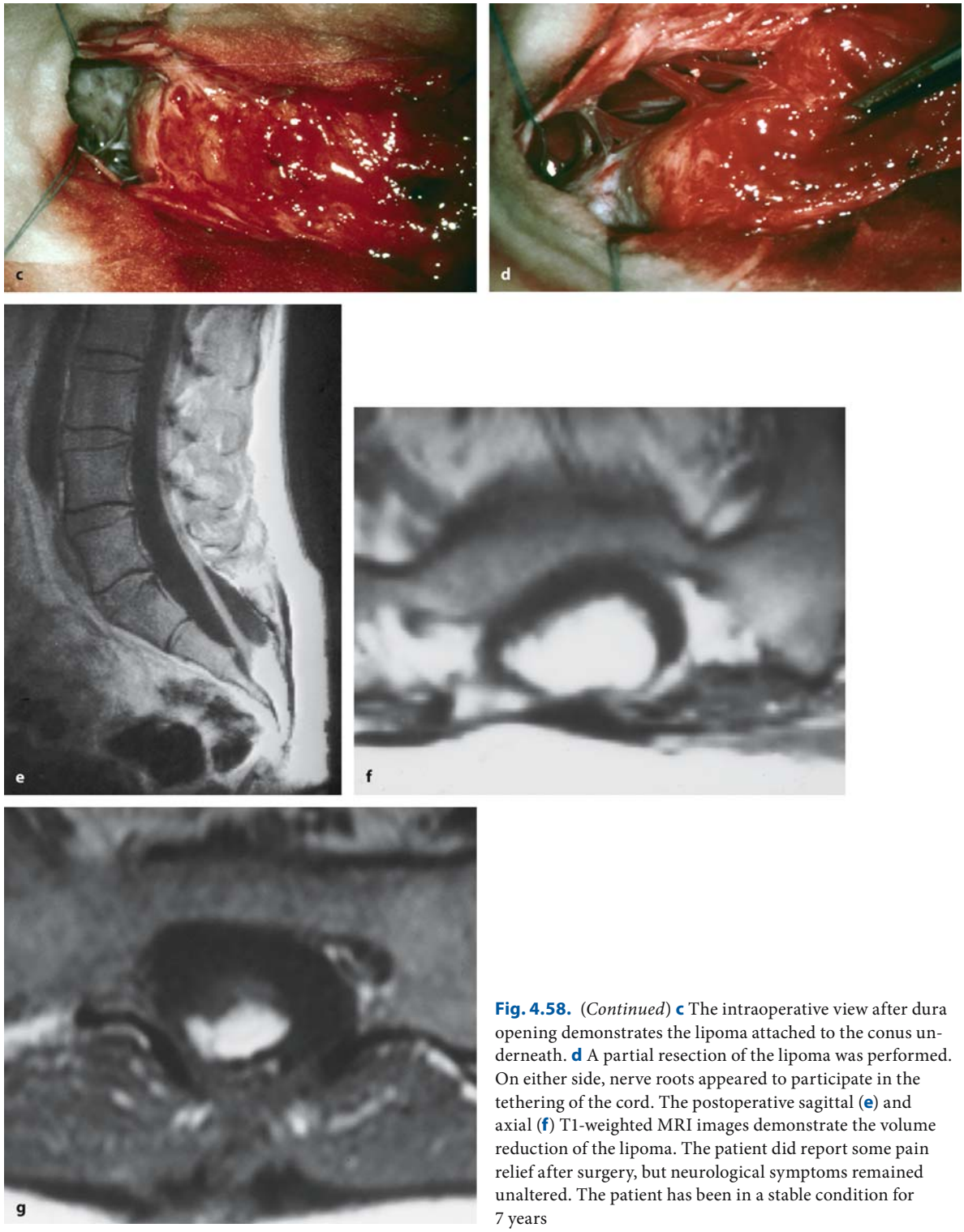

Fig. 4.58. (*Continued*) **c** The intraoperative view after dura opening demonstrates the lipoma attached to the conus underneath. **d** A partial resection of the lipoma was performed. On either side, nerve roots appeared to participate in the tethering of the cord. The postoperative sagittal (**e**) and axial (**f**) T1-weighted MRI images demonstrate the volume reduction of the lipoma. The patient did report some pain relief after surgery, but neurological symptoms remained unaltered. The patient has been in a stable condition for 7 years

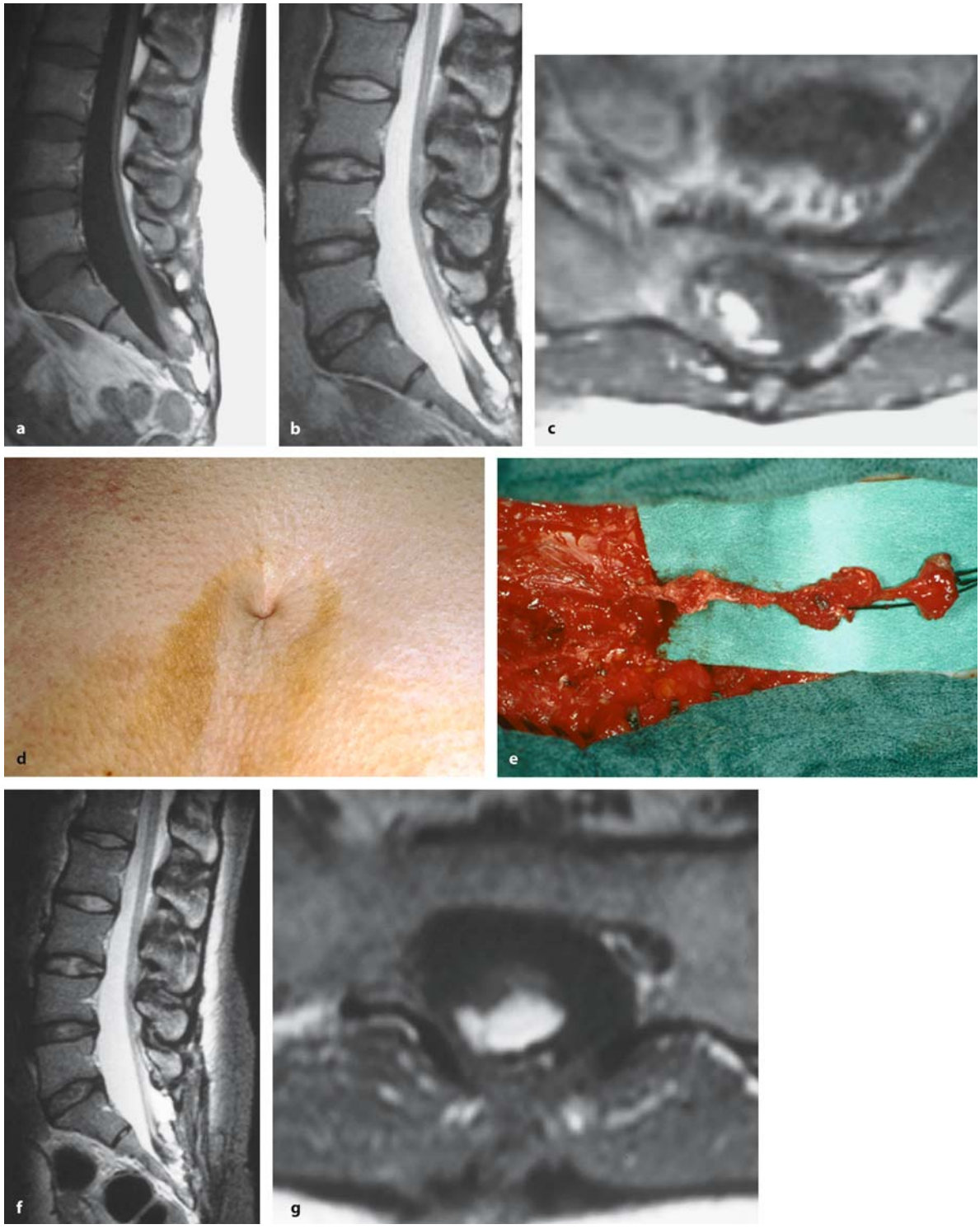

Fig. 4.59. Sagittal T1- (**a**) and T2-weighted (**b**) MRI scans of a sacral conus lipoma in a 31-year-old woman with a 9-month history of progressive paraparesis and sphincter disturbances. **c** The axial scan shows the conus turned in clockwise direction anterior to the lipoma. **d** This photograph shows the porus of a dermal sinus. **e** This sinus could be followed to the dura, but there was no communication with the subarachnoid space. After partial resection of the well-vascularized lipoma, tethered nerve roots prevented further intradural dissections and a Gore-Tex® duraplasty was inserted. The postoperative T2- (**f**) and T1-weighted (**g**) MRI images display a good decompression of the conus without adhesion to the graft. Postoperatively, symptoms remained unchanged but stable

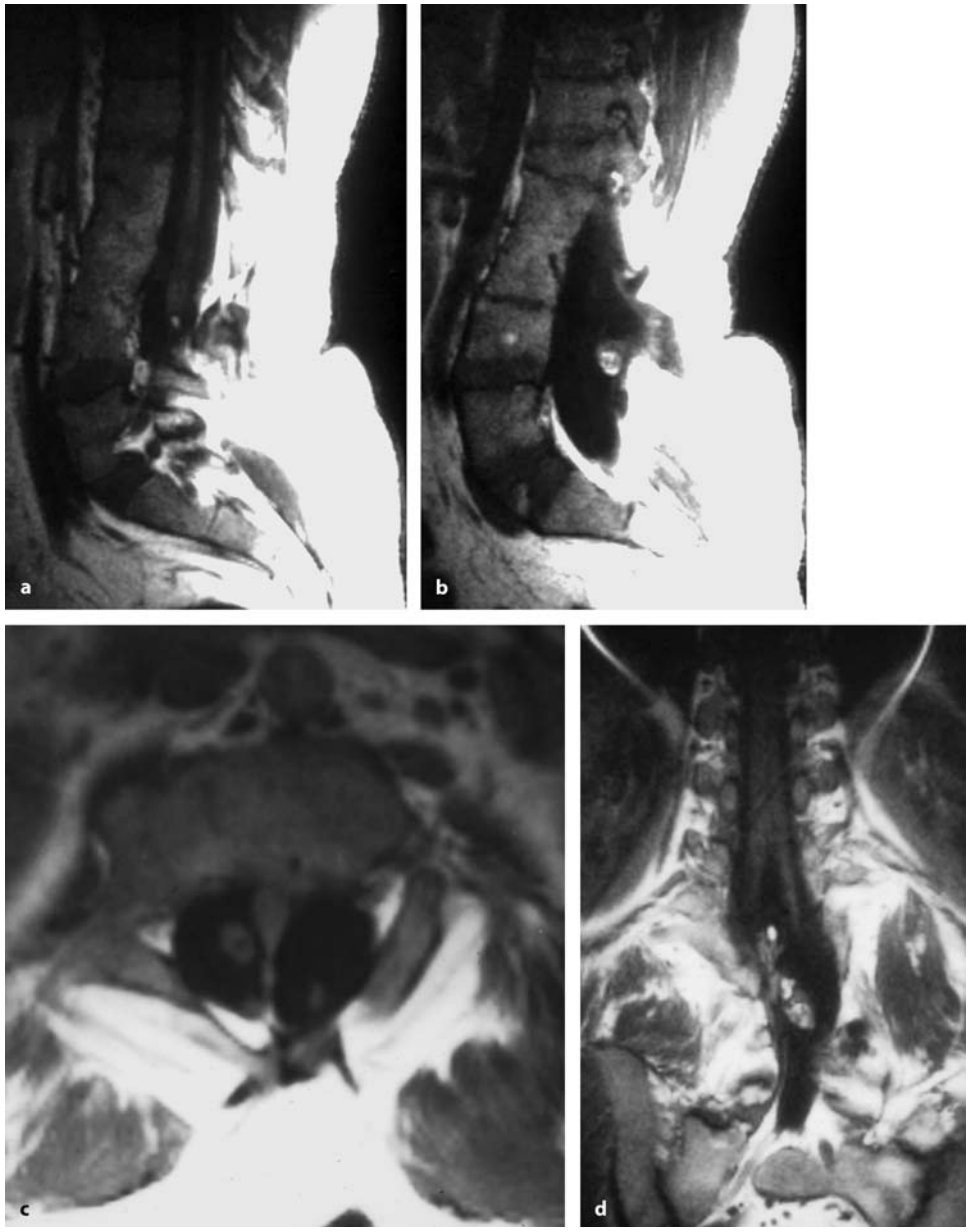

Fig. 4.60. These sagittal T1-weighted MRI scans demonstrate a tethered cord with a conus position at L4 (**a**) and a hamartoma at that level (**b**). L2 and L3 are fused (i.e., Klippel-Feil syndrome). **c** The axial scan shows a bony spur at L3 and a diastematomyelia (i.e. a split-cord malformation type 1). **d** Finally, the coronal scan shows the hamartoma underneath this spur at L4–L5. The patient complained about pain and a slight paresis of his left leg. The patient declined surgery

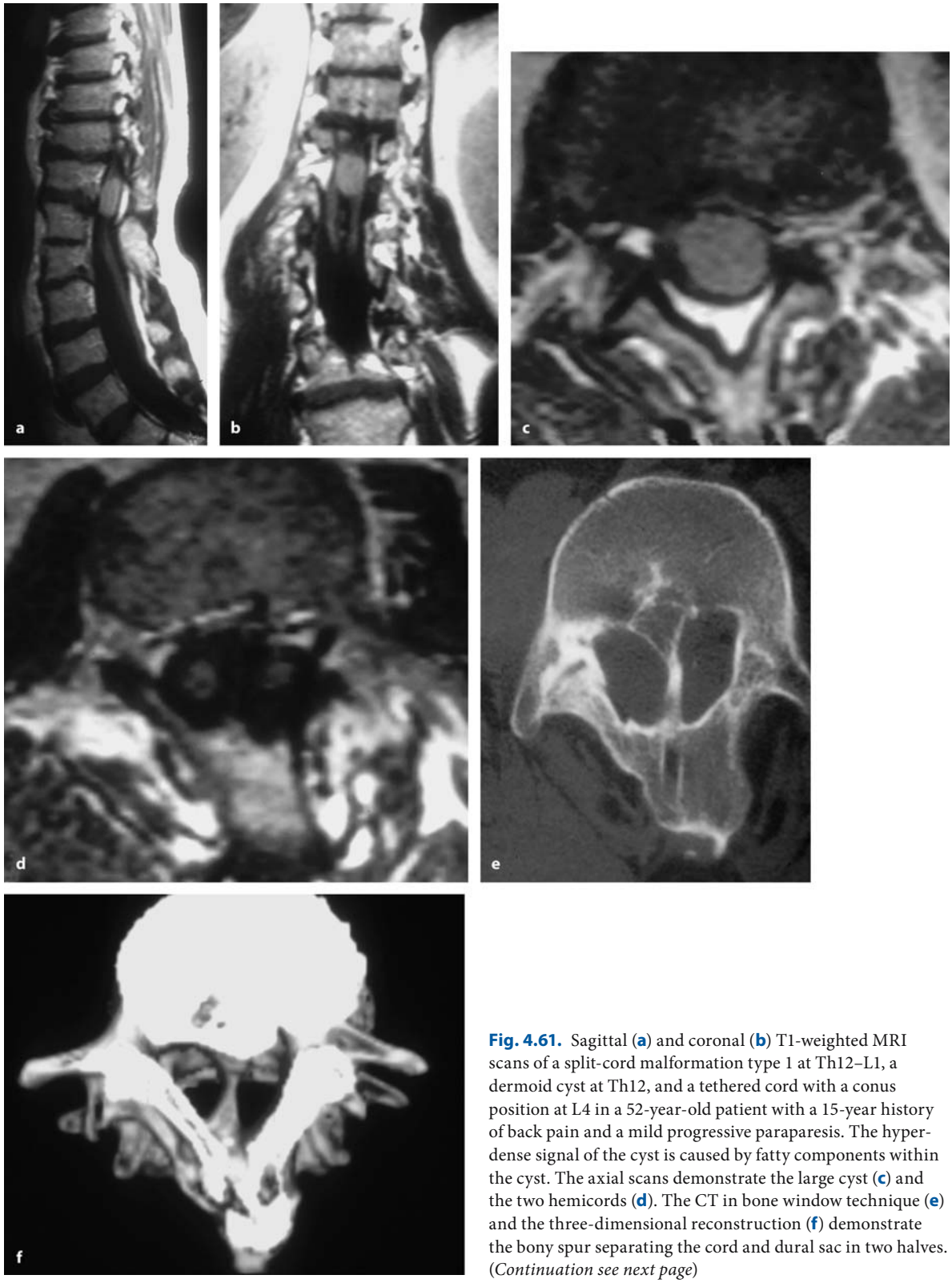

Fig. 4.61. Sagittal (**a**) and coronal (**b**) T1-weighted MRI scans of a split-cord malformation type 1 at Th12–L1, a dermoid cyst at Th12, and a tethered cord with a conus position at L4 in a 52-year-old patient with a 15-year history of back pain and a mild progressive paraparesis. The hyperdense signal of the cyst is caused by fatty components within the cyst. The axial scans demonstrate the large cyst (**c**) and the two hemicords (**d**). The CT in bone window technique (**e**) and the three-dimensional reconstruction (**f**) demonstrate the bony spur separating the cord and dural sac in two halves. (*Continuation see next page*)

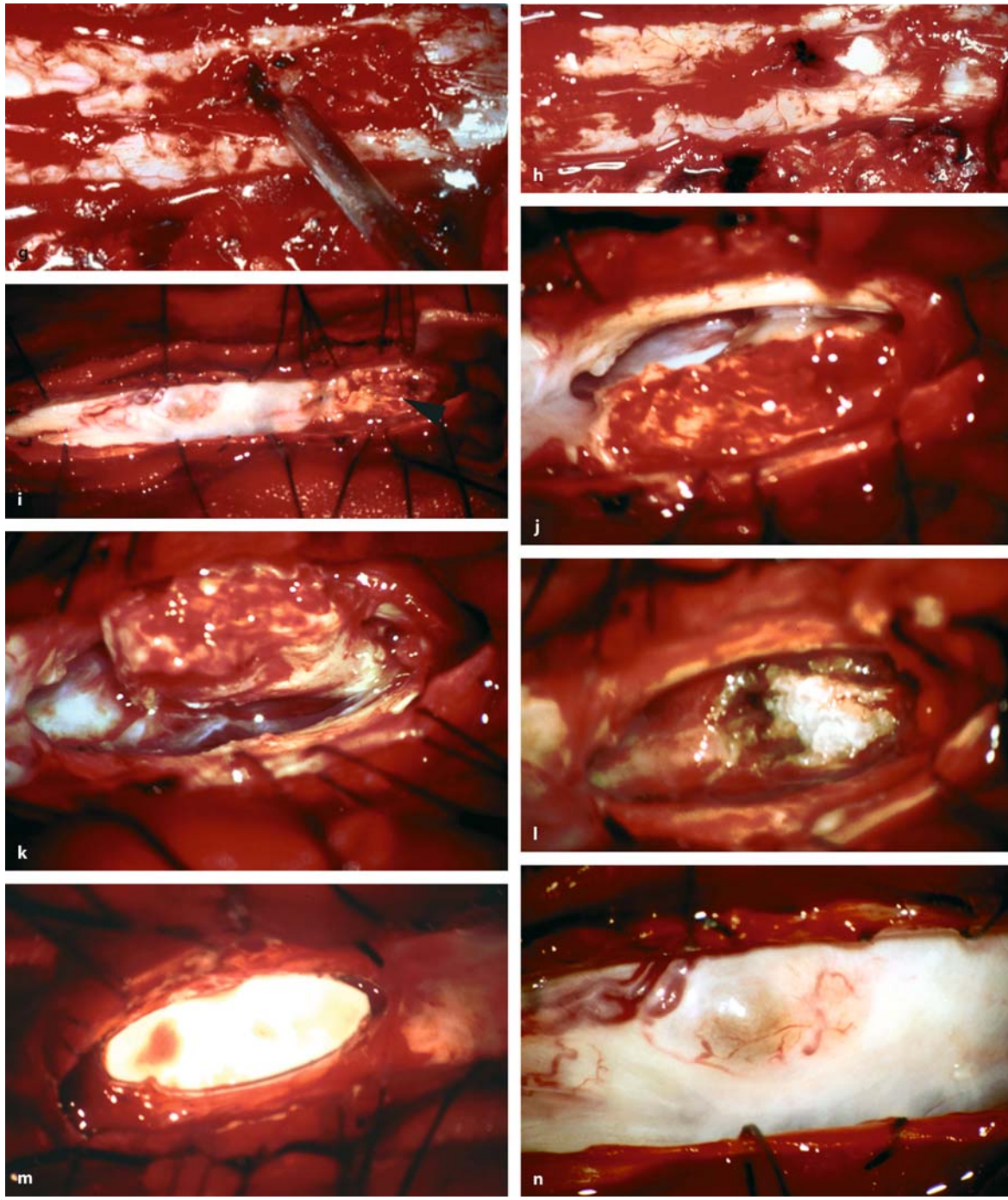

Fig. 4.61. g This intraoperative view shows the removal of the bony spur with a rongeur. After resection of the spur (**h**), the dura is incised (**i**) revealing a considerable amount of arachnoid scarring due to a previous operation that had just punctured the cyst. On the right side the soft tissue between both hemicords marks the former position of the bony spur (*arrow* in **i**). On the left side the dermoid cyst can be seen almost bulging out. **j**, **k** The dura pedicle, which had surrounded the bony spur, is dissected free from both hemicords. **l** This view shows the situation after resection of all soft tissue between both hemicords. **m** The small anterior dura defect is closed with a small patch. **n** This close-up view shows the dermoid cyst surrounded by arachnoid scarring. There appears to be no clearcut demarcation between arachnoid, cyst wall, and spinal cord surface. (*Continuation see next page*)

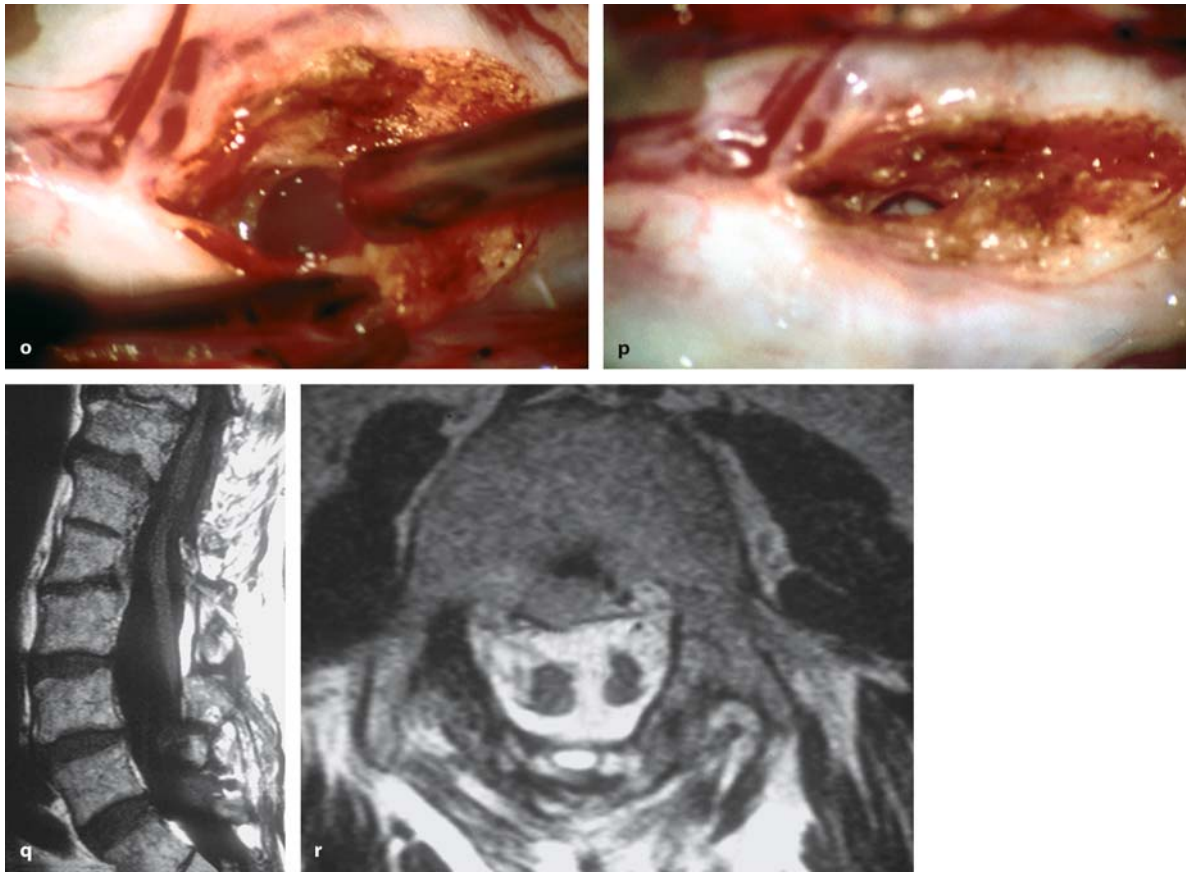

Fig. 4.61. (*Continued*) The cyst was opened revealing mucinous material (**o**) and the cyst wall resected (**p**). The dura was closed with a Gore-Tex® patch. The postoperative sagittal T1- (**q**) and axial T2-weighted (**r**) MRI scans demonstrate the complete resection of the dermoid cyst and untethering of the cord. The filum terminale was transected in a separate operation. Pain improved postoperatively, with stabilization of neurological symptoms for 8 years

Fig. 4.62. Sagittal T1- (**a**) and T2-weighted (**b**) MRI scans of a split-cord malformation type 2 at Th11 associated with a tethered cord, a conus position at L2, and a small syrinx at Th9–Th10 in a 46-year-old woman with a 18-month history of a slight paraparesis accompanied by pain and mild sphincter disturbances. (*Continuation see next page*)

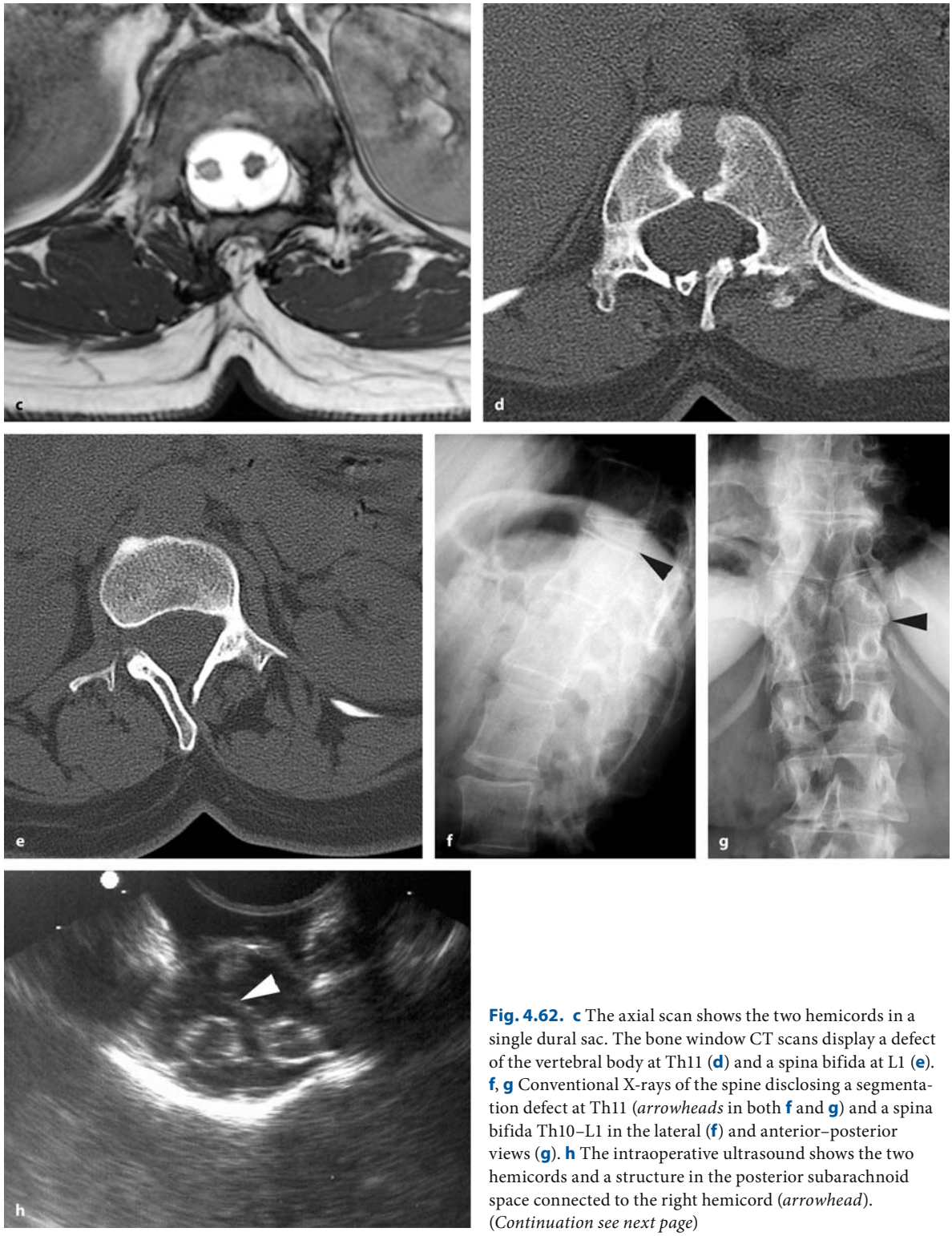

Fig. 4.62. **c** The axial scan shows the two hemicords in a single dural sac. The bone window CT scans display a defect of the vertebral body at Th11 (**d**) and a spina bifida at L1 (**e**). **f**, **g** Conventional X-rays of the spine disclosing a segmentation defect at Th11 (*arrowheads* in both **f** and **g**) and a spina bifida Th10–L1 in the lateral (**f**) and anterior–posterior views (**g**). **h** The intraoperative ultrasound shows the two hemicords and a structure in the posterior subarachnoid space connected to the right hemicord (*arrowhead*). (*Continuation see next page*)

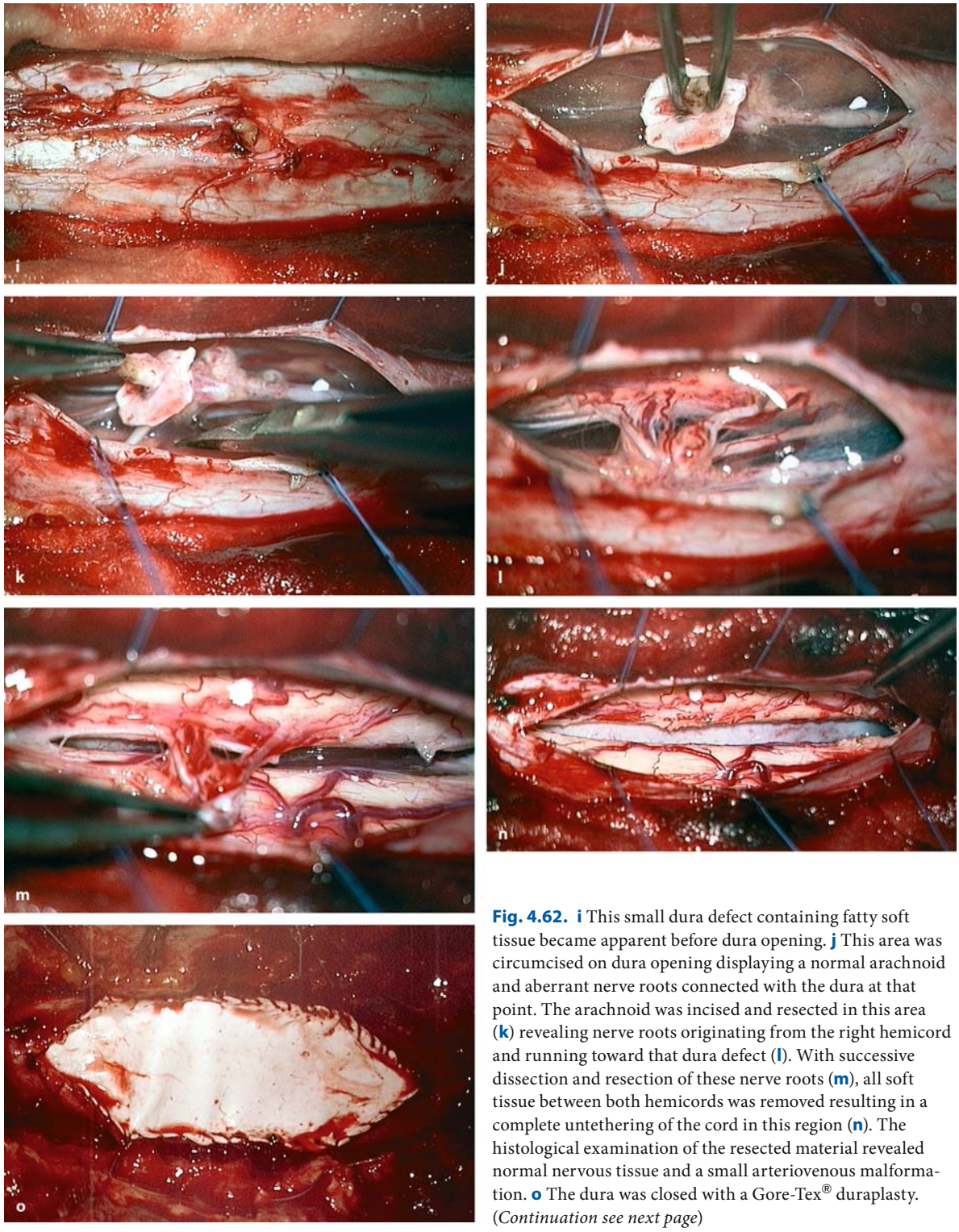

Fig. 4.62. **i** This small dura defect containing fatty soft tissue became apparent before dura opening. **j** This area was circumcised on dura opening displaying a normal arachnoid and aberrant nerve roots connected with the dura at that point. The arachnoid was incised and resected in this area (**k**) revealing nerve roots originating from the right hemicord and running toward that dura defect (**l**). With successive dissection and resection of these nerve roots (**m**), all soft tissue between both hemicords was removed resulting in a complete untethering of the cord in this region (**n**). The histological examination of the resected material revealed normal nervous tissue and a small arteriovenous malformation. **o** The dura was closed with a Gore-Tex® duraplasty. (*Continuation see next page*)

Fig. 4.62. (*Continued*) At L5/S1 the filum terminale was transected as well. The postoperative sagittal (**p**, **q**) and axial (**r**) T2-weighted MRI scans show an unchanged syrinx, a free CSF passage in the operative region, and no adhesion of either hemicord to the dura. The patient reported improvement of pain and dysesthesias and an otherwise unchanged but stable neurological situation

4.3.1.2 Removal of Cystic Tumors

4.3.1.2.1 Removal of Cystic Hamartomas

Cystic hamartomas may present some particular features that demand special surgical measures. Among dysraphic cysts, dermoid (Figs. 4.54, 4.61, and 4.63), neurenteric (Fig. 4.64), and neuroepithelial cysts (Fig. 4.38) can be distinguished. As mentioned earlier for lipomas, cystic hamartomas may also be associated with other dysraphic manifestations such as, for example, a tethered cord (Figs. 4.54 and 4.61) or a split-cord malformation (Fig. 4.61). The strategy for removal of a cyst is different compared to that for a solid tumor. The cyst content may contain irritating substances that should not contaminate the subarachnoid space – this holds particularly true for dermoid cysts (Figs. 4.54, 4.61, and 4.63). The cyst wall may be adherent to the nerve roots and spinal cord, and yet be rather fragile (Figs. 4.38, 4.54, 4.61, and 4.64). Therefore, radicality is not always easy to achieve, nor is it required in each instance [162]. With anteriorly located cysts, an anterior or lateral approach may be useful whenever the cyst can be expected to be adherent to surrounding structures and a radical removal needs to be obtained. Otherwise, the spinal cord may completely obscure the remainder of the cyst wall once part of it is resected and the cyst has collapsed.

With dysraphic cysts, extension over multiple segments is unusual. The cells of the cyst wall may produce substances that may accumulate and cause reformation of the cyst and/or severe arachnoid irritations. Therefore, excision of the entire cyst wall has to be the aim of surgery (Figs. 4.38, 4.53, 4.63, and 4.64). If necessary, sharp dissection is used to mobilize it away from the surrounding structures (Figs. 4.38, 4.53, and 4.63). If the cyst is not amenable to removal in toto, we make a small incision into the cyst wall and remove the content by suction or with forceps (Fig. 4.61). In such a situation, we recommend protection of the surrounding structures with cottonoids. Not too much of the cyst contents should be removed before mobilizing the cyst wall. A completely flaccid cyst wall may be difficult to dissect from nerve roots or other structures. If the cyst wall is densely adherent to nerve roots, vessels, or the cord surfaces, radicality may be impossible to achieve without undue risks; cases of recurrent dysraphic cysts are almost never resected radically. To limit postoperative arachnoid scarring, we again recommend a duraplasty in such instances (Figs. 4.54, 4.61, and 4.63).

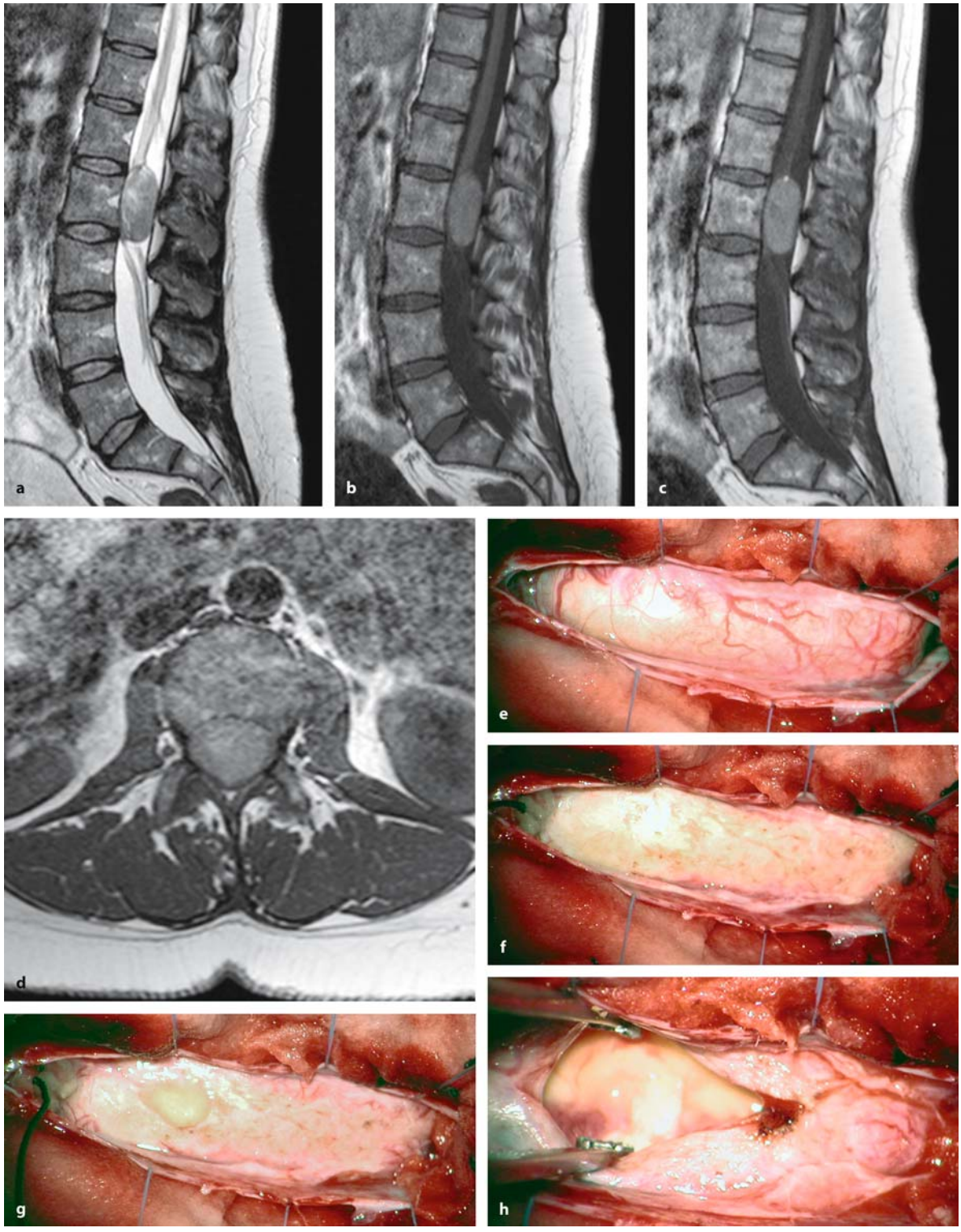

Fig. 4.63. Sagittal T2- (**a**), T1-weighted MRI scan without (**b**) and with contrast (**c**) of a dermoid cyst at L2 in a 40-year-old woman with a 2-year history of pain and slight sphincter problems. **d** The axial scan shows the considerable size of this hamartoma with displacement of the cord to the left. **e** This intraoperative view demonstrates the cyst attached to the spinal cord. **f** After arachnoid dissection and coagulation of surface vessels, this picture displays the capsule of the dermoid. With incision of the capsule a yellowish substance can be evacuated (**g**) and cyst contents emptied with tumor forceps (**h**). (*Continuation see next page*)

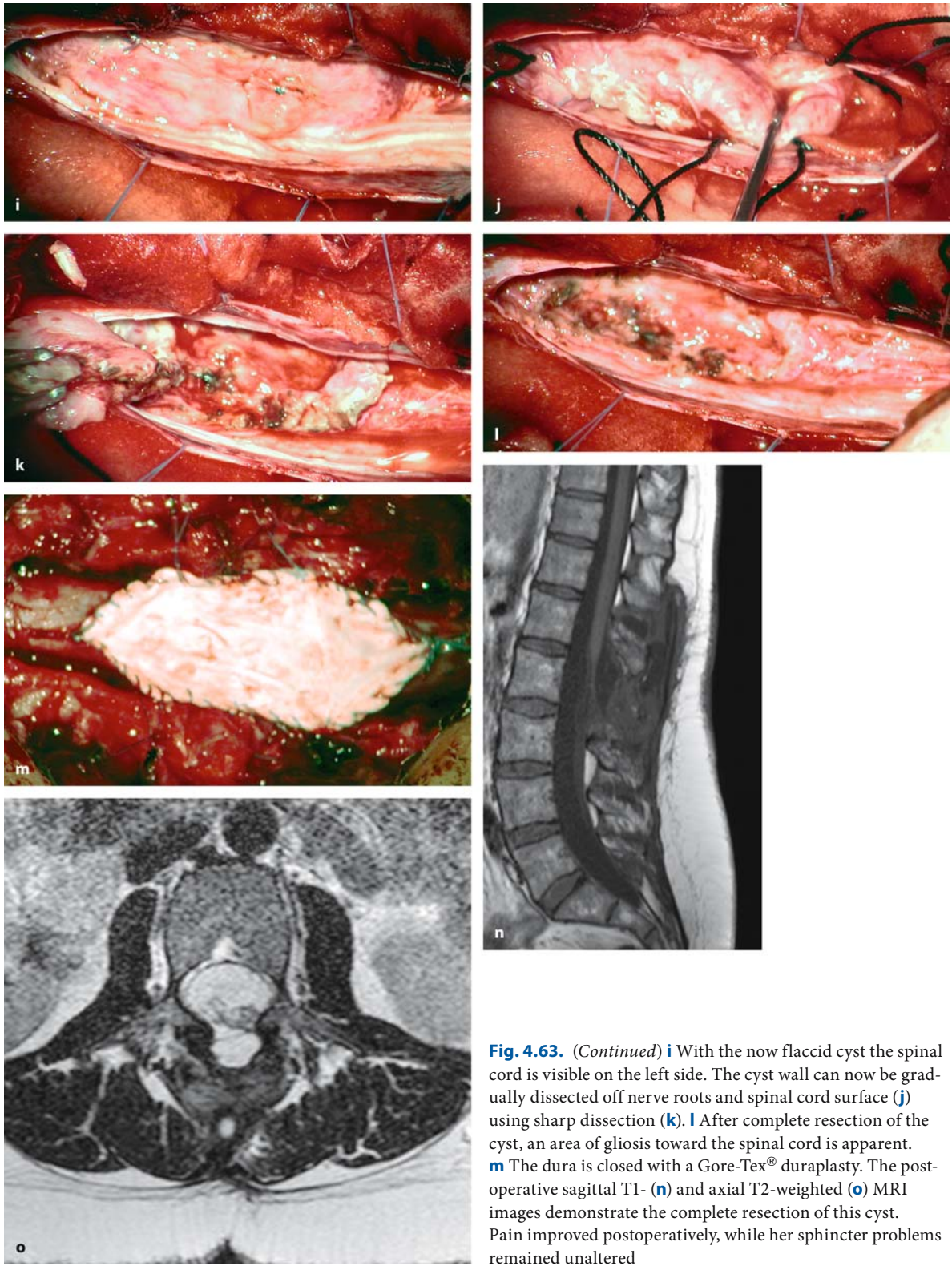

Fig. 4.63. (*Continued*) **i** With the now flaccid cyst the spinal cord is visible on the left side. The cyst wall can now be gradually dissected off nerve roots and spinal cord surface (**j**) using sharp dissection (**k**). **l** After complete resection of the cyst, an area of gliosis toward the spinal cord is apparent. **m** The dura is closed with a Gore-Tex® duraplasty. The postoperative sagittal T1- (**n**) and axial T2-weighted (**o**) MRI images demonstrate the complete resection of this cyst. Pain improved postoperatively, while her sphincter problems remained unaltered

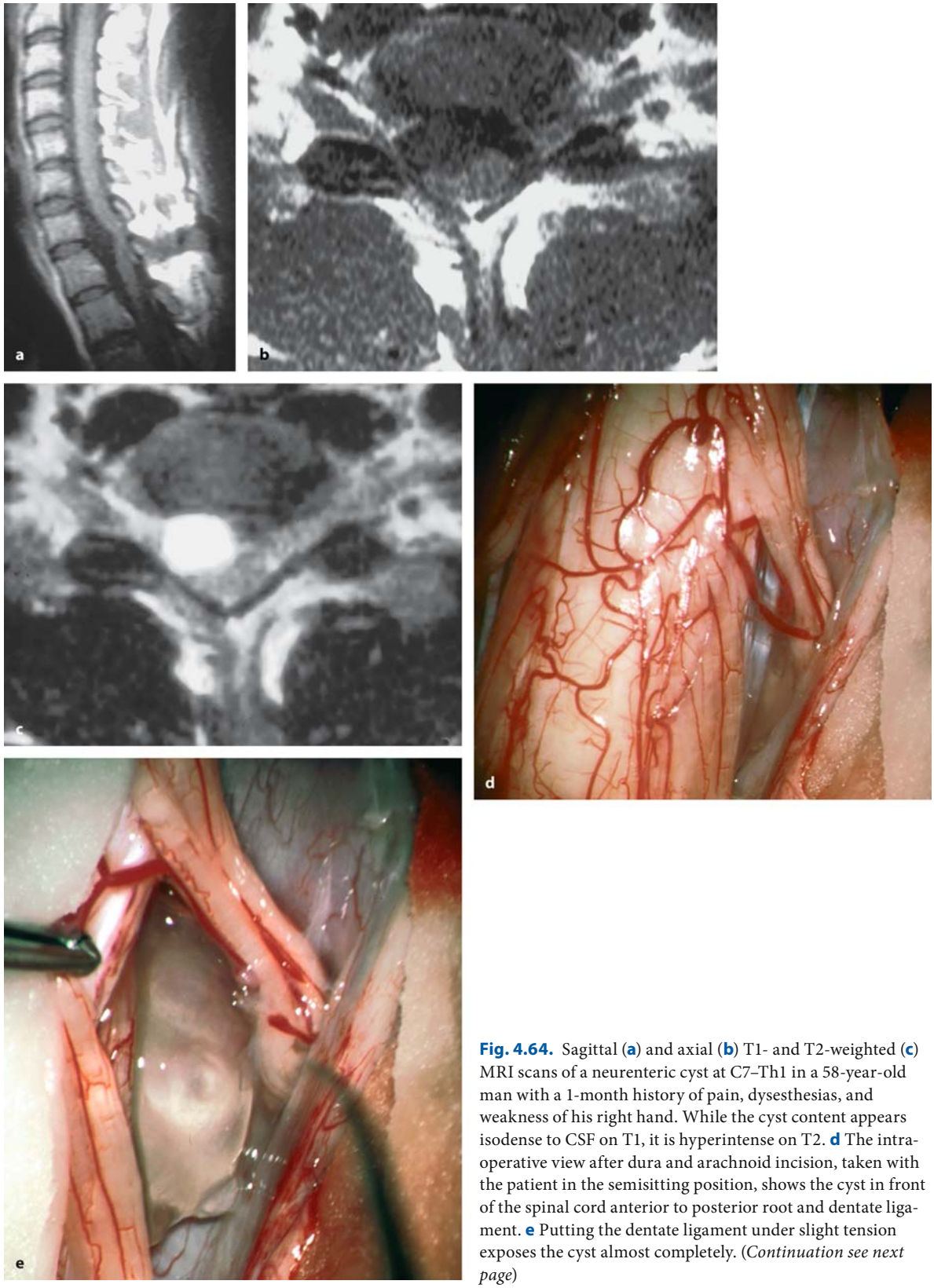

Fig. 4.64. Sagittal (**a**) and axial (**b**) T1- and T2-weighted (**c**) MRI scans of a neurenteric cyst at C7–Th1 in a 58-year-old man with a 1-month history of pain, dysesthesias, and weakness of his right hand. While the cyst content appears isodense to CSF on T1, it is hyperintense on T2. **d** The intraoperative view after dura and arachnoid incision, taken with the patient in the semisitting position, shows the cyst in front of the spinal cord anterior to posterior root and dentate ligament. **e** Putting the dentate ligament under slight tension exposes the cyst almost completely. (*Continuation see next page*)

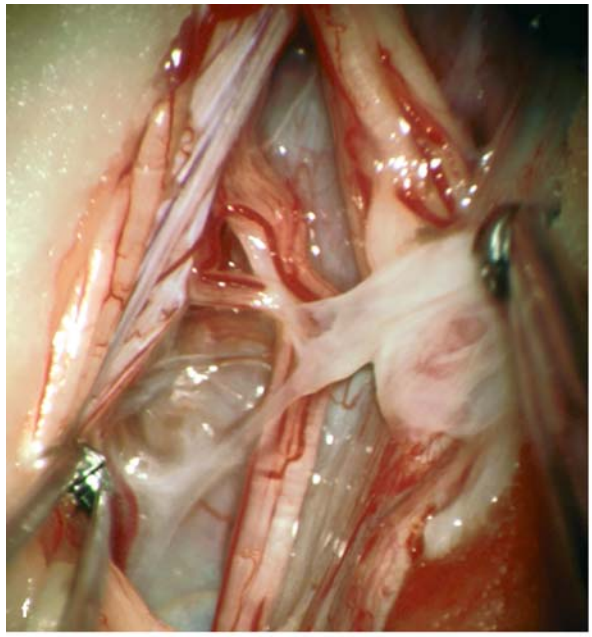

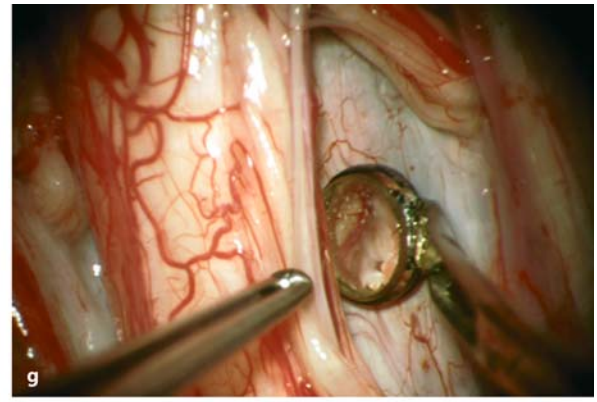

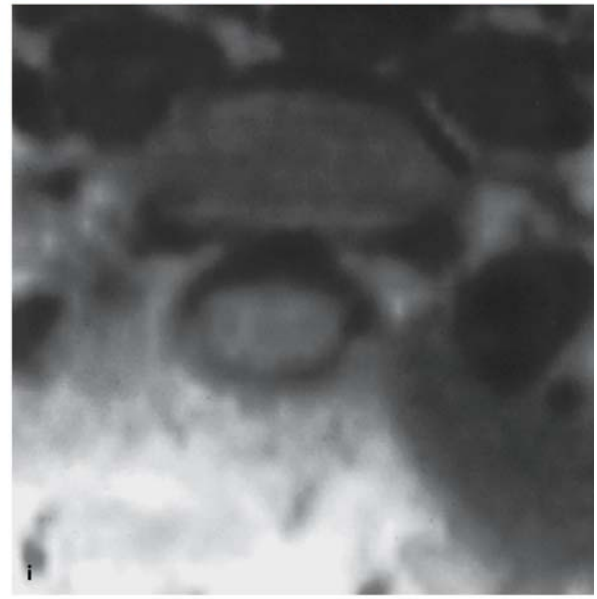

Fig. 4.64. (*Continued*) **f** The cyst has been opened and its wall is now removed with blunt dissection using two fine forceps. **g** After removal, a small mirror is used to ensure a complete resection in the blind angle anteriorly. The postoperative sagittal (**h**) and axial (**i**) T1-weighted images demonstrate a complete resection of the cyst. Postoperatively, the patient made a complete recovery and has been free of a recurrence for 10 years

4.3.1.2.2 Surgery for Arachnoid Cysts

With arachnoid cysts the objective is a wide fenestration of the cyst wall to ensure decompression of the spinal cord and a permanent unobstructed flow of CSF. Excision of the entire cyst wall is performed in small cysts only (Figs. 4.34 and 4.65). In particular, it is not advisable to remove parts of the cyst wall, which are adherent to major cord vessels, cervical or lumbar nerve roots, or the spinal cord surface, and represent the intermediate leptomeningeal layer, as outlined in the anatomy section. However, the long-term success of the operation not only requires a sufficient decompression of the cord and establishment of a free CSF passage, but also minimization of postoperative arachnoid adhesions. These may give rise to CSF flow obstructions, formation of arachnoid pouches, or even reformation of an encapsulated arachnoid cyst. Therefore, we advise focusing arachnoid dissection on a wide fenestration of the cyst wall in an uncritical area (Figs. 4.66 and 4.67). Blunt dissection carries the risk of tearing small vessels embedded in the arach-

Fig. 4.65. Sagittal T1- (**a**) and T2- weighted (**b**) MRI scans of an arachnoid cyst at Th3–Th4 in a 34-year-old woman with a 4-year history of back pain and a slight paraparesis. The T2-image shows the cyst wall quite clearly. **c** The axial image demonstrates the considerable cord compression. **d**, **e** The cardiac gated cine MRI images in systole (**d**) and diastole (**e**) show the corresponding flow disturbances in this area (*arrowheads*). **f** The intraoperative ultrasound demonstrates the pathology and the compressed cord underneath.
(*Continuation see next page*)

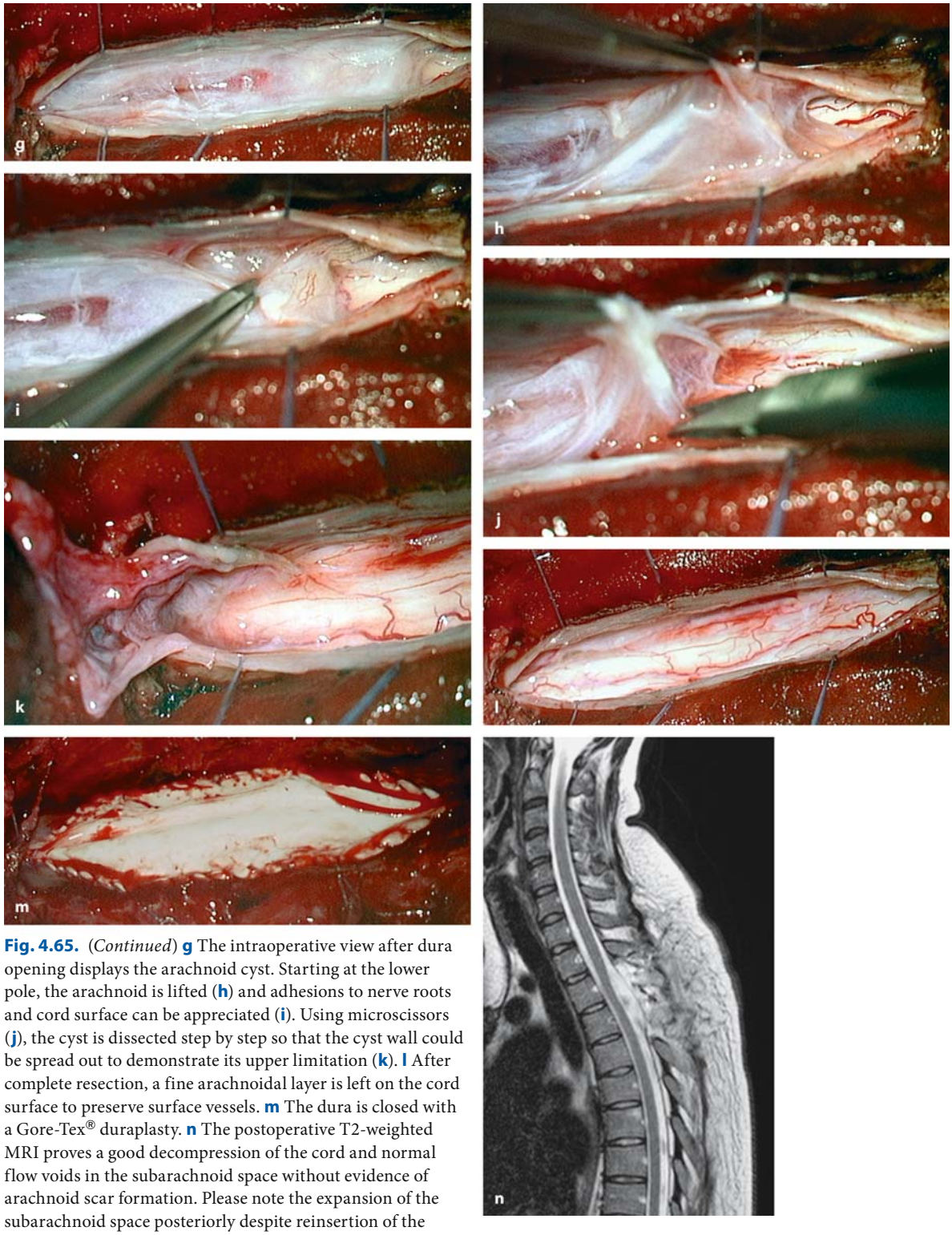

Fig. 4.65. (*Continued*) **g** The intraoperative view after dura opening displays the arachnoid cyst. Starting at the lower pole, the arachnoid is lifted (**h**) and adhesions to nerve roots and cord surface can be appreciated (**i**). Using microscissors (**j**), the cyst is dissected step by step so that the cyst wall could be spread out to demonstrate its upper limitation (**k**). **l** After complete resection, a fine arachnoidal layer is left on the cord surface to preserve surface vessels. **m** The dura is closed with a Gore-Tex® duraplasty. **n** The postoperative T2-weighted MRI proves a good decompression of the cord and normal flow voids in the subarachnoid space without evidence of arachnoid scar formation. Please note the expansion of the subarachnoid space posteriorly despite reinsertion of the laminae. Pain improved postoperatively, while the remaining complaints were left unchanged

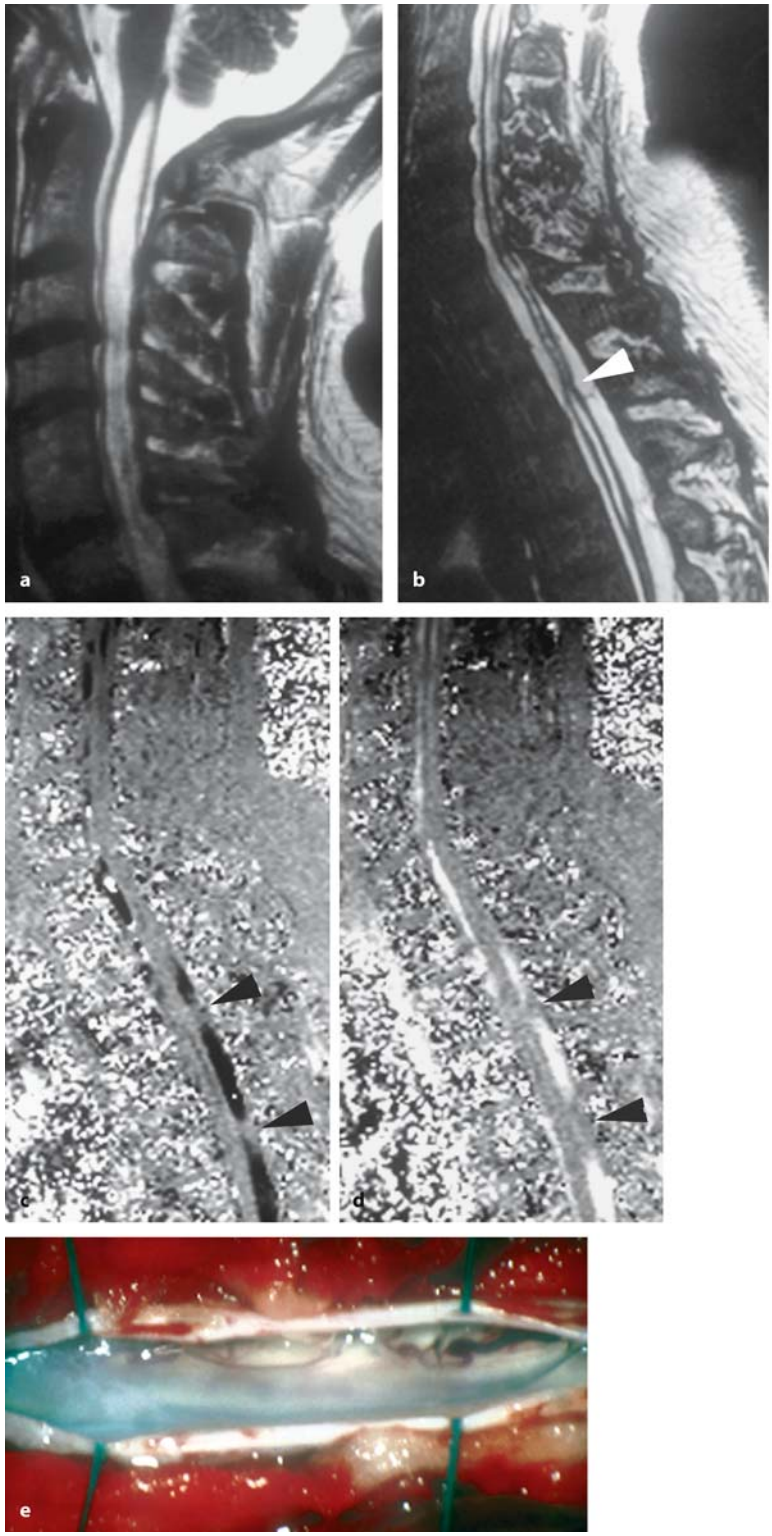

Fig. 4.66. a, b These sagittal T2-weighted MRI scans demonstrate a cervicothoracic syrinx related to an arachnoid cyst at Th2–Th4 in a 48-year-old man with a 4-month history of pain, dysesthesias, and a slight paraparesis. Apart from a little denting of the cord at Th2 (*arrowhead*) there is no cord compression detectable. **c, d** The cardiac gated cine MRI in systole (**c**) and diastole (**d**) demonstrate the extension of the cyst (*arrowheads*). **e** This intraoperative view after dura opening at Th2 shows the upper pole of this arachnoid cyst. (*Continuation see next page*)

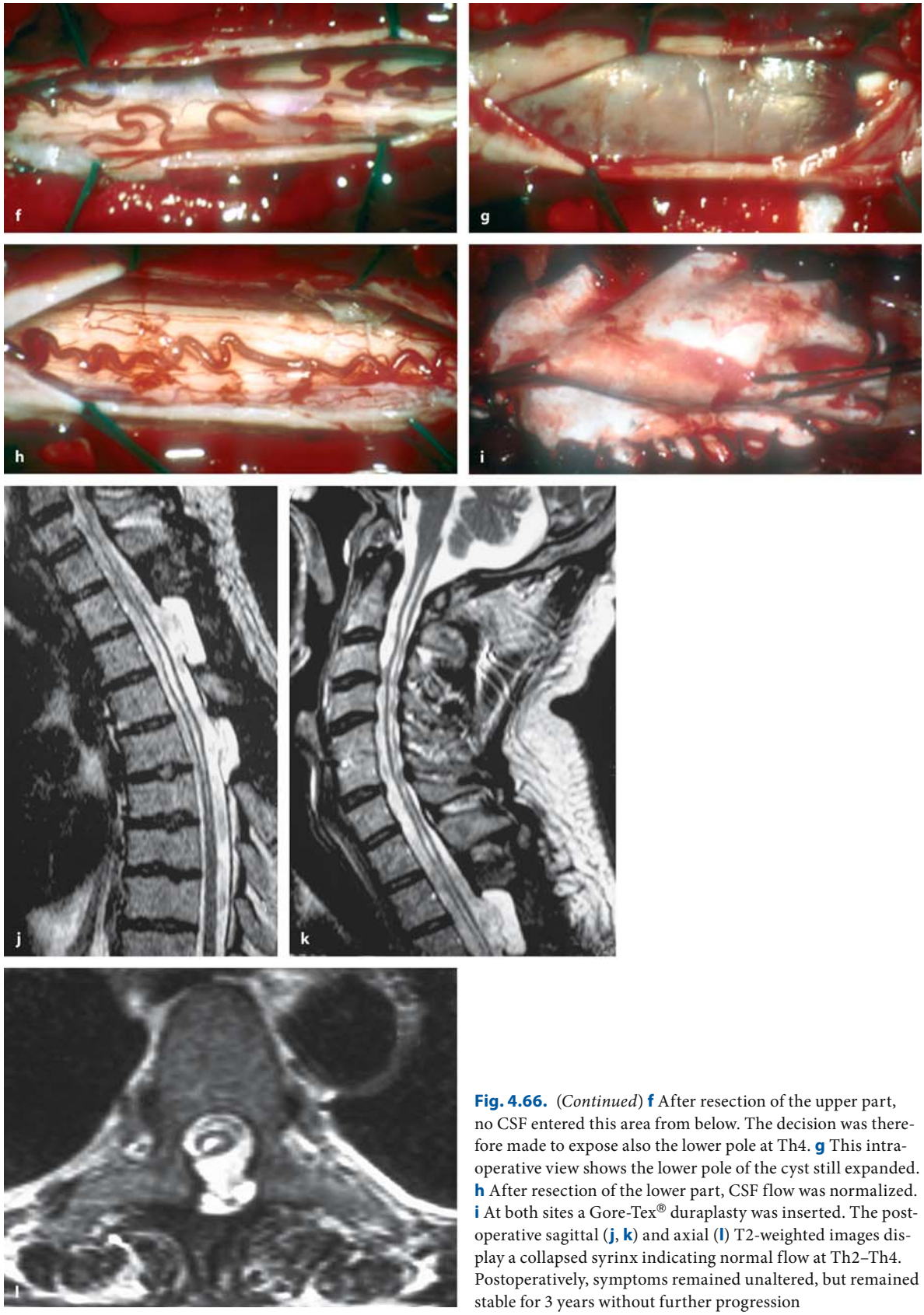

Fig. 4.66. (*Continued*) **f** After resection of the upper part, no CSF entered this area from below. The decision was therefore made to expose also the lower pole at Th4. **g** This intraoperative view shows the lower pole of the cyst still expanded. **h** After resection of the lower part, CSF flow was normalized. **i** At both sites a Gore-Tex® duraplasty was inserted. The postoperative sagittal (**j**, **k**) and axial (**l**) T2-weighted images display a collapsed syrinx indicating normal flow at Th2–Th4. Postoperatively, symptoms remained unaltered, but remained stable for 3 years without further progression

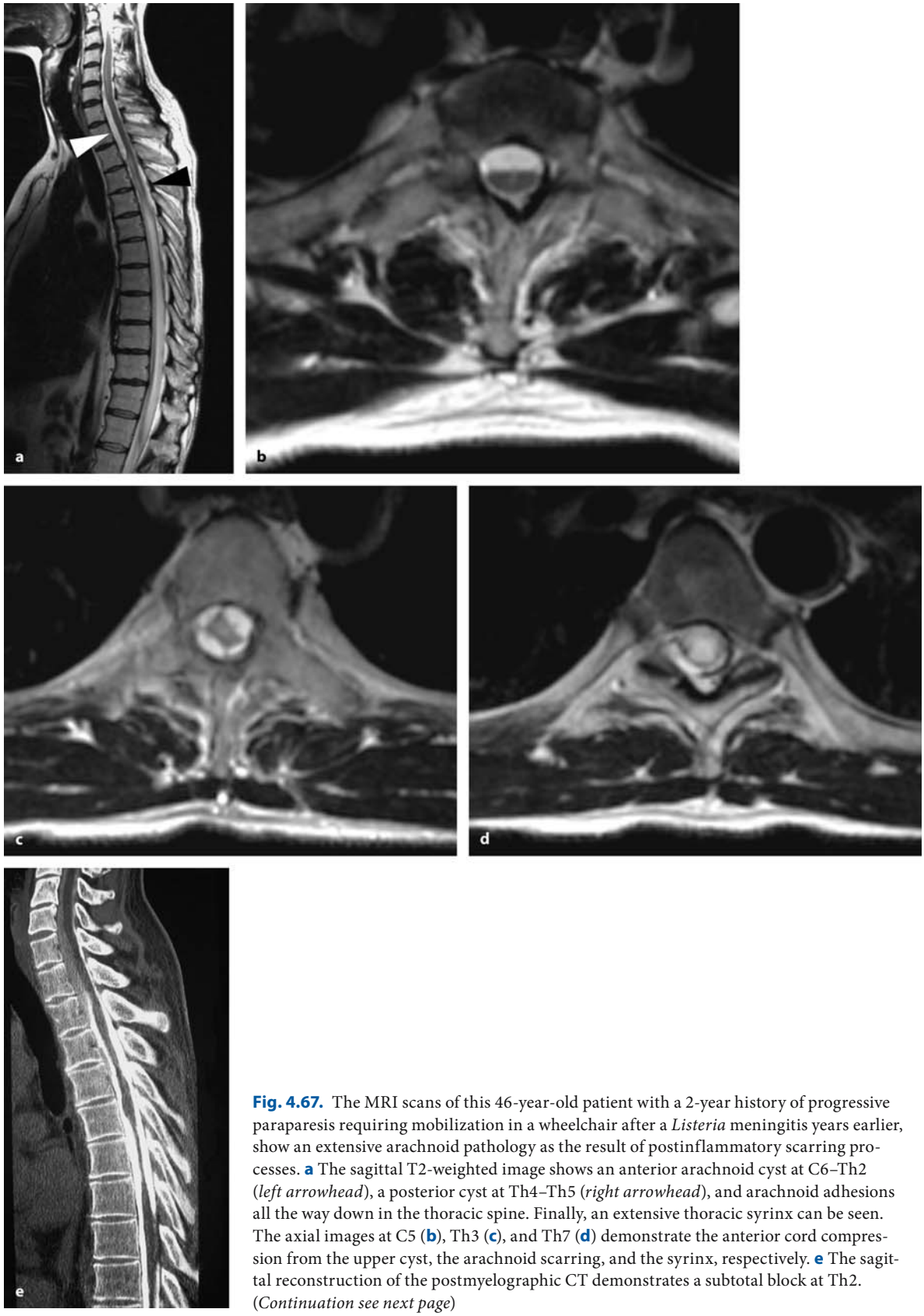

Fig. 4.67. The MRI scans of this 46-year-old patient with a 2-year history of progressive paraparesis requiring mobilization in a wheelchair after a *Listeria* meningitis years earlier, show an extensive arachnoid pathology as the result of postinflammatory scarring processes. **a** The sagittal T2-weighted image shows an anterior arachnoid cyst at C6–Th2 (*left arrowhead*), a posterior cyst at Th4–Th5 (*right arrowhead*), and arachnoid adhesions all the way down in the thoracic spine. Finally, an extensive thoracic syrinx can be seen. The axial images at C5 (**b**), Th3 (**c**), and Th7 (**d**) demonstrate the anterior cord compression from the upper cyst, the arachnoid scarring, and the syrinx, respectively. **e** The sagittal reconstruction of the postmyelographic CT demonstrates a subtotal block at Th2. (*Continuation see next page*)

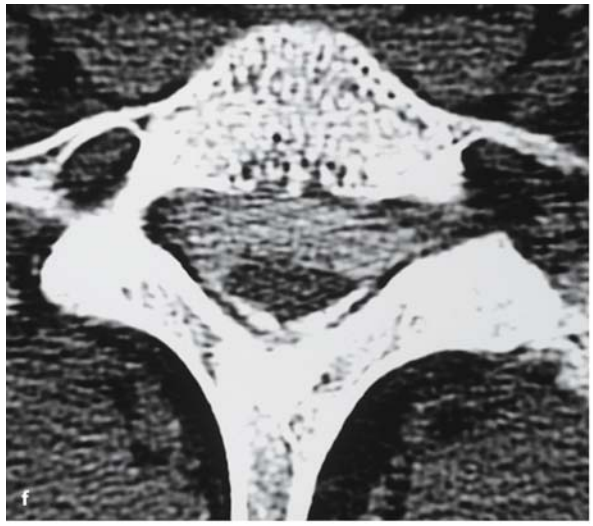

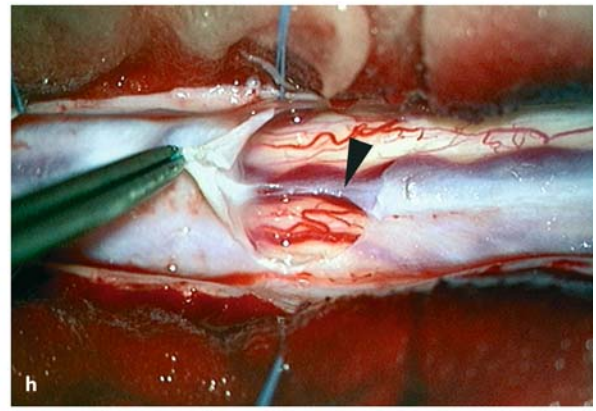

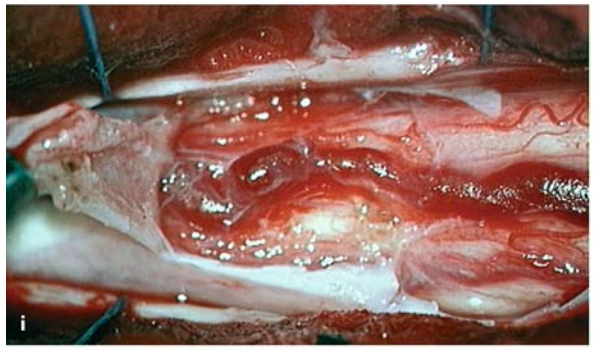

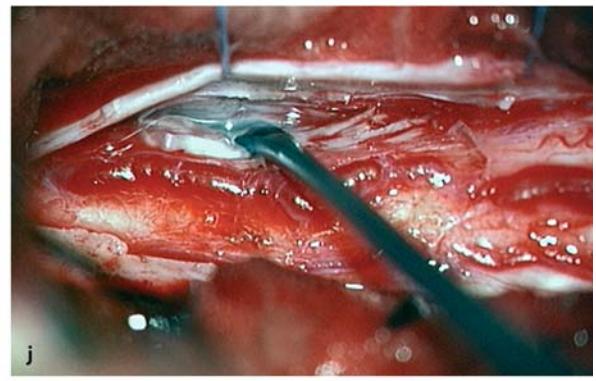

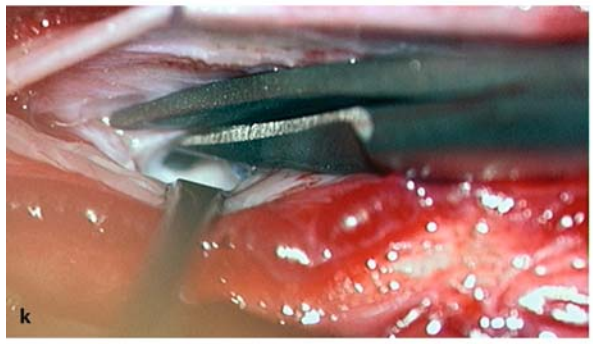

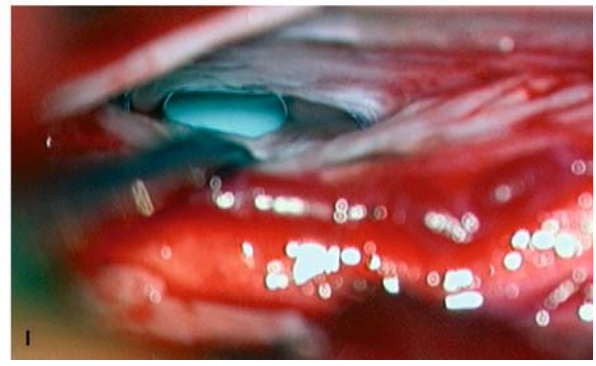

Fig. 4.67. f The axial CT at Th1 shows little amounts of contrast in the anterior arachnoid cyst compared to the subarachnoid space posteriorly. A laminotomy Th2–Th4 was performed. **g** The intraoperative view after dura opening shows the thick arachnoid scarring, which appears most pronounced at Th2. **h**, **i** Starting at Th4 the arachnoid is gradually resected preserving the surface vessels on the spinal cord by sharp dissection. In this way the posterior cyst is removed. Please note the posterior arachnoid septum in the midline connected to the midline spinal cord vein (*arrowhead* in **h**). The wall of the anterior arachnoid cyst can now be visualized on the right side at Th2 with the aid of a microdissector (**j**) and fenestrated (**k**). The final views show the communication of the anterior cyst with the subarachnoid space (**l**) and the situation at the end of the intradural dissection (**m**). (*Continuation see next page*)

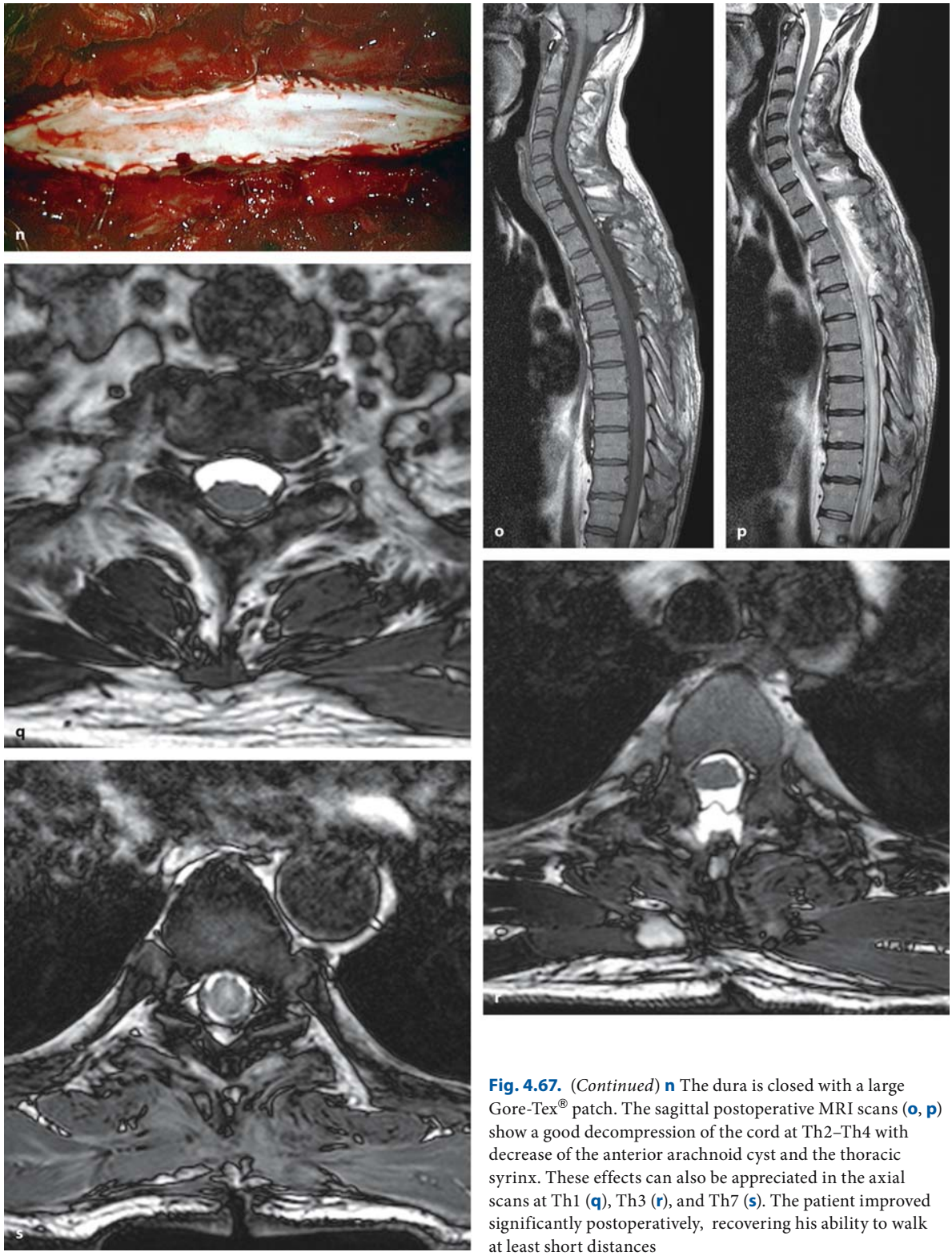

Fig. 4.67. (*Continued*) **n** The dura is closed with a large Gore-Tex® patch. The sagittal postoperative MRI scans (**o**, **p**) show a good decompression of the cord at Th2–Th4 with decrease of the anterior arachnoid cyst and the thoracic syrinx. These effects can also be appreciated in the axial scans at Th1 (**q**), Th3 (**r**), and Th7 (**s**). The patient improved significantly postoperatively, recovering his ability to walk at least short distances

noidal layer and on the cord surface. Sharp dissection avoids this problem. Bipolar coagulation should be used sparsely and only on small vessels in the arachnoid. This strategy limits the risk of injury to sensory spinal cord pathways in particular. If the cyst extends over several spinal segments, we fenestrate the cyst only at the lower or upper pole (Fig. 4.67). Rarely, septations of a cyst require fenestrations at both ends (Fig. 4.66). With anteriorly placed cysts it may be difficult to gain sufficient access from a posterior approach. In such cases, the dentate ligaments can be cut and the cord gently mobilized. However, this should only be attempted in situations where the arachnoid appears relatively normal (i.e., not grossly thickened as a result of previous operations or inflammatory processes; Fig. 4.67). After arachnoid dissection in the posterior subarachnoid space, we do not recommend a primary dura suture but insertion of a Gore-Tex® duraplasty to ensure persistent CSF flow at that spinal level [275].

4.3.2 Closure

Once the tumor or cyst is removed, some authors resuture the arachnoid membrane to avoid scarring and cord tethering [279]. We have not done this regularly. In most instances just the dura is closed with a running suture. Whenever the arachnoid membrane is part of the pathology (i.e., extramedullary cysts or recurrent tumors), we use a Gore-Tex® duraplasty to limit postoperative arachnoid scarring and to maintain CSF flow during surgery. With tenting sutures along the suture line, the duraplasty can be lifted off the spinal cord avoiding scar formation between the spinal cord and suture material in particular (Figs. 4.34, 4.53, 4.55, 4.56, 4.59, 4.61, 4.63, and 4.65–4.67). Finally, the laminae are fixed with titanium miniplates and the wound is closed as described for intramedullary tumors.

4.3.3 Adjuvant Therapy

The treatment of choice in patients with an extramedullary tumor is surgery aiming at complete removal of the tumor. Currently, only WHO grade III and IV tumors are irradiated postoperatively at our institution. In our series, 11 (2%) were classified as WHO grade III tumors and 23 (4%) as WHO grade IV tumors. 94% of extramedullary tumors were benign, requiring surgery only.

4.4 Postoperative Results and Outcome

Cervical and thoracic tumors differed significantly in terms of histological types. In the cervical region, meningiomas (40%) and schwannomas (52%) made up more than 90% of the pathology. In the thoracic region, meningiomas were more common (53%) compared to schwannomas (22%) and arachnoid cysts (12%). In the lumbar canal, schwannomas (39%) were the commonest type, followed by ependymomas (22%), hamartomas (19%), and meningiomas (11%; Table 4.5; chi square test: $p<0.0001$) [34].

4.4.1 Tumor Resection

Overall, 77% of extramedullary tumors in our series were removed completely. A subtotal resection was done in 20%, whereas 3% were decompressed. Resection rates varied considerably in relation to tumor histology and corresponding surgical strategies, as outlined above. A comparison of results for tumors with and without extradural extension revealed no statistically significant difference, although there was a trend toward a lower rate of complete resections with extradural extension (66% compared to 79%; Table 4.6). There was a significantly lower rate of complete resections for patients with recurrent tumors compared to first surgical attempts (53% compared to 84%, respectively; chi square test: $p<0.0001$).

Table 4.5. Histologies of extramedullary tumors related to spinal level

Histology	Cervical	Thoracic	Lumbo-sacral
Meningioma	40%	53%	11%
Nerve sheath tumor	52%	22%	39%
Arachnoid cyst	2%	12%	2%
Hamartoma	3%	3%	19%
Ependymoma	–	–	22%

Table 4.6. Surgical results for extramedullary tumors

Surgery	Intra	Intra-Extra	Total
Complete	305 (79%)	40 (66%)	345 (77%)
Subtotal	68 (18%)	20 (33%)	88 (20%)
Decompression/ Biopsy/Cystostomy	12 (3%)	1 (2%)	3 (3%)

4.4.2 Clinical Results

The successful removal of an extramedullary tumor is one of the most gratifying procedures in neurosurgery. Almost all preoperative symptoms and signs can be expected to improve postoperatively [204]. Quite often, even complete resolutions are obtained. This statement even holds for elderly patients with significant preoperative deficits, so that surgery for extramedullary tumors should be recommended regardless of age [35, 44, 223].

Table 4.7 gives an overview of clinical outcomes for individual symptoms in the first postoperative year for extramedullary tumors. All symptoms showed significant improvements during this time, regardless of extradural extensions. As radicular symptoms rather than more advanced symptoms of medullary compression predominate in patients with dumbbell tumors, clinical results are even better for this group, even though they are surgically more difficult to manage. The average Karnofsky score improved for all extramedullary tumors from 70±15 to 81±16 (without extradural extension 70±15 to 80±17, with extradural extension from 73±12 to 87±10).

An analysis of clinical results with respect to the amount of tumor resected demonstrated worse out-

Table 4.7. Clinical course for patients with extramedullary tumors related to tumor extension

Symptom	Preoperative status	Postoperative status	3 Months postop.	6 Months postop.	1 Year postop.
Pain					
Intra	3.4±1.1	4.0 ±0.8	4.3±0.7	4.4±0.8	4.3±0.9**
Intra-Extra	3.5±1.0	3.9±0.8	4.3±0.5	4.5±0.5	4.5±0.5**
Total	3.4±1.1	3.9±0.8	4.3±0.7	4.4±0.8	4.4±0.9**
Hypesthesia					
Intra	3.5±1.0	3.8±1.0	4.1±1.0	4.1±1.1	4.1±1.1**
Intra-Extra	3.5±0.9	3.9±1.0	4.4±0.7	4.5±0.7	4.5±0.7**
Total	3.5±1.0	3.8±1.0	4.1±1.0	4.2±1.0	4.2±1.1**
Dysesthesias					
Intra	4.0±1.0	4.4±0.8	4.5±0.7	4.5±0.7	4.5±0.8**
Intra-Extra	4.1±1.0	4.4±0.7	4.8±0.4	4.8±0.4	4.8±0.4**
Total	4.0±1.0	4.4±0.8	4.5±0.7	4.6±0.7	4.5±0.8**
Gait					
Intra	3.6±1.2	3.7±1.2	4.1±1.1	4.2±1.1	4.2±1.1**
Intra-Extra	4.0±0.9	4.1±0.8	4.4±0.7	4.5±0.7	4.6±0.6**
Total	3.7±1.2	3.8±1.2	4.1±1.1	4.2±1.0	4.3±1.1**
Motor power					
Intra	3.5±1.2	3.8±1.2	4.1±1.0	4.2±1.1	4.2±1.1**
Intra-Extra	3.8±1.1	3.9±0.9	4.4±0.7	4.6±0.7	4.6±0.7**
Total	3.6±1.2	3.8±1.1	4.2±1.1	4.3±1.1	4.3±1.1**
Sphincter function					
Intra	4.2±1.1	4.2±1.2	4.4±1.0	4.5±1.0	4.5±1.1**
Intra-Extra	4.4±0.9	4.7±0.5	4.9±0.5	4.9±0.5	4.9±0.5**
Total	4.2±1.1	4.2±1.2	4.5±1.0	4.5±0.9	4.5±1.0**
Karnofsky score					
Intra	70±15	72±17	77±16	80±16	80±17**
Intra-Extra	73±12	76±12	83±11	85±11	87±10**
Total	70±15	72±16	78±15	80±15	81±16**

Statistically significant difference between preoperative status and 1 year postoperatively: *$p<0.05$, **$p<0.01$; abbreviation: Postop. = postoperatively

Table 4.8. Clinical course for patients with extramedullary tumors related to type of surgery

Symptom	Preoperative status	Postoperative status	3 Months postop.	6 Months postop.	1 Year postop.
Pain					
Complete	3.4±1.0	4.0 ±0.7	4.4±0.6	4.5±0.6	4.5±0.7**
Subtotal	3.4±1.2	3.8±1.0	4.0±1.0	3.9±1.0	3.7±1.4
Hypesthesia					
Complete	3.5±0.9	3.9±0.9	4.2±0.8	4.3±0.8	4.4±0.8**
Subtotal	3.4±1.3	3.4±1.4	3.6±1.4	3.7±1.5	3.5±1.5
Dysesthesias					
Complete	4.0±1.0	4.3±0.8	4.6±0.6	4.6±0.7	4.6±0.7**
Subtotal	4.1±1.1	4.4±0.8	4.5±0.7	4.5±0.8	4.2±1.0
Gait					
Complete	3.7±1.1	3.9±1.1	4.3±0.9	4.4±0.8	4.5±0.8**
Subtotal	3.5±1.3	3.5±1.3	3.6±1.3	3.7±1.4	3.6±1.5
Motor power					
Complete	3.7±1.1	4.0±1.0	4.3±0.8	4.5±0.8	4.5±0.7**
Subtotal	3.3±1.3	3.5±1.3	3.7±1.4	3.8±1.4	3.6±1.5
Sphincter function					
Complete	4.4±0.9	4.4±1.0	4.7±0.6	4.7±0.6	4.8±0.5**
Subtotal	3.8±1.3	3.7±1.4	3.9±1.3	3.8±1.4	3.7±1.6
Karnofsky score					
Complete	71±15	74±16	80±14	83±13	84±13**
Subtotal	67±14	66±16	71±19	72±19	70±21

Statistically significant difference between preoperative status and 1 year postoperatively: *$p<0.05$, **$p<0.01$

comes after subtotal resections. For this group, only marginal changes were observed within the first postoperative year, with a trend toward deterioration after only 6 months. After complete resections, excellent results can be expected (Table 4.8).

To predict a high postoperative Karnofsky score after 1 year, we performed a multiple regression analysis. The strongest predictors were a high preoperative Karnofsky score and no postoperative dysesthesia syndrome. Less important factors were the absence of NF-2, a short history, or the absence of arachnoid scarring at surgery (Table 4.9).

If we then look at the clinical results as a function of the preoperative Karnofsky score, it becomes clear that patients with more severe preoperative deficits still profit enormously from surgery, with significant improvements of every symptom. However, full recovery does occur only rarely once severe deficits have developed. Comparing results for patients with preoperative Karnofsky scores above and below 70 shows that all clinical scores fall short for the latter group. Significant improvements of the Karnofsky score, however, could be observed independent of the preoperative score (77±7 to 85±12 and 49±11 to 67±19 for

Table 4.9. Multivariate analysis for prediction of a high postoperative Karnofsky score for patients with extramedullary tumors

Factor	β-value
Preop. Karnofsky score	0.4688
No dysesthesia syndrome	0.3596
No neurofibromatosis	0.1939
Short history	0.1754
No arachnoid scarring	0.1034

Correlation: $r=0.7959$, $p<0.0001$, abbreviation: Preop. = preoperative

Table 4.10. Clinical course for patients with extramedullary tumors related to preoperative Karnofsky score

Symptom	Preoperative status	Postoperative status	3 Months postop.	6 Months postop.	1 Year postop.
Pain					
≥70	3.5±1.0	4.1±0.6	4.4±0.6	4.5±0.7	4.5±0.8**
<70	3.2±1.2	3.5±0.9	4.0±0.8	4.1±1.0	4.0±1.1**
Hypesthesia					
≥70	3.6±0.9	4.0±0.8	4.0±0.8	4.3±0.8	4.3±0.8**
<70	3.0±1.0	3.3±1.3	3.6±1.4	3.6±1.4	3.6±1.5**
Dysesthesias					
≥70	4.1±0.9	4.4±0.7	4.6±0.6	4.6±0.6	4.6±0.7**
<70	3.7±1.2	4.1±0.9	4.4±0.8	4.3±0.9	4.2±1.0**
Gait					
≥70	4.1±0.8	4.2±0.9	4.4±0.8	4.5±0.8	4.5±0.8**
<70	2.2±1.0	2.5±1.1	3.0±1.2	3.3±1.3	3.4±1.4**
Motor power					
≥70	4.0±0.9	4.1±0.9	4.4±0.9	4.5±0.8	4.5±0.9**
<70	2.8±1.0	2.8±1.1	3.2±1.2	3.5±1.3	3.6±1.4**
Sphincter function					
≥70	4.5±0.9	4.5±1.0	4.7±0.8	4.7±0.8	4.7±0.8**
<70	3.5±1.3	3.5±1.3	3.9±1.2	4.0±1.1	4.0±1.1*
Karnofsky score					
≥70	77±7	79±11	83±11	85±11	85±12**
<70	49±11	52±13	60±15	66±18	67±19**

Statistically significant difference between preoperative status and 1 year postoperatively: *$p<0.05$, **$p<0.01$; abbreviations: ≥70 = preoperative Karnofsky score, equal or higher than 70, <70 = preoperative Karnofsky score less than 70

patients with preoperative scores above and below 70, respectively; Table 4.10) [34].

For recurrent tumors, however, the situation is more complex in terms of radicality and potential for postoperative improvements. Pain syndromes in particular rarely improve even after radical resection of a recurrent tumor. This is illustrated in Table 4.11, which demonstrates worse clinical outcomes for surgery of recurrent extramedullary tumors compared to a first surgical attempt. As a general rule, the neurological result will be unchanged postoperatively for the majority of these patients.

Table 4.11. Course for patients with extramedullary tumors related to previous operations

Symptom	Preoperative status	Postoperative status	3 Months postop.	6 Months postop.	1 Year postop.
Pain					
First surgery	3.4±1.0	4.0 ±0.7	4.4±0.7	4.5±0.7	4.5±0.7**
Recurrent tumor	3.4±1.2	3.8±0.8	4.1±0.8	3.9±0.9	3.7±1.3
Hypesthesia					
First Surgery	3.5±0.9	4.0±0.8	4.3±0.8	4.3±0.8	4.4±0.8**
Recurrent tumor	3.2±1.2	3.3±1.4	3.4±1.5	3.4±1.5	3.3±1.5
Dysesthesias					
First surgery	4.0±1.0	4.4±0.8	4.6±0.6	4.6±0.6	4.6±0.7**
Recurrent tumor	4.1±1.1	4.4±0.8	4.4±0.7	4.3±0.9	4.2±1.0
Gait					
First surgery	3.7±1.2	3.8±1.1	4.2±1.0	4.4±0.9	4.4±0.9**
Recurrent tumor	3.5±1.2	3.5±1.4	3.6±1.3	3.6±1.4	3.5±1.5
Motor power					
First surgery	3.7±1.1	3.9±1.0	4.3±0.8	4.5±0.8	4.5±0.7**
Recurrent tumor	3.2±1.4	3.3±1.5	3.4±1.5	3.4±1.5	3.3±1.6
Sphincter function					
First surgery	4.4±1.0	4.4±1.0	4.7±0.7	4.7±0.7	4.7±0.7**
Recurrent tumor	3.8±1.4	3.6±1.5	3.8±1.4	3.7±1.4	3.6±1.6
Karnofsky score					
First surgery	71±15	74±16	79±14	83±14	84±14**
Recurrent tumor	68±13	66±17	70±18	70±17	68±20

Statistically significant difference between preoperative status and 1 year postoperatively: *$p<0.05$, **$p<0.01$

4.4.3 Complications

4.4.3.1 Short-Term Complications

Complications were encountered in 10% of patients, with no differences between tumors with and without extradural extension (Table 4.12). A special comment is warranted regarding the risk of a postoperative paraparesis due to the semisitting position. Apart from air embolism, this is the most serious complication of this position. To minimize this risk, we advise performing X-rays of the cervical spine in anteflexion and retroflexion to rule out instabilities, to apply moderate extension on the cervical spine during positioning, and to use somatosensory evoked potential (SEP) monitoring during the positioning maneuver. Among several hundred operations performed with the patient in the semisitting position each year, we have corrected the positioning as a consequence of changes in SEP on various occasions and have not seen such a complication again. Furthermore, like any other monitoring method, SEP recording is a good tool to learn how this maneuver is performed safely.

Surgical mortality was 1.4% (five patients). In three of these five patients the tumor was located in the high cervical region: one patient with a recurrent arachnoid cyst at C1, one patient with a recurrent meningioma at C1/2, and one patient with a recurrent meningioma at C1–C5. The other two harbored a meningioma at Th1/2 and a malignant thoracic teratoma.

A transient postoperative deterioration is much rarer for patients with extramedullary tumors than for patients with intramedullary processes. It was observed for 10% of patients in this series, with recovery for 81% of these within 3 months, and for the remainder in up to 18 months.

Table 4.12. Complication rates for patients with extramedullary tumors

Type	Intra	Intra-Extra	Total
CSF leak	17	3	20
Wound infection	5	1	6
Hemorrhage	2	1	3
Lamina dislocation	1	–	1
Instability	4	–	4
Raised intracranial pressure	2	–	2
Intracerebral hemorrhage	1	–	1
Incomplete paralysis due to positioning	1	–	1
Urinary tract infection	4	–	4
Aspiration pneumonia	1	1	2
Deep vein thrombosis	1	–	1
Total	**39** **10%**	**6** **10%**	**45** **10%**

4.4.3.2 Long-Term Complications

Late complications may be associated with spinal instability or a postoperative dysesthesia syndrome that may progress to myelopathy. To avoid instabilities, intervertebral joints should be left intact during the exposure and lamina reinserted after tumor removal. However, for tumors growing toward the intervertebral foramen, such as dumbbell schwannomas, it may not be possible to preserve every intervertebral joint. Tumor growth itself may have caused significant bony erosion to such an extent that spinal instability has resulted or is immanent (Fig. 4.53). Four patients in this series developed postoperative instability requiring fusion. Therefore, postoperative monitoring of the spine is recommended – and mandatory in children!

A postsurgical myelopathy may cause progressive neurological deterioration in the absence of a tumor recurrence. A postoperative dysesthesia syndrome may lead to pain and dysesthesias, and may even progress to motor and sensory dysfunctions [171, 253]. We observed a dysesthesia syndrome in eight patients and a postsurgical myelopathy in five patients of our series. Dysesthesias developed after removal of meningiomas in four patients. In two of these, a myelopathy followed, of which one was related to a concomitant cervical stenosis. The other dysesthesia syndromes were observed after surgery for a lipoma, an angioblastoma, an arachnoid cyst, and a schwannoma. The remaining three instances of postsurgical myelopathy were related to lipomas and associated tethered cord syndromes.

4.4.4 Morbidity, Recurrences, and Survival

We observed permanent surgical morbidity in 2.3% of cases. Combined with the aforementioned rate for transient postoperative neurological deterioration in 10% of patients, these figures combine to 12.3% of patients who experience an immediate postoperative worsening of neurological functions. Of these, about 82% will regain their preoperative status.

Permanent surgical morbidity was lowest in the cervical and thoracic regions (1.7% each) compared to tumors in the cauda equina (3.7%). Primary surgeries were associated with a morbidity of 1.5%, compared to 5.3% for recurrent tumors (p=0.05).

The long-term results can be analyzed according to clinical and radiological recurrence rates. The former describe the rate of patients who experience progressive neurological problems, the latter is determined by calculating the rate of patients with progressive tumor growth due to a recurrent tumor or growth of a tumor remnant. Compared to purely intradural extramedullary tumors, we observed no differences in clinical or radiological recurrence rates for tumors with extradural extension (i.e., dumbbell tumors). Therefore, analyses in this section are for both groups combined.

According to Kaplan-Meier statistics, the overall recurrence rates for all tumors were 13%, 25%, and 32% after 1, 5, and 10 years, respectively. Schick et al. [231] determined the rate of recurrences for extramedullary tumors as 14 out of 158 operated tumors (i.e. 8.9%). However, this figure is misleading and too low because survival statistics were not employed (i.e., varying follow-up times were not accounted for).

A multiple regression analysis was performed to predict a low tumor recurrence rate after resection of an extramedullary tumor. The strongest predictor was a benign histological grade (Fig. 4.68). The other major influence was first rather than secondary surgery on a particular tumor (Fig. 4.69). Less important factors were the absence of arachnoid scarring, a short history, and a complete resection (Fig. 4.70; Tables 4.13 and 4.14). These figures indicate that complete resection of an extramedullary tumor does not automatically indicate cure of the patient [247].

The worse results for recurrent tumors can be attributed to a more aggressive tumor behavior on one side and the lower rate of complete resections on the

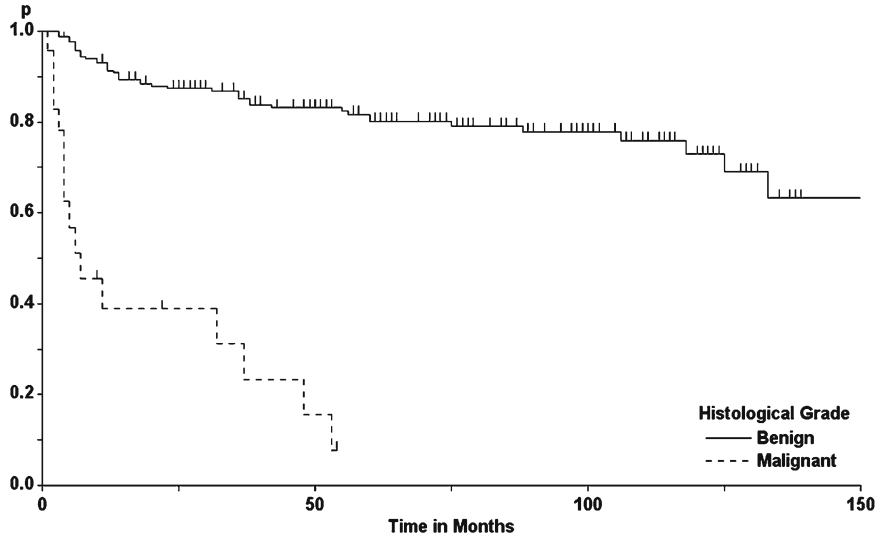

Fig. 4.68. Tumor recurrence rates for patients with extramedullary tumors as a function of histological grade (log-rank test: $p<0.0001$)

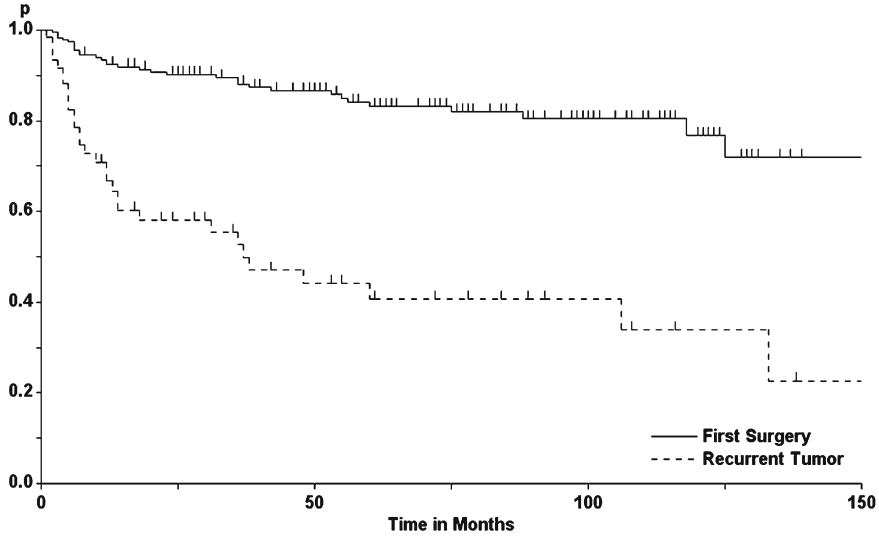

Fig. 4.69. Tumor recurrence rates for patients with extramedullary tumors as a function of first or secondary surgery (log-rank test: $p<0.0001$)

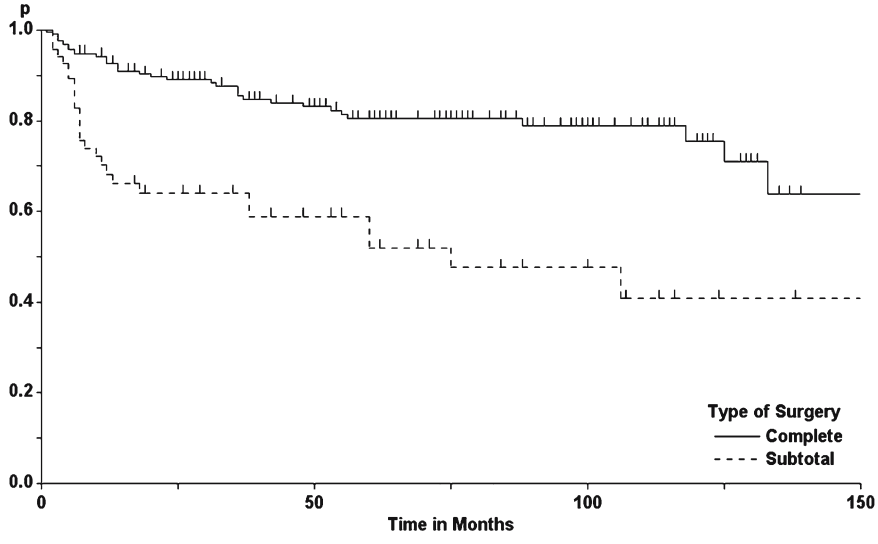

Fig. 4.70. Tumor recurrence rates for patients with extramedullary tumors as a function of extent of tumor resection (log-rank test: $p<0.0001$)

Table 4.13. Multivariate analysis for prediction of a low recurrence rate for patients with extramedullary tumors

Factor	β-value
Benign grade	0.2025
First surgery	0.1084
No arachnoid scarring	0.0729
Short history	0.0679
Complete resection	0.0651

Correlation: r=0.3621, p<0.0001

Table 4.14. Tumor recurrence rates for patients with extramedullary tumors

Group	1 Year	5 Years	10 Years
Benign grade	9%	20%	27%
Malignant grade	61%	92%	
First surgery	8%	17%	23%
Recurrent tumor	33%	59%	66%
Complete removal	7%	20%	25%
Subtotal removal	31%	48%	59%

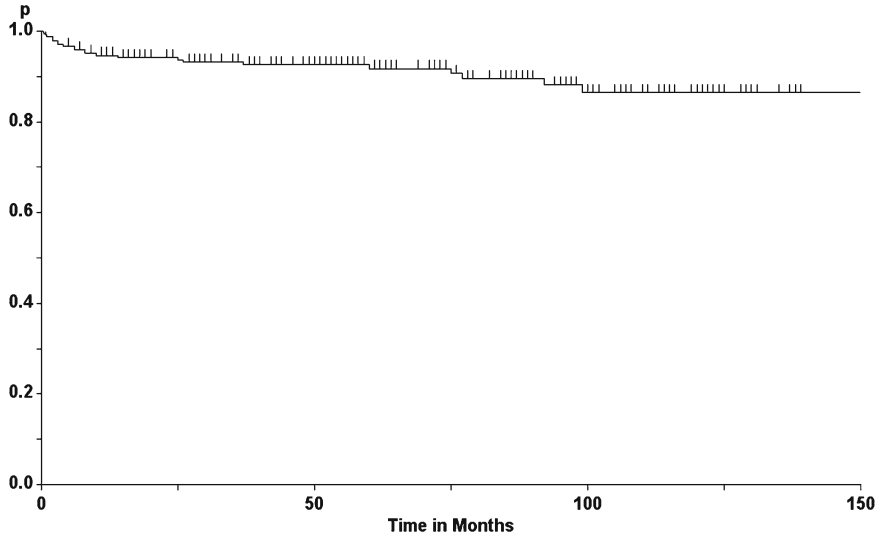

Fig. 4.71. Survival rate for patients with extramedullary tumors

other. Complete resections of recurrent tumors are often made difficult by tremendous arachnoid scarring resulting from the previous operation. In order to preserve function, incomplete resections were sometimes the consequence.

Arachnoid adhesions may not only be related to previous surgeries (81%), but may accompany even unoperated extramedullary tumors (19%; $p<0.0001$). They may obscure the cleavage plane between the tumor and the surrounding soft tissue – in lipomas and meningiomas in particular – and may cause postoperative morbidity independent of the tumor due to interference with spinal cord microcirculation or mobility (i.e., a postoperative tethered cord).

After 5 years, we observed recurrence rates for completely resected tumors of 20%, 48% after subtotal removal, and 100% for decompressed tumors. After 10 years, the corresponding figures were 25%, 59%, and 100%, respectively (Table 4.14).

Looking at clinical recurrence rates, the low number of patients affected by postoperative dysesthesia syndromes and myelopathies warranted no separate analysis. The results for malignant extramedullary tumors were frustrating. Whereas the overall clinical recurrence rate after 5 years was 20% for benign tumors, 61% of malignant tumors were associated with progressive neurological problems within 1 year and 92% within 5 years.

Overall survival for extramedullary tumors could be calculated as 95% for 1 year and 93% and 87% for 5 and 10 years, respectively (Fig. 4.71). Mortality figures were also analyzed with multiple regression. The strongest predictors of survival were a complete resection (Fig. 4.72) and a benign grade (Fig. 4.73). Less important were female sex, a short history, first surgery, young age, and absence of a local recurrence (Table 4.15).

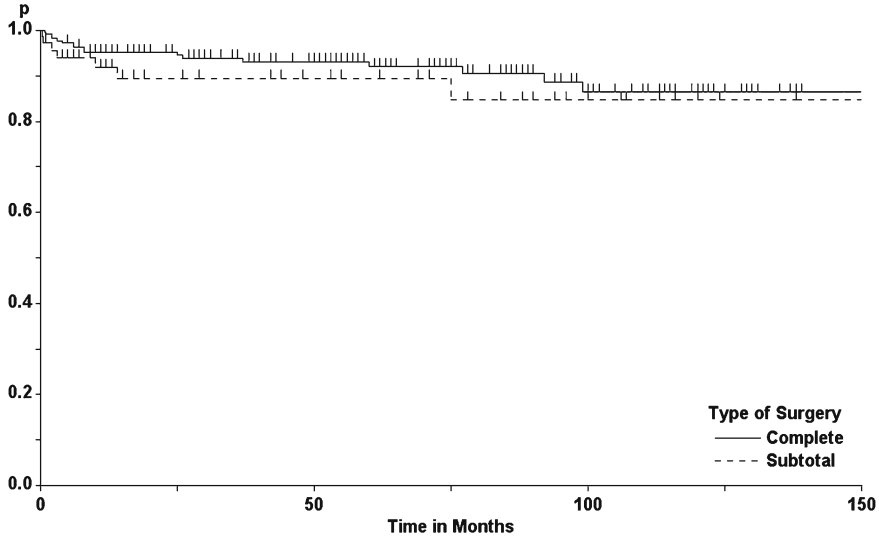

Fig. 4.72. Survival rates for patients with extramedullary tumors as a function of extent of tumor resection (log-rank test: not significant)

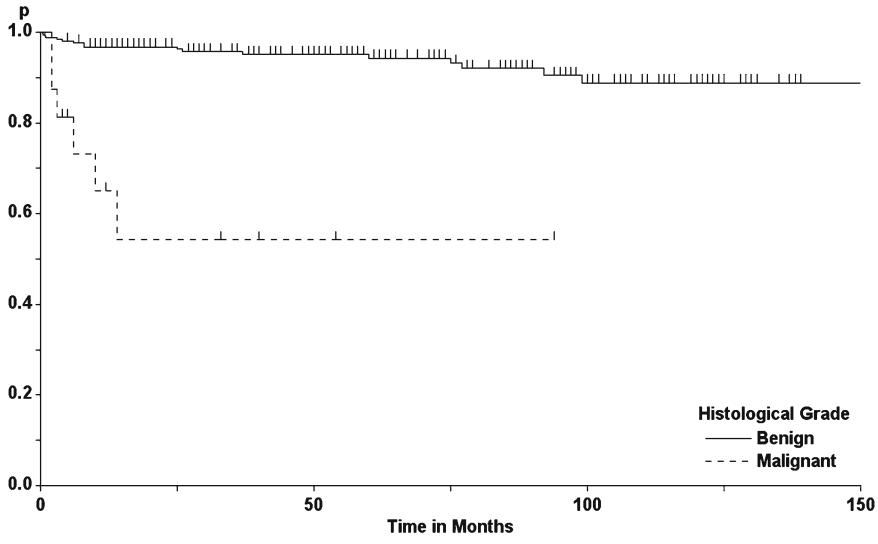

Fig. 4.73. Survival rates for patients with extramedullary tumors as a function of histological grade (log-rank test: $p<0.0001$)

Table 4.15. Multivariate analysis for prediction of a high survival rate for patients with extramedullary tumors

Factor	β-value
Complete resection	0.5352
Benign grade	0.5158
Female sex	0.3706
Short history	0.3332
First surgery	0.2889
Young age	0.1968
No tumor recurrence	0.1559

Correlation: $r=0.7682$, $p=0.0010$

4.5 Specific Entities

4.5.1 Meningiomas

Meningiomas are the commonest extramedullary intradural tumors. We have performed surgery on 180 spinal meningiomas in 167 operations. Overall, 22 operations dealt with recurrent meningiomas. Eight patients presented with multiple meningiomas and 17 patients with NF-2 [48]. In the literature, spinal meningiomas account for 25–46% of spinal tumors, with 7.5–12.7% of all meningiomas occurring in the spinal canal [94].

Extradural extensions do exist in a small number of cases (Fig. 4.74) and even completely extradural

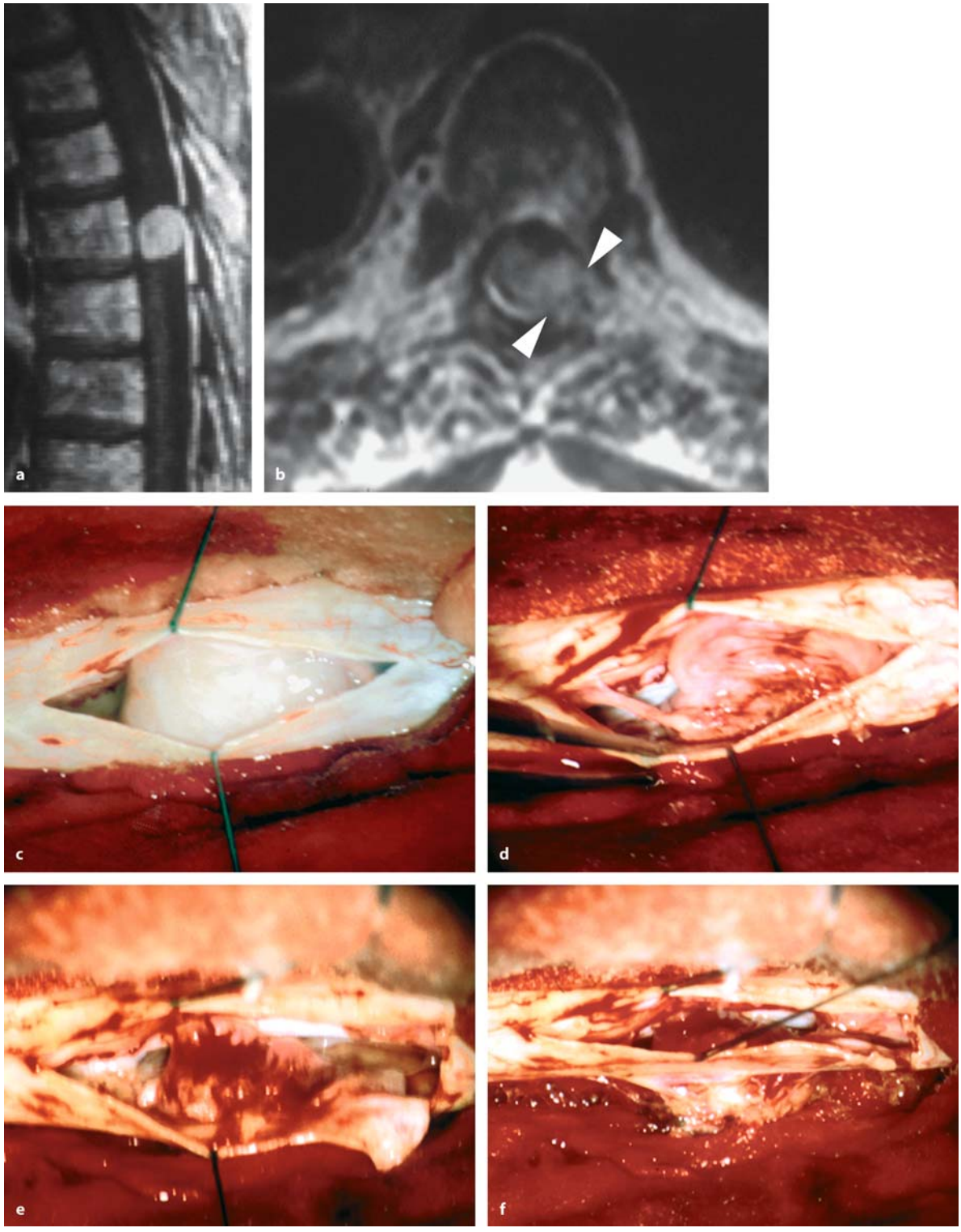

Fig. 4.74. Sagittal (**a**) and axial (**b**) T1-weighted MRI scans with contrast of a meningioma at Th6 in a 67-year-old man with a 3-month history of dysesthesias and a progressive paraparesis. The axial view demonstrates extradural extension of the tumor on the left side (*arrowheads* in **b**). **c** This intraoperative view after dura opening shows the tumor well encapsulated and the spinal cord displaced to the right. After debulking of the tumor (**d**), the remainder of the meningioma can be removed by resecting the dural attachment zone (**e**) together with the extradural component (**f**). (*Continuation see next page*)

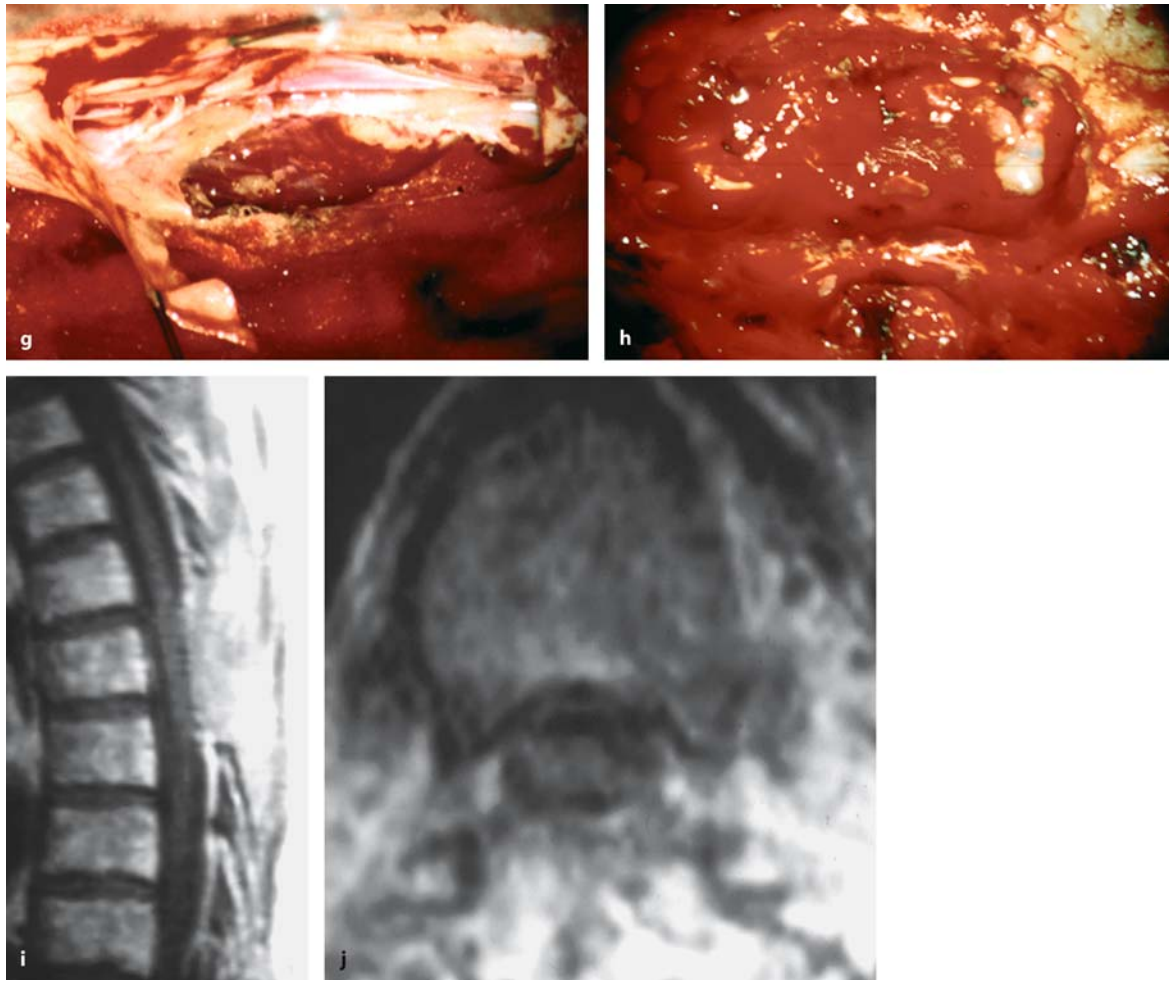

Fig. 4.74. (*Continued*) The resulting dura defect after complete resection (**g**) is closed with a fascia lata patch (**h**). **i**, **j** The postoperative T1-weighted MRI scans show a complete resection of the tumor. Please note, however, the dense adhesions between graft and spinal cord (see Fig. 4.44 for comparison). Neurological symptoms improved considerably postoperatively

varieties have been described [3, 89, 138, 175]. King et al. [138] found 2 epidural and 2 intra-extradural meningiomas among a total of 78 patients. Extradural components are more common in younger patients [48]. We have seen 14 meningiomas with extradural extension (8%).

Patients with meningiomas tend to be the oldest among those with extramedullary tumors (mean±SD age 58±16 years; range 11–94 years). Meningiomas predominated among women, the ratio of females to males being 3.5:1. The average history until admission for surgery was 17±28 months (maximum 18 years). With the more widespread availability of MRI scanners since 1988, meningiomas tend to be diagnosed earlier now. Even though the average age has remained the same, the mean preoperative history has decreased significantly (31±46 months between 1977 and 1985, and 12±14 months between 1986 and 2003; *t*-test: $p<0.01$). Patients were followed for 34±42 months (maximum 13 years).

The majority of patients demonstrated a slowly progressive course and 51% described pain and/or dysesthesias as the first symptoms. The remaining patients complained of motor weakness and gait disturbances (36%) or sensory changes (12%) as the first symptom (Table 4.16).

On admission, the clinical picture was dominated by problems of motor power and/or gait in 67% of patients. Thirty-three patients presented acutely with severe walking disability. For only 30% of patients was pain and/or dysesthesias still the major complaint. Table 4.17 gives an overview of clinical symptoms at presentation. The average Karnofsky score on admission was 67±16 (range 30–100). Since 1986, a

Table 4.16. Initial symptoms of spinal meningiomas

First symptom	Encapsulated	En plaque	Total
Pain	35%	54%	39%
Gait ataxia	21%	9%	19%
Motor weakness	18%	14%	17%
Sensory deficits	12%	18%	12%
Dysesthesias	12%	5%	12%
Sphincter problems	–	–	–

Table 4.17. Symptoms for spinal meningiomas at presentation

Symptom	Encapsulated	En plaque	Total
Pain	70%	74%	71%
Gait ataxia	85%	78%	81%
Motor weakness	78%	74%	75%
Sensory deficits	87%	87%	85%
Dysesthesias	43%	48%	44%
Sphincter problems	37%	57%	40%

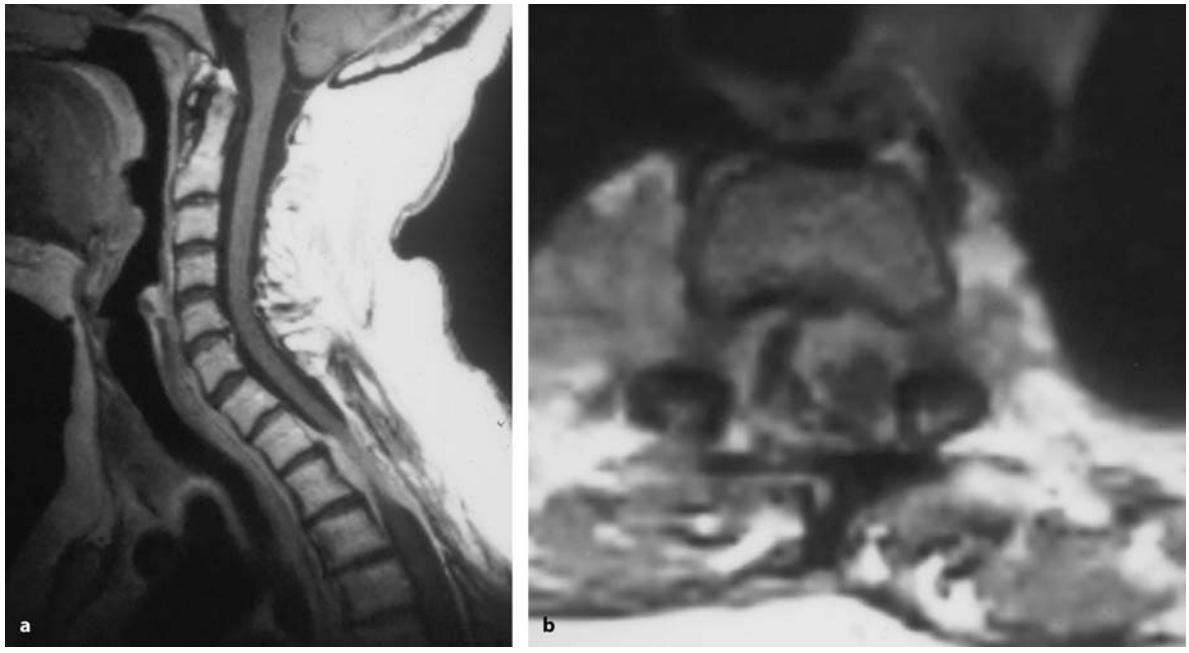

Fig. 4.75. Sagittal (**a**) and axial (**b**) T1-weighted MRI scans with contrast of a recurrent en plaque growing meningioma at Th1–Th3 in a 57-year-old woman with a 15-month history of progressive paraparesis. The meningioma has grown all around the spinal cord and is spreading out cranially and caudally

highly significant increase in the preoperative Karnofsky score has been observed (59±15 in 1977–1985 and 70±15 in 1986–2003; *t*-test: $p<0.0001$).

Meningiomas are observed predominantly in the cervical (28%) and thoracic spine (64%). Lumbar meningiomas are rare (8%). They are evenly distributed around the spinal cord and may be located anteriorly (26%; Fig. 4.40), posteriorly (25%) (Fig. 4.35), or laterally (48%) (Figs. 4.32, 4.44, and 4.74) [89, 94, 181]. In the cervical area, anterior meningiomas are more common than in the thoracic spine (47% and 18%, respectively), whereas most of the thoracic meningiomas are located laterally compared to the cervical area (55% and 38%, respectively). In the lumbar region, 55% were located posteriorly (chi-square test: $p=0.0033$). This distribution differs from a series by King et al. [138], who found predominantly lateral meningiomas (i.e., in 70.5% of cases). Cohen-Gadol et al. [48] observed a higher proportion of cervical meningiomas in younger patients compared to elderly patients. In our series, this was not the case.

Of the tumors observed in our series, 76% demonstrated a tumor capsule, whereas 13% showed an en plaque growth pattern (Figs. 4.43 and 4.75) [80]. The highest number of en plaque growing tumors was encountered in the thoracic spine (83%). We also observed 15 atypical (8%; Fig. 4.76) and 4 malignant meningiomas (2%). Caroli et al. [29] described a lower

percentage (3.1%) of en plaque meningiomas among their series of 225 spinal meningiomas. All of these were in the thoracic spine. Evidence of arachnoid scarring was observed in 20% (9% of previously unoperated tumors and 86% of recurrent tumors; $p<0.0001$). Encapsulated tumors showed a significantly lower tendency for arachnoid scarring than en plaque growing tumors (11% and 44%, respectively; $p=0.005$) [29].

Among patients with meningiomas, four groups can be distinguished according to the growth pattern and histology of the tumor: encapsulated, en plaque growing, atypical, and malignant meningiomas. They differ in clinical, surgical, and postoperative features. With encapsulated meningiomas, the preoperative history is almost twice as long as compared to the remaining groups. Of patients with encapsulated meningiomas, 72% complain about gait and motor deficits as their major concern at the time of surgery [138]; just 25% mention pain or dysesthesias as their major problem. With en plaque growing tumors, the situation is quite different, as pain and dysesthesias become more predominant: 45% complained of pain and/or dysesthesias as their major clinical problem and 55% considered gait disturbances or motor deficits as their most important problem [48]. With atypical meningiomas, 71% are mainly concerned about pain and dysesthesias, while 29% are disabled by gait problems. With malignant meningiomas, 50% are troubled by pain, and the other half by gait ataxia.

Complete tumor removal of a meningioma requires removal of the tumor mass with either resection or coagulation of the dural attachment. This was achieved for 90% of all meningiomas. Corresponding figures in the recent and older literature vary between 78% and 98% [20, 89, 93, 94, 96, 138, 156, 178, 181, 186, 247] and do not suggest a higher cure rate due to improved preoperative imaging and earlier diagnosis in recent years.

Rates of resection vary among first and secondary operations (95% of previously unoperated patients and 59% of recurrent tumors) and differed according to the growth pattern. With encapsulated tumors, the rate for complete resections was 98% and dropped to 57% for en plaque growing tumors [29], but is still quite high for atypical and malignant tumors, with 75% complete resections.

Surgical results were not significantly influenced by tumor position. Complete resections were achieved for 95% of posterior, 90% of lateral, and 86% of anterior located meningiomas. For patients with complete removal, the tumor matrix was resected in 57% and coagulated in 42%. A duraplasty was inserted in 31% of cases.

Fourteen meningiomas demonstrated some degree of extradural extension. This is not restricted to the

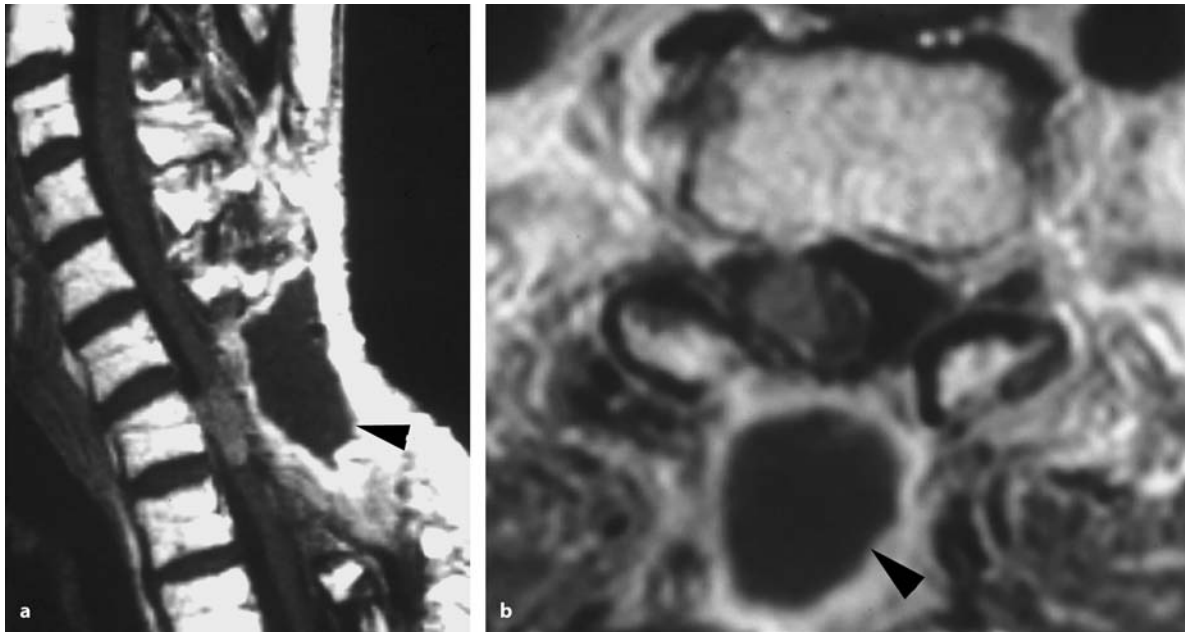

Fig. 4.76. Sagittal (**a**) and axial (**b**) T1-weighted, contrast-enhanced MRI images of a recurrent atypical meningioma at C7 in a 57-year-old patient with a history progressive paraparesis and pain requiring six operations over a period of 13 years. As a result of previous surgeries, a CSF collection is visible posteriorly (*arrowheads*). (*Continuation see next page*)

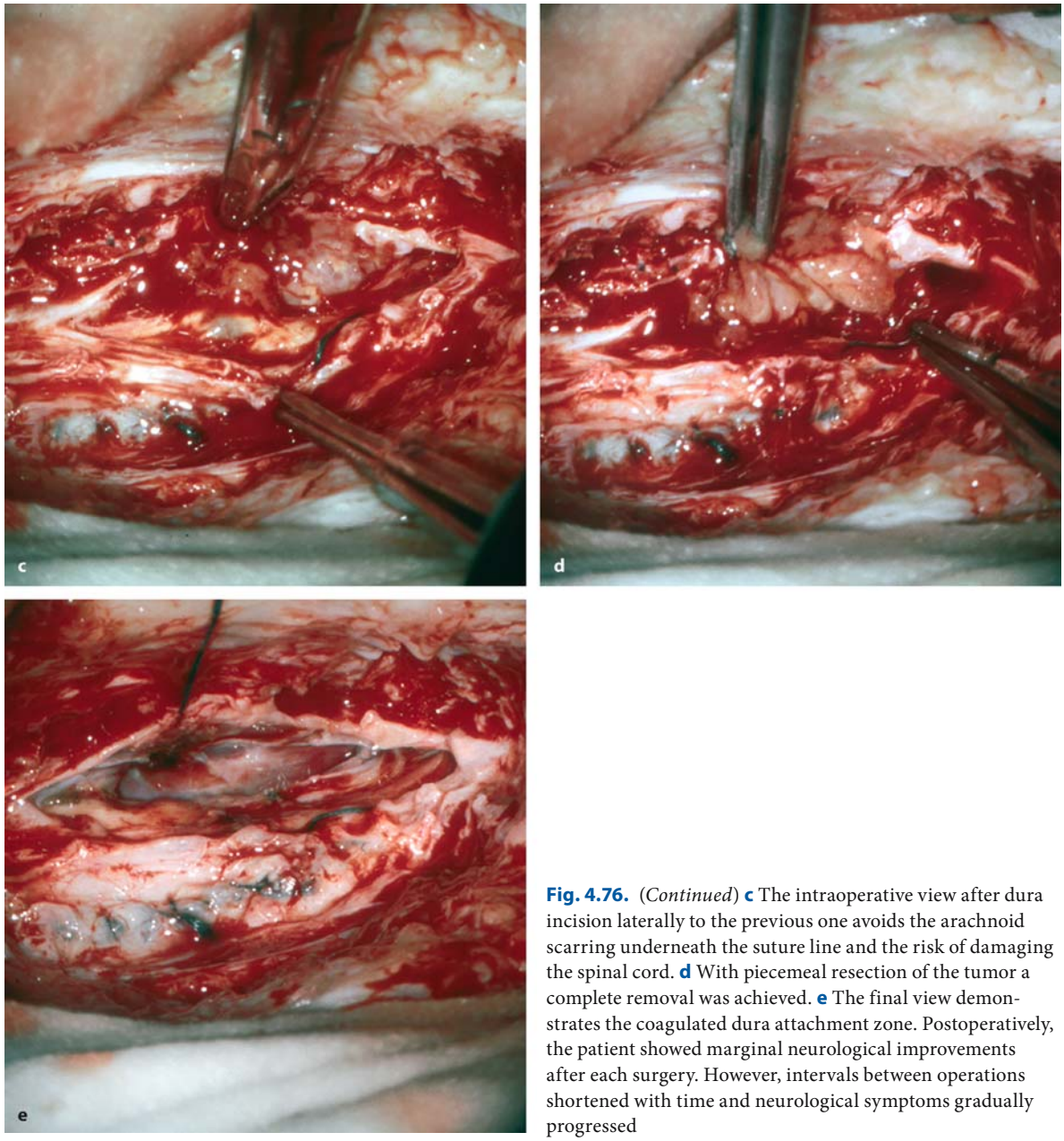

Fig. 4.76. (*Continued*) **c** The intraoperative view after dura incision laterally to the previous one avoids the arachnoid scarring underneath the suture line and the risk of damaging the spinal cord. **d** With piecemeal resection of the tumor a complete removal was achieved. **e** The final view demonstrates the coagulated dura attachment zone. Postoperatively, the patient showed marginal neurological improvements after each surgery. However, intervals between operations shortened with time and neurological symptoms gradually progressed

spinal root sheath (Fig. 4.77) as in schwannomas, but may occur anywhere (Fig. 4.74). We observed no intraosseous tumor growth, although the bone was found to be eroded in some of these patients. Removal of these meningiomas required a duraplasty to reconstruct the inevitable dura defect in laterally located tumors only. With anterior dura defects, no reconstruction was required.

About 20% of meningiomas in our series were accompanied by arachnoid scarring. This figure was lower for encapsulated tumors (11%), but considerably higher for en plaque (44%) or recurrent tumors (86%; Fig. 4.78). Apart from postsurgical arachnoid scarring, we consider mechanical irritation of the leptomeninges due to spinal cord movements as the most likely explanation for arachnoid changes in unoperated patients [156]. Such arachnoid scarring can make dissection of a meningioma quite difficult as it may obscure the exact tumor limits or engulf important spinal cord vessels. Therefore, the rate of complete resections is lower in this subgroup (72%). Arachnoid scarring may cause spinal cord tethering and contrib-

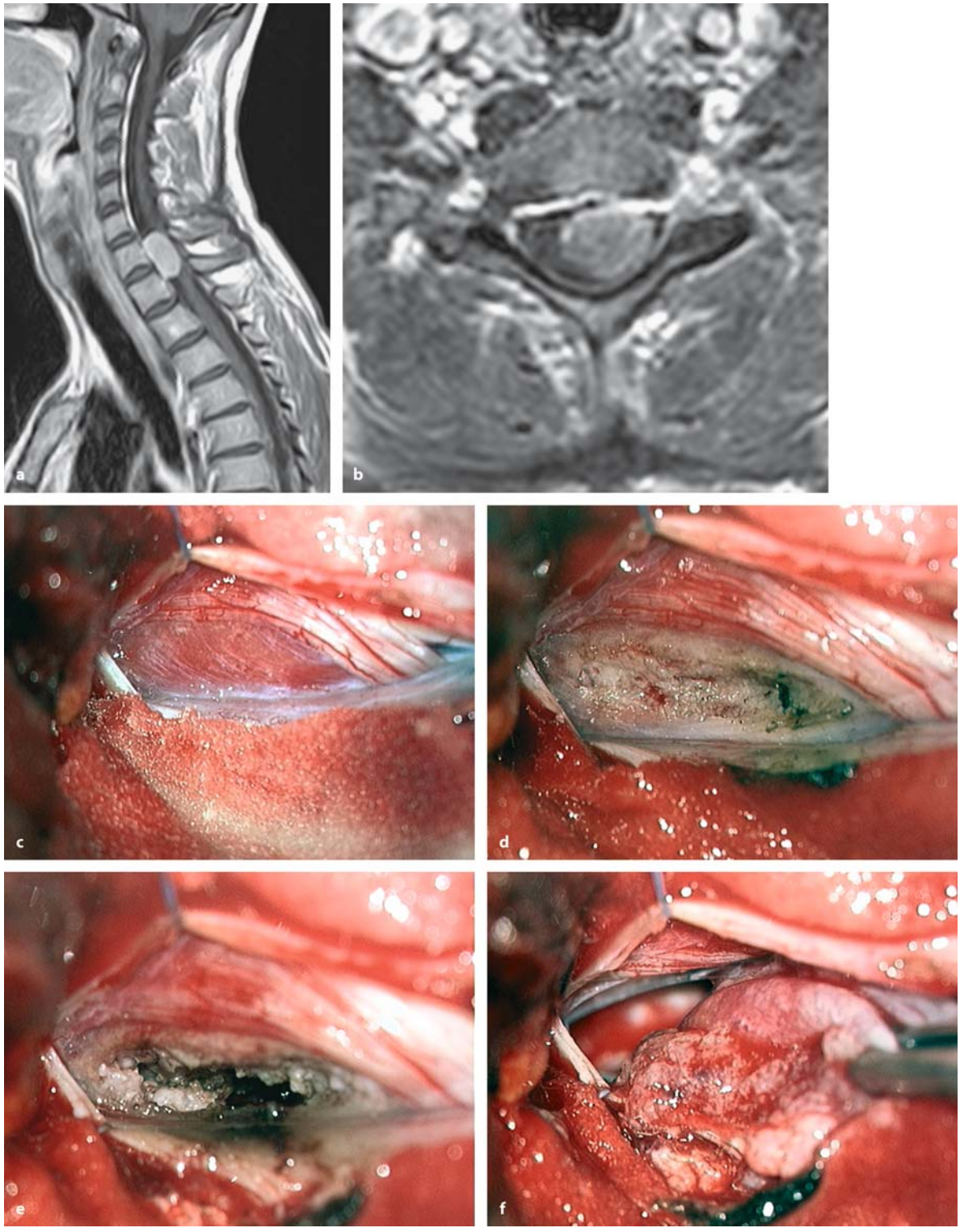

Fig. 4.77. Sagittal (**a**) and axial (**b**) T1 weighted, contrast-enhanced MRI images of a meningioma at C7–Th1 on the left side in a 41-year-old woman with a 6-month history of pain and a slight gait ataxia. **c** This intraoperative view after hemilaminectomy, and dura and arachnoid opening shows the tumor between the posterior and anterior nerve root. After coagulation of the capsule (**d**) and debulking (**e**), the tumor mass could be removed (**f**). (*Continuation see next page*)

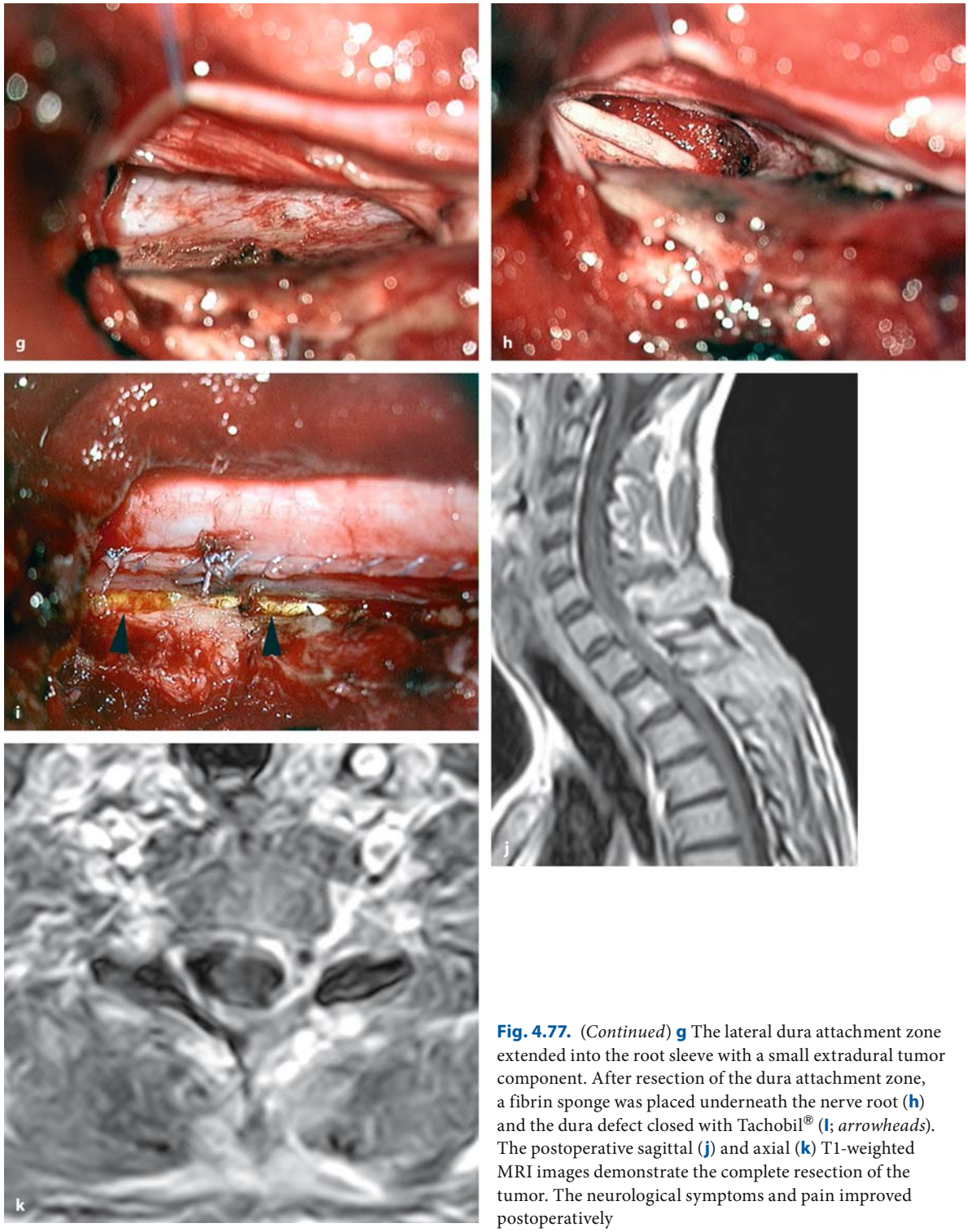

Fig. 4.77. (*Continued*) **g** The lateral dura attachment zone extended into the root sleeve with a small extradural tumor component. After resection of the dura attachment zone, a fibrin sponge was placed underneath the nerve root (**h**) and the dura defect closed with Tachobil® (**l**; *arrowheads*). The postoperative sagittal (**j**) and axial (**k**) T1-weighted MRI images demonstrate the complete resection of the tumor. The neurological symptoms and pain improved postoperatively

ute to neurological symptoms independently from the meningioma. It may lead to pain, dysesthesias, or progressive spinal cord damage due to interference with spinal cord blood flow [129, 156, 163, 219] and meningeal irritation. Postoperatively, it may even mimic a tumor recurrence with progressive motor weakness and sensory disturbances [150, 163, 247, 251, 272]. Such a dysesthesia syndrome was observed in four patients, and progressed to myelopathy in two patients of this study.

Complications occurred in 9% of patients and were more common in secondary operations due to a higher proportion of CSF fistulas (8% with first operations and 23% with recurrent tumors). A transient postoperative worsening of symptoms was experienced by 14% of patients, but all recovered within 6 months after surgery. The rate of permanent surgical morbidity was 1.2% for all meningiomas combined. For encapsulated meningiomas, this figure was 0.8%, for en plaque meningiomas 4.3%, and for recurrent meningiomas 9.1%. For first operations on a particular tumor there was no permanent morbidity at all. The surgical mortality rate was 2.8%. In the literature, mortality rates vary between 1.0% and 5.3% [48, 89, 93, 96, 119, 186, 247].

In general, patients benefited considerably from surgery. For each and every symptom, postoperative improvements can be expected. Significant recoveries were observed for patients with severe preoperative deficits even before the advent of the operative microscope [20, 21, 40, 44, 48, 52, 53, 89, 94, 96, 114, 119, 131, 138, 150, 171, 181, 186, 251]. Likewise, elderly patients can expect a favorable prognosis with resection of a spinal meningioma. In a series of 30 patients over 70 years of age, every patient showed neurological improvement postoperatively [181].

In this series of 33 patients unable to walk preoperatively, 18 regained this ability within a few days or after rehabilitation programs within 1 year. Even two of three patients with no preoperative motor function demonstrated some postoperative recovery, but not to an extent that allowed walking. Of 17 patients with severe preoperative bladder dysfunctions, seven regained control postoperatively.

However, there are risk factors that may argue against such a favorable outcome (Table 4.18): arachnoid scarring, a tumor recurrence, a dysesthesia syndrome, an anteriorly located tumor, a low preoperative Karnofsky score, a short history, and a cervical level predict a worse postoperative Karnofsky score after 1 year.

Table 4.19 provides an overview of the postoperative course of spinal meningiomas related to their localization. It appears that anterior meningiomas have a slightly worse outcome and that patients with posterior meningiomas recover faster compared to the other subgroups.

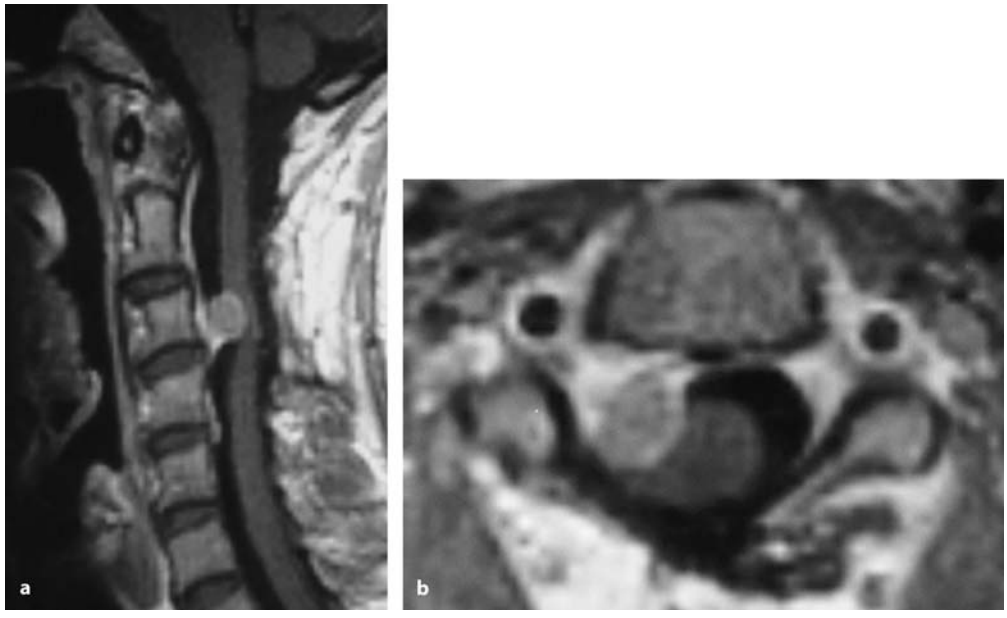

Fig. 4.78. Sagittal (**a**) and axial (**b**) T1 weighted, contrast-enhanced MRI images of a recurrent meningioma at C3 in a 44-year-old woman with a 4-month history of motor weakness of her right arm. (*Continuation see next page*)

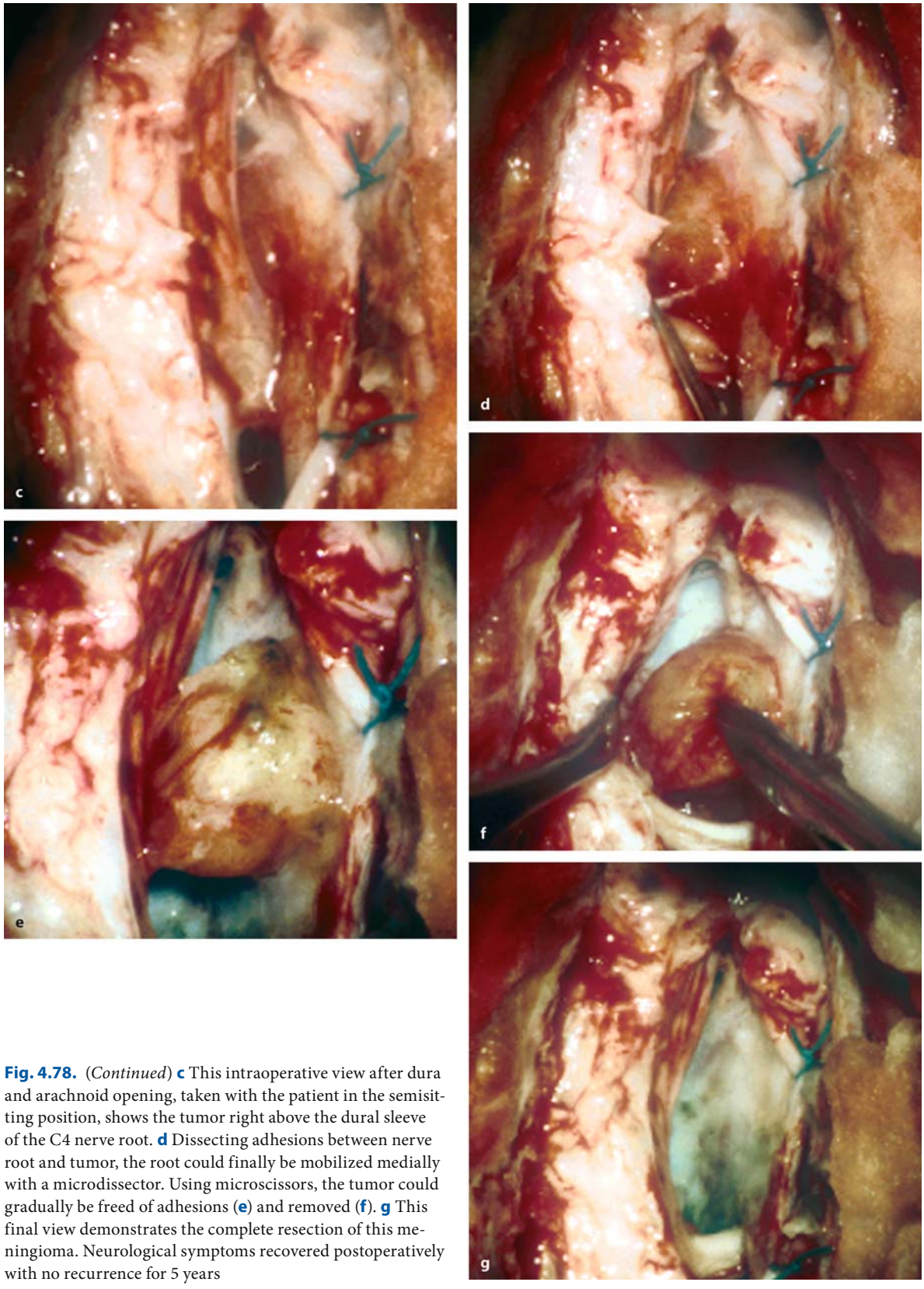

Fig. 4.78. (*Continued*) **c** This intraoperative view after dura and arachnoid opening, taken with the patient in the semisitting position, shows the tumor right above the dural sleeve of the C4 nerve root. **d** Dissecting adhesions between nerve root and tumor, the root could finally be mobilized medially with a microdissector. Using microscissors, the tumor could gradually be freed of adhesions (**e**) and removed (**f**). **g** This final view demonstrates the complete resection of this meningioma. Neurological symptoms recovered postoperatively with no recurrence for 5 years

Table 4.18. Multivariate analysis for prediction of a high postoperative Karnofsky score for patients with spinal meningiomas

Factor	β-value
No arachnoid scarring	0.5029
No tumor recurrence	0.3217
No dysesthesia syndrome	0.2916
Posterior localization	0.2621
High preoperative Karnofsky score	0.2134
Short history	0.1977
Low spinal level	0.1893

Correlation: r=0.8690, p=0.0002

Table 4.19. Clinical course for patients with spinal meningiomas related to tumor position

Symptom	Preoperative status	Postoperative status	3 Months postop.	6 Months postop.	1 Year postop.
Pain					
Anterior	3.2±1.0	3.8±0.7	4.1±0.7	4.1±0.7	4.0±1.0**
Lateral	3.7±1.1	4.2±0.7	4.4±0.7	4.5±0.8	4.4±1.0**
Posterior	3.9±1.0	4.2±0.8	4.5±0.6	4.5±0.6	4.5±0.7*
Hypesthesia					
Anterior	3.3±1.1	3.6±1.2	3.9±1.2	3.9±1.2	3.9±1.3**
Lateral	3.1±1.1	3.4±1.3	3.9±1.4	4.0±1.4	4.1±1.4**
Posterior	3.3±0.7	4.0±0.8	4.4±0.7	4.4±0.8	4.4±0.9**
Dysesthesias					
Anterior	4.0±1.1	4.4±0.9	4.6±0.7	4.6±0.7	4.6±0.9**
Lateral	4.0±1.1	4.4±0.8	4.5±0.7	4.5±0.8	4.4±0.9*
Posterior	4.1±0.9	4.4±0.7	4.6±0.5	4.6±0.5	4.6±0.6**
Gait					
Anterior	3.2±1.3	3.4±1.3	3.9±1.2	3.9±1.3	3.9±1.2**
Lateral	3.5±1.2	3.7±1.3	4.1±1.2	4.2±1.0	4.3±1.0**
Posterior	3.3±1.0	3.8±0.7	4.2±0.9	4.4±1.1	4.3±1.2**
Motor power					
Anterior	3.4±1.2	3.7±1.1	4.1±1.1	4.3±1.0	4.3±1.0**
Lateral	3.5±1.3	3.8±1.3	4.2±1.1	4.4±1.0	4.4±1.0**
Posterior	3.4±1.1	4.0±0.7	4.3±0.7	4.5±0.8	4.4±1.2**
Sphincter function					
Anterior	4.6±0.7	4.3±1.2	4.8±0.7	4.7±0.7	4.6±0.9
Lateral	4.1±1.2	4.3±1.1	4.5±0.9	4.6±0.8	4.6±0.9**
Posterior	4.3±0.9	4.5±0.7	4.6±0.7	4.6±0.8	4.5±1.2
Karnofsky score					
Anterior	64±19	65±18	72±17	75±16	74±18*
Lateral	69±16	73±17	78±16	80±16	82±17**
Posterior	68±13	73±11	77±15	83±15	83±17**

Statistically significant difference between preoperative status and 1 year postoperatively: *p<0.05, **p<0.01

Table 4.20. Multivariate analysis for prediction of a low recurrence rate for spinal meningiomas

Factor	β-value
Histological grade	0.2997
No arachnoid scarring	0.1501
Complete resection	0.1099
Long history	0.0906
Posterior localization	0.0860
High preoperative Karnofsky score	0.0816
Female sex	0.0546

Correlation: r=0.4631, p<0.0001

Table 4.21. Recurrence rates for spinal meningiomas

Group	1 Year	5 Years	10 Years
Total	11%	25%	31%
Complete ± dura resection	7%	17%	25%
Complete ± dura coagulated	6%	22%	22%
Subtotal	47%	79%	79%
First surgery	5%	17%	24%
Recurrent tumor	50%	75%	75%
Encapsulated	1%	8%	17%
En plaque	34%	59%	59%
Atypical	50%	100%	
Malignant	50%	100%	

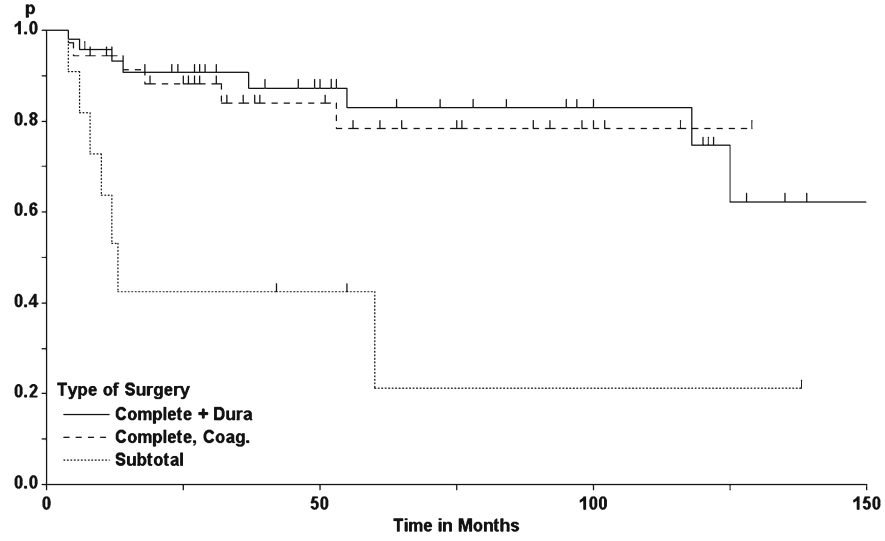

Fig. 4.79. Tumor recurrence rates for spinal meningiomas as a function of extent of tumor resection (log-rank test: p=0.0004)

Predisposing factors for recurrences of spinal meningiomas are: a high histological grade, arachnoid scarring at surgery, subtotal resection, a short history, a ventral localization of the tumor, a low preoperative Karnofsky score, surgery on a recurrent tumor, and female sex (Table 4.20). Table 4.21 provides an overview of recurrence rates of spinal meningiomas and their subgroups. For all meningiomas combined, recurrence rates of 11%, 25%, and 31% were calculated after 1, 5, and 10 years, respectively. These recurrence rates are similar to those for intracranial meningiomas, even though spinal meningiomas appear to display less proliferative potential, as determined by proliferation markers [221]. For completely resected meningiomas, no difference appeared related to the way the dura attachment was handled (Fig. 4.79) [20, 138, 247]. A tremendous difference in recurrence rates appeared when comparing first and secondary operations (Fig. 4.80) and encapsulated, en plaque, atypical, and malignant meningiomas (Fig. 4.81). According to these analyses, the best results can be expected for encapsulated tumors. For recurrent meningiomas, regardless of localization, 42% required another operation within 5 years and 56% within 10 years.

Parsa et al. [204] described higher recurrence rates for patients under 50 years of age (20%) compared to older patients (5%). Similar figures were described by Cohen-Gadol et al. [48], with recurrence rates of 22% and 5%, respectively. Both studies concluded that younger patients have a worse long-term prognosis compared to patients of advanced age. In our analysis, age did not evolve as an independent factor. Schick et

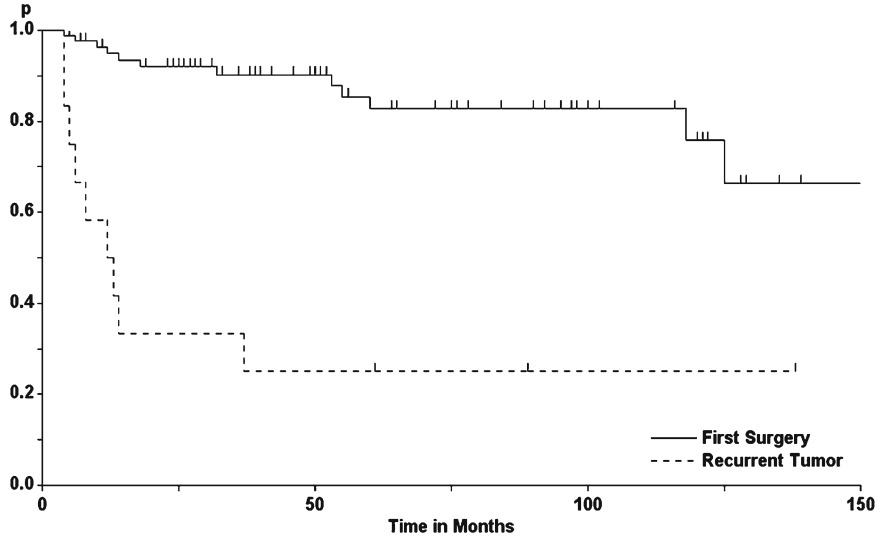

Fig. 4.80. Tumor recurrence rates for spinal meningiomas after first or secondary surgery (log-rank test: $p<0.0001$)

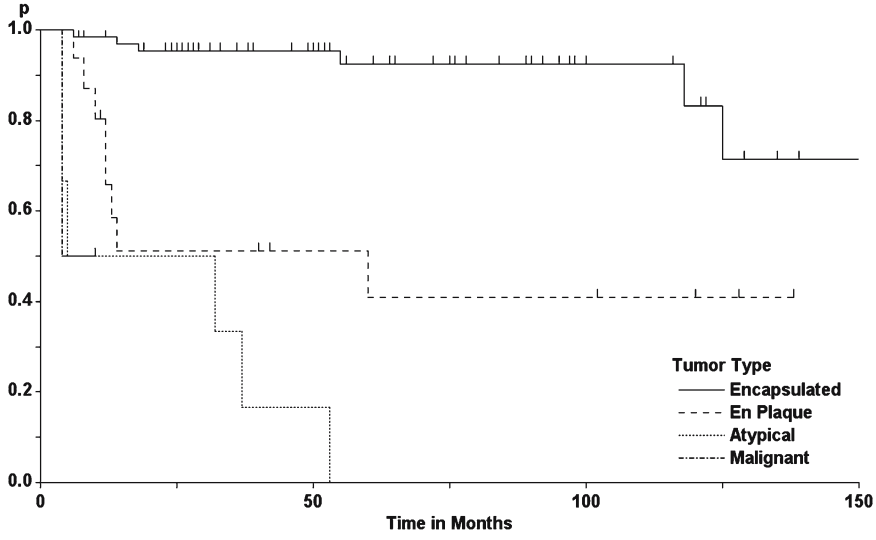

Fig. 4.81. Tumor recurrence rates for spinal meningiomas as a function of growth pattern and histological grade (log-rank test: $p<0.0001$)

al. [231] reported a figure of 8.9%, with recurrences occurring between 29 to 118 months after surgery. They did not apply Kaplan-Meier statistics, however. King et al. [138] observed one recurrence among 78 operated tumors, 14 years after surgery. Solero et al. [247] reported a tumor recurrence rate of 6% for completely and 17% for partially removed tumors. McCormick et al. [171] described a recurrence rate of 10–15%. Using Kaplan-Meier analysis to determine tumor recurrence rates, Mirimanoff et al. [178] gave a figure of 0% after 5 years, but 13% after 10 years. They observed lower recurrence rates for spinal as compared to intracranial meningiomas, due to the higher rate of complete resections in spinal cases.

The first surgeon to operate on a meningioma will have the best chance to provide a long-term benefit for the patient. With each subsequent operation, the chances for improving or at least stabilizing the patient's condition will diminish.

4.5.2 Nerve Sheath Tumors

We have observed a total of 225 extramedullary nerve sheath tumors. Of these, 158 were located intradurally and the remaining 67 tumors extended extradurally (i.e., dumbbell tumors). Schwannomas and neurofibromas can be distinguished in this category. Apart from patients with NF type 1 (NF-1) who presented neurofibromas, schwannomas were encountered in the remainder. The average patient age was 44±16 years (range 10–79 years) [50]. We observed an

equal sex distribution. The average patient history until surgery was 23±33 months (maximum 15 years). The average Karnofsky score was 72±14. Patients were followed for 43±47 months (maximum 15 years).

Schwannomas did not occur along the entire spinal axis in equal proportions. Cervical and lumbar localizations predominate this series: 41% of operations were performed in the cervical, 29% in the thoracic, 29% in the lumbar, and 1% in the sacral region. Similar distributions have been reported in the literature [6, 24, 27, 33, 50, 61, 82, 97, 119, 157, 191, 226]. Intradural schwannomas were slightly more common in the thoracic and lumbar spine, whereas dumbbell tumors were encountered predominantly in the cervical area [61, 100, 127].

With nerve sheath tumors, two patient and two tumor populations have to be distinguished: those with and without NF, and intradural and dumbbell schwannomas. Forty-six operations dealt with schwannomas in NF-2 patients, and 10 surgeries were performed for patients with NF-1 harboring neurofibromas [188]. Patients with NF-2 were significantly younger than those without (29±12 and 49±15 years, respectively; $p<0.0001$), the average history until admission for surgery was significantly shorter (11±22 months and 27±35 months, respectively; $p=0.0008$), and the preoperative Karnofsky score lower (68±15 and 74±13, respectively; $p=0.0137$).

Most patients without NF demonstrated a slowly progressive course. One patient presented a history of 15 years. For the majority of patients, the first symptom noted was pain (77%) [24, 33, 50, 61, 71, 75, 82, 97, 100, 103, 113, 127, 157, 161, 191, 219, 234], with all other symptoms rarely reported as the first indicator of the tumor (Table 4.22). On admission, 63% of patients still reported pain as their main concern. For the remainder, gait ataxia (24%), motor weakness (8%), or dysesthesias (3%) predominated.

Whereas schwannomas are encountered in patients with NF-2 and in patients without NF, neurofibromas are found in patients with NF-1 [102]. NF-1 is an autosomal dominant disease that is linked to a genetic defect on chromosome 17 [184, 187, 210, 263]. Tumors of the spinal canal are not a regular feature of NF-1 [191]. Huson et al. [116] described 2 spinal neurofibromas among 135 patients with NF-1. However, multiple spinal neurofibromas do occur (Fig. 4.82), and in patients with additional spinal deformities, the incidence of spinal tumors was found to be higher (37%) [215]. Apart from neurofibromas, malignant nerve sheath tumors, optic nerve gliomas, rhabdomyosarcomas, pheochromocytomas, and carcinoid tumors are described [203]. Of patients in our series with NF-1, 40% complained about pain as their first manifestation, while 30% mentioned gait and motor deficits as the first symptom. On admission, 40% were concerned about gait ataxia and 30% about motor deficits or pain.

NF-2 is an autosomal dominant disorder that is linked to a genetic defect on chromosome 22 [184, 187, 211]. Spinal tumors can be found in about 90% of patients with NF-2 [169, 205]. Schwannomas are the commonest spinal nerve sheath tumor in NF-2 [56, 102, 169]. Other tumors associated with NF-2 are acoustic schwannomas, neurofibromas, ependymomas, astrocytomas, and meningiomas [56, 203]. The phenotypic expression of the NF-2 gene varies from patient to patient, and so the clinical courses of patients harboring multiple spinal schwannomas vary. Therefore, patients with NF-2 should undergo yearly MRI scans of the entire spinal canal. Genotypic subtyping has not provided additional prognostic information that could be used in the management of these patients [56]. Spinal deformities and instabilities are common and may require additional stabilizations [137] (Fig. 4.83).

In our opinion, diagnosis of a spinal schwannoma in NF-2 patients does not imply an indication for surgery per se. Often, multiple tumors will be encountered throughout the entire spinal canal without apparent growth for several years or corresponding neurological deficits [56, 65, 169]. In a large analysis on NF-2, Mautner et al. [169] reported that only 33% of spinal tumors actually caused symptoms. In a British study on 41 patients with NF-2 and spinal tumors, extramedullary tumors larger than 5 mm showed a

Table 4.22. Initial symptoms for spinal nerve sheath tumors.

First symptom	Intra	Dumbbell	No NF-2	NF-2	Total
Pain	68%	63%	77%	43%	67%
Gait ataxia	16%	15%	9%	33%	16%
Motor weakness	8%	10%	5%	17%	8%
Sensory deficits	3%	–	2%	2%	2%
Dysesthesias	5%	10%	8%	2%	6%
Sphincter problems	–	2%	–	2%	1%

Abbreviation: NF-2 = neurofibromatosis type 2

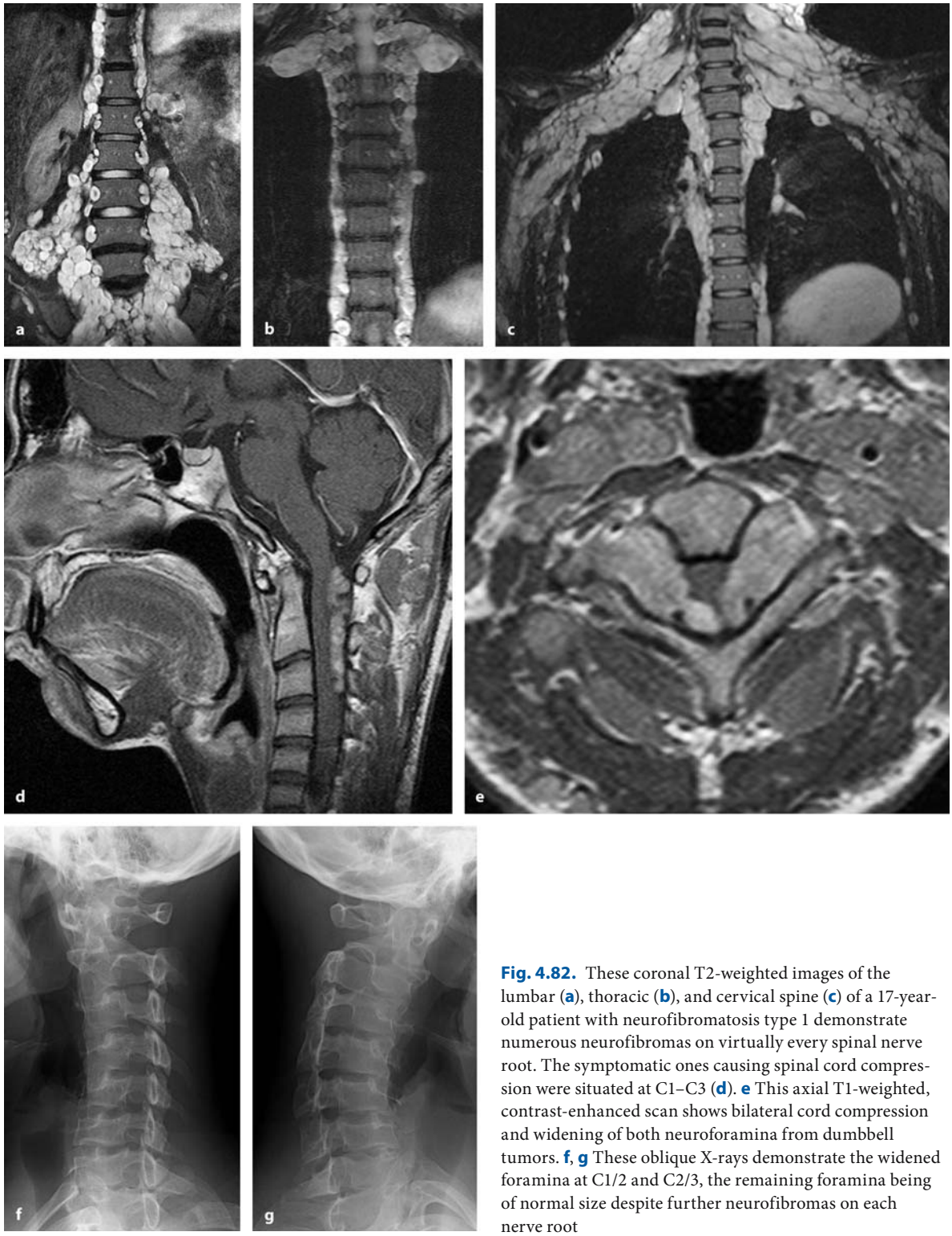

Fig. 4.82. These coronal T2-weighted images of the lumbar (**a**), thoracic (**b**), and cervical spine (**c**) of a 17-year-old patient with neurofibromatosis type 1 demonstrate numerous neurofibromas on virtually every spinal nerve root. The symptomatic ones causing spinal cord compression were situated at C1–C3 (**d**). **e** This axial T1-weighted, contrast-enhanced scan shows bilateral cord compression and widening of both neuroforamina from dumbbell tumors. **f**, **g** These oblique X-rays demonstrate the widened foramina at C1/2 and C2/3, the remaining foramina being of normal size despite further neurofibromas on each nerve root

Fig. 4.83. This 29-year-old patient with NF-2 and multiple schwannomas in his upper cervical spine compressing the cord from both sides, as seen on these sagittal (**a**) and axial (**b**) T1-weighted, contrast-enhanced MRI scans, underwent cervical laminectomies and subtotal resections of these tumors. Within a few weeks after surgery he developed a swan neck deformity, requiring extensive cervical fusion (**c**)

higher likelihood of progression than smaller tumors (36% and 0%, respectively). We recommend observation of patients clinically and neuroradiologically using MRI with gadolinium enhancement [56, 65, 158, 169, 184, 233] with absent or mild neurological symptoms in 6- to 12-month intervals. If neurological signs clearly progress, surgery should be targeted at the tumor that is most likely responsible for it. Likewise, significant tumor growth proven by repeated MRI scans provides an indication for surgery. Radiological follow up should cover the entire spine [56, 169].

The NF2-patient should be informed that symptomatic schwannomas tend to grow faster and are more likely to infiltrate nerve roots, and thus tend to progress to severe neurological deficits sooner. Due to their larger size and multiplicity, complications are more likely and issues such as postoperative instability or vertebral anomalies requiring additional stabilizing operations will need to be addressed subsequently (Fig. 4.83) [113, 158, 184, 225, 233].

Pain was noted as the first symptom in only 43% of NF-2 patients, while gait ataxia (33%) or motor weakness (17%) were mentioned more often from the be-

ginning ($p<0.0001$; Table 4.22). On admission, 55% of NF-2 patients complained about gait ataxia as the major problem, 31% about pain, and 10% about motor weakness ($p=0.0027$). NF-2 patients were more likely to present a significant neurological deficit than patients without NF-2. The average scores for motor weakness (3.7±1.1 and 4.1±1.0, respectively; $p=0.046$) and gait ataxia (3.7±1.1 and 4.1±1.0, respectively; $p=0.025$) were significantly lower for NF-2 patients, while the score for pain was significantly higher compared to patients without NF-2 (3.7±1.0 and 3.1±0.8, respectively; $p<0.0001$). The average Karnofsky score on admission was significantly lower for NF-2 patients (68±15 and 74±13, respectively; $p=0.0097$), indicating that 86% of patients without NF-2 were still able to ambulate without assistance, whereas 33% of NF-2 patients were not.

Table 4.23 gives an overview of the clinical presentations of patients with spinal schwannomas. We observed no significant differences in clinical history and presentation between schwannomas with and without extradural extension. Jinnai et al. [127] presented a series of 149 patients with spinal schwannomas and reported that intradural tumors were more likely to present myelopathic problems, whereas tumors with extradural extension showed radicular deficits.

In NF-2, 95 schwannomas were removed in 43 operations, with multiple tumors encountered during 20 operations (Figs. 4.83–4.85). In 7 NF-1 patients, 20 neurofibromas were resected in 10 operations (Fig. 4.82). In 86 patients without NF, only 3 patients were observed with 2 schwannomas each (Fig. 4.86). Overall, 23 operations dealt with a recurrent schwannoma (Fig. 4.87). Arachnoid scarring associated with the tumor was encountered during 21% of operations for intradural and 17% for dumbbell tumors. They were particularly common with recurrent tumors (65%).

Whether dumbbell schwannomas can be removed via standard posterior approaches or require modified approaches or even staged operations from anterior and posterior depends on the extent of the intra- and extradural portion of the tumor. Most of them can be managed with standard posterior operations (Figs. 4.39, 4.47, 4.85, and 4.87). However, in rare instances dumbbell schwannomas may not present as encapsulated tumors, but may almost appear to infiltrate surrounding structures (Fig. 4.88). In our series, all but one dumbbell schwannoma at C4/5 were removed posteriorly. For significant extradural extensions, techniques have been described to avoid a staged operation and to achieve an entire resection with one approach. Ryu et al. [224] removed the intradural part of a cervical tumor at C4/5 via the grossly enlarged neuroforamen, avoiding any posterior bony removal. George described an anterolateral approach to the cervical spine that he has used for a number of pathologies including dumbbell schwannomas. In this book, this approach is described in the section on bone tumors [85–88]. Fiumara et al. [72], Grillo et al. [98], and Shadmehr et al. [237] described a combined approach for the removal of thoracic tumors with excellent results. McCormick [170] described a series of 12 thoracic and lumbar tumors of this type that were managed from a lateral extracavitary approach. They succeeded in achieving a complete resection in 11 instances. Shadmehr et al. [237] used a posterior thoracotomy combined with foraminotomy, hemilaminectomy, or laminectomy to achieve complete resections in single-stage operations of 13 thoracic dumbbell tumors of spinal nerve sheaths.

In our series, complete tumor removal was achieved for 87% of patients, with subtotal removals in 12% and decompressions in 1% [61]. The affected nerve root was resected with the tumor in 86% of cases (Figs. 4.37, 4.41, 4.45, and 4.47) and preserved in 14% of cases (Figs. 4.36, 4.39, 4.46, 4.84, 4.85, and 4.87). A duraplasty was inserted in 23% of all operations – mostly in recurrent tumors and dumbbell tumors (Figs. 4.39 and 4.85).

Analyses of subgroups among schwannomas showed that complete removals were obtained for 63% with arachnoid scarring, 52% of recurrent

Table 4.23. Symptoms for spinal nerve sheath tumors at presentation

Symptom	Intra	Dumbbell	No NF-2	NF-2	Total
Pain	87%	85%	93%	71%	87%
Gait ataxia	62%	59%	56%	73%	61%
Motor weakness	63%	68%	62%	71%	64%
Sensory deficits	73%	78%	75%	73%	74%
Dysesthesias	42%	44%	49%	27%	43%
Sphincter problems	28%	22%	31%	15%	27%

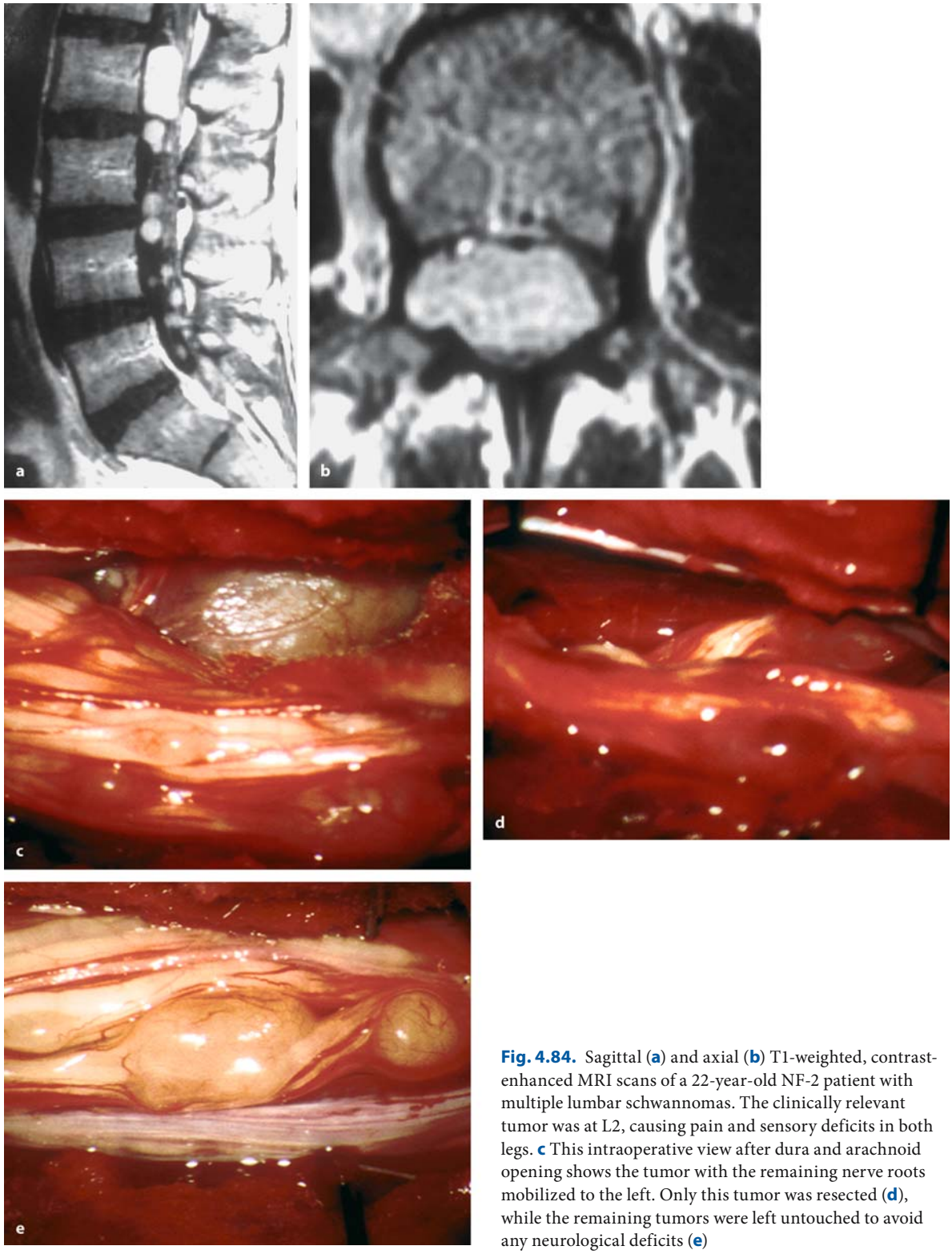

Fig. 4.84. Sagittal (**a**) and axial (**b**) T1-weighted, contrast-enhanced MRI scans of a 22-year-old NF-2 patient with multiple lumbar schwannomas. The clinically relevant tumor was at L2, causing pain and sensory deficits in both legs. **c** This intraoperative view after dura and arachnoid opening shows the tumor with the remaining nerve roots mobilized to the left. Only this tumor was resected (**d**), while the remaining tumors were left untouched to avoid any neurological deficits (**e**)

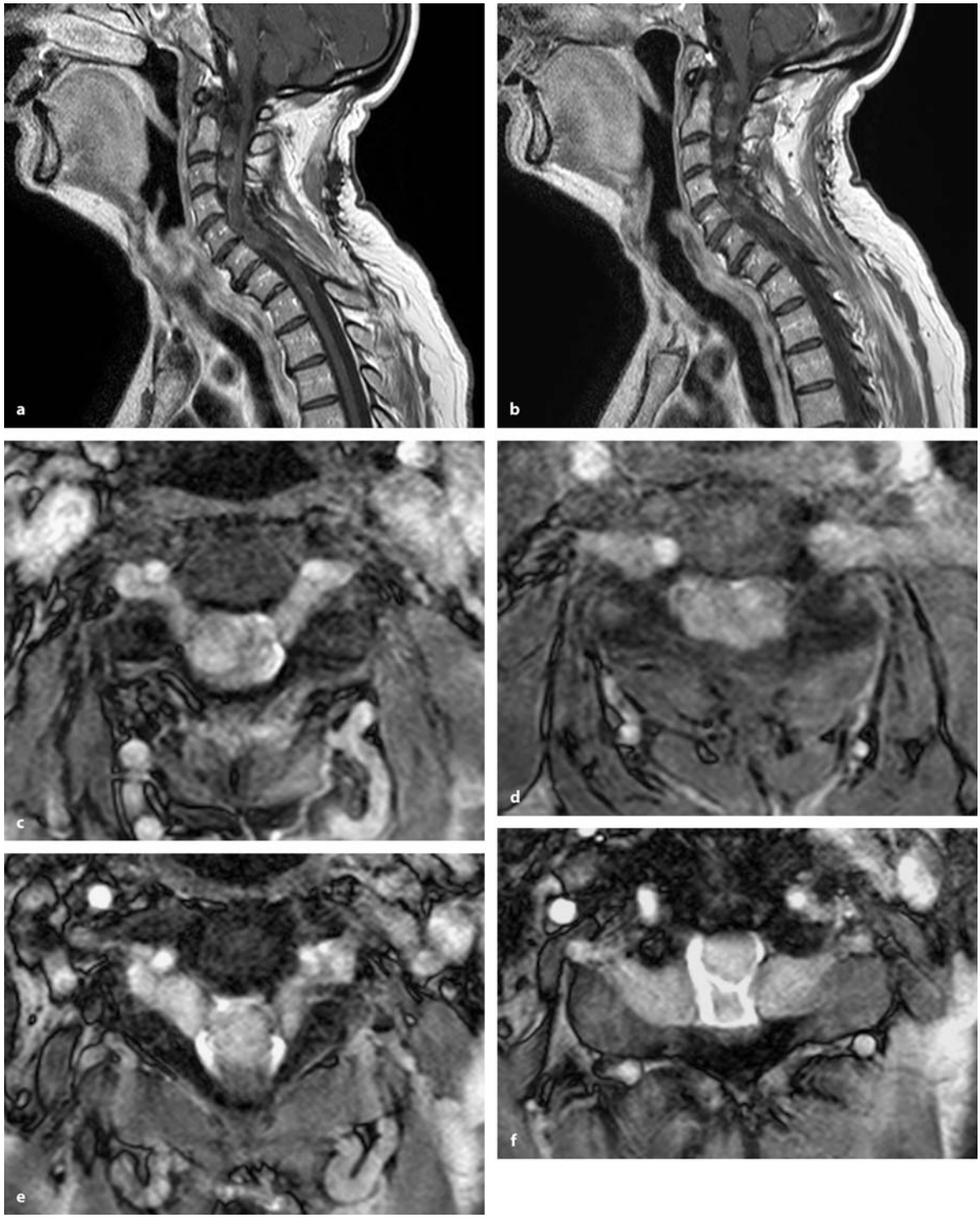

Fig. 4.85. Sagittal midline (**a**) and paramedian (**b**) T1-weighted, contrast-enhanced MRI scans of multiple cervical dumbbell schwannomas in a 66-year-old NF-2 patient with a 6-month history of progressive tetraparesis. The axial T2-weighted scans at C4 (**c**) and C5 (**d**) show tumors compressing the cord bilaterally. At C2/3 (**e**) and C1/2 (**f**), ventral dumbbell tumors push the spinal cord posteriorly. (*Continuation see next page*)

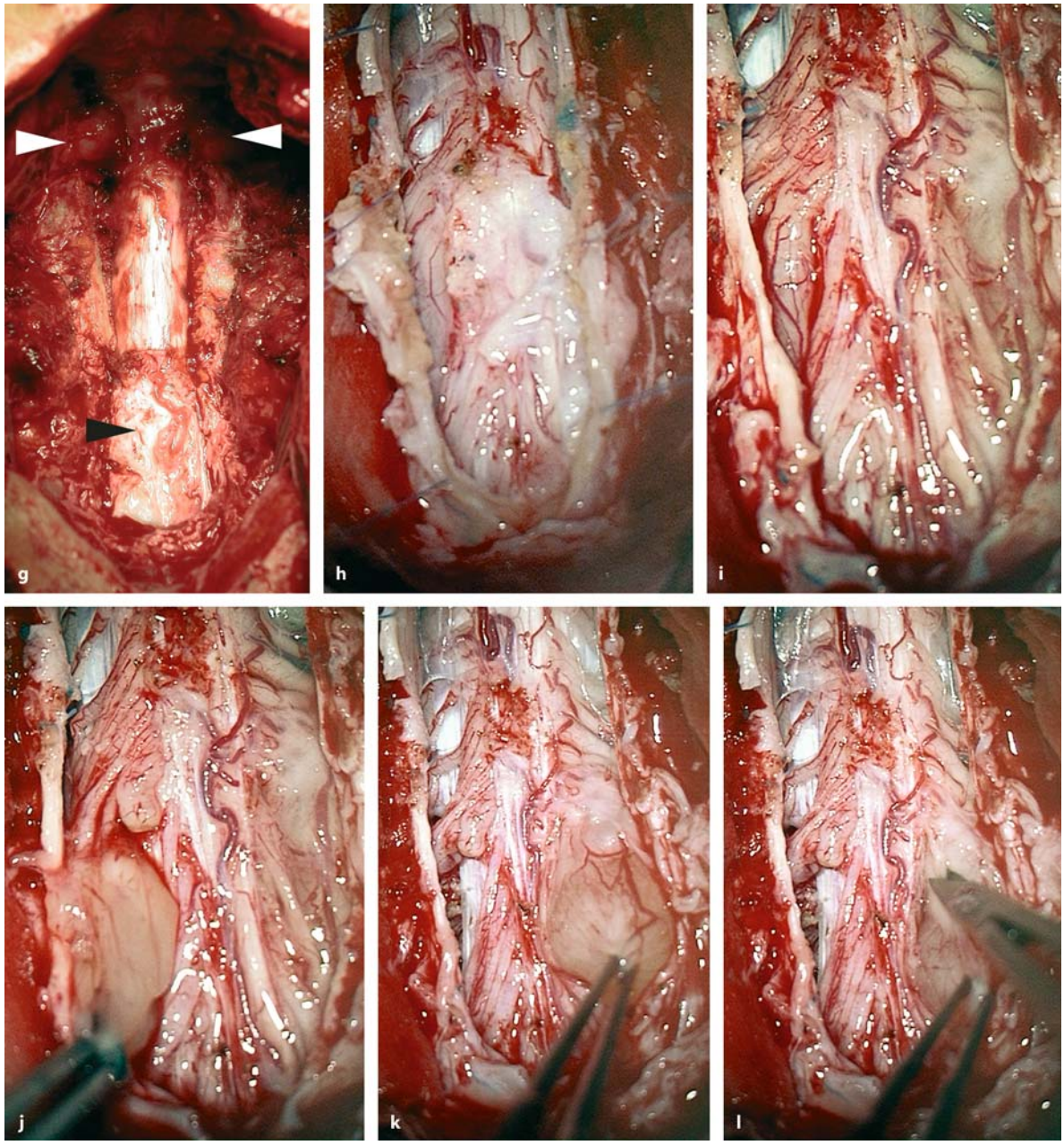

Fig. 4.85. **g** This intraoperative overview, taken with the patient in the semisitting position after laminotomy at C1–C4 and reexposure at C5 and C6, demonstrates the epidural scarring in the lower half (*black arrowhead*) and the enlarged C2 nerve roots bilaterally (*white arrowheads*). **h** After dura opening in the midline, dense adhesions were found underneath the suture line. These had to be resected. **i** After arachnoid dissection at the level of the previous surgery, the tumors underneath the posterior nerve roots were visible compressing the cord from both sides. **j** With transection of the tumorous posterior rootlet on the left side, the first schwannoma could be mobilized, debulked, and resected. Mobilization of the tumor on the right (**k**) exposed the originating rootlet of this tumor (**l**). (*Continuation see next page*)

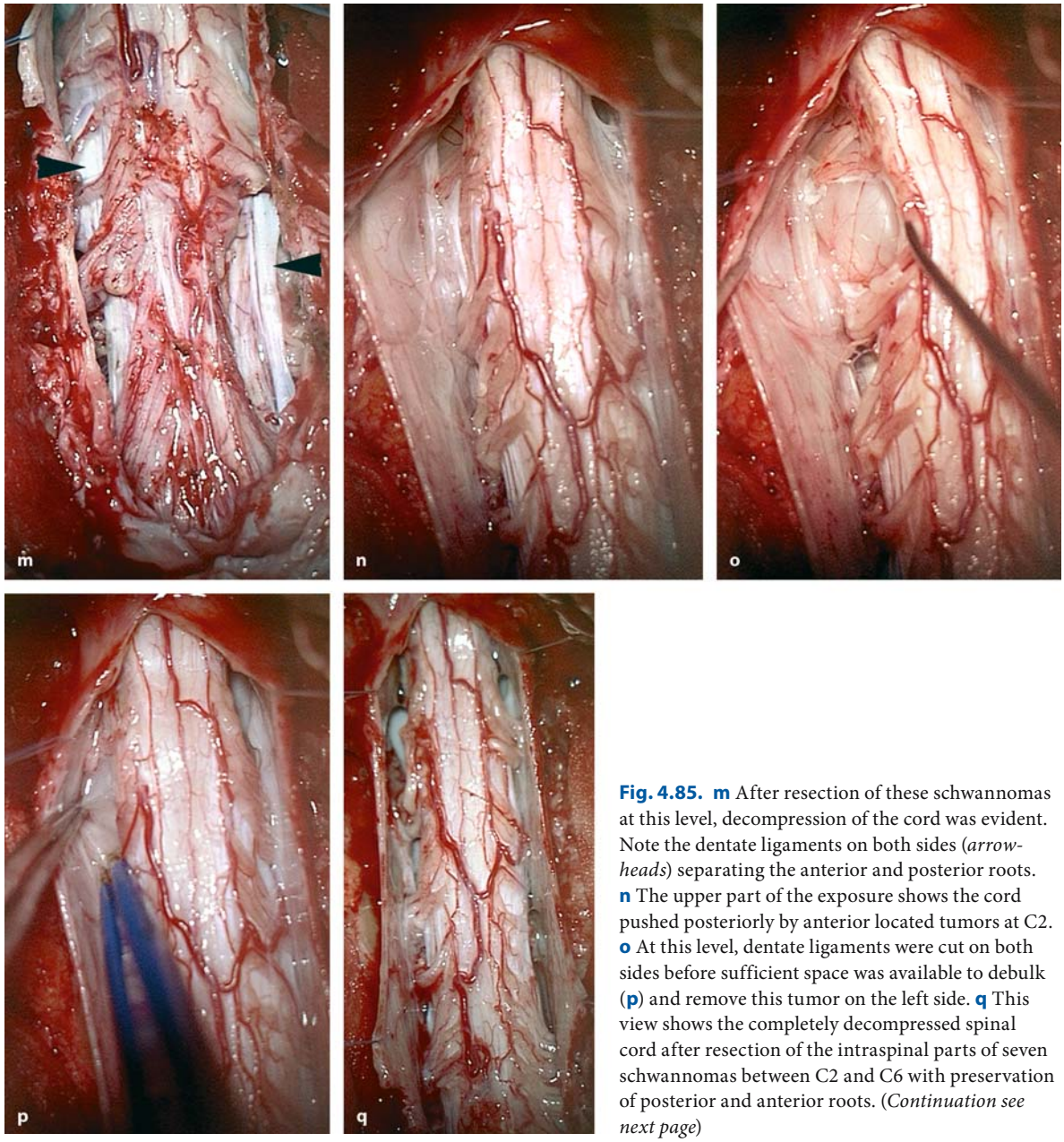

Fig. 4.85. **m** After resection of these schwannomas at this level, decompression of the cord was evident. Note the dentate ligaments on both sides (*arrowheads*) separating the anterior and posterior roots. **n** The upper part of the exposure shows the cord pushed posteriorly by anterior located tumors at C2. **o** At this level, dentate ligaments were cut on both sides before sufficient space was available to debulk (**p**) and remove this tumor on the left side. **q** This view shows the completely decompressed spinal cord after resection of the intraspinal parts of seven schwannomas between C2 and C6 with preservation of posterior and anterior roots. (*Continuation see next page*)

schwannomas, 74% of dumbbell tumors, and 87% of patients with NF-2. Without these features, a complete resection was achieved for 98% of patients. The results for NF-2 patients reflect our more conservative strategy for these patients compared to those without NF-2. In the former, the systemic disease may affect any nerve root any time, regardless of the surgical result for a particular tumor. Therefore, we consider it unjustifiable to expose a patient with NF-2 to unnecessary risks to loose function as a result of surgery. Quite commonly, one will find that multiple nerve roots are affected with tumors or appear abnormal on inspection. In NF-2, preservation of function is the major objective and not radicality for an individual tumor (Figs. 4.39 and 4.85).

Complications occurred in 12% of operations. We observed a trend for higher complication rates in NF-2 patients (16%). A transient postoperative neurological worsening was observed in 10% of patients, with recovery within a maximum of 6 months [40].

We have resected a cervical or lumbar nerve root together with the tumor in 89 instances. A transient

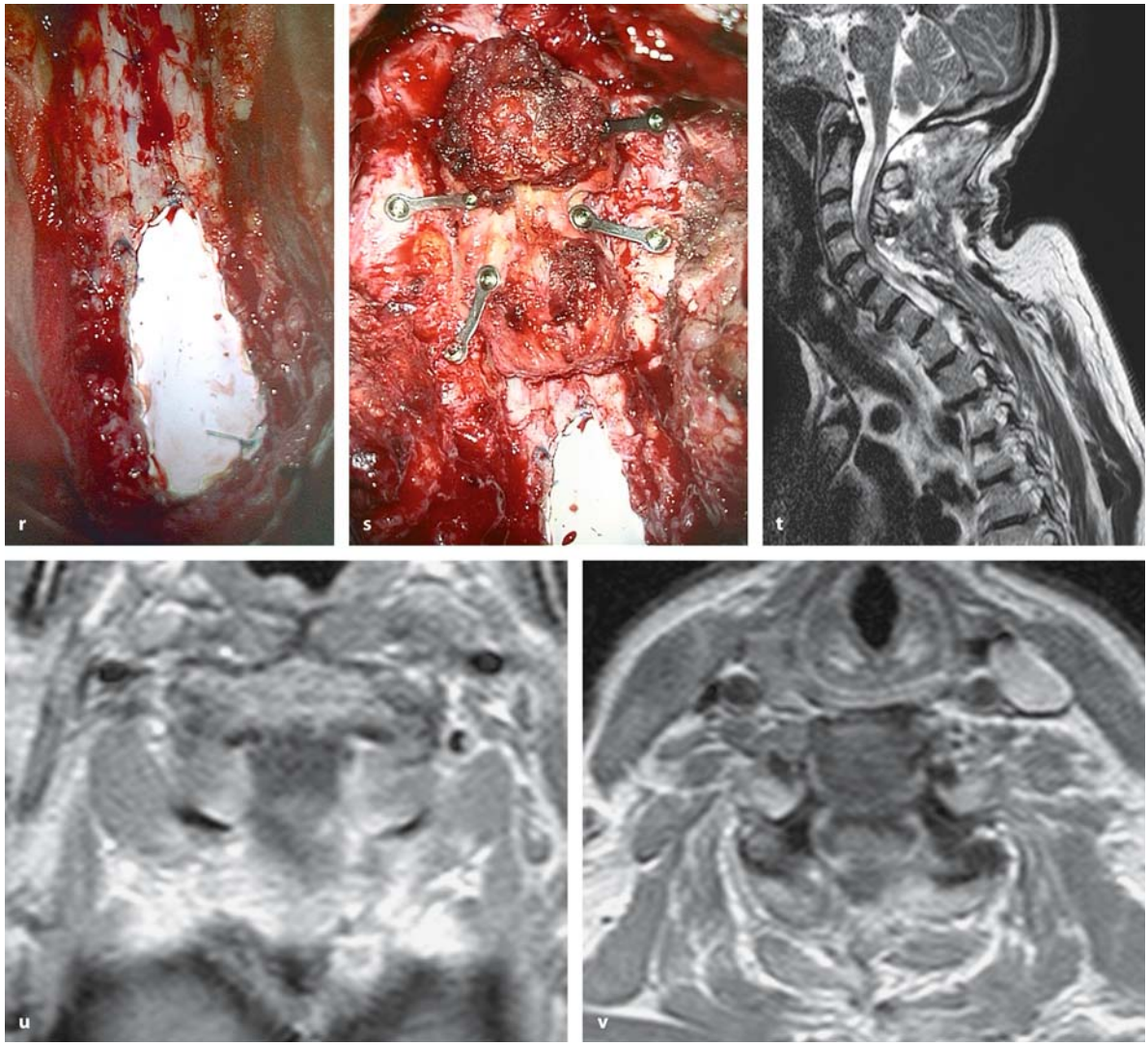

Fig. 4.85. (*Continued*) A Gore-Tex® duraplasty was inserted in the lower part of the exposure (**r**) and the laminae of C2 and C3 reinserted with miniplates (**s**). The postoperative sagittal (**t**) and axial MRI scans at C2 (**u**) and C5 (**v**) show no residual tumors. Postoperatively, the patient demonstrated an aggravation of her ataxia on the left side with subsequent recovery

neurological deficit was observed in 9% of these patients and a permanent deficit in 1 patient. No permanent postoperative morbidity occurred in patients in whom the nerve root could be preserved. These figures correspond to those in the literature documenting that transection of a nerve root in the cervical or lumbar area will not be followed by an additional, permanent neurological deficit in the overwhelming number of cases [33, 103, 157, 170, 179, 234] even after resection of dorsal and posterior roots [179]. McCormick [170] did not observe permanent deficits after transection of nerve roots carrying even dumbbell tumors. Destruction of the root by the schwannoma and concomitant innervation from neighboring nerve roots seem to offer the best explanations for this observation [105, 179, 234]. This hypothesis has been substantiated recently by a neuropathological analysis of nerve stumps removed with spinal schwannomas in 13 patients. Tumor-carrying nerves are in a process of degeneration, with signs of attempted regeneration and remyelination [105]. Furthermore, the overwhelming majority of tumors originate from posterior nerve roots. Jinnai et al. [127] found 6 schwannomas of ventral nerve roots compared to 170 tumors of posterior roots.

However, in a patient with a preoperative motor deficit attributable to the root carrying the tumor, the situation may be more complex. Especially with extradural extension and patients with NF-2, the likeli-

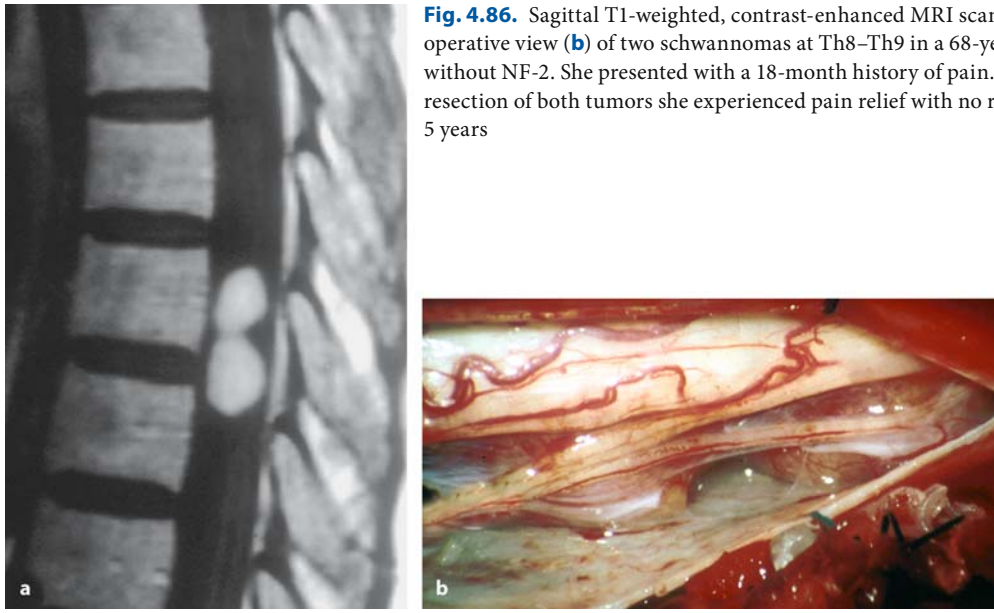

Fig. 4.86. Sagittal T1-weighted, contrast-enhanced MRI scan (**a**) and intraoperative view (**b**) of two schwannomas at Th8–Th9 in a 68-year-old woman without NF-2. She presented with a 18-month history of pain. After complete resection of both tumors she experienced pain relief with no recurrence for 5 years

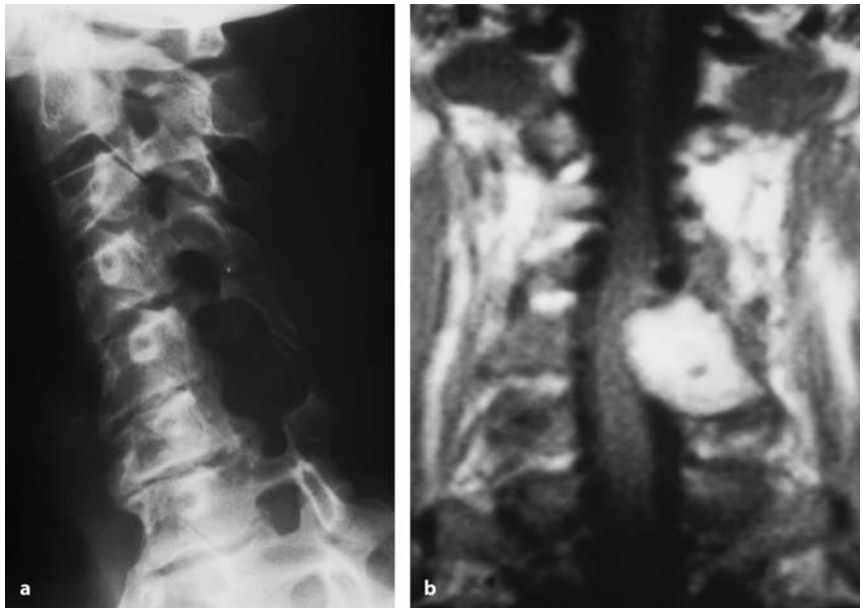

Fig. 4.87. Oblique X-ray of the cervical spine (**a**) and coronal T1-weighted, contrast-enhanced MRI (**b**) of a recurrent dumbbell schwannoma at C5/6 on the right side in a 56-year-old patient with a 9-month history of radicular pain, and sensory and motor disturbances. (*Continuation see next page*)

hood of a permanent deficit with resection of that root or even spinal nerves will be higher. It should be discussed with the patient before operation how to proceed if preservation of function is only possible for the price of incomplete resection. Several points have to be considered in this instance. On the one hand, transection carries the risk of a permanent, possibly significant neurological deficit. Most patients with NF-2 and multiple neurological problems associated with other tumors will not accept additional deficits from surgery. On the other hand, recurrence of the tumor with permanent complete damage of that root at some time in the future is inevitable after incomplete removal of the schwannoma, and chances for radical resection are considerably reduced at a subsequent second attempt.

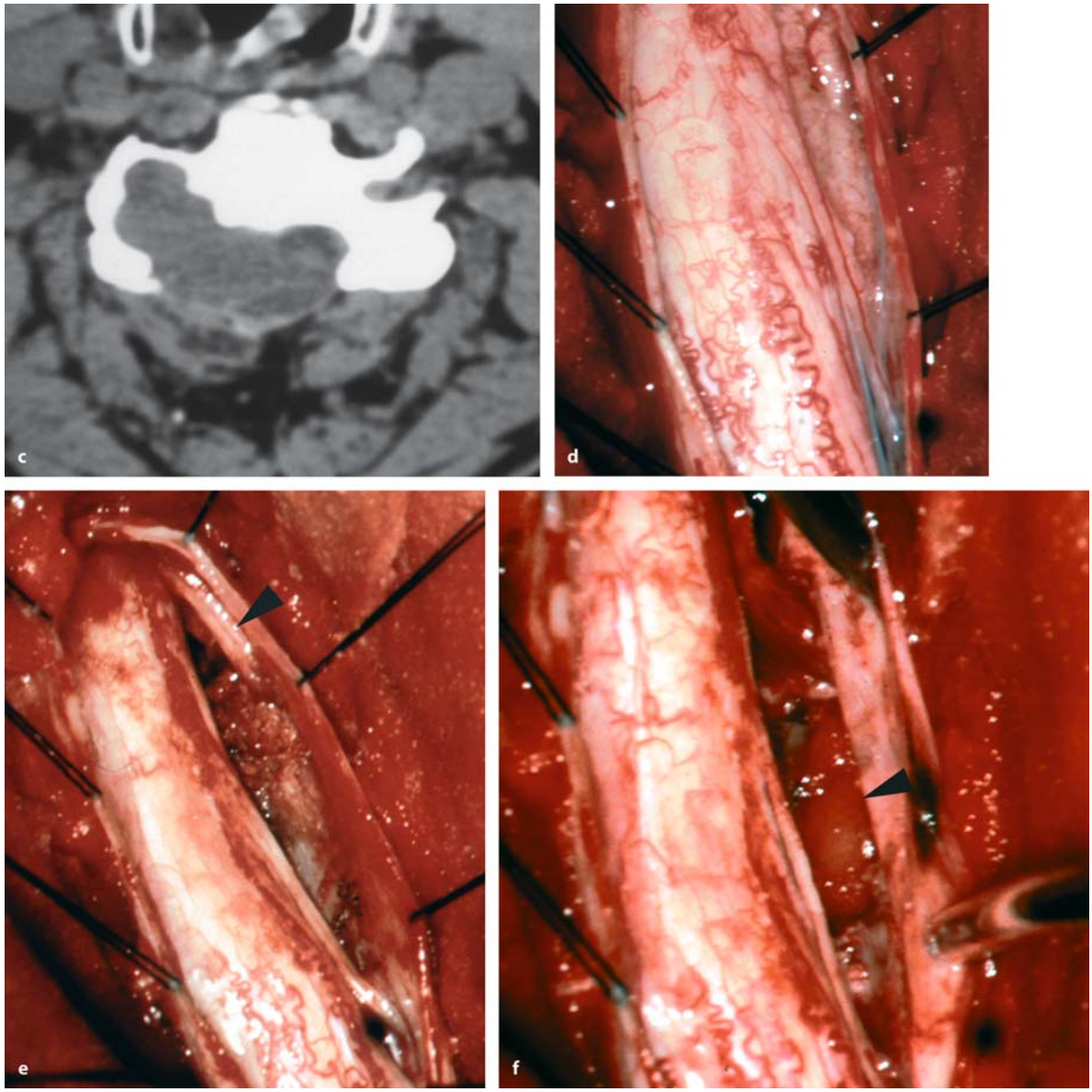

Fig. 4.87. (*Continued*) **c** This CT demonstrates bony erosion on the right side involving the canal of the vertebral artery. **d** This intraoperative view after dura and arachnoid opening in the semisitting position shows the intradural component of this schwannoma compressing the spinal cord. After resection of this part with preservation of the root (**e**; *arrowhead*) the epidural component was removed and the dural sleeve packed with a fibrin sponge (**f**; *arrowhead*) for hemostasis. The neurological symptoms improved postoperatively

Overall surgical morbidity was 2.3%, with no differences between patients with or without NF-2. Surgical morbidity was slightly higher for tumors with extradural extension compared to purely intradural tumors (3.4% and 1.9%, respectively). There was no surgical mortality among extramedullary schwannomas.

To predict a high postoperative Karnofsky score after 1 year, a multiple regression analysis was applied. Independent factors are the absence of NF-2, a high preoperative Karnofsky score, first surgery on a nerve sheath tumor, young age, no arachnoid scarring [113, 150], and no tumor recurrence (Table 4.24). Table 4.25 gives an overview of the clinical outcome in the first postoperative year for patients with and without NF-2. Without NF-2, surgery of a spinal extramedullary schwannoma is one of the most gratifying operations, with postoperative improvements for each

Fig. 4.88. Sagittal (**a**), coronal (**b**), and axial (**c**) T1-weighted MRI scans of a dumbbell schwannoma at Th2–Th5 in a 37-year-old woman with a 4-month history of pain and a slight paraparesis. This tumor displays a diffuse infiltrative pattern growing around the dural sac and spreading caudally and cranially similar to an en plaque meningioma. After complete resection pain improved, leaving the remaining neurology unchanged. A recurrence occurred after 3 years, requiring a second operation

Table 4.24. Multivariate Analysis for prediction of a high postoperative Karnofsky score for spinal nerve sheath tumors

Factor	β-value
No NF-2	0.5992
High preoperative Karnofsky score	0.3224
First surgery	0.3098
Young age	0.2482
No arachnoid scarring	0.1236
No recurrence	0.1079

Correlation: r=0.8162, p<0.0001

symptom [50, 61, 127]. The Karnofsky score increased significantly postoperatively in patients without NF-2 (73±13 to 89±9; p<0.0001, t-test for paired variables). In patients with NF-2, postoperative clinical results were not as favorable compared to patients without NF-2 [50]. Even though patients with NF-2 demonstrated more advanced neurological deficits, they still benefited significantly from operation. The average Karnofsky score increased from 68±16 to 75±17.

A multiple regression analysis was performed to determine the risk factors for a tumor recurrence (Table 4.26). A complete resection was by far the most important determinator (Fig. 4.89). Preservation of the nerve root was not associated with an increased risk for recurrence if the tumor had been resected completely. Other factors predicting a low recurrence rate were first surgery (Fig. 4.90), high spinal level, no NF-2 (Fig. 4.91), intradural tumor (Fig. 4.92), and a

Table 4.25. Clinical course for patients with extramedullary nerve sheath tumors

Symptom	Pre-operative status	Post-operative status	3 Months postop.	6 Months postop.	1 Year postop.
Pain					
No NF-2	2.9±0.8	3.7 ±0.6	4.4±0.5	4.6±0.5	4.6±0.5**
NF-2	3.7±1.0	4.1±0.6	4.4±0.6	4.4±0.6	4.3±0.9*
Hypesthesia					
No NF-2	3.6±0.9	4.0±0.8	4.3±0.8	4.4±0.8	4.4±0.7**
NF-2	3.7±0.8	3.9±1.0	4.1±1.0	4.1±1.0	4.1±1.2
Dysesthesias					
No NF-2	3.9±1.0	4.2±0.7	4.6±0.6	4.6±0.6	4.6±0.7**
NF-2	4.4±1.0	4.7±0.6	4.9±0.3	4.9±0.3	4.9±0.3*
Gait					
No NF-2	4.0±1.0	4.0±1.0	4.4±0.8	4.5±0.7	4.7±0.6**
NF-2	3.7±1.0	3.9±1.0	4.0±0.9	4.1±0.9	4.1±1.1
Motor power					
No NF-2	3.8±1.0	4.0±1.1	4.4±0.9	4.6±0.8	4.6±0.8**
NF-2	3.5±1.1	3.8±1.0	4.0±1.0	4.0±1.1	4.0±1.3*
Sphincter function					
No NF-2	4.4±0.9	4.5±0.9	4.7±0.6	4.7±0.6	4.8±0.6**
NF-2	4.7±0.7	4.8±0.5	4.9±0.4	4.9±0.5	4.8±1.0
Karnofsky score					
No NF-2	73±13	76±15	84±11	87±9	89±9**
NF-2	68±16	71±17	73±15	75±14	75±17*

Statistically significant difference between preoperative status and 1 year postoperatively: *$p<0.05$, **$p<0.01$

Table 4.26. Multivariate analysis for prediction of a low recurrence rate for spinal nerve sheath tumors

Factor	β-value
Complete resection	0.4392
First surgery	0.1949
High spinal level	0.1323
No NF-2	0.1306
Intradural tumor	0.0964
Short history	0.0778

Correlation: $r=0.6032$, $p<0.0001$

short history. Table 4.27 gives an overview of tumor recurrence rates for these subgroups of nerve sheath tumors. The overall recurrence rates for schwannomas after 1, 5, and 10 years were 8%, 17%, and 20%, respectively. Recurrence rates for schwannomas and neurofibromas were given by Schick et al. [231]. Without applying Kaplan-Meier statistics, they obtained a rate of 9.1%.

Finally, we have encountered a malignant schwannoma between Th1 and Th5 in a 62-year-old woman with a 3-month history of pain and moderate sensory loss. After subtotal resection of this tumor the patient improved with postoperative chemo- and radiotherapy. However, a recurrence caused a rapid paraparesis after 7 months, necessitating a second operation. This operation again obtained a subtotal resection. However, the postoperative stabilization of her neurological status was short lived. She developed another regrowth and finally died 14 months after the first operation.

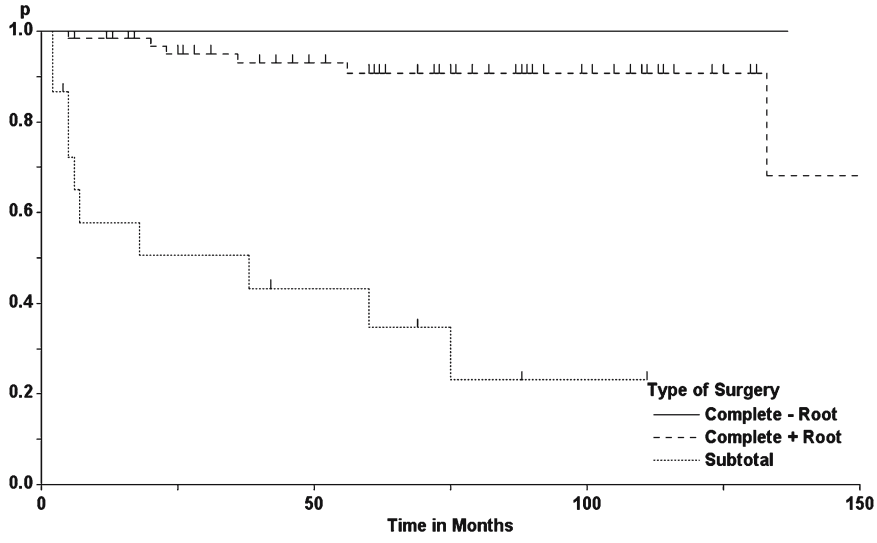

Fig. 4.89. Tumor recurrence rates for spinal nerve sheath tumors as a function of the amount of tumor resected (log-rank test: $p<0.0001$)

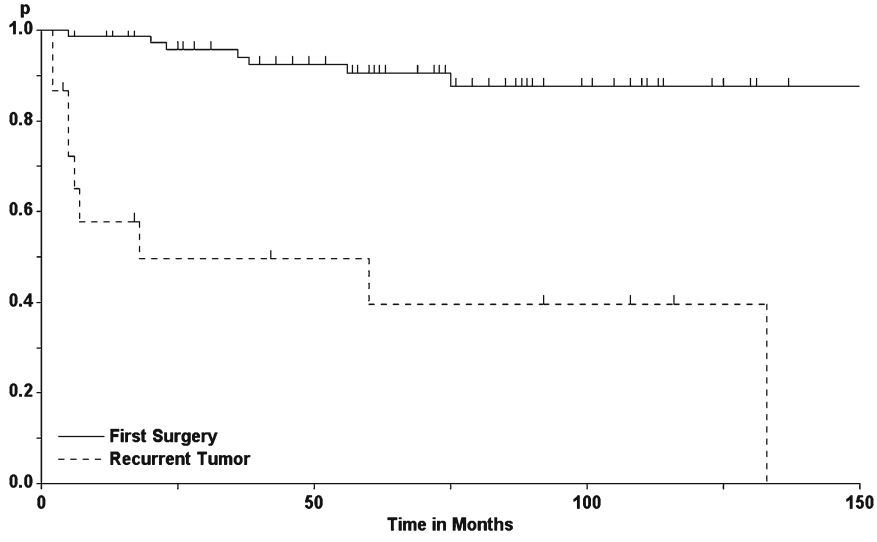

Fig. 4.90. Tumor recurrence rates for spinal nerve sheath tumors as a function of first or secondary surgery (log-rank test: $p<0.0001$)

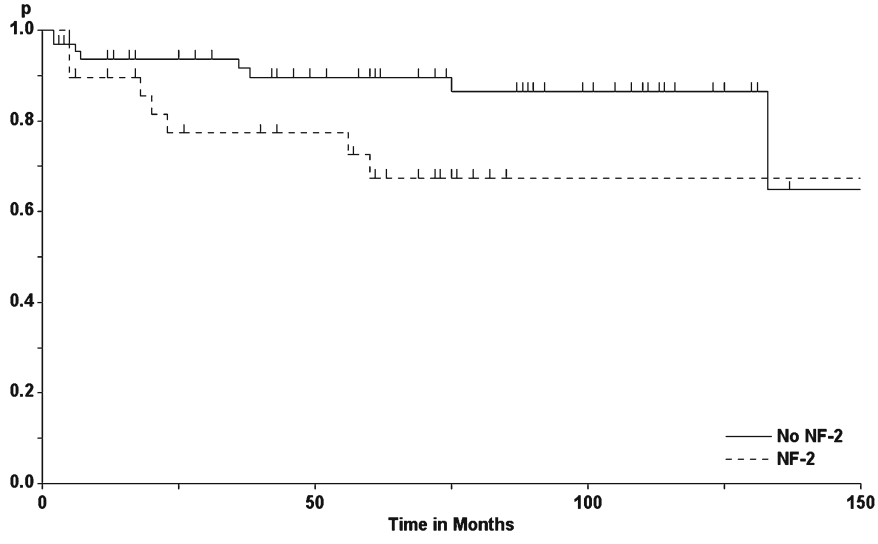

Fig. 4.91. Tumor recurrence rates for spinal nerve sheath tumors as a function of presence of NF-2 (log-rank test: $p=0.05$)

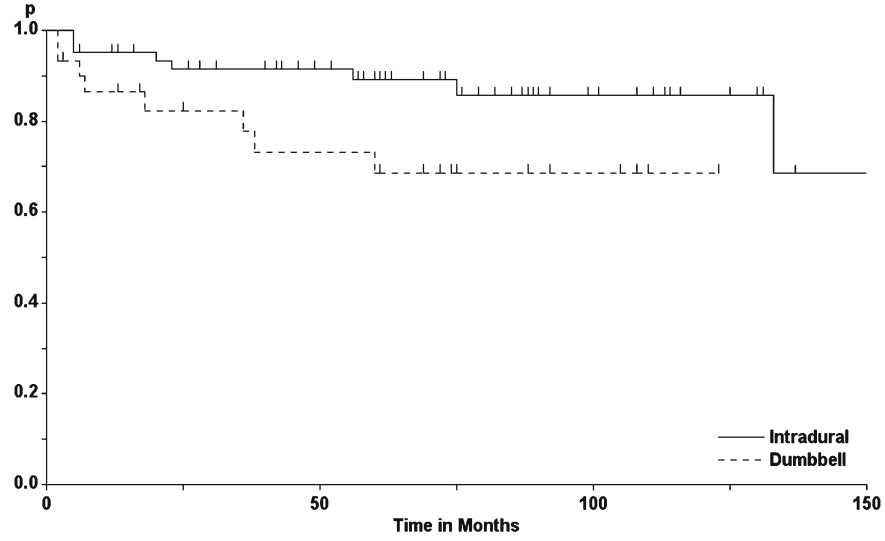

Fig. 4.92. Tumor recurrence rates for extramedullary nerve sheath tumors as a function of extradural extension (log-rank test: p=0.047)

Table 4.27. Tumor recurrence rates for spinal nerve sheath tumors

Group	1 Year	5 Years	10 Years
Total	8%	17%	20%
Complete + root resected	2%	9%	9%
Complete + root preserved	0%	0%	0%
Subtotal	42%	65%	77%
First surgery	1%	10%	12%
Recurrent tumor	42%	60%	60%
No NF-2	6%	10%	14%
NF-2	10%	33%	33%
Intradural	5%	11%	14%
Dumbbell	14%	31%	31%

4.5.3 Arachnoid Cysts

Depending on their size and location, arachnoid cysts may compress the cord (Figs. 4.65 and 4.67), irritate nerve roots (Fig. 4.93), or just interfere with CSF flow and, thus, be responsible for a syrinx (Figs. 4.34, 4.66, and 4.93) [46, 118, 139, 166, 275]. They may be caused by trauma (Fig. 4.34) or other disease processes, leading to arachnoid scarring, such as meningitis (Fig. 4.67), subarachnoid hemorrhage (Fig. 4.94), or surgery to mention just a few [10, 17, 26, 60, 73, 128, 132, 133, 146, 193, 275]. Gellad et al. [84] reported three patients with arachnoid cysts after gunshot injuries, Nogues et al. [192] three, and Sklar et al. [245] eight patients who developed intradural arachnoid cysts as a complication of epidural anesthesia. Multiple lumbar arachnoid cysts have been described in patients with ankylosing spondylitis [220, 241]. Congenital cysts and cysts associated with a variety of malformations have also been described [18, 110, 122, 193, 274], suggesting that at least some of them represent a developmental abnormality [74, 206]. They have been reported even in very young children and newborns [83, 106].

Arachnoid cysts may communicate with the subarachnoid space or be completely separated from it [133]. Depending on the communication with the subarachnoid space, cyst pressure and, thus, clinical symptoms may vary during the patient's course [4]. In rare instances, intradural arachnoid cysts are associated with dura defects and spinal cord herniation [244, 246, 268]. Arachnoid cysts may be located posteriorly in the midline (Figs. 4.65 and 4.66) or may be confined to either side of the posterior medial arachnoid septum, affecting just one side of the posterior subarachnoid space (Fig. 4.93) [206]. In general, anterior cysts appear to be the result of a disease process such as trauma, a hemorrhage, or meningitis (Figs. 4.67 and 4.94).

With these variations in mind the clinical picture is quite variable, too. We observed 35 arachnoid intradural cysts in 32 patients. Six were related to trauma, four to meningitis, and one patient each had developed this arachnoid pathology due to previous surgery, a subarachnoid hemorrhage, or contamination of the subarachnoid space with an irritating substance during peridural anesthesia. For the remainder, the etiology remained obscure.

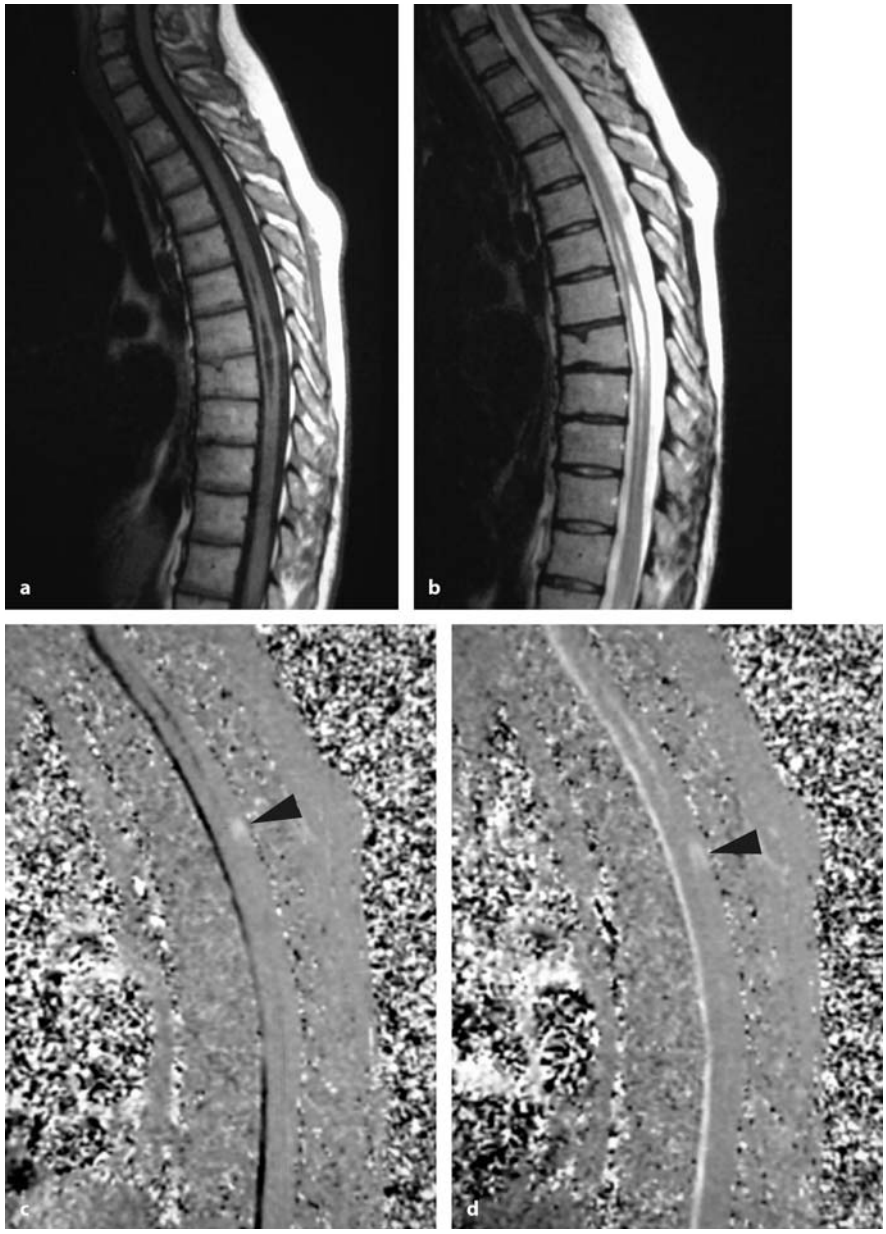

Fig. 4.93. Sagittal T1- (**a**) and T2-weighted (**b**) MRI scans of an arachnoid cyst at Th6 in a 41-year-old woman with an 8-month history of right-sided pain and gait ataxia. A syrinx is visible from Th6–Th9. There appears to be no cord compression, with the cyst completely invisible on these images. With cardiac gated cine MRI scans in systole (**c**) and diastole (**d**) a flow abnormality appears at Th6 (*arrowheads*). (*Continuation see next page*)

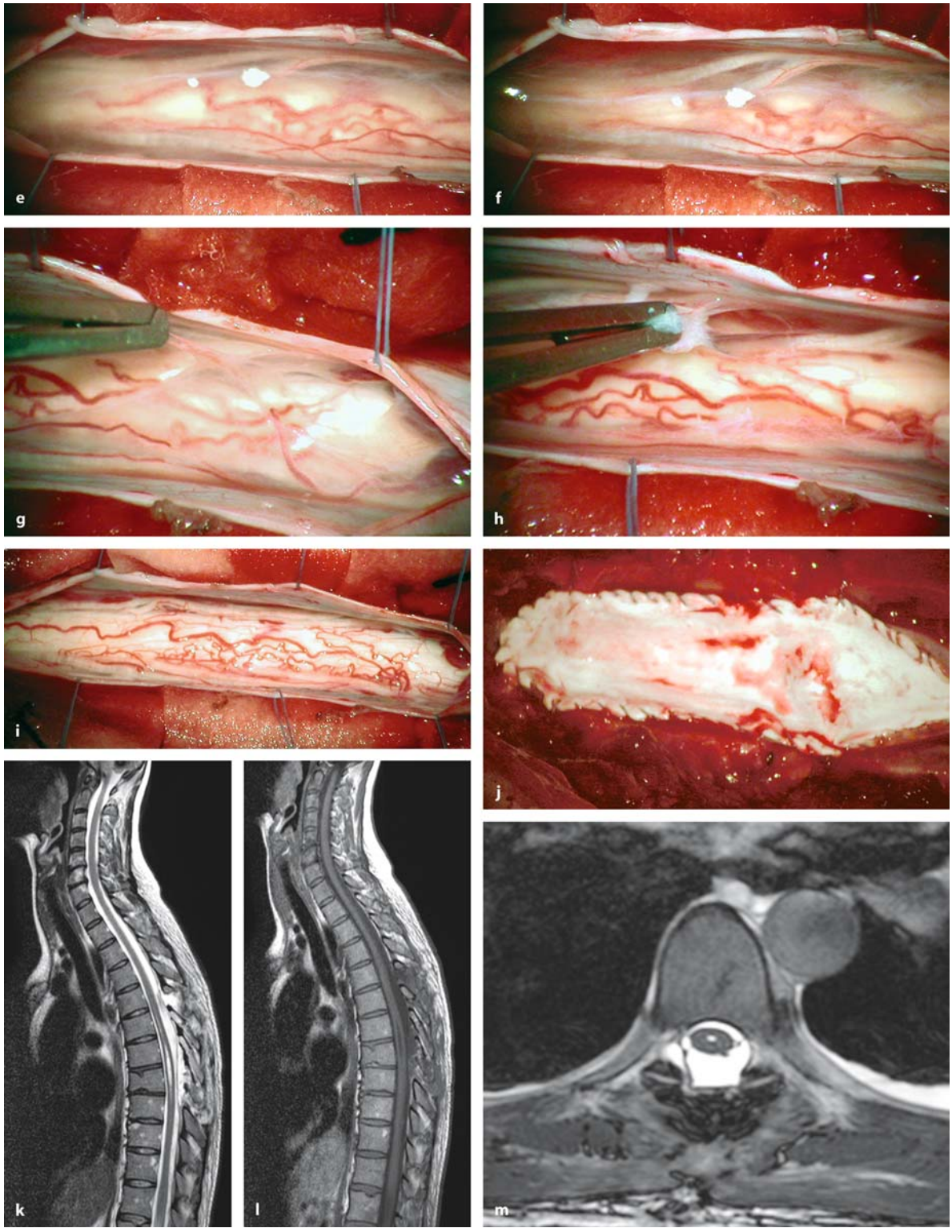

Fig. 4.93. (*Continued*) **e**, **f** These intraoperative views after dura opening at Th6 demonstrate how the wall of the cyst elevates nerve roots on the right side according to respiration-dependent flow changes. Putting the arachnoid under slight tension (**g**), the cyst can be resected (**h**). After complete resection (**i**) the dura is closed with a Gore-Tex® patch (**j**). The postoperative sagittal (**k**, **l**) and axial (**m**) MRI scans demonstrate a wide subarachnoid space at Th6 and a reduction of the syrinx. Postoperatively, pain improved but the ataxia remained unaltered

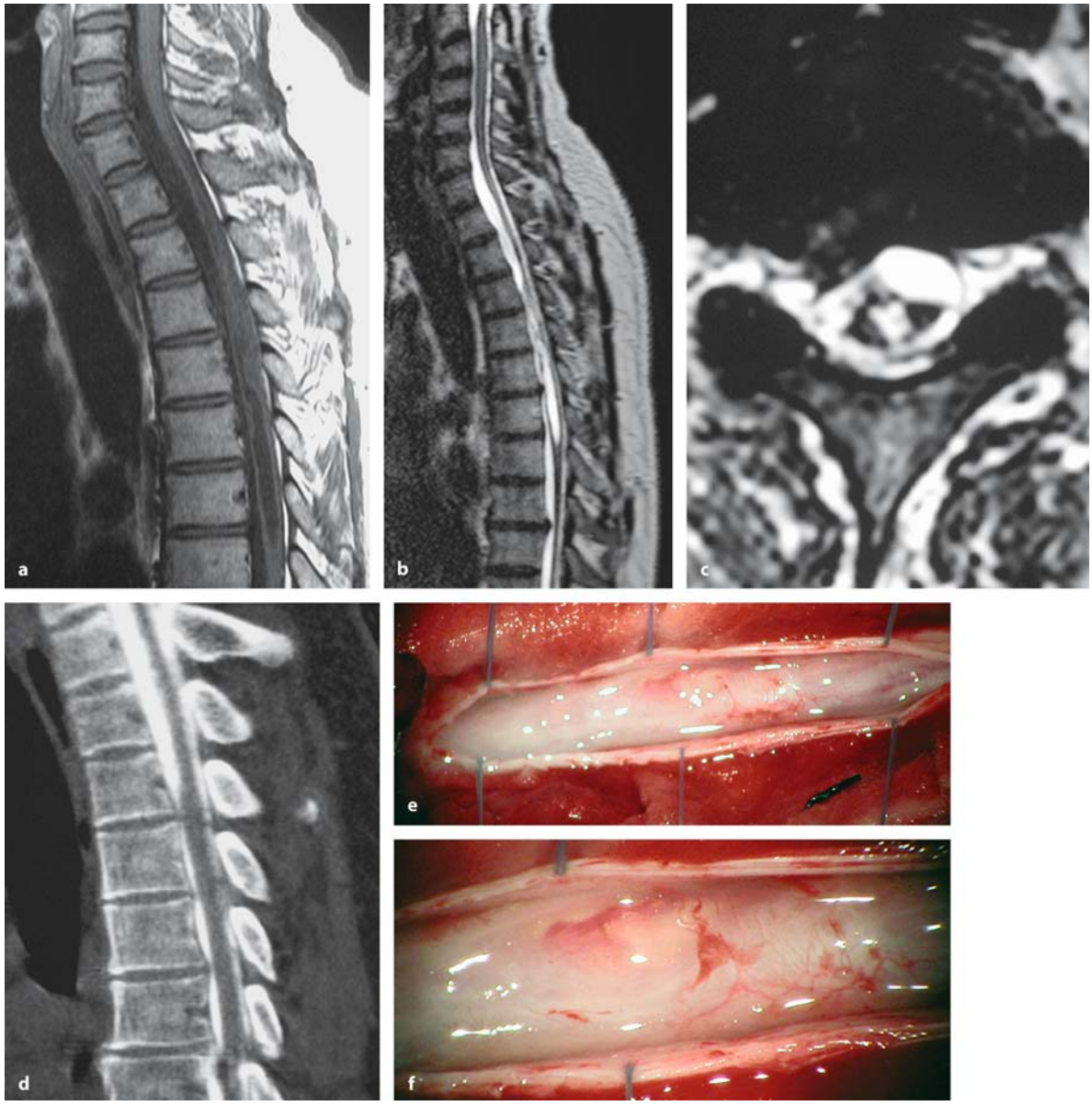

Fig. 4.94. Sagittal T1- (**a**) and sagittal (**b**) and axial (**c**) T2-weighted MRI scans of a ventral arachnoid cyst on the left side at C7–Th2 in a 47-year-old man with a 12-month history of progressive severe paraparesis, which began 20 years after surgery for a ruptured vertebral artery aneurysm. The subarachnoid hemorrhage had caused thoracic arachnoiditis and the development of a cervicothoracic arachnoid cyst. **d** Sagittal reconstruction of the postmyelographic CT demonstrates a good filling of the cyst, which causes ventral compression of the spinal cord. Intraoperative overview (**e**) and close-up (**f**) after dura opening, display a diffusely thickened arachnoid layer. (*Continuation see next page*)

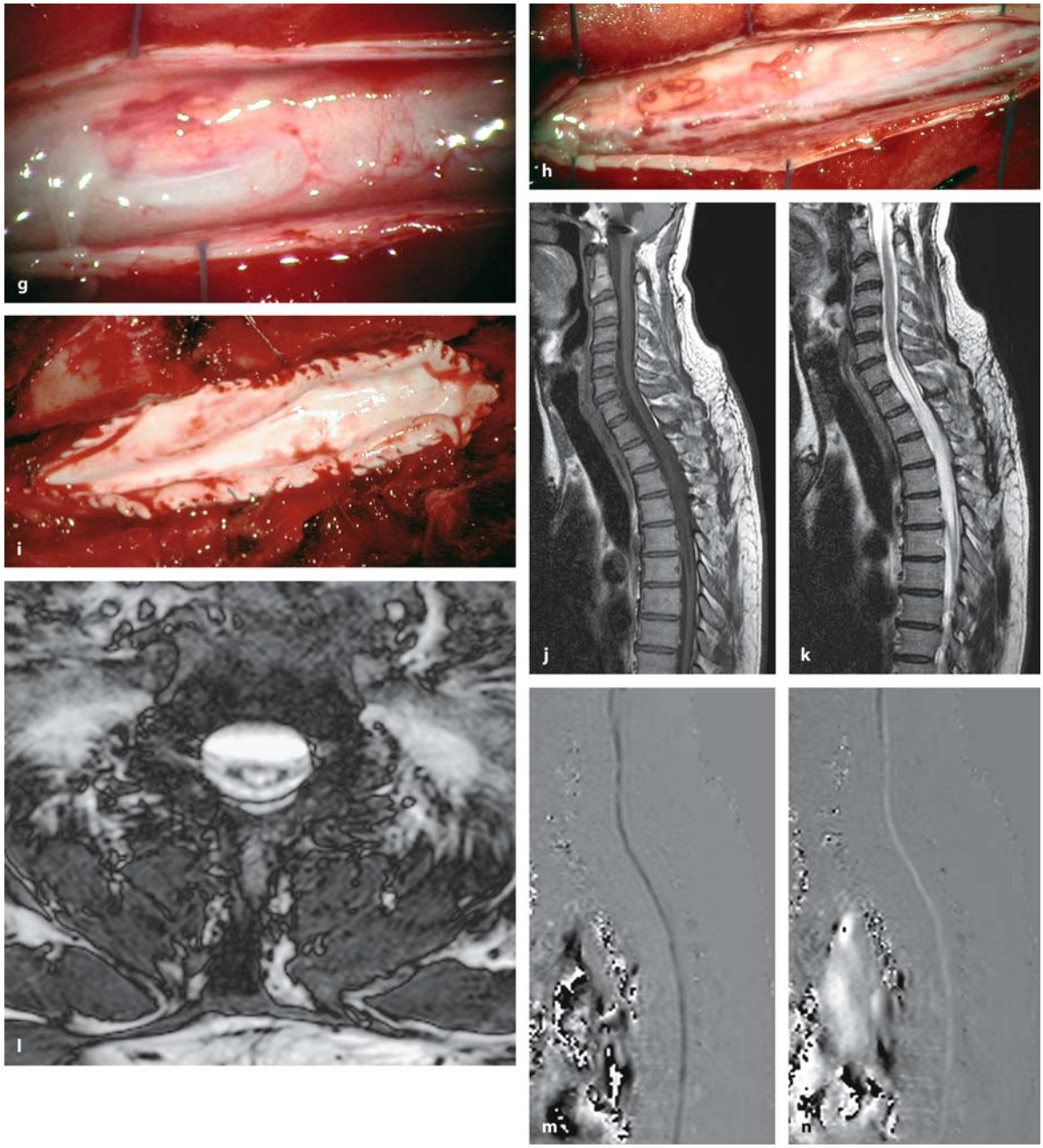

Fig. 4.94. (*Continued*) **g** With sharp dissection, the arachnoid was resected posteriorly layer by layer leaving the final arachnoid layer on the cord surface to avoid any damage to blood vessels thereon. On the left side, the cyst wall could be fenestrated, releasing CSF. **h** This final overview shows the situation before dura closure with a Gore-Tex® patch (**i**). The postoperative sagittal (**j**, **k**) and axial (**l**) MRI scans show a decompression of the cyst and a decrease of the syrinx. The cardiac gated cine MRI scans in systole (**m**) and diastole (**n**) demonstrate free CSF flow in the anterior subarachnoid space of the cervicothoracic junction, but no flow signals posterior of the cord. The patient recovered his walking abilities within a few weeks of rehabilitation, with no recurrence in 18 months

Even though most patients develop signs of a progressive myelopathy due to cord compression [193], one of the characteristic clinical features is the undulating clinical course [74, 197]. Patients describe stepwise progressions followed by transient improvements until the next phase, when new clinical problems occur. Sudden deteriorations, however, have also been described [254]. In some patients, minor traumas have initiated the development of neurological symptoms [74, 112, 132, 155]. Valls et al. [269] described a patient with a thoracic arachnoid cyst that decompensated after surgery for lumbar stenosis.

Patients may present with signs of either cord compression or radicular irritation [17]. A gradual, continuous deterioration, as observed for other extramedullary tumors, may be absent for this entity. Symptoms may vary according to the patient's position. Pain, for instance, may subside by lying down [74]. Therefore, quite a few patients are regarded as neurotic or misdiagnosed for a great variety of diseases, such as multiple sclerosis, before the correct diagnosis is made [1].

In our series, patients presented at an average age of 52±13 years, after a clinical history of 73±116 months, and were followed for 33±34 months (maximum 10 years). The problems with a correct diagnosis are reflected in the great variability of the patient history, which varied between 2 months and 47 years in one particular case [11].

At the beginning, clinical symptoms begin quite variably, but favor gait problems (34%) and motor dysfunctions (22%), or pain (20%), sensory disturbances (12%), and dysesthesias (10%). At presentation, 51% were mainly affected by gait disturbances, 17% by motor weakness, and the remaining patients by pain (24%) or dysesthesias (7%). Overall, 93% showed some degree of gait ataxia, 76% had sensory problems, and 68% motor weakness, while 66% complained about pain, 51% about dysesthesias, and 37% about sphincter disturbances (Table 4.28) [11, 17, 133]. The average preoperative Karnofsky score was 69±15.

This group of patients poses significant diagnostic problems, as extramedullary arachnoid cysts may not only cause fluctuating neurological symptoms, but may also be virtually invisible on standard MRI scans and yet extend over several spinal segments. In our series 50% were associated with syringomyelia (Figs. 4.34, 4.66, 4.67, 4.93, 4.94, and 4.95) [10]. If cyst walls are not visible on MRI, indirect signs of an intradural arachnoid cyst may be displacement or compression of the spinal cord (Figs. 4.65, 4.67, 4.94, and 4.95) [193] and atypical flow void signals in the subarachnoid space on T2-weighted images. In rare cases, the vertebral body may be eroded [28]. However, these indicators are not reliable. We recommend cardiac gated cine MRI examinations, which we consider to be the most sensitive imaging modality in these cases. Any arachnoid pouch or cyst will cause disruptions, turbulences, or a block of CSF flow to some degree (Figs. 4.34, 4.65, 4.66, 4.67, 4.93, and 4.94) [64, 78, 243, 275]. To distinguish between arachnoid and epidermoid cysts, flair sequences are recommended [101]. Conventional myelograms are the alternative method and have sometimes been used to confirm MRI findings (Fig. 4.34) [17, 60, 107]. However, a free passage of contrast does not rule out an arachnoid cyst completely, as only a particular segment of the subarachnoid space may be involved, leaving the remainder unaltered (Fig. 4.93), resulting in a negative myelogram. Therefore, a postmyelographic CT of the suspected spinal segments should always be performed and can sometimes pick up a cyst that was not seen on myelography (Fig. 4.34) [1, 90, 121, 124, 135, 145, 190, 194].

Table 4.28. Symptoms for spinal arachnoid cysts

Symptom	First symptom	At presentation
Pain	20%	66%
Gait ataxia	34%	93%
Motor weakness	22%	68%
Sensory deficits	12%	76%
Dysesthesias	10%	51%
Sphincter problems	–	37%

The overwhelming majority (88%) of the 35 intradural arachnoid cysts in this series were observed in the thoracic area [197]. Cervical (6%) and lumbar (6%) cysts made up for the rest [193]. The majority were located posteriorly and only three anteriorly. In the largest series on arachnoid cysts published to date by Wang et al. [275] on 21 patients, and Bassiouni et al. [17] on 16 patients, found similar distribution with more than 80% occurring in the thoracic spine.

The aim of surgery is to provide a sufficient decompression of nervous structures and a free CSF passage. It is not necessary to expose the entire cyst or to perform a radical resection, even though this is recommended by some authors [7, 148, 155]. In cases with multisegmental extension or anteriorly located cysts, a wide fenestration of the cyst wall at the lower or upper pole is sufficient (Figs. 4.67 and 4.94) [10, 17, 123, 132, 136, 193, 197, 213, 275]. In patients with multiple arachnoid cysts [109, 117, 194], each cyst needs fenestration.

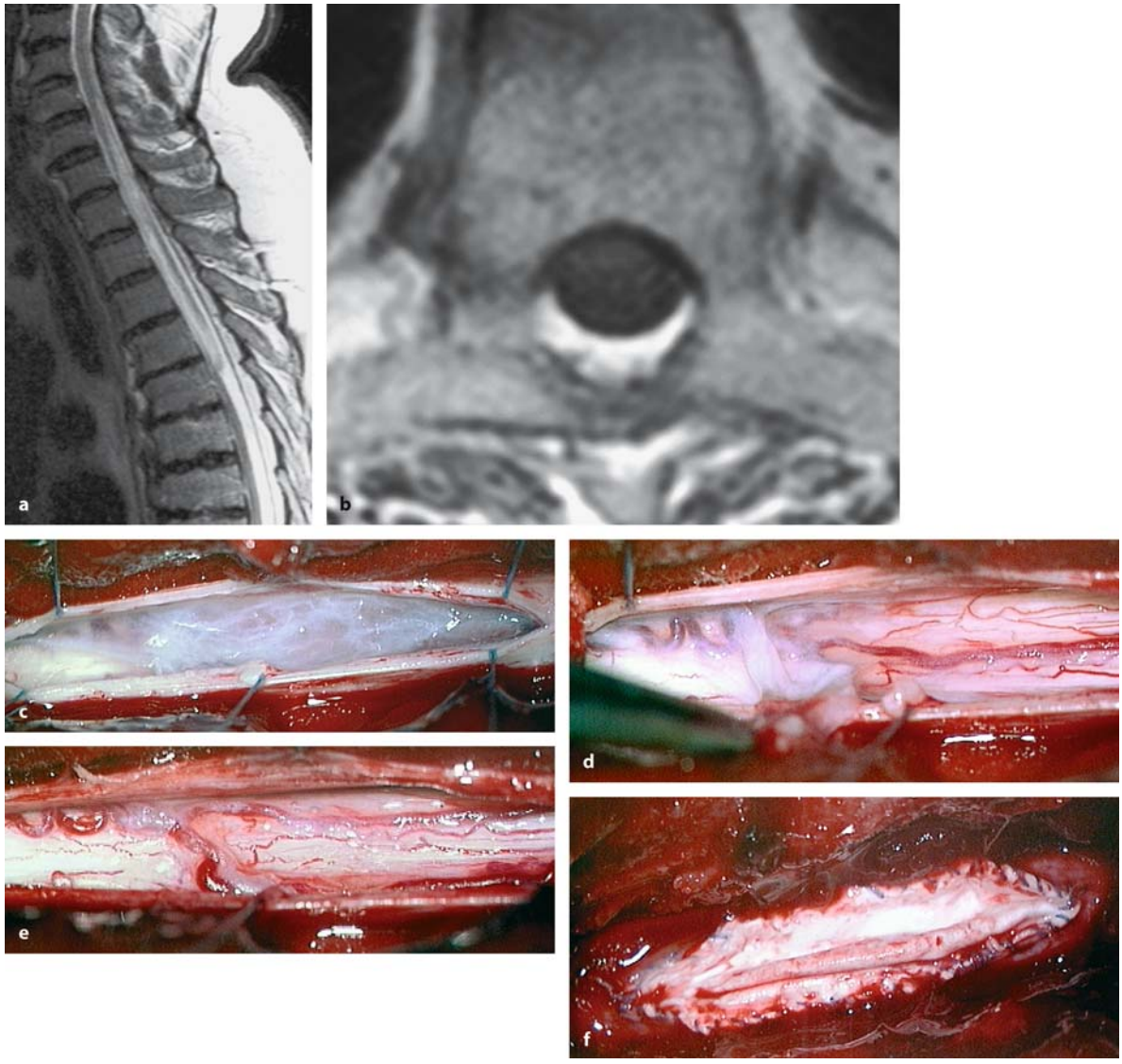

Fig. 4.95. **a** Sagittal T2-weighted MRI scan of a syrinx C5–Th5 in a 58-year-old man with a history of dysesthesias and sensory deficits in his right arm. **b** The axial T1-weighted scan shows an area of cord compression from posterior at Th5. The somewhat blurred image of the cord is related to the arachnoid pathology and flow disturbances at this level. **c** The intraoperative view after dura opening shows the arachnoid cyst. **d** The cyst is resected with sharp dissection. **e** This view demonstrates a complete resection of the cyst. Please note the thin layer of arachnoid membrane left on the cord surface to protect the posterior cord vessels. **f** The dura is closed with a Gore-Tex® patch. (*Continuation see next page*)

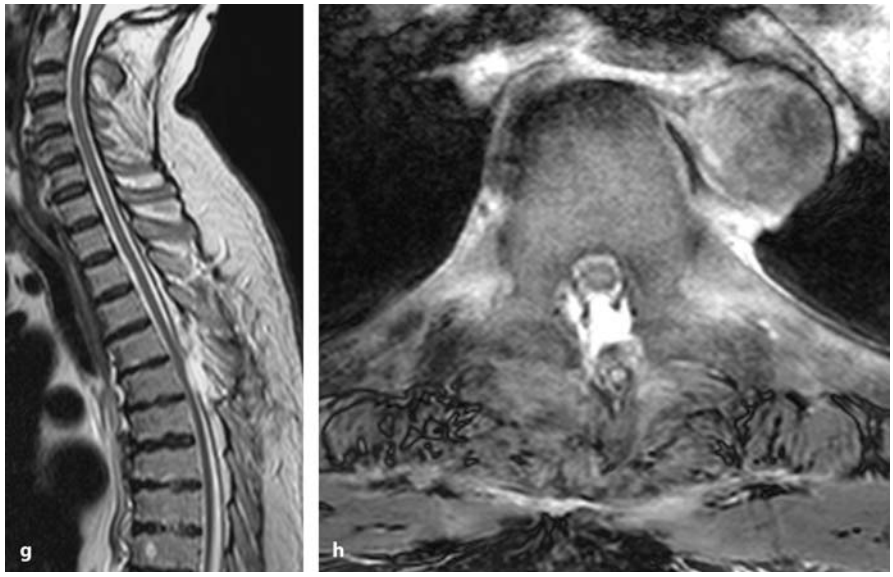

Fig. 4.95. (*Continued*) The postoperative T2-weighted sagittal (**g**) and axial (**h**) MRI scans show no more cord compression at Th5 and a complete disappearance of the syrinx. The patient's symptoms resolved completely

An associated syrinx was observed in 55% of patients [275]. No additional surgical steps, such as a syrinx shunt or myelotomy, are required for these patients [166, 259]. Decompression of the spinal cord and establishment of normal CSF flow are sufficient for treatment of the syrinx as well (Figs. 4.34, 4.66, 4.67, and 4.93–4.95). The intraoperative use of ultrasound is recommended to demonstrate the extent and dynamics of an arachnoid cyst (Figs. 4.34 and 4.65) [10]. In this way, dura opening can be performed right on the correct spot, thus limiting the amount of arachnoid exposure and dissection to the absolute minimum.

Endoscopes have been employed to explore the subarachnoid space in such instances for diagnostic purposes [58, 265]. Tanaka et al. [261] and Warnke et al. [276] propagated endoscopic surgery for arachnoid cysts. Takahashi et al. [258] even reported a patient with a cervical arachnoid cyst that he fenestrated percutaneously under MRI guidance. We would like to advise against such techniques, as there is a considerable risk of injury of spinal cord vessels in particular. Several patients presented at our institution with a severe paraparesis after such endoscopic endeavors.

Alternatively, shunting of the cyst has been advocated, particularly for anterior arachnoid cysts [10, 47, 109, 123, 126, 182, 213, 255, 275, 282]. We have not used this technique. Insertion of a foreign body into the subarachnoid space may cause significant problems with arachnoid scarring and cord tethering. If an anterior cyst is not accessible from posterior we rather approach such a cyst anteriorly [16], as was done for a cervical arachnoid cyst in our series (Fig. 4.96).

We have performed 15 cyst resections, combined with duraplasties in 12 operations, and 20 cyst fenestrations, combined with duraplasties in 14 operations. Complications occurred after 10% of operations. For those patients with additional syringomyelia, postoperative MRI examinations indicated a decrease of the syrinx for 56%, no change for 31%, and subsequent increases for 13%.

Immediately after surgery, 14 operations were followed by some moderate improvement of neurological functions, whereas stabilization was achieved with 20 operations. One patient deteriorated. Table 4.29 shows the postoperative course for the 1st year for patients after cyst resections and fenestrations. Both treatment modalities provide similar results, with moderate increases of scores for each symptom [17, 275]. Due to the limited number of patients, these do not reach statistical significance. Wang et al. [275] observed favorable results for motor weakness and sphincter dysfunctions, but less good outcomes for pain and hypesthesia.

Most authors reported postoperative improvements of neurological symptoms [7, 10, 17, 109, 110, 112, 123, 132, 136, 148, 182, 193, 202, 212, 213, 254,

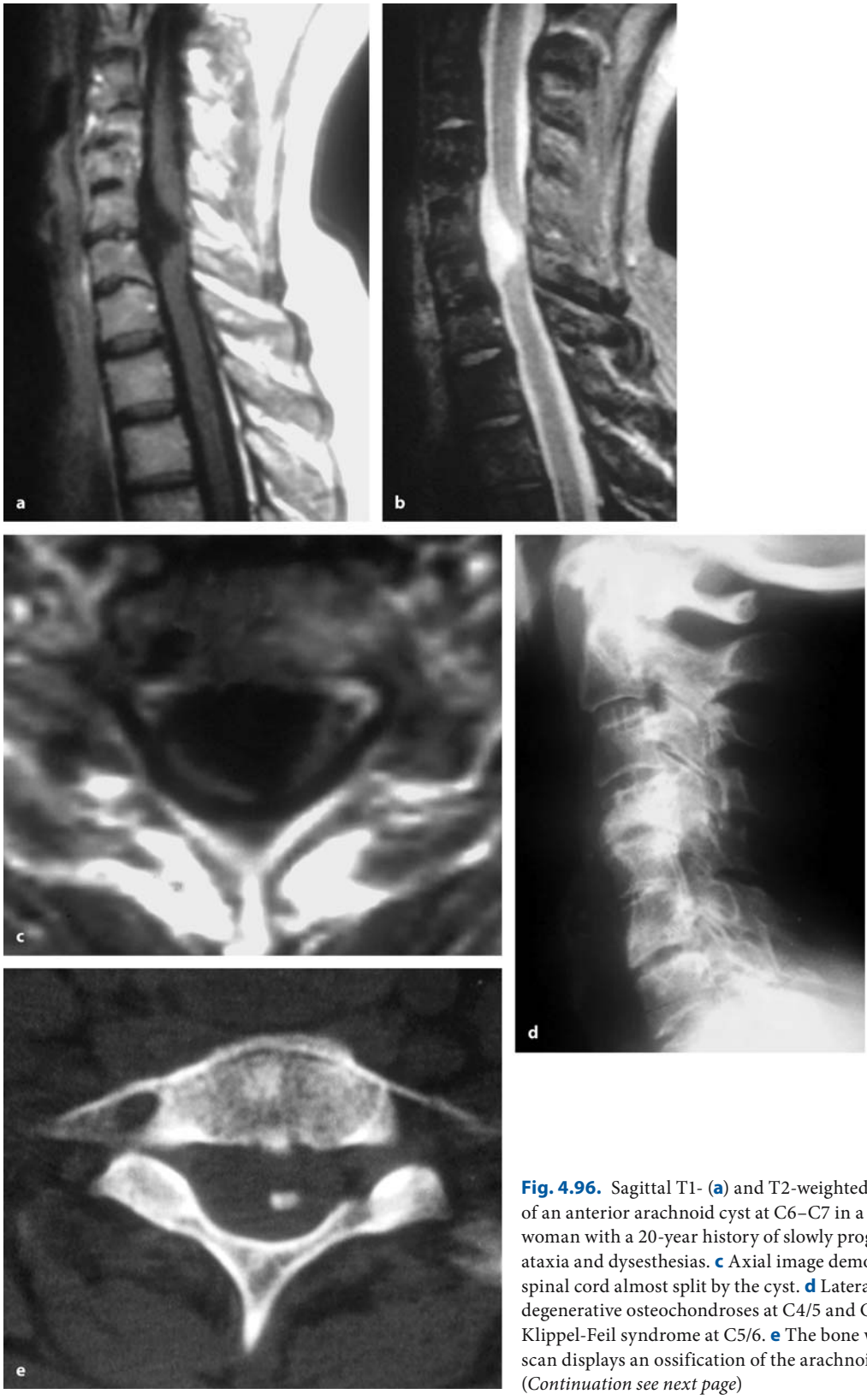

Fig. 4.96. Sagittal T1- (**a**) and T2-weighted (**b**) MRI scan of an anterior arachnoid cyst at C6–C7 in a 61-year-old woman with a 20-year history of slowly progressive gait ataxia and dysesthesias. **c** Axial image demonstrating a spinal cord almost split by the cyst. **d** Lateral X-ray showing degenerative osteochondroses at C4/5 and C6/7 and a Klippel-Feil syndrome at C5/6. **e** The bone window CT scan displays an ossification of the arachnoid membrane. (*Continuation see next page*)

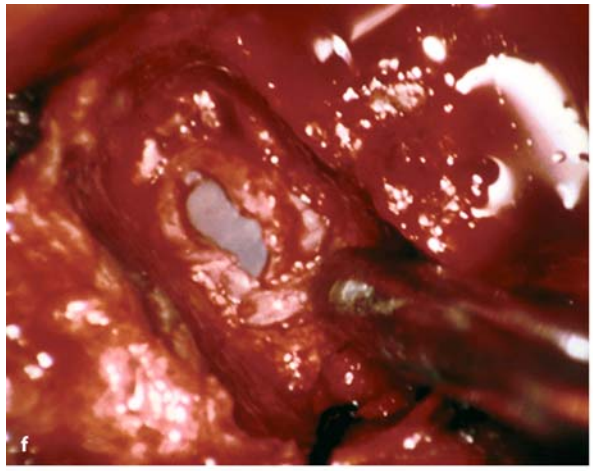
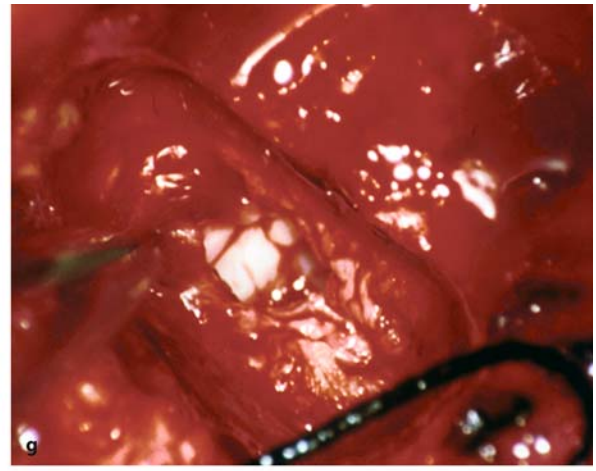


Fig. 4.96. (*Continued*) **f** This intraoperative view, taken after discectomy C6/C7 and dura opening, shows the anterior arachnoid cyst wall. **g** After fenestration of the cyst wall the cyst collapsed and the anterior aspect of the spinal cord became visible. **h** Postoperative X-ray demonstrating ventral fusion with the iliac crest bone and ventral plating at C5–C7. Symptoms improved postoperatively, but the gait ataxia did not resolve completely. The patient has been free of a recurrence for 9 years. Due to subsequent placement of a cardiac pacer, no postoperative MRI scans are available

255, 259, 275]. However, these results reflect only the immediate postoperative effect of cord decompression. Long-term results depend on the degree of preexisting arachnoiditis [133] and postoperative arachnoid scar formation, which may lead to CSF flow obstruction with resulting cord tethering, or reocclusion of arachnoid septations leading to a new arachnoid cyst. The more extensive the intradural exposure has to be for treating a particular cyst, the higher the risk for such postoperative arachnoid problems will be.

Cyst recurrences occurred within the first postoperative year and have not been observed at later stages. Overall, long-term recurrence rates indicate clinical stability for 79% of patients within 10 years after surgery. There was no significant difference in recurrence rates between patients undergoing cyst resection and those undergoing fenestration only (Fig. 4.97), even though there was a trend favoring cyst resections (11% compared to 31% after fenestrations). The major factor determining outcome was the question of arachnoid adhesions after surgery. With a permanently free CSF passage, clinical recurrences were seen in just 6% of cases, whereas the rate rose to 54% with formation of visible arachnoid adhesions on MRI (Fig. 4.98).

Most authors do not mention long-term results and recurrence rates. El Mahdi [60] reported one recurrence among his series of seven intradural arachnoid cysts. Osenbach et al. [193] detected 3 recurrences among 11 operated arachnoid cysts. Bassiouni et al. [17] observed no recurrence after a mean follow up of 3.2 years and a maximum follow up of 7.5 years. They had either fenestrated or

Table 4.29. Clinical course for patients with intradural arachnoid cysts

Symptom	Preoperative status	Postoperative status	3 Months postop.	6 Months postop.	1 Year postop.
Pain					
Resection	3.5±1.3	4.0 ±0.8	4.1±0.8	4.0±1.1	4.0±1.1
Fenestration	4.4±0.8	4.0±1.4	4.2±1.3	4.2±1.3	4.0±1.3
Hypesthesia					
Resection	3.1±0.4	3.6±0.7	3.6±0.7	3.6±0.7	3.6±0.7
Fenestration	3.5±0.8	4.0±0.7	4.2±0.8	4.2±0.8	4.0±0.9
Dysesthesias					
Resection	3.5±0.9	3.9±1.0	4.1±0.8	4.3±0.9	4.3±0.9*
Fenestration	4.3±1.0	4.5±0.8	4.6±0.8	4.6±0.8	4.4±0.9
Gait					
Resection	3.4±0.7	3.6±1.2	3.6±0.9	3.6±0.9	3.6±0.9
Fenestration	2.8±1.2	3.1±1.3	3.3±1.4	3.4±1.5	3.3±1.4
Motor power					
Resection	3.5±0.9	3.9±1.0	3.9±1.0	3.9±1.0	4.0±0.8
Fenestration	3.3±1.4	3.5±1.5	3.7±1.5	3.8±1.5	3.6±1.4
Sphincter function					
Resection	4.5±1.1	4.1±1.4	4.4±0.9	4.4±0.9	4.4±0.9
Fenestration	3.7±1.6	3.7±1.6	3.8±1.6	3.8±1.6	3.8±1.6
Karnofsky score					
Resection	68±10	69±17	70±19	71±16	71±16
Fenestration	66±17	68±19	73±22	75±22	72±20

Statistically significant difference between preoperative status and 1 year postoperatively: *p<0.05, **p<0.01

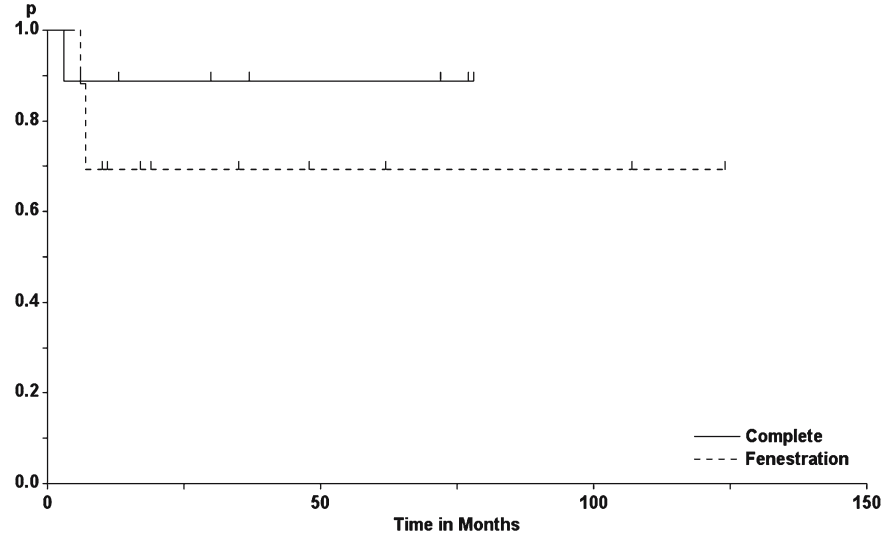

Fig. 4.97. Tumor recurrence rates for intradural arachnoid cysts as a function of type of surgery (log-rank test: not significant)

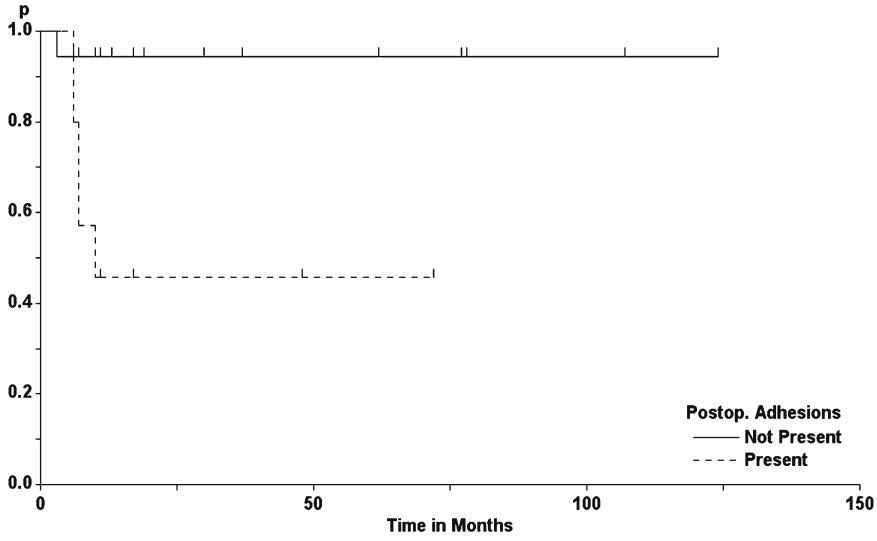

Fig. 4.98. Clinical recurrence rates for intradural arachnoid cysts as a function of postoperative arachnoid scarring (log-rank test: p=0.0128)

removed the cysts completely without applying a duraplasty. Likewise, Wang et al. [275] denied any recurrence among their 21 patients, with a mean follow up of 17 months, as did Alvisi et al. [7] for 10 patients followed to between 2 an 23 years.

4.5.4 Hamartomas

In this group we have encountered lipomas, dermoid cysts, neurenteric cysts, and neuroepithelial cysts. Whereas neurenteric and neuroepithelial cysts always presented without other features of dysraphism in this series, lipomas and dermoids were generally associated with complex spinal malformations leading to a tethered cord syndrome, such as varying degrees of spina bifida, a low conus medullaris, a thick filum terminale, or a split-cord malformation. Therefore, the neuroradiological workup is often very complex for extramedullary hamartomas. Not too rarely, the hamartoma is clinically insignificant and the clinical problems are related to a tethered cord: a dermoid cyst in the thoracic area may be associated with a thick filum and a low conus or a split-cord malformation, for instance. Therefore, the entire spinal axis should be analyzed with plain X-rays as well as MRI before a surgical strategy can be planned, which will often require a CT scan with bone window technique for the targeted spinal segment. In most patients, hamartoma removal and untethering can then be performed in one operation.

We analyze and discuss separately the following groups of patients:

1. Cystic hamartomas: neurenteric cysts, neuroepithelial cysts, and dermoid cysts
2. Solid hamartomas: lipomas of the conus, lipomas of the filum terminale, and lipomas of the cervical and thoracic cord

4.5.4.1 Cystic Hamartomas

With neurenteric, neuroepithelial, and dermoid cysts, surgery is recommended as soon as signs of spinal cord or nerve root compression are present and symptoms appear. Surgery has to achieve a complete resection to avoid local recurrences.

Dermoids may rupture spontaneously and irritating substances may contaminate the subarachnoid space, resulting in severe arachnoiditis [162, 168] or even abscess formation [267]. In such instances, debulking of the hamartoma may be all that is possible without injury to the nerve roots or spinal cord. Likewise, recurrent dermoid cysts may be extremely difficult to remove so that postoperative radiotherapy has been recommended in such instances [23]. Most of the dermoid cysts are reported in the lumbosacral area (Figs. 4.54, 4.60, 4.61, 4.63, and 4.99) [162]. While dissecting a dermoid cyst, the surrounding intradural structures should be covered by cottonoids so that the cyst material can be sucked away without exposing it to the subarachnoid space. Debulking of the cyst contents should be done from a small incision in the capsule. The capsule can then be grasped with tumor forceps and dissection can be performed bluntly with microdissectors and forceps, or sharply with micro-

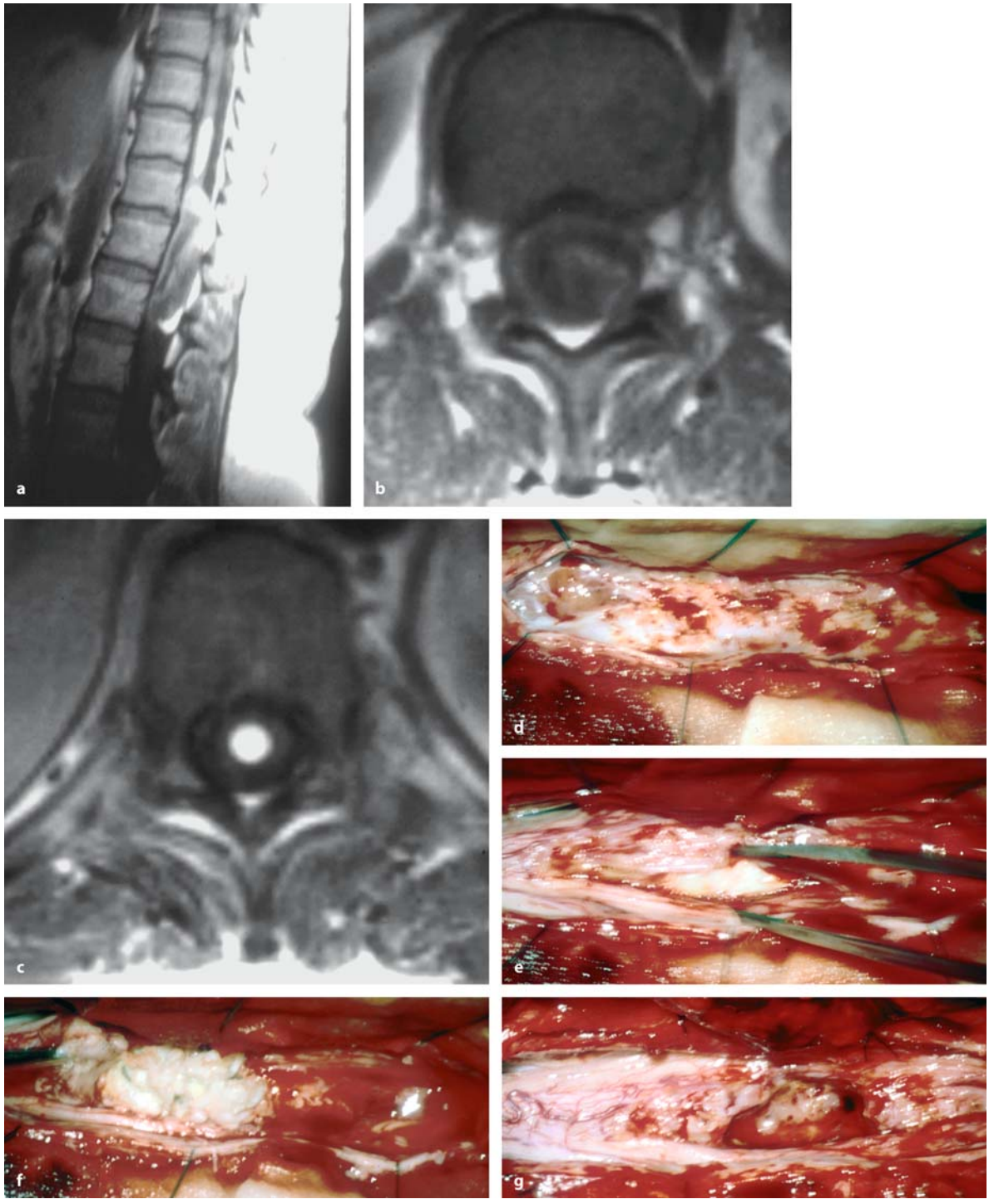

Fig. 4.99. Sagittal (**a**) and axial (**b**) T1-weighted MRI scans of a dermoid cyst at Th11–L2 in a 42-year-old woman with a 4-year history of pain and progressive sphincter disturbances. **c** At Th10 there is an additional intramedullary lipoma. **d** This intraoperative view after dura opening demonstrates a significant amount of arachnoid scarring associated with this lesion. With opening of the cyst (**e**) its contents are removed (**f**). **g** After most of the dermoid is resected, a thick gliotic layer adherent to the cyst wall and the conus becomes apparent. A subtotal resection was achieved. (*Continuation see next page*)

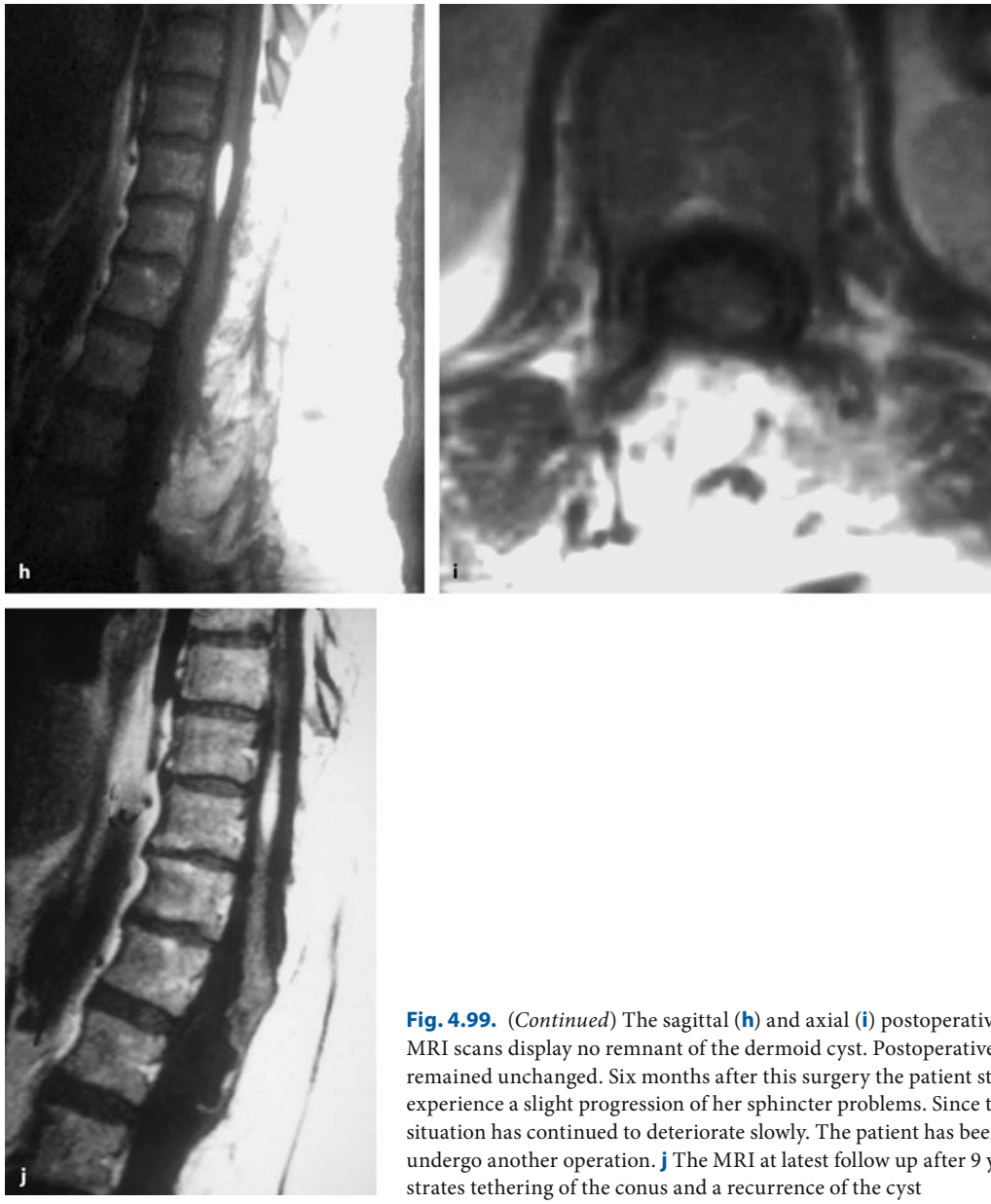

Fig. 4.99. (*Continued*) The sagittal (**h**) and axial (**i**) postoperative T1-weighted MRI scans display no remnant of the dermoid cyst. Postoperatively, symptoms remained unchanged. Six months after this surgery the patient started to experience a slight progression of her sphincter problems. Since then, the clinical situation has continued to deteriorate slowly. The patient has been reluctant to undergo another operation. **j** The MRI at latest follow up after 9 years demonstrates tethering of the conus and a recurrence of the cyst

scissors. To prevent recurrences, a complete resection of the capsule is required. An area of gliosis may be encountered toward the spinal cord. This layer should be preserved as it prevents injury to the spinal cord during dissection (Figs. 4.54, 4.61, and 4.63). In cases of severe adherence to nerve roots or conus medullaris, however, it may be safer to leave parts of the capsule in place (Fig. 4.99) [162, 165, 168]. It has been estimated that no more than 40% of dermoid cysts are totally resectable [23].

We have encountered 14 patients with extramedullary dermoid cysts of the spinal canal. Of these, three chose not to undergo surgery. Twelve dermoid cysts were operated in 11 patients, with 1 patient operated twice for a subsequent recurrence. Three patients presented a combination with a split-cord malformation (Figs. 4.60 and 4.61), three a dermal sinus and seven a tethered cord syndrome (Figs. 4.54, 4.60, 4.61, and 4.63). Finally, one patient presented a combination with a conus lipoma (Fig. 4.54). Table 4.30 gives an overview on this patient group. In one half of these

Table 4.30. Overview of patients with extramedullary dermoid cysts

Sex	Age (years)	Level	Dysr. Man.	History (months)	Symptoms	Surgery	Outcome
F	39	L2–L3	Dia, DS, TCS	216	Dysesth., Pain, Sphincter	Subtotal	Improved No Rec. 84 Months Det. 7 Months
F	59	L3–L4	DS, TCS	336	Gait, Pain, Motor, Sphincter	Subtotal	Improved No Rec. 26 Months Det. 3 Months
F	30	C1–C2	DS	3	Hypesth., Gait, Motor	Complete duraplasty	Improved No Rec. 28 Months
M	30	Th9–L1		84	Hypesth., Gait, Pain, Motor, Sphincter	Dec. duraplasty	Worse Lost to Follow Up
F	42	L2		54	Hypesth., Gait, Pain, Sphincter	Subtotal duraplasty	Unchanged Rec. 106 Months Det. 6 Months
M	19	Th12–L1		36	Hypesth., Gait, Dysesth., Motor	Complete duraplasty	Unchanged No Rec. 6 Months
M	52	Th12–L1	Dia, TCS	168	Hypesth., Gait, Dysesth., Pain, Motor, Sphincter	Complete	Unchanged Rec. 88 Months Det. 3 Months
	59	Th12–L1	Dia, TCS	46	Hypesth., Gait, Dysesth., Pain, Motor, Sphincter	Subtotal duraplasty	Improved No Rec. 4 Months
F	4	L1–L4	Dia, TCS	42	Hypesth., Gait, Motor, Sphincter	Dec. duraplasty	Improved No Rec. 12 Months
F	51	L1	TCS	2	Hypesth., Pain	Complete duraplasty	Improved No Rec. 3 Months
M	55	L2	TCS	6	Pain	Complete duraplasty	Worse No Rec. 3 Months
F	40	L2	TCS	24	Pain, Sphincter	Complete duraplasty	Improved No Rec. 5 Months

Abbreviations: Dysr. Man. = dysraphic manifestations, Dia = diastematomyelia, DS = dermal sinus, TCS = tethered cord syndrome, M = male, F = female, Hypesth. = hypesthesia, Dysesth. = dysesthesia, Motor = motor weakness, Gait = gait ataxia, Sphincter = sphincter disturbances, Rec. = tumor recurrence, Dec. = decompression, Det. = clinical recurrence

patients, pain was the dominating problem leading to surgery. Gait ataxia was the major concern in 31%. Sphincter problems, although present in 7 out of 11 operated patients, was the main problem in only 1 patient [162]. Six cysts were resected completely and four subtotally. In the remainder, a combination of arachnoid dissection, untethering, and decompression was performed. Postoperatively, six operations led to improvement, while three left the patients unchanged and two caused worsening of neurological symptoms. During follow up we observed two recurrences after 88 and 106 months, respectively.

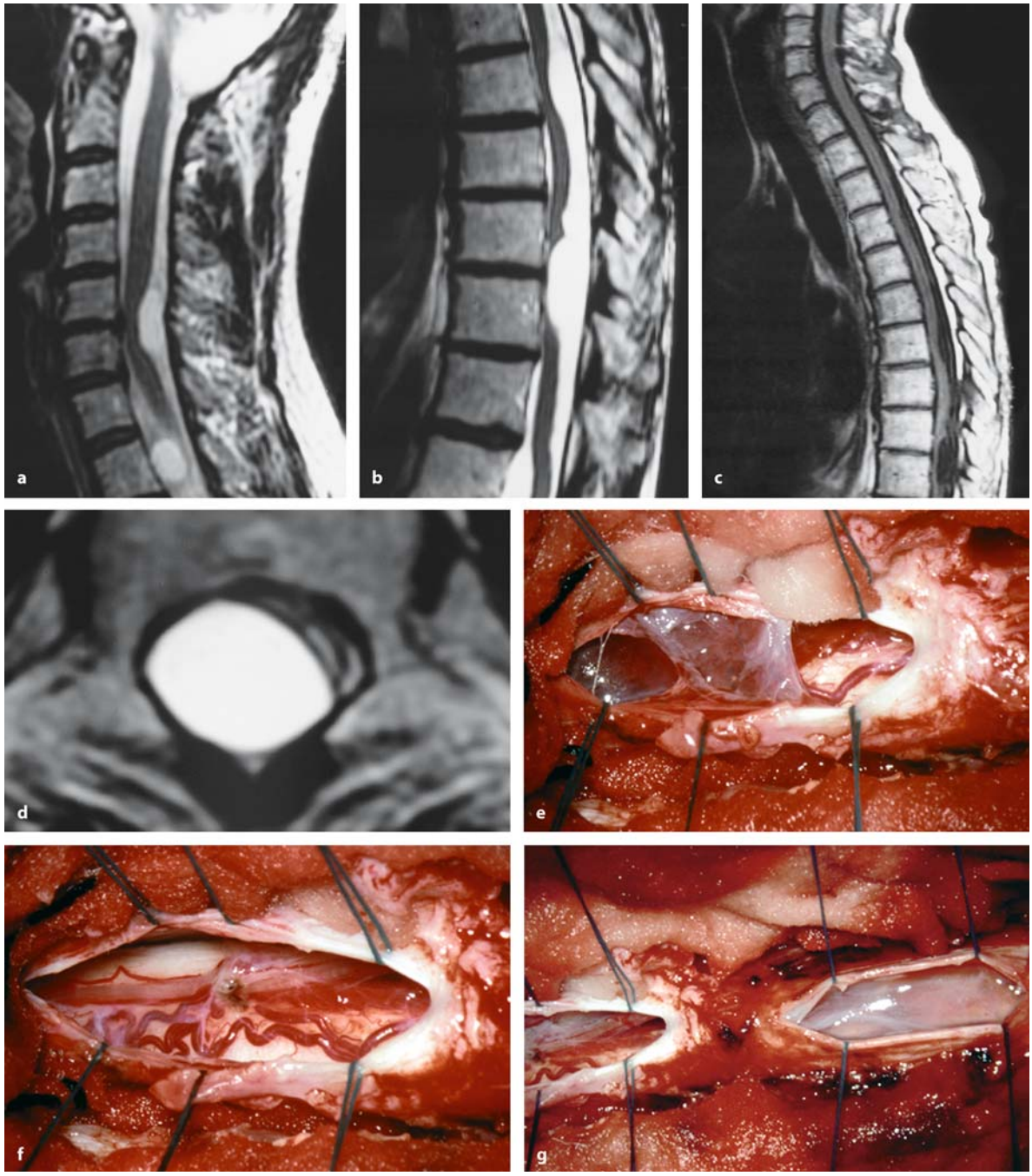

Fig. 4.100. Sagittal T2-weighted MRI scans of the cervical (**a**) and thoracic spine (**b**) demonstrating multiple neuroepithelial cysts at C5–C6, Th1, Th7, Th9–Th10, and Th12 in a 45-year-old woman with a 9-month history of progressive paraparesis. At another institution, fenestrations of the cervical and thoracic cysts at Th1, Th7, and Th9–Th10 were performed endoscopically. **c** This preoperative T1-weighted image shows a good result for the upper cysts, but relapses of the lesions at Th7 and Th9–Th10. **d** The axial T2-weighted scan at Th9 demonstrates the enormous cord compression caused by this hamartoma. **e** Intraoperative view at Th7 taken after dura and arachnoid opening, showing the neuroepithelial cyst. **f** This view demonstrates the spinal cord after complete resection at this level. **g** At Th9–Th10 the dura has been opened with the arachnoid still intact. (*Continuation see next page*)

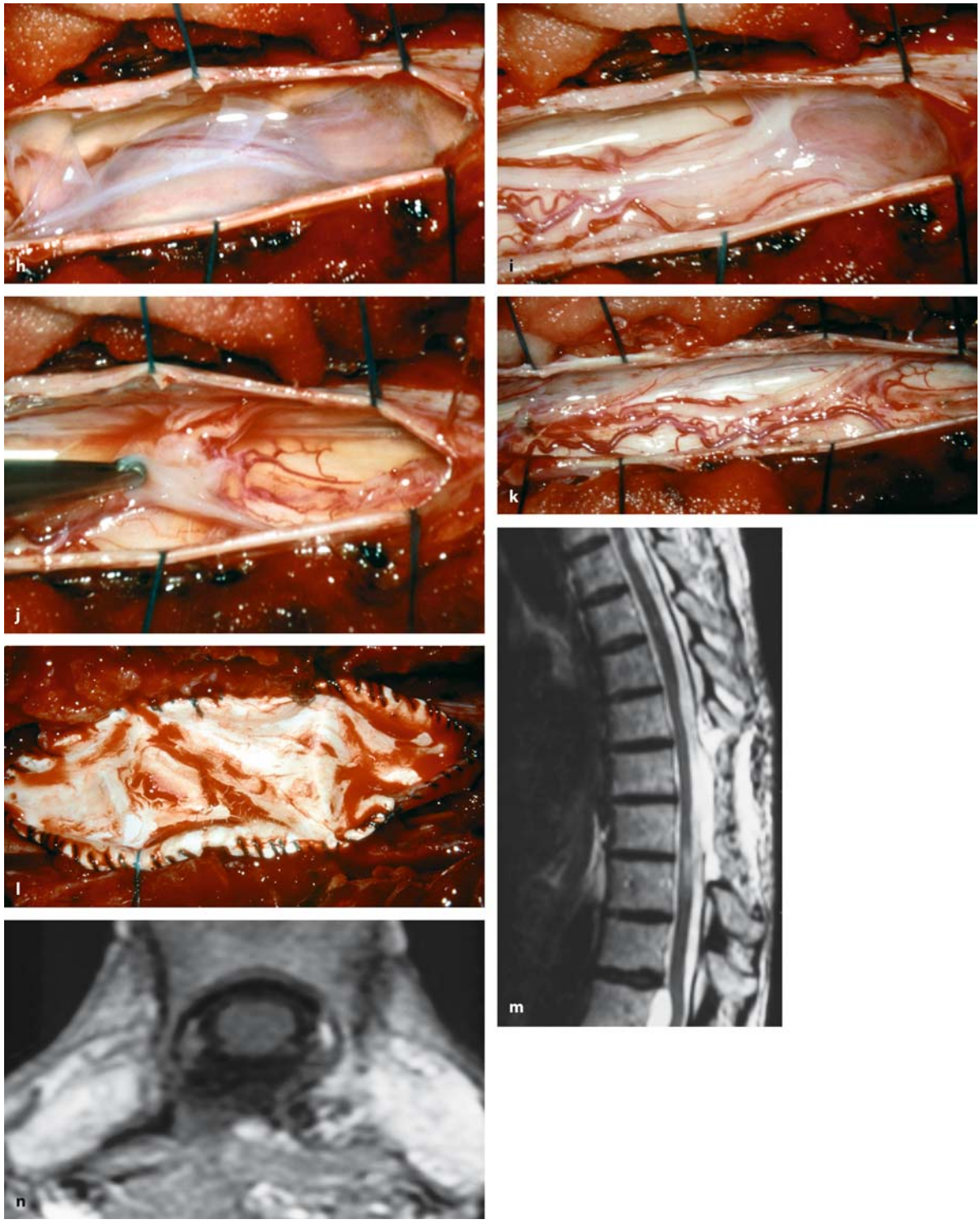

Fig. 4.100. (*Continued*) **h** The close-up view displays the lobulated cyst and the displacement of nerve roots attached to the cyst wall. After resection of the cranial part (**i**), the caudal segment of the cyst is removed, detaching it from the adherent nerve root (**j**). **k** This view demonstrates the situation after complete resection of the cysts at Th7–Th10. **l** The dura is closed with a Gore-Tex® duraplasty. The postoperative sagittal (**m**) and axial (**n**) MRI scans show a complete decompression at Th7–Th10 with a free CSF passage posteriorly. The patient improved postoperatively and has been free of a recurrence for 2 years. The cyst at Th12 is being monitored and will be operated as soon as new symptoms start to appear

The long-term clinical course, however, was not related to recurrences, but to problems of dysesthesias and myelopathy associated with retethering and arachnoid scarring. This caused significant morbidity in four instances, usually beginning within a few months after surgery. Mathew and Todd [168] achieved a complete excision for 6 out of 21 patients with dermoid cysts in the cauda equina area. Improvements were obtained for pain and motor weakness, but sphincter problems remained unchanged. Lunardi et al. [162] achieved a complete resection in three out of eight patients with dermoid cysts.

A much better result could be obtained for neurenteric (Fig. 4.64) and neuroepithelial cysts (Fig. 4.38). These may be associated with bony abnormalities or a tethered cord and are positioned anterior or anterolateral of the cord, as in the four patients of this series. The cysts may occur as single or multiple lesions (Fig. 4.100) so that examination of the entire spinal canal is recommended. The commonest localizations are in the cervical spine anterior to the cord (Figs. 4.38 and 4.64) and the conus region [5, 12, 74]. Neurenteric cysts are related to split-cord malformations. Paolini et al. [201] observed a patient with a neurenteric cyst associated with an anterior spinal-cord cleft at Th8/9. The cyst was embedded in this incomplete anterior diastematomyelia and almost completely surrounded by spinal cord tissue. Soni et al. [249] reported a similar patient with a thoracic split-cord malformation and a neurenteric cyst below the bony spur. Mooney et al. [180] demonstrated five children with thoracic neurenteric cysts associated with anterior vertebral defects and pointed out that severe spinal deformities may complicate the surgical management of these cysts, especially in children. Combined approaches and additional stabilizations may be required. Trehan et al. [266] also showed a patient with a thoracic neurenteric cyst associated with a cleft vertebra. According to Rauzzino et al. [216], the majority do demonstrate signs of occult dysraphism such as cutaneous abnormalities. In the series of Kumar and Nayak [149], signs of dysraphism were detectable in three out of six patients.

We observed neurenteric cysts at the craniocervical junction, cervical (Fig. 4.23) and thoracic spine. Their clinical data are presented in Table 4.31. As the cyst wall is somewhat thicker than the wall of an arachnoid cyst and the cyst content different from CSF, the diagnosis can sometimes be suspected before surgery [17]. However, the cyst may also appear as an arachnoid cyst [149]. The preoperative symptoms involve mainly radicular pain and gait problems [5, 36, 74, 154]. All the cysts could be removed completely with excellent postoperative clinical results and no recurrences [5, 17, 36, 154, 201]. Recurrences do occur after incomplete resections [74]. As the majority of papers describe single cases without adequate follow up, it is difficult to estimate the recurrence rate. Kumar and Nayak [149] achieved only one complete resection among six operations, with no subsequent recurrence after a short follow up of up to 2 years. A series of 13 patients with spinal neurenteric cysts, of which 4 were located intramedullary, reported five recurrences (i.e., a rate of 27%) related to incomplete resections [216]. Chavda et al. [39] presented a series of eight patients and reported a recurrence rate of 37%. Arai et al. [12] presented two patients with subtotal removal of cervical neurenteric cysts.

Multiple neuroepithelial cysts were encountered in the cervical and thoracic spine in a 45-year-old wom-

Table 4.31. Overview of patients with extramedullary neurenteric cysts

Sex	Age (Years)	Level	History (Months)	Symptoms	Surgery	Outcome
M	21	C4–6	18	Hypesth., Gait, Dysesth., Pain, Motor	Complete	Improved No Rec. 137 Months
M	58	C7–Th1	1	Hypesth., Gait, Dysesth., Pain, Motor	Complete	Improved No Rec. 115 Months
M	25	C1	2	Pain	Complete	Improved No Rec. 100 Months
F	45	Th7–10	9	Hypesth., Gait, Pain, Sphincter	Complete duraplasty	Improved No Rec. 12 Months

an with progressive gait ataxia. After endoscopic fenestration of these cysts, the thoracic cysts reappeared, leading to new clinical problems. After open surgery and resection of the three largest cysts at the level of Th7–Th10, the patient recovered with no clinical deterioration for 2 years (Fig. 4.100).

4.5.4.2 Lipomas

With spinal lipomas, the preoperative evaluation and general management become a lot more complex due to associated features of spinal dysraphism in a significant number of patients. The incidence of spinal lipomas is estimated to be somewhere between 1:4000 and 1:25,000 births [42]. The overwhelming majority of spinal lipomas are located in the lumbosacral region (Figs. 4.54–4.59) [264]. However, lipomas may occur in the cervical canal [141], even with extension into the posterior fossa [55, 68] and the thoracic region (Fig. 4.53) [8, 91, 95, 173]. Depending on the complexity of associated malformations, lipomas may compromise spinal cord function not only by mass effect, but also by cord tethering (Figs. 4.54–4.59). The pathophysiology of the tethered cord syndrome has been elegantly studied by Yamada et al. [278].

We still lack precise information on the natural history of these malformations. Consequently, the controversy concerning prophylactic surgery of these lesions remains to be resolved. As far as surgical treatment is concerned, what is required? Is a decompression and untethering enough, or do we need to excise as much of the lipoma as possible? This debate started as early as 1918, when Brickner suggested operating on asymptomatic infants in the hope of preventing future deterioration [22]. A review on 29 patients published in 1945 [59] already mentioned the absence of proliferative potential of intradural and extradural spinal lipomas. Before the introduction of the operative microscope, Giuffre [91] reviewed 99 patients from the literature and a personal case. The patients had either become symptomatic within the first 5 years of life (24.1%), the second and third decades (54.9%), or the fifth decade (16%). He emphasized the long clinical history and the absence of a cleavage plane toward the spinal cord, preventing a complete excision in almost all instances. Nevertheless, postoperative improvements were reported for most surgical interventions. In a later report on the experience a the Mayo Clinic, Thomas and Miller [264] stated that in their 60 patients stabilization of clinical symptoms was the commonest postoperative outcome, with no deterioration after surgery in more than 80% of cases.

Nowadays, some authors recommend prophylactic surgery [143, 152, 153, 172, 207, 256, 277, 283], others advocate an operation only for symptomatic patients [151, 209, 214, 270, 273] or reserve prophylactic surgery for infants and operate on adolescents and adults only if symptoms progress [41]. On comparison of results for infants and adults, it appears that postoperative improvements are more common in children, while neurological signs usually remain unchanged in adults [41, 228]. To justify prophylactic surgery, it has to be established that almost all patients eventually become symptomatic, postoperative improvements are unlikely, surgical morbidity is very low, and that deteriorations do not occur once surgery has been undertaken.

If we look at these points, then the only undisputed fact is that long-term improvements cannot be obtained with surgery for a significant number of symptomatic patients. This certainly calls for early surgery before significant deficits have occurred. In terms of natural history and the long-term results of prophylactic surgery, however, the information from the literature is conflicting. Considering the preoperative course of patients, differing statements appear in the literature. In a study by Koyanagi et al. [143] on 34 patients with a tethered cord between 1 month and 47 years of age, 32 had a lumbosacral lipoma. Just eight (24%) patients under the age of 5 years were asymptomatic; 26 patients (76%) showed signs of a neurogenic bladder, and 24% motor deficits with sphincter problems appearing before motor weakness during the clinical course. These authors concluded that neurological symptoms will almost always appear in early childhood. On the other hand, La Marca et al. [152] observed asymptomatic patients in their group of 213 children up to 12.6 years of age and stated that patients with filum terminale lipomas tend to develop neurological symptoms later than patients with conus lipomas. Pierre-Kahn et al. [210] reported on 291 lipomas and described the onset of neurological symptoms to occur at a mean age of 5 years.

The results of our series and those on adults with occult spinal dysraphism tell another story. In a series of 54 operated adult patients with a tethered cord syndrome, Hüttmann et al. [115] found 32 lipomas, a tight filum in 28 patients, and a diastematomyelia and secondary adhesions in 12 patients; 77% complained about pain, 70% presented with sphincter problems, 57% with motor weakness, and 75% with sensory deficits. Seventeen of these 54 patients (30%) had been asymptomatic in childhood, while 46% were symptomatic but stable during childhood and developed

exacerbations in adulthood, and the remaining 23% had progressive problems since childhood.

We have seen a total of 100 patients with spinal dysraphism; 85% were in the adult age group, 10% even older than 60 years. Of this group, 45 patients harbored an extramedullary hamartoma and 38 were affected by a tethered cord only. The remainder had other manifestations such as an epidural hamartoma, a meningocele, a dermal sinus, or a complex bony malformation. Of 83 adult patients with intradural pathologies associated with spinal dysraphism, 32 patients (39%), chose not to undergo surgery because they were asymptomatic or considered their symptoms as too minor to warrant surgery. Seventeen of these patients were affected by a tethered cord without an additional hamartoma, while 14 had a combination of a tethered cord with a hamartoma, and 1 patient a hamartoma only. These numbers indicate that 45% of the patients in our series with a tethered cord and 33% of those with a hamartoma chose not to be operated. These numbers suggest that not all patients will become symptomatic to a degree that would justify surgery.

Are neurological deteriorations excluded if patients are operated prophylactically? Here we have to look at surgical morbidity and the neurological course in the long term. Surgical morbidity is related to the complexity of the malformation and arachnoid adhesions [210]. Late deteriorations may develop at any time due to retethering of the cord, which is estimated to occur in about 10–20% of patients [42, 49]. For the diagnosis of a retethered cord, MRI and special examinations made with the patient in the prone position are of no use [271], so that a retethered cord is defined clinically by progressive symptoms in the absence of other causes [108].

In the study of Koyanagi et al. [144] on 34 patients with lumbosacral lipomas, 1 of 8 asymptomatic patients (22%) and 6 of 26 symptomatic patients (23%) deteriorated after untethering. They observed a trend for worse results for more complex lesions. In the report of Van Calenbergh et al. [270] on 32 patients with lumbosacral lipomas with 26 children and 6 adults, only symptomatic patients were operated. Permanent morbidity was inflicted in one patient. Postoperative improvements were seen for pain in 28% of patients, for motor function in 31%, and for sphincter functions in 41%. Late deteriorations were seen in 9% with respect to urinary symptoms and 15% for motor weakness. In other words, untethering of the cord did not protect every patient from late deterioration.

It appears that lipomas of the cervical or thoracic cord, the filum terminale and conus lipomas have to be differentiated [152, 210, 277]. Xenos et al. [277] presented their series of 59 children with lipomas – 18 of the filum and 41 of the conus; 32% were asymptomatic before surgery and 26% deteriorated after surgery at late follow up, with filum lipomas demonstrating better outcomes as compared to conus lipomas. Although postoperative improvements can occur, the majority of patients were left unchanged following surgery. Arai et al. [13] reported on 120 patients with lumbosacral lipomas. Of these, 47 were asymptomatic. All patients were operated on, aiming at untethering of the cord, which was sometimes precluded by tethering nerve roots. Twelve patients were functionally worse immediately after surgery. The authors recommended prophylactic surgery for anatomically simple malformations such as a filum lipoma, but found no significant prophylactic effect after surgery of more complex hamartomas. In summary, these smaller studies do not support the concept of prophylactic surgery.

Pierre-Kahn et al. [210] analyzed a large cohort of 291 patients with lumbosacral lipomas operated between 1972 and 1994 to evaluate the results of prophylactic surgery compared to patients operated for symptomatic lesions. The average age at onset of neurological symptoms was 5 years. Postoperative improvements were seen for the majority of patients with lipomas of the filum and 50% of cases with lipomas of the conus. In 93 patients the postoperative follow up exceeded 5 years; 39 of these had been asymptomatic before surgery, but just 53.1% were still free of symptoms at the latest follow up if the lipoma was connected to the conus. A prophylactic effect could only be confirmed for lipomas of the filum terminale. In a subsequent report from this group, Kulkarni et al. [147] reported follow-up results for 53 asymptomatic patients with conus lipomas without surgery since 1994 and compared them with the results for prophylactically operated patients between 1972 and 1994. They observed neurological worsening without prophylactic surgery in 25% of patients during a mean period of 4.4 years. According to Kaplan-Meier analysis, the risk of deterioration within 9 years was 33% for conservatively managed patients and 46% for surgically treated patients. This difference was not statistically significant, but the results certainly do not support prophylactic surgery for conus lipomas.

La Marca et al. [152] performed a similar analysis on 213 patients undergoing 270 surgeries between 1975 and 1995. Of this cohort, 55 presented a lipoma of the filum terminale and 158 with lipoma of the conus. Asymptomatic patients were encountered in the filum group in 50.9% of cases, and in the conus group

in 44.9%. In the filum group, no patient worsened due to surgery and all remained asymptomatic in the long term (mean follow up 3.4 years). In the conus group, nine of the asymptomatic patients (12.7%) deteriorated later (mean follow up 6.2 years), of which four could be stabilized with a second operation. Looking at symptomatic patients, again filum lipomas showed better outcomes, with no long-term deteriorations and improvement to normal in 9% of cases. In comparison, conus lipomas deteriorated at a rate of 41% despite surgery. Applying Kaplan-Meier statistics to calculate clinical recurrence rates after 15 years for patients with conus lipomas revealed deteriorations for 20% of preoperatively asymptomatic and for 60% for symptomatic patients after surgery. Even though these numbers are comparable to those of Pierre-Kahn et al. [210], the authors came to the opposite conclusion and recommended prophylactic surgery on all spinal lipomas.

Considering these analyses, we find it hard to justify prophylactic surgery for patients with spinal hamartomas for the following reasons: a significant number of patients with conus lipomas do reach adult age either without neurological symptoms or consider their symptoms to be so minor that they reject surgery. Surgery is not without risks; morbidity for complex malformations can be considerable. Finally, a significant percentage of patients will experience new or aggravated neurological symptoms despite surgery in the long term. In conclusion, we suggest operating on spinal hamartomas as soon as symptoms develop and advise regular clinical examinations in asymptomatic patients and those who are reluctant to undergo surgery.

In this series, the great majority of patients (85%) were in the adult age group, with a mean age of 39±16 years (Table 4.32). Patients with lipomas of the lower spinal canal tend to become symptomatic earlier than those with lipoma of the cervical or thoracic cord [264]. About 50% complained of pain as their initial symptom, while 32% reported motor weakness or gait problems at the beginning. Just 8% observed sphincter problems at the start. Symptoms may be initiated by sudden efforts, exaggerated bending of the back, trauma, obesity, or pregnancy [115, 210]. On presentation, 55% still considered pain as their major problem, whereas 42% were worried about their motor functions. Sphincter problems were the major complaint for 3% of our series only, even though 48% of our patients did have considerable bladder problems at presentation. In contrast to small children with these disorders, pain is a more common symptom in adults with spinal hamartomas [115, 153].

A similar clinical presentation was documented by Sattar et al. [229] in 50 patients with occult spinal dysraphism. They distinguished cutaneous abnormalities, foot deformities, neurological deficits, sphincter problems, and back or leg pain as the most characteristic features. Most patients presented more than one of them. In only 7 of these 50 patients did the cord end at a normal level above L2; 23 patients had a lipoma, 15 a diastematomyelia, 6 a Chiari malformation, 4 an intradural dermoid cyst, and 20 an associated syrinx. Just 5 patients had a single dysraphic manifestation. Pain was the commonest symptom, but was rarely observed in patients younger than 5 years of age. Sphincter problems were present in 22 patients, cutaneous lesions were demonstrated 35, foot deformities in 28, and signs of muscle wasting in 24 [229]. In the series by Pierre-Kahn et al. [210] on lumbosacral lipomas, 31% had signs of motor weakness, 27.7% sensory deficits, 13.2% complained about pain, and 42% had sphincter disturbances. At least one cutaneous manifestation was observed in 89%, with a subcutaneous lump being the commonest in 64%; 40% had a foot deformity and 36% atrophy of leg muscles. Similar figures were presented by La Marca et al. [152].

As lipomas do not proliferate – changes of volume are correlated with changes in total body fat [62, 210] – the question arises as to whether a lipoma should be resected at all. Extramedullary lipomas may show considerable extension and may pose significant surgical challenges. While one lipoma may be located entirely within the filum terminale and be easily removed (Fig. 4.55), another will be attached to the spinal cord without a dissection plane (Figs. 4.54, 4.58, and 4.59) or a nerve root (Fig. 4.101), and the next may transgress the dura and extend into the epidural space (Fig. 4.56) or even penetrate the fascial layer into the subcutaneous tissue (Fig. 4.57). Such extensive lipomas may not only compress the cord, but also exert a tethering effect, fixing it at the site of dura penetration (Figs. 4.56 and 4.57). Furthermore, arachnoid changes may accompany these lipomas, making it even more difficult to preserve nerve roots and blood vessels during dissection [260].

For filum lipomas we recommend a complete or subtotal resection. With resection of filum and lipoma, the cord is untethered and the surrounding nerve roots are decompressed (Fig. 4.55). For conus lipomas on the other hand, our surgical strategy was to concentrate on untethering of the cord and to debulk a lipoma only to such a degree that conus and lipoma could be accommodated comfortably in the spinal canal (Figs. 4.54, 4.56–4.59, and 4.101). With dense attachment and infiltration into the spinal cord, complete resections

Table 4.32. Overview of patients with extramedullary lipomas

Sex	Age (Years)	Level	Dysr. Man.	History (Months)	Symptoms	Surgery	Outcome
M	44	L4–S2	Filum	180	Hypesth., Gait, Dysesth., Motor, Sphincter	Subtotal duraplasty	Unchanged Lost to follow up
F	32	S1–S5	Filum	108	Hypesth., Pain, Motor, Sphincter	Subtotal duraplasty	Improved No Det. 29 Months
F	44	L1–L3	Filum	12	Gait, Pain	Subtotal duraplasty	Unchanged No Det. 8 Months
F	39	L2–L3	Conus Dia., DS	216	Dysesth., Pain, Sphincter	Partial	Improved No Rec. 84 Months Det. 7 Months
M	23	S1–S5	Conus DS	132	Pain, Motor, Sphincter	Partial	Improved No Rec. or Det. 84 Months
F	67	L4	Conus Dia., Extra	20	Gait, Dysesth., Motor, Sphincter	Partial duraplasty	Unchanged Det.12 Months
F	44	L2–L3	Conus	312	Hypesth., Gait, Dysesth., Motor, Sphincter	Dec. duraplasty	Improved No Det. 24 Months
M	38	L5–S4	Conus Extra	50	Hypesth., Gait, Pain, Motor, Sphincter	Partial duraplasty	Improved Det. 33 Months
	42	L5–S4	Conus	22	Hypesth., Gait, Pain, Motor, Sphincter	Dec. duraplasty	Worse Lost to Follow Up
F	33	L3–S1	Conus Extra	30	Hypesth., Gait, Motor, Sphincter	Partial duraplasty	Unchanged Det. 4 Months
F	28	L5–S1	Conus	3	Hypesth., Gait, Dysesth., Motor, Sphincter	Dec. duraplasty	Improved Det. 10 Months
M	66	Th12	Conus	60	Pain	Partial duraplasty	Unchanged Lost to Follow Up
M	34	L3–S2	Conus Extra	12	Hypesth., Gait, Pain, Motor, Sphincter	Dec. Duraplasty	Unchanged Det. 7 Months
F	49	L3–L5	Conus Extra	8	Hypesth., Gait, Pain, Motor, Sphincter	Partial Duraplasty	Improved No Det. 2 Months
M	48	Th12–L1	Conus	18	Hypesth., Pain, Motor	Partial Duraplasty	Improved Lost to Follow Up
F	32	Th1–Th6		5	Hypesth., Gait, Motor	Duraplasty	Improved Det. 44 Months
M	35	Th1–Th4		6	Hypesth., Gait, Dysesth., Pain, Motor, Sphincter	Duraplasty	Improved Det. 12 Months

Abbreviations: Extra = extradural extension, Filum = lipoma of filum terminale, Conus = conus lipoma

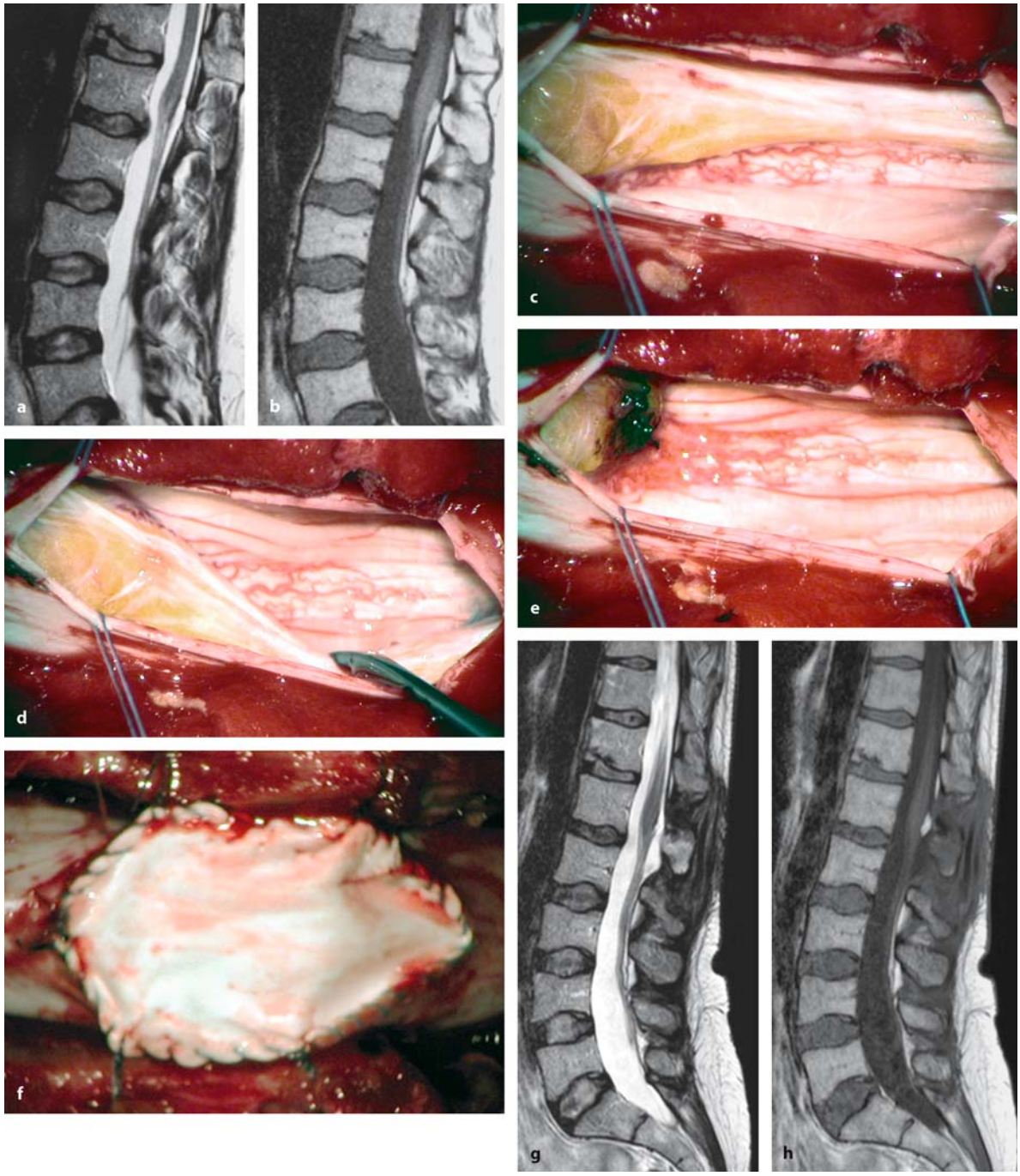

Fig. 4.101. Sagittal T2- (**a**) and T1-weighted (**b**) MRI scans of an extramedullary lipoma at L1–L3 in a 44-year-old woman with a 1-year history of pain and slight gait ataxia. **c** Intraoperative view taken after dura and arachnoid opening, demonstrating the lipoma as part of a caudal nerve root on the right side. **d** The conus can be easily mobilized from this lipomatous root. After subtotal resection of the lipoma and the affected root, the conus is visible underneath (**e**). The dura is closed with a Gore-Tex® patch (**f**). The postoperative T2- (**g**) and T1-weighted (h) MRI scans demonstrate the subtotal removal and a free CSF pathway in the area of surgery. Postoperatively, pain improved but the gait ataxia remained. The patient has been free of a recurrence for 1 year

should not even be attempted. If such a lipoma is small, clinical symptoms will be caused by other factors such as cord tethering, and treatment is concentrated on that issue. If the lipoma is of considerable size, however, we debulk it, leaving the outer part or capsule untouched and closing it at the end with a suture. That way, we try to minimize postoperative arachnoid scarring and, thus, cord retethering (Figs. 4.53 and 4.54). With debulking of the tumor, profuse bleeding may occur so that several authors prefer the use of lasers for this particular surgery. Furthermore, nerve roots may be transgressing the lipoma. Preoperative sagittal and axial MRI scans have to be studied in detail to determine the relationship between lipoma, cord, and nerve roots. If the lipoma is lying on the posterior surface of the cord with all nervous structures displaced anteriorly, the situation is rather straightforward (Figs. 4.53, 4.54, and 4.101). With so-called transitional lipomas, however, the cord and nerve roots will be intertwined in the hamartoma, with considerable risks of damage when resection is attempted (Figs. 4.56–4.59).

Lipomas with epidural extension are managed by circumcising the dura at the site of penetration and transection of the lipoma at that point. After that, the intradural part can be dealt with as described and the epidural and subcutaneous part can be easily resected, bearing in mind, however, that a not too large soft tissue defect should be created with extensive subcutaneous resections, as this may cause wound problems, especially with sacral lipomas (Figs. 4.56 and 4.57) [210].

As a general rule, we have closed the dura with a Gore-Tex® duraplasty to prevent retethering. In two patients with an associated syrinx, no additional measures for the syrinx were taken (Fig. 4.57). We do not recommend any additional shunting as others have done [230]. The postoperative course of the syrinx is related to CSF flow and cord tethering. With obstructed flow and retethering, the syrinx may reexpand. Otherwise, it either remains unchanged or decreases. Thus, if the underlying pathology is treated, no further measures for the syrinx are required [152, 189, 210, 277].

Postoperative outcome was directly correlated to the complexity of associated malformations [130]. Three patients harbored lipomas of the filum terminale, which could be subtotally resected with a satisfactory outcome and no subsequent clinical relapse (Fig. 4.55). Lipomas of the cervical or thoracic cord were associated with widened spinal canals, but no further malformations in our series. Their postoperative course was favorable after decompression with a duraplasty (Fig. 4.53) [68, 95, 264]. In the literature, most authors performed partial resections of cervical and thoracic lipomas, reporting favorable results [8, 55, 95, 141, 173, 264]. Thomas and Miller [264] observed comparable outcomes for patients undergoing decompressive laminectomies alone or additional subtotal removals.

With conus lipomas (Figs. 4.54 and 4.56–4.59), the immediate postoperative situation was characterized by improvement after eight operations, an unchanged state after four, and worsening after one operation (Table 4.32) [153, 199, 283]. The average Karnofsky score increased slightly from 69±17 to 73±22, without statistical significance, in the first postoperative year. However, 40% developed new neurological symptoms within 1 year and 70% within 5 years of surgery, i.e. clinical reccurences (Fig. 4.102). These deteriorations

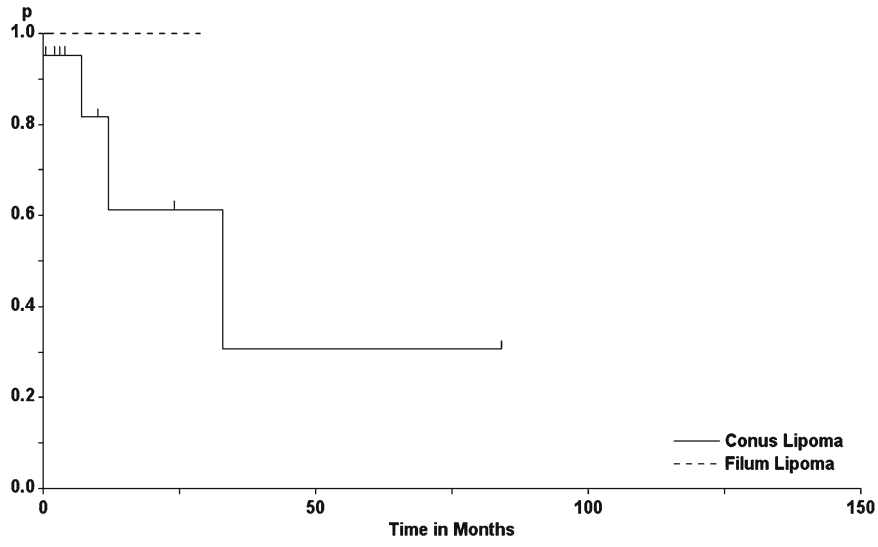

Fig. 4.102. Clinical recurrence rates for extramedullary lipomas (log-rank test: not significant)

can be attributed to retethering and arachnoid scarring [108, 115]. Whenever postoperative arachnoid scarring was evident on MRI, clinical progression was the likely course [9, 63, 67, 242].

In the long term, stabilization of the preoperative neurological status has been found in most studies reporting on children with spinal dysraphism after a follow up of several years [111, 143, 151, 165, 207, 232, 256, 283]. In a series of 341 tethered cord releases, 153 patients – most of them children - were operated for retethering [108]. Among these retethered cords, 53 had occurred after surgery on a conus or filum terminale lipoma, most of them performed at other institutions. These authors claimed a rate of just 6 retetherings out of 160 personally operated patients with spinal lipomas. The diagnosis of retethering was made clinically. Intraoperatively, severe arachnoid adhesions and residual lipoma complicated dissection. Four out of 53 patients could not be untethered sufficiently. Complications occurred in 13% related to wound problems. Just over half of these patients experienced postoperative neurological improvements. Late deteriorations were not observed in the group with lipomas.

Overall, our surgical results for this predominantly adult population are considerably worse compared to these reports for pediatric patients [228]. We attribute this to degenerative changes, to problems achieving a sufficient untethering at surgery or to rethering. In their study on 54 adults, Hüttmann et al. [115] obtained postoperative improvements for 85%, stabilizations in 7%, and observed deteriorations in 7% of their patients. Untethering had been successful in 82% of operations. With complete untethering, the authors observed a clinical recurrence rate of 16%, whereas with incomplete untethering the figure rose to 80%. The authors concluded that surgery provided a long-term benefit for those patients in whom untethering could be achieved.

Maiuri et al. [165] published a series of 15 adults with spinal hamartomas (7 lipomas, 4 epidermoid cysts, 3 dermoid cysts, and 1 teratoma), of which 14 were operated. Ten became initially symptomatic with pain, while hypesthesias were the initial clinical symptom in the remainder. At presentation, six had motor weakness and five had sphincter problems. Two lipomas of the filum, three epidermoid and three dermoid cysts were removed radically, while two were removed subtotally and four partially. Outcome was not analyzed relative to completeness of resection, but was given for the total group. Radicular pain was stated as improved in all patients, motor weakness in five out of six, and sphincter problems in four out of six patients.

Of particular concern is the postoperative outcome for sphincter control. Improvements can only be expected for patients without complex malformations [142]. Otherwise, stabilization of the preoperative status is the commonest result [111, 199, 283]. On the other hand, results of conservative treatment of sphincter disturbances may not be as bad as most neurosurgeons tend to believe, especially in patients with sphincter hyperreflexia [140].

Pierre-Kahn et al. [210] achieved subtotal removals in 66% and partial resections in 34% of cases. In just four patients, removal was minimal. Decompression and untethering was judged to be sufficient in 80% of cases. They found no correlation between postoperative results and the amount of lipoma resection. With filum terminale lipomas, they observed no complications or surgical morbidity. With conus lipomas, however, local complications were observed in 20% with meningoceles, CSF leaks, and wound infections (wound nonunion being the commonest). One of these patients was treated with a lumbar drain and 23 required secondary operations. Neurological aggravations were seen in 10.9% of operations: in 7.5% these aggravations were transient, but in 3.5% they were permanent. These neurological complications were mostly related to arachnoid adhesions and abnormal roots. Similar figures were given by Xenos et al. [277], with a complication rate of 18% and permanent surgical morbidity of 3%.

Looking at results after 1 year for filum terminale lipomas, Pierre-Kahn et al. [210] observed postoperative improvements in 53% of cases. With conus lipomas, 6.4% of asymptomatic and 9% of symptomatic lipomas worsened postoperatively. With long-term follow up, 95.2% of asymptomatic patients with filum lipomas remained intact. In symptomatic patients with filum lipomas, symptoms remained as they were after 1 year. With conus lipomas, 23.9% of preoperatively asymptomatic patients had deficits after 1 year, while 76.1% were still asymptomatic. At maximum follow up, a further 17.5% of patients had worsened. With symptomatic patients, 50% were improved, 29.9% unchanged, and 20.1% were worse than preoperatively. At long term, 11.1% showed deterioration [210].

With respect to patients with conus lipomas and more than 5 years of follow up, 32 were asymptomatic before surgery. In the long term, just 53.1% of these were still asymptomatic, although 93.6% were neurologically normal after 1 year. This outcome was related mainly to the complexity of the malformation, but not to age, and only in asymptomatic cases to the quality of surgery [210].

In conclusion, we recommend: (1) that surgery should be recommended only for symptomatic patients with spinal lipomas, (2) that sizeable lipomas should be debulked, (3) that surgery has to limit postoperative arachnoid scarring (i.e., no unnecessary dissections, careful handling of the arachnoid, and duraplasty with Gore-Tex®), and (4) that surgery on small lipomas should be concentrated on untethering the cord.

4.5.5 Ependymomas of the Filum Terminale

Twenty-nine ependymomas in 26 patients were encountered, and 26 operations were performed. Three patients with extensive ependymomas over several spinal segments rejected surgery. Patients presented at an average age of 36±12 years (range 13–57 years) after a mean history of 25±44 months [30, 34, 218, 235, 250]. Ependymomas of the filum terminale occurred in children at between 10 and 14 years of age [79, 250]. These tumors may be associated with quite long clinical histories of several years [30, 235, 250]. The longest preoperative history in our series was over 8 years.

Pain was the commonest initial symptom and was reported by 74% of these patients (Table 4.33) [30, 218, 235, 250]. Other symptoms were rare as initial complaints. At presentation, 70% still regarded pain as their main concern, with 11% each naming gait ataxia or motor weakness as the major symptom. Only 7% considered sphincter problems as the main symptom, even though 52% did have some problems with bladder function [77]. These tumors may contain hemorrhages [218] and may even present with subarachnoid bleeding [30, 77].

Extramedullary ependymomas arise from the ependyma of the filum terminale. Histologically, the overwhelming majority are myxopapillary. The main bulk of the tumor is located in the lumbar canal below the conus medullaris. Extension in the thoracic spine was observed in 31% of cases (Figs. 4.18, 4.49, and 4.103), and 24% presented with extension into the sacrum (Figs. 4.18 and 4.19). Some may fill the entire lumbosacral canal. These tumors may spread due to subarachnoid seeding [236]. We have not seen a patient with a spinal metastasis of a fourth ventricular ependymoma. Nevertheless, a cranial CT or MRI should be performed in every such patient to rule out this possibility. With primary ependymomas of the filum terminale, however, seeding was observed into other areas of the spinal canal (Figs. 4.18 and 4.19).

Table 4.33. Symptoms of patients with ependymomas of the filum terminale

Symptom	First symptom	At presentation
Pain	74%	85%
Gait ataxia	4%	37%
Motor weakness	7%	44%
Sensory deficits	4%	41%
Dysesthesias	4%	22%
Sphincter problems	7%	52%

The diagnosis can usually be made with gadolinium-enhanced MRI. Extramedullary ependymomas, like their intramedullary counterparts, enhance brightly with contrast. Enhancement may be homogeneous or patchy, as these neoplasms may be associated with small intratumoral cysts and hemorrhages.

Removal of ependymomas in the lumbar and sacral region may be quite difficult as these tumors are well vascularized and may not display a capsule (Figs. 4.49 and 4.50), so that they may completely encase nerve roots of the cauda equina [34, 250]. Chang et al. [37] obtained complete resection for only 40% of cases. Celli et al. [30] reported complete resections for 71% of tumors, Cervoni et al. [34] in 69% of patients, and Rivierez et al. [218] in 75%. In a literature review, Lonjon et al. [160] analyzed reports on 278 ependymomas and determined a complete resection rate of 72%. Nerve roots and the spinal cord may be very adherent to or even infiltrated by the tumor [30, 34, 79]. In the series of Celli et al. [30], 2 patients died postoperatively, 8 improved, 7 were left unchanged, and 11 were worse postoperatively. Surgical morbidity for these tumors is considerably higher compared to other extramedullary pathologies [203]. For this reason, 20 tumors (76%) were removed completely and the remaining 6 (24%) subtotally in our series [235]. Three patients with incomplete resections underwent postoperative radiation without subsequent tumor recurrence. Two of these had been operated on recurrent tumors [69, 167, 236, 240].

Radiotherapy appears to have an effect on incompletely resected ependymomas of the filum terminale [250]. In a literature review of 278 tumors, complete resections were associated with a recurrence rate of 15% and partial resections with a rate of 43%. With radiotherapy and partial resections, the recurrence rate was significantly lower than after partial resections alone (33% and 55%, respectively). Kaplan-Meier statistics, however, were not applied [160]. Similarly, Sonneland et al. [250] reported a recurrence rate of

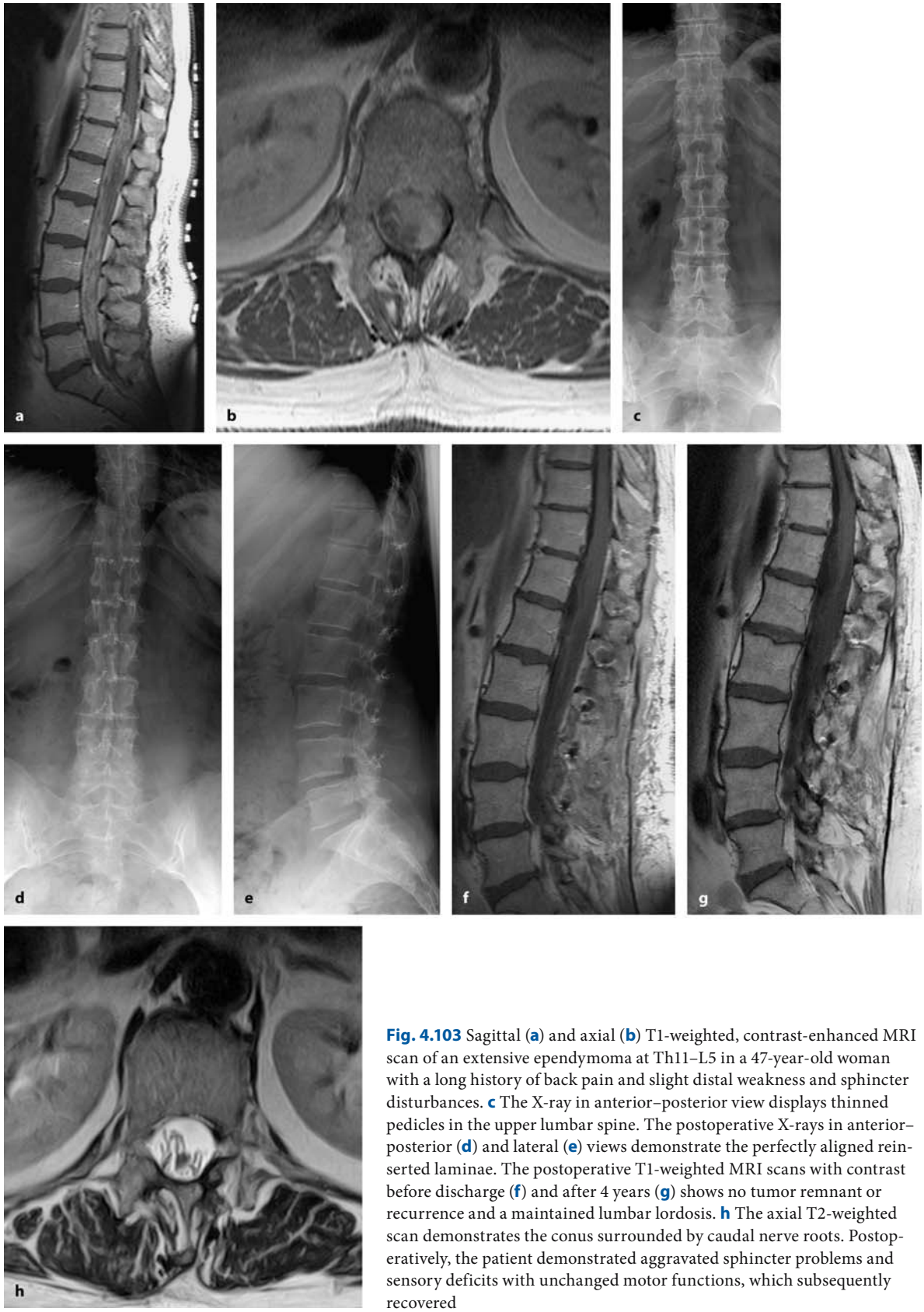

Fig. 4.103 Sagittal (**a**) and axial (**b**) T1-weighted, contrast-enhanced MRI scan of an extensive ependymoma at Th11–L5 in a 47-year-old woman with a long history of back pain and slight distal weakness and sphincter disturbances. **c** The X-ray in anterior–posterior view displays thinned pedicles in the upper lumbar spine. The postoperative X-rays in anterior–posterior (**d**) and lateral (**e**) views demonstrate the perfectly aligned reinserted laminae. The postoperative T1-weighted MRI scans with contrast before discharge (**f**) and after 4 years (**g**) shows no tumor remnant or recurrence and a maintained lumbar lordosis. **h** The axial T2-weighted scan demonstrates the conus surrounded by caudal nerve roots. Postoperatively, the patient demonstrated aggravated sphincter problems and sensory deficits with unchanged motor functions, which subsequently recovered

Symptom	Preoperative status	Postoperative status	3 Months postop.	6 Months postop.	1 Year postop.
Pain	3.3±0.8	3.9±0.6	4.3±0.6	4.3±0.6	4.3±0.8**
Hypesthesia	4.0±1.1	4.3±1.0	4.4±1.0	4.5±0.9	4.5±0.9*
Dysesthesias	4.7±0.6	4.5±0.7	4.6±0.6	4.7±0.6	4.7±0.6
Gait	4.2±1.0	4.1±1.2	4.3±1.1	4.5±1.1	4.5±0.8
Motor power	4.0±1.0	4.0±1.3	4.3±1.2	4.3±1.1	4.4±0.9
Sphincter function	3.9±1.5	3.7±1.6	4.0±1.4	4.1±1.4	4.1±1.4
Karnofsky score	76±6	75±14	79±14	81±12	84±11**

Table 4.34. Clinical course for patients with ependymomas of the filum terminale

Statistically significant difference between preoperative status and 1 year postoperatively: *$p<0.05$, **$p<0.01$

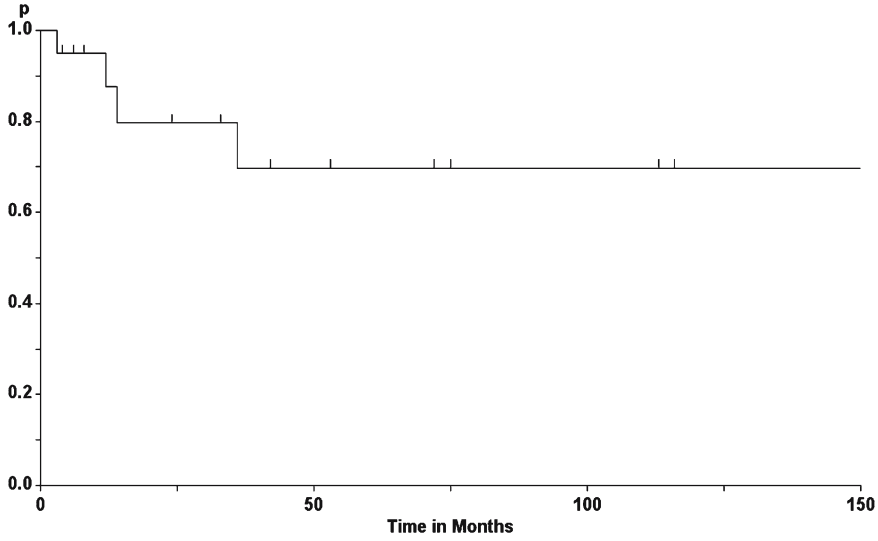

Fig. 4.104. Tumor recurrence rate for ependymomas of the filum terminale

10% after complete resections, 34% after piecemeal, and 41% after partial removals. Cervoni et al. [34] observed 14 recurrences in a series of 36 patients. Eleven of these had undergone subtotal resections due to nerve root infiltrations. In another paper, Cervoni et al. [32] determined a long history, incomplete resection, and infiltration of nerve roots as independent factors for a tumor recurrence in a series of 78 ependymomas. Before the introduction of microsurgery, a recurrence rate of 53% was determined. With microsurgery, a slight decrease to 47% was observed. One paper even reported lower recurrence rates after partial resections followed by radiotherapy as opposed to complete resections alone [79], whereas the recurrences in the aforementioned study by Cervoni et al. [34] had developed despite radiotherapy. Therefore, complete resections should be attempted whenever possible [30, 160, 185].

Within the first postoperative year, we have seen significant

improvements for sensory disturbances and pain, and a significant increase of the Karnofsky score (76±6 preoperatively to 84±11 after 1 year; Table 4.34). In their series of 15 patients, Schweitzer and Batzdorf [235] obtained excellent results in 53%. Outcome was better for patients presenting predominantly with pain rather than neurological deficits.

In our series, the overall tumor recurrence rates were 12% and 30% within the 1st year and after 10 years, respectively (Fig. 4.104). In the literature, recurrences have been described after as long as 42 years following a complete resection [31]. From a literature analysis, these authors estimated a recurrence rate of 19% (without applying survival statistics). In an earlier paper, they had described 11 recurrences among 28 patients [30].

4.5.6 Metastases

Extramedullary as well as intramedullary metastases of carcinomas are rare. We have encountered ten intradural extramedullary metastases in seven patients undergoing eight operations without predilection for a particular primary tumor (three bronchial, two thyroid, one breast, one melanoma, one hypernephroma, one unknown primary tumor) [177].

In our series, two patients reported pain as the major complaint, while the remainder were concerned mainly about gait problems and motor weaknesses.

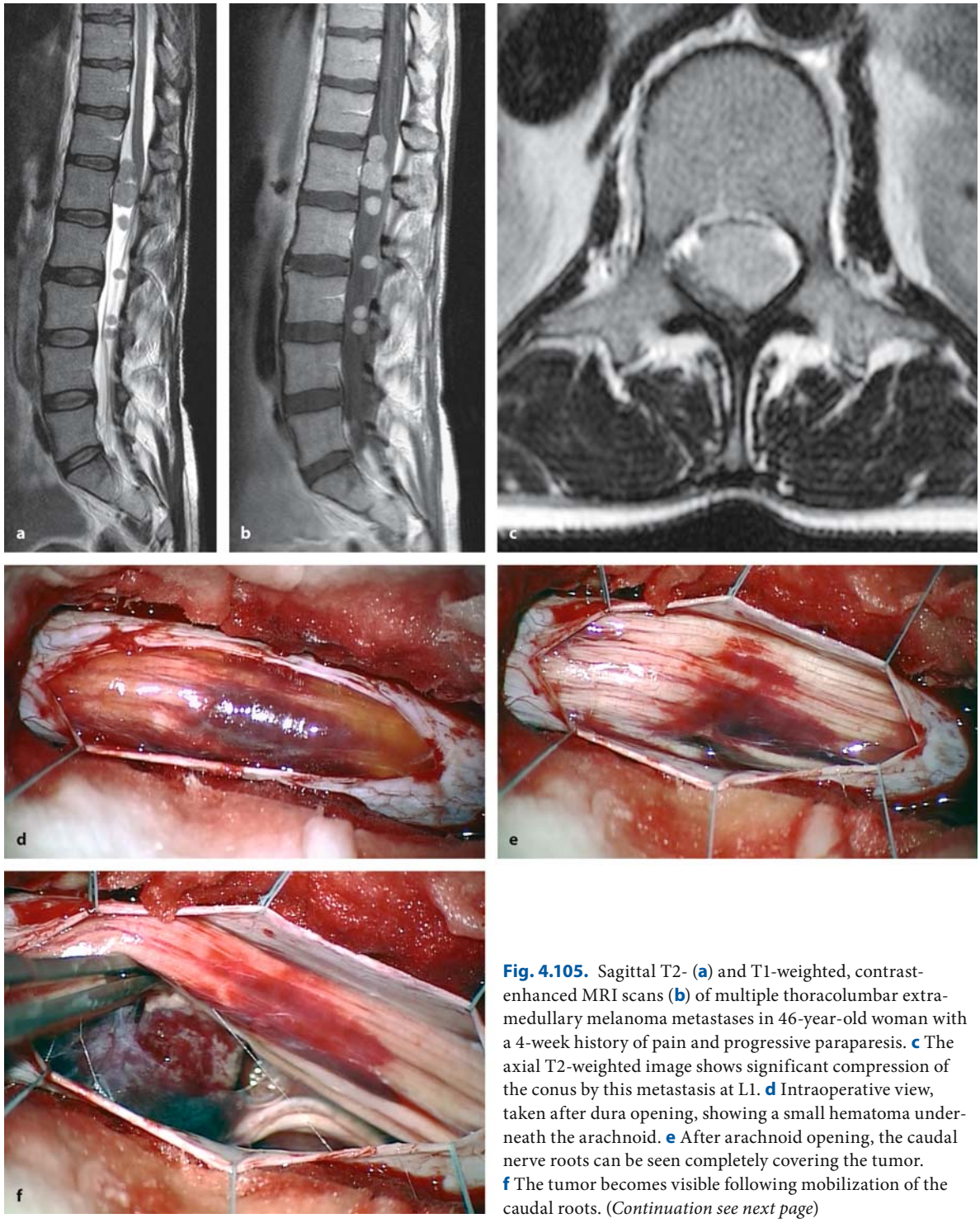

Fig. 4.105. Sagittal T2- (**a**) and T1-weighted, contrast-enhanced MRI scans (**b**) of multiple thoracolumbar extramedullary melanoma metastases in 46-year-old woman with a 4-week history of pain and progressive paraparesis. **c** The axial T2-weighted image shows significant compression of the conus by this metastasis at L1. **d** Intraoperative view, taken after dura opening, showing a small hematoma underneath the arachnoid. **e** After arachnoid opening, the caudal nerve roots can be seen completely covering the tumor. **f** The tumor becomes visible following mobilization of the caudal roots. (*Continuation see next page*)

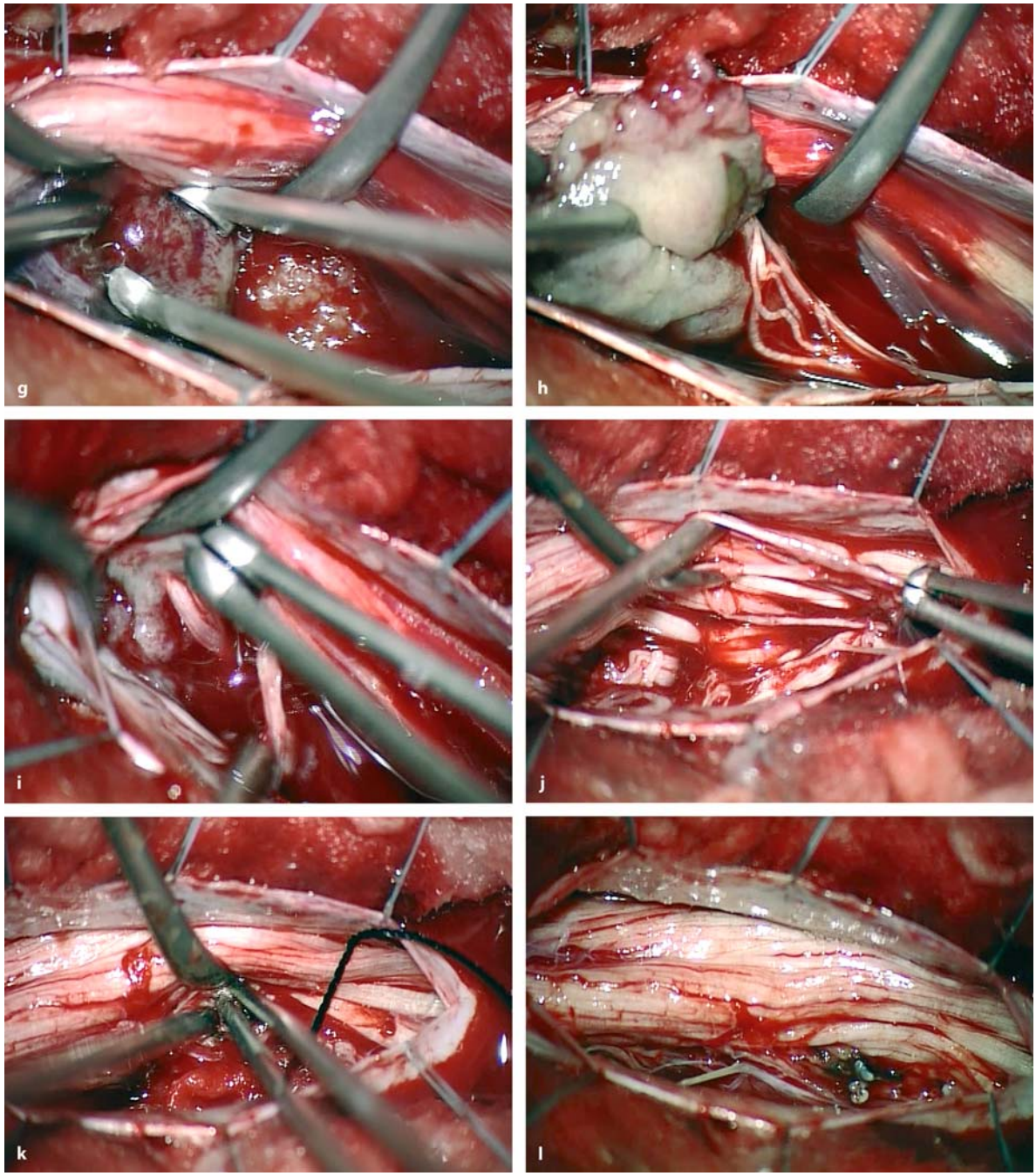

Fig. 4.105. With debulking of the tumor (**g**), it becomes apparent that several nerve roots are attached (**h**) and infiltrated by the tumor (**i**). **j** Each root was dissected free with tumor forceps. **k** The tumor-feeding arteries attached to the nerve roots were coagulated. **l** This final photograph shows the situation after complete resection of the tumor. (*Continuation see next page*)

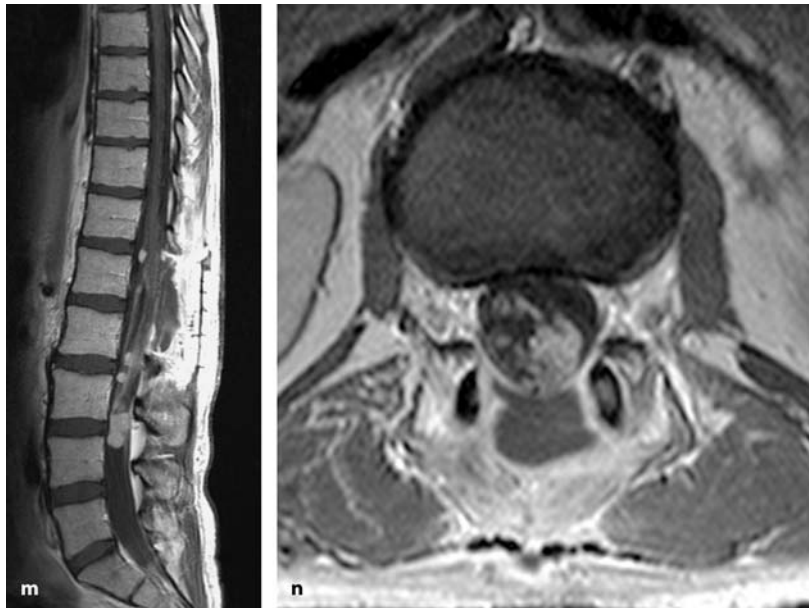

Fig. 4.105. (*Continued*) The postoperative sagittal (**m**) and axial (**n**) T1-weighted, contrast-enhanced scans demonstrate the complete resection at L1 and a small epidural CSF collection. The patient was unchanged postoperatively and referred for further chemotherapy

Four surgeries resulted in complete resections; the remainder were partial removals. Patients with incomplete resections underwent postoperative local radiation. Postoperative clinical results were disappointing, without even short-lived improvements.

From our experience we would question the value of surgery of these lesions. Similar to intramedullary metastases, it appears that extramedullary spread of carcinomas indicates a final stage of the disease in the majority of cases, half of patients dying within 6 months after surgery [177]. Therefore, surgery should be reserved for patients with a single metastasis and otherwise good control of the carcinoma, or as a palliative measure for patients with significant local symptoms but no alternative therapeutic option (Fig. 4.105).

4.5.7 Angioblastomas

Four patients were encountered with extramedullary, intradural angioblastomas (Figs. 4.51 and 4.52). Two of these had von-Hippel-Lindau disease (VHL). Like patients with NF-2, all VHL patients should undergo yearly MRI examinations of the entire neuraxis. All but one tumor in this series were localized in the thoracic spine. However, other localizations and angioblastomas with extradural extension have been described [92]. The problem with these tumors is achieving a correct preoperative diagnosis. As mentioned for the much larger group of intramedullary angioblastomas, attempts to remove the tumor in a piecemeal fashion should be avoided, as profuse bleeding will be encountered. In other words, mistaking this tumor for a schwannoma, for instance, and entering the tumor capsule for debulking will result in a very unpleasant situation. In patients with known VHL, the correct diagnosis will not be a problem. In sporadic cases, however, MRI angiography or spinal angiography would probably be required, and these are not performed before surgery on a routine basis.

The average age in our small series was 43±17 years, with a preoperative history of 25±31 months and a preoperative Karnofsky score of 63±29. Postoperatively, the neurological situation was improved for three and unchanged for the remaining patient. All tumors were removed completely, with no recurrences so far. With sizeable tumors, preoperative embolization may be helpful and was used in one of our patients (Fig. 4.52).

4.5.8 Cavernomas

Cavernomas are rare tumors of the spinal canal. Most are reported to occur in the spinal cord, with only exceptional cases in the extramedullary location. According to one review, most extramedullary cavernomas were reported in males at the thoracolumbar region [196].

We observed two such lesions in this series. Both demonstrated a short history of a few weeks with sudden onset of pain without any other neurological deficits. Both processes – one at Th3 and the other at L3 – were removed completely with good pain relief. With bipolar coagulation the lesion could be shrunk, allowing safe dissection of surrounding structures and radical removal. Sharma et al. [239] and Acciarri et al. [2] observed two extramedullary cavernomas, each with good results, except for one patient with persistent sphincter dysfunctions related to a cauda equina cavernoma [239].

4.5.9 Sarcomas

One patient was operated twice within 8 months on a recurrent sarcoma with intra- and extradural extension in the upper thoracic spine. The tumor had progressed despite a combination of radiotherapy and chemotherapy. While the patient came to us first for the relief of pain, the second operation was performed to prevent a complete paralysis. After sufficient pain relief initially, the second operation was not able to prevent further deterioration and the patient lost her capacity to walk 2 months later.

Surgery on such an extensive malignant tumor, which progresses despite adjuvant therapy, is always an uphill battle. However, if all other options have been taken and surgery is the only chance to preserve neurological function at least for some time, it is hard to refuse an operation if the patient is desperate to keep his self-supporting capacity.

4.5.10 Hemangiopericytomas

Hemangiopericytomas – formerly named angioblastic meningiomas – are highly vascularized tumors that may occur in the spinal canal in the vertebral body, or more commonly, attached to the meninges [159]. Most of the cases described in the literature were located extradurally, with only a few intradural cases reported. In a review article, Betchen et al. [19] found just 5 intradural cases among 39 spinal hemangiopericytomas.

The radiological features are indistinguishable from other extramedullary tumors. They brightly enhance with gadolinium. Due to their vascularization, preoperative embolization may be helpful in selected patients [43, 183].

In a study on 94 hemangiopericytomas of the entire nervous system, Mena et al. [174] determined a metastasis rate of 23.4%. Hemangiopericytomas are prone to local recurrences, regardless of localization [19]. Therefore, en bloc resection should be considered where possible [19] and most authors regard postoperative radiotherapy as being essential [43, 99, 174, 183], whereas the role of chemotherapy is not fully established.

In our series, one hemangiopericytoma, which transgressed the dura at the C5/6 level, was operated in a 58-year-old patient. This tumor had been operated on twice with postoperative radiotherapy at another institution and was located in the dural sleeve of the C6 root and very adherent to it. To preserve nerve function, a small tumor remnant had to be left in place. Postoperatively, motor function of the C6 root deteriorated slightly, but dysesthesias and pain improved.

4.5.11 Exophytic Astrocytomas

One may argue that extramedullary astrocytomas do not exist. However, we have encountered a patient with an astrocytoma at the C1–C3 level, which is believed to have grown exophytically out of the spinal cord. But intraoperatively, no clear connection with the cord was identified. It can only be speculated that a small pedicle of tissue had existed, which disconnected during dissection. The tumor was removed completely with no subsequent recurrence or evidence of an intramedullary counterpart on MRI.

4.5.12 Tumors with Subarachnoid Seeding

In this subgroup, 44 tumors in 18 patients were treated in 26 surgeries. All of the involved histologies were malignant. Recurrence rates differed somewhat for these patients depending on the tumor type. But overall, 51% recurred within 1 year and 92% within 5 years (Fig. 4.106). 55% of patients died within 1 year, with a long-term survival of 37% for 10 years (Fig. 4.107). A significant effect of surgery was a reduction of pain, which was the major problem for 41% of patients at the time of the operation. Another 41% were operated for a rapidly progressing paraparesis, which was improved significantly in the majority of cases.

In other words, surgery is not curative, and one may argue that surgery is of little value in this group of patients. But we do not think, that a categorical

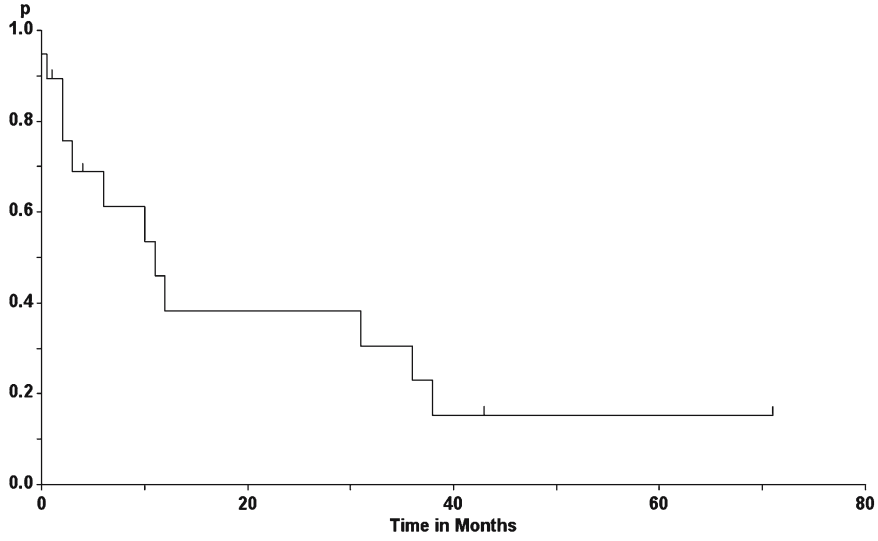

Fig. 4.106. Overall tumor recurrence rate for extramedullary tumors with subarachnoid seeding

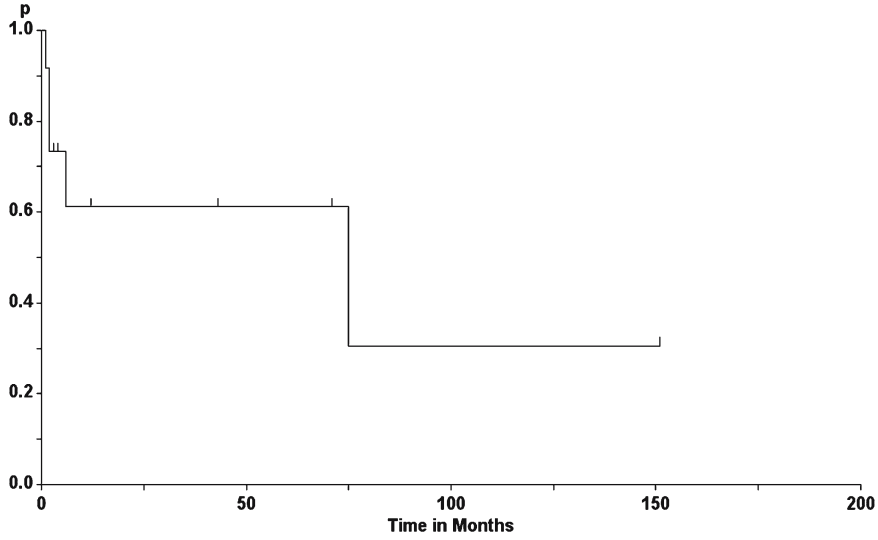

Fig. 4.107. Overall survival rate for extramedullary tumors with subarachnoid seeding

statement is warranted. Treatment of these patients has to be considered on an individual basis: What is the overall prognosis? What adjuvant therapies are available? How is the general health status of the patient? How much is the quality of life affected by the spinal process? What does the patient expect? These are some of the cardinal questions that need to be answered before a decision to operate or not to operate can be made. In terms of surgical management, the same aspects apply as described for other extramedullary tumors.

4.5.12.1 Neuroblastomas

Twelve neuroblastomas were operated on 3 patients in 3 operations. All surgeries had to deal with multiple tumors in patients with subarachnoid seeding of intracranial tumors, resulting in incomplete resections and subsequent recurrences within 6 months, except for the patient undergoing postoperative local radiation, which was followed by a recurrence-free interval of 5 years. All patients had neurological symptoms, but the major preoperative concern for all three patients was radicular pain. Postoperative clinical results were characterized by improvements in pain but unchanged neurological symptoms and slightly improved Karnofsky scores.

4.5.12.2 Melanocytomas

Melanocytomas occur predominantly in the posterior fossa and spinal canal, with a female predominance [45]. Other terms used for these tumors are melanotic meningioma, melanotic schwannoma, and meningeal melanocytoma. As the differential diagnosis to melanoma metastases may be difficult, it appears reasonable to refer patients with these tumors to a thorough dermatological examination.

Eight extramedullary melanocytomas were operated in two patients with subarachnoid seeding of these lesions (Fig. 4.108). One of these patients was presented in a case report in 1992 [262]. Gait problems were the major clinical problem in two instances, while the remainder were troubled by pain or dysesthesias. Tumor recurrences occurred after each operation within 3 years, even though six operations had resulted in what appeared to be a complete resection. Again, local infiltration, high vascularity, and the dissemination of tumor cells limit surgical success. The value of postoperative radiation of the entire neuraxis is still not completely clarified [45].

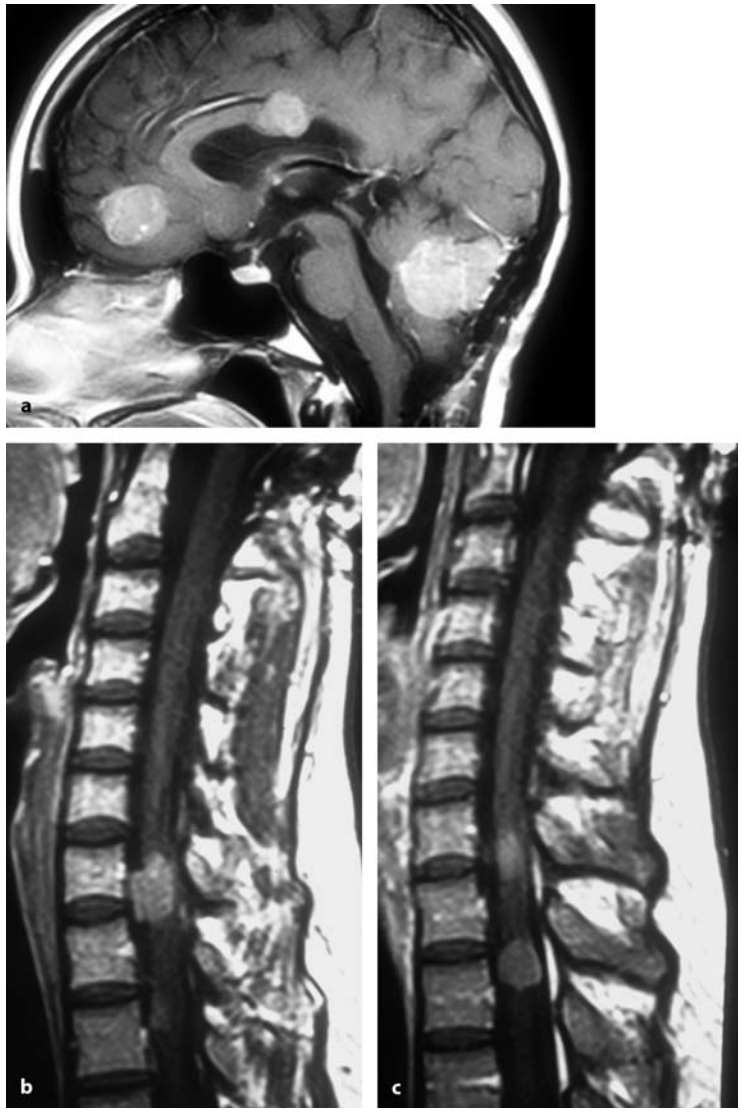

Fig. 4.108. Cranial (**a**) and spinal (**b**, **c**) sagittal T1-weighted, contrast-enhanced MRI scans of a disseminating melanocytoma in a 33-year-old woman with a 4-month history of progressive paraparesis. She had undergone surgery and radiotherapy for a melanocytoma of the posterior fossa years earlier. Apart from a local recurrence and intracranial tumors, spinal melanocytomas were detected at C7, Th1, and Th2. (*Continuation see next page*)

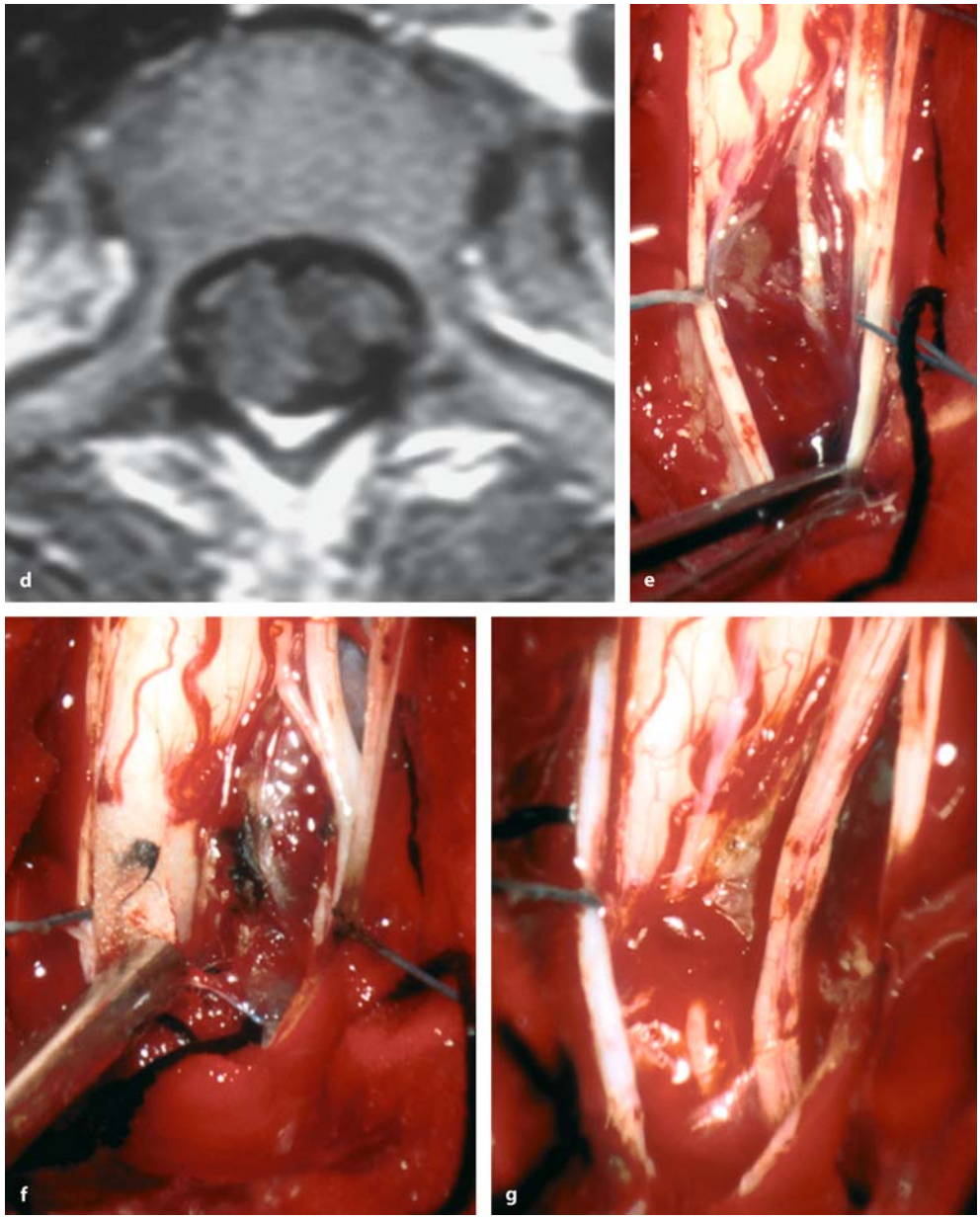

Fig. 4.108. d Axial scan showing compression of the cord from both sides at Th1. **e** Intraoperative view taken with the patient in the semisitting position after dura and arachnoid opening, showing the tumor at C7 anterior to the posterior roots on the right side. With piecemeal removal (**f**) the tumor that did not display a capsule was resected (**g**). (*Continuation see next page*)

4.5.12.3 Teratomas

In one 20-year-old patient, six malignant extramedullary teratomas in the thoracic and lumbar spine were resected completely in a single operation after chemotherapy had failed to control the clinical situation. The patient did not benefit from surgery and died 1 month later. Sharma et al. [238] reported on a series of ten spinal teratomas. None of them was classified as malignant, seven were associated with stigmata of spina bifida, and just one recurrence was observed after seven complete and three partial resections.

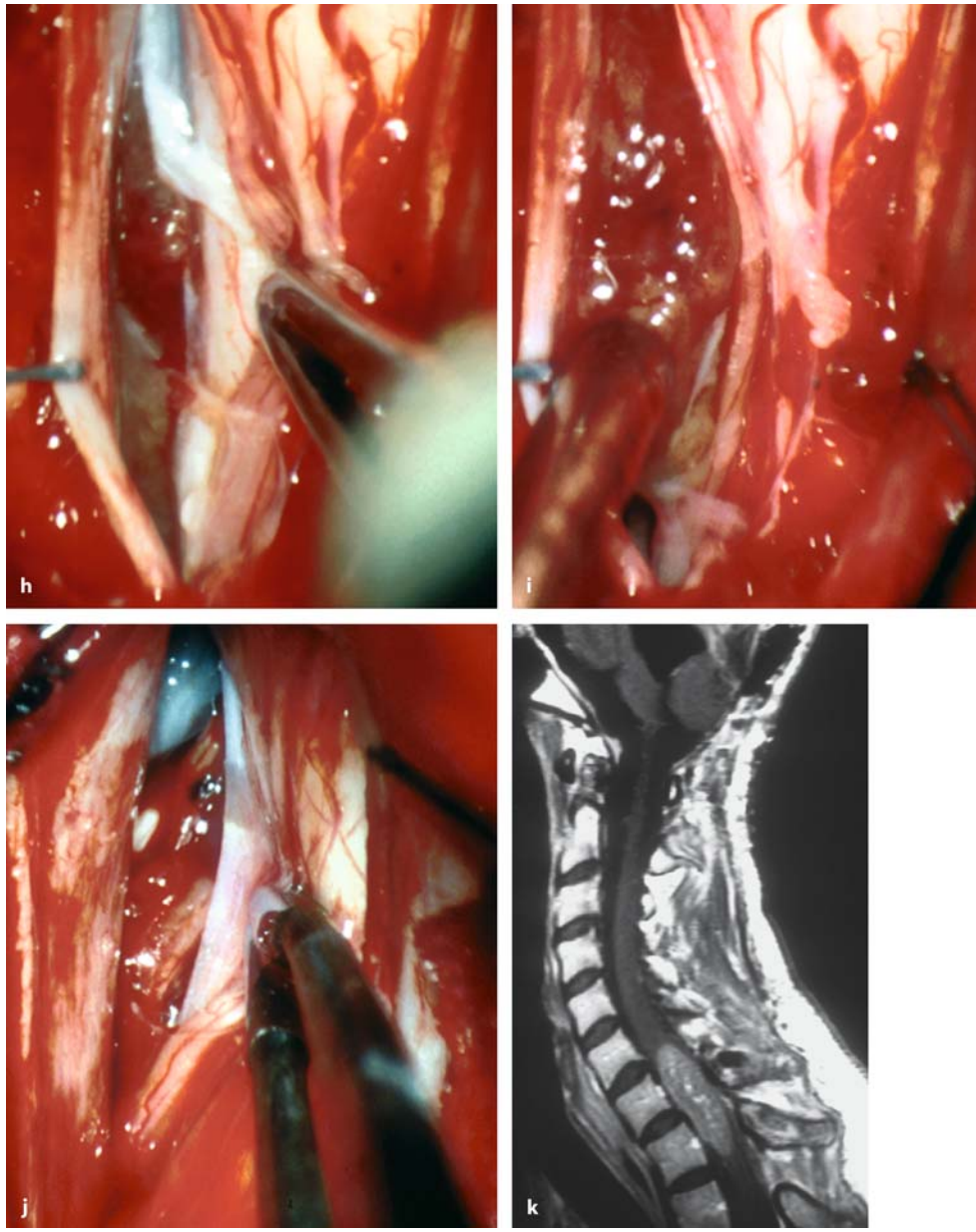

Fig. 4.108. (*Continued*) **h** A similar situation appears at Th2 on the left side. Again, the tumor was removed, applying suction on a low setting (**i**) to achieve a good decompression (**j**). Postoperatively, the patient recovered her neurological functions; 11 months later, a large local recurrence appeared at C7–Th1 (**k**)

4.5.12.4 Chordomas

Asano et al. [15] observed a 53-year-old patient with multiple chordoma metastasis in the thoracic and lumbar spinal canal 11 years after initial surgical treatment of a clivus chordoma, which had been operated upon five times via extra- and intradural approaches over the years. Among a series of 82 patients with skull-base chordomas, Arnautovic and Al-Mefty [14] observed seeding to various locations in six patients, mostly related to surgical maneuvers at the initial operation.

We have operated on five extramedullary chordomas in two patients in three surgeries. All patients underwent postoperative radiation therapy after partial resections of these tumors. Chordomas develop

primarily from remnants of the notochord. Subarachnoid spread usually indicates a more aggressive tumor and may indicate rapid progression, with penetration of the dura and consequently a poor prognosis. One patient died within 2 months of surgery, while the other survived 6 years with a disease-free interval of 3 years.

4.5.12.5 Medulloblastomas

Subarachnoid seeding of a medulloblastoma is a poor prognostic sign indicating widespread disease. Two patients were operated with such extramedullary tumors in the spinal canal and received postoperative adjuvant therapy. Both patients died within 1 year of the spinal operation. Whether surgery of a spinal metastasis influences overall morbidity and survival is a matter of discussion.

4.5.12.6 Germinomas

One germinoma metastasis at the fourth thoracic level was operated in a 22-year-old patient with a rapidly progressive paraparesis that had evolved within 1 week. After partial resection and a duraplasty the patient underwent radiotherapy without neurological recovery.

4.6 Management of Recurrent Extramedullary Tumors

Even though the great majority of extramedullary tumors are benign and can be resected completely, a significant proportion of them may recur. These cases pose some additional problems that we would like to comment on. The clinical and radiological diagnosis of a recurrent extramedullary tumor is usually straightforward. Patients should undergo regular neurological check ups and MRI controls after a first operation. In our series, local recurrences of benign extramedullary tumors occurred anytime throughout the first 10 years – 20% within the first 5 years, 36% after 10 years (Fig. 4.68). With yearly checks, most recurrences can be picked up before symptoms have developed.

Meningiomas, schwannomas, hamartomas, arachnoid cysts, and ependymomas are the commonest histologies in this category. Overall, 85 operations dealt with recurrent extramedullary tumors (Figs. 4.43, 4.76, 4.78, and 4.85). In terms of the clinical presentation, we could not detect a significant difference compared to patients operated on for the first time. Even the preoperative histories (26±50 months and 24±52 months for first and recurrent tumors, respectively) and Karnofsky scores (70±15 and 67±14 for first and recurrent tumors, respectively) were comparable.

Surgery on recurrent extramedullary tumors faces several obstacles: the problems of spinal stability and epidural scar formation have already been dealt with. Intradurally, the big difference with a first operation is the arachnoidal layer. Whereas preservation of the arachnoid membrane during the initial dissection after dural opening allows a safe, first orientation in a primary operation, arachnoid scarring may interfere with the dissection and precise localization of tumor boundaries significantly. Therefore, it is mandatory to start the dural incision and intradural dissection above and below the previous exposure before attempting dissection of a recurrent tumor. Doing so allows to use of the unaltered arachnoid as a guide during dissection toward the tumor and prevents injury to the cord and its vessels. Once the tumor boundaries have been defined, debulking is the next step. Finally, the tumor capsule or remaining tumor parts are removed provided they can be safely dissected off the nerve roots and spinal cord. Here again, arachnoid scarring may obscure the exact outlines of a tumor, making this last part difficult or even impossible without undue risks to important structures. Whenever arachnoid scarring is part of the pathology, we recommend a duraplasty to limit postoperative cord tethering.

With recurrent tumors, just 51% could be resected completely, compared to 81% during first surgeries (chi-square test: $p<0.0001$). On average, patients with recurrent tumors did not demonstrate clinical improvements postoperatively. Therefore, for each clinical sign and symptom, the postoperative result after 1 year was significantly worse compared to patients after a first operation, who demonstrated clinical improvements regularly (Table 4.11). This difference is not attributable to a higher surgical morbidity, but to a significantly higher recurrence rate in the first postoperative year (33% and 8% for recurrent and primary operations, respectively; log-rank test: $p>0.0001$; Table 4.14 and Fig. 4.69).

4.7 Conclusions

Complete resection of extramedullary tumors should be attempted as soon as the diagnosis is made. In general, postoperative outcome and further prognosis are excellent.

Patients with systemic diseases such as NF-2 and VHL, who demonstrate spinal manifestations, require regular MRI examinations of the entire spine at 6- to 12-month intervals to detect individual tumors that may compromise neurological function, in order to preserve functional status and quality of life before severe deficits have developed.

Surgical therapy should be followed by thorough rehabilitation programs for patients with severe preoperative neurological deficits, as significant functional improvements can be expected even for patients in advanced age.

Infiltrative and recurrent extramedullary tumors show differences in clinical presentation, are more difficult to resect, and carry a worse prognosis than the more common encapsulated tumors. They remain a major surgical challenge.

Patients with spinal hamartomas associated with complex malformations should be referred to neurosurgeons experienced with their management.

References

1. Abou-Fakhr FS, Kanaan SV, Youness FM, Hourani MH, Haddad MC (2002) Thoracic spinal intradural arachnoid cyst: report of two cases and review of literature. Eur Radiol 12:877–882
2. Acciarri N, Padovani R, Giulioni M, Gaist G (1993) Surgical treatment of spinal cavernous angiomas. J Neurosurg Sci 37:209–215
3. Achari G, Behari S, Mishra A, Pandey R, Jain VK (2000) Extradural meningioma en-plaque of the cervical cord. Neurol Res 22:351–353
4. Agnoli AL (1984) [Computer tomographic detection of an intraspinal arachnoid cyst]. Rontgenblatter 37:391–393
5. Agnoli AL, Laun A, Schönmayr R (1984) Enterogenous intraspinal cysts. J Neurosurg 61:834–840
6. Alter M (1975) Statistical aspects of spinal cord tumors. In: Vinken PJ, Bruyn GW (eds) Handbook of Clinical Neurology. Vol. 19. Tumours of the Spine and Spinal Cord. Part I. North Holland, Amsterdam, pp 1–22
7. Alvisi C, Cerisoli M, Giulioni M, Guerra L (1987) Long-term results for surgically treated congenital intradural spinal arachnoid cysts. J Neurosurg 67:333–335
8. Ammerman BJ, Henry JM, De Girolami U, Earle KM (1976) Intradural lipomas of the spinal cord. A clinicopathological correlation. J Neurosurg 44:331–336
9. Anderson FM (1975) Occult spinal dysraphism: a series of 73 cases. Pediatrics 55:826–835
10. Andrews BT, Weinstein PR, Rosenblum ML, Barbaro NM (1988) Intradural arachnoid cysts of the spinal canal associated with intramedullary cysts. J Neurosurg 68:544–549
11. Aoyagi N, Hayakawa I, Takizawa T, Matsumoto M (1985) [Clinical study of spinal intradural arachnoid cyst]. No Shinkei Geka 13:1205–1212
12. Arai Y, Yamauchi Y, Tsuji T, Fukasaku S, Yukota R, Kudo T (1992) Spinal neurenteric cyst. Report of two cases and review of forty-one cases reported in Japan. Spine 17:1421–1424
13. Arai H, Sato K, Okuda O, Miyajima M, Hishii M, Nakanishi H, Ishii H (2001) Surgical experience of 120 patients with lumbosacral lipomas. Acta Neurochir (Wien) 143:857–864
14. Arnautovic KI, Al-Mefty O (2001) Surgical seeding of chordomas. J Neurosurg 95:798–803
15. Asano S, Kawahara N, Kirino T (2003) Intradural spinal seeding of clival chordoma. Acta Neurochir (Wien) 145:599–603
16. Banczerowski P, Lipoth L, Vajda J, Veres R (2003) Surgery of ventral intradural midline cervical spinal pathologies via anterior cervical approach: our experience. Ideggyogy Sz 56:115–118
17. Bassiouni H, Hunold A, Asgari S, Hübschen U, König HJ, Stolke D (2004) Spinal intradural juxtamedullary cysts in the adult: surgical management and outcome. Neurosurgery 55:1352–1360
18. Baysefer A, Izci Y, Erdogan E (2001) Lateral intrathoracic meningocele associated with a spinal intradural arachnoid cyst. Pediatr Neurosurg 35:107–110
19. Betchen S, Schwartz A, Black C, Post K (2002) Intradural hemangiopericytoma of the lumbar spine: case report. Neurosurgery 50:654–657
20. Boccardo M, Ruelle A, Mariotti E (1985) Personal experience with the surgery of spinal meningiomas. Ital J Neurol Sci 6:29–35
21. Bret P, Lecuire J, Lapras C, Deruty R, Dechaume JP, Arsaad A (1976) Les meningiomas intra-rachidiens. Reflexions apropos d'une serie de 60 observations. Neurochirurgie 22:5–22
22. Brickner WM (1918) Spina bifida occulta. Am J Med Sci 155:474
23. Bristow RG, Laperriere NJ, Tator C, Milosevic M, Wong CS (1997) Post-operative radiotherapy for recurrent dermoid cysts of the spine: a report of 3 cases. J Neurooncol 33:251–256
24. Broager B (1953) Spinal neurinoma. 44 cases with discussion of histologic origin and with special reference to differential diagnosis against spinal glioma and meningioma. Acta Psychiatr Neurol Scand 85 Suppl:11–241
25. Brooks BS, Duvall ER, El Gammal T, Garcia JH, Gupta KL, Kapila A (1993) Neuroimaging features of neurenteric cysts: analysis of nine cases and review of the literature. AJNR Am J Neuroradiol 14:735–746
26. Buczek M, Jagodzinski Z (1994) [Diagnosis and treatment of central nervous system arachnoid cyst]. Neurol Neurochir Pol 28:211–220
27. Bull JWD (1953) Spinal meningiomas and neurofibromas. Acta Radiol 40:283–300

28. Byrne E, McNeill P, Gilford E, Wright C (1985) Intradural cyst with compression of the cauda equina in ankylosing spondylitis. Surg Neurol 23:162–164
29. Caroli E, Acqui M, Roperto R, Ferrante L, D'Andrea G (2004) Spinal en plaque meningiomas: a contemporary experience. Neurosurgery 55:1275–1279
30. Celli P, Cervoni L, Cantore G (1993) Ependymoma of the filum terminale: treatment and prognostic factors in a series of 28 cases. Acta Neurochir (Wien) 124:99–103
31. Celli P, Cervoni L, Salvati M, Cantore G (1997) Recurrence from filum terminale ependymoma 42 years after 'total' removal and radiotherapy. J Neurooncol 34:153–156
32. Cervoni L, Celli P, Fortuna A, Cantore G (1994) Recurrence of spinal ependymoma. Risk factors and long-term survival. Spine 19:2838–2841
33. Cervoni L, Celli P, Scarpinati M, Cantore G (1994) Neurinomas of the cauda equina. Clinical analysis of 40 surgical cases. Acta Neurochir 127:199–202
34. Cervoni L, Celli P, Cantore G, Fortuna A (1995) Intradural tumors of the cauda equina: a single institution review of clinical characteristics. Clin Neurol Neurosurg 97:8–12
35. Champion G, Brophy B (1987) Spinal cord meningiomas in the elderly. Age Ageing 16:383–387
36. Chang IC (2004) Surgical experience in symptomatic congenital intraspinal cysts. Pediatr Neurosurg 40:165–170
37. Chang UK, Choe WJ, Chung SK, Chung CK, Kim HJ (2002) Surgical outcome and prognostic factors of spinal intramedullary ependymomas in adults. J Neurooncol 57:133–139
38. Chapman P, Stieg PE, Magge S, Barnes P, Feany M (1999) Spinal lipoma controversy. Neurosurgery 44:186–193
39. Chavda SV, Davis AM, Cassar-Pullicino VN (1985) Enterogenous cysts of the central nervous system: a report of eight cases. Clin Radiol 36:245–251
40. Chern SH, Lin SM, Tseng SH, Tu YK, Yang LS, Kao MC, Hung CC (1993) Prognostic factors of intraspinal neurilemmoma and meningioma with severe preoperative motor deficits. J Formos Med Assoc 92:227–230
41. Choux M, Lena G, Genitori L, Foroutan M (1994) The surgery of occult spinal dysraphism. Adv Tech Stand Neurosurg 21:188–238
42. Chumas PD (2000) The role of surgery in asymptomatic lumbosacral spinal lipomas. Br J Neurosurg 14:301–304
43. Ciappetta P, Celli P, Palma L, Mariottini A (1985) Intraspinal hemangiopericytomas. Report of two cases and review of the literature. Spine 10:27–31
44. Ciapetta P, Domenicucci M , Raco A (1988) Spinal meningiomas: prognosis and recovery factors in 22 cases with severe motor deficits. Acta Neurol. Scand 77:27–30
45. Clarke DB, Leblanc R, Bertrand G, Quartey GR, Snipes GJ (1998) Meningeal melanocytoma. Report of a case and a historical comparison. J Neurosurg 88:116–121
46. Clifton AG, Ginsberg L, Webb WJ, Valentine AR (1987) Idiopathic spinal arachnoid cyst and syringomyelia. Br J Radiol 60:1023–1025
47. Coffin CM, Weill A, Miaux Y, Srour A, Cognard C, Dubard T, Savin D, Chiras J (1996) Posttraumatic spinal subarachnoid cyst. Eur Radiol 6:523–525
48. Cohen-Gadol AA, Zikel OM, Koch CA, Scheithauer BW, Krauss WE (2003) Spinal meningiomas in patients younger than 50 years of age: a 21-year experience. J Neurosurg (Spine 3) 98:258–263
49. Colak A, Pollack IF, Albright AL (1998) Recurrent tethering: a common long-term problem after lipomyelomeningocele repair. Pediatr Neurosurg 29:184–190
50. Conti P, Pansini G, Mouchaty H, Capuano C, Conti R (2004) Spinal neurinomas: retrospective analysis and long-term outcome of 179 consecutively operated cases and review of the literature. Surg Neurol 61:34–44
51. Crockard HA, Bradford R (1985) Transoral transclival removal of a schwannoma anterior to the craniocervical junction. Case report. J Neurosurg 62:293–295
52. Cushing H, Eisenhardt L (1938) Meningiomas. Their Classification, Regional Behaviour, Life History, and Surgical End Results. CC Thomas, Springfield
53. Davis RA, Washburn PL (1970) Spinal cord meningioma. Surg Gynecol Obstet 131:15–21
54. Dickman CA, Apfelbaum RI (1998) Thoracoscopic microsurgical excision of a thoracic schwannoma. Case report. J Neurosurg 88:898–902
55. Drapkin AJ (1974) High cervical intradural lipoma. J Neurosurg 41:699–704
56. Dow G, Biggs N, Evans G, Gillespie J, Ramsden R, King A (2005) Spinal tumors in neurofibromatosis type 2. Is emerging knowledge of genotype predictive of natural history? J Neurosurg Spine 2:574–579
57. Dyck P (1992) Intramedullary lipoma. Diagnosis and treatment. Spine 17:979–981
58. Eguchi T, Tamaki N, Kurata H (1999) Endoscopy of the spinal cord: cadaveric study and clinical experience. Minim Invasive Neurosurg 42:146–151
59. Ehni G, Love JG (1945) Intraspinal lipomas. Report of cases; review of the literature, and clinical and pathologic study. Arch Neurol Psych 53:1–28
60. El Mahdi MA (1977) Arachnoid cyst and cord compression in association with tangential shrapnel injuries of the spine. Neurochirurgia (Stuttg) 20:1–7
61. El-Mahdy W, Kane PJ, Powell MP, Crockard HA (1999) Spinal intradural tumours: part I – extramedullary. Br J Neurosurg 13:550–557
62. Endoh M, Iwasaki Y, Koyanagi I, Hida K, Abe H (1998) Spontaneous shrinkage of lumbosacral lipoma in conjunction with a general decrease in body fat: case report. Neurosurgery 43:150–151; discussion 151–152
63. English JE, Maltby GL (1967) Diastematomyelia in adults. J Neurosurg 27:260–264
64. Enzmann DR, Rubin JB, DeLaPaz R, Wright A (1986) Cerebrospinal fluid pulsation: benefits and pitfalls in MR imaging. Radiology 161:773–778
65. Espinal JB, Indakoetxea B, Lopez de Munain A, Marti-Masso JF, Riu I (1991) Multiple nerve root tumors and neurofibromatosis: contribution of magnetic resonance imaging. Neurologia 6:142–147
66. Evans A, Stoodley N, Halpin S (2002) Magnetic resonance imaging of intraspinal cystic lesions: a pictorial review. Curr Probl Diagn Radiol 31:79–94

67. Fain B, Vellet D, Hertzanu Y (1985) Adult tethered cord syndrome. A case report. S Afr Med J 67:985–986
68. Fan CJ, Veerapen RJ, Tan CT (1989) Case report: subdural spinal lipoma with posterior fossa extension. Clin Radiol 40:91–94
69. Fassett DR, Schmidt MH (2003) Lumbosacral ependymomas: a review of the management of intradural and extradural tumors. Neurosurg Focus 15:Article 13
70. Feiring EH, Barron K (1962) Late recurrence of spinal cord meningioma. J Neurosurg 19:652–656
71. Fields WS, Zuelch KJ, Maslenikov V (1972) High cervical neurinoma. Special neurologic and radiologic features. Zentralbl Neurochir 33:89–102
72. Fiumara E, D'Angelo V, Florio FP, Nardella M, Bisceglia M (1996) Preoperative embolization in surgical treatment of spinal thoracic dumbbell schwannoma. A case report. J Neurosurg Sci 40:153–156
73. Fobe JL, Nishikuni K, Gianni MA (1998) Evolving magnetic resonance spinal cord trauma in child: from hemorrhage to intradural arachnoid cyst. Spinal Cord 36:864–866
74. Fortuna A, Mercuri S (1983) Intradural spinal cysts. Acta Neurochir (Wien) 68:289–314
75. Fortuna A, Nolletti A, Nardi P, Caruso R (1981) Spinal neurinomas and meningiomas in children. Acta Neurochir (Wien) 55:329–341
76. Freidberg SR (1972) Removal of an ossified ventral thoracic meningioma. Case report. J Neurosurg 37:728–730
77. Friedman DP, Hollander MD (1998) Neuroradiology case of the day. Radiographics 18:794–798
78. Fujimura M, Tominaga T, Koshu K, Shimizu H, Yoshimoto T (1996) Cine-mode magnetic resonance imaging of a thoracic intradural arachnoid cyst: case report. Surg Neurol 45:533–536
79. Gagliardi FM, Cervoni L, Domenicucci M, Celli P, Salvati M (1993) Ependymomas of the filum terminale in childhood: report of four cases and review of the literature. Childs Nerv Syst 9:3–6
80. Gamache FW Jr, Wang JC, Deck M, Heise C (2001) Unusual appearance of an en plaque meningioma of the cervical spinal canal: a case report and literature review. Spine 26: E87–E89
81. Gambardella G, Gervasio O, Zaccone C (2003) Approaches and surgical results in the treatment of ventral thoracic meningiomas. Review of our experience with a posterolateral combined transpedicular-transarticular approach. Acta Neurochir (Wien) 145:385–392
82. Gautier-Smith PC (1967) Clinical aspects of spinal neurofibromas. Brain 90:359–394
83. Gelabert-Gonzalez M, Cutrin-Prieto JM, Garcia-Allut A (2001) Spinal arachnoid cyst without neural tube defect. Childs Nerv Syst 17:179–181
84. Gellad FE, Paul KS, Geisler FH (1988) Early sequelae of gunshot wounds to the spine: radiologic diagnosis. Radiology 167:523–526
85. George B, Laurian C (1980) Surgical approach to the whole length of the vertebral artery with special reference to the third portion. Acta Neurochir (Wien) 51:259–272
86. George B, Lot G (1995) Neurinomas of the first two cervical nerve roots: a series of 42 cases. J Neurosurg 82:917–923
87. George B, Laurian C, Keravel Y, Cophignon J (1985) Extradural and hourglass cervical neurinomas: the vertebral artery problem. Neurosurgery 16:591–594
88. George B, Zerah M, Lot G, Hurth M (1993) Oblique transcorporeal approach to anteriorly located lesions in the cervical spinal canal. Acta Neurochir (Wien) 121:187–190
89. Gezen F, Kahraman S, Çanakci Z, Bedük A (2000) Review of 36 cases of spinal cord meningioma. Spine 25:727–731
90. Gindre-Barrucand T, Charleux F, Turjman F, Jouvet A, Confavreux C, Deruty R, Froment JC (1991) Magnetic resonance imaging contribution to the diagnosis of spinal cord compression by a subdural arachnoid cyst. Neuroradiology 33:87–89
91. Giuffre R (1966) Intradural spinal lipomas. Review of the literature (99 cases) and report of an additional case. Acta Neurochir (Wien) 14:69–95
92. Gläsker S, Berlis A, Pagenstecher A, Vougioukas VI, Van Velthoven V (2005) Characterization of hemangioblastomas of spinal nerves. Neurosurgery 56:503–509
93. Goldhahn WE, Schmidt U (1989) Das spinale Meningiom. Zentralbl Neurochir 50:18–23
94. Gottfried ON, Gluf W, Quinones-Hinojosa A, Kan P, Schmidt MH (2003) Spinal meningiomas: surgical management and outcome. Neurosurg Focus 14:Article 2
95. Gower DJ, Engles CF, Friedman ES (1994) Thoracic intraspinal lipoma. Br J Neurosurg 8:761–764
96. Gräwe A, Siedschlag WD, Nisch G, Schulz MR (1986) Meningiome des Spinalkanals. Klinik und Langzeitergebnisse. Zentralbl Neurochir 47:139–143
97. Gräwe A, Siedschlag WD, Nisch G (1988) Neurinome des Spinalkanals. Klinik und Langzeitergebnisse. Zentralbl Neurochir 49:1–6
98. Grillo HC, Ojemann RG, Scannell JG, Zervas NT (1983) Combined approach to "dumbbell" intrathoracic and intraspinal neurogenic tumors. Ann Thorac Surg 36:402–407
99. Grisoli F, Vincentelli F, Sedan R, Hassoun J, Caruso G, Salpietro F (1988) Hemangiopericytomas of the spinal canal. Report of four cases and review of literature. J Neurosurg Sci 32:69–76
100. Ha YS, Yamashita J, Aoyama I, Ishikawa M, Handa H (1982) Clinical analysis of 22 spinal neurinomas – with special reference to CT metrizamide myelography and CO2 laser. No Shinkei Geka 10:709–716
101. Hakyemez B, Yildiz H, Ergin N, Uysal S, Parlak M (2003) [Flair and diffusion weighted MR imaging in differentiating epidermoid cysts from arachnoid cysts]. Tani Girisim Radyol 9:418–426
102. Halliday AL, Sobel RA, Martuza RL (1991) Benign spinal nerve sheath tumors: their occurrence sporadically and in neurofibromatosis types 1 and 2. J Neurosurg 74:248–253
103. Hanakita J, Suwa H, Nagayasu S, Nishi S, Iihara K, Sakaida H (1992) Clinical features of intradural neurinomas in the cauda equina and around the conus medullaris. Neurochirurgia 35:145–149

104. Hasegawa M, Fujisawa H, Hayashi Y, Tachibana O, Kida S, Yamashita J (2001) Surgical pathology of spinal schwannomas: a light and electron microscopic analysis of tumor capsules. Neurosurgery 49:1388–1392; discussion 1392–1383
105. Hasegawa M, Fujisawa H, Hayashi Y, Tachibana O, Kida S, Yamashita J (2005) Surgical pathology of spinal schwannoma: has the nerve of its origin been preserved or already degenerated during tumor growth? Clin Neuropathol 24:19–25
106. Hashimoto K, Hashimoto M, Homma S, Ohsone Y, Hasegawa H, Takei J, Kida Y, Takeuchi Y, Ohba M (1992) Spinal arachnoid cyst in a newborn infant. Acta Paediatr Jpn 34:547–550
107. Haughton VM, Williams AL, Cusick JF, Meyer GA (1978) A myelographic technique for cysts in the spinal canal and spinal cord. Radiology 129:717–719
108. Herman JM, McLone DG, Storrs BB, Dauser RC (1993) Analysis of 153 patients with myelomeningocele or spinal lipoma reoperated upon for a tethered cord. Presentation, management and outcome. Pediatr Neurosurg 19:243–249
109. Herskowitz J, Bielawski MA, Venna N, Sabin TD (1978) Anterior cervical arachnoid cyst simulating syringomyelia: a case with preceding posterior arachnoid cysts. Arch Neurol 35:57–58
110. Hirano A, Hashimoto Y, Hashi K (1995) [Spinal intradural arachnoid cyst associated with enlarged filum terminale]. No Shinkei Geka 23:1011–1015
111. HogenEsch R, Zeilstra DJ, Breukers SME, Wiertsema GPA, Begeer JH, Ter Weeme CA (1990) Tethered cord syndrome following spina bifida aperta. Adv Neurosurg 18:158–162
112. Honda E, Fujisawa H, Koyama T, Oshima Y, Sugita Y, Abe T (1998) Symptomatic spinal arachnoid cyst triggered by seat belt injury – case report. Neurol Med Chir (Tokyo) 38:168–172
113. Hori T, Takakura K, Sano K (1984) Spinal neurinomas. Clinical analysis of 45 surgical cases. Neurol Med Chir 24:471–477
114. Horrax G, Poppen JL, Wu WR, Weadon PR (1949) Meningiomas and neurofibromas of the spinal cord. Certain clinical features and end results. Surg Clin N Am 29:659–665
115. Hüttmann S, Krauss J, Collmann H, Sörensen N, Roosen K (2001) Surgical management of tethered spinal cords in adults: report of 54 cases. J Neurosurg (Spine 2) 95:173–178
116. Huson SM, Harper PS, Compston DAS (1988) Von Recklinghausen neurofibromatosis. A clinical and population study in south-east Wales. Brain 111:1355–1381
117. Inbasekaran V, Kannan M, Kumaravelu S, Saravanan SV (2001) Spinal compression caused by multiple arachnoidal cyst. J Indian Med Assoc 99:646–647
118. Inoue Y, Nemoto Y, Ohata K, Daikokuya H, Hakuba A, Tashiro T, Shakudo M, Nagai K, Nakayama K, Yamada R (2001) Syringomyelia associated with adhesive spinal arachnoiditis: MRI. Neuroradiology 43:325–330
119. Iraci G, Peserico L, Salar G (1971) Intraspinal neurinomas and meningiomas. A clinical survey of 172 cases. Int Surg 56:289–303
120. Irger IM, Petukhov SS (1976) [Diagnosis and surgical treatment of hourglass shaped tumors of cervical localization]. Vopr Neirokhir:7–14
121. Isu T, Iwasaki Y, Akino M, Abe H, Tashiro K, Miyasaka K, Saito H, Nomura M (1987) [Diagnosis of a cystic lesion in the spinal cord – studies on delayed CT myelography and MRI]. No Shinkei Geka 15:725–730
122. Jamjoom AB, Mathew BG, Coakham HB (1991) A variant of the syndrome of spinal arachnoid cysts with multiple congenital defects. Br J Neurosurg 5:77–82
123. Jean WC, Keene CD, Haines SJ (1998) Cervical arachnoid cysts after craniocervical decompression for Chiari II malformations: report of three cases. Neurosurgery 43:941–944; discussion 944–945
124. Jena A, Gupta RK, Sharma A, Prakesh VE, Khushu S (1990) magnetic resonance diagnosis of spinal arachnoid cyst. A report of two cases. Childs Nerv Syst 6:107–109
125. Jenny B, Rilliet B, May D, Pizzolato GP (2002) [Transthoracic transvertebral approach for resection of an anteriorly located, calcified meningioma. Case report]. Neurochirurgie 48:49–52
126. Jensen F, Knudsen V, Troelsen S (1977) Recurrent intraspinal arachnoid cyst treated with a shunt procedure. Acta Neurochir (Wien) 39:127–129
127. Jinnai T, Hoshimaru M, Koyama T (2005) Clinical characteristics of spinal nerve sheath tumors: analysis of 149 cases. Neurosurgery 56:510–515
128. Kang HS, Chung CK, Kim HJ (2000) Spontaneous spinal subdural hematoma with spontaneous resolution. Spinal Cord 38:192–196
129. Kang JK, Kim MC, Kim DS, Song JV (1987) Effects of tethering on regional and spinal cord blood flow and sensory evoked potentials in growing cats. Childs Nerv Syst 3:35–39
130. Kang JK, Lee KS, Jeun SS, Lee IW, Kim MC (2003) Role of surgery for maintaining urological function and prevention of retethering in the treatment of lipomeningomyelocele: experience recorded in 75 lipomeningomyelocele patients. Childs Nerv Syst 19:23–29
131. Katz K, Reichental E, Israeli J (1981) Surgical treatment of spinal meningiomas. Neurochirurgia (Stuttg) 24:21–22
132. Kazan S, Ozdemir O, Akyuz M, Tuncer R (1999) Spinal intradural arachnoid cysts located anterior to the cervical spinal cord. Report of two cases and review of the literature. J Neurosurg Spine 91:211–215
133. Kendall BE, Valentine AR, Keis B (1982) Spinal arachnoid cysts: clinical and radiological correlation with prognosis. Neuroradiology 22:225–234
134. Key EAH, Retzius MG (1875) Studien der Anatomie des Nervensystems und des Bindegewebes. Samson Wallin, Stockholm
135. Khosla A, Wippold FJ 2nd (2002) CT myelography and MR imaging of extramedullary cysts of the spinal canal in adult and pediatric patients. AJR Am J Roentgenol 178:201–207

136. Kim CH, Bak KH, Kim JM, Kim NK (1999) Symptomatic sacral extradural arachnoid cyst associated with lumbar intradural arachnoid cyst. Clin Neurol Neurosurg 101:148–152
137. Kim HW, Weinstein SL (1997) The management of scoliosis in neurofibromatosis. Spine 22:2770–2776
138. King AT, Sharr MM, Gullan RW, Bartlett JR (1998) Spinal meningiomas: a 20-year review. Br J Neurosurg 12:521–526
139. Klekamp J, Samii M (2002) Syringomyelia. Diagnosis and Treatment. Springer, Heidelberg
140. Knoll M, Madersbacher H (1993) The chances of a spina bifida patient becoming continent/socially dry by conservative therapy. Paraplegia 31:22–27
141. Kodama T, Numaguchi Y, Gellad FE, Sadato N (1991) Magnetic resonance imaging of a high cervical intradural lipoma. Comput Med Imaging Graph 15:93–95
142. Kondo A, Kato K, Kanai S, Sakakibara T (1986) Bladder dysfunction secondary to tethered cord syndrome in adults: is it curable? J Urol 135:313–316
143. Koyanagi I, Iwasaki Y, Hida K, Abe H, Isu T, Akino M (1997) Surgical treatment supposed natural history of the tethered cord with occult spinal dysraphism. Childs Nerv Syst 13:268–274
144. Koyanagi I, Iwasaki Y, Hida K, Abe H, Isu T, Akino M, Aida T (2000) Factors in neurological deterioration and role of surgical treatment in lumbosacral spinal lipoma. Childs Nerv Syst 16:143–149
145. Krings T, Lukas R, Reul J, Spetzger U, Reinges MH, Gilsbach JM, Thron A (2001) Diagnostic and therapeutic management of spinal arachnoid cysts. Acta Neurochir (Wien) 143:227–234; discussion 234–225
146. Kriss TC, Kriss VM (1997) Symptomatic spinal intradural arachnoid cyst development after lumbar myelography. Case report and review of the literature. Spine 22:568–572
147. Kulkarni AV, Pierre-Kahn A, Zerah M (2004) Conservative management of asymptomatic spinal lipomas of the conus. Neurosurgery 54:868–875
148. Kumar K, Malik S, Schulte PA (2003) Symptomatic spinal arachnoid cysts: report of two cases with review of the literature. Spine 28:E25–29
149. Kumar R, Nayak SR (2002) Unusual neuroenteric cysts: diagnosis and management. Pediatr Neurosurg 37:321–330
150. Kunicki A, Maciejak A (1965) Results of operative treatment in 154 cases of extramedullary meningiomas and neurinomas. Acta Medica Pol 6:397–404
151. Lagae L, Verpoorten C, Casaer P, Vereecken R, Fabry G, Plets C (1990) Conservative versus neurosurgical treatment of tethered cord patients. Z Kinderchir 45 Suppl 1:16–17
152. La Marca F, Grant JA, Tomita T, McLone DG (1997) Spinal lipomas in children: outcome of 270 procedures. Pediatr Neurosurg 26:8–16
153. Lapsiwala SB, Iskandar BJ (2004) The tethered cord syndrome in adults with spina bifida occulta. Neurol Res 26:735–740
154. Lea ME, Sage MR, Bills D, Brophy B, Blumbergs P (1992) Enterogenous cyst of the cervical spinal canal. Australas Radiol 36:327–329
155. Lee HJ, Cho DY (2001) Symptomatic spinal intradural arachnoid cysts in the pediatric age group: description of three new cases and review of the literature. Pediatr Neurosurg 35:181–187
156. Levy WJ Jr, Bay J, Dohn D (1982) Spinal cord meningioma. J Neurosurg 57:804–812
157. Levy WJ, Latchaw J, Hahn JF, Sawhny B, Bay J, Dohn DF (1986) Spinal neurofibromas: a report of 66 cases and a comparison with meningiomas. Neurosurgery 18:331–334
158. Li MH, Holtas S (1991) MR imaging of spinal neurofibromatosis. Acta Radiol 32:279–285
159. Lin YJ, Tu YK, Lin SM, Shun CT (1996) Primary hemangiopericytoma in the axis bone: case report and review of literature. Neurosurgery 39:397–399; discussion 399–400
160. Lonjon M, Von Langsdorf D, Lefloch S, Rahbi M, Rasendrarijao D, Michiels JF, Paquis P, Grellier P (2001) [Factors influencing recurrence and role of radiotherapy in filum terminale ependymomas. About 14 cases and review of the literature]. Neurochirurgie 47:423–429
161. Love JG, Dodge HW (1952) Dumbbell (hour-glass) neurofibromas affecting the spinal cord. Surg Gynecol Obstet 94:161–172
162. Lunardi P, Missori P, Gagliardi FM, Forntuna A (1989) Long-term results of the surgical treatment of spinal dermoid and epidermoid tumors. Neurosurgery 25:860–864
163. Mackay R (1939) Chronic adhesive spinal arachnoiditis. A clinical and pathologic study. JAMA 112:802–808
164. Maiuri F, Laconetta G, Gallicchio B, Stella L (2000) Intraoperative sonography for spinal tumors. J Neurosurg Sci 44:115–122
165. Maiuri F, Gangemi M, Cavallo LM, De Divitis E (2003) Dysembryogenetic spinal tumors in adults without dysraphism. Br J Neurosurg 17:234–238
166. Mallucci CL, Stacey RJ, Miles JB, Williams B (1997) Idiopathic syringomyelia and the importance of occult arachnoid webs, pouches and cysts. Br J Neurosurg 11:306–309
167. Marks JE, Adler SJ (1982) A comparative study of ependymomas by site of origin. Int J Radiat Oncol Biol Phys 8:37–43
168. Mathew P, Todd NV (1993) Intradural conus and cauda equina tumours: a retrospective review of presentation, diagnosis and early outcome. J Neurol Neurosurg Psychiatry 56:69–74
169. Mautner VF, Lindenau M, Baser ME, Hazim W, Tatagiba M, Haase W, Samii M, Wais R, Pulst SM (1996) The neuroimaging and clinical spectrum of neurofibromatosis 2. Neurosurgery 38:880–886
170. McCormick PC (1996) Surgical management of dumbbell and paraspinal tumors of the thoracic and lumbar spine. Neurosurgery 38:67–74; discussion 74–65

171. McCormick PC, Post KD, Stein BM (1990) Intradural extramedullary tumors in adults. In: Stein BM, McCormick PC (eds) Neurosurgery Clinics in North America. Vol. 1 no. 3. Intradural Spinal Surgery. WB Saunders, Philadelphia, pp591–608
172. McLone DG, Naidich TP (1986) Laser resection of fifty spinal lipomas. Neurosurgery 18:611–615
173. Medjek L, Adjmi M, Hammoum S (1992) [Intradural spinal cord lipomas. Report of 2 cases]. J Radiol 73:653–656
174. Mena H, Ribas JL, Pezeshkpour GH, Cowan DN, Parisi JE (1991) Hemangiopericytoma of the central nervous system: a review of 94 cases. Hum Pathol 22:84–91
175. Messori A, Rychlicki F, Salvolini U (2002) Spinal epidural en-plaque meningioma with an unusual pattern of calcification in a 14-year-old girl: case report and review of the literature. Neuroradiology 44:256–260
176. Mhatre P, Hudgins PA, Hunter S (2000) Dermoid cyst in the lumbosacral region: radiographic findings. A J R 174:874–875
177. Mirimanoff R, Choi NC (1987) Intradural spinal metastases in patients with posterior fossa brain metastases from various primary cancers. Oncology 44:232–236
178. Mirimanoff RO, Dosoretz DE, Lingood RM, Ojemann RG, Martuza RL (1985) Meningioma: analysis of recurrence and progression following neurosurgical resection. J Neurosurg 62:18–24
179. Miura T, Nakamura K, Tanaka H, Kawaguchi H, Takeshita K, Kurokawa T (1998) Resection of cervical spinal neurinoma including affected nerve root: recovery of neurological deficit in 15 cases. Acta Orthop Scand 69:280–282
180. Mooney JF, Hall JE, Emans JB, Millis MB, Kasser JR (1994) Spinal deformity associated with neurenteric cysts in children. Spine 19:1445–1450
181. Morandi X, Haegelen C, Riffaud L, Amlashi S, Adn M, Brassier G (2004) Results in the operative treatment of elderly patients with spinal meningiomas. Spine 29:2191–2194
182. Morio Y, Nanjo Y, Nagashima H, Minamizaki T, Teshima R (2001) Sacral cyst managed with cyst-subarachnoid shunt: a technical case report. Spine 26:451–453
183. Muller JP, Destee A, Verier A, Lesoin F, Krivosic I, Jomin M, Warot P (1986) [Intraspinal hemangiopericytoma. 2 cases and review of the literature]. Neurochirurgie 32:140–146
184. Mulvihill JJ, Parry DM, Sherman JL, Pikus A, Kaiser-Kupfer MI, Eldridge R (1990) NIH conference. Neurofibromatosis 1 (Recklinghausen disease) and neurofibromatosis 2 (bilateral acoustic neurofibromatosis). An update. Ann Int Med 113:39–52
185. Nagib MG, O'Fallon MT (1997) Myxopapillary ependymoma of the conus medullaris and filum terminale in the pediatric age group. Pediatr Neurosurg 26:2–7
186. Namer IJ, Pamir MN, Benli K, Saglam S, Erbengi A (1987) Spinal meningiomas. Neurochirurgia (Stuttg) 30:11–15
187. Narod SA, Parry DM, Parboosingh J, Lenoir GM, Rutledge M, Fischer G, Eldridge R, Martuza RL, Frontali M, Haines J, Gusella JF, Rouleau GA (1992) Neurofibromatosis type 2 appears to be a genetically homogeneous disease. Am J Hum Gen 51:486–496
188. National Institute of Health Consensus Development Conference (1988) Neurofibromatosis. Conference statement. Arch Neurol 45:575–578
189. Ng WH, Seow WT (2001) Tethered cord syndrome preceding syrinx formation – serial radiological documentation. Childs Nerv Syst 17:494–496
190. Nishiura I, Koyama T, Kubo Y, Aii H (1984) [Spinal intradural arachnoid cyst. Report of five cases and a review of the literature]. No Shinkei Geka 12:1385–1392
191. Nittner K (1976) Spinal meningiomas, neurinomas and neurofibromas. In: Vinken PJ, Bruyn GW (eds) Handbook of Clinical Neurology. Vol. 20. Tumours of the Spine and Spinal Cord . Part II. North Holland, Amsterdam, pp 177–322
192. Nogues MA, Merello M, Leiguarda R, Guevara J, Figari A (1992) Subarachnoid and intramedullary cysts secondary to epidural anesthesia for gynecological surgery. Eur Neurol 32:99–101
193. Osenbach RK, Godersky JC, Traynelis VC, Schelper RD (1992) Intradural extramedullary cysts of the spinal canal: clinical presentation, radiographic diagnosis, and surgical management. Neurosurgery 30:35–42
194. Osuka K, Takayasu M, Tanazawa T, Ichihara K, Itoh Y (1997) Multiple communicating intradural arachnoid cysts: usefulness of myelography and myelo-computed tomography using both lumbar and cervical punctures. Case report. Neurosurg Rev 20:94–98
195. O'Toole JE, McCormick PC (2003) Midline ventral intradural schwannoma of the cervical spinal cord resected via anterior corpectomy with reconstruction: technical case report and review of the literature. Neurosurgery 52:1482–1486
196. Pagni CA, Canavero S, Forni M (1990) Report of a cavernoma of the cauda equina and review of the literature. Surg Neurol 33:124–131
197. Palmer JJ (1974) Spinal arachnoid cysts. Report of six cases. J Neurosurg 41:728–735
198. Pang D (1992) Split cord malformation: part II: clinical syndrome. Neurosurgery 31:481–500
199. Pang D, Wilberger JE Jr (1982) Tethered cord syndrome in adults. J Neurosurg 57:32–47
200. Pang D, Dias MS, Ahab-Barmada M (1992) Split cord malformation: part I: a unified theory of embryogenesis for double spinal cord malformations. Neurosurgery 31:451–480
201. Paolini S, Ciappetta P, Domenicucci M, Guiducci A (2002) Intramedullary neurenteric cyst with a false mural nodule: case report. Neurosurgery 52:243–246
202. Paramore CG (2000) Dorsal arachnoid web with spinal cord compression: variant of an arachnoid cyst? Report of two cases. J Neurosurg Spine 93:287–290
203. Parsa AT, Fiore AJ, McCormick PC, Bruce JC (2000) Genetic basis of intramedullary spinal cord tumors and therapeutic implications. J Neurooncol 47:239–251
204. Parsa AT, Lee, J, Parney IF, Weinstein P, McCormick PC, Ames C (2004) Spinal cord and intradural-extraparenchymal spinal tumors: current best care practices and strategies. J Neurooncol 69:291–318

205. Patronas NJ, Courcoutsakis N, Bromley CM, Katzman GL, MacCollin M, Parry DM (2001) Intramedullary and spinal canal tumors in patients with neurofibromatosis 2: MR imaging findings and correlation with genotype. Radiology 218:434–442
206. Perret G, Green D, Keller J (1962) Diagnosis and treatment of intradural arachnoid cysts of the thoracic spine. Radiology 79:425–429
207. Peter JC (1992) Occult dysraphism of the spine. A retrospective analysis of 88 operative cases, 1979–1989. S Afr Med J 8:351–354
208. Pierot L, Dormont D, Oueslati S, Cornu P, Rivierez M, Bories J (1988) Gadolinium-DTPA enhanced MR imaging of intradural neurenteric cysts. J Comp Assist Tomogr 12:762–764
209. Pierre-Kahn A, Lacombe J, Pichon J, Giudicelli Y, Renier D, Sainte-Rose C, Perrigot M, Hirsch JF (1986) Intraspinal lipomas with spina bifida. Prognosis and treatment in 73 cases. J Neurosurg 65:756–761
210. Pierre-Kahn A, Zerah M, Renier D, Cinalli G, Sainte-Rose C, Lellouch-Tubiana A, Brunelle F, Le Merrer M, Giudicelli Y, Pichon J, Kleinknecht B, Nataf F (1997) Congenital lumbosacral lipomas. Childs Nerv Syst 13:298–335
211. Pulst SM, Riccardi VM, Fain P, Korenberg JR (1991) Familial spinal neurofibromatosis: clinical and DNA linkage analysis. Neurology 41:1923–1927
212. Quinones-Hinojosa A, Sanai N, Fischbein NJ, Rosenberg WS (2003) Extensive intradural arachnoid cyst of the lumbar spinal canal: case report. Surg Neurol 60:57–59
213. Rabb CH, McComb JG, Raffel C, Kennedy JG (1992) Spinal arachnoid cysts in the pediatric age group: an association with neural tube defects. J Neurosurg 77:369–372
214. Raimondi AJ (1987) Pediatric Neurosurgery. Theoretic Principles. Art of Surgical Techniques. Springer, New York
215. Ramachandran M, Tsirikos AI, Lee J, Saifuddin A (2004) Whole-spine magnetic resonance imaging in patients with neurofibromatosis type 1 and spinal deformity. J Spinal Disord Tech 17:483–491
216. Rauzzino MJ, Tubbs RS, Alexander E, Grabb PA, Oakes WJ (2001) Spinal neurenteric cysts and their relation to more common aspects of occult spinal dysraphism. Neurosurg Focus 10:Article 2
217. Rifkinson-Mann S, Wisoff JH, Epstein F (1990) The association of hydrocephalus with intramedullary spinal cord tumors: a series of 25 patients. Neurosurgery 27:749–754
218. Rivierez M, Oueslati S, Philippon J, Pradat P, Foncin JF, Muckensturm B, Dorwling-Carter D, Cornu P (1990) [The ependymomas of the intradural filum terminale in adults. Twenty cases]. Neurochirurgie 36:96–107
219. Rogers L (1955) Tumors involving the spinal cord and its nerve roots. Ann R Coll Surg Engl 16:1–29
220. Rosenkranz W (1971) Ankylosing spondylitis: cauda equina syndrome with multiple spinal arachnoid cysts. Case report. J Neurosurg 34:241–243
221. Roser F, Nakamura M, Bellinzona M, Ritz R, Ostertag H, Tatagiba MS (2006) Proliferation potential of spinal meningiomas. Eur Spine J 15:211–215
222. Roth-Vargas AA, Rossitti SL, Balbo RJ, Oliveira MA (1989) So-called tethered cervical spinal cord. Neurochirurgia (Stuttg) 32:69–71
223. Roux FX, Nataf F, Pinaudeau M, Borne G, Devaux B, Meder JF (1996) Intraspinal meningiomas: review of 54 cases with discussion of poor prognosis factors and modern therapeutic management. Surg Neurol 46: 458–463; discussion 463–464
224. Ryu H, Nishizawa S, Yamamoto S (1999) One-stage removal of a large dumb-bell-shaped cervical neurinoma without laminectomy or interbody fusion in a child. Br J Neurosurg 13:587–590
225. Sakaida H, Hanakita J, Suwa H, Nagayasu S, Nishi S, Ohta F (1992) Two cases of von Recklinghausen's disease with multiple brain and spinal tumors. No Shinkei Geka 20:51–56
226. Salah S, Horcajada J, Perneczky A (1975) Spinal neurinomas. A comprehensive clinical and statistical study on 47 cases. Neurochirurgia 18:77–84
227. Salpietro FM, Alafaci C, Lucerna S, Iacopino DG, Tomasello F (1997) Do spinal meningiomas penetrate the pial layer? Correlation between magnetic resonance imaging and microsurgical findings and intracranial tumor interfaces. Neurosurgery 41:254–258
228. Satar N, Bauer SB, Shefner J, Kelly MD, Darbey MM (1995) The effects of delayed diagnosis and treatment in patients with an occult spinal dysraphism. J Urol 154:754–758
229. Sattar MT, Bannister CM, Turnbull IW (1996) Occult spinal dysraphism – the common combination of lesions and the clinical manifestations in 50 patients. Eur J Pediatr Surg 6 Suppl 1:10–14
230. Scatliff JH, Hayward R, Armao D, Kwon L (2005) Pre- and post-operative hydromyelia in spinal dysraphism. Pediatr Radiol 35:282–289
231. Schick U, Marquardt G, Lorenz R (2001) Recurrence of benign spinal neoplasms. Neurosurg Rev 24:20–25
232. Schmidt DM, Robinson B, Jones D (1990) The tethered spinal cord. Etiology and clinical manifestations. Orthop Rev 19:870–876
233. Schreiber D, Quade B (1990) CNS involvement in neurofibromatosis. A postmortem study. Zentralbl Allg Pathol Pathol Anat 136:67–76
234. Schultheiss R, Gullotta G (1993) Resection of relevant nerve roots in surgery of spinal neurinomas without persisting neurological deficit. Acta Neurochir 122:91–96
235. Schweitzer JS, Batzdorf U (1992) Ependymoma of the cauda equina region: diagnosis, treatment, and outcome in 15 patients. Neurosurgery 30:202–207
236. Sgouros S, Malluci CL, Jackowski A (1996) Spinal ependymomas – the value of postoperative radiotherapy for residual disease control. Br J Neurosurg 10:559–566
237. Shadmehr MB, Gaissert HA, Wain JC, Moncure AC, Grillo HC, Borges LF, Mathisen DJ (2003) The surgical approach to "dumbbell tumors" of the mediastinum. Ann Thorac Surg 76:1650–1654
238. Sharma MC, Aggarwal M, Ralte AM, Vaishya V, Suri A, Gupta V, Sarkar C (2003) Clinicopathological study of spinal teratomas. J Neurosurg Sci 47:95–100

239. Sharma R, Rout D, Radhakrishnan VV (1992) Intradural spinal cavernomas. Br J Neurosurg 6:351–356
240. Shaw EG, Evans RG, Scheithauer BW, Ilstrup DM, Earle JD (1986) Radiotherapeutic management of adult intraspinal ependymomas. Int J Radiat Oncol Biol Phys 12:323–327
241. Shaw PJ, Allcutt DA, Bates D, Crawford PJ (1990) Cauda equina syndrome associated with multiple lumbar arachnoid cysts in ankylosing spondylitis: improvement following surgical therapy. J Neurol Neurosurg Psychiatry 53:1076–1079
242. Shikata J, Yamamuro T, Mikawa Y, Kotoura Y (1988) Intraspinal epidermoid and dermoid cysts. Surgical results of seven cases. Arch Orthop Trauma Surg 107:105–109
243. Shimizu H, Tominaga T, Takahashi A, Yoshimoto T (1997) Cine magnetic resonance imaging of spinal intradural arachnoid cysts. Neurosurgery 41:95–100
244. Sioutos P, Arbit E, Tsairis P, Gargan R (1996) Spontaneous thoracic spinal cord herniation. A case report. Spine 21:1710–1713
245. Sklar EM, Quencer RM, Green BA, Montalvo BM, Post MJ (1991) Complications of epidural anesthesia: MR appearance of abnormalities. Radiology 181:549–554
246. Slavotinek JP, Sage MR, Brophy BP (1996) An unusual spinal intradural arachnoid cyst. Neuroradiology 38:152–154
247. Solero CL, Fornari M, Giombini S, Lasio G, Oliveri G, Cimino C, Pluchino F (1989) Spinal meningiomas: review of 174 operated cases. Neurosurgery 25:153–160
248. Song JK, Burkey BB, Konrad PE (2003) Lateral approach to a neurenteric cyst of the cervical spine: case presentation and review of surgical technique. Spine 28:E81–E85
249. Soni TV, Pandya C, Vaidya JP (2004) Split cord malformation with neurenteric cyst and pregnancy. Surg Neurol 61:556–558
250. Sonneland PRL, Scheithauer BW, Onofrio BM (1985) Myxopapillary ependyoma. A clinicopathologic and immunocytochemical study on 77 cases. Cancer 56:883–893
251. Souweidane MN, Benjamin V (1994) Spinal cord meningiomas. Neurosurg Clin N Am 5:283–291
252. Stechison MT, Tasker RR, Wortzman G (1987) Spinal meningioma en plaque. Report of two cases. J Neurosurg 67:452–455
253. Stein BM (1979) Surgery of intramedullary spinal cord tumours. Clin Neurosurg 26:529–542
254. Stern Y, Spiegelmann R, Sadeh M (1991) Spinal intradural arachnoid cysts. Neurochirurgia (Stuttg) 34:127–130
255. Stevens JM, Kendall BE, Davis C, Crockard HA (1987) Percutaneous insertion of the spinal end of a cyst – peritoneal shunt as definitive treatment to relieve cord compression from a spinal arachnoid cyst. Neuroradiology 29:190–195
256. Stolke D, Zumkeller M, Seifert V (1988) Intraspinal lipomas in infancy and childhood causing a tethered cord syndrome. Neurosurg Rev 11:59–65
257. Struffert T, Grunwald I, Roth C, Reith W (2004) Spinal intradurale tumore. Radiologe 44:1211–1228
258. Takahashi S, Morikawa S, Egawa M, Saruhashi Y, Matsusue Y (2003) Magnetic resonance imaging-guided percutaneous fenestration of a cervical intradural cyst. Case report. J Neurosurg Spine 99:313–315
259. Takeuchi A, Miyamoto K, Sugiyama S, Saitou M, Hosoe H, Shimizu K (2003) Spinal arachnoid cysts associated with syringomyelia: report of two cases and a review of the literature. J Spinal Disord Tech 16:207–211
260. Tamaki N, Shirataki K, Kojima N, Shouse Y, Matsumoto S (1988) Tethered cord syndrome of delayed onset following repair of myelomeningocele. J Neurosurg 69:393–398
261. Tanaka T, Sakamoto T, Koyama T, Watanabe K, Tanaka T, Murata K (1997) Endoscopic treatment of symptomatic spinal subarachnoid cysts. AJR Am J Roentgenol 169:1719–1720
262. Tatagiba M, Böker DK, Brandis A, Samii M, Ostertag H, Babu R (1992) Meningeal melanocytoma of the C8 nerve root: case report. Neurosurgery 31:958–961
263. Tatagiba M, Bini W, Sepehrnia A, Eichhorn R, Kleider A, Samii M (1994) Involvement of spinal nerves in neurofibromatosis. Neurosurg Rev 17:43–49
264. Thomas JE, Miller RH (1973) Lipomatous tumors of the spinal canal. A study of their clinical range. Mayo Clin Proc 48:393–400
265. Tobita T, Okamoto M, Tomita M, Yamakura T, Fujihara H, Baba H, Uchiyama S, Hamann W, Shimoji K (2003) Diagnosis of spinal disease with ultrafine flexible fiberscopes in patients with chronic pain. Spine 28:2006–2012
266. Trehan G, Soto-Ares G, Vinchon M, Pruvo JP (2003) [Neurenteric cyst: an unusual congenital malformation of the spinal canal]. J Radiol 84:412–414
267. Tsurubuchi T, Matsumura A, Nakai K, Fujita K, Enomoto T, Iwasaki N, Nose T (2002) Reversible holocord edema associated with intramedullary spinal abscess secondary to an infected dermoid cyst. Pediatr Neurosurg 37:282–286
268. Uchino A, Kato A, Momozaki N, Yukitake M, Kudo S (1997) Spinal cord herniation: report of two cases and review of the literature. Eur Radiol 7:289–292
269. Valls PL, Naul LG, Kanter SL (1990) Paraplegia after a routine lumbar laminectomy: report of a rare complication and successful management. Neurosurgery 27:638–640
270. Van Calenbergh F, Vanvolsen S, Verpoorten C, Lagae L, Casaer P, Plets (1999) Results after surgery for lumbosacral lipoma: the significance of early and late worsening. Childs Nerv Syst 15:439–443
271. Vernet O, O'Gorman AM, Farmer JP, McPhillips M, Montes JL (1996) Use of the prone position in the MRI evaluation of spinal cord tethering. Pediatr Neurosurg 25:286–294
272. Vloeberghs M, Herregodts P, Stadnik T, Goossens A, D'Haens J (1992) Spinal arachnoiditis mimicking a spinal cord tumor: a case report and review of the literature. Surg Neurol 37:211–215

273. Vogel S, Neumaerker K, Klepel K (1990) The optimal time for operative treatment of the tethered cord syndrome. Adv Neurosurg 18:155–157
274. Wakai S, Chiu CW (1984) Rare combination of spinal lesions and spina bifida occulta: case report. Dev Med Child Neurol 26:117–121
275. Wang MY, Levi AD, Green BA (2003) Intradural spinal arachnoid cysts in adults. Surg Neurol 60:49–55; discussion 55–56
276. Warnke JP, Koppert H, Bensch-Schreiter B, Dzelzitis J, Tschabitscher M (2003) Thecaloscopy part III: first clinical application. Minim Invasive Neurosurg 46:94–99
277. Xenos C, Sgouros S, Walsh R, Hockley A (2000) Spinal lipomas in children. Pediatr Neurosurg 32:295–307
278. Yamada S, Iacono RP, Andrade T, Mandybur G, Yamada BS (1995) Pathophysiology of tethered cord syndrome. Neurosurg Clin N Am 6:311–323
279. Yasargil MG, Antic J, Laciga R, De Preux J, Fideler RW, Boone SC (1976) The microsurgical removal of intramedullary spinal hemangioblastomas. Report of twelve cases and a review of the literature. Surg Neurol 6:141–148
280. Zavala LM, Adler JR , Greene CS , Winston KR (1988) Hydrocephalus and intraspinal tumor. Neurosurgery 22:751–754
281. Zide B, Constantini S, Epstein FJ (1995) Prevention of recurrent tethered spinal cord. Pediatr Neurosurg 22:111–114
282. Ziv T, Watemberg N, Constantini S, Lerman-Sagie T (1999) Cauda equina syndrome due to lumbosacral arachnoid cysts in children. Eur J Paediatr Neurol 3:281–284
283. Zumkeller M, Stolke D , Dietz H (1990) Intraspinal lipomas with tethered cord syndrome – results of operative treatment in 30 children. Adv Neurosurg 18:164–169

Epidural Tumors 5

Contents

In this section on extradural tumors of the spinal canal, two groups have to be distinguished: soft-tissue and bone tumors. The latter may again be subdivided into primary and secondary neoplasms. These tumors differ in several important aspects: whereas soft-tissue tumors are predominantly benign and do not destroy the biomechanical properties of the spinal column per se, bone tumors interfere with spinal stability, and malignant entities predominate. During the past years, surgical management of bone tumors has undergone profound changes, with better understanding of spinal biomechanics and improved fusion and reconstruction techniques. In this chapter we provide an overview of clinical presentations, neuroradiological features, surgical techniques, and postoperative results for epidural soft-tissue and bone tumors of the spine. Tables 5.1 and 5.2 give an overview of the different histologies among 329 extradural spinal tumors in this series.

Table 5.1. Epidural soft-tissue tumors

Type of tumor	Number
Nerve sheath tumor	65
Synovial cyst	14
Arachnoid cyst	9
Soft-tissue sarcoma	9
Cavernoma	4
Hamartoma	1
Angiolipoma	1
Hemangiopericytoma	1
Calcified pseudotumor	1
Total	**105**

Table 5.2. Epidural bone tumors

Type of tumor	Number
Metastasis	144
Chordoma	20
Plasmocytoma	19
Chondrosarcoma	13
Lymphoma	8
Osteogenic sarcoma	4
Osteoblastoma	4
Aneurysmatic bone cyst	4
Hemangioma	3
Ewing sarcoma	3
Giant cell tumor	1
Histiocytosis X	1
Total	**224**

Table 5.3. Initial symptoms of epidural spinal tumors

First symptom	Soft-tissue tumor	Bone tumor	Total
Pain	65%	79%	75%
Gait ataxia	10%	8%	9%
Motor weakness	6%	6%	7%
Sensory deficits	3%	1%	2%
Dysesthesias	10%	3%	5%
Sphincter problems	2%	1%	1%
Local swelling	3%	1%	2%

Table 5.4. Symptoms of epidural spinal tumors at presentation

Symptom	Soft-tissue tumor	Bone tumor	Total
Pain	82%	96%	92%
Gait ataxia	47%	67%	61%
Motor weakness	60%	66%	64%
Sensory deficits	66%	74%	72%
Dysesthesias	40%	18%	24%
Sphincter problems	19%	39%	33%

5.1 History and Diagnosis

Most patients with epidural tumors present a classic clinical pattern: local pain, radicular symptoms, and spastic para- or tetraparesis. Overall, we have observed local pain as the first symptom in 75% of patients with epidural tumors (65% with soft-tissue and 79% with bone tumors). Just 9% and 7% of patients reported gait or motor disturbances initially, respectively (Table 5.3). At presentation, major complaints were pain (49%), gait ataxia (39%), or motor weakness (7%). Table 5.4 provides an overview in terms of the neurological picture at the time of surgery. Remarkably, a few patients presented just with a local swelling due to the posterior extraspinal extension of the tumor (Fig. 5.1).

Soft-tissue tumors develop within the epidural space, displace epidural fat and veins and then compress the dura. They tend to grow along and around the dural sac and often proceed toward the intervertebral foramina into the paraspinal spaces. The foramina may then be enlarged due to bony erosion. If a space-occupying process grows slowly enough from early childhood on, vertebral bodies may even become distorted or dysplastic. Clinical symptoms progress gradually and pain is the dominating clinical problem throughout the clinical course in 58% of patients. Other major complaints at presentation were gait ataxia (22%), motor weakness (7%), dysesthesias (4%), hypesthesia (3%), or sphincter problems (2%).

Bony tumors present comparable clinical patterns but tend to either distort or destroy the bony anatomy primarily – depending on the benign or malignant nature of the tumor. Local pain is the predominant first symptom in 79% of patients and is caused by infiltration of bone and periosteum. Once the tumor compresses the intervertebral foramina or breaks out into the soft-tissue, radicular symptoms may develop before the spinal cord finally becomes affected. In a study on spinal metastases, for instance, 80% of patients were found to progress from local pain to neurological symptoms within 2 months [230]. However, as stability of the spine may be compromised by malignant tumors in particular, sudden clinical deteorations due to collapse of a vertebral body and spinal instability are not uncommon. At presentation, 45% of patients with bony tumors were affected predominantly by local pain and gait problems.

Compared to patients with intra- and extramedullary tumors, epidural tumors produce significantly more pain [363, 504]. Furthermore, patients with epidural tumors showed the highest proportion of advanced spinal cord lesions at presentation (i.e., patients unable to walk, 31%, or with bladder and bowel incontinence, 17%). This is due mainly to bony tumors causing sudden cord compression from pathological fractures and the higher incidence of malig-

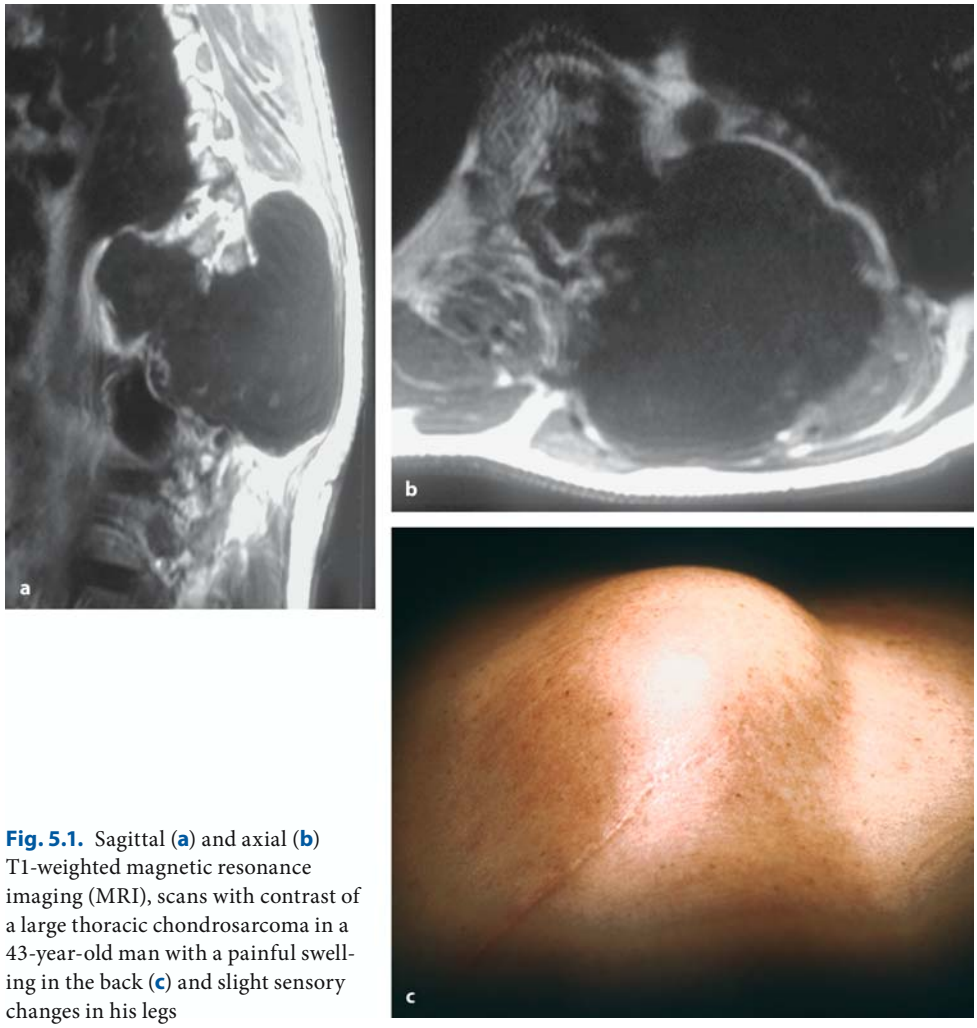

Fig. 5.1. Sagittal (**a**) and axial (**b**) T1-weighted magnetic resonance imaging (MRI), scans with contrast of a large thoracic chondrosarcoma in a 43-year-old man with a painful swelling in the back (**c**) and slight sensory changes in his legs

nant tumors. In other words, the clinical course does not exclusively correlate with tumor growth as in intra- or extramedullary tumors, because symptoms related to spinal instability may take over.

There were significant differences for the average patient history (26±50 months and 6±10 months, respectively; $p<0.0001$) and for the preoperative Karnofsky scores (75±15 and 58±19, respectively; $p<0.0001$) between patients with soft-tissue and bone tumors. This difference is attributable to the higher proportion of malignant tumors in the latter group (4% and 83%, respectively) and is reflected in differences in patient history (21±43 months and 6±12 months, respectively; $p<0.0001$) as well as in the preoperative Karnofsky score (73±15 and 56±19, respectively; $p<0.0001$) in the benign and malignant bone tumor groups, respectively.

5.2 Neuroradiology

Whereas the neuroradiological diagnosis of intra- and extramedullary tumors depends nowadays almost exclusively on magnetic resonance imaging (MRI), the situation is different for extradural tumors, especially bone tumors. Even though modern MRI allows excellent visualization of soft-tissue and bone structures, computed tomography (CT) and plain X-rays are an absolute must for bone tumors of the spine and are recommended for extradural soft-tissue tumors as well.

Neuroradiological examinations of an extradural tumor have to provide information on the following points:

1. Localization and extent of the tumor.
2. Differentiation between soft-tissue and bone tumors.

3. Differentiation between a destructive and displacing tumor.
4. Response of surrounding tissues.
5. Involvement of major vessels.
6. Spinal stability.

5.2.1 Soft-Tissue Tumors

Oblique X-ray studies can visualize the intervertebral foramina. Widening of the foramina may be observed mostly, but not exclusively in schwannomas (Fig. 5.2), as this phenomenon has also been shown for a great variety of histologies such as osteoblastomas, chondrosarcomas, and meningoceles [580].

Within the paraspinal spaces, some epidural tumors may grow to enormous sizes. The visualization of such tumor extensions is the domain of MRI (Fig. 5.3). However, it may be advisable to perform a conventional angiography in selected cases to establish the involvement of major vessels such as the vertebral artery [87, 173, 258, 395]. In highly vascularized tumors, such studies can be combined with preoperative embolization [173, 200].

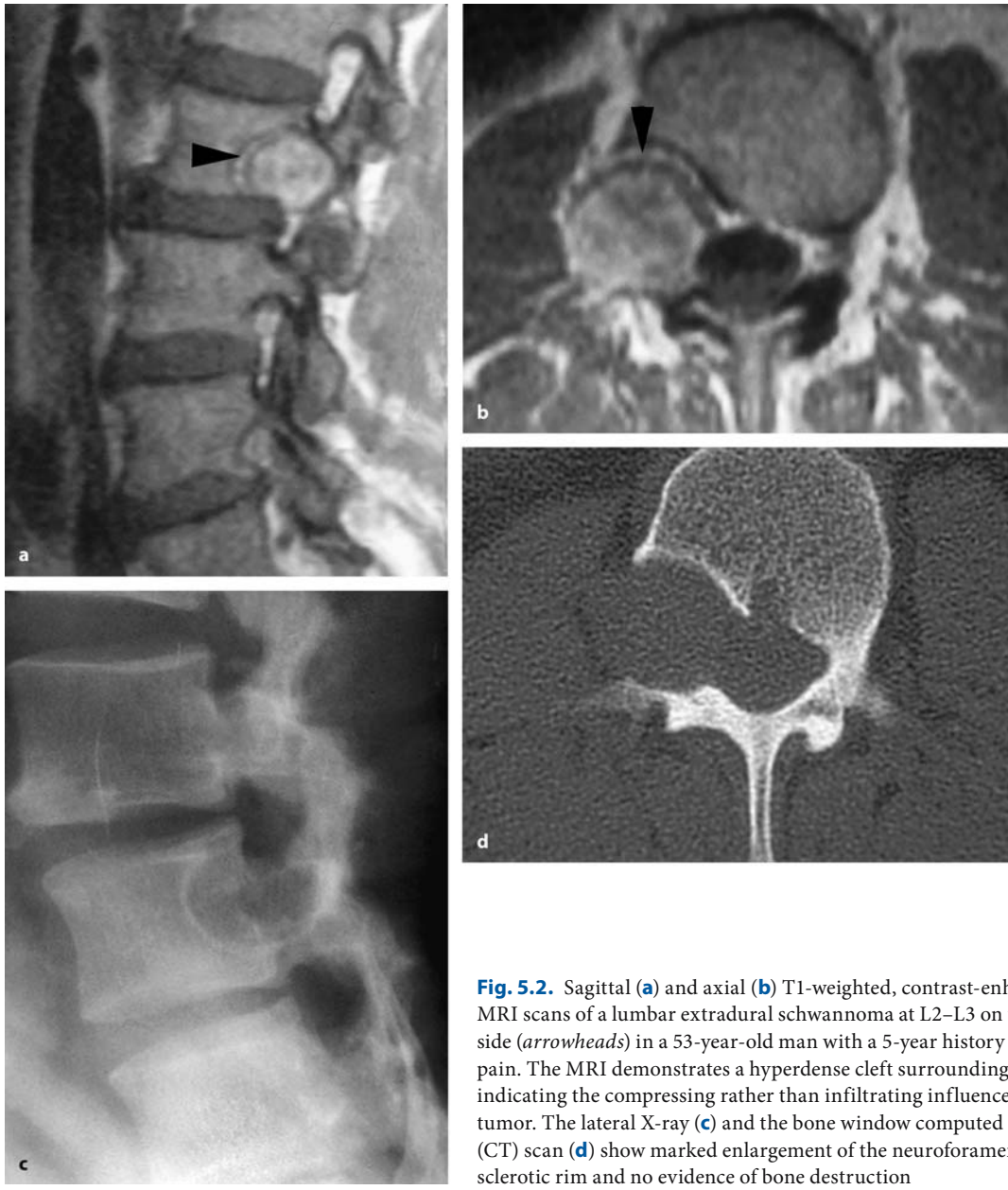

Fig. 5.2. Sagittal (**a**) and axial (**b**) T1-weighted, contrast-enhanced MRI scans of a lumbar extradural schwannoma at L2–L3 on the right side (*arrowheads*) in a 53-year-old man with a 5-year history of radicular pain. The MRI demonstrates a hyperdense cleft surrounding the tumor, indicating the compressing rather than infiltrating influence of this tumor. The lateral X-ray (**c**) and the bone window computed tomography (CT) scan (**d**) show marked enlargement of the neuroforamen with a sclerotic rim and no evidence of bone destruction

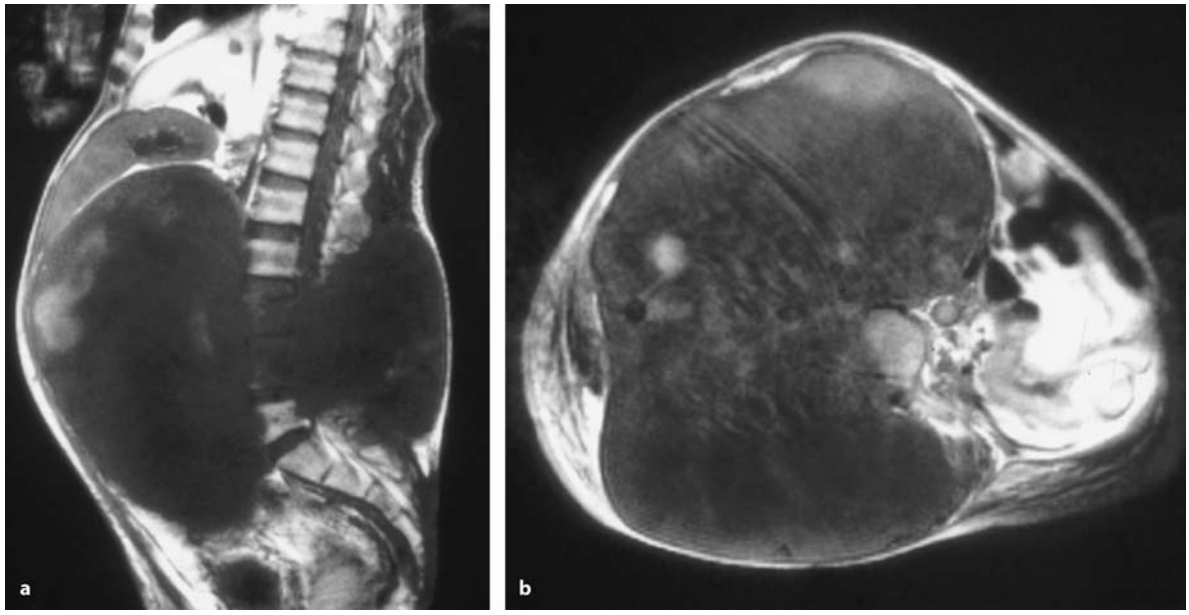

Fig. 5.3. Sagittal (**a**) and axial (**b**) T1-weighted, contrast-enhanced MRI scans of a huge, cystic lumbar schwannoma in a 40-year-old patient with neurofibromatosis type 2 (NF-2) with compression of the entire abdomen

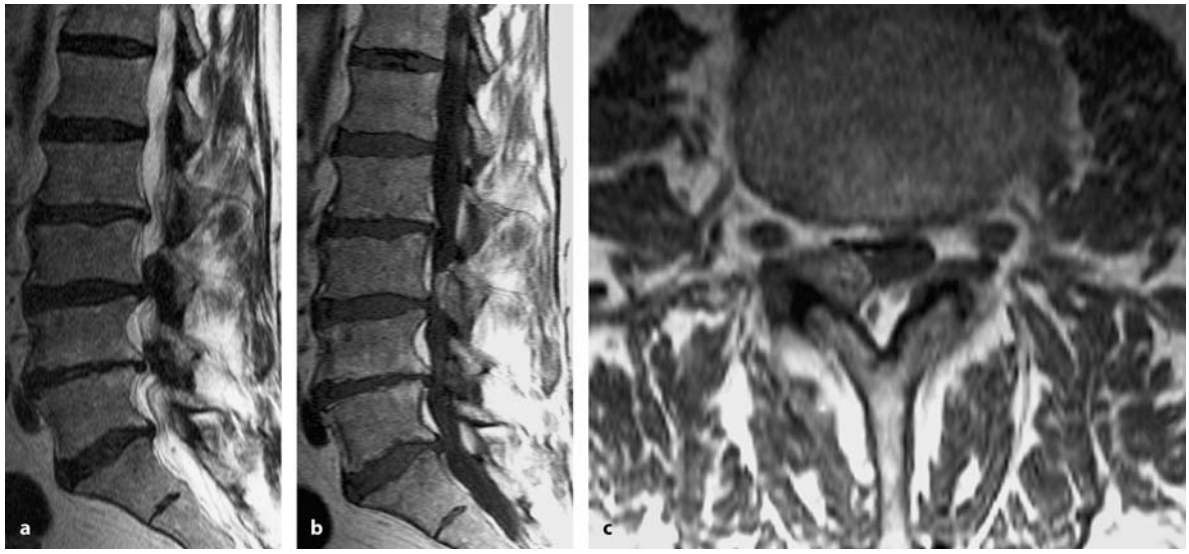

Fig. 5.4. Sagittal T2- (**a**) and T1-weighted, contrast-enhanced MRI scan (**b**) of an epidural cavernoma at L3 in a 73-year-old man with a 10-year history of pain and radicular irritation of the right L4 root. On the T2-weighted image (**a**), the lesion appears hypointense similar to a disc. The T1-image (**b**) shows inhomogenous enhancement with contrast of this sharply demarcated lesion. **c** The axial T1-weighted scan demonstrates the cavernoma in close proximity to the right intervertebral joint compressing the dura

Epidural schwannomas may be solid or cystic with bright contrast enhancement. Usually they are localized laterally, compress the dura, and grow along the nerve sheath through the neuroforamen into the extraspinal space. They enlarge the neuroforamen (Fig. 5.2). In most cases, the extraspinal part is larger than the intraspinal one (Fig. 5.3). Quite often it is not possible to rule out small intradural tumor extensions on MRI, so that the dura has to be opened along the nerve root for intradural inspection in such instances (Fig. 5.2).

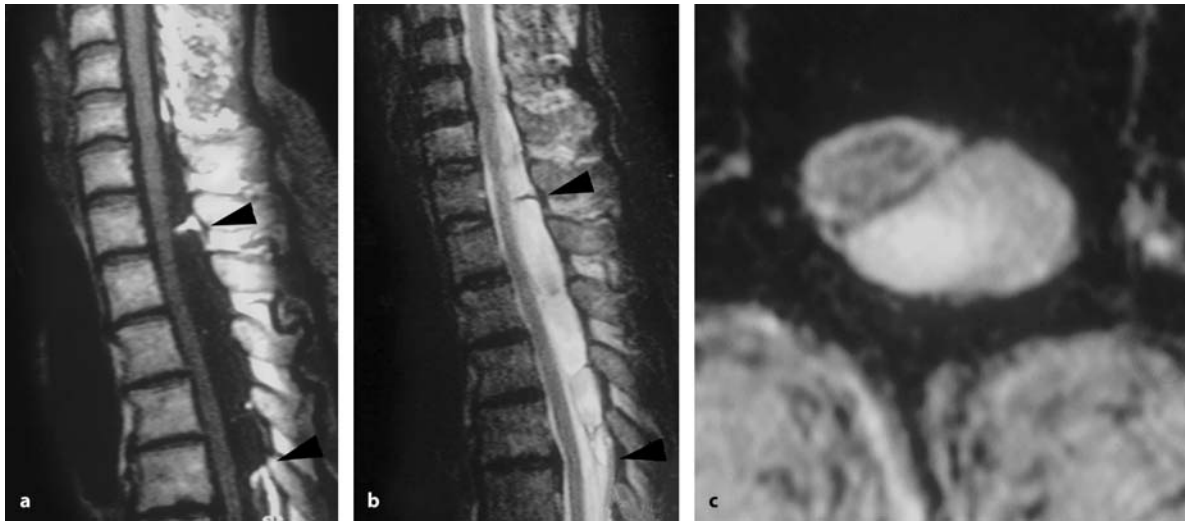

Fig. 5.5. Sagittal T1-weighted, contrast-enhanced MRI scan (**a**) and sagittal (**b**) and axial (**c**) T2-weighted images of an epidural cavernoma with an extensive hemorrhagic cyst at Th2–Th6 (*arrowheads* in **a** and **b**) in a 46-year-old woman with back pain and a slight paresis on the left side. The sagittal T2-weighted image displays septations of the cyst as a result of repeated hemorrhages

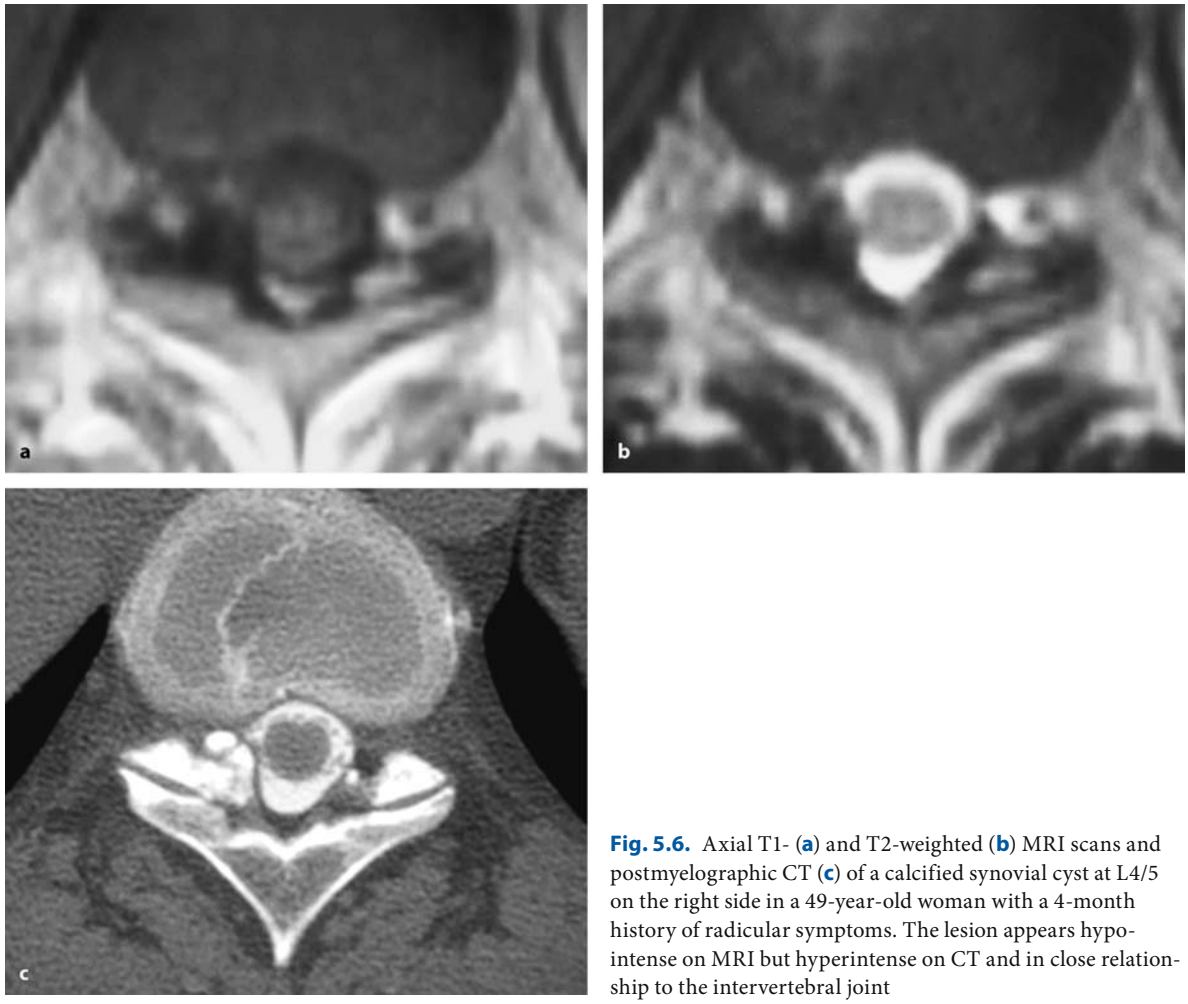

Fig. 5.6. Axial T1- (**a**) and T2-weighted (**b**) MRI scans and postmyelographic CT (**c**) of a calcified synovial cyst at L4/5 on the right side in a 49-year-old woman with a 4-month history of radicular symptoms. The lesion appears hypointense on MRI but hyperintense on CT and in close relationship to the intervertebral joint

Fig. 5.7. Sagittal T2- (**a**) and T1-weighted (**b**) MRI scans of an epidural arachnoid cyst at L1-L2 in a 46-year-old woman complaining about back pain, a slight paraparesis and sphincter problems. On T2, the epidural localization of this cyst is easily detectable with the ventral dura appearing as a dark band (*arrowhead* in **a**). On T1, the relationship between the dura and cyst is not even clear on the axial scan (**c**)

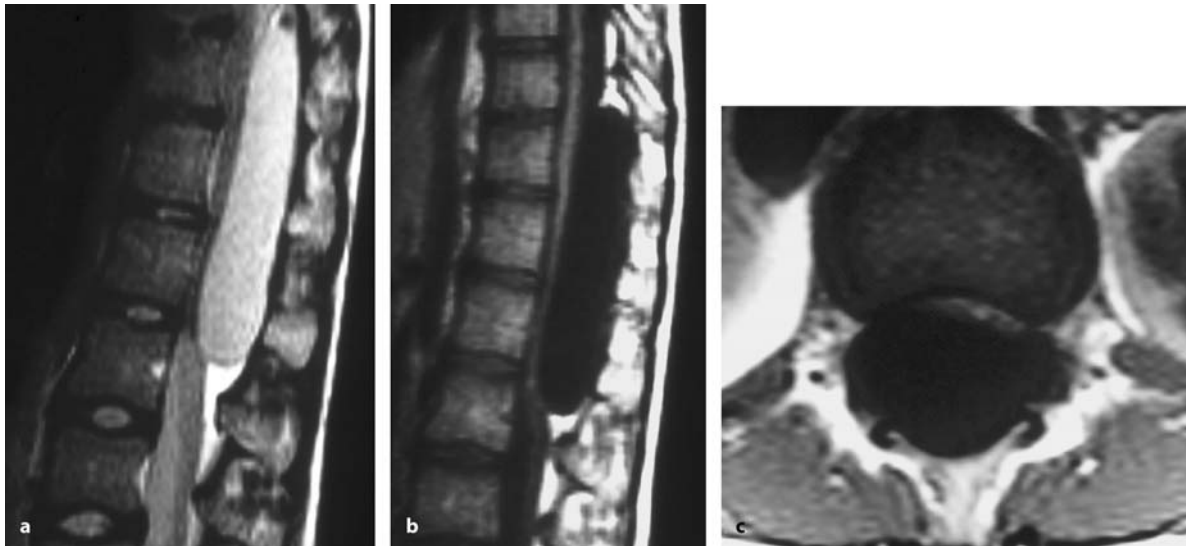

Fig. 5.8. Sagittal T2- (**a**) and T1-weighted (**b**) MRI scans of an epidural arachnoid cyst at Th10–L2 in a 12-year-old girl with a slight, painful paraparesis. The epidural localization can be diagnosed easiest on the T1-image with the epidural space widened at either end of the cyst. Once again, the T2-image displays the dura best. **c** The axial T1-weighted scan indicates an enormous amount of cord compression. The extradural position of the cyst cannot be determined on this scan

Epidural cavernomas demonstrate a varied signal pattern on MRI depending on the amount and chemical state of the hemoglobin derivates associated with smaller hemorrhages (Fig. 5.4). They may be associated with considerable hemorrhagic cysts (Fig. 5.5).

Synovial cysts contain fatty fluid. The signal pattern is inhomogenous on MRI and may resemble a cavernoma. CT demonstrates the connection to the intervertebral joint, making the differential diagnosis quite easy (Fig. 5.6).

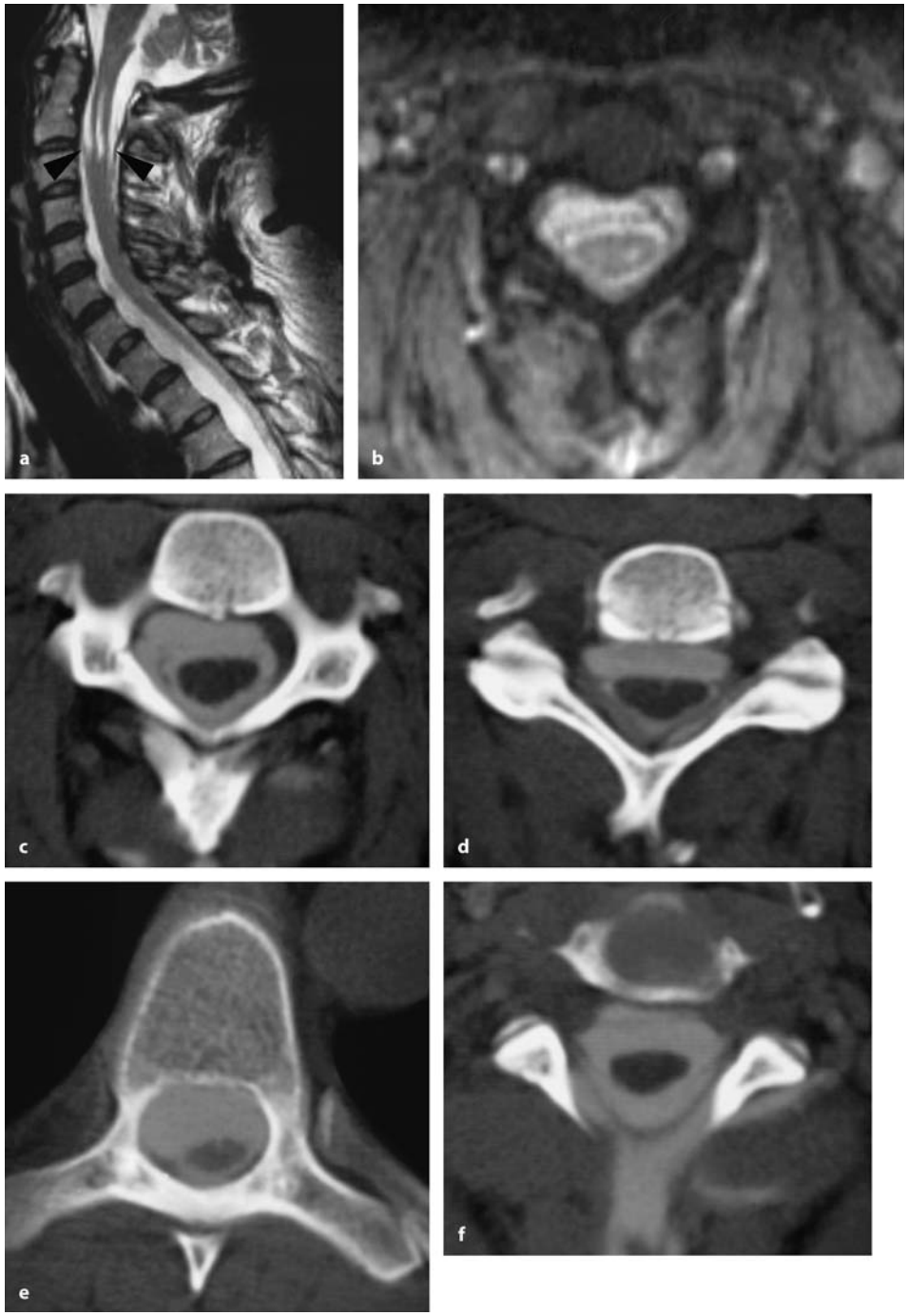

Fig. 5.9 a This sagittal T2-weighted MRI shows a small syrinx at C2/3 and posterior displacement of the cord starting at the cervicothoracic junction in a 46-year-old woman with a previous history of a horse-riding accident several years before developing a slight tetraparesis. Starting at the level of the C2/3 disc space, a dark band appears to converge on the cord anteriorly and posteriorly (*arrowheads*). **b** This axial T2-weighted MRI scan taken at C5 shows the spinal cord surrounded by cerebrospinal fluid (CSF) and an epidural ventral cyst centered on the right side. This cyst was detectable to the level of Th7. **c** This corresponding postmyelographic CT scan displays similar contrast filling in the subarachnoid space and epidural cyst. The lower cervical (**d**) and thoracic scans (**e**) demonstrate the varying amounts of cord compression. **f** At C3, this scan shows extradural accumulation of contrast medium, suggesting a dura defect at this level. In summary, this epidural arachnoid cyst developed as a result of a dura tear along the C3 nerve root on the right side

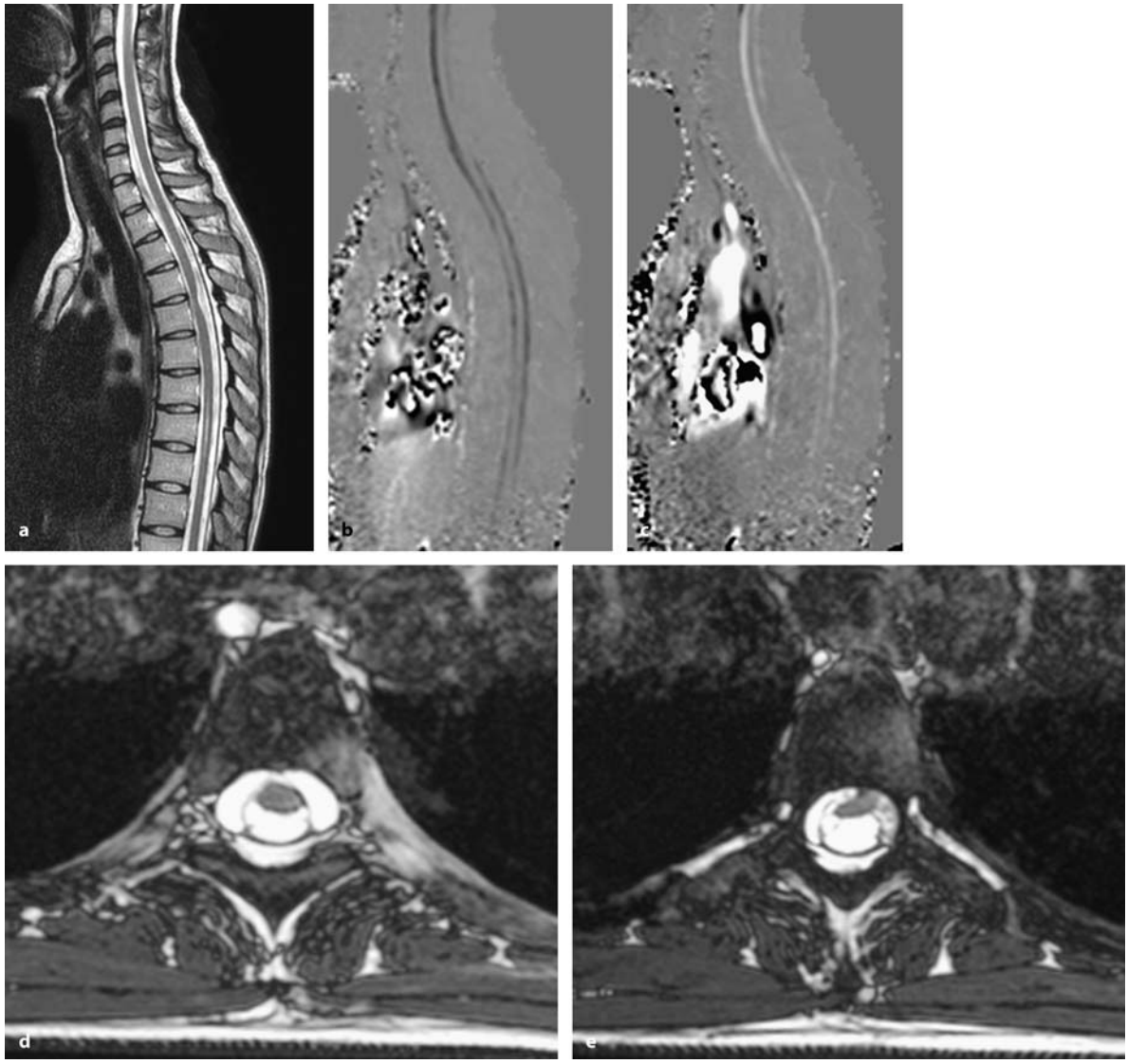

Fig. 5.10 a This sagittal T2-weighted MRI picture shows an area of cord compression at Th4/5 and a small syrinx at Th7–Th8 in a 25-year-old woman with a slight paraparesis. Cardiac gated cine MRI scans taken in systole (**b**) and diastole (**c**) demonstrate a normal flow pattern with no evidence of a CSF flow abnormality. **d** The axial T2-weighted image at Th5 shows ventral displacement of the cord and a ventral arachnoid cyst enclosing three-quarters of the dural sac. **e** At Th4/5 the dura defect responsible for this cyst is visible anteriorly on the left side with the spinal cord herniating into the epidural cyst

Similarly, epidural arachnoid cysts are easy to diagnose. The space-occupying effect of these cysts is variable. Some compress the dura and spinal cord moderately (Fig. 5.7) or enormously (Fig. 5.8), others appear as slit-like dura dissections (Fig. 5.9). The diagnostic challenge is the demonstration of the dura defect and, thus, the site of communication between the subarachnoid space and the cyst. This localization determines the surgical strategy. Most epidural arachnoid cysts are associated with dura defects along a nerve root sleeve, especially where there is a history of trauma. Myelography and postmyelographic CT may be required to demonstrate this communication (Fig. 5.9). In rare instances, the spinal cord may herniate into this dura defect (Fig. 5.10).

Lymphomas and other infiltrating tumors such as soft-tissue sarcomas are iso- or hypointense on T1-weighted images and demonstrate a high signal intensity on T2-weighted images. They grow within the epidural space surrounding the dural sac and accumulate contrast homogenously without destroying bone (Fig. 5.11) [86].

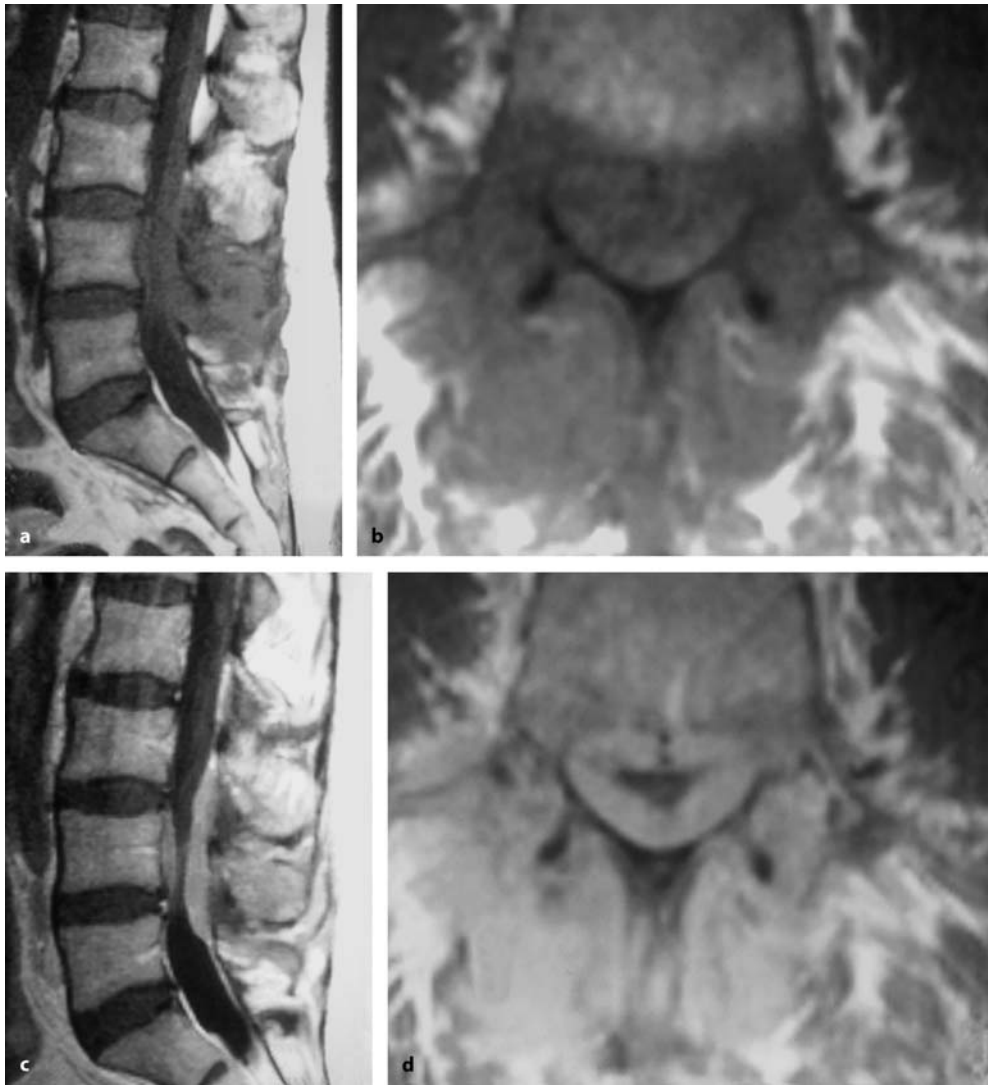

Fig. 5.11. T1-weighted sagittal (**a**) and axial (**b**) MRI scans of a lymphoma at L3–L4 in a 60-year-old woman with back pain and a slight paraparesis. The lesion appears to be diffusely infiltrating with ill-defined borders. On the axial scan, the epidural tumor, dura, and spinal cord appear to be indistinguishable. Likewise, there appears to be considerable diffuse, soft-tissue involvement. With contrast enhancement (**c**, **d**), the corresponding scans demonstrate bright enhancement and marked dural compression, which was not well appreciated on the unenhanced images

Epidural pathologies that could be mistaken for tumors include chronic epidural hematomas, abscesses, disc prolapses, and spinal lipomatosis. Chronic epidural hematomas display varying signal intensities on MRI depending on the age of the hemorrhage (Figs. 5.12 and 5.13). They may extend over several spinal segments in patients with hemorrhagic diatheses (Fig. 5.12) or be locally confined (Fig. 5.13). A history of trauma is not required. Sequential examinations may demonstrate spontaneous resorption (Fig. 5.12).

Spinal epidural abscesses may be caused by hematologic or local spread from a neighboring spondylodiscitis or vertebral abscess. The distinguishing feature from a cystic tumor is the surrounding edema in the epidural space, which gives a somewhat blurred contour of the lesion in T1-weighted images unless gadolinium is given (Fig. 5.14).

Disc prolapses can usually be easily differentiated from epidural neoplasms due to their association with degenerative disc changes and lack of contrast en-

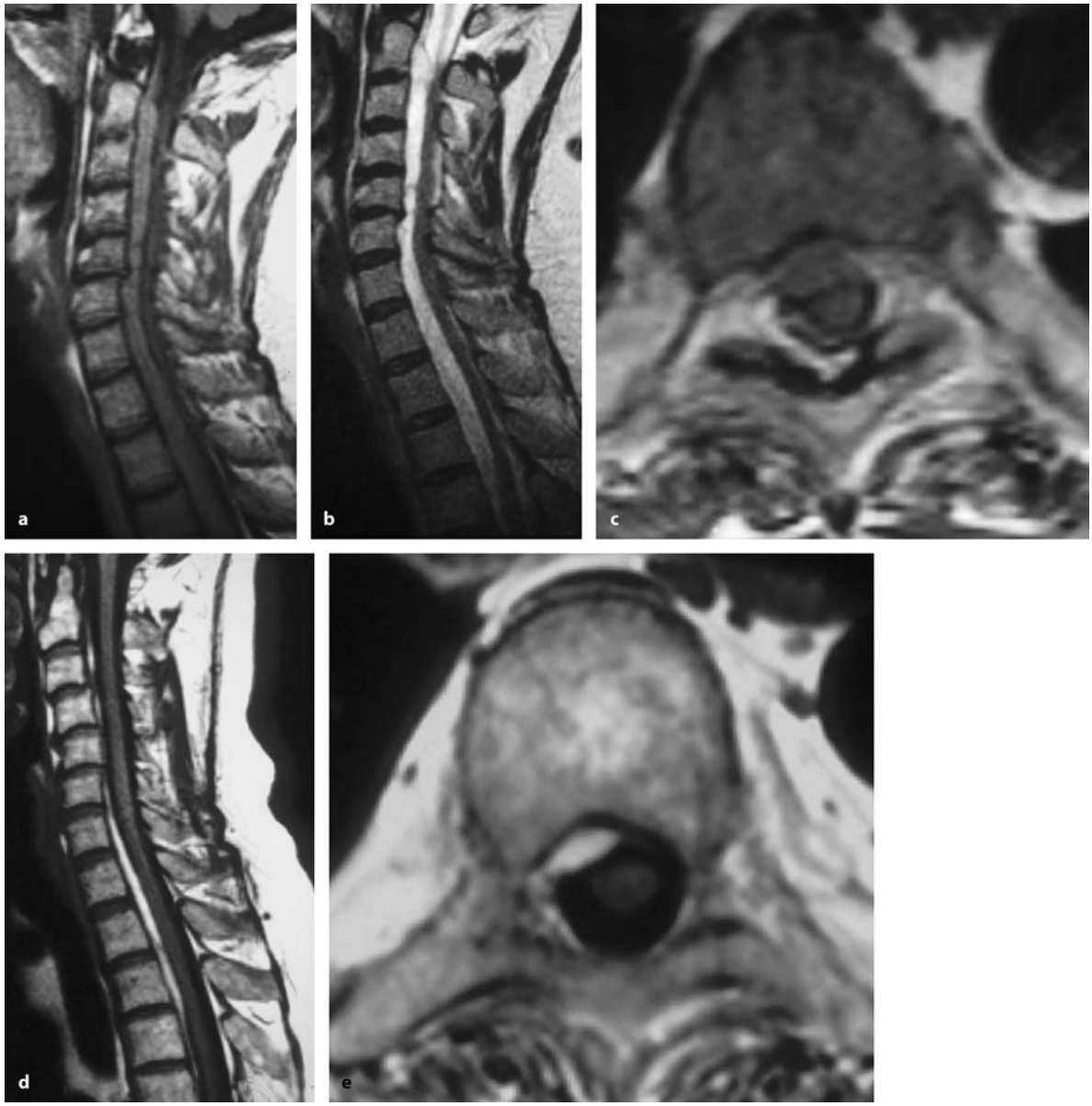

Fig. 5.12. Sagittal T1- (**a**) and T2-weighted (**b**) MRI scans of a 54-year-old woman with chronic alcoholism and a history of sudden tetraparesis that recovered spontaneously over a period of 1 month. A ventral epidural hematoma is visible extending from C2 to Th4. On the T1-weighted image (**a**) the hematoma appears hyperintense and on the T2-weighted image (**b**) the signal is similar to that of CSF. The T2-weighte image (**b**) and the axial T1-weighted image (**c**) indicate the extradural localization of this hemorrhage. After 1 month most of the hematoma has disappeared spontaneously (**d**, **e**). Please note the much brighter signal of the hematoma remnants compared to the initial pattern without application of contrast

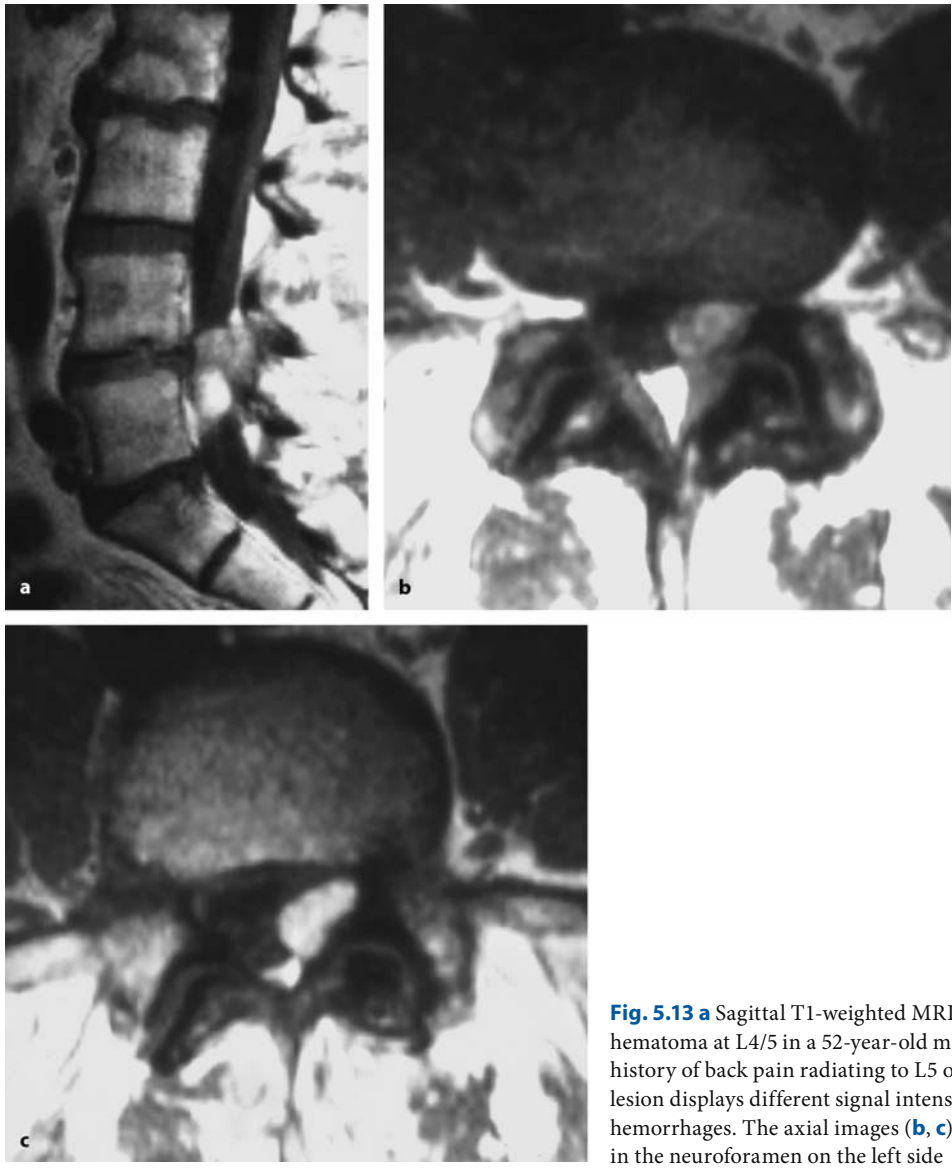

Fig. 5.13 a Sagittal T1-weighted MRI scan of an epidural hematoma at L4/5 in a 52-year-old man with a 6-month history of back pain radiating to L5 on the left side. The lesion displays different signal intensities related to repeated hemorrhages. The axial images (**b**, **c**) show the hematoma in the neuroforamen on the left side

hancement on MRI. However, some sequestrated herniations may pose diagnostic problems if the neighboring disc appears normal and part of the lesion takes up contrast (Fig. 5.15).

Spinal lipomatosis may cause significant dural compression and can be mistaken for a lipoma or an infiltrating epidural tumor. Spinal lipomatosis may be observed in grossly overweight patients, correlating with the amount of body fat. It may also be related to steroid therapy. The distinguishing feature is the concentric compression of the dural sac by fat tissue (Fig. 5.16).

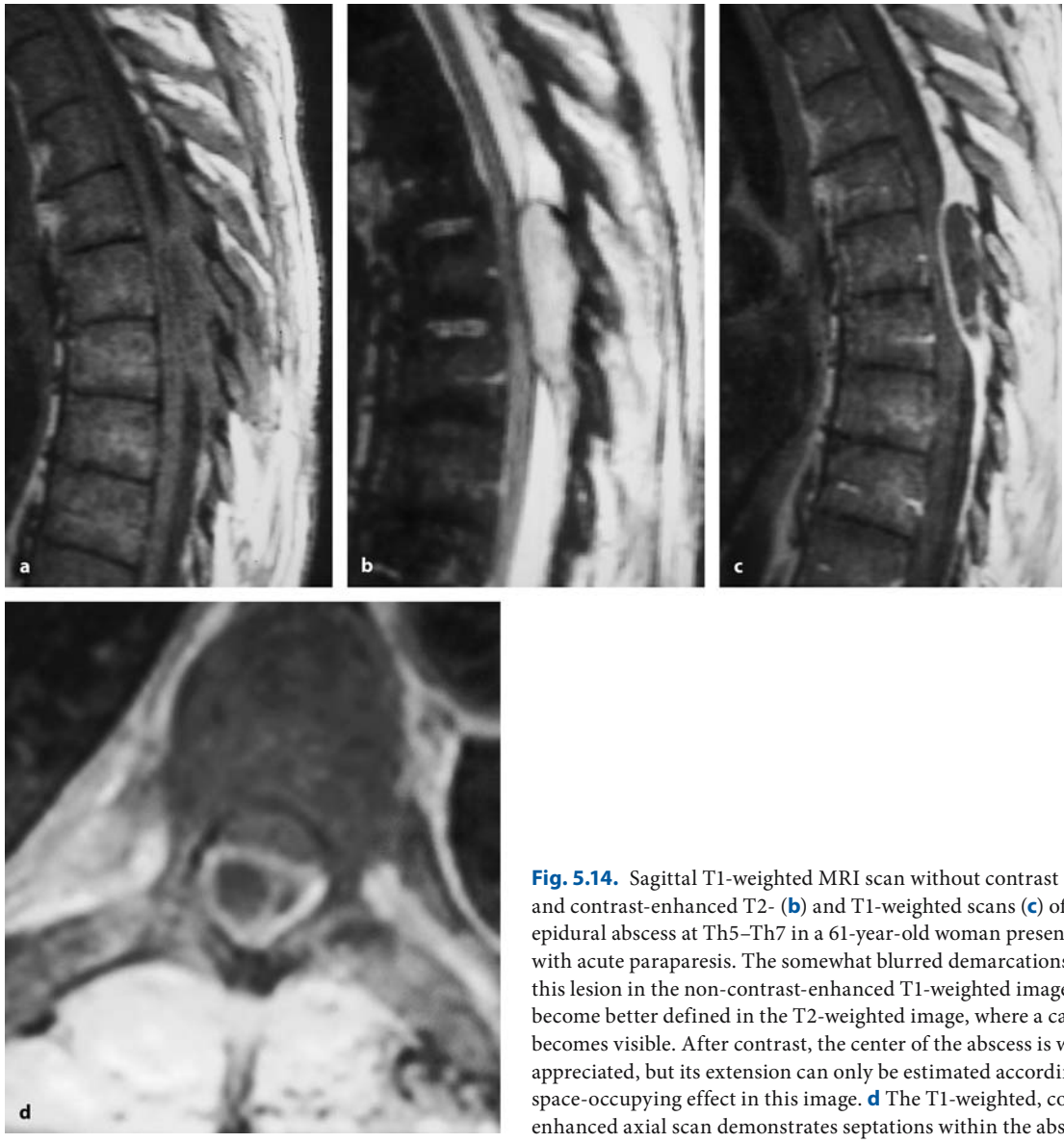

Fig. 5.14. Sagittal T1-weighted MRI scan without contrast (**a**), and contrast-enhanced T2- (**b**) and T1-weighted scans (**c**) of an epidural abscess at Th5–Th7 in a 61-year-old woman presenting with acute paraparesis. The somewhat blurred demarcations of this lesion in the non-contrast-enhanced T1-weighted image become better defined in the T2-weighted image, where a capsule becomes visible. After contrast, the center of the abscess is well appreciated, but its extension can only be estimated according to the space-occupying effect in this image. **d** The T1-weighted, contrast-enhanced axial scan demonstrates septations within the abscess

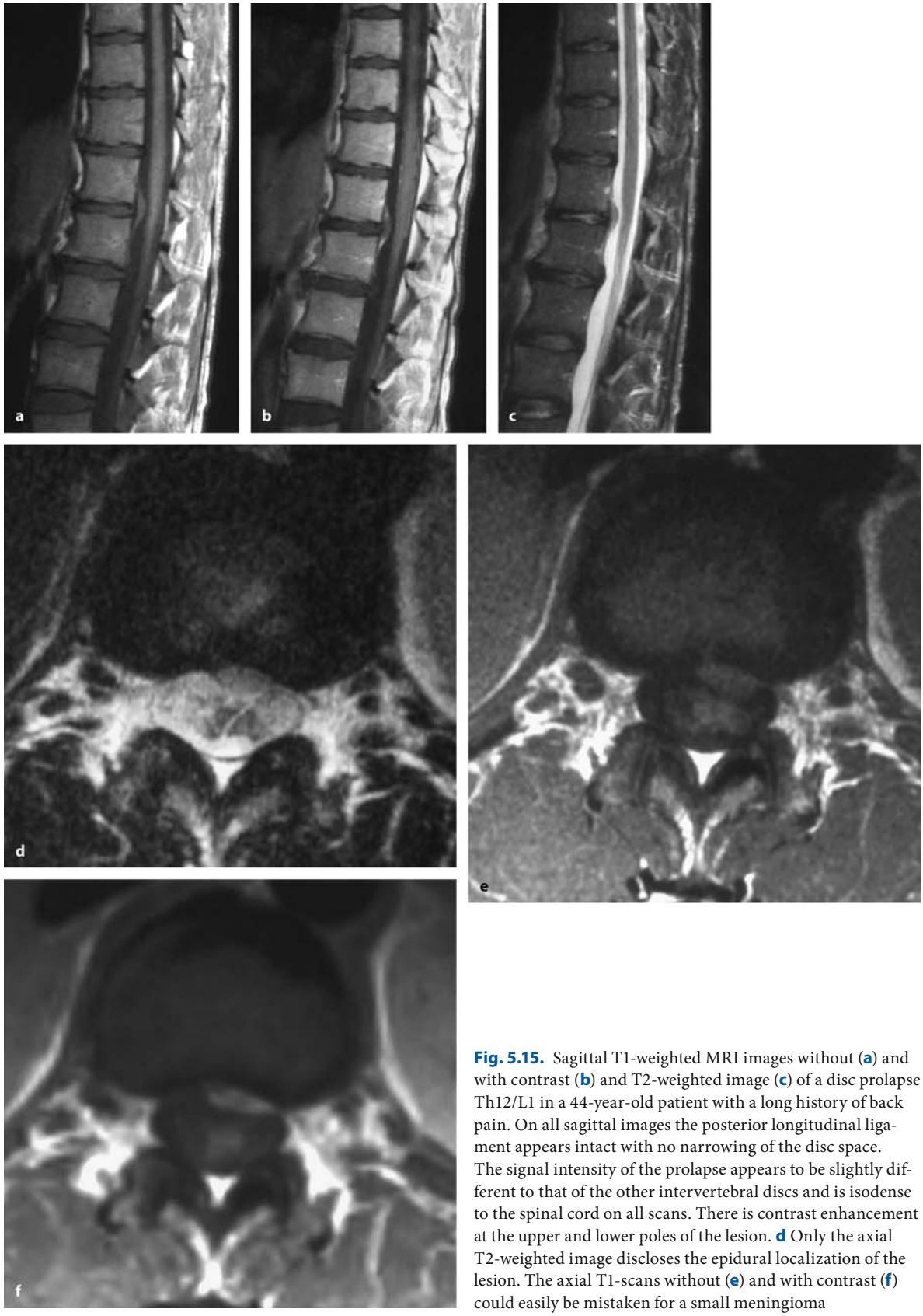

Fig. 5.15. Sagittal T1-weighted MRI images without (**a**) and with contrast (**b**) and T2-weighted image (**c**) of a disc prolapse Th12/L1 in a 44-year-old patient with a long history of back pain. On all sagittal images the posterior longitudinal ligament appears intact with no narrowing of the disc space. The signal intensity of the prolapse appears to be slightly different to that of the other intervertebral discs and is isodense to the spinal cord on all scans. There is contrast enhancement at the upper and lower poles of the lesion. **d** Only the axial T2-weighted image discloses the epidural localization of the lesion. The axial T1-scans without (**e**) and with contrast (**f**) could easily be mistaken for a small meningioma

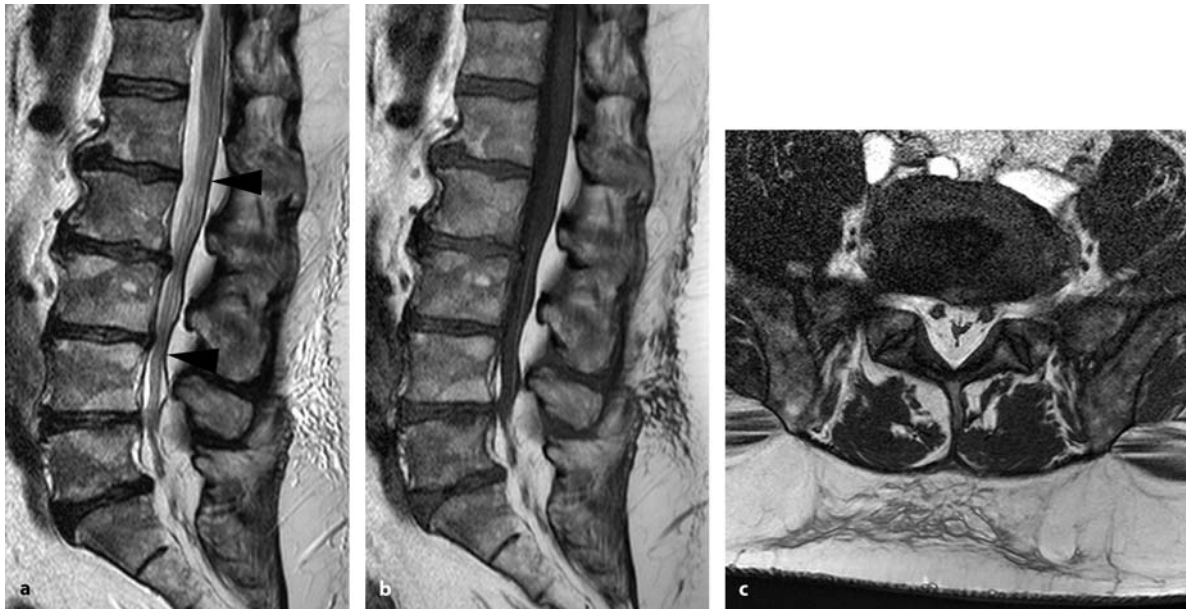

Fig. 5.16. Sagittal T2- (**a**) and T1-weighted (**b**) MRI images of a 66-year-old, overweight man with a history of low back pain and spinal claudication. Starting at L1 and extending into the sacrum, there is profound accumulation of epidural fat with anterior displacement of the dura (*arrowheads* in **a**). **(c)** The axial scan shows the characteristic concentric compression of the dural sac, which appears to be almost completely obstructed

5.2.2 Bone Tumors

With intradural pathologies, which are operated from a standard posterior approach, visualization of the extent and localization of the tumor is sufficient for surgical planning. With epidural bone tumors, however, spine radiographs and CT provide essential information on spinal stability, the response of the surrounding bone and, thus, the biological activity of the tumor. Furthermore, the amount of destruction of bone, intervertebral discs, and joints have to be considered for planning the surgical approach, tumor resection, and – if required – reconstruction and stabilization. CT often allows a distinction between locally destructive, i.e. malignant processes (Fig. 5.17) and displacing and eroding, i.e. benign lesions (Fig. 5.18). It demonstrates more clearly whether adjacent intervertebral joints and vertebral bodies are compromised. A CT in bone-window technique often demonstrates intraosseous tumor extensions clearer than a MRI because signal changes related to the surrounding bone edema may obscure tumor limits.

The neuroradiological diagnosis of bone tumors is especially important for surgical planning. In selected cases, a three-dimensional CT reconstruction of the bony anatomy may be helpful (Fig. 5.19) [474]. In addition to localization and extension of the tumor, stability issues have to be taken into account. Furthermore, the distinction of malignant vs. benign and primary vs. secondary tumors has a profound influence on the treatment strategy. Guidelines and classifications have been introduced for this purpose. According to Boriani et al. [80], who modified the original classification of Enneking [157], benign and malignant bone tumors can be classified according to radiological and clinical criteria. Benign tumors are categorized into three groups. The first group (S1) describes tumors bordered by a true capsule with well-defined margins, which may even be visible on plain X-rays, and represents processes of very limited biological activity with minimal or no symptoms (Fig. 5.20). The second group (S2) describes slow-growing tumors with slowly developing symptoms, which are surrounded by a thin capsule and some reactive tissue, which may be well defined on MRI (Fig. 5.21). The third group of benign tumors (S3) is formed by rapidly growing lesions, which have to be considered as locally aggressive. Capsules are very thin, incomplete, or absent. The tumor invades neighboring structures and may be associated with a hypervascularized pseudocapsule. On X-rays, tumor limits are ill defined (Fig. 5.19).

On the other hand, malignant tumors are subdivided in three major groups, with subgroups A and B. Low-grade tumors (IA and IB) are not accompanied by a true capsule, but a thick pseudocapsule of reac-

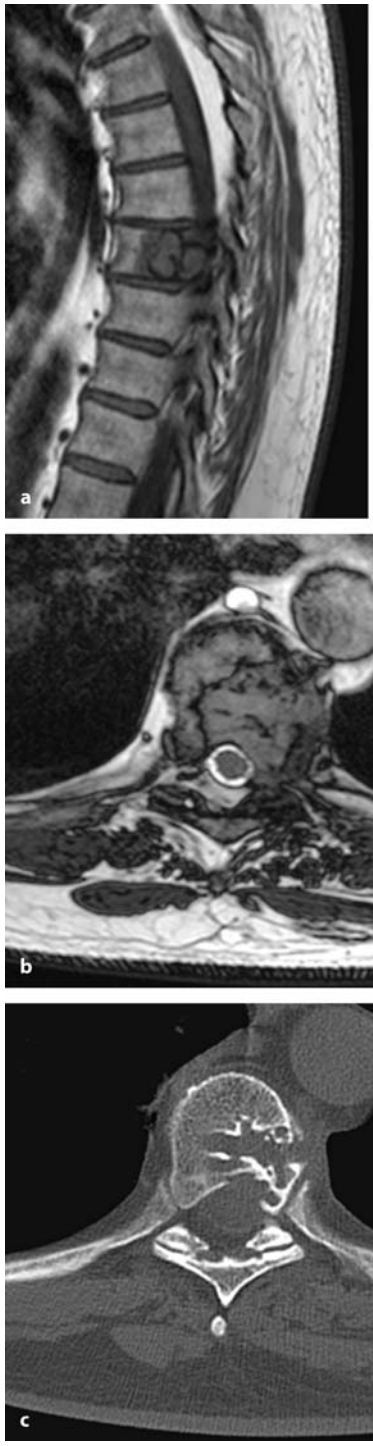

Fig. 5.17. Sagittal T1- (**a**) and axial T2-weighted (**b**) MRI scans of a thoracic plasmocytoma at Th7 in a 62-year-old man with local pain. The MRI demonstrates a lesion inside the vertebral body with surrounding edema and intact intervertebral discs. The spinal cord is not compromised. Compared to the CT in the bone-window technique (**c**), the MRI gives less accurate information as to the amount of bone destruction. The cortical destruction and moth-eaten appearance of the vertebral bone indicate a malignant tumor

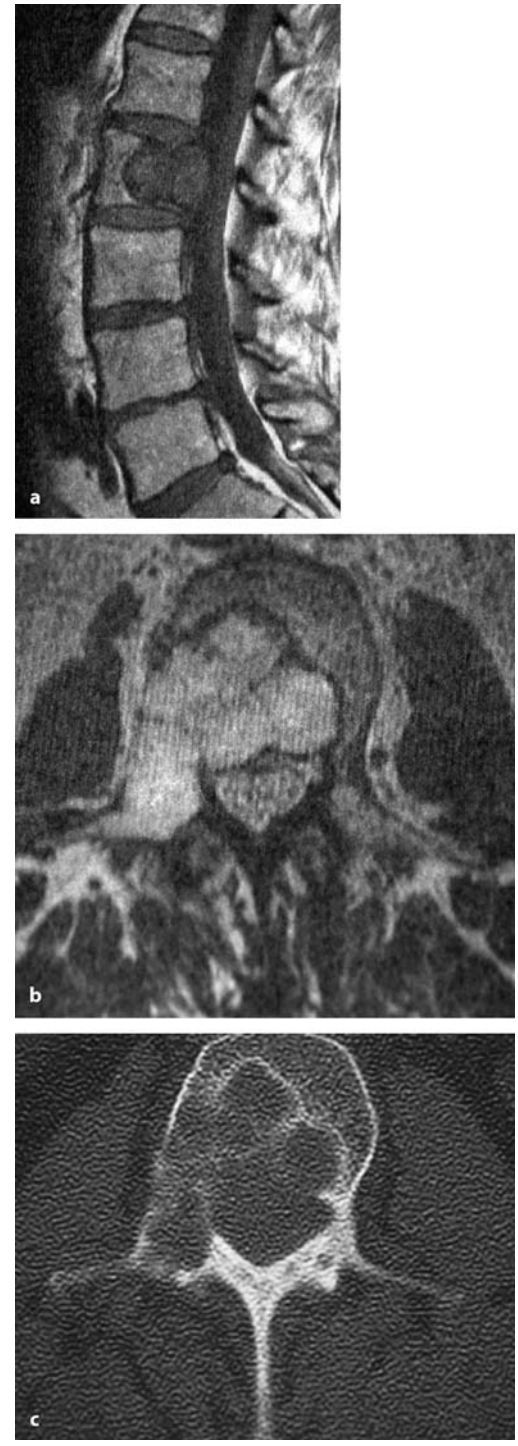

Fig. 5.18. Sagittal T1- (**a**) and axial T2-weighted (**b**) MRI scans of an intraosseous cavernoma at L2 in a 57-year-old woman with a 3-year history of back pain. Apart from the hyperdense signal intensity of this lesion in T2 and the missing edema surrounding the lesion, the cavernoma gives a similar appearance to a metastasis on MRI. **c** The CT in bone-window technique, however, indicates a small sclerotic rim and mostly preserved cortical bone around this lesion, indicating a slow-growing, benign process

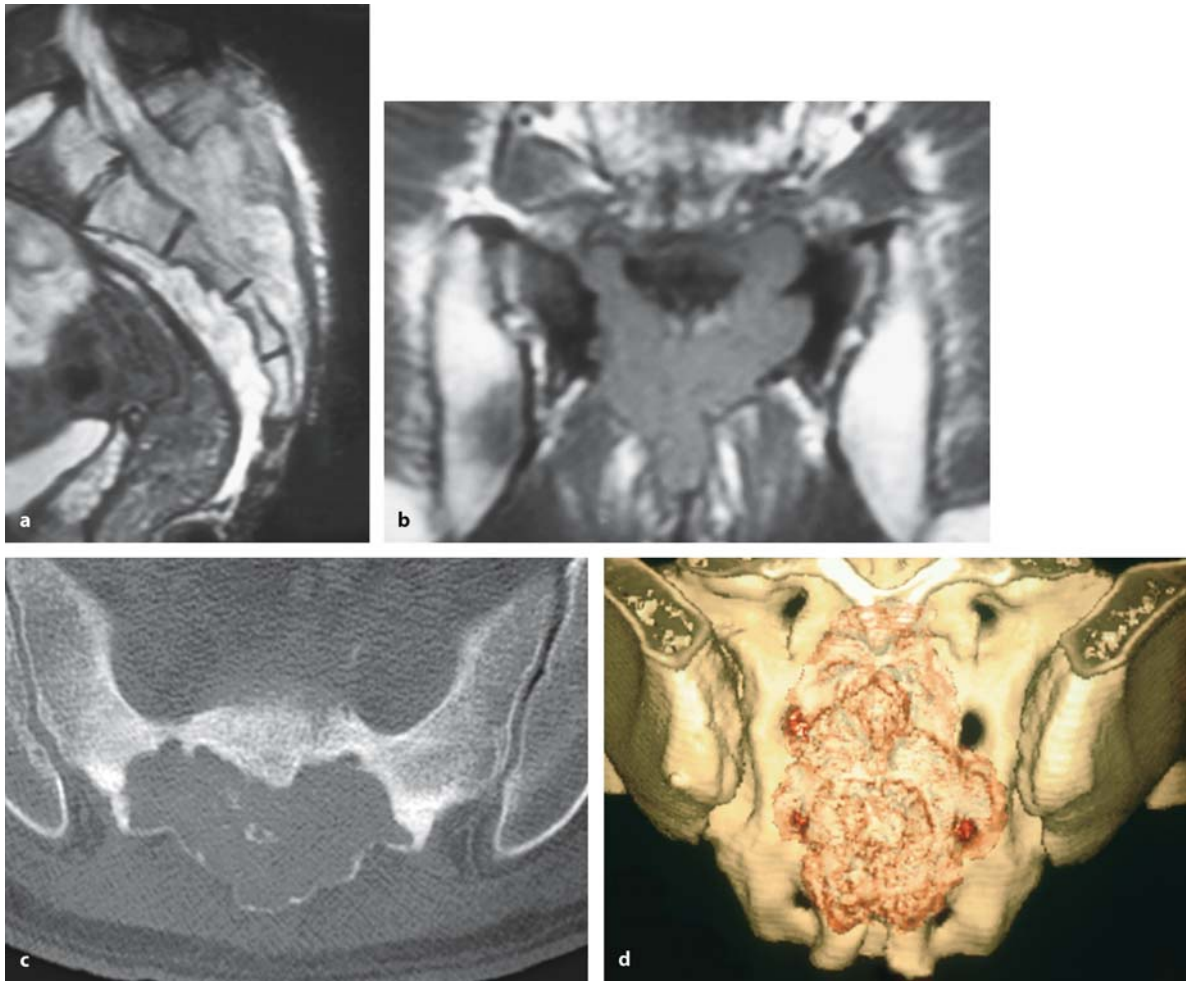

Fig. 5.19. Sagittal T2- (**a**) and coronal T1-weighted (**b**) MRI scans of a sacral infiltrative osteoblastoma in a 22-year-old patient with local pain and slight sphincter disturbances. Whereas the tumor appears well demarcated toward the bone and soft tissues on MRI, the bone-window CT (**c**) demonstrates a thin fragile capsule posteriorly. The lesion appears to be locally destructive and confined to the posterior bony elements. **d** The three-dimensional reconstruction of this tumor provides a good orientation in terms of tumor extension

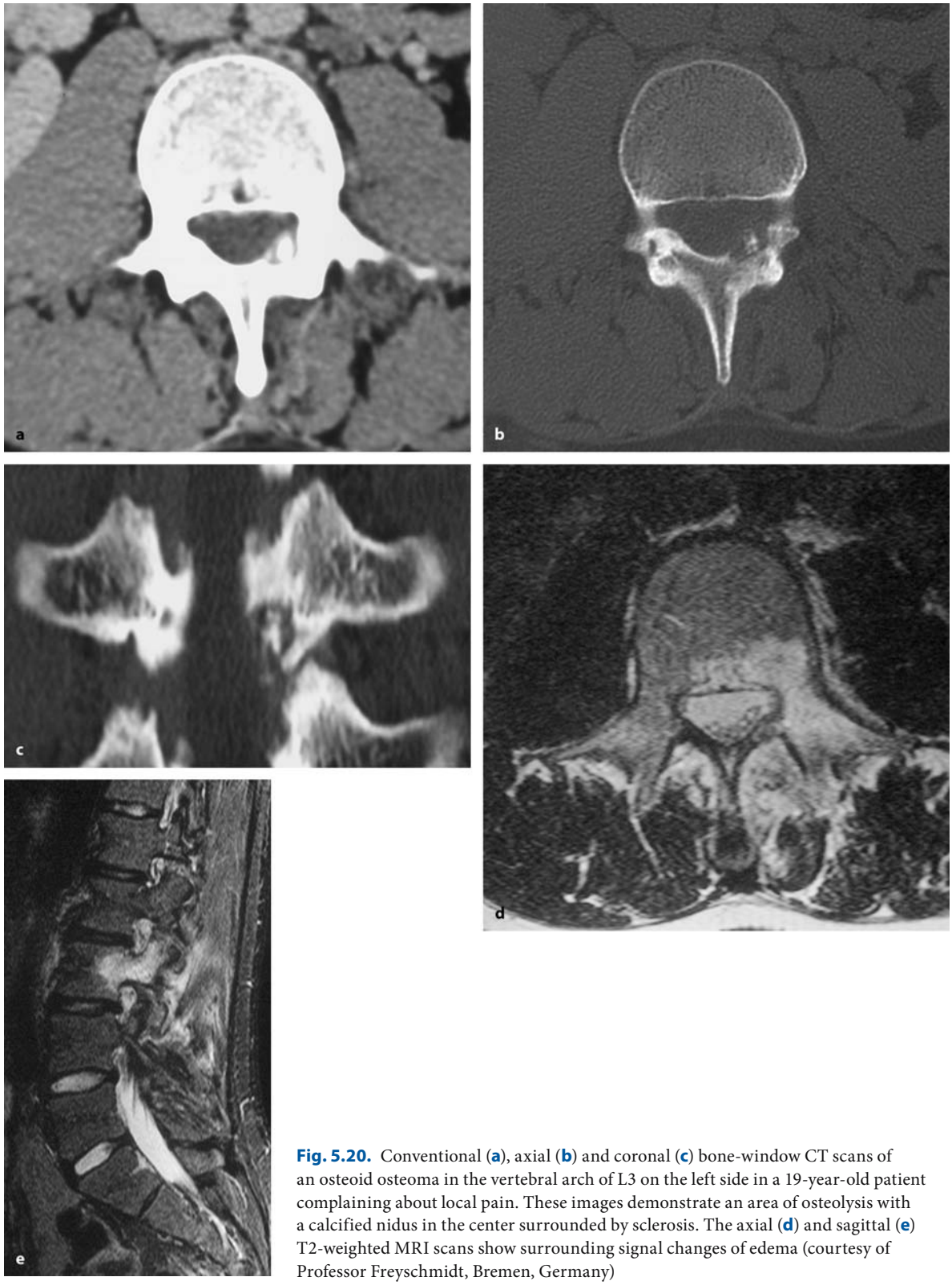

Fig. 5.20. Conventional (**a**), axial (**b**) and coronal (**c**) bone-window CT scans of an osteoid osteoma in the vertebral arch of L3 on the left side in a 19-year-old patient complaining about local pain. These images demonstrate an area of osteolysis with a calcified nidus in the center surrounded by sclerosis. The axial (**d**) and sagittal (**e**) T2-weighted MRI scans show surrounding signal changes of edema (courtesy of Professor Freyschmidt, Bremen, Germany)

Fig. 5.21. Sagittal (**a**) and axial (**b**) T2-weighted MRI scans of an aneurysmatic bone cyst at Th1 in an 11-year-old boy with local pain. The lesion affects posterior elements exclusively and displays a slightly inhomogeneous, hyperdense signal. **c** The bone-window CT image demonstrates the intraosseous localization of this lesion with a thin sclerotic rim surrounding the osteolytic process. **d** On conventional X-rays, the entire lamina appears to be missing

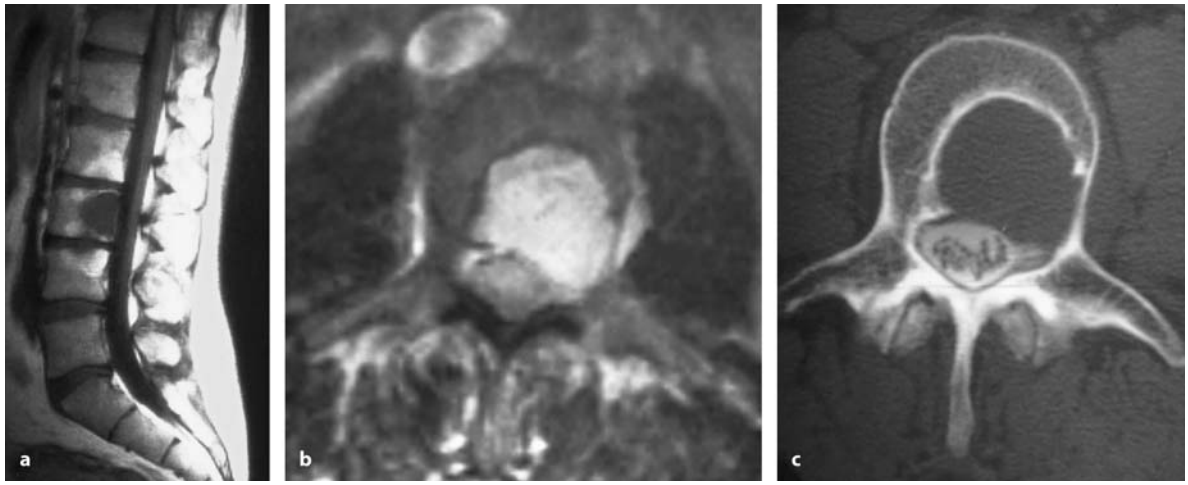

Fig. 5.22. Sagittal T1- (**a**) and axial T2-weighted (**b**) MRI scans of a chordoma at L3 in a 31-year-old man with back pain and radicular symptoms in his left leg. The MRI demonstrates a lesion confined to the vertebral body. There appears to be compression of the recessus on the left side, which explains the neurological symptoms (**b**). **c** The postmyelographic bone-window CT image displays a lytic lesion surrounded by a sclerotic rim toward the vertebral body, but with destruction of cortical bone toward the spinal canal

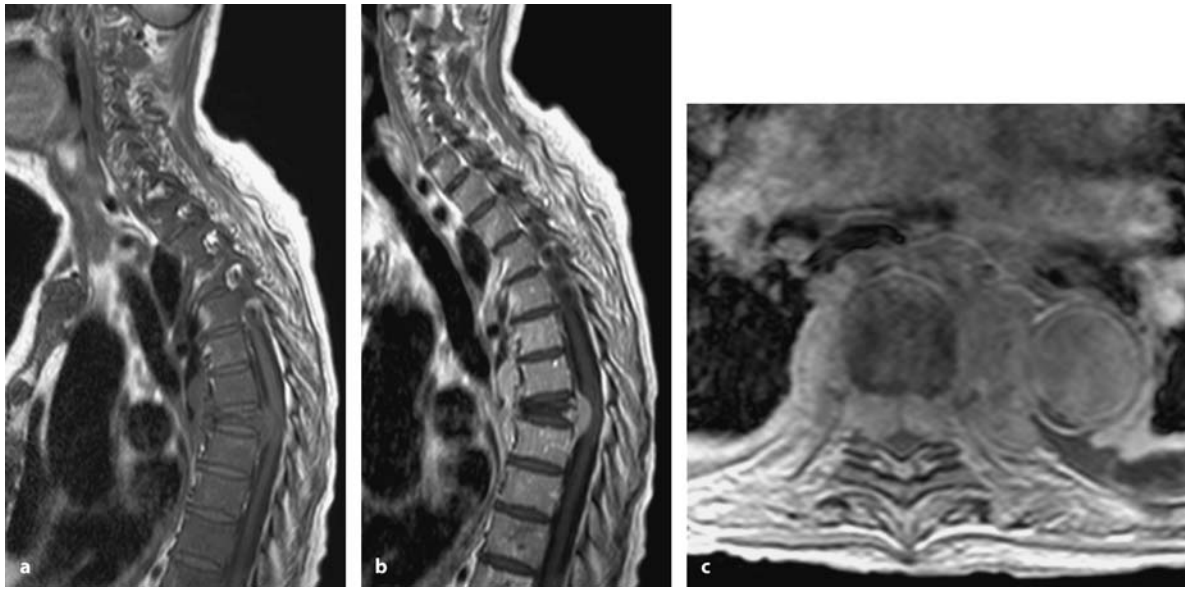

Fig. 5.23. Sagittal T1-weighted MRI scans without (**a**) and with contrast (**b**) of a breast carcinoma metastasis at Th7 in 78-year-old woman with a short history of progressive paraparesis. There is marked compression of the spinal cord by the tumor, which is aggravated by a considerable kyphosis due to collapse of the affected vertebra. **c** This axial scan demonstrates the tumor in the spinal canal extending out of both neuroforaminae into surrounding soft tissues with erosion of the aorta

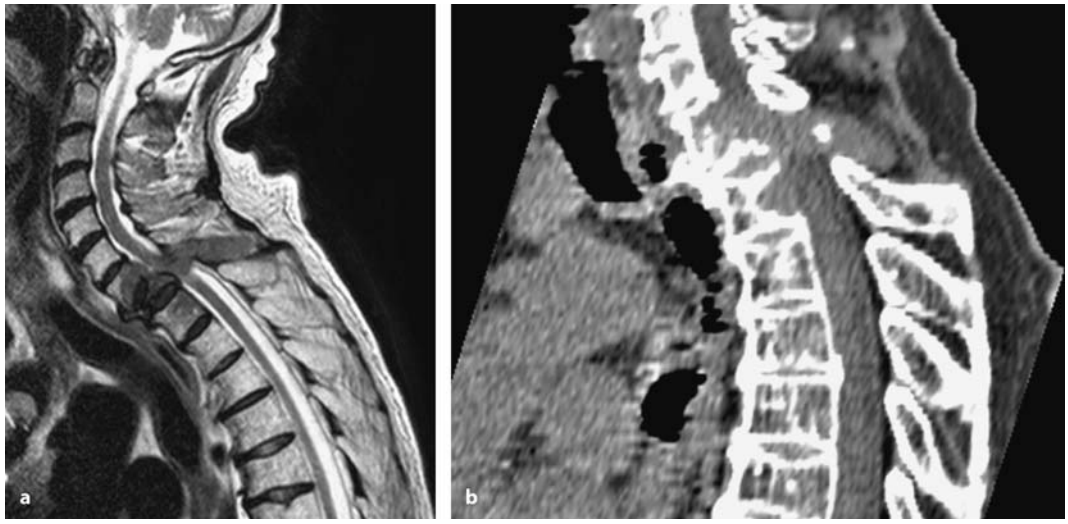

Fig. 5.24. Sagittal T2-weighted MRI scan (**a**) and CT reconstruction (**b**) of a metastasis of an unknown primary tumor at Th1 with complete destruction of Th1 including posterior elements, infiltration of C7, and luxation at C7/Th1 in a 76-year-old man with a severe paraparesis

tive tissue, which may be penetrated by small islands of tumor. Group IA describes tumors that are confined to the vertebra (Fig. 5.22) and IB those invading paravertebral structures (Fig. 5.1). Groups II and III describe high-grade malignancies. Here, the neoplastic growth is so rapid that no reactive tissue is formed around it. Confined to the vertebral body, they are classified as IIA (Fig. 5.17). On plain radiographs, such tumors are detected as radiolucent and destructive lesions and are often accompanied by pathological fractures. Spread into the epidural space may occur rapidly with continuous spreading of these tumors (IIB) (Fig. 5.23), and neoplastic satellites may be seen some distance away from the major tumor. Groups IIIA and IIIB are identical to groups IIA and IIB except for the presence of distant metastases.

Sometimes the most critical diagnostic problem to solve is the question of stability. How can or should it be defined? The most obvious signs of instability (i.e., a luxation or pathological movement on functional X-rays) may not be present or may be impossible to demonstrate. We found it useful to define instability as follows [517]:

1. Pathological movement or dislocation of vertebral bodies (Fig. 5.24).
2. Destruction of the entire vertebral body and/or intervertebral joints (Figs. 5.23–5.26).
3. Obstruction of the spinal canal by a collapsed vertebral body (Figs. 5.23 and 5.26).
4. Affection of neighboring vertebral bodies (Fig. 5.26).

The majority of primary bone tumors are malignant, especially in adults. However, a higher proportion of benign tumors are encountered in children and adolescents [94]. The Bone Tumor Registry of Westphalia, with 7400 tumors and tumor-like lesions of bone, contains among spinal tumors 135 primary neoplasms, 187 metastases, 98 plasmocytomas, and 4 lymphomas. Among adults, the commonest primary spinal bone tumor was the chordoma (35 cases), followed by osteoblastomas (16 cases) eosinophilic granulomas (16 cases), and hemangiomas (12 cases). Furthermore, ten aneurysmatic bone cysts, ten osteochondromas, seven giant cell tumors, five Ewing sarcomas, four osteogenic sarcomas, and three chondrosarcomas were counted. Secondary bone tumors (i.e., metastases) were derived mostly from breast, lung, and prostate [453]. In the clinical practice of a neurosurgeon, however, the ratio between primary and metastatic bone tumors of the spine will favor secondary bone tumors [540]. In our series, metastases accounted for 64% of all spinal bone tumors, with chordomas, chondrosarcomas, and plasmocytomas making up most of the remainder (Table 5.2).

Benezech and Fuentes [50] published a review on 206 primary bone tumors of the spine in France. In children, 45% were malignant, compared to 65% in adults. The commonest diagnoses in adults were chordomas and plasmocytomas, whereas in children osteoblastomas, aneurysmatic bone cysts, and Ewing sarcomas predominated. Furthermore, processes of vertebral bodies are more likely to be malignant than

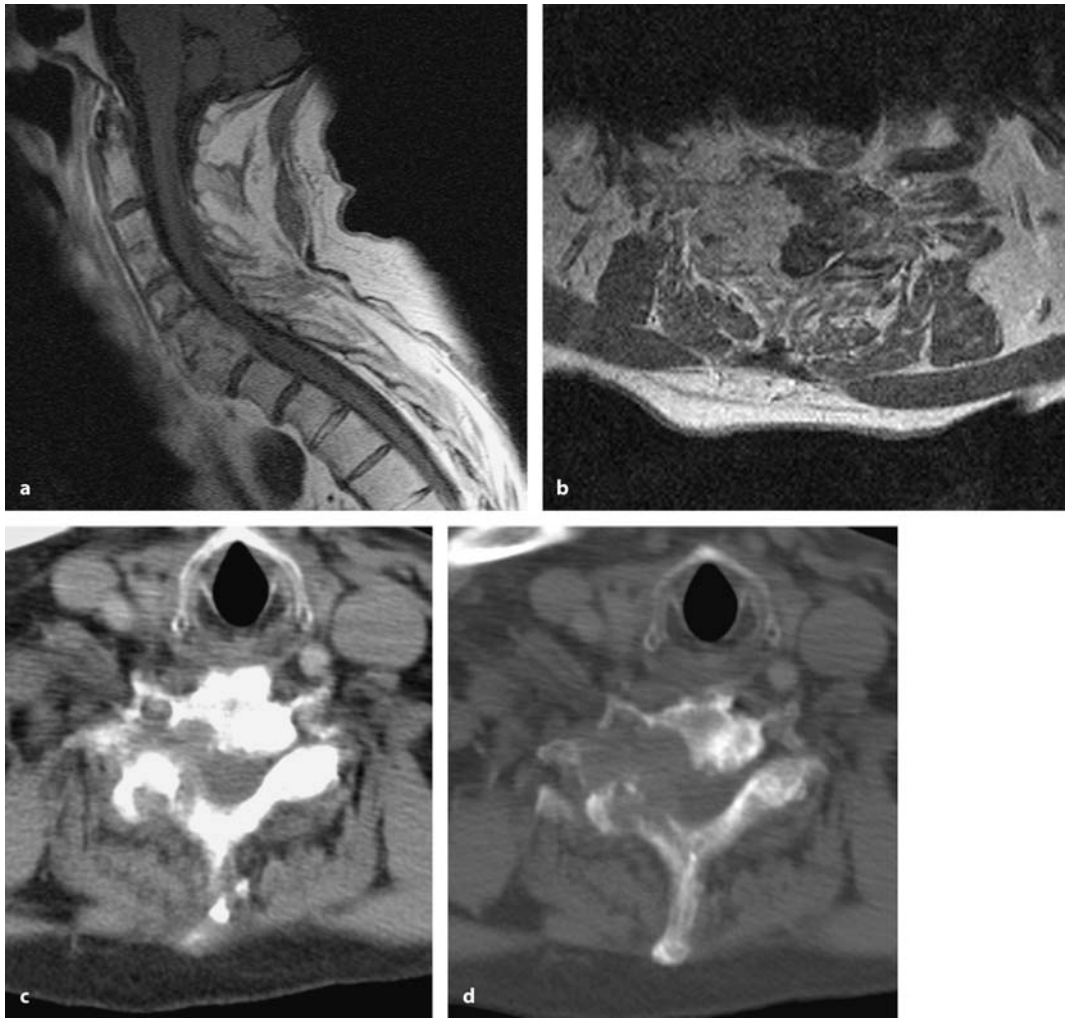

Fig. 5.25. Sagittal (**a**) and axial (**b**) T1-weighted, contrast-enhanced MRI scans of a hypernephroma metastasis at C7 in a 79-year-old man complaining of severe radicular pain. The axial image shows destruction of the right intervertebral joint. Conventional (**c**) and bone-window CT images (**d**) demonstrate the amount of bony destruction and contact with but no compromise of the right vertebral artery

tumors of posterior bone elements [521]. Neuroradiology is often not able to establish a specific diagnosis, but can distinguish between destructive and benign lesions.

Positron emission tomography (PET) can be useful whenever a tumor with high metabolic activity needs to be differentiated from reactive tissue or processes of low metabolic activity. In patients who have undergone chemotherapy or radiotherapy for malignant bone tumors, for instance, PET scans can be extremely helpful to pick up residual or recurrent tumor [521].

For hemangiomas of the vertebral body, the classical vertical striations due to thickened bone trabeculae on plain X-rays and the mineralized dots on CT should provide the diagnosis. Rarely, bone growth surrounding the hemangioma may cause spinal stenosis. On MRI, hemangiomas appear as hyperintense lesions on T1- and T2-weighted images (Fig. 5.27) [178, 321].

Aneurysmatic bone cysts appear as destructive, polycystic, expansile lesions with variable extraosseous extension surrounded by a thin capsule (Fig. 5.21) [1, 174, 272, 321, 328, 391, 435, 521, 553]. They may involve all parts of a vertebra, although anterior elements are mostly involved, and spread to neighboring bones. The intraosseous cysts may be filled with fluid [272, 321, 521, 553]. The lesion is surrounded by a thickened periosteal membrane that may enhance with gadolinium on MRI [174, 391].

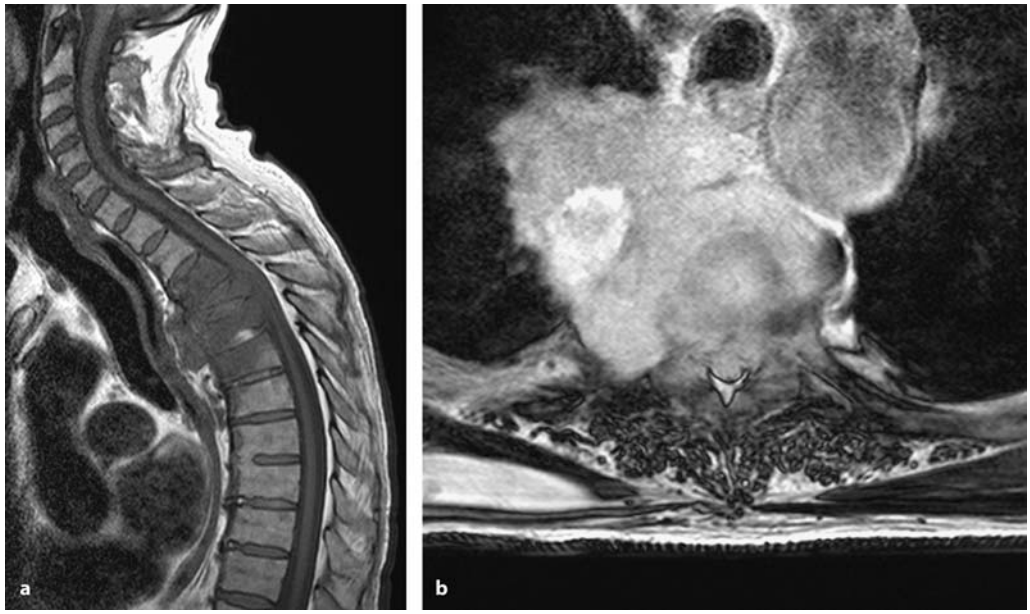

Fig. 5.26 a This sagittal T1-weighted MRI shows a metastasis of a lung carcinoma in a 75-year-old man with pain and a severe paraparesis. The vertebral bodies at Th4 and Th5 have collapsed, with considerable cord compression at Th4. Signal changes representing edema and tumor infiltration have also appeared in Th3, Th6, and Th7. **b** The axial T2-weighted image demonstrates profound extraspinal extension involving the mediastinum and right lung

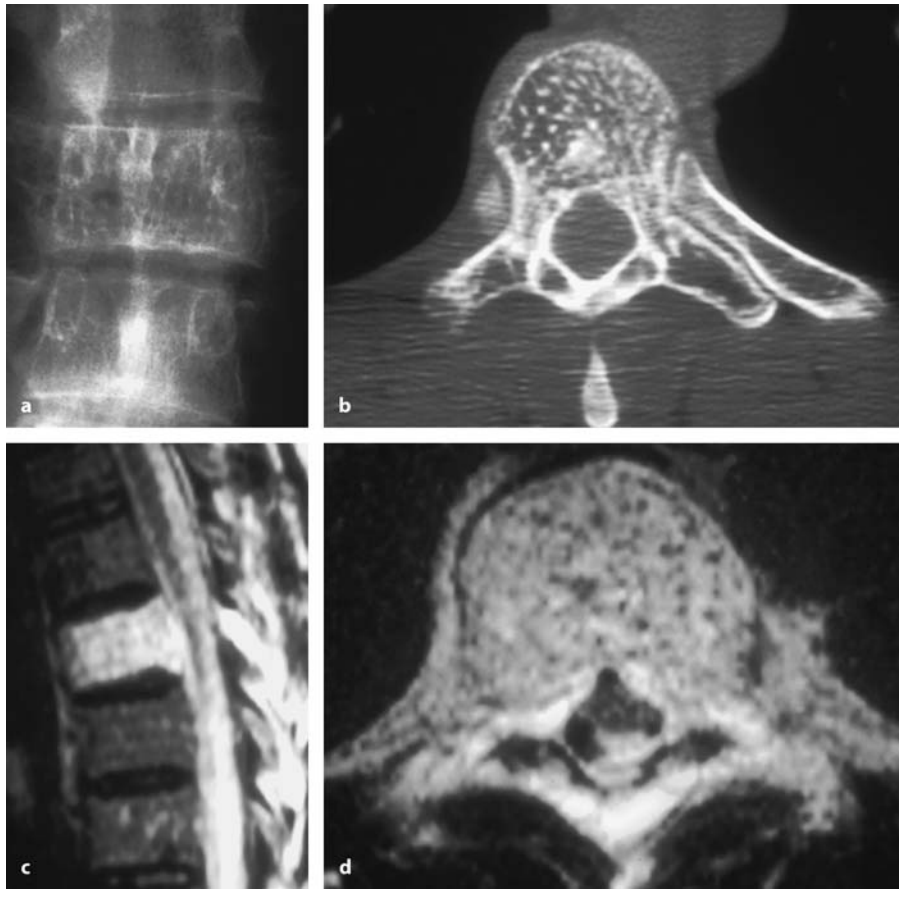

Fig. 5.27 a Spinal anterior–posterior X-ray of a vertebral hemangioma at Th6 in a 34-year-old man with back pain. The vertebral body displays vertical sclerotic signal changes as a result of the thickened trabecula. **b** The bone-window CT is pathognomonic for this entity, showing these trabeculae as mineralized dots. The sagittal (**c**) and axial (**d**) T2- weighted MRI scans demonstrate a hyperdense signal pattern. The bone trabeculae appear as dark dots on the axial image

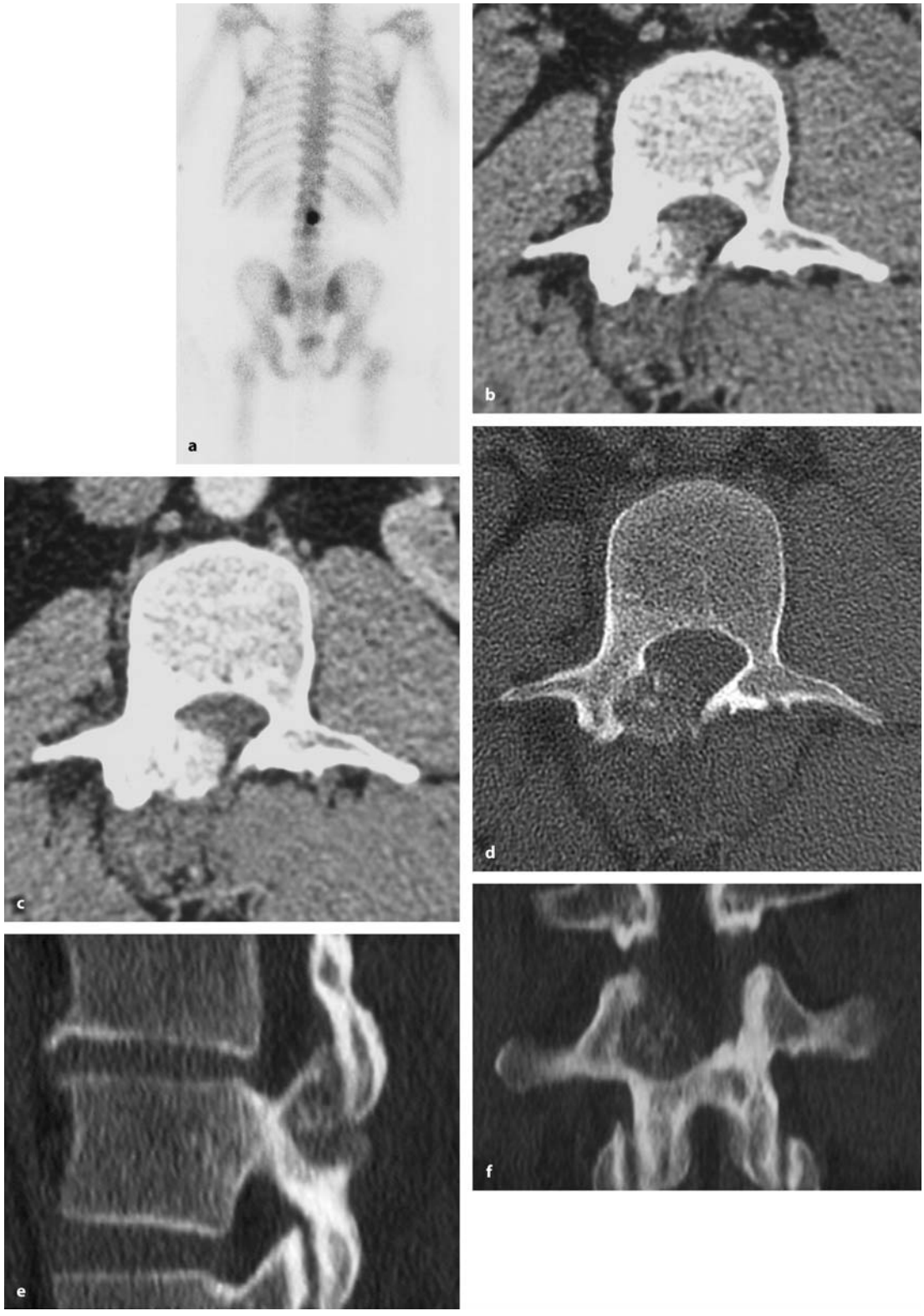

Fig. 5.28. a Bone scintigraphy of a 32-year-old man with a history of severe back pain. It shows a hot spot at L2. The native (**b**) and contrast (**c**) CT scans demonstrate a lytic, partly calcified expansile lesion in the lamina on the right side with bright enhancement. The axial scan (**d**), and sagittal (**e**) and coronal (**f**) reconstructions made using the bone-window technique show that these calcifications are confined to the center of the lesion. The histology disclosed an osteoblastoma (courtesy of Professor Freyschmidt, Bremen, Germany)

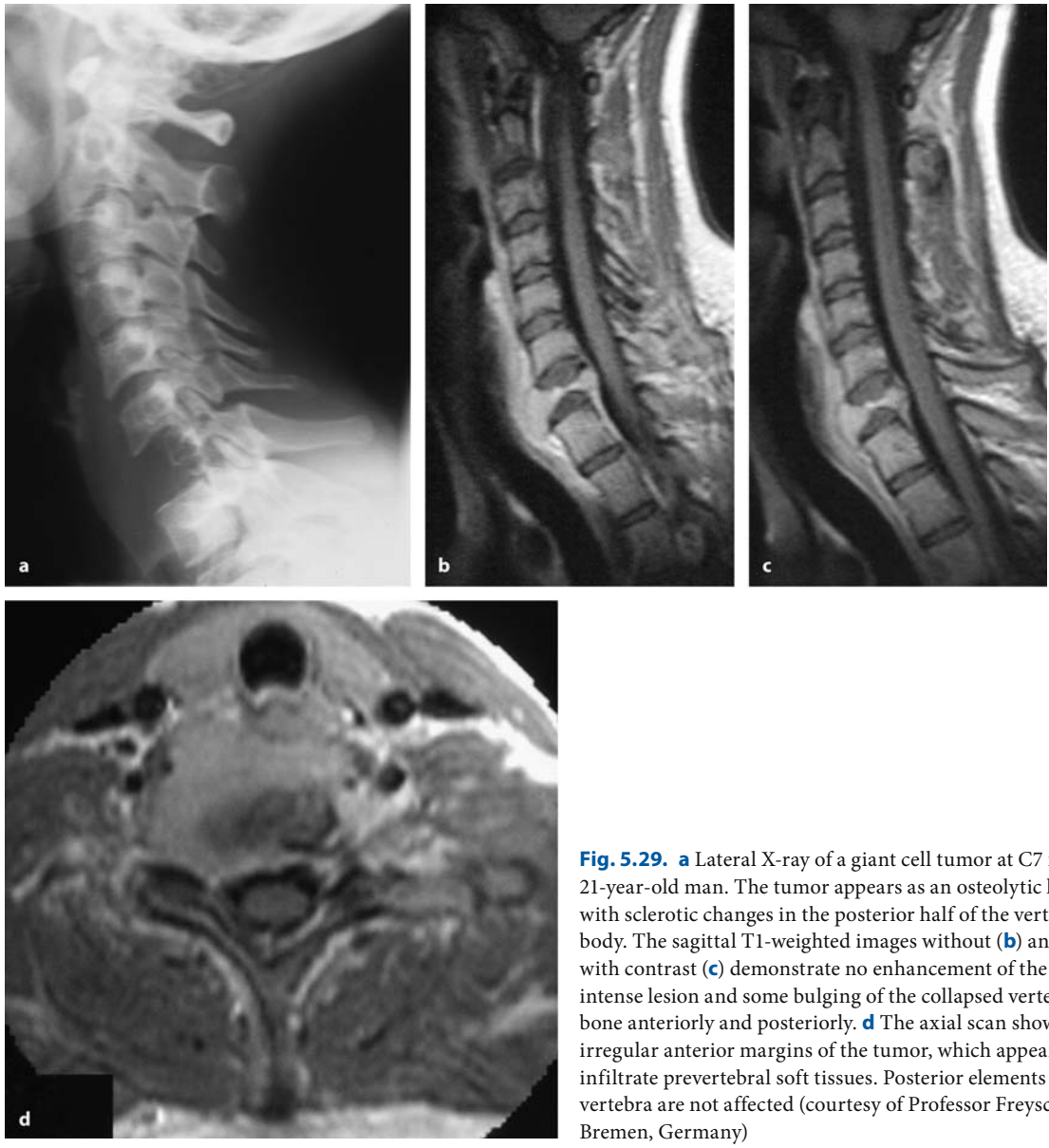

Fig. 5.29. **a** Lateral X-ray of a giant cell tumor at C7 in a 21-year-old man. The tumor appears as an osteolytic lesion with sclerotic changes in the posterior half of the vertebral body. The sagittal T1-weighted images without (**b**) and with contrast (**c**) demonstrate no enhancement of the hyperintense lesion and some bulging of the collapsed vertebral bone anteriorly and posteriorly. **d** The axial scan shows irregular anterior margins of the tumor, which appears to infiltrate prevertebral soft tissues. Posterior elements of the vertebra are not affected (courtesy of Professor Freyschmidt, Bremen, Germany)

Osteoblastomas are benign tumors that may displace bony structures and grow into neighboring soft tissues [521]. Spinal forms predominantly affect posterior elements (Fig. 5.28) [205]. According to their biological behavior, radiological appearances may be quite variable [205, 397]. On conventional X-rays they often give a cloudy, patchy, bone-expanding image with a slight sclerotic rim [174, 205, 326, 391, 397, 488] and multiple calcifications [321]. In other instances, they may appear as pure lytic lesions or present ill-defined margins with soft-tissue extension (Fig. 5.19) [76, 174, 205, 391, 397]. On MRI, the tumor is hypodense on T1- and T2-weighted images [488], or is described as hypo- to isodense on T1-, and iso- to hyperdense on T2-weighted images [205] and shows slight enhancement with contrast [404, 488]. The surrounding bone marrow also may demonstrate some contrast enhancement due to edema [205, 404, 488] that does not correspond to the degree of tumor extension. Therefore, MRI may not be the most accurate imaging modality to define tumor extension, so that CT is still the best imaging method for this entity [488]. Angiography may be helpful to demonstrate the high vascularity of this tumor [55] and can be combined with embolization. Half of these patients present with a painful scoliosis [521].

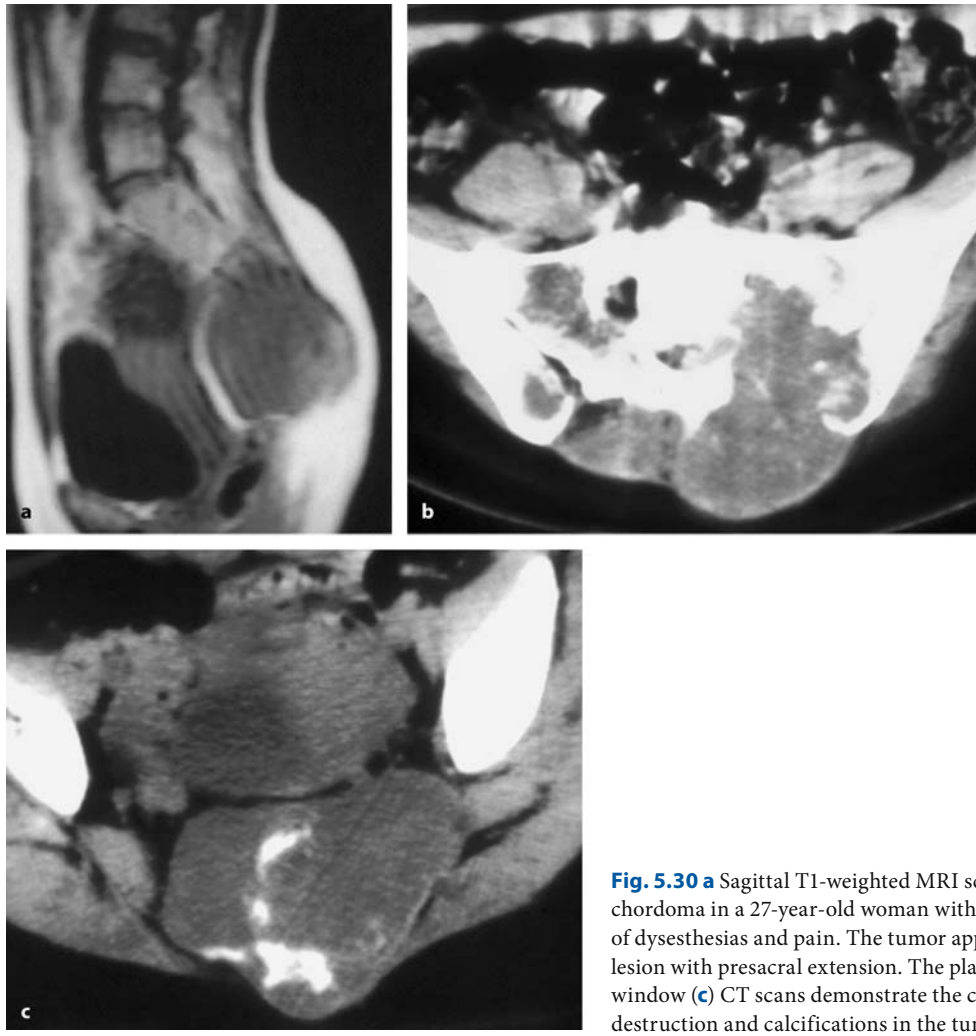

Fig. 5.30 a Sagittal T1-weighted MRI scan of a sacral chordoma in a 27-year-old woman with a 4-month history of dysesthesias and pain. The tumor appears as a greyish lesion with presacral extension. The plain (**b**) and bone-window (**c**) CT scans demonstrate the considerable bone destruction and calcifications in the tumor mass

Giant cell tumors characteristically appear as expansile, lytic, bone-destroying lesions in the anterior elements of the spine (Fig. 5.29) [174, 321, 391, 521]. Mineralizations are not a feature of spinal giant cell tumors. Vertebral collapse and paraspinal soft-tissue extensions are not uncommon. In the sacrum, tumors may cross the sacroiliac joint and disc space. On CT, the tumor may be well defined with a sclerotic rim. Due to tumor hemorrhages, cysts, and areas of necrosis, variable signal intensities may appear on CT and MRI. Due to the collagen content of the tumor, signal intensities may resemble soft-tissue signals [174, 321, 391]. However, differentiation between a malignant tumor and a giant cell tumor may be impossible radiographically.

As far as malignant tumors are concerned, the differentiation between different histological types is limited to a few specific entities. Chordomas are derived from remnants of the notochord. They occur in the clivus, sphenoorbital region, or spine. Most spinal chordomas are encountered in the sacrum (Fig. 5.30). Other vertebrae are rarely affected (Fig. 5.22). Chordomas are midline tumors and their radiological appearance is indistinguishable from chondrosarcomas unless the tumor is located laterally. Chondrosarcomas tend to affect posterior elements more often than chordomas. Chordomas and chondrosarcomas cause lytic, destructive bone lesions with mottled calcifications and additional soft-tissue involvement on CT (Figs. 5.31 and 5.32) [174, 232, 316, 321, 391, 507]. On MRI, both are characterized by a contrast-enhancing capsule and an almost isointense signal of the tumor mass on T1-weighted images, which to a large degree consists of a mucoid, greyish substance, and criss-crossing fibrous septa. They display a high signal intensity on T2-weighted images due to the high fluid

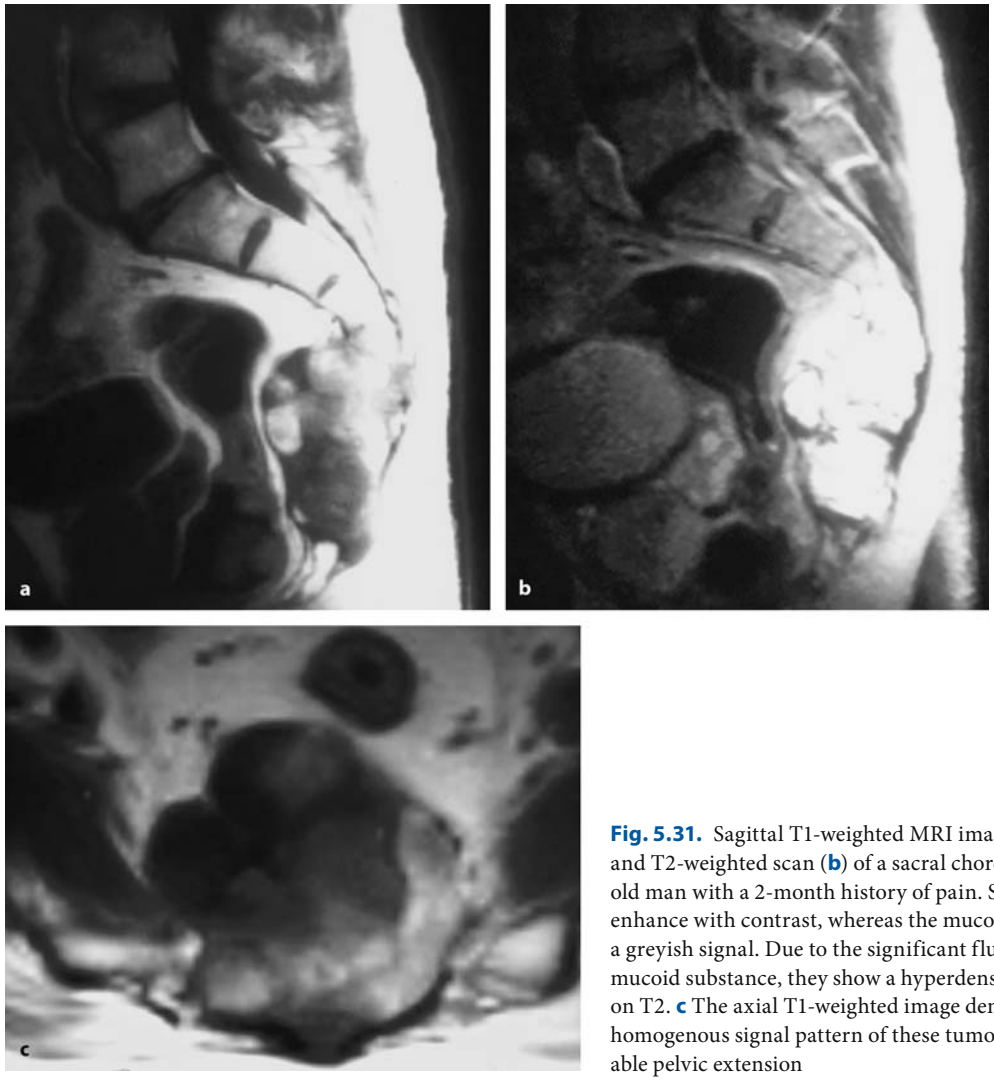

Fig. 5.31. Sagittal T1-weighted MRI image with contrast (**a**) and T2-weighted scan (**b**) of a sacral chordoma in a 62-year-old man with a 2-month history of pain. Solid tumor parts enhance with contrast, whereas the mucoid material displays a greyish signal. Due to the significant fluid content of the mucoid substance, they show a hyperdense signal intensity on T2. **c** The axial T1-weighted image demonstrates the inhomogenous signal pattern of these tumors and the considerable pelvic extension

content. Chordomas and chondrosarcomas may cross the intervertebral disc space to invade neighboring vertebrae (Figs. 5.30–5.32) [174, 321, 391, 507, 523]. Chondrosarcomas present as destructive spine lesions commonly associated with a paraspinal mass, with calcifications that may grow to enormous sizes (Fig. 5.32) [521].

Plasmocytomas typically show up as lytic lesions on plain X-rays. They may appear as round patchy lesions on MRI with a low signal intensity on T1-weighted images and a bright signal on T2 weighted images. Curvilinear low signal-intensity structures may extend through the affected vertebra, representing thickened cortical bone displaced by the slow-growing tumor. The adjacent bone marrow may appear with reduced signal intensity (Fig. 5.33) [310, 550].

Osteogenic sarcomas may appear as sclerotic, mineralized (Fig. 5.34) or – in rarer instances - lytic lesions [249, 281, 315, 321, 431, 521]. The vertebral body is involved in 90% of cases, and pathological fractures have been observed. In the mobile spine, however, it is mainly the posterior elements that are affected (Fig. 5.35) [249]. On MRI, the amount of mineralization determines the signal pattern of the tumor. With nonmineralized tumors having a low signal intensity on T1-weighted images and a high signal intensity on T2-weighted images. With mineralized tumors, dark signals are typical on all images [521]. Vertebral body collapse is quite common, with sparing of the neighboring intervertebral discs [391].

Ewing sarcomas display a moth-eaten appearance of irregular bone destruction with poorly defined margins [521], but often also display osseous expan-

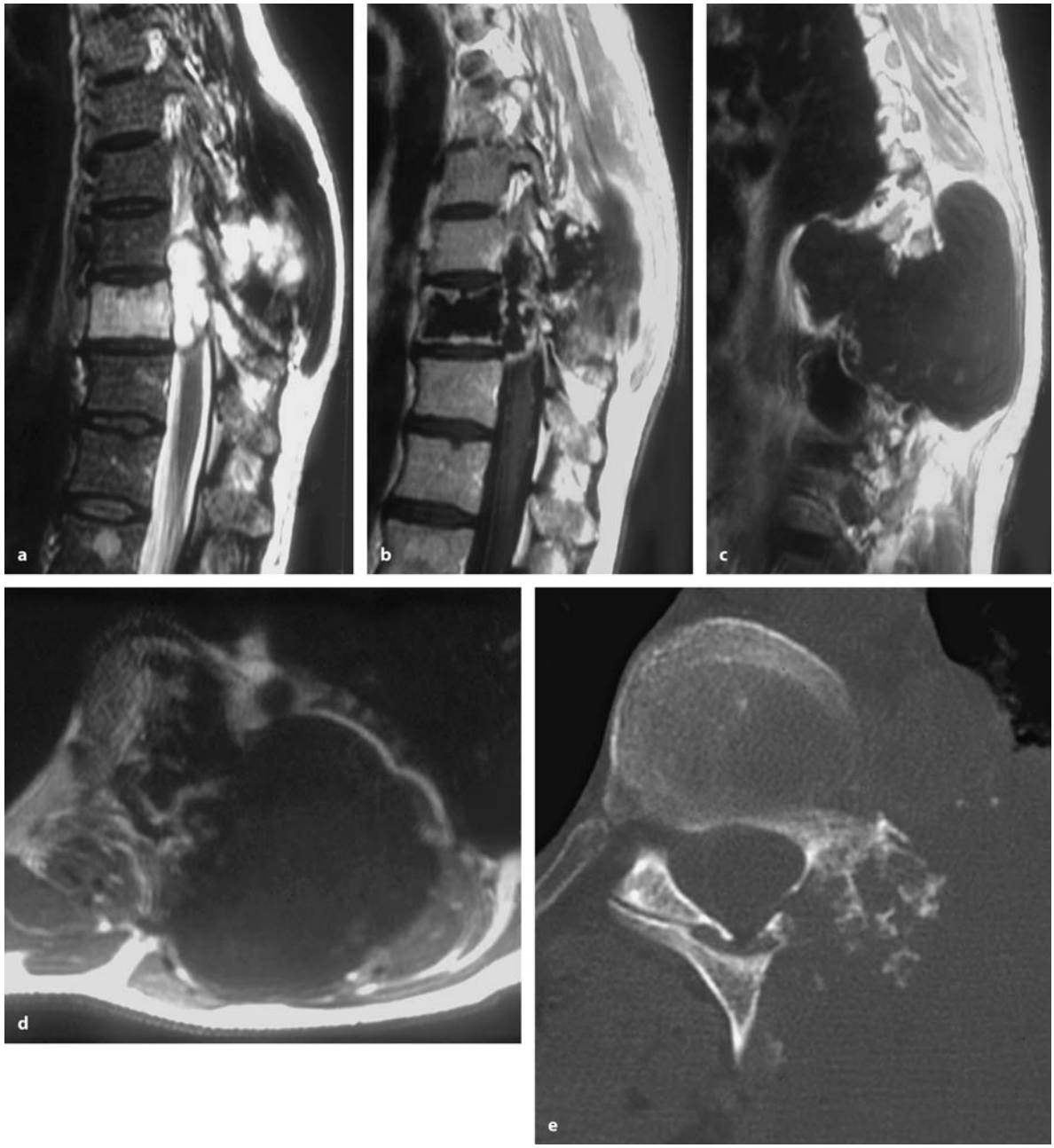

Fig. 5.32 a Sagittal T2-weighted MRI scan of a chondrosarcoma at Th10 in a 43-year-old man with slight sensory changes in his legs. This image demonstrates a hyperdense signal of the entire vertebral body and a cystic-appearing intraspinal lesion with extraspinal extension into the posterior soft tissues. **b** The corresponding T1-weighted, contrast-enhanced scan shows enhancement along the margins of this tumor. The paramedian sagittal (**c**) and the axial (**d**) scan demonstrate the huge extraspinal extension of this mostly cystic-appearing tumor on the left side. **e** The bone-window CT shows calcifications in the solid part of the tumor in the left pedicle and left part of the lamina of Th10

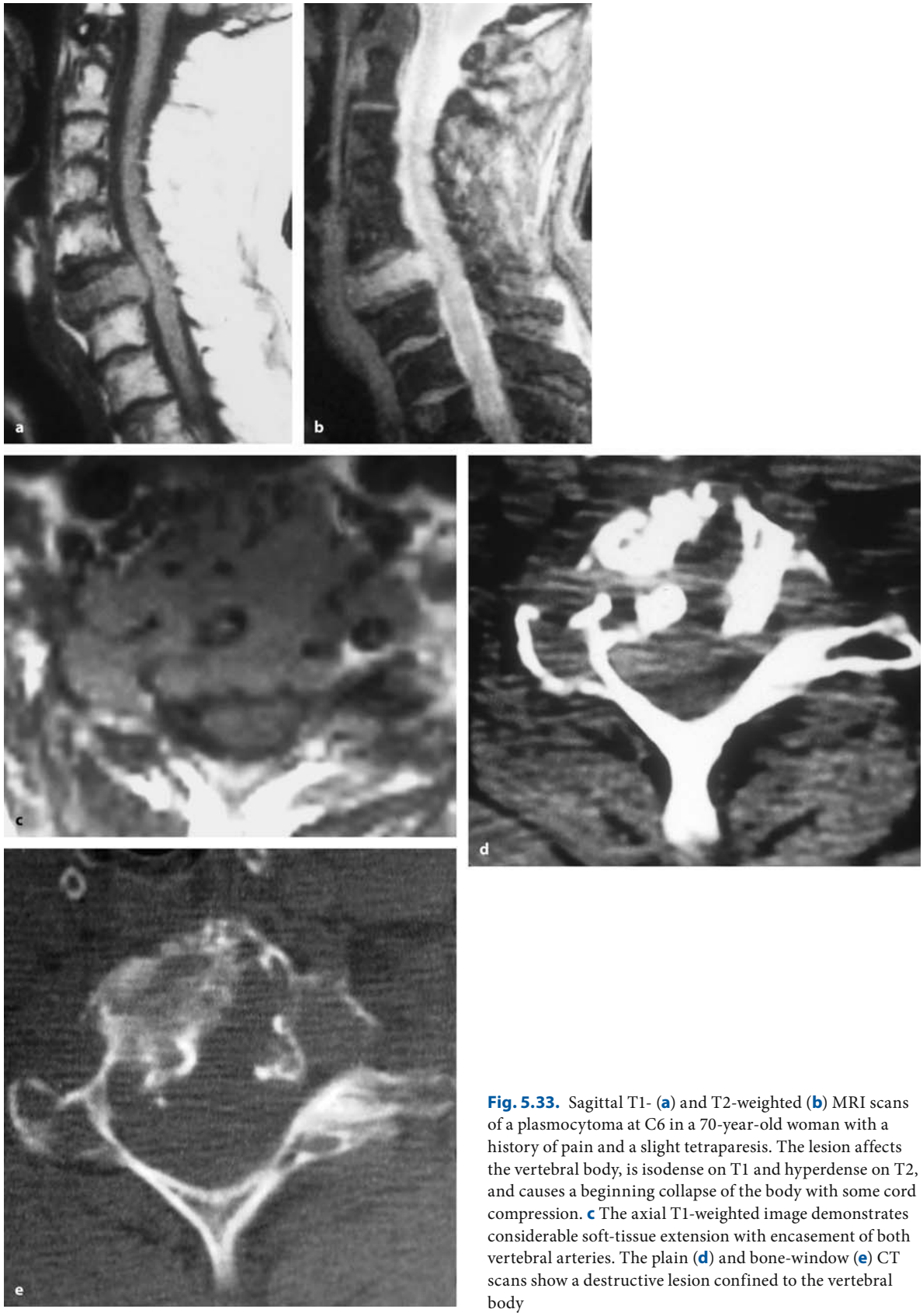

Fig. 5.33. Sagittal T1- (**a**) and T2-weighted (**b**) MRI scans of a plasmocytoma at C6 in a 70-year-old woman with a history of pain and a slight tetraparesis. The lesion affects the vertebral body, is isodense on T1 and hyperdense on T2, and causes a beginning collapse of the body with some cord compression. **c** The axial T1-weighted image demonstrates considerable soft-tissue extension with encasement of both vertebral arteries. The plain (**d**) and bone-window (**e**) CT scans show a destructive lesion confined to the vertebral body

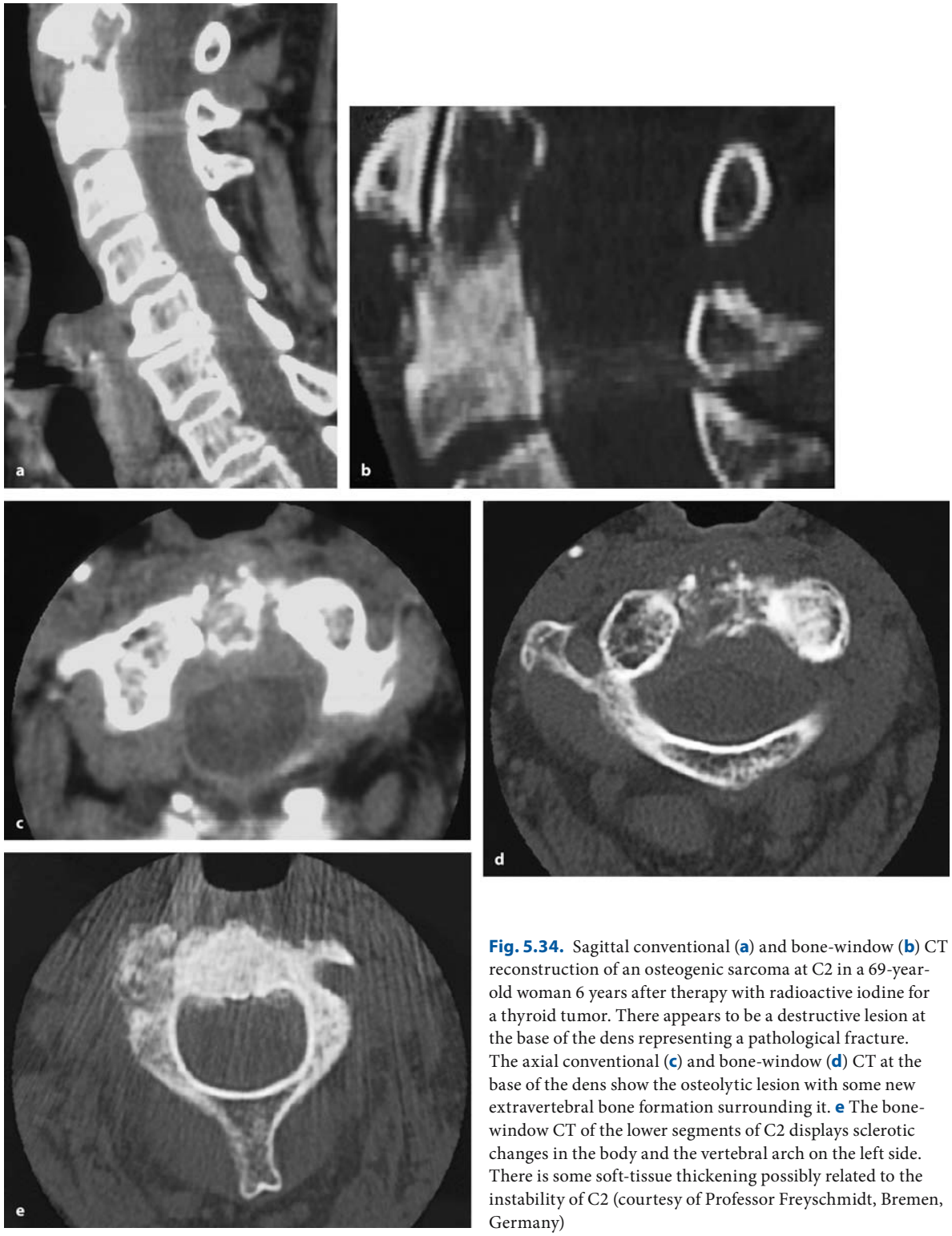

Fig. 5.34. Sagittal conventional (**a**) and bone-window (**b**) CT reconstruction of an osteogenic sarcoma at C2 in a 69-year-old woman 6 years after therapy with radioactive iodine for a thyroid tumor. There appears to be a destructive lesion at the base of the dens representing a pathological fracture. The axial conventional (**c**) and bone-window (**d**) CT at the base of the dens show the osteolytic lesion with some new extravertebral bone formation surrounding it. **e** The bone-window CT of the lower segments of C2 displays sclerotic changes in the body and the vertebral arch on the left side. There is some soft-tissue thickening possibly related to the instability of C2 (courtesy of Professor Freyschmidt, Bremen, Germany)

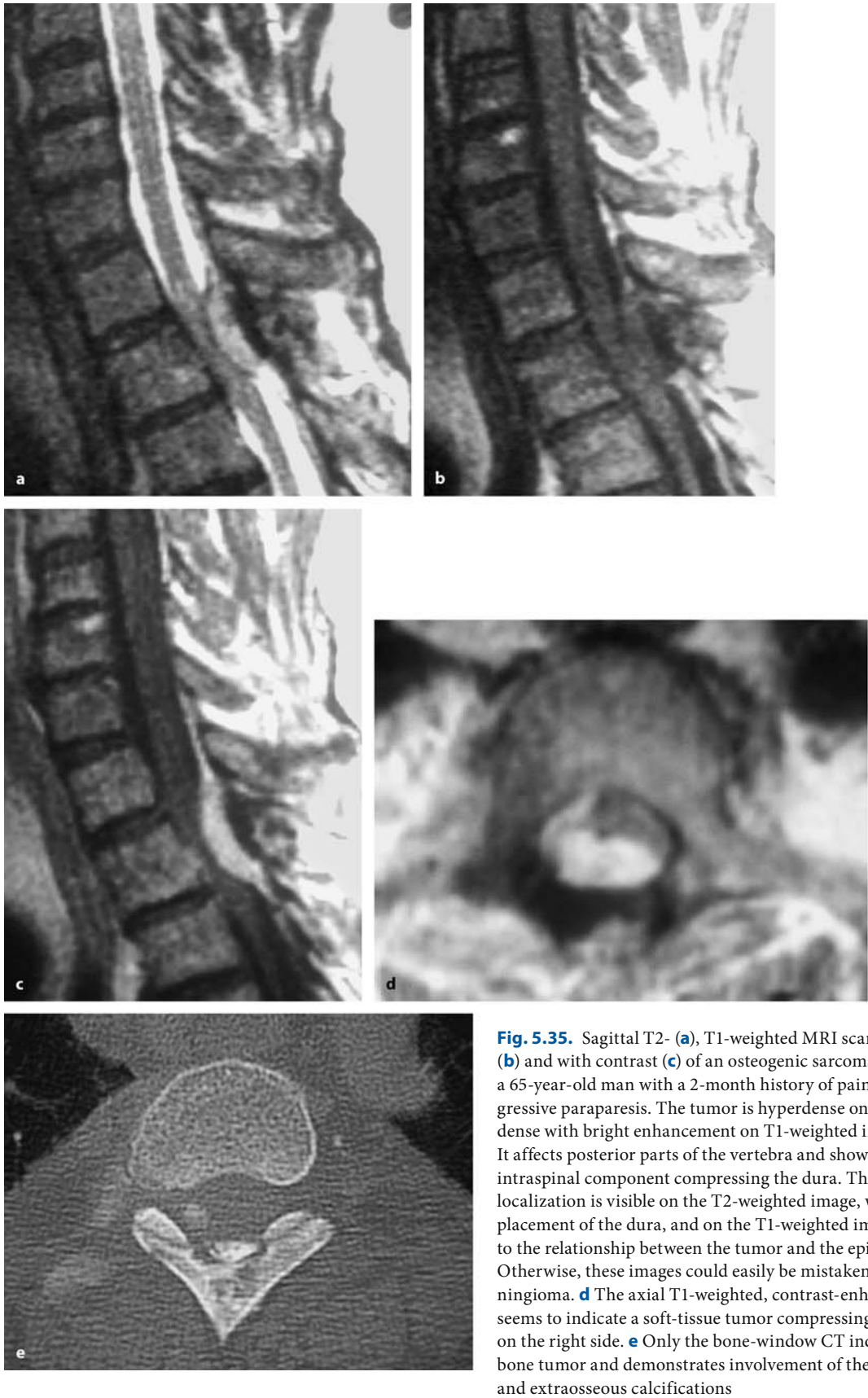

Fig. 5.35. Sagittal T2- (**a**), T1-weighted MRI scans without (**b**) and with contrast (**c**) of an osteogenic sarcoma at Th1 in a 65-year-old man with a 2-month history of pain and progressive paraparesis. The tumor is hyperdense on T2-, isodense with bright enhancement on T1-weighted images. It affects posterior parts of the vertebra and shows a large intraspinal component compressing the dura. The extradural localization is visible on the T2-weighted image, with displacement of the dura, and on the T1-weighted image due to the relationship between the tumor and the epidural fat. Otherwise, these images could easily be mistaken for a meningioma. **d** The axial T1-weighted, contrast-enhanced scan seems to indicate a soft-tissue tumor compressing the dura on the right side. **e** Only the bone-window CT indicates a bone tumor and demonstrates involvement of the lamina and extraosseous calcifications

Fig. 5.36. Sagittal T1- (**a**) and T2-weighted (**b**) MRI scans of a Ewing sarcoma at Th1 in a 26-year-old man with a 4-week history of pain and progressive paraparesis. The tumor appears with varying signal intensity on T1- and T2-weighted images. **c** The axial T1-weighted, contrast-enhanced image shows a patchy enhancement of the tumor inside the vertebral body. **d** This bone-window CT demonstrates the destruction of the body and signal changes in the lamina indicating the beginning affection of the posterior elements

sion and sclerosis on plain X-rays (Fig. 5.36) [174]. Paraspinal extensions may be quite extensive [174, 321, 391].

Spinal metastases grow infiltrative and destroy bone. On conventional X-rays and CT they may appear either as lytic (Fig. 5.37) or sclerotic lesions (Fig. 5.38). In most instances, the metastasis develops in the vertebral body extending toward the pedicles. Therefore, a good screening method for spinal metastases is to look for destruction of the pedicle, paraspinal shadows, and vertebral body collapse on conventional anterior–posterior X-rays (Fig. 5.39) [94, 261]. On MRI, most take up gadolinium peripherally, with somewhat less uptake in the center of the tumor due to inhomogeneous vascularization or necrosis (Fig. 5.23). Others demonstrate homogenous enhancement (Fig. 5.25). In a study of 100 patients with spinal metastases and spinal cord compression, 43 had compression at multiple levels. Isolated involvement of a vertebral body was seen in just 4% of vertebrae, while anterolateral compression occurred in 14% and a more or less circumferential encasement of

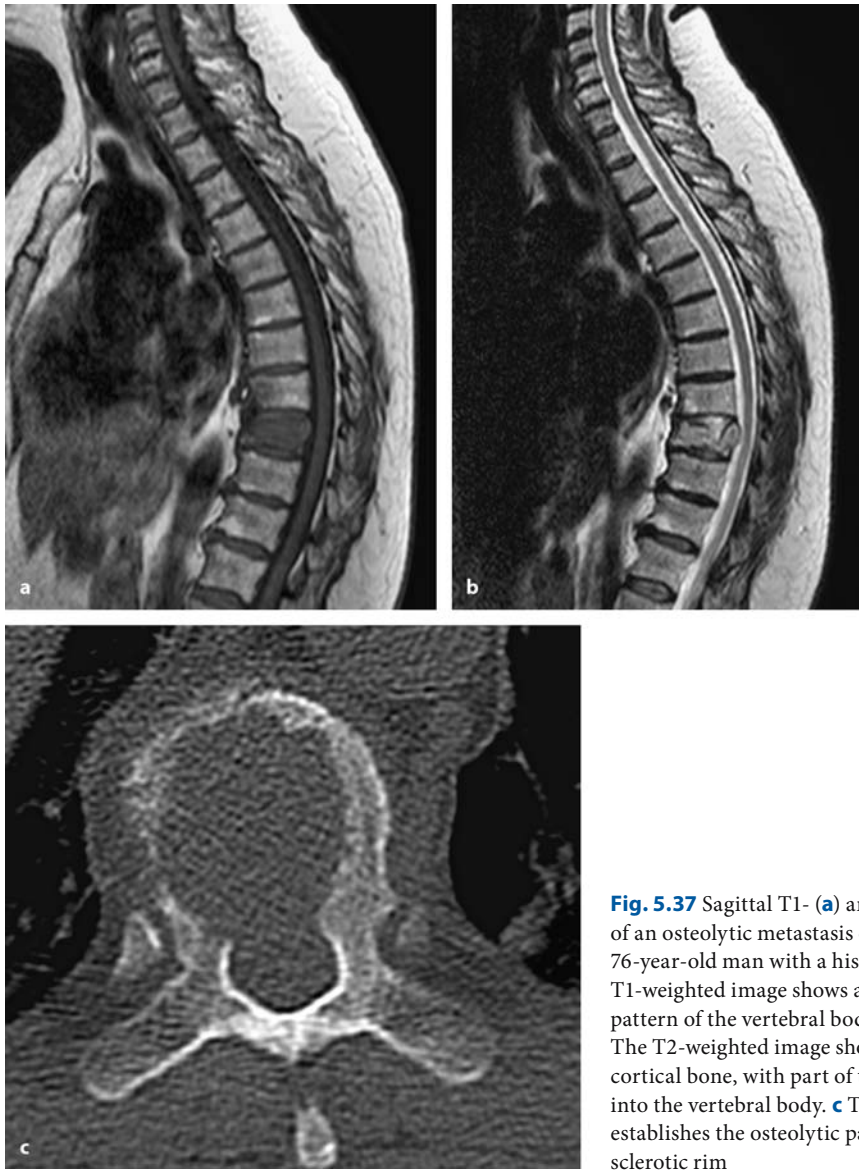

Fig. 5.37 Sagittal T1- (**a**) and T2-weighted (**b**) MRI scans of an osteolytic metastasis of a colon carcinoma at Th9 in a 76-year-old man with a history of local back pain. The T1-weighted image shows a homogenous, isodense signal pattern of the vertebral body and a slight loss of height. The T2-weighted image shows a fracture of the upper cortical bone, with part of the intervertebral disc herniating into the vertebral body. **c** The bone-window CT clearly establishes the osteolytic pattern of this metastasis with no sclerotic rim

Fig. 5.38 a Sagittal T2-weighted MRI scan of a breast carcinoma metastasis at Th5 in a 75-year-old woman with a short history of rapidly progressive paraparesis. The vertebral body has collapsed leading to a subluxation of Th4/5. **b** This axial T1-weighted scan demonstrates tumorous involvement of the entire vertebra and marked cord compression. **c** The plain CT scan demonstrates a sclerotic tumor

the dural sac was seen in 82%; 51% of these vertebrae were fractured [284].

The most important differential diagnoses for a malignant bone tumor are spinal abscesses and osteoporotic fractures. MRI and CT features of an abscess are virtually identical to those of a malignant bone tumor and quite often only systemic symptoms suggesting a septic lesion or a history of a previous intervention provides the decisive clue. However, prominent signal changes in a somewhat widened disc space may point toward spondylodiscitis, and a diffuse surrounding soft-tissue swelling may indicate the inflammatory reaction (Fig. 5.40). Osteoporotic vertebral fractures (Fig. 5.41) can look very similar to a collapsed metastatic vertebra (Fig. 5.39). Features pointing to the correct diagnosis are osteoporotic changes in other levels, the lack of a soft-tissue component, a vacuum phenomenon on CT, fluid signs on MRI, and different signal patterns related to the healing process on repeated MRI scans [44, 45] (Fig. 5.41). However, in selected patients it may be impossible to exclude a metastasis in a patient with an assumed osteoporotic fracture. Another important differential diagnosis for a malignant bone tumor is a vertebral necrosis, which may be observed after previous radiotherapy (Fig. 5.42). Other osseous lesions of the spine, such as ossifications of the posterior longitudinal ligament (Fig. 5.43) or exostoses (Fig. 5.44), should pose no diagnostic problems.

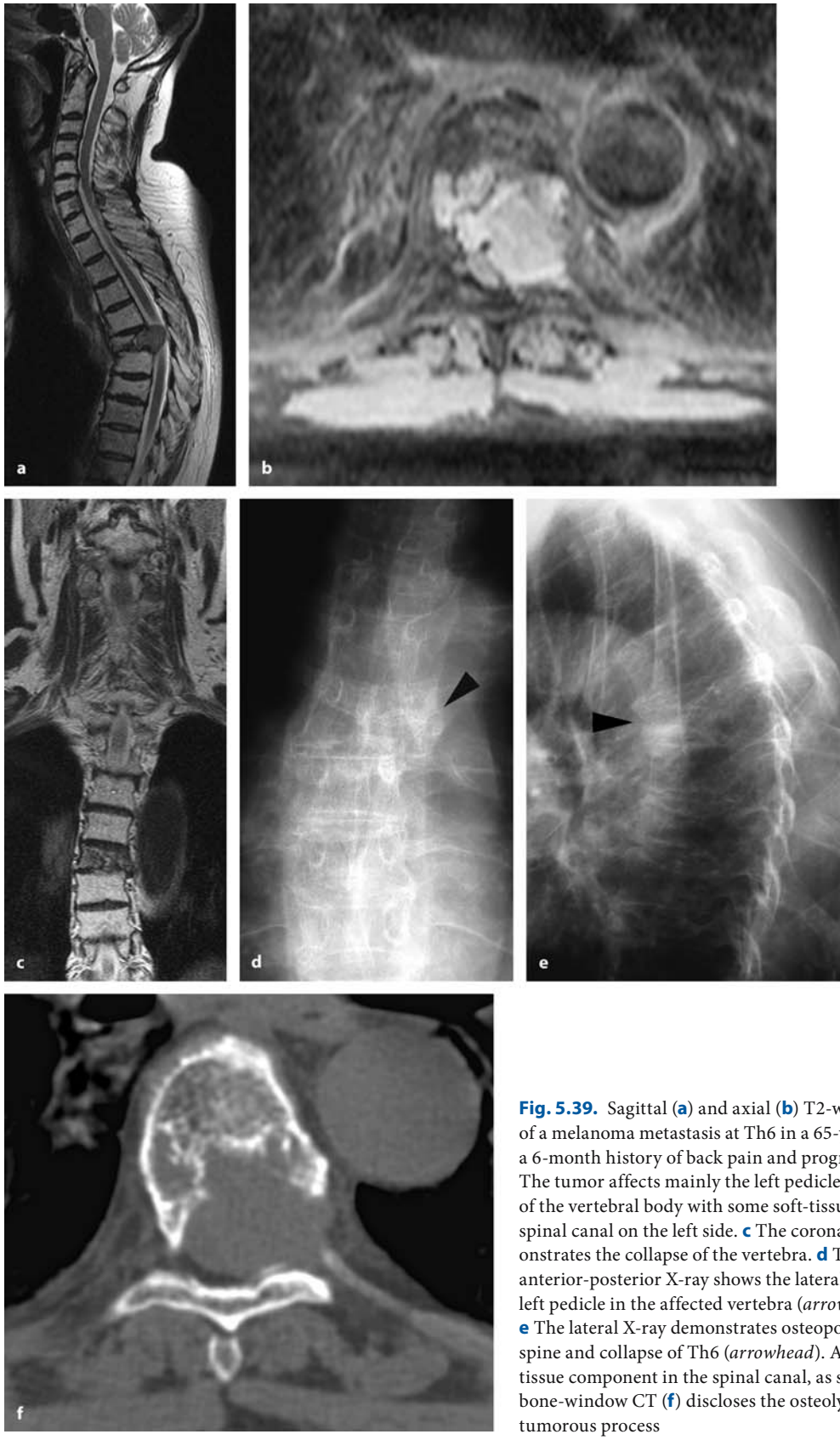

Fig. 5.39. Sagittal (**a**) and axial (**b**) T2-weighted MRI scans of a melanoma metastasis at Th6 in a 65-year-old woman with a 6-month history of back pain and progressive paraparesis. The tumor affects mainly the left pedicle and posterior part of the vertebral body with some soft-tissue extension into the spinal canal on the left side. **c** The coronal MRI scan demonstrates the collapse of the vertebra. **d** The corresponding anterior-posterior X-ray shows the lateral displacement of the left pedicle in the affected vertebra (*arrowhead*). **e** The lateral X-ray demonstrates osteoporosis of the thoracic spine and collapse of Th6 (*arrowhead*). Apart from the soft-tissue component in the spinal canal, as seen on MRI, the bone-window CT (**f**) discloses the osteolytic and destructive tumorous process

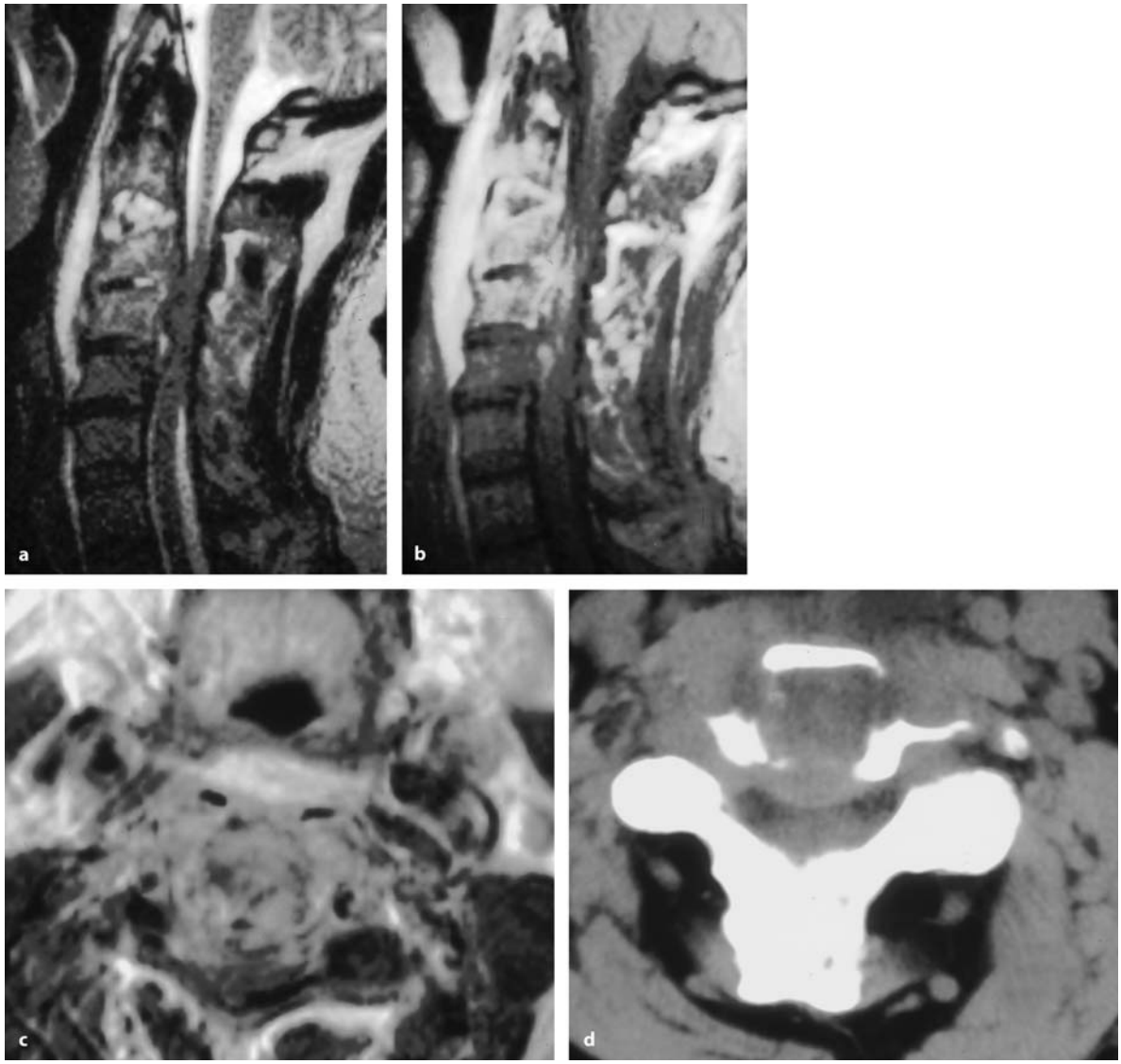

Fig. 5.40. Sagittal T2- (**a**) and T1-weighted, contrast-enhanced MRI images (**b**) of a spontaneous spondylodiscitis at C2/3 in a 55-year-old man with a 2-month history of neck pain and progressive tetraparesis. The most prominent signal changes can be seen in the C2/3 disc space. The remaining abnormalities are secondary changes related to the local spread of the inflammation. There is diffuse uptake of contrast in the neighboring vertebrae and spinal cord compression due to an intraspinal abscess. Signal changes also appear in the posterior soft tissue and there is marked enhancement and thickening of the prevertebral soft tissues. **c** This axial T1-weighted image demonstrates the diffuse signal changes in bone and soft tissues. **d** The plain CT scan at the level of C2/3 shows the soft-tissue component compressing the dura

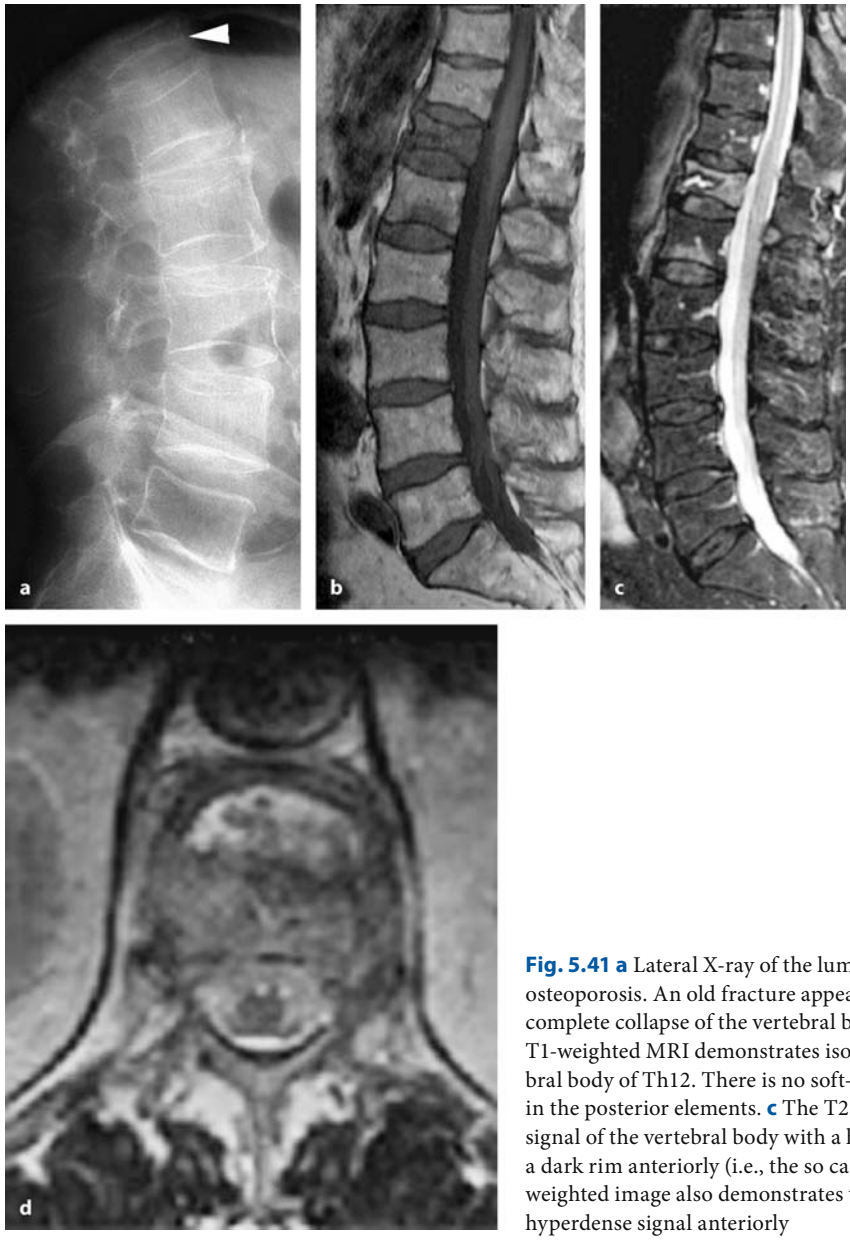

Fig. 5.41 a Lateral X-ray of the lumbar spine in a 69-year-old man with osteoporosis. An old fracture appears at L2 and a fresh lesion causing complete collapse of the vertebral body at Th12 (*arrowhead*). **b** The T1-weighted MRI demonstrates isodense signal changes in the vertebral body of Th12. There is no soft-tissue component and no changes in the posterior elements. **c** The T2-weighted MRI shows the isodense signal of the vertebral body with a hyperdense lesion surrounded by a dark rim anteriorly (i.e., the so called fluid sign). **d** The axial T2-weighted image also demonstrates these signal patterns with the hyperdense signal anteriorly

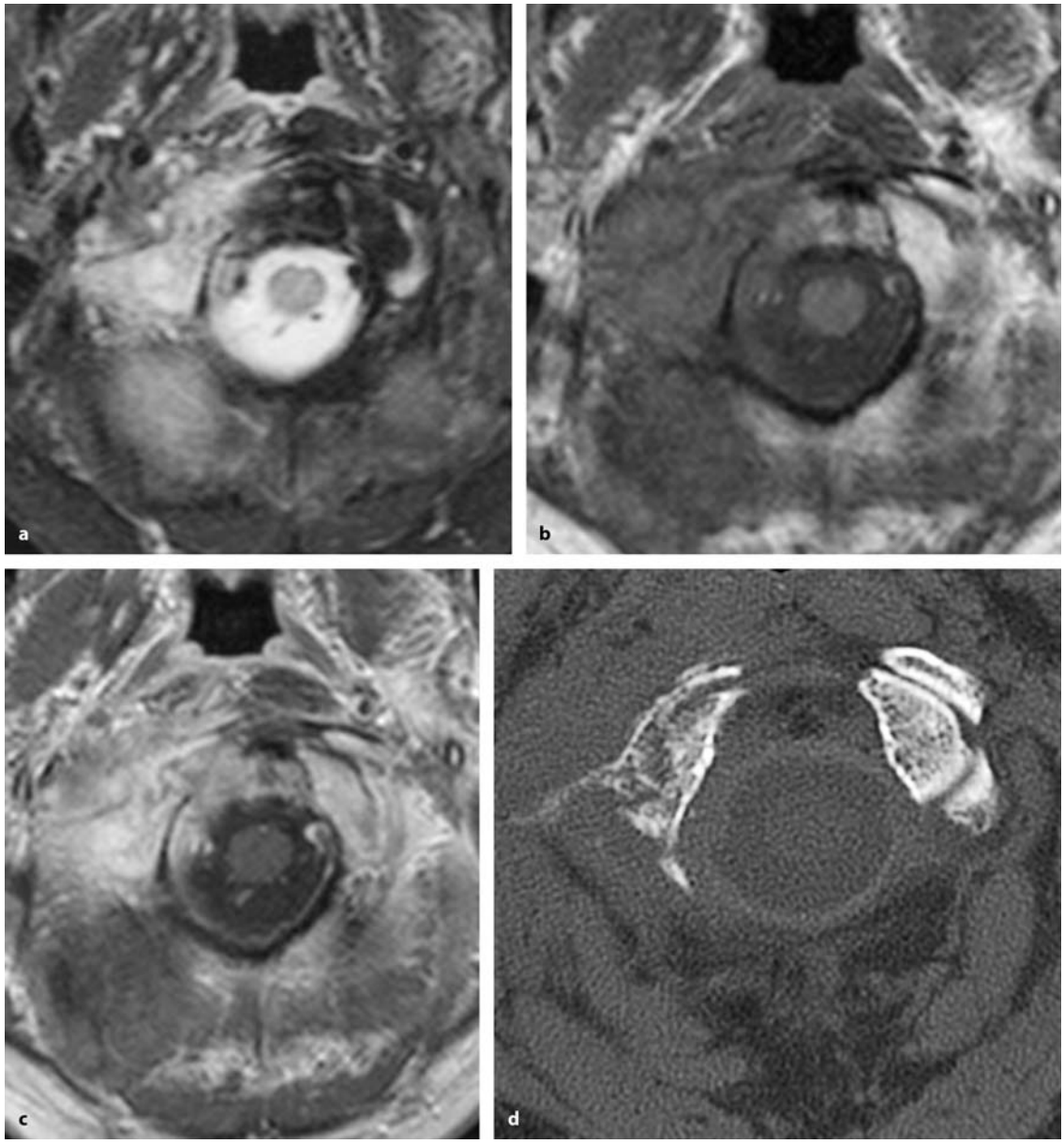

Fig. 5.42. Axial T2- (**a**), T1- without (**b**) and T1-weighted contrast-enhanced MRI scan (**c**) of a 47-year-old man with severe upper neck pain years after radiotherapy for a carcinoma of the tongue. On T2, a hyperdense signal change in the right half of C1 is visible with some extension into the posterior soft tissue. On T1 the lesion appears isodense and brightly enhances with contrast. **d** The bone-window CT discloses an osteolytic process in C1. A CT-guided biopsy procedure was undertaken, which gave the diagnosis of bone necrosis. No surgery was undertaken. Three months later, the pain had completely vanished

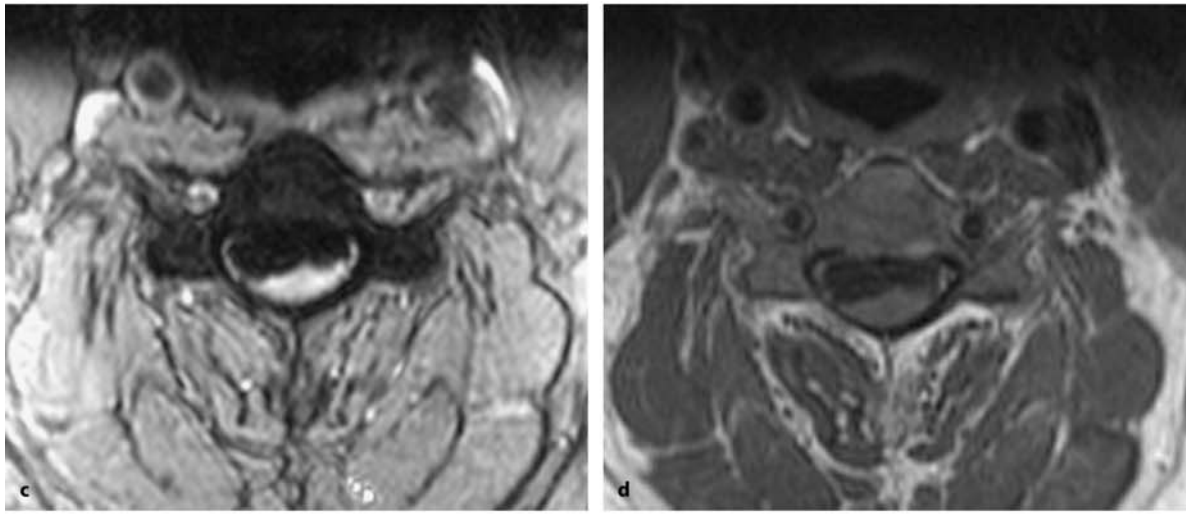

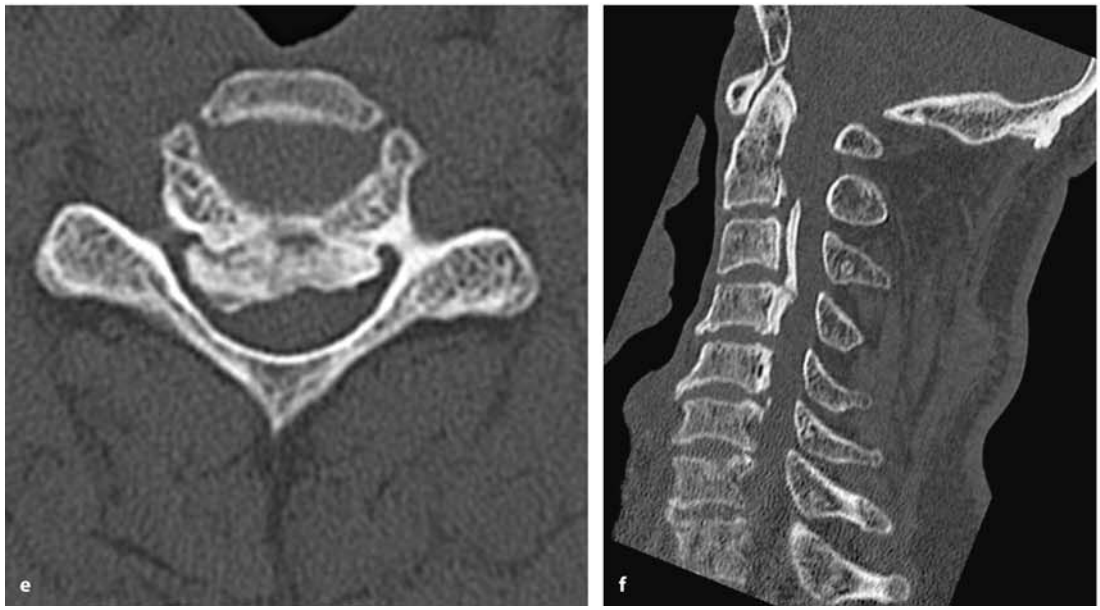

Fig. 5.43. Sagittal T2- (**a**) and T1-weighted (**b**) MRI scans of a 56-year-old man presenting with a severe spastic tetraparesis. At C3/4 there appears to be a hypodense lesion compressing the spinal cord anteriorly. The corresponding axial T2- (**c**) and T1-weighted scans (**d**) demonstrate considerable cord compression. The bone-window CT (**e**) and the sagittal reconstruction (**f**) demonstrate the lesion as an ossified posterior longitudinal ligament

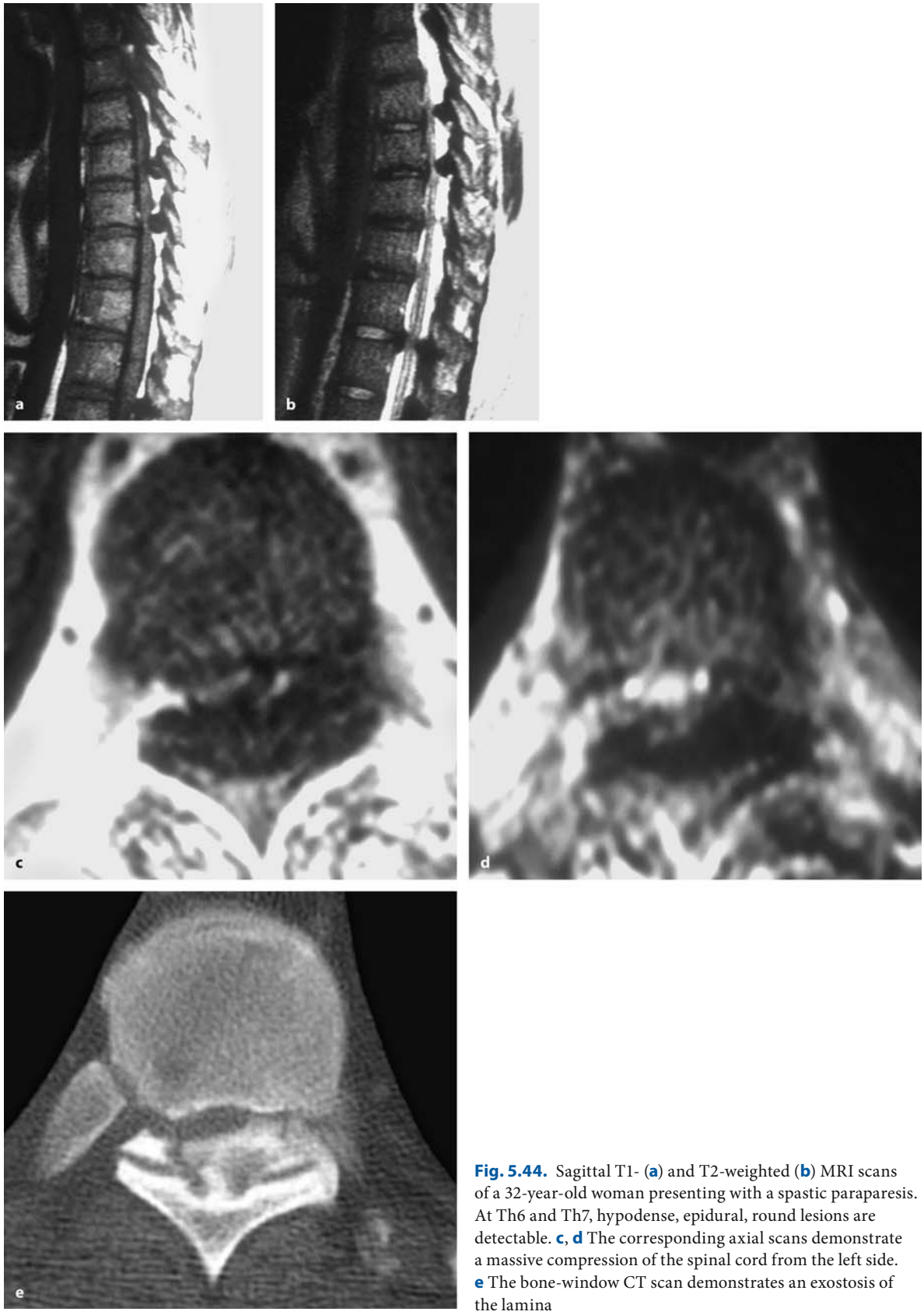

Fig. 5.44. Sagittal T1- (**a**) and T2-weighted (**b**) MRI scans of a 32-year-old woman presenting with a spastic paraparesis. At Th6 and Th7, hypodense, epidural, round lesions are detectable. **c**, **d** The corresponding axial scans demonstrate a massive compression of the spinal cord from the left side. **e** The bone-window CT scan demonstrates an exostosis of the lamina

5.3 Surgery

5.3.1 Soft-Tissue Tumors

5.3.1.1 Exposure

Whereas intra- and extramedullary tumors are operated by a more or less standard posterior approach, epidural tumors may require different strategies. The approach has to consider the intraspinal and extraspinal extension of the tumor and stability aspects. Purely intraspinal tumors restricted to the epidural space can be managed from posterior approaches (i.e., a laminotomy, laminectomy, hemilaminectomy, or interlaminar fenestration) and will not require fusion in the overwhelming majority of cases. With extraspinal extension of an epidural tumor, however, the approach has to extend more laterally so that the tumor can be followed into the paraspinal spaces (Fig. 5.45).

Depending on the extent of intra- and extraspinal parts, it may be advisable to tailor the approach according to the extraspinal component and to use an anterior pathway (Fig. 5.46). However, intraspinal tumor extensions cannot be well controlled by anterior approaches unless a considerable amount of bone is removed, which may then necessitate reconstruction and fusion. Alternatively, it may be wiser to split surgery into an anterior and posterior operation, if the extraspinal part cannot be managed even from a somewhat modified posterior approach alone. On the other hand, en bloc resections may be required for malignant soft-tissue tumors [360, 361].

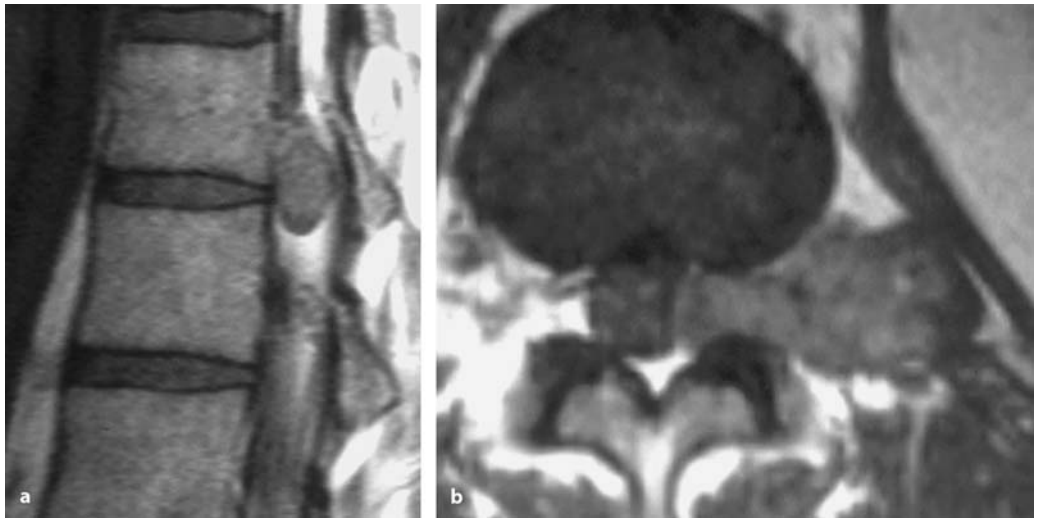

Fig. 5.45. Sagittal (**a**) and axial (**b**) T1-weighted, contrast-enhanced MRI scans of an epidural schwannoma at Th12/L1 in a 41-year-old man with a 2-month history of pain and gait ataxia. The tumor takes up a moderate amount of contrast with the intraspinal part located in the neuroforamen. The extraspinal extension is visible on the axial scan. (*Continuation see next page*)

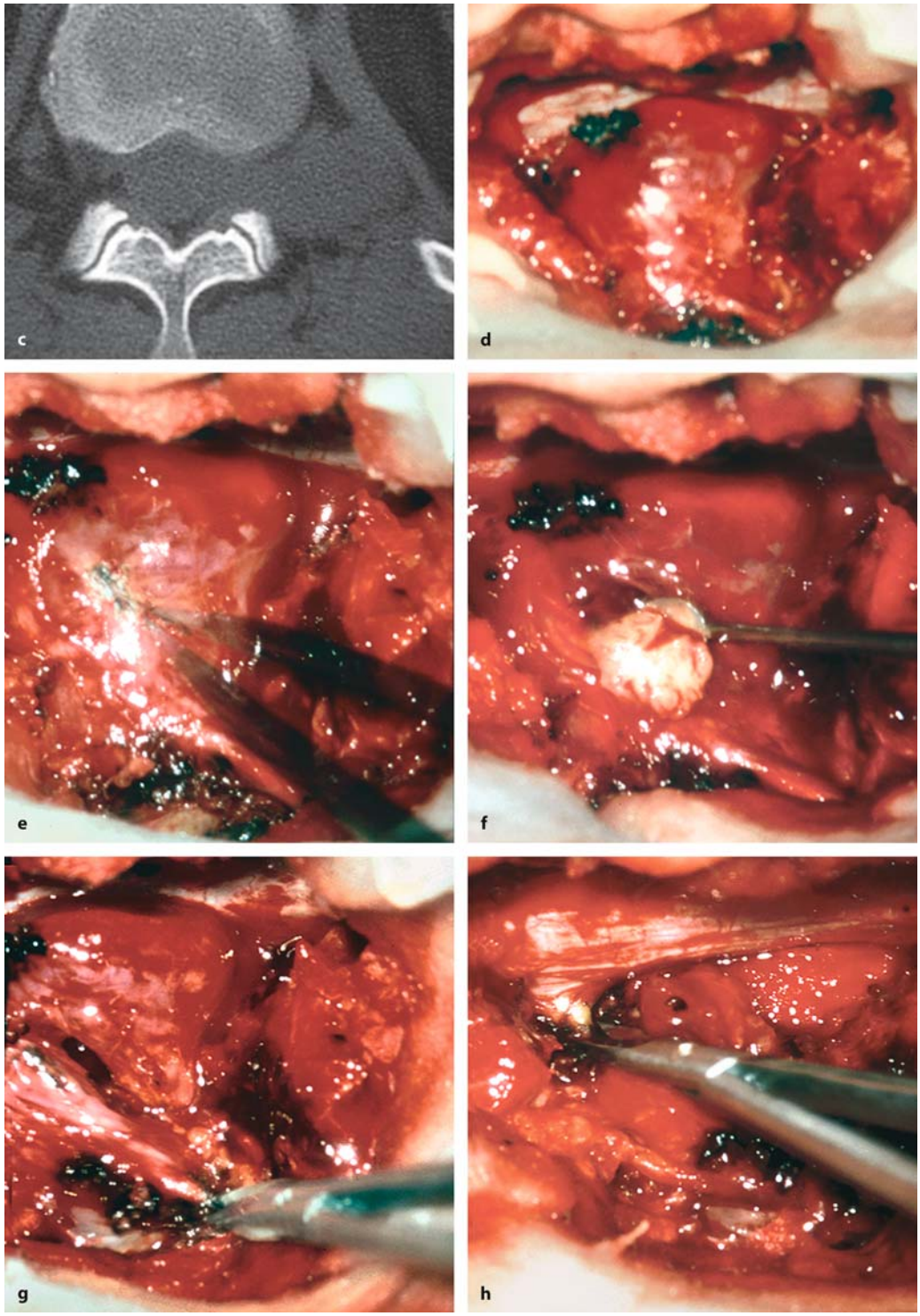

Fig. 5.45. c The bone-window CT demonstrates a slightly enlarged neuroforamen but no bone destruction. **d** This intraoperative view after a hemilaminectomy on the left side shows the epidural tumor compressing the dura. The tumor capsule is coagulated and incised (**e**) for debulking (**f**). Finally, the nerve root is transected distally (**g**) and proximally (**h**) to remove the tumor (**i**). (*Continuation see next page*)

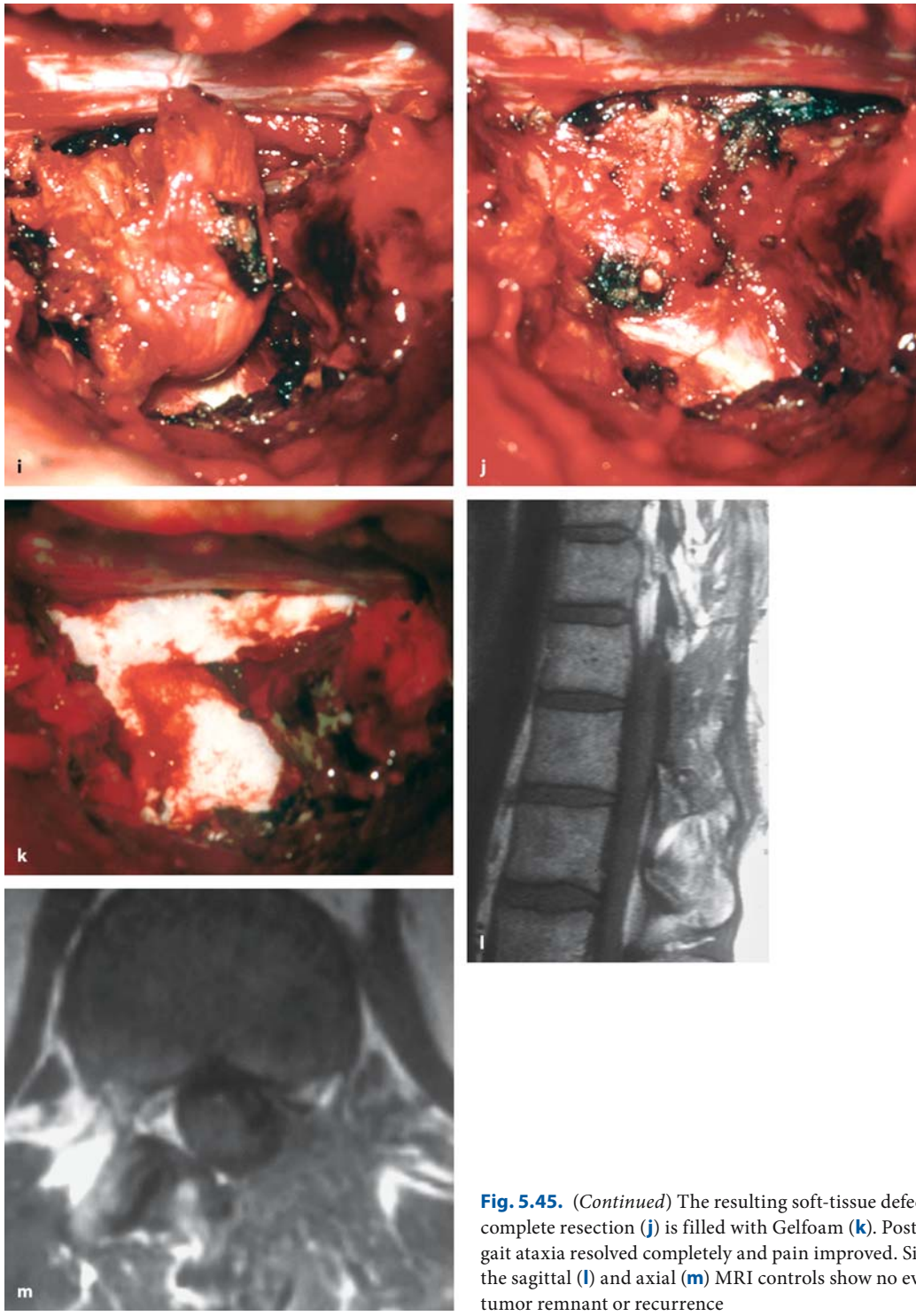

Fig. 5.45. (*Continued*) The resulting soft-tissue defect after complete resection (**j**) is filled with Gelfoam (**k**). Postoperatively, gait ataxia resolved completely and pain improved. Six months later, the sagittal (**l**) and axial (**m**) MRI controls show no evidence of a tumor remnant or recurrence

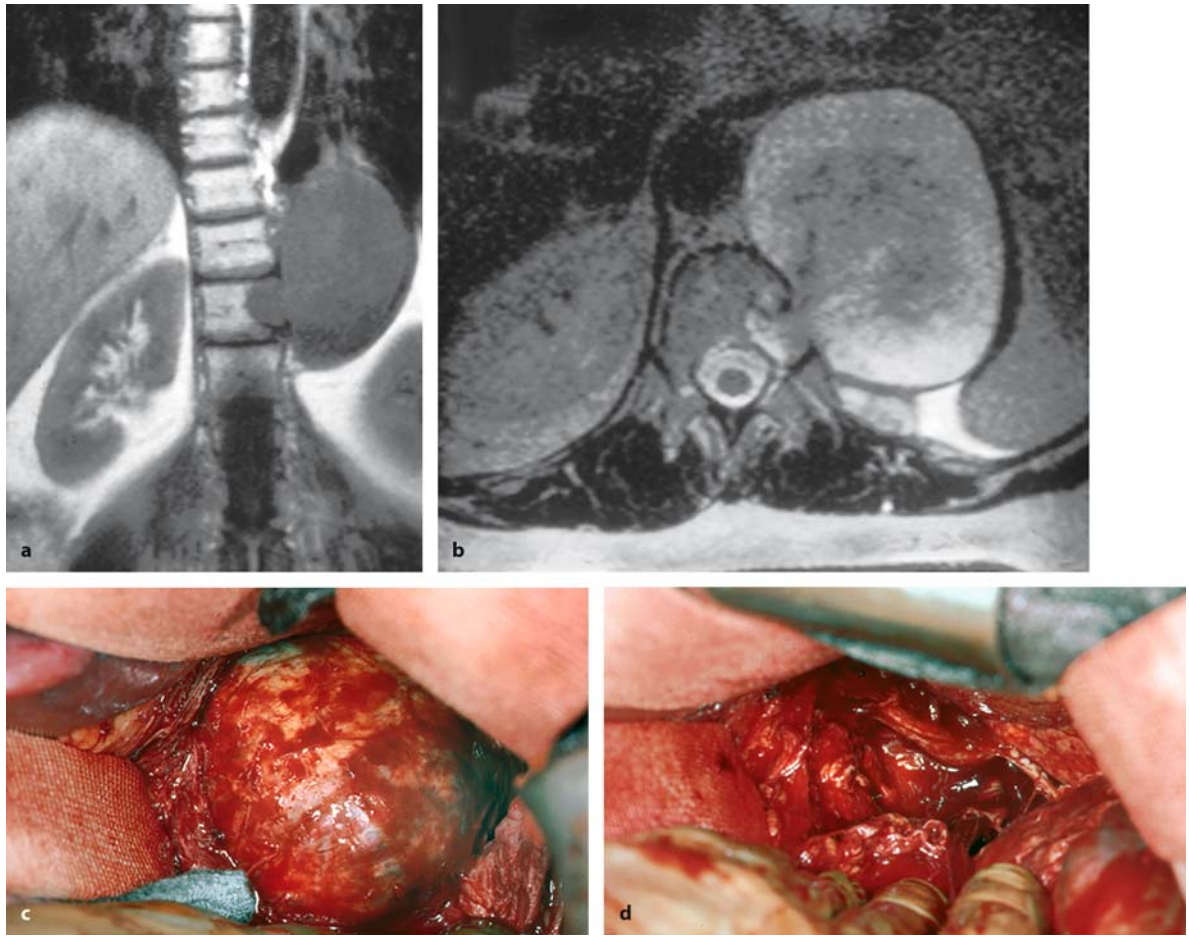

Fig. 5.46. Coronal T1- (**a**) and axial T2-weighted (**b**) MRI scans of an epidural schwannoma at Th11 in a 53-year-old woman with NF-2 and a 1-year history of pain and dysesthesias. The tumor reaches into the neuroforamen but does not cause any dura compression. **c** This intraoperative view shows the huge tumor exposed from a retroperitoneal approach. **d** The tumor was resected in toto. Postoperatively, pain and dysesthesias improved

5.3.1.2 Tumor Removal

Apart from the approach, the surgical removal of epidural neoplasms follows the same principles as outlined for intradural tumors. As a general rule, with posterior approaches the intraspinal tumor part should be removed before attempting excision of the extraspinal portion [253, 335]. If the tumor provides a capsule, this is incised and the tumor reduced with intracapsular removal. Depending on the texture of the capsule and the size of the neoplasm, a more or less large amount of the mass should be taken out before attempting to mobilize and remove the capsule off the dura. With very fragile capsules, its coagulation may help to follow it, while putting cottonoids along the interface toward the epidural tissue. Quite commonly, epidural veins will start to bleed once the decompression has reached a sufficient point. Cottonoids and Gelfoam around the tumor capsule can be used to compress these bleeding veins, thus making it easier to identify and to coagulate them (Fig. 5.45). Regardless of the type of tumor, the spinal dura is a very effective barrier even to malignant tumors. With the exception of epidural schwannomas, which may grow along the nerve sheath into the subarachnoid space, or hamartomas, epidural tumors almost never penetrate the dura. Therefore, it is important to keep the dura intact, with malignant tumors in particular, to prevent intradural spreading. Once the intraspinal tumor part has been removed, the extraspinal part can be attacked along the same lines: intracapsular removal followed by excision of the capsule.

The surgical strategy differs completely for epidural arachnoid cysts. Resection of the entire cyst is not

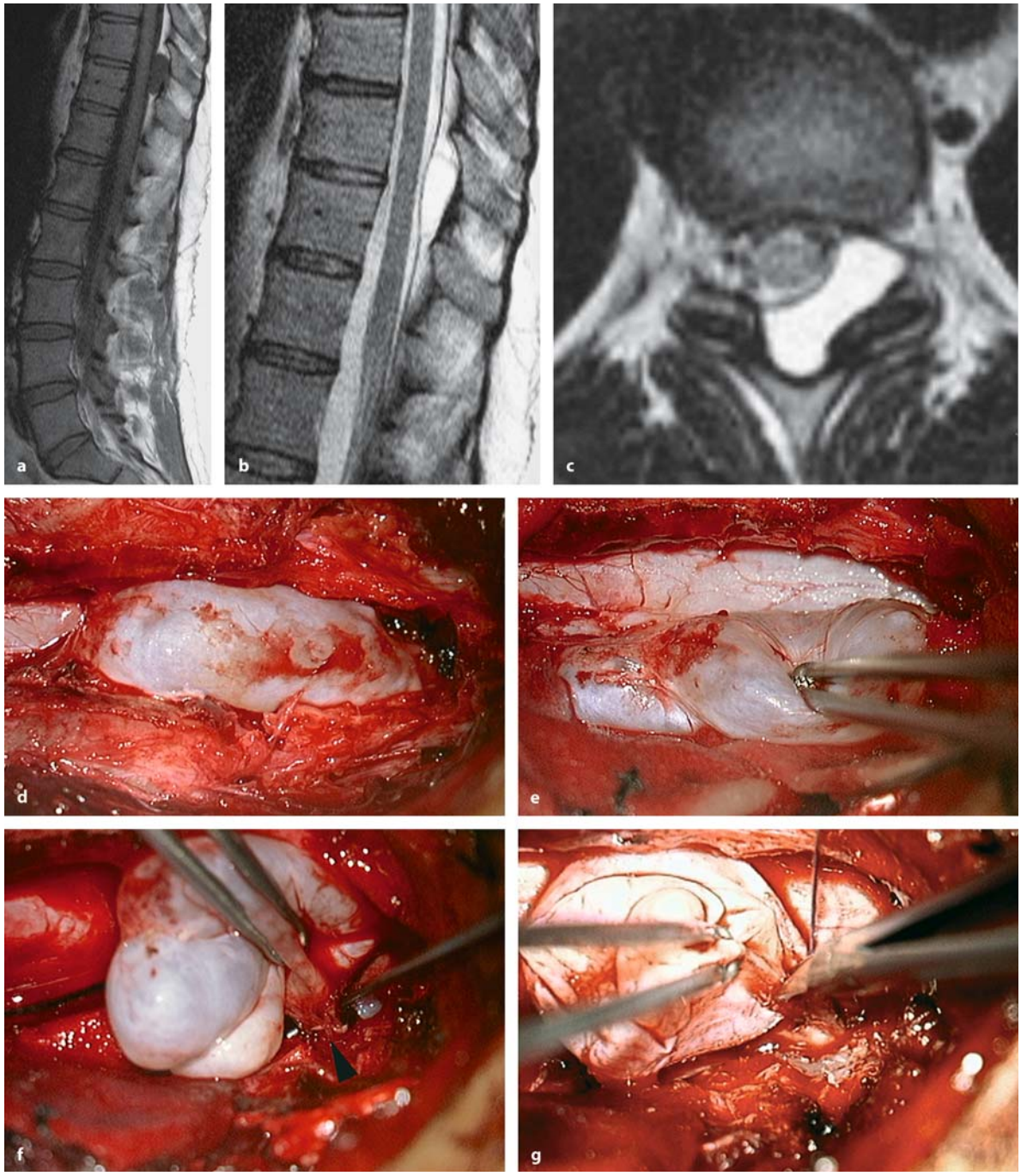

Fig. 5.47. Sagittal T1- (**a**) and T2-weighted (**b**) MRI scans of an epidural arachnoid cyst at Th10/11 in a 42-year-old woman with a 3-month history of radicular pain on the left side. The epidural fat on T1 and the dura appearing as a dark band clearly establish the extradural position of this cyst. **c** The axial T2-weighted image demonstrates the position on the left side in the neuroforamen, suggesting a dura defect in this nerve root sleeve. **d** This intraoperative view after laminotomy Th10 and Th11 demonstrates the cyst. Mobilizing the cyst off the dura (**e**), a small neck can be isolated as the communication with the subarachnoid space (*arrowhead* in **f**). After ligating this neck it can be transected (**g**). (*Continuation see next page*)

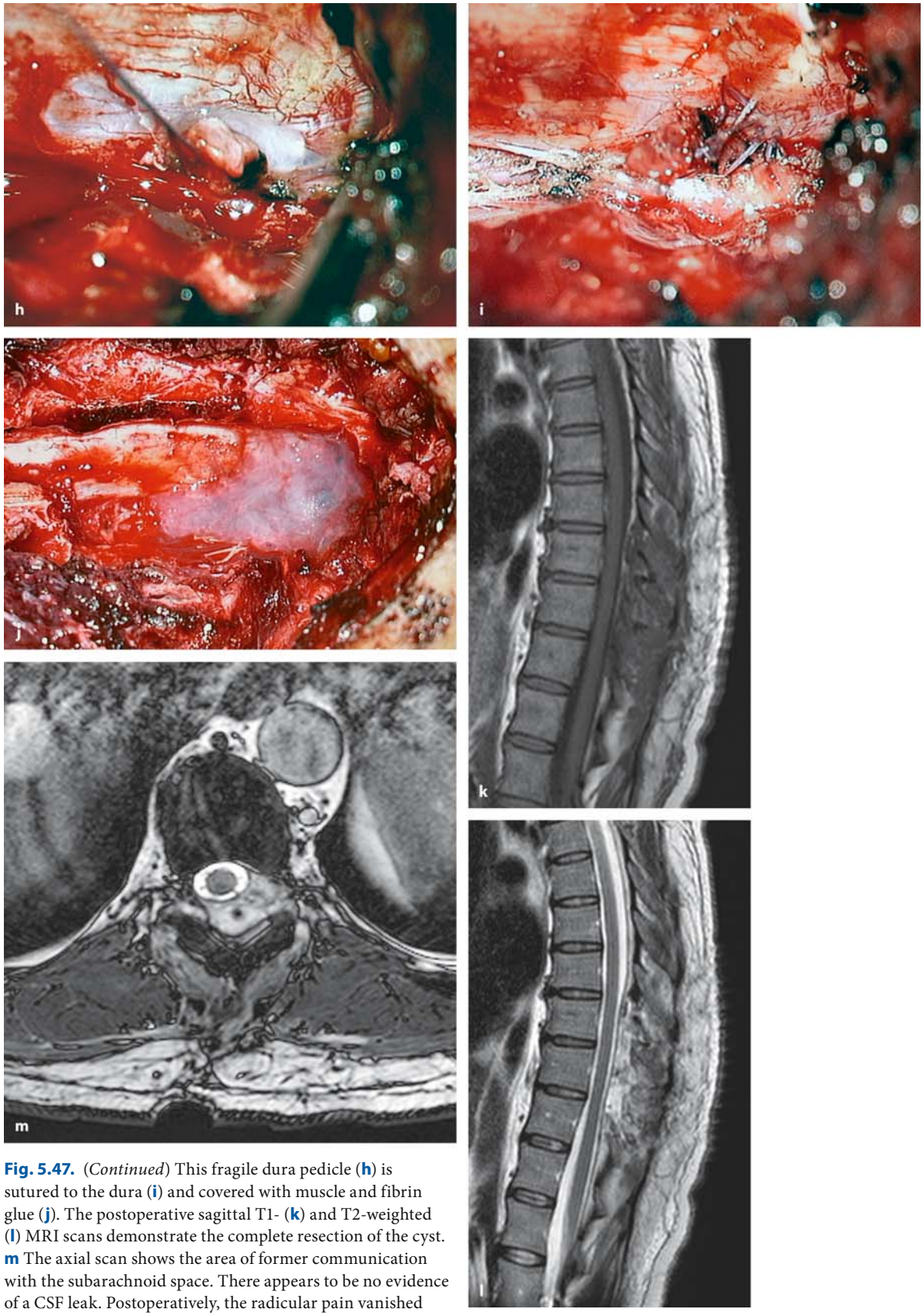

Fig. 5.47. (*Continued*) This fragile dura pedicle (**h**) is sutured to the dura (**i**) and covered with muscle and fibrin glue (**j**). The postoperative sagittal T1- (**k**) and T2-weighted (**l**) MRI scans demonstrate the complete resection of the cyst. **m** The axial scan shows the area of former communication with the subarachnoid space. There appears to be no evidence of a CSF leak. Postoperatively, the radicular pain vanished completely

required, but sufficient occlusion of its communication with the subarachnoid space is. In most instances this communication will be found along a root sleeve. Therefore, the exposure has to be lateral enough to be able to deal with it. Depending on the local condition of the dura, it may be possible to close it with a suture, clip, or muscle and fibrin glue (Fig. 5.47).

Depending on the amount of bony erosion, destruction, or bone removal required for surgical management of an epidural soft-tissue tumor, stabilization may have to follow the resection [362]. McCormick [362] had to stabilize 2 patients from a series of 12 thoracic and lumbar epidural tumors.

5.3.2 Bone Tumors

With bone tumors the surgical strategy used has to take into account the histology, intra- and extraspinal tumor extension, stabilization aspects, and the overall clinical condition of the patient [185, 294]. A large proportion of bone tumors are malignant. With primary bone tumors, the radicality of removal not only determines local control and neurological outcome, but is also a major factor in long-term survival. On the other hand, for secondary bone tumors (i.e., metastases) surgery on a particular spinal metastasis will not influence the survival prognosis of the patient significantly [6]. Once the tumor mass is removed, the efficiency of adjuvant therapies will determine the overall prognosis and not the completeness of resection of a particular spinal lesion. This should be born in mind particularly when planning treatment for cancer patients who are in the advanced stages of their disease. A transthoracic resection may be too much for such a patient and a posterior decompression of the spinal cord with stabilization may be a better choice. Therefore, the surgical planning has to take into account the probable histology as well as the general health status of the patient and his/her prognosis [6, 294]. The better the clinical condition of the patient, the more radically a particular spinal lesion can be treated [6, 296, 538]. In particular, for solitary spinal lesions and no history of cancer, the histology should be determined before planning the definite surgery. Whenever possible, a transpedicular route should be used to obtain tissue, as this limits the risk of contaminating other compartments with tumor tissue, as the approach can be sealed with methylmethacrylate [521].

The foremost decision in planning a surgical procedure is to evaluate whether an intralesional removal or an en bloc removal should be attempted. With benign bone tumors that do not display aggressive patterns (Enneking stages S1 and S2) or highly malignant extensive tumors (Enneking stages IIB, IIIA, and IIIB), intralesional removals can and should be used, because more extensive measures are either not necessary – as in benign tumors – too demanding for the patient, or not indicated, if a curative procedure is no longer possible – as in advanced stages of malignant tumors. On the other hand, benign but locally aggressive tumors (stage S3) or confined highly malignant and low-grade malignant tumors (stages IA, IB, and IIA) are potential candidates for a curative surgical excision. In such cases an en bloc removal should be attempted if the extension of the tumor allows this with acceptable morbidity [185].

The next question is the choice of approach. The answer has to depend on the vertebral parts affected, stability issues, tumor histology, and the clinical condition of the patient. With posterior elements involved exclusively, a simple midline posterior approach can be used and, in general, no stabilization will be required. Purely anterior approaches and stabilizations are sufficient if all posterior elements are intact. Otherwise, a purely ventral stabilization and vertebral reconstruction is bound to fail. With anterior and posterior elements affected, a posterior approach with decompression and transpedicular screw fixation should be done as the first step. This will clarify the histology, decompress neural structures, and provide sufficient short-term stability. As a rule of thumb, such a posterior stabilization should encompass two spinal levels above and below the affected vertebra. Depending on the clinical condition of the patient, the estimated prognosis, and the histological diagnosis, one can then decide to either remove part of the affected vertebra from posterior, filling the defect with polymethylmethacrylate (PMMA) for ventral support as a kind of "low-key" management or to schedule a second operation from anterior with complete resection – marginal or en bloc - and vertebral reconstruction and fusion [296, 521]. Alternatively, en bloc resections of entire vertebrae have also been described from a posterior approach [2, 509, 536, 537] and combined approaches in single-stage operations [2, 72, 81, 84, 126, 228, 279, 301, 352, 449, 536, 537, 573] for any spinal level as well as for mediastinal and thoracic tumors involving the spine secondarily [360].

Depending on the type of tumor, embolization or chemotherapy may be administered before surgery is undertaken. Preoperative embolization is recommended for osteoblastomas, aneurysmatic bone cysts, giant cell tumors, sarcomas, and metastases from thyroid or kidney cancers [143, 200, 345, 371, 435,

521]. With biopsy-proven lymphomas or Ewing sarcomas, preoperative chemotherapy is administered provided the clinical situation does not dictate an urgent operation.

5.3.2.1 Exposure

With resection of bone tumors – the great majority in this group being metastases – several changes regarding surgical strategies have taken place over the years. Early cases in our series were managed almost exclusively from the posterior approach, with sole attention on removal of the intraspinal tumor part, while stability issues were often neglected. With more experience and better visualization of the tumors on MRI in particular, it became apparent that such a strategy is insufficient for most patients. Furthermore, stabilization techniques have improved significantly over the years making fusion techniques safer, faster, and less stressful for the patient. This chapter cannot provide a complete overview on all approaches to and fusion techniques for the spine [12, 72, 218, 287, 314, 327, 517, 559]. We rather prefer to describe those techniques that we have found useful and have used for this series of patients.

For posterior bone tumors of the spine, the classical posterior approach as already described for intra- and extramedullary tumors can be tailored according to the tumor extension to expose transverse processes, costotransverse joints, the posterior part of a rib, and so forth (Fig. 5.48). One should bear in mind that the length of the skin incision has to account for the amount of lateral exposure required. Access to the vertebral body from posterior is possible from an oblique angle with resection of a pedicle or a costotransversectomy. However, it is not possible to visualize the entire vertebral body from this approach and vertebral body reconstruction may be hindered by limited view and maneuverability of cages or bone grafts if nerve roots have to be preserved. In this respect, anterior approaches are easier for the surgeon, but more demanding for the patient.

5.3.2.1.1 Cervical Spine

With tumors rendering the cervical spine unstable, fiber-optic intubation is highly recommended to avoid undue neck movements and spinal cord injury. For the cervical spine, two alternatives to a posterior approach are available: the anterior midline and the anterolateral approach.

The anterior midline approach for C1 and C2 is done transorally with the patient in the supine position and the head fixed in the Mayfield clamp in slight retroflexion and neck extension (Fig. 5.49). Orotracheal intubation can be used, as a tracheostomy is not required for most patients. Topical or systemic corticosteroids can be applied to limit postoperative soft-tissue swelling [388]. The uvula can be elevated with a nasogastric tube (i.e., so-called velotraction), avoiding splitting of the soft palate [388]. Splitting of the soft or even the hard palate should be kept for exceptional cases, as postoperative swallowing problems may be caused (i.e., velopalatine insufficiency) [291]. With introduction of the retractor, the tongue is pushed downward. Care must be taken to avoid injury of the tongue due to compression by the patient's teeth. Depending on tumor extension and destruction or alteration of anatomical landmarks, it may be extremely helpful to use intraoperative X-ray or even navigation techniques for safer orientation. In general, a vertical midline incision is used for the prevertebral soft tissues. Some surgeons prefer a paramedian incision of the mucosa and a median incision for the remaining soft tissues, allowing a two-layer overlapping closure at the end. This may be advantageous if foreign materials for reconstruction and fixation have to be introduced. First the stepwise mobilization of soft tissues and subperiosteal dissection will expose the anterior arch of the atlas and then the lower part of the dens and body of C2 (Fig. 5.49). The superior limitation of this approach is the clivus, the lower limitation is the C2/3 disc, and the lateral limitations are the carotid arteries. Modifying this approach with splitting of the hard palate or the tongue can provide wider angles toward the clivus and adjacent cervical vertebrae. But even with such modifications, only processes confined to the midline are candidates for this technique and a combined anterior and posterior approach is required as soon as the pathology extends lateral of the spinal canal into the transverse processes. As the transoral route is not a sterile avenue and a tight dural closure is difficult given the deep surgical field and the rather thin soft-tissue coverage, intradural pathologies should not be tackled transorally, even though such operations have been described. In these cases, cerebrospinal fluid (CSF) fistulas were prohibited by external CSF drains or eventually by lumboperitoneal shunting [131]. Once tumor removal has been performed, means of stabilization have to be considered. A defect of the body of C2 can be replaced by a titanium cage, a bone graft, or PMMA [472]. Stabilization, however, requires an additional posterior operation. Postoperatively, the patient requires a na-

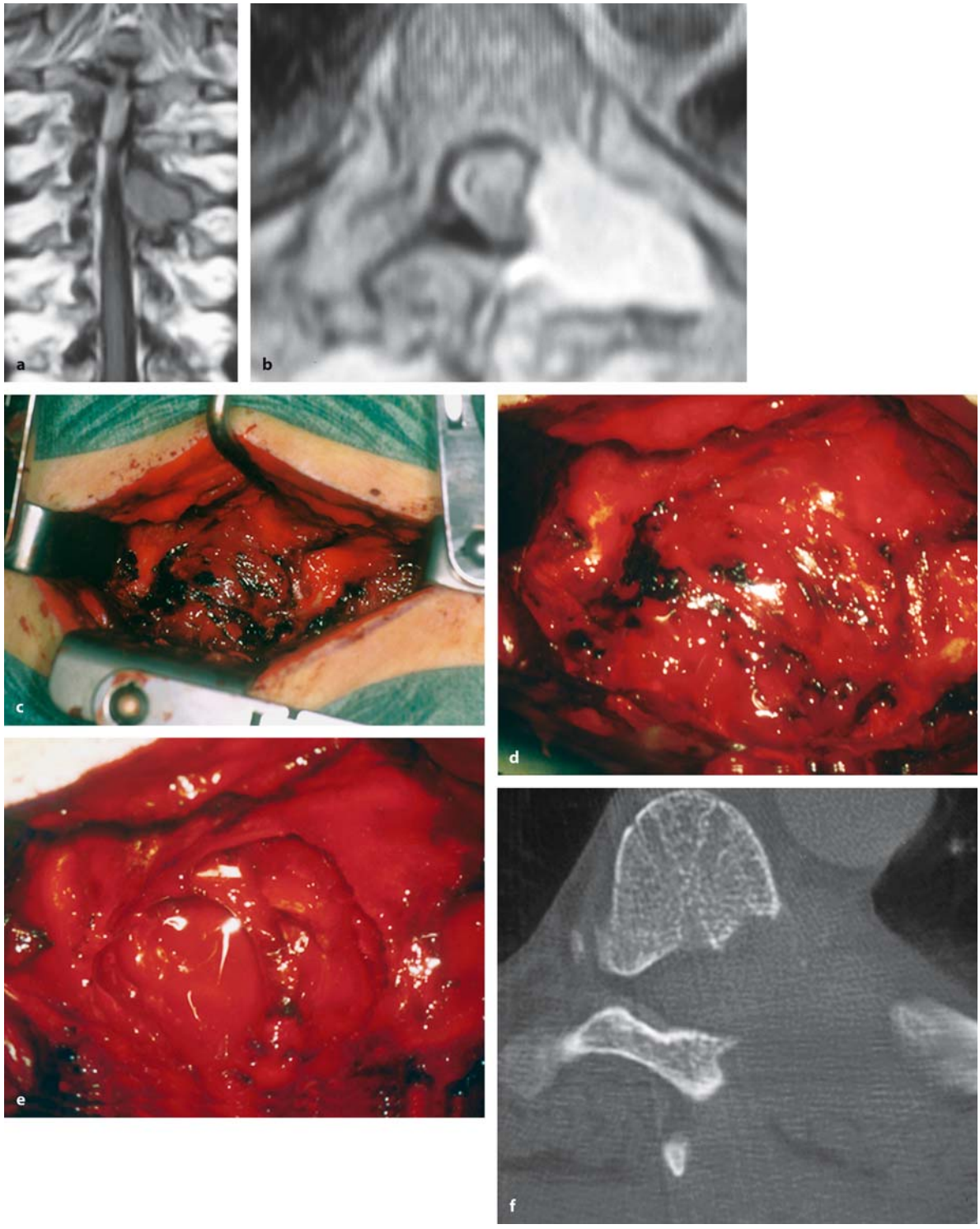

Fig. 5.48. Coronal T1- (**a**) and axial T2-weighted (**b**) MRI scans of a hypernephroma metastasis at Th7 in a 67-year-old man with a 3-month history of pain. This highly vascularized tumor is located posteriorly affecting the left pedicle and left half of the lamina. This intraoperative overview (**c**) and close up image (**d**) show the tumor exposed from a posterior approach. After complete resection (**e**), the postoperative bone-window CT scan (**f**) illustrates the amount of bone removal required for this operation. Pain improved postoperatively. Despite postoperative radio- and chemotherapy, a local recurrence developed 6 months later, which was again removed. No further tumor progression or recurrence has been observed in the 2 years since his last surgery

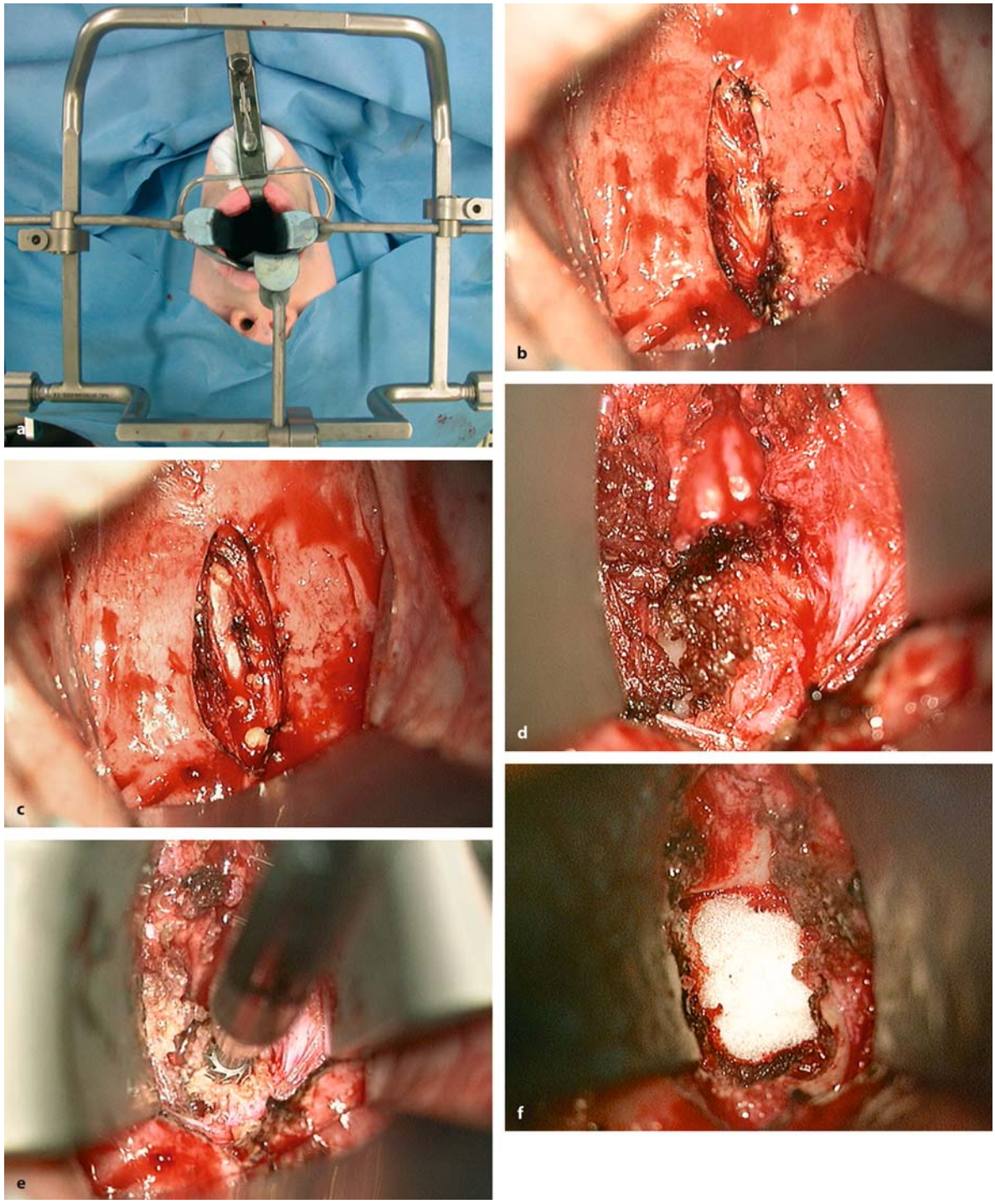

Fig. 5.49. The transoral approach to the upper cervical spine is performed with the head securely fixed in slight retroflexion in a Mayfield clamp. The tongue and soft palate are retracted (**a**). **b** The mucosa and pharyngeal muscles are incised longitudinally down to the periost of the targeted vertebral body. Mobilizing the periost from the midline laterally (**c**) retractors can be put into place to gain access to the anterior surface of the vertebral body. In this case, C1 has been removed to gain access to the dens (**d**). Bone removal is performed using a high-speed drill (**e**). **f** After resection, the defect is filled with Gelfoam. (*Continuation see next page*)

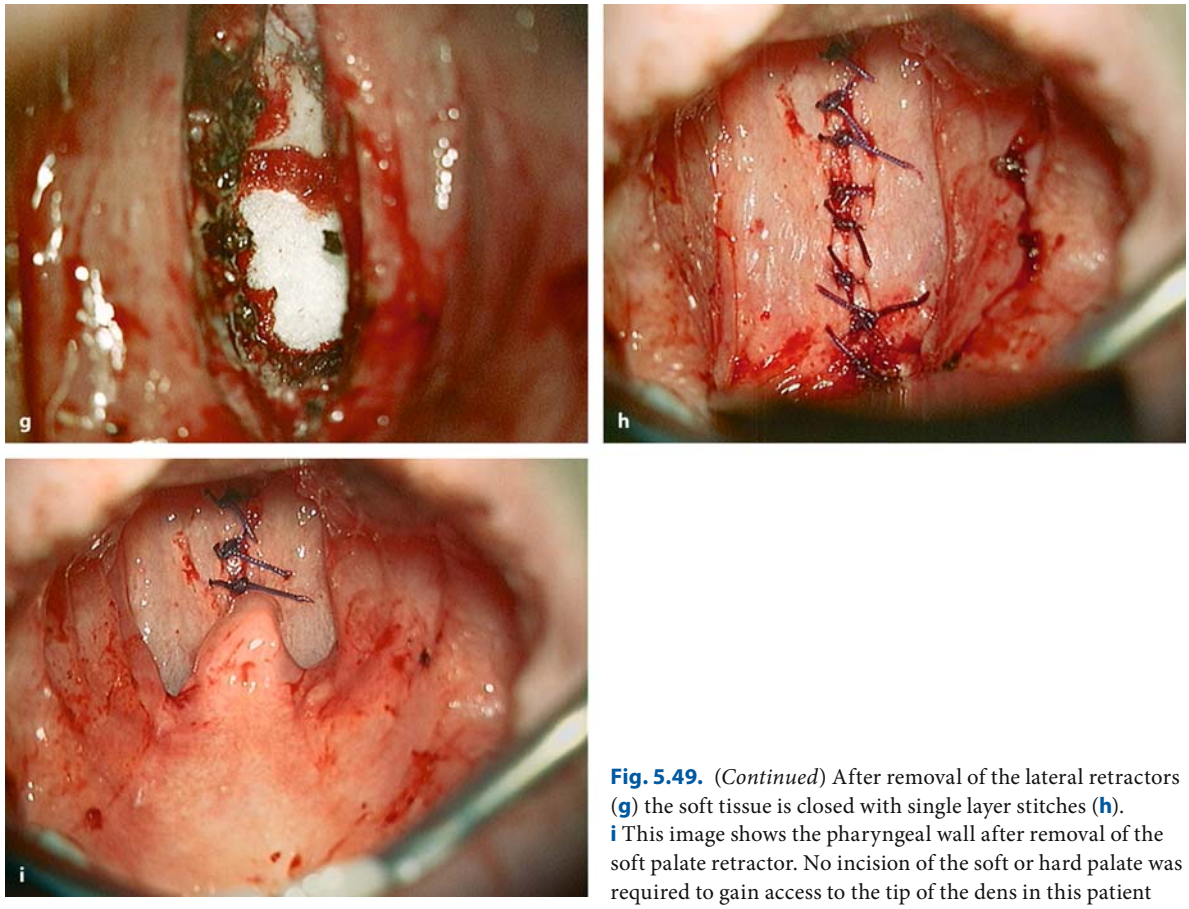

Fig. 5.49. (*Continued*) After removal of the lateral retractors (**g**) the soft tissue is closed with single layer stitches (**h**). **i** This image shows the pharyngeal wall after removal of the soft palate retractor. No incision of the soft or hard palate was required to gain access to the tip of the dens in this patient

sogastric feeding tube for a couple of days, which should be placed under direct vision at the end of the operation.

An anterolateral approach to the upper cervical spine up to C1 is available along the retropharyngeal route. This approach requires complex soft-tissue dissections to preserve facial and hypoglossus nerves to reach C1 and C2 from an oblique angle. The advantage of this approach is the possibility of extending the exposure downward, if lower cervical segments are also involved, and the lower risk for infections if the pathology requires opening of the dura [551]. We have used this approach for several skull-base lesions, but not for spinal tumors.

With tumor processes below the C2/C3 disc, a conventional anterior approach, such as that used for cervical disc disease, can be employed (Fig. 5.50). Depending on the number of vertebra to be exposed, either a horizontal or vertical skin incision along the sternocleidomastoid muscle is performed. After splitting the platysma, dissection continues medial to the sternocleidomastoid muscle, traversing the different fascia layers towards the anterior surface of the spine in a virtually bloodless procedure. The carotid artery is located laterally and esophagus and trachea are mobilized medially. It is important to mobilize these structures sufficiently above and below the affected spinal levels in order to avoid too much traction, which may lead to local swelling and endangers the recurrent laryngeal nerve. For upper cervical levels, the digastric muscle is an important landmark to avoid injury of the hypoglossal nerve, which will be found underneath this muscle. Laryngeal muscles and, in the lower cervical region, the thyroid gland require mobilization to reach the anterior longitudinal ligament. Then the anterior vertebral muscles are detached from the spine to place the retractor blades for lateral traction underneath these muscles. In that way, injury to cervical soft tissues is avoided (Fig. 5.50). In most instances, the anterior ligament is either resected by the tumor or densely infiltrated and thickened, but only rarely traversed by malignant tumor tissue. With incision of the ligament, the entire vertebral body can be resected from this approach. Verti-

cal traction can be applied by screws placed in adjacent vertebral bodies (Fig. 5.50). The lower limitation of this approach is the first thoracic vertebra in most patients, depending on the anatomical relationship between upper thoracic spine and sternum. Eventually, the major cardiac vessels define the lower limit of this approach even with splitting of the sternum. Lateral limitations are the transverse processes and the vertebral arteries on either side. The vertebral artery usually enters the transverse foramen of C6 and leaves at the transverse foramen of C1, running along the upper ridge of the atlas before traversing the cranial dura.

An alternative is the anterolateral approach, as described by George [191–194, 334]. An incision along the sternocleidomastoid muscle is performed, but then dissection continues lateral to the carotid artery allowing an oblique view on the cervical spine. This approach can be used even for tumors extending to the foramen magnum or jugular foramen. An even wider angle can be obtained with division of the mandible. However, care has to be taken to preserve the spinal accessory nerve, which enters the sternocleidomastoid muscle about 3 cm distal to the mastoid tip, and not to put too much traction on the hypoglossal nerve. Then the anterior spine muscles are mobilized and the vertebral artery is exposed by opening the foramina in the transverse processes involved. In this manner, the vertebral artery can be mobilized and tumor removal can be undertaken from an oblique angle including extraspinal extensions on the side of the approach. With partial drilling of the vertebral body from this oblique angle, even intradural extensions of a tumor can be removed from this approach. Likewise, vertebral body reconstruction and fusion can be performed. However, a transient Horner's syndrome is a common sequela of this technique due to traction on the sympathetic chain. Considerable experience is needed during removal of the vertebral body toward the spinal canal as there are no anatomical landmarks.

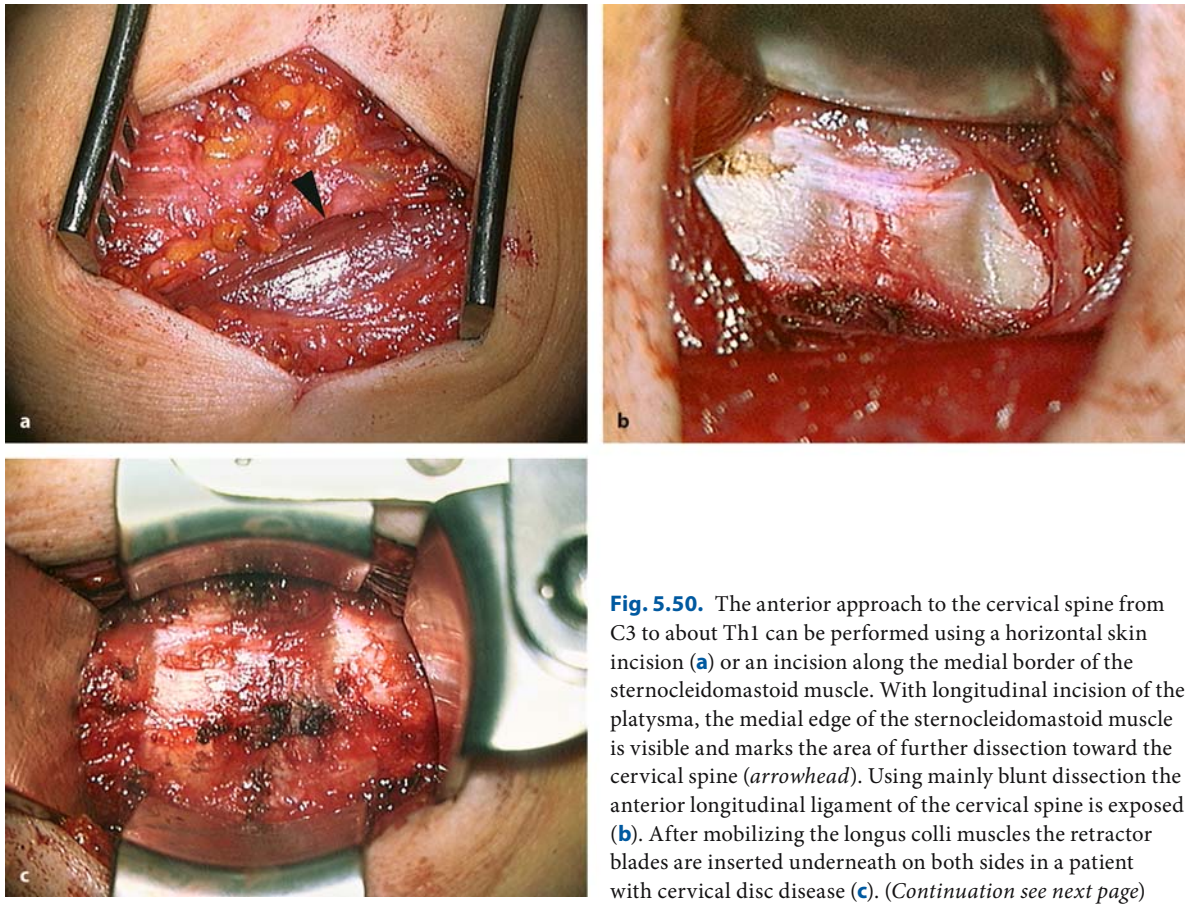

Fig. 5.50. The anterior approach to the cervical spine from C3 to about Th1 can be performed using a horizontal skin incision (**a**) or an incision along the medial border of the sternocleidomastoid muscle. With longitudinal incision of the platysma, the medial edge of the sternocleidomastoid muscle is visible and marks the area of further dissection toward the cervical spine (*arrowhead*). Using mainly blunt dissection the anterior longitudinal ligament of the cervical spine is exposed (**b**). After mobilizing the longus colli muscles the retractor blades are inserted underneath on both sides in a patient with cervical disc disease (**c**). (*Continuation see next page*)

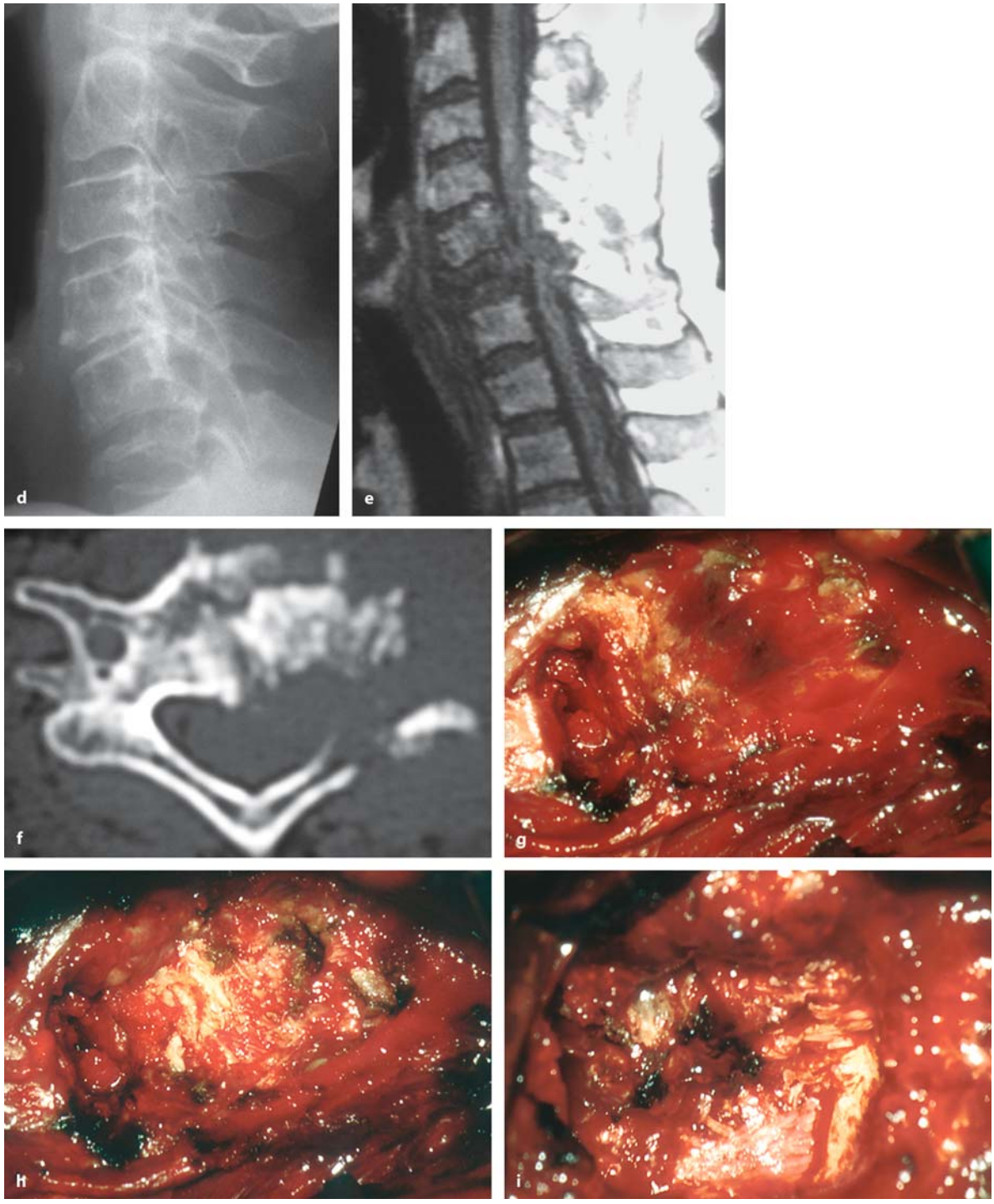

Fig. 5.50. With an underlying tumor, lateral X-ray (**d**), T1-weighted MRI (**e**), and bone-window CT (**f**) show an osteolytic metastasis at C6; the longitudinal ligament is infiltrated by the tumor (**g**) and may bleed profusely. Exposing the tumorous vertebral body (**h**), a vertebrectomy has been performed demonstrating the posterior longitudinal ligament (**i**). (*Continuation see next page*)

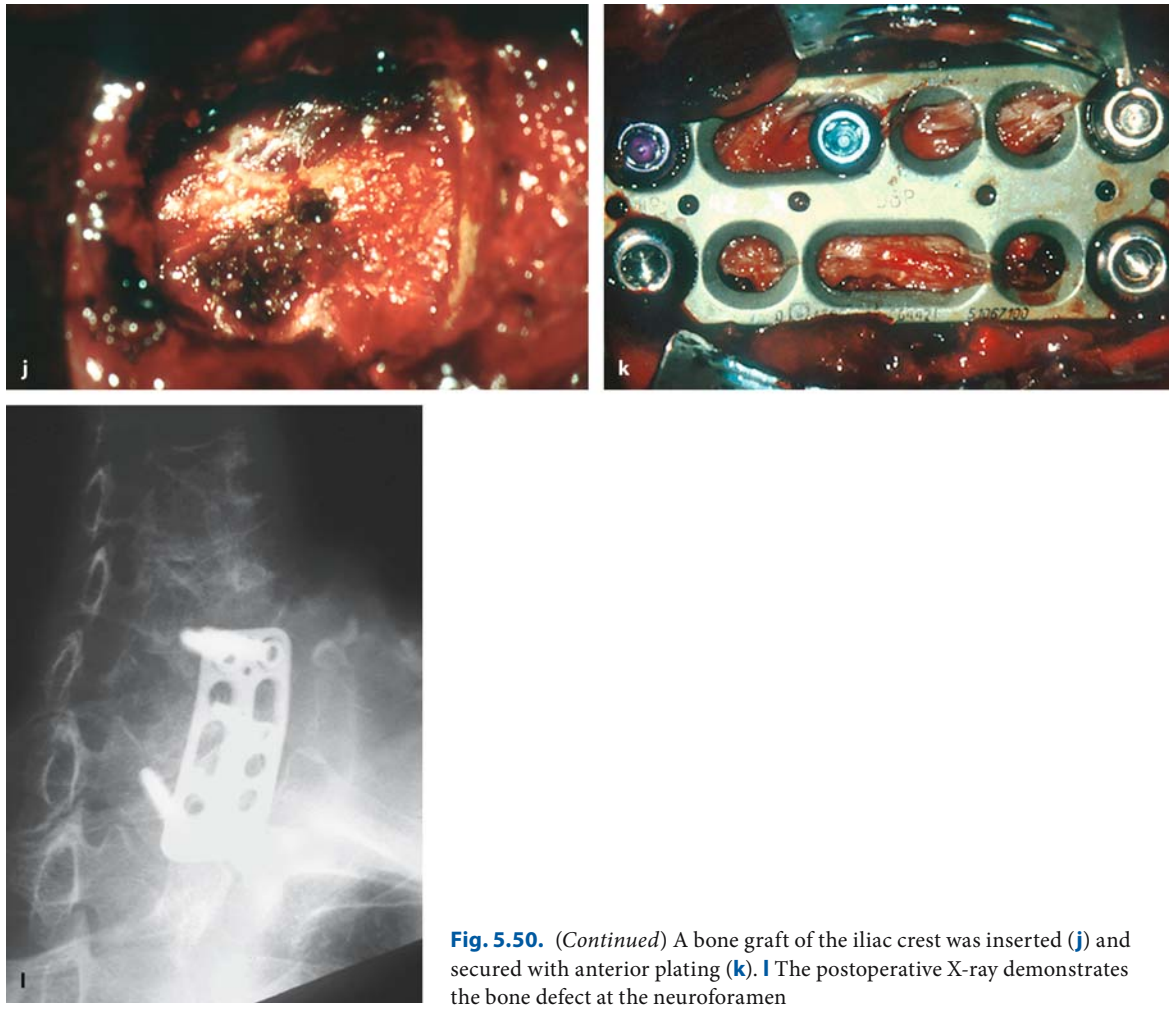

Fig. 5.50. (*Continued*) A bone graft of the iliac crest was inserted (**j**) and secured with anterior plating (**k**). **l** The postoperative X-ray demonstrates the bone defect at the neuroforamen

5.3.2.1.2 Thoracic Spine

With tumors of the cervicothoracic junction or the upper thoracic spine to the level of Th4, anterior approaches are quite demanding due to the restricted prevertebral space, the major thoracic vessels, and the considerable risks of injury to both recurrent laryngeal nerves. Alternatively, a posterior approach with costotransversectomy may be chosen. Others advocate endoscopy-assisted smaller approaches to remove tumors in this area [144, 219].

Anterior approaches to the upper thoracic spine involve either splitting of the sternum or resection of a sternoclavicular joint [510] and should be performed together with a thoracic surgeon (Fig. 5.51). For the latter technique, the patient is positioned supine with a rolled towel for support between both scapulae. The approach should be performed on the left side for lower risks of injury to the laryngeal recurrent nerve on that side. The manubrial and clavicular heads of the sternocleidomastoid muscle are elevated off their attachments and retracted. The medial third of the clavicula is resected and exarticulated from the sternum. Care must be taken to avoid injury to the subclavian vein. Dissection continues between the carotid sheath laterally and the trachea and esophagus medially. The laryngeal nerve courses between the trachea and the esophagus so that medial traction should be applied with care. Blunt retractors should be used to gain access to the anterior cervicothoracic spine between the left carotid sheath and the sternocleidomastoid muscle on the left, and the brachiocephalic vessels of the opposite side.

For an approach with splitting of the sternum, the skin incision over the sternum is extended cranially along the left sternocleidomastoid muscle. After mobilization of retrosternal soft tissues, an oscillating

Fig. 5.51. An anterior approach to the cervicothoracic spine with splitting of the sternum was required for a desmoid tumor at C7–Th2 in a 36-year-old woman with an 18-month history of pain, dysesthesias, and motor weakness in her left arm. The paramedian sagittal (**a**, **b**) and coronal (**c**, **d**) T1-weighted, contrast-enhanced MRI scans demonstrate a tumor with homogeneous contrast enhancement involving the vertebral bodies of C7–Th2 as well as the major thoracic vessels and the brachial plexus on the left side. **e** The axial image at C7 demonstrates the anterior displacement of the left carotid artery (*black arrowhead*) and encasement of the left vertebral artery (*white arrowhead*). The tumor has eroded part of the vertebral body but does not reach into the spinal canal. **f** The axial image at Th2 shows the mediastinal extension and compression of the left lung. (*Continuation see next page*)

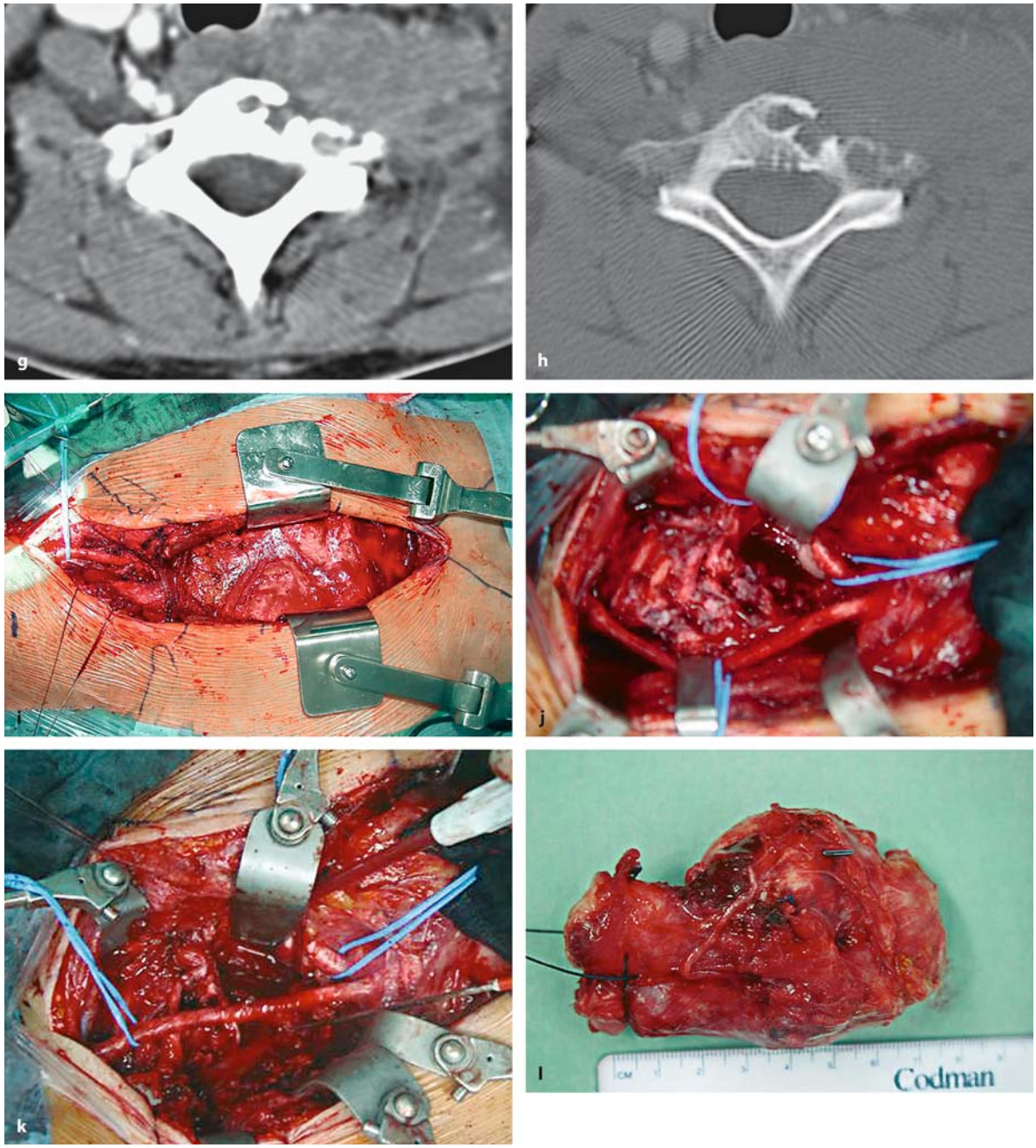

Fig. 5.51. The native (**g**) and bone-window CT (**h**) at C7 demonstrate the amount of bony destruction on the left side. **i** This intraoperative view shows the exposure after splitting the sternum. The right carotid artery has been dissected free. Skin marks demonstrate the position of the clavicles on either side. **j** With mobilization of both carotid arteries, the tumor is displayed. **k** After resection of the tumor sacrificing the left infiltrated C8 nerve root, the resection cavity and bony defect is visible. **l** The tumor specimen was removed in toto. (*Continuation see next page*)

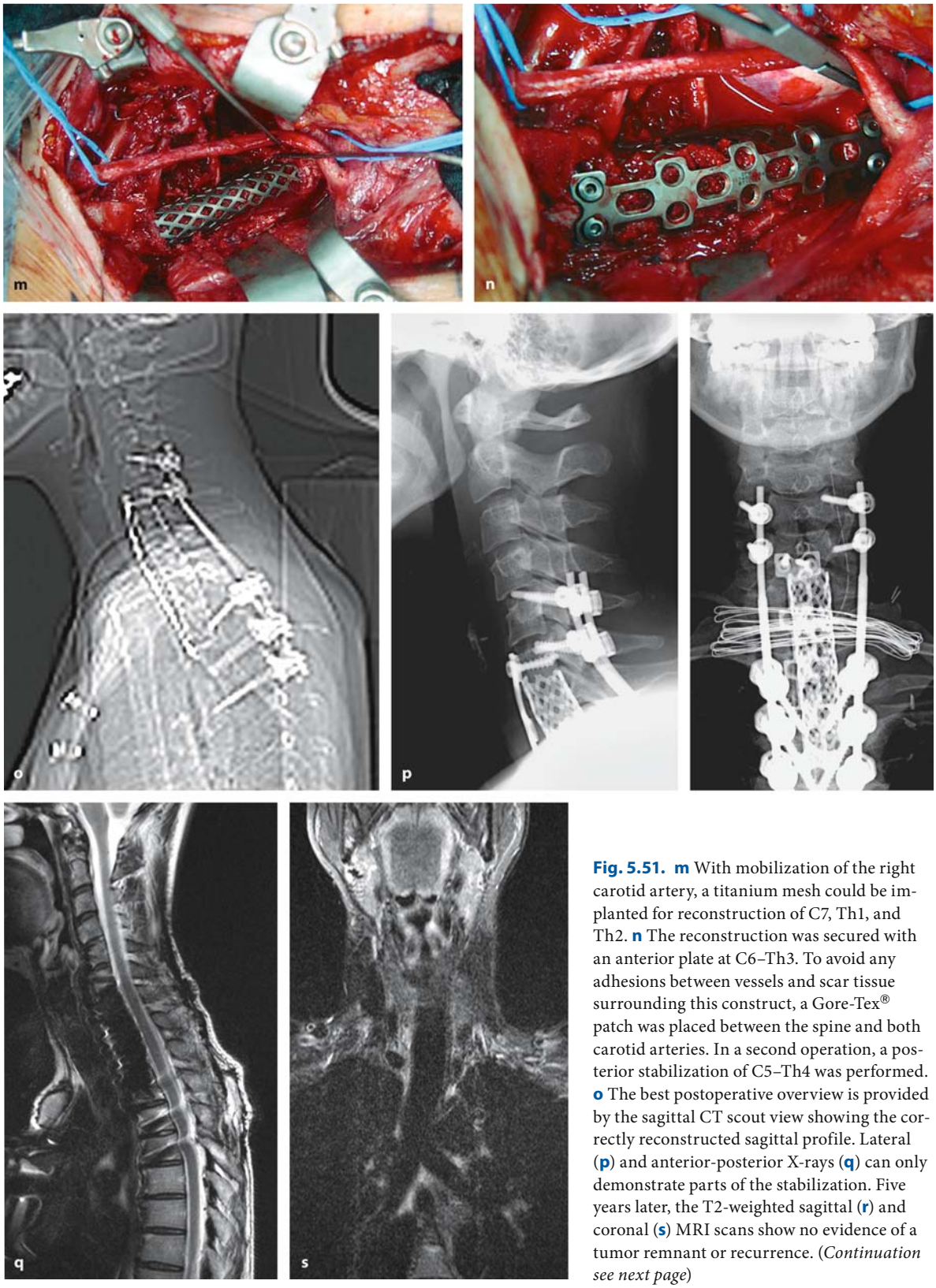

Fig. 5.51. **m** With mobilization of the right carotid artery, a titanium mesh could be implanted for reconstruction of C7, Th1, and Th2. **n** The reconstruction was secured with an anterior plate at C6–Th3. To avoid any adhesions between vessels and scar tissue surrounding this construct, a Gore-Tex® patch was placed between the spine and both carotid arteries. In a second operation, a posterior stabilization of C5–Th4 was performed. **o** The best postoperative overview is provided by the sagittal CT scout view showing the correctly reconstructed sagittal profile. Lateral (**p**) and anterior-posterior X-rays (**q**) can only demonstrate parts of the stabilization. Five years later, the T2-weighted sagittal (**r**) and coronal (**s**) MRI scans show no evidence of a tumor remnant or recurrence. (*Continuation see next page*)

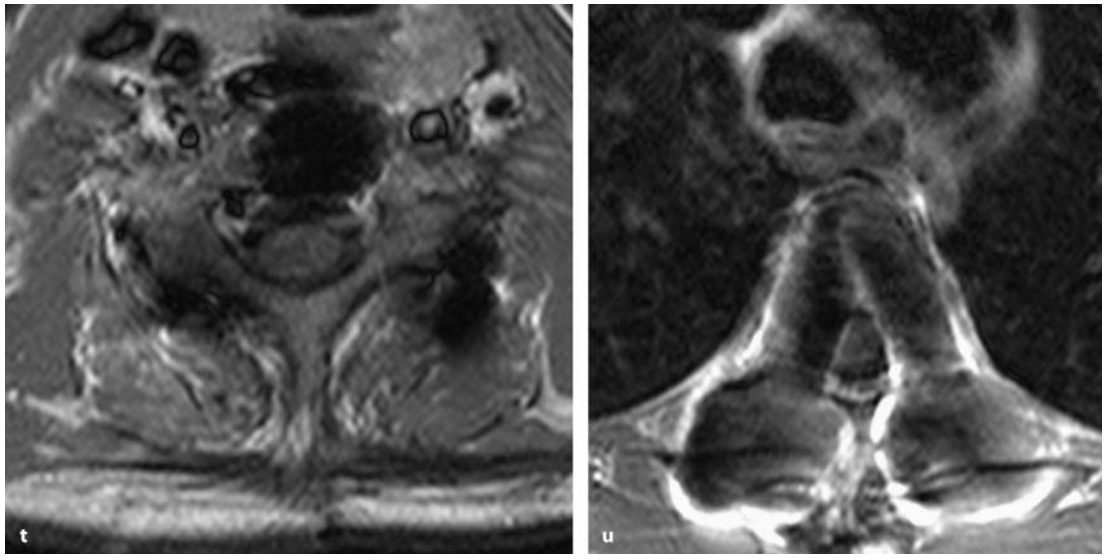

Fig. 5.51. (*Continued*) The axial T1-weighted images at C7 (**t**) and Th3 (**u**) underline this perfect result. Postoperatively, pain and dysesthesias improved, while a Horner syndrome, sensory disturbances, and a slight weakness of her left arm persisted

saw is used to cut the sternum. Combined with the cervical dissection, this will yield a more anterior and wider angle compared to the approach via resection of the sternoclavicular joint (Fig. 5.51). Obviously, these approaches carry the risk of injury to the pleura, thoracic vessels, and thoracic duct, in addition to the aforementioned risk of recurrent laryngeal nerve palsies.

A good alternative for this region is a posterior or posterolateral approach combined with a costotransversectomy (Fig. 5.52). Depending on the amount of spinal canal exposure required, a standard midline incision over the spinous processes or a paramedian incision can be used. With subperiosteal dissection of the vertebral arch, the transverse process, the costotransverse joint, and the proximal rib of each required spinal level, damage to the underlying pleura and neurovascular bundle underneath the rib can be avoided. With distal division of the rib it can be elevated, rotated, and the costotransverse ligaments transected. The transverse process is then resected. For orientation, one should keep in mind that the intervertebral disc space is located under the articulating surface of the transverse process with the rib. With further lateral resection of the rib and identification of the neurovascular bundle, the parietal pleura and sympathetic trunk can be mobilized from the anterolateral surface of the vertebral body to achieve an excavitary anterolateral approach. In this way, sufficient access to processes involving half of the vertebral body and spinal canal can be gained. With more extensive lesions, combinations with other approaches are required.

Tumors between Th4 and Th10 can be reached from anterior rather comfortably by a transthoracic approach (Fig. 5.53) [97]. The lower limitation of this approach is the diaphragm. With a medial diaphragmatic incision, however, this approach provides good access even down to the L2/3 disc space. The patient is positioned in the lateral decubitus position. The site of the skin incision and rib resection is determined according to the spinal level to be targeted. A curved incision along that rib is performed, which inserts at the upper spinal level of the pathology and/or required anterior reconstruction. The incision starts in the anterior axillary line. Depending on the spinal level, parts of the latissimus dorsi, trapezius, and rhomboid muscles need to be transected. The anterior serratus muscle is detached close to its insertion to avoid injury to the long thoracic nerve. After subperiosteal dissection and ligation of the neurovascular bundle underneath the rib, the rib may be resected and a thorax retractor can be inserted. With incision of the pleura, the lung can be retracted and a large space is provided for resection, reconstruction, and stabilization. Care has to be taken to preserve the azygos and hemiazygos veins, and the thoracic duct (Fig. 5.53). The blood supply to the thoracic cord depends on preservation of the artery of Adamkiewicz. This vessel shows considerable variability. It is a branch of a segmental artery that originates at Th8 to Th10 – on the left side in about 80% and on the right

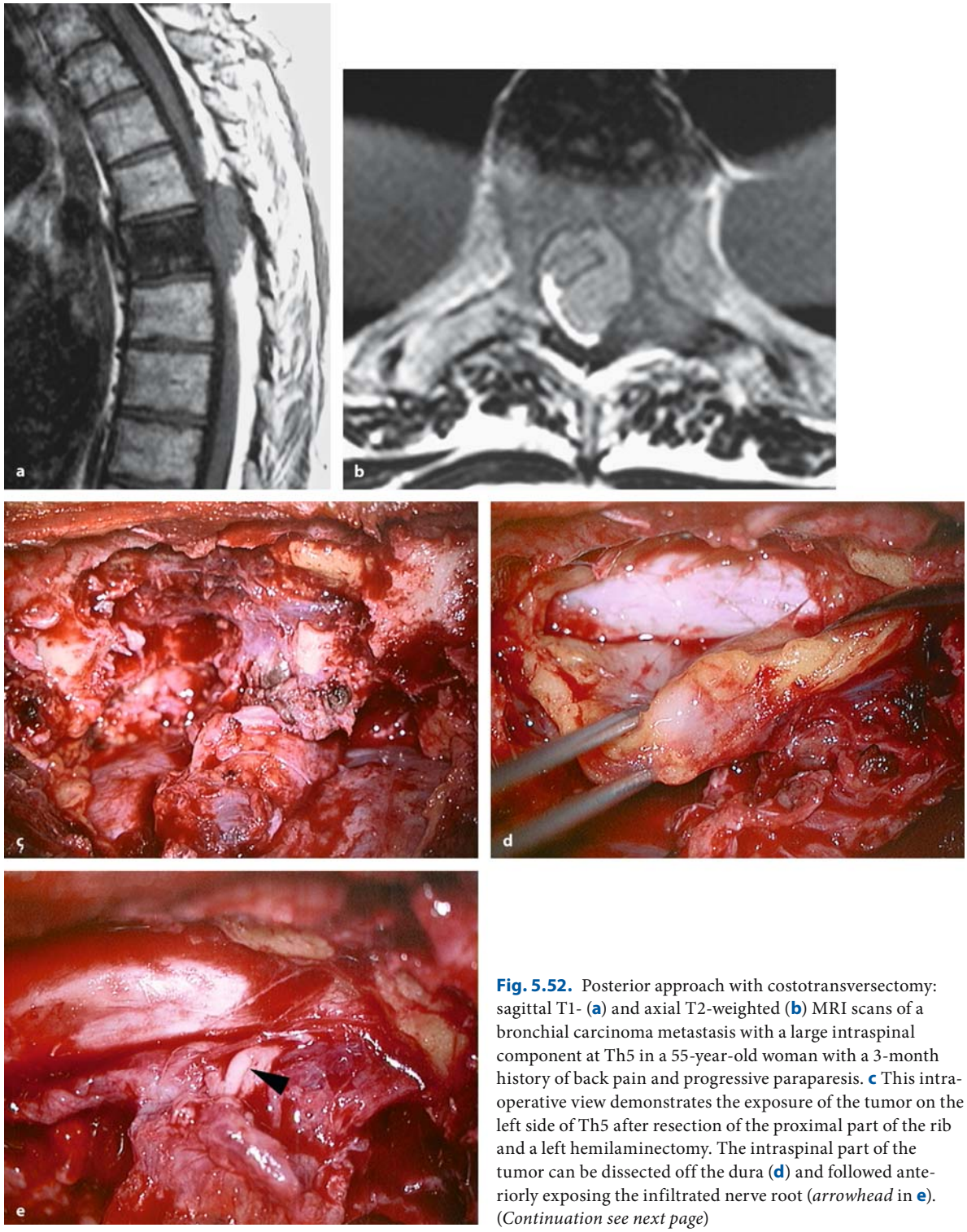

Fig. 5.52. Posterior approach with costotransversectomy: sagittal T1- (**a**) and axial T2-weighted (**b**) MRI scans of a bronchial carcinoma metastasis with a large intraspinal component at Th5 in a 55-year-old woman with a 3-month history of back pain and progressive paraparesis. **c** This intraoperative view demonstrates the exposure of the tumor on the left side of Th5 after resection of the proximal part of the rib and a left hemilaminectomy. The intraspinal part of the tumor can be dissected off the dura (**d**) and followed anteriorly exposing the infiltrated nerve root (*arrowhead* in **e**). (*Continuation see next page*)

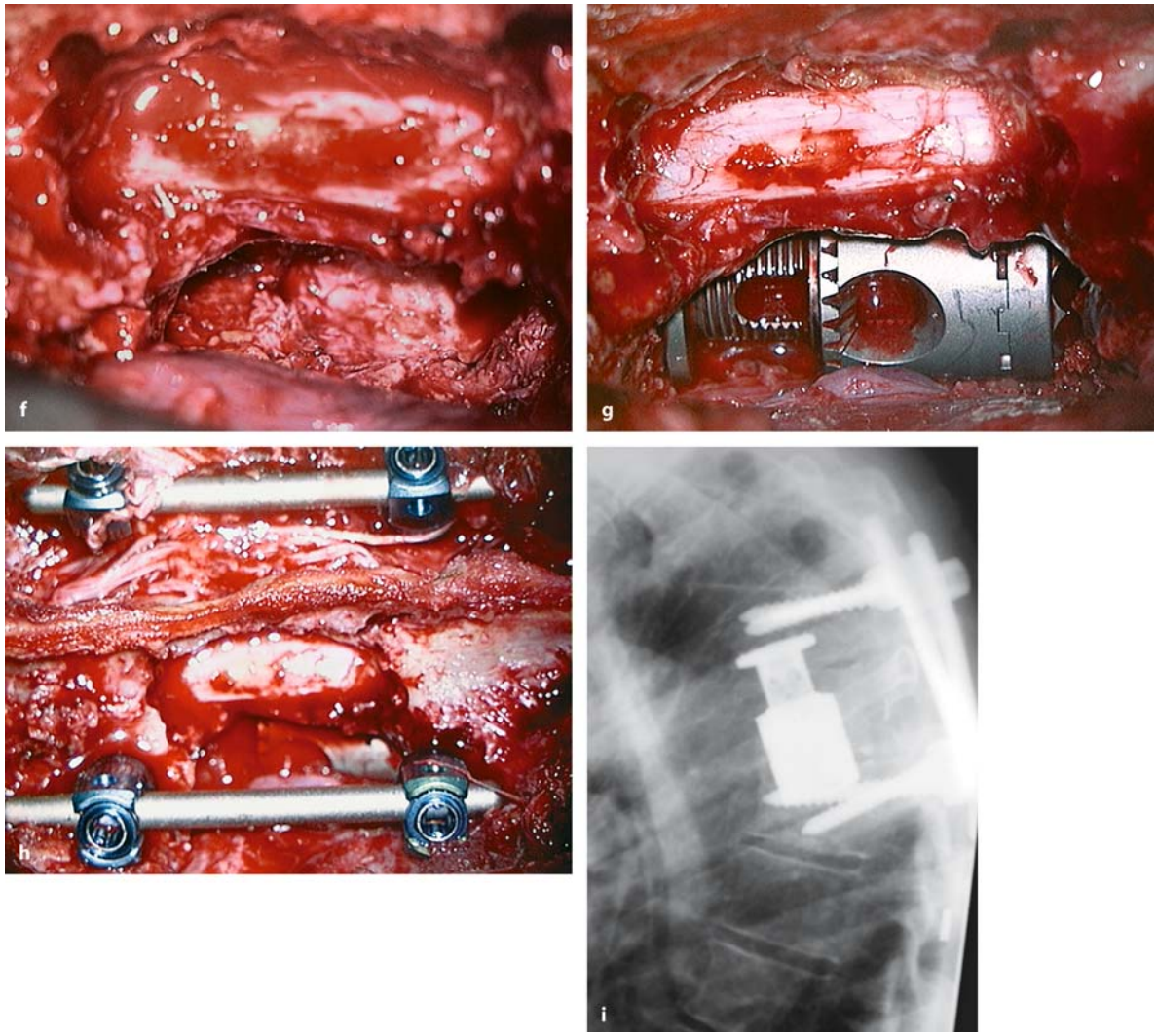

Fig. 5.52. (*Continued*) After tumor resection (**f**) the defect is reconstructed with an expandable titanium cage (**g**). This costotransversectomy approach provides direct access to about the midline of the affected vertebra. Turning the patient to the opposite side and retracting pleura and lung gains further access to the opposite half of the vertebral body. The region underneath the contralateral pedicle, however, remains inaccessible. **h** The posterior transpedicular stabilization from Th4 to Th6 is in place. The lateral X-ray (**i**) demonstrates the postoperative result

side in 20% of cases. Therefore, the segmental arteries at the anterior lateral aspect of lower thoracic vertebral bodies should only be ligated if angiography has localized this artery. Alternatively, monitoring of sensory evoked potentials with test occlusion during surgery has been advocated [313]. Again, this approach provides access to the vertebral body and intervertebral discs, but intraspinal or paraspinal tumor parts may require an additional posterior approach. Patients require a thoracic drain for a few days to facilitate reexpansion of the lung. Endoscopic techniques have been described in addition to such open transthoracic approaches [20, 144].

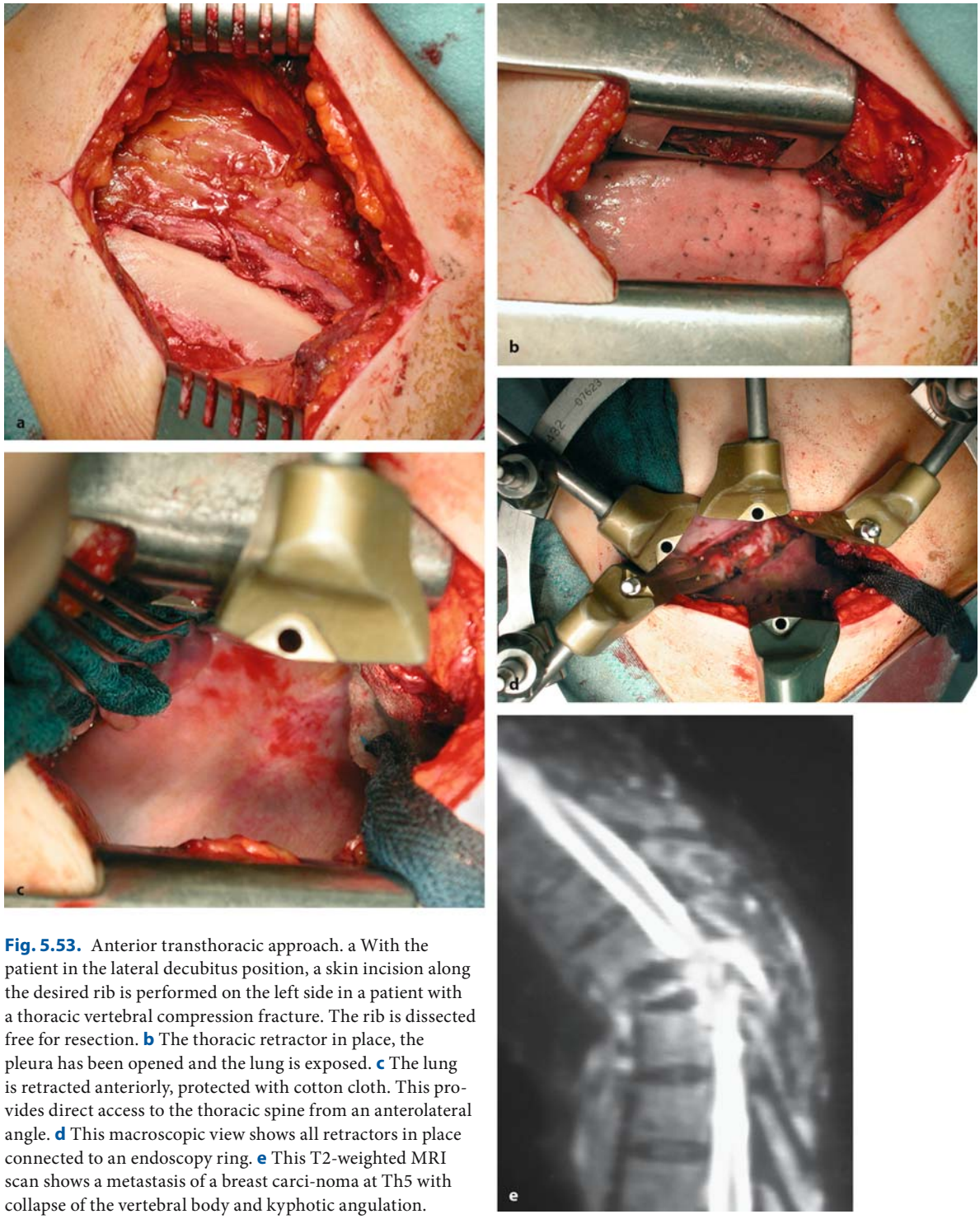

Fig. 5.53. Anterior transthoracic approach. a With the patient in the lateral decubitus position, a skin incision along the desired rib is performed on the left side in a patient with a thoracic vertebral compression fracture. The rib is dissected free for resection. **b** The thoracic retractor in place, the pleura has been opened and the lung is exposed. **c** The lung is retracted anteriorly, protected with cotton cloth. This provides direct access to the thoracic spine from an anterolateral angle. **d** This macroscopic view shows all retractors in place connected to an endoscopy ring. **e** This T2-weighted MRI scan shows a metastasis of a breast carci-noma at Th5 with collapse of the vertebral body and kyphotic angulation.
(*Continuation see next page*)

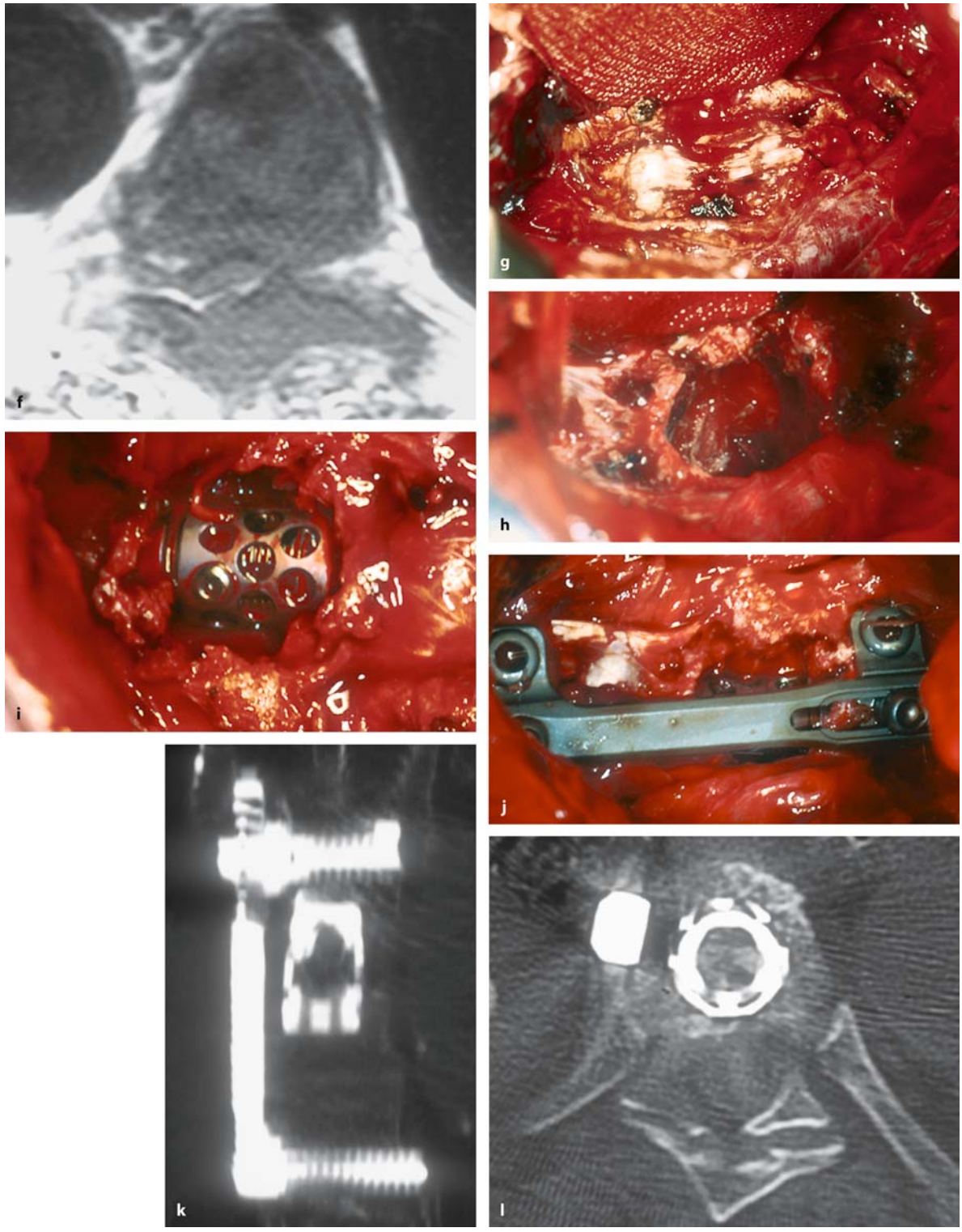

Fig. 5.53. (*Continued*) **f** This axial T1-weighted MRI demonstrates the infiltration of virtually the entire vertebra and considerable cord compression from anterior (see also Fig. 5.38). **g** This intraoperative view shows the tumorous vertebra covered by the anterior longitudinal ligament. With complete resection of the vertebral body (**h**), an expandable cage is implanted (**i**) and combined with an anterior plate (**j**). The postoperative coronal (**k**) and axial (**l**) bone-window CT scans demonstrate a good reconstruction of the spinal profile and decompression of the spinal canal

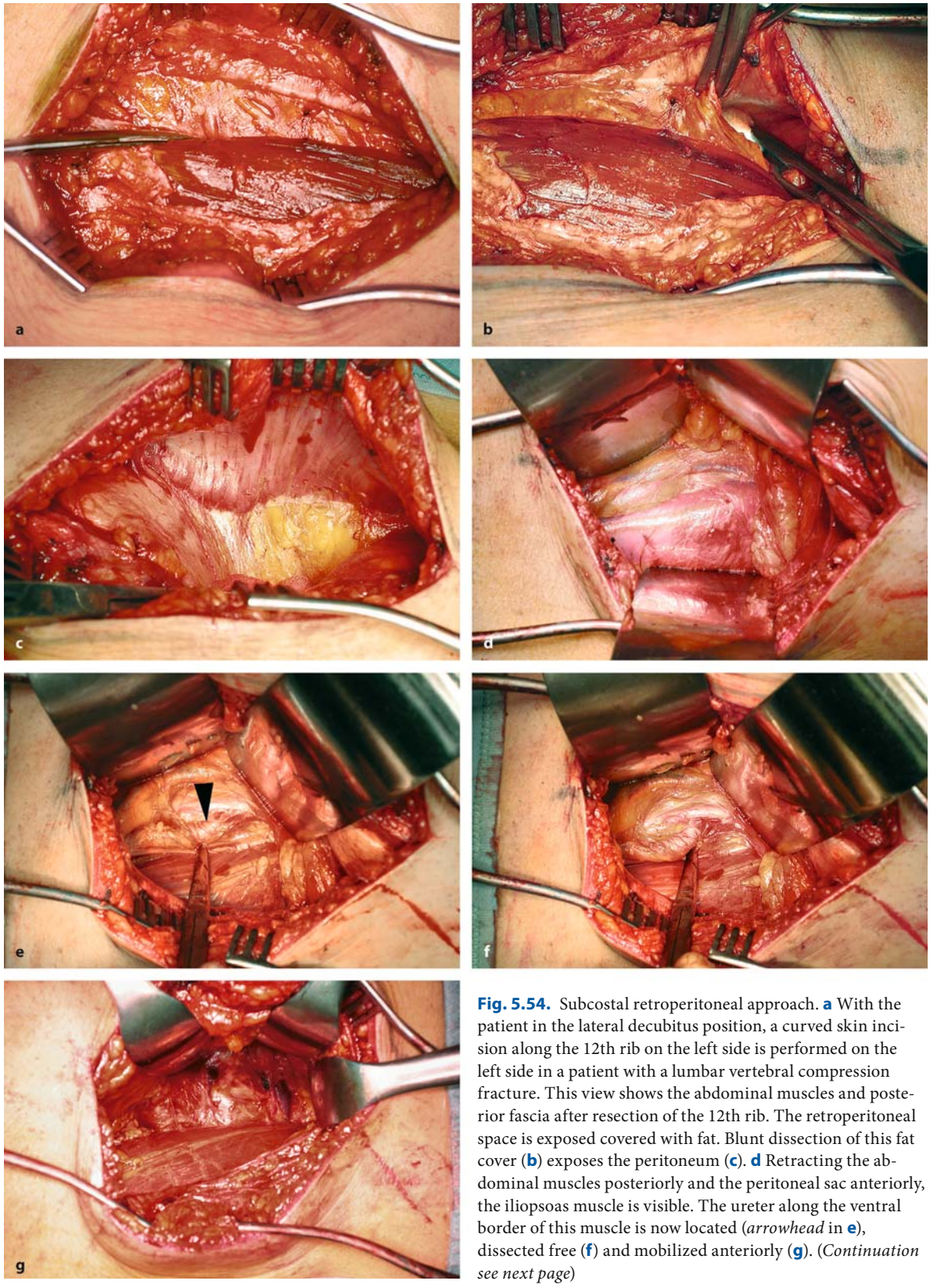

Fig. 5.54. Subcostal retroperitoneal approach. **a** With the patient in the lateral decubitus position, a curved skin incision along the 12th rib on the left side is performed on the left side in a patient with a lumbar vertebral compression fracture. This view shows the abdominal muscles and posterior fascia after resection of the 12th rib. The retroperitoneal space is exposed covered with fat. Blunt dissection of this fat cover (**b**) exposes the peritoneum (**c**). **d** Retracting the abdominal muscles posteriorly and the peritoneal sac anteriorly, the iliopsoas muscle is visible. The ureter along the ventral border of this muscle is now located (*arrowhead* in **e**), dissected free (**f**) and mobilized anteriorly (**g**). (*Continuation see next page*)

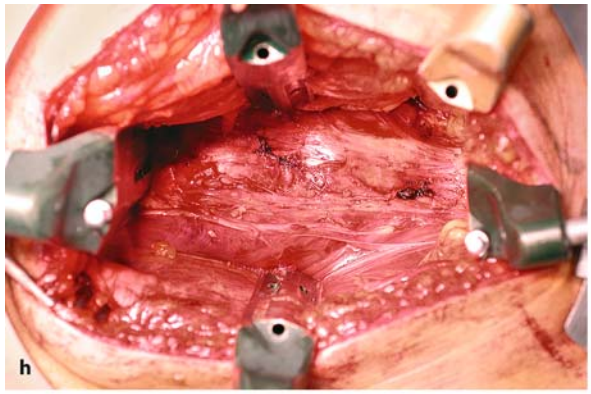

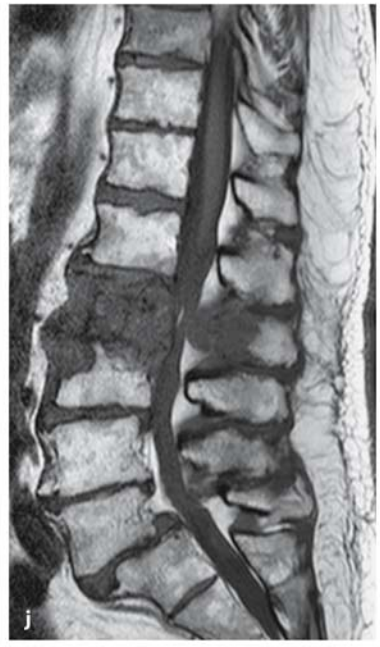

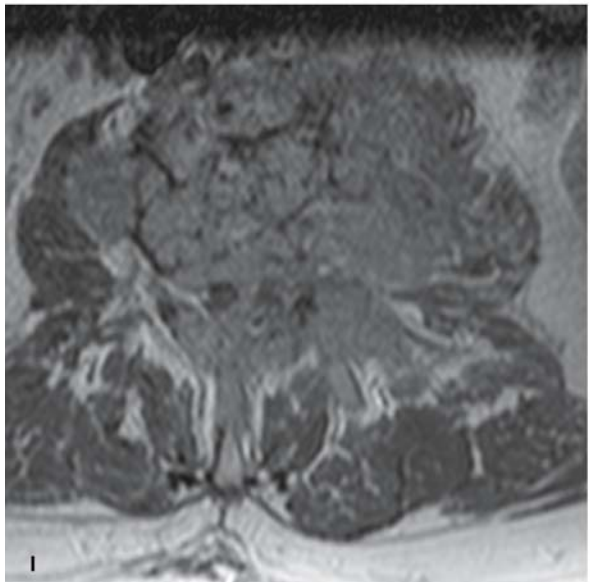

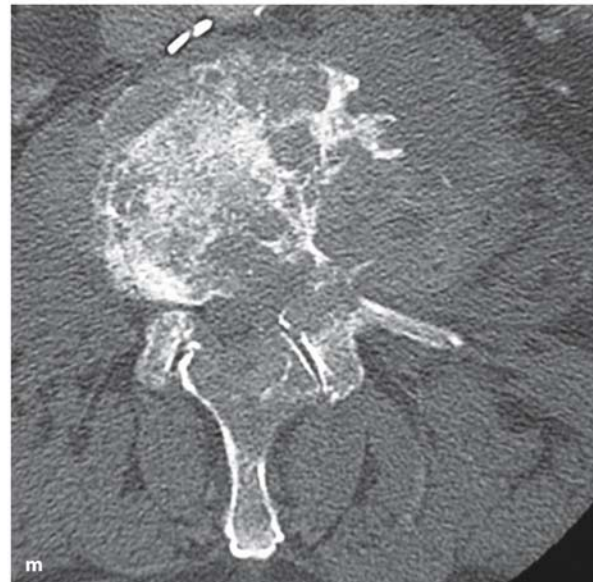

Fig. 5.54. h Finally, the iliopsoas muscle is mobilized posteriorly to expose the vertebral column. These sagittal T2- (**i**), T1- weighted MRI scans without (**j**) and with contrast (**k**) demonstrate a hypernephroma metastasis at L2. The axial T1-weighted MRI (**l**) and bone-window CT scan (**m**) demonstrate circumferential compression of the spinal cord and marked infiltration of the left iliopsoas muscle. (*Continuation see next page*)

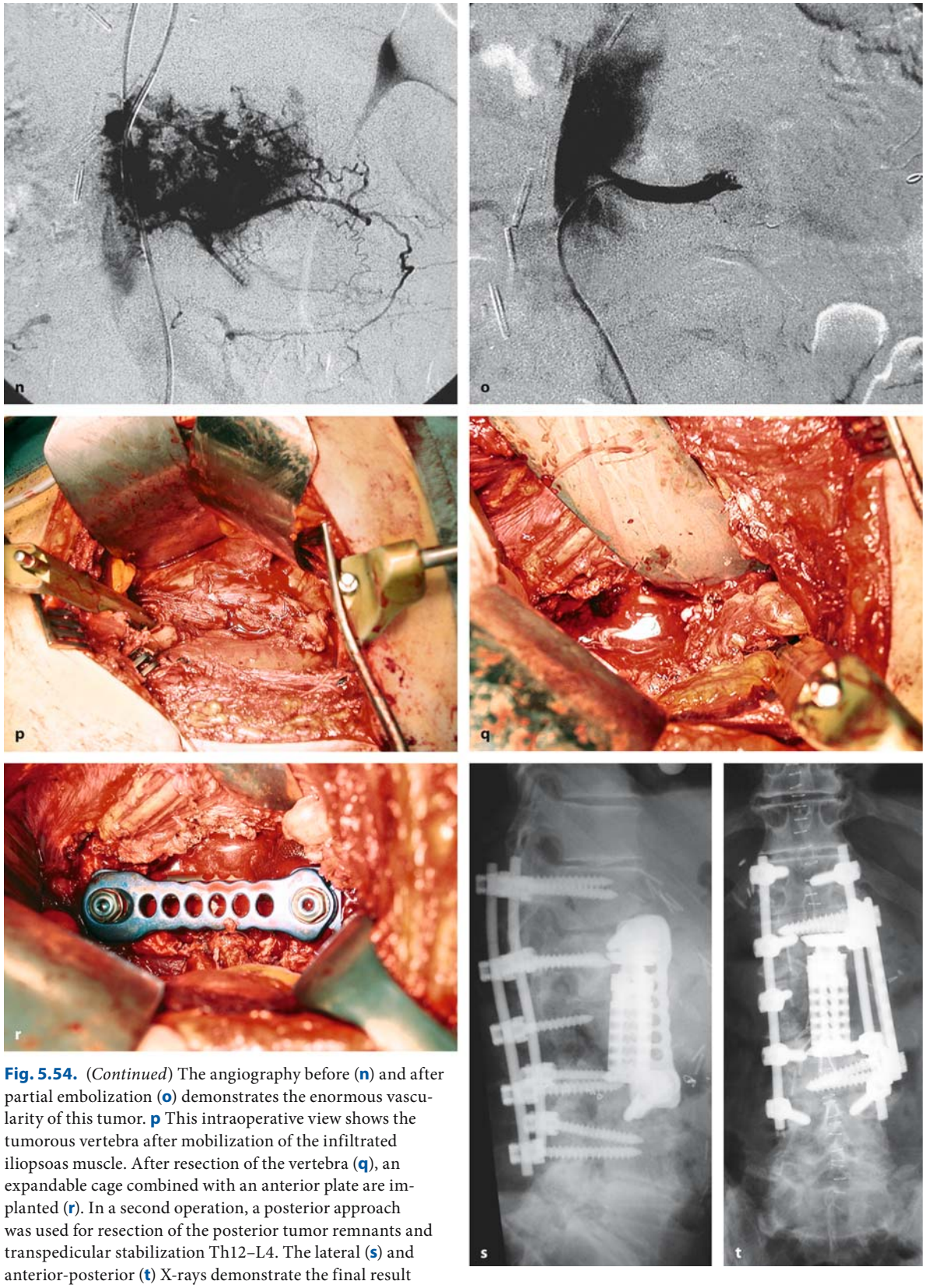

Fig. 5.54. (*Continued*) The angiography before (**n**) and after partial embolization (**o**) demonstrates the enormous vascularity of this tumor. **p** This intraoperative view shows the tumorous vertebra after mobilization of the infiltrated iliopsoas muscle. After resection of the vertebra (**q**), an expandable cage combined with an anterior plate are implanted (**r**). In a second operation, a posterior approach was used for resection of the posterior tumor remnants and transpedicular stabilization Th12–L4. The lateral (**s**) and anterior-posterior (**t**) X-rays demonstrate the final result

5.3.2.1.3 Thoracolumbar and Lumbar Spine

With tumors between Th12 and L2, the transthoracic approach as just described would be our favorite choice for anterior access. Alternatively, a subcostal retroperitoneal approach is available (Fig. 5.54), which can be combined with a diaphragmatic incision to get as high as Th12 (Fig. 5.55). The retroperitoneal approach is our choice for tumors involving the lumbar spine down to L5. Below L4, the iliac vessels may limit this approach depending on the level at which they cross the lumbar spine. But with mobilization of these vessels, the body of L5 can be removed from this approach. The retroperitoneal access provides an anterolateral view, avoiding restrictions of transperitoneal approaches related to the major abdominal vessels. Depending on the spinal level the patient is either in the lateral decubitus or supine position with the table slightly rotated. The table may be slightly bent at the level of the thoracolumbar junction, elevating the lower thorax. The table is rotated slightly to the left so that the abdominal contents can be retracted from the spine more easily. Bending the left leg at the hip relaxes the iliopsoas muscle. A curved lateral incision is made alongside the 12th rib or halfway toward the iliac crest on the left side. Depending on the targeted spinal level, this rib may be resected. The external and internal oblique muscles are transected exposing the transverse abdominal muscle and posterior fascia. With transection of these structures, the retroperitoneum is entered and retroperitoneal fat is seen covering the peritoneum. These are mobilized bluntly from the lateral and posterior abdominal wall. The iliopsoas muscle now covers the lumbar spine. The ureter usually lies near the ventral border of the psoas muscle and can be retracted anteriorly with the

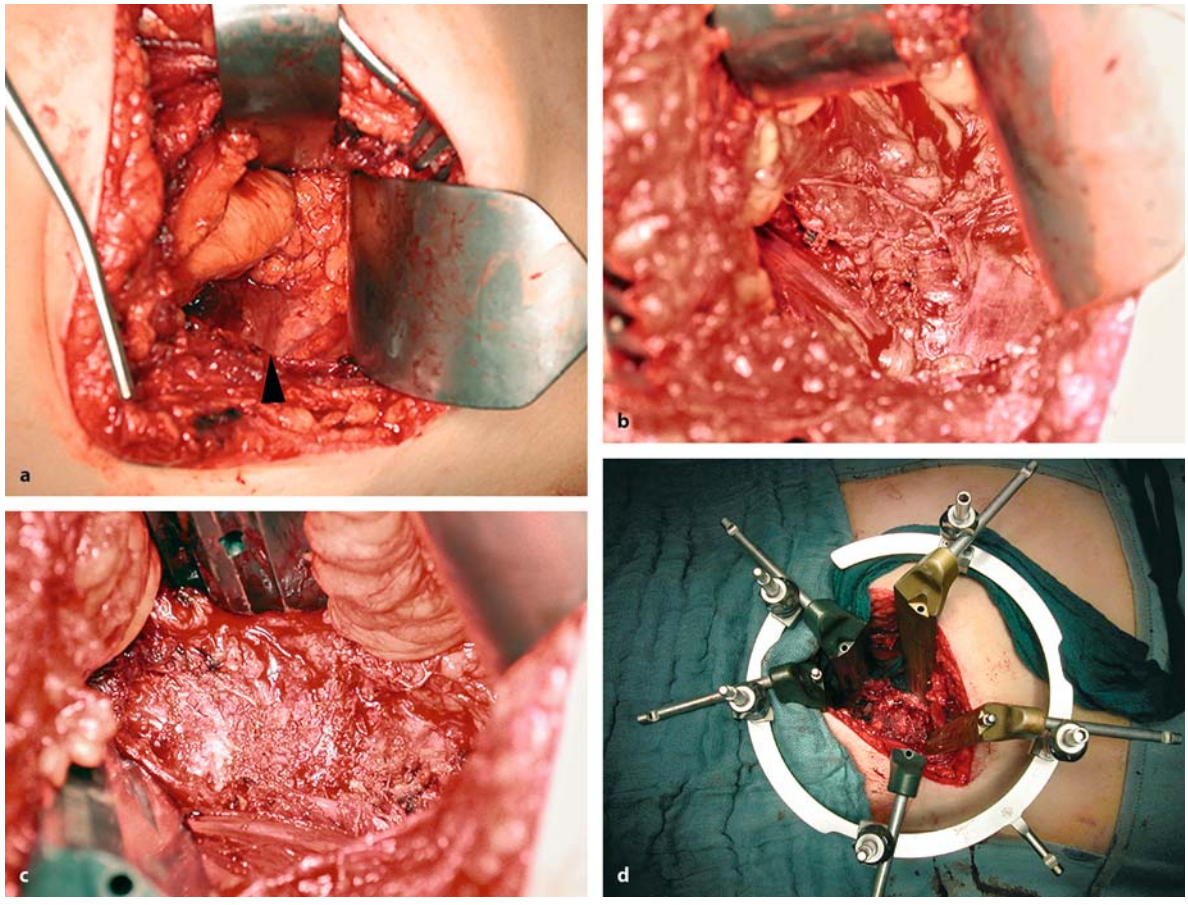

Fig. 5.55 a This intraoperative view represents the state of dissection for a retroperitoneal subdiaphragmatic approach after anterior mobilization of the peritoneal sac (see Fig. 5.53g for comparison). The diaphragmatic insertion at the spinal column is exposed (*arrowhead*). With mobilization of the iliopsoas muscle (**b**) and diaphragmatic insertion (**c**), the vertebral body is visible. **d** This overview demonstrates the exposure with all retractors in place

peritoneal fat. To expose the lumbar spine, the psoas muscle has to be mobilized from anterior to be retracted posteriorly. Some authors caution against splitting this muscle to avoid injury to iliohypogastric, ilioinguinal, genitofemoral, and lateral cutaneous femoral nerves, which course within it at the level of L3 and L4. We regularly split this muscle and have not seen postoperative problems associated with these nerves. Care has to be taken, though, not to compress spinal nerves against transverse processes by retractors. The sympathetic trunk lies along the ventral edge of the psoas muscle and can usually be preserved. This is particularly important at the level of L5, where the sympathetic plexus innervates the urogenital system. With elevation of the psoas the vertebral bodies and segmental vessels can be seen. Posterior exposure should be extended to visualize the lateral wall of the pedicle to provide a landmark for localization of the spinal canal (Fig. 5.54). If the exposure requires access to Th12, the insertion of the diaphragm must be elevated (Fig. 5.55). In such instances, postoperative radiographs should be performed to rule out a pleural tear and pneumothorax.

Alternatively, an anterior retroperitoneal approach can be used to access L4, L5, and the sacrum with the patient in the supine position. From a paramedian incision on the left side along the rectus abdominis muscle, the fascial layers are transected allowing mobilization of the peritoneum to the opposite side, providing a direct anterior angle to the lower lumbar spine. Care has to be taken to identify and transect all minor branches off the iliac veins and arteries before mobilizing these vessels laterally. The feasibility of this approach for tumor removal depends on the relationship between the pathology and the major vessels. With a high-positioned iliac bifurcation, this anterior midline approach has advantages over the anterolateral retroperitoneal approach, as described above.

5.3.2.1.4 Sacrum

For sacral tumors, the size of the tumor and involvement of pelvic organs dictate the approach [582]. With small lesions involving the sacral spinal canal, a standard posterior approach is sufficient (Fig. 5.56). With larger tumors extending into the pelvis, a combined approach from anterior and posterior and cooperation with abdominal surgeons is recommended [211]. Stability requires preservation of S1 and bladder-control preservation of both S1 and S2 roots [245]. Whereas sacral bone tumors in adults almost exclusively consist of either chordomas or metastases, diverse histologies may be found in children [311].

5.3.2.2 Tumor Removal

The strategy for tumor removal has to account for the histology. With metastatic lesions or benign neoplasms, removal can be done intralesionally. After the tumor has been reached, one should expose the neoplasm entirely before starting its removal (Figs. 5.48, 5.50, and 5.52–5.54). Almost all bone tumors are quite vascularized so that it may become difficult to define tumor extensions once the removal and, thus, bleeding has started. Preoperative embolization may be particularly helpful for resection of osteoblastomas, aneurysmatic bone cysts, and thyroid and kidney tumor metastases (Fig. 5.54) [200, 345]. With intratumoral removal, the surgeon may have to work quickly to limit blood loss as the bleeding may not be controllable until the tumor is removed. Quite often the cessation of bleeding is a good indicator that the mass of the tumor has been removed and persistent bleeding indicates that there is still tumor left. The limitations of a bone tumor may be difficult to define inside the vertebral body. The vascularization or consistency of the bone may be the only clues. Bony anatomical landmarks defined on CT can also be used.

With primary malignant or locally aggressive, benign bone tumors, however, a different strategy should be employed whenever possible: en bloc resection with healthy margins (Fig. 5.56). This will provide the only chance for long-term disease-free survival in such patients. An increasing number of publications have appeared describing en bloc resections for tumors of the spine with good postoperative outcomes [2, 72, 81, 84, 126, 228, 279, 300, 301, 449, 509, 536, 573].Planning for an en bloc resection of a vertebral body requires a detailed neuroradiological evaluation. A true en bloc resection of a vertebral body tumor can be achieved if the tumor is centrally located within the vertebral body with at least one pedicle free of tumor [80]. Anterior approaches – even from both sides if appropriate – are chosen for this purpose after a posterior operation has disconnected the posterior elements and stabilized the spine. Discectomies and sectioning of neighboring vertebral bodies with chisels or threadwire saws can be performed under direct vision followed by reconstruction and fusion. Likewise, en bloc resections of posterior elements are possible [80, 301] provided the tumor has not entered the epidural space and does not prog-

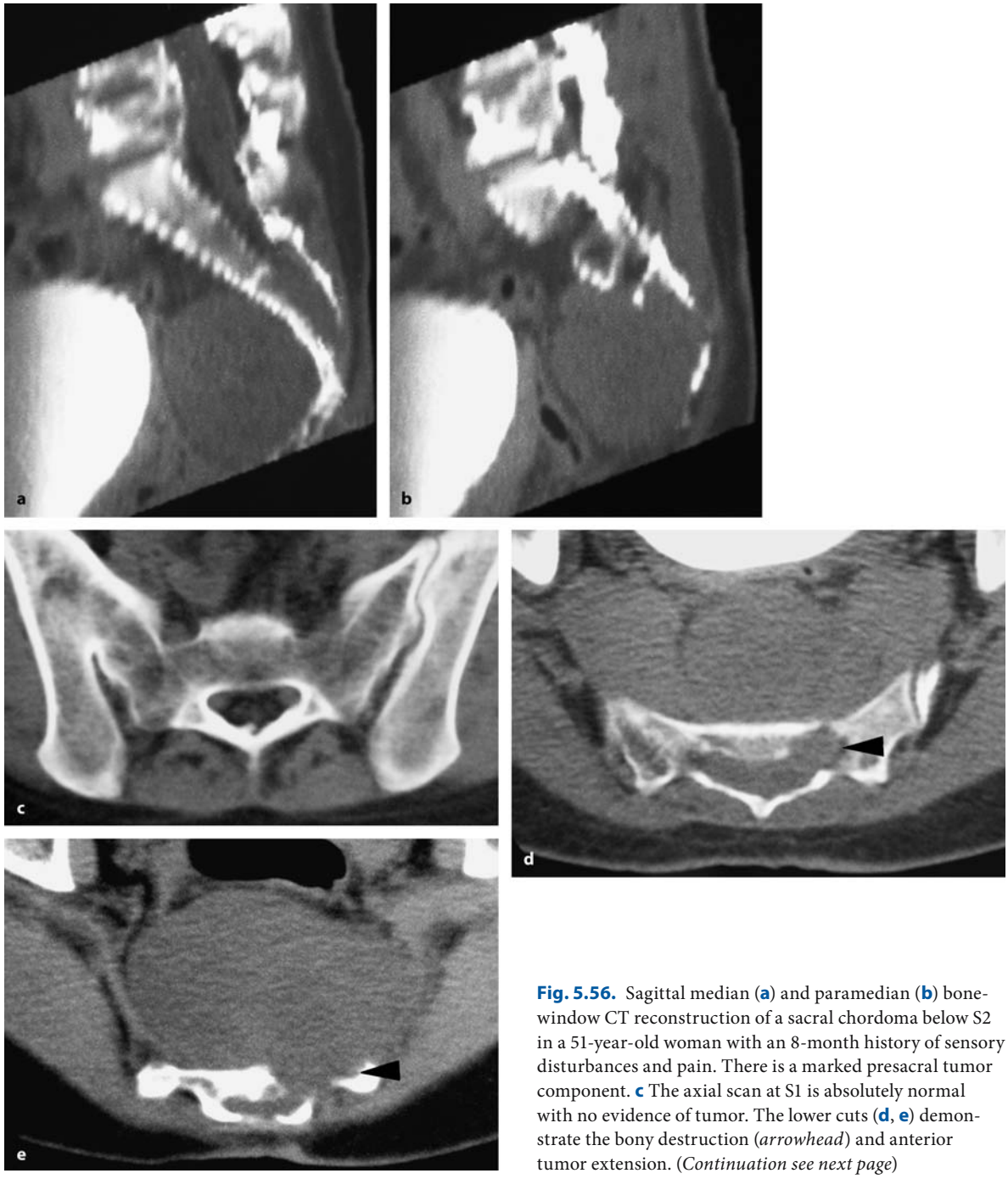

Fig. 5.56. Sagittal median (**a**) and paramedian (**b**) bone-window CT reconstruction of a sacral chordoma below S2 in a 51-year-old woman with an 8-month history of sensory disturbances and pain. There is a marked presacral tumor component. **c** The axial scan at S1 is absolutely normal with no evidence of tumor. The lower cuts (**d**, **e**) demonstrate the bony destruction (*arrowhead*) and anterior tumor extension. (*Continuation see next page*)

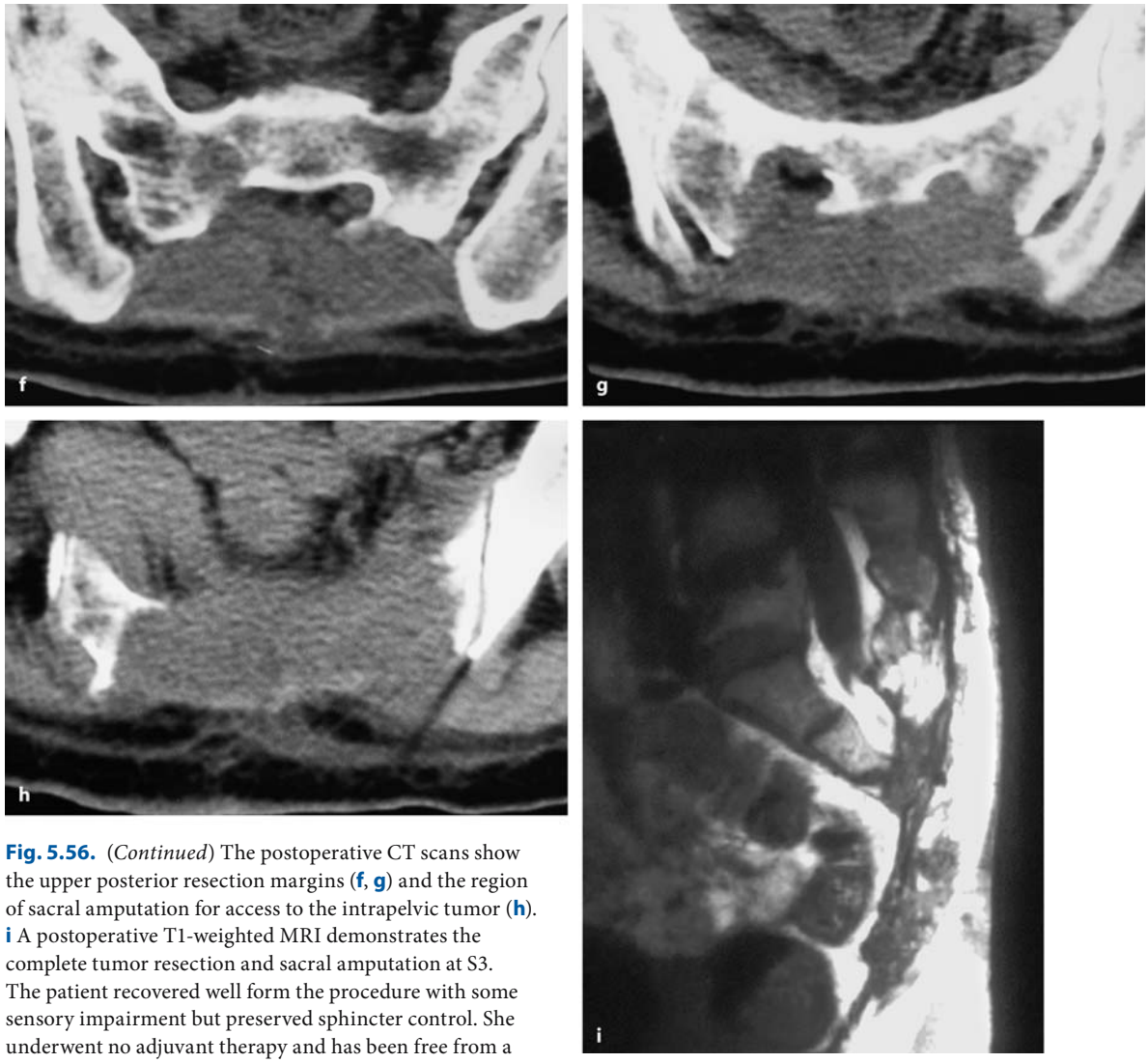

Fig. 5.56. (*Continued*) The postoperative CT scans show the upper posterior resection margins (**f**, **g**) and the region of sacral amputation for access to the intrapelvic tumor (**h**). **i** A postoperative T1-weighted MRI demonstrates the complete tumor resection and sacral amputation at S3. The patient recovered well form the procedure with some sensory impairment but preserved sphincter control. She underwent no adjuvant therapy and has been free from a recurrence for 12 years

ress further into the vertebral body. Whenever tumors do not remain confined to these limits or recurrent tumors have to be operated, we would recommend combined approaches to come as close as possible to an en bloc resection (Fig. 5.57). Compromises are required whenever there is a significant extraosseous extension (i.e., in Enneking stage B tumors), especially into the epidural or intradural spaces. A true oncological resection with preservation of neurological function cannot be achieved in such cases [126]. Boriani et al. described en bloc resections in 29 selected patients and obtained a wide margin in 20 of these operations [77].

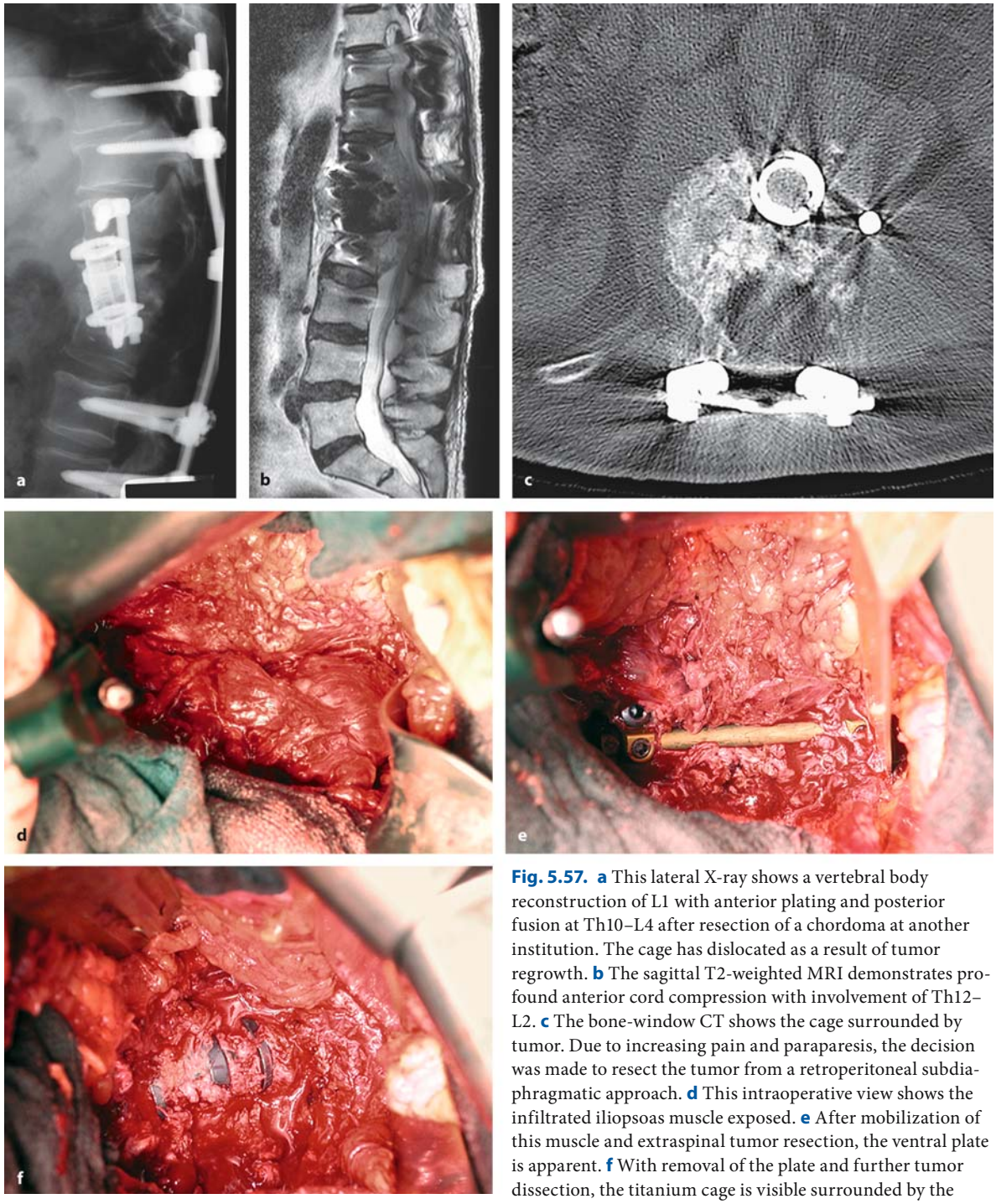

Fig. 5.57. **a** This lateral X-ray shows a vertebral body reconstruction of L1 with anterior plating and posterior fusion at Th10–L4 after resection of a chordoma at another institution. The cage has dislocated as a result of tumor regrowth. **b** The sagittal T2-weighted MRI demonstrates profound anterior cord compression with involvement of Th12–L2. **c** The bone-window CT shows the cage surrounded by tumor. Due to increasing pain and paraparesis, the decision was made to resect the tumor from a retroperitoneal subdiaphragmatic approach. **d** This intraoperative view shows the infiltrated iliopsoas muscle exposed. **e** After mobilization of this muscle and extraspinal tumor resection, the ventral plate is apparent. **f** With removal of the plate and further tumor dissection, the titanium cage is visible surrounded by the tumor. (*Continuation see next page*)

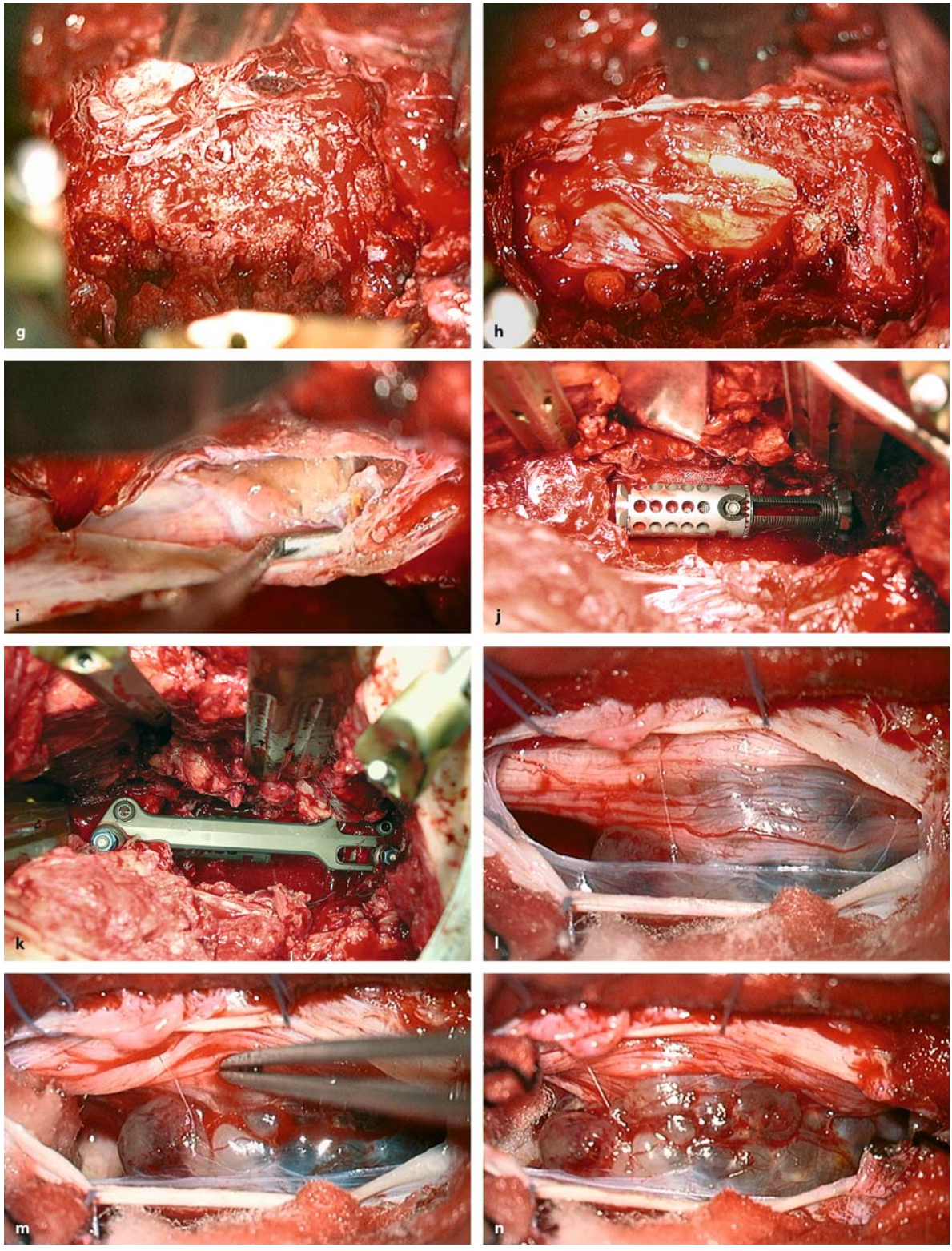

Fig. 5.57. After removal of the cage (**g**), the tumor is resected with removal of Th12, L1, and L2 (**h**). **i** Inspection of the dura discloses an intradural tumor extension at L1. The dura is repaired with fascia and fibrin glue. An expandable cage is implanted (**j**) combined with an anterior plate (**k**). **l** In a second operation from a posterior approach, the intradural tumor is demonstrated. Mobilization of the nerve roots (**m**) exposes the intradural tumor (**n**). (*Continuation see next page*)

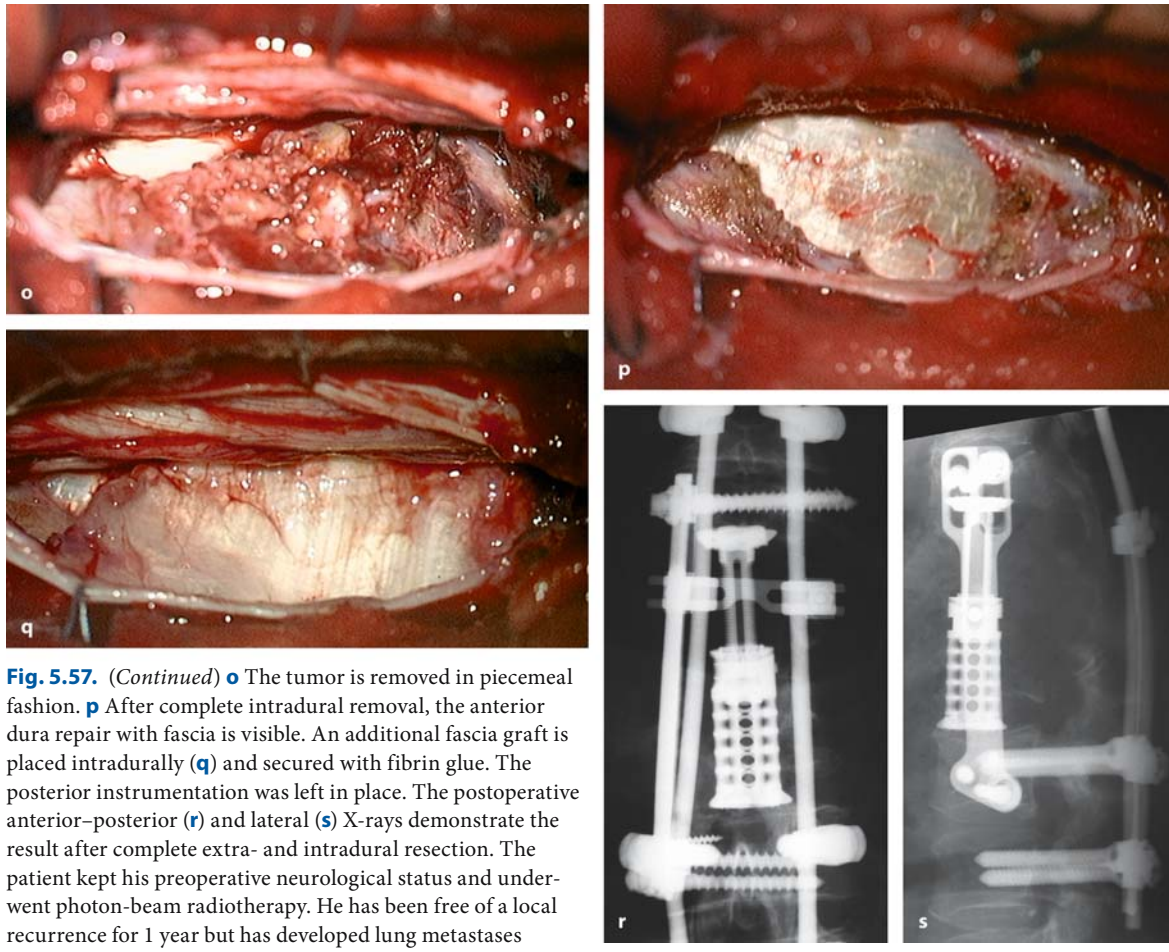

Fig. 5.57. (*Continued*) **o** The tumor is removed in piecemeal fashion. **p** After complete intradural removal, the anterior dura repair with fascia is visible. An additional fascia graft is placed intradurally (**q**) and secured with fibrin glue. The posterior instrumentation was left in place. The postoperative anterior–posterior (**r**) and lateral (**s**) X-rays demonstrate the result after complete extra- and intradural resection. The patient kept his preoperative neurological status and underwent photon-beam radiotherapy. He has been free of a local recurrence for 1 year but has developed lung metastases

5.3.3 Reconstruction, Stabilization, and Closure

Once the process is removed, the resulting defect should be filled with either Gelfoam or other hemostatic materials. Once the bleeding has stopped the defect can then be used for reconstruction of the vertebral body using either PMMA (Fig. 5.58), bone (Fig. 5.50), or a titanium cage (Figs. 5.52–5.54, and 5.57). In recent years, expandable cages have made vertebral body replacement easier, with immediate stability combined with anterior or combined anterior and posterior instrumentation (Figs. 5.52–5.54, and 5.57) [533]. PMMA can be applied as a block (Fig. 5.58) or injected into the remains of the vertebral body during a posterior decompression and instrumentation (i.e., vertebroplasty; Fig. 5.59). With malignant tumors, we prefer PMMA and titanium cages [327, 329]; however, bone grafts can be used as well even if postoperative radio- and chemotherapy are planned (Fig. 5.50). Even though it seems hard to believe, a recent report claimed fusion rates of 93% with bone grafts within 6 months in such instances [324]. In general, bony fusions should be attempted for patients with a life expectancy of more than 6 months [327].

After reconstruction of a vertebral body, additional fixation should be applied. This can be done exclusively from anterior using a plate-and-screw fixation [299, 500, 512, 517] provided all posterior elements are intact (Figs. 5.50, 5.53, and 5.58). With destruction of the posterior elements by tumor or previous operations, a ventral stabilization alone is bound to fail (Fig. 5.60) [327, 329]. Likewise a posterior approach with transpedicular fixation in the thoracic or lumbar spine, or lateral mass fixation in the cervical spine [456, 563] alone will only be successful with appropriate ventral support (Figs. 5.52, 5.59). If this cannot be established from posterior, combined approaches and stabilizations are required (Figs. 5.51, 5.54, 5.57, and 5.60).

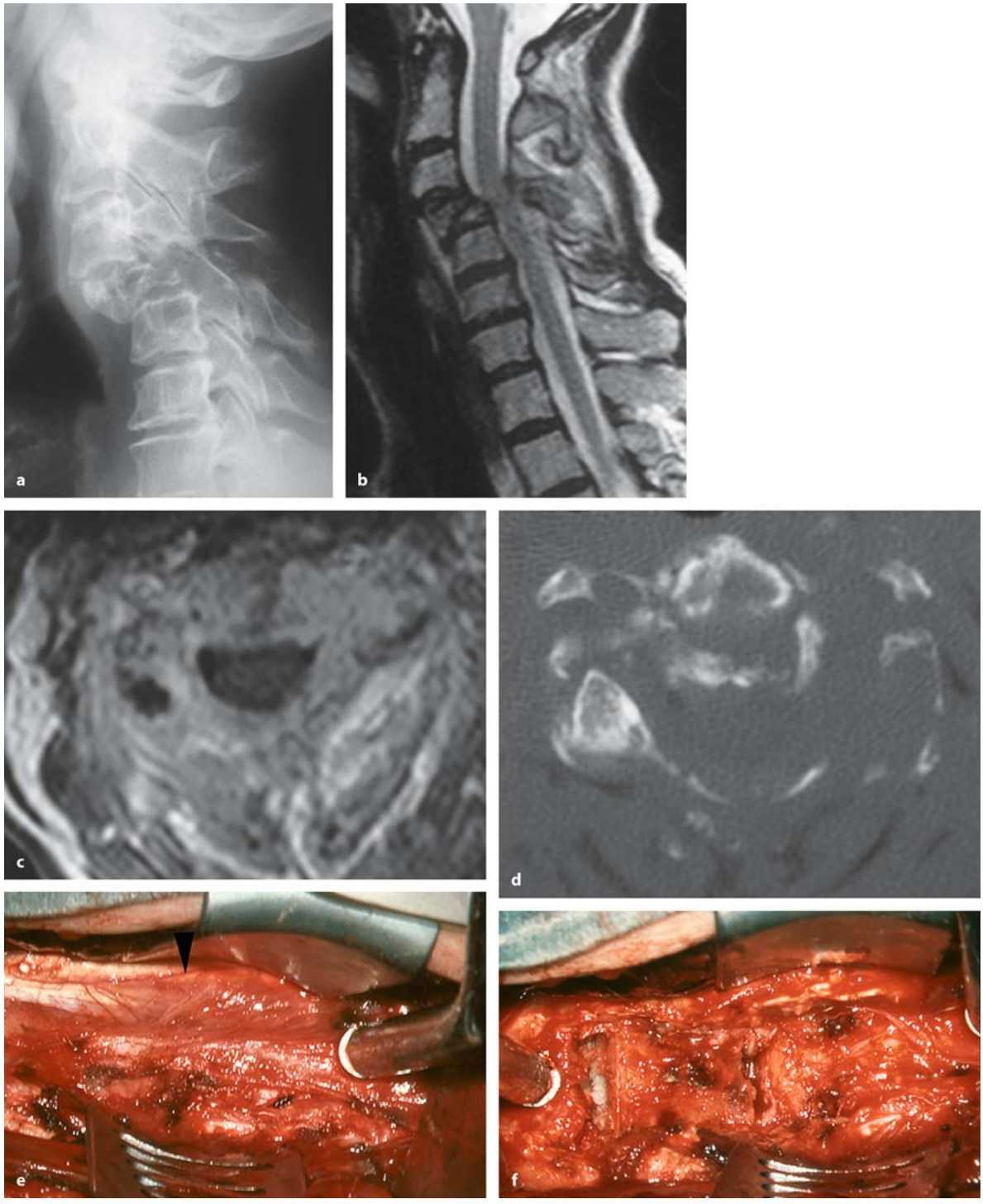

Fig. 5.58. **a** Lateral X-ray of a breast carcinoma metastasis at C4 in a 69-year-old woman and a history of pain and weakness of her left arm. The vertebral body has collapsed leading to anterior luxation. **b** Surprisingly, the sagittal T2-weighted MRI demonstrates only minor compression of the spinal cord. **c** The axial T1-weighted, contrast-enhanced image shows involvement of the entire vertebra but no intraspinal tumor extension. **d** The bone-window CT image demonstrates profound bony destructions of the vertebral body. **e** The intraoperative view shows the anterior longitudinal ligament and the prominent longus colli muscle on the right side (*arrowhead*). **f** The ligament was resected and the discs C3/4 and C4/5 have been removed. (*Continuation see next page*)

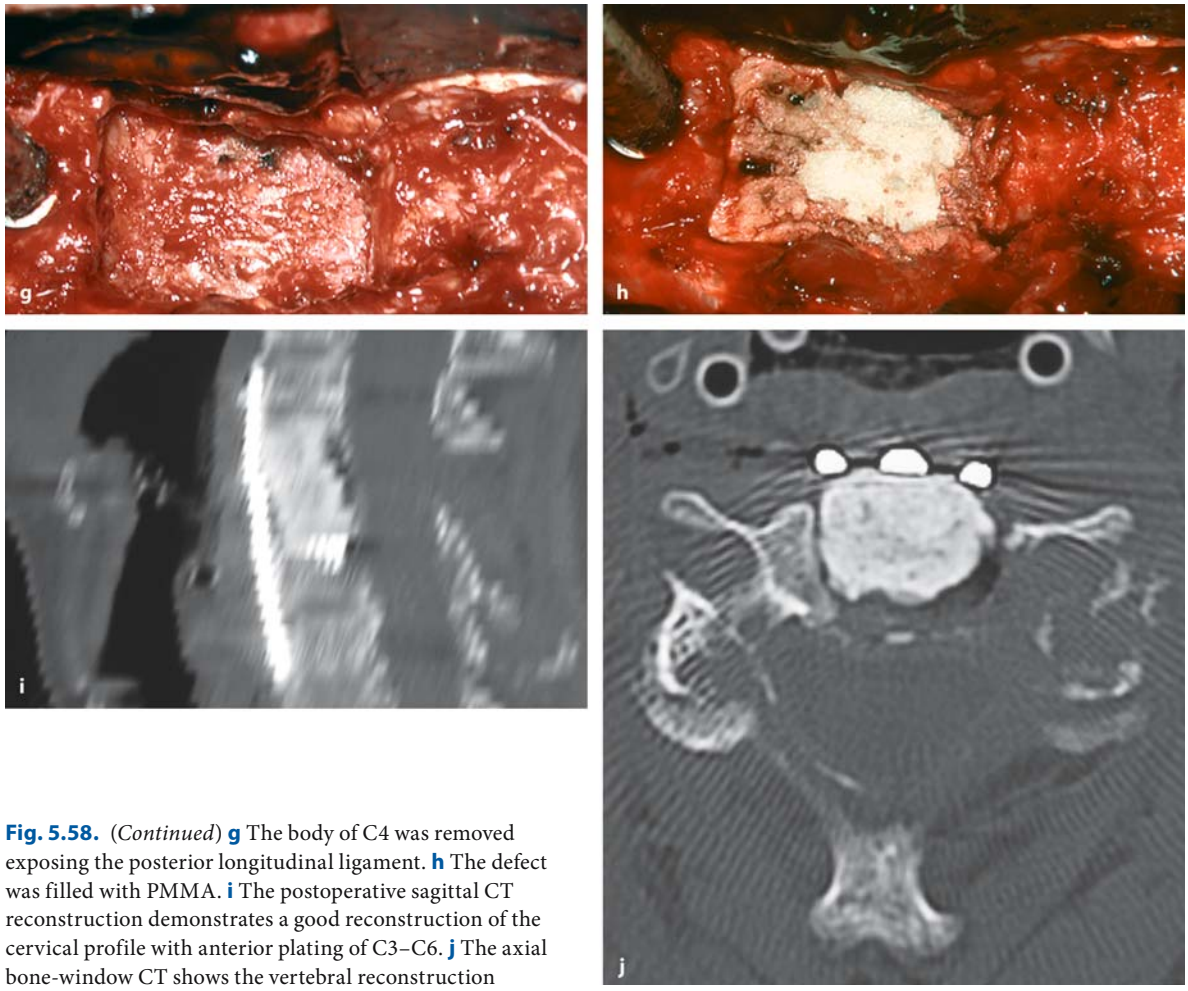

Fig. 5.58. (*Continued*) **g** The body of C4 was removed exposing the posterior longitudinal ligament. **h** The defect was filled with PMMA. **i** The postoperative sagittal CT reconstruction demonstrates a good reconstruction of the cervical profile with anterior plating of C3–C6. **j** The axial bone-window CT shows the vertebral reconstruction

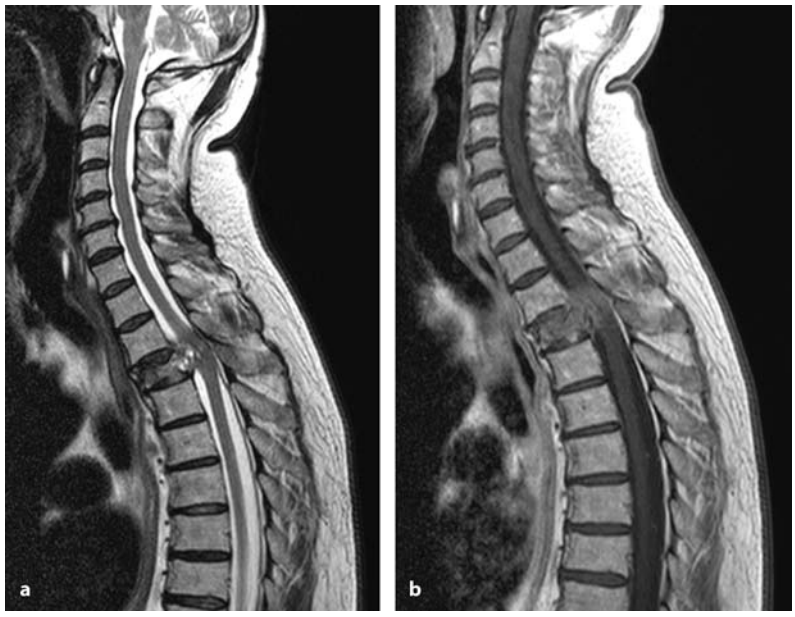

Fig. 5.59. Sagittal T2- (**a**) and T1-weighted MRI scans with contrast (**b**) of a colon carcinoma metastasis at Th3 in a 65-year-old man with a 2-month history of pain and a slight paraparesis. The spinal cord compression occurs exclusively from anterior. (*Continuation see next page*)

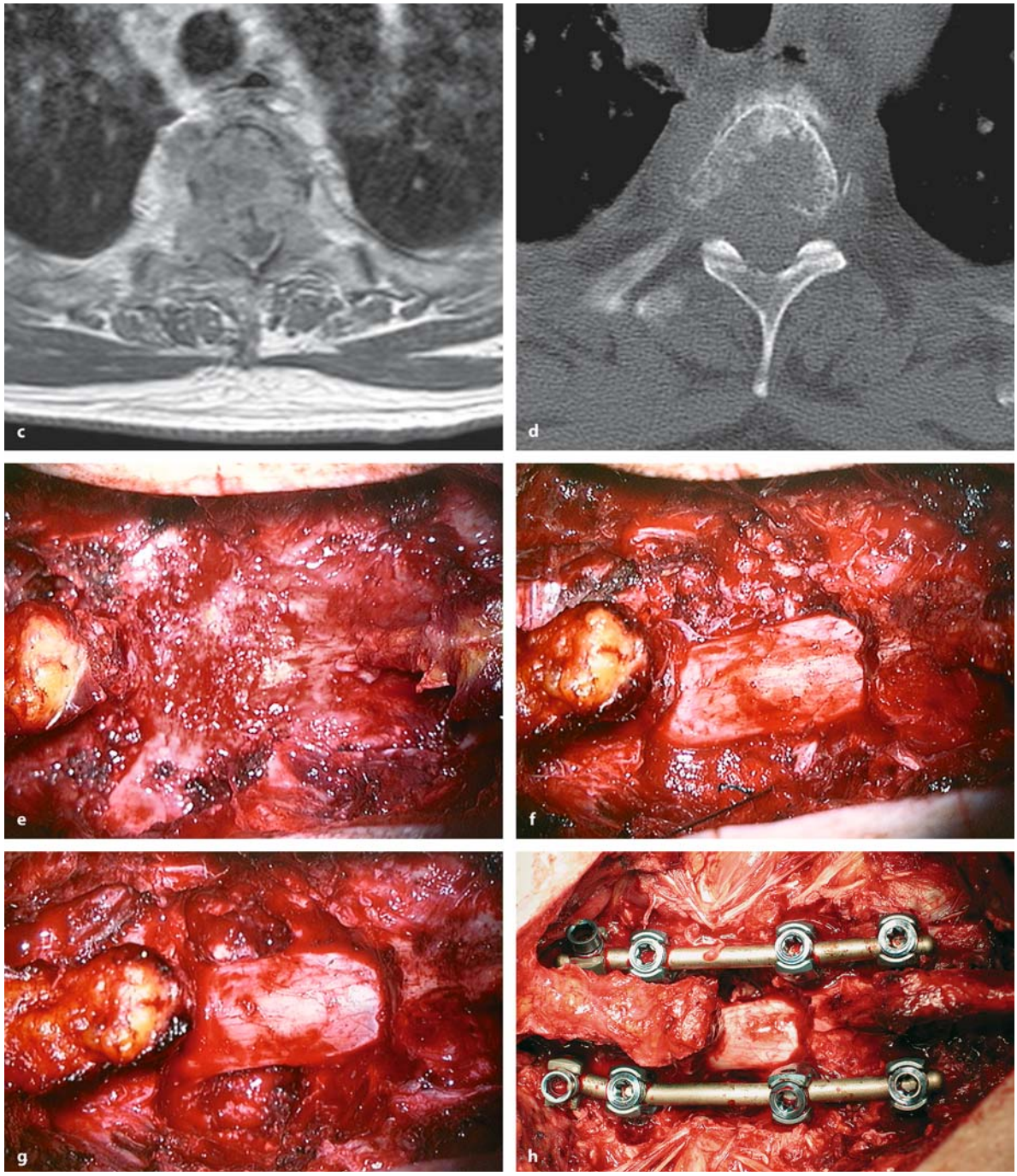

Fig. 5.59. This is underlined by the axial MRI (**c**) and bone-window CT images (**d**). Instead of a demanding anterior approach at this level, a posterior approach was chosen. **e** This intraoperative view demonstrates the situation after removal of the spinous process of Th3. After laminectomy (**f**), both pedicles were removed stepwise providing access to the vertebral body (**g**). After resecting some of the posterior part of the body from both sides, the remainder was filled with PMMA using intraoperative vertebroplasty followed by transpedicular fixation Th1-Th5 (**h**). (*Continuation see next page*)

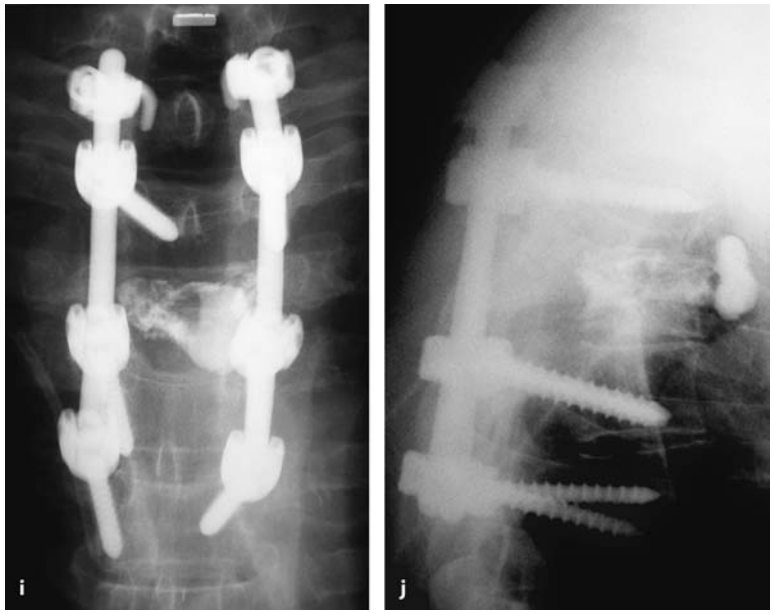

Fig. 5.59. (*Continued*) The postoperative anterior–posterior (**i**) and lateral (**j**) X-rays demonstrate a good realignment of the spinal canal. There is some anterior collection of PMMA without any clinical significance. The patient improved postoperatively in terms of pain relief and his paraparesis and was referred to undergo radiotherapy

The cervicothoracic (Figs. 5.51 and 5.60) and thoracolumbar junctions (Figs. 5.54 and 5.57) offer particular problems of stability as the more rigid thoracic spine is connected here with more mobile spinal segments. As a general rule, longer constructs incorporating posterior instrumentations are required to establish stability in these regions. Shorter and exclusively anterior instrumentations carry the risk of failure in these junctions even with intact posterior elements [314, 329].

Table 5.5 summarizes our current surgical treatment scheme for patients with spinal bone tumors. For patients in bad clinical condition, palliative measures such as vertebroplasty and radio- or chemotherapy are offered depending on the tumor histology. For tumors affecting the cervicothoracic, thoracic, thoracolumbar, and lumbar spine, either combined or posterior approaches are employed depending on the patient's condition, tumor histology, and effectiveness of adjuvant treatment options.

5.3.4 Adjuvant Therapy

For malignant soft-tissue and bone tumors, postoperative radiotherapy and/or chemotherapy are mandatory to ensure a long-lasting local control of the lesion. The modality of treatment needs to be tailored according to local conditions, histology, and oncological status, and should be discussed with oncologists and radiotherapists.

With successful en bloc resections of primary, low-malignant tumors such as chordomas and chondrosarcomas, one may observe the further outcome and reserve radiotherapy for the event of a recurrent tumor.

First reports have now appeared with results for stereotactic radiosurgery of spinal tumors [51, 137, 140, 465]. These studies report good results for pain relief for malignant bone tumors. Whether this modality should be employed for such lesions as intradural schwannomas [51], however, is questionable.

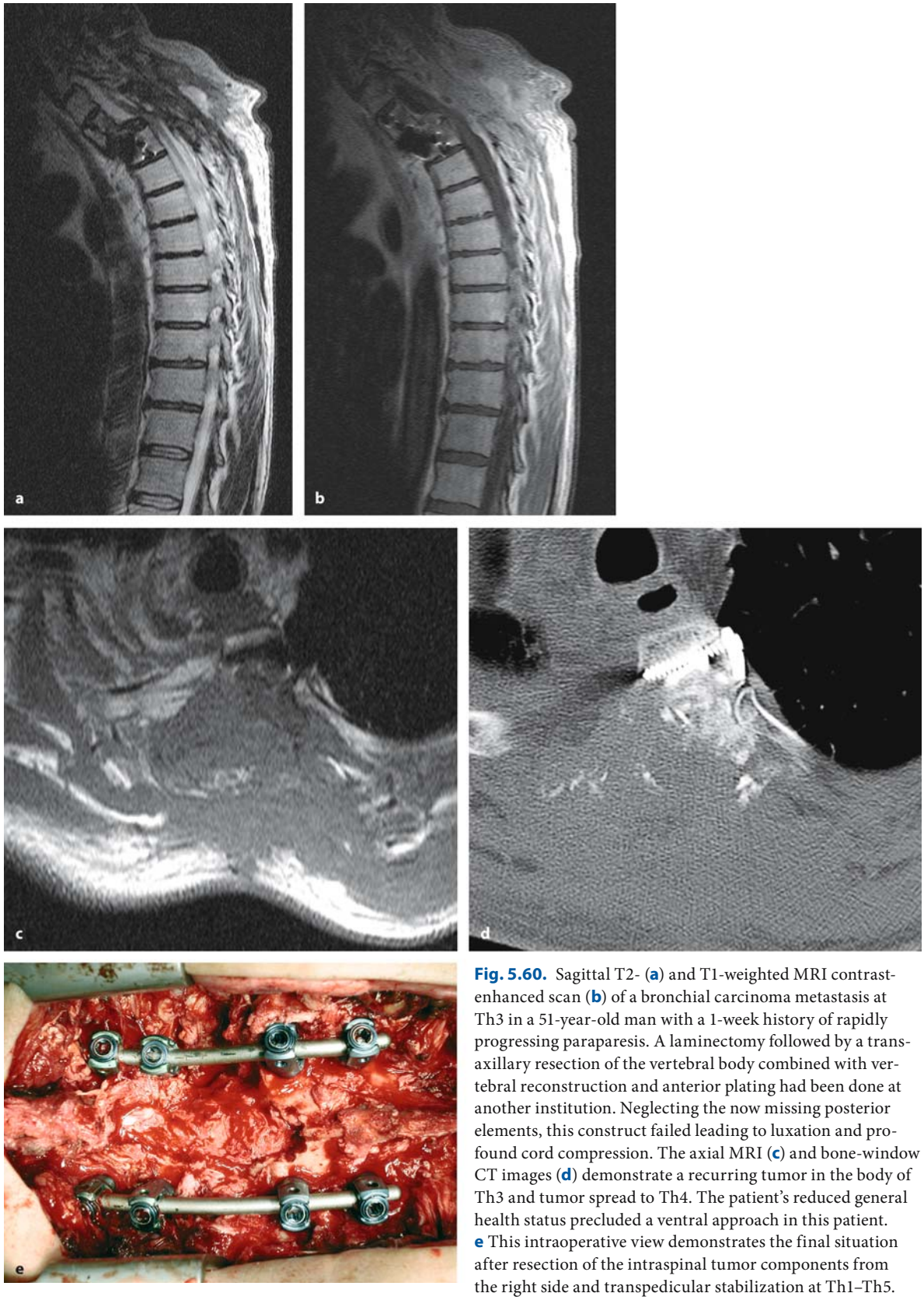

Fig. 5.60. Sagittal T2- (**a**) and T1-weighted MRI contrast-enhanced scan (**b**) of a bronchial carcinoma metastasis at Th3 in a 51-year-old man with a 1-week history of rapidly progressing paraparesis. A laminectomy followed by a transaxillary resection of the vertebral body combined with vertebral reconstruction and anterior plating had been done at another institution. Neglecting the now missing posterior elements, this construct failed leading to luxation and profound cord compression. The axial MRI (**c**) and bone-window CT images (**d**) demonstrate a recurring tumor in the body of Th3 and tumor spread to Th4. The patient's reduced general health status precluded a ventral approach in this patient. **e** This intraoperative view demonstrates the final situation after resection of the intraspinal tumor components from the right side and transpedicular stabilization at Th1–Th5. (*Continuation see next page*)

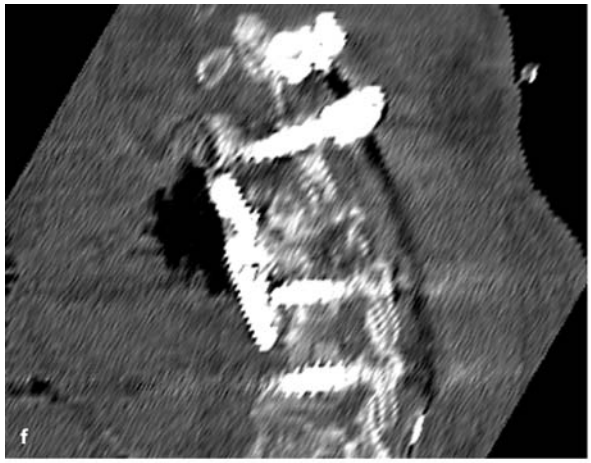

Fig. 5.60. (*Continued*) The postoperative sagittal CT reconstruction (**f**) provides a much better mode of control, demonstrating a good realignment of the sagittal profile compared to the anterior–posterior (**g**) or lateral (**h**) X-rays, which are notoriously difficult to interpret at this level. The patient showed marked improvement of his paraparesis, regaining his ability to walk within a few days

Table 5.5. Surgical strategy for spinal bone tumors

Tumor localization	Approach	Tumor	Reconstruction	Fusion	Option
Cervical Posterior	Posterior	Complete resection	–	Lateral mass screws	
Cervical Anterior	Anterior	Complete resection	Cage or bone	Anterior plating	Lateral mass screws
Cervicothoracic junction Posterior	Posterior	Complete resection	–	Lateral mass + pedicle screws	
Cervicothoracic junction Anterior – Good prognosis	Combined	Complete resection	Cage	Lateral mass + pedicle screws + anterior plating	
Cervicothoracic junction Anterior – Moderate prognosis	Costotrans- versectomy	Complete or subtotal resection	Cage or vertebroplasty	Lateral mass + pedicle screws	
Thoracic Posterior	Posterior	Complete resection	–	–	Pedicle screws
Thoracic Anterior – Good prognosis	Combined	Complete resection	Cage	Pedicle screws	Anterior plating
Thoracic Anterior – Moderate prognosis	Costotrans- versectomy	Complete or subtotal resection	Cage, PMMA or vertebroplasty	Pedicle screws	
Thoracolumbar Posterior	Posterior	Complete resection	–	Pedicle screws	
Thoracolumbar junction Anterior – Good prognosis	Combined	Complete resection	Cage	Pedicle screws	Anterior plating
Thoracolumbar junction Anterior – Moderate prognosis	Posterior ± Costotrans- versectomy	Complete or subtotal resection	Cage, PMMA or vertebroplasty	Pedicle screws	
Lumbar Posterior	Posterior	Complete resection	–	–	Pedicle screws
Lumbar Anterior – Good prognosis	Combined	Complete resection	Cage	Pedicle screws	Anterior plating
Lumbar Anterior – Moderate prognosis	Posterior	Complete or subtotal resection	Cage, PMMA or vertebroplasty	Pedicle screws	
Sacrum	Posterior	Complete or subtotal resection	–	–	Posterior fusion

Abbreviation: PMMA = polymethylmethacrylate

5.4 Postoperative Results and Outcome

Postoperative results are analyzed separately for soft-tissue, benign, and malignant bone tumors.

5.4.1 Tumor Resection and Spinal Instrumentation

Posterior approaches were used for the overwhelming majority (91% for soft-tissue and 80% for bone tumors, respectively). Anterior or combined approaches were applied for the remainder. The only exceptions were cervical bone tumors, which were removed via anterior approaches in 61% of patients (Table 5.6).

Epidural soft-tissue tumors were removed completely in 75% of patients, while subtotal removals were performed in 24% and decompressions in 1%. For benign bone tumors of the spine, the corresponding figures were 38% for complete resections, 46% for subtotal removals, and 15% for decompressions. With malignant bone tumors, 41% were resected completely and 54% subtotally, while 6% were decompressed only (Table 5.7). Examination of the surgical results according to Enneking grades revealed higher rates for complete resection of solitary tumors without soft-tissue extension compared to those with soft-tissue extension or tumors with additional spinal or extraspinal manifestations (p=0.0024; Table 5.8). Combined for all bone tumors, complete resections were obtained for 41% of patients, while subtotal removals and decompressions were performed for 53% and 6%, respectively (Table 5.7).

Looking at spinal bone tumors, biomechanical aspects also had to be addressed. Using the criteria of instability as mentioned in section 5.2, 34% of spinal bone tumors met these criteria for spinal instability. Fusion by either transpedicular fixation, vertebral body reconstruction and anterior plating, or a combination of both was applied in 48% of these patients. Such techniques were also applied in 8% of operations dealing with preoperatively stable situations, if spinal instability was present after tumor removal. For 34%, instrumentation was effected by transpedicular fixation after applying PMMA, a titanium cage, or bone into the vertebral defect; 46% were treated exclusively from anterior by applying a titanium cage or iliac crest bone for vertebral reconstruction and securing this with anterior plating. For the remaining 20%, a combined approach – vertebral reconstruction from anterior and transpedicular fixation from posterior – was used. However, stabilization was not performed for all patients meeting the instability criteria. A pure tumor removal and decompression was performed for 52% of patients in this group (Table 5.9).

Table 5.6. Approaches for epidural spinal tumors

Approach		Soft-tissue tumor					Bone tumors				
		C	Th	L	S	Total	C	Th	L	S	Total
Posterior	n	34	27	23	12	96	9	103	47	21	180
	%	94%	87%	92%	93%	91%	29%	86%	90%	100%	80%
Anterior	n	1	4	2	1	8	19	9	2	-	30
	%	3%	13%	8%	7%	8%	61%	8%	4%	-	13%
Combined	n	1	-	-	-	1	3	8	3	-	14
	%	3%	-	-	-	1%	10%	7%	6%	-	6%

Abbreviations: C = cervical, Th = thoracic, L = lumbar, S = sacral

Table 5.7. Surgical results for epidural spinal tumors

Type of surgery	Soft-tissue tumor	Bone tumor	Total
Complete	79 (75%)	91 (41%)	170 (52%)
Subtotal	25 (24%)	119 (53%)	144 (44%)
Decompression/ biopsy	1 (1%)	14 (6%)	15 (5%)

Table 5.8. Surgical results for spinal bone tumors related to Enneking grades

Enneking classification	Complete	Subtotal	Decompression/biopsy
S1	2 67%	–	1 33%
S2	3 38%	4 50%	1 13%
S3	–	2	–
IA	1	–	–
IB	14 45%	16 52%	1 3%
IIA	28 67%	12 29%	2 5%
IIB	29 31%	61 64%	5 5%
IIIA	4 36%	4 36%	3 27%
IIIB	10 32%	20 65%	1 3%

Table 5.9. Instrumentation for spinal bone tumors

Type of instrumentation	
Unstable	77 (34%)
– Fusion	37 (48%)
– No fusion	40 (52%)
Stable	147 (66%)
– Fusion	13 (9%)
– No fusion	134 (91%)
Transpedicular fixation	17 (34%)
Anterior reconstruction	23 (46%)
Combined reconstruction ± fixation	10 (20%)

5.4.2 Clinical Results

For epidural soft-tissue tumors, clinical improvements for the first postoperative year were observed for all preoperative symptoms. The average Karnofsky score increased from 77±9 to 87±10 ($p<0.01$) in this period (Table 5.10).

For benign bone tumors, significant improvements were seen within the first postoperative year for pain only, as most patients lacked other symptoms preoperatively and remained unchanged neurologically. The average Karnofsky score increased from 80±10 to 90±10; however, due to the limited number of patients, this improvement did not reach statistical significance (Table 5.11).

For malignant bone tumors, significant postoperative improvements for 6 months were obtained for sensory deficits, pain, motor weakness, gait, and sphincter disturbances [299, 456, 512, 514, 563]. However, the Karnofsky score remained almost unchanged (63±17 and 65±23, respectively; Table 5.11). In other words, a good postoperative clinical result for a malignant epidural tumor requires an early intervention [517].

The effect of tumor removal on clinical outcome was analyzed separately for soft-tissue (Table 5.12) and bone tumors (Table 5.13). With complete removals of soft-tissue tumors, significant improvements were obtained within the first postoperative year for each symptom and the Karnofsky score, which increased form 79±9 to 88±9 ($p<0.01$). With incomplete removals, significant improvements were still obtained for pain, sphincter functions, and the Karnofsky score, but postoperative improvements were less pronounced (preoperatively 72±7 and 77±9 after 1 year; $p<0.05$).

We performed a multivariate analysis to predict a high Karnofsky score 1 year after surgery for an epidural soft-tissue tumor. The most important independent factors were a complete tumor resection, a high preoperative Karnofsky score and avoidance of a recurrence ($p<0.0001$; Table 5.14). The length of history, the patient's age, the number of previous operations on that tumor, the histological grade, and the spinal level of the tumor had no significant impact.

Table 5.10. Clinical course for patients with spinal epidural soft-tissue tumors

Symptom	Preop. status	Postop. status	3 Months postop.	6 Months postop.	1 Year postop.
Pain	3.4±1.0	3.8±0.8	4.4±0.8	4.4±0.8	4.4±0.7**
Hypesthesia	3.8±1.0	4.0±0.9	4.2±0.7	4.2±0.7	4.3±0.7**
Dysesthesias	4.2±0.9	4.4±0.8	4.4±0.7	4.5±0.7	4.5±0.7*
Gait	4.4±0.8	4.4±0.8	4.6±0.6	4.6±0.6	4.6±0.6**
Motor power	4.0±1.1	4.1±0.9	4.4±0.8	4.4±0.9	4.4±0.8**
Sphincter function	4.5±1.0	4.7±0.6	4.8±0.5	4.8±0.4	4.9±0.4**
Karnofsky score	77±9	80±8	85±10	87±10	87±10**

Statistically significant difference between preop. status and 1 year postop.: *$p<0.05$, **$p<0.01$; abbreviations: Preop. = preoperative, Postop. = postoperative

Table 5.11. Clinical course for patients with spinal bone tumors

Symptom		Preop. status	Postop. status	3 Months postop.	6 Months postop.	1 Year postop.
Pain	BBT	2.7±0.6	3.3±0.6	4.3±1.2	4.3±1.2	4.7±0.6**
	MBT	2.8±0.8	3.6±0.7	3.8±0.9	3.6±1.2**	
Hypesthesia	BBT	4.7±0.6	4.7±0.6	4.7±0.6	4.7±0.6	4.7±0.6
	MBT	3.6±1.0	4.0±0.9	4.1±0.9	4.0±1.0**	
Dysesthesias	BBT	4.3±0.6	4.7±0.6	4.7±0.6	4.7±0.6	4.7±0.6
	MBT	4.7±0.6	4.9±0.4	4.8±0.5	4.7±0.6	
Gait	BBT	5.0±0.0	5.0±0.0	5.0±0.0	5.0±0.0	5.0±0.0
	MBT	3.5±1.5	3.8±1.3	4.0±1.3	3.7±1.5*	
Motor power	BBT	4.7±0.6	5.0±0.0	5.0±0.0	5.0±0.0	5.0±0.0
	MBT	3.7±1.4	4.0±1.2	4.2±1.1	4.0±1.3**	
Sphincter function	BBT	5.0±0.0	5.0±0.0	5.0±0.0	5.0±0.0	5.0±0.0
	MBT	4.0±1.5	4.2±1.2	4.3±1.2	4.3±1.2*	
Karnofsky score	BBT	80±10	83±6	90±10	90±10	90±10
	MBT	63±17	67±17	68±20	65±23	

Statistically significant difference between preop. status and 1 year postop. and 6 months postop., respectively: *$p<0.05$, **$p<0.01$; abbreviations: BBT = benign bone tumors, MBT = malignant bone tumors

For spinal bone tumors postoperative neurological improvements were not related to the amount of tumor resected. After complete resections, significant improvements for at least 6 months were seen for pain and sensory deficits, with the remaining symptoms unchanged. The Karnofsky score remained virtually unaltered. After incomplete resections, significant improvements for 6 months were observed for pain and motor power, with even slight but insignificant improvements for the remaining symptoms and the Karnofsky score during this period. Comparing the two groups after 6 months, patients with incompletely resected tumors had made up for some of their preoperative deficits, whereas patients with complete resections remained more or less stable (Table 5.13). A multivariate analysis to achieve a high Karnofsky score after 6 months revealed that the preoperative Karnofsky score had by far the greatest predictive power, followed by avoidance of a recurrence, a low spinal level, female sex, and spinal fusion. Less important factors were the completeness of resection, the length of history, number of affected vertebra, and postoperative radiotherapy ($p<0.0001$; Table 5.14). The following factors had no significant, independent influence: the patient's age, the histological grade, the number of affected vertebra, the presence of instability, and further extraspinal lesions.

Table 5.12. Clinical course for patients with epidural soft-tissue tumors related to tumor removal

Symptom	Preop. status	Postop. status	3 Months postop.	6 Months postop.	1 Year postop.
Pain					
Complete	3.6±1.0	3.9±0.8	4.6±0.7	4.6±0.7	4.5±0.7**
Subtotal	2.8±0.7	3.7±0.7	3.8±1.0	3.9±1.1	3.8±0.8**
Hypesthesia					
Complete	4.0±0.9	4.2±0.8	4.4±0.7	4.4±0.6	4.4±0.7**
Subtotal	3.2±0.8	3.2±0.7	3.6±0.5	3.4±0.5	3.4±0.5
Dysesthesias					
Complete	4.2±0.9	4.5±0.8	4.5±0.7	4.5±0.7	4.5±0.7*
Subtotal	4.3±0.9	4.4±0.9	4.4±0.9	4.4±0.9	4.4±0.9
Gait					
Complete	4.3±0.8	4.4±0.7	4.6±0.6	4.6±0.5	4.7±0.5**
Subtotal	4.2±0.7	4.1±0.8	4.2±0.7	4.2±0.7	4.2±0.7
Motor power					
Complete	4.1±1.1	4.2±0.9	4.5±0.8	4.5±0.8	4.5±0.8*
Subtotal	3.6±1.1	4.1±0.8	4.2±0.7	4.1±0.8	4.0±0.7
Sphincter function					
Complete	4.7±0.7	4.9±0.3	5.0±0.2	5.0±0.2	5.0±0.2*
Subtotal	3.6±1.3	4.1±1.1	4.2±0.8	4.3±0.7	4.4±0.7**
Karnofsky score					
Complete	79±9	80±8	86±9	88±9	88±9**
Subtotal	72±7	78±7	79±9	79±9	77±9*

Statistically significant difference between preop. status and 1 year postop.: *$p<0.05$, **$p<0.01$

We have analyzed further the impact of spinal instability and its management on clinical outcome for patients with spinal bone tumors in the first 6 postoperative months (Table 5.15). Examination of the preoperative conditions of patients with and without spinal instability revealed worse scores for patients with additional instablities except for sensory deficits and dysesthesias. For stable patients, postoperative improvements were seen for pain, sensory deficits, motor power, and sphincter functions. The Karnofsky scores increased slightly but insignificantly from 65±18 to 68±23. For patients with additional instabilities, improvements were only obtained for pain, with the remaining symptoms unchanged and Karnofsky scores of 56±17 preoperatively and 55±24 after 6 months. In other words, clinical results were considerably better for patients without additional instability – in terms of the overall clinical condition and the chances for postoperative improvements.

The most interesting question in relation to the surgical management of patients with additional instability relates to the impact of spinal fusion on postoperative clinical outcome compared to patients in whom instability had not been treated. One would expect that neglecting instability and concentrating purely on spinal decompression should come short for these patients.

Our results in this respect reveal that additional fusion of patients with spinal instabilities stabilized the neurological status, with no significant change of the Karnofsky score in the first 6 postoperative months (64±14 to 59±20 after 6 months) and a significant improvement for pain. Without fusion, no significant changes were seen for pain as well as other neurological symptoms and the Karnofsky score (43±10 to 46±30 after 6 months). At each time point, scores for unstable patients were better with spinal fusion compared to those without. However, looking

Table 5.13. Clinical course for patients with spinal bone tumors related to tumor removal

Symptom	Preop. status	Postop. status	3 Months postop.	6 Months postop.
Pain				
Complete	2.8±0.6	3.6±0.7	3.9±1.0	3.5±1.3**
Subtotal	2.6±0.7	3.5±0.7	3.6±0.9	3.5±1.1**
Hypesthesia				
Complete	3.9±1.2	4.3±0.9	4.4±0.9	4.3±0.9*
Subtotal	3.5±0.9	3.8±0.9	3.9±0.9	3.7±1.1
Dysesthesias				
Complete	4.7±0.6	4.8±0.5	4.8±0.5	4.7±0.7
Subtotal	4.7±0.5	4.9±0.3	4.8±0.5	4.8±0.5
Gait				
Complete	3.9±1.4	4.0±1.4	4.2±1.1	3.9±1.3
Subtotal	3.3±1.6	3.7±1.4	3.8±1.5	3.6±1.8
Motor power				
Complete	4.0±1.3	4.1±1.3	4.4±1.0	4.2±1.1
Subtotal	3.3±1.5	3.8±1.3	3.9±1.4	3.8±1.6*
Sphincter function				
Complete	4.4±1.2	4.4±1.2	4.6±1.1	4.5±1.1
Subtotal	3.7±1.6	4.0±1.4	4.0±1.4	4.0±1.4
Karnofsky score				
Complete	67±16	69±19	71±23	66±25
Subtotal	58±18	64±17	66±19	63±23

Statistically significant difference between preop. status and 6 months postop.: *$p<0.05$, **$p<0.01$

Table 5.14. Multivariate analysis for prediction of a high postoperative Karnofsky score for patients with spinal epidural tumors

Factor		β-value
High preop. KS	BT	0.2987
	STT	0.6354
Complete resection	BT	0.3601
	STT	0.1571
Recurrence	BT	0.2954
	STT	0.3511
Low spinal level	BT	–
	STT	0.3083
Female sex	BT	–
	STT	0.2683
Fusion	BT	–
	STT	0.2379
Solitary lesion	BT	–
	STT	0.1647
Short history	BT	–
	STT	0.1382
Postop. radiotherapy	BT	–
	STT	0.1071

Correlation STT: $r=0.6339$, $p<0.0001$; correlation BT: $r=0.8109$, $p<0.0001$; abbreviations: KS = Karnofsky score, BT = bone tumors, STT = Soft-tissue tumors

Table 5.15. Clinical course for patients with spinal bone tumors related to spinal stability

Symptom	Preop. status	Postop. status	3 Months postop.	6 Months postop.
Pain				
Stable	2.8±0.6	3.6±0.7	3.9±0.9	3.6±1.2**
Unstable	2.3±0.5	3.3±0.8	3.3±0.8	3.2±1.0*
– Fusion	2.3±0.5	3.6±0.5	3.5±0.8	3.4±0.8**
– No fusion	2.4±0.5	2.8±0.9	2.9±0.8	3.0±1.2
Hypesthesia				
Stable	3.7±1.0	4.1±0.9	4.2±0.9	4.1±0.9*
Unstable	3.6±1.2	3.9±1.1	4.0±1.1	3.7±1.4
– Fusion	4.0±1.2	4.1±1.1	4.1±1.1	4.1±1.2
– No fusion	2.9±0.6	3.5±1.1	3.6±0.9	3.1±1.6
Dysesthesias				
Stable	4.7±0.6	4.9±0.3	4.8±0.5	4.7±0.6
Unstable	4.8±0.5	4.8±0.5	4.8±0.5	4.8±0.5
– Fusion	4.9±0.4	4.7±0.6	4.7±0.6	4.7±0.6
– No fusion	4.8±0.7	5.0±0.0	5.0±0.0	5.0±0.0
Gait				
Stable	3.7±1.5	4.0±1.3	4.2±1.2	3.9±1.4
Unstable	3.2±1.5	3.4±1.6	3.5±1.6	3.3±1.9
– Fusion	3.9±1.5	3.9±1.8	4.1±1.3	3.9±1.5
– No fusion	2.0±0.5	2.5±0.8	2.4±1.4	2.1±2.0
Motor power				
Stable	3.7±1.4	4.1±1.2	4.3±1.2	4.1±1.3**
Unstable	3.4±1.5	3.6±1.4	3.8±1.3	3.6±1.6
– Fusion	4.1±1.3	4.0±1.6	4.2±1.2	4.0±1.4
– No fusion	2.0±0.8	2.9±0.8	3.0±1.2	2.8±1.6
Sphincter function				
Stable	4.1±1.4	4.3±1.2	4.4±1.1	4.4±1.2*
Unstable	3.9±1.5	3.9±1.7	3.9±1.6	3.9±1.6
– Fusion	4.5±1.1	4.3±1.5	4.3±1.5	4.1±1.6
– No fusion	2.9±1.7	3.1±1.7	3.3±1.7	3.4±1.7
Karnofsky score				
Stable	65±18	69±16	71±21	68±23
Unstable	56±17	59±21	60±19	55±24
– Fusion	64±14	64±20	66±16	59±20
– No fusion	43±10	49±18	51±22	46±30

Statistically significant difference between preop. status and 6 months postop.: *$p<0.05$, **$p<0.01$

at the preoperative conditions of these two subgroups illustrates our intention to tailor the operation to the patient's condition. An average preoperative Karnofsky score of 43±10 for unstable patients who did not undergo fusion indicates that hardly anyone in this group was self ambulatory at the time of presentation so that a limited surgical intervention was all that was undertaken. For patients in whom fusion was performed, on the other hand, the preoperative Karnofsky score was similar to that of patients with a stable spine so that a more extensive operation could be performed to maintain ambulation. Outcome was still worse for unstable patients with spinal fusion compared to those without preoperative instability. This indicates a more aggressive behavior of tumors that compromise spinal stability, as reflected by higher rates for high malignancies and unfavorable Enneking grades.

5.4.3 Complications

5.4.3.1 Short-Term Complications

The overall complication rate for epidural tumors was 12%, with no significant differences between soft-tissue and bone tumors. Soft-tissue tumors were associated with a complication rate of 8%, with two postoperative hematomas and one patient each with a wound infection, CSF leak, instability, injury of the thoracic duct, pneumonia, and a pleural effusion. For benign bone tumors a rate of 10% was observed due to spinal instability in one patient. Malignant bone tumors had a slightly higher complication rate of 15% [64, 296, 518]. The commonest complications in this group were wound infections (11 patients), hematomas (4 patients) and instabilities (4 patients).

In terms of postoperative spinal instability, this was counted as a complication if it became clinically manifest immediately after surgery. Three patients developing this complication had undergone fusion that failed, whereas one patient who was considered as stable developed instability postoperatively.

Other surgical complications that were encountered included a CSF leak, an intercostal neuralgia, a recurrent laryngeal nerve palsy, and a mandibular dislocation. Two patients suffered pulmonary embolisms and six other patients a variety of other medical problems such as pulmonary or urinary infections, deep vein thrombosis, or myocardial infarction (Table 5.16).

Table 5.16. Complications for patients with epidural spinal tumors

Type		Soft-tissue tumors	Bone tumors	Total
Wound infection		1	11	12
CSF leak		1	1	2
Hemorrhage		2	4	6
Instability		1	5	6
Intercostal neuralgia		–	1	1
Recurrent laryngeal palsy		–	1	1
Mandibular dislocation		–	1	1
Thoracic duct injury		1	–	1
Central dysregulation		–	1	1
Pneumonia		1	1	2
Pleural effusion		1	–	1
Deep vein thrombosis		–	1	1
Pulmonary embolism		–	2	2
Myocardial infarction		–	1	1
Urinary tract infection		–	1	1
Septicemia		–	1	1
Total	**n**	**8**	**32**	**40**
	%	**8%**	**14%**	**12%**

Abbreviation: CSF = cerebrospinal fluid

5.4.3.2 Long-Term Complications

Long-term complications may occur due to late-developing spinal instability or a postoperative myelopathy. Postoperative instabilities requiring surgical measures occurred early in the postoperative period and indicated intraoperative misjudgments. We have not seen clinical problems related to late spinal instabilities for patients with spinal bone tumors, even in those cases where preoperative criteria of instability had been present and fusion was not performed. This may be explained by the fact that most of these patients harbored highly malignant tumors and did not survive long enough for this problem to become relevant. We did observe kyphotic angulations in two patients, causing back pain, but neither of these were considered severe enough or responsible for a myelopathy to warrant a reoperation.

The results of our series compare favorably with those of a study describing long-term outcomes after radiotherapy of malignant tumors in children: Butler et al. [93] determined the late consequences of radiotherapy in 143 children: 35% showed spinal scoliosis, 36% a chest asymmetry, 10% kyphotic angulations,

and 16% complained about back pain. Three patients developed radiation-induced tumors. To our knowledge, a comparable study on adults does not exist.

No postoperative myelopathy was observed for patients with epidural tumors in our series, but three patients with epidural schwannomas complained about persistent dysesthesia syndromes, presumably related to radicular irritations by scar tissue.

5.4.4 Morbidity, Recurrences, and Survival

These analyses were done with Kaplan-Meier statistics. Clinical and radiological recurrence rates were identical for epidural tumors, indicating that almost no delayed, tumor-independent morbidity exists, which may be quite significant for intramedullary tumors, for instance.

For epidural soft-tissue tumors, a permanent morbidity of 4% was determined. Within 5 years, 28% and within 10 years, 37% of the tumors had recurred (Fig. 5.61). Analysis of the impact of the amount of tumor resected revealed a significant difference for surgical morbidity, which was 1% after complete and 13% after subtotal resections. Recurrence rates after 5 and 10 years were 18% and 30%, respectively, after complete resections and 54% within 5 years after subtotal resections (Fig. 5.62). A multivariate analysis, however, did not confirm that a complete resection was an independent, significant factor to prevent a recurrence. The strongest independent influence to predict a low recurrence rate was a benign histological grade.

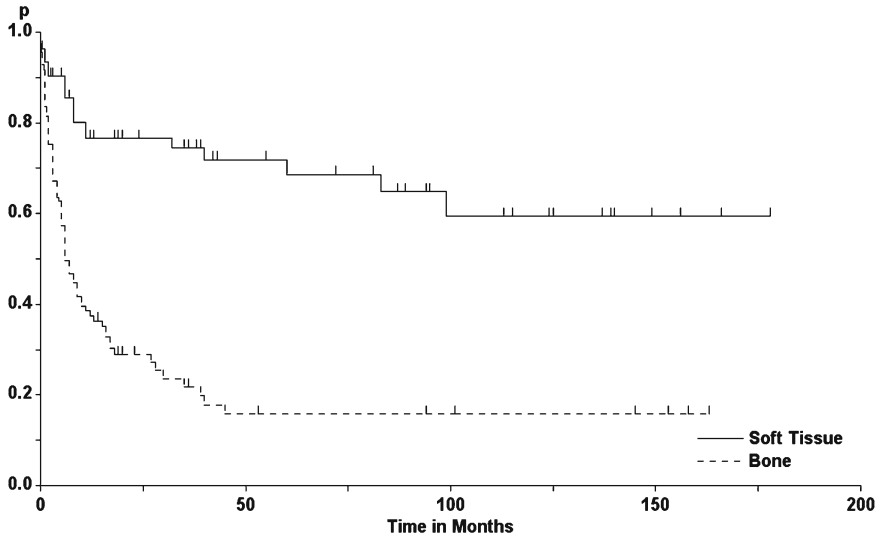

Fig. 5.61. Tumor recurrence rates for epidural soft-tissue and bone tumors (log-rank test: $p<0.0001$)

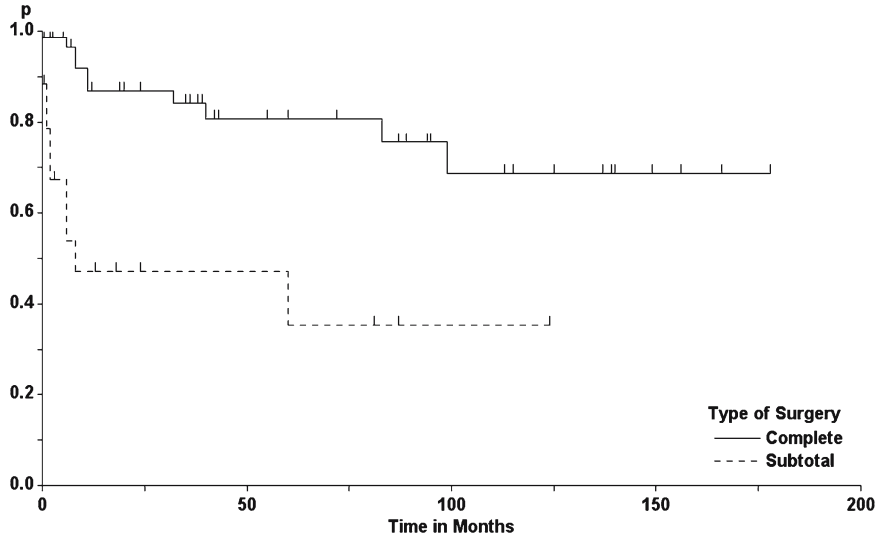

Fig. 5.62. Tumor recurrence rates for spinal soft-tissue tumors as a function of the extent of tumor resection (log-rank test: $p<0.0001$)

Table 5.17. Multivariate analysis for prediction of a high tumor recurrence rate for patients with epidural spinal tumors

Factor		β-value
Malignant grade	BTT	0.6653
	STT	–
Low preoperative Karnofsky score	BT	–
	STT	0.2708
Long history	BT	0.2440
	STT	–
Preoperative radiotherapy	BT	0.2412
	STT	–
No postoperative radiotherapy	BT	0.2335
	STT	–
No fusion	BT	–
	STT	0.1937
Secondary surgery	BT	–
	STT	0.1456
Old age	BT	–
	STT	0.1430
Short history	BT	–
	STT	0.1424
Incomplete resection	BT	–
	STT	0.1341

Correlation STT: r=0.6739, p<0.0001; correlation BT: r=0.4212, p=0.0051

Other independent, but less prominent factors were, in order of importance, a long clinical history, preoperative radiotherapy, and no postoperative radiotherapy (p<0.0001; Table 5.17). No significant influence was effected by the patient's age, the affected spinal level, or the preoperative clinical condition.

For spinal bone tumors, a permanent morbidity of 2% was observed. The recurrence rate after 5 years was calculated as 82%, with no further recurrences thereafter (Fig. 5.61). For ten patients with benign bone tumors, permanent surgical morbidity was observed in one patient, with two tumor recurrences after 7 and 30 months, respectively. For malignant bone tumors, permanent surgical morbidity was determined as 2%, and recurrence rates were calculated after 1 and 5 years as 60% and 85%, respectively (Fig. 5.63).

For spinal bone tumors, surgical morbidity was determined as 1% and 2% after complete and incomplete removals, respectively. Recurrence rates after 5 years were calculated as 80% after complete and 85% after subtotal removals (Fig. 5.64). Again, a multivariate analysis was performed to ascertain the predictors of a low recurrence rate. This analysis showed that the strongest predictor of a recurrence was a low preoperative Karnofsky score (Fig. 5.65). Less important factors were no spinal fusion, a short patient history, surgery on a recurrent tumor, young age, and an incomplete resection (p=0.0051; Table 5.17). Spinal level, number of affected vertebrae, presence of extraspinal lesions, and the presence of instability had no predictive power in this respect.

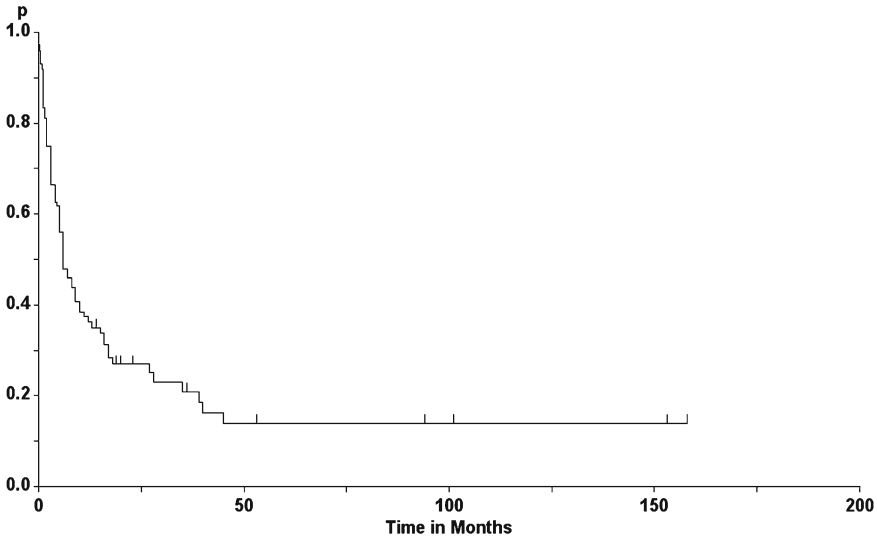

Fig. 5.63. Overall tumor recurrence rate for spinal malignant bone tumors

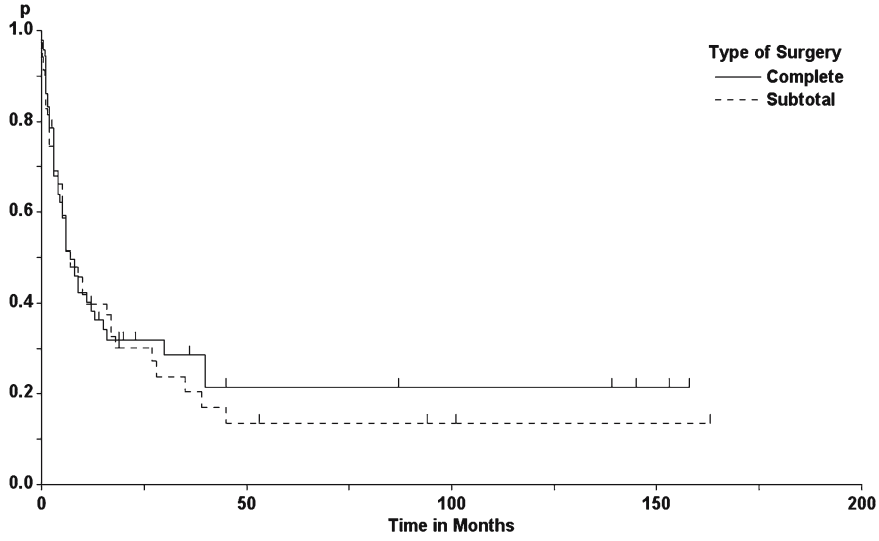

Fig. 5.64. Tumor recurrence rates for spinal bone tumors as a function of the degree of tumor resection (log-rank test: not significant)

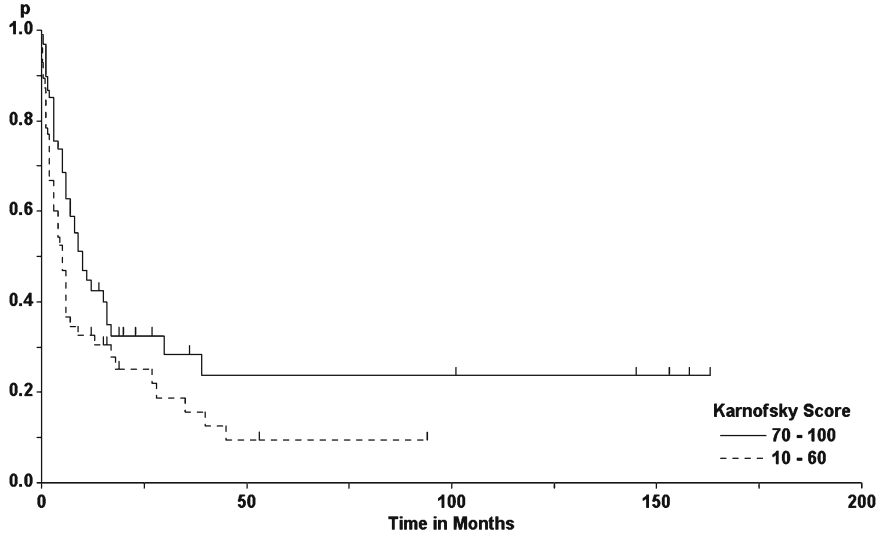

Fig. 5.65. Tumor recurrence rates for spinal bone tumors as a function of the preoperative Karnofsky score (log-rank test: p=0.013)

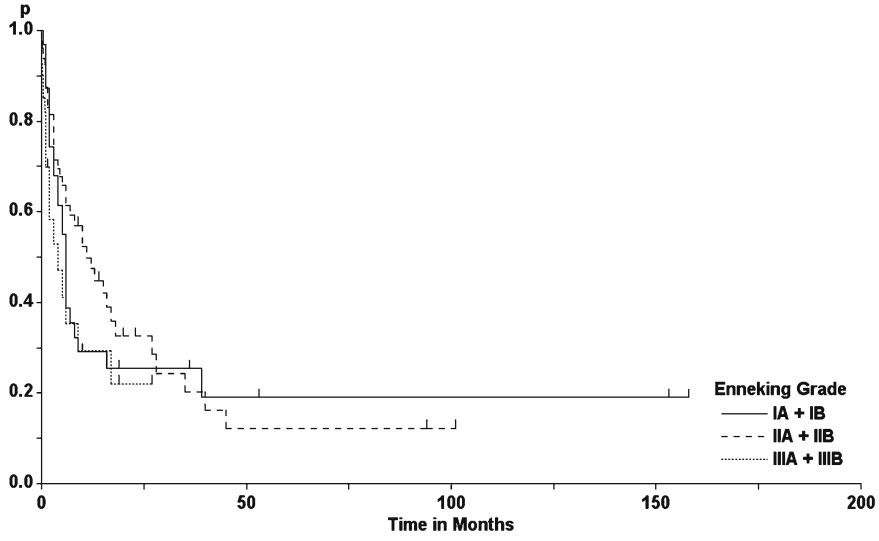

Fig. 5.66. Tumor recurrence rates for malignant spinal bone tumors, as a function of Enneking grades (log-rank test: not significant)

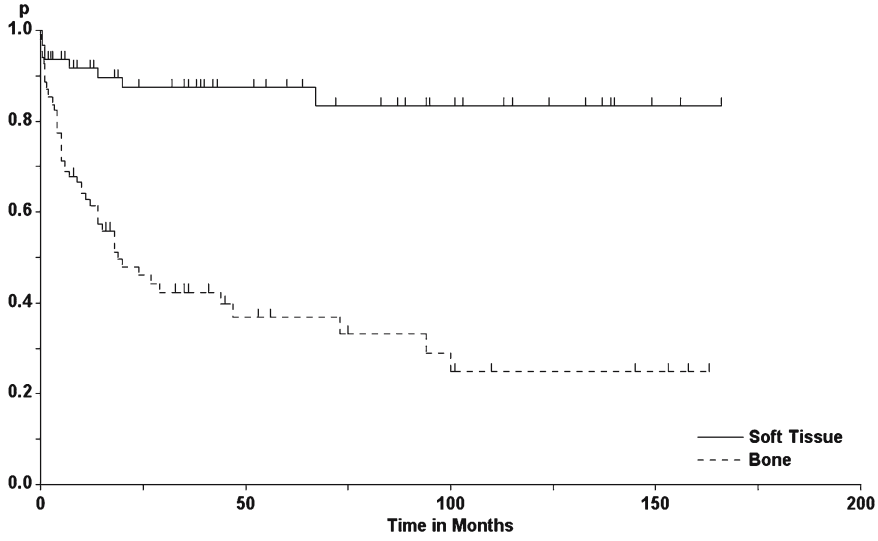

Fig. 5.67. Survival rates for patients with spinal epidural soft-tissue and bone tumors (log-rank test: $p<0.0001$)

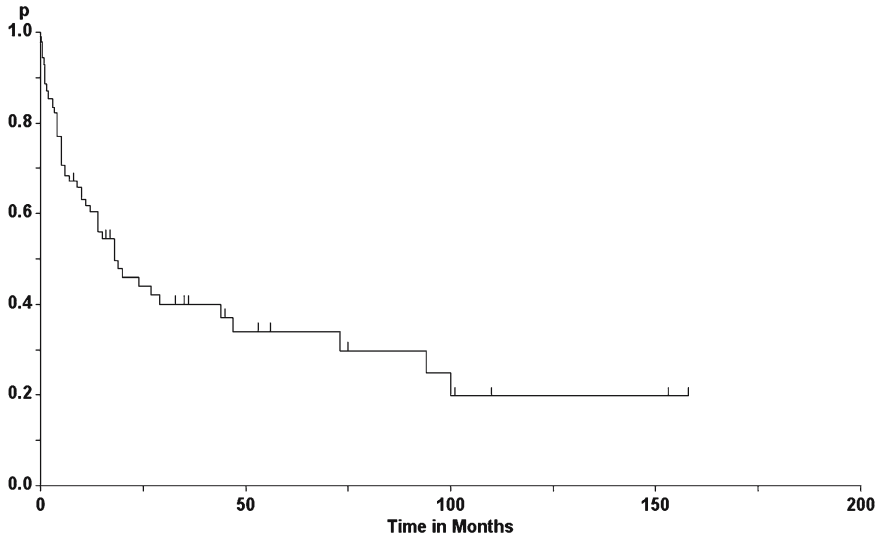

Fig. 5.68. Survival rate for patients with malignant spinal bone tumors

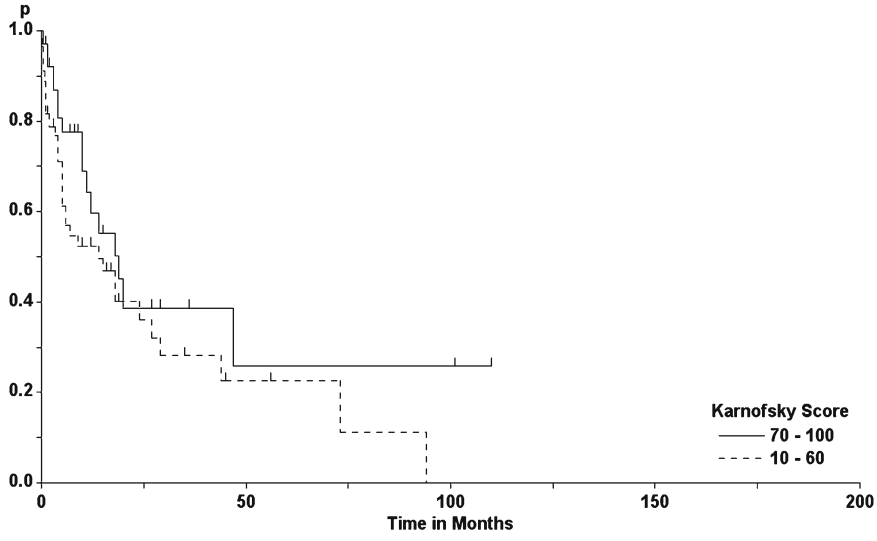

Fig. 5.69. Survival rates for patients with malignant spinal bone tumors, as a function of the preoperative Karnofsky score (log-rank test: $p=0.05$)

We classified the spinal bone tumors of this series according to Enneking's classification [157] to analyze the influence of local soft-tissue extensions and the presence of additional spinal and extraspinal lesions on recurrence rates and survival. Among the benign tumors, three were in class S1, eight were in class S2, and two were in class S3. These numbers did not allow a meaningful statistical analysis for benign tumors. With malignant tumors, 1 tumor was in class IA, 31 were in class IB, 42 were in class IIA, 95 were in class IIB, 11 were in class IIIA, and 31 were in class IIIB. Corresponding to the multivariate analysis, the comparison of local recurrence rates for malignant tumors revealed only slight, but no statistically significant differences between groups IA±IB, IIA±IIB, and IIIA±IIIB (Fig. 5.66).

With respect to surgical mortalities, defined as death within 1 month of operation, a rate of 6% was observed for soft-tissue tumors. This was related to three patients with large epidural schwannomas and two patients with soft-tissue sarcomas. For spinal bone tumors, a surgical mortality of 14% was calculated (Fig. 5.67). Figures did not differ significantly between benign and malignant bone tumors (11% and 15%, respectively).

For malignant bone tumors, survival rates of 59%, 34%, and 26% were observed after 1, 5, and 10 years, respectively (Fig. 5.68) [296]. According to a multivariate analysis, a high mortality figure for malignant bone tumors was predicted mainly by a bad preoperative clinical condition (Fig. 5.69). Other less important predictors were an emergency operation and the presence of extraspinal manifestations ($p<0.0001$; Table 5.18). However, no independent effect was seen for age, spinal level, spinal instability, or the amount of resection (Fig. 5.70) – with the exception of en bloc resections for primary bone tumors. Correspondingly, statistically different survival rates were obtained according to the Enneking classification between low- and high-level malignancies as well as between a localized and a more widespread tumor burden (log rank test: $p=0.0058$; Fig. 5.71).

Boriani et al. [81] advocate en bloc resections for treatment of malignant bone tumors and operated 43 patients with a variety of histologies in this fashion. In this series there were 11 benign tumors, 15 low-level malignancies (i.e., Enneking stages IA or IB), and 17 high-level malignancies. The mean age of their cohort was 35 years. Clinical deteriorations due to metastatic dissemination or local regrowth were seen in 25%, with local recurrences in 9%. Six patients with high-level malignancies died 10–28 months postoperatively, while 77% were disease free at the latest follow up. This study exemplifies the problem of reports advocating aggressive surgical resections: they claim better results in terms of survival with good neurological function compared to standard surgical tech-

Table 5.18. Multivariate analysis for prediction of a high mortality rate for malignant bone tumors

Factor	β-value
Low preoperative Karnofsky score	0.4084
Emergency	0.1367
Extraspinal lesions	0.0798

Correlation: $r=0.4068$, $p<0.0001$

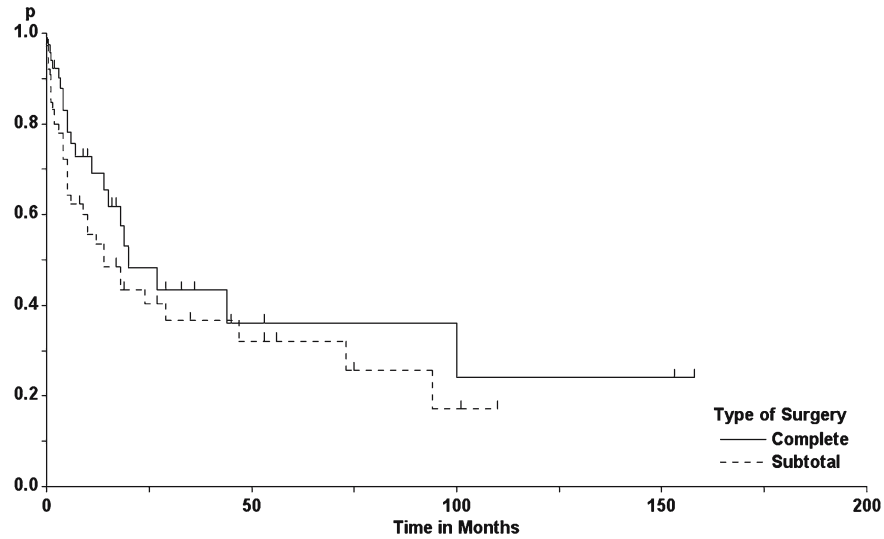

Fig. 5.70. Survival rates for patients with malignant spinal bone tumors, as a function of the extent of tumor resection (log-rank test: not significant)

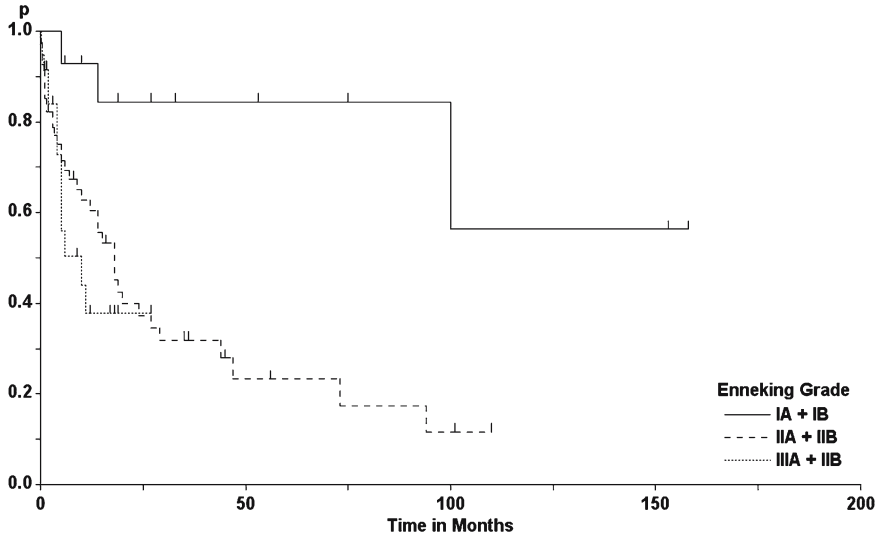

Fig. 5.71. Survival rates for patients with malignant spinal bone tumors, as a function of Enneking grades (log-rank test: p=0.0058)

niques, but mix benign, low-malignant and high-malignant tumors together and do not apply survival statistics. For benign and low-level malignancies, a high survival rate does not require such a radical resection. The major objective is functional preservation. For highly malignant tumors, aggressive surgical strategies may be reasonable if they offer a better chance of survival without inflicting unacceptable morbidity. Here, 6 out of 17 patients reported died within 28 months. The rate of patients surviving 1 or 2 years is not provided, making it impossible to compare these results to those of other studies.

5.5 Specific Entities

5.5.1 Soft-tissue Tumors

5.5.1.1 Nerve Sheath Tumors

Among epidural soft-tissue tumors, nerve sheath tumors were the commonest group. Schwannomas and neurofibromas can be distinguished. Of the 290 spinal nerve sheath tumors in this series, 65 were epidural tumors (22.4%). We encountered 58 schwannomas and 7 neurofibromas. This is the largest reported series of epidural spinal nerve sheath tumors to date. Other series have reported smaller percentages for epidural tumors, mostly below 10% [129, 156], and hardly contained more than a dozen nerve sheath tumors in the epidural group.

Fortuna et al. [175] claimed a higher proportion of epidural nerve sheath tumors in children compared to adults. One such case was even described in a 3-month-old child [546]. However, a higher proportion of epidural nerve sheath tumors in children is not supported by our series, as we could find no difference in age distribution between intradural, extradural, and dumbbell tumors.

The mean age at presentation was 42±17 years, with an average history of 30±57 months. Fourteen patients with neurofibromatosis type 2 (NF-2) harbored 22 schwannomas, 3 patients with neurofibromatosis type 1 (NF-1) had 3 neurofibromas removed, while the remaining 40 patients had single nerve sheath tumors: 36 schwannomas and 4 neurofibromas. Thirty-two tumors were encountered in the cervical (Fig. 5.72), 14 in the thoracic (Figs. 5.45 and 5.46), 10 in the lumbar (Fig. 5.73), and 9 in the sacral spine (Fig. 5.74). This distribution was significantly different compared to intradural or intraextradural schwannomas (chi-square test: p<0.0001) [267]. Whereas dumbbell tumors were more common in the cervical spine, nerve sheath tumors were seen in the sacral area almost exclusively epidurally. The average follow up was 45±52 months. In a series of 16 patients by Celli et al. [105], a completely different distribution was reported, with 14 epidural nerve sheath tumors located in the lumbar or sacral spine and just 2 cervical tumors.

Pain was the initial clinical symptom of an epidural nerve sheath tumor in 68% of patients [105]. Dysesthesias were reported as the initial problem by 12%, with no differences between patients with or without

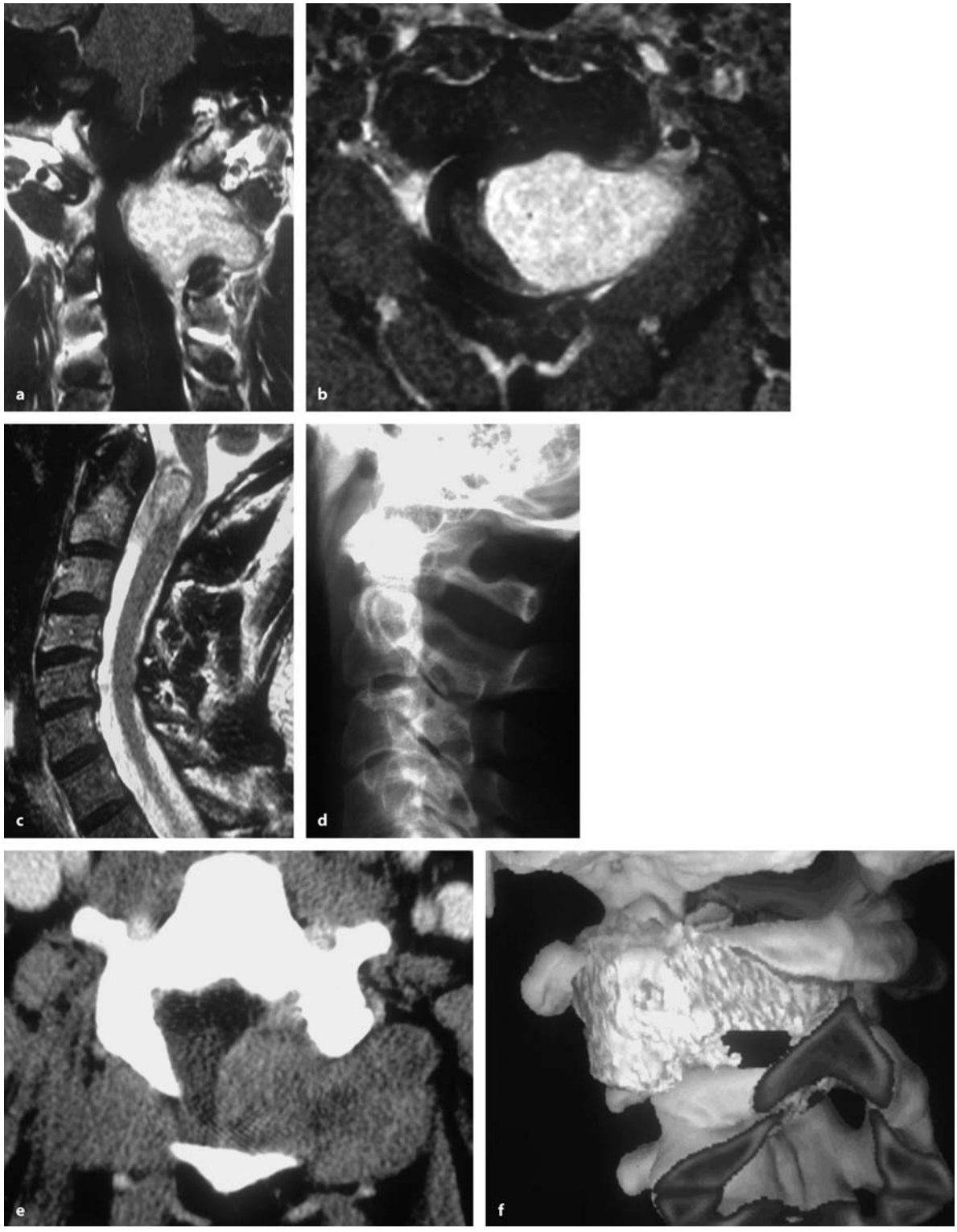

Fig. 5.72. Coronal (**a**) and axial (**b**) T1-weighted, contrast-enhanced MRI scans of an epidural schwannoma at C1/2 on the left side in a 40-year-old man with a progressive tetraparesis and neck pain. **c** The intraspinal component on the T2-weighted sagittal scan causes significant cord compression. None of these images shows clearly whether there is an intradural component. **d** The lateral X-ray demonstrates erosion of the lamina of C2 and a widened neuroforamen. The axial CT (**e**) and the three-dimensional reconstruction (**f**) provide a good orientation, demonstrating bone and tumor. (*Continuation see next page*)

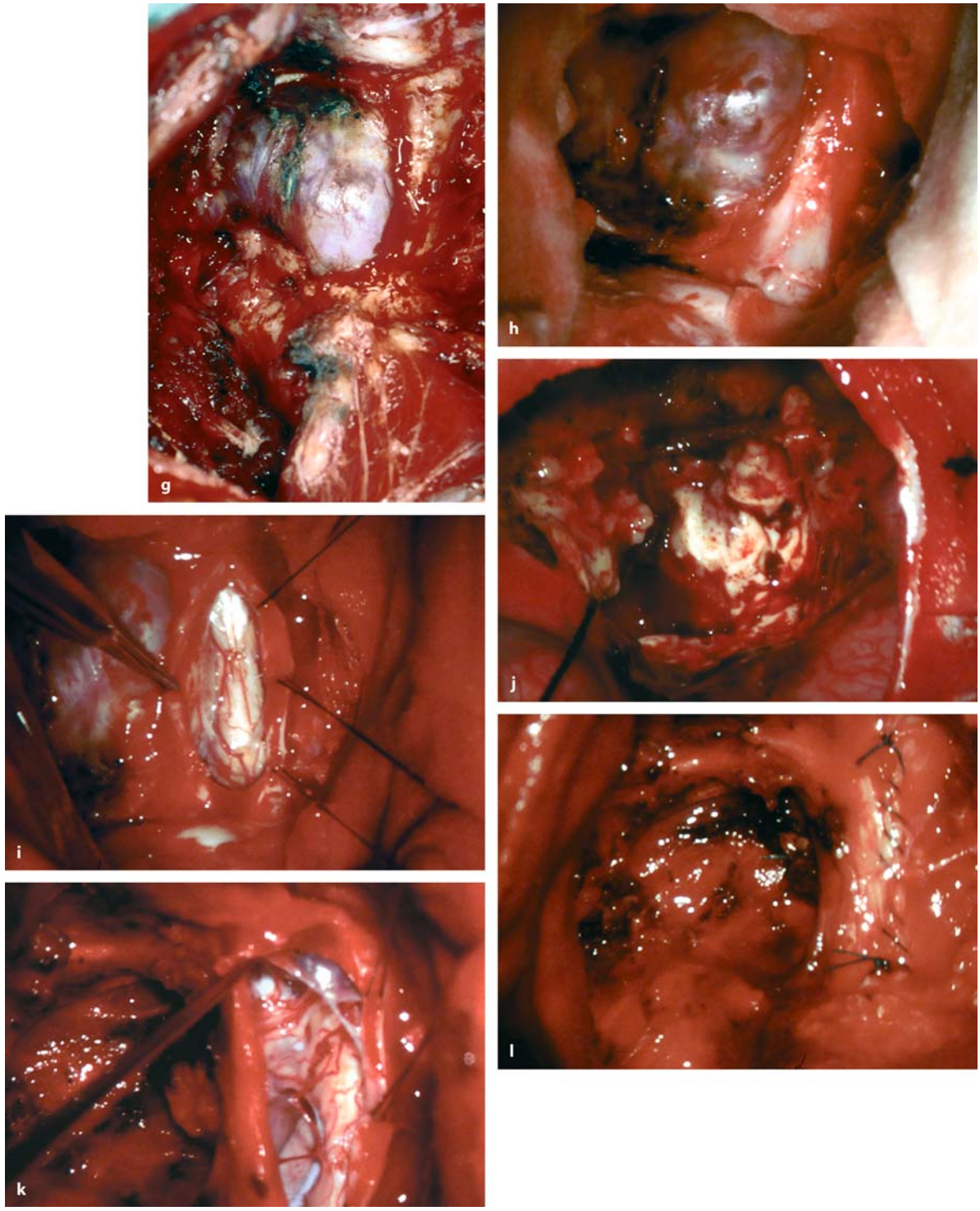

Fig. 5.72. (*Continued*) **g** This intraoperative overview, taken with the patient in the semisitting position shows the epidural tumor after soft-tissue dissection and removal of the lamina at C2. **h** With part of the tumor already removed, this microscopic view shows the connection of the tumor to the dura. **i** Upon dura opening, no intradural tumor is visible. After debulking (**j**), a complete resection is achieved resulting in a complete decompression of the spinal cord (**k**). **l** The dura has been closed and the epidural tumor bed covered with fibrin tissue

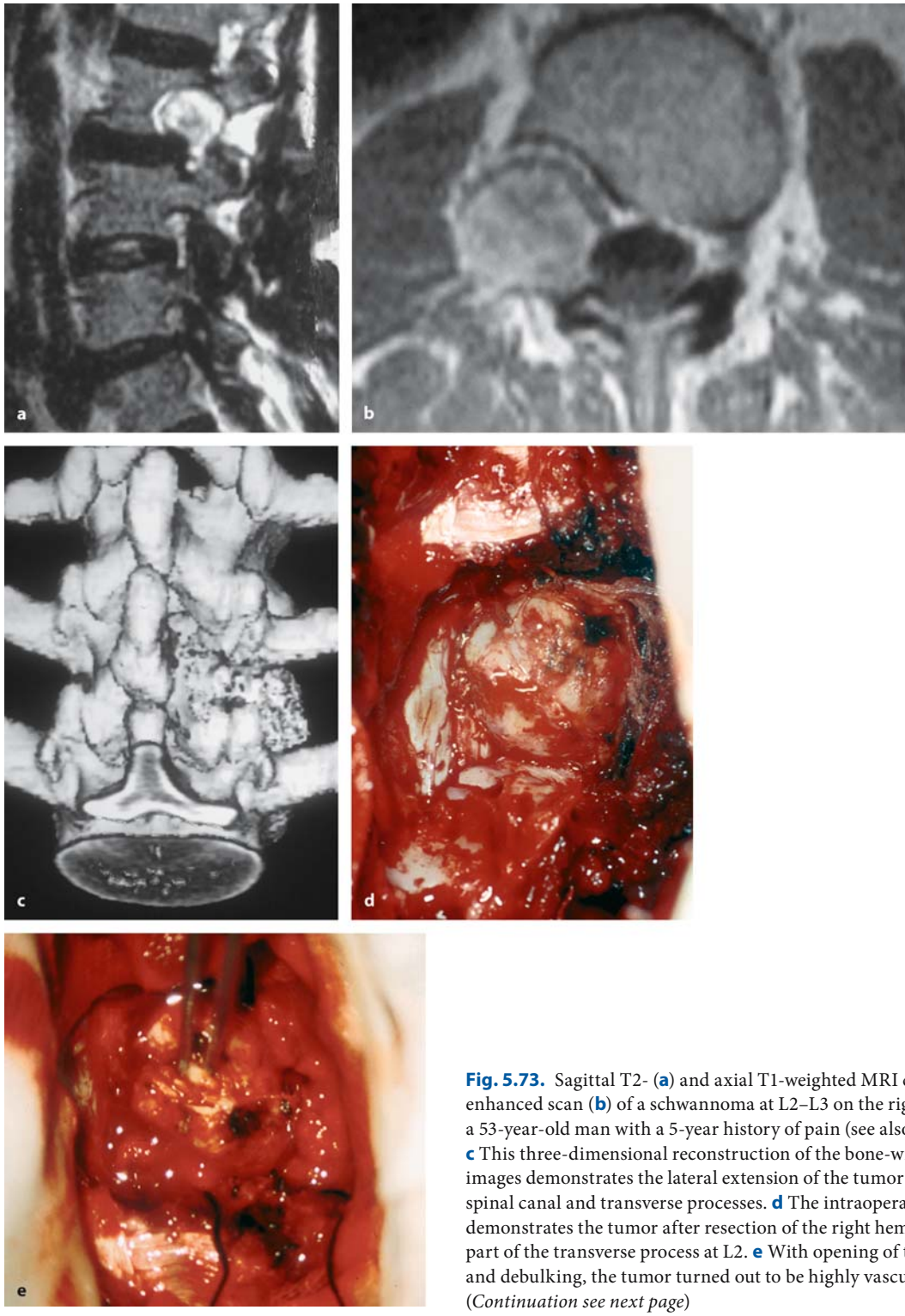

Fig. 5.73. Sagittal T2- (**a**) and axial T1-weighted MRI contrast-enhanced scan (**b**) of a schwannoma at L2–L3 on the right side in a 53-year-old man with a 5-year history of pain (see also Fig. 5.2). **c** This three-dimensional reconstruction of the bone-window CT images demonstrates the lateral extension of the tumor in relation to spinal canal and transverse processes. **d** The intraoperative overview demonstrates the tumor after resection of the right hemilamina and part of the transverse process at L2. **e** With opening of the capsule and debulking, the tumor turned out to be highly vascularized. (*Continuation see next page*)

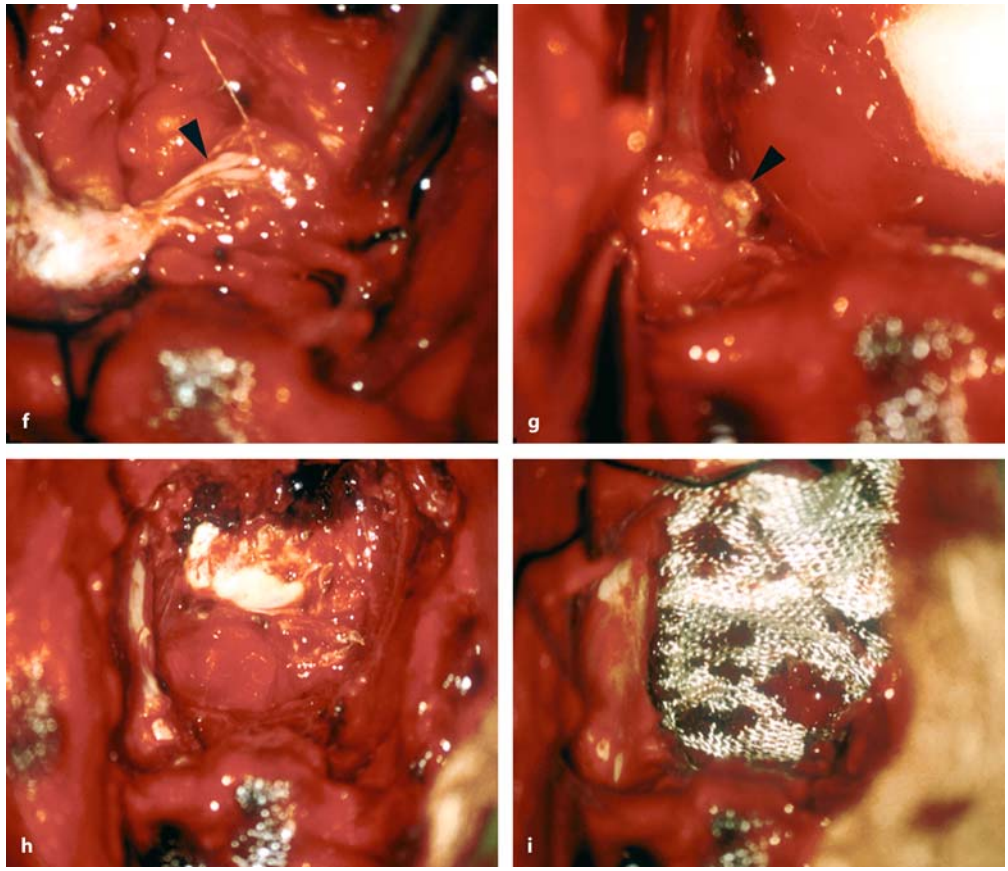

Fig. 5.73. (*Continued*) **f** The nerve root fibers (*arrowhead*) did not display motor responses on stimulation and were transected (*arrowhead* in **g**). **h** This view demonstrates the situation after complete resection of the tumor. **i** The tumor bed was covered with fibrin tissue for hemostasis. Postoperatively, pain improved. No motor deficit developed. However, the patient reported a slight sensory deficit in his right thigh

NF-2. At clinical presentation, pain was still the predominating problem for 61% of patients. However, in 24% of patients gait problems had become the major threat. With regard to neurological signs before surgery, patients without NF-2 were significantly less affected by neurological deficits compared to patients with NF-2, with the exception of pain and dysesthesias, which were about equally severe in both groups (Table 5.19). The preoperative Karnofsky score was significantly lower in patients with NF-2 compared to patients without NF-2 (63±17 and 78±9, respectively; p=0.0044).

Epidural nerve sheath tumors may grow to enormous proportions (Fig. 5.3) [257, 293, 335, 392, 396, 508]. This raises the problem of whether tumors with considerable intra- and extraspinal extension should be operated in a single or staged operation. Single operations with combined approaches from anterolateral and posterior have been used for removal of such tumors [208]. Lot and George [334] have reported excellent results using a modified anterior approach for cervical tumors, achieving a complete resection in 55 of 57 patients. We have used anterior approaches in eight and a combined approach in one patient, splitting surgeries in this case [156]. The remainder were operated via modified posterior approaches [105].

The other problem is radicality. Neuropathological studies have shown that removal of the capsule is mandatory for achieving a complete resection, as the capsule of a spinal schwannoma does contain neoplastic tissue [224]. With growth of such tumors toward the cervical or lumbar plexus, to mention just neural structures, it may become extremely difficult to resect such processes completely without compromising brachial or lumbar plexus, or important vessels, for example.

Radical resections have been advocated for such tumors [105, 257]. Celli et al. [105] preserved just 2 out

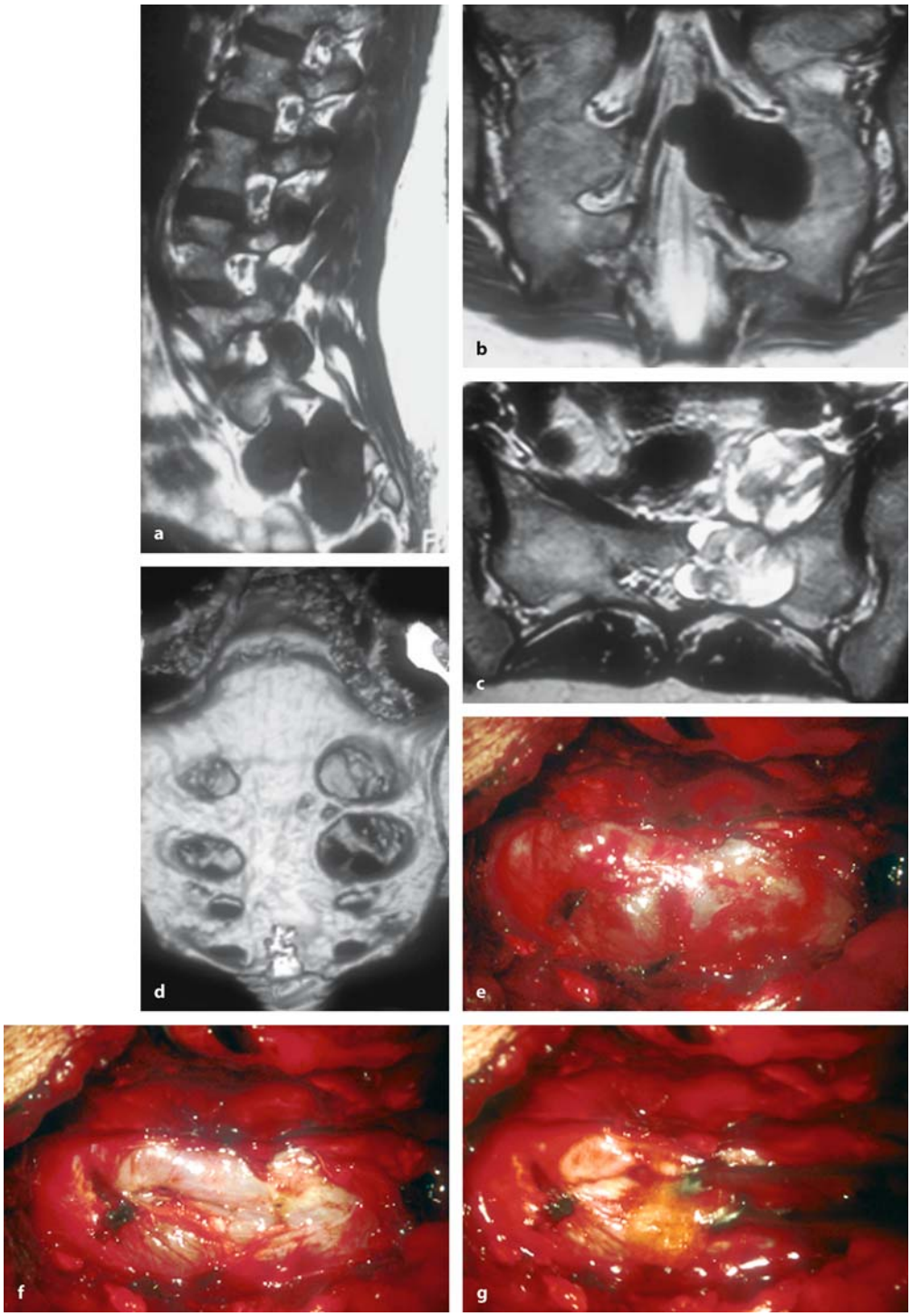

Fig. 5.74. Sagittal (**a**) and coronal (**b**) T1- and axial T2-weighted (**c**) MRI scans of a plexiform neurofibroma at S1–S4 in a 43-year-old woman with an 11-year history of pain and progressive distal paraparesis and complete sphincter control. The tumor has grown along the sacral nerves into the pelvic region. **d** A three-dimensional reconstruction of the bone-window CT scans demonstrates enlarged neuroforamina on the right side. **e** This intraoperative view shows the tumor after removal of the right half of the sacral roof. The tumor capsule is incised (**f**) for debulking (**g**). (*Continuation see next page*)

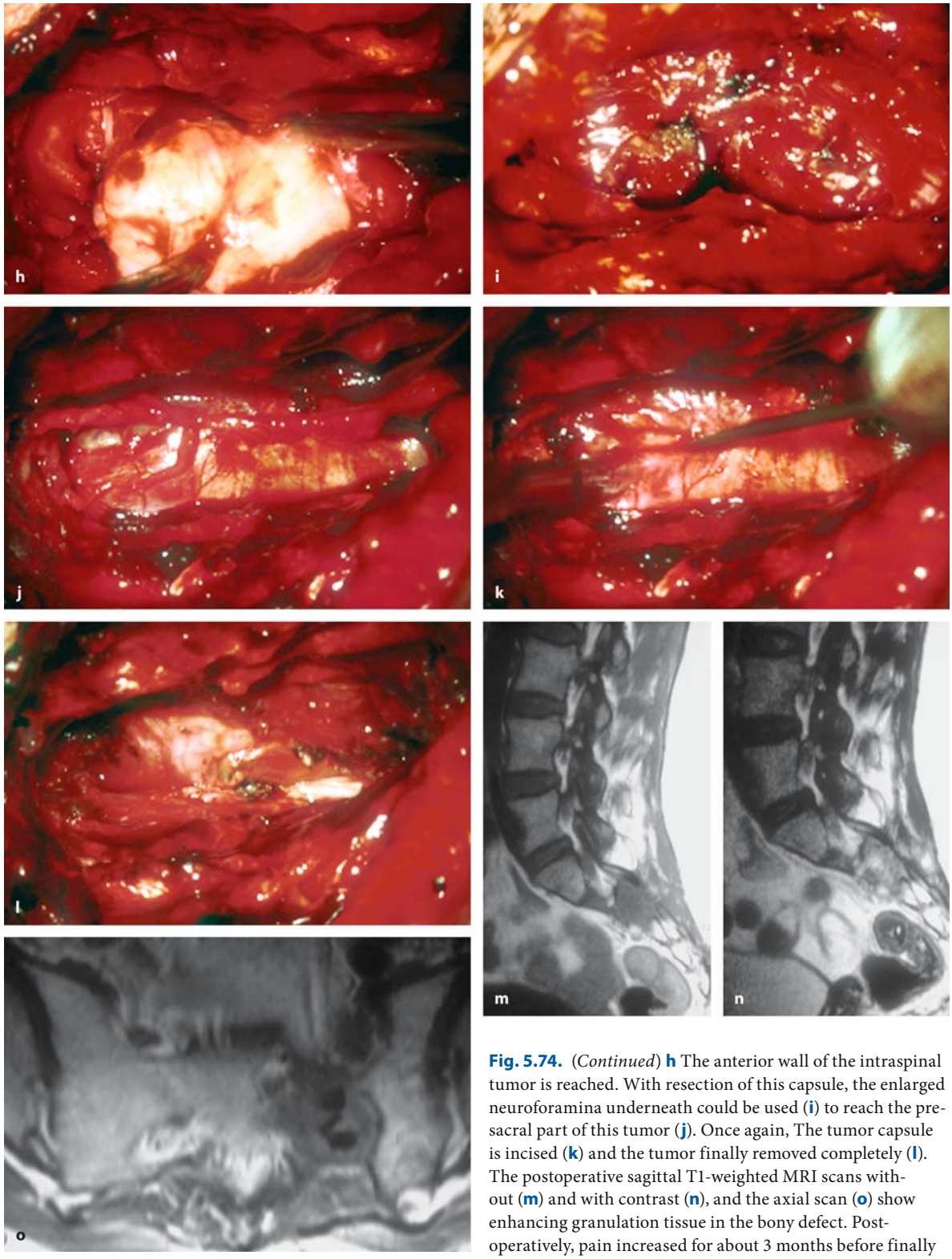

Fig. 5.74. (*Continued*) **h** The anterior wall of the intraspinal tumor is reached. With resection of this capsule, the enlarged neuroforamina underneath could be used (**i**) to reach the presacral part of this tumor (**j**). Once again, The tumor capsule is incised (**k**) and the tumor finally removed completely (**l**). The postoperative sagittal T1-weighted MRI scans without (**m**) and with contrast (**n**), and the axial scan (**o**) show enhancing granulation tissue in the bony defect. Postoperatively, pain increased for about 3 months before finally recovering. Her gait improved immediately and no other neurological deficit developed with the exception of increased sensory disturbances at S1–S5 on the left side

Table 5.19. Symptoms for patients with epidural nerve sheath tumors at presentation

Main symptom	No NF-2	NF-2	Total
Pain	84%	83%	84%
Gait ataxia	42%	75%	48%
Motor weakness	47%	92%	57%
Sensory deficits	58%	83%	65%
Dysesthesias	42%	42%	42%
Sphincter problems	11%	42%	19%

Abbreviation: NF-2 = neurofibromatosis type 2

of 16 nerve roots with this strategy. Their series incorporated only two NF-2 patients. Postoperatively, several patients complained about a radicular dysesthetic burning pain that disappeared after 20 days. One patient suffered a slight, transient L5 palsy, while all patients experienced increased sensory deficits. In an earlier paper, Celli [104] observed persistent motor deficits for two patients with epidural cervical schwannomas and none for intradural schwannomas after radical resection and sacrifice of the originating nerve root, indicating that preservation of the underlying root is important for preservation of function – at least for epidural tumors.

Table 5.20. Clinical course for patients with epidural nerve sheath tumors related to NF-2

Symptom	Preop. status	Postop. status	3 Months postop.	6 Months postop.	1 Year postop.
Pain					
No NF-2	3.2±1.0	3.7±0.8	4.3±0.8	4.4±0.8	4.4±0.7**
NF-2	3.0±1.2	3.6±0.9	4.2±1.3	4.6±1.3	4.6±0.9*
Total	3.2±1.0	3.7±0.8	4.3±0.9	4.4±0.9	4.4±0.8**
Hypesthesia					
No NF-2	4.1±0.9	4.1±0.9	4.2±0.9	4.2±0.9	4.3±0.8
NF-2	2.8±0.5	3.2±0.8	4.0±0.7	4.0±0.7	4.2±0.5*
Total	3.9±1.0	3.9±1.0	4.2±0.8	4.2±0.8	4.2±0.8*
Dysesthesias					
No NF-2	4.2±0.9	4.3±0.9	4.4±0.9	4.4±0.9	4.5±0.8
NF-2	3.8±1.1	4.2±0.8	4.2±0.8	4.2±0.8	4.2±0.8
Total	4.2±0.9	4.3±0.9	4.3±0.8	4.3±0.8	4.4±0.8
Gait					
No NF-2	4.5±0.7	4.3±0.8	4.6±0.6	4.6±0.6	4.6±0.6
NF-2	3.6±0.6	4.0±0.7	4.2±0.5	4.2±0.5	4.2±0.5
Total	4.4±0.8	4.3±0.8	4.6±0.6	4.6±0.6	4.6±0.6
Motor power					
No NF-2	4.0±1.2	4.0±1.3	4.4±1.0	4.3±1.0	4.4±1.0
NF-2	3.4±0.9	3.8±0.5	3.8±0.5	4.0±0.7	4.2±0.5
Total	4.0±1.2	4.0±1.0	4.3±0.9	4.3±0.9	4.3±0.9*
Sphincter function					
No NF-2	4.6±0.9	4.8±0.7	4.8±0.5	4.9±0.4	4.9±0.3
NF-2	4.2±1.1	4.6±0.6	4.6±0.6	4.6±0.6	4.6±0.6
Total	4.6±0.9	4.8±0.6	4.8±0.5	4.8±0.4	4.9±0.4*
Karnofsky score					
No NF-2	78±9	79±9	85±10	86±10	86±10*
NF-2	68±4	72±4	76±9	76±9	76±9*
Total	76±9	78±8	84±10	84±10	84±11*

Statistically significant difference between preop. status and 1 year postop.: *$p<0.05$, **$p<0.01$

From our experience, even an aggressive strategy aiming at radical resection cannot guarantee avoidance of a recurrence. Most patients will not accept radical removal of a benign tumor if that means losing function permanently, even if this incorporates the risk of a recurrence. This has to be taken into account in NF-2 patients in particular. According to our experience, NF-2 patients may harbor tumors on any nerve root and will always place function before radicality [543]. In our series, 72% of epidural nerve sheath tumors were removed completely, while 26% were resected subtotally. For 67% of the tumors, the involved nerve root was resected with the tumor, while it was preserved in 33%. For the majority of subtotal removals, preservation of a functionally relevant nerve root was the reason. For patients with and without NF-2, the rate for complete removals was lower for the former, at 57%, compared to 79% for the latter, reflecting our general policy for NF-2 patients.

Surgical morbidity was 5% related to permanent injury of functionally relevant nerve roots. The overall recurrence rates for epidural nerve sheath tumors were similar to those of their intradural and intra-extradural counterparts, with 26% of tumors recurring within 5 years and 39% recurring within 10 years. The corresponding figures for patients without NF-2 were determined as 10%, 18%, and 25% after 1, 5, and 10 years, respectively, while the figures for NF-patients were 19%, 57%, and 78%, respectively (log-rank test: p=0.0173; Fig. 5.75). Celli et al. [105] lost four patients to follow up and claimed no recurrences for the remaining patients, with a mean follow up of 7 years.

With respect to recurrence rates as a function of the degree of tumor resection, overall recurrence rates

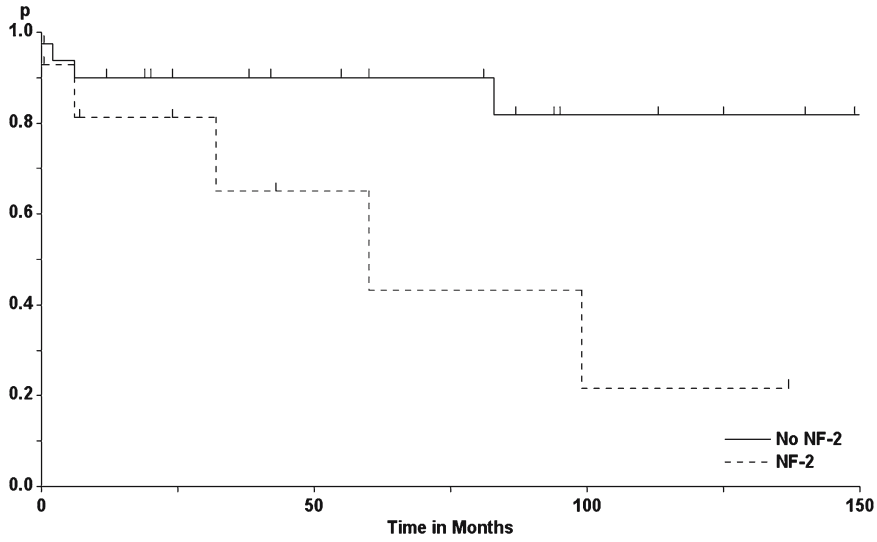

Fig. 5.75. Tumor recurrence rates for patients with epidural nerve sheath tumors, as a function of the presence or absence of NF-2 (log-rank test: p=0.0173)

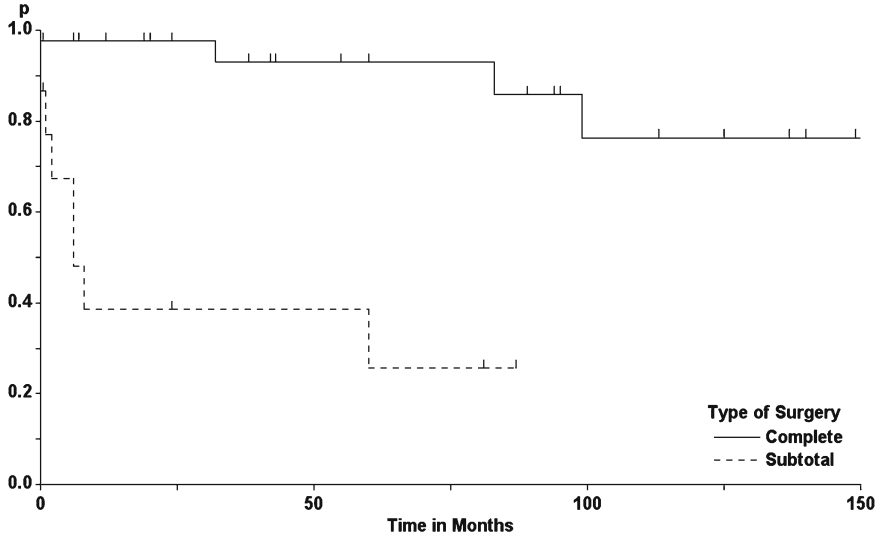

Fig. 5.76. Tumor recurrence rates for epidural nerve sheath tumors, as a function of the extent of tumor resection (log-rank test: p<0.0001)

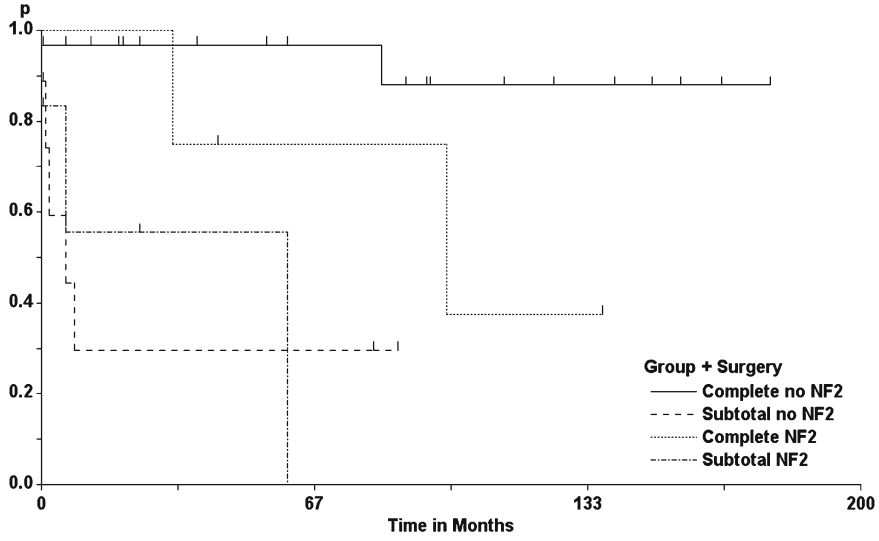

Fig. 5.77. Tumor recurrence rates for epidural nerve sheath tumors, as a function of the extent of tumor resection for patients with and without NF-2 (log-rank test: p=0.0004)

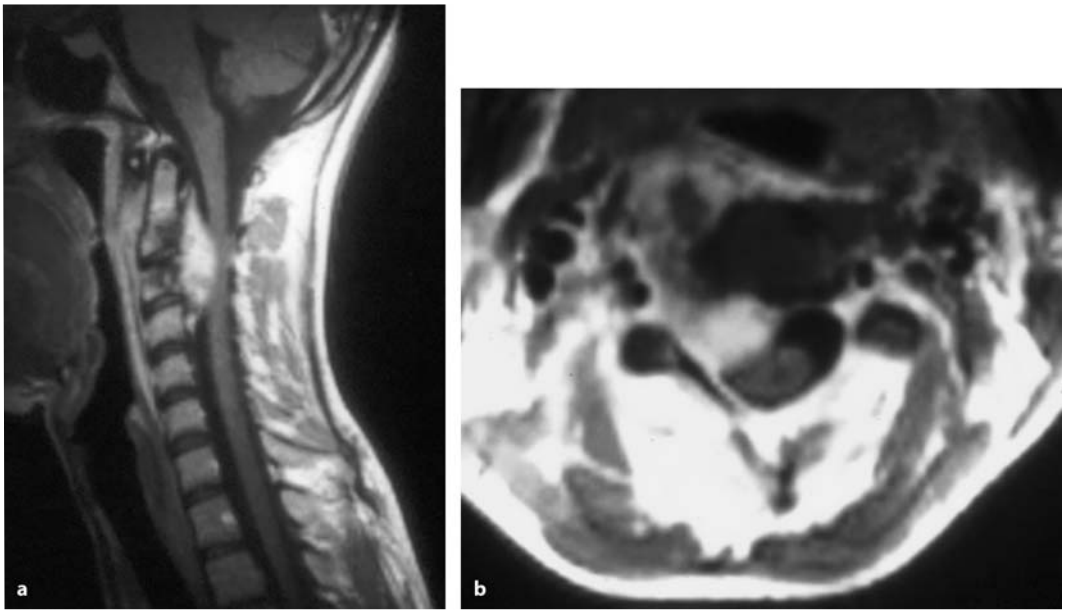

Fig. 5.78. Sagittal (**a**) and axial (**b**) T1-weighted, contrast-enhanced MRI scans of a malignant schwannoma at C2–C4 in a 21-year-old woman with a 14-month history of pain and sensory disturbances., Radiotherapy was applied after resection of the tumor, but a recurrence developed within 8 months. After two subsequent surgeries for recurrences, the patient died 14 months after the first operation

of 7% and 24% were found after complete resections within 5 and 10 years, respectively, and 74% after 5 years following subtotal resection (log-rank test: p<0.0001; Fig. 5.76). Again, splitting these according to the presence and absence of NF-2 showed considerably lower values for the patients without NF-2 after complete compared to subtotal resections, with 3% and 70% recurring after 5 years, respectively (log-rank test: p=0.0002), while for NF-2 patients, corresponding figures after 5 years of 25% and 100% were obtained after complete and subtotal removals, respectively (log-rank test: p=0.0004; Fig. 5.77).

Four operations in two patients dealt with malignant schwannomas. One patient died despite radiotherapy and three operations on a C2/3 tumor 14 months after the initial diagnosis (Fig. 5.78). The other patient underwent complete resection of a Th11/12 schwannoma with postoperative radiotherapy and is in good condition 8 years postoperatively without a recurrence. Mazel et al. [359] reported on

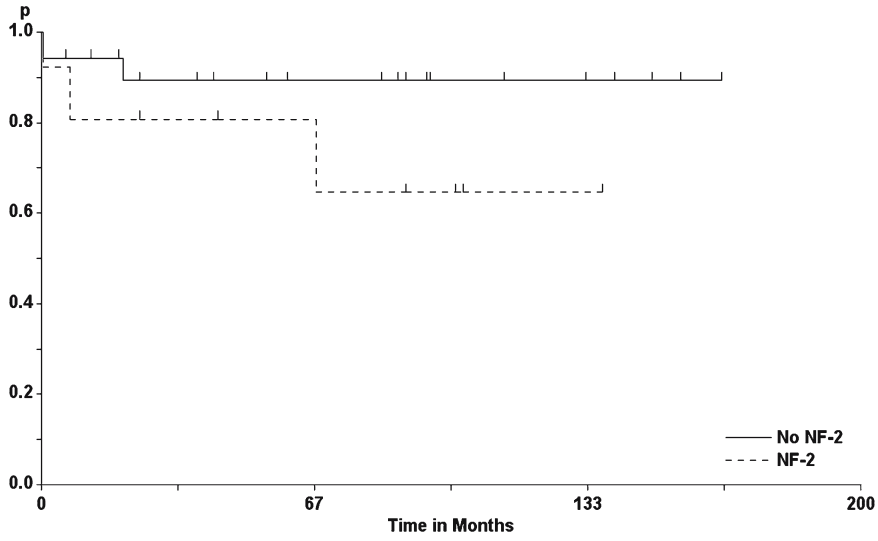

Fig. 5.79. Survival rates for patients with epidural nerve sheath tumors as a function of the presence or absence of NF-2 (log-rank test: not significant)

three malignant schwannomas in the thoracic spine. Despite radical resections, all patients had died within 27 months.

Analysis of mortalities for patients with benign epidural nerve sheath tumors showed higher figures for NF-2 patients, with 35% having died within 7 years after surgery compared to 11% without NF-2 (Fig. 5.79).

5.5.1.2 Synovial Cysts

Synovial cysts are associated with degenerative changes of intervertebral joints [112, 243]. They contain synovial cells with additional proliferative tissue consisting of histiocytes, giant cells, and granulation tissue. They may contain mucinous material or clear cyst fluid [460, 525]. Most of them have been reported to occur in the lumbar spine (Fig. 5.80), predominantly at L4/5, but case reports have been published with synovial joints in the thoracic [148, 202, 332, 337], and more often in the cervical spine (Figs. 5.81 and 5.82) [10, 100, 108, 111, 120, 121, 132, 159, 162, 181, 269, 278, 376, 383, 398, 410, 495, 526, 527, 554, 572, 584]. They are mostly located in an antero- or posterolateral position; however, even far lateral synovial cysts have been observed [432]. Not too rarely, spontaneous regression of synovial cysts has been described [241, 340, 368, 423, 524]. Apart from cysts occurring in association with degenerative spine disease, cases have been associated with trauma [100, 179, 410] and rheumatoid arthritis [383].

Before the advent of MRI, a considerable number of synovial cysts were discovered incidentally during surgery for lumbar discs or spinal stenosis [466]. It has been estimated that up to 1% of all MRI scans for lumbar pain will detect a synovial cyst [217]. On CT, the characteristic finding is a cystic lesion adjacent to an intervertebral joint (Figs. 5.6, 5.80, and 5.82) [92, 478, 548, 557], which may be partly calcified [103, 398, 548, 557] or contain gas [47, 165, 481]. One case was reported with erosion of the vertebral body [269]. The appearance is quite variable on MRI [22], as synovial cysts may contain fluid or solid components intermingled with hemosiderin due to small hemorrhages. Characteristically, the rim of the cyst will be hypointense on T1- and hyperintense on T2-weighted images and may take up gadolinium [31, 163, 184, 217, 330, 383, 478].

We have observed 15 patients with synovial cysts in our series (Table 5.21). The age ranged from 46 to 78 years (mean 62±11 years) [282, 338, 407, 542] and presented after an average history of 7±7 months. Acute presentations may be observed due to sudden hemorrhages into the cyst or even the epidural space [259, 274, 531, 556]. This group was followed for a mean duration of 26±39 months. Three cysts were observed in the cervical region (C1/2, C2 and C7/Th1), one at the thoracolumbar junction, and the remaining 11 in the lumbar spine – 2 at L5/S1 and 9 at L4/5. This distribution is consistent with other reported series [17, 138, 158, 182, 217, 242, 243, 338, 407, 542].

The predominating symptom was pain, which was confined to the back and then followed a radicular distribution in virtually all patients [17, 158, 242, 243, 282, 338, 370]. Additional neurological deficits such

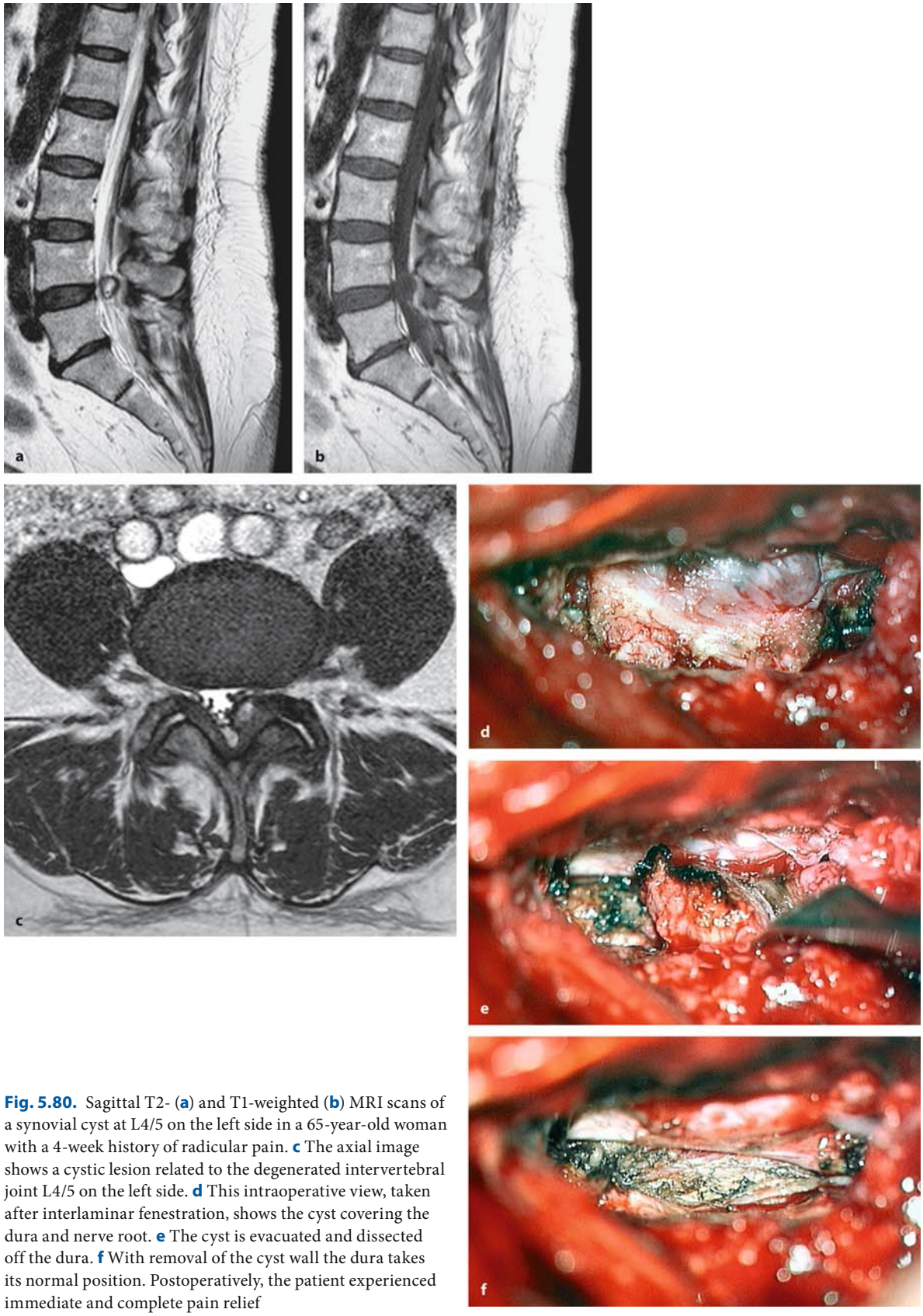

Fig. 5.80. Sagittal T2- (**a**) and T1-weighted (**b**) MRI scans of a synovial cyst at L4/5 on the left side in a 65-year-old woman with a 4-week history of radicular pain. **c** The axial image shows a cystic lesion related to the degenerated intervertebral joint L4/5 on the left side. **d** This intraoperative view, taken after interlaminar fenestration, shows the cyst covering the dura and nerve root. **e** The cyst is evacuated and dissected off the dura. **f** With removal of the cyst wall the dura takes its normal position. Postoperatively, the patient experienced immediate and complete pain relief

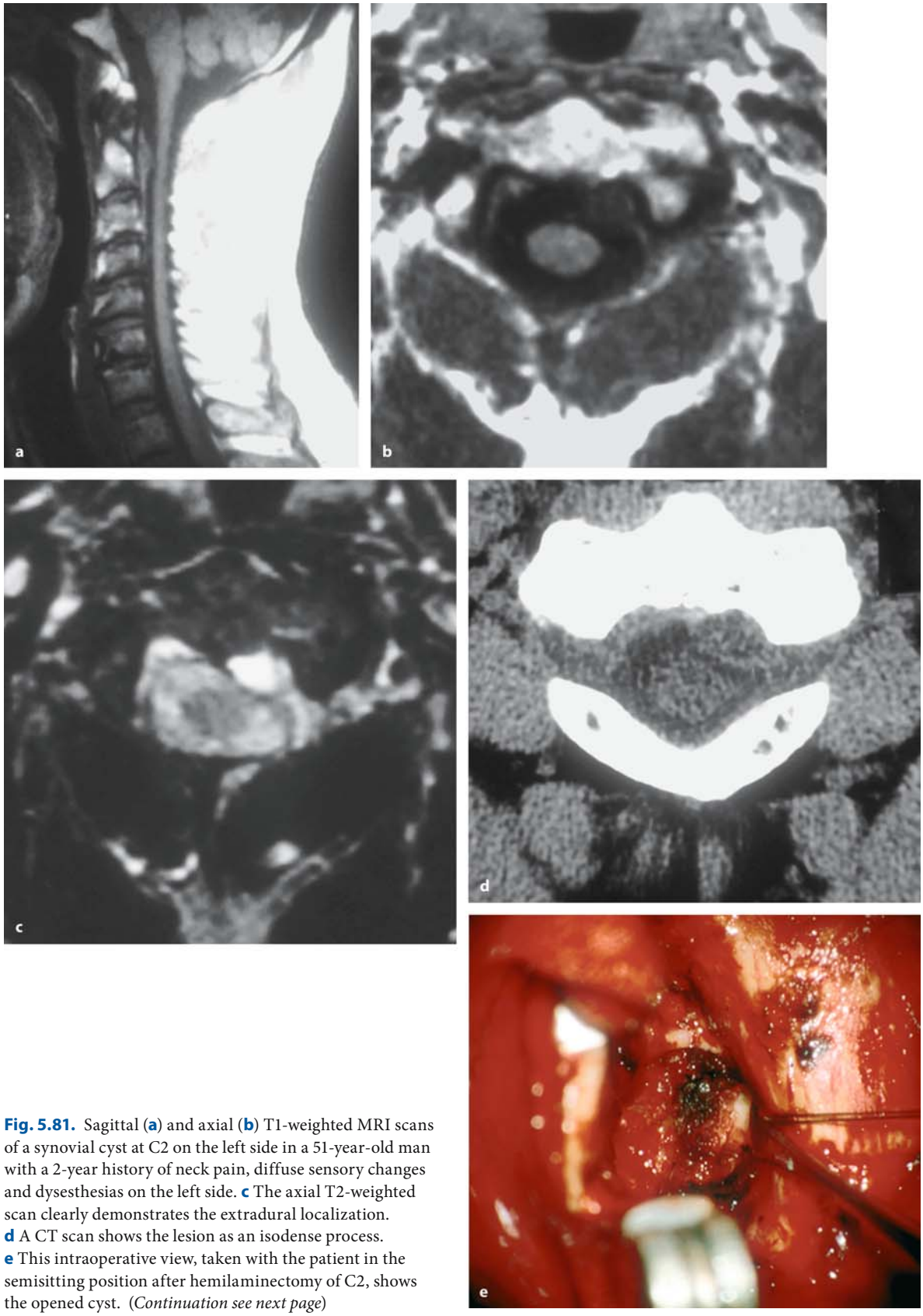

Fig. 5.81. Sagittal (**a**) and axial (**b**) T1-weighted MRI scans of a synovial cyst at C2 on the left side in a 51-year-old man with a 2-year history of neck pain, diffuse sensory changes and dysesthesias on the left side. **c** The axial T2-weighted scan clearly demonstrates the extradural localization. **d** A CT scan shows the lesion as an isodense process. **e** This intraoperative view, taken with the patient in the semisitting position after hemilaminectomy of C2, shows the opened cyst. (*Continuation see next page*)

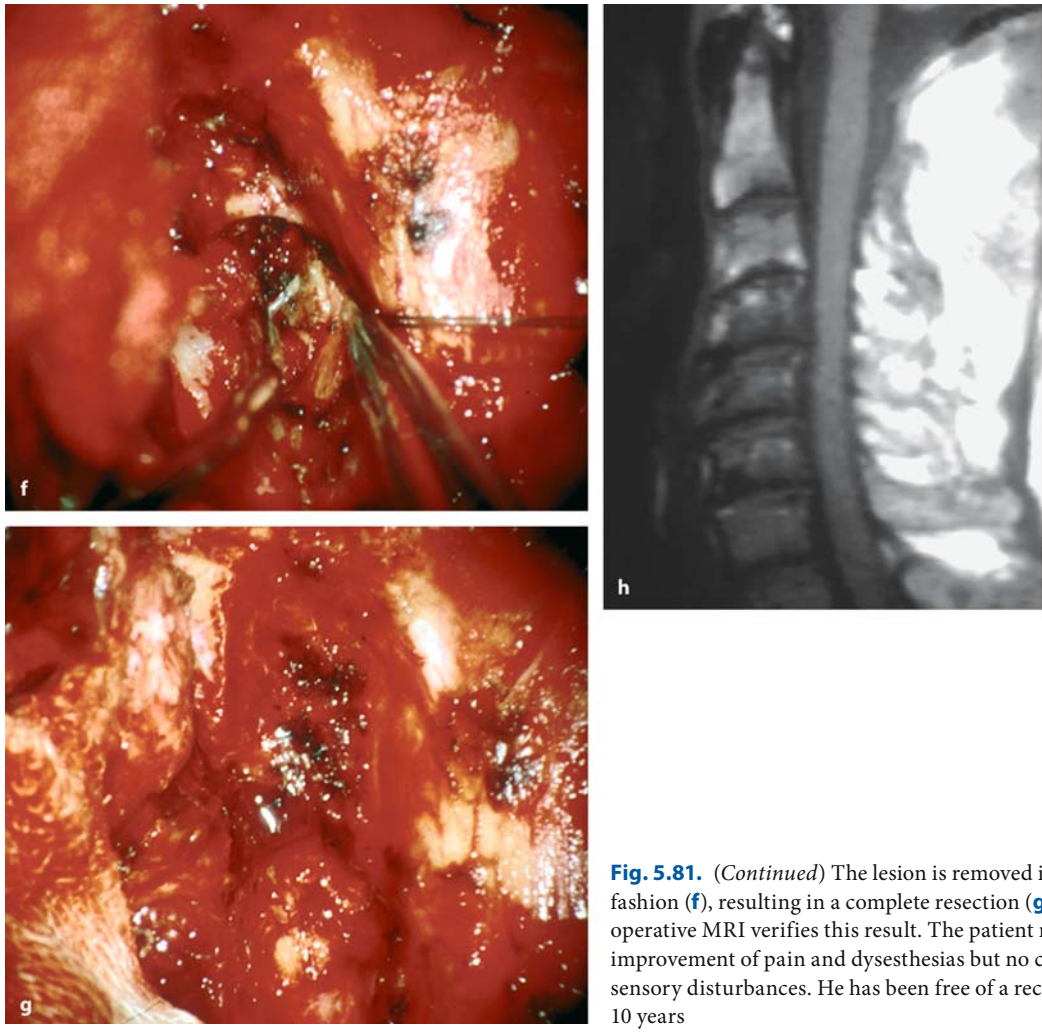

Fig. 5.81. (*Continued*) The lesion is removed in piecemeal fashion (**f**), resulting in a complete resection (**g**). **h** A postoperative MRI verifies this result. The patient reported improvement of pain and dysesthesias but no change of sensory disturbances. He has been free of a recurrence for 10 years

Fig. 5.82. Paramedian sagittal T1-weighted MRI scans without (**a**) and with contrast (**b**) of a synovial cyst involving the atlantodental joint on the right side in a 69-year-old man with a 1-year history of severe neck pain provoked by neck movements. There appears a small contrast-enhancing lesion. (*Continuation see next page*)

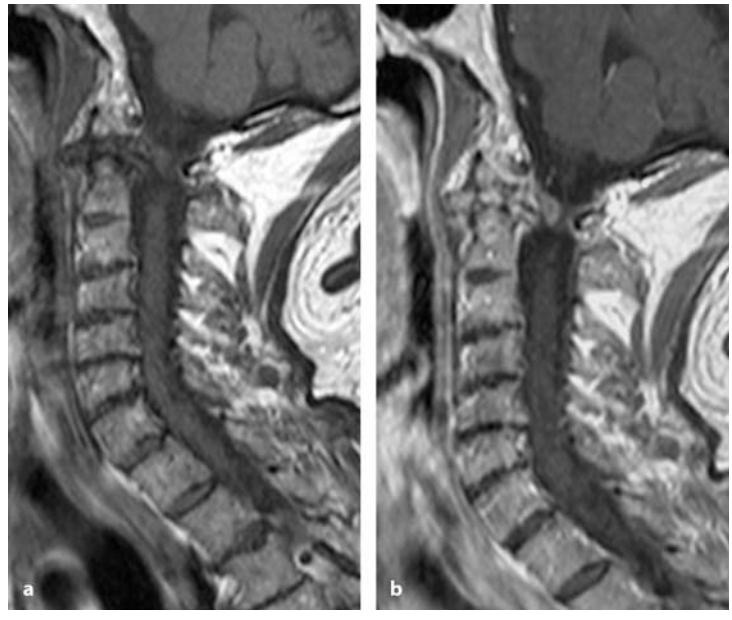

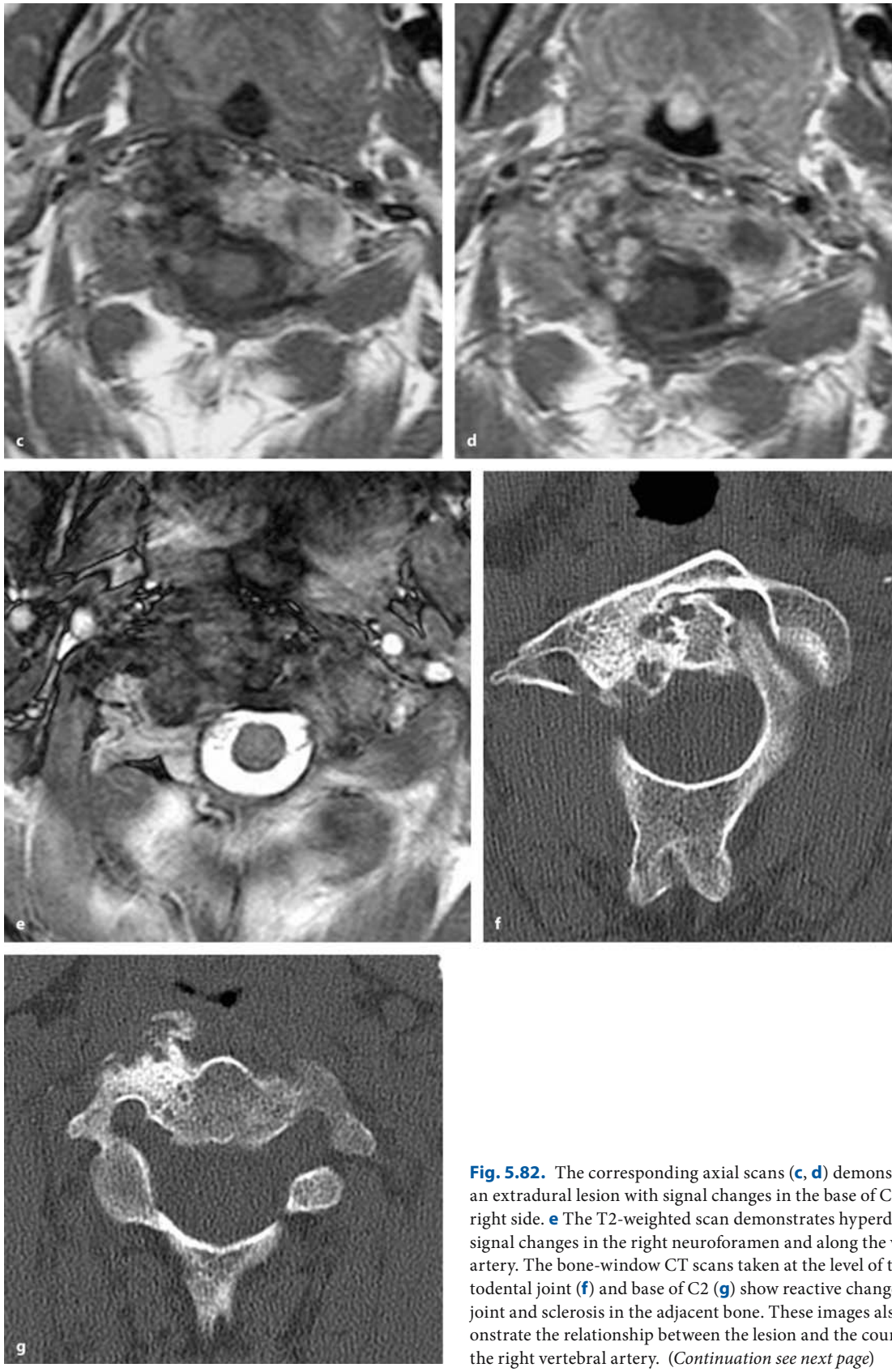

Fig. 5.82. The corresponding axial scans (**c**, **d**) demonstrate an extradural lesion with signal changes in the base of C2 on the right side. **e** The T2-weighted scan demonstrates hyperdense signal changes in the right neuroforamen and along the vertebral artery. The bone-window CT scans taken at the level of the atlantodental joint (**f**) and base of C2 (**g**) show reactive changes of the joint and sclerosis in the adjacent bone. These images also demonstrate the relationship between the lesion and the course of the right vertebral artery. (*Continuation see next page*)

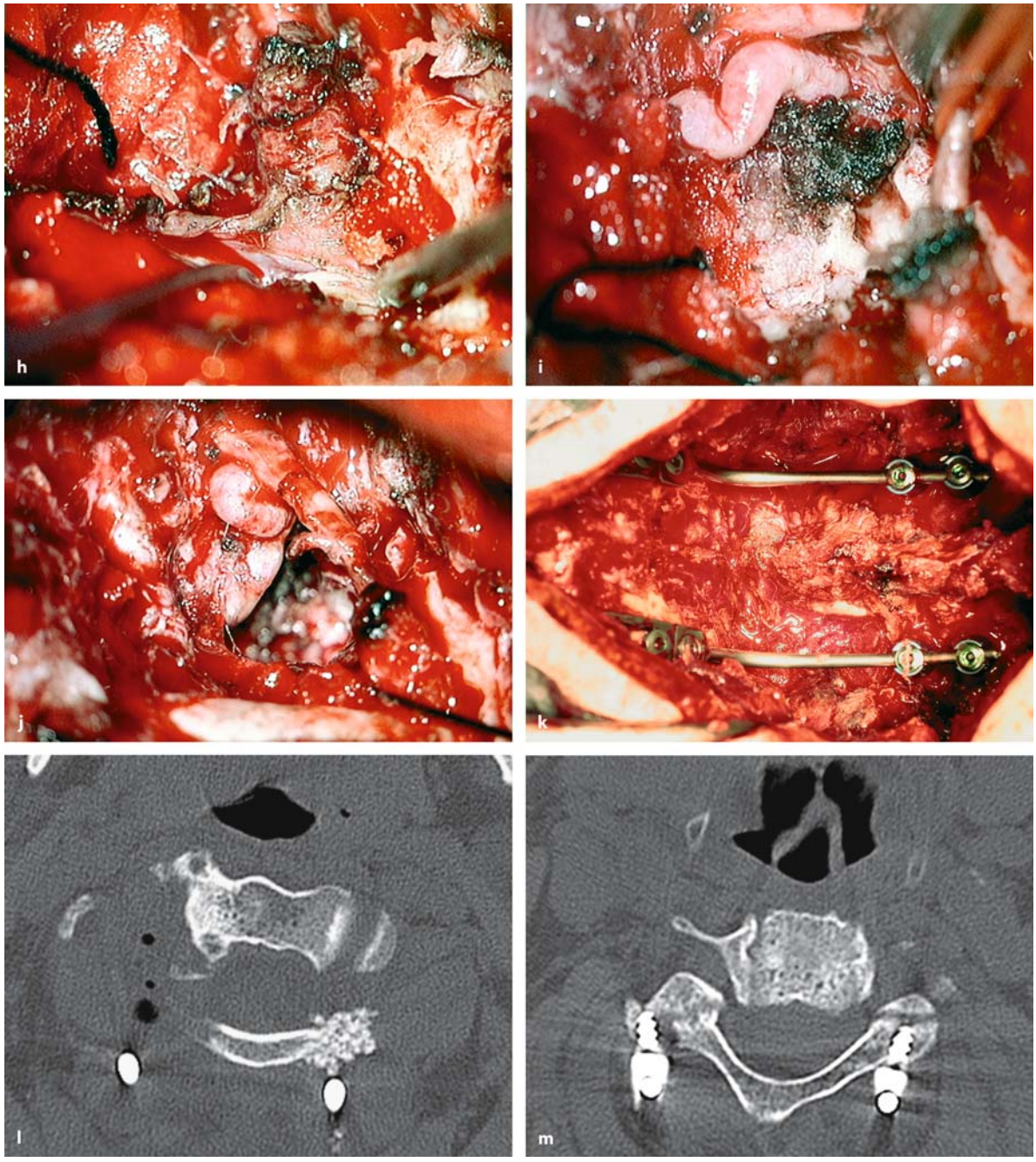

Fig. 5.82. **h** With the patient in the prone position, a hemilaminectomy at C1 and partial hemilaminectomy of C2 on the right side shows reactive soft-tissue changes obscuring the underlying pathology. **i** After dissection of this soft tissue and the vertebral artery, the accompanying veins are covered with fibrin tissues and part of the pathology appears between the dura and the artery. **j** This image shows the situation after removal of the synovial cyst and part of the accompanying soft-tissue changes. **k** The final intraoperative picture displays the occipitocervical fusion to C4 using lateral mass screws. The postoperative bone-window CT images demonstrate the area of resection (**l**) and the position of the screws (**m**). (*Continuation see next page*)

Fig. 5.82. (*Continued*) **n** The lateral X-ray shows the correct position of the implants, but also considerable degenerative disc disease in all cervical segments down to C7. The patient experienced considerable pain relief and has been free of symptoms for 5 months

as sensory deficits (50%), dysesthesias (36%), motor weakness (36%), and gait (14%) or sphincter problems (14%) were rather mild and not functionally significant for most patients [138, 158, 242, 243, 338]. Consequently, the preoperative Karnofsky score of 83±8 was very high compared to of other patients with spinal tumors.

As far as treatment is concerned, three strategies are recommended in the literature. CT-guided aspiration and injection of corticosteroids is reported to produce reasonable results in terms of pain relief [217, 268, 420, 476]. However, if long-term results beyond 6 months are analyzed, only about 30% of patients will still show a satisfactory result. Therefore, this modality will only provide a short-lived benefit [17, 250, 487].

Better long-term results are reported with surgical treatment. Within the neurosurgical literature, cyst resection is favored and produces excellent results for neurological deficits as well as for pain relief (Figs. 5.80 and 5.81) [17, 31, 32, 138, 158, 182, 242, 243, 338, 370, 407, 542].

On the other hand, several authors in the orthopedic literature have emphasized the point that the presence of synovial cysts indicates a compromised intervertebral joint so that the issues of instability and spinal fusion for these patients are raised. At the level of C1/2, several case reports have shown that the cyst will regress if fusion of the affected level is performed [108, 383]. Likewise, the combination of cyst removal and fusion was recommended for lumbar [158, 180, 282] and craniocervical cases (Fig. 5.82) [67]. However, those authors who looked at the incidence of spinal instabilities after a synovial cyst had been resected found that only a small proportion needed such a second intervention [32]. This was even true for a series in which a significant proportion (41%) of patients demonstrated an additional degenerative spondylolisthesis [32].

The largest series on synovial cysts was been published by Lyons et al. [338], who presented the Mayo Clinic experience of 194 patients. They performed a posterior fusion in 18 of their 194 patients because spinal instability was demonstrated in addition to the cyst. The remainder were treated exclusively by cyst resection. Subsequent instabilities occurred in only 4 of these 176 patients. Therefore, they concluded that posterior fixation should not be performed in all patients with synovial cysts, but be reserved for patients with preexisting instability.

For the level of C1/2 at the atlantodental joint, synovial cysts have been managed by transoral resection only [278], transoral resection plus posterior fixation [67], posterior fixation only [108, 383], posterior resection only [67, 162, 181, 526, 584], and posterior resection plus fixation (Fig. 5.82) [10, 410]. Again, the question of stability has to be evaluated preoperatively. If the patient is unstable at C1/2 or reactive inflammatory changes involve intervertebral joints (Fig. 5.82), then the patient will need posterior fixation to achieve a good pain control.

In our series, all patients were operated from a posterior approach with either a laminectomy (2 patients), a laminotomy (1 patient), or hemilaminectomy/interlaminar fenestration (12 patients). All but two synovial cysts could be completely resected. One patient required fusion (Fig. 5.82).

Postoperative clinical results have been excellent for this group of patients. Lyons et al. [338] reported that 91% of their 194 patients experienced marked pain relief in the first postoperative month, and after 6 months, 82% still reported this improvement. In our series, all but one patient reported pain relief for at least 6 months postoperatively with improvement of preoperative neurological symptoms in all but one patient.

The postoperative long-term outcome is characterized by a very low recurrence rate, which is reported to be between zero and 3% [32, 407]. In our series, not a single recurrence was seen.

Table 5.21. Spinal synovial cysts

Sex	Age (years)	Level	History (months)	Symptoms	Surgery	Outcome
M	70	C1/C2	72	Pain	Subtotal + Fusion	Improved No Rec. in 1 month
M	51	C2	24	Hypesth., Dysesth., Pain, Sphincter	Subtotal	Improved No Rec. in 124 months
M	61	L5/S1	?	Pain	Complete	Improved Lost to follow up
M	64	L5/S1	0.5	Dysesth., Motor, Pain	Complete	Improved Lost to follow up
F	50	L4/5	3	Hypesth., Motor, Pain	Complete	Improved Lost to Follow up
F	52	L4/5	14	Hypesth., Pain	Complete	Improved Lost to follow up
M	75	Th12/L1	1	Hypesth., Pain, Sphincter	Complete	Improved No Rec. in 72 months
M	46	L4/5	0.5	Hypesth., Pain	Complete	Improved No Rec. in 40 months
F	78	L4/5	6	Dysesth., Pain	Complete	Improved No Rec. 39 months
F	63	L4/5	12	Pain	Complete	Improved Lost to follow up
F	71	L4/5	5	Hypesth., Dysesth., Pain, Motor	Complete	Improved No Rec. in 32 months
F	64	C7/Th1	1	Hypesth., Motor, Gait, Pain	Complete	Unchanged Lost to follow up
F	60	L4/5	?	Pain	Complete	Improved Lost to follow up
M	55	L4/5	0.5	Pain	Complete	Improved Lost to follow up
F	77	L4/5	12	Dysesth., Motor, Gait, Pain	Complete	Improved Lost to follow up

Abbreviations: M = male, F = female, Hypesth. = hypesthesia, Dysesth. = dysesthesia, Motor = motor weakness, Gait = gait ataxia, Sphincter = sphincter functions, Rec. = recurrence

5.5.1.3 Arachnoid Cysts

Epidural arachnoid cysts are rare spinal pathologies. They require a dural defect so that the arachnoidal layer can herniate through it. This dura defect may be congenital [113] or posttraumatic [115, 155]. They have also been described in association with dysraphic malformations [186, 214, 439] and NF-2 [280].

The communication between cyst and subarachnoid space may be difficult to demonstrate on MRI so that myelography followed by CT can still be regarded as a very useful diagnostic method, especially for epidural cysts that extend over several spinal segments (Figs. 5.83 and 5.84) [147, 150, 155, 265, 280, 302, 419, 452]. Doita et al. [150] demonstrated pressure changes in an epidural arachnoid cyst with kinematic MRI during Valsalva maneuvers, explaining the fluctuating symptoms as posturing or straining in these patients.

Eguchi et al. [152] reported their experience with the use of a small endoscope as a diagnostic tool in

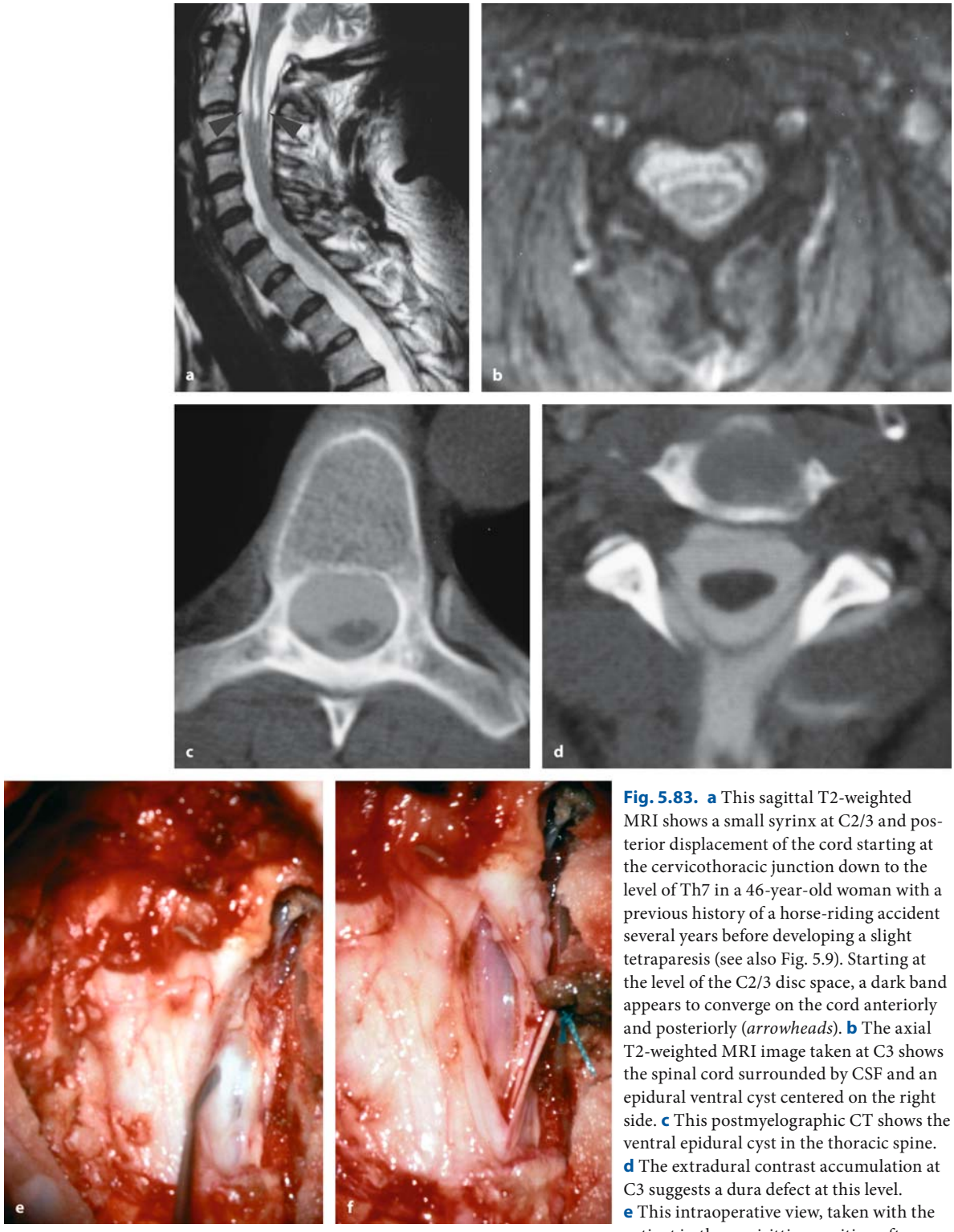

Fig. 5.83. **a** This sagittal T2-weighted MRI shows a small syrinx at C2/3 and posterior displacement of the cord starting at the cervicothoracic junction down to the level of Th7 in a 46-year-old woman with a previous history of a horse-riding accident several years before developing a slight tetraparesis (see also Fig. 5.9). Starting at the level of the C2/3 disc space, a dark band appears to converge on the cord anteriorly and posteriorly (*arrowheads*). **b** The axial T2-weighted MRI image taken at C3 shows the spinal cord surrounded by CSF and an epidural ventral cyst centered on the right side. **c** This postmyelographic CT shows the ventral epidural cyst in the thoracic spine. **d** The extradural contrast accumulation at C3 suggests a dura defect at this level. **e** This intraoperative view, taken with the patient in the semisitting position after laminotomy of C2 and C3, demonstrates the epidural cyst on the right side opened in close proximity to the nerve root sleeve. **f** After paramedian dura opening, the arachnoid is visible and appears normal. (*Continuation see next page*)

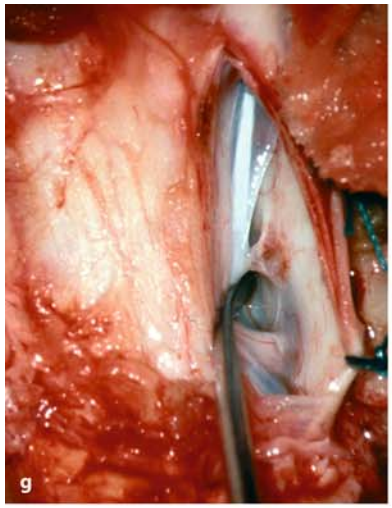

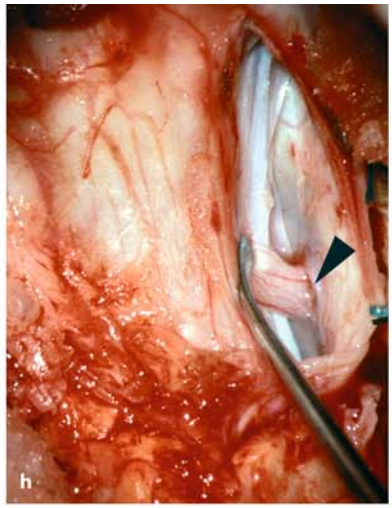

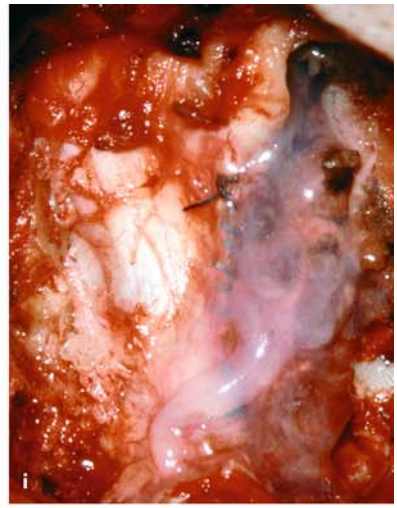

Fig. 5.83. (*Continued*) **g** Inspection of the dura sleeve of the nerve root on the right reveals the white dentate ligament, the posterior root, and an adhesion in the area of the dura sleeve. **h** With transection of this adhesion, the root can be gently mobilized to reveal the communication between the subarachnoid space and the cyst in the root sleeve (*arrowhead*). **i** The dura was closed with a running suture and the dura defect closed with muscle and fibrin glue epidurally. **j** The final intraoperative view shows the reinserted laminae. The postoperative T2-weighted sagittal (**k**) and axial (**l**, **m**) MRI scans show a complete collapse of the cyst with a normal position of the spinal cord in the cervicothoracic spine (**k**), as well as at the level of surgery (**l**). The patient's symptoms improved and there has been no recurrence for 3 years

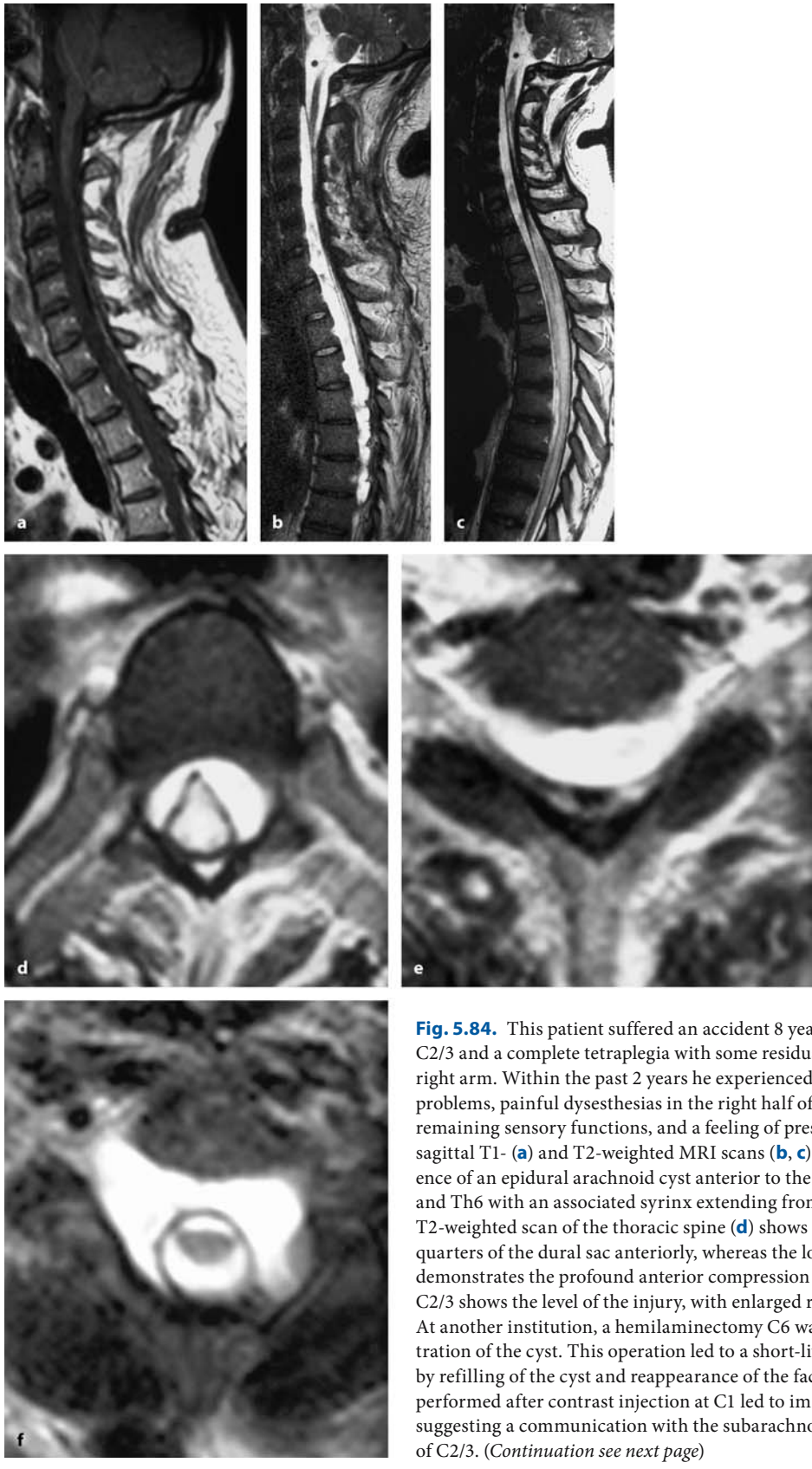

Fig. 5.84. This patient suffered an accident 8 years ago with a luxation C2/3 and a complete tetraplegia with some residual sensory functions in his right arm. Within the past 2 years he experienced increasing swallowing problems, painful dysesthesias in the right half of his face, loss of his remaining sensory functions, and a feeling of pressure in his neck. The sagittal T1- (**a**) and T2-weighted MRI scans (**b**, **c**) demonstrate the presence of an epidural arachnoid cyst anterior to the spinal cord between C2 and Th6 with an associated syrinx extending from Th1 to Th9. The axial T2-weighted scan of the thoracic spine (**d**) shows the cyst encircling three-quarters of the dural sac anteriorly, whereas the lower cervical scan (**e**) demonstrates the profound anterior compression of the cord. **f** The scan at C2/3 shows the level of the injury, with enlarged root sleeves on both sides. At another institution, a hemilaminectomy C6 was performed with fenestration of the cyst. This operation led to a short-lived improvement followed by refilling of the cyst and reappearance of the facial pain. A myelogram performed after contrast injection at C1 led to immediate filling of the cyst, suggesting a communication with the subarachnoid space at the injury level of C2/3. (*Continuation see next page*)

Fig. 5.84. The postmyelographic CT scan in the thoracic spine (**g**) and at C7 (**h**) demonstrate the same features as the MRI scans. Due to obliteration of the subarachnoid space, no subarachnoid contrast was detected below C5. **i** At the injury level, the CT scan suggest a dural defect in both root sleeves. **j** This intraoperative view, taken with the patient in the semi-sitting position, demonstrates the situation after laminotomy of C2 and C3. An epidural scar indicates the level of soft-tissue injury. **k** Upon dissection of this scar, the cyst is entered on the left side. Localization of the dura defect required an intradural inspection. **l** After midline incision of the dura, the left C3 root was followed towards the foramen. Further dissection of the root (**m**) led to the site of communication right above the root in the dural sleeve (**n**). **o** No dura defect could be found on the right side. (*Continuation see next page*)

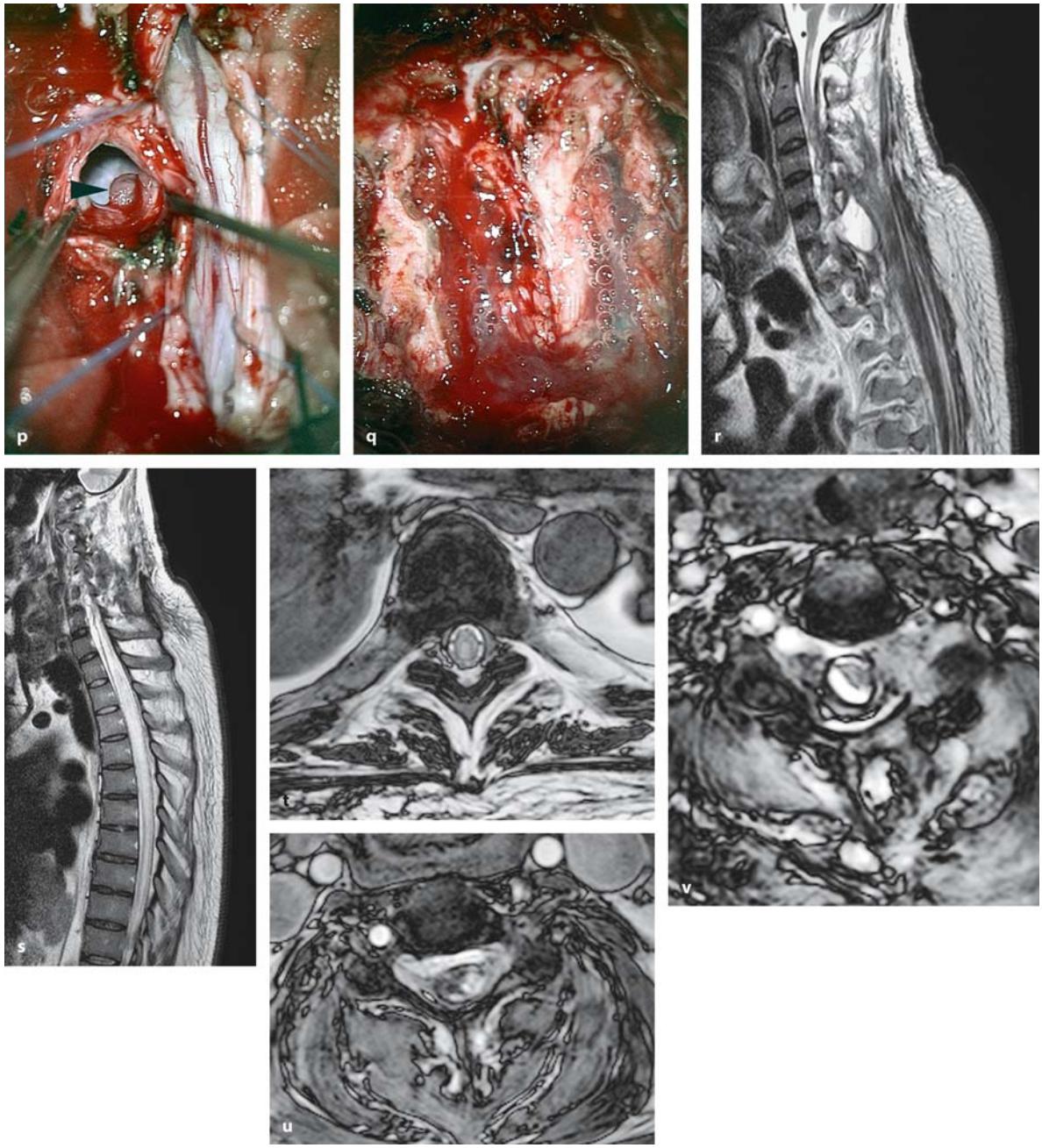

Fig. 5.84. (*Continued*) **p** The defect on the left side was closed with muscle (*arrowhead*) and secured with fibrin glue intradurally and extradurally (**q**). Additional muscle was placed on the right side. **r**, **s** These postoperative sagittal T2-weighted MRI scans show a marked reduction of the cyst size with an unchanged syrinx. The axial images in the thoracic spine (**t**), C7 (**u**), and C2/3 (**v**) demonstrate this postoperative result even better. The patient reported marked improvement of his facial pain and swallowing problems

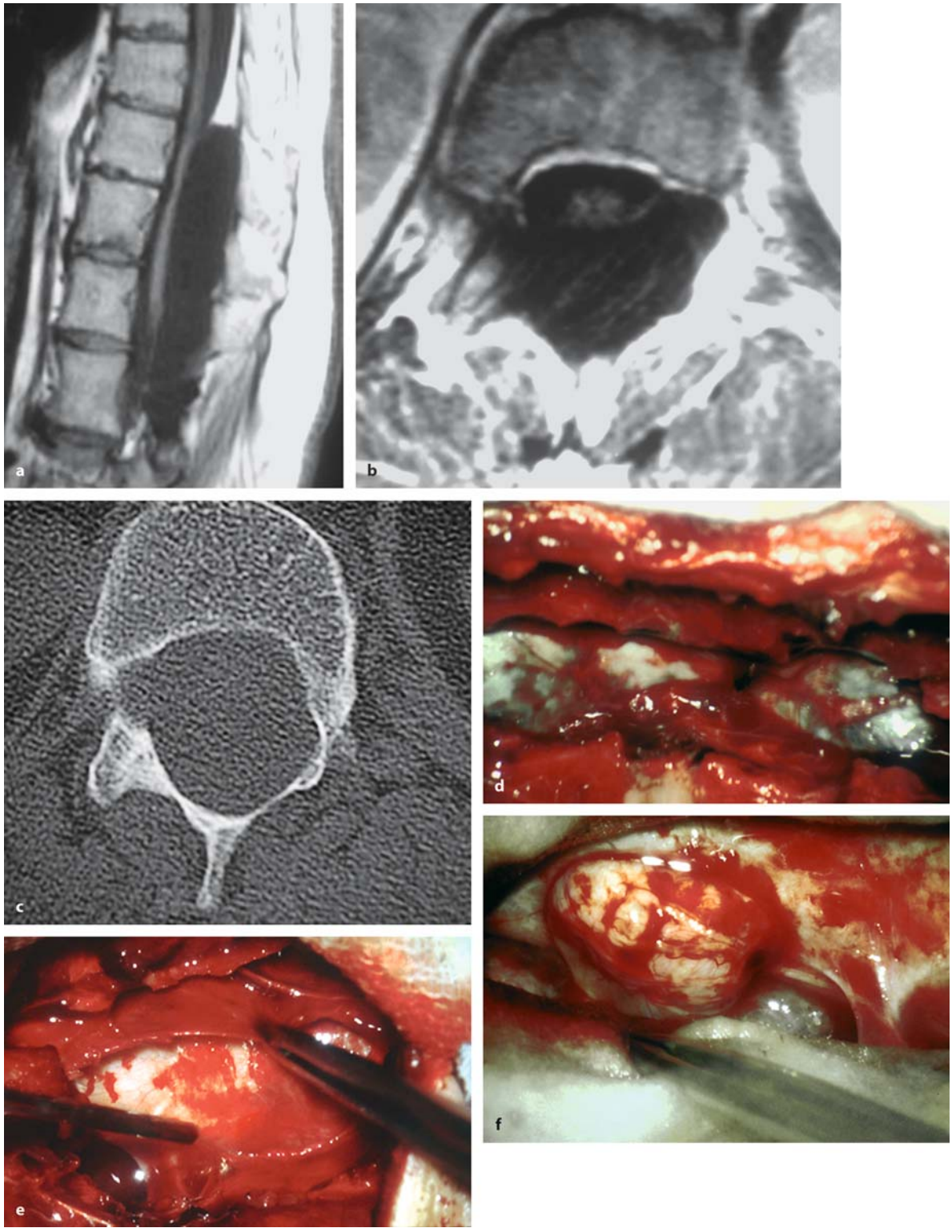

Fig. 5.85. Sagittal (**a**) and axial (**b**) T1-weighted MRI scans of an epidural arachnoid cyst at Th9–Th12 in a 50-year-old man with a 2-year history of progressive paraparesis and pain. **c** The bone-window CT scan demonstrates thinning of the pedicles as a result of long-lasting compression. **d** This intraoperative view shows the posterior cyst wall after removal of the laminae. The cyst could be peeled off the dura (**e**), exposing a large posterior dura defect with the spinal cord herniating through this defect (**f**). (*Continuation see next page*)

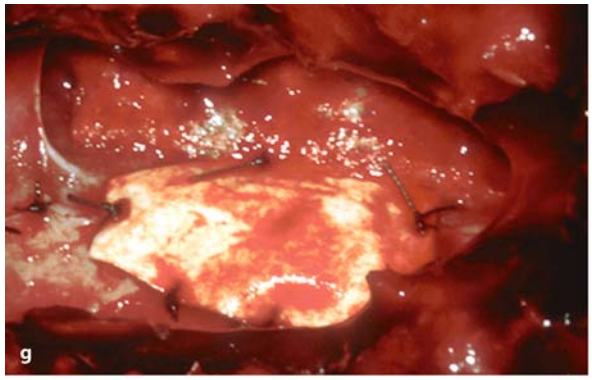

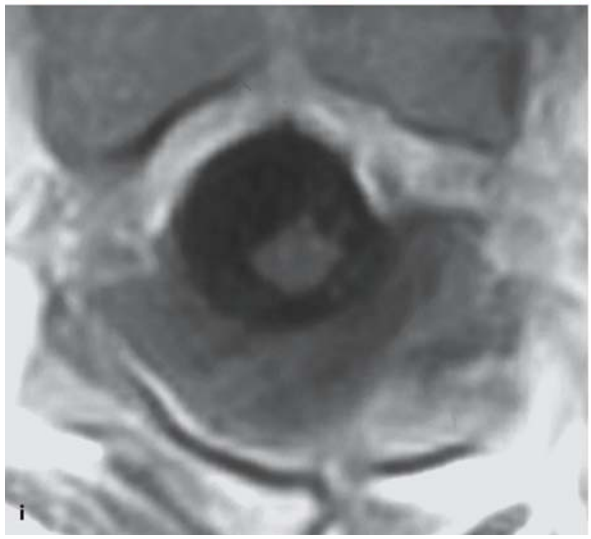

Fig. 5.85. (*Continued*) **g** The cord could be easily mobilized back into the subarachnoid space and the defect was closed with a small patch. The postoperative sagittal T2- (**h**) and axial T1-weighted MRI images (**i**) show a good decompression of the spinal cord with just a little fluid collection in the area of the former cyst. The patient's paraparesis and pain improved postoperatively, and there has been no recurrence for 2 years

order to plan surgery or as an intraoperative adjunct to visualize the effects of surgery distant from the direct surgical field. Amongst other pathologies, they had used it for surgery on an epidural and an intradural arachnoid cyst.

To date, almost nothing but case reports have been published. Charissoux et al. [113] carried out a literature review and found 186 published cases. Rabb et al. [439] described 11 children with arachnoid cysts, of which 2 were extradural. Krings et al. [302] reported seven patients with arachnoid cysts, of which five were extradural, and Kendall et al. [280] provided another six patients.

Epidural arachnoid cysts may extend over a significant number of spinal levels (Figs. 5.83 and 5.84) [186], occur at multiple sites [393], and erode bony structures (Figs. 5.85 and 5.86) [109, 280]. They may expand anywhere inside the spinal canal as well as to the extraspinal spaces [273]. Just like their intradural counterparts, they may be associated with syringomyelia, but in a smaller percentage [255].

We have seen 11 patients with epidural arachnoid cysts, of which 9 were operated. They presented after an average history of 38±45 months (range 5 months to 10 years) with a mean age of 35±18 years (range 12–67 years). The spinal distribution was evenly spread (Table 5.22). In five cases these cysts extended over a maximum of three spinal levels (Figs. 5.47 and 5.86), while extensions over more than four levels were seen in the remainder (Fig. 5.83–5.85), with the largest one extending from C3 to Th7 with an associated syrinx (Fig. 5.83).

Clinical symptoms were caused by cord compression, which may fluctuate according to the cyst pressure [309]. Some patients experience aggravation of neurological symptoms with coughing or Valsalva maneuvers [150]. Commonly, a slowly progressive myelopathy is observed. In their review, Charissoux et al. [113] found just 11% of patients complaining of back pain only.

Pain and gait ataxia were the commonest initial symptoms in four patients each, while the remainder

Table 5.22. Spinal epidural arachnoid cysts

Sex	Age (years)	Level	History (months)	Symptoms	Surgery	Outcome
F	67	L5/S1	6	Hypesth., Dysesth., Motor, Pain	Complete	Improved No Rec. in 115 months
F	14	Th5–7	12	Gait	Complete, Suture	Improved No Rec. in 32 months
F	36	S1–2	120	Hypesth., Pain	Complete	Improved Lost to follow up
F	12	Th10–L2	7	Hypesth., Motor, Gait, Pain	Complete, Muscle	Improved Lost to follow up
M	50	Th9–12	24	Hypesth, Motor, Gait, Pain, Sphincter	Fenestr., Patch	Improved No Rec. in 18 months
M	30	Th8–12	9	Hypesth., Motor, Gait	Complete, Patch	Unchanged Rec. in 8 months
M	18	C4–7	5	Hypesth., Motor	Complete, Muscle	Unchanged Lost to follow up
M	28	C7–Th1	24	Hypesth., Motor, Gait	Complete, Suture	Improved No Rec. in 8 months
F	46	C3–Th7	120	Hypesth., Motor, Gait	Fenestr., Muscle	Improved No Rec. in 13 months

Abbreviation: Fenestr. = fenestration

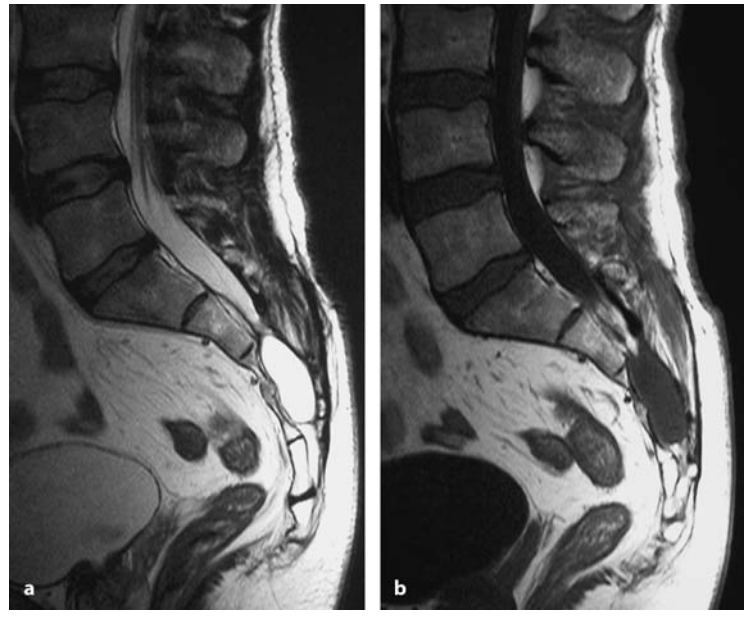

Fig. 5.86. Sagittal T2- (**a**) and T1-weighted (**b**) MRI scans of a sacral epidural arachnoid cyst in a 45-year-old patient with a 6-month history of sphincter problems and loss of erection. The cyst content below S2 has a slightly different signal intensity compared to CSF. (*Continuation see next page*)

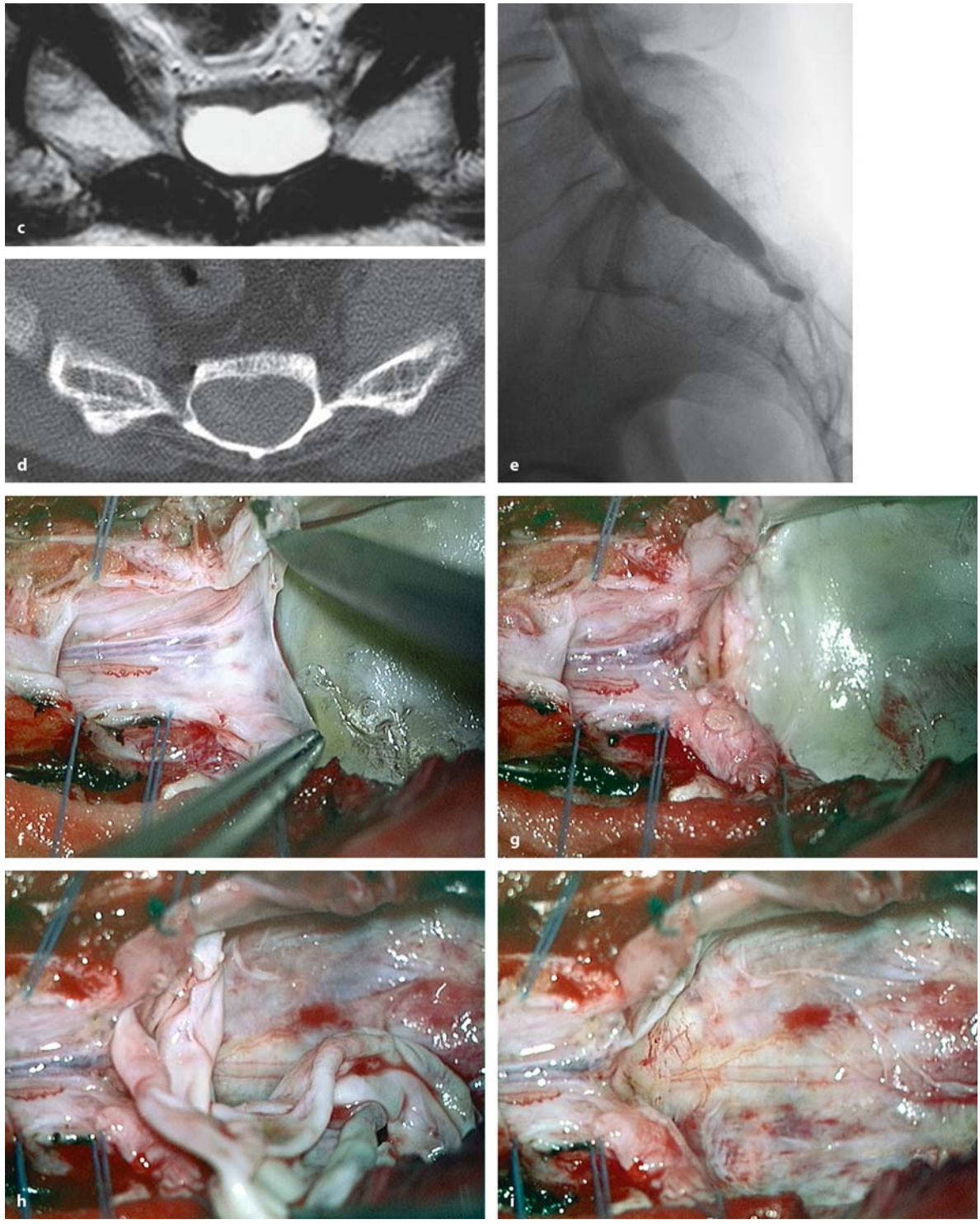

Fig. 5.86. The axial T2-weighted MRI (**c**) and bone-window CT images (**d**) show the enormous widening of the sacral canal. **e** The myelogram demonstrates no communication between the cyst and subarachnoid space. **f** This intraoperative view shows the opened dura at S2 and the upper pole of the cyst wall. The cyst remained under full pressure despite opening the subarachnoid space. A membranous structure connected to the dura is dissected off the cyst wall to expose the interface between the subarachnoid space and cyst. **g** No connection between the subarachnoid space and cyst was detectable. **h** The cyst has been opened and the wall mobilized off the surrounding bone and soft tissue. **i** This view demonstrates the situation after complete removal of the cyst. (*Continuation see next page*)

Fig. 5.86. (*Continued*) The dura was closed and the sacral space filled with muscle (**j**) and fibrin glue (**k**). The patient's symptoms completely disappeared postoperatively. Unfortunately, some of the problems reappeared 8 weeks after the operation. The postoperative sagittal T2- (**l**), and T1-weighted MRI scans without (**m**) and with contrast (**n**) and the axial scan (**o**) all show no evidence of the sacral cyst 3 months after surgery. The residual space in the sacral canal is filled with granulation tissue

reported motor weakness and dysesthesias as the initial signs. At presentation, 89% complained about sensory deficits, 78% about motor weakness, 67% about gait ataxia, 44% about pain, and 11% each about dysesthesias or sphincter problems. However, gait problems and pain were still the two major complaints for most of them [280].

Treatment requires foremost closure of the dura defect [113, 246, 286, 302, 493]. It is not necessary to expose or to resect the entire cyst (Figs. 5.83 and 5.84) [109, 246]. In rare instances, the cord itself may herniate into this dura defect (Figs. 5.10 and 5.85) [118, 256, 307, 355, 357, 377, 406, 425]. The commonest localization for this defect, particularly in posttraumatic cases, is along a root sleeve (Figs. 5.47, 5.83, and 5.84) [374]. The dura defect may be closed from the extradural side (Figs. 5.47 and 5.83) or intradurally (Fig. 5.84).

Radiological examinations must demonstrate the communication adequately so that surgery can be planned accordingly. The defect can only rarely be closed with suturing. The dura around the defect is often thinned and hypoplastic so that sutures are bound to fail. A better alternative is a combination of muscle and fibrin glue (Figs. 5.47, 5.83, 5.84, and 5.86). In the thoracic spine, dura defects along a nerve root may be clipped, sacrificing the nerve root. Rarely, a duraplasty is required (Fig. 5.85).

While a complete cyst resection was done only for small epidural cysts, the dural defect was sutured in two patients and closed with muscle and fibrin glue in three instances, and with a dura patch in two patients. In two instances, no communication was identified after removal of the cyst.

Postoperative results after surgery have been favorable [109, 113, 150, 160, 186, 225, 246, 252, 377, 425, 437, 493]. The patients of this series were followed for up to 10 years (mean 19±35 months). Within the first postoperative year improvements were observed for each preoperative symptom. However, the small number of patients prevented a statistically significant effect. The Karnofsky score did improve significantly from 78±5 to 88±10 ($p<0.05$). We observed a single recurrence after 8 months in a patient with a thoracic cyst, in whom the dura defect had been closed with a dura patch.

5.5.1.4 Soft-Tissue Sarcomas

The majority of epidural soft-tissue sarcomas are metastases from other primary sites so that oncologic resections are not warranted. In a recent study, radiotherapy of metastatic soft-tissue sarcomas resulted in small improvements for pain and Karnofsky score, with a median survival time of 5 months [369]. However, soft-tissue sarcomas can also evolve in the spine primarily and have been described after radiotherapy, for instance [23].

Table 5.23. Spinal soft-tissue sarcomas

Histology	Sex	Age (years)	Level	History (months)	Symptoms	Surgery	Outcome
Fibros.	F	71	L5–S3	3	Hypesth., Motor, Gait, Pain	Subtotal	Worse Dead within 14 months
Rhabdomyos.	F	71	Th2–9	5	Hypesth., Motor, Gait, Pain, Sphincter	Partial	Unchanged Dead within 1 month
Fibros.	M	53	L5	4	Hypesth., Motor, Gait, Pain	Subtotal	Improved Lost to follow up
Lipos.	M	50	Th5–6	0.3	Hypesth., Gait, Pain	Complete	Improved Survival 52 months
		51	Th5–6	1	Hypesth, Gait, Pain	Complete	Unchanged
		52	C7	1	Hypesth., Dysesth., Gait	Complete	Improved
		52	Th9–11	1	Hypesth., Gait	Complete	Improved
		52	Th3–4	1	Hypesth., Dysesth., Motor, Gait	Complete	Unchanged
		53	Th3–4	4	Hypesth, Motor, Gait, Pain	Subtotal	Unchanged

Abbreviations: Fibros. = fibrosarcoma, Rhabdomyos. = rhabdomyosarcoma, Lipos. = liposarcoma

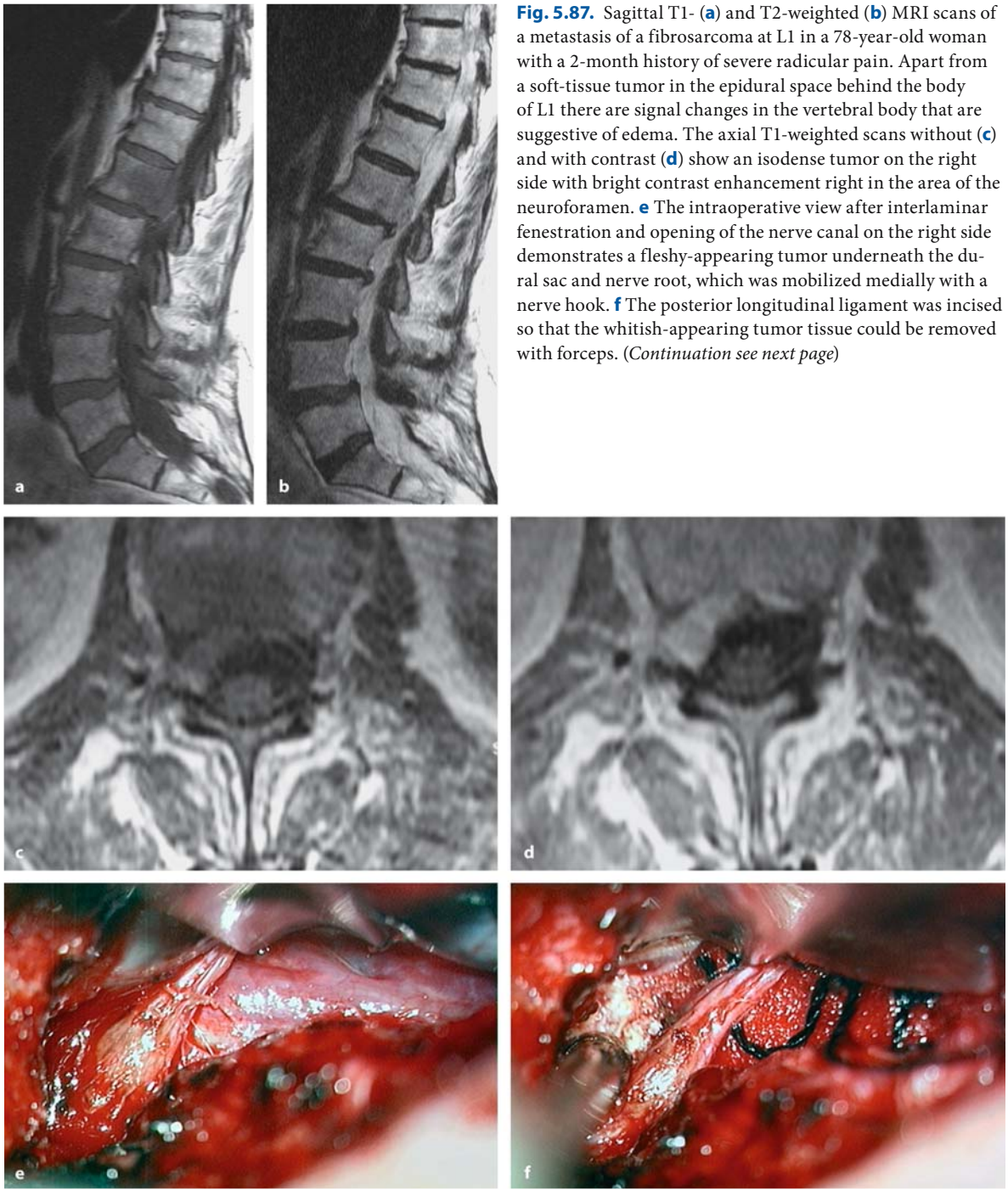

Fig. 5.87. Sagittal T1- (**a**) and T2-weighted (**b**) MRI scans of a metastasis of a fibrosarcoma at L1 in a 78-year-old woman with a 2-month history of severe radicular pain. Apart from a soft-tissue tumor in the epidural space behind the body of L1 there are signal changes in the vertebral body that are suggestive of edema. The axial T1-weighted scans without (**c**) and with contrast (**d**) show an isodense tumor on the right side with bright contrast enhancement right in the area of the neuroforamen. **e** The intraoperative view after interlaminar fenestration and opening of the nerve canal on the right side demonstrates a fleshy-appearing tumor underneath the dural sac and nerve root, which was mobilized medially with a nerve hook. **f** The posterior longitudinal ligament was incised so that the whitish-appearing tumor tissue could be removed with forceps. (*Continuation see next page*)

Fibrosarcomas are not sensitive to radio- or chemotherapy and can be considered as low-grade malignancies in most instances, even though further metastases and local recurrences are common [63, 123, 212, 473]. In a literature review, Chow et al. [123] calculated a recurrence rate of 48%, metastases in 60%, and a mortality rate of 35%. We encountered two fibrosarcomas that both developed primarily in the spine (Table 5.23). A 71-year-old woman presented with a large lumbosacral fibrosarcoma that was resected subtotally. The patient was in bad general health, did not receive any adjuvant therapy, and died 14 months after surgery. The other patient was 53 years of age and presented a 4-month history of pain and an incomplete paraplegia due to a fibrosarcoma at L1 with extension into the right intervertebral

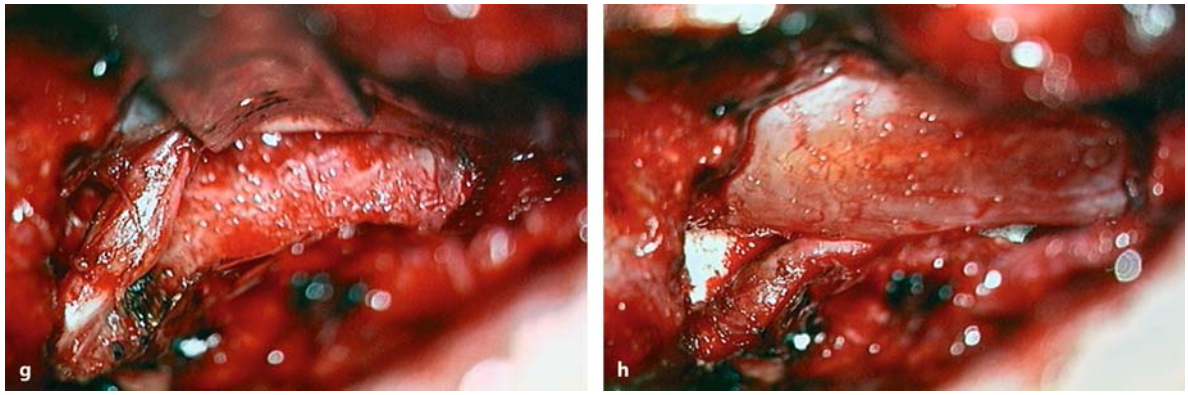

Fig. 5.87. (*Continued*) After complete resection (**g**) the tumor bed was filled with Gelfoam and the nerve hook removed (**h**). Postoperatively, the patient experienced immediate pain relief

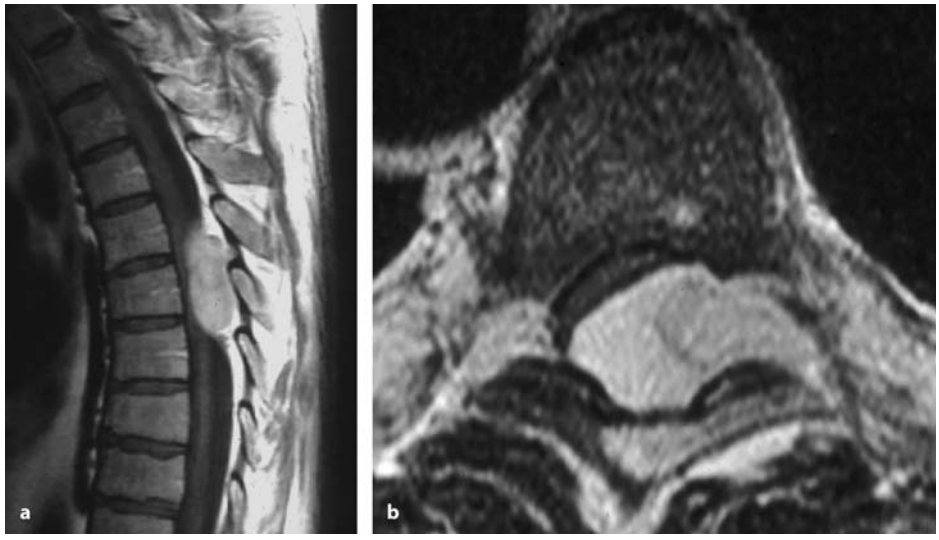

Fig. 5.88. **a** Sagittal T1-weighted MRI with contrast of a liposarcoma at Th5–Th7 in a 50-year-old patient with a rapidly progressive paraparesis. **b** The axial T1-weighted image demonstrates the tremendous compression of the spinal cord

foramen. After subtotal resection, the patient recovered and underwent local radiotherapy (Fig. 5.87).

A similar behavior is observed with liposarcomas, which tend to recur along the entire spinal canal [71, 544] and usually affect the spinal canal as secondary metastases [161, 285], as in the patient of our series (Table 5.23, Fig. 5.88): 13 years prior to presentation a liposarcoma had been resected from the right thigh, with two subsequent local recurrences 11 and 16 years after diagnosis. Despite postoperative radiotherapy, a metastasis was observed at Th5/6 7 months after the last operation on the primary tumor leading to pain and gait ataxia. The tumor was completely resected but not radiated afterwards. A local recurrence developed within 9 months. Again, a complete resection was obtained and local radiotherapy applied. Eight months later, two further epidural liposarcomas appeared at C7 and Th9–Th11, and another one at Th3/4 another 8 months later. Each time, postoperative radiotherapy was applied. A further recurrence at Th3/4 was resected another 9 months later. Chemotherapy with adriamycin was administered after this last spinal operation. During this period further metastases appeared in long bones of both thighs, left humerus, iliac bone, and sigmoid colon. With surgery and radiotherapy of these lesions, this patient retained his independency and a Karnofsky rating of 80 for the entire follow up period of 52 months since our first spinal intervention.

On the other hand, rhabdomyosarcomas carry a bad prognosis [188, 444] and tend to invade the spinal canal through the intervertebral foramen giving the

appearance of a dumbbell tumor [289]. They may invade and destroy bone causing pathological fractures [331]. Subarachnoid seeding has also been described [188, 195, 444, 463, 570]. In a series of ten patients with chest wall sarcomas spreading into the spinal canal, eight males and two females were observed at a median age of 3.5 years. Seven patients were disease free at latest follow up, while three patients had died [443].

In this series, a 71-year-old woman presented with an extensive epidural rhabdomyosarcoma at Th2–Th9 with severe pain, a profound paraparesis, and advanced cachexia. After incomplete resection of this very vascularized tumor the patient died 1 month later due to cardiac arrest (Table 5.23).

5.5.1.5 Cavernomas

Most spinal cavernomas are to be found inside the spinal cord. However, cavernomas may occur anywhere within the central nervous system [222], and on rare occasions have been described extradurally in the spinal canal. On MRI, they are isointense to spinal cord tissue on T1-weighted images and isointense to CSF on T2-weighted images. They enhance with contrast [18, 204, 308, 416, 461, 497, 529, 579]. Homogenous enhancement indicates absence of hemorrhages (Fig. 5.89), whereas a patchy enhancement is related to minor bleedings (Fig. 5.90) [18, 136, 416], which may be localized in the epidural space (Figs. 5.5, 5.89, and 5.90) or in the vertebral body with varying amounts of dura compression (Fig. 5.18) [4, 215, 222, 317, 382], and may even extend into the extraspinal space [4, 29, 46, 438].

Within our series, four cavernomas were observed in the epidural space. They presented at between 37 and 67 years of age after a history of 2–7 months. There were two lumbar cavernomas, one cervicothoracic, and one thoracic cavernoma. Pain was the predominating symptom for two of these patients, whereas motor weakness was the major problem in the other two. All but one had neurological symptoms. All cavernomas were removed completely (Table 5.24). Postoperatively, every symptom improved, with an increase of the Karnofsky score from 77±23 to 93±6 in the 1st year. However, due to the small number of patients, no statistical analysis was applied. No recurrences were observed for this entity, within a mean follow up of 65±22 months (maximum 7.5 years).

Aoyagi et al. [18] reported a personal case and reviewed the literature on 53 further patients with extradural cavernous hemangiomas. The majority were male (male:female ratio – 36:18) and had a mean age of 47 years (5–78 years). Of the cavernomas described, 80% were localized in the thoracic spine, with 93% oriented posteriorly. The typical clinical course was slowly progressive and somewhat different from that of intradural cavernomas, which tend to progress in a stepwise fashion related to multiple bleedings.

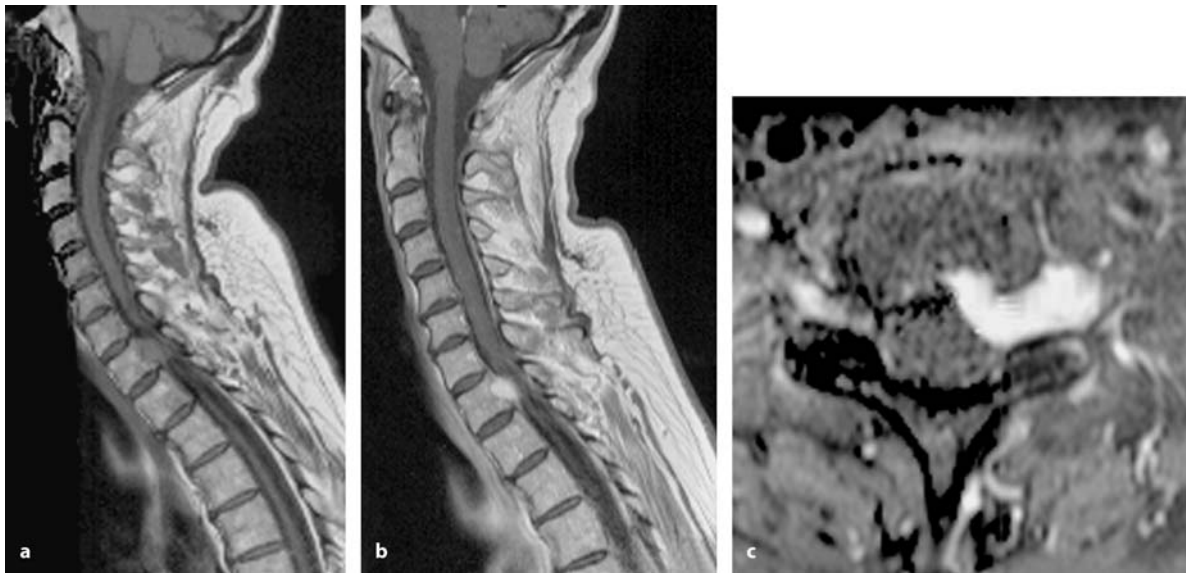

Fig. 5.89. Sagittal T1-weighted MRI scan without (**a**) and with contrast (**b**) of an epidural cavernoma at Th1 in a 70-year-old woman. **c** The axial scan demonstrates the extradural localization of this cavernoma that had expanded along the nerve root on the left side and into the vertebral body of Th1. The homogeneous contrast enhancement indicates no previous hemorrhage

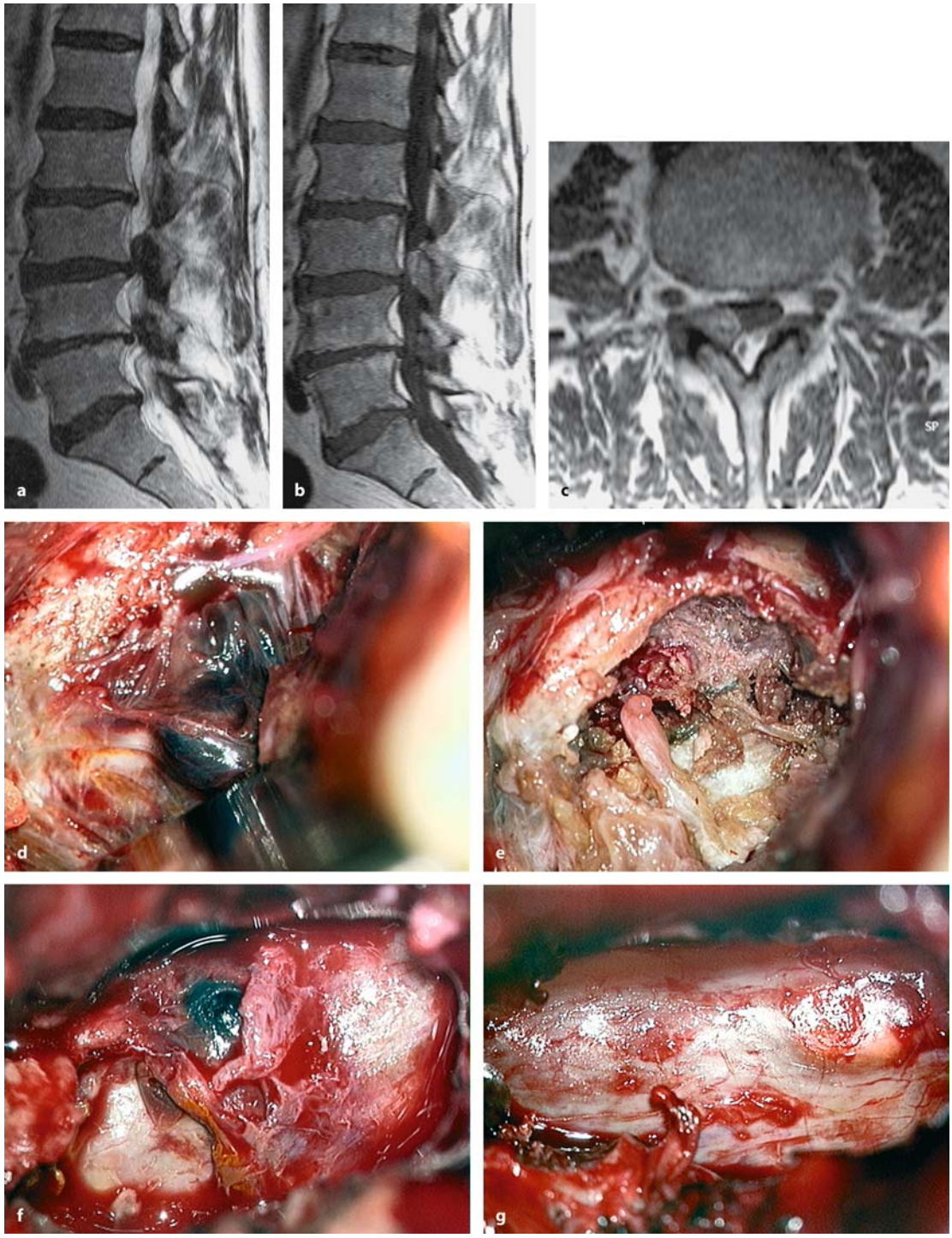

Fig. 5.90. Sagittal T2- (**a**) and T1-weighted MRI with contrast (**b**) of a cavernoma at L3 in a 73-year-old man with a 10-year history of sensory disturbances in his right leg and recent motor weakness and pain. **c** The axial image shows a contrast-enhanced, inhomogeneous lesion similar to a synovial cyst (see also Fig. 5.79). **d** The intraoperative image after interlaminar fenestration L3/4 on the right side demonstrates a dark vascular structure adherent to the dura surrounded by reactive soft tissue. **e** With coagulation and stepwise removal, different compartments of this lesion are encountered as a result of repeated minor hemorrhages. **f** This photograph shows the last part of the cavernoma adherent to the dura. **g** This final view shows the normal-appearing dura after complete resection. Postoperatively, neurological symptoms and pain improved

Table 5.24. Spinal epidural cavernomas

Sex	Age (years)	Level	History (months)	Symptoms	Surgery	Outcome
F	67	L4/5	5	Hypesth., Motor, Gait, Pain	Complete	Improved Lost to follow up
M	46	Th6–8	7	Hypesth., Dysesth., Motor, Gait, Sphincter	Complete	Improved No Rec. in 87 months
F	46	C4–Th6	6	Hypesth., Motor, Gait, Pain	Complete	Improved No Rec. in 43 months
M	37	L4	2	Pain	Complete	Unchanged No Rec. in 64 months

Guthkelch [215] described nine patients with epidural hemangiomas, four of which extended from a vertebral body into the epidural space, while the remaining five did not involve the bone. All but one patient presented with pain of several months duration. In one case, symptoms were precipitated by pregnancy.

Graziani et al. [204] described seven patients with neurological symptoms related to extradural cavernomas. Two patients demonstrated epidural hematomas, indicating that major hemorrhages may occur with this entity. Postoperative results were excellent.

Talacchi et al. [529] described five patients with epidural cavernomas. They emphasized that hemorrhages are less frequent with this localization compared to intramedullary cavernomas, for instance. Radical removal was achieved with good postoperative results.

Padovani et al. [417] reported five such lesions, of which three were located inside the vertebral body and two in the epidural space. One epidural cavernoma was resected completely, while the remainder were removed subtotally and radiated postoperatively. Zevgaridis et al. [579] contributed further three patients with good recovery after complete resections of their lesions, two of which had extended into a neuroforamen.

Hillman and Bynke [236] reported another five patients who presented with histories of repeated hemorrhages leading to neurological symptoms in four patients and just one patient with a slowly progressive course. One cavernoma extended into the thoracic cavity and was adherent to the pleura. All but one cavernoma was resected completely, with good neurological recovery in three patients.

5.5.1.6 Hamartomas

The overwhelming majority of spinal hamartomas occur intradurally. They may protrude through the dura into the epidural space. Purely extradural hamartomas of the spinal canal are rare. To be distinguished are patients with epidural lipomatosis [11], which is often related to corticosteroid therapy.

We have removed one extradural lipoma among our series of 329 extradural tumors. A 52-year-old patient complained about thoracic pain and dysesthesias due to an epidural lipoma between the 6th and 9th thoracic vertebra. With complete resection of the lipoma and reinsertion of the laminae, symptoms improved postoperatively.

5.5.1.7 Angiolipomas

Angiolipomas are rarely reported in the spinal canal. Most of them occur in the trunk and limbs. Two case reports described spinal angiolipomas in the thoracic spine [305, 421]. In both instances, metastatic disease had been suspected and the correct diagnosis was made histologically. Postoperative results have been excellent in these two patients.

The 61-year-old patient of our series presented with a 1-year history of a progressive paraparesis, rendering her unable to walk by the time of presentation. The vascularized tumor at Th6 was completely removed and the patient recovered walking within 3 months (Fig. 5.91).

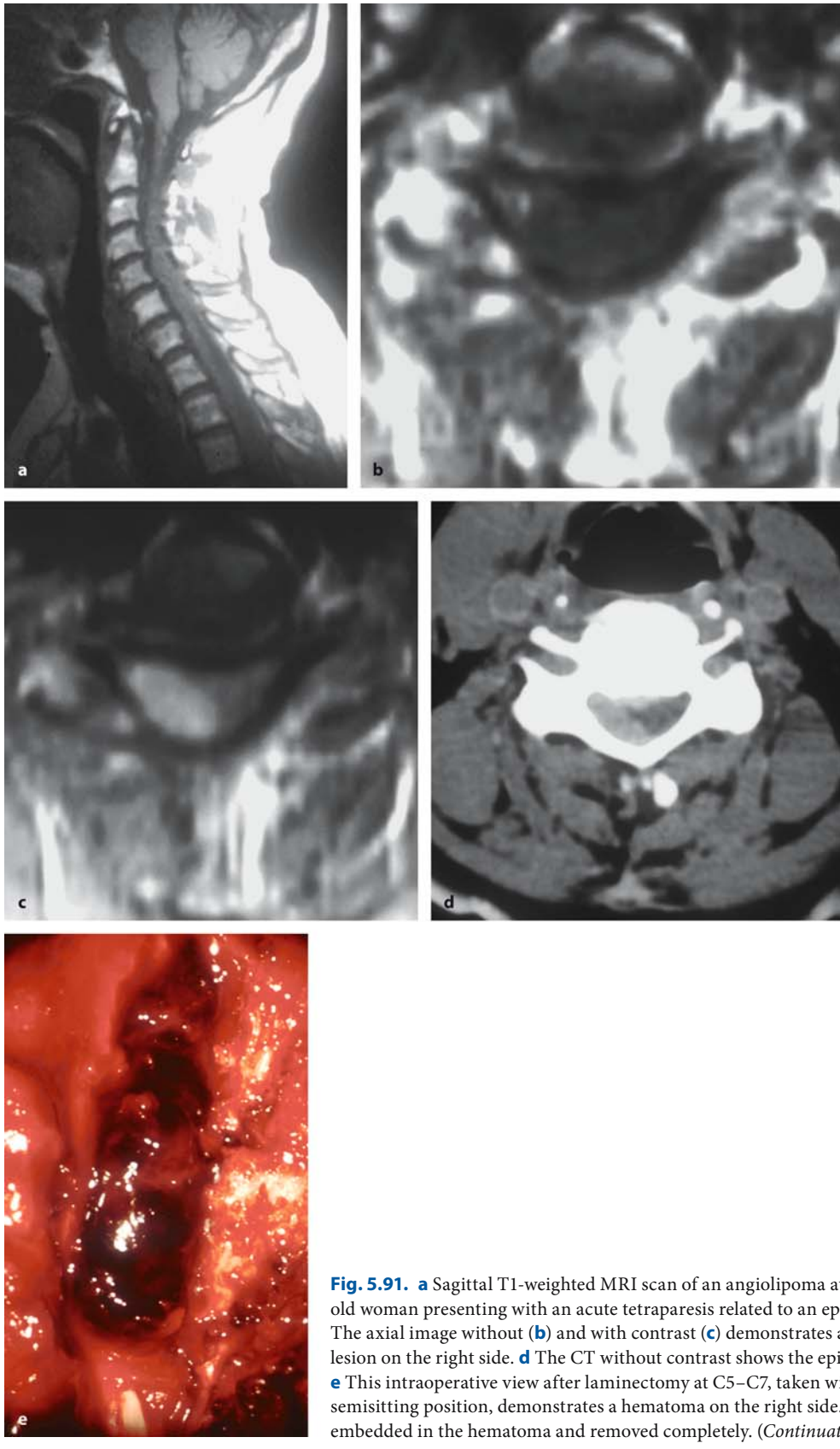

Fig. 5.91. **a** Sagittal T1-weighted MRI scan of an angiolipoma at C5–C7 in a 67-year-old woman presenting with an acute tetraparesis related to an epidural hemorrhage. The axial image without (**b**) and with contrast (**c**) demonstrates a contrast-enhancing lesion on the right side. **d** The CT without contrast shows the epidural hemorrhage. **e** This intraoperative view after laminectomy at C5–C7, taken with the patient in the semisitting position, demonstrates a hematoma on the right side. The tumor was embedded in the hematoma and removed completely. (*Continuation see next page*)

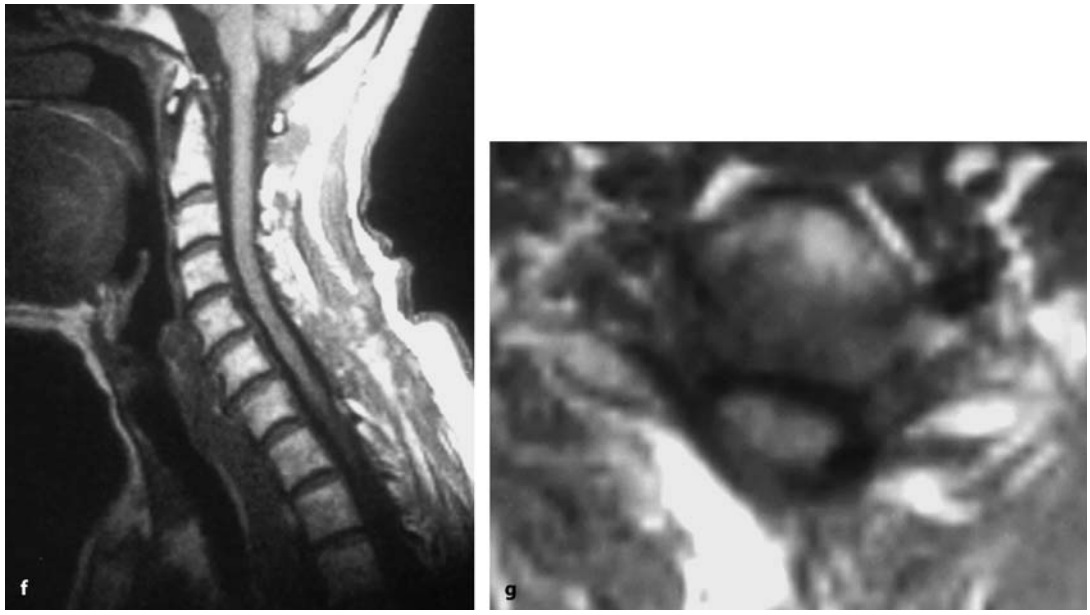

Fig. 5.91. (*Continued*) The postoperative sagittal (**f**) and axial (**g**) MRI scans show the complete resection of this tumor. Postoperatively, the patient made an incomplete recovery

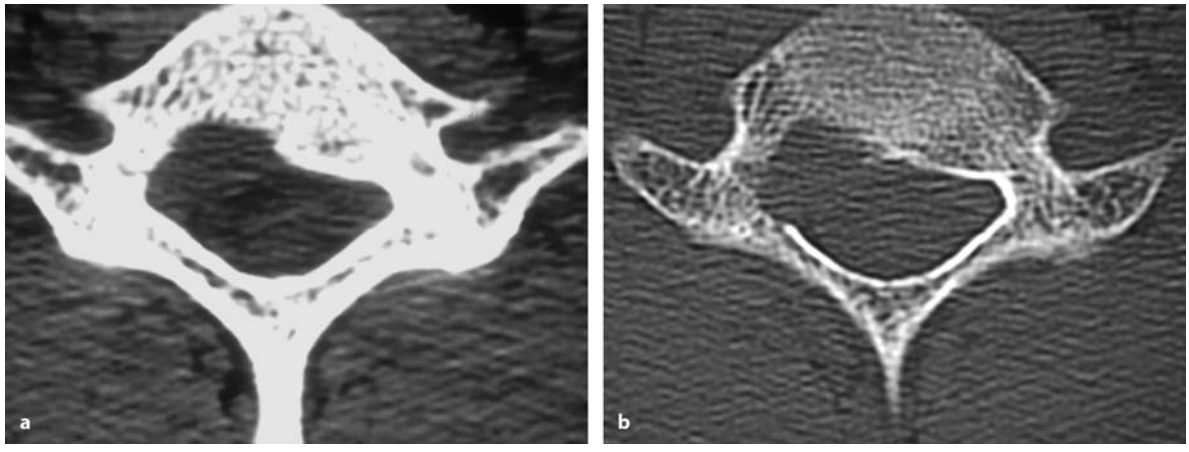

Fig. 5.92. These native (**a**) and bone-window CT images (**b**) demonstrate an epidural tumor at C6–C7 in a 48-year-old patient with a 1-month history of dysesthesias, radicular neurological deficits, and pain. The tumor is isodense and erodes the vertebral body. The quite vascular tumor was removed completely and diagnosed as a hemangiopericytoma. Postoperatively, no neurological improvements were noted except for the sensory deficits. The patient received no postoperative radiotherapy and has been free of recurrence for 3 years

5.5.1.8 Hemangiopericytomas

Hemangiopericytomas – formerly known as angioblastic meningiomas – are highly vascularized tumors that may occur in the spinal canal primarily or as metastases from intracranial tumors [16, 306, 400, 468, 484]. Spinal hemangiopericytomas may be localized in the vertebral body or be more commonly attached to the meninges [325]. One patient was described presenting with a Pancoast tumor that turned out to be a hemangiopericytoma [122].

The radiological features are indistinguishable from other neoplastic pathologies. They brightly enhance with gadolinium on MRI. Due to their vascularization, preoperative embolization may be helpful [124, 387, 390].

In a study on 94 hemangiopericytomas of the entire nervous system, Mena et al. [367] determined me-

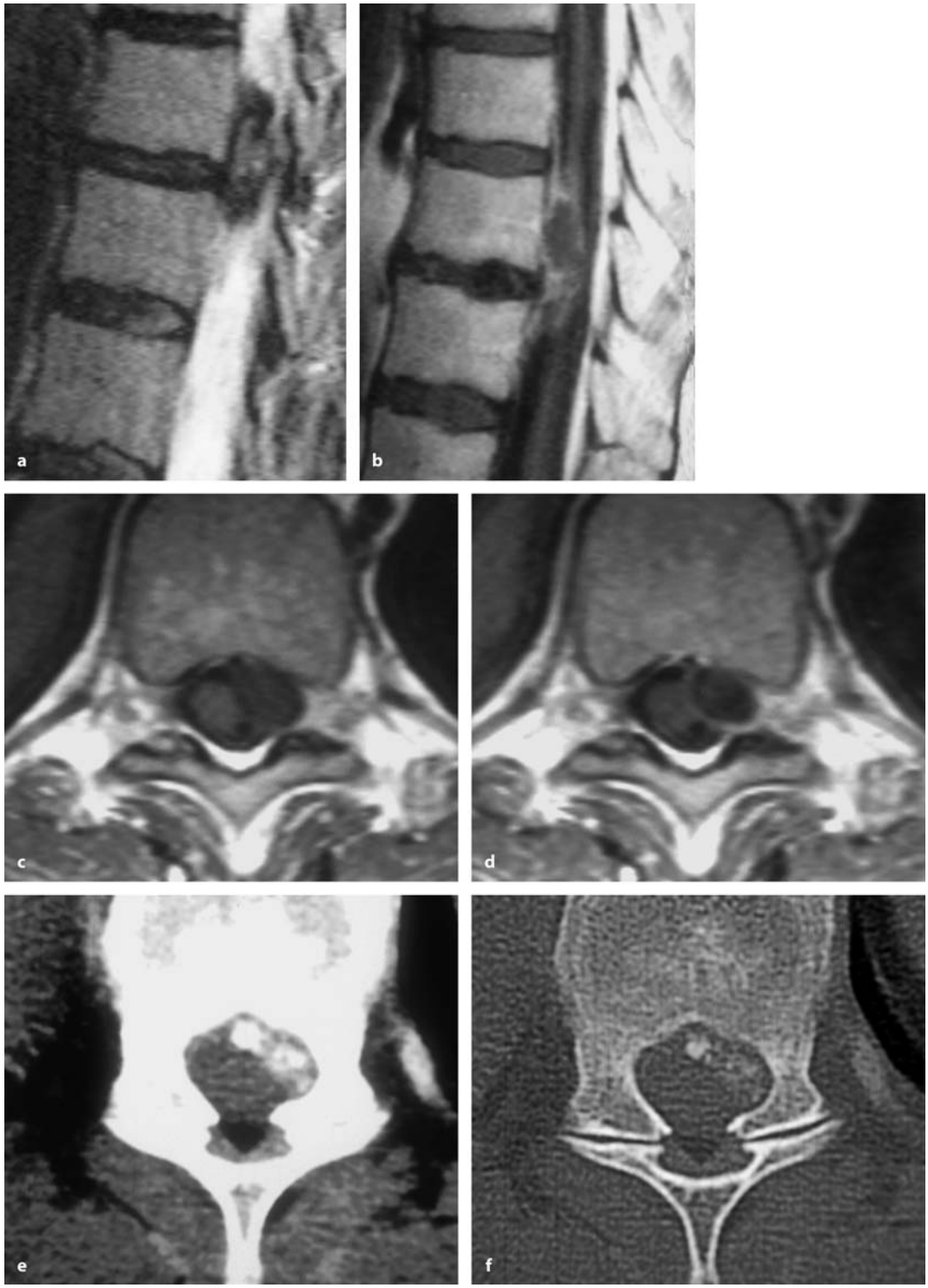

Fig. 5.93. Sagittal T2- (**a**) and T1-weighted MRI contrast-enhanced scans (**b**) of a lesion at Th10–Th11 in a 55-year-old man with a 3-month history of pain and dysesthesias. On T2, the tumor appears like a cyst with an isodense center and a hypodense capsule. On T1, the capsule enhances contrast and there is no sharp demarcation towards the surrounding tissue. The axial T1-weighted images without (**c**) and with contrast (**d**) demonstrate the tumor with a hypodense center in the neuroforamen on the left side. Native (**e**) and bone-window CT images (**f**) display calcifications but no reactive bone changes. (*Continuation see next page*)

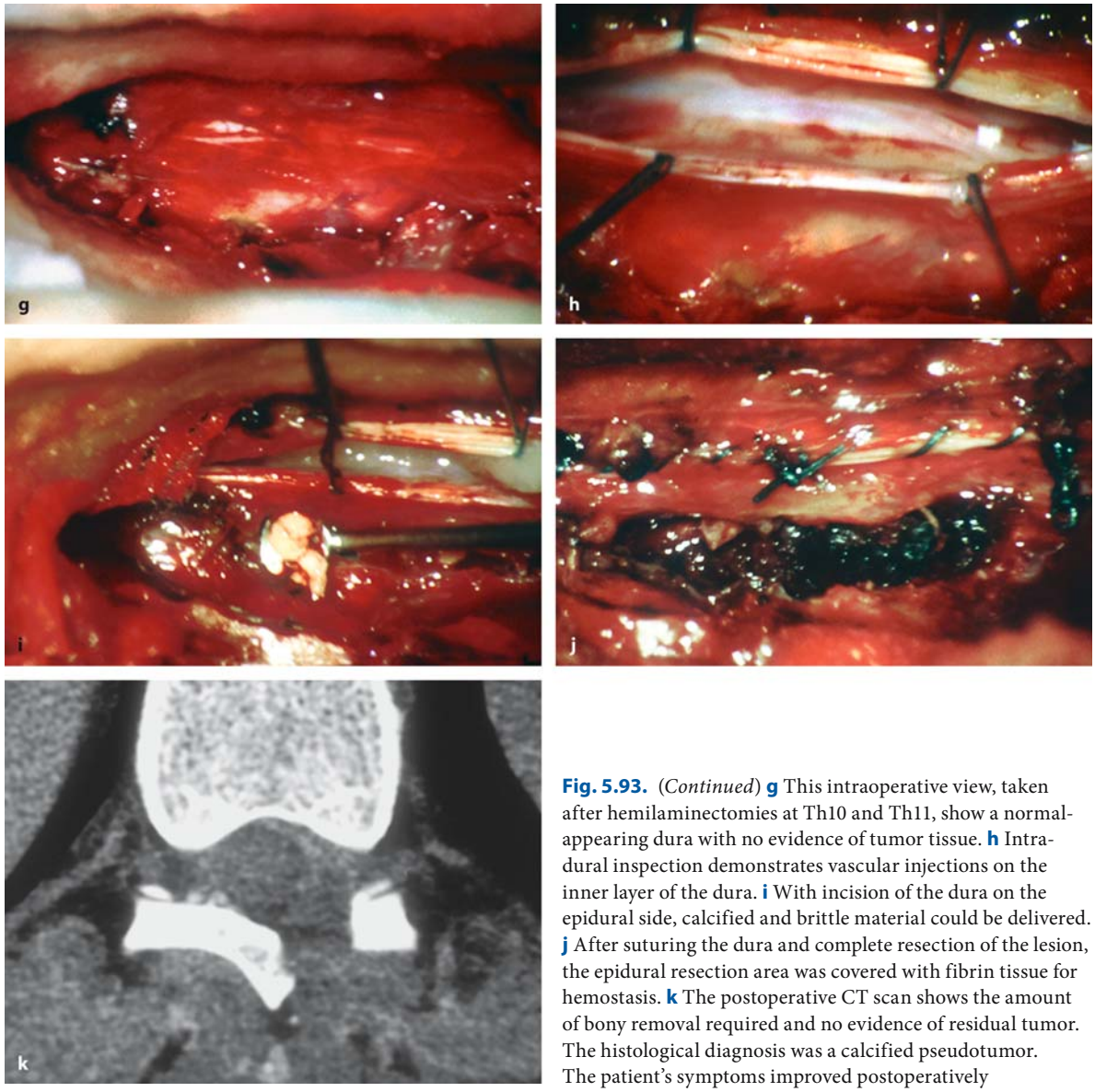

Fig. 5.93. (*Continued*) **g** This intraoperative view, taken after hemilaminectomies at Th10 and Th11, show a normal-appearing dura with no evidence of tumor tissue. **h** Intradural inspection demonstrates vascular injections on the inner layer of the dura. **i** With incision of the dura on the epidural side, calcified and brittle material could be delivered. **j** After suturing the dura and complete resection of the lesion, the epidural resection area was covered with fibrin tissue for hemostasis. **k** The postoperative CT scan shows the amount of bony removal required and no evidence of residual tumor. The histological diagnosis was a calcified pseudotumor. The patient's symptoms improved postoperatively

tastases at a rate of 23.4%. Hemangiopericytomas are prone to local recurrences regardless of their localization [56]. Therefore, en bloc resection should be considered where possible [56] and most authors regard postoperative radiotherapy as essential [9, 75, 124, 209, 221, 367, 387], whereas the role of chemotherapy is not fully established. However, after complete resections, long disease-free intervals have also been reported without postoperative radiotherapy [247, 325].

In the patient of this study, a 48-year-old man presented with a 3-week history of dysesthesias, pain, and slight motor weakness of the right arm due to an extradural tumor in the neuroforamen of C6/7 extending into the vertebral body of C7 (Fig. 5.92). After complete resection of the tumor no radiotherapy was administered. The patient's symptoms improved with no evidence of a recurrence for 3 years.

5.5.1.9 Calcified Pseudotumors

This entity is a rare space-occupying lesion of the meninges that is characterized by an infiltrate of histiocytes, plasma cells, and lymphocytes. Two case reports described thoracic lesions that had led to myelopathy [153, 375]. The etiology is unclear. It has been speculated that they resemble plasma cell granu-

lomas or an immune response related to a meningioma [375]. The 55-year-old patient in this series harbored this lesion at the level of Th10/11 and presented with radicular pain and dysesthesias of 3 months duration. The process was located between both dura layers and resected completely (Fig. 5.93). Postoperatively, symptoms recovered.

5.5.2 Bone Tumors

5.5.2.1 Metastases

At autopsy, up to 70% of cancer patients demonstrate spinal metastases [294, 426, 427]. However, it is estimated that only 5–10% of them actually cause symptoms [261, 426, 427]. However, once local tenderness and pain occur, up to 80% will develop neurological deficits within 2 months [230]. In the United States, 12,700 patients are compromised by metastatic spinal cord compression each year [3]. The commonest primary sites are breast, lung, and prostate, which account for about 50% of the total [6, 27, 263, 294]. Almost every metastasis produces severe local pain at the beginning of spinal manifestation [27, 28, 37, 70, 74, 220, 347, 426, 427, 506, 520]. Especially in patients with known cancerous disease, local pain should lead to an immediate examination of the affected spinal area. In a study of 317 consecutive patients with back pain and a history of cancer, spinal imaging detected metastases in 157 patients [578]. Even though MRI has proven to be particularly valuable in establishing the diagnosis and possible extension of the metastasis into neighboring soft tissues [127] and is considered as sensitive and more specific than scintigraphy [541], conventional plain X-rays will already show the metastasis in a significant number of cases (Figs. 5.39, 5.50, and 5.57) [426, 436].

The treatment of patients with spinal metastases has been, and still is, discussed quite controversially. A considerable number of studies recommend radiotherapy for this group of patients and reserve surgery for patients with unknown primary tumor, failed radiotherapy, or spinal instability. They claim that surgery followed by radiotherapy does not offer any additional benefit compared to radiotherapy alone [74, 166, 171, 198, 203, 266, 288, 347–350, 354, 412, 427, 577]. Even prophylactic radiation of the spine has been advocated [30]. Radiotherapy studies report average survival times of 2.3 months [28], 3.6 months [288], 5 months [577], 6 months [347], and 7 months [348], or give percentages of 30% [28, 198] or 45% of cases [277] surviving 1 year. The study by Katagiri et al. [277] distinguished between responders and nonresponders of radiotherapy with corresponding 1-year survival rates of 76% and 16%, respectively. Zaidat and Ruff [578] reported results of 139 patients undergoing radiotherapy and distinguished between ambulatory and nonambulatory patients. The former lived for an average period of 104 months while the latter had a mean survival of just 6 weeks after treatment. Maranzano et al. [349] gave an overall figure of 55% surviving 1 year for a series of 61 patients; however, they excluded five early fatalities from their analysis. In a final paper, 255 patients received radiotherapy alone; 25 early deaths were taken out of the analysis and a survival rate of 28% for 1 year was reported [347]. From our point of view, such early fatalities can not be eliminated from such an analysis. Including them would lead to considerably lower survival rates.

Studies claiming that surgery does not offer an additional benefit except for selected cases refer to an outdated surgical concept of pure posterior decompression by laminectomy. As most spinal metastases originate in the vertebral body, a posterior approach may be sufficient to decompress the dural sac. However, the anterior tumor is not addressed and combined with disruption of posterior spinal elements, there is a considerable risk for postoperative kyphosis, instability, and cord compression. Sherman and Waddell [492] compared 111 patients treated with a pure laminectomy to 23 patients with posterior decompression and fusion. Both groups of patients were similar in terms of preoperative status. Patients undergoing additional fixation had better ambulatory status, pain control, and sphincter function. Additional radiotherapy had no significant influence on these differing outcomes.

Surgery for spinal metastases has changed considerably in recent years, with a better understanding of spinal biomechanics and introduction of new reconstructive and stabilization techniques. Several authors [27, 28, 196, 312, 500, 512, 518, 520, 561] concluded that surgery followed by radiotherapy gives superior results compared to radiotherapy alone in terms of neurological outcome and survival. Furthermore, the rate of complications was found to be higher if surgery was employed as the second line of treatment. Sundaresan et al. [512, 520] emphasized the high rate of complications and a considerably shorter survival for patients who were operated after they had received radiotherapy compared to those who first underwent surgery. Ghogawala et al. [196] reported a complica-

tion rate of 32% for patients undergoing surgery after radiotherapy as compared to 12% for those operated primarily. In terms of functional outcomes, this study found a higher percentage of patients keeping their self ambulatory status in the surgical as compared to the radiotherapy group for 30 days (75% and 50%, respectively). In another recent study, patients were randomized to either undergo decompressive surgery and stabilization followed by radiotherapy or radiotherapy alone. The trial had to be stopped after 101 patients because an interim analysis at midpoint already demonstrated significant functional advantages for surgically treated patients. A higher percentage of patients undergoing surgery regained the ability to walk (56% and 19%, respectively), retained walking ability longer (126 and 35 days, respectively), required less analgesics, and maintained continence and functional grades longer compared to radiated patients. Survival times, however, were equal in both treatment groups [447].

It is obvious that treatment for a systemic, malignant disease has to be tailored individually to each patient [90, 95]. A wide spectrum of surgical options for spinal metastases exist: for posteriorly located metastases a purely posterior approach and tumor removal is sufficient and no additional measures for stabilization are generally required (Fig. 5.48). For the great majority, however, the major problems are anterior compression of the spinal cord and either imminent or already present instability of the affected spinal segment. Almost always, decompression of the spinal cord in these settings has to be combined with stabilization techniques, which also have to involve some form of vertebral augmentation or reconstruction in the majority of patients. This may be done purely from the anterior approach – if posterior elements are intact – (Figs. 5.50, 5.53, and 5.58) or purely from the posterior approach, using either cages (Fig. 5.52), PMMA (Figs. 5.94 and 5.95), or intraoperative vertebroplasty (Figs. 5.59 and 5.96) for anterior support. In specific settings, such as the cervicothoracic (Figs. 5.60 and 5.97) and thoracolumbar region (Fig. 5.54), a combined anterior and posterior approach may be required to provide sufficient stability for patients with a comparably good prognosis.

Even en bloc resection of entire vertebrae with reconstruction and fusion using combined approaches as the maximal procedure are advocated by some authors [536, 573]. It seems that surgery for spinal metastases has gone from one extreme – just a laminectomy for decompression – to the other, with studies even suggesting cure of the metastatic disease with aggressive surgical regimens [573]. In the same article, however, long-term results are equal to more conservative strategies, with 15–20% of patients in good preoperative condition surviving 5 years [573]. With more than 80% dying of the disease during follow up, we suggest refraining from such terms as “cure” or “radical resections” when dealing with spinal metastases, which always represent a disseminated disease process. We are treating patients who suffer a systemic and consuming disease that will finally be fatal. Treatment of a particular local problem will hardly ever change the patient’s life expectancy.

Further alternatives, which have been introduced recently, incorporate minimally invasive techniques such as endoscopic approaches [66] or the injection of bone cement into cancerous vertebrae (i.e., vertebroplasty) [36, 177, 262, 356, 433]. Using inflatable balloons, even a restoration of vertebral body height, a so-called kyphoplasty, can be achieved [189]. These modalities are associated with a complication rate of around 10% [433] and are suitable for patients with severe pain but no instability, who are poor candidates for surgery. Jang and Lee [262] used a combination of vertebroplasty and radiotherapy for osteolytic spinal metastases. All 28 patients showed evidence of vertebral body collapse or movement-induced local pain but no neurological symptoms. Follow up ranged from 3 to 15 months, with good pain relief and no patient developing further instability.

Some authors have tried to provide criteria to select the right therapy regimen for a particular patient with a spinal metastasis. The aforementioned grading of Enneking [157] and the scoring systems of Tokuhashi et al. [534] and Tomita et al. [538] offer classifications that can be transformed into particular treatment schemes. Tomita et al. [538] differentiate between slowly, moderately, and rapidly growing metastases and consider the presence of visceral and multiple bone metastases to determine a score, which translates into treatment goals of long-term local control (requiring a wide or marginal excision), middle-term local control (requiring marginal or intralesional excision), or short-term palliation with palliative surgery or terminal care. A series of 61 patients who were stratified in this manner has been reported. Twenty-eight patients were treated with wide or marginal excisions, with a mean survival of 38.2 months and 26 patients achieving local control. Thirteen patients underwent intralesional surgery and survived an average period of 21.5 months, with 9 successful local controls. Eleven patients underwent palliative surgery, with a mean survival of 10.1 months and 8 successful local controls. Nine patients treated with supportive care had a mean survival of 5.3 months.

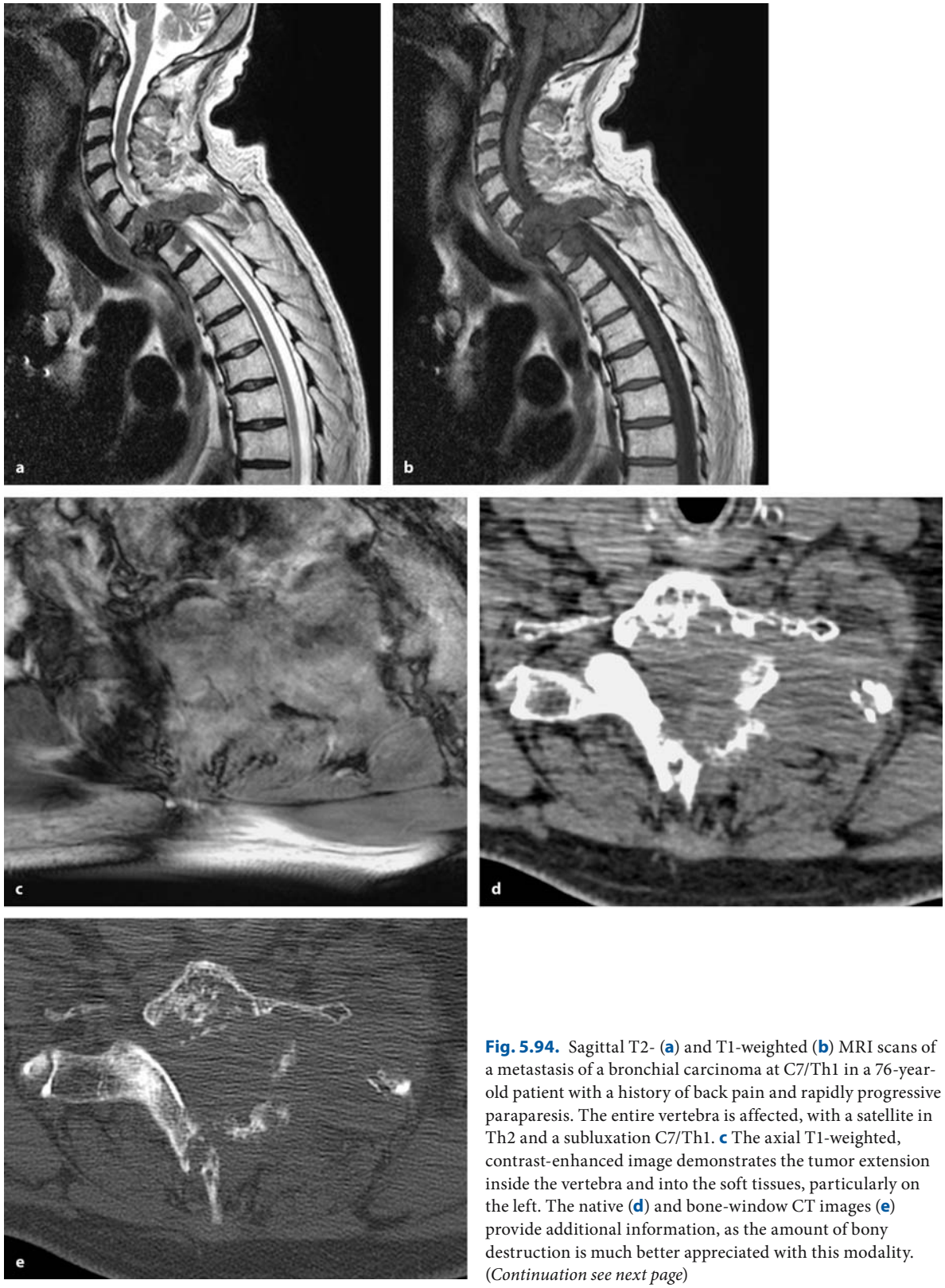

Fig. 5.94. Sagittal T2- (**a**) and T1-weighted (**b**) MRI scans of a metastasis of a bronchial carcinoma at C7/Th1 in a 76-year-old patient with a history of back pain and rapidly progressive paraparesis. The entire vertebra is affected, with a satellite in Th2 and a subluxation C7/Th1. **c** The axial T1-weighted, contrast-enhanced image demonstrates the tumor extension inside the vertebra and into the soft tissues, particularly on the left. The native (**d**) and bone-window CT images (**e**) provide additional information, as the amount of bony destruction is much better appreciated with this modality. (*Continuation see next page*)

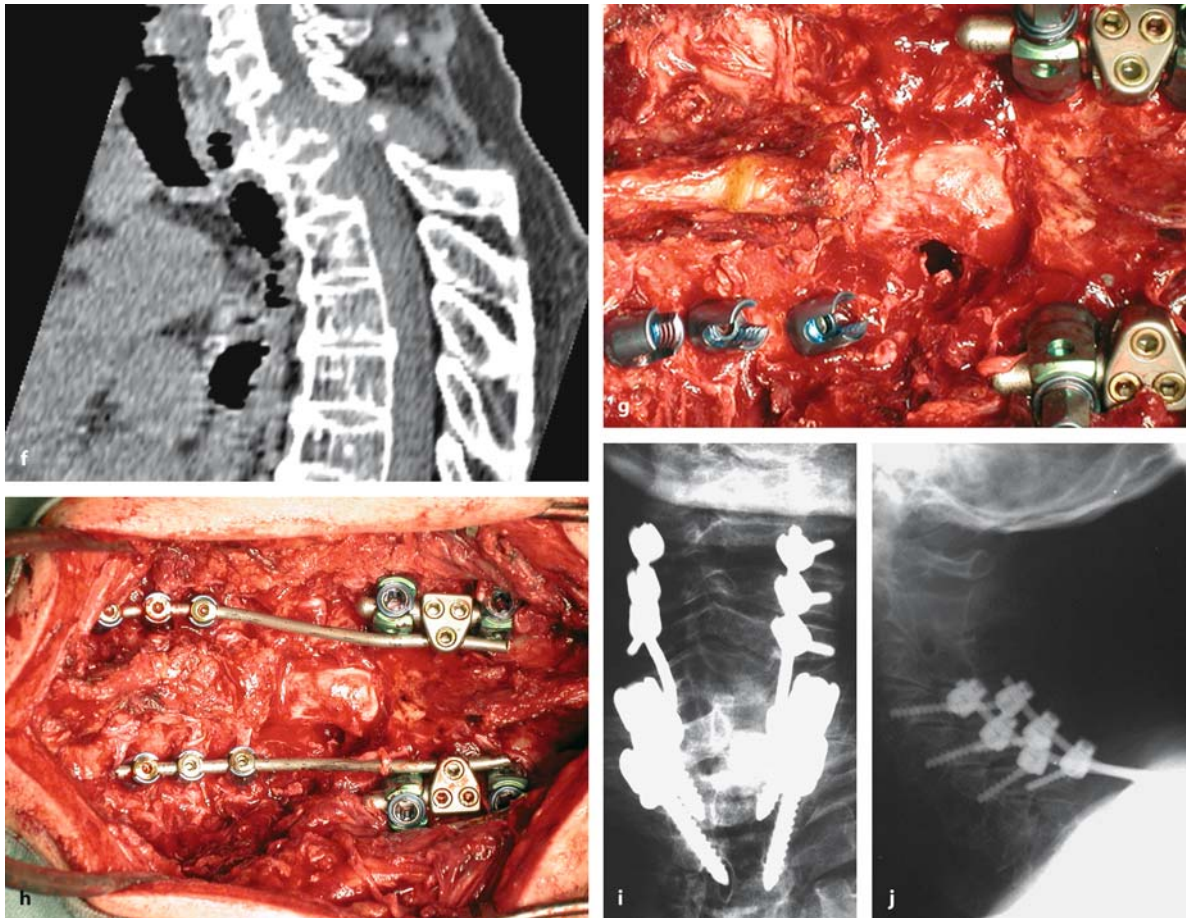

Fig. 5.94. (*Continued*) **f** The sagittal reconstruction demonstrates the C7/Th1 luxation with narrowing of the spinal canal. **g** This intraoperative view shows the situation after laminectomy C7 and transpedicular resection of part of the vertebral body at C7 from the left side after some lateral mass screws in the cervical and transpedicular screws in the thoracic spine had already been placed. **h** The final intraoperative photograph demonstrates the posterior fixation between C4 and Th3 after filling the vertebral defect with PMMA. The postoperative anterior–posterior X-ray (**i**) shows the position of the screws and the PMMA, while the lateral view (**j**) indicates a reasonable realignment at the cervicothoracic junction. The patient experienced a remarkable neurological recovery

Combining all surgically treated patients, 74% experienced postoperative neurological improvement. However, as the rates of local control are similar among all subgroups, these data also show that local control is not primarily related to the amount of resection, but to the biological behavior of the particular cancer.

Tokuhashi et al. [534] considered the patient's general condition, the number of extraspinal bone metastases, the extent of vertebral involvement, the presence of epidural or paravertebral extension, the number of spinal metastases, the number of metastases to other organs, the primary site, and the severity of neurological compromise to calculate a score. This score allowed prediction of the prognosis of the patient. Based on this score, the authors selected 64 patients to either undergo excisional or palliative operations.

It was the general policy in our series to offer surgery as primary treatment if neurological deficits or spinal instabilities were present, or the primary tumor was not known, provided the general health status allowed surgery. Furthermore, surgery was indicated after radio- or chemotherapy had failed to control a metastasis. On the other hand, radiotherapy, or chemotherapy if applicable, were recommended for patients in bad health condition and for patients without neurological deficits or instabilities. No surgery was undertaken in cases where there was com-

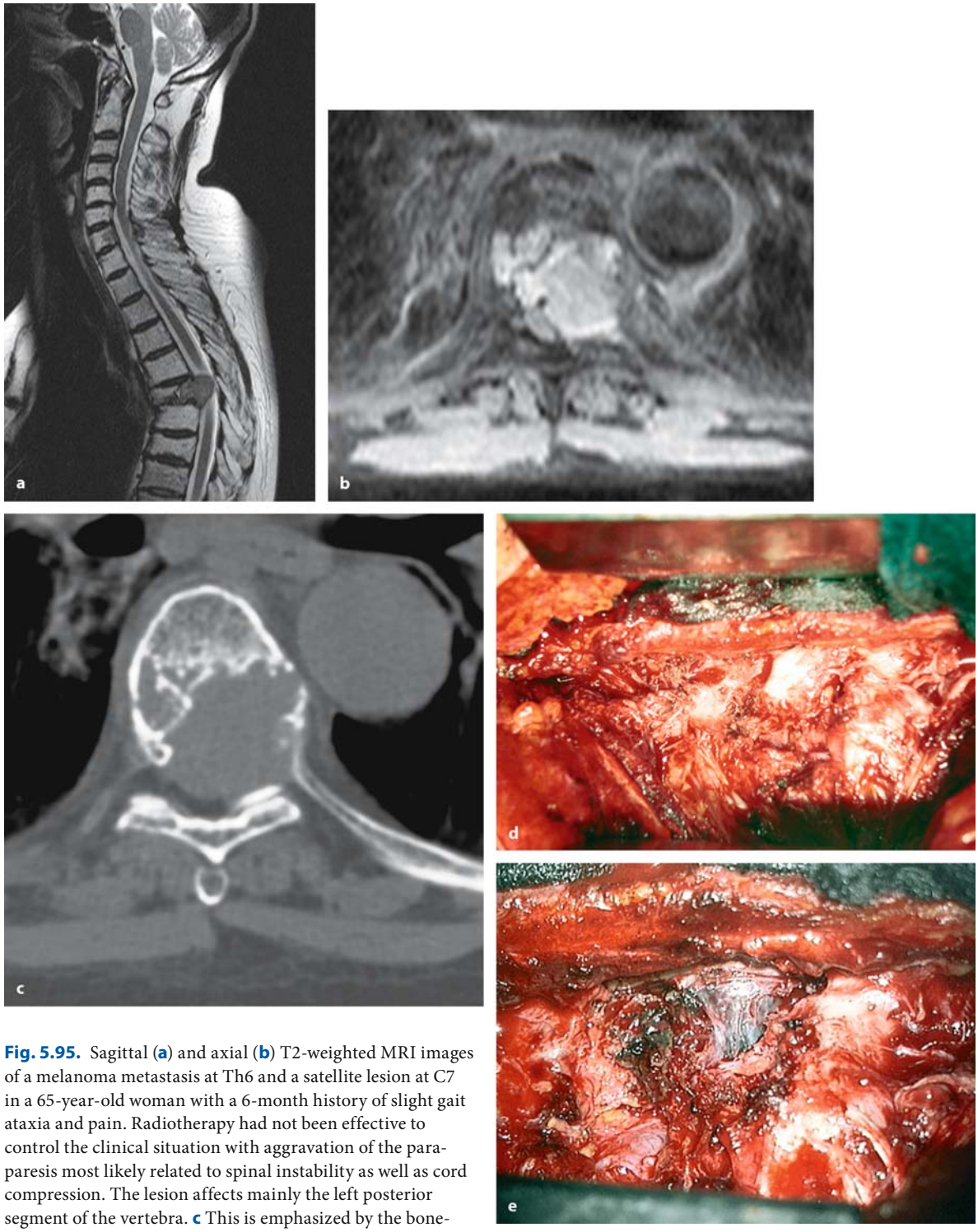

Fig. 5.95. Sagittal (**a**) and axial (**b**) T2-weighted MRI images of a melanoma metastasis at Th6 and a satellite lesion at C7 in a 65-year-old woman with a 6-month history of slight gait ataxia and pain. Radiotherapy had not been effective to control the clinical situation with aggravation of the paraparesis most likely related to spinal instability as well as cord compression. The lesion affects mainly the left posterior segment of the vertebra. **c** This is emphasized by the bone-window CT scan, which demonstrates an osteolysis in this area (see also Fig. 5.39). **d** This intraoperative view, taken after proximal costotransversectomy on the left side, demonstrates the operative approach in this case. **e** After removal of part of the hemilamina, the black tumor is visible.
(*Continuation see next page*)

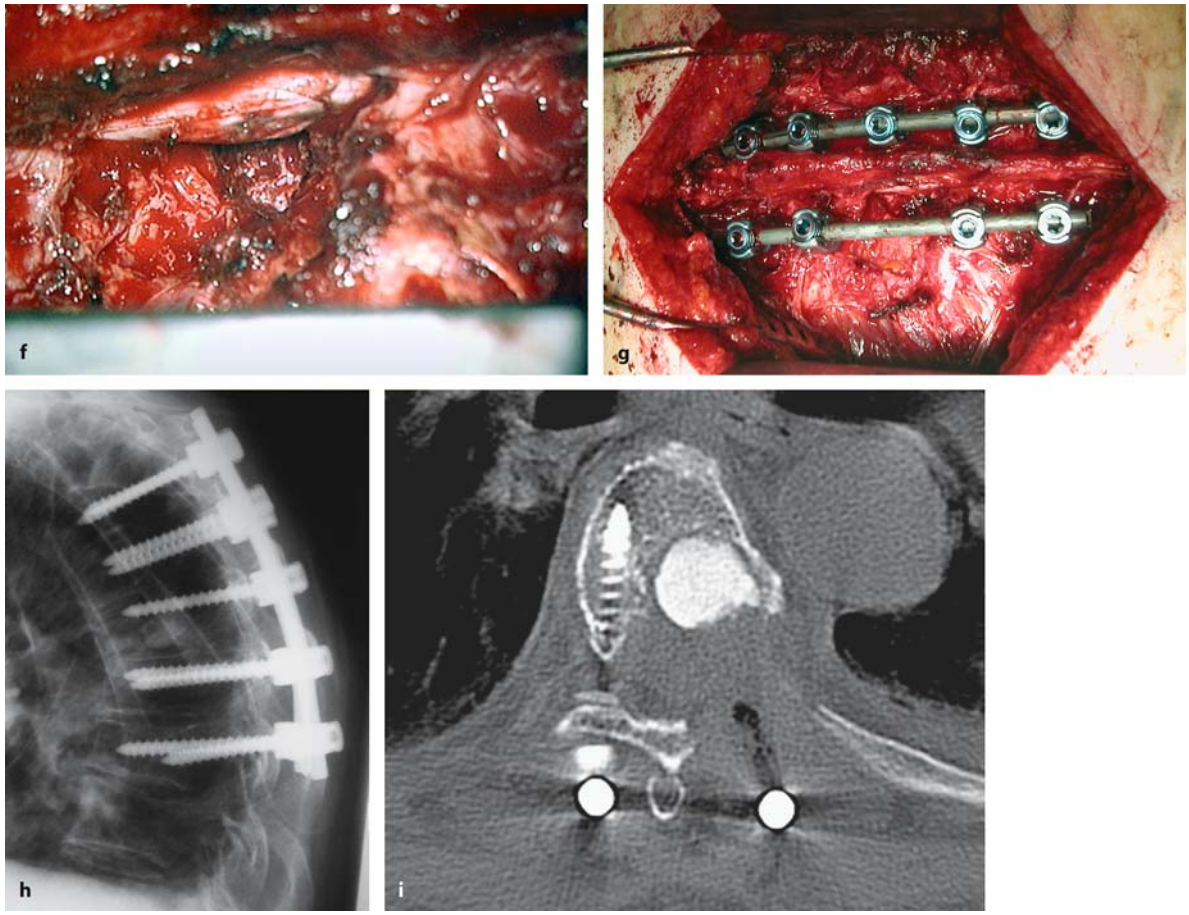

Fig. 5.95. (*Continued*) After subtotal resection of the tumor (**f**), the defect is filled with PMMA and a transpedicular fixation Th4–Th8 is in place (**g**). The postoperative lateral (**h**) X-ray and the bone-window CT image (**i**) show the correct position of the implants with reconstruction of the sagittal profile. The patient's ataxia and pain improved considerably after surgery

Fig. 5.96. Anterior–posterior (**a**) and lateral X-ray (**b**) of a hypernephroma metastasis at Th11 in a 68-year-old woman with a short history of pain and sphincter disturbances. These pictures demonstrate an osteolytic lesion predominantly affecting the posterior half of the vertebra, with destruction of cortical bone and infiltration of both pedicles (*arrowheads*). (*Continuation see next page*)

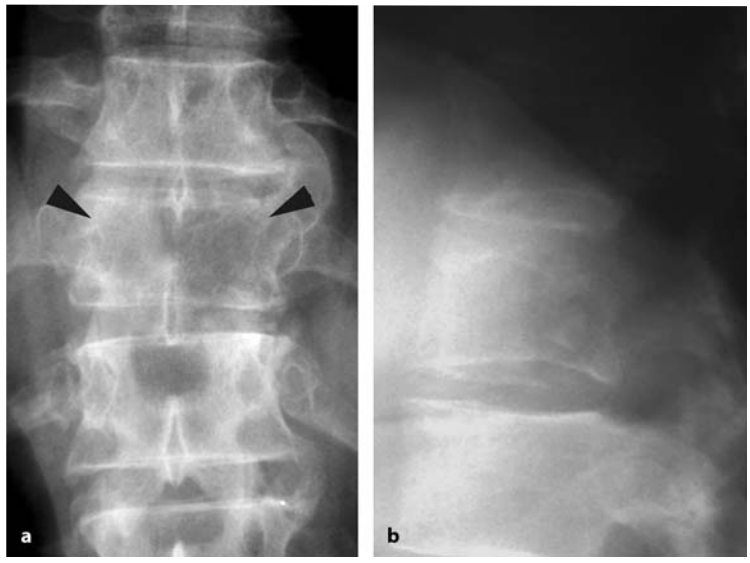

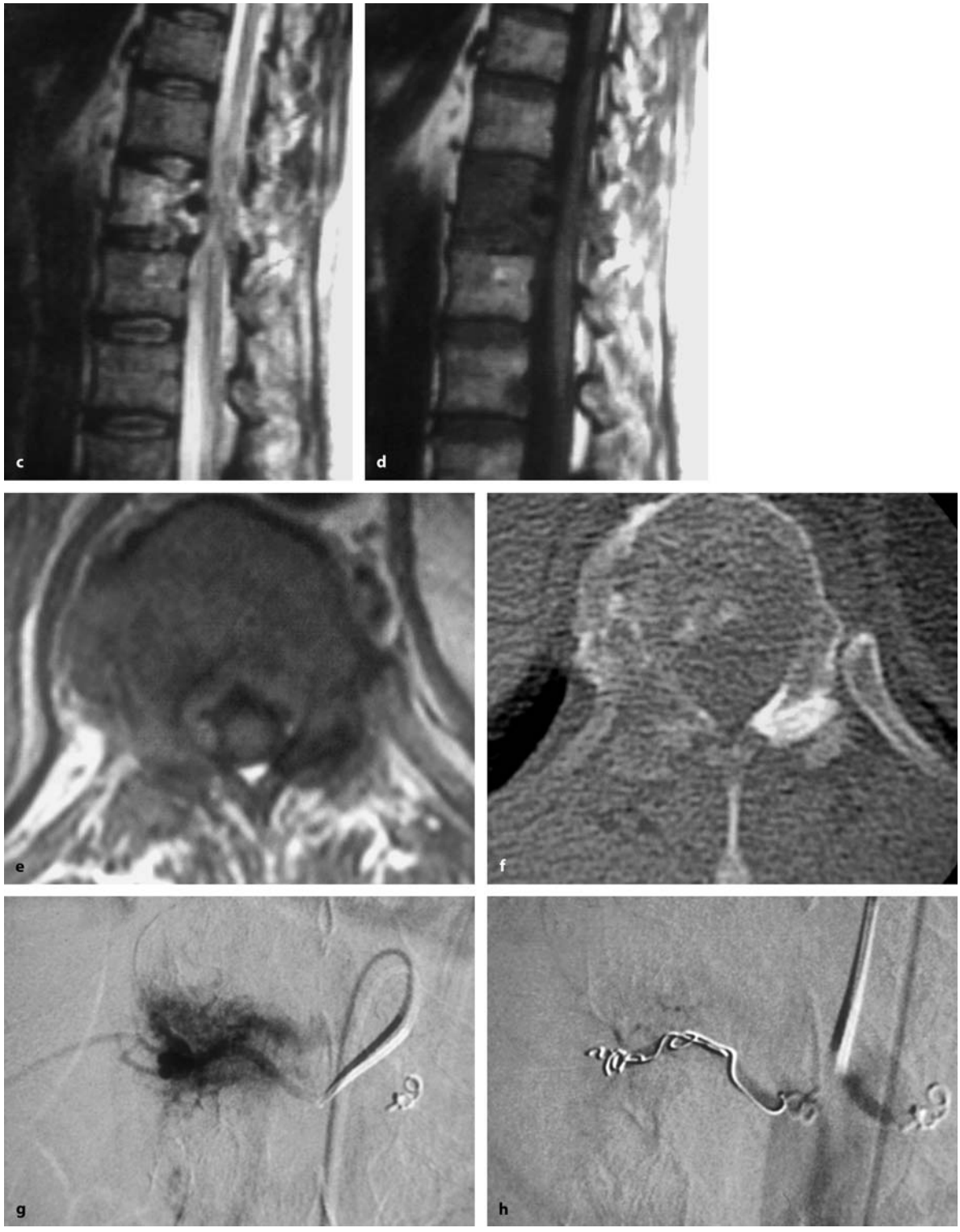

Fig. 5.96. The sagittal T2- (**c**) and T1-weighted (**d**) MRI scans demonstrate compression of the dura anteriorly. **e** An axial T1-weighted scan showing an intraspinal soft-tissue component almost encircling the dura. **f** The bone-window CT scan demonstrates the osteolytic changes predominating in the right pedicle. This highly vascularized metastasis (**g**) was embolized preoperatively (**h**). (*Continuation see next page*)

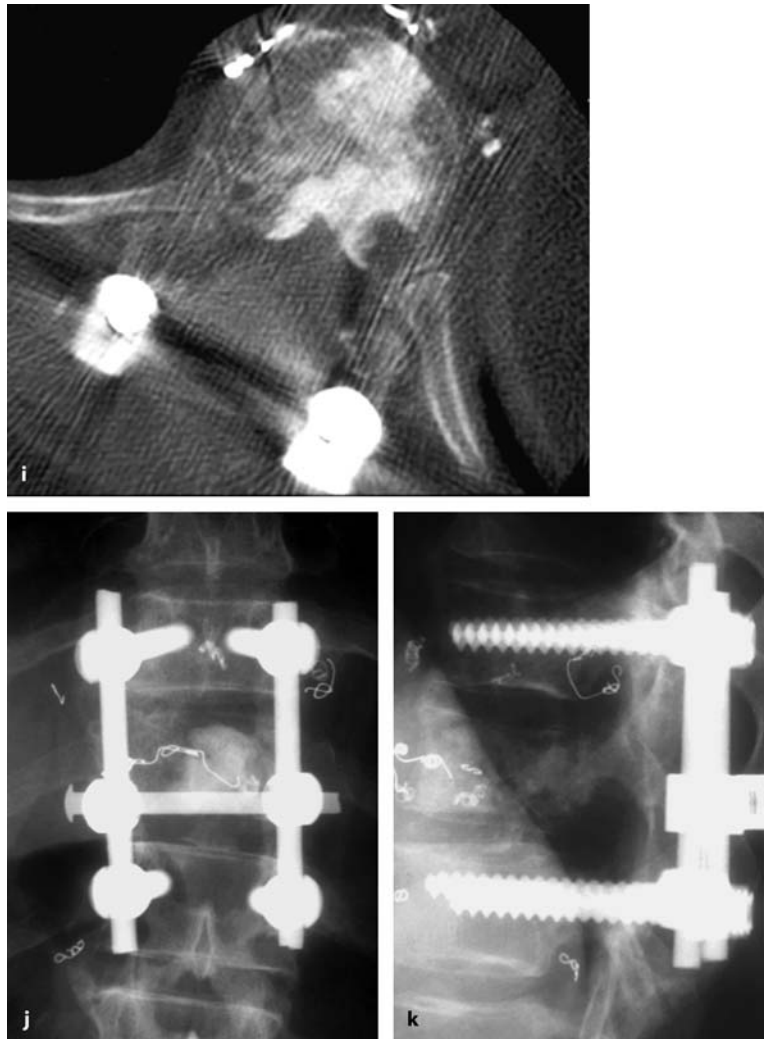

Fig. 5.96. (*Continued*) The patient underwent a laminectomy for removal of intraspinal tumor combined with intraoperative vertebroplasty and posterior transpedicular stabilization at Th10–Th12, as demonstrated on the bone-window CT scan (**i**), anterior–posterior image (**j**), and lateral (**k**) X-ray. Postoperatively, pain improved, but sphincter problems persisted

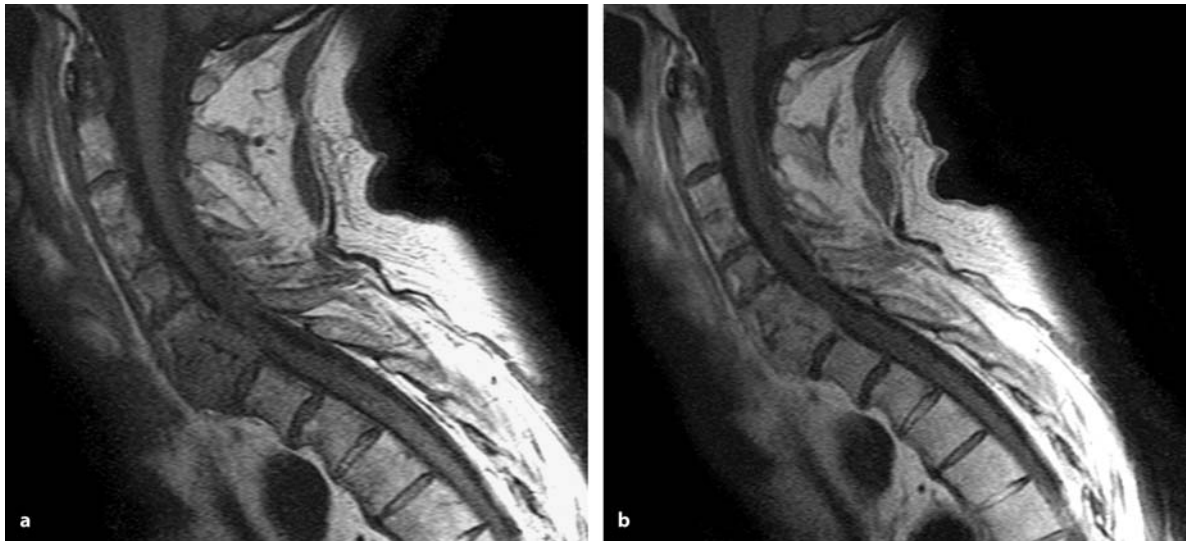

Fig. 5.97. Sagittal T1-weighted MRI scans without (**a**) and with contrast (**b**) of a hypernephroma metastasis at C7 in a 79-year-old patient with a 3-month history of pain. (*Continuation see next page*)

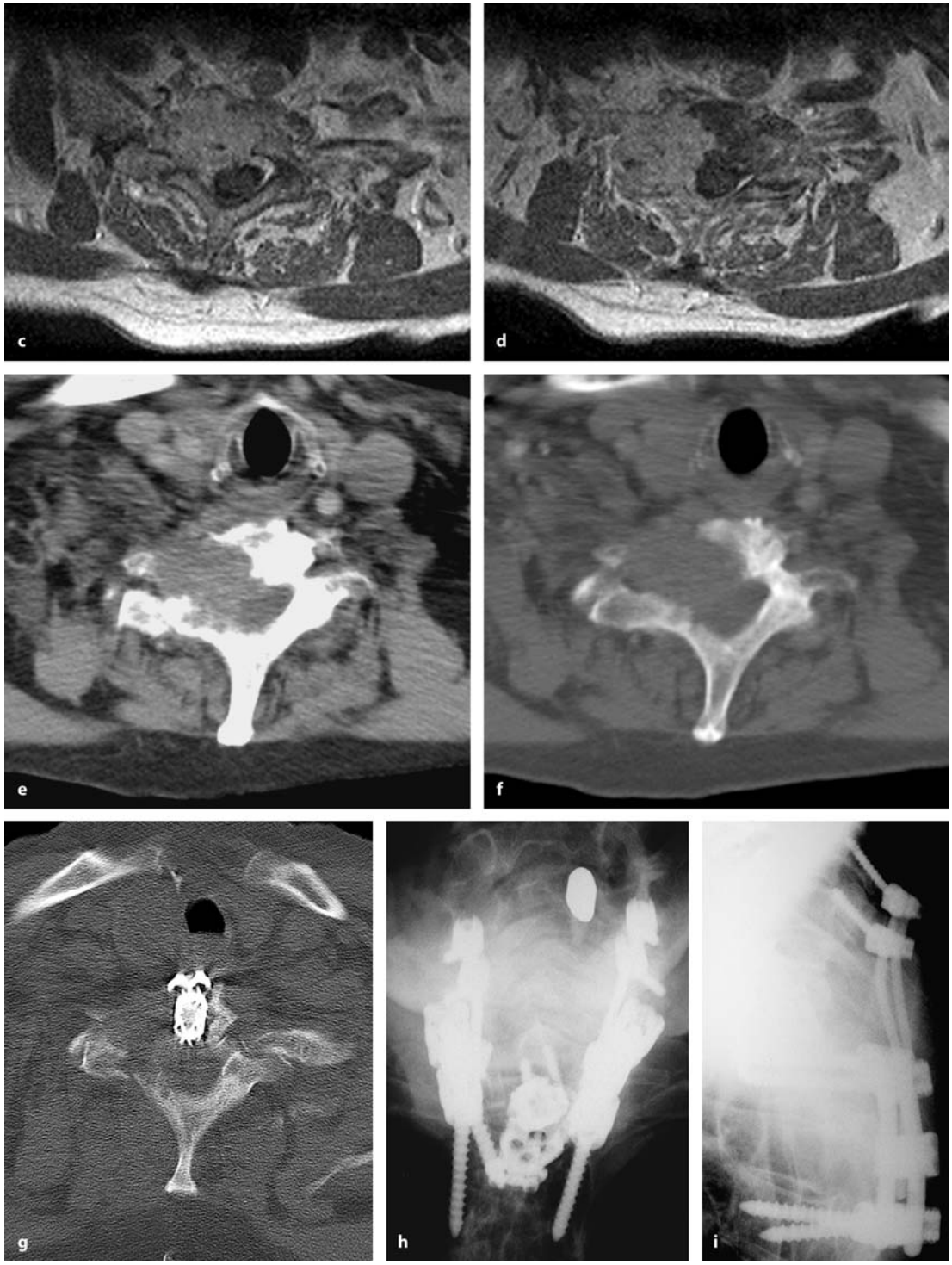

Fig. 5.97. (*Continued*) There is a slight narrowing of the spinal canal anteriorly with no involvement of the posterior elements. **c**, **d** These axial MRI images show predominant involvement of the anterior right part of the vertebra. The native (**e**) and bone-window (**f**) CT scans show the degree of bony destruction. The patient underwent anterior tumor removal, vertebral reconstruction with a cage, anterior plating, and posterior tumor resection and fusion of C5–Th3. **g** This postoperative CT shows the reconstruction and anterior plating, while the anterior–posterior (**h**) and lateral X-rays (**i**) demonstrate a good sagittal profile of the cervicothoracic junction and position of the implants. The patient reported marked pain relief after these two operations

plete paraplegia for more than 24 h [261]. The type of surgery was chosen according to the patient's general health status, urgency of required treatment, oncological status, response to adjuvant therapy, extent and localization of the lesion, and biomechanical requirements.

We encountered 19 cervical, 83 thoracic, 38 lumbar, and 4 sacral metastases; 80% of metastases were located predominantly anterior to the spinal cord in the vertebral bodies, while 10% each were situated laterally or posteriorly. In total, 45% fulfilled the criteria of spinal instability before surgery. Ninety-two patients were operated under emergency conditions, while 52 patients underwent elective tumor removals. For 24% of patients, the primary tumor was not known at the time of surgery. Table 5.25 gives an overview of the primary tumors encountered in our series.

The preoperative Karnofsky score for all patients with spinal metastases was 52±19, indicating that the majority of patients were not ambulatory. They presented at an average age of 62±12 years after a history of 4±5 months (maximum 3 years). The first symptom noted by 80% of patients was local pain at the affected spinal level. For 12%, gait ataxia was the first sign of spinal metastasis. Other complaints were rarely mentioned as the first symptom (Table 5.26). At presentation, this situation had shifted. Only 39% still considered pain as the major problem, while 54% were affected mainly by gait problems and 5% by motor weakness. In all, 97% reported local pain, 78% sensory deficits, 73% motor weakness, 68% walking difficulties, 45% sphincter dysfunction, and 13% complained about dysesthesias (Table 5.27). Seventy-one patients were unable to walk, 11 of them with a severe paraparesis (i.e., minimal muscle innervation but no contraction), while 18 patients were paraplegic. Thirty-four patients were incontinent for urine prior to surgery and 66 patients suffered from severe pain that was incapacitating despite analgesic medication. Thirty-one patients had been treated with radiotherapy, chemotherapy, or both before they underwent surgery.

Analyzing clinical presentations further, two groups could be differentiated: patients undergoing elective surgery (52 patients) and patients admitted as emergencies (92 patients). Their clinical courses differed markedly. Patients presenting as emergencies showed a shorter clinical history (3±6 compared to 5±4 months, respectively; p=0.0462), were older (59±11 and 63±13 years, respectively; p=0.0157), and were less effected by pain but demonstrated more severe neurological deficits (Tables 5.26 and 5.27). Seventy-eight of them were not walking (8% in the elective group; chi square test: p<0.0001) and 36% were incontinent for urine (6% in the elective group; chi square test: p<0.0001). Consequently, their preoperative mean Karnofsky score was significantly lower (43±12 compared to 69±16; p<0.0001). However, there was no difference in the rate of spinal instabilities between these two groups (44% and 45% for elective and emergency operations, respectively).

Table 5.25. Histologies of spinal metastases

Histology	n
Lung	23
Prostate	22
Breast	22
Renal	18
Thyroid	10
Gastrointestinal tract	8
Urothelium	3
Melanoma	1
Seminoma	1
Pleuramesothelioma	1
Unknown primary tumor	35

Table 5.26. Initial symptoms of spinal metastases

First symptom	Elective surgery	Emergency surgery	Total
Pain	94%	73%	80%
Gait ataxia	–	18%	12%
Motor weakness	2%	6%	4%
Sensory deficits	–	2%	1%
Dysesthesias	4%	–	1%
Sphincter problems	–	1%	1%

Chi square test: p=0.005

Table 5.27. Symptoms for spinal metastases at presentation

Symptom	Elective surgery	Emergency surgery	Total
Pain	98%	97%	97%
Gait ataxia	31%	88%	68%
Motor weakness	46%	87%	73%
Sensory deficits	56%	90%	78%
Dysesthesias	15%	12%	13%
Sphincter problems	8%	66%	45%

In other words, the more dramatic course of emergency patients is not predominantly related to spinal instability, but can be attributed to a more aggressive cancerous disease and worse general health condition of the patient. Patients with elective surgeries were more likely to harbor kidney, breast, or thyroid cancers, whereas in emergency patients the underlying tumor was more often located in the prostate and gastrointestinal tract, or was not known (chi square test: p=0.0132). Lung cancers were evenly distributed in both groups. In the elective group, 87% of the metastases were restricted to one vertebra compared to 46% in the emergency group (chi square test: p<0.0001), were more commonly confined to the vertebra without soft-tissue involvement (44% compared to 21%; chi square test: p=0.0035), and multiple spinal lesions were less likely (6% compared to 22%, respectively; chi square test: p=0.0096). However, the number of extraspinal metastases was similar in both groups.

Except for 30 patients, all metastases (i.e., 79%) were operated via a posterior or posterolateral approach. Nineteen patients were operated from an anterior approach only (13%), while 11 patients (8%) underwent a combined approach with anterior tumor removal and vertebral reconstruction and additional posterior tumor removal and fusion.

Management differed between elective and emergency operations. For elective operations, 63% were operated from posterior approaches compared to 88% in emergency situations (chi square test: p<0.0001) (Table 5.28). A similar policy has been described by Jansson and Bauer [263].

A reconstruction of the vertebral body was performed in 49 patients: PMMA as a block or in form of a vertebroplasty was employed in 32 instances. Bone was used for reconstruction in 11 patients, and titanium and carbon cages in 6 patients. Posterior fusion with pedicle screw fixation or anterior screw fixation and plating was used in 48 patients and combined with vertebral body reconstruction in 45 patients. Autologous bone was used for patients with a long survival prognosis, and artificial implants for the remainder.

Again, elective surgeries incorporated vertebral reconstruction and fusion significantly more often than emergency operations (chi square test: p<0.0001). The rate of complete resection was 71% in elective operations compared to 24% for emergencies (chi square test: p<0.0001). Overall, complete resections were achieved for 41% of metastases, while 52% were removed partially and 7% were decompressed (Table 5.28). Anterior vertebral tumors with soft-tissue extensions were those most likely to be resected incompletely.

Table 5.28. Surgical management of spinal metastases

Approach		Elective surgery	Emergency surgery	Total
Posterior	n	33	81	114
	%	63%	88%	79%
Anterior	n	16	3	19
	%	31%	3%	13%
Combined	n	3	8	11
	%	6%	9%	8%
Stability				
Stable	n	29	51	80
	%	56%	55%	56%
Unstable	n	23	41	64
	%	44%	45%	44%
Fusion	n	32	16	48
	%	62%	17%	33%
No Fusion	n	20	76	96
	%	38%	83%	67%
Resection				
Complete	n	37	22	59
	%	71%	24%	41%
Subtotal	n	10	65	75
	%	19%	71%	52%
Decompression/biopsy	n	5	5	10
	%	10%	5%	7%
Vertebral reconstruction				
PMMA	n	20	12	32
	%	38%	13%	22%
Bone	n	9	2	11
	%	17%	2%	8%
Cage	n	5	1	6
	%	10%	1%	4%

There was a trend toward lower complication rates in elective operations compared to emergencies, but this was not significant (12% and 20%, respectively). Sundaresan et al. [520] observed complications in 15% of de–novo-operated patients, compared to 40% for patients with preoperative radiotherapy. We did not observe such a difference [558]. Overall, complications were encountered in 17% of operations (Table 5.29) [65, 263, 555, 558, 562]. In a study comparing anterior and posterolateral approaches to the thoracic

Table 5.29. Complications for patients with spinal metastases

Type		Elective surgery	Emergency surgery	Total
Wound infection		1	8	9
CSF leak		1	–	1
Hemorrhage		2	2	4
Instability		–	3	3
Intercostal neuralgia		–	1	1
Mandibular dislocation		1	–	1
Deep vein thrombosis		–	1	1
Pulmonary embolism		–	1	1
Myocardial infarction		–	1	1
Urinary tract infection		–	1	1
Septicemia		1	–	1
Total	**n**	**6**	**18**	**24**
	%	**12%**	**20%**	**17%**

Table 5.30. Multivariate analysis for prediction of a high postoperative Karnofsky score for patients with spinal metastases

Factor	β-value
High preoperative Karnofsky score	0.8086
Posterior localization	0.2793
Spinal fusion	0.2614
First surgery	0.1619
Complete resection	0.1379

Correlation: r=0.7618, p<0.0001

spine, similar complication rates of 38.8% and 37.9%, respectively, were observed for both approaches [564]. Holman et al. [239] gave a complication rate of 32% for lumbar metastases.

Overall, surgical mortality within 30 days of surgery was 14% (elective surgeries 6% and emergency operations 18%; log-rank test: not significant) [62]. Jansson and Bauer [263] observed a mortality figure of 13% among 282 operated patients. Patients with independent ambulation preoperatively demonstrated no surgical mortality, compared to 21% for dependent patients (log-rank test: p=0.0065). The average follow-up period was 7±15 months (maximum 9 years and 2 months). In a series of 96 patients, Vrionis and Small [555] reported a surgical mortality of 4.1%; in another series on 76 patients, a figure of 7% was given [562].

In the literature, improvement of neurological function has been observed for 50–85% of patients after surgery [5, 8, 28, 35, 42, 59, 62, 65, 101, 116, 169, 196, 199, 229, 231, 239, 240, 263, 290, 299, 312, 313, 351, 380, 401, 455, 456, 470, 496, 506, 511, 519, 520, 530, 534, 536, 558, 562, 563] and for between 33% and 75% after radiotherapy [74, 171, 266, 347, 348, 440, 577, 578].

For analysis of clinical results in our series, a multivariate analysis was performed. With respect to factors predictive of a high postoperative Karnofsky score 3 months after surgery, the preoperative Karnofsky score was by far the strongest [196]. Other less important independent factors were posterior localization of the tumor, spinal fusion, first surgery on a tumor, and complete resection (p<0.0001; Table 5.30). The number of affected vertebrae, the presence of extraspinal metastases or elective vs. emergency operations were not significant independent factors for clinical outcome. In other words, for any given preoperative status, the type of surgical management determines clinical outcome and requires the resection of as much tumor as possible and to treat spinal instability! Treatment of spinal instability and achieving a complete resection do have a favorable impact on postoperative clinical outcome for patients with spinal metastases, but the major determinant is still the preoperative status. This finding is consistent with almost every series on spinal metastases, irrespective of treatment modality [8, 27, 28, 62, 65, 74, 90, 116, 128, 171, 198, 199, 203, 229, 239, 240, 261, 263, 288, 290, 294, 299, 312, 313, 347, 349, 354, 380, 401, 470, 506, 534, 549, 555, 558, 562, 577, 578].

In a radiotherapeutic series of 96 patients with neurological deficits due to spinal metastasis, ambulatory status was regained in 89% if radiotherapy was instituted in patients with a neurological history of at least 14 days, whereas just 12% improved with a shorter history of neurological deterioration [440]. In other words, rapid neurological deteriorations carry a bad prognosis in terms of functional recovery, regardless of treatment modality.

The preoperative status is related predominantly to the activity of the cancerous disease, which differs according to the primary tumor. According to average survival times for individual cancer groups, one can distinguish between primary tumors associated with a comparably long survival and those with a short survival probability. We have divided the patients of this series into these two groups and analyzed their postoperative clinical course separately. Table 5.31 gives an overview of the postoperative clinical scores for the first 6 months after surgery for patients with

Table 5.31. Clinical course for patients with spinal metastases related to survival prognosis and type of presentation

Symptom	Preop. status	Postop. status	3 Months postop.	6 Months postop.
Pain				
Total	2.5±0.5	3.3±0.8	3.4±1.0	3.2±1.2*
Long survival	2.5±0.5	3.3±0.8	3.6±0.8	3.5±1.1**
Short survival	2.3±0.5	3.3±0.9	2.6±1.1	2.1±1.3
Elective	2.5±0.5	3.6±0.7	3.7±0.9	3.3±1.3*
Emergency	2.4±0.5	3.1±0.8	3.2±1.0	3.1±1.2*
Hypesthesia				
Total	3.5±1.1	3.9±1.1	4.0±1.0	3.9±1.2*
Long survival	3.5±1.2	3.9±1.1	4.1±1.0	4.0±1.3*
Short survival	3.5±0.9	3.8±0.9	3.8±0.9	3.5±1.1
Elective	3.9±1.3	4.2±0.9	4.5±0.7	4.3±0.8
Emergency	3.2±1.1	3.7±1.1	3.7±1.0	3.6±1.4
Dysesthesias				
Total	4.8±0.5	4.9±0.4	4.9±0.4	4.8±0.5
Long survival	4.8±0.5	4.9±0.4	4.9±0.4	4.9±0.4
Short survival	4.9±0.4	4.9±0.4	4.9±0.4	4.6±0.7
Elective	4.8±0.6	4.9±0.3	4.9±0.3	4.9±0.3
Emergency	4.9±0.5	4.9±0.5	4.9±0.5	4.8±0.6
Gait				
Total	3.3±1.5	3.5±1.5	3.7±1.5	3.3±1.7
Long survival	3.2±1.6	3.5±1.4	3.7±1.4	3.5±1.7
Short survival	3.4±1.3	3.5±1.7	3.5±1.8	2.9±1.7
Elective	4.1±1.4	4.2±1.5	4.5±1.0	4.3±1.1
Emergency	2.7±1.4	3.1±1.3	3.1±1.5	2.6±1.7
Motor power				
Total	3.4±1.5	3.7±1.3	3.9±1.2	3.7±1.5
Long survival	3.3±1.5	3.6±1.3	3.9±1.3	3.9±1.5*
Short survival	3.8±1.4	3.9±1.3	4.0±0.9	3.3±1.3
Elective	4.2±1.3	4.3±1.2	4.5±0.8	4.6±0.7
Emergency	2.9±1.4	3.3±1.2	3.5±1.3	3.2±1.6
Sphincter function				
Total	3.8±1.6	4.0±1.4	4.0±1.5	4.0±1.5
Long survival	3.9±1.5	4.0±1.3	4.1±1.4	4.1±1.4
Short survival	3.6±1.9	3.8±1.9	3.8±1.8	3.6±1.9
Elective	4.4±1.5	4.7±0.9	4.7±0.8	4.7±0.8
Emergency	3.4±1.5	3.5±1.6	3.5±1.6	3.5±1.6
Karnofsky score				
Total	57±18	60±19	59±22	55±26
Long survival	58±19	61±20	61±23	59±26
Short survival	55±14	58±20	51±17	38±21*
Elective	68±18	71±18	67±24	65±24
Emergency	50±13	53±17	53±20	47±26

Statistically significant difference between preop. status and 6 months postop.: *$p<0.05$, **$p<0.01$

favorable primary tumors (i.e., thyroid, kidney, breast, and prostate cancer), and those with less favorable histologies (i.e., lung, gastrointestinal tract, or unknown primary tumors). A second line of analyses compares elective and emergency operations.

Comparing preoperative and postoperative scores after 6 months, all patients showed improvements for pain, sensory deficits, motor weakness, and sphincter function. A significant difference, however, was seen for pain only. The Karnofsky score remained stable throughout this time (57±18 and 55±26, respectively). The best results were obtained for patients with a long survival prognosis. Significant improvements for this subgroup were obtained for pain, sensory deficits, and motor weakness, whereas minor improvements were seen for dysesthesias, and gait and sphincter functions. Likewise, no significant change of the Karnofsky score was observed (58±19 and 59±26, respectively). On the other hand, patients with a short survival prognosis had a very short-lived benefit from surgery. Within 6 months, the Karnofsky score had declined significantly from 55±14 to 38±21 (Table 5.31).

A comparison of elective and emergency operations revealed similar postoperative changes in both groups. However, emergency patients were in a worse preoperative neurological situation, and most of them did not fully catch up with their elective counterparts. Therefore, at each given time their scores were lower compared to those of patients undergoing planned operations (Table 5.31). Of the electively operated patients, 90% were able to walk postoperatively and 95% had sphincter control, compared to 50% and 73%, respectively, in the emergency group (chi-square test: $p<0.0001$).

These results underline the overwhelming impact of the preoperative status for a satisfactory postoperative outcome. Analysis of individual clinical symptoms demonstrated that 97% of patients who could walk preoperatively kept this ability postoperatively for at least 3 months. At 6 months, 14% had experienced a deterioration in this respect. At 1 year, 88% were still able to walk by themselves [263]. However, of 72 patients unable to walk preoperatively, only 16 (22%) patients regained walking capacity. After 3 months, this number had dropped to eight patients, and after 1 year just five were still able to walk. Although a slight improvement of motor function was observed for four paraplegic patients, none regained walking ability postoperatively.

Correspondingly, 91% of patients remained continent for urine for 3 months after surgery and 82% for 1 year, while only 11 of 37 incontinent patients (30%) regained sphincter control after an operation. After 1 year, just 4 of these 11 patients still had sufficient bladder control [6, 27].

Better overall results were observed for pain. Here, patients benefited the most, so that after 6 months, all treatment groups except patients with a short survival prognosis had similar and sufficient pain control (Table 5.31) [8, 59, 62, 95, 101, 116, 169, 199, 239, 240, 290, 299, 312, 313, 333, 351, 358, 380, 455, 456, 470, 496, 506, 512, 520, 536, 555, 558, 562, 563]. However, similar effects for pain control can be obtained using radiotherapy [51, 140, 171, 198, 266, 347–349, 465, 535, 549, 578]. As most patients underwent postoperative radiation, some of the pain relief probably has to be attributed to radiation. First reports have now appeared with results on stereotactic radiosurgery of spinal metastases, showing a good response at least for pain control [51, 137, 140, 465].

The majority of spinal metastases originate in the vertebral body [13, 128, 294, 320], with spinal cord compression from the anterior. Instability due to vertebral body collapse, fracture, or kyphotic angulation may contribute to anterior compression of the cord. Impressive results have been reported with fixations using anterior approaches [65, 116, 169, 199, 220, 239, 240, 297, 299, 313, 358, 380, 500, 506, 512, 518–520, 536, 562] and with posterior fixations [8, 35, 42, 62, 65, 89, 95, 101, 134, 164, 239, 263, 295, 456, 491, 496, 558, 563]. Even though most of the metastases involve predominantly the anterior elements, no study has proven so far that anterior approaches provide better results than posterior ones [227].

Several studies emphasizing stability issues documented favorable results with vertebrectomies, vertebral body reconstruction, and fusion [8, 62, 65, 95, 116, 134, 199, 220, 229, 239, 240, 299, 358, 380, 455–457, 500, 506, 511, 512, 518–520, 536, 558, 560, 562].

Holman et al. [239] reported on 139 patients with lumbar metastases operated from a variety of approaches; of these, 79% of nonambulatory patients regained walking ability. Mean survival was 14.8 months, with 54% surviving 1 year and 23% for 5 years.

Solini et al. [506] operated on 139 of 151 cervical metastases using an anterior approach, with vertebral body reconstruction and fusion in the overwhelming majority. All patients reported improvement of pain and neurological recovery was seen in 81% of affected patients. The 2-year survival rate was 49%.

Hosono et al. [240] reported 82 patients with spinal metastases, with vertebral body replacements using anterior or anterolateral approaches. Pain relief was obtained in 94% and motor function improved in

81%, resulting in improved ambulation for 64% of patients. Complications were observed in 16%. Maintenance of ambulation required a favorable histology and local control of the metastasis. A total of 78% of patients survived for 6 months.

Weigel et al. [562] presented a series of 76 patients undergoing 86 surgical procedures favoring anterior approaches. The mean postoperative survival was 13.1 months, with functional improvement in 58% and pain relief in 89% of patients. Complications occurred in 19%, with a surgical mortality of 7%. Survival was influenced by tumor histology, age, presence of extraspinal metastases, and the preoperative Karnofsky score.

Gokaslan et al. [199] presented a series of 72 patients operated transthoracically for spinal metastases. Seven patients with thoracolumbar and cervicothoracic lesions required additional posterior instrumentation. Thirty-four out of 46 patients with neurological deficits improved significantly. Complications occurred in 21 patients (29%), with a 1-year survival rate of 62%.

Heidecke et al. [229] presented 62 patients with cervical metastases operated from the anterior approach, with tumor removal, vertebral body replacement, and fusion. Complications occurred in 29%, with 93% demonstrating improvement or an unchanged neurological status after surgery. The 1-year survival rate was 58% and the 2-year survival rate was 21% (survival statistics not applied).

Sundaresan et al. [518] described 54 patients who were operated mainly via anterior approaches. Before surgery, 44% were nonambulatory. Except for a surgical mortality of 6%, all remaining patients became ambulatory after surgery. Twenty-five patients survived for at least 2 years, and 23 of these were still self ambulatory. However, these excellent results are also attributable to the heterogeneity of histologies, with a significant percentage of low-level malignancies such as chordomas and chondrosarcomas. Subsequently, 23% of patients underwent multiple operations for local recurrences or at other spinal levels. Similar results were provided in a later report on 110 patients by this group [519]. The overall median survival in this study was 16 months, which again incorporated a mixture of different histologies, making it difficult to compare these results with those of other studies. With their rather aggressive surgical strategy and a high percentage of patients with combined anterior and posterior approaches (48%), a surgical mortality of 5% and a high complication rate of 48% did not interfere with the overall favorable results for 82% of patients, with 46% surviving for 2 years. A favorable functional result was defined as becoming ambulatory after surgery for previously nonambulatory patients or remaining ambulatory postoperatively for patients who were in good preoperative condition. Excluding low malignant tumors from this calculation reduced the 2-year survival rate to 36%.

In a more recent study from this group [520], 80 patients with solitary metastases were reported. Half of these patients underwent combined anterior and posterior procedures and 32 were managed from an anterior approach only. En bloc resections were obtained in six instances; 32% of these patients were operated again for recurrent disease. The overall median survival was 30 months, with 18% surviving 5 years.

Bilsky et al. [65] presented a series of 33 cervical metastases operated via anterior, posterior, and combined approaches, with neurological improvements seen in 88% of patients and a complication rate of 24%. The overall mean survival was 8.6 months.

In Tomita's series [536] of 21 patients with spinal metastases undergoing en bloc spondylectomies and fusion, there was one operative death. A postoperative improvement was seen for 18 patients. No local recurrence was observed. Among 10 surviving patients, 7 survived for more than 1 year, while 11 patients died, mostly within 1 year of surgery. In other words, en bloc resections do not prolong the survival of patients with metastases but may achieve very good clinical results in suitable patients.

Casadei et al. [101] achieved pain relief in 85% and functional improvements for 52% of patients with pathological fractures due to thoracolumbar metastases using posterior decompression and fusion. Mean survival was 12 months.

As impressive as such results for aggressive surgical strategies are, there can be no doubt that anterior approaches to the thoracic and lumbar spine are quite demanding for these patients. This is even more pronounced if we consider that additional posterior fusion is also required for a significant proportion of these patients. Not every patient with metastatic disease is suitable for such a regimen [95, 496, 563]. An alternative surgical approach is to concentrate on spinal cord decompression and posterior fusion for palliation.

Applying mainly posterior approaches, Jansson and Bauer [263] reported on their experience with 282 spinal metastases. Neurological conditions were found to have improved postoperatively in 70% of patients, with 80% being able to walk for at least 6 months. Similarly, Wang et al. [558] reported the results of 140 patients after posterolateral operations with decompression, vertebral body reconstruction,

and posterior fusion; 90% achieved good functional scores. All of these patients had been able to care for themselves preoperatively at least partially.

Rompe et al. [457] presented results for 106 patients with spinal metastases operated via posterolateral approaches with decompression and stabilization; 61% of patients not able to walk regained walking capacity. Survivors kept this ability for 1 year in 96% of cases with a 1-year survival rate of 50%.

Schoeggl et al. [479] described 84 patients with spinal metastases who were considered not suitable for extensive anterior operations, but who were decompressed from a posterior approach for progressive neurological deficits. Just 20% were able to walk preoperatively and 55% had significant sphincter problems. After decompression, 45% were able to walk provided at least some residual motor power had been present preoperatively, and 18% of the patients with micturition problems reported improvements provided they had not required catheterization preoperatively. In conclusion, the authors recommended posterior decompression for patients with progressive neurological symptoms but significant residual function as a palliative measure to improve quality of life.

Bauer et al. [42] reported on 67 patients treated with posterior decompression and stabilization. The 1-year survival rate was 22%, with 76% experiencing postoperative neurological improvement. The latest study of this group incorporated these patients and described 282 patients undergoing treatment with this strategy. The 1-year survival rate has since been determined as 30% [263].

Akeyson and McCutcheon [8] described a series of 25 patients operated in this fashion and achieved neurological improvements in 56%. Bilsky et al. [62] also presented their experience with posterolateral decompressions and fusions in 25 patients. All patients had postoperative pain relief and 23 either improved or maintained their neurological status.

Mühlbauer et al. [385] were similarly successful in 17 patients. PMMA was used for vertebral reconstruction with posterior instrumentation in most patients. After 1 month, 14 patients (82%) showed neurological improvement, and out of 10 preoperative nonambulators, 7 regained their ability to walk. One local recurrence was observed. Nevertheless, 14 patients died after a mean time of 8 months (1–21 months), with 3 survivors after 10, 4, and 3 months.

Cahill and Kumar [95] presented results for nine patients with spinal metastases who they considered ineligible for anterior surgery. These patients were managed with a posterior approach via costotransversectomy, subtotal vertebrectomy, and posterior fusion.

In our series, the overall local recurrence rates, as determined by the Kaplan-Meier method, were 54% after 6 months, 64% after 1 year, and 95% after 4 years (Fig. 5.98) [290, 500, 518]. Multiple regression analyses revealed that an independent preoperative status of ambulation, favorable tumor histology, low spinal level, low number of affected vertebral bodies, and elective surgery were significant, independent predictors of a low rate of local metastatic recurrence. A good preoperative clinical status (Fig. 5.99) and a planned operation were by far the strongest predictors for a long period of local control (Table 5.32).

Any metastasis provides evidence that the patient suffers from a malignant disease that is no longer

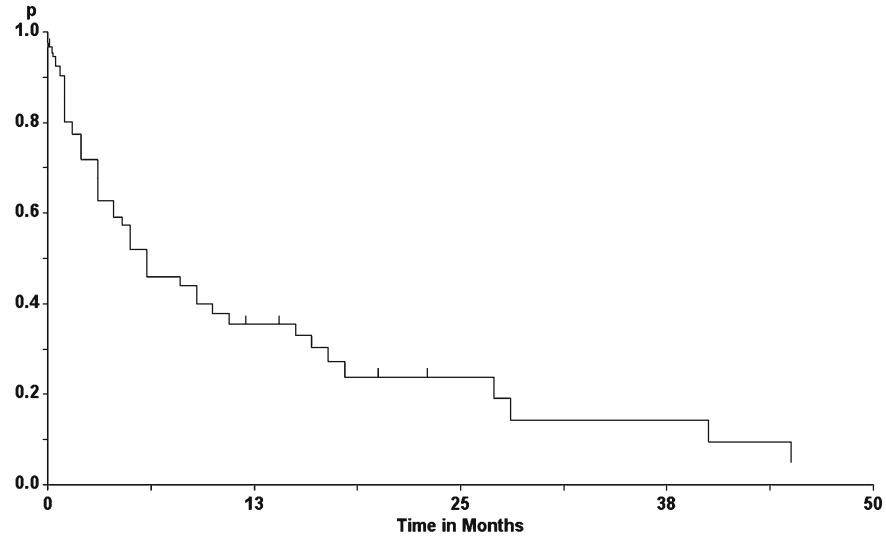

Fig. 5.98. Tumor recurrence rate for patients with spinal metastases

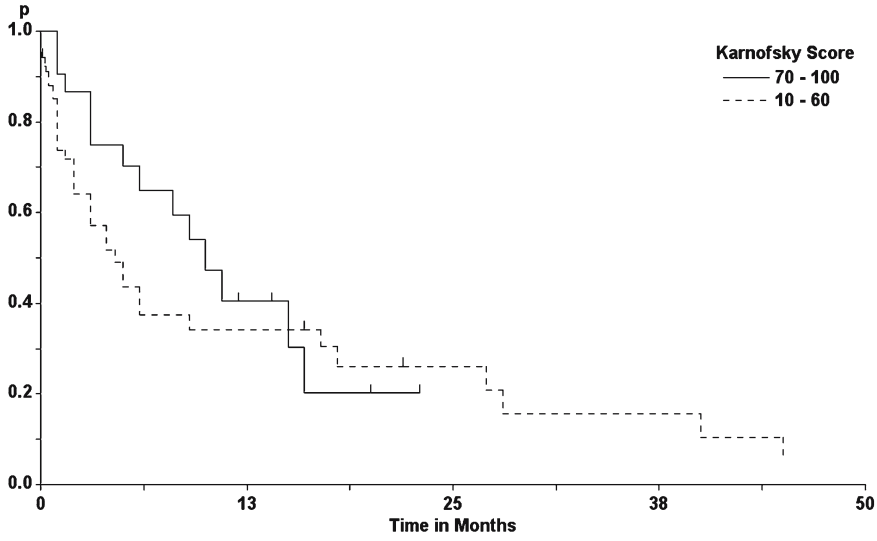

Fig. 5.99. Tumor recurrence rates for patients with spinal metastases as a function of preoperative Karnofsky score (log-rank test: not significant)

Table 5.32. Multivariate analysis for prediction of a local recurrence for spinal metastases

Factor	β-value
Low preoperative Karnofsky score	0.4983
Emergency surgery	0.3750
No fusion	0.2494
High spinal level	0.2313

Correlation coefficient: r=0.5301, p<0.0001

confined to a single organ [203]. Local control of a spinal metastasis alone will be unlikely to change the survival prognosis significantly [6]. The biological behavior of the primary tumor, its response to adjuvant therapy, and the general health status of the patient will have a much more prominent influence on survival.

The overall survival rates for patients in this series, again determined by Kaplan-Meier analysis, were 53% after 6 months, 47% after 1 year, and 16% after 4 years (Fig. 5.100) [239, 558, 562]. The longest postoperative survival was observed for patients with metastases from the thyroid, kidney, breast, and prostate cancer (80%, 83%, 59%, and 44% surviving for 1 year, respectively). These patients were considered to have a good survival prognosis. For these patients, surgical mortality was 9%; 65% survived 6 months and 62% were still alive after 1 year (Fig. 5.101). Similar figures after surgical therapy are reported in the literature [5, 65, 197, 239, 244, 263, 290, 341, 358, 401, 402, 455, 456, 500, 511, 512, 520, 530, 534, 536, 558, 561, 562].

On the other hand, patients with metastases from lung or gastrointestinal cancer or an unknown primary tumor showed a worse outcome in terms of survival and were considered to have a poor survival prognosis [347, 520, 562]. Just 27% of patients with metastases from lung cancer survived for at least 3 months. The 3-month survival for patients with unknown primary tumors was 34%. All patients with metastasis from gastrointestinal cancer died within 6 months of surgery. Overall surgical mortality in the group with a poor survival prognosis was significantly higher, at 22% (log-rank test: p=0.0153; Fig. 5.101) [239].

These figures compare favorably with radiotherapy series such as the study by Maranzano and Latini [347] with 255 patients. For patients with favorable histologies a 1-year survival rate of 41% was observed, whereas just 9% of patients with unfavorable histologies survived 1 year.

Van der Linden et al. [549] treated 342 patients with painful spinal metastases with radiotherapy. The median survival was 7 months; 3% developed spinal cord compression after radiotherapy. Predictors of longer survival were a high Karnofsky score, a favorable primary tumor, and absence of visceral metastases. Based on these factors, patients were divided in three groups with resulting median survival times of 3 months, 9 months, and 18.7 months.

A multiple regression analysis was performed in order to determine other factors that have an independent influence on postoperative survival. This analysis predicts longer survival of patients with local control of the spinal metastasis (Fig. 5.102) and in a

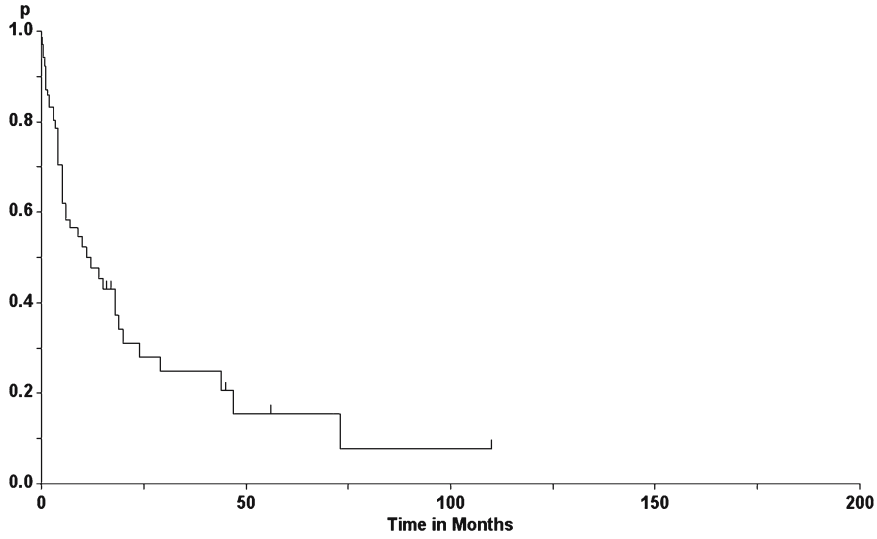

Fig. 5.100. Overall survival rate for patients with spinal metastases

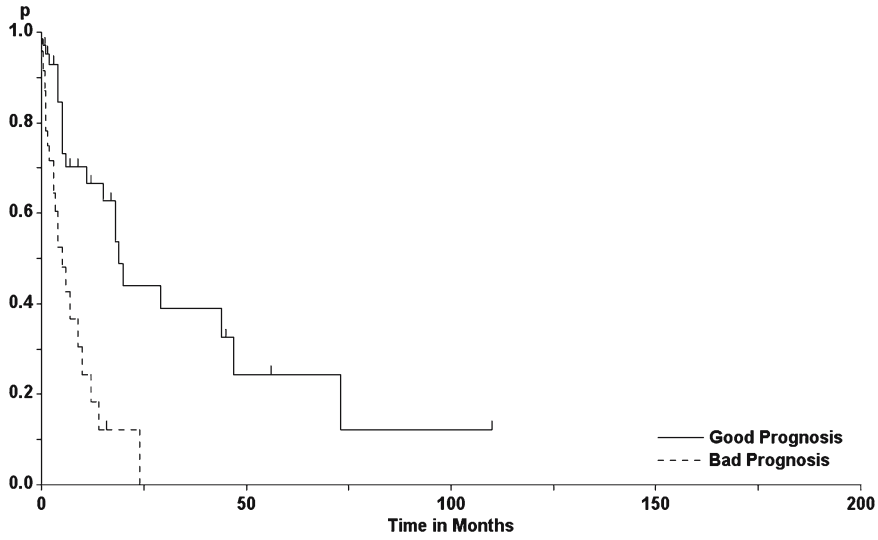

Fig. 5.101. Survival rates of patients with spinal metastases as a function of histology (log-rank test: $p<0.0001$)

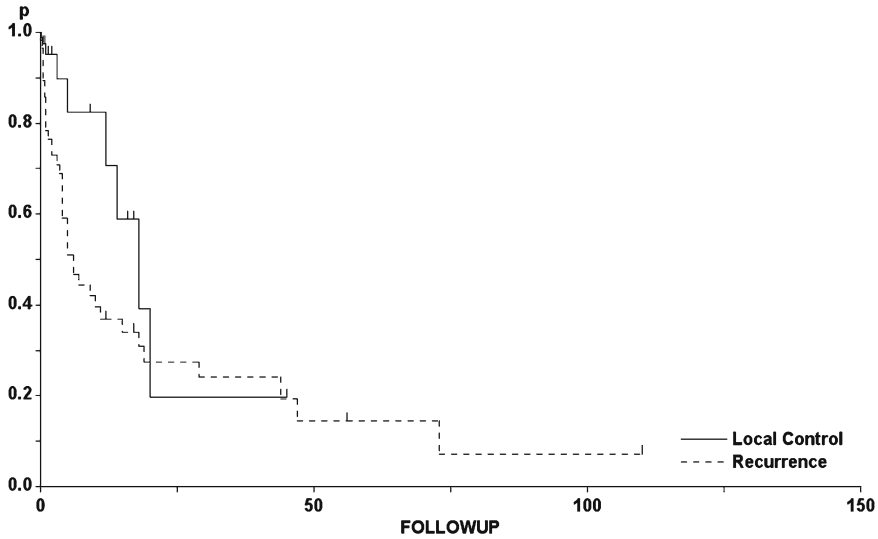

Fig. 5.102. Survival rates of patients with spinal metastases, as a function of local metastatic control (log-rank test: $p=0.023$)

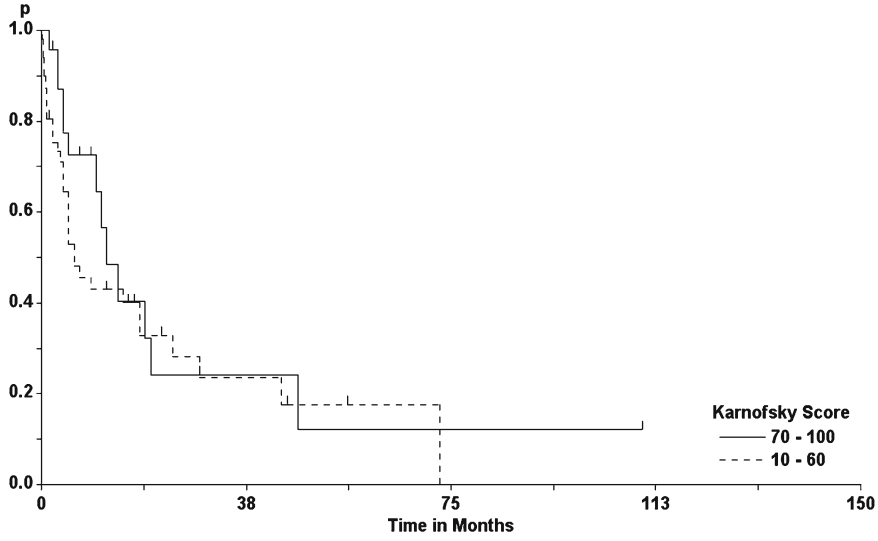

Fig. 5.103. Survival rates of patients with spinal metastases, as a function of preoperative Karnofsky score (log-rank test: not significant)

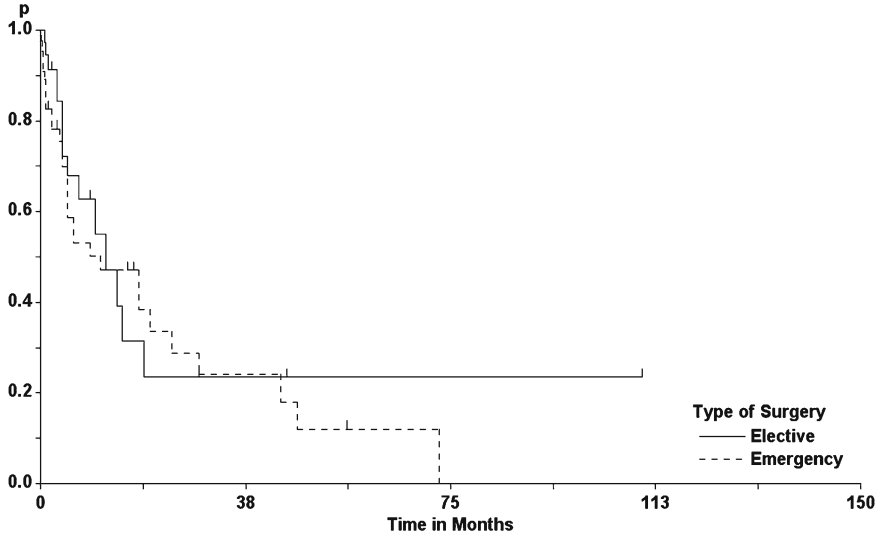

Fig. 5.104. Survival rates of patients with spinal metastases, as a function of elective or emergency surgery (log-rank test: not significant)

good preoperative clinical status (Fig. 5.103) [229, 239, 347, 534, 562]. Less important factors were a low spinal level of the metastasis, administration of postoperative radiotherapy, and elective surgery (Fig. 5.104; Table 5.33). Spinal instability and its management did not have an impact on postoperative survival in our experience. One study claimed that a rapidly progressing severe neurological deficit, a complete block on myelography, a pathological fracture, or additional metastases in other organs indicated a particularly bad prognosis [534]. This was not substantiated by our analysis. However, these factors do have a profound influence on the postoperative clinical course of the patient, as mentioned above. North et al. [401]

Table 5.33. Multivariate analysis for prediction of a long postoperative survival for spinal metastases

Factor	β-value
No local recurrence	0.4263
High preoperative Karnofsky score	0.2481
Low spinal level	0.1776
Elective surgery	0.1480
Radiotherapy	0.1082

Correlation coefficient: $r=0.6767$, $p<0.0001$

determined that surgery over more than two spinal segments, recurrent disease after radiotherapy, and cervical metastases as factors predicting a short postoperative survival time.

According to this analysis, we suggest the following guidelines for treatment of spinal metastases:

1. Patients in good health condition and living independently should undergo surgery for spinal metastasis if neurological symptoms are present. Postoperatively, adjuvant therapy should be initiated.
2. Patients with neurological symptoms but in a bad health condition requiring hospitalization for their cancerous disease independent of the spinal metastasis should not be operated, but offered vertebroplasty, radiotherapy, and/or chemotherapy as palliative measures.
3. Patients with spinal instability due to metastatic disease require stabilization to achieve a satisfactory neurological outcome. However, the surgical procedure has to be tailored according to the life expectancy and health status of the patient.
4. Patients without neurological symptoms or instability should undergo radiotherapy primarily unless the tumor is radioresistant.
5. Patients who deteriorate after or despite primary radiotherapy may be candidates for surgery. But higher complication and surgical mortality rates may have to be anticipated.

5.5.2.2 Chordomas

Chordomas arise from cell remnants of the notochord, and are found at autopsy in about 2% of patients [517]. They are slow-growing, malignant bone tumors with a high propensity for local recurrence. Systemic metastases occur in about 5–43% of patients [69, 133, 235, 271, 316, 336, 451, 475, 480, 517, 566]. They represent 2% of spinal tumors [517] and about 1–4% of malignant bone tumors [517]. In a survey of 400 patients with chordomas treated in the United States between 1973 and 1995, a male predominance was found and the incidence calculated as 0.08/100000 [366]. About half of them are encountered in the sacrum (Figs. 5.30, 5.31, and 5.56), 35% in the area of the clivus and the remaining 15% in the mobile segments of the spine (Fig. 5.57) [24, 99, 226, 271, 366, 517, 540]. The incidence of chordomas increases with age, but they may affect patients of all ages with a male predominance [15, 24, 69, 226, 235, 271, 339, 366, 469, 475, 480, 517, 522]. Sacral chordomas tend to affect mainly elder patients, whereas younger patients more commonly present with clivus chordomas [366].

Local pain is the predominant symptom for most patients with chordomas of the spine. About two-thirds develop additional neurological symptoms, as the tumor may display a significant soft-tissue extension and infiltrate the nerve sheaths of spinal nerves [521, 576].

In this series, a total of 20 operations for spinal chordomas in 9 patients (3 females and 6 males) were performed, representing 6% of the spinal tumors encountered. We observed 1 cervical, 4 thoracic, 3 lumbar (Fig. 5.57), and 12 sacral chordomas (Figs. 5.30, 5.31, and 5.56; Table 5.34).

The first symptom noted for 17 tumors was local pain. Sensory deficits, dysesthesias, or sphincter disturbances were mentioned once each. After an average period of 7±13 months, all but one tumor had caused progressive neurological symptoms with either a sensory deficit (14 patients), motor weakness (9 patients), sphincter disturbances (9 patients), or gait ataxia (8 patients; Table 5.34).

Chordomas are notoriously difficult to remove radically [254, 576]. They infiltrate and destroy bone. Soft-tissue extensions are delineated by a pseudocapsule. Inside the vertebral body, the tumor may be multilobulated, with nests of chordoma cells occurring between parts of healthy bone. The consistency of the tumor can be quite variable, from firm, ossified lesions to extremely soft tumors with cystic components harboring a mucoid substance [521]. During surgery, tumor cells may contaminate the surgical field. Therefore, no surgeon can be assured of a radical removal if the tumor is removed along macroscopic tumor margins or in piecemeal fashion (Figs. 5.30, 5.31, and 5.57).

The only chance for cure is an en bloc resection with a margin of healthy tissue [33, 176, 254, 271, 413, 509, 521, 571, 582]. In general, this can be achieved without significant morbidity below S3, provided the nerve roots of S1–S3 can be preserved at least on one [226, 339], but preferably on both sides (Fig. 5.56) [33, 117, 167, 176, 213, 413, 458, 469, 582]. Once the roots of S1 and S2 have to be sacrificed, a significant number of patients will develop persistent sphincter problems [117]. With resection involving the sacroiliac joint, lumbosacral stability and gait may be severely compromised. With even higher-reaching tumors, radical resections require sophisticated reconstructions and are associated with a significant number of patients remaining permanently immobilized. If pelvic organs are involved or the tumor extends into the lumbar spine, surgery will be unlikely to result in cure. There-

Table 5.34. Spinal chordomas

Sex	Age (years)	Level	History (months)	Symptoms	Therapy	Outcome
F	51	S3–S5	8	Hypesth., Dysesth., Pain, Sphincter	En bloc	Improved No Rec. in 153 months
M	62	S2–S5	2	Pain	En bloc	Improved No Rec. in 158 months
F	27	S1–S5	4	Dysesth., Pain	Complete	Improved Rec. in 4 months
	27	S1–S5	4	Hypesth., Dysesth., Pain	Complete	Improved Rec. in 1 month
	28	S1–S5	2	Pain, Sphincter	Complete	Improved Rec. in 6 months
	28	S1–S5	2	Hypesth., Motor, Pain	Subtotal, Radioth.	Improved Rec. in 42 months
	33	S1–S5	48	Hypesth., Dysesth., Motor, Pain	Decomp.	Unchanged Died 101 months after 1st surgery
M	69	S1–S5	10	Hypesth., Pain, Sphincter	Subtotal Radioth.	Improved No Rec. in 53 months
	72	Th8–Th9	3	Hypesth., Dysesth., Pain, Motor, Gait, Sphincter	Subtotal Radioth.	Improved No Rec. in 16 months
F	43	S4–S5	60	Hypesth., Pain	Subtotal	Improved Rec. in 1 month
	44	S4–S5	9	Hypesth., Pain	Subtotal Radioth.	Improved Rec. in 39 months
	47	S4–S5	3	Hypesth., Pain, Sphincter	Subtotal	Improved Rec. in 9 months
	48	S2–S5	6	Hypesth., Sphincter	Subtotal	Unchanged No Rec. in 10 months
M	31	L3	3	Hypesth., Dysesth., Pain, Motor, Gait	Complete	Improved No Rec. in 6 months
M	75	L2–L3	8	Pain, Motor, Gait	Subtotal	Unchanged Rec. in 2 months
	75	L2	1	Hypesth., Pain, Motor, Gait, Sphincter	Subtotal	Unchanged Died 14 months after 1st surgery
M	55	Th2–Th3	1	Hypesth., Pain, Motor, Gait, Sphincter	Complete	Improved Rec. in 6 months
	56	Th2–Th3	3	Motor, Gait, Pain, Sphincter	Complete Radiother.	Improved Rec. in 7 months
	57	Th2–Th3	2	Motor, Gait, Pain	Complete	Improved No Rec. in 36 months
M	28	C2–C4	8	Hypesth., Pain, Gait	Complete	Improved Rec. in 2 months Died after 8 months

Abbreviations: Radioth. = radiotherapy, Decomp. = decompression

fore, a surgical strategy should be chosen that ensures preservation of function in these cases. These require a combined approach, first anteriorly to secure the pelvic structures, and then posteriorly to remove the mass [57, 213, 429, 517].

En bloc resections for high-located sacral chordomas are controversial due to the associated morbidity and considerable complication rates of around 50% [33, 149, 176, 485, 509, 567, 569, 582]. From our point of view, such surgical strategies could only be justified if a high cure rate can be achieved. According to the reported numbers, however, this seems not to be the case:

Zileli et al. [582] performed 11 sacrectomies above S2. These operations took an average time of 13.4±4.4 h and were associated with a mean blood loss of 4518±1773 ml. Surgical mortality was 27%, with nine further complications. Overall, just 3 of these 11 patients are still alive with no disease. This type of surgery clearly demands a very high price from every patient.

Xu et al. [571] reported 41 sacral chordomas among a series of 87 patients with a mixture of different histologies. Twenty-five of the chordomas were located below S3 and removed using a posterior approach, while the remaining 16 above this level were operated with combined approaches. Survival statistics were not applied to determine recurrence or survival rates. Surgical mortality was 11.15% and there were six subsequent tumor recurrences in this series.

Bergh et al. [52] published their experience with 39 chordomas, of which 30 were located in the sacral and the remaining 9 in the mobile spine. Surgical margins were wide in 23, marginal in 6, and intralesional in 10 patients, with all but 4 operations intended as en bloc resections of the tumor. Local recurrences occurred in 40% of sacral and 55% of chordomas of the mobile spine, and metastases developed in 28%. No survival statistics were applied. There were ten tumor-related and ten tumor-unrelated deaths. Of the remaining 19 patients, 2 are living with disease and the remaining 17 without evidence of tumor. All but six of the survivors had undergone wide resections. In other words, with wide resections 12 of 23 patients, (52%) survived, compared to 6 of 16 (38%) after marginal or intralesional removals. The estimated 5- and 10-year survival rates were 84% and 64%, respectively. The authors strongly advocated aggressive surgical strategies with sacrifice of sacral nerve roots and considered the functional losses for their patients as acceptable.

York et al. [576] reported a series of 27 patients with sacral chordomas. These patients underwent a total of 67 surgical procedures. Twenty-eight operations were judged as radical resections, with the remaining 39 being subtotal removals. The median survival was 7.38 years, with four patients developing systemic metastases and five patients dying of unrelated causes. A total of 47 local recurrences were observed. The recurrence free-interval was correlated with the amount of resection and postoperative radiotherapy. After radical resections, the disease-free interval was 2.27 years, and after subtotal resections it was 8 months. With additional radiotherapy, the interval increased for subtotally removed chordomas to 2.12 years.

Baratti et al. [33] reported on 28 sacral chordomas. Surgical margins were wide in 11, marginal in 13, and intralesional in 4 patients; 17 recurrences were seen during a follow up of 15–200 months. Ten patients died, while nine patients currently remain free of disease. Wide resection margins were not associated with a lower recurrence rate compared to marginal resections combined with radiotherapy.

Cheng et al. [117] presented a series of 23 lumbosacral chordomas. Wide excisions were achieved in 7, resections with positive margins in 5, and intralesional resections in 11 patients. Overall, 86% survived for 5 years and there was a local recurrence rate of 40%. Survival was correlated with the upper limit of the tumor. Radicality influenced local recurrence rates only in nonradiated patients. Patients treated with postoperative radiotherapy showed similar recurrence rates than patients with wide excisions.

Ozaki et al. [413] reported 12 sacral chordomas, with radiotherapy applied to 1 unoperated patient only, who died of the disease 22 months later. Five had intralesional removals and the other six marginal resections. Five of these six patients are free of recurrence, with a follow up of 2–7.5 years, whereas four of those with intralesional resections are either dead or alive with a recurrence within 4 years after surgery.

With chordomas of the mobile spine, results for en bloc resections have also been published [2, 187, 346, 352, 449]. Boriani et al. [79] described 21 such patients and obtained their best results with en bloc resection followed by radiotherapy. In their series, 10 patients died 1–137 months postoperatively (mean 65 months), with 11 survivors, of which 7 were free of tumor recurrence.

Carpentier et al. [99] reported on 36 cervical chordomas and emphasized the importance of aggressive surgical strategies for long-term control and survival of these patients. Oncologic resections were not usually performed in their patients, but the vertebral artery and/or cervical roots were sacrificed in selected cases. Compared to more conservative strategies aiming at functional preservation, patients with aggres-

sive tumor removal had better long-term control (70% and 0% recurrence-free after 5 years, respectively) and survival rates (80% and 50% surviving 5 years, respectively). However, 2 early deaths were taken out of the analysis in the aggressively treated group of 22 patients!

Except for the cervical tumor, all chordomas in our series were removed via posterior approaches. En bloc resections were attempted if the tumor was localized in the sacrum but did not extend higher than S1 or into the pelvis. Whenever the tumor did not confine to these limits, en bloc resection was not intended. Preservation of sacral nerve roots S1–S3 for at least one side was attempted in every case. With this policy, two tumors were removed en bloc with a safety margin of healthy tissue (Fig. 5.56), eight tumors were removed completely along tumor margins (Figs. 5.30, 5.31, and 5.57), and the remaining ten tumors were removed subtotally. For three out of five patients with sacral tumors, repeated surgeries for a total of eight recurrences were performed. For two out of four patients with chordomas of the mobile spine, three tumor recurrences were operated subsequently. All of the patients retained sphincter control throughout their clinical course despite repeated surgeries. With the exception of one preoperatively paraplegic patient, all remained self ambulatory postoperatively. However, with each subsequent surgery, improvements of function were less pronounced and intervals until the next recurrence progressively shortened (Table 5.34). Unlike the case for chordomas of the clivus [73], a higher rate of complications was not seen for patients operated for a recurrent chordoma after previous radiotherapy. Except for one wound infection, no complications were encountered. Five operations were followed by radiotherapy using neutron, photon-beam, or conventional radiotherapy at dosages of 60–70 Gy. The average follow-up times were 64±58 months per patient and 31±45 months per tumor.

The postoperative course during the 1st year was analyzed for tumors with and without radiotherapy. Without radiotherapy, slight but not significant changes for pain, sensory deficits, and dysesthesias could be demonstrated. The Karnofsky score remained unchanged during this period (69±18 and 69±23, respectively). With radiotherapy, slight but not significant improvements were seen for pain, motor weakness, gait, sphincter functions, and the Karnofsky score, which increased from 60±14 to 75±10. This effect of radiation was mainly a consequence of prolonging the disease-free interval, as many tumors had recurred within a few months in nonradiated patients.

The overall 1- and 5-year recurrence rates for spinal chordomas were 65% and 75%, respectively (Fig. 5.105). A high preoperative and postoperative Karnofsky score, a sacral level of the tumor [235], a complete resection [24, 271, 517], and postoperative radiotherapy predicted a long recurrence-free interval according to our analysis. Almost every tumor eventually recurred unless en bloc resection or radiotherapy had been performed. Without radiotherapy, 75% of the tumors had recurred by 1 year, compared to 25% for patients who had received postoperative radiotherapy. Several studies have demonstrated the beneficial effects of postoperative high-dose radiotherapy for spinal chordomas [15, 24, 33, 119, 207, 235, 336, 342, 399, 403, 424, 429, 454, 475], particularly after the first operation [15, 403]. A dose-dependent response of chordomas to radiotherapy was emphasized repeatedly [342, 424, 454] and a total dose of at least 50–70 Gy is currently widely recommended [15, 102, 336, 342, 424, 454, 469, 480]. Postoperative radiotherapy also had a favorable influence on pain and neurological function [133, 342, 454, 480]. Gutin et al. [216] described their results with brachytherapy involving I^{125}, and reported stabilization of three out of five patients with chordomas.

To facilitate the application of high local radiation without damaging neighboring structures such as sacral nerve roots or the rectum, modern forms of radiotherapy such as proton-beam and photon-beam radiation are advocated [21, 102, 342, 389, 399, 403, 429, 450, 475, 480]. For cervical chordomas, a 10-year rate for local control of 54% was reported after proton-beam radiation [389]. Noel et al. [399] published a 3-year control rate of 71% and a 3-year survival rate of 75%. Rhomberg et al. [450] used photon-beam radiation augmented by a sensitizing agent in five patients. With a median follow up of 10 years, three of those patients currently remain alive and free of disease, with a minimum period of local control of 5 years. Catton et al. [102] treated 41 chordoma patients after surgery with photon-beam irradiation. A palliative effect for symptomatic patients was seen for pain only. Median survival in this group was 62 months, and the median time to clinical or radiological progression 35 months.

Promising results have been obtained recently with carbon ion radiotherapy [251, 482]. Schulz-Ertner et al. [482] reported a control rate of 81% for 3 years. Imai et al. [251] concentrated on 30 sacral chordomas and obtained a control rate of 96% for 5 years. These results indicate a superior effect for this modality compared to photon-beam radiation.

However, every radiated tumor except one had recurred after 39 months in our series (Fig. 5.106). This

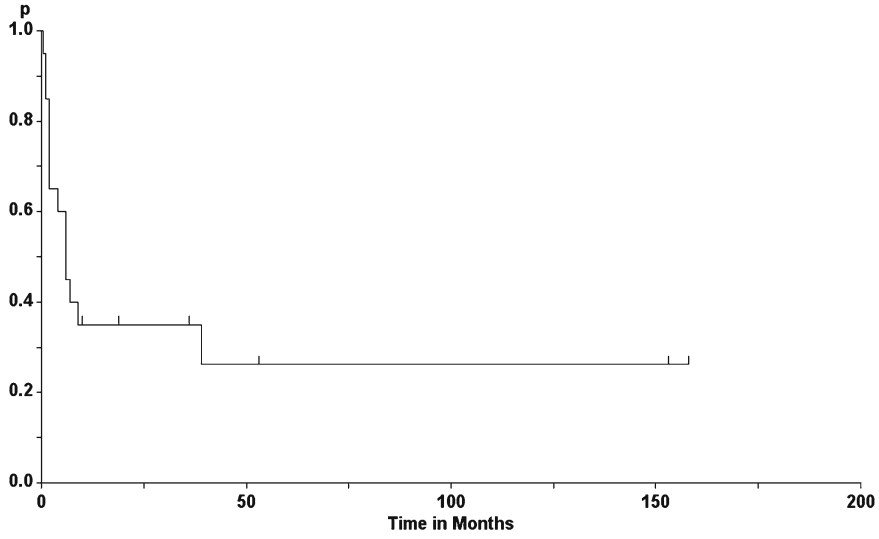

Fig. 5.105. Tumor recurrence rate for spinal chordomas

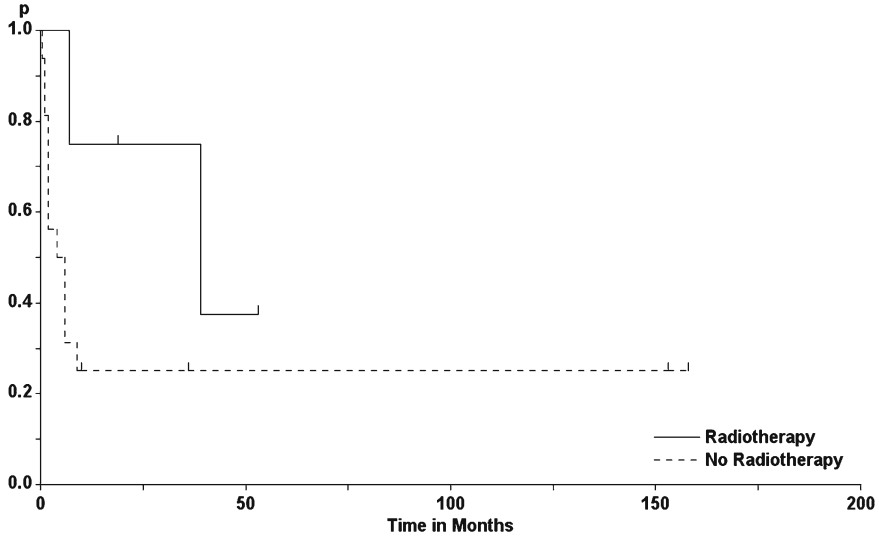

Fig. 5.106. Tumor recurrence rates for spinal chordomas, as a function of postoperative radiotherapy (log-rank test: not significant)

emphasizes the importance of a radical en bloc excision, even though such a resection does not guarantee recurrence-free survival: Kaiser et al. [271] reported a recurrence rate of 28% after successful en bloc resections. Similarly high recurrence rates are reported in the remaining literature [24, 33, 57, 69, 79, 119, 133, 176, 235, 254, 339, 342, 403, 411, 454, 475, 480, 515, 517].

Three patients in this series developed systemic metastases during their course of illness. They died from their disease 5, 14, and 101 months following their first operation. According to a Kaplan-Meier analysis, 5- and 10-year survival rates of 80% and 53%, respectively, were calculated.

Reviewing data of the National Cancer Institute in the United States, a survey of 400 patients treated between 1973 and 1995 for spinal as well as cranial chordomas were analyzed together [366]. The authors observed no significant differences between different tumor sites and calculated a median survival of 6.29 years, a 5-year survival rate of 67.6%, and a 10-year survival rate of 39.9%. For sacral chordomas, a recent report documented 5- and 10-year survival rates of 87.8% and 48.9%, respectively [33]. In the study by Cheng et al. [117], 86% of patients with lumbosacral chordomas survived for 5 years.

In summary, the reviewed literature and the results of our series support our strategy to perform en bloc

Fig. 5.107. Sagittal T1-weighted MRI with contrast (**a**) and T2-weighted (**b**) scan of a plasmocytoma at C2 with atlantoaxial dislocation in a 61-year-old man with multiple myeloma presenting with a short history of progressive swallowing problems and neck pain. **c** Axial T2-weighted image demonstrating the compression of the spinal cord. **d** Cranial T1-weighted contrast-enhanced scan disclosing another tumor in the parietal bone on the right side. The patient underwent occipitocervical fusion of C0–C5. The postoperative lateral (**e**) and anterior–posterior (**f**) X-rays show the position of the implants with a corrected position of C1 and C2. (*Continuation see next page*)

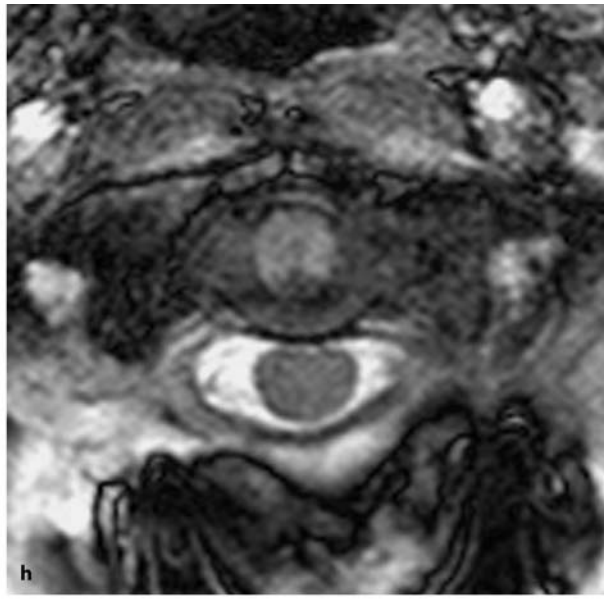

Fig. 5.107. (*Continued*) The postoperative sagittal (**g**) and axial (**h**) T2-weighted scans demonstrate a good decompression of the spinal cord. The patient's symptoms improved postoperatively. He was referred for radio- and chemotherapy

resections for tumors of the lower sacrum, and resections aiming at completeness of resection with preservation of function in the remaining cases. Postoperative radiotherapy should be applied whenever an en bloc resection is not performed.

5.5.2.3 Plasmocytomas

Plasmocytomas are malignant tumors that are derived from plasma cells and may occur either as solitary or multiple lesions (i.e., multiple myeloma). Plasmocytomas may involve any bone of the body. Even though they occur predominantly in elderly patients, children may also be affected [418, 483]. Among primary tumors of the spine, plasmocytomas account for up to 5% [540]. The majority of spinal plasmocytomas involve the thoracic spine [25, 110].

In general, patients with multiple myeloma are treated with radiotherapy and chemotherapy and are no candidates for surgical interventions unless a particular lesion has caused spinal instability (Fig. 5.107) [40, 503] or severe local pain requires a vertebroplasty [40, 189, 238, 442]. In a series of 114 patients with multiple myeloma, just 19 showed some degree of spinal cord compression [88]. In a more recent series, 20% of patients with multiple myeloma demonstrated cord compression [428].

On the other hand, Bataille et al. [41] described 114 patients with solitary plasmocytomas. Compared to patients with multiple myelomas, these patients were younger, predominantly male, and presented no monoclonal component on plasma electrophoresis [41, 106].

The radiological features on CT and X-ray studies may demonstrate a lytic lesion, a polycystic appearance, or a vertebral collapse (Figs. 5.107–5.109) [168]. Among patients with solitary plasmocytomas, between 30% and 50% will develop systemic disease after intervals of 1–8 years [26, 168, 298, 364]. With careful MRI examinations, Pertuiset et al. [428] observed multiple bone lesions in up to 30% of patients with assumed solitary plasmocytomas. MRI has to be considered the most effective imaging modality to detect further lesions in patients with plasmocytomas [49, 384]. MRI characteristics for plasmocytomas are low signal intensity on T1-weighted images, high signal intensity on T2-weighted images, curvilinear demarcations, and cortical irregularities [486].

Unfortunately, most studies combine patients with solitary lesions and multiple myeloma. Bisagni-Faure et al. [68] examined 184 patients with plasmocytomas and determined 22 with lesions causing spinal cord compression. One-half were treated with surgery followed by radio- and chemotherapy and the other half

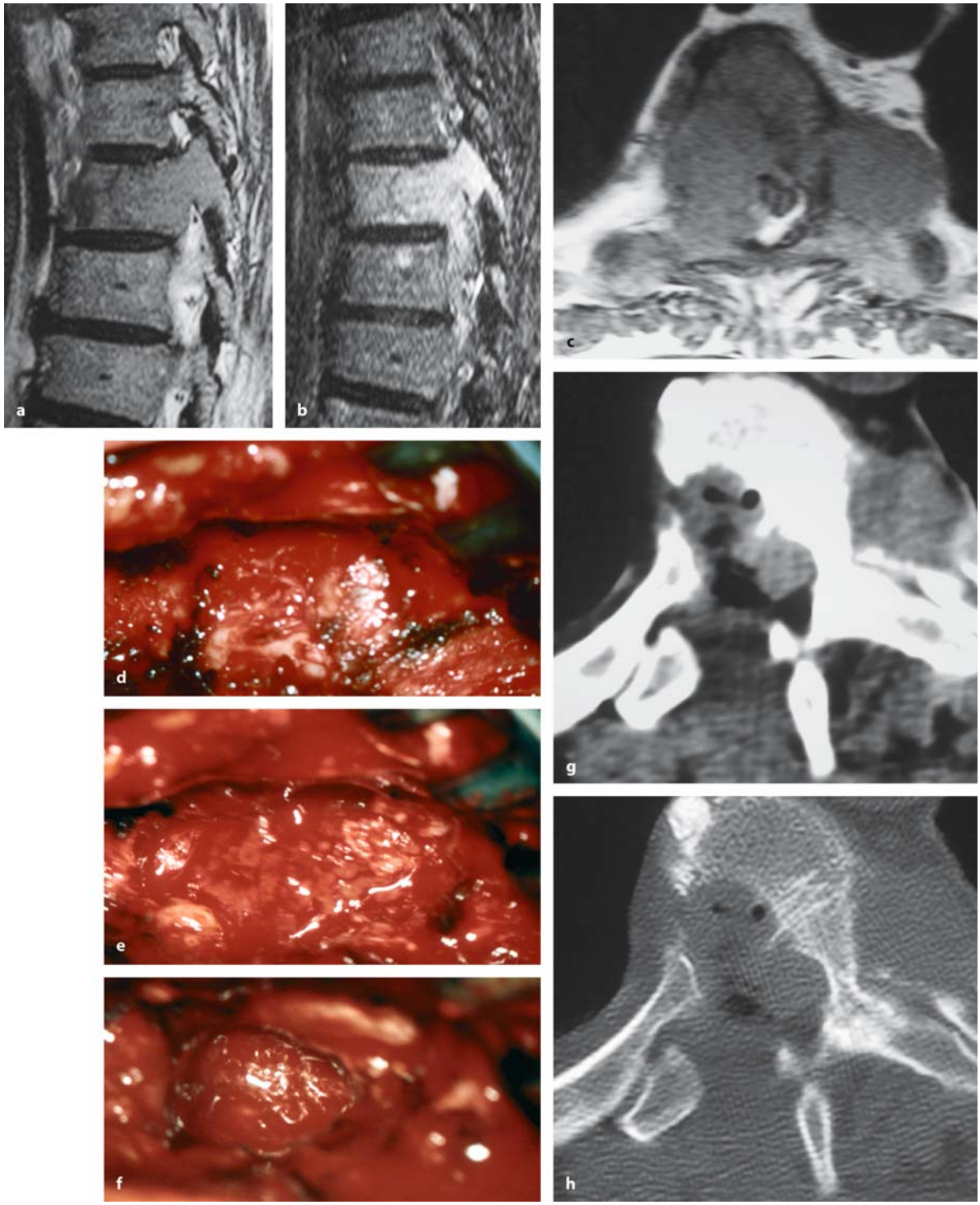

Fig. 5.108. Sagittal T1- (**a**) and T2-weighted (**b**) MRI scans of a solitary plasmocytoma at Th6 in a 68-year-old man with a short history of pain and progressive paraparesis. The tumor infiltration appears to be confined to the bone on these images. **c** Axial T1-weighted scan demonstrating considerable extraosseous extension with involvement of both pedicles and intraspinal tumor parts on the right side. **d** This intraoperative view after hemilaminectomy at Th6 demonstrates the epidural tumor part adherent to the dura. With resection of this part, the tumorous, enlarged pedicle (**e**) provides access for subtotal removal of tumor extensions in the vertebral body (**f**). The postoperative native (**g**) and bone-window CT scans (**h**) show the decompression of the spinal cord and degree of tumor resection. The patient improved postoperatively and underwent radio- and chemotherapy

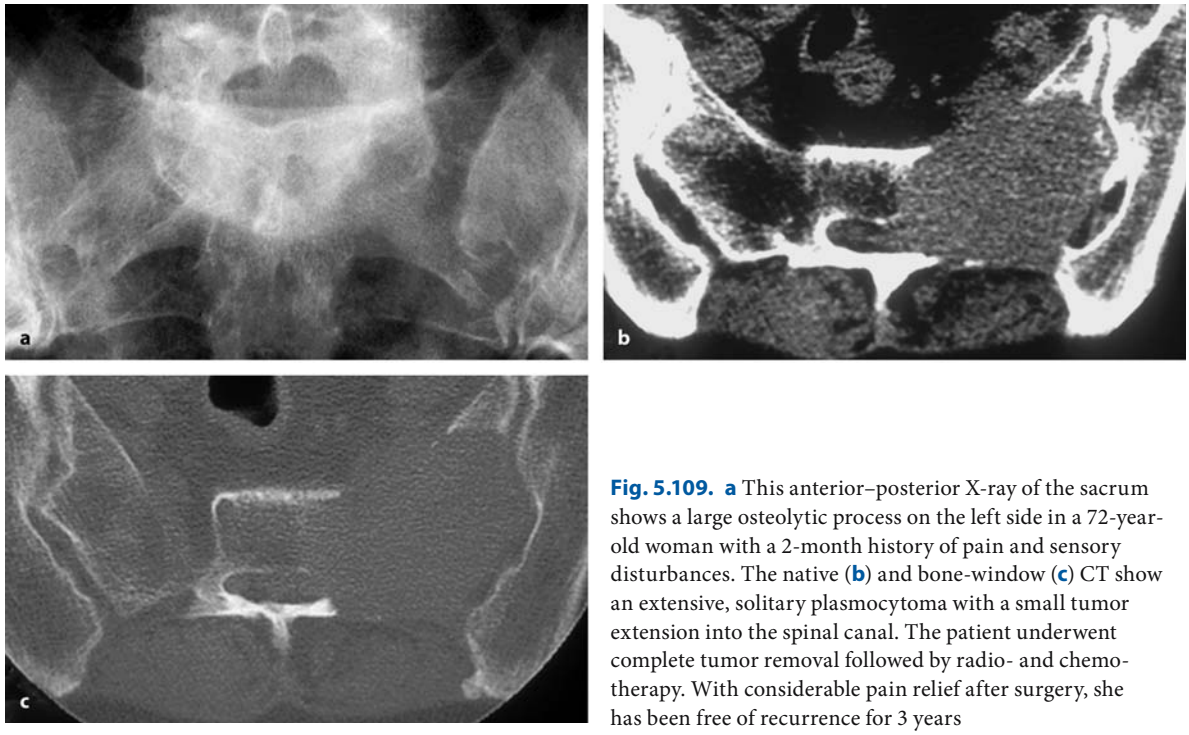

Fig. 5.109. a This anterior–posterior X-ray of the sacrum shows a large osteolytic process on the left side in a 72-year-old woman with a 2-month history of pain and sensory disturbances. The native (**b**) and bone-window (**c**) CT show an extensive, solitary plasmocytoma with a small tumor extension into the spinal canal. The patient underwent complete tumor removal followed by radio- and chemotherapy. With considerable pain relief after surgery, she has been free of recurrence for 3 years

by radio- and chemotherapy only. Except for patients with paraplegia, who did not recover regardless of the treatment modality, functional outcomes were better for the surgical group. The median survival time for this group was 30 months. Mill and Griffith [372] presented a series of 128 patients with multiple myeloma and 16 solitary plasmocytomas treated with radiotherapy. For solitary cases, mean survival was 5.5 years. Camacho et al. [96] observed 32 patients with spinal involvement among a total of 110 plasmocytomas. Among these, 3 had solitary and the remaining 29 had multiple lesions. Twelve patients demonstrated spinal cord compression and required surgical intervention. Mühlbauer et al. [385] described 17 patients who they operated from the posterior approach in a single stage involving tumor removal, spinal reconstruction, and fusion. One month after surgery, 82% were improved neurologically, with seven out of ten patients regaining their ability to walk. However, the mean survival was only 8 months in this group. Chataigner et al. [114] operated on 18 patients with plasmocytomas, of which 5 were solitary lesions. All complained of local pain, and seven patients presented with neurological deficits. Six operations were done from the anterior approach, five from a posterior approach, and seven as combined procedures. Postoperatively, nine patients died and there was a median survival of 15.4 months; the other nine patients are currently alive after a mean follow up of 57 months. Neurological symptoms improved in five of the seven patients, and the Karnofsky scores increased from 50 preoperatively to 77 at the latest follow up.

A few series focus on solitary plasmocytomas. Bacci et al. [26] presented a series of 15 patients; of these, 11 had spinal cord compression. Eleven patients were treated with radiotherapy alone, while 4 underwent surgery before radiotherapy. Seven patients are alive 3–9 years later, while the other eight progressed to multiple myeloma and died. Chang et al. [110] presented a series of 19 solitary plasmocytomas treated with radiotherapy. They claimed local control in all cases and observed two patients progressing to multiple myeloma, with 9 survivors for 7–77 months. They concluded that radiotherapy is the treatment of choice and recommended chemotherapy for recurrences and disseminated lesions.

A comparison of the results of different series leaves no doubt that the best outcome is achieved with a multimodality treatment [323]. In the series of Delauche-Cavallier et al. [139] describing 19 patients with solitary lesions, 11 were operated, 18 underwent radiotherapy, and 8 underwent chemotherapy; 85% of these patients were alive 10 years later. Local recur-

Table 5.35. Spinal plasmocytomas

Sex	Type	Age (years)	Level	History (months)	Symptoms	Therapy	Outcome
M	Multiple myeloma	56	C3 Unstable	1 Preop. Radiother.	Pain	Subtotal Recon. + Fusion	Improved Lost to follow up
F	Multiple myeloma	70	C5–C6 Unstable	60	Motor, Gait, Pain	Subtotal Recon. + Fusion; Chemo. + Radiother.	Improved No Rec. in 27 months
F	Solitary	71	Th4	2	Hypesth., Dysesth., Pain, Motor, Gait	Subtotal; Chemo + Radiother.	Improved No Rec. in 2 months
F	Solitary	57	C2 Unstable	24	Pain	Subtotal Recon. + Fusion; Chemo	Improved Rec. in 35 months
F	Solitary	72	L5–S5	2	Motor, Gait, Pain	Complete; Chemo. + Radiother.	Improved Rec. in 13 months Died after 27 months
M	Multiple myeloma	67	Th9	0.5	Hypesth., Motor, Gait, Pain, Sphincter	Subtotal	Surgical mortality
M	Solitary	39	L1	8	Pain	Subtotal	Surgical mortality
M	Solitary	65	Th6	2	Hypesth., Motor, Gait, Pain	Subtotal; Chemo. + Radioth.	Improved No Rec. in 12 months
F	Solitary	60	Th3–Th5	1	Hypesth., Gait, Pain	Subtotal; Chemo. + Radioth.	Improved No Rec. in 8 months
F	Solitary	64	Th6–Th9	0.5	Hypesth., Motor, Gait, Pain, Sphincter	Subtotal; Chemo.	Improved No Rec. in 5 months
M	Solitary	67	C6–Th2 Unstable	0.2	Hypesth., Motor, Gait, Pain	Subtotal Recon. + Fusion; Chemo. + Radioth.	Improved Lost to follow up
M	Multiple myeloma	53	C6–Th2 Unstable	4 Preop. Radiother.	Gait	Complete Recon. + Fusion; Chemo.	Improved Lost to follow up
F	Solitary	46	C2 Unstable	1	Pain	Subtotal Fusion; Radiother.	Improved Rec. in 17 months Died after 18 months
F	Solitary	72	S1–S3	2	Hypesth., Gait, Pain	Complete; Chemo. + Radiother.	Improved Rec. in 3 months Alive after 36 months

Abbreviations: Chemo. = chemotherapy, Recon. = vertebral reconstruction

Table 5.35. (*Continued*)

Sex	Type	Age (years)	Level	History (months)	Symptoms	Therapy	Outcome
M	Solitary	61	Th2	36	Pain, Gait	Subtotal; Chemo. + Radiother.	Unchanged Lost to follow up
M	Multiple myeloma	56	L5	36	Pain, Gait	Subtotal; Chemo. + Radiother.	Unchanged Lost to follow up
F	Multiple myeloma	74	C2 Unstable	0.5	Dysesth., Pain, Gait	Subtotal Fusion	Surgical mortality
F	Solitary	66	Th4 Unstable	12	Pain	Complete Recon. + Fusion; Radiother.	Improved
M	Solitary	68	Th6	2	Hypesth., Motor, Gait, Pain, Sphincter	Complete; Chemo. + Radiother.	Improved Lost to follow up

rences were seen in 13 patients, mostly within 5 years. Again, plasma electrophoresis was helpful to determine those patients likely to develop systemic disease [139, 565].

In a series of 12 patients and a literature analysis of another 72 cases, McLain and Weinstein [364] determined a mean disease-free interval for patients with solitary plasmocytomas of 76 months and a 5-year disease-free survival rate of 60%. A total of 44% developed systemic disease 2–13 years after diagnosis. The authors recommended radiotherapy as the treatment of choice.

We have treated 19 patients with spinal plasmocytomas, of which 6 had multiple lesions at the time of presentation. Among the 13 patients with solitary plasmocytomas, three developed multiple myeloma at a later stage. We observed an equal sex distribution, and the mean age at diagnosis was 62±10 years after an average history of 11±17 months. No difference in preoperative clinical data was found on comparing patients with solitary lesions and those with multiple myeloma, with the exception of instability, which was encountered more often in multiple myeloma patients and reflects our surgical policy to treat only patients with instability. With the exception of one patient describing motor weakness as the first symptom, all others complained about local pain as the first clinical manifestation of the spinal tumor. By the time of the operation, pain was still the predominating clinical problem for 69%, with 26% and 5% complaining mainly about gait problems and motor weakness, respectively. We encountered five cervical (Fig. 5.107), two cervicothoracic, eight thoracic (Fig. 5.108), two lumbar tumors, one lumbosacral, and one sacral tumor (Fig. 5.109). Two patients had undergone radiotherapy before. The plasmocytomas were removed completely in 26% of cases, and the remainder were removed subtotally. Vertebral reconstruction was done in seven patients with either iliac crest bone (four patients), PMMA (two patients), or a titanium cage (one patient). Eight patients presented with spinal instability and underwent fusion. Postoperatively, ten patients received a combination of radio- and chemotherapy after surgery, while the remainder underwent either chemo- or radiotherapy (Table 5.35).

Due to the limited number of patients, no separate analyses were performed for solitary plasmocytomas and multiple myelomas. The average preoperative Karnofsky score of 66±17 improved postoperatively to 76±8 after 1 year (p=0.0309). Significant improvements were observed during this period for gait ataxia and pain (Table 5.36). According to Kaplan-Meier analysis, the local tumor recurrence rate was 20% within 1 year. Unfortunately, three patients died in the immediate postoperative period, due to pulmonary embolism in two instances and fatal septicemia in the third patient. The proportions of those patients still alive at 1 and 3 years postoperatively were 84% and 52%, respectively (Fig. 5.110).

Symptom	Preop. status	Postop. status	3 Months postop.	6 Months postop.	1 Year postop.
Pain	2.3±0.5	3.6±0.5	3.9±0.4	4.1±0.7	3.9±0.7**
Hypesthesia	4.1±1.1	4.4±0.8	4.4±0.8	4.4±0.8	4.4±0.8
Dysesthesias	5.0	5.0	5.0	5.0	5.0
Gait	3.6±1.6	4.1±1.2	4.3±1.0	4.3±1.0	4.3±1.0*
Motor power	4.3±1.0	4.6±0.8	4.9±0.4	4.9±0.4	4.9±0.4
Sphincter function	5.0	5.0	5.0	5.0	5.0
Karnofsky score	66±17	71±15	74±10	77±8	76±8*

Statistically significant difference between preop. status and 1 year postop. and 6 months postoperatively, respectively: *p<0.05, **p<0.01

Table 5.36. Clinical course for patients with spinal plasmocytomas

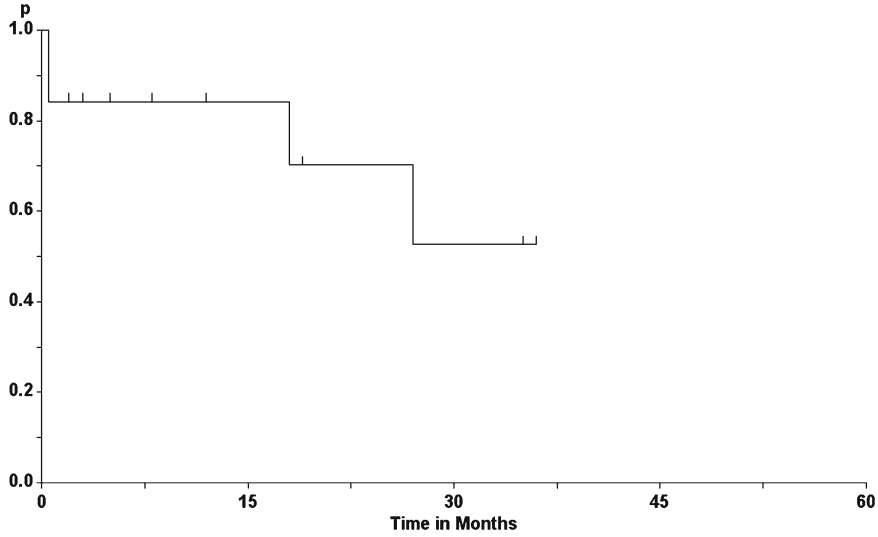

Fig. 5.110. Survival rate for spinal plasmocytomas

5.5.2.4 Chondrosarcomas

Chondrosarcomas are chondrogenic tumors and affect either the skull base (in 90% of cases) or the mobile spine (in about 10% of patients) [82]. They occur predominantly in males and local recurrences are common [53]. Chondrosarcomas affect predominantly adults, but have been described in children [19, 303]. They primarily involve bony structures, but may demonstrate considerable extraspinal extensions (Figs. 5.111 and 5.112) [1] or may metastasize to the epidural space [319, 434, 448]. Spinal involvement is associated with a bad prognosis compared to cranial forms. In recurrent cases, chemotherapy and radiotherapy are recommended [19]. The proliferation marker Ki 67 appears to have prognostic significance [464]. The tumors may display myxoid changes, calcifications, and ossifications [521].

We have observed six patients with chondrosarcomas of the spine. Four involved the thoracic spine (Figs. 5.111 and 5.112) and one each the cervical and lumbar spine. They presented at an average age of 51±10 years after a history of 3±3 months. The clinical course was quite variable, with patients complaining about pain (38%), motor weakness (23%), gait problems (15%), a local swelling (15%), or dysesthesias (8%) as the first clinical symptom. At presentation, gait problems were the major concern for three patients and pain for the remainder. The mean Karnofsky rating at presentation was 59±19. Posterior spinal elements were mainly affected in all but one tumor, which was removed via a combined transthoracic approach and followed with posterior fusion (Table 5.37).

In our series, complete resections at first surgery were obtained in all three instances, while secondary

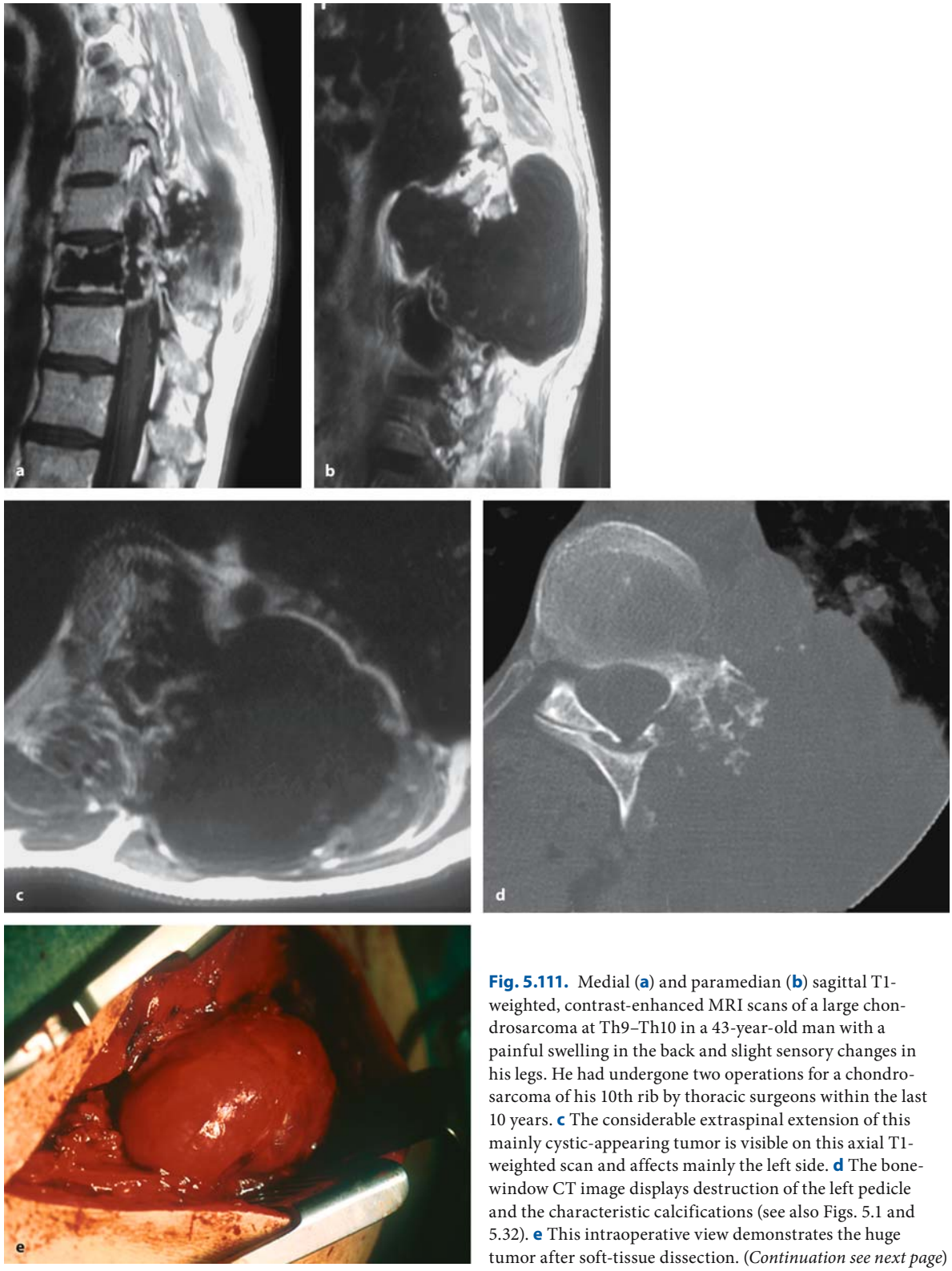

Fig. 5.111. Medial (**a**) and paramedian (**b**) sagittal T1-weighted, contrast-enhanced MRI scans of a large chondrosarcoma at Th9–Th10 in a 43-year-old man with a painful swelling in the back and slight sensory changes in his legs. He had undergone two operations for a chondrosarcoma of his 10th rib by thoracic surgeons within the last 10 years. **c** The considerable extraspinal extension of this mainly cystic-appearing tumor is visible on this axial T1-weighted scan and affects mainly the left side. **d** The bone-window CT image displays destruction of the left pedicle and the characteristic calcifications (see also Figs. 5.1 and 5.32). **e** This intraoperative view demonstrates the huge tumor after soft-tissue dissection. (*Continuation see next page*)

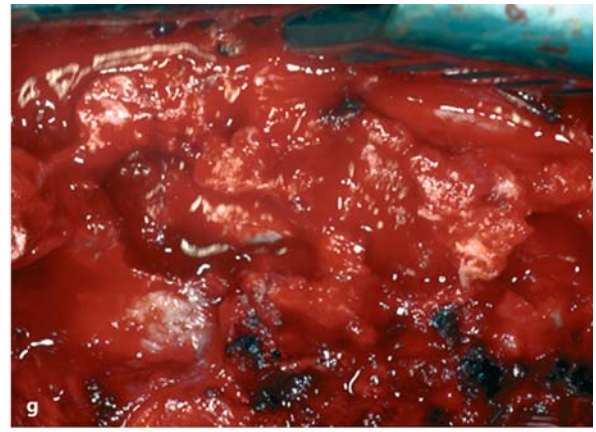

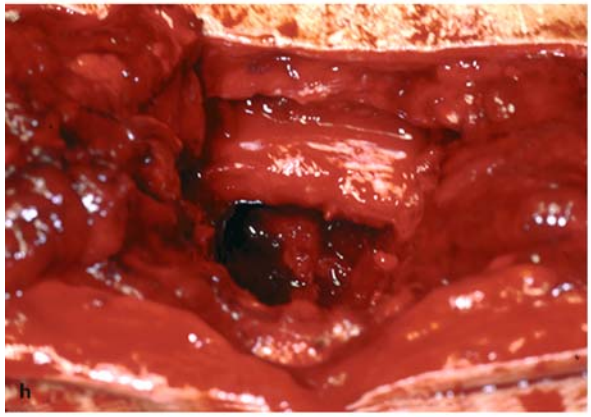

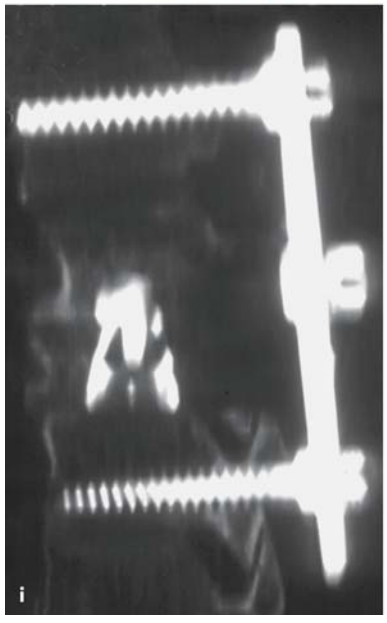

Fig. 5.111. (*Continued*) The large cystic mass was evacuated (**f**) and removed to gain access to the left pedicle of Th10 and the intraspinal tumor at Th9 (**g**). After resection of the epidural part and most of the body of Th10 (**h**), a cage was implanted followed by transpedicular fixation of Th8–Th11. **i** The postoperative sagittal CT reconstruction demonstrates a good decompression of the spinal canal. The patient experienced considerable pain relief with unaltered sensory changes. **j** Despite postoperative photon-beam radiation, an intraspinal epidural recurrence developed 6 months later

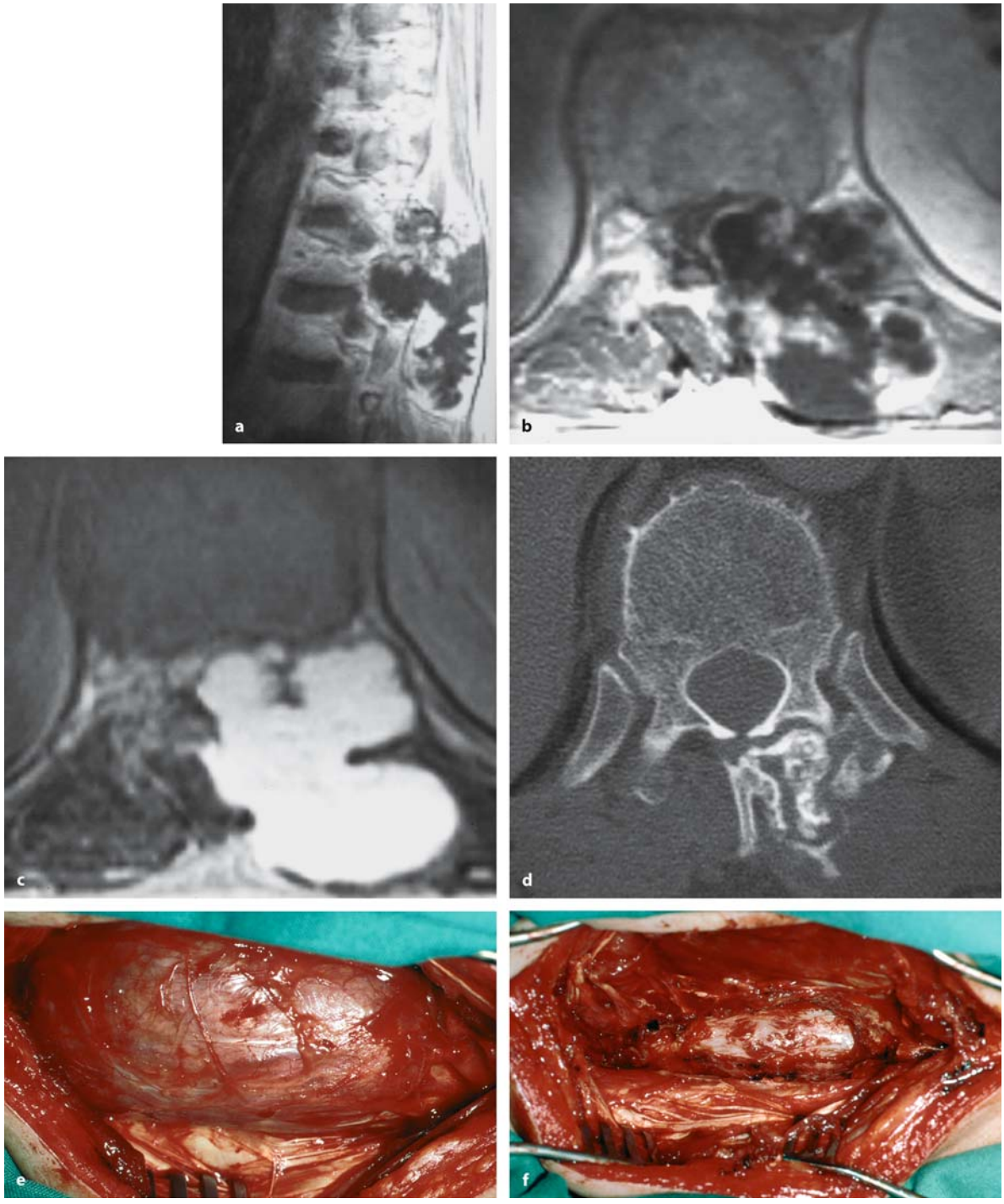

Fig. 5.112. Sagittal (**a**) and axial (**b**) T1-weighted, contrast-enhanced MRI scans of a chondrosarcoma at Th10–Th12 in a 66-year-old man with a 6-month history of pain and a slight paraparesis. The axial T1- (**b**) and T2-weighted (**c**) images show the amount of cord compression and extraspinal extension. **d** The bone-window CT image shows remarkably few osteolytic changes with extraosseous calcifications. **e** The intraoperative view demonstrates the large tumor after soft-tissue dissection. **f** This final intraoperative view demonstrates the complete resection of this tumor with what appears to be healthy margins. (*Continuation see next page*)

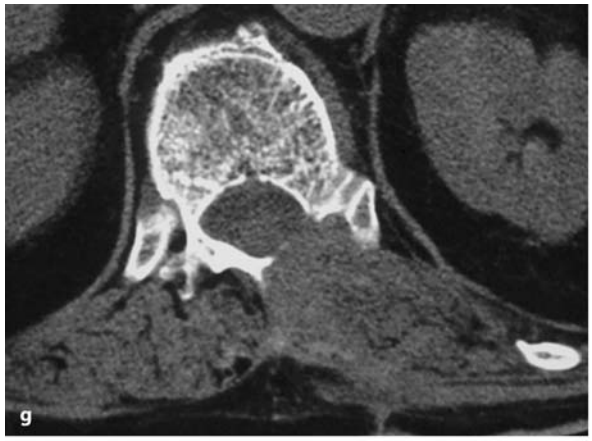

Fig. 5.112. (*Continued*) The postoperative CT (**g**) and T1-weighted MRI images (**h**) show a complete tumor resection. Postoperatively, the patient's symptoms improved; however, a local recurrence developed despite radiotherapy within 10 months

Table 5.37. Spinal chondrosarcomas

Sex	Age (years)	Level	History (months)	Symptoms	Therapy	Outcome
M	45	L2–3	12	Pain	Complete; Radiother.	Improved No Rec. in 19 months
F	64	Th11	3	Hypesth., Motor, Gait, Pain	Complete	Improved Rec. in 1 month
M	51	Th6 3 operations	8	Hypesth., Dysesth., Gait, Pain	Complete	Unchanged Rec. in 3 months
M	66	Th10–12	6	Hypesth., Motor, Gait, Pain, Sphincter	Complete	Improved Rec. in 3 months
	66	Th10–11	1	Hypesth., Motor, Gait, Pain	Complete	Unchanged Rec. in 5 months
	67	Th10	1	Hypesth., Motor, Gait, Pain, Sphincter	Subtotal	Unchanged
M	45	C7 3 operations Preop. Radiother.	0.5	Hypesth., Dysesth., Motor, Gait, Pain	Subtotal	Improved Rec. in 5 months
	46	C4–7	3	Hypesth., Dysesth., Motor, Gait, Pain	Subtotal	Unchanged Rec. in 16 months
	47	C2–Th1 Unstable	3	Hypesth., Motor, Gait, Pain, Sphincter	Subtotal Fusion	Unchanged Rec. in 6 months
M	42	Th9–11 2 operations	6	Dysesth., Pain	Complete	Improved Rec. in 8 months
	42	Th10	2	Hypesth., Dysesth., Motor, Gait, Pain, Sphincter	Subtotal Recon. ± Fusion; Radiother.	Improved Rec. in 6 months
	43	T10–L3	1	Hypesth., Dysesth., Motor, Gait, Pain, Sphincter	Subtotal; Radiother.	Improved Rec. in 4 months
	44	Th11–L5	0.5	Hypesth., Dysesth., Motor, Gait, Pain, Sphincter	Subtotal	Unchanged

Table 5.38. Clinical course for patients with spinal chondrosarcomas

Symptom	Preop. status	Postop. status	3 Months Postop.	6 Months postop.
Pain	3.7±0.5	4.0±0.6	4.2±0.4	3.8±0.8
Hypesthesia	3.5±1.1	3.8±1.0	4.0±0.9	3.5±1.2
Dysesthesias	4.3±0.5	4.5±0.6	4.5±0.6	4.5±0.6
Gait	3.7±1.4	4.0±1.1	4.2±0.8	3.8±1.5
Motor power	3.7±1.2	3.8±1.0	4.2±0.8	3.7±1.2
Sphincter function	4.5±1.2	4.7±0.8	4.8±0.4	4.5±1.2
Karnofsky score	70±17	72±13	77±10	70±19

Statistically significant difference between preop. status and 6 months postop. and 6 months postop., respectively: $^{*}p<0.05$, $^{**}p<0.01$

surgeries resulted in three complete (Fig. 5.112) and seven subtotal resections (Fig. 5.111). The postoperative benefits of surgery, however, were rather short-lived and not significant during the first 6 postoperative months. The average Karnofsky score of 70±17 improved for about 3 months, only to drop back to 70±19 after 6 months (Table 5.38).

The course of spinal chondrosarcomas is extremely variable depending on the biology of the tumor and the mode of treatment. With recurrent tumors, transformations to a more malignant histological and clinical picture have been described. Therefore, resection has to be as complete as possible the first time – preferably en bloc. If this cannot be done without unacceptable morbidity, postoperative radiotherapy with proton- and photon-beam radiation is recommended [521].

Shives et al. [498] reported the Mayo Clinic series of 20 patients with spinal chondrosarcomas treated with conventional surgery. Just 5 patients received postoperative radiotherapy; 15 of these patients died due to local progression after a mean survival period of 6 years. The 5-year survival rate in this series was just 55%. Likewise, Bergh et al. [53] observed a 5-year survival rate of 72% and a 10-year survival for 67%. On the other hand, Hirsh et al. [237] described a patient with involvement of the upper thoracic spine who survived for 18 years, requiring repeated operations illustrating a more benign behavior of some of these tumors.

Longer survival rates have been described after en bloc resections with adequate margins. Boriani et al. [82] observed 3 local recurrences among 15 patients undergoing en bloc resection of their tumors, with all but 1 patient alive at the follow up. On the other hand, intralesional surgery was invariably followed by recurrence, with eight out of ten patients dying in this series [82].

In another series of 21 spinal chondrosarcomas, 7 radical and 21 subtotal resections were achieved. Median survival was 6 years. Radiotherapy was administered in ten patients and prolonged the average disease-free interval from 16 to 44 months [575].

As for chordomas, proton- and photon-beam radiation has been recommended for chondrosarcomas of the skull base as well as of the spine [21, 389, 399, 521]. Unfortunately, many studies mix chordomas and chondrosarcomas together in their analyses. Compared to chordomas, the results of radiotherapy have been superior for chondrosarcomas [54, 389, 399]. Noel et al. [399] described a local control rate of 85% for 3 years and a 3-year survival rate of 88% after proton-beam radiation. Promising results have also been obtained with carbon ion radiotherapy [482].

In our series, all tumors recurred despite complete resections within 8 months unless postoperative radiotherapy was administered. For all subtotally resected tumors, recurrences were observed within 16 months with or without postoperative radiotherapy. Due to the small number of patients and the rather short follow up of 14±13 months, we cannot make any comments on postoperative survival figures for this group.

5.5.2.5 Lymphomas

The role of surgery in the treatment of spinal lymphomas is limited to establish an exact histological diagnosis and – on rare occasions – to achieve a rapid decompression of the spinal canal (Figs. 5.113 and 5.114) or stability of the spine (Fig. 5.115). The radiological features are quite variable. Lymphomas may appear like a metastasis with bone destruction and soft-tissue invasion (Fig. 5.115). Others look almost like a well-encapsulated epidural tumor (Fig. 5.114) or

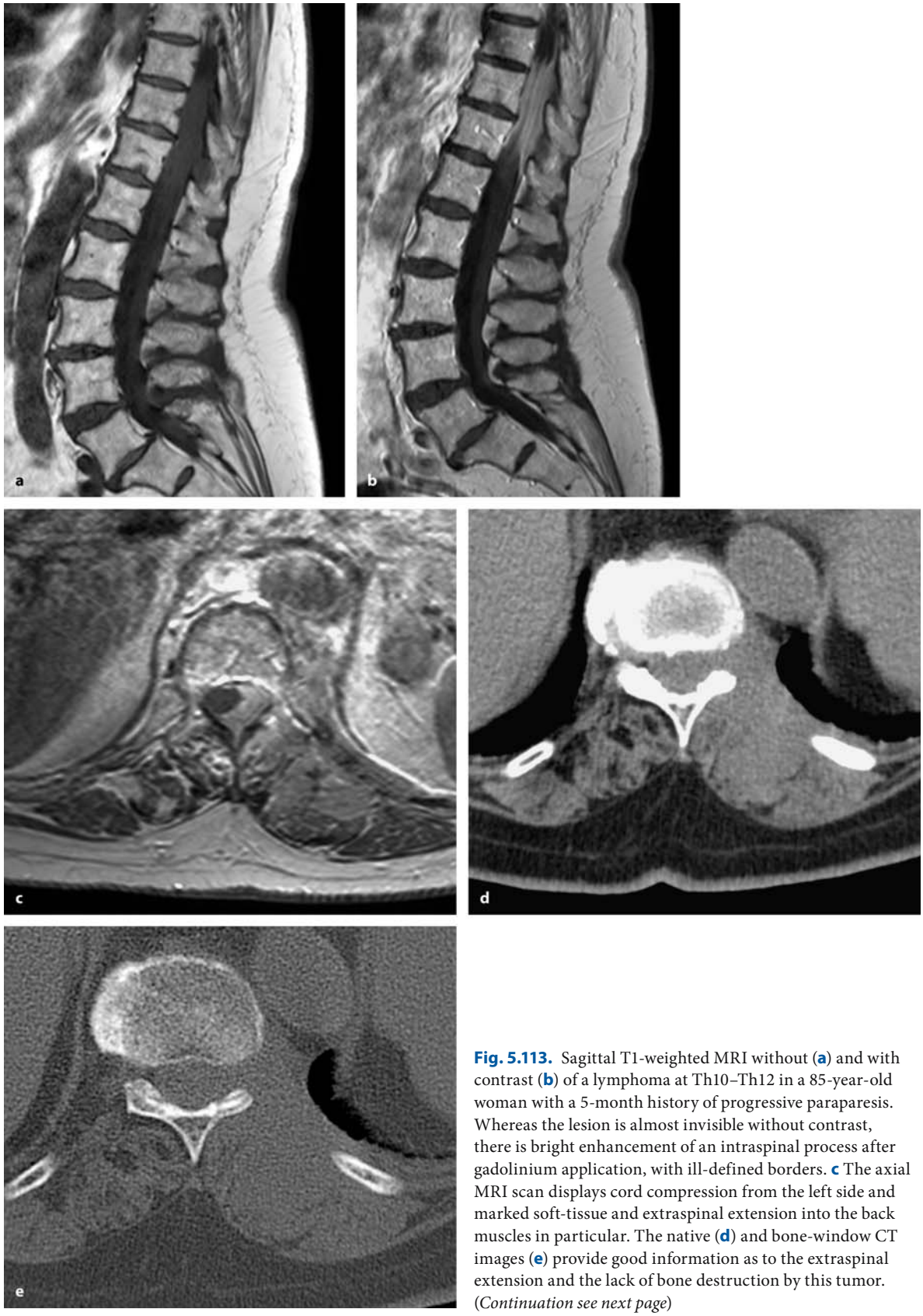

Fig. 5.113. Sagittal T1-weighted MRI without (**a**) and with contrast (**b**) of a lymphoma at Th10–Th12 in a 85-year-old woman with a 5-month history of progressive paraparesis. Whereas the lesion is almost invisible without contrast, there is bright enhancement of an intraspinal process after gadolinium application, with ill-defined borders. **c** The axial MRI scan displays cord compression from the left side and marked soft-tissue and extraspinal extension into the back muscles in particular. The native (**d**) and bone-window CT images (**e**) provide good information as to the extraspinal extension and the lack of bone destruction by this tumor. (*Continuation see next page*)

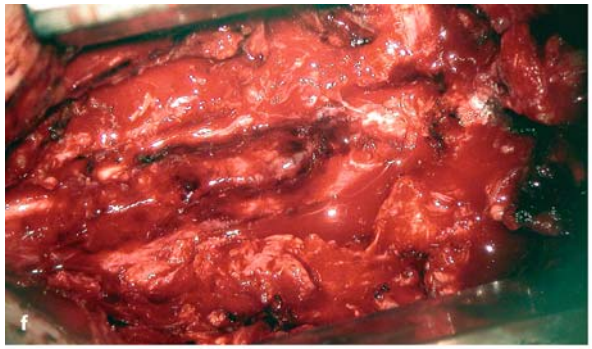

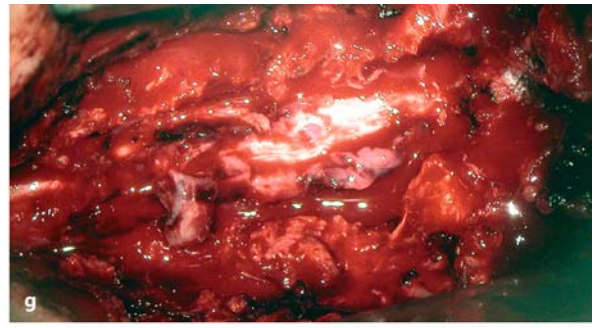

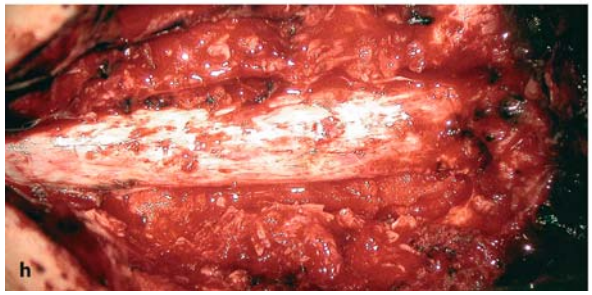

Fig. 5.113. (*Continued*) **f** This intraoperative view after laminectomy at Th10 and Th11 demonstrates the epidural space filled with tumor. With blunt dissection, this tumor could be separated form the dura (**g**) and the intraspinal part resected completely (**h**). Postoperatively, the patient showed neurological improvement, regained her walking ability, and underwent radiotherapy. Unfortunately, recurrent disease appeared after 5 months

Fig. 5.114. **a** Sagittal T1-weighted MRI scan of a lymphoma at Th3–Th4 in a 54-year-old man with a 4-week history of pain and slight gait ataxia. The lesion could be easily mistaken for an epidural schwannoma except for the signal changes in neighboring interspinous ligaments. The T2- (**b**) and T1-weighted, contrast-enhanced scans (**c**) demonstrate the lymphoma as a well demarcated solitary tumor in the spinal canal, but also diffuse tumor infiltration of the entire spine. (*Continuation see next page*)

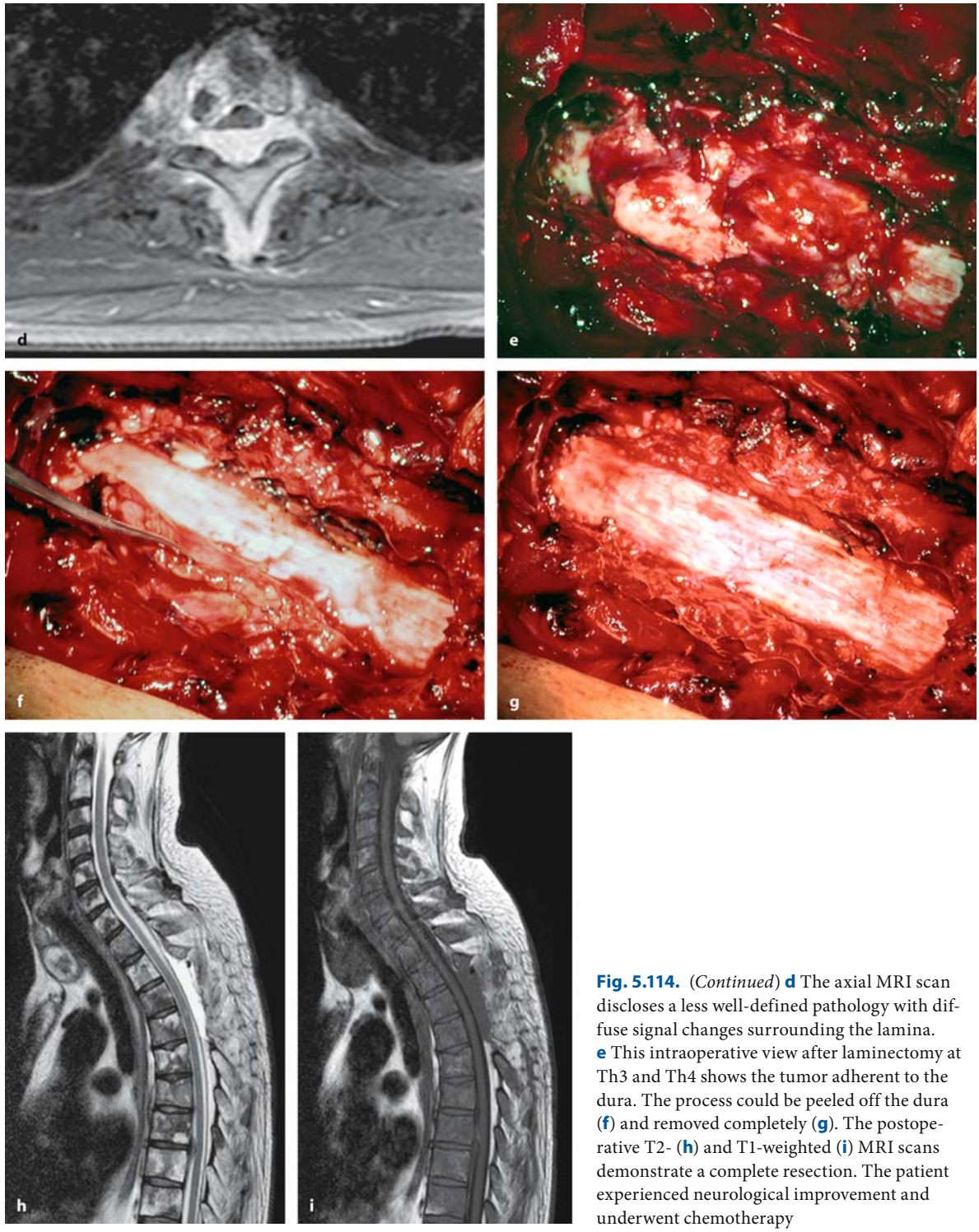

Fig. 5.114. (*Continued*) **d** The axial MRI scan discloses a less well-defined pathology with diffuse signal changes surrounding the lamina. **e** This intraoperative view after laminectomy at Th3 and Th4 shows the tumor adherent to the dura. The process could be peeled off the dura (**f**) and removed completely (**g**). The postoperative T2- (**h**) and T1-weighted (**i**) MRI scans demonstrate a complete resection. The patient experienced neurological improvement and underwent chemotherapy

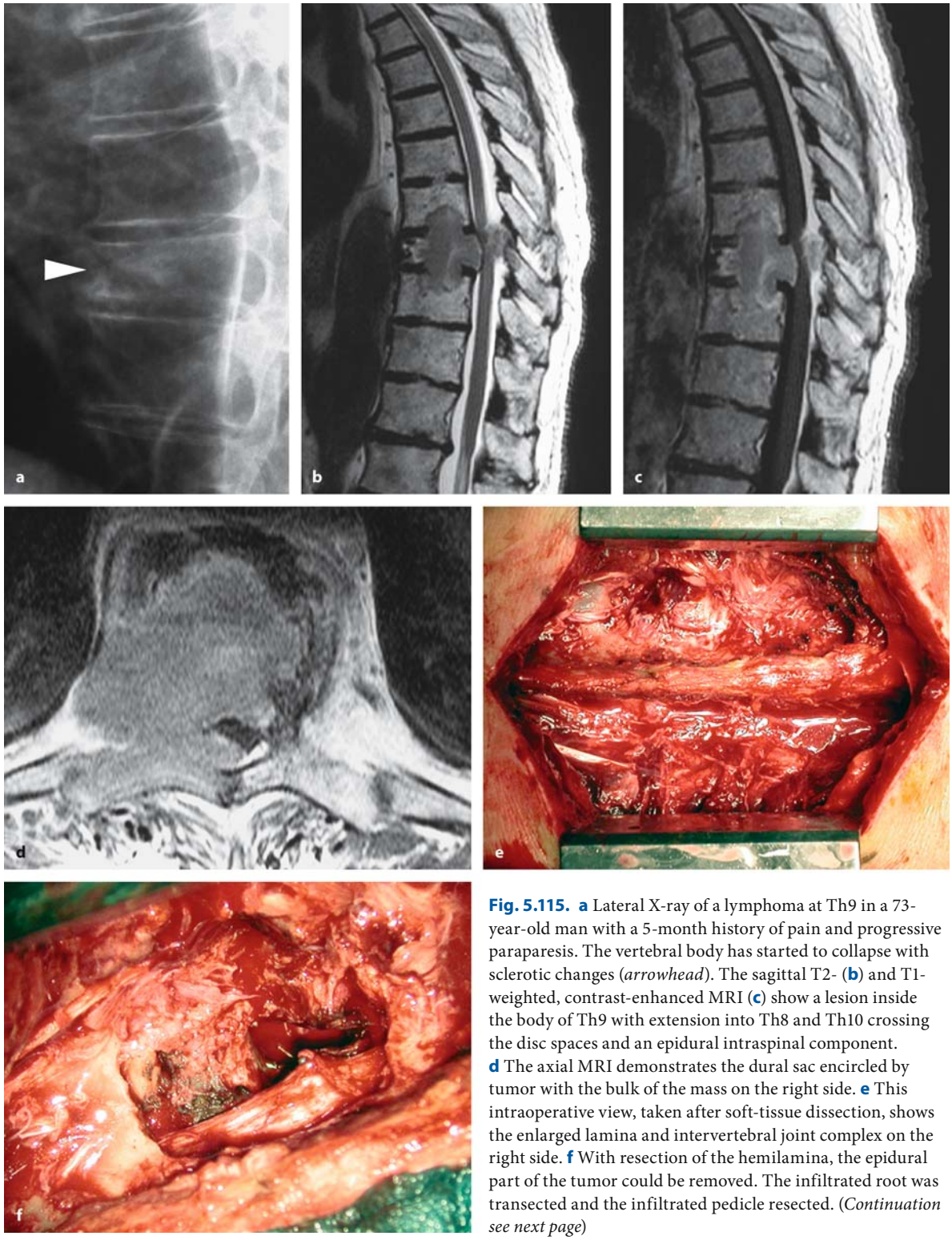

Fig. 5.115. **a** Lateral X-ray of a lymphoma at Th9 in a 73-year-old man with a 5-month history of pain and progressive paraparesis. The vertebral body has started to collapse with sclerotic changes (*arrowhead*). The sagittal T2- (**b**) and T1-weighted, contrast-enhanced MRI (**c**) show a lesion inside the body of Th9 with extension into Th8 and Th10 crossing the disc spaces and an epidural intraspinal component. **d** The axial MRI demonstrates the dural sac encircled by tumor with the bulk of the mass on the right side. **e** This intraoperative view, taken after soft-tissue dissection, shows the enlarged lamina and intervertebral joint complex on the right side. **f** With resection of the hemilamina, the epidural part of the tumor could be removed. The infiltrated root was transected and the infiltrated pedicle resected. (*Continuation see next page*)

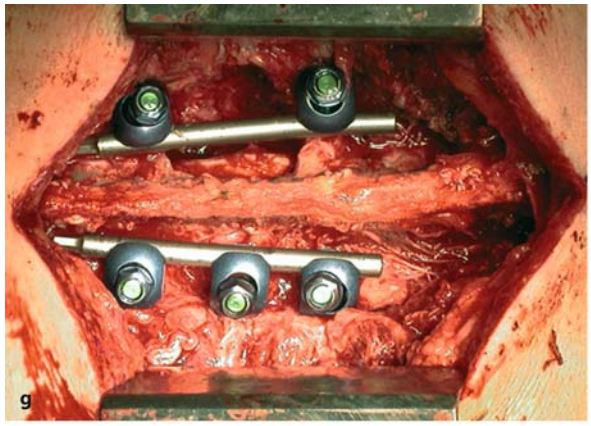

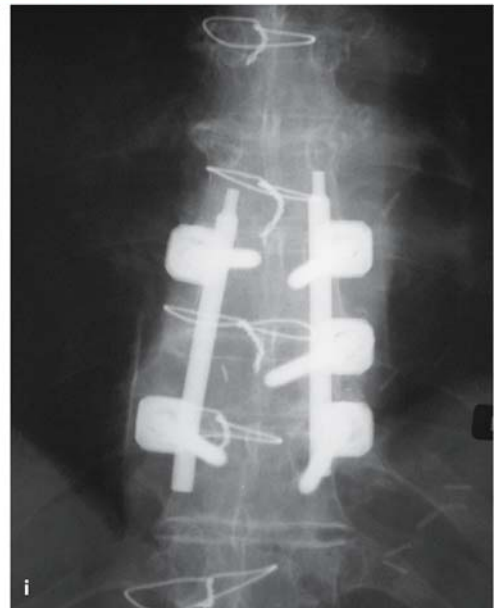

Fig. 5.115. (*Continued*) **g** Finally, a transpedicular stabilization of Th8–Th10 was performed. The postoperative lateral (**h**) and anterior–posterior (**i**) X-rays show the correct position of all implants. The wires were placed during a previous sternotomy for cardiac surgery. The patient experienced marked pain relief and neurological improvement after surgery and underwent radiotherapy

display ill-defined margins (Fig. 5.113). Osteolytic bone destruction, however, is absent. Radiotherapy and chemotherapy are the treatment modalities of choice [183]. A spinal presentation has been described in 4% of patients with lymphomas in a major series [107]. Zimmermann [583] examined 7000 tumors of the central nervous system and determined 208 lymphomas (3%) among these; 50% of the lymphomas were located in the brain. There were 57 spinal cases, either epidurally or in the vertebral bone, with primary as well as secondary metastases from other sites. The majority of spinal lymphomas are of the B-cell type [483]. A wide variety of ages may be affected, with children as well as people of advanced age [483]. Most lymphomas affect the thoracic spine [183].

In our series of eight patients, seven lymphomas were of the B-cell type, and one T-cell lymphoma was encountered. Patients presented at an average age of 56±15 years after a rather short history of 4±2 months. Half of the processes affected the thoracic spine (Fig. 5.113–5.115) and the other half the lumbar spine. All but one patient complained about pain initially. At presentation, every patient had developed rapidly deteriorating neurological deficits. A severe paraparesis was present in one patient. Except for one patient with multiple lymphomas, all others showed single lesions. The postoperative course is not related to the amount of resection. While two lymphomas were resected completely, six were subtotally removed to achieve a sufficient decompression of the spinal cord. All patients underwent postoperative oncological treatment (Table 5.39). Follow up was 14±35 months, with a maximum of 9 years. With one patient dying 6 weeks postoperatively, the small number of patients did not allow a meaningful analysis of local recurrence rates or survival figures.

Table 5.39. Spinal lymphomas

Sex	Type	Age (years)	Level	History (months)	Symptoms	Therapy	Outcome
M	B-cell Solitary	36	Th8–9	0.05	Hypesth., Motor, Gait	Subtotal; Chemo. + Radiother.	Improved No Rec. in 2 months
M	B-cell Multiple	68	Th5–7	6	Hypesth., Motor, Gait, Pain, Sphincter	Subtotal; Radiother.	Improved No Rec. in 2 months
F	T-cell Solitary	77	L4–5	6	Pain, Motor, Gait	Subtotal; Chemo + Radiother.	Improved Lost to follow up
F	B-cell Solitary	71	Th10–11	2	Motor, Gait, Pain	Subtotal; Chemo. + Radiother.	Unchanged Rec. + Died 2 months
M	B-Cell Solitary	46	L4–5	2	Dysesth., Gait, Pain	Complete; Chemo.	Improved Lost to follow up
F	B-cell Solitary	52	Th9–12	2	Hypesth., Gait, Pain	Complete; Radiother.	Improved Lost to follow up
F	B-Cell Solitary	41	L4–5	6	Dysesth., Motor, Pain	Subtotal; Chemo. + Radiother.	Improved No Rec. in 101 months
F	B-cell Solitary	60	L4–5	6	Motor, Gait, Pain	Subtotal; Chemo. + Radioth.	Improved Lost to follow up

5.5.2.6 Osteogenic Sarcomas

Among primary osteogenic sarcomas, spinal involvement is rare and found in only 2–4% of patients [233, 249, 431]. Barwick et al. [38] reviewed 1000 osteogenic sarcomas and observed 10 sarcomas in the spinal column. Three of those were related to Paget's disease. It is estimated that up to 10% of patients with Paget's disease will eventually develop an osteogenic sarcoma [145]. As Paget's disease rarely causes neurological symptoms, the appearance of neurological problems in a patient with this disorder should lead to further diagnostic measures [315]. Osteogenic sarcomas have been described after radiotherapy [513] and in former workers of plutonium plants [373]. Radiation-induced sarcomas tend to be associated with a particularly bad prognosis [513].

In a review on 4887 cases of osteogenic sarcomas treated in the Mayo Clinic, 4% (198) evolved primarily in the spine with an equal sex distribution [249]. The average age at presentation was 34.5 years, ranging from 8–80 years. Twenty-seven involved the cervical spine, 66 the thoracic, 64 the lumbar, and 41 the sacral spine. Two levels were affected in 17% of patients. Nonsacral tumors tended to affect the posterior elements predominantly (44 of 56); 84% invaded the spinal canal [249, 431].

We observed four patients with osteogenic sarcomas at ages 16, 45, 48, and 65 years. There was one Pancoast tumor extending from C7 to Th3, one extensive thoracic tumor at Th1/2 after radiotherapy for a thyroid carcinoma, one tumor involving the posterior elements of Th2 and Th3 (Fig. 5.116), and one large sacral sarcoma below S2 with intrapelvic extension. All patients presented with a rapidly progressive paraparesis and/or severe pain. The cervicothoracic tumors were resected partially in either a single or three subsequent operations. The thoracic and sacral tumors were removed completely using a marginal resection for the thoracic tumor and an en bloc resection for the sacral tumor. All patients underwent postoperative chemotherapy. The two partially resected tumors showed no response to adjuvant therapy and progressed within 7 months, leading to death 15 months after surgery in both instances. The two patients with completely resected tumors were free of disease 3 and 36 months after surgery (Table 5.40).

Even though isolated reports demonstrated a good response to chemotherapy alone [408], several studies have shown that en bloc resections of the involved vertebrae followed by adjuvant multimodality treatment provide the best chances of survival [2, 61, 126, 414, 537]. The best regimen may be a combination of preoperative chemotherapy after the diagnosis is proven by biopsy, followed by surgery – provided the clinical situation allows such a strategy [521].

Conventional radiotherapy has only a palliative effect [142]. A trial with charged particle radiotherapy

Fig. 5.116. Sagittal T2- (**a**), T1-weighted MRI scans without (**b**) and with contrast (**c**) of an osteogenic sarcoma at Th1 in a 65-year-old man with a 2-month history of pain and progressive paraparesis. On the T2-weighted image, the tumor appears as a hyperintense, circumscribed, epidural, intraspinal tumor with no apparent bone involvement. On T1, the tumor is isodense with bright, homogeneous contrast enhancement and a dural tail sign. **d** The axial scan discloses cord compression from posterior and the right side. **e** The bone-window CT scan shows calcifications in this tumor, but again no apparent bone destruction. (*Continuation see next page*)

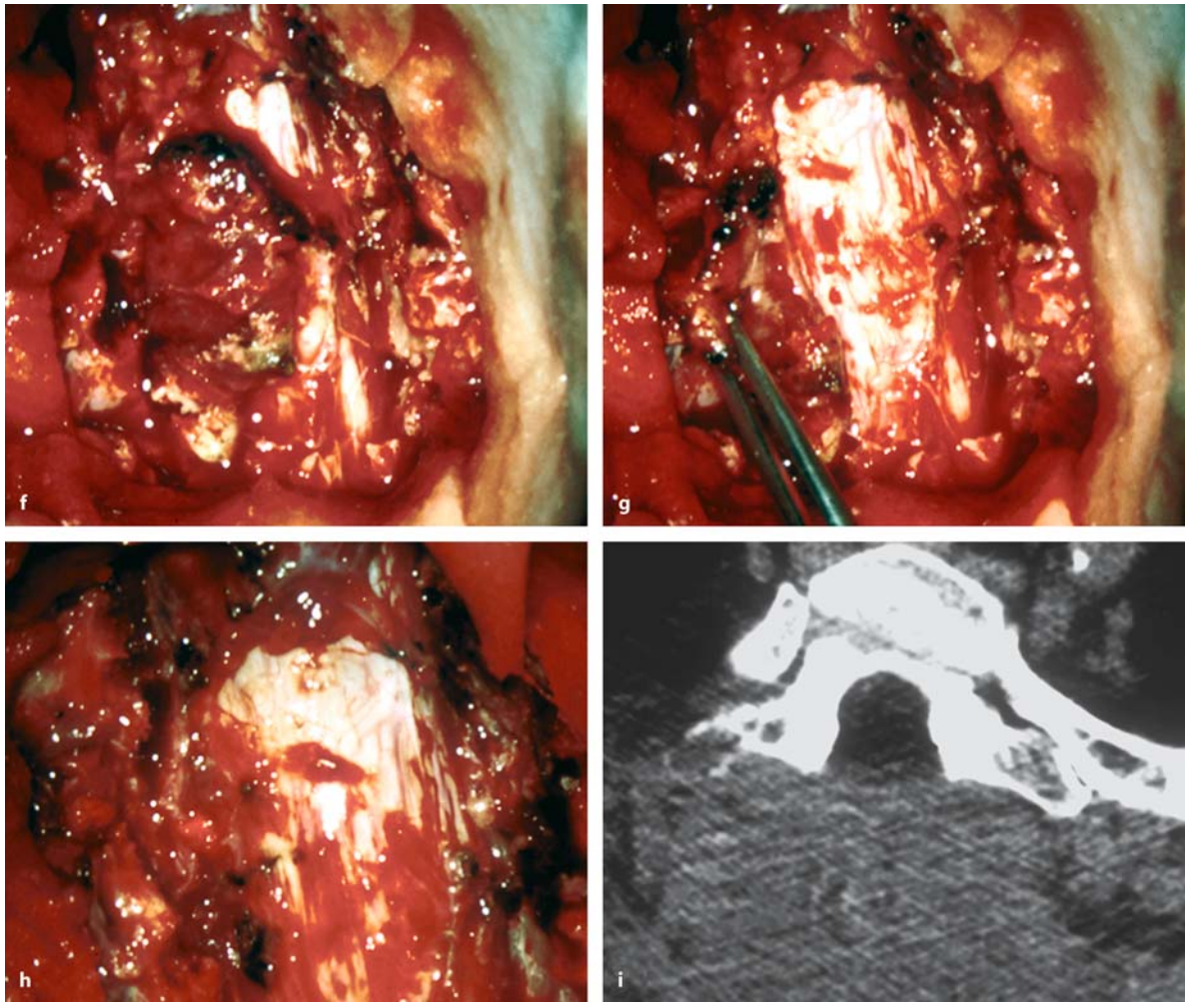

Fig. 5.116. (*Continued*) **f** This intraoperative view, taken with the patient in the semisitting position after laminectomy of Th1, demonstrates a well-demarcated tumor adherent to the dura. Blunt dissection of the tumor (**g**) allowed what appeared to be a complete resection (**h**). **i** The postoperative CT shows the surgical result. The patient improved postoperatively and was referred for further oncological treatment

achieved a 5-year local control rate of 48% [547]. Intralesional resections are followed by recurrences and further spreading of the tumor. Wide resection margins are advocated in case reports, even for secondary sarcomas [43]. However, metastases have been observed in patients with spinal osteogenic sarcomas in significant percentages of up to 34% [61, 414, 431], so that radical resections with the potential for cure can be reserved for patients with solitary tumors that do not show wide extensions into paraspinal tissues.

The most effective treatment for advanced and metastatic sarcomas is chemotherapy [414, 459]. In a study of 105 such patients responses were observed in 47% of patients. A tumor size of less than 5 cm and a history no longer than 1 year were factors predicting a good response with a median survival of 16 months [154]. In a more recent study on 22 cases, a median survival of 23 months was observed [414].

In a series of 66 primary osteogenic sarcomas of the spine, 80% demonstrated neurological symptoms, with a mean history of 7 months. The lumbar spine was the commonest localization. En bloc resections were performed for 25% of these patients and were preceded by chemotherapy. The largest group of osteogenic sarcomas were of the osteoblastic type and survived for a mean period of 17 months [281].

Bilsky et al. [64] reviewed 59 spinal sarcomas; of these, 7 were osteogenic sarcomas. Only nine cases were amenable to en bloc resections so that the overwhelming majority underwent intralesional resec-

Table 5.40. Spinal osteogenic sarcomas

Sex	Age (years)	Level	History (months)	Symptoms	Therapy	Outcome
M	16	C7–Th3 Pancoast tumor	1	Hypesth., Dysesth., Motor, Gait, Pain, Sphincter	Partial; Chemo.	Improved Rec. in 5 months Died after 15 months
F	45	Th1–2 Radiation-induced	3	Hypesth., Motor, Pain	Subtotal; Chemo.	Improved Rec. in 7 Months Died after 15 months
M	65	Th2–3	8	Hypesth., Dysesth., Motor, Gait, Pain, Sphincter	Complete; Chemo.	Unchanged No Rec. in 3 months
M	48	S2–S5	6	Pain	En bloc; Chemo.	Improved No Rec. in 36 months

tions. Thirty-five patients were operated once and 24 required repeated operations. The median age was 42 years, ranging from 6 to 79 years, with 25 primary spinal sarcomas and 34 metastatic lesions. After surgery 95% were ambulatory. The median disease-free period was 13 months and median survival 18 months, reflecting the small proportion (15%) of en bloc resections.

Talac et al. [528] observed a close correlation between surgical radicality and survival in their series of 30 patients with spinal sarcomas, in whom en bloc removals were obtained in 12 patients and piecemeal resections in 18 patients. Positive resection margins increased by fivefold the likelihood for a local recurrence, with 92% of patients with local recurrences dying within a mean interval of 16.6 months. Median survival times were 37 and 62 months for patients after piecemeal and en bloc resections, respectively.

Sundaresan et al. [516] published their series of 24 osteogenic sarcomas of the spine. Patient age ranged between 13 and 71 years, and 67% presented neurological symptoms. In 13 patients, partial resections were followed by radiotherapy. This strategy proved to be ineffective. In the second group of 11 patients, radical resections were obtained followed by chemotherapy and radiotherapy. One patient in this group developed metastases and five long-term survivors were observed.

5.5.2.7 Osteoblastomas

Osteoblastomas may occur in the spine and long bones of the lower extremities [353]. Patients under the age of 30 years are affected predominantly [326, 353, 581], but these tumors have also been described in elderly patients [343]. They occur more frequently in males compared to females by a ratio of 2:1 [76, 353, 397]. In most instances the posterior elements are involved (Fig. 5.117) [14, 205, 394, 397, 521, 581], whereas the vertebral body may be more commonly affected in the cervical spine [581].

Pain is the predominant clinical problem, and in young patients it is often accompanied by scoliosis [7, 378, 521]. The average history is 1.5 years [76, 353, 581]. With resection of the tumor, preoperative pain should be reduced dramatically [292, 353, 394]. Most studies emphasize that total removal has to be achieved to ensure local control [14, 322, 353, 521, 581], particularly for aggressive forms [477, 539]. With aggressive osteoblastomas, complete resections with a margin of healthy tissue have been recommended to prevent recurrence [539]. As these tumors may be extremely vascularized, preoperative embolization can be helpful [501]. On the other hand, several authors have also described good outcomes after incomplete resections [98, 353, 365, 394].

Despite being considered as benign tumors, osteoblastomas may behave as locally aggressive [48, 477] and progress to sarcomas [14]. In a review of 184 osteoblastomas, transformation to sarcomas was seen in 5 cases and were not restricted to radiated tumors. The overall recurrence rate was determined as 9.8% for osteoblastomas of all localizations, but was restricted to patients with incomplete resections. No recurrence was observed for completely resected tumors [260]. Late recurrences have been described to occur up to 17 years after surgery [48]. Radiotherapy is not effective [260, 353].

Nemoto et al. [397] reviewed 75 spinal osteoblastomas. Eighteen patients presented with neurological deficits and 17 with a scoliosis. They encountered 29 cervical, 16 thoracic, 17 lumbar, and 13 sacral tumors. With a short patient history, the chances of improv-

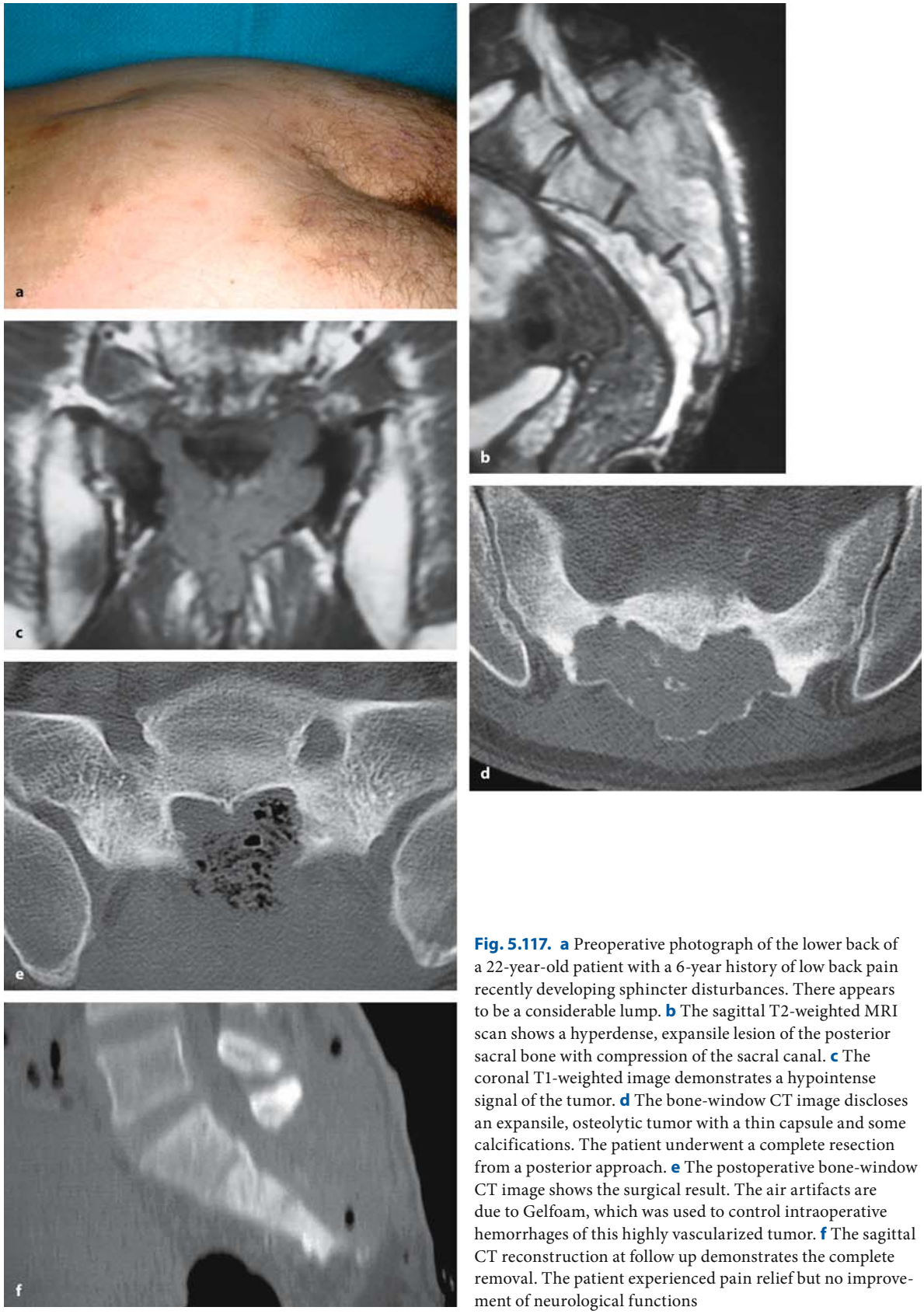

Fig. 5.117. **a** Preoperative photograph of the lower back of a 22-year-old patient with a 6-year history of low back pain recently developing sphincter disturbances. There appears to be a considerable lump. **b** The sagittal T2-weighted MRI scan shows a hyperdense, expansile lesion of the posterior sacral bone with compression of the sacral canal. **c** The coronal T1-weighted image demonstrates a hypointense signal of the tumor. **d** The bone-window CT image discloses an expansile, osteolytic tumor with a thin capsule and some calcifications. The patient underwent a complete resection from a posterior approach. **e** The postoperative bone-window CT image shows the surgical result. The air artifacts are due to Gelfoam, which was used to control intraoperative hemorrhages of this highly vascularized tumor. **f** The sagittal CT reconstruction at follow up demonstrates the complete removal. The patient experienced pain relief but no improvement of neurological functions

Table 5.41. Spinal osteoblastomas

Sex	Age (years)	Level	History (months)	Symptoms	Therapy	Outcome
F	20	Th9	15	Hypesth., Dysesth., Pain	Subtotal	Improved No Rec. in 163 months
F	5	C5	9	Dysesth., Motor, Pain	Complete	Improved No Rec. in 145 months
M	23	C2	60	Pain	Subtotal	Improved Lost to follow up
M	22	S1–S5	56	Hypesth., Pain, Sphincter	Complete	Improved Lost to follow up

ing a scoliosis by tumor removal are favorable [7, 430].

In a series on 30 spinal osteoblastomas, Boriani et al. [76] observed 16 tumors in the lumbar region, 8 in the thoracic region, and 6 in the cervical region, mainly involving posterior elements. Twelve patients presented with a painful scoliosis. Fourteen tumors were well defined and restricted to spinal bone, whereas 16 demonstrated some soft-tissue extension and ill-defined margins. Surgical results with intralesional resections were very good for all circumscribed tumors. For extensive tumors, additional radiotherapy was employed in nine patients. Radiation-induced ossification of the tumor remnants was seen in 80% of cases and considered a healed lesion. Sometimes this process was even sufficient to achieve a bony fusion. Nevertheless, aggressive forms were associated with a recurrence rate of 19%.

With respect to osteoblastomas in children, Amacher and Eltomey [14] reported eight patients with spinal osteoblastomas all of whom presented with local pain followed by either scoliosis or some other form of a pathological posture. Total excision prevented a recurrence in this series. All three incomplete resections were followed by recurrences within 2 years.

Rechl et al. [446] reported two patients with osteoblastomas of the sacrococcygeal region. Both patients underwent complete resections with immediate postoperative pain relief and no recurrences.

We have observed four patients (two males and two females) with osteoblastomas at ages 5, 20, 22, and 23 years. One tumor each was located in the thoracic spine and sacrum (Fig. 5.117) and two cervical tumors were encountered. All four patients complained predominantly about pain, with just three patients suffering minor neurological problems with preoperative Karnofsky scores between 70 and 80. Two tumors were resected completely and two subtotally. All patients showed postoperative improvement of pain and neurological symptoms (Table 5.41). In our series, all tumors underwent intralesional resection and curettage. While one cervical and the sacral tumor were removed completely, the other two underwent subtotal resection. No recurrences were observed with a maximum follow up of 14 years.

5.5.2.8 Aneurysmatic Bone Cysts

Aneurysmatic bone cysts affect children and young adults with a slight female predominance [275, 553]. Long bones, flat bones, and the spine may be affected [553]. The current concept considers this entity as a primarily vascular lesion [275] and describes it as an arteriovenous fistula that creates a reactive bone lesion related to hemodynamic forces [521]. Due to considerable bone destruction, vertebral fractures may occur [83, 328, 553]. The histological differentiation to osteoblastomas and giant cell tumors may be difficult [146, 371]. Posterior elements are affected predominantly, with expansion of the vertebral contour [83, 521].

We have seen four spinal aneurysmatic bone cysts in three patients: one child of 11 years and two adults in their 20s, of whom one had to be operated a second time on a recurrent tumor 30 months after a complete resection. Three tumors were located in the cervical spine (Fig. 5.118) and one in the upper thoracic spine. All patients were affected by local pain and just one presented with additional neurological symptoms (Table 5.42).

Complete resection is the treatment of choice and can be performed intralesionally [83, 275], although en bloc resections have also been advocated [328, 553].

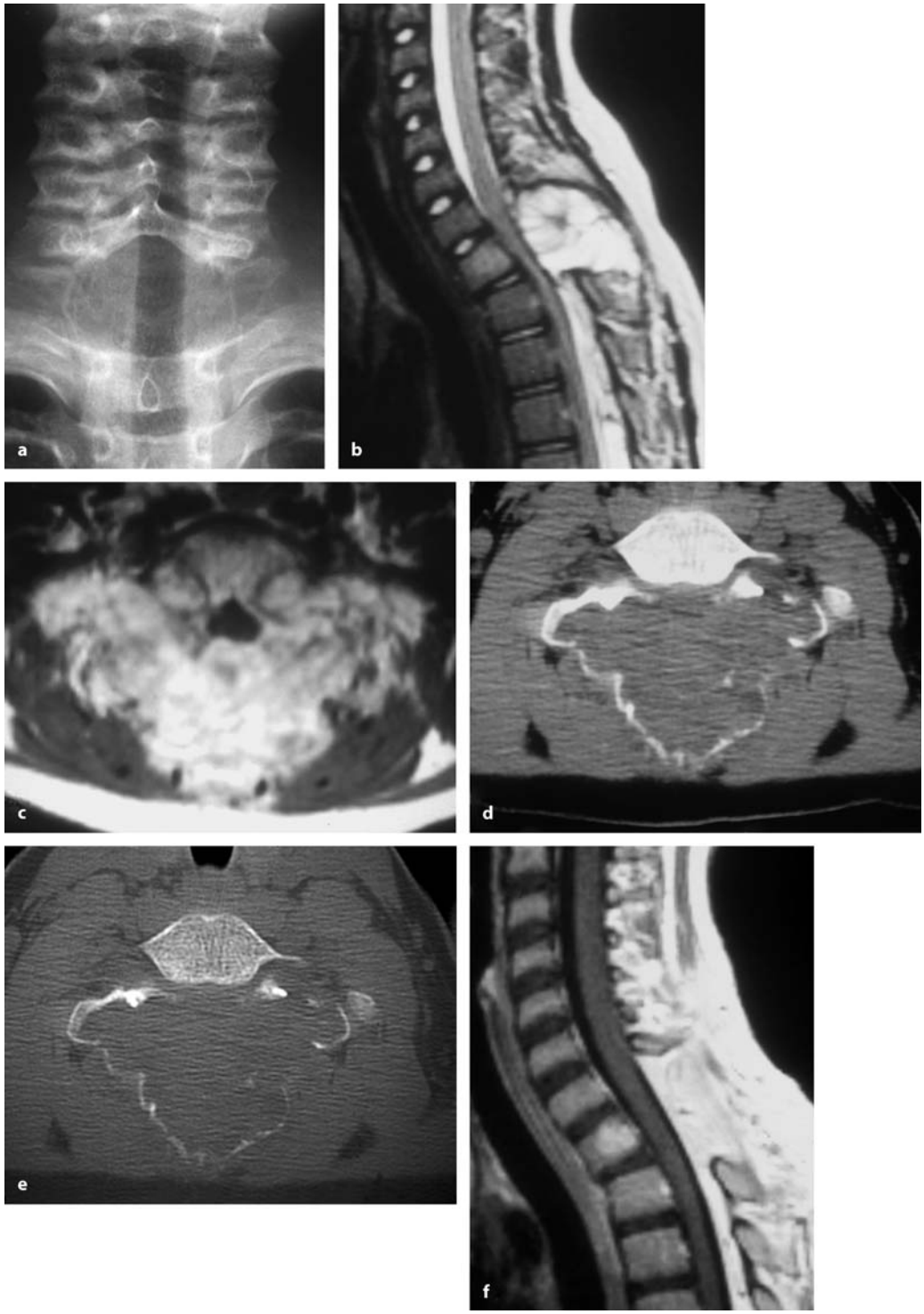

Fig. 5.118. **a** Anterior–posterior X-ray of the cervical spine of a 11-year-old boy with a 4-month history of pain and paraparesis. The X-ray shows complete absence of the lamina of Th1. **b** The sagittal T2-weighted MRI scan demonstrates a hyperintense tumor in the posterior elements of Th1 with compression of the spinal cord and the beginnings of kyphotic angulation and luxation. **c** The axial T1-weighted image with contrast demonstrates the extension of this aneurysmatic bone cyst, which involves both pedicles but leaves out the anterior components of Th1. Native (**d**) and bone-window CT images (**e**) show an expansile, osteolytic tumor in the lamina of Th1 with a thin sclerotic rim. The patient underwent a complete resection of the tumor, as demonstrated by the postoperative T1-weighted MRI (**f**). The patient improved postoperatively and underwent anterior fusion C7–Th2 in a separate operation

Table 5.42. Spinal aneurysmatic bone cysts

Sex	Age (years)	Level	History (months)	Symptoms	Therapy	Outcome
F	25	C2	12	Pain	Subtotal	Improved Lost to follow up
M	11	Th1	4	Hypesth., Motor, Gait, Pain	Complete	Improved Lost to follow up
M	24	C3–5	6	Pain	Subtotal Recon. + Fusion	Improved Rec. in 30 months
	27	C4	3	Pain	Complete Recon. + Fusion	Improved Rec. in 7 months

Preoperative embolization is recommended for large tumors [83, 143, 371, 435] and may be curative in some instances [83, 521]. Spontaneous regressions after partial resections have been described [275], but recurrences of at least 20–30% must be expected after partial resections [328, 521, 553]. In a large review on the Mayo Clinic series of 238 aneurysmal bone cysts of various locations, 19% recurred after intralesional surgery. Most recurrences were observed in the first 2 years [553]. Radiotherapy is not recommended as it carries the risk of sarcomatous transformation [275].

Boriani et al. [83] reported on 41 patients with spinal aneurysmatic bone cysts and concluded that embolization should be offered as the first line of treatment except for patients with vertebral fractures. If surgery is required, intralesional surgery achieved excellent results, with two recurrences observed for one embolized and one surgical patient each.

In our series, two complete and two subtotal resections were performed with vertebral body reconstruction and fusion in one patient. Preoperative embolization was applied in one patient. One patient experienced a recurrence 30 months after a complete resection with vertebral reconstruction and fusion, and required a second operation, which was subtotal leading to another recurrence 7 months later. At that stage, the tumor was again embolized and completely resected at another institution (Table 5.42).

5.5.2.9 Ewing Sarcomas

Ewing sarcomas are among the commonest primary bone tumors in children and young adults [85], but may also occur in the epidural space in rare instances [172, 270, 276, 381, 386]. Lactic dehydrogenase (LDH) may be used as a serum marker and can be monitored to control the effect of treatment [521]. The best treatment approach for neurologically stable patients is chemotherapy followed by surgery and further oncologic treatment [489, 521].

In the literature, all patients with Ewing sarcomas in the epidural space complained of local pain and 83% demonstrated neurological deficits. Less than half of these tumors could be resected completely so that chemo- and radiotherapy was administered after surgery. Local recurrences and metastases led to a mortality rate of 63% within 4 years of diagnosis [276].

In a literature review, Morandi et al. [381] found a male predominance of 2:1 and a mean age of 16 years (range 4 –30 years) for Ewing sarcomas in the epidural space. Twelve of 21 patients had died within 4 1/2 years (mean survival 18 months) despite multimodality treatment.

Ilaslan et al. [248] reviewed the Mayo Clinic's series of 1277 Ewing sarcomas between 1936 and 2001. Of these, 9.8% (125 patients) originated primarily in the spine. The mean age was 19.3±10.7 years (range 4–54 years) and there was a slight male predominance. The sarcomas were located predominantly in the sacrum (53.2%), the remainder with decreasing frequency in the lumbar (25%), thoracic (10.5%), and cervical spine (3.2%); 8% had more than one vertebra affected and 93% showed a lytic lesion on X-ray or CT. With respect to the nonsacral tumors, 14 out of 20 affected mainly the posterior elements, while 6 involved the vertebral body predominantly. In this review, 91% of spinal Ewing sarcomas demonstrated involvement of the spinal canal, with 40% having neurological deficits. Local pain was present in all patients. The average history was 7 months (range 1–30 months). All 125 patients underwent radiotherapy, but 70% also had chemotherapy and 25 patients underwent surgery in terms of partial removals and decompressive laminectomies. The 5-year disease-free survival rate was 53%, with sacral tumors having a slightly better prognosis (5-year disease-free survival: 60% compared to 45%).

Razek et al. [445] presented a series of 193 patients with Ewing sarcomas of various localizations who underwent radiotherapy and were then randomized to receive different chemotherapy regimens. Local control was achieved in 96% of patients, with a median survival of 43 months.

Grubb et al. [210] presented a series of 36 patients with Ewing sarcomas of the spine. There were 17 sacral tumors with decreasing involvement towards cranial spinal levels. The mean age was 17 years, with patients between 5 and 40 years being affected with a male predominance of 2:1. Neurological symptoms were observed in 58%. All were treated with radiotherapy; 17 out of 21 patients with neurological symptoms underwent a decompressive laminectomy and 32 received chemotherapy. The 5-year survival rate was 33%, with a mean survival of 2.9 years.

In a series of 33 patients treated with a combination of chemo- and radiotherapy, 48.1% survived overall for 5 years and 35.6% were disease-free [552].

Barbieri et al. [34] reported 28 patients (mean age 19.5 years) with spinal involvement. All underwent a combination of chemo- and radiotherapy, and 50% were also operated. The mean follow up was 59 months. The majority of tumors affected the lumbosacral spine. The 5-year survival rate was 43.5%; 20% developed cerebral metastases and 50% developed skeletal metastases.

Sharafuddin et al. [489] described 7 patients with primary Ewing sarcomas of the spine among 47 patients with Ewing sarcomas of various locations. The mean clinical history was 4 months (range 1–10 months). It started with pain in every patient and progressed to severe neurological deficits in five out of seven patients. Six patients were operated (four posterior decompressions, one posterior en bloc removal, and one anterior removal and fusion), while the seventh patient was biopsied only. Six patients underwent radiotherapy and all seven were administered chemotherapy. The authors observed one local recurrence and two distant metastases within 10 months of surgery, with the remainder free of disease for up to 10 years.

In our small group of three male patients aged 14, 26, and 32 years, one sacral and two thoracic Ewing sarcomas (Fig. 5.119) were seen. All were affected by pain and presented with neurological symptoms for 1, 3, and 24 months, respectively. The sacral tumor and one thoracic tumor were resected completely, the latter with a combined approach including vertebral reconstruction, and anterior and posterior fusion, whereas the other thoracic tumor was resected subtotally. All patients underwent postoperative radio- and chemotherapy. We observed one recurrence after 1 year for the sacral tumor, whereas the other two have been free of local recurrences for 3 months and 8 years after complete and subtotal removals, respectively.

5.5.2.10 Hemangiomas

Most vertebral hemangiomas are incidental findings on radiographs and are asymptomatic [31, 532]. According to autopsy series, the estimated incidence in the population is 10–12% [178]. Problems may arise if they expand toward the spinal canal [215, 304, 422] or cause vertebral collapse and instability [215]. If vertebral hemangiomas become symptomatic then most of the patients present with local pain. Pregnancy may initiate local pain due to intra-abdominal hemodynamic changes [178, 215, 422]. A progression to neurological symptoms occurs in only a small percentage [178, 462, 532]. Apart from surgery, embolization, vertebroplasty, percutaneous alcohol injections, and radiotherapy are therapeutic alternatives [521, 532].

Fox and Onofrio [178] followed 59 patients with vertebral hemangiomas over a 10-year period. Thirty-five were asymptomatic at the time of diagnosis, 13 presented with pain, and 11 presented with neurological deficits. Of those patients without neurological deficits at the time of diagnosis, three developed neurological symptoms. The authors concluded that regular clinical and radiological studies should be recommended for patients with local pain, but are unnecessary for asymptomatic patients until pain develops. Females are more likely to develop clinical problems than males.

We encountered three patients with vertebral hemangiomas at ages 16, 57, and 70 years. Two were located in the thoracic spine at Th6 (Fig. 5.120) and Th6/7, and one at L2. All presented with severe local pain, with additional neurological symptoms in patients with thoracic lesions. For the lumbar tumor, only part of the vertebral body was affected. After complete resection, the defect was filled with PMMA. The patient improved and is free of recurrence. The thoracic tumor in the 16-year-old patient was resected completely via a posterior approach followed by fusion. The patient has been free of symptoms for 11 years (Fig. 5.120). The other thoracic tumor was treated by decompression as this 70-year-old patient was in poor general health. She showed marginal improvement postoperatively.

Pastushyn et al. [422] observed 86 patients with vertebral hemangiomas, 64 of whom presented with

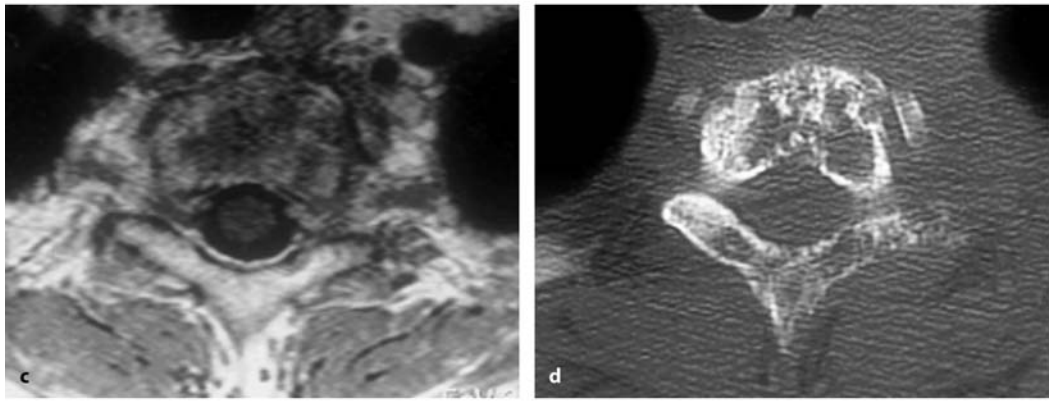

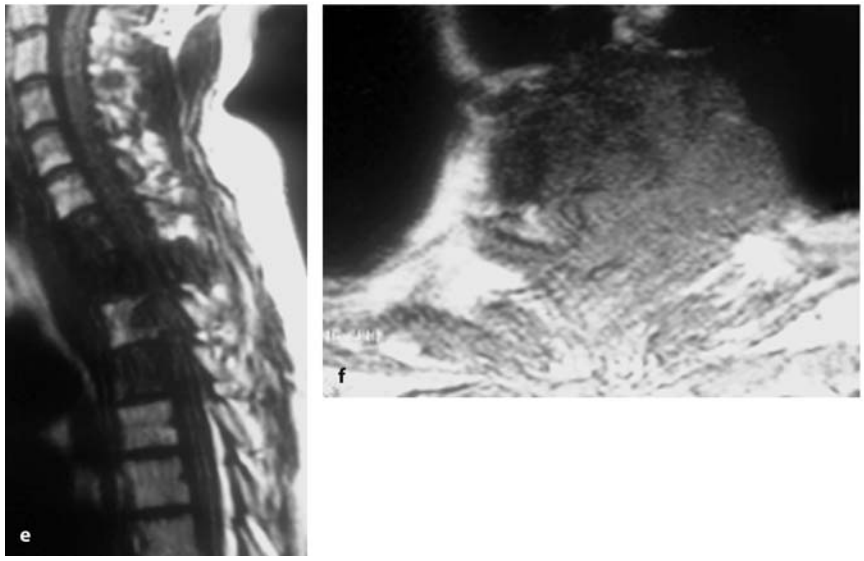

Fig. 5.119. Sagittal T1- (**a**) and T2-weighted (**b**) MRI scans of a 26-year-old patient with a Ewing sarcoma at Th1 6 months before presentation to our clinic. **c** At that time, the axial MRI demonstrated patchy destruction of the vertebral body, sparing posterior elements. **d** The bone-window CT scan also disclosed an osteolytic process of the body. However, the beginnings of destruction of the lamina on the left side could be appreciated that was not detectable on MRI. At this stage, he underwent chemotherapy before developing a progressive paraparesis and pain. **e** At the time of presentation at our clinic, the new MRI now shows affection of Th1–Th4 and a beginning kyphosis at Th2/3. **f** The axial T1-weighted MRI image demonstrates extensions of the tumor into the spinal canal and extraspinal soft tissues on the left side. (*Continuation see next page*)

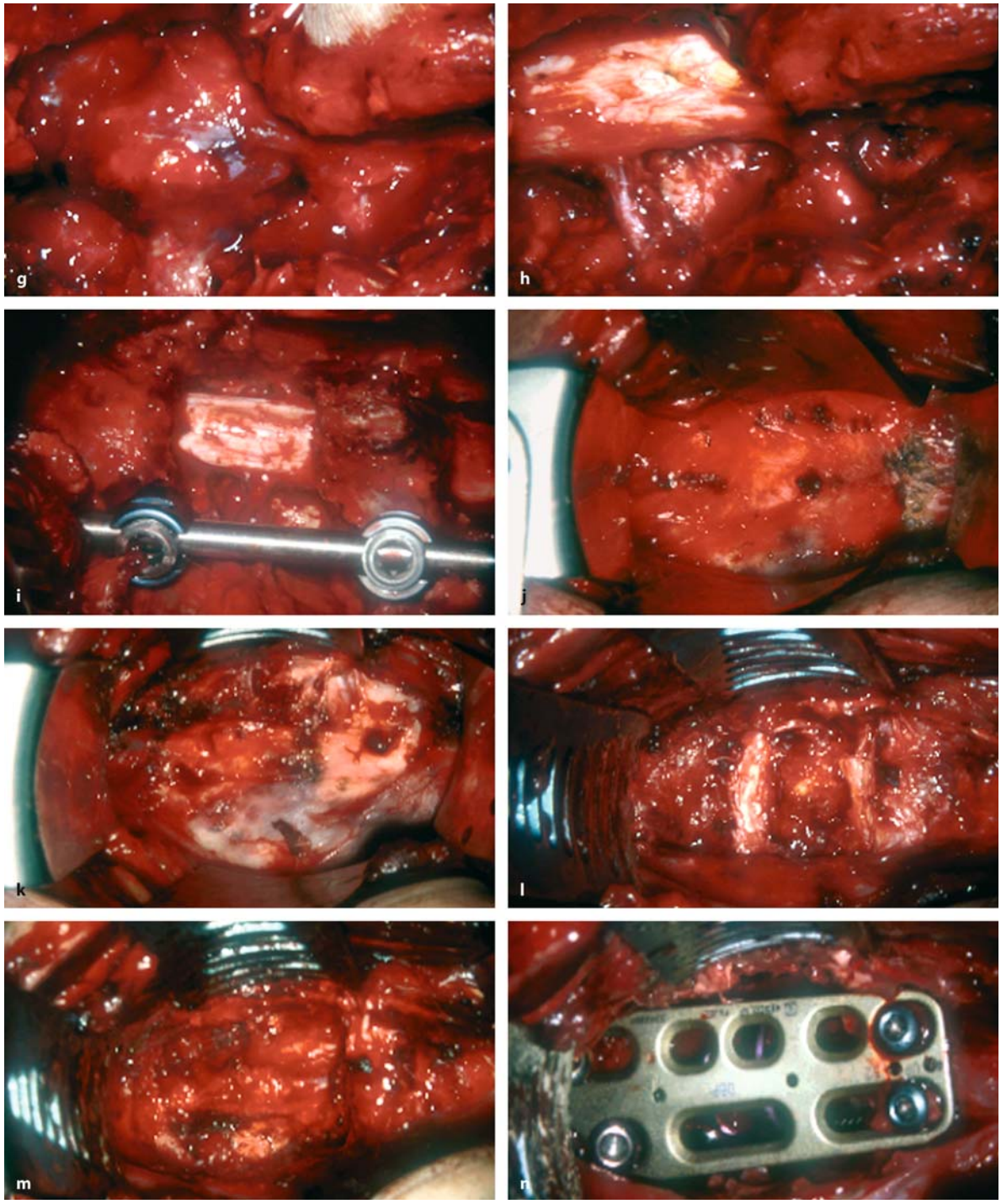

Fig. 5.119. (*Continued*) **g** The intraoperative view, taken after laminectomy of Th1, shows the intraspinal tumor component obscuring the dura. **h** After resection of the epidural tumor, part of the pedicle of Th1 on the left side is removed and the nerve root is freed from tumor. At Th4, the pedicle on the left was resected to remove the tumor in that vertebra. The defect was filled with PMMA. **i** A posterior transpedicular fixation of C7–Th5 was performed. **j** In a separate ventral approach, the infiltrated anterior longitudinal ligament is visible. **k** With resection of the ligament, the underlying infiltrated bone is visible (**l**). Using intervertebral discs as landmarks (**m**), anterior tumor resection was performed removing the vertebral bodies of Th1 and Th2. Reconstruction was achieved with a titanium cage. **n** Anterior plating of C7–Th3 was possible without splitting the sternum in this patient. Postoperatively, the patient showed no neurological change and was referred for further oncological treatment with no recurrence in 3 months

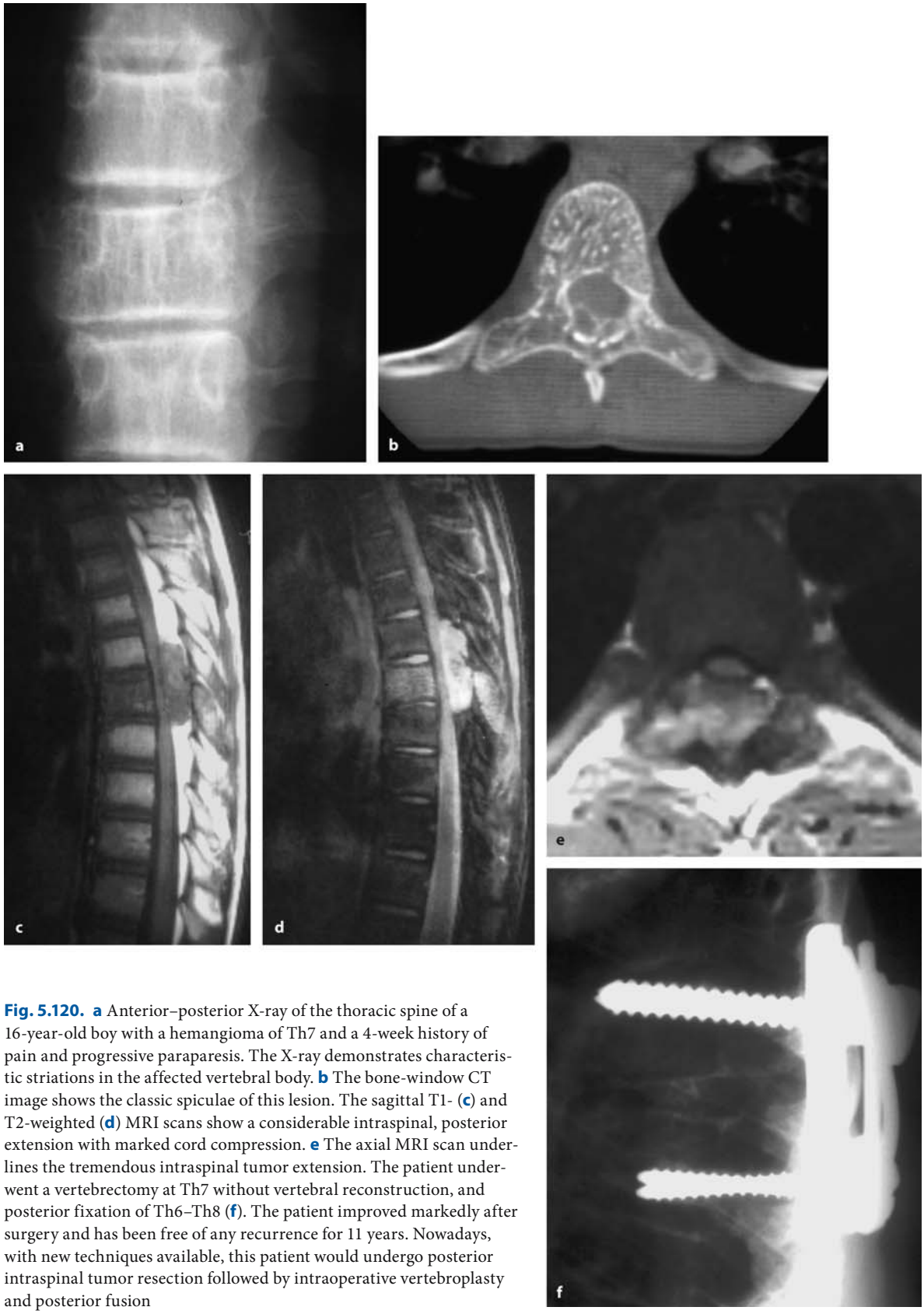

Fig. 5.120. **a** Anterior–posterior X-ray of the thoracic spine of a 16-year-old boy with a hemangioma of Th7 and a 4-week history of pain and progressive paraparesis. The X-ray demonstrates characteristic striations in the affected vertebral body. **b** The bone-window CT image shows the classic spiculae of this lesion. The sagittal T1- (**c**) and T2-weighted (**d**) MRI scans show a considerable intraspinal, posterior extension with marked cord compression. **e** The axial MRI scan underlines the tremendous intraspinal tumor extension. The patient underwent a vertebrectomy at Th7 without vertebral reconstruction, and posterior fixation of Th6–Th8 (**f**). The patient improved markedly after surgery and has been free of any recurrence for 11 years. Nowadays, with new techniques available, this patient would undergo posterior intraspinal tumor resection followed by intraoperative vertebroplasty and posterior fusion

clinical and radiological signs of cord compression and were operated. Twenty-five were operated only, and the remainder were treated with surgery and postoperative radiotherapy. Capillary and cavernous types were distinguished with better neurological outcomes (i.e., 55.3% and 78% with functional recovery, respectively) and lower recurrence rates (i.e., 37.3% and 16.7%, respectively) for capillary hemangiomas.

Fox and Onofrio [178] operated on 11 patients with neurological symptoms out of their series of 59 cases with vertebral hemangiomas. Only one lesion was completely resected, all others were removed subtotally. Intraoperative blood loss was considerable and a postoperative epidural hematoma occurred in one patient. Neurological symptoms recovered in each patient. Postoperative radiotherapy was administered in five of the subtotally removed cases and two patients were embolized. Three of the 11 operated patients developed clinical recurrences after a mean period of 9.3 years after subtotal removals.

Alternatively, vertebroplasties can achieve good results for patients with vertebral hemangiomas suffering severe pain but no neurological deficits. Cohen et al. [125] published their experience with 192 vertebroplasties. Among these, 31 patients underwent 43 procedures for vertebral hemangiomas with a high success rate.

Brunot et al. [91] presented their results on vertebroplasties in 19 patients with 21 lesions treated. All had presented with local pain. After a mean follow up of 38.6 months, 56.2% were asymptomatic and 31.2% experienced occasional back pain.

Bas et al. [39] treated 18 patients with direct ethanol injections into the hemangioma. After a mean follow up of 2 years, no complications had occurred. Doppman et al. [151] treated 11 patients in this manner. Angiography proved complete obliteration in all instances. Five of six patients with severe paraparesis recovered completely and the other is walking with assistance. Likewise, radicular symptoms responded in four of five patients; however, two patients receiving the largest injections developed vertebral fractures 4 and 16 weeks afterwards, suggesting that the injection dose be limited to about 15 ml. Goyal et al. [201] presented results for 14 patients treated with ethanol injections. Of these, 13 presented with neurological deficits. Eleven patients showed a sustained improvement at follow up after 5–31 months. They mentioned vertebral collapse and infections as possible risks associated with this modality.

Another option is embolization. Jayakumar et al. [264] treated 12 patients with spinal cord compression due to vertebral hemangiomas with particulate embolization of the feeding arteries. Eleven of these underwent subsequent posterior decompression. Eleven patients had improved neurologically after 8 months follow up, but the condition of one patient remained unchanged.

Radiotherapy for this benign disorder is met with considerable scepticism due to the risk of inducing malignant tumors. Beyzadeoglu et al. [58] calculated a risk of 0.6% for single radiation portals and 0.9% for double irradiation portals on the basis of a dose of 20–30 Gy. With doses of 30 Gy, a review of 327 cases reported complete pain relief in 54% and partial relief in 32%, with 11% not responding. They advised against higher doses to avoid late side effects and induction of malignancies [234].

In a series of 117 patients treated with radiotherapy, a dose-dependent effect was observed and a total dose of 36–40 Gy was recommended to achieve sufficient pain relief in 82% [441]. Sakata et al. [467] achieved excellent success rates after radiation doses of 36 Gy for 14 patients.

In conclusion, radiotherapy seems to provide no advantages compared to vertebroplasty, but carries the risk of inducing malignant tumors. This risk, although small, appears hardly acceptable for treatment of an absolutely benign lesion when an equally or even better alternative exists. Therefore, we recommend vertebroplasty if pain becomes unbearable in patients without neurological symptoms, and surgery once neurological symptoms or instability have developed [304, 318, 409, 462, 532, 574].

5.5.2.11 Giant Cell Tumors

Giant cell tumors rarely affect the spine, representing 1.3–9.3% of all giant cell tumors [60], and are considered as benign tumors. However, malignant transformations of giant cell tumors have been described [130, 379, 471] as well as metastases to the lung in rare instances [141, 344, 379]. Anterior spinal elements are predominantly involved and they are highly vascularized so that preoperative angiography and embolization are recommended [521].

In terms of surgical strategy for spinal giant cell tumors, two lines of thought exist: some authors advocate en bloc surgical resections to prevent local recurrence [2, 170, 405, 494, 509, 537] and to avoid radiotherapy, which is known to produce sarcomatous transformations in a significant number of patients. Mondal et al. [379] observed 5 sarcomas leading to death within months among 39 radiated giant cell tumors, emphasizing the need for life-long control of

radiated patients. However, this strategy may inflict significant morbidity, especially when dealing with sacral tumors. On the other hand, "conservative" surgical approaches are recommended to preserve neurological function [415, 471, 490, 505]. These authors emphasize the often indolent nature of tumor remnants and the better prognosis of spinal giant cell tumors compared to other locations [135, 146, 283, 505] even if they have metastasized [344, 499, 568].

We have seen a giant cell tumor of the thoracic spine in a 27-year-old female patient with a 3-month history of local pain and no neurological symptoms. She underwent subtotal resection from a posterior approach with no subsequent radiotherapy.

Hart et al. [223] reported 36 giant cell tumors of the spine. He observed a recurrence rate of 18% among primary cases and 83% among pretreated patients. Another prognostic factor was the localization of the tumor: if anterior elements were affected exclusively, no recurrence was seen after surgery. With anterior and posterior involvement, this rate rose to 24%. Purely intraspinal tumors were associated with a recurrence rate of 10%, with extraspinal infiltration of soft tissues, 21% recurred.

Reviewing the Mayo Clinic series of 24 giant cell tumors treated between 1955 and 1989, Sanjay et al. [471] observed a marked male predominance (17 males, 7 females); the average age was 30 years. Half of the patients showed neurological symptoms. They found an even distribution along the spine, whereas others reported them preferentially in the sacrum [190, 502]. In the Mayo Clinic series, seven patients underwent radiotherapy after incomplete resections. Overall, 10 of 24 tumors recurred within an average follow up of 12.4 years. The likelihood of a recurrence corresponded to the extent of the tumor and, thus, with the completeness of resection. The authors concluded, that radiotherapy should be administered only to incompletely resected or recurring tumors [471].

Boriani et al. [78] described 23 giant cell tumors of the mobile spine followed for an average period of 9 years. They found a favorable outcome after intralesional surgery, and reserved more extensive approaches with en bloc resections followed by radiotherapy for aggressive forms.

Dahlin [135] reported 31 sacral giant cell tumors and recommended a combined therapy of surgery and radiotherapy. Turcotte et al. [545] followed 26 sacral giant cell tumors for an average period of 7.8 years. Sixteen were operated primarily, while 10 tumors had recurred; 21 received radiotherapy. He observed pulmonary metastases in three cases and a recurrence rate of 33% after curettage of the tumor. In another series of 13 sacral giant cell tumors, 7 recurrences were seen and 5 patients died of this disease [502].

Fidler [170] reported nine patients with spinal giant cell tumors. He recommended en bloc resections and emphasized the use of extralesional dissection for removal of the tumor capsule. He observed one local recurrence and one death due to pulmonary metastases.

Analyzing giant cell tumors with pulmonary metastases, Maloney et al. [344] found metastases after a mean period of 3.2 years and up to 10 years after diagnosis of the primary tumor. Local recurrences at the original site were detected in 63% of cases; 16% of these patients died. Surgery was still considered as the treatment of choice even for the metastases [344, 499], and radiotherapy was recommended as adjuvant therapy. Similar results were published by Siebenrock et al. [499], who studied 23 metastasizing giant cell tumors. Metastases were observed after an average interval of 11.9 years (the longest time span was 24.5 years) with 83% having local recurrences at the original bone site.

5.5.2.12 Histiocytosis X

Histiocytosis X is a systemic disease of the reticuloskeletal system that may affect children as well as adults. Granulomas of histiocytes are mostly observed in the skull bone, but may also occur in the spine causing a locally destructive lesion. Greinacher and Gutjahr [206] described 15 children with this rare lesion. Of these, three demonstrated spinal involvement, emphasizing that even with severe destruction of bone neurological symptoms can be absent.

We have seen one such lesion in the thoracic spine of a 41-year-old male patient with a 5-year history of pain and progressive myelopathy. Despite subtotal resection, the medical condition of this patient deteriorated further and he died just 2 weeks later.

5.6 Conclusions

Epidural tumors of the spine may lead to neurological symptoms due to the compression of nervous structures or interference with spinal stability. Consequently, surgical treatment has to account for both aspects.

If removed completely, benign epidural soft-tissue tumors carry a similarly favorable prognosis as intradural extramedullary tumors. The prognosis of malignant soft-tissue tumors depends foremost on the

completeness of resection. If a curative procedure is not possible, the clinical condition of the patient and the effectiveness of adjuvant therapies determine the further course.

Primary benign bone tumors of the spine can be removed with standard surgical techniques and carry a good prognosis. Locally aggressive forms and primary malignant tumors require en bloc resections to provide a chance for cure and long-term survival. These patients should be referred to experienced spine surgeons.

For primary malignant bone tumors of the spine not feasible for en bloc resections as well as for spinal metastases, surgical strategies have to account for the overall prognosis and general condition of the patient. As curative procedures are not available for these tumors, surgery has foremost to ensure neurological function and quality of life. The survival of these patients is determined by the behavior of the tumor and effectiveness of adjuvant therapies and not by the completeness of resection.

References

1. Abdelwahab IF, Casden AM, Klein MJ, Spollman A (1991) Chondrosarcoma of a thoracic vertebra. Bull Hosp Jt Dis Orthop Inst 51:34–39
2. Abe E, Sato K, Tazawa H, Murai H, Okada K, Shimada Y, Morita H (2000) Total spondylectomy for primary tumor of the thoracolumbar spine. Spinal Cord 38:146–152
3. Abraham JL (2004) Assessment and treatment of patients with malignant spinal cord compression. J Support Oncol 2:377–288, discussion 391
4. Acciarri N, Padovani R, Giulioni M, Gaist G (1993) Surgical treatment of spinal cavernous angiomas. J Neurosurg Sci 37:209–215
5. Acikgoz B, Akkurt C, Erbengi A, Bertan V, Oezgen T, Oezcan O (1989) Metastatic spinal cord tumors. Paraplegia 27:359–363
6. Aebi M (2003) Spinal metastasis in the elderly. Eur Spine J 12:S202–S213
7. Akbarnia BA, Rooholamini SA (1981) Scoliosis caused by benign osteoblastoma of the thoracic or lumbar spine. J Bone Joint Surg Am 63:1146–1155
8. Akeyson EW, McCutcheon IE (1996) Single-stage posterior vertebrectomy and replacement combined with posterior instrumentation for spinal metastasis. J Neurosurg 85:211–220
9. Akhaddar A, Chakir N, Amarti A, El Hassani MR, El Khamlichi A, Jiddane M, Boukhrissi N (2002) Thoracic epidural hemangiopericytoma. Case report. J Neurosurg Sci 46:89–92; discussion 92
10. Akiyama H, Tamaki N, Kondoh T, Nagashima T (1999) Craniocervical junction synovial cyst associated with atlanto-axial dislocation – case report. Neurol Med Chir (Tokyo) 39:539–543
11. Akiyama N, Takeuchi M, Shibagaki Y, Uchiyama S, Iwata M (1999) [Two cases of spinal epidural lipomatosis]. Rinsho Shinkeigaku 39: 634–638
12. Albert TJ, Balderston RA, Northrup BE (1997) Surgical Approaches to the Spine. WB Saunders, Philadelphia
13. Algra RR, Heimans JJ, Valk J, Nauta JJ, Lachniet M, Van Kooten B (1992) Do metastases in vertebrae begin in the body or the pedicles? Imaging study in 45 patients. AJR Am J Roentgenol 158:1275–1279
14. Amacher AL, Eltomey A (1985) Spinal osteoblastoma in children and adolescents. Childs Nerv Syst 1:29–32
15. Amendola BE, Amendola MA, Oliver E, McClatchey KD (1986) Chordoma: role of radiation therapy. Radiology 158:839–843
16. Anderson C, Rorabeck CH (1980) Skeletal metastases of an intracranial malignant hemangiopericytoma. Report of a case. J Bone Joint Surg Am 62:145–148
17. Antoniadis G, Richter HP, Kast E, Treugut H (1997) [Juxtafacet cysts as space-occupying intraspinal processes]. Nervenarzt 68:515–520
18. Aoyagi N, Kojima K, Kasai H (2003) Review of spinal epidural cavernous hemangioma. Neurol Med Chir (Tokyo) 10:471–475; discussion 476
19. Aprin H, Riseborough EJ, Hall JE (1982) Chondrosarcoma in children and adolescents. Clin Orthop Relat Res 166:226–232
20. Assaker R, Fromont G, Reyns N, Louis E, Chastanet P, Lejeune JP (2001) [Video-assisted thoracoscopic surgery]. Neurochirurgie 47:93–104
21. Austin JP, Urie MM, Cardenosa G, Munzenrider JE (1993) Probable causes of recurrence in patients with chordoma and chondrosarcoma of the base of skull and cervical spine. Int J Radiat Oncol Biol Phys 25:439–444
22. Awwad EE, Martin DS, Smith KR Jr, Bucholz RD (1990) MR imaging of lumbar juxtaarticular cysts. J Comput Assist Tomogr 14:415–417
23. Aydin F, Ghatak NR, Leshner RT (1995) Possible radiation-induced dural fibrosarcoma with an unusually short latent period: case report. Neurosurgery 36:591–594; discussion 594–595
24. Azzarelli A, Quagliuolo V, Cerasoli S, Zucali R, Bignami P, Mazzaferro V, Dossena G, Gennari L (1988) Chordoma: natural history and treatment results in 33 cases. J Surg Oncol 37:185–191
25. Baba H, Maezawa Y, Furusawa N, Wada M, Kokubo Y, Imura S, Imamura Y, Yamada Y (1998) Solitary plasmacytoma of the spine associated with neurological complications. Spinal Cord 36:470–475
26. Bacci G, Savini R, Calderoni P, Gnudi S, Minutillo A, Picci P (1982) Solitary plasmacytoma of the vertebral column. A report of 15 cases. Tumori 68:271–275
27. Bach F, Larsen BH, Rohde K, Borgesen SE, Gjerris F, Boge-Rasmussen T, Agerlin N, Rasmusson B, Stjernholm P, Sorensen PS (1990) Metastatic spinal cord compression. Occurrence, symptoms, clinical presentations and prognosis in 398 patients with spinal cord compression. Acta Neurochir (Wien) 107:37–43

28. Bach F, Agerlin N, Soerensen JB, Rasmussen TB, Dombernowsky P, Soerensen PS, Hansen HH (1992) Metastatic spinal cord compression secondary to lung cancer. J Clin Oncol 10:1781–1787
29. Badinand B, Morel C, Kopp N, Tran Min VA, Cotton F (2003) Dumbbell-shaped epidural capillary hemangioma. AJNR Am J Neuroradiol 24:190–192
30. Bagshaw MA, Kaplan ID, Valdagni R, Cox RS (1992) Radiation treatment of prostate bone metastases and the biological considerations. Adv Exp Med Biol 324:255–268
31. Bandiera S, Campanacci L, De Iure F, Bertoni F, Picci P, Boriani S (1999) Hemorrhagic synovial lumbar cyst: a case report and review of the literature. Chir Organi Mov 84:197–203
32. Banning CS, Thorell WE, Leibrock LG (2001) Patient outcome after resection of lumbar juxtafacet cysts. Spine 26:969–972
33. Baratti D, Gronchi A, Pennacchioli E, Lozza L, Colecchia M, Fiore M, Santinami M (2003) Chordoma: natural history and results in 28 patients treated at a single institution. Ann Surg Oncol 10:291–296
34. Barbieri E, Chiaulon G, Bunkeila F, Putti C, Frezza G, Neri S, Boriani S, Campanacci M, Babini L (1998) Radiotherapy in vertebral tumors. Indications and limits: a report on 28 cases of Ewing's sarcoma of the spine. Chir Organi Mov 83:105–111
35. Barcena A, Lobato RD, Rivas JJ, Cordobes F, De Castro S, Cabrera A, Lamas E (1984) Spinal metastatic disease: analysis of factors determining functional prognosis and the choice of treatment. Neurosurgery 15:820–827
36. Barr JD, Barr MS, Lemley TJ, McCann RM (2000) Percutaneous vertebroplasty for pain relief and spinal stabilization. Spine 25:912–928
37. Barron KD, Hirano A, Araki S, Terry RD (1959) Experiences with metastatic neoplasms involving the spinal cord. Neurology 9:91–106
38. Barwick KW, Huvos AG, Smith J (1980) Primary osteogenic sarcoma of the vertebral column: a clinicopathologic correlation of ten patients. Cancer 46:595–604
39. Bas T, Aparisi F, Bas JL (2001) Efficacy and safety of ethanol injections in 18 cases of vertebral hemangioma: a mean follow-up of 2 years. Spine 26:1577–1582
40. Basic-kes V, Basic-Jukic N, Kes P, Demarin V, Labar B (2002) [Neurologic sequelae of bone changes in multiple myeloma and its therapy]. Acta Med Croatica 56:103–107
41. Bataille R, Sany J, Serre H (1981) [Apparently isolated plasmacytoma of bone. Clinical and prognostic data. 114 cases and review of literature (author's transl)]. Nouv Presse Med 10:407–411
42. Bauer HC (1997) Posterior decompression and stabilization for spinal metastases. Analysis of sixty-seven consecutive patients. J Bone Joint Surg Am 79:514–522
43. Bauernhofer T, Stoger H, Kasparek AK, Ploner F, Kuss I, Pieber TR, Kotz R, Samonigg H (1999) Combined treatment of metastatic osteosarcoma of the spine. Oncology 57:265–268
44. Baur A, Stabler A, Bruning R, Bartl R, Krodel A, Reiser M, Deimling M (1998) Diffusion-weighted MR imaging of bone marrow: differentiation of benign versus pathologic compression fractures. Radiology 207:349–356
45. Baur A, Stabler A, Arbogast S, Duerr HR, Bartl R, Reiser M (2002) Acute osteoporotic and neoplastic vertebral compression fractures: fluid sign at MR imaging. Radiology 225:730–735
46. Bavbek M, Yurt A, Caner H, Altinors N (1997) An unusual dumbbell form of cavernous hemangioma of the cervical spine. Kobe J Med Sci 43:57–63
47. Beatty RA (1987) Sciatica and epidural gas. Neurosurgery 21:537–539
48. Beauchamp CP, Duncan CP, Dzus AK, Morton KS (1992) Osteoblastoma: experience with 23 patients. Can J Surg 35:199–202
49. Bellaiche L, Laredo JD (1994) [Value of magnetic resonance imaging in myeloma]. Presse Med 23:315–317
50. Benezech J, Fuentes JM (1989) [Primary tumors of the spine. A multicenter cooperative study]. Neurochirurgie 35:317–322
51. Benzil DL, Saboori M, Mogilner AY, Rocchio R, Moorthy CR (2004) Safety and efficacy of stereotactic radiosurgery for tumors of the spine. J Neurosurg 101:413–418
52. Bergh P, Kindblom LG, Gunterberg B, Remotti F, Ryd W, Meis-Kindblom JM (2000) Prognostic factors in chordoma of the sacrum and mobile spine. Cancer 88:2122–2134
53. Bergh P, Gunterberg B, Meis-Kindblom JM, Kindblom LG (2001) Prognostic factors and outcome of pelvic, sacral, and spinal chondrosarcomas: a center-based study of 69 cases. Cancer 91:1201–1212
54. Berson AM, Castro JR, Petti P, Phillips TL, Gauger GE, Gutin P, Collier JM, Henderson SD, Baken K (1988) Charged particle irradiation of chordoma and chondrosarcoma of the base of skull and cervical spine: the Lawrence Berkeley Laboratory experience. Int J Radiat Oncol Biol Phys 15:559–565
55. Bessou P, Lefournier V, Ramoul A, Vasdev A, Boubagra K, Crouzet G (1998) [Benign vertebral osteoblastoma. Report of 6 cases]. J Neuroradiol 25:21–31
56. Betchen S, Schwartz A, Black C, Post K (2002) Intradural hemangiopericytoma of the lumbar spine: case report. Neurosurgery 50:654–657
57. Bethke KP, Neifeld JP, Lawrence W (1991) Diagnosis and management of sacrococcygeal chordoma. J Surg Oncol 48:232–238
58. Beyzadeoglu M, Dirican B, Oysul K, Surenkok S, Pak Y (2002) Evaluation of radiation carcinogenesis risk in vertebral hemangioma treated by radiotherapy. Neoplasma 49:338–341
59. Bhojraj SY, Dandawate AV, Ramakantan R (1992) Preoperative embolisation, transpedicular decompression and posterior stabilisation for metastatic disease of the thoracic spine causing paraplegia. Paraplegia 30:292–299
60. Bidwell JK, Young JW, Khalluff E (1987) Giant cell tumor of the spine: computed tomography appearance and review of the literature. J Comput Tomogr 11:307–311

61. Bielack SS, Wulff B, Delling G, Gobel U, Kotz R, Ritter J, Winkler K (1995) Osteosarcoma of the trunk treated by multimodal therapy: experience of the Cooperative Osteosarcoma study group (COSS) Med Pediatr Oncol 24:6–12
62. Bilsky MH, Boland P, Lis E, Raizer JJ, Healey JH (2000) Single-stage posterolateral transpedicle approach for spondylectomy, epidural decompression, and circumferential fusion of spinal metastases. Spine 25:2240–2250
63. Bilsky MH, Schefler AC, Sandberg DI, Dunkel IJ, Rosenblum MK (2000) Sclerosing epithelioid fibrosarcomas involving the neuraxis: report of three cases. Neurosurgery 47:956–959; discussion 959–960
64. Bilsky MH, Boland PJ, Panageas KS, Woodruff JM, Brennan MF, Healey JH (2001) Intralesional resection of primary and metastatic sarcoma involving the spine: outcome analysis of 59 patients. Neurosurgery 49:1277–1286; discussion 1286–1287
65. Bilsky MH, Boakye M, Collignon F, Kraus D, Boland P (2005) Operative management of metastatic and malignant primary subaxial cervical tumors. J Neurosurg Spine 2:256–264
66. Binning MJ, Gottfried ON, Klimo P, Schmidt MH (2004) Minimally invasive treatments for metastatic tumors of the spine. Neurosurg Clin N Am 15:459–465
67. Birch BD, Khandji AG, McCormick PC (1996) Atlantoaxial degenerative articular cysts. J Neurosurg 85:810–816
68. Bisagni-Faure A, Ravaud P, Amor B, Menkes CJ (1991) [Myeloma and epidural invasiveness. Clinical and therapeutic aspects (a study of 22 cases)]. Rev Rhum Mal Osteoartic 58:501–506
69. Bjornsson J, Wold LE, Ebersold MJ, Laws ER (1993) Chordoma of the mobile spine. A clinicopathologic analysis of 40 patients. Cancer 71:735–740
70. Black P (1979) Spinal metastases: current status and recommended guidelines for management. Neurosurgery 5:726–746
71. Bogoch ER, English E, Perrin RG, Tator CH (1983) Successful surgical decompression of spinal extradural metastases of liposarcoma. Spine 8:228–235
72. Bohinski RJ, Rhines LD (2003) Principles and techniques of en bloc vertebrectomy for bone tumors of the thoracolumbar spine: an overview. Neurosurg Focus 15:Article 7
73. Böker DK, Sepehrnia A, Samii M (1992) Skull-base chordomas: operative strategies and clinical results. First International Skull Base Congress, Hanover, June 14–20
74. Boogerd W, Van der Sande JJ, Kroeger R (1992) Early diagnosis and treatment of spinal epidural metastasis in breast cancer: a prospective study. J Neurol Neurosurg Psychiatr 55:1188–1193
75. Borg MF, Benjamin CS (1995) Haemangiopericytoma of the central nervous system. Australas Radiol 39:36–41
76. Boriani S, Capanna R, Donati D, Levine A, Picci P, Savini R (1992) Osteoblastoma of the spine. Clin Orthop 278:37–45
77. Boriani S, Biagini R, De Lure F, Bertoni F, Malaguti MC, Di Fiore M, Zanoni A (1996) En bloc resections of bone tumors of the thoracolumbar spine: a preliminary report on 29 patients. Spine 21:1927–1931
78. Boriani S, Biagini R, Laus M, De Lure F, Campanacci L (1996) Giant cell tumor of the vertebral column. Chir Organi Mov 81:233–245
79. Boriani S, Chevalley F, Weinstein JN, Biagini R, Campanacci L, De Lure F, Piccill P (1996) Chordoma of the spine above the sacrum. Treatment and outcome in 21 cases. Spine 21:1569–1577
80. Boriani S, Weinstein JN, Biagini R (1997) Primary bone tumors of the spine. Terminology and surgical staging. Spine 22:1036–1044
81. Boriani S, Biagini R, De Lure F, Bandiera S, Di Fiore M, Bandello L, Malaguti MC, Picci P, Bacchini P (1998) Resection surgery in the treatment of vertebral tumors. Chir Organi Mov 83:53–64
82. Boriani S, De Lure F, Bandiera S, Campanacci L, Biagini R, Di Fiore M, Bandello L, Picci P, Bacchini P (2000) Chondrosarcoma of the mobile spine: report on 22 cases. Spine 25:804–812
83. Boriani S, De Lure F, Campanacci L, Gasbarrini A, Bandiera S, Biagini R, Bertoni F, Picci P (2001) Aneurysmal bone cyst of the mobile spine: report on 41 cases. Spine 26:27–35
84. Bosma JJ, Pigott TJD, Pennie BH, Jaffray DC (2001) En bloc removal of the lower lumbar vertebral body for chordoma. Report of two cases. J Neurosurg 94:284–291
85. Bouffet E, Marec-Berard P, Thiesse P, Carrie C, Risk T, Jouvet A, Brunat-Mentigny M, Mottolese C (1997) Spinal cord compression by secondary epi- and intradural metastases in childhood. Childs Nerv Syst 13:383–387
86. Boukobza M, Mazel C, Touboul E (1996) Primary vertebral and spinal epidural non-Hodgkin's lymphoma with spinal cord compression. Neuroradiology 38:333–337
87. Bozzao L, Fantozzi L, Di Lorenzo N (1977) Angiographic features of upper cervical extradural neurinoma. Case Report. Acta Neurochir (Wien) 39:269–273
88. Brenner B, Carter A, Tatarsky I, Gruszkiewicz J, Peyser E (1982) Incidence, prognostic significance and therapeutic modalities of central nervous system involvement in multiple myeloma. Acta Haematol 68:77–83
89. Bridwell KH, Jenny AB, Saul T, Rich KM, Grubb RL (1988) Posterior segmental spinal instrumentation (PSSI) with posterolateral decompression and debulking for metastatic thoracic and lumbar spine disease. Limitations of the technique. Spine 13:1383–1394
90. Brihaye J, Ectors P, Lemort M, Van Houte P (1988) The management of spinal epidural metastases. Adv Techn Stand Neurosurg 16:122–176
91. Brunot S, Berge J, Barreau X, Menegon P, Dousset V (2005) [Long term clinical follow up of vertebral hemangiomas treated by percutaneous vertebroplasty]. J Radiol 86:41–47
92. Budris DM (1991) Radiologic case study. Intraspinal lumbar synovial cyst. Orthopedics 14:613, 618–620
93. Butler MS, Robertson WW Jr, Rate W, D'Angio GJ, Drummond DS (1990) Skeletal sequelae of radiation therapy for malignant childhood tumors. Clin Orthop:235–240
94. Cahill DW (1996) Surgical management of malignant tumors of the adult bony spine. South Med J 89:653–665

95. Cahill DW, Kumar R (1999) Palliative subtotal vertebrectomy with anterior and posterior reconstruction via a single posterior approach. J Neurosurg 90:42–47
96. Camacho J, Arnalich F, Anciones B, Pena JM, Gil A, Barbado FJ, Puig JG, Vazquez JJ (1985) The spectrum of neurological manifestations in myeloma. J Med 16:597–611
97. Cancrini A Jr, Bellotti C, Santoro A, Quagliarini L, Tossini A, Ciappetta P, Delfini R (1993) [Anterior approaches to the spinal column: considerations of the surgical technique]. G Chir 14:92–98
98. Capanna R, Ayala A, Bertoni F, Picci P, Calderoni P, Gherlinzoni F, Bettelli G, Campanacci M (1986) Sacral osteoid osteoma and osteoblastoma: a report of 13 cases. Arch Orthop Trauma Surg 105:205–210
99. Carpentier A, Polivka M, Blanquet A, Lot G, George B (2002) Suboccipital and cervical chordomas: the value of aggressive treatment at first presentation of the disease. J Neurosurg 97:1070–1077
100. Cartwright MJ, Nehls DG, Carrion CA, Spetzler RF (1985) Synovial cyst of a cervical facet joint: case report. Neurosurgery 16:850–852
101. Casadei R, Greggi T, Miglietta A, Perozzi M, Barchetti M, Parisini P (1998) Posterior surgery for the treatment of thoracolumbar pathologic fractures in metastatic patients. Chir Organi Mov 83:149–158
102. Catton C, O'Sullivan B, Bell R, Laperriere N, Cummings B, Fornasier V, Wunder J (1996) Chordoma: long-term follow-up after radical photon irradiation. Radiother Oncol 41:67–72
103. Cauhape P, Soubrier M, Ristori JM, Bussiere JL (1993) [Massive calcinosis of a spinal synovial cyst after intra-articular injection of long-acting corticosteroid]. Rev Rhum Ed Fr 60:177–179
104. Celli P (2002) Treatment of relevant nerve roots involved in nerve sheath tumors: removal or preservation? Neurosurgery 51:684–692
105. Celli P, Trillo G, Ferrante L (2005) Extrathecal intraradicular nerve sheath tumor. J Neurosurg Spine 3:1–11
106. Cervoni L, Celli P, Salvati M, Tarantino R, Fortuna A (1995) Solitary plasmacytoma of the spine: relationship of IGM to tumour progression and recurrence. Acta Neurochir (Wien) 135:122–125
107. Chahal S, Lagera JE, Ryder J, Kleinschmidt-DeMasters BK (2003) Hematological neoplasms with first presentation as spinal cord compression syndromes: a 10-year retrospective series and review of the literature. Clin Neuropathol 22:282–290
108. Chang H, Park JB, Kim KW (2000) Synovial cyst of the transverse ligament of the atlas in a patient with os odontoideum and atlantoaxial instability. Spine 25:741–744
109. Chang IC, Chou MC, Bell WR, Lin ZI (2004) Spinal cord compression caused by extradural arachnoid cysts. Clinical examples and review. Pediatr Neurosurg 40:70–74
110. Chang MY, Shih LY, Dunn P, Leung WM, Chen WJ (1994) Solitary plasmacytoma of bone. J Formos Med Assoc 93:397–402
111. Chaoui FM, Njee-Bugha T, Figarella-Branger D, Peragut JC (2000) [Synovial cyst of cervical spine]. Neurochirurgie 46:391–394
112. Charest DR, Kenny BG (2000) Radicular pain caused by synovial cyst: an underdiagnosed entity in the elderly? J Neurosurg Spine 92:57–60
113. Charissoux JL, Dunoyer J, Arnaud JP, Pecout C, Huc H (1992) [Extradural spinal cysts: an uncommon cause of back pain. Review of the literature apropos of a case]. Rev Chir Orthop Reparatrice Appar Mot 78:51–57
114. Chataigner H, Onimus M, Polette A (1998) [Surgical treatment of myeloma localized in the spine]. Rev Chir Orthop Reparatrice Appar Mot 84:311–318
115. Chen HJ, Chen L (1996) Traumatic interdural arachnoid cyst in the upper cervical spine. Case report. J Neurosurg 85:351–353
116. Chen LH, Chen WJ, Niu CC, Shih CH (2000) Anterior reconstructive spinal surgery with Zielke instrumentation for metastatic malignancies of the spine. Arch Orthop Trauma Surg 120:27–31
117. Cheng EY, Özerdemoglu RA, Transfeldt EE, Thompson RC Jr (1999) Lumbosacral chordoma: prognostic factors and treatment. Spine 24:1639–1645
118. Cheng MH (1996) Intraspinal extradural arachnoid cyst with spinal cord herniation. J Formos Med Assoc 95:712–714
119. Chevalier X, Voisini MC, Brugieres P, Ducoup-Lepointe H, Avonac B, Marty M, Martigny J, Hernigou PH, Gontallier D, Villiaumey J, Larget-Petit B (1990) Chordomes du rachis mobile. A propos de neuf cas. Revue de la literature. Rev Rhumatisme 57:767–778
120. Cho BY, Zhang HY, Kim HS (2004) Synovial cyst in the cervical region causing severe myelopathy. Yonsei Med J 45:539–542
121. Choe W, Walot I, Schlesinger C, Chambi I, Lin F (1993) Synovial cyst of dens causing spinal cord compression. Case report. Paraplegia 31:803–807
122. Chong KM, Hennox SC, Sheppard MN (1993) Primary hemangiopericytoma presenting as a Pancoast tumor. Ann Thorac Surg 55:9
123. Chow LT, Lui YH, Kumta SM, Allen PW (2004) Primary sclerosing epithelioid fibrosarcoma of the sacrum: a case report and review of the literature. J Clin Pathol 57:90–94
124. Ciappetta P, Celli P, Palma L, Mariottini A (1985) Intraspinal hemangiopericytomas. Report of two cases and review of the literature. Spine 10:27–31
125. Cohen JE, Lylyk P, Ceratto R, Kaplan L, Umanskyt F, Gomori JM (2004) Percutaneous vertebroplasty: technique and results in 192 procedures. Neurol Res 26:41–49
126. Cohen ZR, Fourney DR, Marco RA, Rhines LD, Gokaslan ZL (2002) Total cervical spondylectomy for primary osteogenic sarcoma. Case report and description of operative technique. J Neurosurg (Spine 3) 97:386–392
127. Colletti PM, Siegel HJ, Woo MY, Young HY, Terk MR (1996) The impact on treatment planning of MRI of the spine in patients suspected of vertebral metastasis: an efficacy study. Comput Med Imaging Graph 20:159–162
128. Constans JP, Divitiis E, Donizelli R, Spaziante R, Meder JF, Haye C (1983) Spinal metastasis with neurological manifestations: review of 600 cases. J Neurosurg 59:111–118

129. Conti P, Pansini G, Mouchaty H, Capuano C, Conti R (2004) Spinal neurinomas: retrospective analysis and long-term outcome of 179 consecutively operated cases and review of the literature. Surg Neurol 61:34–43; discussion 44
130. Crew JP, Flannery M, Manners B, Coates CJ (1995) Malignant transformation in a fatal case of giant cell tumour of the sacrum. Postgrad Med J 71:301–302
131. Crockard HA, Bradford R (1985) Transoral transclival removal of a schwannoma anterior to the craniocervical junction. Case report. J Neurosurg 62:293–295
132. Cudlip S, Johnston F, Marsh H (1999) Subaxial cervical synovial cyst presenting with myelopathy. Report of three cases. J Neurosurg Spine 90:141–144
133. Cummings BJ, Hodson DI, Bush RS (1983) Chordoma: the results of megavoltage radiation therapy. Int J Radiat Oncol Biol Phys 9:633–642
134. Cybulski GR, Stone JL, Opesanmi O (1992) Spinal cord decompression via a modified costotransversectomy approach combined with posterior instrumentation for management of metastatic neoplasms of the thoracic spine. Surg Neurol 35:280–285
135. Dahlin DC (1977) Giant-cell tumor of vertebrae above the sacrum: a review of 31 cases. Cancer 39:1350–1956
136. D'Andrea G, Ramundo OE, Trillo G, Roperto R, Isidori A, Ferrante L (2003) Dorsal foramenal extraosseous epidural cavernous hemangioma. Neurosurg Rev 26:292–296
137. Degen JW, Gagnon GJ, Voyadzis JM, McRae DA, Lunsden M, Dieterich S, Molzahn I, Henderson FC (2005) CyberKnife stereotactic radiosurgical treatment of spinal tumors for pain control and quality of life. J Neurosurg Spine 2:540–549
138. Deinsberger W, Schindler C, Böker DK (1997) [Juxta-facet cysts. Pathogenesis, clinical symptoms and therapy]. Nervenarzt 68:825–830
139. Delauche-Cavallier MC, Laredo JD, Wybier M, Bard M, Mazabraud A, Le Bail Darne JL, Kuntz D, Ryckewaert A (1988) Solitary plasmacytoma of the spine. Long-term clinical course. Cancer 61:1707–1714
140. De Salles AAF, Pedroso AG, Medin P, Agazaryan N, Solberg T, Cabatan-Awang C, Espinosa DM, Ford J, Selch MT (2004) Spinal lesions treated with Novalis shaped beam intensity-modulated radiosurgery and stereotactic radiotherapy. J Neurosurg (Spine 3) 101:435–440
141. De Smedt M, Copin G, Boeri C, Dosch JC, Dupuis M, Marcellin L (1999) [A case of a aggressive giant-cell tumor with multiple bone metastases]. Rev Chir Orthop Reparatrice Appar Mot 85:293–296
142. Deutsch M, Tersak JM (2004) Radiotherapy for symptomatic metastases to bone in children. Am J Clin Oncol 27:128–131
143. Dick HM, Bigliani LU, Michelsen WJ, Johnston AD, Stinchfield FE (1979) Adjuvant arterial embolization in the treatment of benign primary bone tumors in children. Clin Orthop 139:133–141
144. Dickman CA, Apfelbaum RI (1998) Thoracoscopic microsurgical excision of a thoracic schwannoma. Case report. J Neurosurg 88:898–902
145. Dieckmann C, Bruns J, Maas R (1996) [Secondary osteosarcoma in Paget disease]. Aktuelle Radiol 6:191–193
146. Di Lorenzo N, Spallone A, Nolletti A, Nardi P (1980) Giant cell tumors of the spine: a clinical study of six cases, with emphasis on the radiological features, treatment, and follow-up. Neurosurgery 6:29–34
147. DiSclafani A II, Canale DJ (1985) Communicating spinal arachnoid cysts: diagnosis by delayed metrizamide computed tomography. Surg Neurol 23:428–430
148. Doherty PF, Sherman BA, Stein C, White R (1993) Bilateral synovial cysts of the thoracic spine: a case report. Surg Neurol 39:279–281
149. Doita M, Harada T, Iguchi T, Sumi M, Sha H, Yoshiya S, Kurosaka M (2003) Total sacrectomy and reconstruction for sacral tumors. Spine 28:E296–E301
150. Doita M, Nishida K, Miura J, Takada T, Kurosaka M, Fujii M (2003) Kinematic magnetic resonance imaging of a thoracic spinal extradural arachnoid cyst: an alternative suggestion for exacerbation of symptoms during straining. Spine 28:E229–E233
151. Doppman JL, Oldfield EH, Heiss JD (2000) Symptomatic vertebral hemangiomas: treatment by means of direct intralesional injection of ethanol. Radiology 214:341–348
152. Eguchi T, Tamaki N, Kurata H (1999) Endoscopy of the spinal cord: cadaveric study and clinical experience. Minim Invasive Neurosurg 42:146–151
153. Eimoto T, Yanaka M, Kurosawa M, Ikeya F (1978) Plasma cell granuloma (inflammatory pseudotumor) of the spinal cord meninges: report of a case. Cancer 41:1929–1936
154. Elias A, Ryan L, Sulkes A, Collins J, Aisner J, Antman KH (1989) Response to mesna, doxorubicin, ifosfamide, and dacarbazine in 108 patients with metastatic or unresectable sarcoma and no prior chemotherapy. J Clin Oncol 7:1208–1216
155. El-Mahdi MA (1977) Arachnoid cyst and cord compression in association with tangential shrapnel injuries of the spine. Neurochirurgia (Stuttg) 20:1–7
156. El-Mahdy W, Kane PJ, Powell MP, Crockard HA (1999) Spinal intradural tumours: part I – extramedullary. Br J Neurosurg 13:550–557
157. Enneking WF (1986) A system of staging musculoskeletal neoplasms. Clin Orthop 204:9–24
158. Epstein NE (2004) Lumbar laminectomy for the resection of synovial cysts and coexisting lumbar spinal stenosis or degenerative spondylolisthesis: an outcome study. Spine 29:1049–1055; discussion 1056
159. Epstein NE, Hollingsworth R (1993) Synovial cyst of the cervical spine. J Spinal Disord 6:182–185
160. Ersahin Y, Yildizhan A, Seber N (1993) Spinal extradural arachnoid cyst. Childs Nerv Syst 9:250–252
161. Estourgie SH, Nielsen GP, Ott MJ (2002) Metastatic patterns of extremity myxoid liposarcoma and their outcome. J Surg Oncol 80:89–93
162. Eustacchio S, Trummer M, Unger F, Flaschka G (2003) Intraspinal synovial cyst at the craniocervical junction. Zentralbl Neurochir 64:86–89

163. Evans A, Stoodley N, Halpin S (2002) Magnetic resonance imaging of intraspinal cystic lesions: a pictorial review. Curr Probl Diagn Radiol 31:79–94
164. Faccioli F, Lima J, Bricolo A (1985) One-stage decompression and stabilization in the treatment of spinal tumors. J Neurosurg Sci 29:199–205
165. Fardon DF, Simmons JD (1989) Gas-filled intraspinal synovial cyst. A case report. Spine 14:127–129
166. Faul CM, Flickinger JC (1995) The use of radiation in the management of spinal metastases. J Neurooncol 23:149–161
167. Feldenzer JA, McGanley JL, McGillicuddy JE (1989) Sacral and presacral tumors: problems in diagnosis and management. Neurosurgery 25:884–891
168. Feldmann JL, Guedri M, Ohana N, Menkes CJ, Amor B (1984) [Solitary spinal plasmacytoma]. Ann Med Interne (Paris) 135:259–264
169. Fidler MW (1986) Anterior decompression and stabilization of metastatic spinal fractures. J Bone Joint Surg 68:83–90
170. Fidler MW (2001) Surgical treatment of giant cell tumours of the thoracic and lumbar spine: report of nine patients. Eur Spine J 10:69–77
171. Findlay GFG (1984) Adverse effects of the management of malignant spinal cord compression. J Neurol Neurosurg Psychiatr 47:761–768
172. Fink LH, Meriwether MW (1979) Primary epidural Ewing's sarcoma presenting as a lumbar disc protrusion. Case report. J Neurosurg 51:120–123
173. Fiumara E, D'Angelo V, Florio FP, Nardella M, Bisceglia M (1996) Preoperative embolization in surgical treatment of spinal thoracic dumbbell schwannoma. A case report. J Neurosurg Sci 40:153–156
174. Flemming DJ, Murphey MD, Carmichael BB, Bernard SA (2000) Primary tumors of the spine. Semin Musculoskelet Radiol 4:299–320
175. Fortuna A, Nolletti A, Nardi P, Caruso R (1981) Spinal neurinomas and meningiomas in children. Acta Neurochir (Wien) 55:329–341
176. Fourney DR, Gokaslan ZL (2003) Current management of sacral chordoma. Neurosurg Focus 15:Article 9
177. Fourney DR, Schomer DF, Nader R, Chlan-Fourney J, Suki D, Ahrar K, Rhines LD, Gokaslan ZL (2003) Percutaneous vertebroplasty and kyphoplasty for painful vertebral body fractures in cancer patients. J Neurosurg (Spine 1) 98:21–30
178. Fox M, Onofrio B (1993) The natural history and management of symptomatic and asymptomatic vertebral hemangiomas. J Neurosurg 78:36–45
179. Franck JI, King RB, Petro GR, Kanzer MD (1987) A posttraumatic lumbar spinal synovial cyst. Case report. J Neurosurg 66:293–296
180. Franke J, Mahlfeld K, Grasshoff H (2002) [Results after resection of juxta-facet-cysts – Which role does a segmental instability play?]. Zentralbl Chir 127:497–502
181. Fransen P, Pizzolato GP, Otten P, Reverdin A, Lagier R, de Tribolet N (1997) Synovial cyst and degeneration of the transverse ligament: an unusual cause of high cervical myelopathy. Case report. J Neurosurg 86:1027–1030
182. Freidberg SR, Fellows T, Thomas CB, Mancall AC (1994) Experience with symptomatic spinal epidural cysts. Neurosurgery 34:989–993; discussion 993
183. Friedman M, Kim TH, Panahon AM (1976) Spinal cord compression in malignant lymphoma. Treatment and results. Cancer 37:1485–1491
184. Fritz RC, Kaiser JA, White AH, DeLong WB, Gamburd RS (1994) Magnetic resonance imaging of a thoracic intraspinal synovial cyst. Spine 19:487–490
185. Fuentes JM, Benezech J (1989) [Strategy of the surgical treatment of primary tumors of the spine]. Neurochirurgie 35:323–327, 352
186. Fujimura M, Kusaka Y, Shirane R (2003) Spinal lipoma associated with terminal syringohydromyelia and a spinal arachnoid cyst in a patient with cloacal exstrophy. Childs Nerv Syst 19:254–257
187. Fujita T, Kawahara N, Matsumoto T, Tomita K (1999) Chordoma in the cervical spine managed with en bloc excision. Spine 24:1848–1851
188. Gaiger AM, Soule EH, Newton WA Jr (1981) Pathology of rhabdomyosarcoma: experience of the Intergroup Rhabdomyosarcoma Study, 1972–78. Natl Cancer Inst Monogr:19–27
189. Gaitanis IN, Hadjipavlou AG, Katonis PG, Tzermiadianos MN, Pasku DS, Patwardhan AG (2005) Balloon kyphoplasty for the treatment of pathological vertebral compression fractures. Eur Spine J 14:250–260
190. Garcia-Bravo A, Sanchez-Enriquez J, Mendez-Suarez JL, Melian-Suarez A, Miranda-Calderin G (2002) Secondary tetraplegia due to giant-cell tumors of the cervical spine. Neurochirurgie 48:527–532
191. George B, Laurian C (1980) Surgical approach to the whole length of the vertebral artery with special reference to the third portion. Acta Neurochir (Wien) 51:259–272
192. George B, Lot G (1995) Neurinomas of the first two cervical nerve roots: a series of 42 cases. J Neurosurg 82:917–923
193. George B, Laurian C, Keravel Y, Cophignon J (1985) Extradural and hourglass cervical neurinomas: the vertebral artery problem. Neurosurgery 16:591–594
194. George B, Zerah M, Lot G, Hurth M (1993) Oblique transcorporeal approach to anteriorly located lesions in the cervical spinal canal. Acta Neurochir (Wien) 121:187–190
195. Gerson JM, Jaffe N, Donaldson MH, Tefft M (1978) Meningeal seeding from rhabdomyosarcoma of the head and neck with base of the skull invasion: recognition of the clinical evolution and suggestions for management. Med Pediatr Oncol 5:137–144
196. Ghogawala Z, Mansfield FL, Borges LF (2001) Spinal radiation before surgical decompression adversely affects outcomes of surgery for symptomatic metastatic spinal cord compression. Spine 26:818–824
197. Giehl JP, Kluba T (1999) Metastatic spine disease in renal cell carcinoma – indication and results of surgery. Anticancer Res 19:1619–1624
198. Gilbert RW, Kim JH, Posner JB (1978) Epidural spinal cord compression from metastatic tumor; diagnosis and treatment. Ann Neurol 3:40–51

199. Gokaslan ZL, York JE, Walsh GL, McCutcheon IE, Lang FF, Putnam JB Jr, Wildrick DM, Swisher SG, Abi-Said D, Sawaya R (1998) Transthoracic vertebrectomy for metastatic spinal tumors. J Neurosurg 89:599–609
200. Gottfried ON, Schloesser PE, Schmidt MH, Stevens EA (2004) Embolization of metastatic spinal tumors. Neurosurg Clin N Am 15:391–399
201. Goyal M, Mishra NK, Sharma A, Gaikwad SB, Mohanty BK, Sharma S (1999) Alcohol ablation of symptomatic vertebral hemangiomas. AJNR Am J Neuroradiol 20:1091–1096
202. Graham E, Lenke LG, Hannallah D, Lauryssen C (2001) Myelopathy induced by a thoracic intraspinal synovial cyst: case report and review of the literature. Spine 26: E392–394
203. Grant R, Papadopoulos SM, Sandler HM, Greenberg HS (1994) Metastatic epidural spinal cord compression: current concepts of treatment. J Neurooncol 19:79–92
204. Graziani N, Bouillot P, Figarella-Branger D, Dufour H, Peragut JC, Grisoli F (1994) Cavernous angiomas and arteriovenous malformations of the spinal epidural space: report of 11 cases. Neurosurgery 35:856–863; discussion 863–854
205. Greenspan A (1993) Benign bone-forming lesions: osteoma, osteoid osteoma, and osteoblastoma. Clinical, imaging, pathologic, and differential considerations. Skelet Radiol 22:485–500
206. Greinacher I, Gutjahr P (1978) [Vertebral changes in histiocytosis x]. Radiologe 18:228–232
207. Griffet J, Perraud L, Lacour C, Paquis P, Grellier P (1987) Chordome du rachis cervical. Rev Chir Orthop Suppl II 74:299–301
208. Grillo HC, Ojemann RG, Scannell JG, Zervas NT (1983) Combined approach to "dumbbell" intrathoracic and intraspinal neurogenic tumors. Ann Thorac Surg 36:402–407
209. Grisoli F, Vincentelli F, Sedan R, Hassoun J, Caruso G, Salpietro F (1988) Hemangiopericytomas of the spinal canal. Report of four cases and review of literature. J Neurosurg Sci 32:69–76
210. Grubb MR, Currier BL, Pritchard DJ, Ebersold MJ (1994) Primary Ewing's sarcoma of the spine. Spine 19:309–313
211. Grundfest-Broniatowski S, Fazio V, Marks K, Levin H (1988) [Diagnosis and treatment of sacral and retrorectal tumors. II]. Chirurg 59:343–348
212. Guest C, Wang EH, Davis A, Langer F, O'Sullivan B, Noria S, Bell RS (1993) Paraspinal soft-tissue sarcoma. Classification of 14 cases. Spine 18:1292–1297
213. Guo W, Xu WP, Yang RL, Tang XD (2003) [The surgical management of sacral tumors]. Zhonghua Wai Ke Za Zhi 41:827–831
214. Gupta RK, Phadke RV, Srivastava DN, Jain VK, Gujral RB (1992) CT demonstration of complex dorsal spinal dysraphism. Australas Radiol 36:2–3
215. Guthkelch AN (1948) Haemangiomas involving the spinal epidural space. J Neurol Neurosurg Psychiatry 11:199–210
216. Gutin PH, Leibel SA, Hosobuchi Y, Crumley RL, Edwards MS, Wilson CB, Lamb S, Weaver KA (1987) Brachytherapy of recurrent tumors of the skull base and spine with iodine-125 sources. Neurosurgery 20:938–945
217. Hagen T, Daschner H, Lensch T (2001) [Juxta-facet cysts: magnetic resonance tomography diagnosis]. Radiologe 41:1056–1062
218. Haher TR, Merola AA (2003) Surgical techniques for the spine. Thieme, New York
219. Han PP, Dickman CA (2002) Thoracoscopic resection of thoracic neurogenic tumors. J Neurosurg (Spine 3) 96:304–308
220. Harrington KD (1984) Anterior cord compression and spinal stabilization for patients with metastatic lesions of the spine. J Neurosurg 61:107–117
221. Harris DJ, Fornasier VL, Livingston KE (1978) Hemangiopericytoma of the spinal canal. Report of three cases. J Neurosurg 49:914–920
222. Harrison MJ, Eisenberg MB, Ullman JS, Oppenheim JS, Camins MB, Post KD (1995) Symptomatic cavernous malformations affecting the spine and spinal cord. Neurosurgery 37:195–204; discussion 204–195
223. Hart RA, Boriani S, Biagini R, Currier B, Weinstein JN (1997) A system for surgical staging and management of spine tumors. A clinical outcome study of giant cell tumors of the spine. Spine 22:1773–1782; discussion 1783
224. Hasegawa M, Fujisawa H, Hayashi Y, Tachibana O, Kida S, Yamashita J (2001) Surgical pathology of spinal schwannomas: a light and electron microscopic analysis of tumor capsules. Neurosurgery 49:1388–1392; discussion 1392–1383
225. Hatashita S, Kondo A, Shimizu T, Kurosu A, Ueno H (2001) Spinal extradural arachnoid cyst – case report. Neurol Med Chir (Tokyo) 41:318–321
226. Healey JH, Lane JM (1989) Chordoma: a critical review of diagnosis and treatment. Orthop Clin North Am 20:417–426
227. Heary RF, Bono CM (2001) Metastatic spinal tumors. Neurosurg Focus 11:Article 1
228. Heary RF, Vaccaro AR, Benevenia J, Cotler JM (1998) "En-bloc" vertebrectomy in the mobile lumbar spine. Surg Neurol 50:548–556
229. Heidecke V, Rainov NG, Burkert W (2003) Results and outcome of neurosurgical treatment for extradural metastases in the cervical spine. Acta Neurochir (Wien) 145:873–881
230. Helweg-Larsen S, Sorensen PS (1994) Symptoms and signs in metastatic spinal cord compression: a study of progression from first symptom until diagnosis in 153 patients. Eur J Cancer 30A:396–398
231. Heppner F, Clarici G (1984) Die operative Therapie der Wirbeltumoren aus neurochirurgischer Sicht. In: Die Wirbelsäule in Forschung und Praxis. Band 103. Tumoren der Wirbelsäule. Schmitt E (ed) Hippokrates Verlag, Berlin, pp 175–182
232. Hermann G, Sacher M, Lanzieri CF, Anderson PJ, Rabinowitz JG (1985) Chondrosarcoma of the spine: an unusual radiographic presentation. Skeletal Radiol 14:178–183

233. Hervas Benito I, Perez Velasco R, Vera Espallardo F, Bello Arques P, Saura Quiles A, Gonzalez Cabezas P, Mateo Navarro A (2001) [Bone scintigraphy in two cases of primary vertebral osteosarcoma in adults]. Rev Esp Med Nucl 20:299–304
234. Heyd R, Strassmann G, Filipowicz I, Borowsky K, Martin T, Zamboglou N (2001) [Radiotherapy in vertebral hemangioma]. Röntgenpraxis 53:208–220
235. Higginbotham NL, Phillips RF, Farr HW, Hustu HO (1967) Chordoma: thirty-five year study at Memorial Hospital. Cancer 20:1841–1850
236. Hillman J, Bynke O (1991) Solitary extradural cavernous hemangiomas in the spinal canal. Report of five cases. Surg Neurol 36:19–24
237. Hirsh LF, Thanki A, Spector HB (1984) Primary spinal chondrosarcoma with eighteen-year follow-up: case report and literature review. Neurosurgery 14:747–749
238. Hoffmann RT, Jakobs TF, Wallnofer A, Reiser MF, Helmberger TK (2003) [Percutaneous vertebroplasty (pv): indications, contraindications, and technique]. Radiologe 43:709–717
239. Holman PJ, Suki D, McCutcheon I, Wolinsky JP, Rhines LD, Gokaslan ZL (2005) Surgical management of metastatic disease of the lumbar spine: experience with 139 patients. J Neurosurg Spine 2:550–563
240. Hosono N, Yonenobu K, Fuji T, Ebara S, Yamashita K, Ono K (1995) Vertebral body replacement with a ceramic prosthesis for metastatic spinal tumors. Spine 20:2454–2462
241. Houten JK, Sanderson SP, Cooper PR (2003) Spontaneous regression of symptomatic lumbar synovial cysts. Report of three cases. J Neurosurg Spine 99:235–238
242. Howington JU, Connolly ES, Voorhies RM (1999) Intraspinal synovial cysts: 10-year experience at the Ochsner Clinic. J Neurosurg Spine 91:193–199
243. Hsu KY, Zucherman JF, Shea WJ, Jeffrey RA (1995) Lumbar intraspinal synovial and ganglion cysts (facet cysts) Ten-year experience in evaluation and treatment. Spine 20:80–89
244. Hu YG (1993) Intraspinal tumor in the higher cervical region. Chung Hua Wai Ko Tsa Chih 31:73–75
245. Huth JF, Dawson EG, Eilber FR (1984) Abdominosacral resection for malignant tumors of the sacrum. Am J Surg 148:157–161
246. Ido K, Matsuoka H, Urushidani H (2002) Effectiveness of a transforaminal surgical procedure for spinal extradural arachnoid cyst in the upper lumbar spine. J Clin Neurosci 9:694–696
247. Ijiri K, Yuasa S, Yone K, Matsunaga S, Ryoki Y, Taniguchi N, Yonezawa S, Komiya S (2002) Primary epidural hemangiopericytoma in the lumbar spine: a case report. Spine 27:E189–192
248. Ilaslan H, Sundaram M, Unni KK, Dekutoski MB (2004) Primary Ewing's sarcoma of the vertebral column. Skeletal Radiol
249. Ilaslan H, Sundaram M, Unni KK, Shives TC (2004) Primary vertebral osteosarcoma: imaging findings. Radiology 230:697–702
250. Imai K, Nakamura K, Inokuchi K, Oda H (1998) Aspiration of intraspinal synovial cyst: recurrence after temporal improvement. Arch Orthop Trauma Surg 118:103–105
251. Imai R, Kamada T, Tsuji H, Yanagi T, Baba M, Miyamoto T, Kato S, Kandatsu S, Mizoe J, Tsuji H, Tatezaki S (2004) Carbon ion radiotherapy for unresectable sacral chordomas. Clin Cancer Res 10:5741–5746
252. Inoue H, Nishinaka K, Urushitani M, Udaka F, Kameyama M (1996) [A case of a thoracic extradural arachnoid cyst presenting with slowly progressive muscle weakness in the right upper and lower limbs]. Rinsho Shinkeigaku 36:47–51
253. Irger IM, Petukhov SS (1976) [Diagnosis and surgical treatment of hourglass shaped tumors of cervical localization]. Vopr Neirokhir 6:7–14
254. Ishii K, Chiba K, Watanabe M, Yabe H, Fujimura Y, Toyama Y (2002) Local recurrence after S2–3 sacrectomy in sacral chordoma. Report of four cases. J Neurosurg (Spine 1) 97:98–101
255. Isu T, Iwasaki Y, Akino M, Abe H, Tashiro K, Miyasaka K, Saito H, Nomura M (1987) [Diagnosis of a cystic lesion in the spinal cord – studies on delayed CT myelography and MRI]. No Shinkei Geka 15:725–730
256. Isu T, Iizuka T, Iwasaki Y, Nagashima M, Akino M, Abe H (1991) Spinal cord herniation associated with an intradural spinal arachnoid cyst diagnosed by magnetic resonance imaging. Neurosurgery 29:137–139
257. Iwasaki M, Nakamura K, Takeshita K, Kawaguchi H, Akune T, Hoshino Y (1998) Surgical management of giant schwannoma in the lumbosacral region. J Spinal Disord 11:444–447
258. Iwasaki Y, Nakagawa T, Koiwa M (1978) [A case of cervical extradural neurinoma with vertebral artery occlusion]. No Shinkei Geka 6:701–705
259. Jabre A, Shahbabian S, Keller JT (1987) Synovial cyst of the cervical spine. Neurosurgery 20:316–318
260. Jackson RP (1978) Recurrent osteoblastoma: a review. Clin Orthop 131:229–233
261. Jacobs WB, Perrin RG (2001) Evaluation and treatment of spinal metastases: an overview. Neurosurg Focus 11: Article 10
262. Jang JS, Lee SH (2005) Efficacy of percutaneous vertebroplasty combined with radiotherapy in osteolytic metastatic spinal tumors. J Neurosurg Spine 2:243–248
263. Jansson KA, Bauer HC (2006) Survival, complications and outcome of 282 patients operated for neurological deficit due to thoracic or lumbar spinal metastases. Eur Spine J 15:196–202
264. Jayakumar PN, Vasudev MK, Srikanth SG (1997) Symptomatic vertebral haemangioma: endovascular treatment of 12 patients. Spinal Cord 35:624–628
265. Jena A, Gupta RK, Sharma A, Prakesh VE, Khushu S (1990) Magnetic resonance diagnosis of spinal arachnoid cyst. A report of two cases. Childs Nerv Syst 6:107–109
266. Jeremic B, Grujicic D, Cirovic V, Djuric L, Mijatovic L (1991) Radiotherapy of metastatic spinal cord compression. Acta Oncol 30:985–986

267. Jinnai T, Hoshimaru M, Koyama T (2005) Clinical characteristics of spinal nerve sheath tumors: analysis of 149 cases. Neurosurgery 56:510–515
268. Job-Deslandre C, Gagnerie F, Revel M, Chevrot A, Amor B, Menkes CJ (1989) [Sciatica caused by a posterior articular cyst. Apropos of 8 cases]. Rev Rhum Mal Osteoartic 56:731–734
269. Jost SC, Hsien Tu P, Wright NM (2003) Symptomatic intraosseous synovial cyst in the cervical spine: a case report. Spine 28:E344–346
270. Kadri PA, Mello PM, Olivera JG, Braga FM (2002) [Primary lumbar epidural Ewing's sarcoma: case report]. Arq Neuropsiquiatr 60:145–149
271. Kaiser TE, Pritchard DJ, Unni KK (1984) Clinicopathological study of sacrococcygeal chordoma. Cancer 53:2574–2578
272. Kalinichenko LV, Vesnin AG, Murenkov OV, Kochnev VA (1988) [Difficulties of differential roentgeno-diagnosis of aneurysmal cysts and tumors of flat bones and the spine]. Vopr Onkol 34:1166–1171
273. Kamata M, Satomi K, Hirabayashi K, Ueno M, Asazuma T, Fujimura Y (1992) A congenital spinal arachnoid diverticulum expanded into the retropleural cavity. A case report and short literature review. Spine 17:854–857
274. Kaneko K, Inoue Y (2000) Haemorrhagic lumbar synovial cyst. A cause of acute radiculopathy. J Bone Joint Surg Br 82:583–584
275. Karparov M, Kitov D (1977) Aneurysmal bone cyst of the spine. Acta Neurochir (Wien) 39:101–113
276. Kaspers GJ, Kamphorst W, van de Graaff M, van Alphen HA, Veerman AJ (1991) Primary spinal epidural extraosseous Ewing's sarcoma. Cancer 68:648–654
277. Katagiri H, Takahashi M, Inagaki J, Kobayashi H, Sugiura H, Yamamura S, Iwata H (1998) Clinical results of nonsurgical treatment for spinal metastases. Int J Radiat Oncol Biol Phys 42:1127–1132
278. Kaufmann AM, Halliday WC, West M, Fewer D, Ross I (1996) Periodontoid synovial cyst causing cervico-medullary compression. Can J Neurol Sci 23:227–230
279. Kawahara N, Tomita K, Matsumoto T, Fujita T (1998) Total en bloc spondylectomy for primary malignant vertebral tumors. Chir Organi Mov 83:73–86
280. Kendall BE, Valentine AR, Keis B (1982) Spinal arachnoid cysts: clinical and radiological correlation with prognosis. Neuroradiology 22:225–234
281. Khalfallah M, Malca S, Roche PH, Duffaud F, Soumare O, Garbe L, Pellet W (1997) [Primary spinal osteosarcomas]. Neurochirurgie 43:28–34
282. Khan AM, Synnot K, Cammisa FP, Girardi FP (2005) Lumbar synovial cysts of the spine. An evaluation of surgical outcome. J Spinal Disord Tech 18:127–131
283. Khan DC, Malhotra S, Stevens RE, Steinfeld AD (1999) Radiotherapy for the treatment of giant cell tumor of the spine: a report of six cases and review of the literature. Cancer Invest 17:110–113
284. Khaw FM, Worthy SA, Gibson MJ, Gholkar A (1999) The appearance on MRI of vertebrae in acute compression of the spinal cord due to metastases. J Bone Joint Surg Br 81:830–834
285. Khurana JS, Rosenthal DI, Rosenberg AE, Mankin HJ (1989) Skeletal metastases in liposarcoma detectable only by magnetic resonance imaging. Clin Orthop Relat Res 243:204–207
286. Kim CH, Bak KH, Kim JM, Kim NK (1999) Symptomatic sacral extradural arachnoid cyst associated with lumbar intradural arachnoid cyst. Clin Neurol Neurosurg 101:148–152
287. Kim DH, Henn JS, Vaccaro A, Dickmann CA (2005) Surgical anatomy and techniques to the spine. WB Saunders, Philadelphia
288. Kim RY, Smith JW, Spencer SA, Meredith RF, Salter MM (1993) Malignant epidural spinal cord compression associated with a paravertebral mass: its radiotherapeutic outcome on radiosensitivity. Int J Radiat Oncol Biol Phys 27:1079–1083
289. Kimura S, Kawaguchi S, Wada T, Nagoya S, Yamashita T, Kikuchi K (2002) Rhabdomyosarcoma arising from a dormant dumbbell ganglioneuroma of the lumbar spine: a case report. Spine 27:E513–517
290. King GJ, Kostuik JP, McBroom RJ, Richardson W (1991) Surgical management of metastatic renal carcinoma of the spine. Spine 16:265–271
291. Kingdom TT, Nockels RP, Kaplan MJ (1995) Transoral-transpharyngeal approach to the craniocervical junction. Otolaryngol Head Neck Surg 113:393–400
292. Kirwan EO, Hutton PA, Pozo JL, Ransford AO (1984) Osteoid osteoma and benign osteoblastoma of the spine. Clinical presentation and treatment. J Bone Joint Surg Br 66:21–26
293. Kitamura J, Hida K, Seki T, Iwasaki Y (2002) [Giant, invasive sacral schwannoma extending to the 4th lumbar spine]. No Shinkei Geka 30:1203–1208
294. Klimo P, Schmidt MH (2004) Surgical management of spinal metastases. Oncologist 9:188–196
295. Klimo P, Dailey AT, Fessler RG (2004) Posterior surgical approaches and outcomes in metastatic spine-disease. Neurosurg Clin N Am 15:425–435
296. Kluger P, Korge A, Scharf HP (1997) Strategy for the treatment of patients with spinal neoplasms. Spinal Cord 35:429–436
297. Knöringer P (1986) Osteosynthesis in patients with malignant tumors of the cervical vertebral column: indications, technique, and results. Adv Neurosurg 14:125–132
298. Kochbati L, Ben Romdhane NK, Mrad K, Nasr C, Ben Salah DE, Ben Romdhane K, Maalej M (2004) [Solitary bone plasmocytoma: treatment and outcome features]. Cancer Radiother 8:70–74
299. Kostuik JP, Errico TJ, Gleason TF, Errico CC (1988) Spinal stabilization of vertebral column tumors. Spine 13:250–256
300. Krepler P, Windhager R, Bretschneider W, Toma CD, Kotz R (2002) Total vertebrectomy for primary malignant tumours of the spine. J Bone Joint Surg Br 84:712–715
301. Krepler P, Windhager R, Toma CD, Kitz K, Kotz R (2003) Dura resection in combination with en bloc spondylectomy for primary malignant tumors of the spine. Spine 28:E334–338

302. Krings T, Lukas R, Reul J, Spetzger U, Reinges MH, Gilsbach JM, Thron A (2001) Diagnostic and therapeutic management of spinal arachnoid cysts. Acta Neurochir (Wien) 143:227–234; discussion 234–225
303. Kruse R, Simon RG, Stanton R, Grissom LE, Conard K (1997) Mesenchymal chondrosarcoma of the cervical spine in a child. Am J Orthop 26:279–282
304. Kuga D, Shono T, Miyazono M, Sasaki T (2004) [Vertebral hemangioma extending into the spinal canal: case report]. No Shinkei Geka 32:43–47
305. Kujas M, Lopes M, Lalam TF, Fohanno D, Poirier J (1999) Infiltrating extradural spinal angiolipoma. Clin Neuropathol 18:93–98
306. Kumar PP, Good RR, Skultety FM, Masih AS, McComb RD (1987) Spinal metastases from pituitary hemangiopericytic meningioma. Am J Clin Oncol 10:422–428
307. Kumar R, Taha J, Greiner AL (1995) Herniation of the spinal cord. Case report. J Neurosurg 82:131–136
308. Kurose K, Kishi H, Sadatoh T (1989) [Spinal epidural cavernous hemangioma. Case report]. Neurol Med Chir (Tokyo) 29:538–542
309. Labauge R, Pages M, Testard D, Privat JM (1989) [Extradural arachnoid cyst of the dorsal region with relapsing and recurrent development]. Rev Neurol (Paris) 145:405–407
310. Lafforgue P, Clairet D, Chagnaud C, Toussirot E, Daumen-Legre V, Schiano A, Bayle O, Kasbarian M, Acquaviva PC (1992) [Aspects and role of spinal MRI in the assessment of solitary plasmacytoma and multiple myeloma. Apropos of 11 cases]. Rev Rhum Mal Osteoartic 59:317–326
311. Lam CH, Nagib MG (2002) Nonteratomatous tumors in the pediatric sacral region. Spine 27:E284–287
312. Landmann C, Hünig R, Gratzl O (1992) The role of laminectomy in the combined treatment of metastatic spinal cord compression. Int J Radiat Oncol Biol Phys 24:627–631
313. Landreneau FE, Landreneau RJ, Keenan RJ, Ferson PF (1995) Diagnosis and management of spinal metastases from breast cancer. J Neurooncol 23:121–134
314. Le H, Balabhadra R, Park J, Kim D (2003) Surgical treatment of tumors involving the cervicothoracic junction. Neurosurg Focus 15:Article 3
315. Le Breton C, Meziou M, Laredo JD, Amouroux J, Mazabraud A, Bigot JM, Tubiana JM (1993) [Sarcoma of the spine in Paget's disease of bone. Apropos of 8 cases]. Rev Rhum Ed Fr 60:16–22
316. Le Charpentier Y, Bellefqih S, Boisnic S, Roy-Camille R (1988) [Chordomas]. Ann Pathol 8:25–32
317. Lee JP, Wang AD, Wai YY, Ho YS (1990) Spinal extradural cavernous hemangioma. Surg Neurol 34:345–351
318. Lee S, Hadlow AT (1999) Extraosseous extension of vertebral hemangioma, a rare cause of spinal cord compression. Spine 24:2111–2114
319. Lee ST, Lui TN, Tsai MD (1989) Primary intraspinal dura mesenchymal chondrosarcoma. Surg Neurol 31:54–57
320. Leeson MC, Zechmann JP (1993) Metastatic carcinoma of the spine with neurologic complications: an autopsy review. Orthopedics 16:1119–1122
321. Leone A, Costantini A, Guglielmi G, Settecasi C, Priolo F (2000) Primary bone tumors and pseudotumors of the lumbosacral spine. Rays 25:89–103
322. Lepage J, Rigault P, Nezelof C, Padovani JP, Pierre-Kahn A, Guyonvarc'h G (1984) [Benign osteoblastoma in children. Apropos of 8 cases, 4 with spinal localization]. Rev Chir Orthop Reparatrice Appar Mot 70:117–127
323. Lesoin F, Bonneterre J, Lesoin A, Jomin M (1982) [Neurologic manifestations of spinal plasmacytomas]. Neurochirurgie 28:401–407
324. Lewandrowski KU, Hecht AC, DeLaney TF, Chapman PA, Hornicek FJ, Pedlow FX (2004) Anterior spinal arthrodesis with structural cortical allografts and instrumentation for spine tumor surgery. Spine 29:1150–1158; discussion 1159
325. Lin YJ, Tu YK, Lin SM, Shun CT (1996) Primary hemangiopericytoma in the axis bone: case report and review of literature. Neurosurgery 39:397–399; discussion 399–400
326. Lingg G, Roessner A, Telgmann CL, Karbowski A, Peters PE, Grundmann E (1986) [X-ray morphology and pathologic anatomy of osteoblastoma]. ROFO Fortschr Geb Rontgenstr Nuklearmed 145:49–56
327. Liu JK, Apfelbaum RI, Chiles BW III, Schmidt MH (2003) Cervical spinal metastasis: anterior reconstruction and stabilization techniques after tumor resection. Neurosurg Focus 15:Article 2
328. Liu JK, Brockmeyer DL, Dailey AT, Schmidt MH (2003) Surgical management of aneurysmatic bone cysts of the spine. Neurosurg Focus 15:Article 4
329. Liu JK, Apfelbaum RI, Schmidt MH (2004) Surgical management of cervical spinal metastasis: anterior reconstruction and stabilization techniques. Neurosurg Clin N Am 15:413–424
330. Liu SS, Williams KD, Drayer BP, Spetzler RF, Sonntag VK (1989) Synovial cysts of the lumbosacral spine: diagnosis by MR imaging. AJNR Am J Neuroradiol 10:1239–1242
331. Locatelli F, Tonani P, Porta F, Zecca M, Beluffi G, Fiori P, Rosso R, Paulli M, Basso G, Invernizzi R, et al (1991) Rhabdomyosarcoma with primary osteolytic lesions simulating non-Hodgkin's lymphoma. Pediatr Hematol Oncol 8:159–164
332. Lopes NM, Aesse FF, Lopes DK (1992) Compression of thoracic nerve root by a facet joint synovial cyst: case report. Surg Neurol 38:338–340
333. Loquet E, Thibaut R, Thibaut H, Hendrickx M (1993) Surgical treatment of spinal metastases. Acta Orthop Belg 59:79–82
334. Lot G, George B (1997) Cervical neuromas with extradural components: surgical management in a series of 57 patients. Neurosurgery 41:813–820; discussion 820–812
335. Lucas S, Cendan E, Auque J, Civit T, Caremelle S, Braun D (1992) [Asymptomatic giant thoracic dumbbell neurinoma. Apropos of a case]. J Chir (Paris) 129:81–87
336. Lybeert MLM, Meerwaldt JH (1986) Chordoma. Report on treatment results in eighteen cases. Acta Radiol Oncol 25:41–43

337. Lynn B, Watkins RG, Watkins RI, Williams LA (2000) Acute traumatic myelopathy secondary to a thoracic cyst in a professional football player. Spine 25:1593–1595
338. Lyons MK, Atkinson JL, Wharen RE, Deen HG, Zimmerman RS, Lemens SM (2000) Surgical evaluation and management of lumbar synovial cysts: the Mayo Clinic experience. J Neurosurg Spine 93:53–57
339. MacCarthy CS, Waugh JM, Coventry MB, O'Sullivan DC (1961) Sacrococcygeal chordomas. Surg Gynecol Obstet 113:551–554
340. Maezawa Y, Baba H, Uchida K, Furusawa N, Kubota C, Yoshizawa K (2000) Spontaneous remission of a solitary intraspinal synovial cyst of the lumbar spine. Eur Spine J 9:85–87
341. Magerl F, Jeanneret B (1988) Surgical management of tumor-related spinal instability. Recent Results Cancer Res 108:163–171
342. Magrini SM, Papi MG, Marletta F, Tomaselli S, Cellai E, Mungai V, Biti G (1992) Chordoma – natural history, treatment and prognosis. The Florence Radiotherapy Department experience (1956–1990) and a critical review of the literature. Acta Oncol 31:847–851
343. Maheshwari V, Srivastava VK (1997) Benign osteoblastoma mimicking malignancy of the spine. J Postgrad Med 43:78–80
344. Maloney WJ, Vaughan LM, Jones HH, Ross J, Nagel DA (1989) Benign metastasizing giant-cell tumor of bone. Report of three cases and review of the literature. Clin Orthop Relat Res 243:208–215
345. Manke C, Bretschneider T, Lenhart M, Strotzer M, Neumann C, Gmeinwieser J, Feuerbach S (2001) Spinal metastases from renal cell carcinoma: effect of preoperative particle embolization on intraoperative blood loss. AJNR Am J Neuroradiol 22:997–1003
346. Manzone P, Fiore N, Forlino D, Alcala M, Cabrera CF (1998) Chordoma of the lumbar L2 vertebra: case report and review of the literature. Eur Spine J 7:252–256
347. Maranzano E, Latini P (1995) Effectiveness of radiation therapy without surgery in metastatic spinal cord compression: final results from a prospective trial. Int J Radiat Oncol Biol Phys 32:959–967
348. Maranzano E, Latini P, Checcaglini F, Ricci S, Panizza PM, Aristei C, Perrucci E, Beneventi S, Corgna E, Tonato M (1991) Radiation therapy in metastatic spinal cord compression. A prospective analysis of 105 consecutive patients. Cancer 67:1311–1317
349. Maranzano E, Latini P, Checcaglini F, Perrucci E, Aristei C, Panizza BM, Ricci S (1992) Radiation therapy of spinal cord compression caused by breast cancer: report of a prospective trial. Int J Radiat Oncol Biol Phys 24:301–306
350. Maranzano E, Trippa F, Chirico L, Basagni ML, Rossi R (2003) Management of metastatic spinal cord compression. Tumori 89:469–475
351. Marchesi DG, Boos N, Aebi M (1993) Surgical treatment of tumors of the cervical spine and first two thoracic vertebrae. J Spinal Disord 6:489–496
352. Marmor E, Rhines LD, Weinberg JS, Gokaslan ZL (2001) Total en bloc lumbar spondylectomy. J Neurosurg 95:264–269
353. Marsh BW, Bonfiglio M, Brady LP, Enneking WF (1975) Benign osteoblastoma: range of manifestations. J Bone Joint Surg Am 57:1–9
354. Martenson JA, Evans RG, Lie MR, Ilstrup D, Dinapoli RP, Ebersold MJ, Earle JD (1985) Treatment outcome and complications in patients treated for malignant epidural cord compression. J Neurooncol 3:77–84
355. Martin G (2000) Spinal cord herniation into an extradural arachnoid cyst. J Clin Neurosci 7:330–331
356. Martin JB, Wetzel SG, Seium Y, Dietrich PY, Somon T, Gailloud P, Payer M, Kelekis A, Ruefenacht DA (2003) Percutaneous vertebroplasty in metastatic disease: transpedicular access and treatment of lysed pedicles – initial experience. Radiology 229:593–597
357. Masuzawa H, Nakayama H, Shitara N, Suzuki T (1981) Spinal cord herniation into a congenital extradural arachnoid cyst causing Brown-Sequard syndrome. Case report. J Neurosurg 55:983–986
358. Matsui H, Tatezaki S, Tsuji H (1994) Ceramic vertebral body replacement for metastatic spine tumors. J Spinal Disord 7:248–254
359. Mazel C, Topouchian V, Grunenwald D (2002) Effectiveness of radical resections in malignant dumbbell tumors of the thoracic spine: review of three cases. J Spinal Disord Tech 15:507–512
360. Mazel C, Grunenwald D, Laudrin P, Marmorat JL (2003) Radical excision in the management of thoracic and cervicothoracic tumors involving the spine: results in a series of 36 cases. Spine 28:782–792; discussion 792
361. Mazel C, Hoffmann E, Antonietti P, Grunenwald D, Henry M, Williams J (2004) Posterior cervicothoracic instrumentation in spine tumors. Spine 29:1246–1253
362. McCormick PC (1996) Surgical management of dumbbell and paraspinal tumors of the thoracic and lumbar spine. Neurosurgery 38:67–74; discussion 74–75
363. McCormick PC, Post KD, Stein BM (1990) Intradural extramedullary tumors in adults. Neurosurg Clin N Am 1:591–608
364. McLain RF, Weinstein JN (1989) Solitary plasmacytomas of the spine: a review of 84 cases. J Spinal Disord 2:69–74
365. McLeod RA, Dahlin DC, Beabout JW (1976) The spectrum of osteoblastoma. Am J Roentgenol 126:321–325
366. McMaster ML, Goldstein AM, Bromley CM, Ishibe N, Parry DM (2001) Chordoma: incidence and survival patterns in the United States, 1973–1995. Cancer Causes Control 12:1–11
367. Mena H, Ribas JL, Pezeshkpour GH, Cowan DN, Parisi JE (1991) Hemangiopericytoma of the central nervous system: a review of 94 cases. Hum Pathol 22:84–91
368. Mercader J, Munoz Gomez J, Cardenal C (1985) Intraspinal synovial cyst: diagnosis by CT. Follow-up and spontaneous remission. Neuroradiology 27:346–348
369. Merimsky O, Kollender Y, Bokstein F, Issakov J, Flusser G, Inbar MJ, Meller I, Bickels J (2004) Radiotherapy for spinal cord compression in patients with soft-tissue sarcoma. Int J Radiat Oncol Biol Phys 58:1468–1473

370. Metellus P, Flores-Parra I, Fuentes S, Dufour H, Adetchessi T, Do L, Bouvier C, Manera L, Grisoli F (2003) [A retrospective study of 32 lumbar synovial cysts. Clinical aspect and surgical management]. Neurochirurgie 49:73–82
371. Meyer S, Reinhard H, Graf N, Kramann B, Schneider G (2002) Arterial embolization of a secondary aneurysmatic bone cyst of the thoracic spine prior to surgical excision in a 15-year-old girl. Eur J Radiol 43:79–81
372. Mill WB, Griffith R (1980) The role of radiation therapy in the management of plasma cell tumors. Cancer 45:647–652
373. Miller SC, Lloyd RD, Bruenger FW, Krahenbuhl MP, Polig E, Romanov SA (2003) Comparisons of the skeletal locations of putative plutonium-induced osteosarcomas in humans with those in beagle dogs and with naturally occurring tumors in both species. Radiat Res 160:517–523
374. Miravet E, Sinisterra S, Birchansky S, Papazian O, Tuite G, Grossman JA, Alfonso I (2002) Cervicothoracic extradural arachnoid cyst: possible association with obstetric brachial plexus palsy. J Child Neurol 17:770–772
375. Mirra SS, Tindall SC, Check IJ, Byrnes RK, Moore WW (1983) Inflammatory meningeal masses of unexplained origin: an ultrastructural and immunological study. J Neuropathol Exp Neurol 42:453–468
376. Miwa M, Doita M, Takayama H, Muratsu H, Harada T, Kurosaka M (2004) An expanding cervical synovial cyst causing acute cervical radiculopathy. J Spinal Disord Tech 17:331–333
377. Miyake S, Tamaki N, Nagashima T, Kurata H, Eguchi T, Kimura H (1998) Idiopathic spinal cord herniation. Report of two cases and review of the literature. J Neurosurg 88:331–335
378. Mohan V, Sabri T, Marklund T, Sayed M, Gupta RP (1991) Clinicoradiological diagnosis of benign osteoblastoma of the spine in children. Arch Orthop Trauma Surg 110:260–264
379. Mondal A, Kundu B, Gupta S, Biswas J (2002) Secondary malignant giant cell tumour of bone – a study of five cases with short review of literature. Indian J Pathol Microbiol 45:273–275
380. Moore AJ, Uttley D (1989) Anterior decompression and stabilization of the spine in malignant disease. Neurosurgery 24:713–717
381. Morandi X, Riffaud L, Haegelen C, Lancien G, Kerbrat P, Guegan Y (2001) [Extraosseous Ewing's sarcoma of the spinal epidural space]. Neurochirurgie 47:38–44
382. Morello A, Tumbiolo A, Pinto G, Lo Duca B (1991) Cavernous angioma of the spinal dura. J Neurosurg Sci 35:31–35
383. Morio Y, Yoshioka T, Nagashima H, Hagino H, Teshima R (2003) Intraspinal synovial cyst communicating with the C1–C2 facet joints and subarachnoid space associated with rheumatoid atlantoaxial instability. Spine 28: E492–495
384. Moulopoulos LA, Dimopoulos MA, Weber D, Fuller L, Libshitz HI, Alexanian R (1993) Magnetic resonance imaging in the staging of solitary plasmacytoma of bone. J Clin Oncol 11:1311–1315
385. Mühlbauer M, Pfisterer W, Eyb R, Knosp E (2000) Noncontiguous spinal metastases and plasmocytomas should be operated on through a single posterior midline approach, and circumferential decompression should be performed with individualized reconstruction. Acta Neurochir (Wien) 142:1219–1230
386. Mukhopadhyay P, Gairola M, Sharma M, Thulkar S, Julka P, Rath G (2001) Primary spinal epidural extraosseous Ewing's sarcoma: report of five cases and literature review. Australas Radiol 45:372–379
387. Muller JP, Destee A, Verier A, Lesoin F, Krivosic I, Jomin M, Warot P (1986) [Intraspinal hemangiopericytoma. 2 cases and review of the literature]. Neurochirurgie 32:140–146
388. Mummaneni PV, Haid RW (2005) Transoral odontoidectomy. Neurosurgery 56:1045–1050
389. Munzenrider JE, Liebsch NJ (1999) Proton therapy for tumors of the skull base. Strahlenther Onkol 175 Suppl 2:57–63
390. Muraszko KM, Antunes JL, Hilal SK, Michelsen WJ (1982) Hemangiopericytomas of the spine. Neurosurgery 10:473–479
391. Murphey MD, Andrews CL, Flemming DJ, Temple TH, Smith WS, Smirniotopoulos JG (1996) From the archives of the AFIP. Primary tumors of the spine: radiologic pathologic correlation. Radiographics 16:1131–1158
392. Muzumdar D, Desai K, Goel A, Shenoy A (2000) Unusual massive neurinoma in the suboccipital region – case report. Neurol Med Chir (Tokyo) 40:280–282
393. Myles LM, Gupta N, Armstrong D, Rutka JT (1999) Multiple extradural arachnoid cysts as a cause of spinal cord compression in a child. Case report. J Neurosurg Spine 91:116–120
394. Myles ST, MacRae ME (1988) Benign osteoblastoma of the spine in childhood. J Neurosurg 68:884–888
395. Nagasawa S, Ohtsuki H (1991) [A case of C2 neurinoma suffering syncopal episodes]. No Shinkei Geka 19:589–593
396. Nagasawa S, Ohta T, Kajimoto Y, Aoki J, Onomura T, Miyaji Y (1994) Giant neurinoma occupying the holocervical and upper thoracic regions: case report. Surg Neurol 42:157–159
397. Nemoto O, Moser RP Jr, Van Dam BE, Aoki J, Gilkey FW (1990) Osteoblastoma of the spine. A review of 75 cases. Spine 15:1272–1280
398. Nijensohn E, Russell EJ, Milan M, Brown T (1990) Calcified synovial cyst of the cervical spine: CT and MR evaluation. J Comput Assist Tomogr 14:473–476
399. Noel G, Habrand JL, Jauffret E, de Crevoisier R, Dederke S, Mammar H, Haie-Meder C, Pontvert D, Hasboun D, Ferrand R, Boisserie G, Beaudre A, Gaboriaud G, Guedea F, Petriz L, Mazeron JJ (2003) Radiation therapy for chordoma and chondrosarcoma of the skull base and the cervical spine. Prognostic factors and patterns of failure. Strahlenther Onkol 179:241–248

400. Nonaka M, Kohmura E, Hirata M, Hayakawa T (1998) Metastatic meningeal hemangiopericytoma of thoracic spine. Clin Neurol Neurosurg 100:228–230
401. North RB, LaRocca VR, Schwartz J, North CA, Zahurak M, Davis RF, McAfee PC (2005) Surgical management of spinal metastases: analysis of prognostic factors during a 10-year experience. J Neurosurg Spine 2:564–573
402. Nottebaert M, Von Hochstetter AR, Exner GU, Schreiber U (1987) Metastatic carcinoma of the spine. A study of 92 cases. Int Orthop 11:345–348
403. Nowakowski VA, Castro JK, Petti PL, Collier JM, Dattari I, Ahn D, Gauger G, Sutin P, Linstadt DE, Phillips TL (1991) Charged particle radiotherapy of paraspinal tumors. Int J Radiat Oncol Biol Phys 22:295–303
404. Obenberger J, Seidl Z, Plas J (1999) Osteoblastoma in lumbar vertebral body. Neuroradiology 41:279–282
405. Oda Y, Miura H, Tsuneyoshi M, Iwamoto Y (1998) Giant cell tumor of bone: oncological and functional results of long-term follow-up. Jpn J Clin Oncol 28:323–328
406. Oe T, Hoshino Y, Kurokawa T (1990) [A case of idiopathic herniation of the spinal cord associated with duplicated dura mater and with an arachnoid cyst]. Nippon Seikeigeka Gakkai Zasshi 64:43–49
407. Oertel MF, Ryang Y, Ince A, Gilsbach JM, Rohde V (2003) Microsurgical therapy of symptomatic lumbar juxta facet cysts. Minim Invasive Neurosurg 46:349–353
408. Ogihara Y, Sekiguchi K, Tsuruta T (1984) Osteogenic sarcoma of the fourth thoracic vertebra. Long-term survival by chemotherapy only. Cancer 53:2615–2618
409. Ogura T, Mori M, Hayashida T, Osawa T, Hase H (2002) Spinal reconstruction for symptomatic thoracic haemangioma using a titanium cage. Postgrad Med J 78:559–561
410. Okamoto K, Doita M, Yoshikawa M, Manabe M, Sha N, Yoshiya S (2004) Synovial cyst at the C1–C2 junction in a patient with atlantoaxial subluxation. J Spinal Disord Tech 17:535–538
411. O'Neill P, Bell BA, Miller JD, Jacobson I, Guthrie W (1985) Fifty years of experience with chordomas in Southeast Scotland. Neurosurgery 16:166–170
412. Osborn JL, Getzenberg RH, Trump DL (1995) Spinal cord compression in prostate cancer. J Neurooncol 23:135–147
413. Ozaki T, Hillmann A, Winkelmann W (1997) Surgical treatment of sacrococcygeal chordoma. J Surg Oncol 64:274–279
414. Ozaki T, Flege S, Liljenqvist U, Hillmann A, Delling G, Salzer-Kuntschik M, Jurgens H, Kotz R, Winkelmann W, Bielack SS (2002) Osteosarcoma of the spine: experience of the Cooperative Osteosarcoma Study Group. Cancer 94:1069–1077
415. Ozaki T, Liljenqvist U, Halm H, Hillmann A, Gosheger G, Winkelmann W (2002) Giant cell tumor of the spine. Clin Orthop 401:194–201
416. Padolecchia R, Acerbi G, Puglioli M, Collavoli PL, Ravelli V, Caciagli P (1998) Epidural spinal cavernous hemangioma. Spine 23:1136–1140
417. Padovani R, Acciarri R, Giulioni M, Pantieri R, Foschini MP (1997) Cavernous angiomas of the spinal district: surgical treatment of 11 patients. Eur Spine J 6:298–303
418. Panteli K, Tsiara S, Bourantas KL (2002) Solitary bone plasmacytoma in a young patient. J Exp Clin Cancer Res 21:139–141
419. Parlier-Cuau C, Wybier M, Laredo JD (1997) [Secret information provided by lumbosacral myelography]. Ann Radiol (Paris) 40:215–224
420. Parlier-Cuau C, Wybier M, Nizard R, Champsaur P, Le Hir P, Laredo JD (1999) Symptomatic lumbar facet joint synovial cysts: clinical assessment of facet joint steroid injection after 1 and 6 months and long-term follow-up in 30 patients. Radiology 210:509–513
421. Pasquier B, Vasdev A, Gasnier F, Chirossel JP, Keddari E, Pasquier D, Crouzet G, Couderc P (1984) [Epidural angiolipoma: a rare and curable cause of spinal cord compression]. Ann Pathol 4: 365–369
422. Pastushyn AI, Slin'ko EI, Mirzoyeva GM (1998) Vertebral hemangiomas: diagnosis, management, natural history and clinicopathological correlates in 86 patients. Surg Neurol 50:535–547
423. Patel SC, Sanders WP (1988) Synovial cyst of the cervical spine: case report and review of the literature. AJNR Am J Neuroradiol 9:602–603
424. Pearlman AW, Friedman M (1970) Radical radiation therapy of chordoma. AJR Am J Roentgenol 108:333–341
425. Pereira P, Duarte F, Lamas R, Vaz R (2001) Idiopathic spinal cord herniation: case report and literature review. Acta Neurochir (Wien) 143:401–406
426. Perrin RG, Laxton AW (2004) Metastatic spine disease: epidemiology, pathophysiology, and evaluation of patients. Neurosurg Clin N Am 15:365–373
427. Perrin RG, McBroom RJ, Perrin RG (1991) Metastatic tumors of the cervical spine. Clin Neurosurg 37:740–755
428. Pertuiset E, Bellaiche L, Liote F, Laredo JD (1996) Magnetic resonance imaging of the spine in plasma cell dyscrasias. A review. Rev Rhum Engl Ed 63:837–845
429. Peters ND (1987) Chordomas: a review. Early diagnosis and complete removal offer potential for cure. R I Med J 70:173–176
430. Pettine KA, Klassen RA (1986) Osteoid-osteoma and osteoblastoma of the spine. J Bone Joint Surg Am 68:354–361
431. Peyrade F, Bondiau PY, Lebrun C, Pivot X, de Jaureguibery JP, Thyss A (1995) [Vertebral osteosarcoma. Review of the literature apropos of a case]. Bull Cancer 82:551–556
432. Phuong LK, Atkinson JL, Thielen KR (2002) Far lateral extraforaminal lumbar synovial cyst: report of two cases. Neurosurgery 51:505–507; discussion 507–508
433. Pilitsis JG, Rengacharya SS (2001) The role of vertebroplasty in metastatic spinal disease. Neurosurg Focus 11: Article 9
434. Platania N, Nicoletti G, Lanzafame S, Albanese V (2003) Spinal meningeal mesenchymal chondrosarcoma. Report of a new case and review of the literature. J Neurosurg Sci 47:107–110
435. Pogoda P, Linhart W, Priemel M, Rueger JM, Amling M (2003) Aneurysmal bone cysts of the sacrum. Clinical report and review of the literature. Arch Orthop Trauma Surg 123:247–251

436. Portenoy RK, Lipton RB, Foley KM (1987) Back pain in the cancer patient: an algorithm for evaluation and management. Neurology 37:134–138
437. Prevo RL, Hageman G, Bruyn RP, Broere G, van de Stadt J (1999) Extended extradural spinal arachnoid cyst: an unusual cause of progressive spastic paraparesis. Clin Neurol Neurosurg 101:260–263
438. Puvaneswary M, Cuganesan R, Barbarawi M, Spittaler P (2003) Vertebral haemangioma causing cord compression: MRI findings. Australas Radiol 47:190–193
439. Rabb CH, McComb JG, Raffel C, Kennedy JG (1992) Spinal arachnoid cysts in the pediatric age group: an association with neural tube defects. J Neurosurg 77:369–372
440. Rades D, Blach M, Nerreter V, Bremer M, Karstens JH (1999) Metastatic spinal cord compression. Influence of time between onset of motoric deficits and start of irradiation on therapeutic effect. Strahlenther Onkol 175:378–381
441. Rades D, Bajrovic A, Alberti W, Rudat V (2003) Is there a dose–effect relationship for the treatment of symptomatic vertebral hemangioma? Int J Radiat Oncol Biol Phys 55:178–181
442. Rand T, Lomoschitz F, Cejna M, Grohs A, Kettenbach J (2003) [Percutaneous radiologically-guided vertebroplasty in the treatment of osteoporotic and tumorous spinal body lesions]. Radiologe 43:723–728
443. Raney RB, Ragab AH, Ruymann FB, Lindberg RD, Hays DM, Gehan EA, Soule EH (1982) Soft-tissue sarcoma of the trunk in childhood. Results of the intergroup rhabdomyosarcoma study. Cancer 49:2612–2616
444. Raney RB, Ater JL, Herman-Liu A, Leeds NE, Cleary KR, Womer RB, Rorke LM (1994) Primary intraspinal soft-tissue sarcoma in childhood: report of two cases with a review of the literature. Med Pediatr Oncol 23:359–364
445. Razek A, Perez CA, Tefft M, Nesbit M, Vietti T, Burgert EO Jr, Kissane J, Pritchard DJ, Gehan EA (1980) Intergroup Ewing's Sarcoma Study: local control related to radiation dose, volume, and site of primary lesion in Ewing's sarcoma. Cancer 46:516–521
446. Rechl H, Plotz W, Gradinger R, Hipp E (1992) Osteoblastoma of the coccyx. A report of two cases. Arch Orthop Trauma Surg 112:36–38
447. Regine WF, Tibbs PA, Young A, Payne R, Saris S, Kryscio RJ, Patchell RA (2003) Metastatic spinal cord compression: a randomized trial of direct decompressive surgical resection plus radiotherapy vs. radiotherapy alone. Int J Radiat Oncol Biol Phys 57 Suppl:S125
448. Rengachary SS, Kepes JJ (1969) Spinal epidural metastatic "mesenchymal" chondrosarcoma. Case report. J Neurosurg 30:71–73
449. Rhines LD, Fourney DR, Siadati A, Gokaslan ZL (2005) En bloc resection of multilevel cervical chordoma with C-2 involvement. Case report and description of operative technique. J Neurosurg Spine 2:199–205
450. Rhomberg W, Bohler FK, Novak H, Dertinger S, Breitfellner G (2003) A small prospective study of chordomas treated with radiotherapy and razoxane. Strahlenther Onkol 179:249–253
451. Rich TA, Schiller A, Suit HD, Mankin HJ (1985) Clinical and pathological review of 48 cases of chordoma. Cancer 56:182–187
452. Rimmelin A, Clouet PL, Salatino S, Kehrli P, Maitrot D, Stephan M, Dietemann JL (1997) Imaging of thoracic and lumbar spinal extradural arachnoid cysts: report of two cases. Neuroradiology 39:203–206
453. Roessner A, Bosse A, Wuisman P, Erlemann R, Grundmann E (1987) [Pathology of tumors of the spinal column]. Orthopäde 16:358–370
454. Romero J, Cardenes H, La Torre A, Valcarel F, Magallon R, Regneiro C, Aragon G (1993) Chordoma: results of radiation therapy in eighteen patients. Radiother Oncol 29:27–32
455. Rompe JD, Eysel P, Hopf C, Heine J (1993) Metastatic spinal cord compression – options for surgical treatment. Acta Neurochir 123:135–140
456. Rompe JD, Eysel P, Hopf C , Heine J (1993) Decompression/stabilization of the metastatic spine. Cotrel-Dubousset-Instrumentation in 50 patients. Acta Orthop Scand 64:3–8
457. Rompe JD, Hopf CG, Eysel P (1999) Outcome after palliative posterior surgery for metastatic disease of the spine – evaluation of 106 consecutive patients after decompression and stabilisation with the Cotrel-Dubousset instrumentation. Arch Orthop Trauma Surg 119:394–400
458. Rosell Pradas J, Ruiz Morales M, Guerrero Fernandez JA, Vara-Thorbeck R (1991) Das sakrokokzygeale Chordom. Ergebnisse nach Radikaloperation. Zentralbl Chir 116:1253–1257
459. Rosen G, Tefft M, Martinez A, Cham W, Murphy ML (1975) Combination chemotherapy and radiation therapy in the treatment of metastatic osteogenic sarcoma. Cancer 35:622–630
460. Rousseaux P, Durot JF, Pluot M, Bernard MH, Scherpereel B, Bazin A, Peruzzi P, Baudrillard JC (1989) [Synovial cysts and synovialomas of the lumbar spine. Histo-pathologic and neuro-surgical aspects apropos of 8 cases]. Neurochirurgie 35:31–39
461. Rovira A, Rovira A, Capellades J, Zauner M, Bella R, Rovira M (1999) Lumbar extradural hemangiomas: report of three cases. AJNR Am J Neuroradiol 20:27–31
462. Rudnick J, Stern M (2004) Symptomatic thoracic vertebral hemangioma: a case report and literature review. Arch Phys Med Rehabil 9:1544–1547
463. Rumboldt Z, Jednacak H, Talan-Hranilovic J, Kalousek V (2004) Spinal epidural rhabdomyosarcoma. Acta Neurochir (Wien) 146:195–197
464. Rushing EJ, Armonda RA, Ansari Q, Mena H (1996) Mesenchymal chondrosarcoma: a clinicopathologic and flow cytometric study of 13 cases presenting in the central nervous system. Cancer 77:1884–1891
465. Ryu S, Rock J, Rosenblum M, Kim JH (2004) Patterns of failure after single-dose radiosurgery for spinal metastasis. J Neurosurg (Suppl 3) 101:402–405
466. Sachdev VP, Savitz MH, Hindi AI, Goldstein HB (1991) Synovial cysts of the lumbar facet joint. Mt Sinai J Med 58:125–128

467. Sakata K, Hareyama M, Oouchi A, Sido M, Nagakura H, Tamakawa M, Akiba H, Morita K (1997) Radiotherapy of vertebral hemangiomas. Acta Oncol 36:719–724
468. Salvati M, Ciappetta P, Artico M, Raco A, Fortuna A (1991) Intraspinal hemangiopericytoma: case report and review of the literature. Neurosurg Rev 14:309–313
469. Samson IR, Springfield DS, Suit HD, Mankin HJ (1993) Operative treatment of sacrococcygeal chordoma. A review of twenty-one cases. J Bone Joint Surg Am 75:1476–1484
470. Sanguinetti C, Aulisa L, Valassina A, D'Arienzo M (1998)The surgical treatment of spinal cord compression caused by tumorous metastases. A review of 91 cases. Chir Organi Mov 83:113–126
471. Sanjay BK, Sim FH, Unni KK, McLeod RA, Klassen RA (1993) Giant-cell tumours of the spine. J Bone Joint Surg Br 75:148–154
472. Sar C, Eralp L (2001) Transoral resection and reconstruction for primary osteogenic sarcoma of the second cervical vertebra. Spine 26:1936–1941
473. Sar C, Eralp L (2002) Metastatic spinal neurofibrosarcoma. Arch Orthop Trauma Surg 122:106–108
474. Satake K, Matsuyama Y, Yoshihara H, Yanase M, Miura Y (2004) Three-dimensional images for surgical plan of giant sacral schwannoma. Spinal Cord 42:368–370
475. Saunders WM, Castro JR, Chen GTY, Sutin PH, Collier JM, Zink SR, Phillips TL, Gauger GE (1986) Early results of ion beam radiation therapy for sacral chordoma. A Northern California Oncology Group study. J Neurosurg 64:243–247
476. Sauvage P, Grimault L, Ben Salem D, Roussin I, Huguenin M, Falconnet M (2000) [Lumbar intraspinal synovial cysts: imaging and treatment by percutaneous injection. Report of thirteen cases]. J Radiol 81:33–38
477. Schajowicz F, Lemos C (1976) Malignant osteoblastoma. J Bone Joint Surg Br 58:202–211
478. Schmid G, Willburger R, Jergas M, Pennekamp W, Bickert U, Koster O (2002) [Lumbar intraspinal juxtafacet cysts: MR imaging and CT-arthrography]. Rofo Fortschr Geb Rontgenstr Neuen Bildgeb Verfahr 174:1247–1252
479. Schoeggl A, Reddy M, Matula C (2002) Neurological outcome following laminectomy in spinal metastases. Spinal Cord 40:363–366
480. Schoenthaler R, Castro JR, Petti PL, Baken-Brown K, Phillips TL (1993) Charged particle irradiation of sacral chordomas. Int J Radiat Oncol Biol Phys 26:291–298
481. Schulz EE, West WL, Hinshaw DB, Johnson DR (1984) Gas in a lumbar extradural juxtaarticular cyst: sign of synovial origin. AJR Am J Roentgenol 143:875–876
482. Schulz-Ertner D, Nikoghosyan A, Thilmann C, Haberer T, Jakel O, Karger C, Kraft G, Wannenmacher M, Debus J (2004) Results of carbon ion radiotherapy in 152 patients. Int J Radiat Oncol Biol Phys 58:631–640
483. Schwechheimer K, Hashemian A, Ott G, Muller-Hermelink HK (1996) Primary spinal epidural manifestation of malignant lymphoma. Histopathology 29:265–269
484. Scott M, Kellett G, Peale A (1974) Angioblastic meningioma (hemangiopericytoma) of the cerebellar fossa with metastases to the temporal bone and the lumbar spine. Surg Neurol 2:35–38
485. Senegas J (1989) [Extensive resection of primary malignant tumors of the sacrum]. Neurochirurgie 35:337–341, 353–334
486. Shah BK, Saifuddin A, Price GJ (2000) Magnetic resonance imaging of spinal plasmacytoma. Clin Radiol 55:439–445
487. Shah RV, Lutz GE (2003) Lumbar intraspinal synovial cysts: conservative management and review of the world's literature. Spine J 3:479–488
488. Shaikh MI, Saifuddin A, Pringle J, Natali C, Sherazi Z (1999) Spinal osteoblastoma: CT and MR imaging with pathological correlation. Skeletal Radiol 28:33–40
489. Sharafuddin MJA, Haddad FS, Hitchon PW, Haddad SF, El-Khoury GY (1992) Treatment options in primary Ewing's sarcoma of the spine: report of seven cases and review of the literature. Neurosurgery 30:610–619
490. Sharma RR, Mahapatra AK, Pawar SJ, Sousa J, Dev EJ (2002) Craniospinal giant cell tumors: clinicoradiological analysis in a series of 11 cases. J Clin Neurosci 9:41–50
491. Shaw B, Mansfield FL, Borges L (1989) One-stage posterolateral decompression and stabilization for primary and metastatic vertebral tumors in the thoracic and lumbar spine. J Neurosurg 70:405–410
492. Sherman R, Waddel J (1986) Laminectomy for metastatic epidural spinal cord tumors. Posterior stabilisation, radiotherapy, and postoperative assessment. Clin Orthop 207:55–63
493. Shih DY, Chen HJ, Lee TC, Chen L (1990) Congenital spinal arachnoid cysts: report of 2 cases with review of the literature. J Formos Med Assoc 89:588–592
494. Shikata J, Yamamuro T, Shimizu K, Shimizu K, Kotoura Y (1992) Surgical treatment of giant-cell tumors of the spine. Clin Orthop 278:29–36
495. Shima Y, Rothman SL, Yasura K, Takahashi S (2002) Degenerative intraspinal cyst of the cervical spine: case report and literature review. Spine 27:E18–22
496. Shimizu K, Shikata J, Iida H, Iwasaki R, Yoshikawa J, Yamamuro T (1992) Posterior decompression and stabilization for multiple metastatic tumors of the spine. Spine 17:1400–1404
497. Shin JH, Lee HK, Rhim SC, Park SH, Choi CG, Suh DC (2001) Spinal epidural cavernous hemangioma: MR findings. J Comput Assist Tomogr 25:257–261
498. Shives TC, McLeod RA, Unni KK, Schray MF (1989) Chondrosarcoma of the spine. J Bone Joint Surg Am 71:1158–1165
499. Siebenrock KA, Unni KK, Rock MG (1998) Giant-cell tumour of bone metastasising to the lungs. A long-term follow-up. J Bone Joint Surg Br 80:43–47
500. Siegal T, Siegal T (1985) Surgical decompression of anterior and posterior malignant epidural tumors compressing the spinal cord: a prospective study. Neurosurgery 17:424–432

501. Silva ML, Brunelle F (1996) Embolisation of vascular lesions of the spinal column in childhood: a report of three cases. Neuroradiology 38:809–811
502. Smith J, Wixon D, Watson RC (1979) Giant-cell tumor of the sacrum. Clinical and radiologic features in 13 patients. J Can Assoc Radiol 30:34–39
503. Smith SR, Saunders PW, Todd NV (1995) Spinal stabilisation in plasma cell disorders. Eur J Cancer 31A:1541–1544
504. Solero CL, Fornari M, Giombini S, Lasio G, Oliveri G, Cimino C, Pluchino F (1989) Spinal meningiomas: review of 174 operated cases. Neurosurgery 25:153–160
505. Solini A, Gargiulo G (1998) Giant cell tumor of the spine. Surgical findings. Chir Organi Mov 83:35–42
506. Solini A, Gargiulo G, Ruggieri N (1998) The surgical treatment of cervical metastases. Chir Organi Mov 83:139–147
507. Soo MYS (2001) Chordoma; review of clinicoradiological features and factors affecting survival. Australas Radiol 45:427–434
508. Stappenbeck L (1972) [Unusual big hour-glass neurinoma]. Fortschr Geb Rontgenstr Nuklearmed 116:274–276
509. Stener B (1989) Complete removal of vertebrae for extirpation of tumors. A 20-year experience. Clin Orthop 245:72–82
510. Sundaresan N, Shah J, Foley KM, Rosen G (1984) An anterior approach to the upper thoracic vertebrae. J Neurosurg 61:686–690
511. Sundaresan N, Galicich JH, Lane JM, Bains MS, McCormack P (1985) Treatment of neoplastic epidural cord compression by vertebral body resection and stabilization. J Neurosurg 63:676–684
512. Sundaresan N, Digiacinto GV, Hughes JEO (1986) Surgical treatment of spinal metastases. Clin Neurosurg 33:503–522
513. Sundaresan N, Huvos AG, Rosen G, Lane JM (1986) Postradiation osteosarcoma of the spine following treatment of Hodgkin's disease. Spine 11:90–92
514. Sundaresan N, Scher H, DiGiacinto GV, Yagoda A, Whitmore W, Choi IS (1986) Surgical treatment of spinal cord compression in kidney cancer. J Clin Oncol 4:1851–1856
515. Sundaresan N, Huvos AG, Krol G, Lang JM, Brennan M (1987) Surgical treatment of spinal chordomas. Arch Surg 122:1479–1482
516. Sundaresan N, Rosen G, Huvos AG, Krol G (1988) Combined treatment of osteosarcoma of the spine. Neurosurgery 23:714–719
517. Sundaresan N, Schmidek HH, Schiller AL, Rosenthal DI (1990) Tumors of the Spine. Diagnosis and Clinical Management. WB Saunders, Philadelphia
518. Sundaresan N, Digiacinto GV, Hughes JEO, Cafferty M, Vallejo A (1991) Treatment of neoplastic spinal cord compression: results of a prospective study. Neurosurgery 29:645–650
519. Sundaresan N, Steinberger AA, Moore F, Sachdev VP, Krol G, Hough L, Kelliher K (1996) Indications and results of combined anterior-posterior approaches for spine tumor surgery. J Neurosurg 85:438–446
520. Sundaresan N, Rothman A, Manhart K, Kelliher K (2002) Surgery for solitary metastases of the spine: rationale and results of treatment. Spine 27:1802–1806
521. Sundaresan N, Boriani S, Rothman A, Holtzman R (2004) Tumors of the osseous spine. J Neurooncol 69:273–290
522. Sung HW, Shu WP, Wang HM, Yuai SY, Tsai YB (1987) Surgical treatment of primary tumors of the sacrum. Clin Orthop 215:91–98
523. Sung MS, Lee GK, Kang HS, Kwon ST, Park JG, Suh JS, Cho GH, Lee SM, Chung MH, Resnick D (2005) Sacrococcygeal chordoma: MR imaging in 30 patients. Skeletal Radiol 34:87–94
524. Swartz PG, Murtagh FR (2003) Spontaneous resolution of an intraspinal synovial cyst. AJNR Am J Neuroradiol 24:1261–1263
525. Sze CI, Kindt G, Huffer WB, Chang M, Wang M, Kleinschmidt-DeMasters BK (2004) Synovial excrescences and cysts of the spine: clinicopathological features and contributions to spinal stenosis. Clin Neuropathol 23:80–90
526. Tabaddor K, Sachs D, Llena JF, Testaiuti MA (1996) Ganglion cyst of the odontoid process. Case report and review of the literature. Spine 21:2019–2022
527. Takano Y, Homma T, Okumura H, Takahashi HE (1992) Ganglion cyst occurring in the ligamentum flavum of the cervical spine. A case report. Spine 17:1531–1533
528. Talac R, Yaszemski MJ, Currier BL, Fuchs B, Dekutoski MB, Kim CW, Sim FH (2002) Relationship between surgical margins and local recurrence in sarcomas of the spine. Clin Orthop:127–132
529. Talacchi A, Spinnato S, Alessandrini F, Iuzzolino P, Bricolo A (1999) Radiologic and surgical aspects of pure spinal epidural cavernous angiomas. Report on 5 cases and review of the literature. Surg Neurol 52:198–203
530. Tatsui H, Onomura T, Morishita S, Oketa M, Inoue T (1996) Survival rates of patients with metastatic spinal cancer after scintigraphic detection of abnormal radioactive accumulation. Spine 21:2143–2148
531. Tatter SB, Cosgrove GR (1994) Hemorrhage into a lumbar synovial cyst causing an acute cauda equina syndrome. Case report. J Neurosurg 81:449–452
532. Templin CR, Stambough JB, Stambough JL (2004) Acute spinal cord compression caused by vertebral hemangioma. Spine J 4:595–600
533. Thongtrangan I, Balabhadra RSV, Le H, Park J, Kim DH (2003) Vertebral body replacement with an expandable cage for reconstruction after spinal tumor resection. Neurosurg Focus 15:Article 8
534. Tokuhashi Y, Matsuzaki H, Toriyama S, Kawano H, Ohsaka S (1990) Scoring system for the preoperative evaluation of metastatic spine tumor prognosis. Spine 15:1110–1113
535. Tombolini V, Zurlo A, Montagna A, Notarianni E, Osti MF, Enrici RM, Pirolli C (1994) Radiation therapy of spinal metastases: results with different fractionations. Tumori 80:353–356
536. Tomita K, Toribatake Y, Kawahara N, Ohnari H, Kose H (1994) Total en bloc spondylectomy and circumspinal decompression for solitary spinal metastasis. Paraplegia 32:36–46

537. Tomita K, Kawahara N, Baba H, Tsuchiya H, Fujita T, Toribatake Y (1997) Total en bloc spondylectomy. A new surgical technique for primary malignant vertebral tumors. Spine 22:324–333
538. Tomita K, Kawahara N, Kobayashi T, Yoshida A, Murakami H, Akamaru T (2001) Surgical strategy for spinal metastases. Spine 26:298–306
539. Tonai M, Campbell CJ, Ahn GH, Schiller AL, Mankin HJ (1982) Osteoblastoma: classification and report of 16 patients. Clin Orthop Relat Res 167:222–235
540. Touboul E, Khelif A, Guerin RA (1989) [Primary tumors of the spine. Initial oncologic aspects: epidemiology, anatomo-prognostic and therapeutic classification]. Neurochirurgie 35:312–316, discussion 351–312
541. Traill ZC, Talbott D, Golding S, Gleeson FV (1999) Magnetic resonance imaging versus radionucleide screening for bone metastases. Clin Radiol 54:448–451
542. Trummer M, Flaschka G, Tillich M, Homann CN, Unger F, Eustacchio S (2001) Diagnosis and surgical management of intraspinal synovial cysts: report of 19 cases. J Neurol Neurosurg Psychiatry 70:74–77
543. Tsukigi M, Kubota Y, Iijima Y, Yaguchi H, Tateno T, Suzuki T, Sasagawa I, Nakada T (2002) Retroperitoneal schwannoma extending into the intravertebral foramen. Urol Int 69:75–77
544. Turanli S, Ozer H, Ozyurekoglu T, Cakiroglu E (2000) Liposarcoma in the epidural space. Spine 25:1733–1735
545. Turcotte RE, Sim FH, Unni KK (1993) Giant cell tumor of the sacrum. Clin Orthop:215–221
546. Ueda S, Hirose A, Miwa M, Sakai N (1975) [Spinal cord tumor of children – a cured case of infantile spinal cord tumor and review of domestic literature (author's transl)]. No Shinkei Geka 3:501–507
547. Uhl V, Castro JR, Knopf K, Phillips TL, Collier JM, Petti PL, Daftari I (1992) Preliminary results in heavy charged particle irradiation of bone sarcoma. Int J Radiat Oncol Biol Phys 24:755–759
548. Vallee C, Chevrot A, Benhamouda M, Gires F, Wybier M, Sellier N, Pallardy G (1987) [X-ray computed tomographic aspects of lumbar articular synovial cysts with intraspinal development]. J Radiol 68:519–526
549. Van der Linden YM, Dijkstra SP, Vonk EJ, Marijnen CA, Leer JW (2005) Prediction of survival in patients with metastases in the spinal column: results based on a randomized trial of radiotherapy. Cancer 103:320–328
550. Van Goethem JWM, Van den Houwe L, Özsarlak Ö, De Schepper AMA, Parizel PM (2004) Spinal tumors. Eur J Radiol 50:159–176
551. Vardiman AB, Dickman CA, Sonntag VKH (1998) Modified anterolateral approach to the craniocervical junction. In: Dickman CA, Spetzler RF, Sonntag VKH (eds) Surgery of the Craniocervical Junction. Thieme, Stuttgart, pp 419–431
552. Venkateswaran L, Rodriguez-Galindo C, Merchant TE, Poquette CA, Rao BN, Pappo AS (2001) Primary Ewing tumor of the vertebrae: clinical characteristics, prognostic factors, and outcome. Med Pediatr Oncol 37:30–35
553. Vergel De Dios AM, Bond JR, Shives TC, McLeod RA, Unni KK (1992) Aneurysmal bone cyst. A clinicopathologic study of 238 cases. Cancer 69:2921–2931
554. Vergne P, Bonnet C, Zabraniecki L, Bertin P, Moreau JJ, Treves R (1996) Synovial cyst at the C1–C2 junction and spondyloarthropathy. J Rheumatol 23:1438–1440
555. Vrionis FD, Small J (2003) Surgical management of metastatic spinal neoplasms. Neurosurg Focus 15: Article 12
556. Wait SD, Jones FD, Lonser RR, Lee KS (2005) Symptomatic epidural hematoma caused by lumbar synovial cyst rupture: report of two cases and review of the literature. Neurosurgery 56:1157
557. Wang AM, Haykal HA, Lin JC, Lee JH (1987) Synovial cysts of the lumbar spine: CT evaluation. Comput Radiol 11:253–257
558. Wang JC, Boland P, Mitra N, Yamada Y, Lis E, Stubblefield M, Bilsky MH (2004) Single-stage posterolateral transpedicular approach for resection of epidural metastatic spine tumors involving the vertebral body with circumferential reconstruction: results in 140 patients. J Neurosurg 3:287–298
559. Watkins RG (2003) Surgical Approaches to the Spine. Springer, New York
560. Weidner A (1986) Extradural tumors of the spine. Adv Neurosurg 14:10–15
561. Weidner A, Immenkamp M (1984) Ergebnisse der operativen Therapie von malignen Wirbelsäulentumoren. In: Schmitt E (ed) Die Wirbelsäule in Forschung und Praxis. Band 103. Tumoren der Wirbelsäule. Hippokrates Verlag, Berlin, pp 203–206
562. Weigel B, Maghsudi M, Neumann C, Kretschmer R, Müller FJ, Nerlich M (1999) Surgical management of symptomatic spinal metastases: postoperative outcome and quality of life. Spine 24:2240–2246
563. Weller SJ, Rossitch E Jr (1995) Unilateral posterolateral decompression without stabilization for neurological palliation of symptomatic spinal metastasis in debilitated patients. J Neurosurg 82:739–744
564. Wiggins GC, Mirza S, Bellabarba C, West GA, Chapman JR, Shaffrey CI 2001) Perioperative complications with costotransversectomy and anterior approaches to thoracic and thoracolumbar tumors. Neurosurg Focus 11: Article 4
565. Wilder RB, Ha CS, Cox JD, Weber D, Delasalle K, Alexanian R (2002) Persistence of myeloma protein for more than one year after radiotherapy is an adverse prognostic factor in solitary plasmacytoma of bone. Cancer 94:1532–1537
566. Winnem MF (1987) Intraspinal chordomas. Paraplegia 25:406–408
567. Wirbel RJ, Schulte M, Mutschler W (1998) [Primary malignant tumors of the sacrum]. Langenbecks Arch Chir Suppl Kongressbd 115:1324–1327
568. Wray CC, Macdonald AW, Richardson RA (1990) Benign giant cell tumour with metastases to bone and lung. One case studied over 20 years. J Bone Joint Surg Br 72:486–489

569. Wuisman P, Lieshout O, Sugihara S, van Dijk M (2000) Total sacrectomy and reconstruction: oncologic and functional outcome. Clin Orthop:192–203
570. Xu F, De Las Casas LE, Dobbs LJ Jr (2000) Primary meningeal rhabdomyosarcoma in a child with hypomelanosis of Ito. Arch Pathol Lab Med 124:762–765
571. Xu WP, Song XW, Yue SY, Cai YB, Wu J (1990) Primary sacral tumors and their surgical treatment. A report of 87 cases. Chinese Med J 103:879–884
572. Yamamoto A, Nishiura I, Handa H, Kondo A (2001) Ganglion cyst in the ligamentum flavum of the cervical spine causing myelopathy: report of two cases. Surg Neurol 56:390–395
573. Yao KC, Boriani S, Gokaslan ZL, Sundaresan N (2003) En bloc spondylectomy for spinal metastases.: a review of techniques. Neurosurg Focus 15:Article 6
574. Yazici M, Iyigun OL, Gulman B, Rakunt C, Cizmeli O (1996) Vertebral hemangioma presenting with intermittent claudication. Eur Spine J 5:131–133
575. York JE, Berk RH, Fuller GN, Rao JS, Abi-Said D, Wildrick DM, Gokaslan ZL (1999) Chondrosarcoma of the spine: 1954 to 1997. J Neurosurg Spine 90:73–78
576. York JE, Kaczaraj A, Abi-Said D, Fuller GN, Skibber JM, Janjan NA, Gokaslan ZL (1999) Sacral chordoma: 40-year experience at a major cancer center. Neurosurgery 44:74–80
577. Young RF, Post EM, King GA (1980) Treatment of spinal epidural metastases. Randomized prospective comparison of laminectomy and radiotherapy. J Neurosurg 53:741–748
578. Zaidat OO, Ruff RL (2002) Treatment of spinal epidural metastasis improves patient survival and functional state. Neurology 58:1360–1366
579. Zevgaridis D, Buttner A, Weis S, Hamburger C, Reulen HJ (1998) Spinal epidural cavernous hemangiomas. Report of three cases and review of the literature. J Neurosurg 88:903–908
580. Zibis AH, Markonis A, Karantanas AH (2000) Unusual causes of spinal foraminal widening. Eur Radiol 10:144–148
581. Zileli M, Cagli S, Basdemir G, Ersahin Y (2003) Osteoid osteomas and osteoblastomas of the spine. Neurosurg Focus 15(5): Article 5
582. Zileli M, Hoscoskun C, Brastianos P, Sabah D (2003) Surgical treatment of primary sacral tumors: complications associated with sacrectomy. Neurosurg Focus 15:Article 9
583. Zimmerman HM (1975) Malignant lymphomas of the nervous system. Acta Neuropathol Suppl (Berl) 6:69–74
584. Zorzon M, Skrap M, Diodato S, Nasuelli D, Lucci B (2001) Cysts of the atlantoaxial joint: excellent long-term outcome after posterolateral surgical decompression. Report of two cases. J Neurosurg Spine 95:111–114

Subject Index

E

F

G

H

I